



18th WORLD CLEAN
AIR CONGRESS 2019

WCAC'19

23-27 September 2019
ISTANBUL / TURKEY

PROCEEDINGS



Editors:

Melik KARA, Yetkin DUMANOĞLU, Gizem TUNA TUYGUN,
Abdurrahman BAYRAM, Tolga ELBİR



Turkish National Committee for Air Pollution Research and Control (TUNCAP)

Proceedings of the
18th World Clean Air Congress 2019

23-27 September 2019
Hilton Istanbul Maslak Hotel - Istanbul, Turkey

organized by

**Turkish National Committee for
Air Pollution Research and Control (TUNCAP)**

and

**The International Union of Air Pollution Prevention and Environmental
Protection Associations (IUAPPA)**

in collaboration with

ITU – Istanbul Technical University
DEU – Dokuz Eylul University
EFCA - The European Federation of Clean Air and Environmental Protection Associations
MyCAS - Clean Air Forum Society of Malaysia
CAA - Clean Air Asia
WB - The World Bank

Editors:

**M. Kara, Y. Dumanoglu, G. Tuna Tuygun,
A. Bayram, T. Elbir**

The Proceedings of the 18th World Clean Air Congress 2019 is printed from the original manuscripts provided by the authors. No responsibility is assumed by the publisher for any injury and/or damage to persons or property as a matter of the products liability, negligence or otherwise, or from any use or operation of any methods, products, instructions or ideas contained in the material herein.

Proceedings of the 18th World Clean Air Congress 2019

Editors: Melik Kara, Yetkin Dumanoglu, Gizem Tuna Tuygun,
Abdurrahman Bayram, Tolga Elbir

Copyright © 2019

Turkish National Committee for Air Pollution Research
and Control (TUNCAP), Izmir-Turkey

ISBN 978-975-00331-2-4

Correspondance Address:

Prof.Dr. Abdurrahman Bayram
Dokuz Eylul University, Department of Environmental Engineering
Tinaztepe Campus, Izmir-Turkey
Tel: +90 232 3017113
Fax: +90 232 4530922
e-mail: abdurrahman.bayram@deu.edu.tr

INTERNATIONAL PROGRAM COMMITTEE

Prof. Abdurrahman Bayram -Turkey
Prof. Alan Gertler - USA
Prof. Ali Deniz - Turkey
Assoc. Prof. Arnis Asmat - Malaysia
Prof. Aysen Muezzinoglu - Turkey
Prof. Aysel Atımtay - Turkey
Prof. Carlos Borrego - Portugal
Dr. Ceyhan Kahya - Turkey
Dr. Deniz Demirhan - Turkey
Prof. Ekrem Ekinici - Turkey
Dr. Gordona Pehnec - Croatia
Prof. Gulen Gullu - Turkey
Dr. Hanlie Liebenberg-Enslin - South Africa
Prof. Hasancan Okutan Turkey
Prof. Huseyin Toros - Turkey
Prof. Hyo Choi – Korea
Prof. Ji Hyeon Song - Korea
Dr. John Murlis - United Kingdom
Assoc. Prof. Juliana Jalaludin - Putra Malaysia
Prof. Mete Tayanc - Turkey
Dr. Murad Qureshi - United Kingdom
Dr. Noor Zaitun Binti Yahaya - Malaysia
Prof. Pavlos Kassomenos - Greece
Dr. Richard Mills - United Kingdom
Dr. Sebnem Aksayoglu - Switzerland
Prof. Sema Topcu -Turkey
Prof. Sermin Ornektekin -Turkey
Dr. Sven-Erik Gryning - Denmark
Dr. Talat Odman - USA
Prof. Tayfun Kindap -Turkey
Prof. Tolga Elbir -Turkey
Dr. Yetkin Dumanoglu - Turkey
Prof. Young Sunwoo - Korea

INTERNATIONAL ADVISORY COMMITTEE

Dr. Markus Amann - IIASA, Austria
Prof. Paulo Artaxo - Brazil
Prof. Alexander Baklanov - WMO
Prof. Robert Bornstein - USA
Prof. Greg Carmichael - USA
Dr. Beatriz Cardenas - Mexico
Dr. Judith Chow - USA
Prof. Tuncay Dogeroglu - Turkey
Prof. Hartmut Herrmann - Germany
Dr. Mark Hibbert - Australia
Dr. Andrzej Jagusiewicz - Poland
Prof. Mehmet Karaca - Turkey
Dr. Kil-Choo Moon - Korea
Prof. George Kallos - Greece
Prof. Gongwoong Lee - Korea
Prof. Menachem Luria - Israel
Prof. Lidia Morawska - Australia
Dr. Nguyen Thi Kim Oanh - Thailand
Prof. Mustafa Odabası - Turkey
Dr. Anumita Roy Chowdhury - New Delhi, India
Prof. Bob Scholes - South Africa
Prof. John H. Seinfeld - USA
Prof. Drew Shindell - USA
Dr. Andreas Skouloudis - Italy
Dr. Youba Sokona - Mali
Prof. Katsunori Suzuki - Japan
Prof. Gurdal Tuncel - Turkey
Dr. Michael P. Walsh - USA
Dr. Martin Williams - UK
Prof. Orhan Yenigun - Turkey
Prof. Tong Zhu – China

PREFACE

18th World Clean Air Congress was held from 23 to 27 September 2019 in Istanbul, Hilton Maslak Hotel. The Congress was organized by the Turkish National Committee for Air Pollution and Control (TUNCAP) and International Union of Air Pollution Prevention Associations (IUAPPA) in collaboration with regional air pollution control organizations from around the world.

The 18th Congress, held in Istanbul, follows earlier congresses which have been held in the worldwide. For example, in 2016 it was held in Busan, Korea, preceded by Cape Town, South Africa in 2013, and before that Vancouver, Canada, Brisbane, Australia, and London, in the UK, in 2004. Next World Clean Air Congress will be held in Singapore in 2021.

The 18th World Clean Air Congress, as one of the premier events in the field, provided a worldwide platform for scientists, policy makers and industrialists to discuss state-of-the-art scientific knowledge and latest progress and technical solutions in improving air quality. The declaration of the last World Clean Air Congress, in Busan, South Korea in 2016, was focused on identifying the impact of air pollution on health and climate, achieving climate mitigation targets, the adopting two-pronged approaches in to achieve climate targets and the sustainable development goals at the local, regional and global levels. This Congress had extended these efforts, while seeking to develop integrated strategies to improve air quality under changing climate. For these reasons the main theme of the 18th World Clean Air Congress was selected as “One Atmosphere: Integrating Climate and Air Pollution Science and Policy”.

The 5-day conference had about 300 participants from 44 countries in 5 continents. In total 20 plenary talks and 168 oral and 32 poster papers were given. Six major side events were organized by the international institutions during the world conference. We would like to convey my thanks and appreciation to the World Bank, European Federation for Clean Air and Environmental Protection Associations, Clean Air Asia and Malaysian Clean Air Association and World Resources Institute for their contributions by performing the Side Events. Special thanks to International Advisory Committee, Program Committee, reviewers, Session Chairs, and student volunteers who contributed to the success of this Conference. I also thank to the Scientific and Technological Research Council of Turkey, Istanbul Technical University, Dokuz Eylul University and for their support.

Finally, we would thank to all participants and sponsors without them we would not have been able to organize this outstanding conference.

We sincerely hope that this congress has been a place to enhance mutual understanding and deepen friendship, and promote cooperation among all participants and participating countries.



Selahattin Incecik
Congress Chair



**18th WORLD CLEAN
AIR CONGRESS 2019**

WCAC'19

**23-27 September 2019
ISTANBUL / TURKEY**

TABLE OF CONTENTS

International Program Committee	iii
International Advisory Committee	iv
Preface	v
Table of Contents	vii
Evaluating the performance of ANN in predicting the concentrations of ambient air pollutants in Nicosia, North Cyprus	1
<i>Sedef Cakir, Moro Sita</i>	
Comparing the performance of entrained mixing reactor applied to the dry scrubbing of gaseous SO₂ and HCl with hydrated lime	13
<i>Young Ok Park, Jea Won Han, Jea Rang Lee, Naim Hassoli, Kang San Lee, HeaTaik Kim, Kwang Duek Kim</i>	
Investigation of the effect of air cleaning devices on air quality in the intensive care unit	27
<i>Sanaz Lakestani, Ibrahim Cakir, Hasan Tahsin Gozdas, Isa Yildiz, Abdullah Demirhan</i>	
Heavy metal exposure monitoring of residents of Slavonski Brod	38
<i>Valjetic Marijana, Ćosić Vesna, Orct Tatjana, Kosanović Cleo, Jurčev Savičević Anamarija, Cvitković Ante</i>	
Integrating citizen's behaviour and air quality management to raise public awareness in European cities	49
<i>Enda Hayes, Joanna Barnes, Andy King, Kris Vanherle, Alastair Callum, Eva Csobod, Laura De Vito, Iason Diafas, Laura Fogg-Rogers, Willem Himpe, Trond Husby, Olga Ivanova, Peter Papics, Jim Longhurs</i>	
Emergency interventions and air pollution in Slavonski Brod, Croatia	57
<i>Ante Cvitković, Vesna Ćosi, Marijana Valjetic</i>	
Intraday and interday variations of 69 volatile organic compounds (BVOCs and AVOCs) and their source profiles at a semi-urban site	63
<i>Serpil Yenisoj Karakas, Melike Dorter, Mustafa Odabasi</i>	
Necessity of improved ammonia emission inventory in agriculture	73
<i>Sung-Chang Hong, Eun-Suk Jang, Sun-Young Yu, Gyu-Hyen Lee, Kyeong-Sik Kim, Sae-Nun Song</i>	
Nickel, arsenic, cadmium, and lead in PM₁ fraction in Zagreb, Croatia	76
<i>Jasmina Rinkovec, Gordana Pehnac, Silva Zužul</i>	
Source apportionment of biogenic and anthropogenic VOCs in Bolu Plateau	84
<i>Melike Dorter, Mustafa Odabasi, Serpil Yenisoj Karakas</i>	
Carbon content in PM_{2.5} at a coastal measuring site in Croatia	94
<i>Ranka Godec, Iva Simić, Martina Silović Hujic, Ivan Bešlić, Silvije Davila, Martin Mihaljević</i>	

PAHs in PM₁ particle fraction at an urban location in Croatia.....	105
<i>Ivana Jakovljević, Zdravka Sever Strukil, Ranka Godec, Gordana Pehnec</i>	
Comparison of electro-chemical sensors for air quality monitoring with reference methods in Zagreb	112
<i>Silvije Davila, Ivan Bešlić, Marko Marić Ivana Hrga</i>	
Ionic composition of PM_{2.5} particle fraction at a coastal urban background site in Croatia	123
<i>Valentina Gluščić, Mirjana Cačković, Gordana Pehnec, Ivan Bešlić</i>	
Atmospheric deposition of organic compounds	129
<i>Iva Simić, Gordana Mendaš, Gordana Pehnec</i>	
Carcinogenic organic content of particulate matter at urban locations with different pollution sources	137
<i>Gordana Pehnec, Ivana Jakovljević, Ranka Godec, Sabina Zero, Jasna Huremović, Katja Džepina</i>	
An integrated analysis of dust transport over Turkey.....	146
<i>Efem Bilgic, Gizem Tuna Tuygun, Orhan Gunduz</i>	
Spatial distribution of health risks associated with PM_{2.5} in Turkey and Iran using satellite and ground observations	160
<i>Burcak Kaynak, Ezgi Akyuz, Mehrdad Samavati</i>	
Long-term analysis of the columnar-surface aerosol relationship with Planetary Boundary Layer Height at southern coastal site of Turkey	172
<i>Gizem Tuna Tuygun, Tolga Elbir</i>	
Location optimization for future coal-fired power plants using geographical information system and dispersion model.....	184
<i>Baris Saridikmen, Ezgi Akyuz, Burcak Kaynak</i>	
Evaluation of hourly based precipitation chemistry in suburban site of Bolu	196
<i>Hatice Karadeniz, Serpil Yenisoay Karakas</i>	
Effects of long-term exposure to PM_{2.5} air pollution on life expectancy of elderly population in Taiwan	203
<i>Jing-Shiang Hwang, Tsuey-Hwa Hu</i>	
Near-real time low-cost PM source apportionment using microscopic chemical imaging	214
<i>Alan W. Gertler, Danny Moshe</i>	
Analysis of NO₂ and SO₂ in Marmara Region	225
<i>Seda Nur Suer, Ceyhan Kahya</i>	
Size-segregated particulate matter down to PM_{0.1} and carbon content during a haze episode in Sumatra Island, Indonesia	244
<i>Muhammad Amin, Rahmi Mulia Putri, Suthida Piriyaakarsakul, Andre Rizky, Aulia Ullah, Worradorn Phairuang, Fumikazu Ikemori, Mitsuhiro Hata, Masami Furuuchi</i>	

Air Pollution reduction with intelligent transportation systems: Dilovası scenario	265
<i>Zubeyde Ozturk, Onur Alp Arslantas, Hande Emanet Beba, Merve Yılmaz, Huseyin Toros</i>	
Determination of greenhouse gas reduction potential for solid fuel based power plants in Turkey	274
<i>Ece Gizem Cakmak, Hasancan Okutan</i>	
Ambient air polybrominated diphenyl ether (PBDE) concentrations in Urla, İzmir, and back trajectory modelling	282
<i>Ilknur Ayri, Mesut Genisoglu, Aysun Sofuoglu, Perihan B. Kurt-Karakus, Askin Birgul, Sait C. Sofuoglu</i>	
Indoor air gas-particulate partitioning of synthetic musk compounds.....	288
<i>Esin Balci, Mesut Genisoglu, Aysun Sofuoglu, Sait C. Sofuoglu</i>	
Air quality level, emission sources and control strategies in Bursa.....	296
<i>Burak Caliskan, Nihan Ozengin, S. Siddik Cindoruk</i>	
Application of reduction scenarios on traffic related NO_x emissions in Trabzon, Turkey	306
<i>Melike Nese Tezel, Deniz Sari, Nesimi Ozkurt, S. Sinan Keskin</i>	
Seasonal variations of organochlorine pesticides (OCPs) in air samples during day and night periods in Bursa, Turkey	321
<i>Gizem Eker Sanli, Yucel Tasdemir</i>	
Determination of fluxes and mass transfer coefficients of Polychlorinated Biphenyls (PCBs).....	330
<i>Ahmet Egemen Sakin, Yucel Tasdemir</i>	
Dust and radon levels on the West Coast of Namibia – what did we learn?	340
<i>Hanlie Liebenberg-Enslin, Detlof von Oertzen, Norwel Mwananawa</i>	
Modeling of greenhouse gas emissions from the transportation sector in Istanbul	349
<i>Tugba Dogan Guzel, Kadir Alp</i>	
Impact on urban and regional air quality from unconventional energy production of shale gas in North Texas.....	359
<i>Guo Quan Lim, Kuruvilla John</i>	
Modeling of PM₁₀ emissions from motor vehicles in Zonguldak, Turkey	370
<i>Ozgur Zeydan, Elif Ozturk</i>	
Estimating particulate matter (PM) concentrations from a meteorological index for data-scarce regions: a pilot study	378
<i>Anzel de Lange, Rebecca M. Garland, Liesl L. Dyson</i>	
Experimental investigation of co-combustion of biocoal with Soma lignite in a 30 kWth circulating fluidized bed	389
<i>Babak Keivani, Hayati Olgun, Aysel T. Atimtay</i>	

Integrated air quality assessment of Konya in terms of meteorology, topography and emission sources	399
<i>Mete Tayanc, Ismail Sezen, Ezgi Akyuz, Burcak Kaynak, Metin Baykara, Alper Unal</i>	
Analysis of surface ozone levels in the forest and vegetation areas in Northwest Anatolia.....	412
<i>Deniz Sari, Selahattin Incecik, Nesimi Ozkurt</i>	
Success of volatile organic compounds (VOCs) emission reduction and challenges for oil and gas sector in Thailand	425
<i>Vichuda Tipsunave, Wasin Pinprateep, Ekkapat Mahasurachaikul, Nathasith Chiarawatchai, Chanansiri Panpanit</i>	
A study of metallic composition in the daily PM_{2.5} samples at Kirklareli, Turkey	431
<i>Halil N. Oruc, Huseyin Ozdemir, Rosa M. Flores, Ismail Sezen, Bulent Akkoyunlu, Goksel Demir, Alper Unal, Mete Tayanc</i>	
Seasonality of PM_{2.5} and its organic fraction in a traffic site in Besiktas, Istanbul.....	447
<i>Rosa M. Flores, Elif Mertoglu, Huseyin Ozdemir, Bulent Akkoyunlu, Alper Unal, Mete Tayanc</i>	
Dispersion modeling and air quality measurements to evaluate the odor impact of a wastewater treatment plant in İzmir	457
<i>Faruk Dincer, Fatih Kemal Dincer, Deniz Sari, Ozcan Ceylan, Ozgen Ercan</i>	
Determination of PM₁₀ and deposited dust dispersion on the settlement areas from Aksa Goynuk coal (lignite) fueled thermal power plant	467
<i>Ozgen Ercan, Faruk Dincer, Deniz Sari, Ozcan Ceylan, Fatih Kemal Dincer</i>	
Indoor air VOC levels associated with the use of bleach containing toilet-bowl cleaners and the effect of ventilation	476
<i>Ilknur Ayri, Mesut Genisoglu, Handan Gaygisiz, Aysun Sofuoglu, Sait C. Sofuoglu</i>	
Black carbon evaluation in an urban side of Istanbul atmosphere during spring and summer seasons	483
<i>S. Levent Kuzu, Elif Yavuz, Ezgi Akyuz, Arslan Saral, Bulent Akkoyunlu, Huseyin Ozdemir</i>	
Wintertime urban air pollution in Macedonia – composition and source contribution of air particulate matter.....	492
<i>Dejan Mirakovski, Blazo Boev, Ivan Boev, Marija Hadzi Nikolova, Afrodita Zendelska, Tena Shijakova</i>	
Assessment of the levels of trace elements and ions in rainwater samples in Pamukkale, Denizli, Turkey...	501
<i>Sibel Cukurluoglu</i>	
An improved high pressure CO₂ capture technology for oxy-fuel combustion.....	509
<i>Hande Cukurlu, Yasemen Kuddusi, Baris Oktay, Hasancan Okutan, Husnu Atakul</i>	
Non-ignorable pollution source: airborne microplastics.....	518
<i>Emine Can-Guven</i>	

Long-term airborne monitoring of lead pollution by lichen <i>Flavoparmelia caperata</i> in Ramsar region, north of Iran.....	525
<i>Ahmad Jahangiri, Amin Dalvand, Reza Ghasemi</i>	
Forecasting of PM₁₀ concentrations in Istanbul using backpropagation neural network	533
<i>Elif Palaz, Tolga Elbir</i>	
Microbial study of airborne microorganisms in indoor air of hospital in Northern Algeria	544
<i>Amina Djadi, F. Benadda, Farid Agouilla, Amel Kaced, Abdelkader Lemou, Nabila Ait Ouakli, Nabila Cherifi, Riad Ladj</i>	
Genotoxicity of polycyclic aromatic hydrocarbons (PAHs) in size segregated PM samples collected from a thermal power plant area.....	554
<i>Eftade Odaman Gaga, Pelin Ertürk Arı, Gonca Cakmak, Akif Arı, Roel Schins, Mustafa Odabasi, Yetkin Dumanoglu, Sema Burgaz</i>	
Assessment of PM_{2.5} concentrations in indoor and outdoor environments of different workplaces	560
<i>Fatma Nur Eraslan, Ozlem Ozden Uzmez, Eftade O. Gaga</i>	
Waterborne transport in Venice lagoon: a problem of sustainability	567
<i>Eliana Pecorari, Giancarlo Rampazzo, Antonio Ferrari, Giovanni Giuconi, Gianluca Cuzzolin</i>	
Linkage among ambient air quality measurements, air quality models, and respiratory symptoms and diseases in different locations of Canakkale, Turkey	576
<i>Sibel Mentese, Nihal Arzu Mirici, Tolga Elbir, Gizem Tuna Tuygun, Coskun Bakar, Sibel Oymak, Muserref Tatman Otkun</i>	
A long-term multi-parametric indoor air quality (IAQ) monitoring study on respiratory diseases and Sick building syndrome (SBS) linkages.....	582
<i>Sibel Mentese, Elif Palaz, Deniz Tasdibi Mumcuoglu, Osman Cotuker, Nihal Arzu Mirici, Coskun Bakar, Sibel Oymak, Muserref Tatman Otkun, Tolga Elbir</i>	
Comparison of BTEX exposure of commuters due to on-road traffic around Canakkale and Kilitbahir Harbors	591
<i>Bahar Akca, Sibel Mentese</i>	
Bibliometric analysis on use of mosses in air pollution studies and possibility of use of mosses for passive monitoring of PM₁₀	597
<i>Bihter Olgun, Feyza Bingol, Cansu Misirlioglu, Selcen Dogan, Ayca Erdem, Cigdem Moral, Guray Dogan</i>	
Gene-environment interaction: the evaluation of chromosomal damage among urban traffic policemen exposed to benzene in relation to <i>NQO1</i>, <i>GSTT1</i>, and <i>GSTM1</i> Polymorphisms.....	603
<i>Noor Fatimah Mohamad Fandi, Juliana Jalaludin, Suhaili Abu Bakar, Mohd Talib Latif</i>	
Sustainable cement sector strategies to control emissions and combat climate change	616
<i>Canan Derinoz Gencel, M. Emre Erguclu, Yasin Yigit</i>	

Metal emissions characterization of piston engine aircraft in general aviation	627
<i>Soner Ozenc Ilhan, Eftade O. Gaga, Gurkan Acikel, Duran Calisir, Mustafa Odabasi, Akif Ari, Gulzade Artun, Emre Can, Enis T. Turgut</i>	
Spatial and temporal variation of AERONET aerosol optical depth over Turkey and its surrounding	635
<i>Esra Ozdemir, Gizem Tuna Tuygun, Fehmican Unsalan, Tolga Elbir</i>	
An overview of WRI experiences in impacts assessment on air quality and personal exposure to air pollutants of mobility interventions.....	647
<i>Tugce Uzumoglu, Cristina Albuquerque, Beatriz Cardenas, Seth Contreras, Luisa Oliveira, Jessica Seddon, Walter Simoni</i>	
Dynamic spatio-temporal health impact assessments using geolocated population-based data: the PULSE project.....	654
<i>Domenico Vito, Riccardo Bellazzi, Vittorio Casella, Cristiana Larizza, Andrea Pogliaghi, Daniele Pala</i>	
Temporal and spatial variability of atmospheric ammonia in the Lombardy region (Northern Italy).....	674
<i>Giovanni Lonati, Stefano Cernuschi</i>	
Particle number concentrations in the Po valley (Northern Italy) in wintertime: comparison between urban and rural sites	684
<i>Giovanni Lonati, Arianna Trentini</i>	
Towards low carbon mobility in a developing country	693
<i>Mohamed Rehan Muhammad Saifuddin, Mohamed Rehan Karim</i>	
Site-specific variation in ambient nanoparticles (PM_{0.1}) in North Sumatra Province-Indonesia	703
<i>Rahmi Mulia Putri, Muhammad Amin, Tetra F. Suciari, Al Fattah Faisal M, Astri Novarina, Sri Rafiah Nam Bintang, Fumikazu Ikemori, Masashi Wada, Mitsuhiro Hata, Masami Furuuchi</i>	
Commuter exposure to black carbon, fine particulate matter and particle number concentration in public marine transport in Istanbul	715
<i>Burcu Onat, Ulku Alver Sahin, Burcu Uzun, Ozcan Akin, Fazilet Ozkaya, Coskun Ayvaz</i>	
Computational fluid dynamics modelling of air distributions and optimization of indoor air quality in classrooms	725
<i>Norhayati Mahyuddin</i>	
Spatial variations of linear and cyclic volatile methyl siloxanes in a river basin and their air-water exchange patterns.....	732
<i>Baris Yaman, Hakan Erkuzu, Fulya Okan, Mustafa Odabasi</i>	
Monitoring and mapping of hydrogen sulphide emissions in a geothermal area in Turkey	742
<i>Yetkin Dumanoglu</i>	
Indoor air THM levels in an olympic and a semi-olympic swimming pool.....	749
<i>Mesut Genisoglu, Yetkin Dumanoglu, Ersan Gunel, Ceren Nurlu, Begum Unsal, Merve Yolcular, Aysun Sofuoglu, Sait C. Sofuoglu</i>	

Investigation of the effects of atmospheric particulate matter transported from deserts on photovoltaic module performance in Sanliurfa, Turkey	755
<i>Tuba Rastgeldi Dogan, Nurettin Besli, Mehmet Azmi Aktacir, Merne Nur Dinc, Mehmet Akif Ilkhan, Fatma Ozturk, Melek Yildiz</i>	
Comparison of MODIS collection 6.1 and 6 aerosol optical depth based on finer resolution dark target dataset over Turkey	764
<i>Gizem Tuna Tuygun, Esra Ozdemir, Tolga Elbir</i>	
An ecological assessment on the air pollution environment of Akhisar	778
<i>M. Dogan Kantarci, Arzu Yucel</i>	
Source apportionment of fine particles simultaneously sampled at rural area versus urban area using receptor model application	797
<i>Orhan Sevimoglu, Wolfgang F. Rogge</i>	
AUTHOR INDEX	809
KEYWORD INDEX.....	813



**18th WORLD CLEAN
AIR CONGRESS 2019**

WCAC'19

**23-27 September 2019
ISTANBUL / TURKEY**



Evaluating the performance of ANN in predicting the concentrations of ambient air pollutants in Nicosia, North Cyprus

Sedef Cakir¹ and Moro Sita²

¹Cyprus International University, Environmental Engineering Department, Nicosia-North Cyprus

²Cyprus International University, Environmental Science Master Program, Nicosia-North Cyprus

scakir@ciu.edu.tr

Abstract. Air pollution is a key concern that has been impacting human health, agricultural harvests, forestry, animals as well as the environment. Indigenous environmental or health organizations regularly make daily air contamination predictions for public awareness and for use in making decisions concerning reduction methods in addition to the management air quality. Predictions are customarily based on statistical associations between meteorological conditions and ambient air contamination concentrations. Multiple linear regression (MLR) models have been extensively utilized. The aim of this work is to ascertain the better technique between MLR (linear method) and Artificial Neural Network (ANN) (non-linear method) models for forecasting concentrations of PM₁₀, NO₂ and O₃ in Nicosia. Multiple regression models and neural networks were investigated for Nicosia using the similar input and output parameters, allowing a comparative study of the two methods. Data from 2012-2015 was used in this research. Previous day's pollutant concentration, atmospheric pressure, wind speed, relative humidity and temperature used as an input parameters. The reliability and strength of the models were evaluated via root mean square error, mean absolute error and Pearson correlation coefficient. The results obtained indicate that MLR did better than ANN except in a few cases where ANN had better predictive performances. The results obtained indicate that MLR did better than ANN except in a few cases where ANN had better predictive performances. However, the Backpropagation (BP) models of all three pollutants developed in this research were found to be in agreement with other studies in the literature proving that the BPANN models built in this study can be used for the prediction of NO₂, O₃ and PM₁₀.

Keywords: Air pollutants, Artificial Neural Network, Linear Regression, Meteorological Parameters.

1. Introduction

Air pollution is an extremely significant issue that should be focused on all around the globe as it affects human health, ecosystems and the environment. It is defined as a condition, in which the substances that result from both natural and anthropogenic activities are present in the air at concentrations sufficiently high above their normal ambient levels producing considerable impacts on humans, animals, vegetation, or materials (Seinfeld and Pandis, 1998). It is important to minimizing the adverse effects by providing proper actions and controlling strategies. This can be done by predicting air quality exactly.

Air pollution is greatly correlated with meteorological conditions. Actually, contaminants are usually trapped into the planetary boundary layer (PBL), which is the lowermost part of the atmosphere and it

is directly affected by its interaction with the ground. In this particular layer, physical factors such as, temperature, moisture, flow velocity and pollutants show rapid fluctuations or turbulence and vertical mixing is strong as well (Cogliani, 2001). Meteorological elements have a relationship with the air pollutants and as such provide vital information about air pollution, in the sense that they are involved in the dispersal and/or production of pollutants. Temperature (sunlight) plays a pivotal role in the formation of photochemical smog. This is due to the fact that a photochemical smog is formed as a result of a combination of pollutants such as nitrogen oxides and volatile organic compounds (VOCs) reacting with sunlight (temperature) to form a brown haze over cities. This occurs predominantly in summer since that is when temperatures are highest (Colbeck and Mackenzie, 1994). Another case of the association between temperature and contaminants is in the formation of ozone. The formation of ozone in the troposphere arises when ozone precursors such as volatile organic compounds (VOCs), carbon monoxide (CO) and when nitrogen oxides (NO_x) undergo an atmospheric reaction in the presence of sunlight (temperature) (Reeves et al., 2002).

A set of observed data from air monitoring and meteorological stations have been analysed using some statistical techniques such as Pearson linear correlation coefficient and regression analysis to determine whether a relationship exist among the meteorological parameters and the pollutants (Bhardwaj and Pruthi, 2016; Abdullahi, 2017). According to Ocak and Turalioglu (2008), the relationship between temperature and air contaminants such as NO, CO, O₃ is important. For example at lower air temperatures, higher concentrations of CO and NO_x have been observed, in winter. However the amount of O₃ is high at higher temperature. Previous day's concentration has an effect on air pollutants concentrations as well as the impact of daily meteorological parameters (Ocak, 1997) and its a useful predictor for contaminants.

Several studies on air quality prediction using multiple linear regression and artificial neural networks (ANN) have been done (Barai et al., 2003; Wang et al., 2003; Hassan and Li, 2008; Nidzgorska-Lencewicz and Czarnecka, 2015) Computation and implementation of regression models are simple which are advantages of MLR. Although regression techniques have an extensive history of application as predicting tools in various areas including air pollution, regression models may not offer precise predictions in some complex circumstances such as non-linear data and extreme values data. The reason for this is that linear relations are tried to be obtained between parameters in linear regression analysis. Another limitation of regression models is that the necessity to satisfy regression assumptions and multiple collinearity between independent and dependent variables results in the failure of regression model (Molazem et al., 2002; Ul- Saufie et al., 2011; Zaefizadah et al., 2011). On the other hand ANNs are well suited to the extraction of information from vague and non-linear data which makes them valuable tools for forecasting. ANNs have application in vast array of tasks which can be classified as forecasting, function estimation or pattern taxonomy. Forecasting has to do with prediction of prospective trends with the aid of time series of information given using present and past parameters. Function estimation on the other hand deals with modelling the association amongst parameters whereas pattern taxonomy comprises categorizing information into distinct groups (Gardner and Dorling, 1998). It is thus imperative to perform a comparative analysis between ANN and MLR to ascertain the better forecasting tool. There are such studies done to predict PM₁₀ Papanastasiou et al., 2007; (Ul- Saufie et al., 2011).

The objective of this study is to design an ANN pollutant predictor model of air contaminants (O₃, PM₁₀, NO₂) utilizing historical data from the year 2012 to 2015. Thus, separate ANN model was developed for each pollutant of O₃, PM₁₀ and NO₂. Besides, a comparative analysis between a linear (MLR) and a non-linear (ANN) method of pollutant modelling in order to ascertain the better air quality forecasting tool was performed.



2. Data and methodology

Nicosia is the capital and largest city on the island of Cyprus, located at latitude 35°10'31"N, and longitude 33°21'51"E with an elevation of 220 m above the sea level. This area of study has a hot semi-dry weather owing to its low yearly rainfall totals. The city experiences extended, hot, arid summers, and cool to slight winters, with maximum of the rainfall taking place in winter. Nicosia has mean annual high and low temperature of 26.2 and 13.2 °C respectively. The data used in this study include the daily average of meteorological parameters (temperature, relative humidity (RH), wind speed and atmospheric pressure) and hourly concentrations of O₃ and NO₂ as well as daily concentrations of PM₁₀ all of which span from 2012 to 2015. The meteorological data were obtained from the Meteorological Department whilst the air quality data was provided by the Environmental Protection -Air Emission - Department of Northern Cyprus.

Organizing data for the neural network, data analysis is an imperative and crucial stage that has a massive influence on the success as well as the performance of the ANN results (Yu et al., 2006). The data set was examined for missing data. If there are missing data for any parameter due to the calibration or faults in the measuring instruments, all the other parameters observed on same date supposed to be deleted. The data used in this study were separated into two sets, learning set (2014-2015) for training the ANN and simulation set (2012-2013) for validating the efficacy and accuracy of the developed model. As there is no general laws to determine the size of subdivisions, the data set for this study was arbitrarily subjected to a ratio of 1:1 for training and simulation sets respectively (Sita, 2019). 2012-2013 period selected as simulation because this is the similar period of data which is used in multiple linear regression analysis done by Cakir and Abdullahi (2017).

2.1. ANN model development

The development of ANN was inspired by the human nervous system and mathematical operators are used to simulate this system by using predictors and predictand which are act as inputs and output, respectively (Cakir et al., 2013). There are several types of ANNs based on their architecture, such as Multilayer Perceptron (MLP), Elman Recurrent Network, and the Radial Basis Function Network.

There are two main steps in ANN, training and testing. During the training process, the network analyses the training data and adjusts the weights between network units until a desirable error between calculated outputs and observed outputs is achieved. Then, the network tests the unused data using final weights to measure the performance of the network. Out of the several learning algorithms, back-propagation algorithm is the most widespread and the most implemented for the purpose of training feed-forward neural systems. Hidden and output layers include activation functions that are various kinds of nonlinear functions (sigmoid, hyperbolic tangent, etc.). This is the part that makes the neural networks more powerful compared to linear methods.

In order to develop the prediction model for air pollutants, MATLAB Neural Network Toolbox was utilized as it is a simple and user-friendly. The Neural Network Toolbox exhibits a wide range of parameters for neural network development which can be selected (Koshand et al., 2017).

In this study the feedforward Back Propagation (BP) MLP architecture was designated for the air quality modelling since BP is one of the most prevalent training procedures, used for non-linear models (Figure 1). Also among different BP algorithms, the Levenberg Marquardt method is employed because of its demonstrated fast learning rate.

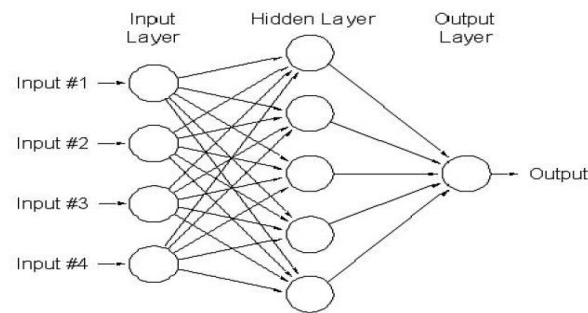


Figure 1. Multilayer perceptron. Source: Cilimkovic (2015)

Specifically, MATLAB simulator was run to train and simulate the network. Table 1 displays the designated contaminants and meteorological parameters used as input parameters for each pollutants model. Where PDC is previous day's concentration, WS is wind speed, P is pressure, T is temperature, RH is Relative Humidity.

In the current research, the MLP models were run in a supervised method based on trial and error system and several different modifications were integrated to increase the model performance. These modifications comprised alternative utilization of different number of nodes in the hidden layer, diverse epochs, different input parameter as well as use of diverse activation functions. The neural network training continued till attaining the maximum correlation between the measured and predicted output or until a desirable error between calculated outputs and observed outputs is achieved. The performance functions used to assess the efficacy of the model are correlation coefficient (r), RMSE, MAE. As seen from Table 1, for all three pollutants same meteorological parameters and PDC are utilized as input because it is observed that different input configurations did not cause significant differences in performances.

Table 1. Input and output parameters proposed for each pollutant ANN model

	Model 1	Model2	Model 3
	O ₃ PDC	PM ₁₀ PDC	NO ₂ PDC
Input Parameters	WS	WS	WS
	P	P	P
	T	T	T
	RH	RH	RH
	NO ₂	-	-
Output Parameters	O ₃	PM ₁₀	NO ₂

2.2. Multiple linear regression

Regression is a statistical procedure used to determine the relationships that exist between two or more variables and it is predominantly used for estimation. Among the different types of regression analysis linear regression method is widely used by the scientist to show the linear relations between variables. General multiple linear regression equation, used for more than one independent variable, which for three independent variable is given in Equation (1) as:

$$Y = A + B_1X_1 + B_2X_2 + B_3X_3 + E \quad (1)$$

Where, Y is the predicted/dependent variable, A is the constant of regression B_i is the regression coefficient of ith independent variable, X_i is the ith independent variable. Coefficient of determination (R²) is used to show goodness of fit of regression model.

In this study, stepwise multiple linear regression equations (Equation (2) to (12)) developed by Cakir and Abdullahi (2017) for Nicosia, for the period of 2012-2014 were used to simulate 2012-2013 data which were used to simulate ANN models. NO₂, O₃ and PM₁₀ has different MLR equation for each season. As can be seen from the equations below, among the different meteorological parameters (pressure, RH, temperature, wind speed) and previous day's concentration, variables with p<0.05 were selected as independent variable by Cakir and Abdullahi (2017). PDC is a common parameter in all.

According to the R² values obtained by Cakir and Abdullahi (2017), at most 70% of the O₃ and NO₂ can be determined by given Equations (5), (6), or (10). However, PM₁₀ is not predictable by given equations below.

$PM_{10} = 1637.29 - 1.57(P) + 0.31(PDC)$	Spring	R ² = 0.14	(1)
$PM_{10} = -5.99 + 1.75 (WS) + 0.91(T) + 0.40(PDC)$	Summer	R ² = 0.22	(2)
$PM_{10} = 72.83 - 5.10 (WS) - 2.26 (T) + 0.38 (PDC)$	Winter	R ² = 0.25	(3)
$O_3 = 50.72 - 0.36 (RH) + 1.65 (WS) + 0.44(PDC)$	Spring	R ² = 0.47	(4)
$O_3 = 537.59 - 0.45 (P) - 0.47(RH) + 2.05 (WS) - 1.33(T) + 0.54(PDC)$	Summer	R ² = 0.70	(5)
$O_3 = 9.67 - 0.14 (RH) + 3.54 (WS) + 0.75(T) + 0.40(PDC)$	Fall	R ² = 0.70	(6)
$O_3 = 283.88 - 0.25 (P) - 0.29 (RH) + 3.17 (WS) + 0.61 (T) + 0.38(PDC)$	Winter,	R ² = 0.48	(7)
$NO_2 = 16.26 - 0.06 (RH) - 1.26(WS) - 0.12 (T) + 0.53(PDC)$	Spring	R ² = 0.35	(8)
$NO_2 = 7.97 - 0.098 (RH) - 0.961 (WS) + 0.795(PDC)$	Summer	R ² = 0.69	(9)
$NO_2 = 57.23 + 0.14 (RH) - 3.93(WS) - 1.02(T) + 0.30 (PDC)$	Fall	R ² = 0.69	(10)
$NO_2 = 14.87 - 1.70 (WS) + 0.60(PDC)$	Winter	R ² = 0.41	(11)

3. Results and Discussion

3.1. Statistical analysis of the data sets

Statistical analyses which include mean, standard deviation (Std dev), minimum (min) and maximum (max) were carried out on the entire dataset for O₃, PM₁₀ and NO₂, and the results are displayed in Table 2. The mean daily concentration of O₃ is 49.19 µg/m³ with a standard deviation of 18.12 µg/m³. The minimum and maximum observed concentrations of O₃ are 9.14 and 97.60 µg/m³ respectively. The average daily PM₁₀ concentration is 52.25 µg/m³ with a standard deviation of 37.63 µg/m³. The minimum and maximum concentrations are 15.80 and 912.70 µg/m³ respectively. The maximum PM₁₀ concentration was recorded during the dust storm transportation in September 2015. From the Table 2 the mean NO₂ concentration is 19.80 µg/m³ with a standard deviation of 10.90 µg/m³. The minimum and maximum concentrations are 1.00 and 79.06 µg/m³ respectively.

The correlations between O₃, PM₁₀, NO₂ and atmospheric parameters (pressure, RH, temperature, wind speed) and previous day's concentration were evaluated for 4 year period, 2012-2015 and displayed in

Table 3. According to Pearson correlation coefficient (r), there is a significant relation between pollutant concentrations and meteorological parameters. It was found that pressure and RH have similar effects on pollutants. They have a moderate positive relation with NO₂, weak positive relation with PM₁₀ but there is a moderate negative relation with O₃. Wind speed has a moderate positive relationship with O₃, but moderate negative relationship with NO₂ concentration. Increasing temperature cause an increasing concentrations for O₃ but decreasing concentrations for NO₂. However, there is a weak negative relationship amongst PM₁₀, temperature and wind speed. All the findings about relationship between meteorological parameters and pollutants at this research are similar to ones in the other studies (Ocak and Turalioglu, 2008).

Table 2. Statistical analysis of PM₁₀, NO₂ and O₃ concentration between 2012-2015

	PM ₁₀ (µg/m ³)	NO ₂ (µg/m ³)	O ₃ (µg/m ³)
Mean	52.25	19.80	49.19
Std dev	37.63	10.90	18.12
Min	15.80	1.00	9.14
Max	912.70	79.06	97.60
# of data	1270	1347	1194

Table 3. Correlation between pollutants and meteorological parameters and previous day's concentration

Pollutant	P (mbar)	RH (%)	T (°C)	WS (m/s)	PDC (µg/m ³)
NO ₂	0.57**	0.42**	-0.51**	-0.54**	0.80**
O ₃	-0.45**	-0.67**	0.57**	0.50**	0.86**
PM ₁₀	0.24*	0.15**	-0.23*	-0.23**	0.33**

** Correlation is significant at the 0.01 level (2-tailed).

* Correlation is significant at the 0.05 level (2-tailed).

3.2. ANN model performances

ANNs were trained with different neuron numbers and different transfer functions used in hidden layer. In all algorithms purelin which is linear transfer function was used in output layer. Some of the algorithm results and performances are in Table 4. It is evident that each configuration has different performance for pollutants. Among the O₃ predictions ANN5 has the best performance, while according to RMSE, MAE and (r) ANN10 has the best performance for PM₁₀ predictions. There is no significant differences between given performances for NO₂ prediction but ANN10 has the lower MAE.

Table 4. Performances of different training configurations for O₃, PM₁₀ and NO₂

ANN model	TF (H/O)	# of epochs	RMSE	MAE	r
			O ₃ / PM ₁₀ / NO ₂	O ₃ / PM ₁₀ / NO ₂	O ₃ / PM ₁₀ / NO ₂
ANN5	Tansig/Purelin	50	9.12 / 29.38 / 6.10	7.05 / 17.58 / 4.90	0.87 / 0.35 / 0.85
ANN10	Logsig/Purelin	100	9.80 / 27.29 / 5.90	7.77 / 16.56 / 4.36	0.86 / 0.47 / 0.84
ANN15	Logsig/Purelin	150	11.22 / 28.11 / 5.76	8.70 / 16.69 / 4.54	0.80 / 0.44 / 0.86
ANN20	Tansig/Purelin	200	9.84 / 29.72 / 6.66	7.52 / 17.51 / 5.16	0.85 / 0.37 / 0.80

3.2.1. Comparing ANN prediction performances with other studies.

Best models for predicting O₃, PM₁₀ and NO₂ concentrations were determined as ANN5, ANN10 and ANN10 configurations respectively. Details about this configurations are seen in Table 4.

Table 5 shows O₃, PM₁₀ and NO₂ simulation performances of selected ANNs in this study together with other studies. Levenberg Marquardt (LM) training algorithm was used in all of the presented studies, as well as in this study. This study totally have 4 years data in which years 2012 and 2013 were completely used for simulation. RMSE, MAE and (r) values obtained from ANN predictions and observations for 2012-2013 period are presented in Table 5.

As seen in Table 5, O₃ predictions using ANN algorithms have a strong correlation with observed concentrations. ANN performances obtained in this study are similar to the results of other studies. Regarding to r values, Cai et al. (2009) had obtained the best predictions for O₃ and NO₂. Considering the accuracies of O₃ and NO₂ predictions this study has a better performance when compared to the ones of Hrust et. al. (2009) and Ding et al. (2016).

Hrust et al. (2009) used ANN to obtain predictions for PM₁₀ also, but according to error calculations accuracy in PM predictions is worse than in O₃ and NO₂ predictions. Similar findings with Hrust et. al. (2009) were obtained in this study. However, studies done by Cai et al. (2009) and Chaloulakou and Grivas (2006) have good performances also in prediction of PM₁₀.

Table 5. ANN performances in this study and other studies

Pollutant	Researcher	# of Data	Hidden Layer:Nodes	RMSE	MAE	r
O ₃	This study	4 years	1:5	9.12	7.05	0.87
	Hrust et al. (2009)	3	2:(24)(10)	18.16	14.01	0.73
	Cai et al. (2009)	2	1:20	10.30	7.5	0.94
	Ding et al. (2016)	2	1:25	15.90	12.60	0.65
PM ₁₀	This study	4 years	1:10	21.10	15.22	0.56
	Hrust et al.(2009)	3	2:(24)(12)	18.54	12.42	0.47
	Cai et al. (2009)	2	1:20	20.70	15.15	0.96
	Grivas and Chaloulakou (2006)	18 months	1:15	26.06	19.1	0.80
NO ₂	This study	4 years	1:10	5.90	4.37	0.84
	Hrust et al.(2009)	3	2:(24)(8)	6.04	8.86	0.82
	Cai et al. (2009)	2	1:20	21.90	14.90	0.87
	Ding et al. (2016)	2	1:25	20.20	16.3	0.67

The observed and predicted O₃, PM₁₀ and NO₂ values were matched graphically for the simulation data (2012-2013) as given in Figures 2 to 4. Extremum PM₁₀ values (<140 µg/m³) were not included to graphs as well as the accuracy analysis. As can be seen from the graphs, there is a relationship between the observed and predicted values, but the ANN overestimated some values while underestimated some others.

It can be observed from the Figure 2 that the observed and predicted O₃ values are very close to each other with the exception of some days during summer and fall seasons. During these seasons there are some significant differences between the observed and predicted values.

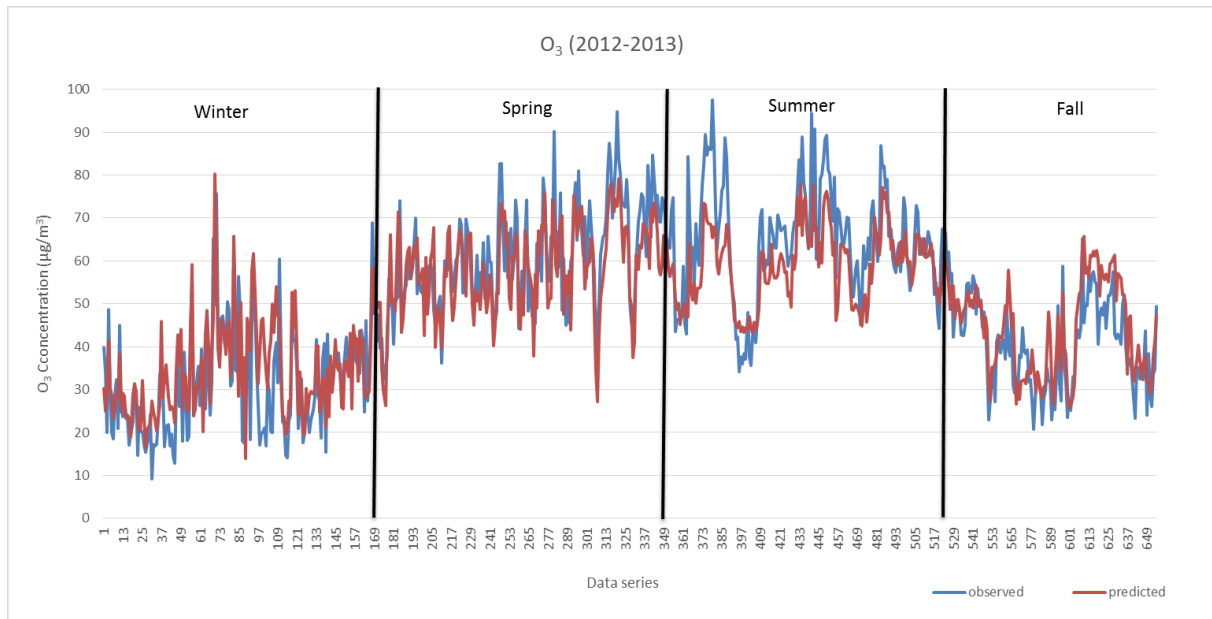


Figure 2. Observed and predicted O₃ concentrations using ANN5 model

ANN predictions for the PM₁₀ concentrations (Figure 3) appear as matched with observations but especially winter season predicted values are less than the observed values. According to the Figure 4, NO₂ predictions underestimates the concentrations especially for the higher values observed in winter season while, there are some overestimations during summer.

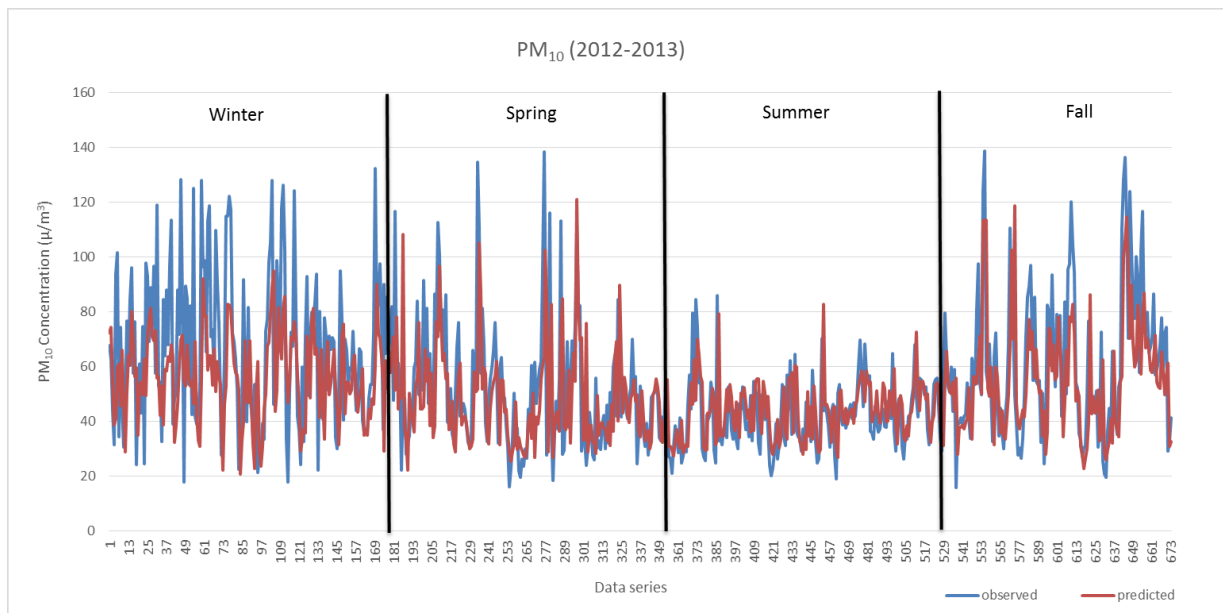


Figure 3. Observed and predicted PM₁₀ concentrations using ANN10 model

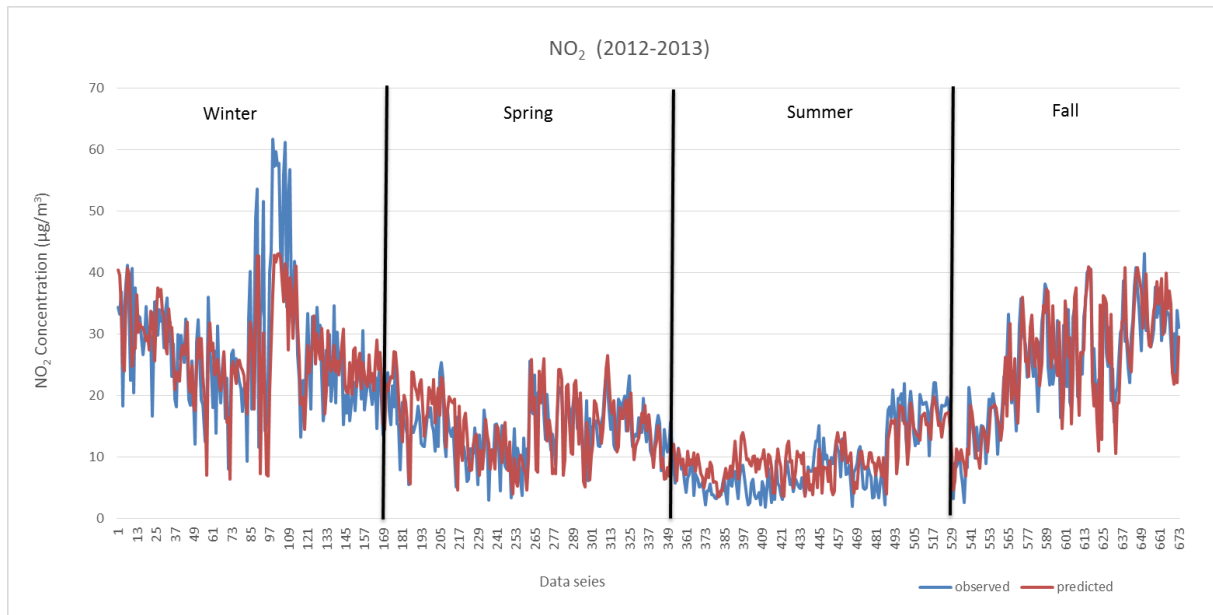


Figure 4. Observed and predicted NO₂ concentrations using ANN10 model

3.3. Comparison between ANN and simulated Cakir and Abdullahi (2017)'s MLR performances

In this study, Cakir and Abdullahi (2017) MLR equations obtained for the Nicosia were used to predict NO₂, O₃ and PM₁₀ only for the period of 2012-2013. Same data sets used to simulate both ANN and MLR but predictors used in ANN are not exactly same with the independent variables of regression equations. During the model development, independent variables of the MLR equations were used as a predictor in different ANN configurations however the obtained performances were not better than ANN trained with predictors given in Table 1.

Seasonal ANN performances were compared with MLR performances in Table 6 to Table 8 for each pollutant. Table 6 shows that the MLR model has lower RMSE and higher correlation values than ANN and it has a better performance than the ANN model to predict the O₃. The error measure (RMSE) of the ANN model is less than that of MLR model only for spring season as seen in Table 7. There is no significant differences between MLR and ANN model performances for winter and summer. In this study ANN and MLR models did not exhibit good performance in PM₁₀ predictions, however Ul-Saufi et al. (2011) stated that MLR and ANN can be used to predict PM₁₀. Papanastasiou et al. (2007) also concluded that neural network can predict PM slightly better than multiple regressions.

It can be seen from the Table 8 that the MLR model for NO₂ has higher correlation coefficient except for spring and lower RMSE values except for summer. However, there are no significant differences between accuracy of the predictions.

Table 6. Comparison between ANN and MLR analysis for O₃ (2012-2013)

	Winter		Spring		Summer		Fall	
	RMSE	r	RMSE	r	RMSE	r	RMSE	r
This study	9.47	0.69	8.70	0.73	10.37	0.77	7.39	0.81
Cakir and Abdullahi (2017)(MLR model)	7.75	0.75	7.70	0.77	6.72	0.86	5.77	0.85
# of Data	167		177		175		135	

Table 7. Comparison between ANN and MLR analysis for PM₁₀ (2012-2013)

	Winter		Spring		Summer		Fall	
	RMSE	r	RMSE	r	RMSE	r	RMSE	r
This study	26.63	0.46	21.81	0.47	12.82	0.41	20.94	0.65
Cakir and Abdullahi (2017) (MLR Model)	24.51	0,45	32.19	0.26	11.39	0.38	-	-
# of Data	174		180		172		147	

Table 8. Comparison between ANN and MLR analysis for NO₂ (2012-2013)

	Winter		Spring		Summer		Fall	
	RMSE	r	RMSE	r	RMSE	r	RMSE	r
This study	8.36	0.64	4.71	0.60	3.69	0.74	6.21	0.79
Cakir and Abdullahi (2017) (MLR Model)	8.20	0.65	3.85	0.58	3.92	0.85	5.85	0.82
# of Data	169		182		177		145	

4. Conclusion

Main objectives of this study were performing the multiple linear regression and Multi-layer perceptron-ANN models for predicting O₃, PM₁₀ and NO₂ in Nicosia, Northern Cyprus and comparing the performances by error statistics. In MLR models, depending on their significance's independent parameters were selected from meteorological parameters (pressure, temperature, RH, wind speed) and previous days's concentration. Different MLR models were obtained for each pollutant and each season. In ANN models all the meteorological parameters and previous day's concentration were used as an input for all pollutants. Parameter selection may cause a differences between MLR and ANN models.

In general, the ANN model results obtained for NO₂ and O₃ are similar to other studies in the literature. ANN model which is a non-linear method did not produce more accurate or more significant predictions than MLR except for some seasons. Whereas it was expected to yield more successful results. If these two models are developed with completely same parameters results may change. Developing the MLR models for each season separately may have led to an improvement in MLR predictions.

5. References

- Abdullahi, A.H., 2017. The impacts of meteorological parameters on air pollution in Nicosia, TRNC. Master Thesis, Cyprus International University, Nicosia, Cyprus, 112 pages.
- Barai, S.V., Dikshit, A.K., Sharma, S., 2003. Neural network models for air quality prediction: a comparative study. *Soft. Comput. Ind. Appl.* 39, 209–305.
- Bhardwaj, R., Pruthi, D., 2016. Time series and predictability analysis of air pollutants in Delhi. In *Next Generation Computing Technologies (NGCT), 2nd International Conference on Next Generation IEEE*, pp. 553-560.
- Cai, M., Yin, Y., Xie, M., 2009. Prediction of hourly air pollutant concentrations near urban arterials using artificial neural network approach. *Transportation Research Part D: Transport and Environment.* 14(1), 32-41.
- Cakir, S., Kadioglu, M., Cubukcu, N., 2013. Multischeme ensemble forecasting of surface temperature using neural network over Turkey. *Theor. Appl. Climatol.* 111, 703–711.
- Cakir, S., Abdullahi, A.H., 2017. Hava kirletici konsantrasyonlarının meteorolojik parametrelere dayali çoklu-lineer regresyonla analizi: Kuzey Kıbrıs Örneği. VII. Ulusal Hava Kirliliği ve Kontrolü Sempozyumu, 1-3 Kasım 2017, Antalya, Turkey.

- Chaloulakou, A., Grivas, G., 2006. Artificial Neural Network Models for Prediction of PM₁₀ Hourly Concentrations, in the Greater Area of Athens, Greece. *Atmospheric Environment*. 40, 1216-1229.
- Cilimkovic, M., 2015. Neural networks and back propagation algorithm. Institute of Technology Blanchardstown, Blanchardstown Road North Dublin, 15.
- Cogliani, E., 2001. Air pollution forecast in cities by an air pollution index highly correlated with meteorological variables. *Atmos. Environ.* 35(16), 2871-2877.
- Colbeck, I., Mackenzie, A.R., 1994. Air pollution by photochemical oxidants. *Air Quality Monographs*. Vol. 1, Elsevier, Netherlands.
- Ding, W., Zhang, J., Leung, Y., 2016. Prediction of air pollutant concentration based on sparse response back-propagation training feedforward neural networks. *Environmental Science and Pollution Research*. 23(19), 19481-19494.
- Gardner, M.W., Dorling, S.R., 1998. Artificial neural networks (the multilayer perceptron)- A review of applications in the atmospheric sciences. *Atmospheric Environment*. 32(14-15), 2627-2636.
- Grivas, G., Chaloulakou, A., 2006. Artificial neural network models for prediction of PM₁₀ hourly concentrations, in the Greater Area of Athens, Greece. *Atmospheric Environment*. 40(7), 1216-1229.
- Hassan, M.R., Li, M., 2010. Urban air pollution forecasting using artificial intelligence-based tools. *Air Pollution*, In Tech, Chapter 9, pp. 195-219.
- Hrust, L., Klaić, Z.B., Križan, J., Antonić, O., Hercog, P., 2009. Neural network forecasting of air pollutants hourly concentrations using optimised temporal averages of meteorological variables and pollutant concentrations. *Atmospheric Environment*. 43(35), 5588-5596.
- Khoshand, A., Sehrani, M.S., Kamalan, H., Bodaghpour, S., 2017. Prediction of Ground-Level Air Pollution Using Artificial Neural Network in Tehran. 1(1), 61-67.
- Molazem, D., Valizadeh M., Zaefizadeh M., 2002. North West of genetic diversity of wheat. *J. Agricultural Sciences*. 20, 353-431.
- Nidzgorska-Lencewicz, J., Czarnecka, M., 2015. Winter weather conditions vs. air quality in Tricity, Poland. *Theoretical and Applied Climatology*. 119(3-4), 611-627
- Ocak S., 1997. Erzurum'da Hava Kirliliği, Değerlendirmesi ve Atmosferik Parametrelerle İlişkilendirilmesi, Master Thesis, Atatürk University, Erzurum.
- Ocak S., Turalioglu, F.S., 2008. Effect of meteorology on the atmospheric concentrations of traffic related pollutants in Erzurum, Turkey. *J. Int. Environmental Application & Science*. 3(5), 325-335.
- Papanastasiou, D., Melas D., and Kioutsioukis I., 2007. Development and Assessment of Neural Network and Multiple Regression Models in Order to Predict PM₁₀ Levels in a Medium-sized Mediterranean City. *Water, Air & Soil Pollution*. 182(1), 325-334.
- Reeves, C.E., Penkett, Stuart A., Bauguitte, S., Law, K.S. Evans, M.J., Bandy, B.J., Monks, P.S., Edwards, G.D., Phillips, G., Barjat, H., Kent, J., Dewey, K., Schmitgen, S., Kley, D. 2002. Potential for photochemical ozone formation in the troposphere over the North Atlantic as derived from aircraft observations during ACSOE. *Journal of Geophysical Research*. 107 (D23), 4707, ACH14 1-14.
- Seinfeld, J.H., Pandis, S.N., 1998. *Atmospheric Chemistry and Physics: From air pollution to climate change*. John Wiley and Sons, New York.
- Sita, M., 2019. Evaluating the performance of a non-linear method (Artificial Neural Networks) in predicting the concentrations of ambient air pollutants in Nicosia, TRNC. Master Thesis. Cyprus International University, Nicosia, 87 page.



18th World Clean Air Congress, 23-27 September 2019, Istanbul
organized by TUNCAP and IUAPPA

Ul-Saufie, A.Z., Yahya, A.S., Ramli, N.A., Hamid, H.A., 2011. Comparison between multiple linear regression and feed forward back propagation neural network models for predicting PM₁₀ concentration level based on gaseous and meteorological parameters. *International Journal of Applied*. 1(4), 42-49.

Wang, W., Xu, Z., Lu, J.W., 2003. Three improved neural network models for air quality forecasting. *Engineering Computations*. 20(2), 192-210.

Yu L., Wang S., Lai K.K., 2006. An integrated data preparation scheme for neural network data analysis. *IEEE Trans. Knowl. Data Eng.* 18, 217-230.

Zaefizadah M., Khayatnezhad M., Ghlaomin M., 2011. Comparison of Multiple Linear Regression (MLR) and Artificial Neural Network (ANN) in Predicting the Yield Using its Components in the Hulless Barley. *J. Agriculture and Environmental Sciences*. 10(1), 60-64.

Comparing the performance of entrained mixing reactor applied to the dry scrubbing of gaseous SO₂ and HCl with hydrated lime

Young Ok Park^{1,2}, Jea Won Han^{2,3}, Jea Rang Lee¹, Naim Hassoli¹, Kang San Lee¹, HeaTaik Kim² and Kwang Duek Kim¹

¹Clean Fuel Research Laboratory, Korea Institute of Energy Research, Deajeon Korea.
²SN Co., Ltd. Ansan, Korea. ³Department of Material and Chemical Engineering, University of Hanyang, Ansan, Korea

kdkim@kier.fe.kr

Abstract. Entrained mixing reaction system, combining a numerical optimized entrained mixing up flow reactor with a rectifier for homogeneous flue gas flow distribution were developed as reaction chambers for the dry scrubbing of gaseous SO₂ and HCl with solid hydrated lime particles. The performance of this technology was experimented at the test unit of business model scale with 0.3m in diameter and 6.0 m in height. Three kind of solid hydrated limes with different surface area and pore volume were injected with carrier compressed air into the reaction chamber for absorption of acid gaseous. The experimental conditions were the following: reaction temperature 180°C, gas flow rate 1,800 Nm³/h and SO₂ and HCl concentration in inlet gas 300 ppm, respectively, giving different values for the ratio the amount of fresh hydrated lime and acid gaseous concentration at the inlet of reaction chamber and that corresponding to the stoichiometric molar ratio (SR). The gaseous SO₂ and HCl removal efficiencies ranged from 95 to 99 %, and the best performance were obtained for high surface area and pore volume of the hydrated lime. Increased the surface area and pore volume of hydrated lime improved the performance of the gaseous SO₂ and HCl removal as well as the solid reactant conversion.

Keywords: Entrained mixing reactor, Hydrate lime, SO₂ removal, HCl removal, Dry scrubbing

1. Introduction

Environmental quality is a key issue of human society. Due to the important role of industry in economic development, industrial plants should operate while minimizing the aggression to the environment. In order to guarantee the human welfare in the future, governments are establishing increasingly rigorous regulations, and industry has to make severe economic efforts to comply. Therefore new technological alternatives have to be developed to ensure industry's ability in complying with new standards in environmental performance.

The incineration of solid wastes (municipal, hazardous, industrial,...) and the combustion of certain solid fuels (coal, biomass,...) are environmental menaces since these processes may produce large amounts of air pollutants (HCl, SO_x, HF, CO, NO_x, VOCs, heavy metals, fine particulate matter), which are important sources of local and global environmental pollution (Bode'nan and Deniard, 2003; Chiang et al., 2003; Koch et al., 2005; Verdone and Filippis, 2006). Among these pollutants, acid gases such as HCl, SO_x, and HF are causes of acid rain and fog, which are harmful to human life, modifying the lungs'

defenses and aggravating cardiovascular or chronic lung diseases (Mura and Lallai, 1994; Chiang et al., 2003).

The processes used for acid gas removal in gaseous emissions are classified as “wet”, “semidry”, or “dry”. Although wet scrubbing technologies have proven to be more efficient for acid gas cleaning purposes, this technology implies the generation of a wastewater problem and has economical drawbacks when compared to dry or semidry processes. Acid gas cleaning with dry or semidry technologies are becoming more widespread since they are easy to use, efficient, and of simple implementation (Chiang et al., 2003; Chin et al., 2005; Koch et al., 2005). Dry sorbent injection can be performed at low (150 °C) or moderate (200-315 °C) temperature in the so-called in-duct injection or directly in the combustion chamber at higher temperatures (750-1100 °C) (Verdone and Filippis, 2006).

Calcium compounds such as $\text{Ca}(\text{OH})_2$, CaO , and CaCO_3 are sorbents frequently used in dry scrubbing due to their low cost and high efficiency (Chiang et al., 2003; Fujita et al., 2003; Chin et al., 2005). Nevertheless, the dry scrubbing process needs to be improved since the very short contact time available for the sorbent and acid gases to react results in low sorbent conversion efficiencies (< 25%) and generates a large amount of solid particles (Chin et al., 2005). Moreover, in order to improve the sorbent conversion and to achieve the increasing stringent emission limits set by regulations, the partially spent sorbent should be recirculated (Garea et al., 2001) or new sorbents with higher removal efficiencies should be used (Heap, 1996; Verdone and Filippis, 2006; Shemwell et al., 2011).

In the dry scrubbing process, the gases are removed through adsorption and chemical reaction at the solid's surface and a dry powdery product results. This product is usually separated downstream the reactor chamber from the cleaned flue gas by bag filters or electrostatic precipitators. The promotion of the dry scrubbing and the dust removal processes in the same equipment would have considerable practical and economical implications, and in the authors' opinion this can be made possible using an entrained mixing reactor.

The entrained mixing reactor is a new technology with longer contact time for the sorbent and acid gases to react results in higher sorbent conversion efficiencies (> 50%) and generates a lower amount of solid particles.

Figure 1 illustrates the field of application for three main scrubbing technologies. Compared to the semi-dry reactor, the dry sorbent mixing reactor can achieve higher acid gas removal capacity at lower acid gas to sorbent molar ratio as described in the figure 1 (b). This in return means that the dry sorbent mixing reactor will require less sorbent amount for the high acid gas loading and generates a lower solid particles.

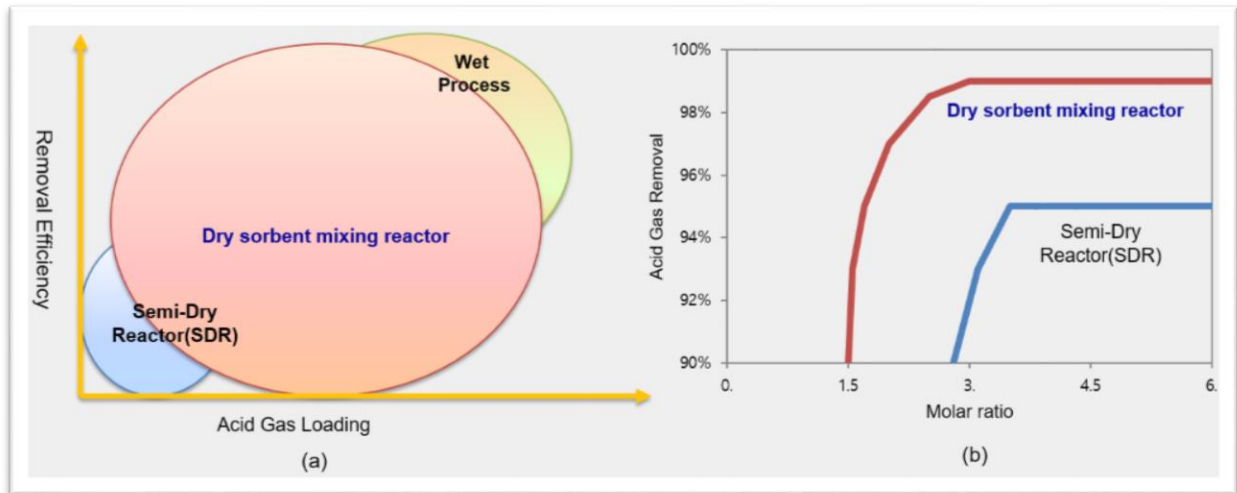


Figure 1. Acid gas removal capacities of three scrubbing technologies according to acid gas loading (a) and acid gas to sorbent molar ratio (b).

The three stage of development process for increasing of entrained mixing reactor performance were conducted to have longer contact time with sorbent particles and acid gas as shown in Figure 2. The 3rd generation of entrained mixing reactor has an advantage of higher sorbent conversion efficiencies at the lower acid gas to sorbent molar ratio. This is mainly due to its simple inner structure and longer residence time of sorbent particles and acid gas in inside of reactor. Dry sorbent mixing reactors can achieve high acid gas removal efficiencies at the acid gas to sorbent molar ratio compare to other similar dry scrubbing reactors.

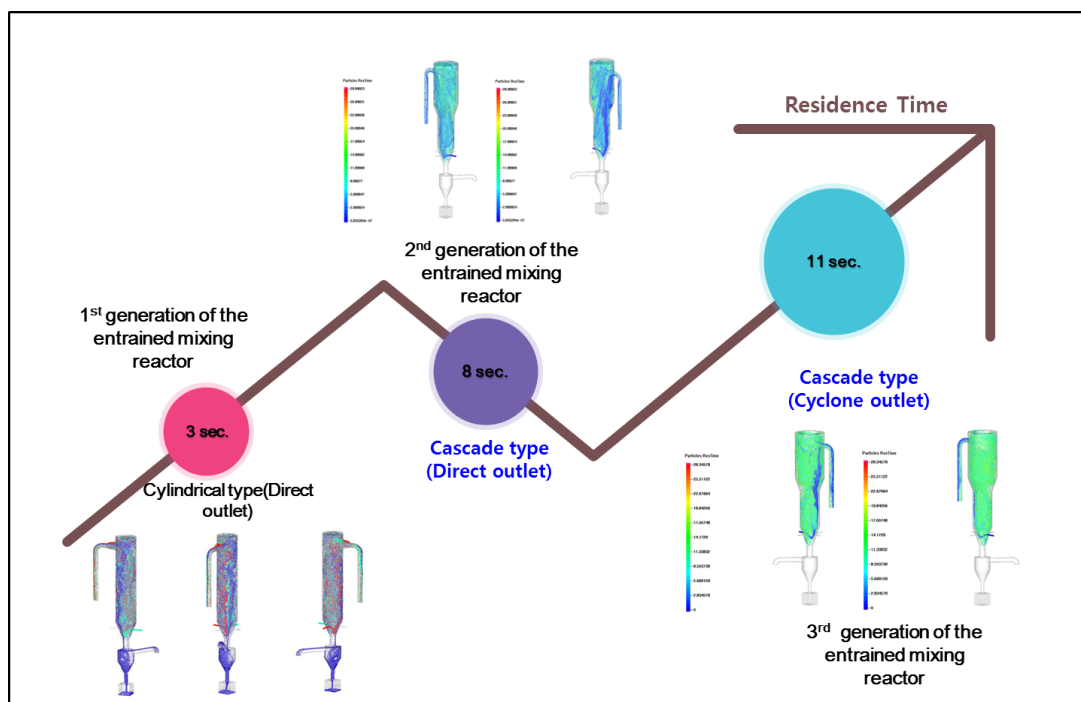


Figure 2. Process of development for changing of entrained mixing reactor structures.

Dry sorbent mixing reactor was developed to increase the acid gas removal efficiency at the lower range of sorbent feeding amount. Higher acid gas removal efficiency can be reached by well mixing with sorbent particles and acid gas inside of reactor chamber to react results in higher sorbent conversion efficiencies. Due to its simple structure, the reactor can easily be applied to replace existing spray dry reactors and wet scrubbers in an existing acid gas treatment system or apply it for completely new flue gas treatment process. Furthermore, in combination with bag filter, the overall acid gas removal efficiency can be increased (Grisholm and Rochelle, 1999; Tseng et al., 2003). During the development process, various operating conditions were tested to ensure that the reactor is fit for application in industrial sites with highest performance. As hardware, the reactor has so far been well optimized and it remains to be checked how the performance is dependent on the sorbent properties and its reactivity. The various structures of the entrained mixing reactor were tested and the changing of residence time displayed in Figure 2. By further optimization of the structure of reaction chamber, reaction with sorbent particles and acid gas can be accelerated and the residence time of sorbent particles inside the reactor chamber can be increased. In case of our developed reactor, at the final development stage, the average sorbent residence time was 11 seconds.

The aim of this study is to verify, at the pilot scale test unit, the extent of the effect of the acid gas and sorbent particles contact time in process of dry scrubbing of SO₂ and HCl with three grades of Ca(OH)₂ in the entrained mixing reactor.

2. Experimental Set Up and Methods

2.1. Experimental Set Up

The schematic diagram of business model scale test units is shown in Figure 3. This test unit consists of the following functional units. Flue gas generation parts include gas burner, force draft fan, burner and the water injection unit for steam generation. The entrained mixing reactor as a dry scrubbing equipment (ERx) includes settling chamber, sorbent injection ports, and temperature and pressure drop sensors. The sorbent feeding unit includes solid particle feeder, particle ejector and high pressure purified compressed air lines. The bag filter unit consists of bag filter cases, pleated filter bags, bag cleaning unit, and collected dust box with rotary valve and temperature and pressure drop sensors. The flue gas flow control unit includes average pitot tube for measuring flow rate, pressure sensor, temperature sensor and pressure drop sensor, frequency inverter, induced draft fan and stack. The system also includes the gas sampling ports where the concentration of acid gases contained in the composition of flue gas is online measured by the portable FTIR gas analyser (DX4000, Gaset Technologies Inc.). The acid gas sampling ports indicated in Figure 3. These ports are used for online measurements alternatively to check the base inlet acid gas concentration, without injection of sorbent, and the continuous concentration, by injecting the sorbent at certain sorbent to acid gas (Ca/S) molar ratios. A real image of the pilot scale entrained mixing reactor test system is depicted in Figure 4.

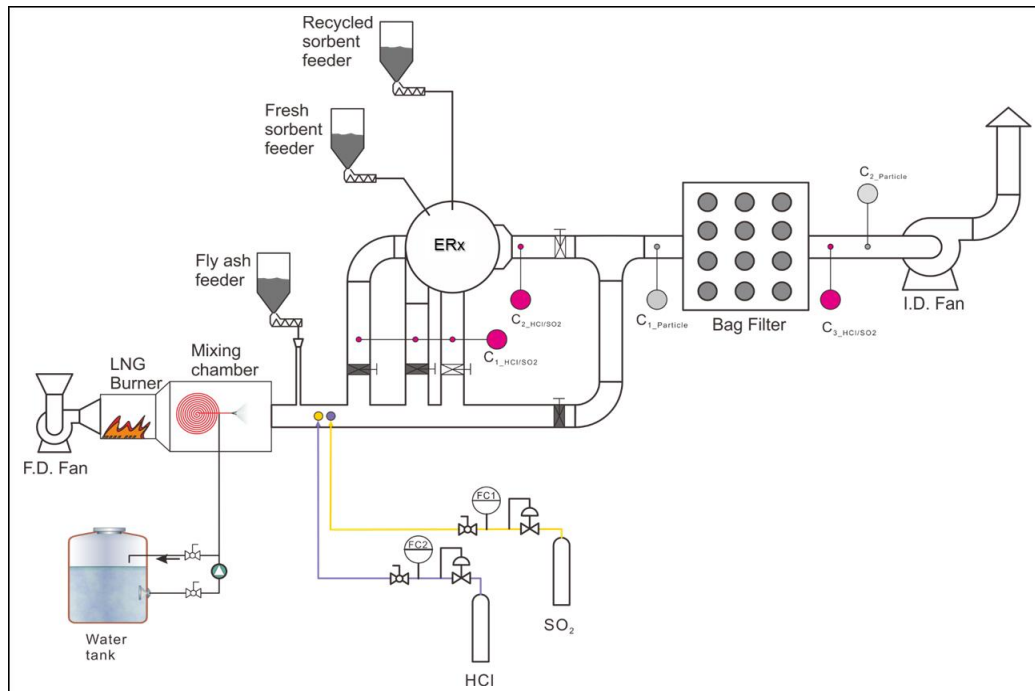


Figure 3. Schematic diagram of business model scale test unit.

The business model scale entrained mixing reactor, used as reaction chamber, is a 0.3m in inside diameter, 6.0m in high. The cone angle in spout bed formation zone at bottom of chamber is 60°. The range of experimental conditions for dry scrubbing test is listed in Table 1.

Table 1. Experimental conditions for the dry scrubbing test

Inlet SO ₂ concentration, C _{in}	250 ppm
Inlet HCl concentration, C _{in}	250 ppm
Stoichiometric ratio, SR	1.0 - 3.0
Reaction temperature	180 °C
Inlet gas flow rate	1,800 Nm ³ /hr
Operation time	Max. 24 hours



Figure 4. Real image of the business model scale test unit.

2.2. Test material

Table 2 gives the physical properties and chemical analysis of the SO₂ and HCl sorbents as the sample A, B and C. Particularly, the active surface area for sorption, based on the considered Brunauer-Emmett-Teller (BET) theory as one of most important properties for adsorption process. SEM images of the sorbent samples A, B and C are displayed in the Figure 5.

Table 2. Physical properties of test sorbents

Sample/ Parameter	A	B	C
CaO, %	73.0	62.8	51.5
Ca(OH) ₂ , %	96.5	86.1	74.5
Mean particle size (Dp ₅₀), μm	6.8	8.4	16.1
H ₂ O (300°C), %	1.1	1.6	1.91
Bulk density, g/ml	0.584	0.450	0.430
Tap. density, g/ml	0.657	0.540	0.460
BET Surface area, m ² /g	41.6	36.152	16.384
BJH Pore volume, cm ³ /g	0.29	0.21	0.12
BET Pore Size, Å	172.21	168.21	98.21

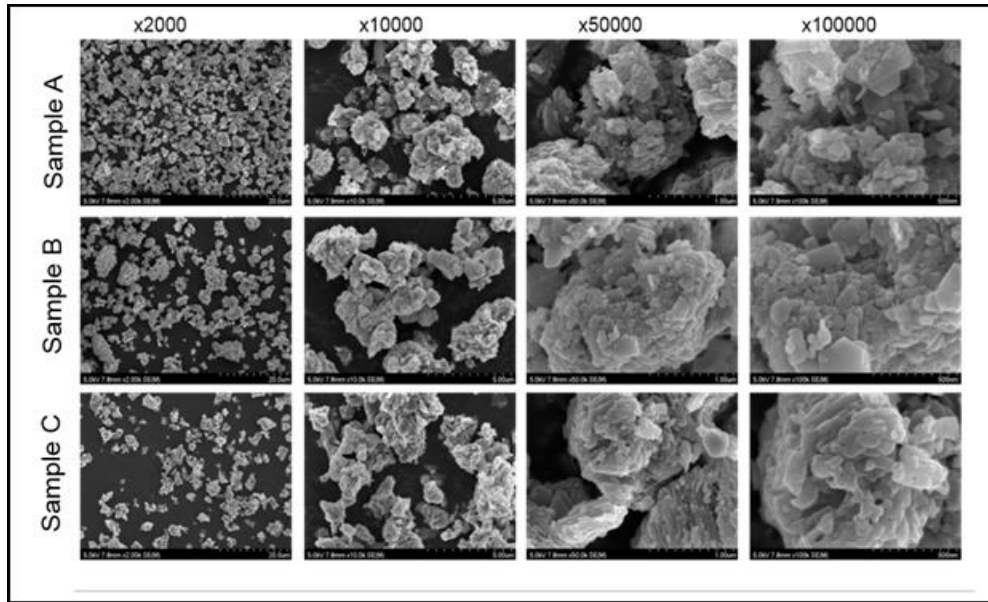


Figure 5. SEM Images of test sorbents used in pilot scale entrained mixing reactor.

The ratio SR(or Ca/HCl molar ratio) is calculated through the expression:

$$\text{SR or Ca/HCl molar ratio} = (W_{\text{Ca(OH)}_2}) / (QC_{\text{HCl}}) / (M_{\text{Ca(OH)}_2} / 2) \quad (1)$$

where $W_{\text{Ca(OH)}_2}$ is the sorbent feed rate at the inlet of the entrained mixing reactor, C_{HCl} and Q are respectively the HCl concentration and the gas flow rate at the same location, and $M_{\text{Ca(OH)}_2}$ is the molar mass of Ca(OH)_2 . The experimental variable SR(or Ca/HCl molar ratio) can be manipulated either by changing the solids feed rate or by changing the HCl concentration, or both.

The SO_2 and HCl removal efficiency is defined as

$$\text{SO}_2 \text{ and HCl removal efficiency} = ((C_{\text{in}} - C_{\text{out}}) / C_{\text{in}}) \times 100 \quad (2)$$

where C_{in} are inlet SO_2 and HCl concentration at the upstream of entrained mixing reactor and bag filter and C_{out} are the outlet SO_2 and HCl concentration at the downstream of entrained mixing reactor and bag filter, respectively.

3. Results and Discussions

3.1. SO_2 removal characteristics

In this study three different sorbents were used to investigate the effect of Ca/S molar ratio on SO_2 removal. The effect of Ca/S molar ratio on SO_2 concentration in downstream of the bag filter and SO_2 removal efficiency are shown in Figure 6. As one would expect, SO_2 removal efficiency increases with increase in the ratio since a larger Ca/S molar ratio means that more SO_2 sorbents per unit time are fed into the reactor for a given inlet SO_2 concentration in the flue gas. It is also seen from this figure that SO_2 concentration in downstream of bag filter decreases rapidly with increasing Ca/S molar ratio. The

SO₂ removal efficiency with the sample A, B and C are 99%, 94% and 93% could achieved at 3.0 of Ca/S molar ratio, respectively. When the sorbent has lager BET surface area and pore volume, which leads to higher contact efficiency and faster reaction between hydrated lime and SO₂ gas than lower BET surface area and pore volume of the hydrated limes. It is generally considered that the reaction of SO₂ gas with hydrated lime mainly occurs on the internal surface and pore of unreacted hydrated lime.

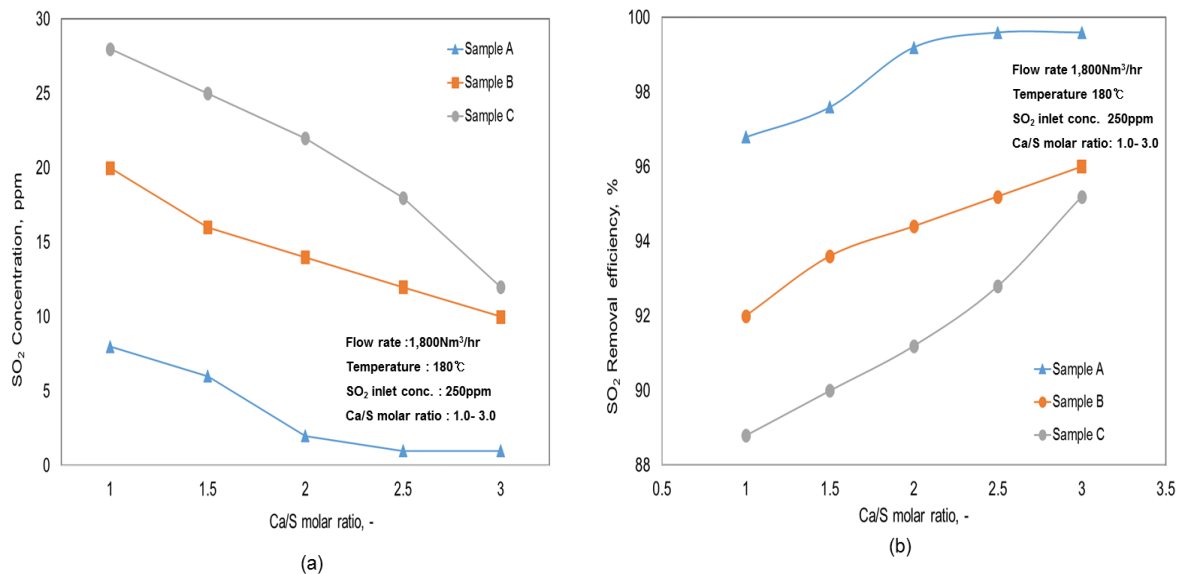


Figure 6. Effect of Ca/S molar ratio on SO₂ concentration (a) and SO₂ removal efficiency according to the types of hydrated lime.

3.2. HCl removal characteristics

The three grades of hydrated lime are used for dry scrubbing test in the business model scale trained mixing reactor. Figure 7 shows the comparison of HCl concentration in downstream of bag filter and SO₂ removal efficiency between sample A, and sample B and sample C of hydrated lime. It is also seen from this figure that HCl concentration in downstream of bag filter decreases rapidly with increasing Ca/S molar ratio. The HCl removal efficiency with the sample A, B and C are 99%, 96% and 92% could achieved at 3.0 of Ca/S molar ratio, respectively. The hydrated lime with high BET surface area, ore volume and quality possesses higher acid gas removal capacity and better reactivity with acid gas at low reaction temperature. With regard to the relationship between the reactivity of acid gas sorbents at low temperature and their structural properties, the BET surface area, pore volume and pore size distribution, are generally concerned.

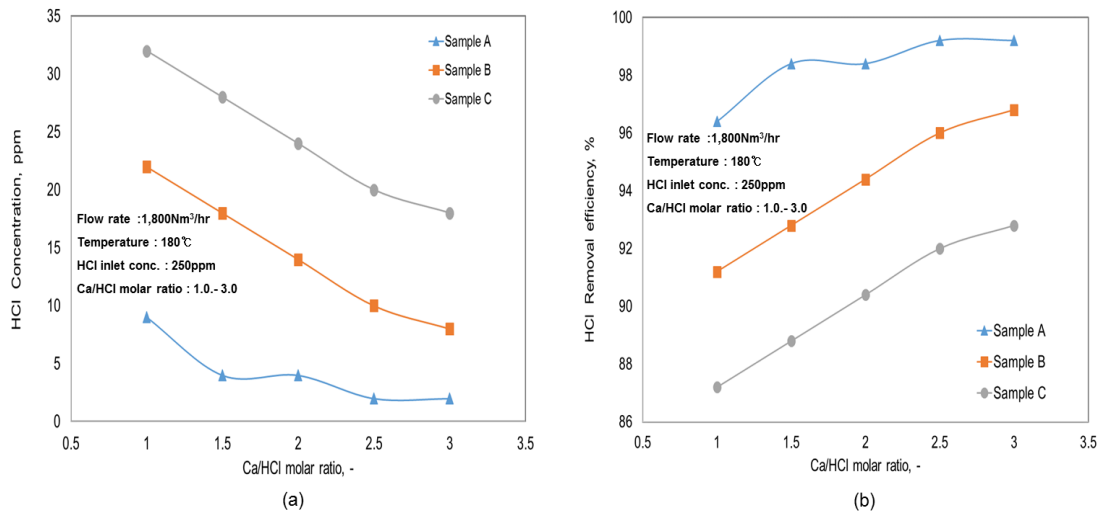


Figure 7. Effect of Ca/HCl molar ratio on HCl concentration (a) and HCl removal efficiency according to the types of hydrated lime.

3.3. Effect of operating time on acid gas concentration in downstream

The three grades of hydrated lime are used for dry scrubbing test in the business model scale entrained mixing reactor. The sample A of hydrated lime is used in the business model sale entrained mixing reactor for long time test of acid gas dry scrubbing. Figure 8 shows the effect of operating time on SO₂ and HCl gas concentration in downstream of bag filter with sample A of hydrated lime. The sample A has inherently high specific surface area and abundant pores in the reactive form. Only when apply the entrained mixing reactor is done to enhance the reactivity of the hydrated lime a high acid gas removal will be reached.

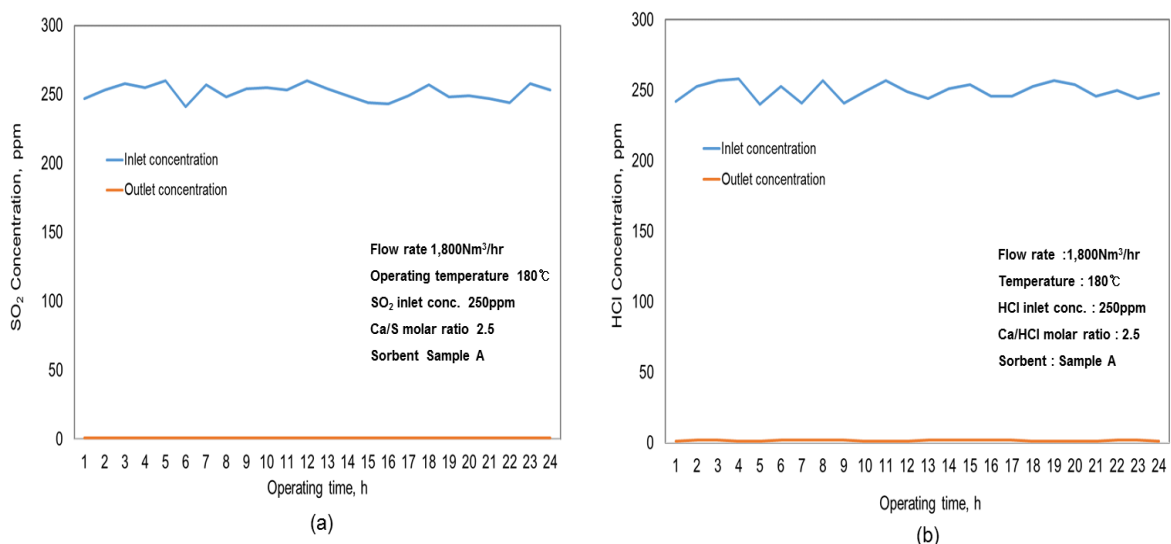


Figure 8. Variation of SO₂ and HCl concentration in inlet and outlet varying the operating time with sample A.

3.4. Acid gas concentration in downstream

The combination of the dry scrubbing system and bag filter are also important process. In the this study, the effect of them on acid gas removal with high quality hydrated lime were investigated as parameter of acid gas to molar ratio since their variations mainly result in different sorbent conversion efficiencies

in the entrained mixing reactor. Figure 9 shows the acid gas concentration in downstream of the entrained mixing reactor (ERx) and bag filter at different acid gas to sorbent molar ratio. The acid gas to sorbent molar ratio was changed by adjusting the sorbent feed rate. The acid gas concentration in downstream of entrained mixing reactor and bag filter decreased with increased of acid gas to sorbent molar ratio, which indicates that either increase in sorbent feed rate can make acid gas removal efficiency increase in both units. For a higher acid gas to sorbent molar ratio can enhance the contact number of acid gas with sorbent particles in the reactor and on the surface of filter bags, which increases the contact time and reaction time between acid gas and the hydrated lime in the reactor and on the surface of filter bags.

3.5. Total acid gas removal efficiency

Figure 10 shows the total SO₂ and HCl removal efficiency with changes to the acid gas to sorbent molar ratio for the different types of hydrated lime. The SO₂ and HCl total removal efficiency increases with increase in the acid gas to sorbent molar ratio since a larger acid gas to sorbent molar ratio means that sorbent per unit time are fed into the reaction chamber and more unreacted sorbent are flowed in the bag filter for a given inlet SO₂ and HCl concentration in the flue gas. It is also seen from this SO₂ and HCl removal efficiency increases rapidly with increasing acid gas to sorbent molar ratio, and then tends to level off as acid gas to sorbent molar ratio more than 2.0 in case of sample A. Further increase in acid gas to sorbent molar ratio of sample A can not enhance acid gas removal efficiency.

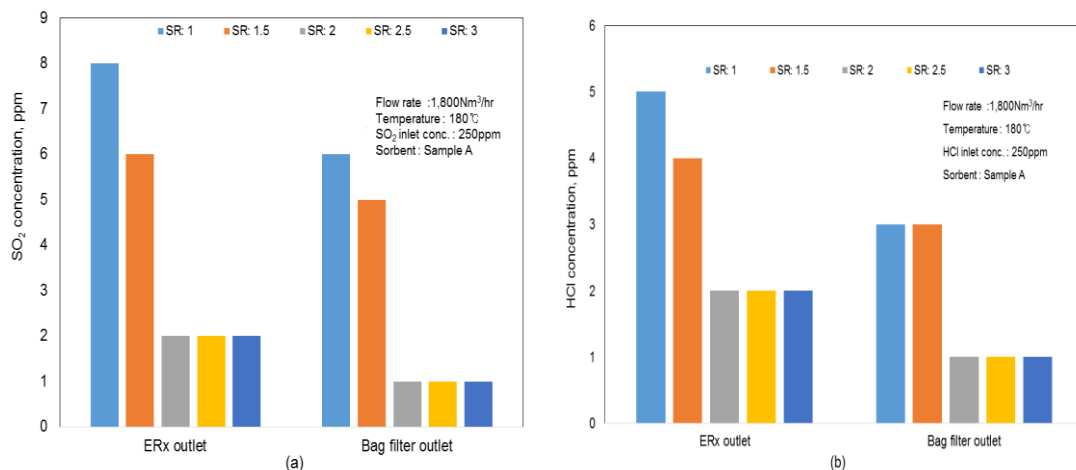


Figure 9. Variation of acid gas concentration in downstream of entrained mixing reactor (ERx) and bag filter with changes to the acid gas to sorbent molar ratio.

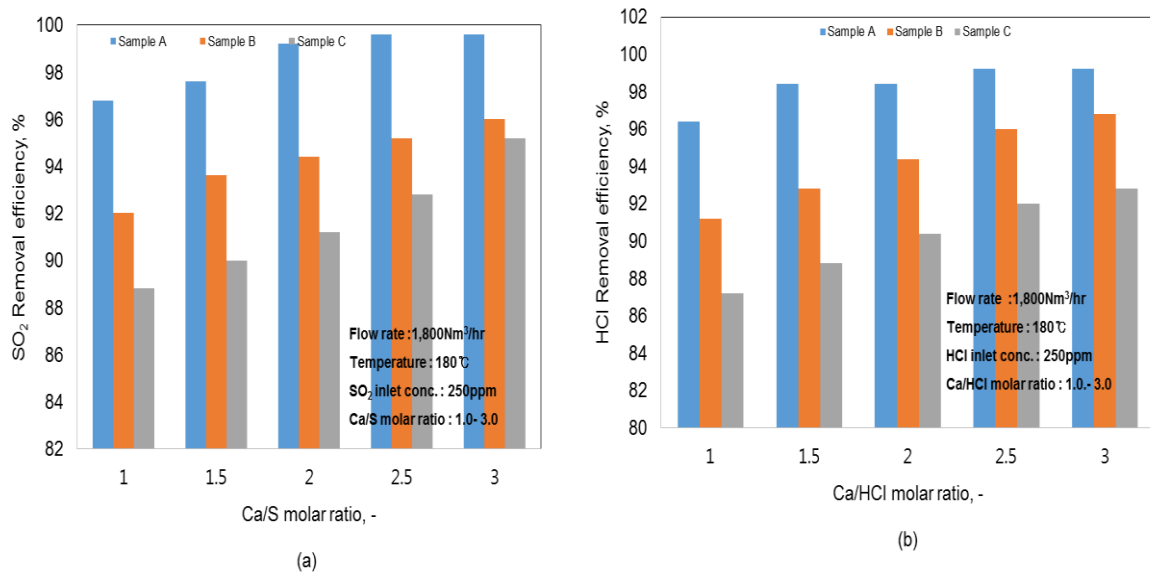


Figure 10. Total acid gas removal efficiencies with changes to the acid gas to sorbent molar ratio for the different types of hydrated lime.

The most important requirement in considering dry scrubbing technologies to comply with more severe emission standards for the limited remaining life of existing power plant and waste incineration plant is a low capital and operating cost. For this purpose, the entrained mixing reaction process with the high quality of hydrated lime should be an attractive candidate, taking advantages of its more compact size, lower capital and operating costs compared with semi dry scrubbers and wet scrubbers, and less environmental impact (e.g., no wastewater).

The entrained mixing reactor is a dry sorbent scrubber that deals with the raw flue gases from waste incineration by means of a specially designed reactor and fabric filter. This technology uses the basic principles of spouted beds and circulating fluid beds. The use of this technology has led to the successful demonstration of its simplified and efficient process which has led to higher availability and lower residue levels.

The entrained mixing reaction process is based on the raw flue gases from incineration being directly ducted into the bottom of the reactor. As the flue gases move up the reactor vessel they are mixed with dry powdered hydrated lime and recirculated fabric filter residues. As the flue gas exits the reactor and enters into the fabric filter, the additives and pollutants form a product that is captured on the bags while the cleaned flue gas exits the system and can then be released to the atmosphere through the use of an induced draft fan and stack. However, the residues captured on the fabric filter bags are then re-circulated back to the reactor via a screw conveyor and re-introduced into the reaction chamber. This recirculation allows for the maximum utilization of all additives injected into the reaction chamber. The standard entrained mixing reaction system consists of four (4) main pieces of equipment: the reactor, the fabric filter, the recirculation conveyor, and the sorbent storage and injection system.



Figure 11. Real plants of the entrained mixing reaction process in site installed.

Total acid gas removal efficiencies with changes to the acid gas to sorbent molar ratio for the different types of hydrated lime.

There are four (4) main advantages to this type of system: the high reliability, the zero waste water discharge, the compact design, and the low additive consumption. The entrained mixing reaction system has a high reliability and availability for all the different loads because it controls on many different variables, such as temperature, pressure, and emissions. In addition, the minimal amount of moving/rotating mechanical parts contributes to the minimization of operation and maintenance costs.

Another of the main advantages is that the system does not create any waste water discharge; therefore removing the need to have any on-site water treatment. Not only does the system not create any waste water. Also, the elevated fabric filter provides abundant unused floor space for other equipment. The last main advantage of the entrained mixing reaction system is the low reagent consumption because of the recirculation of fabric filter residues (the stoichiometric ratio in this system is typically in the order of 1.5 to 1.9). This not only leads to lower reagent cost, but will also decrease the residues produced and therefore, the residue disposal costs.

4. Conclusions

Effects of the acid gas to sorbent molar ratio parameters on SO₂ and HCl removal efficiency of three different type of hydrated lime were investigated in a new dry scrubbing process with a new entrained mixing reaction process. SO₂ and HCl removal efficiency are affected by the acid gas to sorbent molar ratio, the approach to BET surface area, pore volume and contents of CaO in the hydrated lime.



Using sample A as the sorbent in the present process, SO₂ and HCl removal efficiency of up to 98% can be achieved when the acid gas to sorbent molar ratio is 1.5. The SO₂ and HCl removal efficiency for using sample B and are 92%, 88% when the acid gas to sorbent molar ratio is 1.5, respectively. The acid gas removal efficiency of sample B and C are naturally lower than that of sample A but considerably enhanced in this new dry scrubbing process. More than anything else, using high quality of hydrated lime would substantially lower the costs of the new dry scrubbing process.

The Korea government continues to tighten regulations in the energy and environment industry it becomes more and more important to find the right technology to meet the every growing need to reduce emissions. In order to meet the ever growing need it will become important to be open minded regarding new technologies to meet the decreasing emissions levels and to maintain the concept of BACT.

5. References

- Bode'nan, F. Deniard, 2003. Characterization of Flue Gas Cleaning Residues from European Solid Waste Incinerators: Assessment of Various Ca-based Sorbent Processes. *Chemosphere*, 51, 335.
- Chiang, B. C., Wey, M. Y., Yeh, C. L., 2003. Control of Acid Gases using a Fluidized Bed Absorber. *J. Hazard. Mater.*, 101, 259.
- Chin, T., Yan, R., Liang, D. T., Tay, J. H., 2005. Hydrated Lime Reaction with HCl under Simulated Flue Gas Conditions. *Ind. Eng. Chem. Res.*, 44, 3742.
- Fujita, S., Suzuki, K., Shibasaki, Y., Mori, T., 2003. A New Technique to Remove Hydrogen Chloride Gas at High Temperature Using Hydrogrossular. *Ind. Eng. Chem. Res.*, 42, 1023.
- Garea, A., Herrera, J. L., Marques, J. A., Irabien, 2001. A Kinetics of Dry Flue Gas Desulfurization at Low Temperatures using Ca(OH)₂: Competitive Reactions of Sulfation and Carbonation. *Chem. Eng. Sci.*, 56, 1387.
- Grisholm P. N., and Rochelle G. T., 1999. *J. Ind. Eng. Chem. Res.*, 38, 625.
- Heap, B. M., 1996. The Continuing Evolution and Development of the Dry Scrubbing Process for the Treatment of Incinerator Flue Gases. *Filtr. Sep.*, 33, 375.
- Koch, M., Zhang, X., Deng, J., Kavouras, A., Krammer, G., Xu, J., Ge, L., 2005. Reaction Mechanism of a Single Calcium Hydroxide Particle with Humidified HCl. *Chem. Eng. Sci.*, 60, 5819.
- Lee D. S., Yoon O. S., Shim S. H., and Lee B. J., 2005. Proc. Korea Society of Waste Management, spring academic research 2005, 550.
- Mangun C. L., and Debarr J. A., Carbon 2001, 39, 1689.
- Mura, G., Lallai, A., 1994. Reacting Kinetics of Gas Hydrogen Chloride and Limestone. *Chem. Eng. Sci.*, 49, 4491.
- Shemwell, B., Levensis, Y. A., Simons, G. A., 2001. Laboratory study on the high-temperature capture of HCl gas by dry-injection of calciumbased sorbents. *Chemosphere*, 42, 785.
- Stein, J., Kind, M., Schlunder, E. U., 2002. The Influence of HCl on SO₂ Absorption in the Spray Dry Scrubbing Process. *Chem. Eng. J.*, 86, 17.
- Tseng H. H., Wey M. Y., Liang Y. S., and Chen K. H., Carbon 2003, 41, 1079.
- Wey M. Y., Fu C. H., Tseng H. H., and Chen K. H., Fuel 2003, 8, 2, 2285.
- Wu C., Khang S. J., Keener T. C., and Lee S, K., 2004. Adv. Environ. Res., 8, 655.
- Verdone, N., Filippis, P., 2006. Reaction Kinetics of Hydrogen Chloride with Sodium Carbonate. *Chem. Eng. Sci.*, 61, 7487.



18th World Clean Air Congress, 23-27 September 2019, Istanbul
organized by TUNCAP and IUAPPA

Acknowledgments

This study was supported by the Korea Ministry of Environment as “Eco Business Advancement Technology Development Program” from the Korea Environmental Industry and Technology Institute (KEITI) and by the Korea Institute of Energy Technology Evaluation and Planning (KETEP) and the Ministry of Trade, Industry & Energy (MOTIE) of the Republic of Korea. The SN Co., Ltd. thanks for supplying the acid gas sorbents.

Investigation of the effect of air cleaning devices on air quality in the intensive care unit

Sanaz Lakestani¹, Ibrahim Cakir¹, Hasan Tahsin Gozdas², Isa Yildiz³ and Abdullah Demirhan³

¹Bolu Abant Izzet Baysal University, Scientific Industrial and Technological Application and Research Center, Gölköy 14030 Bolu/Turkey

²Bolu Abant Izzet Baysal University, Medical Faculty, Infectious Diseases, Gölköy 14030 Bolu/Turkey

³Bolu Abant Izzet Baysal University, Medical Faculty, Anesthesiology and Reanimation Gölköy 14030 Bolu/Turkey

sanazlakestani@ibu.edu.tr

Abstract. In this study the effect of air cleaning devices in the changing of the concentration of bio-aerosols (bacteria) in the indoor air was determined. Air quality monitoring carried out at the hospital in two different places including Intensive Care Unit (ICU) and isolated room. Bacteria were collected on %5 sheep blood agar for pathogen determination and plate count agar for total bacteria count. The measurements were done in 3 weeks for 3 times per a day (In the morning when doctors controlled patients, Patients relatives visit time, and afternoon). On each study day, 24 samples were collected. In both the working and non-working conditions of the air cleaning devices, bio-aerosols samples were taken with Biomerieux sampler pump and the concentration change of the bacteria in the environment was monitored. Indoor levels of bio-aerosols were identified with MALDI-TOF MS instrument. The dominant bacteria in the air of examined area are *Staphylococcus hominis*, *Micrococcus luteus*, *Staphylococcus capitis*, *Staphylococcus epidermidis*, *Corynebacterium afermentans* and *Staphylococcus haemolyticus*. The highest levels of bacteria were measured in the mornings. The number of bacteria was increased, especially when there are more people in the room. In this study the efficacy of a hydroxyl radical air disinfection system in reducing the number of airborne bacteria was assessed in the ICU. According to the results, it was determined that air cleaning devices were effective in decreasing the concentration of microorganisms in the ICU. The study was also provides information on the sources and mitigation measures can be applied for the pollutants that are associated with health problems. Reduction of hospital infections and other diseases due to environmental factors through air cleaning devices in the hospital environment provided extensive impact on the society by reducing expenditures on health.

Keywords: Intensive Care Unit, Bio-aerosols, MALDI-TOF MS, Air Cleaning Devices

1. Introduction

People spend about 90% of their life in indoor environments (Lin Huang et al., 2017). There is an increase in the number of evidences indicating increase rate of health problems associated with environmental pollution.

Indoor airborne biological pollutants have numerous sources, including outdoor air, human bodies, wallpaper, carpet, resuspended particles, air conditioning systems, and animal waste (Lindemann et al.,

1982; Pastuszka et al., 2000; Chao et al., 2002; Hargreaves et al., 2003; Kalogerakis et al., 2005; Tseng et al., 2011; Hospodsky et al., 2012; Lin Huang et al., 2017; Xu et al., 2017). The health effects of indoor air pollutants are not fully understood, but indoor air quality has been linked with a wide array of health outcomes including deficits in lung function, chronic respiratory disease, lung cancer, heart disease, developmental disorders, and damage to the brain, nervous system, liver, or kidneys (Wang and Pinkerton, 2007; Weschler, 2011; Lakestani et al., 2013).

Environmental contaminations caused by bio-aerosols is thought to play a role in the spread of infections in hospitals and to prevent or decrease this infections interest in new air disinfection systems has increased (Wong et al., 2008). Air cleaning devices used in the indoor environment can be helpful to control the range of pollutants such as allergens, particulate matter, bio-aerosols and odor (Babai et al., 2017).

Indoor air pollutants including particulate matter, gases, fumes, biological pollutants and fibers might have adverse impacts on health. Maintaining high levels of indoor air quality in hospitals is important for protecting both staff and patients (Jung et al., 2015). Bioaerosol may cause health effects, such as SBS, allergies, asthma, poisoning, infection, and even cancer (Douwes et al., 2003; Schleibinger et al., 2004; Bowers et al., 2011).

Bioaerosols consists of aerosols containing microorganisms (bacteria, fungi, viruses) or organic compounds derived from microorganisms (endotoxins, metabolites, toxins and other microbial fragments) (Heikkien et al., 2005). The concentration of airborne bacteria or fungi was calculated by dividing numbers of colonies growth on the culture medium by air volume (m^3), therefore, the unit of bioaerosol concentration is expressed as the colony forming unit ($CFU m^{-3}$) (Lin Huang et al., 2017).

The sampling and analysis of airborne microorganisms in indoor air has received attentions in recent years (Kim and Kim, 2007; Stanley et al., 2008). Bioaerosols contribute to about 5 to 34% of indoor air pollution (Srikanth, 2008). The best way to decrease the indoor air pollution's risk is controlling the sources of the pollutants and ventilate the area. Air cleaning devices used in the indoor environment can be helpful to control the range of pollutants such as allergens, particulate matter, bioaerosols and odor (Babai et al., 2017).

Several studies have suggested that environmental contamination may play a role in the spread of infection (Rampling et al., 2001; Hota, 2004).

A number of air decontamination products have been shown to reduce environmental contamination in patient isolation rooms, including a portable high efficiency particulate air (HEPA) filtration unit and a dry mist hydrogen peroxide delivery system (Boswell and Fox 2006; Shapey et al., 2008).

In this study for decrease the indoor air pollution we used Aerte AD 2.0 air cleaning devices. The Air Disinfection Units (AD) have been developed in conjunction with British microbiologists, infection control experts and engineers to replicate the way in which the natural environment protects and cleaning the air in open spaces.

Hydroxyl radicals work by neutralizing any dangerous bacteria and viruses, altering their molecular structures so that they become nonviable by neutralizing 99.99% of bacteria and viruses in the air. The reason the process is so effective is because hydroxyl radicals are highly reactive molecules missing a hydrogen atom, meaning they can traverse an entire room virtually instantly (in less than a second), continuing its search until it encounters a hydrogen atom forcibly removing it from any organic material and inexorably changing the compounds molecular structure (Medical Technology Business Europe, 2011). Hydroxyl radicals have been implicated in the oxidation of a large number of biomolecules, including protein and DNA (Miller and Britigan, 1997).

The mechanism of DNA damage is through DNA strand breakage (Babior, 2000). Once formed, the hydroxyl radical is likely to travel only a short distance before it encounters an oxidisable substrate (Medical Technology Business Europe, 2011). Aims of this study is to evaluate the effectiveness of the air cleaning devices in reducing total airborne microbial counts and environmental contamination in the Intensive Care Unit (ICU).

2. Experimental methods and data processing

2.1. Sampling Place

This study was conducted in an ICU at a hospital in Bolu, Turkey. In this project collected bioaerosols (bacteria) samples from the ICU and the isolated room.

ICU consisted of 12 beds, 11 beds were in one room and 1 bed was in isolated room. The size of this ICU is approximately 250 m². The nurse's office was located in the corner of the ICU. High Efficiency Particulate Air filters (HEPA) were located above the 12 beds in two rooms. Generally, (HEPA) filters were changed after 1-2 years. Over a one-week the effect of the air cleaning devices were assessed in two rooms: ICU and isolated room.

2.2. Air Cleaning Device

The air cleaning devices have been developed in conjunction with British microbiologists, infection control experts and engineers to replicate the way in which the natural environment protects and cleaning the air in open spaces. The technology reproduces these effects in any enclosed environment such as hospitals, wards, schools or theatres, neutralizing airborne pathogens.

The air cleaning device (Aerte AD 2.0) is designed to be used with a consumable cartridge containing a reagent, which is ionized and reacted with traces of ozone, resulting in the generation of hydroxyl 'free radicals' (Figure 1)



Figure 1. Air Cleaning Device (Aerte AD 2.0)

3. Data Collection

3.1. Indoor Bioaerosols

Sampling of bioaerosols was carried out according to NIOSH Method-0800 (Andersen, 1958; NIOSH, 1998). Indoor bioaerosol samples were collected by using a BioMerieux air sampler at the rate of 100 L/min for 1 min. Pump was calibrated prior to sampling for accuracy in the rate of air sampling. Media used for sampling were Sheep Blood Agar (SBA) and Plate Count Agar (PCA) for aerobic bacteria. Air samples were collected 1.5 meters above the floor.

Sampling was performed 3 times daily for 3 weeks in the morning, noon and afternoon. PCA and SBA were used for determine the total number of bacteria and the identification of bacteria species.

For each day, 24 samples were collected. The number of person, the activity in the ICU and cleaning program were recorded. At the morning doctors, interns and nurses moving around the bed, the patients were examined, about 10 o'clock washing/turning/transferring of patients, changing bed clothes and cleaning the beds and floor were performed. About 13:00 was the patient visiting time; generally, two or three relatives were around the patients. At the evening patients were asleep or resting and two or three nurse were in the ICU.

During the sampling, at the first week the air cleaning devices were turn off, second week the air cleaning devices were turn on and the third week the air cleaning devices were turn off, totally 216 samples were collected.

4. Analyses of Bioaerosol

After collecting samples, they were placed in a cooler box and were transported to the laboratory for analysis. All analysis were down in Scientific, Industrial and Technological Applications and Research Centre in Bolu Abant Izzet Baysal University. The plates were incubated at 37 °C for 24 hours. Colonies were counted after 24 hours. Colonies were specified and expressed as colony forming units per cubic meter of air CFU m⁻³).

4.1. Microbial Sample Preparation for Matrix Assisted Laser Desorption Ionization Time of Flight Mass Spectrometry (MALDI-TOF MS)

Identification based on the analysis of mass spectra was performed by MALDI TOF/TOF MS (Autoflex Speed from Bruker Daltonics, Germany) with MALDI Biotyper 3.4 software package. Calibration of mass spectrometer was performed with the Bruker's bacterial test standard (Bruker Daltonics GmbH, Germany). For each sample, the MS-signals were acquired in linear positive mode in the 2000–20.000 Da m/z range by summing 500 laser-shot spectra, according to the manufacturer's automatic method MBT_FC. par. Laser intensity was used between 50 and 60%.

4.2. Identification of colonies using the MALDI-TOF MS

According Bruker direct transfer method; Smear bacteria as a thin film directly onto spot a MALDI target plate. Overlay the spot with 1 μ L of HCCA (α -Cyano-4-hydroxycinnamicacid) solution and allowed to dry room temperature (Figure 2). The steel target was air-dried for 10 minutes and placed in the MALDI Biotyper for analysis.

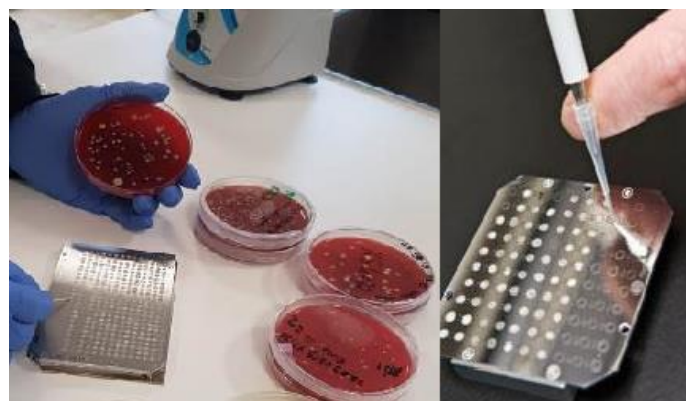


Figure 2. Direct Transfer onto spot a MALDI target

5. Results and Discussion

5.1. Effect of the air cleaning device on bacteria

Monitoring for indoor air quality was conducted in the ICU for one month in a hospital in Bolu-Turkey. Table 1 summarize the mean, maximum and minimum of concentrations (CFU/m³) in the ICU in the March 2019.

Table 1. Mean, Max and Min of concentration of bacteria when the air cleaning devices (ACD) were on/off

Time	ACD off CFU/m ³			
	N	Mean	Max.	Min.
Morning	9	600	1060	180
Noon	9	370	830	130
Afternoon	9	440	810	350
	ACD on CFU/m ³			
	N	Mean	Max.	Min.
Morning	9	320	610	120
Noon	9	280	380	30
Afternoon	9	340	470	40
	*ACD off CFU/m ³			
	N	Mean	Max.	Min.
Morning	9	510	1210	240
Noon	9	280	380	200
Afternoon	9	340	500	180

*Turning off the device after one week "on" period

Maximum concentrations of bacteria were seen in the morning as 1210 CFU/m³ after turning off the air cleaning devices. Because during the sampling nurses were cleaning the patients. Minimum concentrations of bacteria was seen in the noon as 30 CFU/m³ when the air cleaning devices were active. Concentrations of bacteria were change in different times and when air cleaning devices were turning on/off (Figure 3).

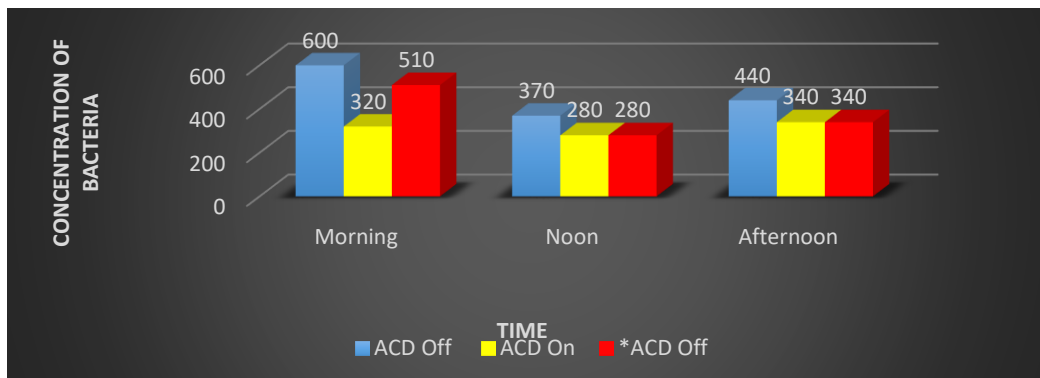


Figure 3. Concentration of bacteria when the air cleaning devices were turn on/off (*Turning off the device after one week "on" period)

5.2. Indoor airborne bacteria

216 samples were collected from ICU. Bacteria identification by MALDI -TOF MS. Table 2 were shown the species of bacteria, sources and health effects on human that obtained in indoor environment.

Table 2. Identifications species of bacteria with MALDI-TOF MS, Source and Health

Bacteria	Gram Positive	Gram Negative	Source	Health	Reference
<i>Acinetobacter baumannii</i>		G (-)	Soil samples, isolated from hospital environments	Important as a hospital-derived (nosocomial) infection	
<i>Staphylococcus capitis</i>	G (+)		Normal flora of the skin of the human scalp, face, neck, and ear	Pathogen	Kreiswirth et al., 2009.
<i>Staphylococcus epidermidis</i>	G (+)		Normal flora of the skin, and less commonly the mucosal flora	Patients with compromised immune systems are at risk of developing infection	
<i>Staphylococcus hominis</i>	G (+)		Usually iso-lated from the axillae and glabrous skin of arms, legs and trunk of humans	common species encountered in the clinical samples, an Opportunistic Pathogen, Patients with compromised immune systems are at risk of infection	Jiang et al., 2012
<i>Staphylococcus haemolyticus</i>	G (+)		Isolated from human blood cultures	Important hospital pathogen	Barros et al., 2012.
<i>Enterococcus faecium</i>	G (+)		Commensal (innocuous, coexisting organism) in the gastrointestinal tract of humans and animals	It may also be pathogenic, causing diseases such as neonatal meningitis or endocarditis.	
<i>Micrococcus luteus</i>	G (+)		Found in soil, dust, water and air, and as part of the normal flora of the mammalian skin	Patients with compromised immune systems are at risk of infection	Hadano et al., 2012.
<i>Moraxella osloensis</i>		G (-)	Isolated from environmental sources in hospitals and from the normal human respiratory tract	As rare causative pathogen of infections in humans	Fox-Lewis et al., 2016.
<i>Corynebacterium afermentans</i>	G (+)		Isolated from human blood cultures.	Caused prothetic valve endocarditis	Sewell et al., 1995.
<i>Acinetobacter lwoffii</i>		G (-)	Normal flora of the oropharynx and skin	Pathogen in patients with impaired immune systems	Regalado et al., 2009.

Common bacteria species were *Acinetobacter baumannii*, *Staphylococcus capitis*, *Staphylococcus epidermidis*, *Staphylococcus hominis*, *Staphylococcus haemolyticus*, *Enterococcus faecium*, *Micrococcus luteus*, *Moraxella osloensis*, *Corynebacterium afermentans*, *Acinetobacter lwoffii*. *Staphylococcus capitis*, *Moraxella osloensis* and *Staphylococcus haemolyticus* were important hospital pathogens. Other bacteria were pathogen in patients with impaired immune systems. The amounts of all types of bacteria have decrease after turning on the air cleaning devices except *Micrococcus luteus*. The percent of decrease rate of bacteria shown in Table 3.

Maximum amount of *Staphylococcus capitis*, *Staphylococcus epidermidis* and *Staphylococcus hominis* were 12%, 9% and 13% before turning on the air cleaning devices minimum amount were 2%, 2% and 3% after air cleaning devices were on.

Table 3. Percentage of bacteria when air cleaning devices were on/off

Bacteria	Cleaning Devices Off (%)	Cleaning Devices On (%)	*Cleaning Devices Off (%)
<i>Acinetobacter baumannii</i>	4	2	3
<i>Staphylococcus capitis</i>	12	2	2
<i>Staphylococcus epidermidis</i>	9	2	3
<i>Micrococcus luteus</i>	6	4	2
<i>Staphylococcus hominis</i>	13	3	3
<i>Enterococcus faecium</i>	3	-	2
<i>Moraxella osloensis</i>	2	2	-
<i>Corynebacterium afermentans</i>	2	-	2
<i>Staphylococcus haemolyticus</i>	4	2	2
<i>Acinetobacter lwoffii</i>	6	2	-

*Turning off the device after one week "on" period

5.3. The number of people and activity

Data entry and data interpretation done by using Statgraphics Centruion XV statistical package program. The P-value of the F-test is less than 0.05, there was a statistically significant difference between the mean of concentration of bacteria with Number of person in ICU.

Number of person during the sampling was affected the indoor concentration of bacteria levels because of the variations of indoor activities like;

- At the morning doctors, interns and nurses moving around the bed, the patient is examined.
- About 10 o'clock washing/turning/transferring patient, changing bed clothes and cleaning the beds and floor were done.
- About 13:00 patient visiting times; generally, two or three relatives were around the patient.
- At the evening Patient were asleep or resting and two or three nurse were in the ICU.

Number of person during the sampling when >14 in ICU colony forming unites of bacteria were the highest amount.

In Figure 4 shown the box and whisker plot of concentrations of bacteria and the number of person in ICU.

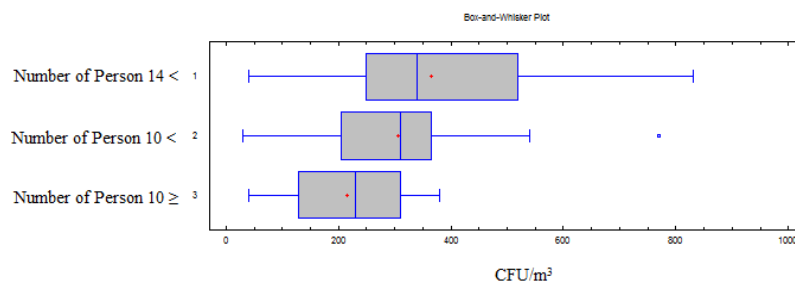


Figure 4. The box and whisker plot of concentrations of bacteria and the number of person

The P-value of the F-test was greater than 0.05, there was not a statistically significant difference between the mean concentrations of bacteria with number of patients in ICU. The box and whisker plot of concentrations of bacteria was shown in Figure 5. The concentration of total bacteria was significantly high when the number of patients was more than 6 people.

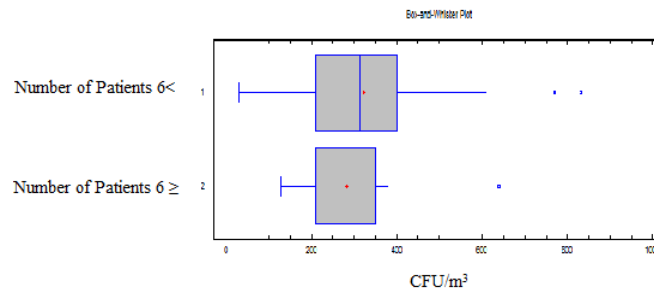


Figure 5. The box and whisker plot of concentrations of bacteria and the number of patients

6. Maximum Acceptable Levels of Bacteria Concentrations from WHO and Countries

There is no international standard available on levels and acceptable maximum bioaerosol concentrations (Mandal and Brandl, 2011). In table 4 shown guideline values of concentration of bacteria in different countries and world health organization (WHO).

Table 4. Guideline values of concentration of bacteria

Institution / Country	CFU/m ³	Reference
WHO	500	WHO 2002, 19970
European Union	2000	Wanner et al., 1994
China	2500	Gorny, 2004
Finland	4500	Neväläinen, 1989

The maximum concentration of bacteria in this study in the mornings were 1060 CFU m⁻³, 610 CFU m⁻³ and 1210 CFU m⁻³, in the noons and afternoons were 830 CFU m⁻³ and 810 CFU m⁻³, these concentration were higher than the WHO's limited (Figure 6).

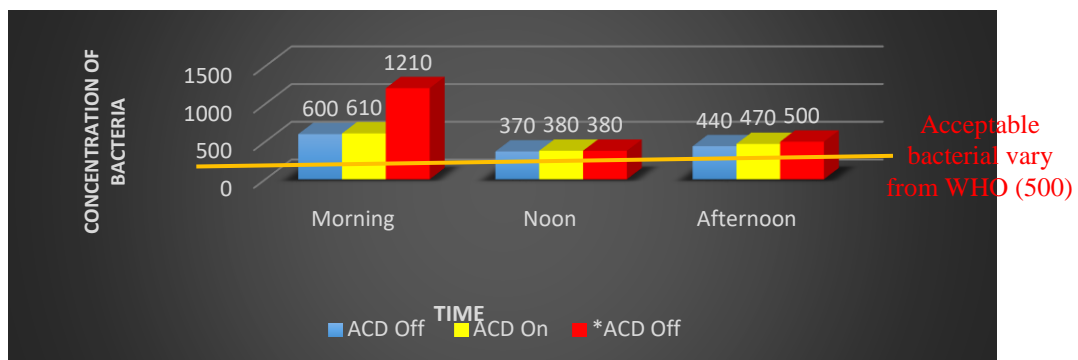


Figure 6. Maximum CFU m⁻³ of bacteria in this study and WHO's limited (*Turning off the device after one week "on" period)

7. References

- Babior BM. 2000. Phagocytes and oxidative stress. *The American Journal of Medicine*, 109:33e44.
- Boswell TC, Fox PC. 2008 Reduction in MRSA environmental contamination with a portable HEPA-filtration unit. *Journal of Hospital Infection*, 63:47-54.
- Barros E. M., Ceotto H., Bastos M. C. F., dos Santos K. R. N. and Giambiagi-de Marva M. 2012. *Staphylococcus haemolyticus* as an Important Hospital Pathogen and Carrier of Methicillin Resistance Genes. *Journal of Clinical Microbiology*, 50(1): 166-168.
- Bowers, R.M., Sullivan, A.P., Costello, E.K., Collett, J.L., Knight, R. and Fierer, N., 2011. Sources of bacteria in outdoor air across cities in the midwestern United States. *Appl. Environ. Microbiol.* 77: 6350-6356.
- Douwes, J., Thorne, P., Pearce, N. and Heederik, D. 2003. Bioaerosol health effects and exposure assessment: Progress and prospects. *Ann. Occup. Hyg.* 47: 187-200.
- Fox-Lewis A., Coltart G., Rice S. Sen R., Gourtsoyannis Y., Hyare H., Gupta R.K. 2016. Extensive subclinical sinusitis leading to *Moraxella osloensis* meningitis. *IDCases.* 6:39-42. doi: 10.1016/j.idcr.2016.08.007.
- Goh, I., Obbard, J.P., Viswanathan, S. and Huang, Y. 2000. Airborne bacteria and fungal spores in the indoor environment. A case study in Singapore. *Acta Biotechnol.* 200: 67-73.
- Jung, C.C., Wu, P.C., Tseng, C.H., Su, H.J. 2015. Indoor air quality varies with ventilation types and working areas in hospitals. *Build. Environ.* 85: 190-195.
- Gorny RL. 2004. Biologiczne czynniki szkodliwe: normy, zalecenia I propozycje wartosci dopuszczalnych. *Podstawy i Metody Oceny Srodowiska Pracy.* 3: 17-39.
- Hadano Y., Ito K., Suzuki J., Ichiro Kawamura I., Kurai H., and Ohkusu K. 2012. *Moraxella osloensis*: an unusual cause of central venous catheter infection in a cancer patient. *International Journal of General Medicine*, 5: 875-877.
- Hargreaves, M., Parappukaran, S., Morawska, L., Hitchins, J., He, C. and Gilbert, D. 2003. A pilot investigation into associations between indoor airborne fungal and non-biological particle concentrations in residential houses in Brisbane, Australia. *Sci. Total Environ.* 312: 89-101.
- Heikkienien MSA, Hjelmroos-Koski MK, Haggblom MM, MacherJM. Bioaerosols. In: Ruzer LS, Harley NH, Eds. 2005. *Aerosols Handbook*. Boca Raton: CRC Press, pp. 291-342.
- Hospodsky, D., Qian, J., Nazaroff, W.W., Yamamoto, N., Bibby, K., Rismani-Yazdi, H. and Peccia, J. 2012. Human occupancy as a source of indoor airborne bacteria. *PLoS One* 7: e34867.
- Hota B. 2004. Contamination, disinfection, and cross-colonisation: are hospital surfaces reservoirs for nosocomial infection? *Clin Infect Dis*, 39:1182-1189.
- Huang, H.L., Lee, M.K., Shih H.W. 2017. Assessment of Indoor Bioaerosols in Public Spaces by Real-Time Measured Airborne Particles. *Aerosol and Air Quality Research*, 17: 2276-2288.
- Jiang S, Zheng B, Ding W, Lv L, Ji J, Zhang H, Xiao Y, Li L. 2012. Whole-genome sequence of *Staphylococcus hominis*, an opportunistic pathogen. *Journal of Bacteriology*, 194 (17): 4761-2.



- Kalogerakis, N., Paschali, D., Lekaditis, V., Pantidou, A., Eleftheriadis, K. and Lazaridis, M. 2005. Indoor air quality-bioaerosol measurements in domestic and office premises. *J. Aerosol Sci.*, 36: 751–761.
- Kim, KY, Kim CN. 2007. Airborne microbiological characteristics in public building of Korea. *Build Environ*, 42: 2188-96.
- Kreiswirth BN, Mathema B, Mediavilla JR, Chen L. 2009. The evolution and taxonomy of staphylococci. In: Crossley KB, Jefferson KK, Archer GL, Fowler VG (eds) *Staphylococci in human disease*, 2nd edn. Wiley-Blackwell, Chichester.
- Lakestani S., Karakaş B., Acar Vaizoğlu S., Guçiz Doğan B., Çağatay G., Şekerel B., Taner A., Gullu G. 2013. Comparison of Indoor and Outdoor Air Quality in Children Homes at Prenatal Period and One Year Old. *International Journal of Civil, Environmental, Structural, Construction and Architectural Engineering*, 7.6. ISSN 2010-374X.
- Lindemann, J., Constantinidou, H.A., Barchet, W.R. and Upper, C.D. 1982. Plants as sources of airborne bacteria, including ice nucleation-active bacteria. *Appl. Environ. Microbiol.* 44: 1059-1063.
- Mandal J. and Brandl H. 2011. Bioaerosols in Indoor Environment - A Review with Special Reference to Residential and Occupational Locations, *Environmental & Biological Monitoring Journal*, 4: 83-96.
- Medical Technology Business Europe. 2011, Aerte launches revolutionary free-radical based air disinfection device 14 Nov.
- Miller RA, Britigan BE. 1997. Role of oxidants in microbial pathophysiology. *Clinical Microbiology Rev*, 10:1-18.
- Neväläinen A. 1989. Bacterial aerosols in indoor air. Dissertation, Helsinki, Finland, National Public Health Institute.
- Pastuszka, J.S., Paw, U.K.T., Lis, D.O., Wlazło, A. and Ulfig, K. 2000. Bacterial and fungal aerosol in indoor environment in Upper Silesia, Poland. *Atmos. Environ.* 34: 3833-842.
- Ramplung A, Wiseman S, Davis L. 2001 Evidence that hospital hygiene is important in the control of methicillin-resistant *Staphylococcus aureus*. *Journal of Hospital Infection*, 49: 109-116.
- Regalado NG, Martin G, Antony SJ. 2009. *Acinetobacter lwoffii*: Bacteremia associated with acute gastroenteritis. *Travel Medicine and Infectious Disease – Journal*, 7(5): 316-7.
- Schleibinger, H., Keller, R. and Rüdén, H. 2004. In: *The handbook of environmental chemistry*, Vol. 4, Pluschke, P. (Eds.), Springer-Verlag Berlin Heidelberg New York, pp. 149-177.
- Sewell D. L., Coyle M. B., and Funke G. 1995. Prosthetic valve endocarditis caused by *Corynebacterium afermentans* subsp. *lipophilum* (CDC coryneform group ANF-1). *Journal of Clinical Microbiology Journal of Clinical Microbiology*, 33(3): 759-761.
- Shapey S, Machin K, Levi K, Boswell TC. 2008 Activity of a dry mist hydrogen peroxide system against environmental *Clostridium difficile* contamination in elderly care wards. *Journal of Hospital Infection*, 70: 136-141.



Srikanth P, Sudharsanam S, Steinberg R. 2008. Bioaerosols in indoor environment: Composition, health effects and analysis. *Indian J Med Microbial*, 26: 302-12.

Stanley NJ, Kuehn TH, Kim SW, Raynor P.C., Anantharaman S., Ramakrishnan M.A., Goyal S.M. 2008. Background culturable bacteria aerosol in two large public buildings using HVAC filters as long term, passive, high-volume air samplers. *J Environ Monit*, 10: 474-81.

Tseng, C.H., Wang, H.C., Xiao, N.Y. and Chang, Y.M. 2011. Examining the feasibility of prediction models by monitoring data and management data for bioaerosols inside office buildings. *Build. Environ.* 46: 2578-2589.

Wang L., Pinkerton K.E. 2007. Air pollutant effects on fetal and early postnatal development. *Birth Defects Res. Part C, Embryo Today: Rev.* 81: 144-154.

Wanner HU, Verhoff A, Colombi A, et al. 1994. Biological particles in indoor environments. European Collaborative Action "Indoor air quality and its impact on man". Commission of the European Communities, Report no. 12. Luxembourg.

Weschler C.J. 2011. Chemistry in indoor environments: 20 years of research. *Indoor Air* 21: 205-218.
Wong V., Staniforth K., Boswell T.C. 2011. Environmental contamination and airborne microbial counts: a role for hydroxyl radical disinfection units? *Journal of Hospital Infection*, 78 ;194e199.

World Health Organization (WHO).1990. Indoor air quality: Biological contaminants. Copenhagen, European Series, No. 31.

World Health Organization (WHO). 2002. Guidelines for concentration and exposure-response measurements of fine and ultra-fine particulate matter for use in epidemiological studies. Geneva, Switzerland.

Xu, C., Wu, C.Y. and Yao, M. 2017. Fluorescent bioaerosol particles resulting from human occupancy with and without respirators. *Aerosol Air Qual. Res.* 17: 198-208.

Acknowledgments

This study was supported by grants obtained by Bolu Abant Izzet Baysal University Scientific Research Projects (BAP Project Number: 2018.31.01.1336).

Heavy metal exposure monitoring of residents of Slavonski Brod

Valjetić Marijana¹, Ćosić Vesna², Orcić Tatjana³, Kosanović Cleo⁴, Jurčević Anamarija⁵ and Cvitković Ante^{1,2,6}

¹Institute of Public Health Brod-Posavina County

²Josip Juraj Strossmayer University of Osijek Faculty of Dental Medicine and Health

³Institute for Medical Research and Occupational Health

⁴Croatian Meteorological and Hydrological Service

⁵Institute of Public Health, Split-Dalmatia County

⁶Josip Juraj Strossmayer University of Osijek Faculty of Medicine

ante.cvitkovic@sb.t-com.hr

Abstract. The objective of this study was to evaluate the exposure of heavy metals of the inhabitants of Slavonski Brod, Croatia, living within close proximity and somewhat further away from an oil refinery. Concentrations of Ni, Cr, V, Mn, Tl and Pb were analyzed in blood/serum, urine and hair and results were compared between these two groups of subjects. In 2018, heavy metals were analyzed in 40 subjects from Slavonski Brod. The study subjects were divided into two gender- and age-matched groups, assigned as "exposed" (N=20; 16 women and 4 men, aged 52.4±13.8 years) and control or "less exposed" (N=20; 16 women and 4 men, aged 54.9±16.1 years), according to the proximity of the oil refinery and meteorological data on wind directions (wind rose plot). The Ni, Cr, V, Mn, Tl and Pb concentrations were analyzed in whole blood or serum, urine and hair using inductively coupled plasma mass spectrometry (ICP-MS). The reference values used for evaluation of metal exposure were from the German Biomonitoring Commission, the Mayo Medical Laboratories and the ARUP Laboratories (USA), London Pathology and Laboratory Medicine (Canada) and Medizinische Labor Bremen (Germany). The difference between the groups was tested using student t-test, after logarithmic transformation of variables that did not follow normal distribution. The concentrations of the analyzed elements in blood, serum, urine and hair were generally within the expected reference ranges, except for Pb, which was > 90 µg/L in 4 subjects in the "exposed" group. There were statistically significant differences between the control and "exposed" subjects for Pb in serum (0.047 [0.023-0.113] µg/L vs. 0.056 [0.028-0.267] µg/L; t=-2.07; p<0.05), Pb in urine (0.68 [0.10-1.92] µg/g crea vs. 1.02 [0.35-8.39] µg/g crea; t=-2.59; p<0.02), V in hair (20.8±10.2 µg/L vs. 13.8±9.15; t=2.30; p<0.027), Mn in blood (9.18 [6.12-30.3] µg/L vs. 8.31 [4.57-10.9]; t=2.64; p<0.02). There was no difference in the concentrations of other metals in urine, hair, serum and blood between the groups. Significant differences were found for several metals between the groups of subjects living in Slavonski Brod and at different distances from an oil refinery. However, to evaluate the possible impact of the refinery on metal exposure, a larger number of the city's residents as well as additional groups of subjects living at greater distances from the refinery should be included.

Keywords: heavy metals, oil refinery, Croatia

1. Introduction

Air pollution recently became a major environmental problem around the world due to rapid industrialization, urbanization and growth of the global population (Soleimani et al., 2018). In his observations, Prasad (2004) argues that anthropogenic heavy metal emissions, linked to industrialization and urbanization, have been result of both developed and developing countries race to exploit as much

natural resources as possible worldwide to create a thriving and fast-growing economy. As reported (Leili et al., 2008; Park et al., 2008; Xu et al., 2010), heavy metals emissions can be a consequence of various sources such as fossil fuel combustion in power plants, refineries, mining industry, motor vehicles, forest fires, industrial metallurgical processes.

Heavy metal is defined in the literature as a natural element with a high atomic mass and density five times greater than water (Banfalvi, 2011). Among all pollutants, heavy metals have received enormous attention from environmental chemists due to their toxic nature. Many heavy metals are toxic even at very low concentrations (Herawati et al., 2000). In their study, Salomons et al. (1995) confirmed that metals such as mercury, arsenic, cadmium, lead, zinc, nickel, selenium, chromium and cobalt are very toxic in small quantities, and pointed to discharge of metal-containing effluents from industries into fresh water without proper treatment, as the significant source for heavy metals amount increase in our resources.

Heavy metals may enter the human body through water, food, air or absorption through the skin when they come in contact with humans through agriculture, manufacturing, pharmaceutical, industrial or residential settings (Figure1). Industrial exposure accounts for a common route of exposure for adults while ingestion is the most common route of exposure in children. Natural and human activities contaminate the environment and its resources and more is being discharged than what the environment can handle (Herawati et al., 2000; He et al., 2005).

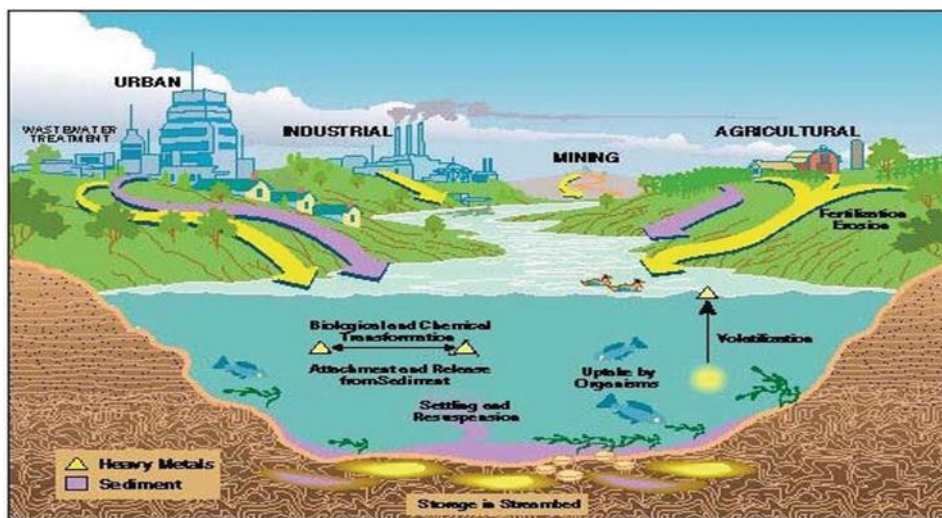


Figure 1. Sources and sinks of heavy metals (Garbarino et al., 1995).

Heavy metal pollution is one of the biggest threats for the environment that has been increasing since the mid-nineteenth century until the end of the 20th century, when these emissions had started to decrease in most developed countries. Still, exceptions exist in highly industrialized areas with outdated technologies (Nriagu, 1996).

The oil refinery in the town of Brod (Bosnia and Herzegovina) was established in 1892 with an oil refining capacity of 25,000 tons per year. In 1991, with the start of the civil war in the former Socialist Federal Republic of Yugoslavia, the refinery was shut down. At the end of the war, the damage was repaired and the refinery revitalized. Following privatization, the refinery's production facilities went into operation in 2008 and a new refining line was launched, with a capacity of 1.2 million tonnes of oil refined per year. This oil refinery is only a few hundred meters away from the town of Slavonski Brod (Croatia).

Due to multiple sources of exposure, heavy metals also represent one of the most serious threats to human health. Studies conducted over the last decade or two suggest that epigenetic mechanisms may play a role in metal-induced carcinogenesis (Figure 2), (Arita and Costa, 2009; Szewczyk, 2013).

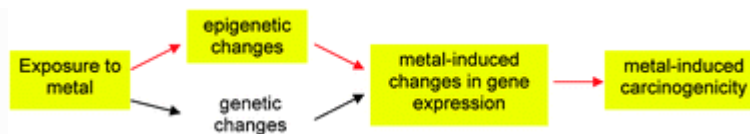


Figure 2. Epigenetics in metal carcinogenesis, (Arita & Costa, 2009).

Trace elements, occurring in the human body in amounts < 0.01 % of body weight, are essential for many physiological processes. However, when present at increased levels, they may produce different adverse conditions and diseases, including neurodegenerative diseases as Parkinson's disease, Down syndrome, and Alzheimer's disease (Fido and Al-Saad, 2005).

In the EUROPE-HRAPIE project, relevant stakeholders and experts identified six categories of sources of air polluting emissions: agriculture (5.3%), metal industry (6.2%), energy production and distribution (6.2%), shipping (8.8%), air conditioning and space heating (15.0%) and road transport, (40.7%). In the case of metals, several are particularly prominent: nickel (2.3%), iron (2.0%), vanadium (2.0%), lead (1.7%), manganese (1.6%), copper (1.4%), cadmium (1.3%), zinc (1.0%), arsenic (1.1%), mercury (0.8%), aluminum (0.1%), and transition metals in general (0.3%) (Henschel and Chan, 2013).

In a study by Al-Jebouri (2014) conducted in Iraq, it was found that concentrations of heavy metals in the soil and water of the oil refinery were higher than the maximum allowable levels recommended by the WHO. These high levels metals suggest a lack of efficient control measures in the refinery. Consequently, this situation might lead to pathophysiological changes in human body systems, particularly the respiratory tract, in refinery workers and in the nearby community.

Yuan et al. (2019) studied relation between toxicity and the combined effects of PM-bounded metals in human lung epithelial cells (A549). Results showed that six heavy metals (Cr, Zn, Cu, Fe, Mn and Pb) among the eleven elements tested (Cr, Zn, Cu, Fe, Mn, Pb, Ni, As, Se, Sr and Cd) might account for PM toxicity in A549 cells and that their exposure led to high A549 cell mortality ($36.5 \pm 7.3\%$), confirming potential adverse effects of heavy metals and their interactions to PM toxicity.

In a study conducted in Chicago between 2005 and 2008, breast cancer cases were investigated. Logistic regression models were used to examine whether the airborne heavy metal associations differed by tumor ER/PR status. Principal component analysis was performed to assess associations by metal co-exposures. In women with diagnosed breast cancer, air pollution (including metallic air pollutants) has been associated with an increased chance of developing ER/PR-negative breast cancer (Kresovich et al., 2019).

The European Parliament and the countries of the European Council have adopted Directive 2008/50/EC on ambient and cleaner air quality for Europe in order to improve ambient air quality. Continuous ambient air quality monitoring, as a part of general environmental monitoring, is essential due to constant changes of the ambient air caused by aerogenic pollutants (Baltrėnaitė et al., 2014).

The 2015 annual report of the Agency for Environment and Nature, Croatia on air quality in Slavonski Brod, showed that the air was polluted (second category according to Croatian legislation) for the

following three parameters: H₂S, PM₁₀ and PM_{2.5}. The situation was similar in previous years. In a report of the Institute for Medical Research and Occupational Health (for the period 7 November 2013 - 8 August 2014), air pollution monitoring in the city of Slavonski Brod, contributions of possible sources (from biomass burning, traffic, industry and oil refinery) to levels of different inorganic and organic pollutants were studied. It was shown that the oil refinery, which predominantly contributed to sulphur compounds, also contributed to the number of elements (Ni 84.9%, Cr 73.9%, Pb 2.7%, Mn 8.5%, V 57.6%, La 81.5%).

2. Aim

The objective of this study was to evaluate exposure to heavy metals of the residents of Slavonski Brod, Croatia, living within close proximity and somewhat further away from the oil refinery. Concentrations of Ni, Cr, V, Mn, Tl and Pb were analyzed in blood/serum, urine and hair and results were compared between these two groups of subjects.

3. Subjects and Methods

3.1. Subject selection

The Institute of Public Health of the County of Brod-Posavina selected the respondents. The samples were collected in November 2018. Respondents were divided into two groups matched by gender and age, classified as "exposed" (N = 20; 16 women and 4 men, aged 52.4 ± 13.8 years) and control or "less exposed" (N = 20; 16 females and 4 males, aged 54.9 ± 16.1 years), according to the proximity of the oil refinery and data from the Croatian Meteorological and Hydrological Institute on wind direction (flat wind rose). The participants in the "exposed" group lived in the range of about 1-2.5 km, and the participants of the "less exposed" group on the route lived approximately 7.7 km from the Brod oil refinery. In selecting the subjects for the analysis of metals in blood/serum, urine and hair, certain criteria were applied. Respondents who did not work in the metal industry, non-smokers and participants who did not dye their hair, could participate. All respondents provided written consent for voluntary and anonymous participation in the survey. The Ethics Committee of the "Dr. Josip Benčević" General Hospital approved the study.

3.2. Metal analysis

The Institute for Medical Research and Occupational Health analyzed the concentrations of Ni, Cr, V, Mn, Tl and Pb in whole blood or serum, urine and hair using inductively coupled plasma mass spectrometry (ICP-MS) on an Agilent 7500cx device (Agilent Technologies, Japan). The reference values for the metal exposure assessment were used primarily from the literature of the German Biomonitoring Commission, Mayo Medical Laboratories and ARUP Laboratories (USA), London Pathology and Laboratory Medicine (Canada) and Medizinisches Labor Bremen (Germany), since no studies have been conducted in Croatia on the general population to determine metal reference values in blood, urine and hair samples. The accuracy of the analysis was confirmed by analysis of reference blood samples (Seronorm™ Trace Element Whole Blood Level I, II and Level III (Sero AS, Norway) and ClinChek Whole Blood Control, Level I, II and Level III, ClinChek® Controls - RECIPE Chemicals + Instruments GmbH), serum and plasma (Seronorm™ Trace Element Serum and Seronorm™ Trace Element Plasma Level I and Level II (Sero AS, Norway) and ClinChek Serum Control and ClinChek Plasma Control, Levels I and Level II, ClinChek® Controls - RECIPE Chemicals + Instruments GmbH), urine (Seronorm Urine, Levels I and Level II, Sero Norway and ClinChek Urine Control, Levels I and Level II, RECIPE Chemicals + Instruments GmbH) and hair (NIES CRM No 13 Human Hair, National Institute for Environmental Studies, Japan). Urine creatinine concentration, which was used to normalize the concentration of metal in urine, was determined by spectrophotometry (Cary 50, Varian, Australia), using the standard Jaffé method. Test accuracy was confirmed using a reference urine sample of Seronorm (Nycomed, Norway) with a certified creatinine concentration.

3.3. Statistical analysis

Data are presented as the mean \pm SD for variables following normal distribution (according to the Kolmogorov-Smirnov test), and as the median and range (or the lowest to the highest value) for the asymmetric variables. Differences between the defined groups were tested by Student's t-test for independent samples after the data in the variables with asymmetric logarithmic distribution were transformed to follow normal distribution. The level of statistical significance was set at 5% ($p < 0.05$). Statistical analysis was performed using the data analysis software system Dell Statistica, version 13 (Dell Inc., USA).

4. Results

There was no statistically significant difference in age between the groups (less exposed 54.9 ± 16.1 ; more exposed 52.4 ± 13.8 ; $t=0.516$; $p=0.608$). The age of the respondents ranged in the exposed group within 31-75 years, in the less exposed group 30-76 years. Table 1 shows the results of the analysis of the concentrations of Pb, Ni, Cr, V, Mn and TI in whole blood (Pb-B, Ni-B, Cr-B, V-B, Mn-B, TI-B) or serum (Pb-S, Ni-S, Cr-S, V-S, Mn-S, TI-S), urine (Pb-U, Ni-U, Cr-U, V-U, Mn-U, TI-U) and hair (Pb-Hair, Ni-Hair, Cr-Hair, V-Hair, Mn-Hair, TI-Hair) with participants living near (Group II) or at a greater distance from the oil refinery (Group I). The concentrations of the analyzed elements in blood, serum, urine and hair were generally within the expected reference ranges, except for Pb, which was $>90 \mu\text{g/L}$ in 4 subjects (3 female, 1 male) in the "exposed" group. There were statistically significant differences between the control and "exposed" subjects for Pb (Figure 3) in serum ($0.047 [0.023-0.113] \mu\text{g/L}$ vs. $0.056 [0.028-0.267] \mu\text{g/L}$; $t=-2.07$; $p<0.05$), Pb in urine ($0.68 [0.10-1.92] \mu\text{g/g creat}$ vs. $1.02 [0.35-8.39] \mu\text{g/g creat}$; $t=-2.59$; $p<0.02$), V in hair ($20.8 \pm 10.2 \mu\text{g/L}$ vs. 13.8 ± 9.15 ; $t=2.30$; $p < 0.027$), Mn in blood ($9.18 [6.12-30.3] \mu\text{g/L}$ vs. $8.31 [4.57-10.9]$; $t=2.64$; $p<0.02$). There was no difference in the concentrations of other metals in urine, hair, serum and blood between the groups.

Table 1. Concentrations of analyzed indicators in blood (B), urine (U) and hair of subjects from two different areas of Slavonski Brod, Croatia: Group I from the northern part (less exposed); Group II from center and south, near Oil Refinery (exposed).

	GROUP I (N=20)	GROUP II (N=20)	t	p
Age	54.9±16.1	52.4±13.8	0.516	>0.608
Pb-B (µg/L)	15.2 (10.1-75.0)	21.4 (9.02-131)	-1.863	>0.070
Pb-S (µg/L)	0.047 (0.023-0.113)	0.056 (0.028-0.267)	-2.072	<0.05
Pb-U (µg/L)	1.16 (0.11-3.39)	1.45 (0.22-10.1)	-1.051	>0.300
Pb-U (µg/g creat)	0.68 (0.10-1.92)	1.02 (0.35-8.39)	-2.594	<0.02
Pb-Hair (µg/kg)	337 (97.6-3558)	334 (88.9-8794)	-1.179	>0.245
Ni-B (µg/L)	0.86±0.21	0.87±0.18	-0.208	>0.836
Ni-S (µg/L)	0.81±0.13	0.78±0.08	0.802	>0.081
Ni-U (µg/L)	2.87±1.53	2.72±1.98	0.269	>0.789
Ni-U (µg/g creat)	1.76±0.72	1.90±0.84	-0.565	>0.575
Ni-Hair (µg/kg)	63.7 (33.2-177)	67.6 (27.8-293)	-0.377	>0.707
	78.5±40.1	90.1±68.2	-0.656	>0.516
Cr-B (µg/L)	0.51±0.17	0.52±0.23	-0.182	>0.193
Cr-S (µg/L)	0.52±0.09	0.57±0.08	-1.947	>0.058
Cr-U (µg/L)	0.93±0.35	0.91±0.46	0.176	>0.861
Cr-U (µg/g creat)	0.58±0.19	0.73±0.40	-1.540	>0.131
Cr-Hair (µg/kg)	86.9 (15.2-205)	47.8 (13.3-203)	1.505	>0.141
	88.4±47.8	70.5±54.1	1.110	>0.274
V-B (µg/L)	0.71±0.032	0.73±0.03	-2.022	>0.05
V-U (µg/L)	0.92±0.24	1.01±0.45	-0.804	>0.426
V-U (µg/g creat)	0.61±0.28	0.84±0.46	-1.886	>0.066
V-Hair (µg/kg)	18.2 (12.8-57.6)	11.9 (1.70-42.2)	3.198	<0.003
	20.8±10.2	13.8±9.15	2.304	<0.027
Mn-B (µg/L)	9.18 (6.12-30.3)	8.31 (4.57-10.9)	2.636	<0.02
Mn-S (µg/L)	0.47±0.10	0.45±0.11	0.562	>0.577
Mn-U (µg/L)	0.121 (0.034-0.544)	0.116 (0.013-1.15)	0.557	>0.581
	0.16±0.12	0.18±0.24	-0.273	>0.786
Mn-U (µg/g creat)	0.072 (0.023-0.223)	0.098 (0.008-0.513)	-0.551	>0.585
	0.10±0.07	0.14±0.13	-1.075	>0.289
Mn-Hair (µg/kg)	161 (28.4-815)	134 (19.4-447)	1.245	>0.221
	243±227	155±119	1.530	>0.134
Tl-B (µg/L)	0.031 (0.018-0.073)	0.036 (0.022-0.116)	-1.873	>0.069
Tl-S (µg/L)	0.014±0.002	0.015±0.002	-1.788	>0.08
Tl-U (µg/L)	0.23±0.09	0.20±0.10	1.064	>0.294
Tl-U (µg/g creat)	0.14±0.05	0.16±0.06	-0.731	>0.469
Tl-Hair (µg/kg)	0.36 (0.14-2.58)	0.57 (0.11-6.50)	-1.413	>0.166

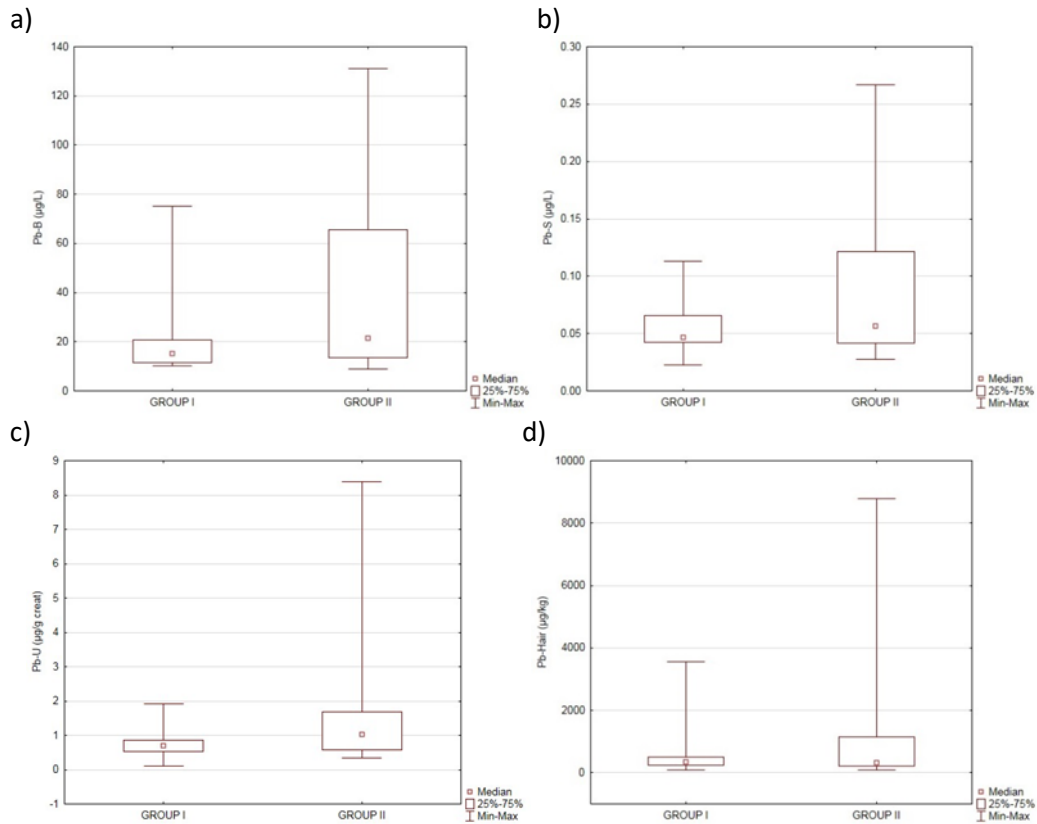


Figure 3. Graphical representation of the measured concentrations of Pb in blood (a), serum (b), urine (c) and hair (d) in the examined two groups of respondents of Slavonski Brod population by place of residence (Group I from the northern part (less exposed) and Group II from center and south, near the Oil Refinery (exposed)).

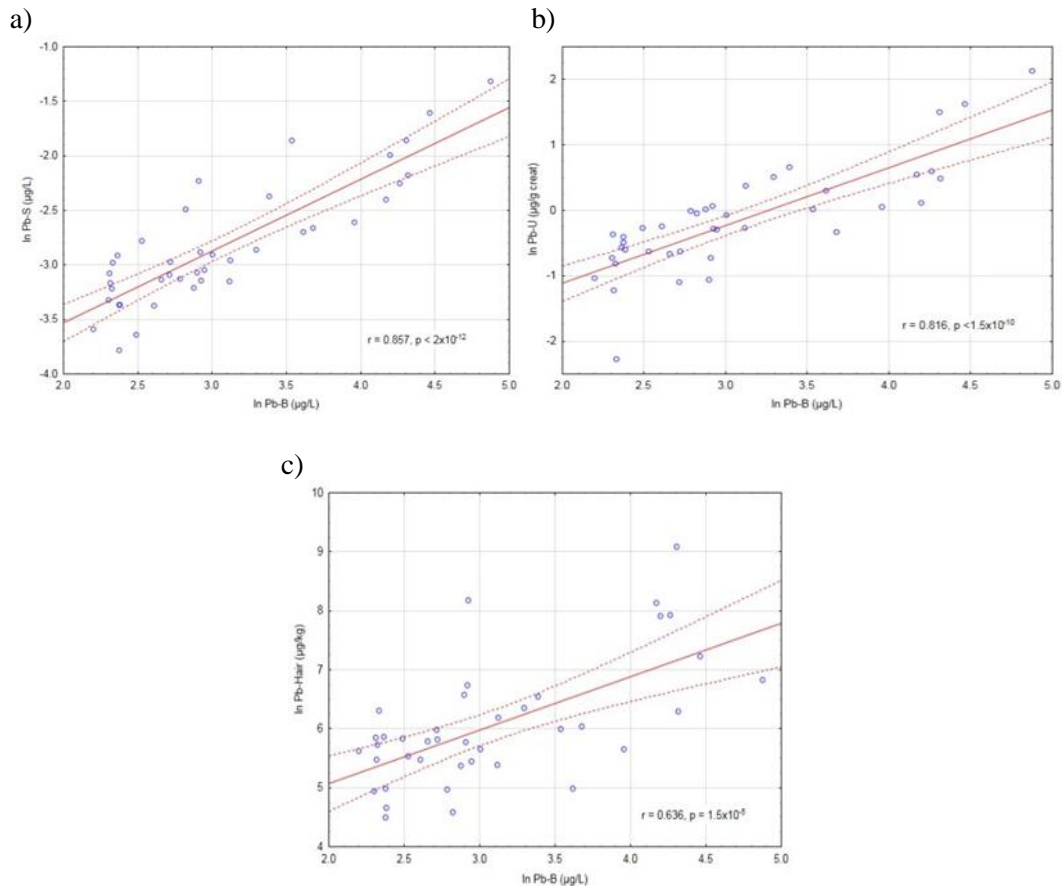


Figure 4. Correlations between Pb concentration in serum (a), urine (b) and hair (c) of subjects obtained by Pearson linear correlation test (after logarithmic transformation of skewed variables to obtain normal distribution).

5. Discussion

The main objective of this pilot study was to investigate the potential impact of the oil refinery on the health of the people in its vicinity, and to examine the concentrations of metals of Pb, Ni, Cr, V, Mn and Ti in blood /serum, urine and hair. The concentrations of the analyzed elements in blood, serum, urine and hair were generally within the expected reference ranges, except for Pb, which was $> 90 \mu\text{g/L}$ in 4 subjects in the “exposed” group. There was no difference in the concentrations of other metals in urine, hair, serum and blood between the groups. The elevated levels of Pb, V and Mn in several participants may be attributed to specific eating or lifestyle habits. Pb level was significantly higher in urine (expressed in $\mu\text{g/L}$) in group II compared with group I. The relevant indicator of total body load with Pb and the most potent indicator for biological monitoring is considered to be Pb in the blood, while urine concentration reflects recent exposure and is significantly more variable with respect to individual fluid intake and renal function as indicated in the Mayo Clinic, Interpretive Handbook, (2019). No statistically significant difference was found between the two groups in Pb level in blood and hair, but given the apparent increase in Pb in the blood and urine of subjects living near the oil refinery relative to distant subjects, more detailed studies are needed. A statistically significant difference was found between groups in concentration V in hair, elevated values were in group I and in group II, but not toxicologically relevant. In the absence of criteria for levels V in Croatia, an accurate interpretation of the measured values is not possible. The concentration of Mn in the blood was higher in Group I and a statistically significant difference was found between the groups. The levels of Mn in the hair of the

three subjects in Group I were above the reference values, but no statistically significant difference was found as in serum and urine. Sanders et al. (2009) argues that biological monitoring is very useful for assessing the risk of toxic agents in the environmental impact of human health. This pilot study of biological monitoring of metals in Slavonski Brod showed an increase in the concentration of several analyzed metals in the subjects, but we still could not assess whether the increased concentration of metals in the subjects was related to the proximity of the oil refinery. The results of this study, conducted in 2016, showed that there were several participants with elevated levels of Pb, Cd, and Hg in blood, urine and hair, As in urine and Mn in hair. There was a significantly higher median Pb concentration in urine, As and Tl in the blood of the exposed group compared to the less exposed group. The concentration of Mn in urine was higher at less exposed group. Statistically significant differences between the groups were not toxicologically significant because they are within the reference values and ranges for the general population (Cvitković et al., 2017). Due to the great dissatisfaction of the citizens, it is certainly necessary to continue with research and increase the number of respondents, to the extent to which financial resources allow, and with the support of the Croatian Ministry of Health try to determine whether the individual metals associated with the oil refinery or we should attribute them to food intake or lifestyle.

6. Conclusion

Air pollution is not a new phenomenon, because it existed even before man became aware of nature, but the sources of this pollution need to be explored in order to reduce it. This study is a step in the direction of estimates of air pollution and its impact on human health (Ugya et al., 2017). A multidisciplinary approach through clinical, epidemiological, and environmental expertise could allow integrating information and ameliorate risk assessment. Overall, new efforts should be performed in order to confirm the role of metals as etiological agents and accelerate translation of science into prevention (Gorini et al., 2014). Significant differences were confirmed for several metals between the groups of subjects living in Slavonski Brod and at different distance from an oil refinery. However, to evaluate the possible impact of the refinery on metal exposure, a larger number of the city's residents as well as additional groups of subjects living at greater distances from the refinery should be included.

7. References

- Annual Report on Air Quality Monitoring in the Republic of Croatia for 2015. Zagreb. Croatian Environmental and Nature Agency. <http://iszz.azo.hr/iskzl/file?id=31863>, accessed in 2019.
- Arita, A., & Costa, M., 2009. Epigenetics in metal carcinogenesis: nickel, arsenic, chromium and cadmium. *Metallomics* 1, 222–228.
- Baltrėnaitė, E., Baltrėnas, P., Lietuvninkas, A., Serevičienė, V. & Zuokaitė, E., 2014. Integrated evaluation of aerogenic pollution by air-transported heavy metals (Pb, Cd, Ni, Zn, Mn and Cu) in the analysis of the main deposit media. *Environ Sci Pollut Res Int* 21, 299-313.
- Banfalvi, G., 2011. *Cellular Effects of Heavy Metals*. Netherlands, London, New York. Springer.
- Cvitković, A., Capak, K., Jurasović, J., Barišin, A., Ivić-Hofman, I., Poljak, V., Valjetić M., 2017. Metal Concentration Study In A Population Living In The Vicinity Of An Oil Refinery. *WIT Transactions on Ecology and the Environment*, 211, 255-261.
- Fido, A., & Al-Saad, S., 2005. Toxic trace elements in the hair of children with autism. *Autism* 9, 290–298.



- Garbarino, JR., Hayes, HC., Roth, DA., Antweiler, RC., Brinton, TI., Taylor, HE., 1995. Contaminants in the Mississippi River: Heavy metals in the Mississippi River. U.S. Geological Survey Circular. Reston, Virginia, pp. 1133.
- Gorini, F., Muratori, F., Morales, M.A., 2014. Review Journal of Autism and Developmental Disorders. 1. 4, pp 354–372.
- He, ZL., Yang, XE., Stoffella, PJ., 2005. Trace elements in agroecosystems and impacts on the environment. Journal of Trace Elements in Medicine and Biology 19, 125-140.
- Henschel, S., & Chan, G., 2013. Health risks of air pollution in Europe –HRAPIE project. World Health Organization, Copenhagen. www.euro.who.int/en/health-topics/environment-and-health/air-quality/publications/2013/health-risks-of-air-pollution-in-europe-hrapie-project.-new-emerging-risks-to-health-from-air-pollution-results-from-the-survey-of-experts., accessed in September 2019.
- Herawati, N., Suzuki, S., Hayashi, K., Rivai, IF., Koyoma, H., 2000. Cadmium, copper and zinc levels in rice and soil of Japan, Indonesia and China by soil type. Bulletin of Environmental Contamination and Toxicology 64, 33-39.
- Herawati, N., Suzuki, S., Hayashi, K., Rivai, IF., Koyoma, H., 2000. Cadmium, copper and zinc levels in rice and soil of Japan, Indonesia and China by soil type. Bulletin of Environmental Contamination and Toxicology 64, 33-39.
- Institute for Medical Research and Occupational Health, Environmental Hygiene Unit. Report on Air Pollution Monitoring at the Temporary Station of the State Air Quality Monitoring Network - Slavonski Brod (for the period 7 November 2013 - 8 August 2014) .Croatia. [iszz.azo.hr/iskzl/file?id= 19,830th](http://iszz.azo.hr/iskzl/file?id=19,830), accessed in 2019.
- Jerome, o. Nriagu., 1996. A History of Global Metal Pollution. Science 272, 223-224.
- Kresovich, JK., Erdal, S., Chen, HY., Gann, PH., Argos, M., Rauscher, GH., 2019. Metallic air pollutants and breast cancer heterogeneity. Environ Res. 8, 108639.
- Leili, M., Naddafi, K., Nabizadeh, R., Yunesian, M., 2008. The Study of TSP and PM10 Concentration and Their Heavy Metal Content in Central Area of Tehran Iran. Air Quality, Atmosphere & Health 1, 159-166.
- Mayo Clinic. Mayo Medical Laboratories, Interpretive Handbook.
- Mohemid, Al-Jebouri., 2014. Estimation of Environmental Chemical Pollution of Al-Baiji Oil Refinery in Iraq. Current Journal of Applied Science and Technology 4, 2223-2230.
- Online: <http://www.mayomedicallaboratories.com/interpretive-guide/index.html>. accessed in 2019.
- Park, K., Heo, Y., Putra, HE., 2008. Ultrafine Metal Concentration in Atmospheric Aerosols in Urban Gwangju, Korea. Aerosol and Air Quality Research 8, 411-422.
- Prasad, R.,2004. Urban Air Quality—Some Interesting Observations. Our Earth. 1, 8-11.
- Salomons, W., Forstner, U., Mader, P., 1995. Heavy Metals: Problems and Solutions. Berlin, Germany. Springer-Verlag.
- Sanders, T., Liu, Y., Buchner, V., Tchounwou P.B, 2009. Neurotoxic Effects and Biomarkers of Lead Exposure: A Review. Rev Environ Health 24, 15–45.
- Soleimani, M., Amini, N., Sadeghian, B., Wang, D., Fang, L., 2018. Heavy metals and their source identification in particulate matter (PM_{2.5}) in Isfahan City, Iran. J. Environ. Sci. 72, 166-175.
- Szewczyk, B., 2013. Zinc homeostasis and neurodegenerative disorders. Front Aging Neurosci. 19, 5-33.



18th World Clean Air Congress, 23-27 September 2019, Istanbul
organized by TUNCAP and IUAPPA

Ugya, A.Y., Imam,T.S., Priatamby. A., 2017. The effect of heavy metal air pollution arising from local metallurgical activities on albino rat. *American Journal of Preventive Medicine and Public Health* 1, 10-19.

Xu, YH., Wu, JH., Feng, YC., Dai, L., Bi, XH., Li, X., Zhu, T., Tang, SB., Chen, MF., 2010. Source Characterization and Apportionment of PM10 in Panzhi-hua, China. *Aerosol and Air Quality Research* 10, 367- 377.

Yuan, Y., Wu, Y., Ge, X., Nie, D., Wang, M., Zhou, H., Chen, M., 2019. In vitro toxicity evaluation of heavy metals in urban air particulate matter on human lung epithelial cells. *Sci Total Environ.* 15, , 301-308.

Acknowledgments

The authors would like to thank all the staff of the Department of Epidemiology and Public Health, Institute of Public Health Brod-Posavina County for their efforts and support for this project. We would also like to thank the Croatian Ministry of Health for the financial support and all external associates of the Institute who contributed to the implementation of this project.

Integrating citizen's behaviour and air quality management to raise public awareness in European cities

Enda Hayes¹, Joanna Barnes¹, Andy King¹, Kris Vanherle², Alastair Callum¹, Eva Csobod³, Laura De Vito¹, Iason Diafas⁴, Laura Fogg-Rogers¹, Willem Himpe², Trond Husby⁴, Olga Ivanova⁴, Peter Papics² and Jim Longhurst¹

¹ University of the West of England Bristol, Coldharbour Lane, Bristol, United Kingdom.

² Transport Mobility Leuven, Leuven, Belgium.

³ The Regional Environmental Centre for Central and Eastern Europe, Szentendre, Hungary

⁴ PBL Netherlands Environmental Assessment Agency, The Hague, The Netherlands

enda.hayes@uwe.ac.uk

Abstract. Despite many years of efforts to reduce air pollution to safe ambient concentrations, levels of several pollutants still contravene health-based guidelines across many European cities. Traditional government policy has had a very techno-centric view of air pollution sources resulting in a primary focus on technological policies and solutions. This has resulted in a general apathy and disconnect among citizens towards air pollution and subsequently a lack of ownership of the problem and solutions. This paper argues the need for a broader approach to air quality management, one that places a greater emphasis on the social factors that contribute to emissions such as the daily behaviours, practices and activities of people (e.g. commuting, leisure, shopping etc.), not just technologies (e.g. Euro standards). Drawing from evidence collated across six European cities as part of the ClairCity Project (www.claircity.eu), this paper will illustrate how an enhance qualitative and quantitative understanding of the role of citizen's behaviour in generating pollution, married with innovate public engagement activities, can be used to create a shift in public debate surrounding causes of poor air quality. The public engagement activities include a Delphi process in which citizens were given a platform to explore the reasons for their entrenched behaviour and decision making and the ClairCity Skylines App that utilised game technology to engage citizens and 'crowd-source' public perceptions and acceptability of air pollution policies. These engagement activities are reinforced by the source apportionment of pollution by people's behaviour and motives rather than technology thereby making the data more relevant to people and their daily lives. By putting citizens' behaviour and activities at the heart of policymaking, citizens are empowered to visualise clean, low carbon, healthy futures for their city.

Keywords: Citizen behaviour, Air pollution, Cities, Public engagement, Source apportionment

1. Introduction

A lack of civic engagement in air quality management to date lies partially in the absence of 'people' in the data, evidence, models and policy narratives used to estimate, predict and communicate air pollution data and its impacts. There is a growing volume of scientific evidence on the health effects of air pollution, which is being shared by the main stream media in many countries, and the health impact of air pollution is further exacerbated due to the inter-relationships with other social determinants of health creating a disproportionate risk and burden (EEA, 2018a). Transport is a major source of poor



air quality across European cities (EEA, 2018b) and interventions to improve the efficiency of vehicles can go some way to ameliorate the situation, but reducing the number of vehicles on the roads is also a crucial element in any air quality strategy that seeks to identify and reduce root causes of poor air quality whilst simultaneously addressing related issues, for example reducing carbon emissions and increasing the physical activity and wellbeing of a population. The UK Committee on Climate Change report on achieving net-zero found that 38% of shifts required would be wholly based on the uptake of low-carbon technologies but the remaining 62% of emission reductions would require some degree of societal and individual behaviour change (CCC, 2019).

The ClairCity project (www.claircity.eu), funded by EU Horizon 2020 (Project Ref: 689289), aims to provide a new perspective for citizens and a new geography of pollution based on ‘activities, behaviour and practices’ which will allow the connection to be made between pollution and behaviour, and link these to the various practices that constitute everyday life within our cities. In other words, air pollution and carbon management are no longer to be addressed as separate and rather technical policy topics, but to be regarded as part of wider concerns of city inhabitants about their quality of life and healthy futures. The ClairCity project creates a new platform to stimulate discussion and engage citizens across Europe in a democratic debate about how their cities develop in a manner that protects the local and global environments and puts their health and well-being at the heart of policymaking.

With a particular focus on transport and domestic energy use, new modes of engaging citizens, stakeholders and policymakers have placed ‘people’ within our data and models and stimulated the public engagement necessary to tackle our challenging emissions problems through the development of a range of citizen-led future scenario and policy packages. Using an innovative quantification and engagement toolkit to facilitate multi-stakeholder dialogue in six European pilot cities and regions, (Bristol, United Kingdom; Amsterdam, Netherlands; Ljubljana, Slovenia; Sosnowiec, Poland; Aveiro, Portugal; and Liguria, Italy) we can integrate the findings to obtain a qualitative and quantitative understanding of the public perceptions of existing policy options (Skylines Game), the constraints that entrench people in repetitive patterns of behaviour (Delphi) and the source apportionment emissions by those behaviours. Using the Bristol city data as an exemplar, and focussing on transport behaviour, this paper will illustrate how these datasets can come together to raise public awareness and also allow for targeted air quality management interventions by city policy makers that enable wider societal change required to meet the air quality and carbon challenges that modern European cities now face.

2. Methodology

2.1. Understanding the public acceptability of policies using the ClairCity Skylines Game

The ClairCity Skylines Game created a serious game experience to actively engage city citizens and stakeholders providing an enhanced understanding of the air quality, carbon, economic and health issues within cities (Hayes et al., 2018). The ClairCity Skylines Game gave players (citizens and key stakeholders) the power to augment a stylised ‘living city’. The local look and feel of the Game (e.g. the game platform for Bristol was styled to look like Bristol) allowed the player to feel comfortable and connected with their gaming environment. The game engine made it possible to visualise when, where and why any player made key decisions and the behavioural choices that led to the overall success or failure of their pathway in terms of air quality, economy, carbon footprint and health. The ClairCity Skylines Game has a comprehensive policy library (the ClairCity Policy Library (CPL)) underpinned the “ideas” that are presented to the players. Each of the > 500 environmentally positive and negative “ideas” in the CPL has been mined and adapted from a number of existing databases such as JOAQUIN (www.joaquin.eu) and the FAIRMODE Catalogue of Air Quality Measures (<http://fairmode.jrc.ec.europa.eu/measure-catalogue/>). Each individual “idea” has been scored (+/- 10 points) for both the short and long term impacts against four key attributes – climate/carbon, air quality/health, citizen satisfaction/happiness and city economy.

Players, acting as the Mayor, move around their stylised city to recognisable landmarks where they are randomly presented “ideas” from the CPL and they must choose the “ideas” they like. Chosen “ideas” are then promoted to “policies” by the player every five years with the aim to improve air quality, carbon and health in the city while maintaining citizen satisfaction and the city economy. At the end of each play (win or fail) the “ideas” and “policies” are recorded and can then be assessed to understand the broader public perception and acceptability of specific policies thereby allowing ClairCity to “crowd-source” potential citizen-led policy pathways and scenarios. To enhance the playability of the game the attribute scores (i.e. how well or how bad a player is doing against each of the four attributes) is linked to the game world effects so that the game world can either decay or regenerate. Finally, players provide some simple personal demographic data (e.g. age, gender and rate their knowledge of air pollution) that will allow the project to undertake case attribute analysis of the results in the future that will allow for demographically targeted scenarios and policy development.

2.2. *Generating qualitative evidence - Delphi Study*

The ClairCity project used an open question survey method as part of a Delphi process to collect data from >500 people in Bristol over the summer of 2017, using a sampling method with a mix of online, paper self-complete and interviewer led methods (Boushel et al., 2018). The Delphi process is a mixed method approach, usually using multiple rounds of opinion elicitation to generate and identify consensus over complex topics (Dalkey and Helmer, 1963; Bailey et al., 2012; Brunt et al., 2018). The mixed approach resulted 155 responses completed online (using BOS), 223 questionnaires completed by trained interviewers and a further 122 surveys self-completed by respondents. Events were selected to reach respondents from marginalised groups, those who may be less likely to respond to an online survey or those less likely to be motivated to fill in a survey relating to air quality and carbon emissions. This included community events in deprived neighbourhoods, shopping areas etc. The final sample is not designed to be perfectly representative of the Bristol population, but through a relatively large sample size, purposive sampling and monitoring demographic data our sample is effective for eliciting patterns of behaviour, identifying some common or shared experiences and gives an insight in to citizen behaviour and desires. The data was collated and thematically coded using NVIVO software.

2.3. *Source apportionment by behaviour*

A fine granular dataset of road transport emissions was generated that allowed source apportionment not only at the typical level of mode choice (e.g. car, bus, taxi, cycling, walking etc) but also the underlying behaviour or motive (e.g. shopping, commuting, leisure etc) and socio-economic properties of the people travelling (e.g. gender, age, income etc). The scientifically robust yet flexible methodology is designed to allow it to use different types of public datasets, which can be applied to different cities in similar fashion. The methodology had two primary steps: (1) A simple traffic demand generation and assignment algorithm to establish traffic flows at link level to calculate total emissions; and (2) merging the emission dataset from step 1 with travel survey data holding information on the underlying motives and socio-economic properties of travellers of individual trips.

The trip motive / citizen behaviour activity definitions are taken from the UK National Travel Survey (HM Government, 2018). These are defined as:

- **Commuting:** trips to a usual place of work from home, or from work to home;
- **Business:** personal trips in course of work, including a trip in course of work back to work. This includes all work trips by people with no usual place of work (e.g. site workers) and those who work at or from home;
- **Other:** trips to work from a place other than home or in course of work, e.g. coming back to work from going to the shops during a lunch break. In most tables this is included with 'personal business';
- **Education:** trips to school or college, etc. by full time students, students on day-release and part time students following vocational courses;

- Shopping: all trips to shops or from shops to home, even if there was no intention to buy;
- Personal business: visits to services, e.g. hairdressers, launderettes, dry-cleaners, betting shops, solicitors, banks, estate agents, libraries, churches; or for medical consultations or treatment; or for eating and drinking, unless the main purpose was entertainment or social;
- Leisure: visits to meet friends, relatives, or acquaintances, both at someone's home or at a pub, restaurant, etc.; all types of entertainment or sport, clubs, and voluntary work, non-vocational evening classes, political meetings, etc.;
- Escort: used when the traveller has no purpose of his or her own, other than to escort or accompany another person; for example, taking a child to school. 'Escort commuting' is escorting or accompanying someone from home to work or from work to home. Similarly, other escort purposes are related to the purpose of the person being escorted.

3. Case Study Results and Discussion

3.1. Skyline Game

The Bristol version of the Skylines Game had been downloaded >750 times with a play rate of 3.2 players per download (i.e. approximately 2,400 individual play sessions). During these plays, >37,500 "ideas" were presented, >18,000 individual "ideas" were collected for future consideration and >10,000 ideas were enacted into "policies". When exploring the enacted policies in more detail we see a shallow but wide variety of preferred policies being chosen by the Bristol players (Figure 1). These specific policies, while interesting in their own right, also illustrate the main policies areas of importance for citizens in that city. Additionally, this evidence is not viewed in isolation but also cross-referenced against the findings of the ClairCity Delphi process and the source apportionment data. Indicative results for Bristol point to three main areas of concern (Figure 1) but when we look at the key enacted policies we see a clear preference for transport and land-use policies. Indicative policy areas and policy preferences include: Transport (60.1%): Citizens/players enacted policies addressed active travel (26%) and public transport (25%); Energy/Other (39%): Citizens/players enacted energy policies addressed energy alternatives such as renewables (22%) and energy efficiency measures (18%); and "Other" policies addressed green infrastructure / green space (17.2%) (Figure 1).

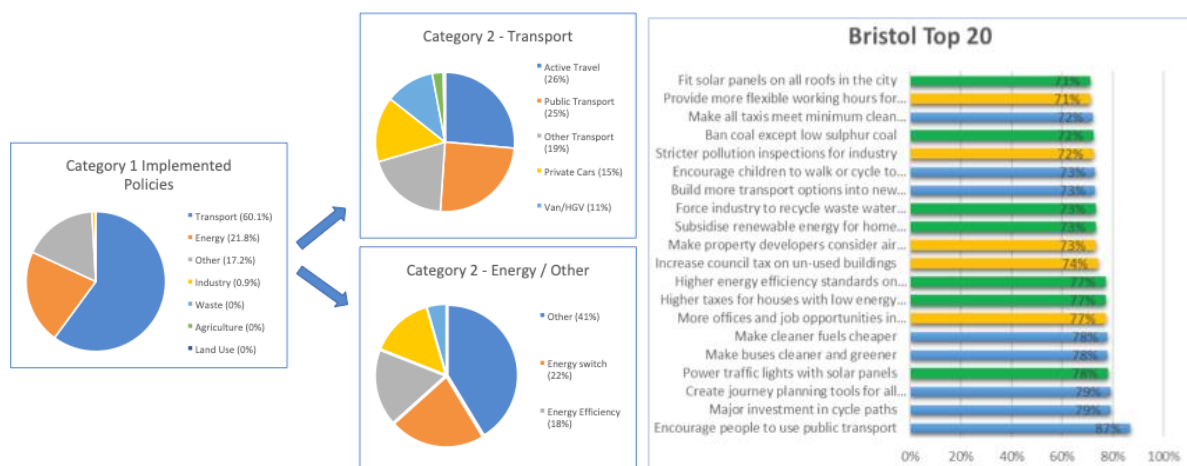


Figure 1. ClairCity Skylines policy choices for Bristol

3.2. Delphi Data

In the Delphi process, citizens were asked to what extent they wanted to change their own transport (and heating behaviour) in the future. Regarding commuting, almost three-quarters of respondents wanted to travel to work in the future either by public transport or active travel (walking, cycling). This is a substantial change compared to their stated present modes of transport for commuting, where only 54%

rely solely on public transport or active travel. For the rest, 29% presently commute by car all the time, 17% use a mix of conventional car and other modes (public transport or active travel). This increase in interest in less polluting transport came from those who solely rely on a car for their commute, as well as from those who already used a mix of transport modes. 20% of the respondents who currently only commuted by car (85 respondents in total) stated they would like to use at least some public transport, active travel or “cleaner” vehicle. Asked for reasons why they presently felt unable to change, the most commonly stated reason was poor public transport, need for flexibility or convenience, required for work and other perceived constraints such as cost and safety (Figure 2).

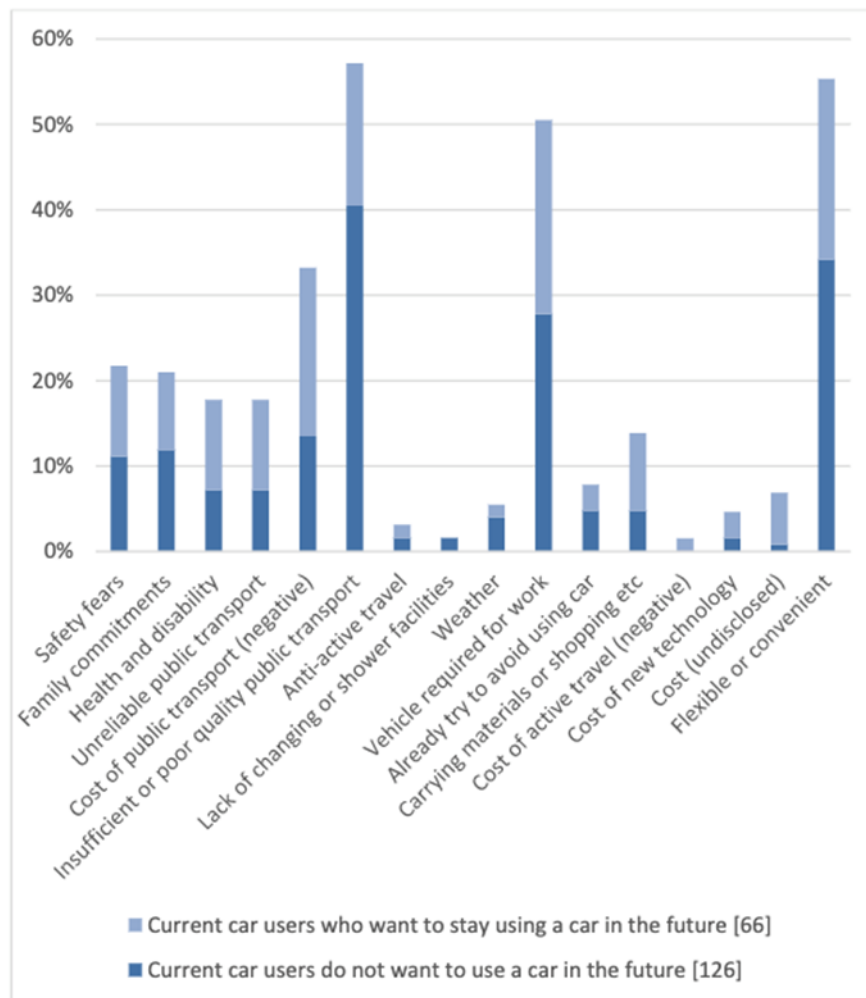


Figure 2. Reasons why car used feel they cannot or do not want to change their mode of comment in Bristol (Boushel et al., 2018)

3.3. Source Apportionment Data

The source apportionment data illustrates transport emissions of NO_x for the Bristol population. The data is primarily presented as mode choice and trip motive/behaviour (Figure 3) but can be further disaggregated to explore the impact of gender, age, income, car ownership and time of day on the total emissions. Freight emissions, which account for 30% of the total emissions, are not included in this data as we are primarily concerned with the direct influence of citizen behaviour.

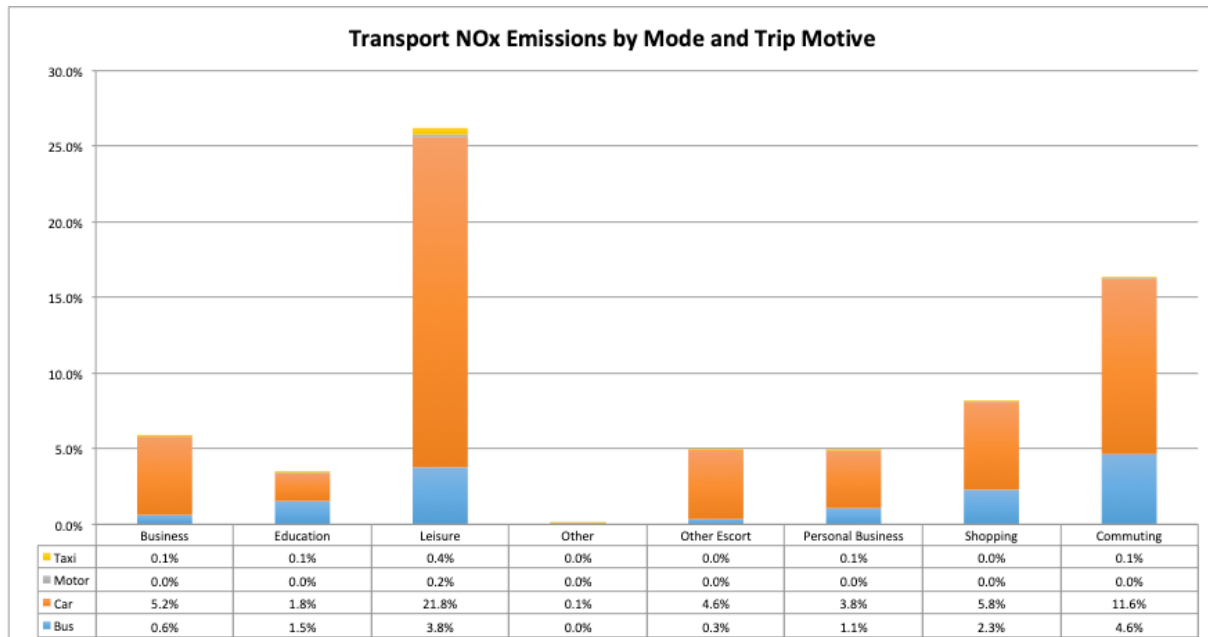


Figure 3. Source apportionment of NO_x emissions from transport in Bristol

3.3.1. Impact of Trip Motive

Traditional air quality management policies are often orientated to addressing commuter traffic (i.e. the morning and afternoon peak congestion) to reduce ambient NO₂ concentrations. The source apportionment data indicates that while commuting by car has a substantial influence, it is actually the use of the car for leisure purposes that has the highest impact on NO_x emissions. Using the car for leisure, commuting, shopping and business purposes dominates the NO_x emission profile for the city. From a behaviour perspective, if a city's air pollution challenge is related to a long term objective (e.g. annual mean) rather than a short term objective (e.g. 1-hour) then a city air quality management focus must include enabling policies and mechanisms that can influence leisure and shopping in addition to commuting and business motives.

3.3.2. Impact of Gender

When the source apportionment data is disaggregated by gender (i.e. male v female) we find that males are responsible for 6% more of the transport NO_x emissions than females (38% and 32% respectively). However, these emission differences are not evenly distributed across the modes and trip motives. Males are responsible for more emissions from 'Business' and 'Commuting' activities ('Business' = M:4.4% v F:1.5% and 'Commuting' = M:10.5% v F:5.7%), while females are responsible for more emissions from 'Education', 'Shopping' and 'Leisure' activities ('Education' = M:1.6% v F:1.9%; 'Shopping' = M:3.4% v F:4.7%; and 'Leisure' = M:13% v F:13.2% respectively). Additionally, males, proportionally, used the car more than public transport for all trip motives and females walk and cycle less than males. There may be a number of reasons for this such as the need for more travel flexibility, family responsibilities, road safety concerns etc. but these gender differences and concerns must be considered when cities are implementing policies and through targeted communication and awareness raising activities to recognise that 'one size does not fit all'.

3.3.3. Impact of Income

When the source apportionment data is disaggregated by income (i.e. three categories: <£25k, £25-50k and >£50k), the data shows that there is an impact of income on the generation of transport NO_x emissions - citizens within the higher income category generate more emissions than those in the lower income category. This finding is also supported by other UK air quality and socio-economic status studies (Brunt et al., 2017; Barnes et al., 2019). For example, citizens earning <£25k generate 13% of



the NO_x emissions by car compared to 19.3% and 22.4% for people earning £25-50 and >£50k respectively. It is also noticeable that people earning <£25k are also those most making greater use of the cheaper travel option such as the bus and active travel options but least use of the train. This illustrates that socio-economic factors and the ability of citizens to adapt to policies must be taken into consideration – this has been a central concern with the implementation of Clean Air Zones in the UK.

4. Conclusions

By bringing a behaviour and social science dimension to the subject area, not only in terms of quantification but also in terms of citizen engagement, we can better represent how citizens see their own lives and can also make it more amenable to representing the significant societal changes and scenarios that are likely to occur. Innovative and immersive engagement platforms, such as the ClairCity Skylines Game, provide a mechanism for citizens to choose solutions while considering not only the personal impact but also to understand the aggregated impacts of their actions at the city level. By putting citizens and their activities at the heart of the debate, the quantification and engagement process goes beyond the traditional attempts to communicate air pollution in terms of ambient concentrations, whilst ensuring that the emphasis is placed on the actual health impacts of pollution on people themselves. In addition to making the information more salient, stronger links can be made to the other negative, non-air quality/carbon, impacts related to relevant activities (such as noise, road safety, community separation etc.), and therefore place these issues and develop scenarios within the bigger picture of overall quality of life.

The ClairCity project creates the evidence to stimulate discussion and engage citizens in a democratic debate about how their cities develop in a manner that protects the local and global environments and puts citizen health and well-being at the heart of policymaking. Through the implementation of innovative and impactful toolkits and methodological approaches, ClairCity has given a voice to citizens and has enabled a new level of comprehensive and in-depth citizen and stakeholder engagement at the city scale, supported by scientifically robust quantitative and policy data and leading to a step change in democratic participation in environmental policymaking.

5. References

Bailey, R., Longhurst, J., Hayes, E., Hudson, L., Ragnarsdottir, K. V., Thumim, J., 2012. Exploring a city's potential low carbon futures using Delphi methods: some preliminary findings. *Journal of Environmental Planning and Management* 55, 1022-1046.

Barnes, J., Chatterton, T., Longhurst, J., 2019, Emissions vs exposure: Increasing injustice from road traffic-related air pollution in the United Kingdom. *Transportation Research Part D: Transport and Environment* 73, 56-66.

Boushel, C., Barnes, J., Chatterton, T., Devito, L., Edwards, A., Rogers, L. F., Leach, M., Prestwood, E., Hayes, E., 2018. "Unfortunately, I use my car": Commuter transport choices in Bristol, UK, *Air Pollution XXVI*, WIT Press, 230, 243-252.

Brunt, H., Barnes, J., Jones, S., Longhurst, J., Scally, G., & Hayes, E., 2017. Air pollution, deprivation and health: Understanding relationships to add value to local air quality management policy and practice in Wales, UK. *Journal of Public Health* 39, 485-497.

Brunt, H., Barnes, J., Longhurst, J., Scally, G., Hayes, E., 2018. Enhancing local air quality management to maximise public health integration, collaboration and impact in Wales, UK: A Delphi study. *Environmental Science and Policy*, 80, 105-116.



CCC (Committee on Climate Change), 2019. Net Zero Technical Report, London, 304 pages.

Dalkey, N. & Helmer, D., 1963, Delphi technique: characteristics and sequence model to the use of experts. *Management Science* 9, 458–467.

EEA (European Environment Agency), 2018a. Unequal exposure and unequal impacts: social vulnerability to air pollution, noise and extreme temperatures in Europe, EEA Report No. 22/2018, Copenhagen, 102 pages.

EEA (European Environment Agency), 2018b. Air quality in Europe – 2018 report, EEA Report No. 12/2018, Copenhagen, 88 pages.

Hayes, E., King, A., Callum, A., Williams, B., Vanherle, K., Boushel, C., Barnes, J., Chatterton, T., Bolscher, H., Csobod, E., Rogers, L. F., Slingerland, S., Longhurst, J., 2018. ClairCity project: Citizen-led scenarios to improve air quality in European cities. *Air Pollution XXVI*, WIT Press, 230, 233-241.

HM Government, 2018, National Travel Survey 2018 Technical Report, Department for Transport, London, 291 pages.

Acknowledgments

This project has received funding from the European Union’s Horizon 2020 research and innovation programme under grant agreement No. 689289. The authors wish to acknowledge the input and support of the wider ClairCity consortium partners and the input from the thousands of European citizens that participated.

Emergency interventions and air pollution in Slavonski Brod, Croatia

Ante Cvitković^{1,2,3}, Vesna Ćosić³ and Marijana Valjetic¹

¹Institute of Public Health Brod Posavina County, Croatia

²Josip Juraj Strossmayer University of Osijek Faculty of Medicine, Croatia

³Josip Juraj Strossmayer University of Osijek Faculty of Dental Medicine and Health, Croatia

ante.cvitkovic@sb.t-com.hr

Abstract. A great risk for global health, recognized by governments, institutions and citizens, is air pollution. Short term and long-term exposure to air pollutants have different health effects. The purpose of this research is to determine whether particulate matter up to 10 µm in size (PM₁₀), particulate matter up to 2.5 µm in size (PM_{2.5}), hydrogen sulphide (H₂S) and meteorological parameters have impact on frequency of urgent interventions in ERs (Institute of Emergency Medicine of Brod-Posavina County and Integrated Emergency Hospital Admission). The observed period is between January 1 and August 31, 2018, in the area of Slavonski Brod (Croatia). Data were collected from four sources: Institute of Emergency Medicine of Brod-Posavina County (Croatia), Integrated Emergency Hospital Admission, Meteorological and Hydrological Service data and Croatian Agency for Environment and Nature. All diseases were included in the analysis. Meteorological and air quality data were added to each day. During the observed period, 40041 interventions in ERs were recorded. Weak but statistically significant positive correlation was established between maximum temperatures (correlation coefficient 0.202; p 0.002), PM₁₀ (correlation coefficient 0.1293; p 0.048), PM_{2.5} (correlation coefficient 0.147; p 0.036) and H₂S (correlation coefficient 0.141; p 0.035) with the number of interventions in ERs. The correlation of mean relative humidity was statistically significant but negative (correlation coefficient -0.172; p 0.007). Connection between minimum and mean pressure values was not established. These results point to the importance of reducing air pollution in Slavonski Brod.

Keywords: Air pollution, Emergency interventions, Hydrogen sulphide, Particulate matters, Slavonski Brod.

1. Introduction

Air pollution is a major health risk to global health, recognized by governments, institutions and citizens (WHO Regional Office for Europe, 2017). The health effects range from increased hospital admissions and emergency room visits, to increased risk of premature death. An estimated 4.2 million premature deaths globally are linked to ambient air pollution, mainly from heart disease, stroke, chronic obstructive pulmonary disease, lung cancer, and acute respiratory infections in children. (WHO, 2019). Pollutants have short-term and long-term effects on human health (WHO Regional Office for Europe, 2013a). Particulate matter up to 10 µm in size (PM₁₀) and particulate matter up to 2.5 µm in size (PM_{2.5}) pass through the respiratory system when inhaled (WHO Regional Office for Europe, 2013b). They can affect human health in both the short-term (hours, days) and long-term (months, years) exposure and can cause: respiratory and cardiovascular morbidity, such as aggravation of asthma, respiratory symptoms and an increase in hospital admissions; mortality from cardiovascular and respiratory diseases and from lung

cancer. PM_{2.5} is a stronger risk factor than the coarse part of PM₁₀ (WHO Regional Office for Europe, 2013b). All-cause daily mortality is estimated to increase by 0.2–0.6% per 10 µg/m³ of PM₁₀. Long-term exposure to PM_{2.5} is associated with an increase in the long-term risk of cardiopulmonary mortality by 6–13% per 10 µg/m³ of PM_{2.5}. Susceptible groups with pre-existing lung or heart disease, as well as elderly people and children, are particularly vulnerable (WHO Regional Office for Europe, 2013b). Hydrogen sulphide is annoying with its smell (WHO, 2003). Long-term exposure to low concentrations of hydrogen sulphide is not completely investigated. (Jaakkola et al., 1990).

Emergency admissions for ischemic heart disease and heart rhythm disturbances were significantly associated with PM₁₀, PM_{2.5}, and NO₂ exposures the week before admission (Devos et al., 2015). Annual reports on air quality in Slavonski Brod, Croatia, show that the atmosphere is polluted with H₂S, PM₁₀ and PM_{2.5} in 2018 (Hrvatska agencija za okoliš i prirodu, 2016). A similar situation was in previous years (Agencija za zaštitu okoliša, 2019).

2. Aim

The aim of this paper is to determine the influence of high concentrations of particulate matters and hydrogen sulphide on the number of emergency interventions.

3. Methods

The analysis was conducted on data regarding Slavonski Brod (Croatia) from January 1st to August 31st 2018 obtained from:

1. Institute of Emergency Medicine of Brod-Posavina County (Croatia) (Croatian acronym ŽZHМ) –emergency medical services interventions in Slavonski Brod (field interventions as well as patients' visits to emergency clinic)
2. Integrated Emergency Hospital Admission - General Hospital Slavonski Brod - patients' visit and interventions (Croatian acronym OHBP)
3. Meteorological and Hydrological Service data (Croatian acronym DHMZ)-data of the temperature per day, pressure and relative humidity
4. Environmental Protection Agency (Croatian acronym HAOP) data regarding air quality for PM_{2.5}, PM₁₀ and H₂S per day from two measuring stations (SL1 and SL2) per day.

OHBP data and data from ŽZHМ were added together and observed in two ways: 1) sum of interventions/visits per day without clearing duplicate records and 2) sum of patients per day (interventions/visits with more than one appearance in ŽZHМ and/or OHBP per patient per day are excluded). Corresponding meteorological data and data on air quality were added to each day. In accordance with the law of The Republic of Croatia and EU Directive on ambient air quality and cleaner air for Europe (2008/50/EC) the limits for H₂S, PM_{2.5} and PM₁₀ were determined. The concentrations of PM_{2.5}, PM₁₀ and H₂S were also analysed depending on the limit values (25 µg/m³ for PM_{2.5}, 50 µg/m³ for PM₁₀ and 5 µg/m³ for H₂S).

According to data distribution, numeric variables were described in the central values and dispersion measure. Continuous variables were tested for normal distribution by Shapiro-Wilks's/Kolmogorov-Smirnov-test. For testing the direction and strength of the association between variables, Spearman correlation coefficient was used. The difference of continuous variables between the two groups was analysed by Mann-Whitney Wilcoxon test. MS Excel and SPSS 23 program package were used for data processing. Ethics Committee of the Croatian Institute of Public Health gave the approval no. 80-436 /1-16 to conduct the research.

4. Results

Total number of interventions analysed was 40041 and total number of patients analysed was 36 501. At OHBP, it was registered 27635 patient visits and total number of interventions in that period was 30220.

Total number of patients analysed was 8866 and total number of medical interventions was 9821 at emergency medical services interventions (ŽZHM). Frequencies of total interventions/visits and distribution for interventions carried out at ŽZHM and OHBP are shown in Table 1. Measures of central tendency and variables dispersion are shown in Table 1.

Table1. Measures of central tendency and variables dispersion

Variable	N		Mean	Median	Std. Dev.	Min	Max
	Valid	Missing					
N_Intervention_ŽZHM	243	0	40.42	40.00	9.95	18.00	73.00
N_Intervention_OHBP	243	0	124.36	123.00	15.93	93.00	171.00
N_patient_Day_ŽZHM	243	0	36.49	36.00	9.15	17.00	68.00
N_patient_Day_OHBP	243	0	113.72	113.00	14.54	83.00	156.00
N_Intervention	243	0	164.78	164.00	21.94	118.00	226.00
N_patient_Day	243	0	150.21	150.00	18.64	111.00	202.00
Temp min	243	0	8.34	10.40	7.84	-17.40	20.00
Temp max	243	0	19.79	23.30	10.53	-5.20	33.60
Pressure_medium	243	0	1003.35	1003.60	5.81	984.60	1023.50
Relative humidity_Medium	243	0	74.93	75.00	10.48	44.00	96.00
SL1_PM _{2.5} µg/m ³	205	38	38.32	27.83	31.96	3.26	193.35
SL2_PM _{2.5} µg/m ³	241	2	22.71	14.21	22.86	0.85	130.36
SL1_PM ₁₀ µg/m ³	240	3	35.71	25.39	30.12	5.04	184.76
SL2_PM ₁₀ µg/m ³	235	8	29.44	22.69	20.97	7.11	124.18
SL1_H ₂ S µg/m ³	228	15	0.81	0.64	0.71	-0.04	5.31
SL2_H ₂ S µg/m ³	214	29	1.98	1.80	1.17	0.20	9.11

The values at the measurement station SL1 in 34.16% were within the limit values for PM_{2.5}, in 77.37% for PM₁₀ and in 93% for H₂S, while at the station SL2, values were within the recommended range in 71.60% for PM_{2.5}, in 83.13% for PM₁₀ and in 86.42% for H₂S. The share of days for which measurements were not recorded at the measuring station SL1 for PM_{2.5} and PM₁₀ is 15.64% and 1.23%, while the share of H₂S days for which measurements are not recorded is 6.17%. The share of days for which measurements were not recorded at the measuring station SL2 for PM_{2.5} and PM₁₀ is 0.82% and 3.29%, while the share of H₂S days for which measurements are not recorded is 11.93%.

In Table 2 there is the correlation between the number of interventions/visit and environmental variables (meteorological data and data on PM_{2.5}, PM₁₀ and H₂S), and the significant correlation with the level of significance of 5% (p < 0.05).

Table 2. The correlation between the number of interventions/visit and environmental variables

	Number of patients per day	p	Number of interventions per day	p
	Correlation coefficient		Correlation coefficient	
Relative humidity medium	-0.191	0.003	-0.172	0.007
Temp _{min}	0.030	0.644	0.090	0.161
Temp _{max}	0.157	0.014	0.202	0.002
Pressure medium	0.006	0.922	-0.018	0.783
SL1_PM _{2.5}	0.186	0.007	0.147	0.036
SL2_PM _{2.5}	0.117	0.069	0.050	0.437
SL1_PM ₁₀	0.147	0.023	0.088	0.176
SL2_PM ₁₀	0.183	0.005	0.129	0.048
SL1_H ₂ S	0.093	0.163	0.141	0.034
SL2_H ₂ S	0.098	0.152	0.149	0.030

5. Discussion

The results of air contaminated with particulate matters and hydrogen sulphide in Slavonski Brod do not show any difference compared to previous years. According to the Croatian legislation, the air in Slavonski Brod is still in the second category for particulate matters and hydrogen sulphide. The first category means the air is unpolluted and the second category means the air is polluted. The PM₁₀, PM_{2.5} and H₂S values reached high concentrations (maximum 184 µg/m³, 193 µg/m³, 9 µg/m³). At the measuring station SL1, there was significant weak positive correlation between PM_{2.5} and PM₁₀ and the number of patients per day. Positive correlation was also determined between PM_{2.5} concentrations on SL1 and the number of emergency interventions as well as between PM₁₀ concentrations on SL2 and the number of patients/number of interventions. Positive correlation between H₂S concentrations and the number of intervention per day was determined for both measuring stations (SL1 and SL2).

Results of this study for 2016, show weak but statistically significant positive correlation between PM₁₀ (correlation coefficient 0.103; p 0.043) and PM_{2.5} (correlation coefficient 0.106; p 0.043) with the number of interventions in ERs. The correlation of mean relative humidity was statistically significant but negative (correlation coefficient -0.109; p 0.038). Connection between minimum and maximum temperature, H₂S and mean pressure values was not established (Cvitković et al., 2018). Positive correlation with maximum temperature and the number of interventions/number of patients is also established in 2018. The results for 2017 show different situation (unpublished date).

The connection of meteorological parameters and air pollution with emergency interventions due to cardiovascular disease was established in Zagreb (Pintarić et al., 2016). The authors found a statistically significant correlation between the number of aggravated chronic obstructive pulmonary disease in adults and the total suspended particles concentrations on the previous day (Pavlović et al., 1997). Among other results, the occurrence of respiratory diseases showed positive Spearman's correlation with the values of air humidity, PM₁₀ and negative correlation with the values of air temperature and pressure. The occurrence of respiratory diseases showed correlation with weather conditions and air pollutants despite the legally permitted values in the region with a humid continental climate [21 days before (r=0.08) ED admission (p<0.05 all) (Knezović et al., 2017). Our research has shown a negative correlation between mean relative humidity and number of interventions per day. Negative correlation was established between mean relative humidity and number of patients per day also.

Maximum, minimum, and mean temperatures were associated similarly with the number of hospitalization (Almagro et al, 2015). Our study showed no association between minimum temperature and pressure with the number of interventions and the number of patients.

The emergency health service in Croatia is organized through a system of emergency clinic and the Integrated Emergency Hospital Admission. Connections with high concentrations of PM_{2.5} and PM₁₀ and emergency interventions were established although the specific reason for patients' emergency visit was not analysed. The results obtained in the study can and should be used for further recommendations and researches that would help the general public in cases when the concentrations of pollutants exceed established threshold or guideline limit values.

Considering constraints (lack of data on residence) and specifics of the sample (the domain of emergency medicine and the logging of visits), test strength and generalisation of conclusions on for the entire population of Slavonski Brod can be limited.

6. Conclusion

The study found a correlation between the maximum temperature and the relative air humidity with the number of patients per day who needed intervention. For temperature, the correlation was positive, and for relative humidity, it was negative. At SL1 station, a weak positive correlation between PM_{2.5} and the number of patients per day/number of interventions per day was determined as well as statistically significant weak positive correlation between PM₁₀ and the number of patients per day and between H₂S and the number of interventions per day. At SL2 station, statistically significant weak positive correlation between PM₁₀ and the number of patients per day/number of interventions per day as well as statistically significant weak positive correlation between H₂S and the number of interventions per day were determined. The correlation was positive, that is, the number of patients per day/number of interventions per day increased as the measuring parameters grew. The established positive relationship is consistent with theoretical assumptions.

It is necessary to continue carrying out further studies, jointly interpret the results of complementary studies and further analyse other parameters, indicators of present pollution.

7. References

- Agencija za zaštitu okoliša, 2019. Godišnja izvješća o praćenju kvalitete zraka na području Republike Hrvatske. Zagreb, Online. <http://iszz.azo.hr/iskzl/godizvrpt.htm?pid=0&t=0> accessed in 14 Sep 2019.
- Almagro P, Hernandez C, Martinez-Cambor P, Tresserras R, Escarrabill J, Seasonality, ambient temperatures and hospitalizations for acute exacerbation of COPD: a population-based study in a metropolitan area. *Environ Res* 2015; 140:554-61, doi: 10.1016/j.envres.2015.05.005.
- Cvitković Ante, Barišin Andreja, Capak Krunoslav, Ivić-Hofman Igor, Vidić Igor, Poljak vedran, Valjetic Marijana. Descriptive analysis of urgent medical interventions based on air pollution in Slavonski Brod, Croatia. *Ecology and Environment* (1743-3541) 230 (2018); 549-556.
- Devos, S., Cox, B., Dhondt, S., Nawrot, T., Putman, K. Cost saving potential in cardiovascular hospital costs due to reduction in air pollution. *Sci Total Environ*, 527-528:413-9. doi: 10.1016/j.scitotenv.2015.04.104,2015.
- Hrvatska agencija za okoliš i prirodu, 2016. Godišnje izvješće za praćenje kvalitete zraka na području Republike Hrvatske za 2015. godinu. Zagreb. <http://iszz.azo.hr/iskzl/datoteka?id=31863>, accessed in 14 Sep 2019.



Jaakkola, J., J., Vilkkka, V., Marttila, O., Jäppinen, P., Haahtela, T., 1990. The South Karelia Air Pollution Study. The effects of malodorous sulfur compounds from pulp mills on respiratory and other symptoms. *The American Review of Respiratory Disease*, 142(6 Pt 1), 1344-1350.

Knezović, M., Pintarić, S., Jelavić, M.M., Neseck, V., Krstačić, G., Vrsalović, M., Šikić, A., Zeljković, I., Pintarić, H., 2017. Correlation between concentration of air pollutants and occurrence of cardiac arrhythmias in a region with humid continental climate. *Acta Clin Croat.*, 56(1):3-9.

Pavlović, M., Simić, D., Hrsak, J., 1997. Emergency cases of chronic obstructive pulmonary disease (COPD) in adults and air pollution in Zagreb. *Arh Hig Rada Toksikol*, 48(4):365-71.

Pintarić, S., Zeljkovic, I., Pehneck, G., Neseck, V., Vrsalović, M., Pintarić, H., 2016 Impact of meteorological parameters and air pollution on emergency department visits for cardiovascular diseases in the city of Zagreb, Croatia. *Arh Hig Rada Toksikol*; 67(3):240-246, doi: 10.1515/aiht-2016-67-2770

WHO, 2019. <https://www.who.int/airpollution/ambient/health-impacts/en/>, accessed in 14.Sep 2019.

WHO, 2003. Hydrogen sulfide: Human health aspects. (Concise International Chemical Assessment Document 53).Geneva. <http://www.who.int/ipcs/publications/cicad/en/cicad53.pdf>, accessed in 14 Sep 2019.

WHO Regional Office for Europe, 2017. Evolution of WHO air quality guidelines: past, present and future. Copenhagen. www.euro.who.int/data/assets/pdf_file/0019/331660/Evolution-air-quality.pdf?ua=1, accessed in 14 Sep 2019.

WHO Regional Office for Europe, 2013a. Review of evidence on health aspects of air pollution – REVIHAAPP Project: Technical Report. Copenhagen. http://www.euro.who.int/__data/assets/pdf_file/0004/193108/REVIHAAP-Final-technical-report-final-version.pdf?ua=1, accessed in 14 Sept, 2019.

WHO Regional Office for Europe, 2013b. Health effects of particulate matter. Policy implications for countries in Eastern Europe, Caucasus and central Asia (2013). http://www.euro.who.int/__data/assets/pdf_file/0006/189051/Health-effects-of-particulate-matter-final-Eng.pdf?ua=1, accessed in 14 Sep 2019.

Acknowledgements

I would like to express my deep gratitude to Mr. Marko Brkić from The Croatian Institute of Public Health who did the statistics. Results shown in this study are a part of Study of impact of environmental factors on human health which is financed by Ministry of Health of the Republic of Croatia.

Intraday and interday variations of 69 volatile organic compounds (BVOCs and AVOCs) and their source profiles at a semi-urban site

Serpil YenisoY Karakas¹, Melike Dörter^{1,2} and Mustafa Odabasi³

¹Department of Chemistry, Bolu Abant İzzet Baysal University, Bolu

²Present address: Department of Pharmacy Services, Yuksek İhtisas University, Ankara

³Department of Environmental Engineering, Dokuz Eylül University, İzmir

yenisoykarakas_s@ibu.edu.tr

Abstract. Atmosphere includes numerous volatile organic compounds (VOCs) which have biogenic and/or anthropogenic origin. VOCs may have adverse effects on human health and ecosystem. The main objective of this study was to examine concentrations, temporal variations and possible sources of VOCs. VOCs were collected in April, in May, in June, in July, in August 2017 and in January 2018 on Tenax-TA sampling tubes using a Perkin Elmer STS25 sequential tube sampler in the Bolu Abant İzzet Baysal University Campus. Daily active sampling was performed for a period of eight days for a month whereas hourly samples were collected every six hours for two days a month. Thermal Desorption Gas Chromatography Mass Spectrometry (TD-GC-MS) system was used in analysis of the samples. Totally 69 VOCs having biogenic (i.e., isoprene, monoterpenes and oxygenated VOCs) and anthropogenic origins were investigated. Biogenic VOC levels and detection frequencies were found to be higher in May, June, July and August when temperature and solar intensity increased, compared to those observed in January and in April. Decanal, benzaldehyde, benzene, phenol and toluene were the anthropogenic VOCs with higher concentrations while alpha-pinene and hexanal were the dominant biogenic compounds. Intraday variations showed that vehicle traffic during working hours lead to increase in VOC levels. Ozone formation potential of isoprene, benzene, toluene, ethylbenzene, m+p xylene, o-xylene, isopropylbenzene, n-propylbenzene, m-ethyltoluene, p-ethyltoluene, 1,2,4-trimethyl benzene, o-ethyltoluene, 1,3,5-trimethylbenzene, gamma-terpinene, dodecane, camphor and naphthalene were found to be significant. As a result of Positive Matrix Factorization (PMF) analyses; solvent evaporation, gasoline-powered vehicle emissions, fossil fuel (residential heating), biogenic (hornbeam, grass, oak, beech), diesel/domestic activities and forested city atmosphere were determined as the main VOC sources. G-score graphs and G-score pollution roses were also used to support the source apportionment.

Keywords: Temporal variations, Anthropogenic VOCs, Biogenic VOCs, Source apportionment, Positive matrix factorization.

1. Introduction

Volatile organic compounds (VOCs) represent a key class of atmospheric pollutants. They have negative impacts, such as stratospheric ozone depletion, tropospheric photochemical ozone (O₃) formation, toxic and carcinogenic human health effects, and enhancement of the global greenhouse effect (Jobson et al., 2004; Ann et al., 2014). It is important to identify concentrations, sources and behaviors of these pollutants. Sources of VOCs can be mainly categorized as emissions from biogenic and anthropogenic

activities. It is asserted that the emissions of biogenic volatile organic compounds (BVOCs) is higher than the anthropogenic volatile organic compounds (AVOCs) on the global scale (Zimmerman, 1979; Lamb et al., 1987; Guenther et al., 1995).

This paper aims to investigate atmospheric VOCs with respect to temporal variability, possible sources and relationship with ozone formation in a semi-urban site. VOCs include hundreds of compounds that differ greatly in source and reactivity. In this context, totally 69 VOCs having biogenic and anthropogenic origins were examined.

2. Materials and methods

2.1. Sampling program, collection and analysis

The study was conducted in Bolu city located in the Western Black Sea Region of Turkey in April, May, June, July, August 2017 and in January 2018. Bolu has a population of around 300000 and an average altitude of 1000 m. Samples were collected at the roof of Bolu Abant İzzet Baysal University rectory building (Figure 1). Bolu city center hosts a small number of industrial sectors including cement, poultry, woodworking, metal and glass (Bolu Environmental Status Report, 2016). Emissions from agricultural activities, vegetation and vehicles are expected to be important VOC sources. Oak, Oriental beech, Scots pine, Juniper, Fir and Hornbeam are the most abundant tree species in city.



Figure 1. The sampling location and sequential active sampler

VOCs were collected on Tenax-TA sampling tubes (Perkin Elmer, USA) using a Perkin Elmer STS-25 sequential tube sampler. Air was passed through the sampling tubes using a vacuum pump (Gilian, LFS 1130) at a flow rate of 250 ml min^{-1} . Daily active sampling was performed for a period of eight days a month whereas hourly samples were collected every six hours for two days a month. The conditioning was carried out at $320 \text{ }^\circ\text{C}$ for 60 minutes under high purity helium gas. The conditioned Tenax-TA tubes were stored in screw-capped falcon tubes with a pack of silica gel and an activated carbon to prevent the humidity and contamination problems, respectively. Following sampling, the samples were analyzed using Thermal Desorption Gas Chromatography Mass Spectrometry (TD-GC-MS, Shimadzu-QP2010SE) system. Hourly ozone and NO_x data were gathered with Environnement 42M O_3 Analyzer and Environnement AC31M NO_x Analyzer, respectively in the same sampling point.

2.2. Positive matrix factorization (PMF)

Positive matrix factorization (PMF) has been widely used as a multivariate factor analysis tool (Amarillo et al., 2017; Sakar et al., 2017; Ashrafi et al., 2018; Zhang et al., 2018). It reduces the large number of variables in complex data sets to combinations of species named source types and source contributions.

The model uses a matrix of speciated sample data into two matrices that are called factor contributions (G) and factor profiles (F) (Norris and Duvall, 2014). Two matrices are derived using the minimized objective function, Q, in the PMF:

$$Q = \sum_{i=1}^n \sum_{j=1}^m \left[\frac{x_{ij} - \sum_{k=1}^p g_{ik} f_{kj}}{u_{ij}} \right]$$

where x is the data matrix of i number of samples by j chemical species which were measured, and u is the uncertainties. PMF solves the problem iteratively and this minimizes the Q.

EPA PMF 5.0 was used to identify the source profiles of active VOCs. The data file contains the results of concentrations and uncertainties. For PMF analysis, a more comprehensive set of data was obtained by combining the concentration of all months of active sampling. Concentrations were substituted with the MDL/2 when concentrations are below the method detection limit (MDL) or there is a missing value. The uncertainty of these concentrations were calculated as: (5/6)xMDL. Other data in the uncertainty file was estimated based on the equation given by Norris et al. (2014):

$$u = \sqrt{((0.1) \times \text{concentration})^2 + (0.5 \times \text{MDL})^2}$$

Compounds having a signal to noise ratio below 0.5, data percentage below detection limit exceeding 30%, low R² values (less than 0.5) and compounds appearing in more than two groups, were not included in PMF analysis. Therefore, sources were explained with 6 factors. Q_{robust} and Q_{true} values were 1020 and 1029. Moreover, residual distributions were approximately symmetric within the range of -3 and +3 that represents a good agreement between the observed and predicted values. Samples that did not comply with these rules were excluded from the analysis.

3. Results and discussion

During entire active sampling period, 54 of 69 analyzed VOCs could be detected. Alpha-terpinene and beta-myrcene were detected only in 4 and 9 samples, respectively. Hexanal (2.535 µg m⁻³) and alpha-pinene (0.113 µg m⁻³) were the biogenic compounds with the higher atmospheric concentrations. Hexane (0.430 µg m⁻³) showed the highest concentration among the anthropogenic VOCs. Concentrations measured in this study are found to be smaller than those reported for urban and semi-urban areas (de Albuquerque et al., 2012; Fernandez-Villarrenaga et al., 2005; Wang et al., 2016; Yurdakul et al., 2013). When the present study compared with Lamas de Olo which is classified as mountainside and rural area, closer and higher results for some VOCs (benzene, ethylbenzene, o-xylene and alpha-pinene) were obtained (Evyugina et al., 2009).

3.1. Temporal variations of VOC concentrations

Concentrations and number of the detected compounds for biogenic VOCs were higher in May, June, July and August compared to January and April (Figure 2).

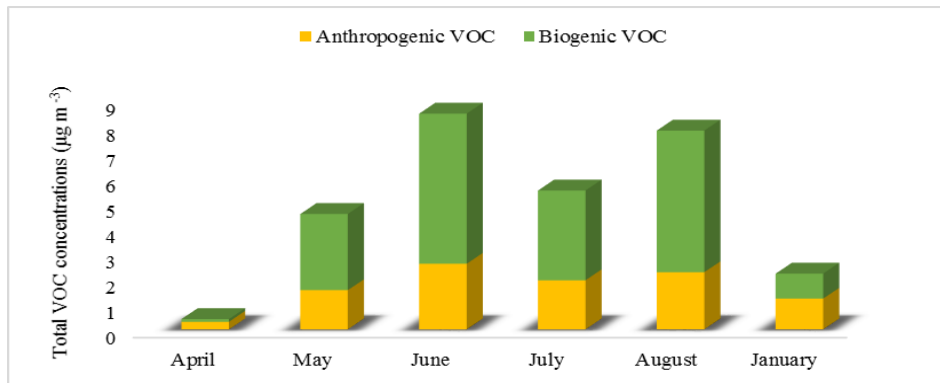


Figure 2. Monthly total VOC (anthropogenic and biogenic) variations

When the hourly changes of VOCs are examined, different trends have been observed (Figure 3). No significant hourly trend was found in April probably due to low VOC levels. In May and June, the highest VOC concentrations were measured during the 11:00-17:00 period when the temperature and the solar intensity were at their maximum. In July, the highest VOC level was detected in the 11:00-17:00 hour interval but there was no sharp difference between time intervals. Remarkably, the highest concentrations were found in August from 05:00 to 11:00. In January, the highest VOC concentrations were measured in the 11:00-17:00 time zone.

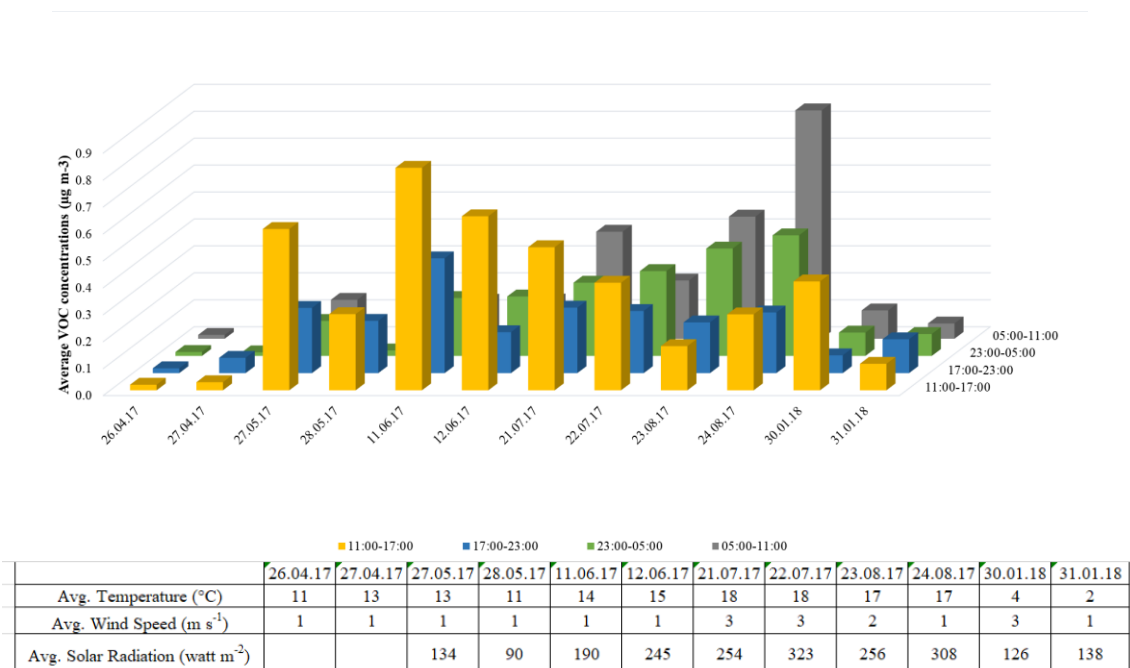


Figure 3. Hourly VOC variations

3.2. Ozone formation potential

In order to investigate the contribution of VOCs to the formation of ozone, statistical relationship between VOC and ozone was examined in Table 1. Both biogenic VOCs and anthropogenic VOCs were found to be related with ozone. It is thought that VOC-ozone negative correlations are seen as a result of the consumption of VOCs through the photochemical reactions. Hence, isoprene, benzene, toluene, ethylbenzene, m+p xylene, o-xylene, isopropylbenzene, n-propylbenzene, m-ethyltoluene, p-ethyltoluene, 1,2,4-trimethyl benzene, o-ethyltoluene, 1,3,5-trimethylbenzene, gamma-terpinene, dodecane, camphor and naphthalene were evaluated as effective VOCs in the ozone formation. Ozone

formation occurs in the presence of sufficient NO_x and VOCs. However, if there is insufficient NO_x in the atmosphere, this will cause the net ozone depletion and a decrease in both will be observed. This can be explained by positive correlations between NO_x and ozone. Assuming that the number of deciduous trees did not change between the examined months (except for January and April), it could be suggested that the NO_x level in the air was an important factor affecting the ozone formation in addition to the solar intensity and temperature.

Table 1. VOC - ozone correlations (p<0.05)

	January	April	May	June	July	August
Isoprene	-0.33	-0.54	-0.62	0.17	0.41	-0.56
Acrylonitrile	0.52					
n-Hexane	0.48	-0.19	-0.12	-0.06	-0.22	0.37
2-Methylfuran	-0.21	-0.61	-0.41	0.77	-0.44	-0.46
Chloroform	0.64	-0.14	-0.13	0.05	-0.25	0.33
Tetrachloromethane	-0.01	-0.07	0.09	0.82	-0.16	0.18
Benzene	-0.59	-0.80	-0.27	0.36	-0.06	-0.28
n-Heptane	-0.36	-0.46	-0.24	-0.12	-0.03	-0.44
Crotonaldehyde	-0.37	-0.45	-0.27	0.24	-0.04	-0.42
n-Octane	-0.19	-0.14	-0.33	-0.14	-0.05	-0.44
Toluene	-0.22	-0.75	0.59	0.36	-0.18	0.23
Hexanal	0.54	0.61	-0.06	0.44	-0.25	-0.26
Chlorobenzene	0.13		0.03	0.69	0.21	-0.12
Ethylbenzene	-0.09	-0.71	0.24	0.50	-0.10	0.20
m+p Xylene	0.08	-0.72	0.18	0.52	-0.09	0.15
o-Xylene	0.16	-0.69	0.11	0.59	-0.09	0.09
Styrene	0.30	-0.34	-0.07	0.55	0.05	0.05
1- Heptanal	0.29	0.53	-0.24	0.71	0.04	-0.17
Alpha-pinene	0.58	-0.43	0.13	0.35	-0.33	0.11
Isopropylbenzene	-0.17	-0.73	0.43	0.65	-0.15	-0.02
Camphene	0.45		-0.04	0.51	-0.22	-0.48
n-Propylbenzene	0.08	-0.66	-0.04	0.52	0.02	0.01
m-Ethyltoluene	-0.15	-0.66	0.10	0.44	0.09	-0.04
p-Ethyltoluene	-0.25	-0.69	-0.05	0.57	0.09	-0.08
Sabinene			0.06	0.40	0.03	-0.41
beta-Myrcene	0.21					
1,2,4-Trimethylbenzene	-0.16	-0.72	0.31	0.67	0.09	-0.06
beta-Pinene	0.29	-0.12	0.12	0.46	-0.21	-0.09
o-Ethyltoluene	-0.19	-0.72	0.37	0.48	0.07	-0.14
3-Carene	0.32		0.11	0.59	-0.08	0.11
1,3,5-Trimethylbenzene	-0.16	-0.69	0.30	0.57	0.14	-0.21
Benzaldehyde	-0.06	0.40	0.16	0.00	0.07	-0.15
Limonene	-0.36		0.09	0.44	-0.07	-0.02
m-Cymene	-0.45		-0.25	0.79	0.06	0.00
p-Cymene	-0.39	0.04	-0.13	0.68	0.19	-0.44

Table 1. Continued

	January	April	May	June	July	August
Eucalyptol	-0.27		-0.30	0.69	0.32	0.19
Ocimene					-0.26	-0.03
1,2,3-Trimethylbenzene	-0.20	-0.51	0.54	0.64	0.28	-0.29
gamma-Terpinene	-0.28		-0.11	0.32	0.23	-0.55
1,3-Diethylbenzene				0.63	-0.40	-0.46
1,4-Diethylbenzene	0.07		0.45	0.67	0.25	-0.29
Phenol	0.31	-0.60	-0.18	0.27	0.02	-0.41
Dihydromyrcenol	-0.15			0.29	-0.12	0.14
Nonanal	0.22	0.45	-0.21	0.63	0.22	-0.32
Acetophenone	-0.15	0.75	0.25	0.75	0.28	-0.53
L-Fenchone	0.24		-0.02	-0.26	0.10	-0.02
n-Dodecane	-0.25	0.00	0.42	0.17	0.36	-0.60
(+)-Camphor	0.09			-0.62	-0.09	-0.19
Decanal	-0.27	0.04	-0.44	0.23	-0.27	-0.09
Alpha-terpineol	0.63		-0.17	0.52	-0.22	-0.23
Naphthalene	-0.19	-0.73	0.40	0.41	0.23	-0.37
n-Tridecane	0.12	0.07	-0.06	0.17	0.25	-0.38
Benzothiazole	-0.25	0.40	0.54	0.37	0.59	-0.23
n-Tetradecane	0.07	0.38	0.18	0.33	0.24	

3.3. Source apportionment

The chemical profiles of the compounds and the literature data were used to identify each factor. Potential sources of VOCs were determined as solvent evaporation, gasoline-powered vehicle emissions, fossil fuel (residential heating), biogenic emission (hornbeam, grass, oak, beech), diesel/domestic activities, and forested city atmosphere. Contribution of sources to the total was 2.5%, 16%, 2.9%, 38.6%, 17.6% and 22.4%, respectively. The compounds explained at least 20% in the factor were given in Table 2.

Table 2. PMF results of VOCs determined in active sampling study (N = 44)

Factors	VOCs	Source
Factor 1	acetophenone, 1,4-diethylbenzene, phenol, 1,2,3-trimethylbenzene	Solvent evaporation
Factor 2	ethylbenzene, xylenes, benzene, toluene	Gasoline-powered vehicle emissions
Factor 3	isoprene, benzene, toluene	Fossil fuel (residential heating)
Factor 4	crotonaldehyde, heptanal, hexanal, nonanal, phenol, beta-pinene, chlorobenzene, decanal	Biogenic emission (hornbeam, /grass, /oak, /beech)
Factor 5	chlorobenzene, decanal, nonanal, naphthalene, tridecane, styrene, 1,3,5-trimethylbenzene, tetradecane, 1,2,3-trimethylbenzene, m-ethyltoluene, 1,2,4-trimethylbenzene, n-propylbenzene, p-cymene, o-ethyltoluene, 1,4-diethylbenzene, isoprene	Diesel/domestic activities (photocopy, plastic usage, wood and biomass combustion)
Factor 6	alpha-pinene, ethyltoluene, n-propylbenzene, 1,2,4-trimethylbenzene, 1,3,5-trimethylbenzene, tridecane, xylene, beta-pinene, 1,2,3-trimethylbenzene, phenol, ethylbenzene, styrene, 1,4-diethylbenzene, tetradecane, naphthalene, toluene, hexanal, p-cymene, acetophenone, heptanal	Forested city atmosphere

In the first factor, highly explained VOCs were acetophenone, 1,4-diethylbenzene, phenol and 1,2,3-triethylbenzene. According to the daily G-score variations, the highest G-score was observed on August 20, 2017 in Figure 4. South-East, West, South-West and West-South-West directions were dominant wind directions. Solvents used in the campus laboratories and even perfumes and other chemicals spread to the atmosphere were the possible effective (EPA, 2000) pollution sources.

Gasoline exhaust marker compounds ethylbenzene, m+p-xylene, o-xylene, benzene and toluene constitute the second factor (Yurdakul et al., 2013; Civan et al., 2015). The highest G-score value of the factor was determined on May 19, 2017 (Figure 4). The predominant G-score values from the West-South-West and South-West directions indicated that campus traffic was more effective. Thus, traffic emissions were identified as the second factor.

Factor 3 is fossil fuel (residential heating) factor. Liu (2008) stated that benzene and toluene which had high percentages in factors are caused by coal combustion. The highest G-score was found on 29 January 2018 (Figure 4). The contribution of residential heating factor increased in January as temperature decreased. The dominant wind sectors were East-North-East (residential areas near the city center) and the West (semi-rural settlements in the west of the campus).

Factor 4 explained the high proportion of crotonaldehyde, heptanal, hexanal, nonanal and beta-pinene. This represented biogenic emissions. On June 08 2017, the highest G-scores was found (Figure 4). Increased temperatures played an active role in the release of biogenic VOCs in warmer months. The air currents coming from the West-South-West (including the campus) reflected the influence of the hornbeam and oak trees that are dominant tree species in this region. Hornbeam is known to emit crotonaldehyde, alpha-pinene, beta-pinene and p-cymene to the atmosphere. Oak is the source of VOCs such as crotonaldehyde, 2-methylfuran, eucalyptol and hexanal (Aydın et al., 2014).

Factor 5 included VOCs that were emitted from the diesel and/or domestic activities (photocopy, plastic usage, wood and biomass combustion) (Dumanoglu et al., 2014; Civan et al., 2015). The highly explained VOCs were chlorobenzene, decanal, nonanal, naphthalene, tridecane, styrene, 1,3,5-trimethylbenzene, tetradecane, 1,2,3-trimethylbenzene, m-ethyltoluene, 1,2,4-trimethylbenzene, n-propylbenzene, p-cymene, o-ethyltoluene, 1,4-diethylbenzene and isoprene. The highest G-score value was determined on 17 August 2017. Dominant wind directions were from West-South-West and from South-West (Figure 4). These directions pointed to the campus and nearby villages.

VOCs representing the forested city atmosphere were gathered under Factor 6. According to G-score results, West-South-West was dominant and the highest value was found on July 11 2017 (Figure 4). Factor contained alpha-pinene, ethyltoluene, n-propylbenzene, 1,2,4-trimethylbenzene, 1,3,5-trimethylbenzene, tridecane, xylene, beta-pinene, 1,2,3-trimethylbenzene, phenol, ethylbenzene, styrene, 1,4-diethylbenzene, tetradecane, naphthalene, toluene, hexanal, acetophenone and heptanal.

4. Conclusions

The ambient VOC concentrations measured in the semi-urban site of Bolu in April, May, June, July, August 2017 and in January 2018, were used to investigate their temporal characteristics, effect on ozone formation and sources. Hexane, heptanal, alpha-pinene, hexanal and nonanal were found as the VOCs with higher atmospheric concentrations. There was a distinct seasonal variation in the VOC concentrations. In summer months, especially BVOCs were observed at higher levels. Although there was no sharp difference in VOC levels, the increase due to vehicle emissions during working hours was observed. Both anthropogenic and biogenic sources were found to be significant in the study area. Solvent evaporation, gasoline-powered vehicle emissions, fossil fuel (residential heating), biogenic emission (hornbeam, grass, oak, beech), diesel/domestic activities and forested city atmosphere were determined as the main VOC sources. Correlations between VOCs and ozone showed that isoprene,

benzene, toluene, ethylbenzene, m+p xylene, o-xylene, isopropylbenzene, n-propylbenzene, m-ethyltoluene, p-ethyltoluene, 1,2,4-trimethyl benzene, o-ethyltoluene, 1,3,5-trimethylbenzene, gamma-terpinene, dodecane, camphor and naphthalene were important contributors for ozone.

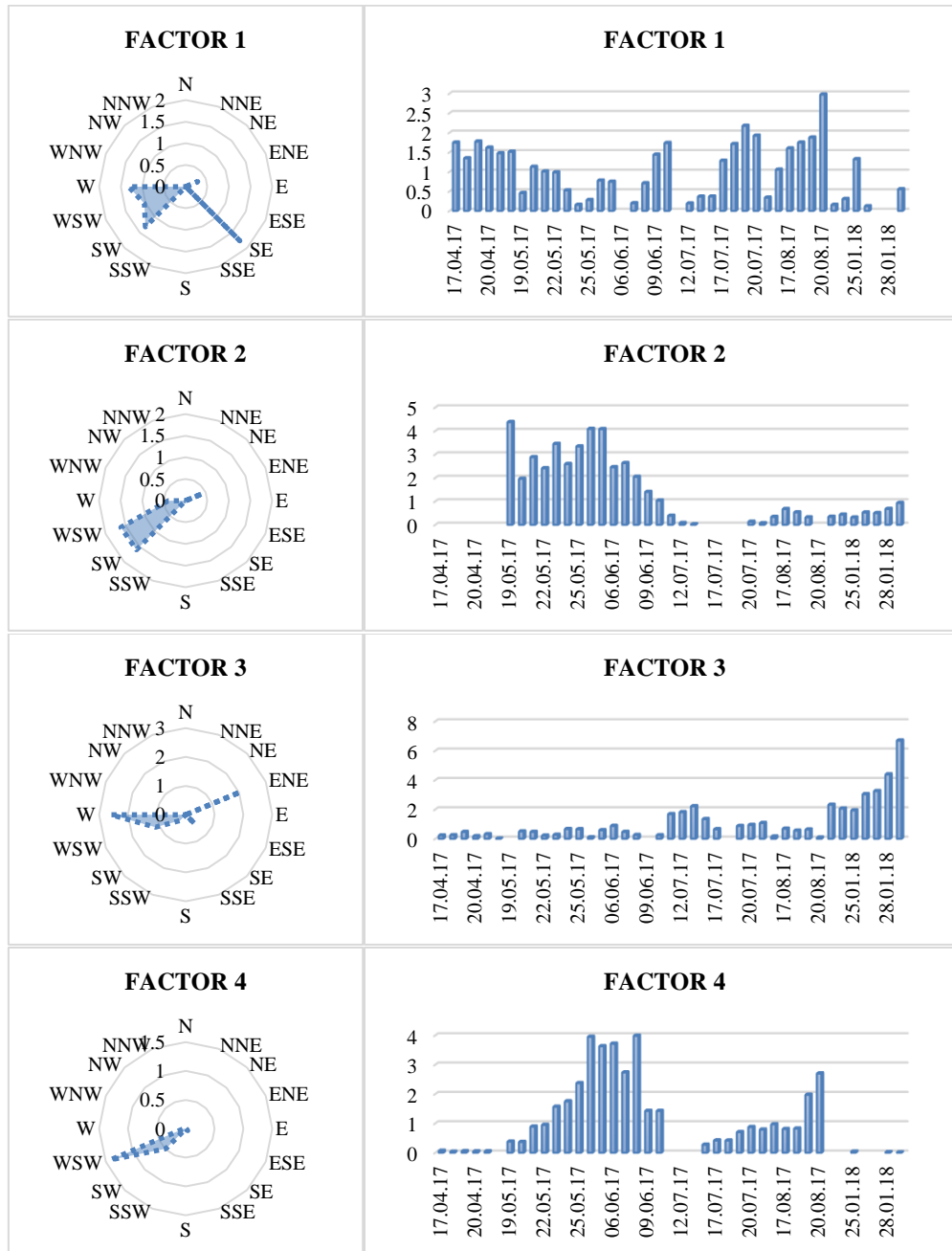


Figure 4. PMF results of factors (G-score daily changes and G-score pollution roses)

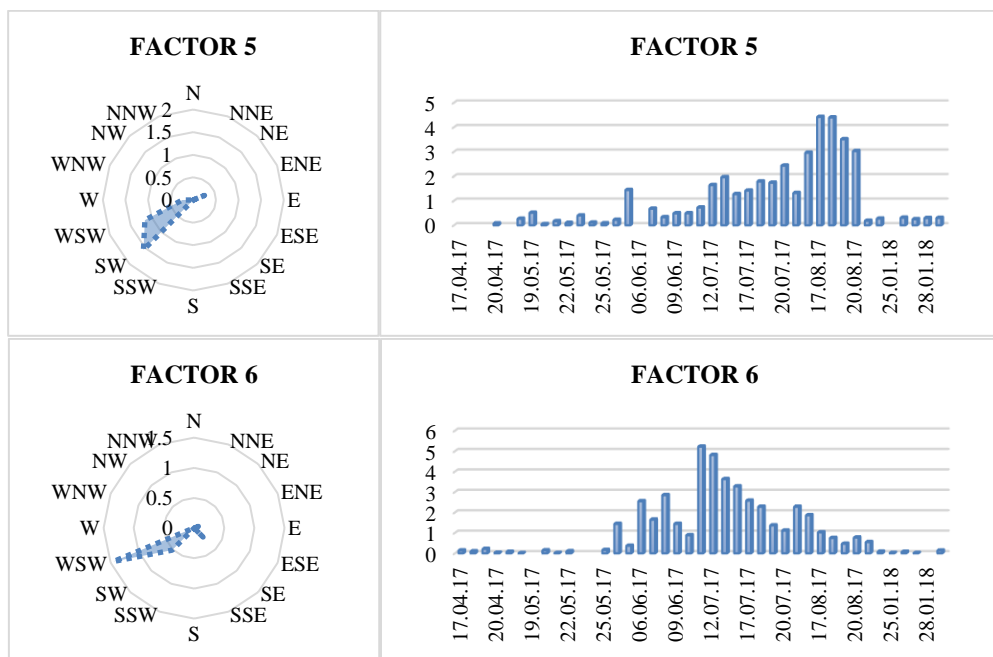


Figure 4. Continued

5. References

- Amarillo, A.C., Mateos, A.C., Carreras, H., 2017. Source apportionment of PM 10-bound polycyclic aromatic hydrocarbons by positive matrix factorization in Cordoba City, Argentina. *Arch. Environ. Con. Tox.* 72, 380-390.
- Ann, J., Zhu, B., Wang, H., Li, Y., Lin, X., Yang, H., 2014. Characteristics and source apportionment of VOCs measured in an industrial area of Nanjing, Yangtze River Delta, China. *Atmos. Environ.* 97, 206-214.
- Ashrafi, K., Fallah, R., Hadei, M., Yarahmadi, M., Shahsavani, A., 2018. Source Apportionment of Total Suspended Particles (TSP) by Positive Matrix Factorization (PMF) and Chemical Mass Balance (CMB) Modeling in Ahvaz, Iran. *Arch. Environ. Con. Tox.* 75, 278-294.
- Aydin, Y.M., Yaman, B., Koca, H., Dasdemir, O., Kara, M., Altiok, H., Dumanoğlu, Y., Bayram, A., Tolunay, D., Odabasi, M., Elbir, T., 2014. Biogenic Volatile Organic Compound (BVOC) Emissions from Forested Areas in Turkey: Determination of Specific Emission Rates for Thirty-one Tree Species. *Sci. Total. Environ.* 490, 239-253.
- Bolu Environmental Status Report, 2016. <http://www.bolukulturturizm.gov.tr/TR-70000/yedigoller-milli-parki.html>, accessed in 2019.
- Civan, M.Y., Elbir, T., Seyfioglu, R., Kuntasal, Ö.O., Bayram, A., Doğan, G., Yurdakul, S., Andiç, Ö., Müezzinoğlu, A., Sofuoğlu, S.C., Pekey, H., Pekey, B., Bozlaker, A., Odabasi, M., Tuncel, G., 2015. Spatial and temporal variations in atmospheric VOCs, NO₂, SO₂, and O₃ concentrations at a heavily industrialized region in Western Turkey, and assessment of the carcinogenic risk levels of benzene. *Atmos. Environ.* 103, 102-113.
- de Albuquerque, É.L., Tomaz, E., de Lima Tresmondi, A.C.C., 2012. VOCs Concentrations at Metropolitan Area of São Paulo, Brazil. In Proceedings of the Air and Waste Management Association's Annual Conference and Exhibition, AWMA.



Dumanoglu, Y., Kara, M., Altıok, H., Odabasi, M., Elbir, T., Bayram, A., 2014. Spatial and seasonal variation and source apportionment of volatile organic compounds (VOCs) in a heavily industrialized region. *Atmos. Environ.* 98, 168-178.

EPA, 2000 – Phenol (108-95-02) –Acetophenone (98-86-2)

Evtyugina, M. G., Nunes, T., Alves, C., Marques, M.C., 2009. Photochemical pollution in a rural mountainous area in the northeast of Portugal. *Atmos. Res.* 92, 151-158.

Fernández-Villarrenaga, V., López-Mahía, P., Muniategui-Lorenzo, S., Prada-Rodríguez, D., 2005. Possible influence of a gas station on volatile organic compound levels in the ambient air of an urban area. *Fresen. Environ. Bull.* 14, 368-372.

Guenther, A.B., Hewitt, C.N., Erickson, D., Fall, R., Geron, C., Graedel, T., Harley, P., Klinger, L., Lerdau, M., MacKay, W.A., Pierce, T., Scholes, B., Steinbrecher, R., Tallamraju, R., Taylor, J., Zimmerman, P.R., 1995. A global model of natural volatile organic compound emissions. *J. Geophys. Res.* 100, 8873-8892.

Jobson, B.T., Berkowitz, C.M., Kuster, W.C., Goldan, P.D., Williams, E., Fesenfeld, F.C., Apel, E.C., Karl, T., Lonneman, W.A., Riemer, D., 2004. Hydrocarbon source signatures in Houston, Texas: influence of the petrochemical industry. *J. Geophys. Res.* 109, 24305-24326.

Lamb, B., Guenther, A.B., Gay, D., Westberg, H., 1987. A national inventory of biogenic hydrocarbon emissions. *Atmos. Environ.* 21, 1695-1705.

Liu, Y., Shao, M., Fu, L., Lu, S., Zeng, L., Tang, D., 2008. Source profiles of volatile organic compounds (VOCs) measured in China: Part I. *Atmos. Environ.* 42, 6247-6260.

Norris, G., Duvall, R., 2014. EPA Positive Matrix Factorization (PMF) 5.0 Fundamentals and User Guide, U.S. Environmental Protection Agency Office of Research and Development Washington, DC 20460.

Norris, G.A., Duvall, R., Brown, S.G., Bai, S., 2014. EPA Positive Matrix Factorization (PMF) 5.0 fundamentals and User Guide Prepared for the US Environmental Protection Agency Office of Research and Development, Washington, DC.

Sarkar, C., Sinha, V., Sinha, B., Panday, A.K., Rupakheti, M., Lawrence, M.G., 2017. Source apportionment of NMVOCs in the Kathmandu Valley during the SusKat-ABC international field campaign using positive matrix factorization. *Atmos. Chem. Phys.* 17, 8129-8156.

Wang, G., Cheng, S., Wei, W., Zhou, Y., Yao, S., Zhang, H., 2016. Characteristics and source apportionment of VOCs in the suburban area of Beijing, China. *Atmos. Pollut. Res.* 7, 711-724.

Yurdakul, S., Civan, M., Tuncel, G., 2013. Volatile organic compounds in suburban Ankara atmosphere, Turkey: sources and variability. *Atmos. Res.* 120, 298-311.

Zhang, X., Wei, S., Sun, Q., Wadood, S.A., Guo, B., 2018. Source identification and spatial distribution of arsenic and heavy metals in agricultural soil around Hunan industrial estate by positive matrix factorization model, principle components analysis and geo statistical analysis. *Ecotox. Environ. Safe.* 159, 354-362.

Zimmerman, P.R., 1979. Testing of hydrocarbon emissions from vegetation, leaf litter and aquatic surfaces and development of a method for compiling biogenic inventories. Report, EPA-450/4-70- 004. US Environmental Protection Agency, Research Triangle Park.

Acknowledgements

This study was financially supported by TÜBİTAK [project number 114Y632] and Bolu Abant İzzet Baysal University Coordination Unit of Scientific Research Projects [project number 2015.09.02.962].

Necessity of improved ammonia emission inventory in agriculture

Sung-Chang Hong, Eun-Suk Jang, Sun-Young Yu, Gyu-Hyen Lee, Kyeong-Sik Kim and Sae-Nun Song

Climate Change & Agroecology Division, National Institute of Agricultural Sciences, RDA, Wanju 55365, Korea

schongcb@naver.com

Abstract. In winter and spring seasons, high concentration particulate matter severely affects human health in Korea. Particulate matter is emitted from various sources and formed from many chemical materials. Increasing use of nitrogen fertilizer during the past 50 years has also increased the agricultural production and induced environmental load in the agricultural environment. In the agricultural sector, non-point source pollutants could be emitted to not only water but also air. Agriculture is a complex system which has a broad border and includes various living organisms. Ammonia emitted from animal feeding operations is an air pollutant contributing to the formation of fine particulate matter. Secondary formation particulate matter is composed of 72% fine particulate matter in 2014. Ammonia is mainly emitted from animal feeding, manure process, fertilizer application, and industrial process. It reacts in the atmosphere with sulfur dioxide (SO₂) and nitrogen oxides (NO_x) to form particles containing ammonium sulfate and ammonium nitrate. An ammonia emission of 78% was found in agriculture through the Clean Air Policy Support System (CAPSS, Ministry of Environment) in 2015. The EU, the USA, and China ammonia emissions in the agricultural sector were 94 %, 86 %, and 82 %, respectively. The livestock sector needs to develop improved emission factor by animal housing type, animal, manure storage method, manure management, and livestock environments. Crop land sector also needs to enhance emission factors by crop, cultivation method, nutrient input material, application time, and cultivation environments. The nitrogen budget of crop land is not reduced by increasing manure application although nitrogen fertilizer application is reduced in Korea. In order to develop the quality emission inventory of ammonia, the activity data (animal number, amount of manure, amount of fertilizer application, crop land area, etc.) should be renewed every year. When the amount of ammonia emission in the agricultural sector is established, one could apply the practical reduction technology of ammonia emission at the agricultural field and could contribute to preserving the sustainability of agriculture and improving air quality.

Keywords: Agriculture, Air quality, Ammonia, Crop land, Inventory, Livestock.

1. Introduction

In recent years, the frequent occurrence of fine dust is very concerned about the adverse effects on health, causing a variety of obstacles in everyday life, the national interest in reducing fine dust becomes very high.

Dust that threatens public health is classified into particulate matter (PM₁₀) of 10 µm or less and fine particulate matter (PM_{2.5}) of 2.5 µm or less. The generation of fine dust is classified into primary generation discharged in the form of solid dust from the source and secondary generation which is discharged as gaseous material from the source and becomes fine dust by chemical reaction with the

material in the air. The secondary generation means that the fine dust production in which sulfite gas from the combustion process of fossil fuels is combined with water vapor and ammonia in the atmosphere, or nitrogen oxides from automobile exhaust gases is combined with water vapor, ozone and ammonia, and fine dust is generated through chemical reactions. Recently, [The Comprehensive Measures for Fine Dust Management (2017)] by the Ministry of Environment stated that secondary generated fine dust accounts for 72% of the total fine dust. Particularly, ammonia (NH_3), which is produced mainly in livestock farming, manure treatment, fertilizer use, and production process facilities in the agricultural sector, reacts with sulfur oxides and nitrogen oxides in the air to produce ultrafine dust such as ammonium sulfate and ammonium nitrate. Ammonium sulfate and ammonium nitrate among the components of the fine dust measured in the capital area make up 25.9 ~ 35.2% of the total fine dust concentration (Ministry of Environment, 2007), it is therefore assumed that ammonia greatly affect the concentration of the fine dust.

2. Ammonia emission

The Ministry of Environment designated 8 emissions such as CO, NO_x , SO_x , TSP, PM_{10} , $\text{PM}_{2.5}$, VOC and NH_3 as air pollutants through the Clean Air Policy Support System (CAPSS) and estimates the emission yearly.

The trend of emissions of major air pollutants published by the Ministry of Environment shows that since 2013 sulfur oxides and fine dust have been decreasing, but ammonia has been repeatedly increasing and decreasing. Nitrogen oxide emissions have been steadily increasing since 2009. According to the yearly ammonia emission trend, 23.31 million tons of ammonia was emitted in 2001, 292 thousand tons in 2014, and 1,014 thousand tons in 2009 and 1,135 thousand tons in 2014. The main sources of ammonia in Korea were 79% from agricultural sector, 14% from the production process, and 7% from the transportation energy and industrial combustion. Especially, the ammonia emissions were attributed by the agricultural sector and production facilities with about 93% of the total with the highest figure from the agricultural sector (Ministry of Environment, 2016).

In the EU, agricultural sector accounted for the largest share with 94% of ammonia emissions (Eurostat, 2015). The ammonia emission trend in USA shows 87% emission from the agricultural sector (EPA, 2018), while in China agricultural sector attributed ammonia emission 87% of the total (Huang et al., 2012).

3. Emission factor

In Korea, statistics on national air pollutant emissions are prepared from the Ministry of Environment. The ammonia emissions for the agricultural sector has been calculated based on livestock raising and livestock facilities statistics. However, the agricultural sector is a complex system with very wide boundaries and containing a variety of organisms. In order to calculate the accurate emission of ammonia generated in the agricultural sector, the emission factor for each sector, such as livestock and breeding, must be developed. Increasing use of nitrogen by fertilizer application has greatly increased agricultural production over the last 50 years and might have attributed to excess nitrogen input into the environment. Particularly, this was done mainly through the ammonia emission into the atmosphere. In order to reduce nonpoint source from farmland, not only nitrogen loss through water, but also air loss should be reduced to improve air quality. Increasing nitrogen utilization in crop cultivation can help improve air quality, reduce greenhouse gas emissions and reduce operating costs. Research has been started from this year on ammonia emissions from rice, field crops and plant cultivation crops. In order to estimate the ammonia emission factor during crop cultivation, ammonia emission should be measured by using the chamber during the crop cultivation period by chemical fertilizer and compost input. In addition, in order to use the ammonia emission factor as the official national emission factor, activity data such as



ammonia emissions for each crop type, crop area, crop fertilizer usage and crop compost consumption must be calculated every year.

For the livestock sector, it is necessary to calculate correct emission factors for each type of livestock by subdividing them into Korean cattle, beef cattle, dairy cows, pigs, chickens and ducks according to the type of livestock.

4. Conclusions

Due to fine dust, which occurs frequently in springs and winters, the public's interest in the health of fine dust has increased. The fine dust that occurs recently in Korea is more concentrated than in the past and has a longer duration, which raises more concern than in the past. Many of the recently generated fine dust is composed of ultra-fine dust, and it is known to be produced by the secondary chemical reaction of ammonia, sulfur oxides and nitrogen oxides in the atmosphere. Since ammonia is mostly generated in agriculture, efforts to estimate and reduce the amount of ammonia produced in agriculture are needed. In the agricultural sector also, accurate emission calculations are needed by developing emission factors for crop cultivation and animal husbandry and securing reliable activity data. Activity data can be collected through sales statistics from government agencies such as the National Statistical Office and the Ministry of Agriculture, Food and Rural Affairs and various associations. However, cooperation with various agricultural material producer associations is essential for details that are missing or to be added. Improved ammonia emission factor and emission inventory should be established as above so that ammonia emission reduction technology can be practically applied in agricultural field. These efforts will help to reduce national ammonia emissions in the agricultural sector and help in implementing national air quality improvement policies.

5. References

Eurostat, 2015. <https://ec.europa.eu/eurostat/statistics-explained/index.php?title=Agri-environmental>, accessed in August 2019

NAPES (National Air Pollutants Emission Service), 2019.

<http://www.airemiss.nier.go.kr/module/statistics/causeStatistics.do?siteId=airemiss&id=aire>, accessed in August 2019

EPA, 2018. <https://www.epa.gov/air-emissions-inventories/air-pollutant-emissions-trends-data>, accessed in August 2019

Huang, X., Song, Y., Li, M., Li, J., Huo, Q., Cai, X., Zhu, T., Hu, M., Zhang, H., 2012. A high-resolution ammonia emission inventory in China. *Global Biogeochemical Cycles*. 26, GB1030, doi:10.1029/2011GB004161

Acknowledgments

This study was carried out with the support of the "Research Program for Agricultural Science & Technology Development (Project No. PJ014205)" of the National Institute of Agricultural Sciences, Rural Development Administration, Republic of Korea.

Nickel, arsenic, cadmium, and lead in PM₁ fraction in Zagreb, Croatia

Jasmina Rinkovec, Gordana Pehnc and Silva Zužul

Institute for medical research and occupational health, Ksaverska cesta 2, Zagreb, Croatia

jrinkovec@imi.hr

Abstract. Fine aerosol particles have been found to play a key role in global climate change, pollution problems and health hazards. PM₁ particles (particulate matter with an aerodynamic diameter of less than 1 μm) are characterized by a high surface-area-to-volume ratio, having great potential negative risks for human health. The metals released by anthropogenic activities, bounded to fine particulate matter, are bioaccumulative and can cause severe ecosystem disturbances. In this study, 24-hour samples of PM₁ were collected at an urban background location in Zagreb, during 2011 and 2016, using a low-volume reference sampler. The collected samples of PM₁ were prepared in nitric acid using a high pressure microwave digestion system. Nickel, arsenic, cadmium and lead were determined by inductively coupled plasma mass spectrometry (ICP MS). The objective of the study was to determine mass concentrations of nickel, arsenic, cadmium and lead in PM₁ fraction in 2011 and 2016 and compare the obtained data sets. The mean annual values were 1.58 ng m⁻³, 0.45 ng m⁻³, 0.21 ng m⁻³ and 5.55 ng m⁻³ in 2011, and 0.14 ng m⁻³, 0.23 ng m⁻³, 0.13 ng m⁻³, and 4.33 ng m⁻³ in 2016 for Ni, As, Cd and Pb, respectively. Statistically significant differences between the years were found for all metals with higher concentrations determined in 2011 compared to 2016. A statistically significant difference was found between seasons as well, except in winter and autumn for As and Pb (in 2011) and As, Ni and Cd (in 2016), and in spring and summer for Ni (in 2011) and Ni, Cd and Pb (in 2016). The highest values during the colder part of the year were found for all of the determined metals which was expected because of the adverse weather conditions that make it difficult to circulate air.

Keywords: ICP MS, Metals, Microwave digestion, Particulate matter.

1. Introduction

Particulate matter (PM) is a mixture of organic and inorganic substances that emerge from a wide range of natural and anthropogenic sources. Numerous and consistent studies show that particulate matter and heavy metals are responsible for the occurrence of a wide range of biological and health effects, and contribute to the degradation of air and human health (Talbi et al., 2017).

Only a limited number of measurements of smaller fractions have been performed so far. (Cheng et al. 2011; Mingulion et.al. 2012; Perrone et al. 2013). Although this number has increased over the last several years because fine particles (like PM₁ – particles with aerodynamic diameter of less than 1μm) can affect the environment and human health due to the fact that: (i) they can remain suspended for longer periods of time in the atmosphere than coarse particles; (ii) they penetrate more effectively into the deep lung; (iii) they can penetrate more readily into indoor environments; (iv) they may be transported over long distances; (v) they tend to carry higher concentrations of more toxic compounds, including acids, heavy metals and organic compounds; and (vi) they have a larger surface area per unit

mass compared to larger particles and can absorb larger amounts of semi-volatile compounds (Squizzato et al., 2016).

Metals are useful tracers and are extensively used to identify sources of emissions. Therefore, monitoring of the metal composition of PM has become a crucial part of air quality programs in countries around the world (Buczynska et al., 2014; Sarti et al., 2015; Samek et al., 2017). Some metals and metalloids associated with airborne particulate matter have been found to be a potential health concern. Certain elements like V, Cu, As, and Pb, were found to be of greater relative concern given their solubility and as such pose an elevated potential to induce pulmonary toxicity. The chemical complexity of airborne particulate matter and its variability highlight the need to assess the impact of exposures to metals as well as other constituents of particulate matter. (Wiseman and Zereini, 2014).

Zagreb is the capital of Croatia, located in the northwest of the country, along the Sava river, at the southern slopes of the Medvednica mountain with a population of 792.875 (the Zagreb metropolitan area has a population of 1.110.517). The city has six local and three national measurement stations for continuous air quality monitoring. The PM₁₀ and PM_{2.5} compositions in the city were the object of several studies in the past (Čačković et al., 2006; Bešlić et al., 2008; Šišović et al., 2008; Vadić et al. 2007, 2010, 2011). This paper presents the results of a comparison of two-year monitoring (2011 and 2016) of metal contents in PM₁ particles in the city of Zagreb.

2. Materials and methods

2.1. Sampling site

The sampling site (N: 45° 50' 9"; E: 15° 58' 59") is located in the residential, northern part of Zagreb, behind the Institute for Medical Research and Occupational Health (IMROH). It is located 15 m from a local road with modest traffic density, and is near a modestly populated residential area. It is classified as an urban background station.

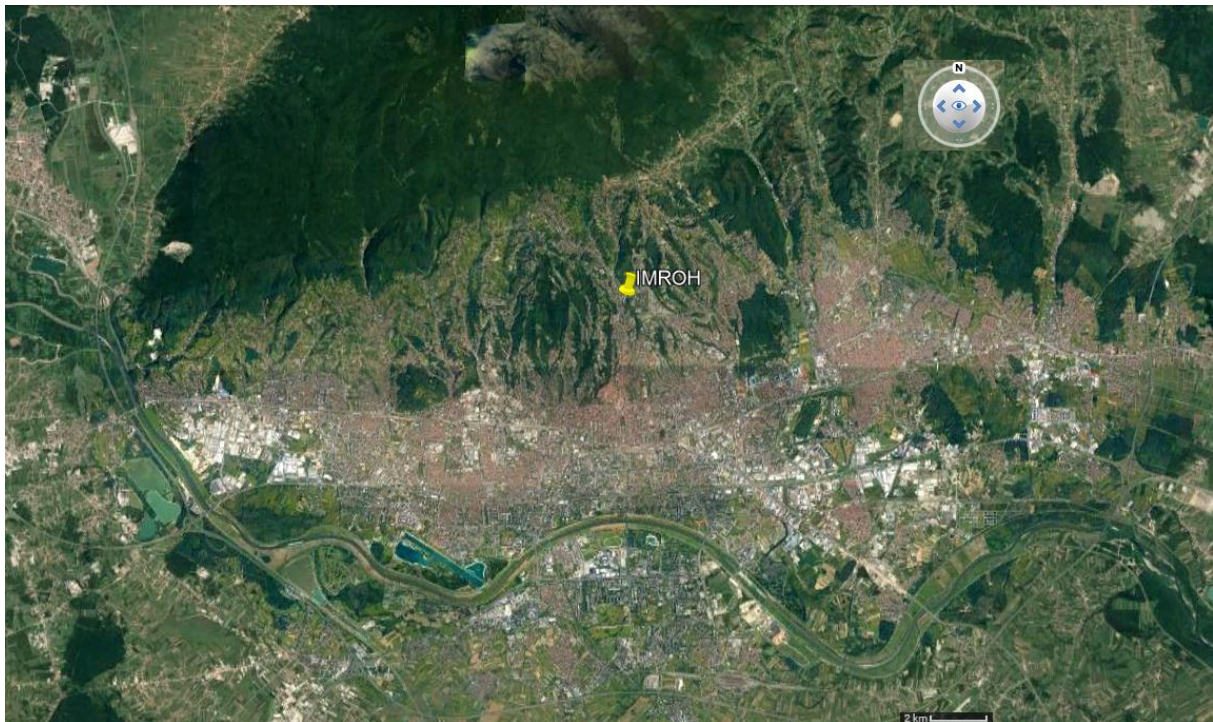


Figure 1. The position of the sampling site in Zagreb

2.2. Sampling method

Sampling was carried out over a two-year period (1st January - 31st December 2011 and 1st January - 31st December 2016). Twenty-four hour samples were collected on 47 mm-diameter quartz fiber filters using a Sven Leckel LVS3 low-volume reference sampler (~50m³ of air / day).

2.3. Preparation and analysis method

After sampling, the filters were prepared for analysis in a high pressure microwave digestion system (Ultraclave IV, Milestone) and analysed using inductively coupled plasma mass spectrometry, ICP-MS (7500cx, Agilent technologies). Isotopes ⁶⁰Ni, ⁷⁵As, ¹¹¹Cd, and ²⁰⁶Pb were selected and the integration time per point was 0.1 s for Ni and Pb and 0.5 for As and Cd, with three acquisition points per peak. Scandium, germanium, and rhodium were added as internal standards during calibration and sample analysis.

The ICP-MS spectrometer was tuned to obtain an oxide ratio and doubly charged ratio < 1.5%. The analysis was made in helium (He) mode. The tuned operating parameters were: RF power 1550 kW, RF matching 1.72 V, carrier gas (Ar 5.0) flow rate 1.12 L/min, helium gas (He 6.0) flow rate 4.5 mL/min in the collision cell. The carrier and make up gas flow rate were optimized to minimize interferences and maximize the sensitivity. Working standards (5% HNO₃(v/v)) were prepared from stock solutions (1000 µg mL⁻¹) of Ni, As, Cd and Pb at eight level concentrations and calibration was carried out every time before sample analysis. The method detection limit for Ni, As, Cd and Pb were 0.82 ng m⁻³, 0.018 ng m⁻³, for Cd 0.004 ng m⁻³ and 0.23 ng m⁻³, respectively. The accuracy of the method was determined by preparing and analysing PM₁₀-like reference materials NIST 1648 (used in 2011) and ERM CZ120 (used in 2016) the same way as the collected samples. The recoveries for NIST 1648 ranged from 89 % to 95 % for Ni, 92 % to 99 % for As, 90 % to 95 % for Cd, and 90 % to 92 % for Pb. The recoveries for ERM CZ120 ranged from 85 % to 95 % for Ni, 92 % to 95 % for As, 98 % to 104 % for Cd, and 90 % to 93 % for Pb.

2.4. Data analysis

Statistica version 13.2 from Dell Inc. was used for processing the measured data. The statistical difference between the two sampling years as well as between seasons was investigated using Student's t-test of independent samples.

3. Results and discussion

The two-year comparison on nickel, arsenic, cadmium and lead levels in PM₁ fraction in the city of Zagreb represents the first analysis of this kind for this area. As shown in Table 1, the mean annual values in 2011 were 1.58 ng m⁻³, 0.45 ng m⁻³, 0.21 ng m⁻³ and 5.55 ng m⁻³ for Ni, As, Cd and Pb, respectively, and 0.14 ng m⁻³, 0.23 ng m⁻³, 0.13 ng m⁻³, and 4.33 ng m⁻³ in 2016 for Ni, As, Cd and Pb, respectively.

Table 1. Descriptive statistic of metal mass concentrations (ng m⁻³) in PM₁ samples in 2011 and 2016

	Sampling year	N	Mean	Minimum	Maximum	SD
Ni	2011	364	1.58	DL	11.93	2.2
	2016	357	0.14	DL	5.07	0.5
As	2011	364	0.45	0.09	2.25	0.4
	2016	357	0.23	0.03	1.36	0.2
Cd	2011	364	0.21	0.03	1.33	0.2
	2016	357	0.13	0.01	1.03	0.1
Pb	2011	364	5.55	0.70	38.32	5.2
	2016	357	4.33	0.33	31.57	4.8

DL - detection limit; SD - standard deviation; N - number of samples



18th World Clean Air Congress, 23-27 September 2019, Istanbul
organized by TUNCAP and IUAPPA

In both sampling years, 2011 and 2016, the highest values were obtained for Pb, and the lowest for Cd. Also, the highest values for all metals were measured in 2011. Figure 2 shows the daily mass concentrations of Ni, As, Cd and Pb for the whole two year sampling period (2011, 2016). In order to determine whether there was a significant difference between the mass concentrations of the elements measured in the 2011 and 2016, and between seasons as well, the data were statistically processed using Student's t-test of independent samples.

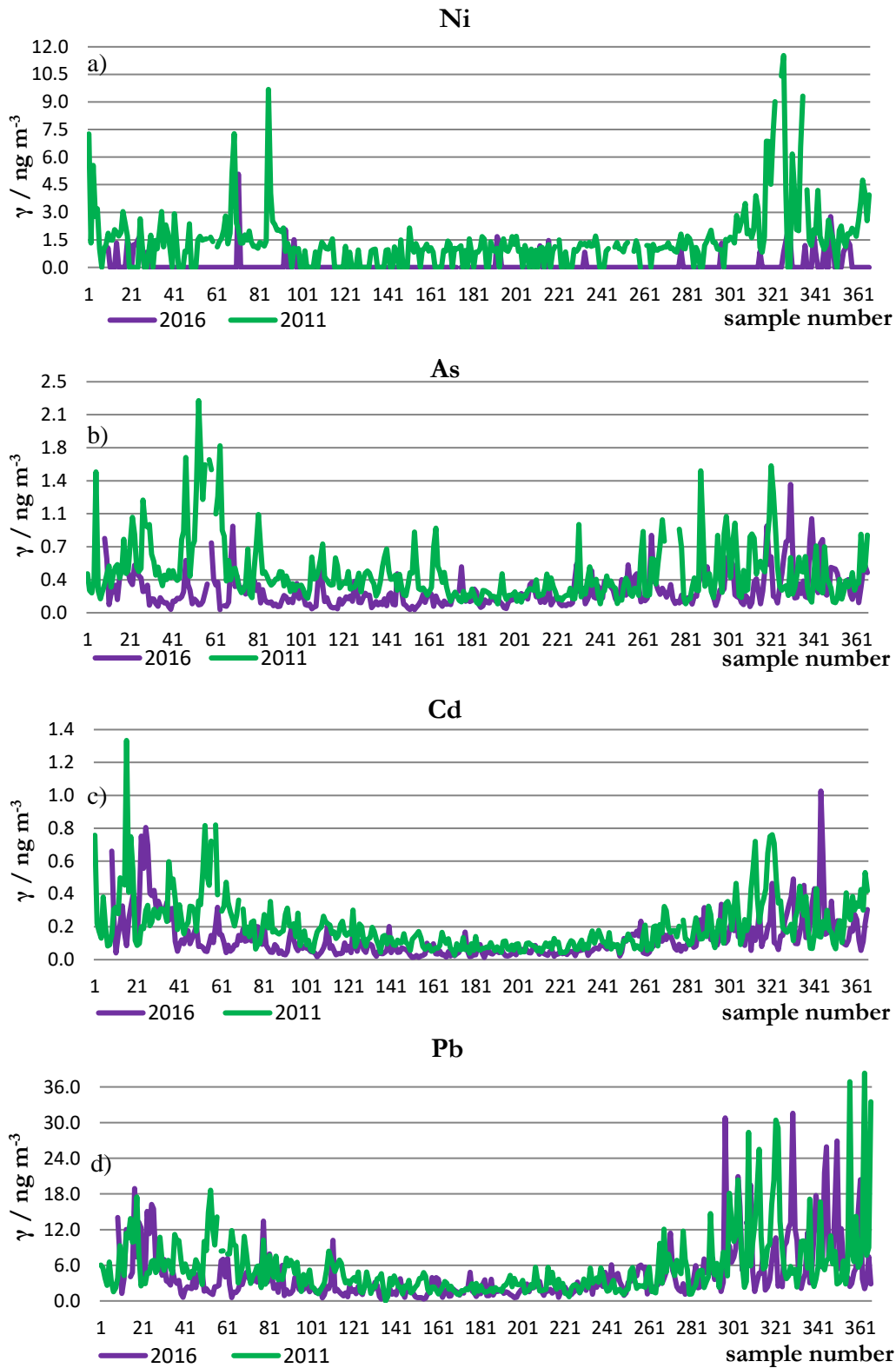


Figure 2. Daily mass concentrations of a) nickel (Ni), b) arsenic (As), c) cadmium (Cd) and d) lead (Pb) in 2011 and 2016.

A statistically significant difference ($p < 0.05$) between mass concentrations in 2011 and in 2016 was found for all metals with higher measured concentrations in 2011 compared to 2016. As seen in Table 1 and Figure 2.a, the mass concentrations of nickel show a substantial difference between the years. The reason for this kind of difference could be the type of material used for heating in the nearby households and the diverse meteorological conditions in those sampling years. Also, quite a lot of samples of Ni in 2016 were below the detection limit which additionally points to low mass concentrations of the mentioned metal in that particular year. Higher values during the colder part of the year were probably due to an increased use of cars, the heating period as well as adverse weather conditions that made it difficult for air to circulate.

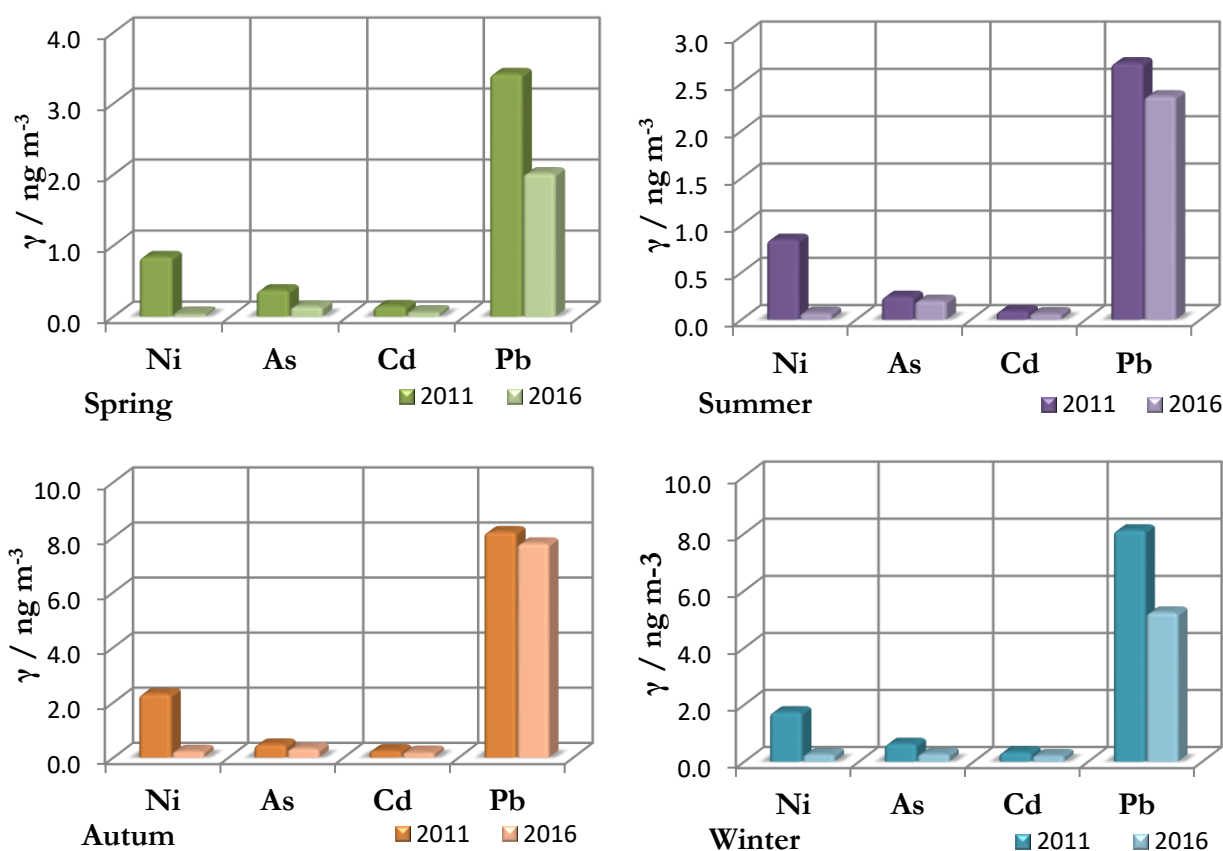


Figure 3. Average seasonal mass concentrations of Ni, As, Cd and Pb in 2011 and 2016

The highest values in every season in both sampling years were found for Pb, and the lowest for Cd. Figure 3 shows the average seasonal mass concentrations of metals for both sampling years. A statistically significant difference was found between seasons as well, except in winter and autumn for As and Pb (in 2011) and As, Ni and Cd (in 2016), and in spring and summer for Ni (in 2011) and Ni, Cd and Pb (in 2016). Similar results regarding nickel (3 ng m^{-3}) and cadmium (0.1 ng m^{-3}) were obtained by Perrone et al. 2013, for a central Mediterranean site in Italy. Squizzato et al. (2016), following measurements at an urban background station in Venice, Italy, in a highly populated residential zone, obtained somewhat higher average mass concentrations for nickel (2.5 ng m^{-3}), arsenic (1.2 ng m^{-3}) and cadmium (1.1 ng m^{-3}), but for lead (7 ng m^{-3}) the results were similar to those presented in this paper.

4. Conclusion

PM₁ samples were collected during 2011 and 2016 in an urban background station in Zagreb. The highest values for all metals were measured in 2011, the highest values were obtained for Pb, and the lowest for Cd. Mass concentrations of nickel showed the biggest differences between the years and the reason for this could have been the type of material used for heating the nearby households and the diverse meteorological conditions between sampling years. The expected results such as the higher values found during the colder part of the year suggest an increased use of cars, an influence from heating as well as impact from the adverse weather conditions that make it difficult to circulate air. As this fraction of particulate matter is smaller and can breach further in the organism, the research of the composition and the effect that it has on the organism should be investigated in the near future.

5. References

- Bešlić I., Šega K., Čačković M., Bencetić-Klaić Z., Bajić A. 2008. Relationship between 4-day air mass back trajectories and metallic components in PM₁₀ and PM_{2.5} particle fractions in Zagreb air, Croatia. *B. Environ. Contam. Tox.* 71, 270-273.
- Buczynska, A.J., Krata, A., van Grieken, R., Brown, A., Polezer, G., De Wael K., Potgieter-Vermaak, S., 2014. Composition of PM_{2.5} and PM₁ on high and low pollution event days and its relation to indoor air quality in a home for elderly. *Sci. Total. Environ.* 490, 134-143.
- Cheng Y., Zou S.C., Lee S.C., Chow J.C., Ho K.F., Watson J.G., Han Y.M., Zhang R.J., Zhang F., Yau P.S., Huang Y., Bai Y., Wu W.J., 2011. Characteristic and source apportionment of PM₁ emissions at a roadside station, *J. Hazard. Mater.* 195, 82-91.
- Čačković M., Šega K., Vadić V., Bešlić I., 2006. Correlation between metallic and acidic components in high-risk particle fraction in Zagreb air. *B. Environ. Contam. Tox.* 76, 1014-1020.
- Perrone M.R., Becagli S., Garzia Orza J.A., Vecchi R., Dinoi A., Udisti R., Cabello M., 2013. The impact of long-range-transport on PM₁ and PM_{2.5} at Central Mediterranean site, *Atmos. Environ.* 71, 176-186.
- Mingulion M.C., Querol X., Baltensperger U., Prevot A.S.H., 2012. Fine and coarse PM composition and sources in rural and urban sites in Switzerland: Local or regional pollution. *Sci. Total. Environ.* 427/428, 191-202.
- Samek, L., Furman, L., Mikrut, M., Regiel-Futyra, A., Macyk W., Stochel, G., Van Eldik, R., 2017. Chemical composition of submicron and fine particulate matter collected in Krakow, Poland. Consequences for the APARIC project. *Chemosphere* 187, 430-439.
- Sarti, E., Pasti, L., Rossi, M., Ascanelli, M., Pagnoni, A., Trombini, M., Remeli, M., 2015. The composition of PM₁ and PM_{2.5} samples, metals and their water soluble fractions in the Bologna area (Italy). *Atmos. Pollut. Res.* 6, 708-718.
- Squizzato, S., Masiol, M., Agostini, C., Visin, F., Formenton, G., Harrison R.M., Rampazzo, G., 2016. Factors, origin and sources affecting PM₁ concentrations and composition at an urban background site, *Atmospheric Res.*, 180, 262-273.
- Šišović A., Bešlić I., Šega K., Vadić V., 2008. PAH mass concentrations measured in PM₁₀ particle fraction. *Environ. Int.* 34, 580-584.



Talbi, A., Kerchich, Y., Kerbachi, R., Boughedaoui, M., 2017. Assessment of annual air pollution levels with PM₁, PM_{2.5}, PM₁₀ and associated heavy metals in Algiers, Algeria. *Environ. Pollut.* 232, 252-263.
Vađić V., Hršak J., Žužul S., 2009. Trends of lead in suspended particulate matter in Zagreb air. *Int. J. Environ. Pollut.* 39, 385-391.

Vađić V., Žužul S., Pehnc G., 2010. Zinc levels in suspended particulate matter in Zagreb air. *B. Environ. Contam. Tox.* 85, 628-631.

Vađić V., Žužul S., Pehnc G. 2011. Manganese Levels in Suspended Particulate Matter in Zagreb Air. *Proceedings of the 2011 International Symposium on Environmental Science and Technology*, June 1-4, 2011, Beijing China, pp. 267-274.

Wiseman, C.L.S., Zereini, F., 2014. Characterizing metal(oid) solubility in airborne PM₁₀, PM_{2.5} and PM₁ in Frankfurt, Germany using simulated

Source apportionment of biogenic and anthropogenic VOCs in Bolu Plateau

Melike Dörter^{1,2}, Mustafa Odabasi³ and Serpil Yenisoğ Karakas¹

¹Department of Chemistry, Bolu Abant İzzet Baysal University, Bolu

²Present address: Department of Pharmacy Services, Yüksek İhtisas University, Ankara

³Department of Environmental Engineering, Dokuz Eylül University, İzmir

melikedrtr@gmail.com

Abstract. Passive sampling provides a cost-effective way to do simultaneous sampling of specific species in rural, regional and global scales. In this study, volatile organic compounds (VOCs) were collected on Tenax-TA tubes during two-week periods in winter (28th January 2017-12nd February 2017) and in summer (7th July 2017-23rd July 2017) passive sampling campaigns in Bolu plateau. Samples were analyzed using Thermal Desorption Gas Chromatography Mass Spectrometry (TD-GC-MS). Investigated 69 VOCs were classified as biogenic (isoprene, monoterpenes and oxygenated VOCs) and anthropogenic VOCs. Benzaldehyde, toluene, phenol, benzene, hexane, decanal, benzothiazole, dodecane and acetophenone were anthropogenic VOCs with higher concentrations. Biogenic VOCs with the higher concentrations were determined as hexanal, alpha-pinene and limonene. Ozone formation potential of VOCs were also determined. Winter and summer seasons showed different trends according to their biogenic VOC percentages. Biogenic VOCs had lower concentrations in winter which was characterized with low solar intensity, temperature and amount of leafy tree species. Spatial distribution maps were drawn for each VOC, and the results were supported with Positive Matrix Factorization (PMF) analyses. Anthropogenic VOCs were found at high levels in regions with industrial activities, traffic and dense population. On the other hand, biogenic VOCs showed higher concentrations correlated with tree species. PMF analyses and G-score distribution maps of the factors revealed that solvent evaporation, wood-coal combustion, biogenic emissions (pine, grain, grass), city atmosphere, biogenic (hornbeam, pine, juniper) and vehicle emissions were the major VOC sources in Bolu plateau.

Keywords: Anthropogenic VOCs, Biogenic VOCs, Seasonal variation, Spatial distribution, Positive matrix factorization (PMF).

1. Introduction

Increased industrialization and urbanization are leading to deterioration of air quality, resulting in increasing levels of pollutants in the environment, with consequences for both ecosystem and human health (Baklanov et al., 2016; Gulia et al., 2015; Kjellstrom et al., 2007; Moore et al., 2003). Volatile organic compounds (VOCs) are one group of the pollutants that lead to many pollution problems including tropospheric photochemical ozone formation, stratospheric ozone depletion, global greenhouse and mutagenic and carcinogenic effects on human health (Ismail and Hameed, 2013). There are various VOCs, and they differ in chemical characteristic. Thus, each one leads to different impacts.

Both dangerous effects and widespread existence of volatile organic compounds make their determination, quantification and source apportionment very essential. In order to determine the

concentrations of the pollutants, first thing is to sample them properly. There are various ways of sampling. Active sampling is one of them. Although active samplers are advantageous in collection of a precise volume of air in a short time, they have a number of limitations. It is difficult to study the multi points and simultaneously because they require equipment and electricity. A passive sampling method which does not involve forced movement of the air through the sampler, is based on taking samples of pollutants in vapour or gas form from the atmosphere at a rate controlled by a physical process, such as diffusion through a static air layer or permeation through a membrane. No requirement for electricity, lower cost and easy portability of passive samplers make them a favored way to survey numerous sampling points simultaneously. In this paper, 69 VOCs having biogenic and anthropogenic origins were investigated according to their spatial distribution, temporal variation, possible sources and ozone production capacities. In determination of possible source sectors, positive matrix factorization (PMF) was applied.

2. Materials and methods

2.1. Sampling program, collection and analysis

The study was conducted in city of Bolu which is in the Western Black Sea Region of Turkey. It has a population of around 300.000 and total area of the city is 832.339 hectare. Bolu city center hosts a small number of industrial sectors including cement, poultry, woodworking, metal and glass (Bolu Environmental Status Report, 2016). However, emissions from agricultural activities, vegetation emission and vehicle traffic are possible important VOC sources. The city was rich in tree species such as Oak, Oriental beech, Scots pine, Juniper, Fir and Hornbeam. General features of sampling area was represented in Figure 1.

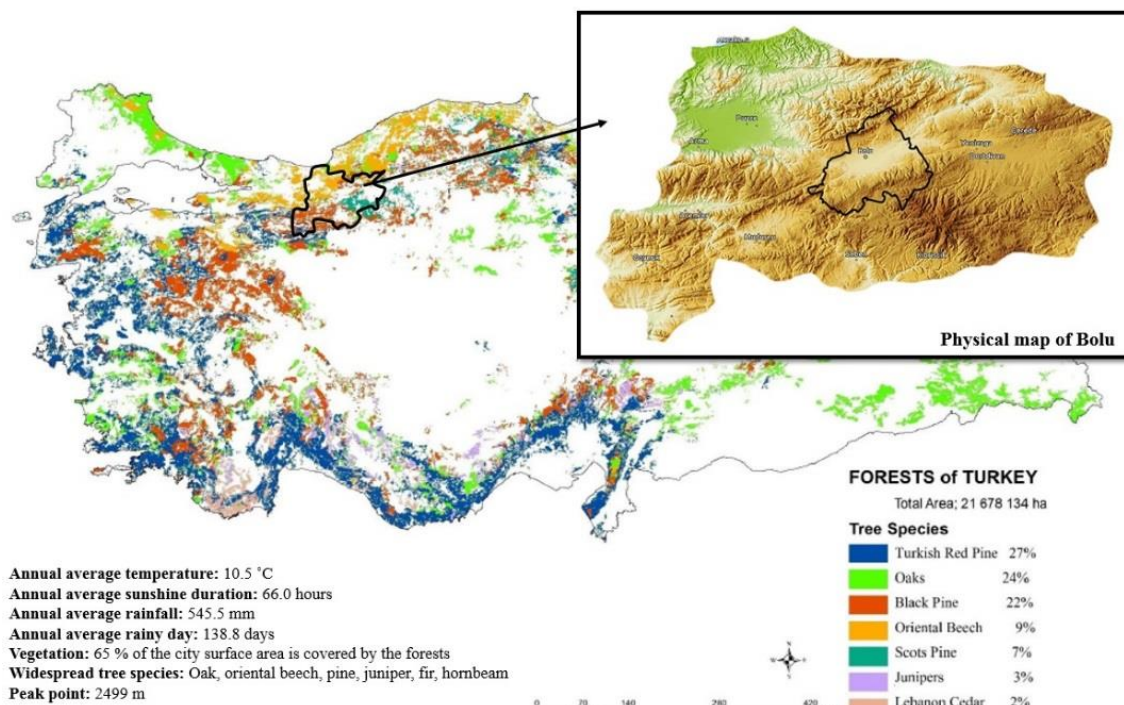


Figure 1. Sampling area (Bolu plateau)

Passive sampling of VOCs was performed at 47 sampling points in winter season (28th January 2017-12nd February 2017) and 63 sampling points in summer season (7th July 2017-23rd July 2017). The sampling points were determined by considering pollution sources and geography of the area. VOCs

were collected on Tenax-TA sampling tubes (Perkin Elmer, USA) that have a length of 89 mm, an outer diameter of 6.4 mm, an inner diameter of 5 mm and a diffusion path length of 15 mm. Before sampling campaigns, the tubes were conditioned at 320 °C for 60 minutes under high purity helium gas. Until sampling, they had been stored in screw-capped falcon tubes which include a pack of silica gel and an activated carbon so as to prevent the humidity and contamination problems, respectively. When they were transported to the sampling point, diffusion headers were fit on sampling tubes and placed vertically with the open end downward in aluminum shelters. After the sampling, the diffusion caps were replaced with the covers of the tubes. They were transported to the laboratory in falcon tubes and stored at -18 °C until analysis. Isoprene, 2-methylfuran, chloroform, 1,2-dichloroethane, crotonaldehyde, benzene, tetrachloromethane, toluene, n-octane, hexanal, ethylbenzene, m-p-xylene, styrene, o-xylene, n-nonane, 1-heptanal, isopropylbenzene, alpha-pinene, camphene, n-propylbenzene, benzaldehyde, 1,2,4-trimethylbenzene, sabinene, beta-pinene, phenol, beta-myrcene, 1,3,5-trimethylbenzene, n-decane, alpha-phellandrene, 3-carene, alpha-terpinen, 1,4-cineole, 4-methylanisole, 1,2,3-trimethylbenzene, m-cymene, p-cymene, eucalyptol, gamma-terpinene, acetophenone, 1-octanol, dihydromyrcenol, 1-fenchone, terpinolene, linalool, nonanal, alloocimene, (+)-camphor, naphthalene, alpha-terpineol, n-dodecane, decanal, benzothiazole, n-tridecane, n-tetradecane, acrylonitrile, 1,1,1-trichloroethane, n-hexane, n-heptane, 1,2-dichlorobenzene, chlorobenzene, o-ethyltoluene, p-ethyltoluene, m-ethyltoluene, 1,4-diethylbenzene, ocimene, limonene, 1-terpinen-4-ol and 1,3-diethylbenzene were the volatile organic compounds under consideration in this study. Thermal Desorption Gas Chromatography Mass Spectrometry (TD-GC-MS) system was used in analyzing of all VOC samples.

2.2. Positive matrix factorization (PMF)

Positive matrix factorization (PMF) has been widely used in source apportionment studies (Amarillo et al., 2017; Ashrafi et al., 2018; Sakar et al., 2017; Zhang et al., 2018). The model uses a matrix of speciated sample data into two matrices that are called factor contributions (G) and factor profiles (F) (Norris and Duvall, 2014). Two matrices are derived using the minimized objective function, Q, in the PMF:

$$Q = \sum_{i=1}^n \sum_{j=1}^m \left[\frac{x_{ij} - \sum_{k=1}^p g_{ik} f_{kj}}{u_{ij}} \right]^2$$

where x is the data matrix of i number of samples by j chemical species which were measured, and u is the uncertainties. PMF solves the problem iteratively and this minimizes the Q.

EPA PMF 5.0 was used to identify the source profiles of passive VOCs. The data file contains the results of concentrations and uncertainties. For PMF analysis, a more comprehensive set of data was obtained by combining the concentration of both seasons. Concentrations were substituted with the MDL/2 when concentrations are below the method detection limit (MDL) or there is a missing value. The uncertainty of these concentrations were calculated as ((5/6)xMDL). Other data in the uncertainty file was estimated based on the equation (Norris et al., 2014):

$$u = \sqrt{((0.1) \times \text{concentration})^2 + (0.5 \times \text{MDL})^2}$$

Compounds having signal to noise ratio below 0.5, data percentage below detection limit exceeding 30%, low R² values (less than 0.5) and compounds appearing in more than two groups, were not included in PMF analysis. Therefore, sources were explained with 6 factors. Q_{robust} and Q_{true} values were 1020 and 1029. Moreover, residual distributions were approximately symmetric within the range of -3 and +3

that represents a good agreement between the observed and predicted values. Samples that did not comply with these rules were excluded from the analysis.

3. Results and discussion

3.1. Temporal variations of VOC concentrations

The anthropogenic VOCs with high concentrations were benzaldehyde ($3.64 \mu\text{g m}^{-3}$), toluene ($2.38 \mu\text{g m}^{-3}$) and benzene ($1.75 \mu\text{g m}^{-3}$) in winter season whereas benzaldehyde ($1.75 \mu\text{g m}^{-3}$), acetophenone ($1.53 \mu\text{g m}^{-3}$) and isoprene ($1.52 \mu\text{g m}^{-3}$) had higher concentrations in summer season. Alpha-pinene was the biogenic VOC with the highest concentration for both winter ($0.21 \mu\text{g m}^{-3}$) and summer ($1.00 \mu\text{g m}^{-3}$) seasons. Although there was no greater variability in types of dominant VOCs, difference was obtained in their atmospheric levels between seasons. In summer period, high mixing height, high solar radiation and high temperatures lead to the reduction of especially anthropogenic VOCs by photochemical reactions, and avoid accumulation of them in the city atmosphere. However, VOCs with biogenic origin showed different trend. Biogenic VOCs had higher percentage and variety in summer period (31% of total VOCs) than winter period (9% of total VOCs). That can be associated with the higher average solar radiation, higher average temperature and high amount of leafy tree species in summer period.

Isoprene which is a compound having both anthropogenic and biogenic origin, was found lower concentrations in winter in Bolu compared to the study performed in Duzce which is a neighbouring city (Bozkurt et al., 2018). However, the concentration of the compound in the Bolu atmosphere was approximately 10 times higher during the summer period. Higher percentage of forest areas in Bolu (64%) than in Duzce (50%) is thought to be effective in the amount of released biogenic VOC (Forest Atlas, 2017). In addition, anthropogenic VOC concentrations obtained in this study had generally lower than found by other studies (Bozkurt et al., 2018; de Albuquerque et al., 2012; Dumanoglu et al., 2014; Nunes et al., 2013; Yurdakul et al., 2017).

3.2. Spatial distribution

For each of the identified VOCs, distribution maps were prepared. They revealed that the components showed significant spatial changes in the city. The pollution distribution maps of some selected VOCs (benzene, m+p xylene, isoprene, crotonaldehyde and alpha-pinene) for both seasons were given in Figure 2.

According to the Figure 2, benzene showed a marked increase in the city center, organized industrial zone and areas including various factories. m+p Xylene which occur mostly as a result of traffic emissions found in higher concentrations in the city center and along TEM and D-100 highways. Also, for winter season, this compound was detected in high levels in Kartalkaya region and its road route, which is an important ski resort area of the country and reflects the emissions from operation and vehicular emission. When the isoprene pollution distribution maps were examined, both biogenic and anthropogenic sources had been found to be effective as expected. The highest isoprene levels was determined in the city center and the regions in which pine trees were common. Crotonaldehyde which is thought to be released from beech, hornbeam and oak had high concentrations in the northern part of the city center where beech is dominant and in villages close to the city center which can represent hornbeam, grass, grain and oak emissions (Aydın et al., 2014; Wildt et al., 2003). Alpha pinene and beta pinene are released from coniferous trees (red pine, black pine, pine, etc.) as well as hornbeam, fir and juniper (Aydın et al., 2014). These VOCs were found in high concentrations at the southern part of the city center of Bolu where pine species are common as given in Figure 1.

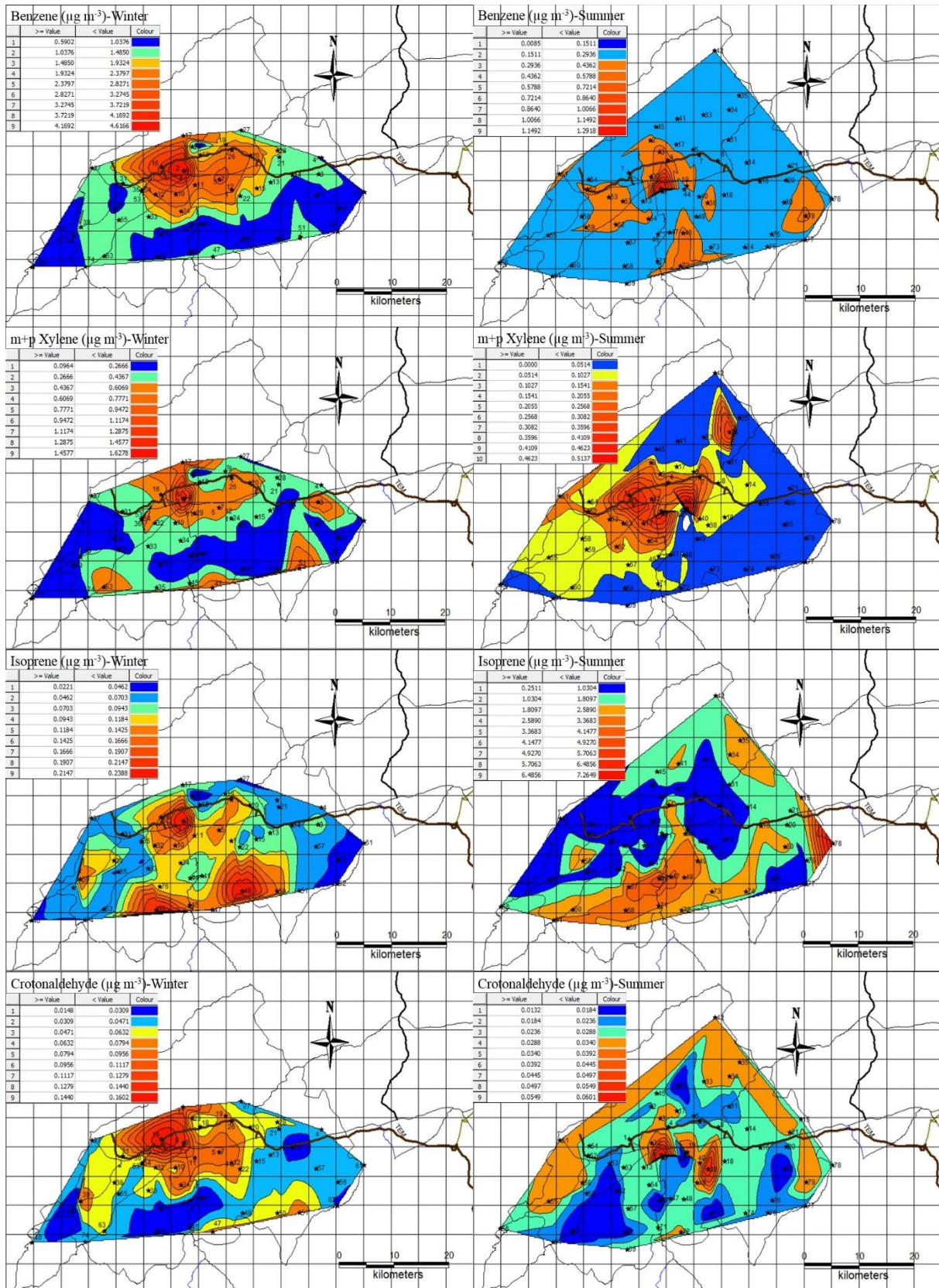


Figure 2. Pollution distribution maps

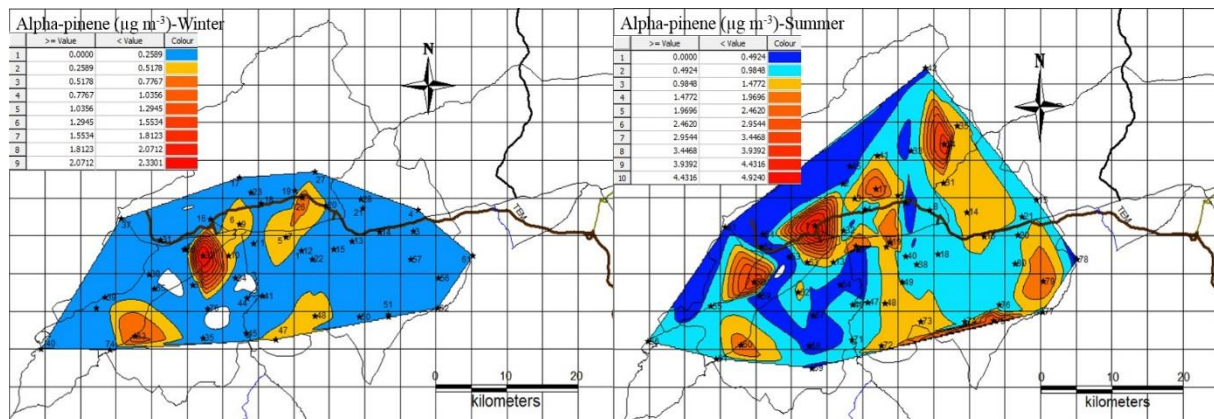


Figure 2. Continued

3.3. Ozone formation potential

Within this scope, ozone (O_3) and nitrogen dioxide (NO_2) were collected simultaneously with VOCs by using passive sampling technique in Bolu plateau. VOC-ozone and VOC- NO_2 binary statistical relations were examined to investigate the contribution of VOCs to ozone formation. It is supposed that VOC-ozone negative correlations are seen as a result of the consumption of VOCs through the photochemical reactions. So, compounds that have similar tendency (increase) with NO_2 and negative tendency towards ozone are determined as effective in ozone formation. The compounds which contribute to the ozone formation were determined as isoprene, n-hexane, beta-pinene, alpha-pinene, 2-methylfuran, benzene, crotonaldehyde, toluene, m+p xylene, limonene, p-cymene, n-propylbenzene, camphene, camphor, styrene and naphthalene.

3.4. Source apportionment

EPA Positive Matrix Factorization (PMF) 5.0 was used to identify the source profile of passive VOCs. In PMF analysis, a large number of samples should be used to ensure that the definition of resources is realistic as indicated by Norris and Duvall (2014). Therefore, PMF analysis was performed by combining all data obtained from summer and winter passive sampling. As a result of running PMF by combining the two data, the factors were clearly resolved and the factors that could be named based on certain marker VOCs were obtained. The chemical profiles of the compounds and the literature were used to identify each factor. Potential sources of VOCs were determined as solvent evaporation, wood-coal combustion, biogenic emissions (pine / grain / grass), city atmosphere, biogenic (hornbeam / pine / juniper) and vehicle emissions (Figure 3). Contribution of sources to the total was 31%, 22%, 8.0%, 8.0%, 13% and 18%, respectively.

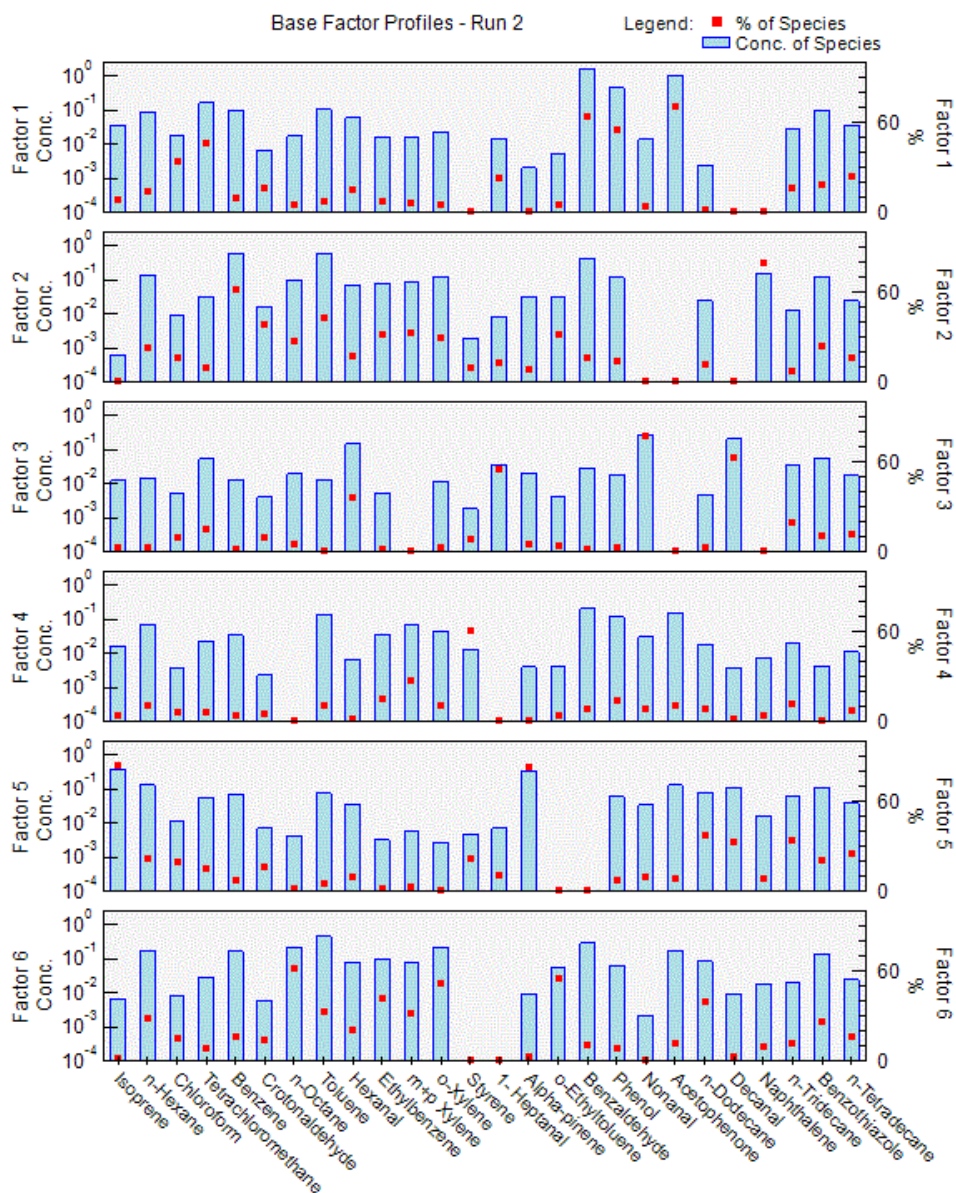


Figure 3. PMF source profiles for VOCs in the Bolu

In the first factor, VOCs with high explained percentages were acetophenone, benzaldehyde, phenol, tetrachloromethane and chloroform. It is known that these compounds were used as solvents in the laboratory / industry and even perfumes and other chemicals spreading to the atmosphere (EPA, 2000). The G-score values of factor 1 were mapped in Figure 4. The highest values were obtained at the sampling points of BAIBU Golkoy Campus.

Factor 2 was named as wood-coal combustion factor. The second factor included high concentrations of naphthalene, benzene, toluene, crotonaldehyde, ethylbenzene, m, p-xylene, o-xylene, octane, ethyltoluene, benzothiazole. Naphthalene, benzene, toluene, ethylbenzene, m,p-xylene and o-xylene are compounds in the structure of coal and released as a result of combustion (Liu et al., 2008). High G-scores were found in densely populated areas (urban and semi-urban) in the factor 2 (Figure 4).

The third factor, which mainly contains decanal, nonanal, heptanal and hexanal compounds, can be called biogenic emissions (pine/grain/grass). Isoprene is known to have both biogenic and anthropogenic origin. Aldehydes (decanal, nonanal, heptanal, hexanal) are also released from plants. Pine, grass and various plants are known to be effective in the release of aldehydes into the atmosphere (Wildt et al., 2003). High values in the G-score map (Figure 4) were determined especially in the southern and northern regions of Bolu. Forest Atlas (2017) stated that black pine and scotch pine trees which are active in the release of related compounds are common in the southern regions of the plateau.

In the fourth factor, the high occurrence of styrene is remarkable. This compound is particularly spread through industrial processes in which styrene and its polymers are studied. Common use in urban areas causes high styrene amounts in city atmosphere (WHO, 1983). In Figure 4, the sampling region with the highest G-score values was found in the city center.

Alpha-pinene and isoprene are the most commonly explained compounds in the fifth factor. Aydın et al. (2014) indicated that pine, hornbeam, juniper, cedar, fir, sycamore and poplar tree species spread significant amount of alpha-pinene to the atmosphere. Isoprene is mostly released from poplar, sycamore, oak, hornbeam, fir and beech trees (Aydın et al., 2014). Among these tree species, pine, hornbeam, juniper and fir are common in the sampling region. This factor is classified as biogenic emission (hornbeam / pine / juniper). High values in the G-score map were determined in the northern and inland regions of Bolu plateau where the related tree species were widespread (Figure 1, Figure 4).

In the last factor, octane, o-xylene, o-ethyltoluene, ethylbenzene, dodecane, m, p-xylene, toluene, hexane and benzothiazole are the compounds that have a high contribution. Liu et al. (2008) has identified o-xylene, ethylbenzene, dodecane, m, p-xylene and toluene compounds as potential trace compounds for mobile sources. According to the G-score map of the Factor 6 given in Figure 4, the highest value was obtained in Kartalkaya region.

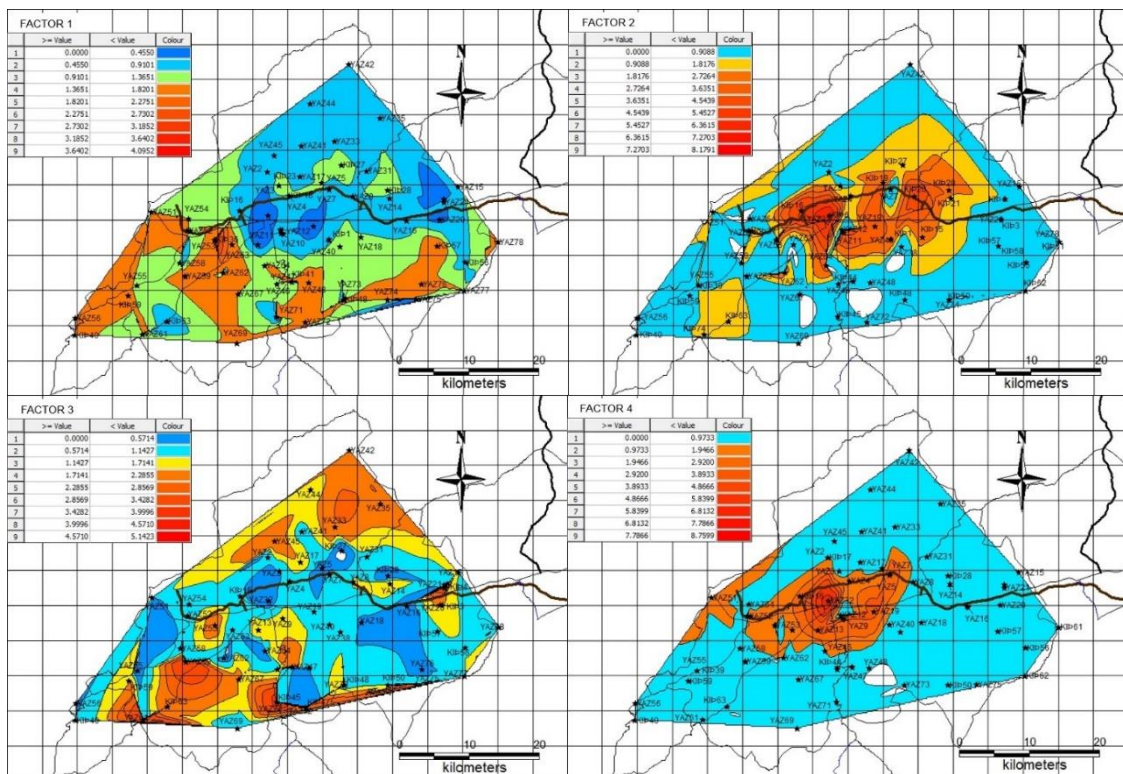


Figure 4. Passive sampling G-score distribution maps

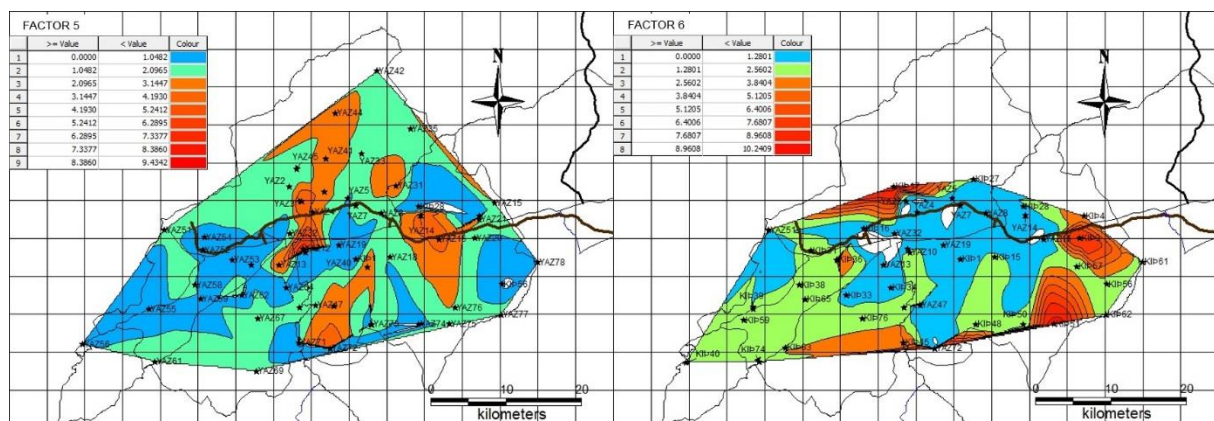


Figure 4. Continued

4. Conclusions

The atmospheric VOC concentrations sampled in Bolu plateau in winter and summer seasons, were used to investigate their spatial distribution, temporal variation, possible sources and ozone production capacities. Benzaldehyde, toluene, benzene, acetophenone, isoprene and alpha-pinene were found as the VOCs with higher atmospheric concentrations. While anthropogenic VOC concentrations were obtained in regions with heavy traffic and dense population, biogenic VOC levels were found to be high in rural and forestry regions. There was a distinct seasonal trend of variation in the VOC concentrations. VOC levels were found to be lower in summer than winter season. However, biogenic VOCs showed higher percentage and variety in summer season. Solvent evaporation, wood-coal combustion, biogenic emission (pine / grain / grass), city atmosphere, biogenic emission (hornbeam / pine / juniper) and vehicle emissions were determined as the main VOC sources. Correlations between VOCs and ozone revealed that isoprene, n-hexane, beta-pinene, alpha-pinene, 2-methylfuran, benzene, crotonaldehyde, toluene, m+p xylene, limonene, p-cymene, n-propylbenzene, camphene, camphor, styrene and naphthalene were important contributors for ozone.

5. References

- Aydin, Y.M., Yaman, B., Koca, H., Dasedemir, O., Kara, M., Altiok, H., Dumanoglu, Y., Bayram, A., Tolunay, D., Odabasi, M., Elbir, T., 2014. Biogenic Volatile Organic Compound (BVOC) Emissions from Forested Areas in Turkey: Determination of Specific Emission Rates for Thirty-one Tree Species. *Sci. Total. Environ.* 490, 239-253.
- Baklanov, A., Molina, L.T., Gauss, M., 2016. Megacities, air quality and climate. *Atmos. Environ.* 126, 235-249.
- Bolu Environmental Status Report, 2016. <http://www.bolukulturturizm.gov.tr/TR-70000/yedigoller-milli-parki.html>, accessed in 2019.
- Bozkurt, Z., Uzmez, O.O., Dogeroglu, T., Artun, G., Gaga, E.O., 2018. Atmospheric concentrations of SO₂, NO₂, ozone and VOCs in Duzce, Turkey using passive air samplers: sources, spatial and seasonal variations and health risk estimation. *Atmos. Pollut. Res.* 9, 1146-1156.
- de Albuquerque, É.L., Tomaz, E., de Lima Tresmondi, A.C.C., 2012. VOCs Concentrations at Metropolitan Area of São Paulo, Brazil. In Proceedings of the Air and Waste Management Association's Annual Conference and Exhibition, AWMA.



Dumanoglu, Y., Kara, M., Altiok, H., Odabasi, M., Elbir, T., Bayram, A., 2014. Spatial and seasonal variation and source apportionment of volatile organic compounds (VOCs) in a heavily industrialized region. *Atmos. Environ.* 98, 168-178.

EPA, 2000 – Phenol (108-95-02) –Acetophenone (98-86-2).

Forest Atlas, <https://www.ogm.gov.tr/ekutuphane/Yayinlar/Orman%20Atlasi.pdf>, accessed in 2017

Gulia, S., Nagendra, S.M.S., Khare, Mukesh, Khanna, I., 2015. Urban air quality management–A review. *Atmos. Pollut. Res.* 6, 286-304.

Ismail, O.M.S., Hameed, R.S.A., 2013. Environmental Effects of Volatile Organic Compounds on Ozone Layer. *Adv. Appl. Sci.Res.* 4, 264-268.

Kjellstrom, T., Friel, S., Dixon, J., Corvalan, C., Rehfuess, E., Campbell-Lendrum, D., Gore, F., Bartram, J., 2007. Urban environmental health hazards and health equity. *J. Urban Health.* 84, 86-97.

Liu, Y., Shao, M., Fu, L., Lu, S., Zeng, L., Tang, D., 2008. Source profiles of volatile organic compounds (VOCs) measured in China: Part I. *Atmos. Environ.* 42, 6247-6260.

Moore, M., Gould, P., Keary, B.S., 2003. Global urbanization and impact on health. *Int. J. Hyg. Environ. Health.* 206, 269-278.

Norris, G., Duvall, R., 2014. EPA Positive Matrix Factorization (PMF) 5.0 Fundamentals and User Guide, U.S. Environmental Protection Agency Office of Research and Development Washington, DC 20460.

Norris, G.A., Duvall, R., Brown, S.G., Bai, S., 2014. EPA Positive Matrix Factorization (PMF) 5.0 fundamentals and User Guide Prepared for the US Environmental Protection Agency Office of Research and Development, Washington, DC.

Nunes, T., Poceiro, C., Evtyugina, M., Duarte, M., Borrego, C., Lopes, M., 2013. Mapping anthropogenic and natural volatile organic compounds around Estarreja Chemical Industrial Complex. *WIT Transactions on Ecology and the Environment*, 174, 55-64.

World Health Organization (WHO), 1983. Environmental Health Criteria, No. 26, Styrene, Geneva.

Wildt, J., Kobel, K., Schuh-Thomas, G., Heiden, A.C., 2003. Emissions of oxygenated volatile organic compounds from plants Part II: emissions of saturated aldehydes. *J. Atmos. Chem.* 45, 173-196.

Yurdakul, S., Civan, M., Ozden, O., Gaga, E., Dogeroglu, T., Tuncel, G., 2017. Spatial variation of VOCs and inorganic pollutants in a university building. *Atmos. Pollut. Res.* 8, 1-12.

Acknowledgments

This study was financially supported by TUBITAK [project number 114Y632] and Bolu Abant İzzet Baysal University Coordination Unit of Scientific Research Projects [project number 2015.03.03.891]. The authors would also like to thank to Duran Karakas, Hatice Karadeniz, Akif Arı, Pelin Erturk Arı, Ercan Berberler, Tugce Demir Berberler, Melike Busra Bayramoglu Karsi, Sait Karsi and Esra Magat Turk for their helps in the sampling campaigns.

Carbon content in PM_{2.5} at a coastal measuring site in Croatia

**Ranka Godec, Iva Simić, Martina Silović Hujčić, Ivan Bešlić, Silvije Davila
and Martin Mihaljević**

Institute for Medical Research and Occupational Health, 10000 Zagreb, Croatia

rgodec@imi.hr

Abstract. Rijeka is the principal seaport and third largest city in Croatia. The city's economy largely depends on shipbuilding and maritime transport. Rijeka has a humid subtropical climate with warm summers and relatively mild winters with frequent rainfall and cold (bura) winds. This study is the first on particulate matter with an equivalent aerodynamic diameter smaller than 2.5 μm (PM_{2.5}) and the carbon content in it at a coastal urban background station. Mass concentrations of elemental (EC), organic (OC) and total carbon (TC) were investigated from January 1st 2017 to August 31st 2019. Sampling was conducted during 24-hour periods from approximately 55 m³ of ambient air on quartz fibre filters pre-fired at 850°C for 3 hours. Mass concentrations of 973 PM_{2.5} samples were determined gravimetrically according to the standard EN 12341:2014. Carbon content was measured by the thermal-optical transmittance method (TOT) using a carbon aerosol analyser with a flame ionization detector and EUSAAR_2 temperature program operating according to the standard EN 16909:2017. The average PM_{2.5} mass concentration (11.1 $\mu\text{g m}^{-3}$) did not exceed the limit value of 25 $\mu\text{g m}^{-3}$ and the maximum was observed in winter (51.3 $\mu\text{g m}^{-3}$). Carbon mass concentrations revealed strong seasonality having its low in summer and high in winter. The average OC/EC mass ratio values of around 6.6 pointed to the influence of secondary organic aerosols. Average TC mass contribution to the total PM_{2.5} mass was 33 %, of which 20 % SOC (secondary OC), 7 % POC (primary OC) and 5 % EC. The high mass contribution of SOC to total OC mass (as much as 74 %) can be explained by the warm climate suitable for photochemical reactions and the formation of SOC from sea spray.

Keywords: EC, OC, OC/EC ratio, POC and SOC.

1. Introduction

1.1. Particulate matter

The term particulate matter (PM) is a general term used for particles suspended in air for longer periods, from several hours to several weeks, even months, caused by various natural or anthropogenic activities. Atmospheric particles originate from primary and secondary sources. Primary particles are those emitted directly from the source, while secondary particles are formed in the atmosphere from gases emitted directly from the source (Pöschl, 2005). PM is characterized according to size, composition, shape, colour, number and balance between the gaseous and particle phase (Šega, 2004).

An individual particle: a small unit of matter, of a regular shape with a density approximately equal to the intrinsic density of the substance from which it is made.

Aggregate: A group of individual particles held together by molecular forces. When moving, they behave like single particles.

Agglomerate: A group of individual particles held together by weaker forces of adhesion and cohesion.

Flocculants: A group of even weaker-bound individual particles that easily break by shaking or shuffling. When moving, it behaves very differently from individual particles.

Fibres: natural (biological or mineral origin) or artificial origin. The following conditions must be satisfied to define the particle as a fiber: $L > 5 \mu\text{m}$ and $L / D > 3$ (Figure 1).

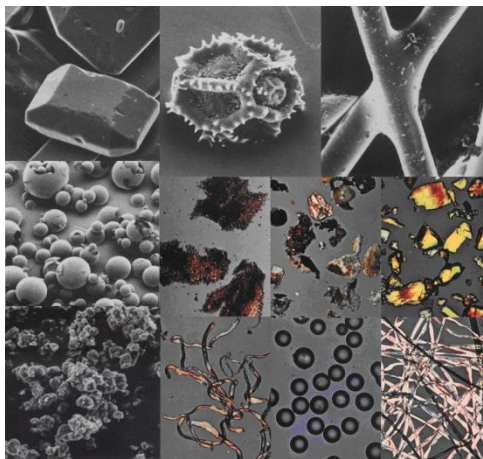


Figure 1. Different types of particulate matter (Šega, 2004)

The harmful action of PM on human health can originate from minor irritation of the upper respiratory tract to chronic respiratory and cardiovascular diseases, lung cancer, and acute respiratory infections in children and chronic bronchitis in adults, aggravating existing heart and lung diseases, or asthmatic seizures (Beugnet and Chalvet-Monfray, 2013; Wu et al., 2016; Bhardawaj et al., 2017; Camatini et al., 2016; Honda et al., 2017; Liang and Gong, 2017; Liu et al., 2017; Malley et al., 2017; Rivas et al., 2017; Segersson et al., 2017; Tobías et al., 2018).

1.2. Carbon in particles

The main forms of carbon in particulate matter are elemental carbon (EC), organic carbon (OC) and carbonate carbon (CC). EC is a visible component of the PM which is inert, non-volatile, insoluble under atmospheric conditions and may be called soot, black carbon (BC) or carbon that absorbs light (LAC) depending which type of analyses is used for its determination. EC has a large specific surface with adsorbed polluting gases and particles on it. These gases and particles may have carcinogenic and mutagenic properties and that is why we investigate EC; because of its potential harmful effects on human health and the environment. EC is a primary pollutant and it is all directly emitted into the atmosphere from various natural and anthropogenic sources, for example: incomplete combustion of fossil and biomass fuels, biomass burning, industrial processes, forest fires, etc. Unlike EC, OC is a fraction of organic matter which is complex and contains hundreds of organic compounds that may have mutagenic and carcinogenic properties. OC can be primary (POC) and secondary (SOC). Sources of primary OC are natural (photochemical oxidation of gaseous organic precursors, emissions of plant, spores and pollen, forest fires, volcanic eruptions) and anthropogenic (combustion of fossil fuels and biomass, etc.). Secondary OC is made by conversion of gaseous pollutants in the air and the condensation of organic compounds onto pre-existing particles (Kumagai et al., 2009; Mkoma et al., 2010; Pio et al., 2011; Park et al., 2012; Karanasiou et al., 2015; Wu and Yu, 2016) (Figure 2).

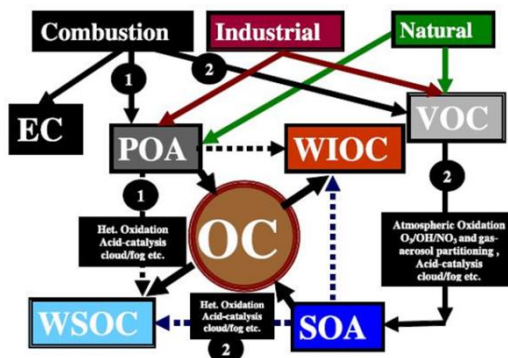


Figure 2. Mechanisms of sources of EC, OC, primary organic aerosol (POA,) secondary organic aerosol (SOA), water soluble (WSOC) and water insoluble organic carbon (WIOC) in the atmosphere (Pathak et al., 2011)

The purpose of this study was to determine and observe if carbon mass contributions to overall PM_{2.5} mass, as well as whether elemental and organic mass concentrations change with seasons and years. Furthermore, this was the first time measurements of EC and OC as well as calculations of POC and SOC were carried out at a coastal urban background site in Croatia.

2. Materials and methods

2.1. Sampling site

Rijeka is the principal seaport and third largest city in Croatia (after Zagreb and Split). It is located in the Primorje-Gorski Kotar County on Kvarner Bay, an inlet of the Adriatic Sea and has a population of about 130000 inhabitants on 44 square km with density about 2923 people per km². Rijeka is the main city and county seat of the Primorje-Gorski Kotar County and is located in western Croatia, 131 kilometres (81 miles) southwest of the capital, Zagreb, on the coast of Kvarner Gulf, in the northern part of the Adriatic Sea. Geographically, Rijeka is roughly equally distant from Milan (485 km), Budapest (502 km), Munich (516 km), Vienna (516 km) and Belgrade (550 km). The Bay of Rijeka, which is bordered by Vela Vrata (between Istria and the island of Cres), Srednja Vrata (between Cres and Krk Island) and Mala Vrata (between Krk and the mainland) is connected to the Kvarner Gulf and is deep enough (about fifty metres) to accommodate large commercial ships. The City of Rijeka lies at the mouth of river Rječina and in the Vinodol micro-region of the Croatian coast. Two important land transport routes start in Rijeka due to its location. The first route is to the Pannonian Basin given that Rijeka is located alongside the narrowest point of the Dinaric Alps (about fifty kilometres). The other route, across Postojna Gate connects Rijeka with Slovenia, Italy and beyond. The city's economy largely depends on shipbuilding and maritime transport. The terrain configuration, with mountains rising steeply just a few kilometres inland from the shores of the Adriatic, provides for some striking climatic and landscape contrasts within a small geographic area. Beaches can be enjoyed throughout summer in a typically Mediterranean setting along the coastal areas of the city to the east (Pećine, Kostrena) and west (Kantrida, Preluk). At the same time, the ski resort of Platak, located only about 10 kilometres from the city, offers alpine skiing and abundant snow during winter months (at times until early May). The Kvarner Bay and its islands are visible from the ski slopes. Rijeka has a humid subtropical climate with warm summers and relatively mild winters with frequent rainfall and cold (bura) winds. The sampling site was located near the historical city center of Rijeka (N: 45° 19' 14.86"; E: 14° 29' 0.64") and altitude of 109 m and as such this station was classified as an urban background sampling site. Meteorological parameters (temperature, relative humidity, wind speed and direction, pressure and precipitation) are obtained from the Croatian Meteorological and Hydrological Service.



Figure 3. Location of Rijeka and sampling site in Rijeka

2.2. Sampling and $PM_{2.5}$ mass concentrations

A sequential low-volume reference sampler SEQ47 / 50 (Sven Leckel Ingenieurbüro, Berlin, Germany) equipped with a $PM_{2.5}$ cut off inlet situated on a building roof, at approximately 5 m horizontal distance from the sidewalk, was used for sample collection. The $PM_{2.5}$ samples were collected during 24 hours every day from January 1st 2017 to August 31st 2019, from approximately 55 m³ of ambient air. Quartz fiber filters (Pallflex Tissuquartz 2500QAT-UP, Pall Life Science, 47 mm) pre-fired at 850 °C for three hours in a furnace to reduce carbon content in filters before collecting $PM_{2.5}$ were used. The $PM_{2.5}$ mass concentrations were determined gravimetrically according to the EN 12341:2014 standard, meaning that filter conditioning and weighing were carried out under conditions of constant temperature (20 ± 1) °C and relative humidity (50 ± 5) %. For filter weighing, Mettler Toledo MX 5 and XP6/M microbalances with resolution of 10^{-6} g and electrostatic charge outflow systems that eliminate static electricity were used. Blanks were analyzed one per each 14 samples, always from the same batch of pre-fired filters, and passed the same procedure of conditioning and weighing. After weighing, the filters were stored in the fridge at 4°C until analysis.

2.3. Carbon analyses

Organic carbon and elemental carbon in $PM_{2.5}$ fraction were determined by thermal-optical transmittance method (TOT), using a Carbon Aerosol Analyzer (Sunset Laboratory Inc.) described by Birch and Cary, 1996; Godec et al., 2016, 2012. Recently, within the framework of the EU-project EUSAAR (European Supersites for Atmospheric Aerosol Research, www.eusaar.net), the thermal-optical analysis protocol EUSAAR_2 was developed (using transmittance for charring correction) for European regional background sites (EMEP network) in order to improve the accuracy of the discrimination between OC and EC. The EUSAAR_2 temperature program is the latest protocol, and it was established so that Europe could standardize analysing techniques and as such is prescribed in the standard EN 16909:2017. The use of lower temperature steps in the He-mode and longer residence times aimed at the reduction of pyrolysis and at a more complete evolution of OC. To ensure QA/QC and prove the consistent operation of the instrument, an inner standard, external sucrose aqueous solution and cross method procedure were used. The results of recovery ranged between 98 % and 102 % with relative standard deviation $RSD < 5$ %. The detection limits expressed in $\mu\text{g m}^{-3}$ in 55 m³ of air were 0.002 $\mu\text{g m}^{-3}$ for EC and 0.04 $\mu\text{g m}^{-3}$ for OC.

3. Results and discussion

Table 1 presents the statistical parameters of the $PM_{2.5}$, EC, and OC (POC and SOC) ratio for the monitoring site in Rijeka from January 1st 2017 to August 31st 2019. Yearly averages of $PM_{2.5}$ mass concentrations were all under the yearly average limit value of 25 $\mu\text{g m}^{-3}$ prescribed by the Directive 2008/50/EC of the European Parliament and of the Council (21st May 2008), and Commission Directive

2015/1480, (28th August 2015), but 35 exceedances were noticed mostly during winter and autumn. The EC and OC mass concentrations determined in Rijeka are comparable with those found in literature for Europe especially for Mediterranean area (Custódio et al., 2016; Jedynska et al., 2014; Khan et al., 2016; Merico et al., 2019; Salma et al., 2004; Viana et al., 2007; Viidanoja et al., 2002).

Table 1. Statistical parameters for PM_{2.5} and carbon species concentrations ($\mu\text{g m}^{-3}$) at the monitoring site in site in Rijeka during the measuring period from January 1st 2017 to August 31st 2019

Statistical parameters	PM _{2.5}	EC	OC	SOC	POC
N	973	973	973	971	973
$\bar{\gamma}$	11.1	0.5	2.9	2.2	0.7
σ_{γ}	6.3	0.3	1.6	1.4	0.4
γ_{min}	1.4	0.0	0.3	0.1	0.0
γ_{25}	6.8	0.3	1.8	1.2	0.4
γ_{50}	9.9	0.4	2.6	2.0	0.6
γ_{75}	13.8	0.6	3.5	2.8	0.8
γ_{max}	51.3	2.1	10.9	8.5	2.9

$\bar{\gamma}$ - average, σ_{γ} - standard deviation, γ_{min} - minimum measured value, γ_{25} - 1st quartile, γ_{50} - median, γ_{75} - 3rd quartile, γ_{max} - maximum measured value, PM_{2.5} - particle matter with an aerodynamic diameter smaller than 2.5 μm , EC - elemental carbon, OC - organic carbon, POC - primary organic carbon, SOC - secondary organic carbon

Figure 4 presented EC and POC mass concentrations for each season at the Rijeka measuring station during the whole sampling period and it shows that during summer POC and EC came from the same source of pollution - traffic. During winter, the POC mass concentrations were twice higher than the EC mass concentrations which indicates another source for POC except traffic.

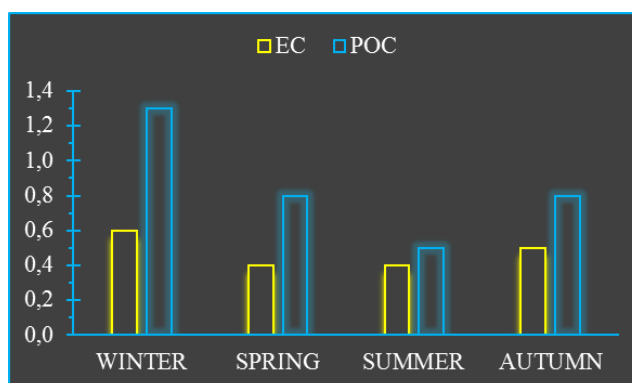


Figure 4. EC and POC mass concentrations ($\mu\text{g m}^{-3}$) for each season at Rijeka during the whole sampling period

Table 2 presents the average and minimum values of OC/EC mass concentration ratio for each season at the Rijeka monitoring site from January 1st 2017 to August 31st 2019. All averages were above 3, which indicates the presence of SOC. SOC was calculated with a minimum OC/EC ratio for each season as described by Castro et al., (1999). Seasonal minimum values of OC/EC mass concentration ratio were lower for warmer period but similar to colder period than those measured at similar place in Southern Italy (Merico et al., 2019). Comparison of POC and COS mass concentrations between different years

of sampling (Figure 5) showed that yearly averages for POC followed the sequence: 2019>2017>2018, while yearly averages for SOC followed the sequence: 2018> 2017>2019.

Table 2. Average and minimum values of OC/EC mass concentration ratio for each season at the monitoring site in Rijeka during the measuring period from January 1st 2017 to August 31st 2019

Statistical parameters	spring	summer	autumn	winter
\bar{x}	6.6	7.9	5.5	6.2
x_{min}	1.8	1.4	1.4	2.1

\bar{x} – average OC/EC ratio, x_{min} – minimum value of OC/EC ratio

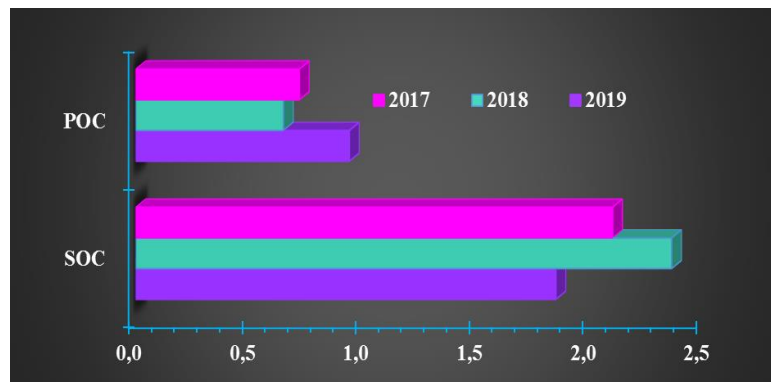


Figure 5. POC and SOC mass concentrations ($\mu\text{g m}^{-3}$) for each sampling year at Rijeka

Seasonal contributions of EC, OC, POC and SOC fractions to the total $\text{PM}_{2.5}$ mass are shown in Figure 6. The highest OC contribution to the total $\text{PM}_{2.5}$ mass was noticed in winter > autumn > summer while the lowest in spring, as expected. EC mass contributions were lowest in summer and spring and were the same, which was not to be expected, and the highest was noticed in autumn. POC mass contribution to total $\text{PM}_{2.5}$ mass was the same in summer and spring, highest in winter, while SOC mass contribution to the total $\text{PM}_{2.5}$ mass was the same in summer and autumn, and lowest in spring. Yearly averages of EC and OC mass contribution to the total $\text{PM}_{2.5}$ mass show slightly downward trend thru years and are similar with those measured in Mediterranean area (Cesari et al., 2018).

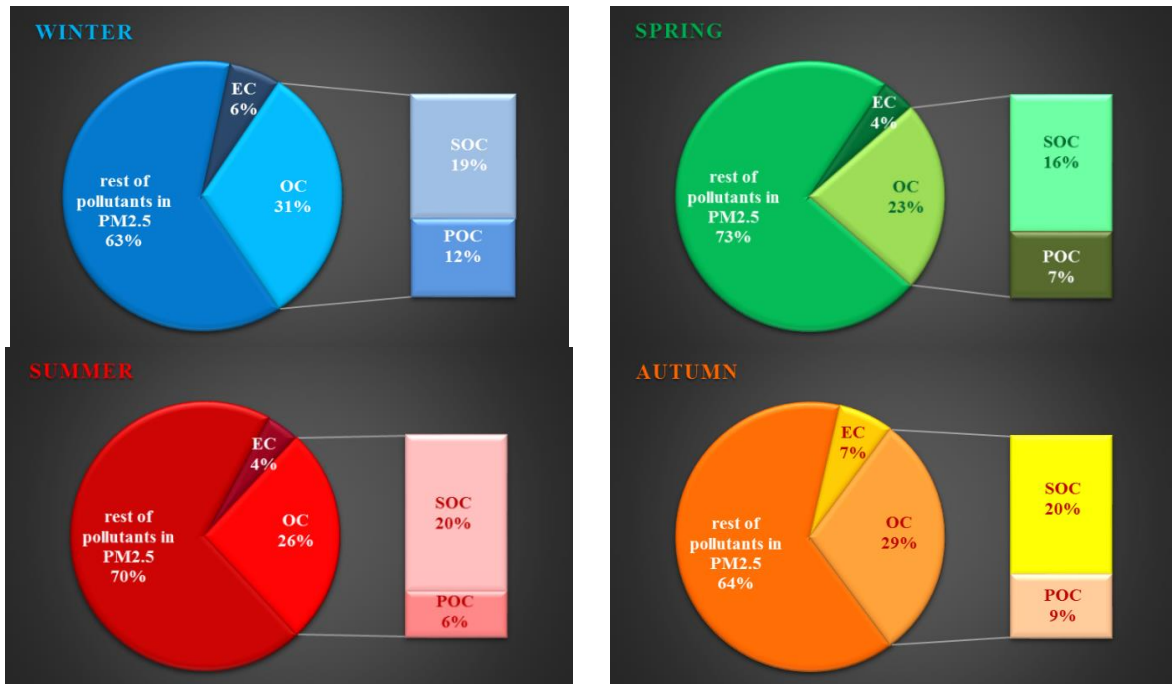


Figure 6. EC and OC mass contribution to the total PM_{2.5} mass in each season during the entire measuring period at Rijeka

Wind roses for PM_{2.5}, EC and OC pollutants showed that pollution came from NW to ENE directions and from SSW to ESE directions (Figure 7). Average wind velocity was 2.5 m s⁻¹ and the most frequent direction was SSE.

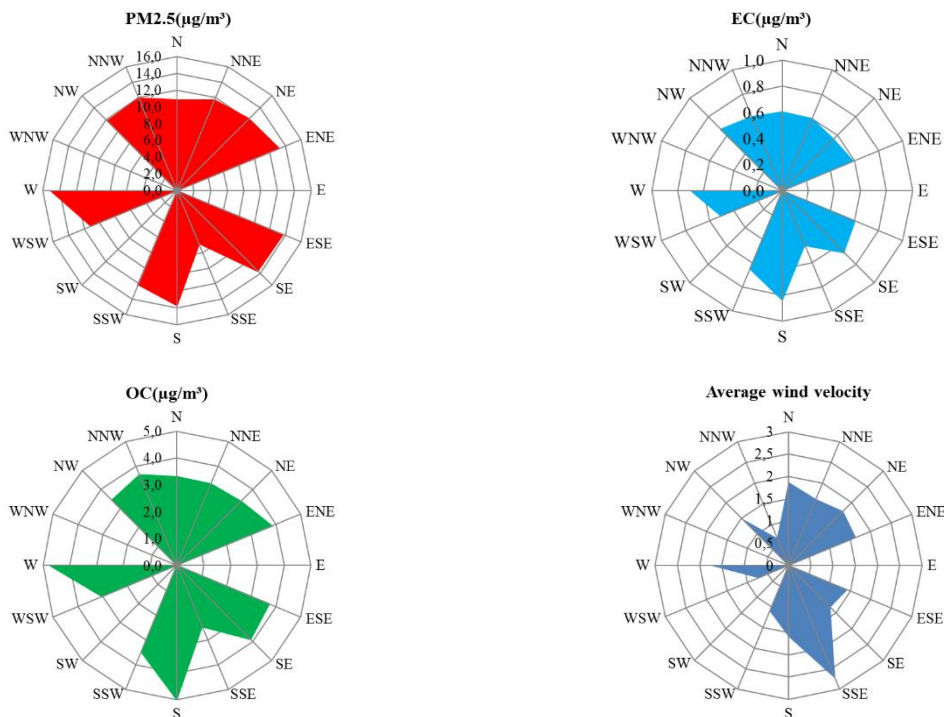


Figure 7. Wind roses for PM_{2.5}, EC and OC mass concentrations and average wind velocity during the entire measuring period at Rijeka

When higher PM_{2.5}, OC and SOC mass concentrations were determined, the trajectories showed that pollutants came from long transport even across the Atlantic Ocean, while for EC mass concentrations trajectories showed that pollution came mostly from Europe and Africa (Figure 8). Trajectories were made for 72 hours back at an altitude of 1500 meters. According to the HYSPLIT model, maximum altitude for trajectories were at 8348 m, with an average altitude of 1656 m.

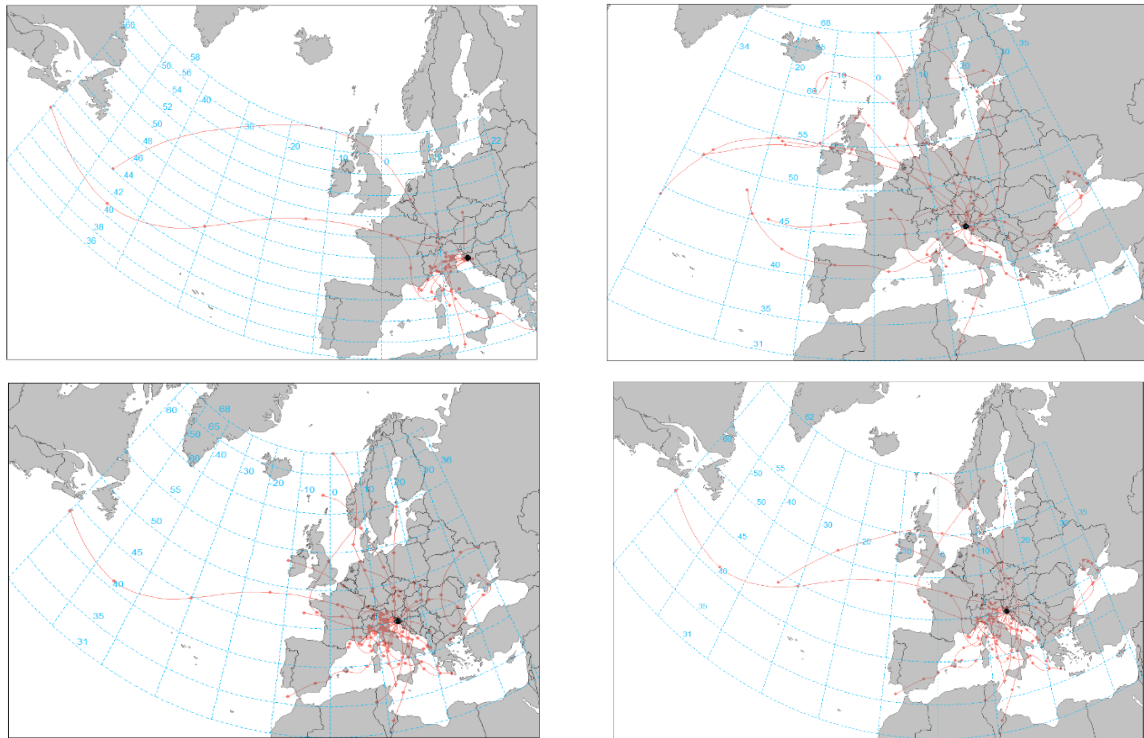


Figure 8. PM_{2.5}, EC, SOC and OC trajectories during the entire measuring period at Rijeka

4. Conclusions

During the measuring period from January 1st 2017 to August 31st 2019, yearly averages of PM_{2.5} mass concentrations were all under the yearly average limit value of 25 µg m⁻³ but 35 exceedances were noticed, mostly during winter and autumn. During summer, POC and EC came from the same source of pollution – traffic, while during winter period POC mass concentrations were twice higher than EC mass concentrations which indicates another source for POC except traffic. EC and OC mass contribution to total PM_{2.5} mass showed a slightly downward trend during the years. SOC mass contribution to the total PM_{2.5} mass was the same (20%) in summer and autumn, while EC mass contribution was lowest in summer and spring and was also the same (4%), which was not expected. All measured pollutants were at this urban background coastal site were similar with those measured in Mediterranean area. Wind roses for PM_{2.5}, EC and OC pollutants showed that pollution came from NW to ENE directions and from SSW to ESE directions. Trajectories showed that higher PM_{2.5}, OC and SOC mass concentrations came from long transport across the Atlantic Ocean, while trajectories for higher EC mass concentrations showed that pollution came mostly from Europe and Africa.

5. References

Beugnet, F., Chalvet-Monfray, K., 2013. Impact of climate change in the epidemiology of vector-borne diseases in domestic carnivores. *Comp. Immunol. Microbiol. Infect. Dis.* 36, 559–566. doi:10.1016/j.cimid.2013.07.003.



- Bhardawaj, A., Habib, G., Kumar, A., Singh, S., Nema, A.K., 2017. A review of ultrafine particle-related pollution during vehicular motion, health effects and control. *J. Environ. Sci. Public Heal.* 1, 268–288. doi:10.26502/JESPH.024.
- Birch, M.E., Cary, R.A., 1996. Elemental Carbon-Based Method for Monitoring Occupational Exposures to Particulate Diesel Exhaust. *Aerosol Sci. Technol.* 25, 221–241. doi:10.1080/02786829608965393.
- Camatini, M., Gualtieri, M., Sancini, G., 2016. Impact of the airborne particulate matter on the human health, in: *Atmospheric Aerosols: Life Cycles and Effects on Air Quality and Climate.* doi:10.1002/9783527336449.ch10.
- Castro, L.M., Pio, C. a., Harrison, R.M., Smith, D.J.T., 1999. Carbonaceous aerosol in urban and rural European atmospheres: Estimation of secondary organic carbon concentrations. *Atmos. Environ.* 33, 2771–2781. doi:10.1016/S1352-2310(98)00331-8.
- Cesari, D., De Benedetto, G.E., Bonasoni, P., Busetto, M., Dinoi, A., Merico, E., Chirizzi, D., Cristofanelli, P., Donato, A., Grasso, F.M., Marinoni, A., Pennetta, A., Contini, D., 2018. Seasonal variability of PM_{2.5} and PM₁₀ composition and sources in an urban background site in Southern Italy. *Sci. Total Environ.* 612, 202–213. doi:10.1016/j.scitotenv.2017.08.230.
- Custódio, D., Cerqueira, M., Alves, C., Nunes, T., Pio, C., Esteves, V., 2016. A one-year record of carbonaceous components and major ions in aerosols from an urban kerbside location in Oporto, Portugal. *Science of the Total Environment A one-year record of carbonaceous components and major ions in aerosols from an urban kerbside lo.* *Sci. Total Environ.* 562, 822–833. doi:10.1016/j.scitotenv.2016.04.012.
- Godec, R., Čačković, M., Šega, K., Bešlić, I., Bešlić, I., 2012. Winter mass concentrations of carbon species in PM₁₀, PM_{2.5} and PM₁ in Zagreb Air, Croatia. *Bull. Environ. Contam. Toxicol.* 89, 1087–1090. doi:10.1007/s00128-012-0787-4.
- Godec, R., Jakovljević, I., Šega, K., Čačković, M., Bešlić, I., Davila, S., Pehnc, G., 2016. Carbon species in PM₁₀ particle fraction at different monitoring sites. *Environ. Pollut.* 216, 700–710. doi:10.1016/j.envpol.2016.06.034.
- Honda, T., Pun, V.C., Manjourides, J., Suh, H., 2017. Anemia prevalence and hemoglobin levels are associated with long-term exposure to air pollution in an older population. *Environ. Int.* 101, 125–132. doi:10.1016/j.envint.2017.01.017.
- Jedynska, A., Hoek, G., Eeftens, M., Cyrus, J., Keuken, M., Ampe, C., Beelen, R., Cesaroni, G., Forastiere, F., Cirach, M., de Hoogh, K., De Nazelle, A., Madsen, C., Declercq, C., Eriksen, K.T., Katsouyanni, K., Akhlaghi, H.M., Lanki, T., Meliefste, K., Nieuwenhuijsen, M., Oldenwening, M., Pennanen, A., Raaschou-Nielsen, O., Brunekreef, B., Kooter, I.M., 2014. Spatial variations of PAH, hopanes/steranes and EC/OC concentrations within and between European study areas. *Atmos. Environ.* 87, 239–248. doi:10.1016/j.atmosenv.2014.01.026.
- Karanasiou, A., Minguillón, M.C., Viana, M., Alastuey, A., Putaud, J.-P., Maenhaut, W., Panteliadis, P., Močnik, G., Favez, O., Kuhlbusch, T.A.J., 2015. Thermal-optical analysis for the measurement of elemental carbon (EC) and organic carbon (OC) in ambient air a literature review. *Atmos. Meas. Tech. Discuss* 8, 9649–9712. doi:10.5194/amtd-8-9649-2015.



- Khan, M.B., Masiol, M., Formenton, G., Di Gilio, A., de Gennaro, G., Agostinelli, C., Pavoni, B., 2016. Carbonaceous PM_{2.5} and secondary organic aerosol across the Veneto region (NE Italy). *Sci. Total Environ.* 542, 172–181. doi:10.1016/j.scitotenv.2015.10.103.
- Kumagai, K., Iijima, A., Tago, H., Tomioka, A., Kozawa, K., Sakamoto, K., 2009. Seasonal characteristics of water-soluble organic carbon in atmospheric particles in the inland Kanto plain, Japan. *Atmos. Environ.* 43, 3345–3351. doi:10.1016/j.atmosenv.2009.04.008.
- Liang, L., Gong, P., 2017. Climate change and human infectious diseases: A synthesis of research findings from global and spatio-temporal perspectives. *Environ. Int.* 103, 99–108. doi:10.1016/j.envint.2017.03.011.
- Liu, L., Urch, B., Szyszkowicz, M., Speck, M., Leingartner, K., Shutt, R., Pelletier, G., Gold, D.R., Scott, J.A., Brook, J.R., Thorne, P.S., Silverman, F.S., 2017. Influence of exposure to coarse, fine and ultrafine urban particulate matter and their biological constituents on neural biomarkers in a randomized controlled crossover study. *Environ. Int.* 101, 89–95. doi:10.1016/j.envint.2017.01.010.
- Malley, C.S., Kuylenstierna, J.C.I., Vallack, H.W., Henze, D.K., Blencowe, H., Ashmore, M.R., 2017. Preterm birth associated with maternal fine particulate matter exposure: A global, regional and national assessment. *Environ. Int.* 101, 173–182. doi:10.1016/j.envint.2017.01.023.
- Merico, E., Cesari, D., Dinoi, A., Gambaro, A., Barbaro, E., Guascito, M.R., Giannossa, L.C., Mangone, A., Contini, D., 2019. Inter-comparison of carbon content in PM₁₀ and PM_{2.5} measured with two thermo-optical protocols on samples collected in a Mediterranean site. *Environ. Sci. Pollut. Res.* doi:10.1007/s11356-019-06117-7.
- Mkoma, S.L., Chi, X., Maenhaut, W., 2010. Characteristics of carbonaceous aerosols in ambient PM₁₀ and PM_{2.5} particles in Dar es Salaam, Tanzania. *Sci. Total Environ.* 408, 1308–1314. doi:10.1016/j.scitotenv.2009.10.054.
- Park, S.S., Cho, S.Y., Kim, K.-W.W., Lee, K.-H.H., Jung, K., 2012. Investigation of organic aerosol sources using fractionated water-soluble organic carbon measured at an urban site. *Atmos. Environ.* 55, 64–72. doi:10.1016/j.atmosenv.2012.03.018.
- Pathak, R.K., Wang, T., Ho, K.F., Lee, S.C., 2011. Characteristics of summertime PM_{2.5} organic and elemental carbon in four major Chinese cities: Implications of high acidity for water-soluble organic carbon (WSOC). *Atmos. Environ.* 45, 318–325. doi:10.1016/j.atmosenv.2010.10.021.
- Pio, C., Cerqueira, M., Harrison, R.M., Nunes, T., Mirante, F., Alves, C., Oliveira, C., Sanchez de la Campa, A., Artíñano, B., Matos, M., 2011. OC/EC ratio observations in Europe: Re-thinking the approach for apportionment between primary and secondary organic carbon. *Atmos. Environ.* 45, 6121–6132. doi:10.1016/j.atmosenv.2011.08.045.
- Pöschl, U., 2005. Atmospheric Aerosols: Composition, Transformation, Climate and Health Effects. *Angew. Chemie Int. Ed.* 44, 7520–7540. doi:10.1002/anie.200501122.
- Rivas, I., Kumar, P., Hagen-Zanker, A., 2017. Exposure to air pollutants during commuting in London: Are there inequalities among different socio-economic groups? *Environ. Int.* 101, 143–157. doi:10.1016/j.envint.2017.01.019.
- Salma, I., Chi, X., Maenhaut, W., 2004. Elemental and organic carbon in urban canyon and background environments in Budapest, Hungary. *Atmos. Environ.* 38, 27–36. doi:10.1016/j.atmosenv.2003.09.047.



Šega, K., 2004. Lebdeće čestice. *Gospod. i okoliš* 66, 11–16.

Segersson, D., Eneroth, K., Gidhagen, L., Johansson, C., Omstedt, G., Nylén, A.E., Forsberg, B., 2017. Health impact of PM₁₀, PM_{2.5} and black carbon exposure due to different source sectors in Stockholm, Gothenburg and Umea, Sweden. *Int. J. Environ. Res. Public Health* 14, 11–14. doi:10.3390/ijerph14070742.

Tobías, A., Rivas, I., Reche, C., Alastuey, A., Rodríguez, S., Fernández-Camacho, R., Sánchez de la Campa, A.M., de la Rosa, J., Sunyer, J., Querol, X., 2018. Short-term effects of ultrafine particles on daily mortality by primary vehicle exhaust versus secondary origin in three Spanish cities. *Environ. Int.* 111, 144–151. doi:10.1016/j.envint.2017.11.015.

Viana, M., Maenhaut, W., ten Brink, H.M., Chi, X., Weijers, E., Querol, X., Alastuey, a., Mikuška, P., Večeřa, Z., 2007. Comparative analysis of organic and elemental carbon concentrations in carbonaceous aerosols in three European cities. *Atmos. Environ.* 41, 5972–5983. doi:10.1016/j.atmosenv.2007.03.035.

Viidanoja, J., Sillanpää, M., Laakia, J., Kerminen, V.M., Hillamo, R., Aarnio, P., Koskentalo, T., 2002. Organic and black carbon in PM_{2.5} and PM₁₀: 1 Year of data from an urban site in Helsinki, Finland. *Atmos. Environ.* 36, 3183–3193. doi:10.1016/S1352-2310(02)00205-4.

Wu, C., Yu, J.Z., 2016. Determination of Primary combustion source organic carbon-to-elemental carbon (OC/EC) ratio using ambient OC and EC measurements: Secondary OC-EC correlation minimization method. *Atmos. Chem. Phys. Discuss.* 2, 1–25. doi:10.5194/acp-2015-997.

Wu, X., Lu, Y., Zhou, S., Chen, L., Xu, B., 2016. Impact of climate change on human infectious diseases: Empirical evidence and human adaptation. *Environ. Int.* 86, 14–23. doi:10.1016/j.envint.2015.09.007

PAHs in PM₁ particle fraction at an urban location in Croatia

Ivana Jakovljević, Zdravka Sever Strukil, Ranka Godec and Gordana Pehcec

Institute for Medical Research and Occupational Health, Ksaverska cesta 2, 10000 Zagreb

ijakovljevic@imi.hr

Abstract. Airborne particles are composed of inorganic species and organic compounds. PM₁ particles, with an aerodynamic diameter smaller than 1 µm, are considered to be important in the context of adverse health effects. The mass concentration of particulate matter (PM) is not the only important parameter for the assessment of health risks of atmospheric pollution. Many compounds bound to particulate matter, such as polycyclic aromatic hydrocarbons (PAH), are suspected to be genotoxic, mutagenic and carcinogenic. In this study, PAHs in PM₁ particle fraction were measured during one year (1/1/2018–31/12/2018). The measuring station was located in the northern residential part of Zagreb, the Croatian capital, close to a street with modest traffic. We collected 24-hour samples of PM₁ particle fraction on quartz filters from about 55 m³ air using a low-volume sampler. The analysis was performed using a high performance liquid chromatograph (HPLC) with a fluorescence detector. Significant differences were found between PAH concentrations during cold (January- March, October-December) and warm (April-September) periods of the year. During the cold period, BbF had the highest mass concentrations (0.215–3.412 ng m⁻³), while during the warm period the highest mass concentrations was recorded for BghiP (0.067–0.277 ng m⁻³). During both periods, DahA had the lowest mass concentrations. The average monthly mass concentrations of BaP ranged from 0.038 ng m⁻³ in June to 2.826 ng m⁻³ in December (the annual average was 0.765 ng m⁻³). In general, during the whole year mass concentrations of PAH characteristic for car exhaust (BghiP, IP, BbF) were higher than concentrations of Flu and Pyr, which originate mostly from domestic heating and biomass burning.

Keywords: BaP; HPLC; Carcinogenic; Diagnostic ratio.

1. Introduction

Particle pollution contains “inhalable coarse particles” with diameters larger than 2.5 µm and smaller than 10 µm and “fine particles” with diameters of 2.5 µm or smaller. Particulate matter (PM) is assumed to be the most hazardous of ambient pollutants. One of the most significant organic groups, bound to PM₁, in terms of health risk are polycyclic aromatic hydrocarbons (PAH). These compounds can exist in the atmosphere in the vapour phase (PAHs with low molecular weight), whereas heavier ones (PAHs with high molecular weight) are mostly adsorbed on the particle phase (Ravindra et al., 2008). PAHs generally occur as complex mixture, they are products of the incomplete combustion processes, and originate from natural and anthropogenic sources (ATSDR, 1995). High PAH levels in ambient air of large metropolitan cities are usually associated with traffic, including diesel and gasoline vehicles (Ströher et al., 2007; Ravindra et al., 2008). Catalytic converters have shown a significant effect on reducing levels of the PAH concentration in exhaust gases, but PAH emission levels continue to increase due to the contribution of other sources, such as traffic congestion (Teixeira et al., 2012). PAHs are always emitted as a mixture, and the molecular concentration ratios are considered to be typical of a

given emission source (Tobiszewski and Namieśnik, 2012). The toxicity, carcinogenicity and mutagenicity of aromatic hydrocarbons have led to increased concerns in human populations. Benzo(a)pyrene (BaP) is the most studied PAH and most data on the toxicity and occurrence of PAHs is correlated to this compound, which was why it was used as an indicator of carcinogenic hazard in polluted environments (WHO, 2000; Delgado-Saborit et al., 2011; Wickramasinghe et al., 2011).

The aim of this paper was to measure the levels of mass concentrations of individual PAHs in urban area and determine potential sources of PAH in this area. For this purpose, we needed to calculate the diagnostic ratios of the selected PAHs. Diagnostic ratios are common tools for the identification of pollution sources (Šišović et al., 2012; Fu et al., 2010; Zhang et al., 2004; Yunker et al., 2002). However, some papers have shown their limitations. Katsoyiannis (2011) demonstrated that due to weathering in the environment, variability in degradation processes, photodegradation, and reaction with ozone and other atmospheric pollutant, the diagnostic ratio cannot always be effective as a marker of sources. Because of this, diagnostic ratios were calculated between PAHs of similar molecular mass, to reduce confounding factors such as differences in volatility, water solubility, and adsorption (Dvorská et al., 2011).

2. Materials and methods

2.1. Location and sampling

Concentrations of eleven PAHs in PM₁ particle fraction were measured continuously from January to December, 24-hours a day. The measuring station was located in the northern residential part of Zagreb, the Croatian capital. It is a low-rise residential area with a low population density and modest traffic. Residential heating relies mostly on gas, but some households still use oil or wood for heating and cooking. Samples of PM₁ particles were collected on quartz filters with low-volume sequential automatic sampler (Sven Leckel). The sampler inlet was located approximately 1.5 m above ground and 15 m away from the road. The samples were kept frozen in aluminium foil at -18 °C until analysis to avoid PAH losses and sample degradation.

2.2. Analysis of PAHs

Filters were extracted with a solvent mixture of toluene and cyclohexane (7:3) in an ultrasonic bath for 1 h, separated from undissolved parts by centrifugation (10 min, 3000 rpm), and evaporated to dryness in a mild stream of nitrogen at 30 °C. They were then re-dissolved in acetonitrile. The analysis was performed using a Agilent Infinity 1260 high-performance liquid chromatography (HPLC) with a fluorescence detector. PAHs were separated on a Zorbax Eclipse PAH column (100×4.6 mm). The mobile phase was a mixture of acetonitrile and water (60:40), and the flow rate was 1 mL min⁻¹ (Jakovljević et al., 2015; Šišović et al., 2012). Samples were analysed for the following PAHs: fluoranthene (Flu), pyrene (Pyr), benzo(a)anthracene (BaA), chrysene (Chry), benzo(j)fluoranthene (BjF), benzo(b)fluoranthene (BbF), benzo(k)fluoranthene (BkF), benzo(a)pyrene (BaP), dibenzo(ah)anthracene (DahA), benzo(ghi)perylene (BghiP), and indeno(1,2,3-cd)pyrene (IP).

3. Results and discussion

3.1. PAH concentrations

Measurements of PAH mass concentrations in PM₁ particle fractions showed differences between the cold (January-March; October-December) and warm (April-September) period of the year with the highest values in cold and the lowest concentrations in warm period. (Fig. 1). The highest average mass concentrations during cold period were recorded for BbF (3.412 ng m⁻³), while during the warm period the highest average mass concentration was determined for BghiP (0.277 ng m⁻³). During both the warm and cold period DahA had the lowest mass concentration. The range of 24-h concentrations for DahA was from 0.010 ng m⁻³ (May) to 0.386 ng m⁻³ (December). The average monthly mass concentrations of

BaP ranged from 0.038 ng m⁻³ (June) to 2.826 ng m⁻³ (December), while the annual mass concentrations was 0.765 ng m⁻³. The target value in the European Union set by Directive 2004/107/EC for BaP content in PM₁₀ fraction only is 1 ng m⁻³ averaged over a calendar year. The relevant literature comprises a very limited number of papers relating to PAHs in PM₁ fractions (Agudelo-Castañeda and Teixeira 2014; Rogula-Kozłowska et al., 2013; Wenger et al., 2009). Rogula-Kozłowska et al. (2013) reported a much higher mass concentration of BaP in PM₁ particle fraction during winter seasons in Poland. PAH concentrations determined in the Metropolitan Area of Porto Alegre, Brazil, were much lower during winter but higher during summer (Agudelo-Castañeda and Teixeira, 2014).

Concentrations of PAH characteristic for domestic heating or biomass burning were lower in the cold period than concentrations of PAH characteristic for car exhaust. This indicated that PAH in PM₁ particle fractions was dominantly from car exhausts.

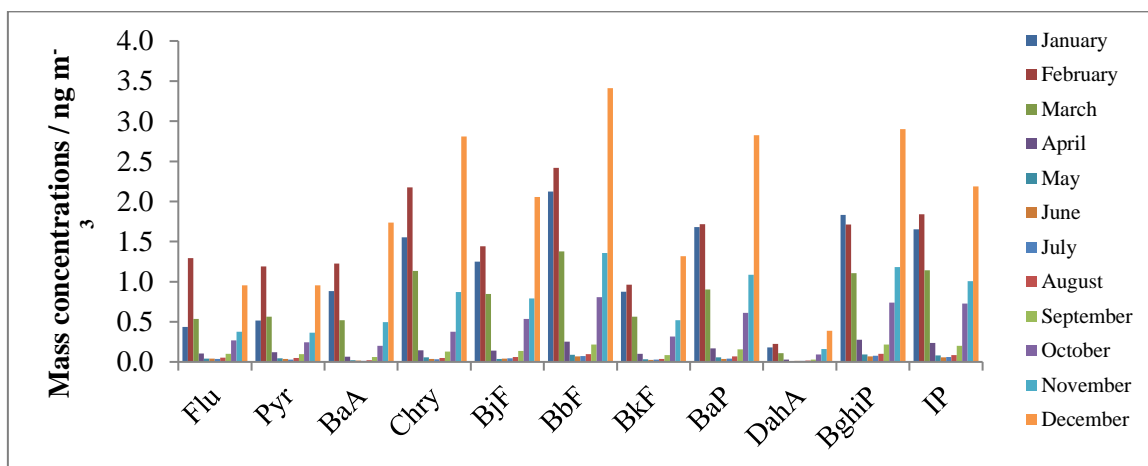


Figure 1. Monthly mass concentrations of PAH measured during one calendar year

PAHs can be classified into two groups: heavy and lighter PAHs. Heavy PAH concentrations was calculated as sum of PAHs with five or more aromatic rings, and lighter PAHs were represented the sum of PAHs with four aromatic rings. Heavy PAHs are usually characteristic for car exhausts, while lighter PAHs originated mostly from domestic heating or biomass burning. During both measured periods, the contributions of heavy PAHs were much higher than those of lighter PAHs (Fig. 2). Fig. 3 shows the monthly mass concentration of these two groups. These results indicated that traffic (diesel or gasoline) was the main pollution source of PAHs in PM₁ in this area. To confirm this we determined the diagnostic ratio to identify possible pollution sources.

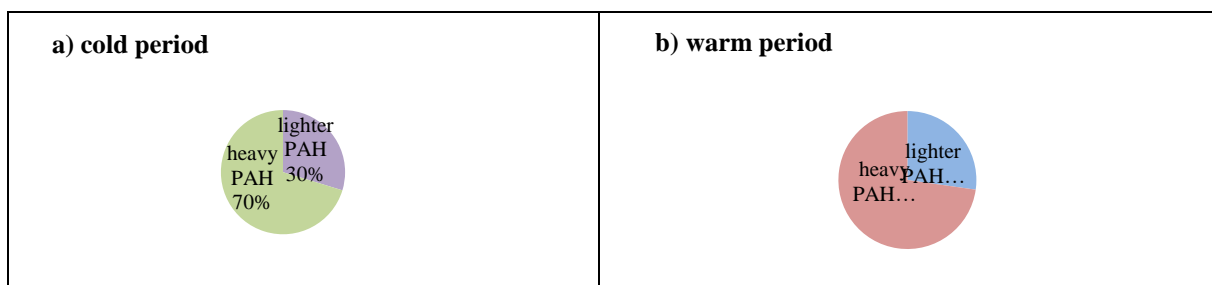


Figure 2. Contribution of lighter and heavy PAH in the sum of measured PAHs during the: a) cold period and b) warm period

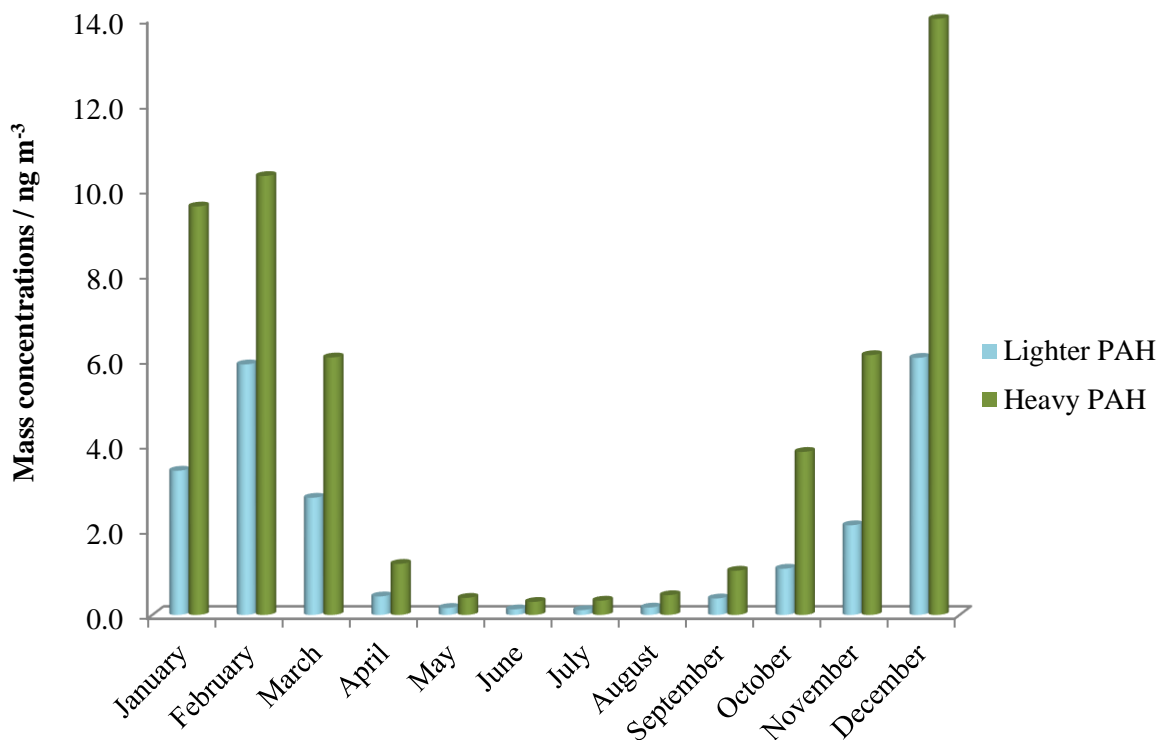


Figure 3. Mass concentrations of lighter and heavy PAHs measured during one calendar year

3.2. Diagnostic ratios

Many authors used diagnostic ratios of PAHs to identify potential pollution sources (Šišović et al., 2012; Fu et al., 2010; Zhang et al., 2004; Yunker et al., 2002). The values determined in this study were compared with the same diagnostic ratios computed from the characterized emission sources based on literature. IP/ (IP+BghiP) ratio values between 0.35 and 0.7 are characteristic for diesel, while a value of 0.56 indicates coal combustion (Agudelo-Castañeda and Teixeira 2014). BaP/BghiP values between 0.3 and 0.4 are characteristic for traffic, 0.46–0.81 for diesel combustion, and 0.9–6.6 for coal combustion (Agudelo-Castañeda and Teixeira, 2014; Hanedar et al., 2014; Fu et al., 2010). A Flu/(Flu+Pyr) ratio between 0.2 and 0.5 indicates diesel, a ratio between 0.4 and 0.5 liquid fossil fuel, while a ratio >0.5 suggests wood combustion (Zhang et al., 2004; Yunker et al., 2002). Finally, a BaP/ (BaP+Chry) ratio of <0.5 indicated diesel, but > 0.5 gasoline (Agudelo-Castañeda and Teixeira, 2014; Teixeira et al., 2012).

In this paper, the average IP/ (IP+BghiP) ratios were 0.5 during all seasons indicating that the PAHs produced stemmed from the emission of diesel vehicles. The mean of the BaP/ (BaP+Chry) and Flu/(Flu+Pyr) ratios were 0.5 during all seasons except ratio BaP/(BaP+Chry) in autumn, which was 0.6. All values for these ratios indicated the influence of emissions from gasoline or diesel vehicles. The BaP/BghiP ratio ranged from 0.6 in summer and spring to 0.9 in winter. Also in all seasons, the value was characteristic for emission from diesel (Table 1). Similar results were reported by Agudelo-Castañeda and Teixeira (2014) and Hanedar et al. (2014). They also found that PAH in PM₁ originated from diesel or gasoline emission.

Table 1. Comparison of PAH mean diagnostic ratios in PM₁ during all seasons, and the main emission sources

Diagnostic ratios	Value	Sources	This study		References
Flu/(Flu+Pyr)	0.2-0.5	diesel	Winter	0.5	Teixeira et al., 2012
	0.4-0.5	Liquid fossil	Spring	0.5	Yunker et al., 2002
	>0.5	fuel Wood combustion	Summer	0.5	Zhang et al., 2004
			Autumn	0.5	
BaP/BghiP	0.3-0.4	traffic	Winter	0.9	Agudelo-Castañeda and Teixeira, 2014
	0.46-0.81	diesel	Spring	0.6	
	0.9-6.6	coal	Summer	0.6	Hanedar et al., 2014
			Autumn	0.8	
BaP/(BaP+Chry)	<0.5	diesel	Winter	0.5	Teixeira et al., 2012
			Spring	0.5	
	>0.5	gasoline	Summer	0.5	Agudelo-Castañeda and Teixeira, 2014
			Autumn	0.6	
IP/(IP+BghiP)	0.35-0.70	diesel	Winter	0.5	Agudelo-Castañeda and Teixeira, 2014
	0.56	coal	Spring	0.5	
			Summer	0.5	
			Autumn	0.5	

4. Conclusion

Measurements of PAHs in PM₁ particle fraction showed seasonal differences with higher mass concentrations of PAH in the cold (autumn and winter) than in the warm (spring and summer) period. The highest mass concentration during the cold period was measured for BbF, while in the warm period the highest mass concentrations were recorded for BghiP. High mass concentrations of BghiP in the warm period in comparison to other hydrocarbons are probably due to BghiP stability at high temperatures.

The lowest mass concentrations for both periods (cold and warm) were determined for DahA. The annual mass concentration for BaP was 0.765 ng m⁻³. During both measured periods, the contributions of heavy PAHs were much higher than those of lighter PAHs. Results of diagnostic ratios showed that the principal emission source of PAHs associated with PM₁ in this study area was engine combustion of diesel or gasoline.

5. References

Agudelo-Castañeda, D.M., Teixeira, E.C., 2014. Seasonal changes, identification and source apportionment of PAH in PM₁₀. Atmos. Environ. 96, 186–200.

ATSDR (Agency for Toxic Substances and Disease Registry). Toxicology profile for polycyclic aromatic hydrocarbons, US Department of Health and Human Services, Atlanta, GA. <http://www.atsdr.cdc.gov/toxprofiles/tp69.pdf>1995

- Delgado-Saborit, J.M., Stark, C., Harrison, R.M. 2011. Carcinogenic potential, levels and sources of polycyclic aromatic hydrocarbon mixtures in indoor and outdoor environments and their implications for air quality standards. *Environ. Int.* 37, 383–392.
- Dvorská, A., Lammel, G., Klánová, J., 2011. Use of diagnostic ratio for studying source apportionment and reactivity of ambient polycyclic aromatic hydrocarbons over Central Europe. *Atmos. Environ.* 45, 420–427.
- Fu, S., Yang, Z.Z., Li, K., Xu, X.B., 2010. Spatial characteristics and major sources of polycyclic aromatic hydrocarbons from soil and respirable particulate matter in a Mega-City, Chin. *Bull. Environ. Contam. Toxicol.* 85, 15–21.
- Hanedar, A., Alp, K., Kaynak, B., Avşar, E., 2014. Toxicity evaluation and source apportionment of Polycyclic Aromatic Hydrocarbons (PAHs) at three stations in Istanbul. Turkey. *Sci. Total. Environ.* 488–489, 437–446.
- Jakovljević, I., Pehneć, G., Vadjjić, V., Šišović, A., Davila, S., Bešlić, I., 2015. Carcinogenic activity of polycyclic aromatic hydrocarbons bounded on particle fraction. *Environ. Sci. Pollut. Res.* 22(20), 15931–15940.
- Katsoyiannis, A., Sweetman, A.J., Jones, K.C., 2011. PAH Molecular diagnostic ratios applied to atmospheric sources: a critical evaluation using two decades of source inventory and air concentration data from the UK. *Environ. Sci. Technol.* 45, 8897–8906.
- Ravindra, K.; Sokhi, R.; Grieken, R.V., 2008. Atmospheric polycyclic aromatic hydrocarbons: Source attribution, emission factors and regulation. *Atmos. Environ.* 42, 2895–2921.
- Rogula-Kozłowska, W., Kozielska, B., Klejnowski, K., Szopa, S., 2013. Hazardous compounds in urban PM in the central part of Upper Silesia (Poland) in winter. *Arch. Environ. Prot.* 39, 53–65.
- Šišović, A., Pehneć, G., Jakovljević, I., Šilović Hujčić, M., Vadjjić, V., Bešlić, I., 2012. Polycyclic aromatic hydrocarbons at different crossroads in Zagreb, Croatia. *Bull. Environ. Contam. Toxicol.* 88, 438–442.
- Ströher, G.L., Poppi, N.R., Raposo Jr., J.L., de Souza, J.B.G., 2007. Determination of polycyclic aromatic hydrocarbons by gas chromatography – ion trap tandem mass spectrometry and source identifications by methods of diagnostic ratio in the ambient air of Campo Grande, Brazil. *Microchem. J.* 86, 112–118.
- Teixeira, E.C., Agudelo-Castañeda, D.M., Fachel, J.M.G., Leal, K.A., Garcia, K.O., Wiegand, F., 2012. Source identification and seasonal variation of polycyclic aromatic hydrocarbons associated with atmospheric fine and coarse particles in the Metropolitan Area of Porto Alegre, RS, Brazil. *Atmos. Res.* 118, 390–403.
- Tobiszewski, M., Namieśnik, J., 2012. PAH diagnostic ratios for the identification of pollution emission sources. *Environ. Pollut.* 162, 110–119.
- Wenger, D., Gerecke, A.C., Heeb, N.V., Hueglin, C., Seiler, C., Haag, R., Naegeli, H., Zenobi, R., 2009. Aryl hydrocarbon receptor-mediated activity of atmospheric particulate matter from an urban and a rural in Switzerland. *Atmos. Environ.* 34, 3556–3562.
- WHO Regional Office for Europe, 2000. Air quality guidelines, 2nd edn. WHO, Copenhagen, Denmark
- Wickramasinghe, A.P., Karunaratne, D.G.G.P., Sivakanesan, R., 2011. PM₁₀-bound polycyclic aromatic hydrocarbons: concentrations, source characterization and estimating their risk in urban, suburban and rural areas in Kandy, Sri Lanka. *Atmos. Environ.* 45, 2642–2650.



18th World Clean Air Congress, 23-27 September 2019, Istanbul
organized by TUNCAP and IUAPPA

Yunker, M.B., Macdonald, R.W., Vingarzan, R., Mitchell, R.H., Goyette, D., Sylvestre, S., 2002. PAHs in the Fraser River basin: a critical appraisal of PAH ratios as indicators of PAH source and composition. *Org. Geochem.* 33, 489–515.

Zhang, Z., Huang, J., Yu, G., Hong, H., 2004. Occurrence of PAHs, PCBs and organochlorine pesticides in the Tonghui River of Beijing, China. *Environ. Pollut.* 130, 249–261.

Acknowledgments

These measurements have been conducted within internal scientific project “Organic content of PM₁ particle fraction” (PI: R. Godec).

Comparison of electro-chemical sensors for air quality monitoring with reference methods In Zagreb

Silvija Davila¹, Ivan Bešlić¹, Marko Marić² and Ivana Hrga²

¹ Institute for Medical Research and Occupational Health (IMROH), Zagreb, Croatia, sdavila@imi.hr

² Educational Institute for Public Health „Dr. Andrija Štampar“, Zagreb, Croatia

sdavila@imi.hr

Abstract. Within the project "Eco Map of Zagreb", 8 sensor sets (type AQMeshPod) were obtained for air quality measurement. Throughout 2018, a set of sensors was set up at an automatic measuring station at the Institute for Medical Research and Occupational Health (IMROH) for comparison with reference methods for air quality measurement. This automatic station is a city background station within the Zagreb network for air quality monitoring, where measurements of SO₂, CO, NO₂, O₃, PM₁₀ and PM_{2.5} are performed using standardized methods accredited to EN ISO / IEC 17025. The paper presents a comparison of mass concentrations of pollutants SO₂, CO, NO₂, O₃, PM₁₀ and PM_{2.5} determined by sensors and reference methods during 2018. For the gases, the hourly averages were compared and for the particle matter, 24-hour averages of concentrations. The raw data of the sensor and validated data of the reference devices were used. Negative data values from the sensor were replaced by the minimum detection limits of the reference methods. Data were compared using Student's t-test dependent samples and regression analysis. A Grubb test was performed to remove the outliers of data pairs from the database. The Grubb test is not applicable for gaseous pollutants due to high dispersion of results. For PM₁₀ and PM_{2.5}, the Grubb test is satisfactorily applied with a critical factor of 5% confidence level. In order to remove large deviations between the results obtained by sensors and by the reference methods for gaseous pollutants and in order to reduce the scattering of the results, data filtering was performed. The results where the deviation between sensors data and reference methods data over 90% were excluded in the filtering process. The Grubb test was performed over the new set of data. A comparison of sensor results with the results of reference methods showed a large scattering of all gaseous pollutants while the comparison for PM₁₀ and PM_{2.5} indicated a satisfactory low dispersion. The results of regression analysis showed a significant seasonal dependence for all pollutants. There was a significant statistical difference between the reference method and sensors for the whole year and in all seasons for all gas pollutants as well as for PM₁₀. For PM_{2.5} there was not a significant statistical difference for the whole year as well as in summer, while for other periods there was a statistically significant difference.

Keywords: Low-cost air sensors, Grubb test, AQMeshPod.

1. Introduction

Zagreb is the capital of Croatia, situated in the north eastern part of the country, at the foot of Mt Medvednica to the north and by the River Sava to the south. The climate is continental. Although measurements of air quality are performed continuously since 1999, till 2018 there were no measurements of air quality with electro-chemical air sensors. Starting from 2018, the project "Eco Map of Zagreb" began, as part of which a total of 8 sensor sets (type AQMeshPod) for air quality monitoring were installed in the city.

2. Methods

From January to December of 2018, a set of sensors was set up at an automatic measuring station at the Institute for Medical Research and Occupational Health (IMROH) for comparison with reference methods for air quality measurement. This automatic station is a city background station within the Zagreb network for air quality monitoring, where measurements of SO₂, CO, NO₂, O₃, PM₁₀ and PM_{2.5} are performed using standardized methods accredited to EN ISO / IEC 17025 in accordance with the Air Protection Act (1) and the Regulation on Air Quality Monitoring (2). The sensor set used in comparison is AQMeshPod, using electrochemical sensors for gas pollutants and optical particle counter for particulate matter.

After one year of parallel measurements, the values were statistically compared. Hourly averages were compared for SO₂, CO, NO₂, and O₃ gases and concentrations of 24 hours averaged for particulate matter. The raw data of the sensor and validated data of the reference devices were used. The periods when the sensors did not work as well as the periods during the calibration and maintenance of the reference devices are excluded from the statistical analysis. Negative data values from the sensor were replaced by the minimum detection limits of the reference methods. Data were compared using Student's t-test dependent samples and regression analysis. A Grubb test was performed to remove the outliers of data pairs from the database. The Grubb test is not applicable for gaseous pollutants due to high dispersion of results. For PM₁₀ and PM_{2.5}, the Grubb test is satisfactorily applied.

In order to eliminate large discrepancies between the results between the sensors and the reference methods for gaseous pollution and to reduce the scatter of the results, data filtering was performed. In the filtering process, pairs of results were eliminated in which the deviation between the results determined by the sensors and the results determined by the reference methods was more than 90%. The newly acquired data set was again subjected to the Grubb test. The Grubb test was run until the critical factor of 5% confidence level.

3. Results and discussion

Table 1 shows the annual statistical parameters for the reference method and sensor during 2018. The data presented in Table 1 are the number of pairs of results, data coverage, lowest concentration in the indicated period, highest concentration in the indicated period and median. The lowest data coverage in the comparative was 77.7 for SO₂, while the highest was 98.9 for PM_{2.5}.

Table 2 shows the annual statistical parameters after the filtration process. It can be seen that the data coverage is the lowest for SO₂ 33.9 and the highest for CO 88.4. The filtering process was not performed for particulate matter.

Table 1. Annual statistical parameters of sensors and reference methods without filtering

		N	DC(%)	Cmin	Cmax	Median
SO ₂	Reference	6809	77.7	1.34 µg/m ³	56.51 µg/m ³	1.10
	Sensor	6809	77.7	0.05 µg/m ³	195.06 µg/m ³	0.10
NO ₂	Reference	6809	77.7	0.0 µg/m ³	114.1 µg/m ³	11.3
	Sensor	6809	77.7	0.0 µg/m ³	127.2 µg/m ³	24.2
O ₃	Reference	7106	81.1	1.2 µg/m ³	157.3 µg/m ³	51.1
	Sensor	7106	81.1	0.0 µg/m ³	187.0 µg/m ³	46.4
CO	Reference	7906	90.3	0.0 mg/m ³	1.73 mg/m ³	0.3
	Sensor	7906	90.3	0.0 mg/m ³	1.75 mg/m ³	0.3
PM ₁₀	Reference	345	94.5	5.0 µg/m ³	97.0 µg/m ³	21.0
	Sensor	345	94.5	7.0 µg/m ³	130.0 µg/m ³	16.0
PM _{2.5}	Reference	361	98.9	3.0 µg/m ³	88.0 µg/m ³	15.0
	Sensor	361	98.9	6.0 µg/m ³	97.0 µg/m ³	14.0

Table 2. Annual statistical parameters of sensors and reference methods after filtering

		N	DC(%)	Cmin	Cmax	Median
SO ₂	Reference	2967	33.9	0.10 µg/m ³	13.87 µg/m ³	0.97
	Sensor	2967	33.9	0.06 µg/m ³	13.10 µg/m ³	0.13
NO ₂	Reference	3401	38.8	0.2 µg/m ³	114.1 µg/m ³	22.5
	Sensor	3401	38.8	0.2 µg/m ³	94.2 µg/m ³	20.9
O ₃	Reference	6805	77.8	1.2 µg/m ³	157.0 µg/m ³	53.0
	Sensor	6805	77.8	0.3 µg/m ³	187.0 µg/m ³	47.8
CO	Reference	7747	88.4	0.08 mg/m ³	1.73 mg/m ³	0.26
	Sensor	7747	88.4	0.03 mg/m ³	1.71 mg/m ³	0.27

Table 3 shows the annual statistical significance for the reference method and sensor during 2018. The data presented in Table 3 are mean difference between pairs, standard deviation, standard error, t-ratio in the t test, correlation coefficient and t-ratio at the given confidence range. Table 4 shows the annual statistical significance after the filtration process. In the filtering process, pairs of results were eliminated in which the deviation between the results determined by the sensors and the results determined by the reference methods was more than 90%. The filtration process was not applied to the particulate matter.

Table 3. Annual statistical significance of sensors and reference methods without filtering

Pollutant	Δ	Std(Δ)	SE(Δ)	t	r	$t_{crit}(P=0.95)$
SO ₂	-5.31	17.913	0.2171	24.456	-0.0118	1.9603
NO ₂	-10.2	18.51	0.224	45.6420	0.3822	1.9603
O ₃	1.5	14.87	0.176	8.4497	0.8980	1.9603
CO	-0.02	0.074	0.0008	18.0604	0.9410	1.9602
PM ₁₀	3.6	12.9	0.694	5.2296	0.6522	1.9669
PM _{2.5}	0.5	11.64	0.613	0.7995	0.7056	1.9666

Table 4. Annual statistical significance of sensors and reference methods after filtering

Pollutant	Δ	Std(Δ)	SE(Δ)	t	r	$t_{crit}(P=0.95)$
SO ₂	0.58	0.556	0.0102	56.797	0.8532	1.9610
NO ₂	1.2	11.31	0.194	6.1689	0.7712	1.9607
O ₃	2.2	14.3	0.174	12.8152	0.9047	1.9603
CO	-0.01	0.065	0.0007	19.1530	0.9527	1.9602

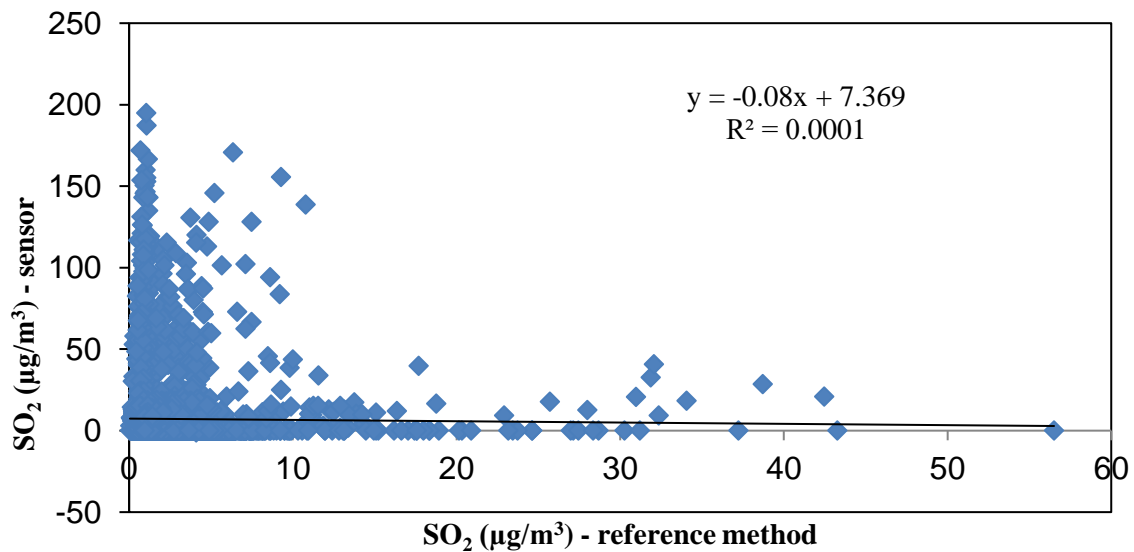


Figure 1. Regression analysis of SO₂ concentrations measured by the reference method and sensors during 2018 before filtering the data

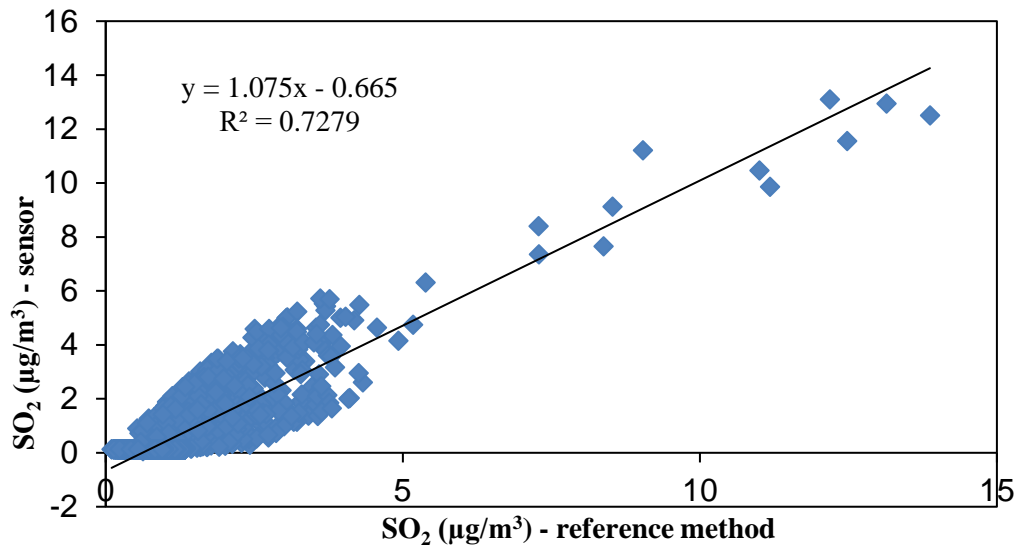


Figure 2. Regression analysis of SO₂ concentrations measured by reference method and sensors during 2018 after data filtering

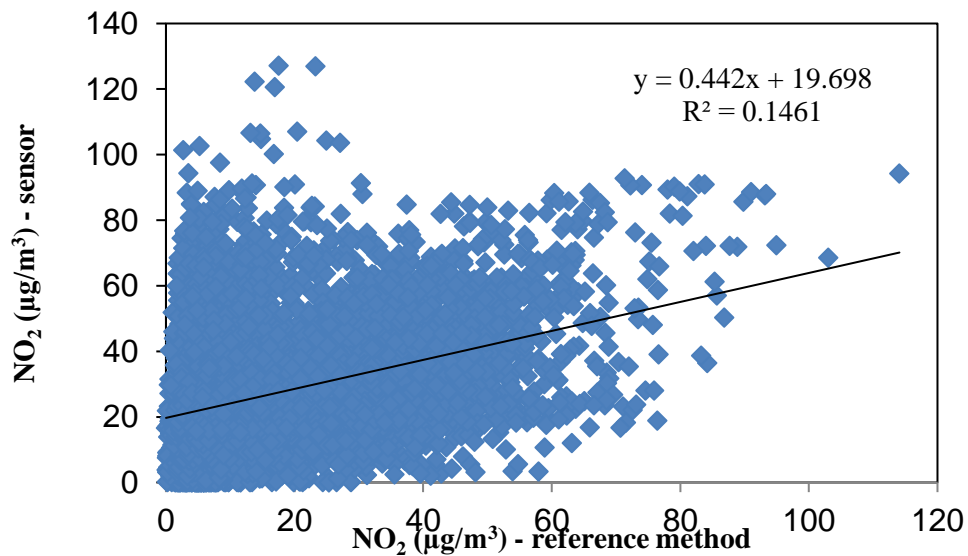


Figure 3. Regression analysis of NO₂ concentrations measured by the reference method and sensors during 2018 before filtering the data

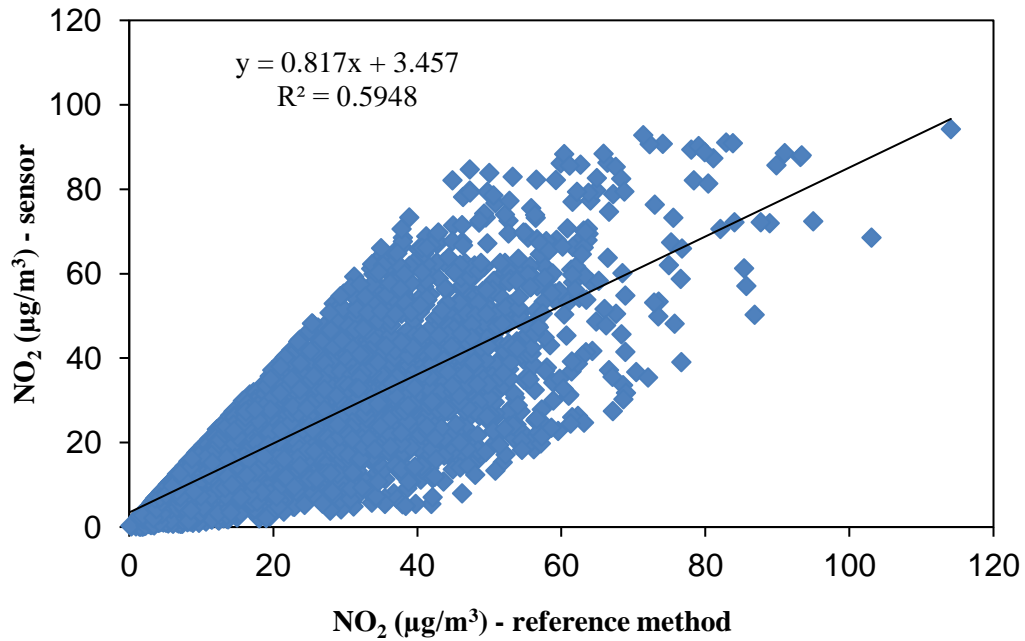


Figure 4. Regression analysis of NO_2 concentrations measured by reference method and sensors during 2018 after data filtering

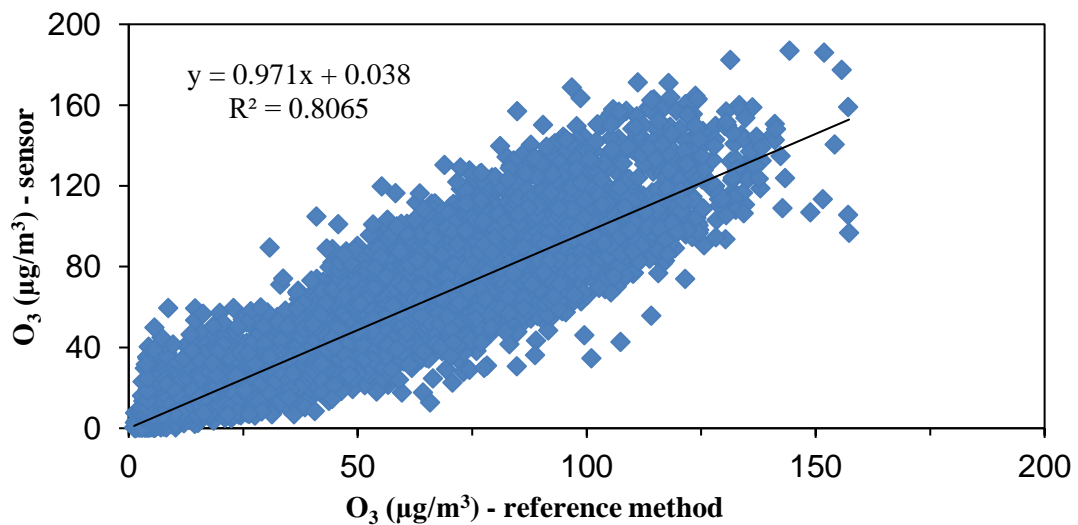


Figure 5. Regression analysis of O_3 concentrations measured by the reference method and sensors during 2018 before filtering the data

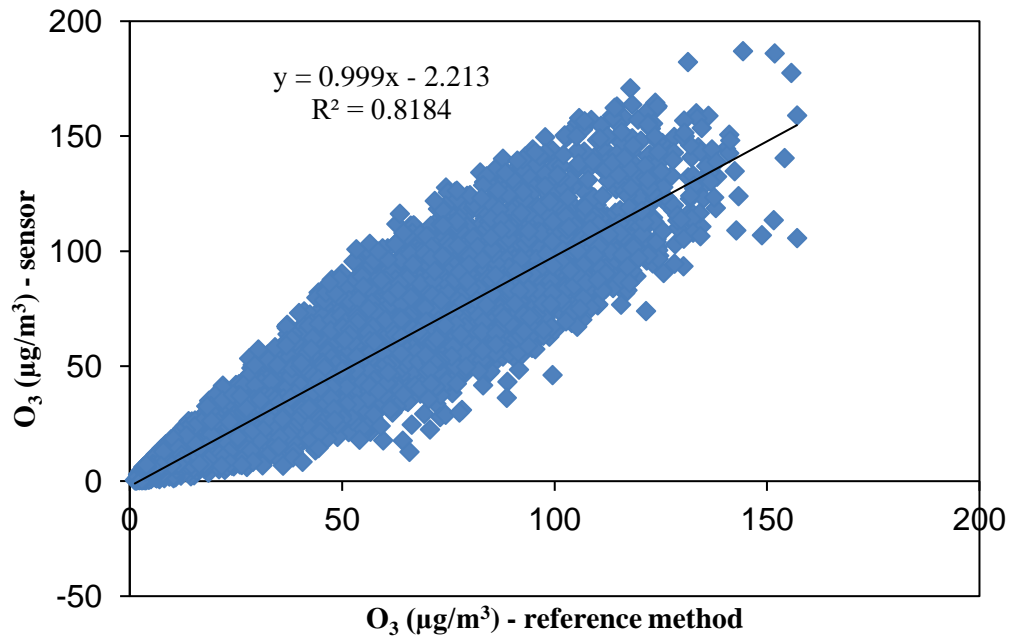


Figure 6. Regression analysis of O₃ concentrations measured by reference method and sensors during 2018 after data filtering

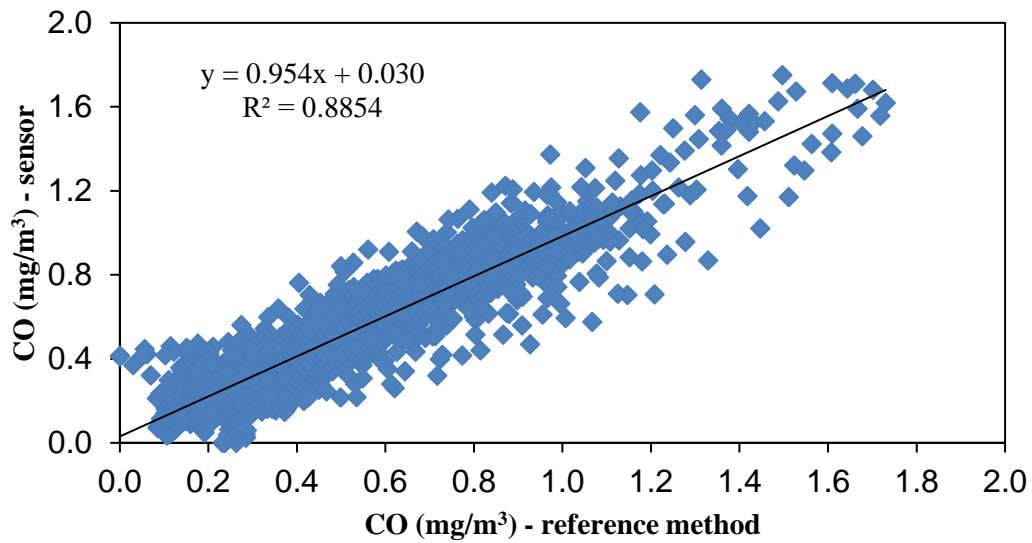


Figure 7. Regression analysis of CO concentrations measured by the reference method and sensors during 2018 before filtering the data

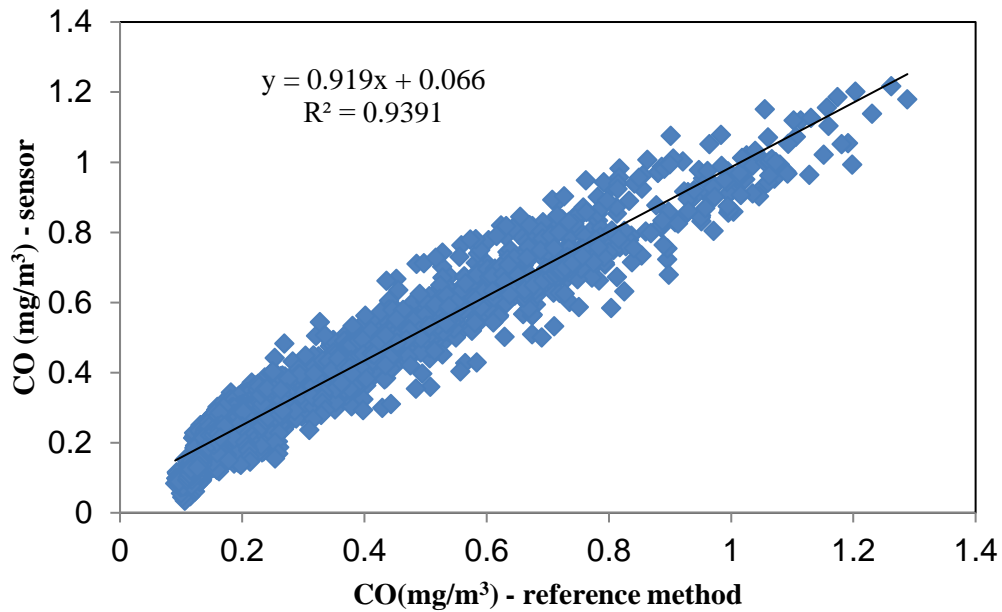


Figure 8. Regression analysis of CO concentrations measured by reference method and sensors during 2018 after data filtering

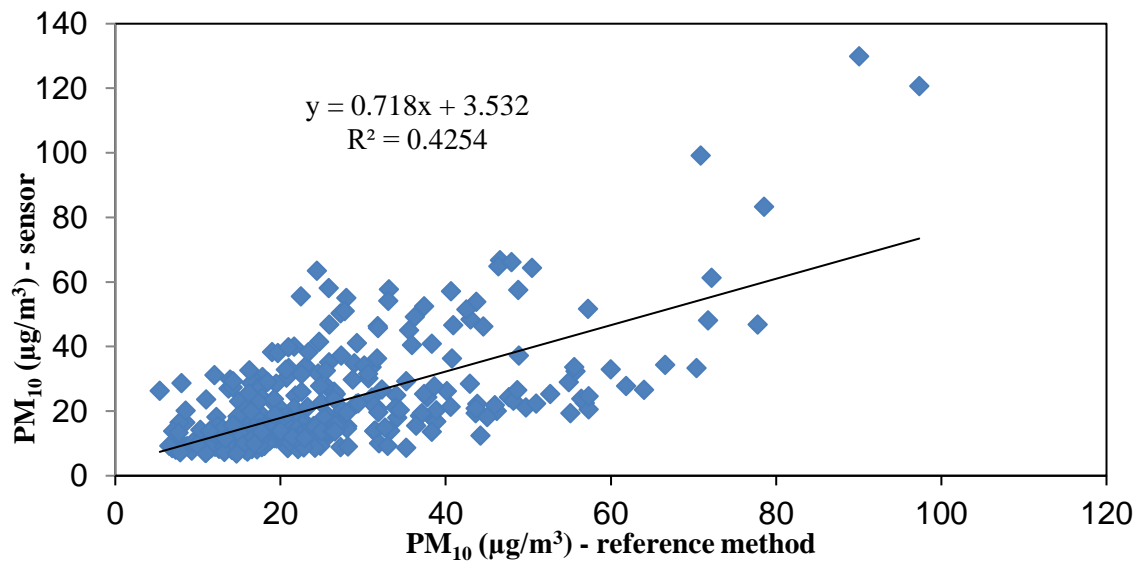


Figure 9. Regression analysis of PM₁₀ concentrations measured by the reference method and sensors during 2018

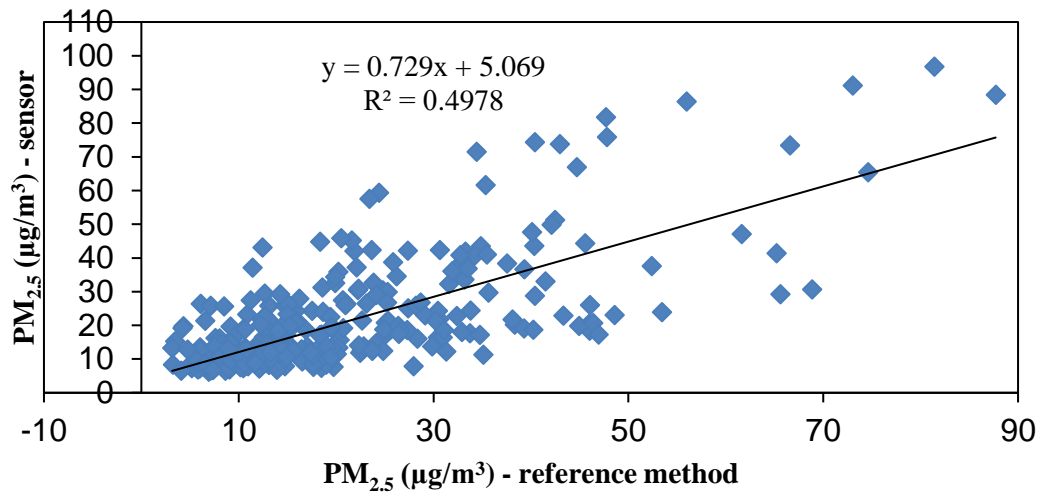


Figure 10. Regression analysis of PM_{2.5} concentrations measured by the reference method and sensors during 2018

Table 5. Statistical significance of sensors and reference methods after filtering for winter of 2018.

Pollutant	Δ	Std(Δ)	SE(Δ)	t	r	t _{crit} (P=0.95)
SO ₂	0.29	0.831	0.0308	9.336	0.6939	1.9630
NO ₂	4.5	10.26	0.305	14.8702	0.8089	1.9621
O ₃	5.0	7.22	0.184	27.1635	0.9605	1.9615
CO	-0.03	0.060	0.0015	19.4703	0.9557	1.9615
PM ₁₀	-12.4	10.05	1.266	9.8223	0.8860	1.9990
PM _{2.5}	-10.8	11.14	1.278	8.4592	0.8264	1.9921

Table 6. Statistical significance of sensors and reference methods after filtering for spring of 2018.

Pollutant	Δ	Std(Δ)	SE(Δ)	t	r	t _{crit} (P=0.95)
SO ₂	0.76	0.421	0.0141	53.7858	0.9125	1.9626
NO ₂	1.7	8.20	0.292	6.0701	0.6404	1.9630
O ₃	-2.7	14.11	0.339	8.1528	0.8609	1.9613
CO	-0.05	0.040	0.0010	55.6158	0.7719	1.9614
PM ₁₀	1.9	8.01	0.839	2.2358	0.5436	1.9867
PM _{2.5}	-1.5	6.40	0.667	2.2003	0.5814	1.9864

Table 7. Statistical significance of sensors and reference methods after filtering for summer of 2018.

Pollutant	Δ	Std(Δ)	SE(Δ)	t	r	$t_{crit}(P=0.95)$
SO ₂	0.67	0.334	0.0109	60.9140	0.8130	1.9624
NO ₂	-3.6	11.57	0.550	6.5378	0.4949	1.9654
O ₃	1.8	18.54	0.398	4.4610	0.8188	1.9611
CO	0.01	0.061	0.0013	10.0311	0.5812	1.9611
PM ₁₀	4.5	6.39	0.659	6.8998	0.3612	1.9858
PM _{2.5}	0.4	5.07	0.553	0.7962	0.3661	1.9858

Table 8. Statistical significance of sensors and reference methods after filtering for autumn of 2018.

Pollutant	Δ	Std(Δ)	SE(Δ)	t	r	$t_{crit}(P=0.95)$
SO ₂	0.51	0.347	0.0177	28.9744	0.9629	1.9661
NO ₂	-2.1	13.0	0.454	4.719	0.7184	1.9629
O ₃	6.3	10.11	0.280	22.4829	0.8557	1.9618
CO	0	0.064	0.014	0.3880	0.9576	1.9611
PM ₁₀	14.7	11.34	1.223	11.9957	0.6856	1.9883
PM _{2.5}	10.5	10.96	1.169	8.9755	0.7594	1.9876

4. Conclusion

Comparison of the results obtained by measurement using sensors with the results obtained by reference methods indicated that the scattering was too large for all the gaseous pollutants determined (SO₂, NO₂, O₃, CO). For this reason, data filtration was performed by rejection from further analysis of pairs of results in which the deviation between the results determined by the sensors and the results determined by the reference methods was more than 90%. Even before filtering, the sensors for SO₂, NO₂ and O₃ did not achieve satisfactory data coverage under the Air Protection Act (1) and the Air Quality Monitoring Regulations (2). After data filtration, the data coverage was between 33.9% (SO₂) and 88.4% (CO).

Comparison of the results determined by the sensors with the results determined by the reference methods for the PM₁₀ and PM_{2.5} particulate matter fractions indicates satisfactory low scattering. For this reason, no data filtering was necessary and the requirement for data coverage under the Air Protection Act (1) and the Air Quality Monitoring Regulation (2) was also satisfied.

The results of the regression analysis showed a strong seasonal dependence for all pollutants. Observing unfiltered data, the highest correlation between sensors and referent methods was obtained for CO and O₃.

For the sulfur dioxide (SO₂) the total data coverage for 2018 before filtering was 77.7%, and after filtering it was 33.9%, which does not satisfy the criterion of data coverage. The statistics show that there is a significant statistical difference between the reference method and the sensors both for the whole year and in all seasons.

For nitrogen dioxide (NO₂) the total data coverage for the year 2018 before filtering was 77.7% and after filtering the data amounted to 38.8%, thus not meeting the criterion of data coverage in accordance with the regulations. The statistics show that there is a significant statistical difference between the reference method and the sensors both for the whole year and in all seasons.



For ozone (O₃) the total data coverage for 2018 was 81.1%, and after filtering the data 77.8%, thus not meeting the data coverage criteria in accordance with the regulations. The statistics show that there is a significant statistical difference between the reference method and the sensors both for the whole year and in all seasons.

For carbon monoxide (CO) the total data coverage for 2018 before filtering was satisfactory (90.3%) but after filtering data it was 88.4% and thus did not meet the minimum data coverage criterion. The statistics show that there is a significant statistical difference between the reference method and the sensor, except in the fall.

For PM₁₀ the total coverage of data for 2018 is 94.5%, thus satisfying the criterion of data coverage according to the Air Protection Act and the Regulation on Air Quality Monitoring (1,2). The statistics show that there is a significant statistical difference between the reference method and the sensor. For PM_{2.5} the total data coverage for 2018 is 98.9%, thus satisfying the data coverage criterion according to the Air Protection Act and the Regulation on Air Quality Monitoring (1,2). The statistics show that there is no significant statistical difference between the reference method and the sensors for the whole year and summer, while in the other seasons (winter, spring, autumn) there is a statistically significant difference.

The results obtained from sensory measurement techniques are highly seasonally dependent, suggesting the sensitivity of meteorological conditions to the measurement technique. Seasonal dependence, as well as poor data coverage due to failures (especially in the determination of SO₂, NO₂ and O₃) and wastefulness of the results, call into question their application in continuous monitoring of air quality. The best agreement with the reference method was shown by the CO sensors and the PM_{2.5} particulate matter fractions, while the PM₁₀ and PM_{2.5} sensors showed the least scatter and satisfactory data coverage.

Future research will focus on determination of sensors sensitivity of metrological conditions, as well as on sensor calibration using seasonal and annual correction factors.

5. References

Air Protection Act of Croatia, Official Gazette no. 130/2011, Official Gazette no. 47/2014, Official Gazette no. 61/2017, Official Gazette no. 118/2018.

Rule book on air quality monitoring of Croatia, Official Gazette no. 79/2017

Ionic composition of PM_{2.5} particle fraction at a coastal urban background site in Croatia

Valentina Gluščić, Mirjana Cačković, Gordana Pehnc and Ivan Bešlić

Institute for Medical Research and Occupational Health, Ksaverska c. 2, 10 000 Zagreb, Croatia

vgluscic@imi.hr

Abstract. The aim of this study was to determine the mass concentration and the content of water-soluble anions (Cl^- , NO_3^- , SO_4^{2-}) and cations (Na^+ , NH_4^+ , K^+ , Mg_2^+ , Ca_2^+) in PM_{2.5} particle fraction, to investigate their relationship and their contribution to the total PM_{2.5} mass measured at site located in Rijeka, Croatia. Rijeka is the third-largest city in Croatia at Kvarner Bay on Adriatic Sea with developed petrochemical and metal industry, shipyards, oil refining and transportation especially maritime. Measuring site is a part of Croatian monitoring network for air quality classified as urban background site. Daily samples of PM_{2.5} particle fraction were collected over a year 2017 on PTFE filters using the low volume sampler Sven Leckel SEQ 47/50. Mass concentration of PM_{2.5} particle fraction was determined by gravimetric according to the standard HRN EN 12341:2014 (EN 12341:2014). The content of water-soluble inorganic anions and cations were determined using Thermo Scientific ICS-5000 capillary ion chromatograph. Results show that annual average PM_{2.5} mass concentration was 9.65 $\mu\text{g}/\text{m}^3$ and didn't exceed limit value of 25 $\mu\text{g}/\text{m}^3$ given by the Regulation on the level of pollutants in air (OG No. 117/12). The annual average mass concentrations of ions in PM_{2.5} particle fraction was in order $\text{SO}_4^{2-} > \text{NH}_4^+ > \text{NO}_3^- > \text{Ca}^{2+} > \text{K}^+ > \text{Na}^+ > \text{Cl}^- > \text{Mg}^{2+}$. Contribution of total anion mass and cation mass to the total PM_{2.5} mass were 25.4% and 12.8%, respectively. Contribution of each anion mass to the total anion mass were 84.8%, 14.2% and 0.9% for SO_4^{2-} , NO_3^- and Cl^- respectively, while contribution of each cation mass to the total cation mass were 6.6%, 72%, 6.2%, 1% and 13.3% for Na^+ , NH_4^+ , K^+ , Mg^{2+} and Ca^{2+} , respectively. The prediction of the pollutant sources we ran the principal component analysis (PCA) which was performed using the statistical packages STATISTICA 13.0. After varimax rotation, the obtained four principal component factors were found to account for 86% of the variance. Factor loadings > 0.7 were considered significant.

Keywords: Measuring site, Anions, Cations, PCA.

1. Introduction

The city of Rijeka is the third-largest city in Croatia with a population of 128.624 inhabitants and is a county seat of the Primorje-Gorski Kotar County. It is situated in the Bay of Rijeka on the coast of Kvarner Gulf under the mountain Učka in the northern part of the Adriatic Sea. The Bay of Rijeka is bordered with peninsula Istria and islands Cres and Krk and is connected to the Kvarner Gulf with three main maritime corridors. It has developed petrochemical and metal industry, shipyards, oil refining and transportation especially maritime.

Because of characteristic location and highly developed industry, particulate matter (PM) expected to be one of dominant pollutants present in Rijeka air. Particulate matter (PM) is the mixture of solid particles, gas phase and liquid droplets suspended in the air that varies in size, chemical composition,

concentration and origin (Čačković et al., 2008). It originates either directly from a variety of natural (e.g. sea spray and mineral dust) and anthropogenic (e.g. vehicular exhaust, shipping emissions, residential wood combustion, industrial emissions, agricultural activities, biomass burning) sources, or as secondary pollutants in chemical reactions of gaseous precursors (nitrogen oxides, sulphur dioxide, ammonia) with reactive species present in atmosphere as ozone and hydroxyl radical (Perrino et al., 2011; Votusa et al., 2013).

Particles with equivalent aerodynamic diameter less than 2.5 μm ($\text{PM}_{2.5}$) also known as fine particulate matter fraction, has long-term persistence in air and an adverse impact on human health and environment. Epidemiological studies have confirmed association between ambient concentrations of $\text{PM}_{2.5}$ and increased appearance of chronic respiratory illness (asthma, chronic obstructive pulmonary disease, lung cancer) and cardiovascular illness (myocardial infarction (MI), cardiac arrhythmias, vascular dysfunction, hypertension and atherosclerosis) listed by Terzano et al. (2010).

According to the literature, the highest contribution to PM mass have organic matter (OM), elemental carbon (EC), and water-soluble inorganic ions sulphates (SO_4^{2-}), nitrates (NO_3^-) and ammonium (NH_4^+). These compounds can alter the chemical properties of particles, they have also ability to scatter light and therefore modify visibility. They can also act as cloud condensation nuclei and thereby directly or indirectly affects the climate and are among the most common substances contributing to the atmospheric acidity (Harrison et al., 2000; Čačković et al., 2009).

The aim of this study was to determine the mass concentration and the content of water-soluble anions (Cl^- , NO_3^- , SO_4^{2-}) and cations (Na^+ , NH_4^+ , K^+ , Mg^{2+} , Ca^{2+}) in $\text{PM}_{2.5}$ particle fraction, to investigate their relationship and their contribution to the total $\text{PM}_{2.5}$ mass measured at site located in Rijeka, Croatia.

2. Materials and methods

Daily samples of $\text{PM}_{2.5}$ particle fraction were collected over a year 2017 at measuring station located in Rijeka (45°20'35.02" N 14°24'33.01" E). Samples were collected on Teflon filters (Whatman PTFE 47 mm, 2 μm) using the low volume sampler Sven Leckel SEQ 47/50. Mass concentration of $\text{PM}_{2.5}$ particle fraction was determined by gravimetric according to the standard HRN EN 12341:2014 (EN 12341:2014). The content of water-soluble inorganic anions and cations were determined using Thermo Scientific ICS-5000 capillary ion chromatograph.

3. Results and discussion

Table 1 shows the statistical parameters: number of samples (N), average values (C_{avg}) and maximum values of mass concentrations of measured species (C_{max}), as well as the mass ratio of $[\text{NO}_3^-]/[\text{SO}_4^{2-}]$ obtained in $\text{PM}_{2.5}$. Results show that annual average $\text{PM}_{2.5}$ mass concentration was 9.65 $\mu\text{g}/\text{m}^3$ and didn't exceed limit value of 25 $\mu\text{g}/\text{m}^3$ given by the Croatian and European Legislation. The annual average mass concentrations of measured ions in $\text{PM}_{2.5}$ particle fraction were in order $\text{SO}_4^{2-} > \text{NH}_4^+ > \text{NO}_3^- > \text{Ca}^{2+} > \text{K}^+ > \text{Na}^+ > \text{Cl}^- > \text{Mg}^{2+}$. Contribution of total cation mass and total anion mass to $\text{PM}_{2.5}$ mass was 12.8% and 25.4%, respectively (Figure 1). Contribution of each anion mass to the total anion mass was in order $\text{SO}_4^{2-} > \text{NO}_3^- > \text{Cl}^-$ (Figures 2) and contribution of each cation mass to the total cation mass was in order $\text{NH}_4^+ > \text{Ca}^{2+} > \text{Na}^+ > \text{K}^+ > \text{Mg}^{2+}$ (Figure 3) The most contributing ion to the $\text{PM}_{2.5}$ mass is SO_4^{2-} with 84.8% then NH_4^+ with 72.8% and NO_3^- and Ca^{2+} with 14.2% and 13.3%, respectively. The similar results were obtained in a research of Votusa et al. (2014).

Table 1. Mass concentrations of measured species ($\mu\text{g}/\text{m}^3$)

Statistical parameters	N	C_{avg}	C_{max}
Cl^-	365	0.02	1.30
NO_3^-	365	0.50	11.71
SO_4^{2-}	365	2.03	10.32
Na^+	365	0.06	1.13
NH_4^+	365	0.92	4.96
K^+	365	0.08	1.40
Mg^{2+}	365	0.01	0.20
Ca^{2+}	365	0.14	1.05
$\text{PM}_{2.5}$	365	9.65	45.68
$[\text{NO}_3^-]/[\text{SO}_4^{2-}]$	365	0.27	4.22

N: number of samples, C_{avg} : average values
 C_{max} : maximum values, $[\text{NO}_3^-]/[\text{SO}_4^{2-}]$: mass ratio

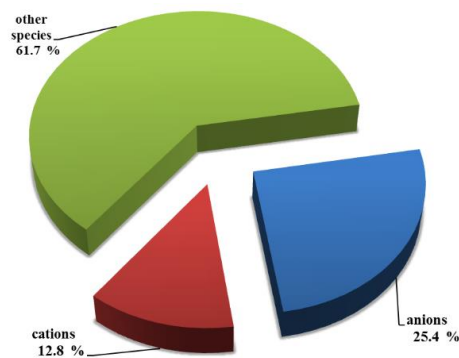


Figure 1. Contribution of total anion mass and total cation mass to the total $\text{PM}_{2.5}$ mass

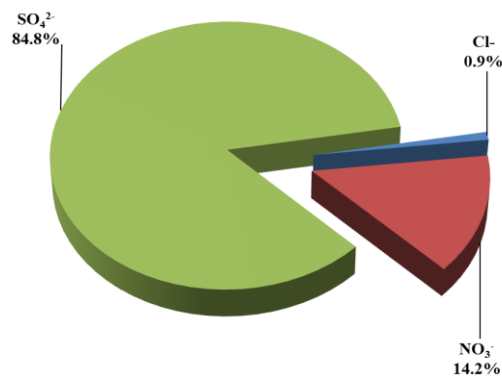


Figure 2. Contribution of each anion mass to the total anion mass in $\text{PM}_{2.5}$

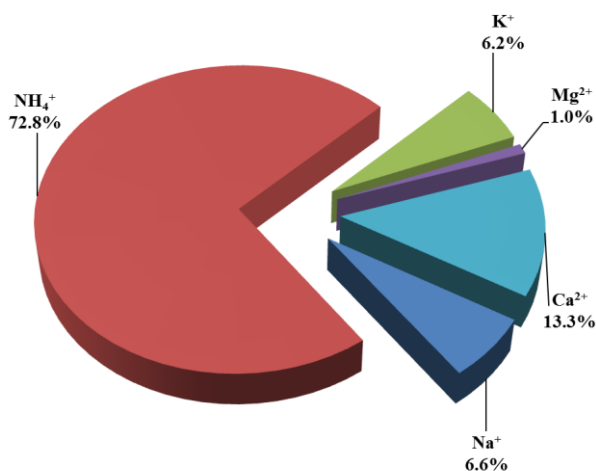


Figure 3. Contribution of each cation mass to the total cation mass in PM_{2.5}

Table 2. The Pearson correlation coefficients between measured species

	Cl ⁻	NO ₃ ⁻	SO ₄ ²⁻	Na ⁺	NH ₄ ⁺	K ⁺	Mg ²⁺	Ca ²⁺
NO ₃ ⁻	0.115*							
SO ₄ ²⁻	-0.052	0.171**						
Na ⁺	0.735**	0.013	0.003					
NH ₄ ⁺	-0.025	0.712**	0.801**	-0.061				
K ⁺	0.225**	0.470**	0.392**	0.037	0.511**			
Mg ²⁺	0.623**	0.015	0.050	0.667**	-0.028	0.272**		
Ca ²⁺	0.098	0.118**	0.299**	0.162**	0.260**	0.212**	0.186**	
PM _{2.5}	0.068	0.710**	0.729**	0.031	0.926**	0.673**	0.075	0.336**

*p<0.05 **p<0.01

The mass ratio of [NO₃⁻]/[SO₄²⁻] was used as an indicator of relative importance of mobile or stationary sources in the atmosphere (Čačković et al., 2009). Our results show (Table 1) that the annual average mass ratio of [NO₃⁻]/[SO₄²⁻] was 0.276 which suggested that the mobile and stationary sources both contributed to PM_{2.5} particle fraction emissions with higher contribution of stationary sources.

Values of correlation coefficients between mass concentrations of measured species in Rijeka are shown in Table 2. Significant correlations were obtained between PM_{2.5} and measured anions and cations, except between mass concentration of PM_{2.5} and ions Cl⁻, Na⁺ and Mg²⁺ indicating that species may have the origin from several sources. Significant correlations between Cl⁻, Na⁺ and Mg²⁺ indicate the same origin of species, probably sea spray. Significant correlations were between NO₃⁻, NH₄⁺ and PM_{2.5} indicating that species may have the origin from vehicular exhaust. Similar results were obtained by Souza et al. (2014). Significant correlation was observed between SO₄²⁻, NH₄⁺, K⁺ and PM_{2.5}. Correlations between this species at urban city port station were described as contribution from fossil fuel combustion and biomass burning (Tolis et al., 2015). Significant correlation was observed between SO₄²⁻, NO₃⁻ and NH₄⁺ indicating similarity of their formation pathways as secondary aerosols. Similar results were obtained by Alebić et al. (2017).

Principal component analysis (PCA) was performed using the statistical packages STATISTICA 13.0 in order to prediction the pollutant sources on measuring site. Table 3 show results of PCA analysis.

Table 3. Factor loadings (PCA analysis)

Variable	Factor 1	Factor 2	Factor 3	Factor 4
Cl ⁻	0.155	0.883*	-0.021	-0.096
NO ₃ ⁻	0.956*	-0.013	0.014	0.002
SO ₄ ²⁻	0.166	-0.007	0.131	0.973*
Na ⁺	-0.043	0.897*	0.070	0.010
NH ₄ ⁺	0.677	-0.090	0.087	0.686
K ⁺	0.671	0.207	0.084	0.296
Mg ²⁺	0.023	0.862*	0.100	0.061
Ca ²⁺	0.108	0.109	0.975*	0.154
PM _{2.5}	0.743*	0.023	0.166	0.613
Expl.Var.	2.442	2.391	1.025	1.917
Prp.Total	0.271	0.266	0.114	0.213
% Total variance	40.680	26.570	11.15	7.980

* Factor loadings > 0.7

After varimax rotation, the obtained four principal component factors (F1 - F4) were found to account for 86% of the variance. Factor loadings > 0.7 were considered significant. Factor F1 was strongly loaded with NO₃⁻ and PM_{2.5} indicates contribution of vehicular exhaust. Factor F2 was strongly loaded with Cl⁻, Na⁺ and Mg²⁺ indicates contribution of sea spray. Factor F3 was strongly loaded with Ca²⁺ indicates contribution of re-suspended mineral dust. Factor F4 was strongly loaded with SO₄²⁻ what suggest contribution of combustion sources using sulphur rich fuels, such as coal and oil in industry or maritime transport. The similar results were reported by Perrone et al. (2013).

4. Conclusions

Annual average PM_{2.5} mass concentration in Rijeka was 9.65 µg/m³ and didn't exceed limit value given by the Croatian and European Legislation (25µg/m³). The annual average mass concentrations of ions in PM_{2.5} particle fraction was in order SO₄²⁻ > NH₄⁺ > NO₃⁻ > Ca²⁺ > K⁺ > Na⁺ > Cl⁻ > Mg²⁺. Contribution of total anion mass to the total PM_{2.5} mass were 25.4% and total cation mass to the total PM_{2.5} mass 12.8%, respectively. Contribution of each anion mass to the total anion mass was in order SO₄²⁻ > NO₃⁻ > Cl⁻ and contribution of each cation mass to the total cation mass was in order NH₄⁺ > Ca²⁺ > Na⁺ > K⁺ > Mg²⁺. PCA extracted four principal component factors that account for 86% of the variance. Factor F1 was strongly loaded with NO₃⁻ and PM_{2.5} pointing contribution of vehicular exhaust. Factor F2 was strongly loaded with Cl⁻, Na⁺, Mg²⁺ and pointing contribution of sea spray. Factor F3 was strongly loaded with Ca²⁺ pointing contribution of mineral dust resuspension. Factor 4 was strongly loaded with SO₄²⁻ pointing combustion of fuels rich with sulphur as well as secondary aerosols.

5. References

- Alebić, A., Mifka, B., 2017. Secondary Sulfur and Nitrogen Species in PM₁₀ from the Rijeka Bay Area (Croatia). Bull. Environ. Contam. Toxicol. 98, 133-140.
- Čačković, M., Šega, K., Vađić, V., Bešlić, I., 2008. Characterisation of Major Acidic Anions in TSP and PM₁₀ in Zagreb Air. Bull. Environ. Contam. Toxicol. 80, 112-114.
- Čačković, M., Vađić, V., Šega, K., Bešlić, I., 2009. Acidic anions in PM₁₀ Particle Fraction in Zagreb Air, Croatia. Bull. Environ. Contam. Toxicol. 83, 188-192.



Croatian Standards Institute, 2014. HRN EN 12341:2014 Ambient air - Standard gravimetric measurement method for the determination of the PM₁₀ or PM_{2.5} mass concentration of suspended particulate matter (EN 12341:2014).

Harrison, R. M., Yin, J., 2000. Particulate matter in the atmosphere: which particle properties are important for its effects on health? *Sci. Total Environ.* 249, 85-101.

Perrino, C., Tiwari, S., Catrambone, M., DallaTorre, S., Rantica, E., Canepari, S., 2011. Chemical characterization of atmospheric PM in Delhi, India, during different periods of the year including Diwali festival. *Atmos. Poll. Research.* 2, 418-427.

Perrone, M. R., Becagli, S., Orza Garcia, J.A., Vecchi, R., Dinoi, A., Udisti, R., Gabello, M., 2013. The impact of long-range-transport on PM₁ and PM_{2.5} at a Centar Mediterranean site. *Atmos. Environ.* 71, 176-186.

Republic of Croatia, Ministry of Environment and Energy, 2012. Regulation on the levels of pollutants in ambient air. OG No. 117/12.

Souza, D.Z., Vasconcellos, P.C., Lee, H., Aurela, M., Karri, S., Teinilä, K., Hillamo, R., 2014. Composition of PM_{2.5} and PM₁₀ Collected at Urban Sites in Brazil. *Aerosol and Air Quality Res.* 14, 168-176.

Terzano, C., Di Stefano, F., Conti, V., Graziani, E., Petroianni, A., 2010. Air pollution ultrafine particles: Toxicity beyond the lung. *Eur. Rev. Med. Pharmacol. Sci.* 14, 809-821.

The European Parliament and the Council of the European Union, 2008. Directive 2008/50/EC of the European Parliament and of the Council of 21 May 2008 on ambient air quality and cleaner air for Europe. Off. J. EU L 152/1.

Tolis, E. I., Saraga, D. E., Lytra, M. K., Papathanasiou, A. C., Bougaidis, P. N., Prekas-Patronakis, O. E., Ioannidis, I. I., Bartzis, J. G., 2015. Concentration and chemical composition of PM_{2.5} for a one year period at Thessaloniki, Greece: A comparison between city and port area. *Atmos. Environ.* 113, 197-2017.

Votusa, D., Smara, C., Manoli, E., Lazarou, D., Tzoumaka, P., 2014. Ionic composition of PM_{2.5} at urban sites of northern Greece: secondary inorganic aerosol formation. *Environ Sci Pollut Res.* 21, 4995-5006.

Atmospheric deposition of organic compounds

Iva Simić, Gordana Mendaš and Gordana Pehnc

Institute for Medical Research and Occupational Health, Ksaverska c. 2, Zagreb,
Croatia

isimic@imi.hr

Abstract. The atmosphere is a carrier by which some natural and anthropogenic pollutants are transported. Deposition events are the most important mechanisms that remove organic compounds from the atmosphere to terrestrial and aquatic ecosystems. A method based on solid phase extraction (SPE), gas chromatography-mass spectrometry (GC-MS/MS) and gas chromatography with electron capture detector (GC-ECD) was developed for the determination of polycyclic aromatic compounds (PAHs) and polychlorinated biphenyls (PCBs) in atmospheric deposition samples. PAH compounds (fluoranthene (FLU), pyrene (PYR), benz(a)anthracene (BaA), chrysene (CHRY), benzo(b)fluoranthene (BbF), benzo(k)fluoranthene (BkF), benzo(j)fluoranthene (BjF), benzo(a)pyrene (BaP), benzo(e)pyrene (BeP), indeno(1,2,3-cd)pyrene (IP), dibenz(a,h)anthracene (DahA) and benzo(g,h,i)perylene (BghiP)) were analysed by GC-MS/MS and six indicator PCB congeners (PCB-28, PCB-52, PCB-101, PCB-138, PCB-153 and PCB-180) were analysed by GC-ECD equipped with two micro electron-capture detectors and two gas chromatographic columns. Solid phase extraction on silica sorbent was suitable for accumulation of PAHs and PCBs from deposited matters. The extraction procedure was based by passing the whole sample volume through a silica cartridge with dichloromethane and *n*-hexane (1:1, v/v) as the eluting solvents. Prior to analysis, the eluate was dried with sodium anhydrous sulphate and evaporated under a stream of nitrogen to 2 mL. The method was applied for analysis of the 12 PAHs and six indicator PCBs in monthly total deposited matters samples collected by bulk method at an urban background station in Zagreb, Croatia during 2018. The levels and occurrence of PCBs corresponded to global environmental pollution with the highest PCB deposition rate determined in December. During the measurement period, the deposition rates of $\sum 12\text{PAHs}$ varied between $132.2 \text{ ng m}^{-2} \text{ d}^{-1}$ and $698.6 \text{ ng m}^{-2} \text{ d}^{-1}$.

Keywords: Bulk, PAH, PCB, Total deposited matter.

1. Introduction

Organic pollutants such as PAHs and PCBs are widespread atmospheric contaminants with harmful impact on human health (Hanedar et al., 2013; Ravindra et al., 2008). Atmospheric deposition represents an important removal mechanism from the atmosphere to the aquatic and terrestrial systems, and therefore is of great environmental concern. Information on atmospheric deposition is necessary for assessing the impact of different organic pollutants on the environment and human health, as well as for source apportionment. Amodio et al. (2014) describe usual sampling procedures and analytical methods for atmospheric deposition of PAHs and PCBs. Much more the attention is focused on the presence of organic pollutants in total deposited matters (Korhonen et al., 2016; Qu et al., 2019; Shahpoury et al., 2015; Xing et al., 2016). The aim of this study was to develop and optimize SPE method for the simultaneous accumulation of 12 PAHs (fluoranthene (FLU), pyrene (PYR), benz(a)anthracene (BaA), chrysene (CHRY), benzo(b)fluoranthene (BbF), benzo(k)fluoranthene (BkF), benzo(j)fluoranthene (BjF), benzo(a)pyrene (BaP), benzo(e)pyrene (BeP), indeno(1,2,3-cd)pyrene (IP),

dibenz(a,h)anthracene (DahA) and benzo(g,h,i)perylene (BghiP)) and 6 indicator PCBs congeners (PCB-28, PCB-52, PCB-101, PCB-138, PCB-153 and PCB-180) from total deposited matter to obtain information about the levels and distribution of atmospheric deposition of organic pollutants in Zagreb, Croatia. To the best of our knowledge, this paper represents the first results of these organic pollutants in atmospheric bulk deposition samples in Croatia.

2. Experimental

2.1. Sampling

Sampling was performed in Zagreb at the Institute for Medical Research and Occupational Health from August to December 2018. Monthly atmospheric deposition samples were collected by a bulk collector consisting of an open cylindrical glass bottle with a diameter of 100 mm wrapped in aluminium foil. The collector was permanently open to the atmosphere at a height of around 2 m above ground and equipped with a device for keeping birds off. Samples were stored at a cool and dark place avoiding exposure to sunlight and contaminants.

2.2. Chemicals and solvents

The solvents (GC and MS grade) dichloromethane, acetone, ethyl acetate and *n*-hexane were obtained from Merck, Germany. Certified standard mixtures of polycyclic aromatic hydrocarbons, perylene-d12 solution, benzo(e)pyrene solution and benzo(j)fluoranthene solution were procured from Supelco, Bellefonte, USA. A mixture of 16 deuterated PAHs was purchased from CPAchem, Bulgaria. Sodium chloride and sodium sulphate were also obtained from Merck, Germany. Strata SI-1 Silica cartridges (1 g, 6 mL) for sample preparation were purchased from Phenomenex, USA.

2.3. Extraction

Sodium chloride and 100 μ L of the surrogate recovery standard (perylene-d12) were added to the sample prior to analysis. Samples were filtrated through the glass fibre filter with a pore size of 2 μ m and the filter was extracted three times with *n*-hexane in an ultrasonic bath for 15 minutes. SPE cartridges were activated with dichloromethane, acetone and high purity water, respectively. A vacuum was applied at a consistent and reduced flow rate of ~1-2 drops/second to ensure optimal retention. Dichloromethane and *n*-hexane were used for the elution of PAHs and PCBs from cartridges. The extract was dried with anhydrous sodium sulphate, evaporated under a stream of nitrogen to dryness and dissolved in 2 mL of *n*-hexane. One millilitre was transferred into a vial and 100 μ L of the internal standards were added before final GC-ECD and GC-MS/MS analysis.

2.4. Analysis

Identification and quantification of the PAHs were performed by gas chromatography with tandem mass spectrometry (Agilent, USA). One microliter of final extract was injected in PTV pulsed splitless mode at 450 °C. A DB-EUPAH capillary column (20 m \times 0.18 mm i.d., 0.14 μ m film thickness; Agilent) was selected for the analysis and the oven temperature was programmed as follows: 58 °C held for 2 min; 45 °C min⁻¹ to 200 °C; 8 °C min⁻¹ to 240 °C; 3 °C min⁻¹ to 275 °C; 2 °C min⁻¹ to 285 °C and 1.5 °C min⁻¹ to 290 °C. Helium (99.9999 %) was used as the carrier gas at a constant flow rate of 1.3 mL min⁻¹. Mass spectrometer was operated in electron impact ionization (EI) mode with the following conditions: transfer line and ion source temperatures at 340 °C, quadrupole temperatures at 180 °C. Multiple reactions monitoring (MRM) mode with unit resolutions for mass quadruples was used for all the analytes and their associated internal standards. The full list of compounds with their retention times, precursor ions, product ions, collision energies and dwell times are shown in Table 1. Quantifications of PAHs were done by calibrating with internal calibration standards mixture which was added to the final extract in the same amount with standards. Mass concentrations of PAHs were calculated using relative response factors and corrected by the recovery efficiency using the surrogate standard method.

Table 1. MS/MS settings for individual PAHs, deuterated internal standards (IS) and surrogate recovery standard (SS)

Time segment	Segment start time (min)	RT (min)	Compounds	Precursor ion (m/z^{-1})	Product ion (m/z^{-1})	Dwell time (ms)	Collision energy (eV)
1	9.00	9.196	fluoranthene-d10 (IS)	212	210	45	50
				212	208	45	50
		9.266	FLU	202	201	45	42
2	9.60			202	200	45	42
		9.812	pyrene-d10 (IS)	212	208	45	50
				212	210	45	42
3	11.50	9.884	PYR	202	201	45	42
				202	200	45	42
		13.294	BaA-d12 (IS)	240	236	45	45
4	16.00	13.431	BaA	228	226	45	40
				228	202	45	40
		13.589	CHRY-d12 (IS)	240	236	45	45
5	19.50	13.746	CHRY	228	226	45	40
				228	202	45	40
		18.192	BbF-d12 (IS)	264	260	25	50
6	20.70	18.379	BbF	252	250	25	50
				252	224	25	50
		18.339	BkF-d12 (IS)	264	260	25	50
7	24.00	18.510	BkF	252	250	25	50
				252	224	25	50
		18.656	BjF	252	250	25	50
8	27.60			252	248	25	50
		20.188	BeP	252	250	30	50
				252	249	30	50
9		20.249	BaP-d12 (IS)	264	260	30	50
				252	250	30	50
		20.447	BaP	252	249	30	50
10		20.959	perylene-d12 (SS)	264	260	100	40
		26.211	IP-d12 (IS)	288	284	45	50
		26.436	IP	276	274	45	50
11		26.374	DahA-d14 (IS)	292	288	45	50
				278	276	45	52
		26.663	DahA	278	276	45	52
12		28.093	BghiP-d12 (IS)	288	284	75	50
		28.356	BghiP	276	274	75	52

Final analysis of PCBs was performed on an Agilent 7890B gas chromatograph equipped with two micro electron-capture detectors and two gas chromatographic columns, HP-5 and SDB-1701, both 30 m × 0.25 mm i.d., 0.25 μm film thickness (Agilent, USA). The column temperature was from 90 °C (with 1 min hold) up to 180 °C at 30 °C min⁻¹ (1 min hold), and then up to 240 °C at 2 °C min⁻¹ with a hold of 20 min and finally up to 260 °C at 5 °C min⁻¹ with 8 min hold. The injectors and detectors temperatures were 270 °C and 300 °C, respectively. The carrier gas was helium with a flow rate of 1.2 mL min⁻¹. Injection volume was 1 μL. Stock solutions were prepared in acetone and further diluted with *n*-hexane as required by the experiment. The mass concentration of a single compound in GC-ECD standards ranged from 0.1 to 5.0 ng mL⁻¹. Calibration lines were obtained in triplicate at five different

concentration levels and were linear in this range. The mass fractions are reported as an average of the result obtained on two different gas chromatographic columns. Each sample was analysed in duplicate.

3. Results and discussion

3.1. Solid-phase extraction and analysis of PAHs and PCBs in total deposited matter

Two different SPE cartridges were compared for accumulation of PAHs and PCBs: silica and C-18. For the extraction recovery experiment, 200 mL Milli-Q water samples were spiked before extraction with a known quantity of all of the analysed compounds (1-10 ng mL⁻¹). The extraction procedure using silica sorbent proved suitable for determination of all of the analysed compounds while the same procedures did not work for the C-18 sorbent therefore further investigations were performed on silica sorbent. Influence of the elution solvent on extraction efficiency was tested with dichloromethane, *n*-hexane, acetone and ethyl acetate where the elution volume was 80 mL (Figure 1). Dichloromethane and *n*-hexane proved to be suitable for the extraction of both PCBs and PAHs with recoveries ranging from 45 % to 75 % and 60 % to 113 % for PCBs and PAHs, respectively. Elution with acetonitrile was not suitable for extraction of PCBs while PAHs recoveries ranged from 47 % to 98 %, except BghiP with recovery less than 20 %. Analysis of extracts with ethyl acetate as eluent resulted in many interfering compounds.

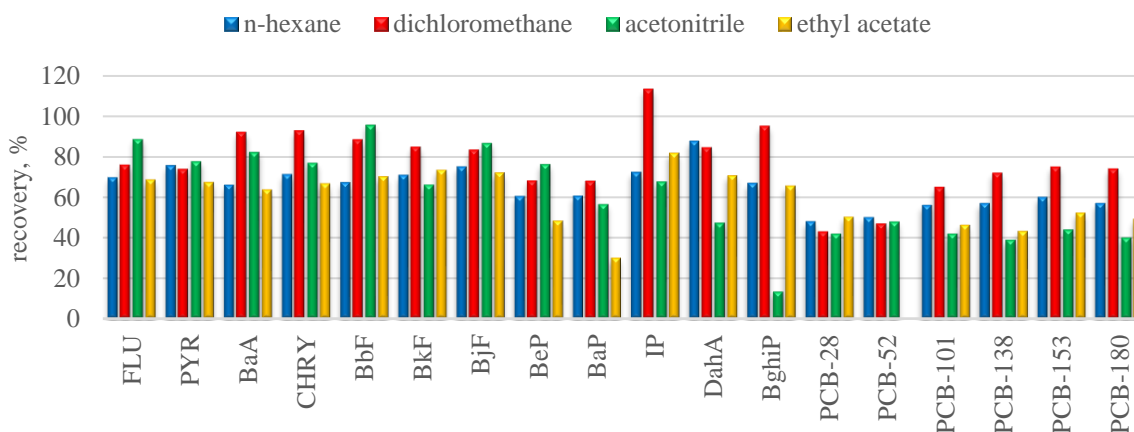


Figure 1. Influence of extraction solvent on extraction efficiency of PAHs and PCBs. Mass concentrations of analytes are from 10 ng mL⁻¹ to 20 ng mL⁻¹

Since the best results were obtained for elution with dichloromethane and *n*-hexane, we further studied successive elution with *n*-hexane and dichloromethane and the influence of the eluents volume (24, 40 and 56 mL) on extraction efficiency. Each fraction was collected separately, evaporated to dryness and redissolved in *n*-hexane prior the analysis. Fractions are analysed separately. The results are shown in Figure 2.

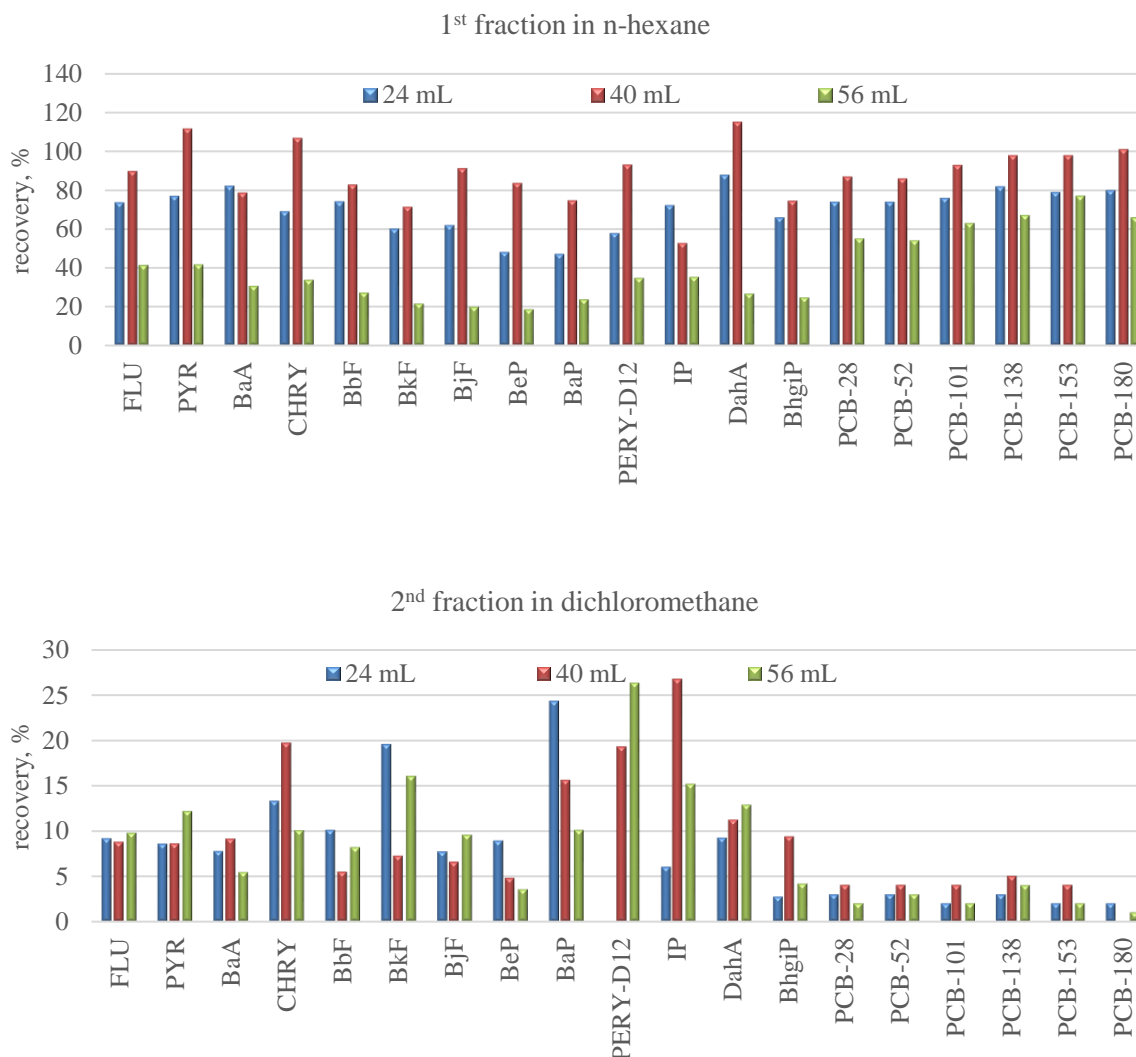


Figure 2. Influence of solvent volume on successive extraction with n-hexane and dichloromethane on extraction efficiency of PAHs and PCBs. Mass concentrations of analytes: 10 - 20 ng mL⁻¹

Elution with 40 mL of *n*-hexane gave the highest recoveries for both PCBs (>80 %) and PAHs (>75 %) except IP (53 %) which was found in the second fraction in >25 %. Elution with 56 mL of *n*-hexane resulted in low recoveries for all PAHs (<40 %). The results indicate that most of the compounds were eluted in the first, *n*-hexane fraction with the exception of IP. Since more than 25 % of IP was desorbed from the column in the second fraction while eluting with 40 mL of dichloromethane, successive elution with 40 mL of *n*-hexane and 40 mL of dichloromethane was selected for PAH and PCB extraction in the total deposited matter sample.

Linearity, accuracy, limits of detection and quantification, and selectivity of the method was determined. Calibration curves were prepared at 5 or 7 levels with internal standards in linearity range shown in Table 2 and each calibration level was injected in triplicate. The correlation coefficients, obtained by linear regression of sample to standard peak area ratio were higher than 0.99. Laboratory blanks were submitted to the analytical protocol to detect possible contamination during the procedure.

Relative standard deviations of average response factors ranged from 5.6 % for pyrene to 10.6 % for benzo(j)fluoranthene over the working range. Samples for which surrogate recoveries were less than 50 % mass fraction should be discarded. In this work, recoveries of perylene-d12 were between 53 % and 61 % so no samples were discarded.

For the recovery test, standard solutions of PAHs and PCBs in the range of 10 ng mL⁻¹ to 20 ng mL⁻¹ were added to 200 mL of high purity water along with surrogate recovery standard. The data showed the recoveries range from 65 % to 124 % for PAHs and from 79 % to 91 % for PCBs respectively as shown in Table 2. The relative standard deviations were below 15 %. The recovery results indicated that the extraction procedure is acceptable.

Influence of the matrix on the accuracy and sensitivity of the method was tested by passing the 200 mL of deposited matter spiked with a known quantity of all of the analyzed compounds.

Table 2. Extraction efficiency of PAHs and PCBs from five spiked deposition samples (10 ng mL⁻¹ to 20 ng mL⁻¹) with dichloromethane and *n*-hexane (1:1, v/v)

Compounds	Recovery ± RSD, %	Linearity, ng mL ⁻¹	Detection limit, ng mL ⁻¹
FLU	73 ± 12	1.80 - 37.04	0.036
PYR	65 ± 11	0.90 - 18.52	0.074
BaA	112 ± 10	0.90 - 18.52	0.062
CHRY	124 ± 15	0.90 - 18.52	0.055
BbF	113 ± 11	1.80 - 37.04	0.024
BkF	117 ± 11	0.90 - 18.52	0.056
BjF	109 ± 11	1.80 - 37.04	0.046
BeP	87 ± 8	0.90 - 18.52	0.050
BaP	86 ± 8	0.90 - 18.52	0.048
IP	110 ± 12	0.90 - 18.52	0.049
DahA	105 ± 8	1.80 - 37.04	0.083
BghiP	108 ± 6	1.80 - 37.04	0.089
PCB-28	80 ± 8	0.10-10.29	0.050
PCB-52	79 ± 7	0.11-10.66	0.050
PCB-101	84 ± 10	0.11-10.26	0.050
PCB-138	87 ± 9	0.12-10.69	0.050
PCB-153	91 ± 10	0.14-11.60	0.050
PCB-180	88 ± 10	0.15-10.89	0.050

3.2. Application of method to real samples

The proposed SPE procedure was applied for determination of PAHs and PCBs in five monthly samples collected in Zagreb in the period from August to December 2018. Table 3 shows the deposition rate expressed in ng m⁻² d⁻¹. The deposition rates of PAHs and PCBs were higher in samples collected in cold period (from November to December). Hussain et al. (2016) reported similar levels for PAHs in samples collected in India. Deposition rates of PCB-52 were below detection limit in samples collected in August and September. The levels and occurrence of PCBs corresponded to global environmental pollution (Blanchard et al., 2006; Hanedar et al., 2017).

Table 3. Deposition of PAHs and PCBs in bulk atmospheric samples collected in 2018 at an urban background station in Zagreb

Compounds	DEPOSITION RATE, ng m ⁻² d ⁻¹					average
	August	September	October	November	December	
FLU	29.9	25.1	76.7	85.5	146.6	72.7
PYR	21.4	17.0	58.4	71.3	99.2	53.5
BaA	9.1	7.2	19.3	27.0	20.8	16.7
CHRY	18.3	12.5	43.1	142.1	89.2	61.0
BbF	21.7	12.6	28.1	94.0	36.3	38.5
BkF	9.1	5.9	18.4	32.9	24.1	18.1
BjF	17.5	12.0	22.9	65.6	26.4	28.9
BeP	9.4	5.6	12.1	39.8	12.7	15.9
BaP	10.4	6.3	14.6	24.4	9.0	13.0
IP	15.8	7.3	16.3	51.6	14.8	21.2
DahA	8.2	8.1	10.4	11.3	9.2	9.4
BghiP	21.1	12.8	23.7	53.0	20.6	26.2
PCB-28	1.8	2.2	1.7	3.3	4.6	2.7
PCB-52	<DL	<DL	0.9	1.5	3.6	2.0
PCB-101	1.1	2.6	1.2	1.3	2.8	1.8
PCB-138	0.9	1.1	1.7	1.9	8.6	2.9
PCB-153	2.7	2.2	1.1	0.9	5.6	2.5
PCB-180	1.5	2.6	1.6	2.0	2.9	2.1

4. Conclusions

The extraction procedure using silica sorbent proved suitable for accumulation of PAHs and PCBs from deposition samples. Elution with *n*-hexane or dichloromethane gave the highest yields for most analytes. The best results were achieved by the extraction of deposition sample with dichloromethane and *n*-hexane (1:1, v/v). The method was successfully applied for PAHs and PCBs determination in total deposited matters collected by bulk method at an urban background station in Zagreb. The highest PCB deposition rate was determined in December, 4.7 ng m⁻² d⁻¹ for ΣPCBs. Deposition rates of PAHs were highest in November, ranged from 11.3 ng m⁻² d⁻¹ for DahA to 142.1 ng m⁻² d⁻¹ for CHRY. The results presented in this study indicate the need for further investigation including influence of different bulk collectors on the levels of PCBs and PAHs in atmospheric deposition samples and monitoring over the whole year period to obtain insight into seasonal and spatial variations of PAHs and PCBs in total deposited matter samples.

5. References

- Amodio, M., Catino, S., Dambruoso, P.R., de Gennaro, G., Di Gilio, A., Giungato, P., Laiola, E., Marzocca, A., Mazzone, A., Sardaro, A., Tutino, M., 2014. Atmospheric Deposition: Sampling Procedures, Analytical Methods, and Main Recent Findings from the Scientific Literature. *Adv. Meteorol.* 161-730.
- Blanchard, M., Teil, M.J., Chevreuril, M., 2006. The Seasonal Fate of PCBs in Ambient Air and Atmospheric Deposition in Northern France. *J. Atmos. Chem.* 53, 123-144.
- Hanedar, A., Alp, K., Kaynak, B., Av, E., 2013. Toxicity evaluation and source apportionment of Polycyclic Aromatic Hydrocarbons (PAHs) at three stations in Istanbul, Turkey. *Sci. Total. Environ.* 488-489, 437-446.
- Hanedar, A., Guneş, E., Kaykioglu, G., Cabi, E., 2017. Determination of Polychlorinated Biphenils In The Soil, Atmospheric Deposition and Bioindicator Samples in The Meric-Ergene River Basin, Turkey. *Acta Scientifica Malaysia.* 1, 1-13.
- Hussain, K., Rahman, M., Prakash, A., Sarma, K.P., Hoque, R.R., 2016. Atmospheric bulk deposition of PAHs over Brahmaputra valley: Characteristics and influence of meteorology. *Aerosol Air Qual. Res.* 16, 1675–1689.
- Korhonen, M., Verta, M., Salo, S., Vuorenmaa, J., Kiviranta, H., 2016. Atmospheric Bulk Deposition of Polychlorinated and Polychlorinated Biphenyls in Finland. *J. Mar. Sci. Eng.* 4, 56.
- Qu, C., Albanese, S., Lima, A., Hope, D., Pond, P., Fortelli, A., Romano, N., Cerino, P., Pizzolante, A., Vivo, B. De., 2019. The occurrence of OCPs , PCBs , and PAHs in the soil , air , and bulk deposition of the Naples metropolitan area , southern Italy : Implications for sources and environmental processes. *Environ. Int.* 124, 89–97.
- Ravindra, K., Sokhi, R., Van Grieken, R., 2008. Atmospheric polycyclic aromatic hydrocarbons: Source attribution, emission factors and regulation. *Atmos. Environ.* 42, 2895–2921.
- Shahpoury, P., Lammel, G., Šmejkalová, A.H., Klánová, J., Příbylová, P., Váňa, M., 2015. Polycyclic aromatic hydrocarbons, polychlorinated biphenyls, and chlorinated pesticides in background air in central Europe - investigating parameters affecting wet scavenging of polycyclic aromatic hydrocarbons. *Atmos. Chem. Phys.* 15, 1795–1805.
- Xing, X., Zhang, Y., Yang, D., Zhang, J., Chen, W., Wu, C., Liu, H., Qi, S., 2016. Spatio-temporal variations and influencing factors of polycyclic aromatic hydrocarbons in atmospheric bulk deposition along a plain-mountain transect in western China. *Atmos. Environ.* 139, 131-138.

Carcinogenic organic content of particulate matter at urban locations with different pollution sources

Gordana Pehnec¹, Ivana Jakovljević¹, Ranka Godec¹, Sabina Zero², Jasna Huremović² and Katja Džepina³

¹Institute for Medical Research and Occupational Health, Ksaverska cesta 2, Zagreb, Croatia

²Department of Chemistry, Faculty of Science University of Sarajevo, Zmaja od Bosne 33-35, Sarajevo, Bosnia and Herzegovina

³Department of Biotechnology University of Rijeka, Ulica Radmile Matejčić 2, Rijeka, Croatia; now at Multiphase Chemistry Department, Max Planck Institute for Chemistry, Hahn-Meitner-Weg 1, Mainz, Germany

gpehnec@imi.hr

Abstract. Polycyclic aromatic hydrocarbons (PAH) are compounds known for their adverse effects on human health. Many of them are proven carcinogens, especially those with 5 and 6 aromatic rings, which are usually in the particle-phase under normal tropospheric conditions. Benzo(a)pyrene (BaP) is often measured as their general representative. Sarajevo, the capital of Bosnia and Herzegovina, is among European cities with the poorest air quality. However, measurements of PAH are not part of routine monitoring. The capital of Croatia, Zagreb, is located approximately 300 km air distance north-west from Sarajevo. PAH mass concentrations in Zagreb have been measured continuously since 1994 within air quality monitoring networks. During winter 2017/2018, the SAFICA project (Sarajevo Canton Winter Field Campaign 2018) was carried out in order to characterise organic and inorganic pollutants in the city of Sarajevo and its surroundings. This paper presents results of PAH measurements at one urban location in Sarajevo. 24-hour samples of the PM₁₀ (particulate matter with aerodynamic diameters ≤ 10 μm) were collected during heating season, from 10 December 2017 to 27 February 2018. PAH mass concentrations in Sarajevo were compared with results obtained in Zagreb during the same period. Average BaP concentrations in Sarajevo and Zagreb were 6.925 ng m⁻³ and 3.109 ng m⁻³, respectively. The contribution of BaP to the sum of PAH mass concentrations was similar at both locations (~11 %). However, much higher contributions of fluoranthene and pyrene were obtained in Sarajevo. Contributions of individual PAH and their diagnostic ratios indicated combustion of gasoline and diesel as a potential source of PAH (traffic) at both locations, as well as combustion of other liquid fossil fuels (petroleum, crude oil). Wood burning was occasionally indicated as a source in Zagreb, while in Sarajevo the contribution of wood and coal combustion was evident. The total carcinogenic potency (TCP) of PAH was estimated using toxic equivalence factors from the literature and it was more than twice higher in Sarajevo compared to Zagreb. BaP had the highest contribution to the TCP at both locations (69 and 67%).

Keywords: Carcinogenic potency, Diagnostic ratio, PM₁₀, Polycyclic aromatic hydrocarbons.

1. Introduction

Chemical composition of airborne particulate matter is of considerable importance regarding human health. Many compounds bound to particulate matter are suspected to be genotoxic, mutagenic and carcinogenic. Polycyclic aromatic hydrocarbons (PAH) are compounds well known for their adverse effects on human health. They are one of the first atmospheric pollutants identified as suspected

carcinogens. In ambient conditions PAHs with smaller molecular weight (2-3 aromatic rings) are present almost exclusively in the gas-phase while those with higher molecular weights (more than 4 rings) are mostly bounded to particles. As the molecular weight of PAH increases, so does the carcinogenicity of PAHs, which means that the recognized carcinogenic PAHs are mostly associated with particulate matter. Benzo(a)pyrene (BaP) is the most often measured PAH and it is usually taken as their representative (Ravindra et al., 2008; Jakovljević and Žužul 2011). Directive 2004/107/EC of the European Union as well as Croatian legislation stipulates the target value only for BaP in the PM₁₀ (particulate matter with aerodynamic diameters $\leq 10 \mu\text{m}$) fraction (1 ng m^{-3} for annual average). As PAHs are formed during incomplete combustion or pyrolysis of organic matter, they originate from numerous anthropogenic sources (traffic, domestic heating, oil refining, waste incineration, industrial activities, agricultural activities, biomass burning etc.) (Yunker et al., 2002; Ravindra et al., 2008; Šišović et al., 2012; Tobiszewski and Namieśnik 2012).

The capital of Croatia, Zagreb, is located in the southeast of Europe at 158 m a.s.l. altitude. It is situated at the foot of the mountain Medvednica (1035 m a.s.l.) to the north and by the River Sava to the south. It has about 800 000 inhabitants and over 350 000 registered vehicles. The climate is continental and the heating season usually lasts from October until April. Newer parts of the city are connected to a central heating system or to a natural gas distribution network. Although most family houses introduced natural gas about 20 years ago, wood furnaces are still in use for heating in a number of households, especially in the city outskirts. PAH mass concentrations have been measured continuously in Zagreb since 1994 within the local and national air quality monitoring network. Several studies concerning PAHs in PM₁₀ (Šišović et al., 2012; Jakovljević et al., 2015) and other fractions were carried out in recent years (Jakovljević et al., 2018; Pehcec and Jakovljević 2018). Measurements have shown much higher PAH concentrations in the colder part of the year (October-March). Traffic and household heating were identified as the main pollution sources of PAHs bounded to airborne particulate matter (Jakovljević et al., 2015; Jakovljević et al., 2018). Annual BaP concentrations in some years exceeded the target value of 1 ng m^{-3} .

Sarajevo, the capital of Bosnia and Herzegovina (B&H), is situated approximately 300 km air distance south-east from Zagreb, within the plain at 518 m a.s.l., surrounded by mountains of the Dinaric Alps (the height of the majority of the mountains is between 1000 and 2500 m a.s.l.). In 2018, Sarajevo had a population of ~450 000 and about 148 945 registered vehicles (BHAS, 2013). The city has one of the poorest European air qualities, mostly due to the extensive use of non-renewable energy sources. Data reported in 2014 to the World Health Organization showed that the annual PM₁₀ average was $55 \mu\text{g m}^{-3}$. Particularly during the winter months, topography and meteorology cause the pollutants to be trapped within the city's plane. Restrained by poor economic conditions after the war ended (1995), coal and wood eventually became important energy sources again, causing hazardous air pollution events (for example, in Sarajevo daily ambient PM₁₀ mass concentration in winter occasionally exceeds $400 \mu\text{g m}^{-3}$). Measurements of PAH are not part of routine monitoring and only limited data are available from previous studies (De Pieri et al., 2014).

During winter 2017/2018, the SAFICA project (Sarajevo Canton Winter Field Campaign 2018) was carried out in order to characterise the organic and inorganic pollutants in the air of Sarajevo and its surroundings. This paper presents results of PAH measurements in the PM₁₀ particle fraction at one urban location in Sarajevo. PAH mass concentrations in Sarajevo were compared with the results obtained in Zagreb during the same period. The study was carried out in order to identify the main pollution sources and estimate PAH carcinogenic potency at both locations.

2. Methods

2.1. Description of measuring sites and sampling of particulate matter

Sarajevo filter samples for PAH analyses were collected during heating season, from 10 December 2017 to 27 February 2018. The sampling site was located at the headquarters of the Federal Hydrometeorological Institute of B&H in Bjelave, Sarajevo (altitude 631 m a.s.l., latitude 43°52'03"N, longitude 18°25'23" E). Bjelave is an urban background site located within mainly residential area with a population of 53 368 in 2018 (Institute for Statistics of FBiH, 2019), and slightly elevated above the city plain. Continuous, 24-hour filter samples of PM₁₀ particle fraction were collected using high-volume sampler (DH77, Digitel-AG, Volketswil, Switzerland) at the flow rate of 70 m³ h⁻¹ on quartz filters (Whatman, QM-A Quartz Microfibre Filters, 150 mm in diameter). The sampler was positioned on the ground in the yard of the Federal Hydrometeorological Institute of B&H, 15 m from the main building and 30 m from the nearest two-lane road. Before sampling, filters were baked for 12 hours at 55°C to reduce carbon content in them.

The measuring site in Zagreb was located in the southern, residential part of the town with high population density and traffic (altitude 116 m a.s.l., latitude 45°46'25" N, longitude 15°59'04" E). The site is influenced by winds from the north (centre of the town) and from the southeast (low-rise residential area with residential heating which relies mostly on gas, oil or, wood). 24-hour samples of PM₁₀ particle fraction were collected on quartz filters (Whatman, QM-A Quartz Microfibre Filters, 47 mm in diameter) using a sequential low-volume reference device Sven Leckel Sequential Sampler SEQ47 / 50 (Sven Leckel, Ingenieurbüro, Berlin, Germany) equipped with a PM₁₀ cut off inlet. The sampler was located approximately 4 m above ground, and about 30 m from the nearest road.

Before and after sampling all Sarajevo and Zagreb filters were wrapped in aluminium foil and kept in a freezer at all times.

2.2. PAH analysis

The analysis of PAHs was carried out in the Environmental Hygiene Unit of the Institute for Medical Research and Occupational Health in Zagreb. Filters were extracted with a solvent mixture of toluene and cyclohexane in an ultrasonic bath, separated from undissolved parts by centrifugation and evaporated to dryness in a mild stream of nitrogen at 30 °C. They were then re-dissolved in acetonitrile. The analysis was performed using an Agilent Infinity 1260 high-performance liquid chromatography (HPLC) with a fluorescence detector (Šišović et al., 2012; Jakovljević et al., 2015). Samples were analysed for the following PAHs: fluoranthene (Flu), pyrene (Pyr), benzo(a)anthracene (BaA), chrysene (Chry), benzo(j)fluoranthene (BjF), benzo(b)fluoranthene (BbF), benzo(k)fluoranthene (BkF), benzo(a)pyrene (BaP), dibenzo(ah)anthracene (DahA), benzo(ghi)perylene (BghiP) and indeno(1,2,3-cd)pyrene (IP).

3. Results and discussion

3.1. PAH levels in Sarajevo and Zagreb

Average PAH mass concentrations in Sarajevo and Zagreb for the period 10 December 2017 - 27 February 2018 are presented in Figure 1. Levels of all PAHs were much higher in Sarajevo compared to Zagreb. For example, average BaP concentrations in Sarajevo and Zagreb were 6.925 ng m⁻³ and 3.109 ng m⁻³, respectively. The differences between some other PAHs (Flu, Pyr, BaA) were even more pronounced. In Sarajevo the highest mass concentration was recorded for Pyr and in Zagreb for BbF. The lowest concentrations at both sites was found for DahA.

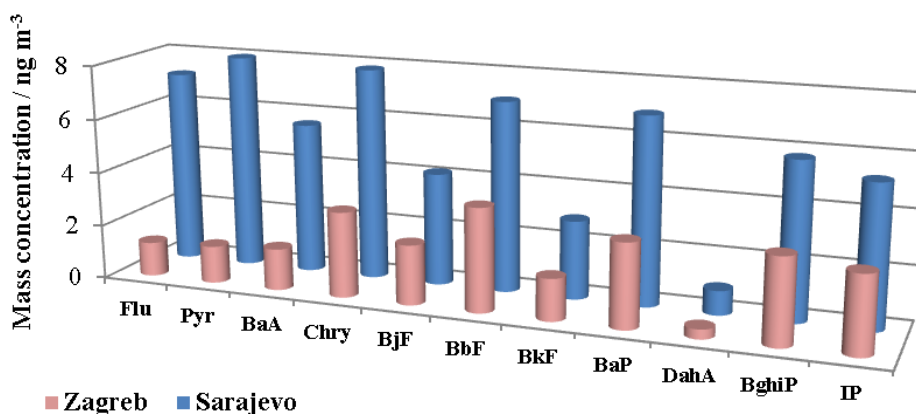


Figure 1. Average PAH mass concentrations in Sarajevo and Zagreb for the period 10 December 2017 – 27 February 2018

In Sarajevo, the average PAH concentrations followed the order: Pyr > Chry > Flu > BbF > BaP > BghiP > BaA > IP > BbF > BkF > DahA, while in Zagreb the order was: BbF > BghiP > Chry > BaP > IP > BbF > BkF > BaA > Pyr > Flu > DahA.

The contributions of the individual PAHs to the sum of total PAH mass concentration were calculated as well (Figure 2).

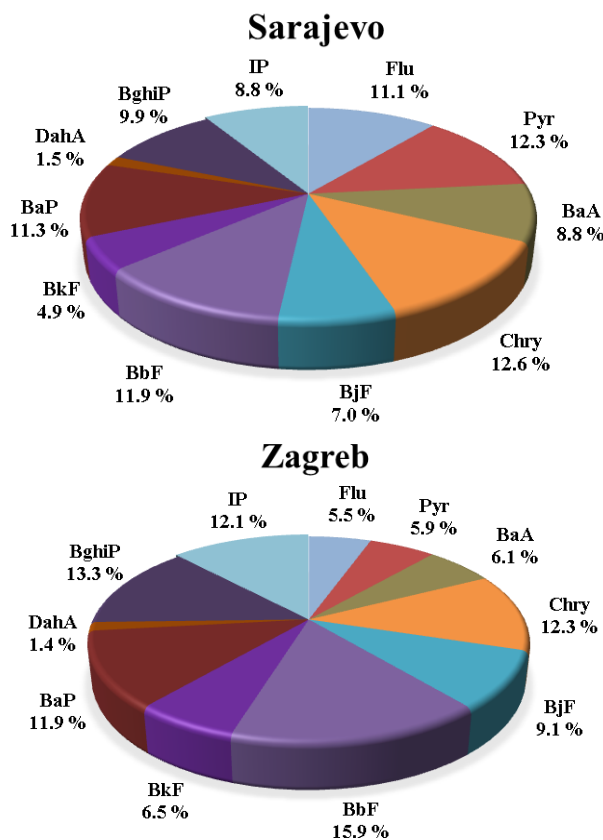


Figure 2. The contributions of the individual PAHs to the sum of total PAH mass concentration

From Figure 2 it is evident that Sarajevo's PAH mixture was characterised by a much higher contribution of four-ring PAHs (Flu, Pyr and BaA) - PAHs that originate from coal and wood combustion processes, while in Zagreb there was a high contribution of 6-ring (BghiP, IP) and some 5-ring PAHs (BjF, BbF, BkF) characteristic for vehicle exhaust emission. However, the contribution of BaP to the sum of PAH mass concentrations was similar at both locations (~ 11 %), which confirm that BaP is a good representative of the PAH atmospheric mixture. Contributions of Flu and Pyr similar to those in Sarajevo were found in Poland, probably as the result of the widespread use of wood and coal during heating season in Poland. (Rogula-Kozłowska et al., 2013).

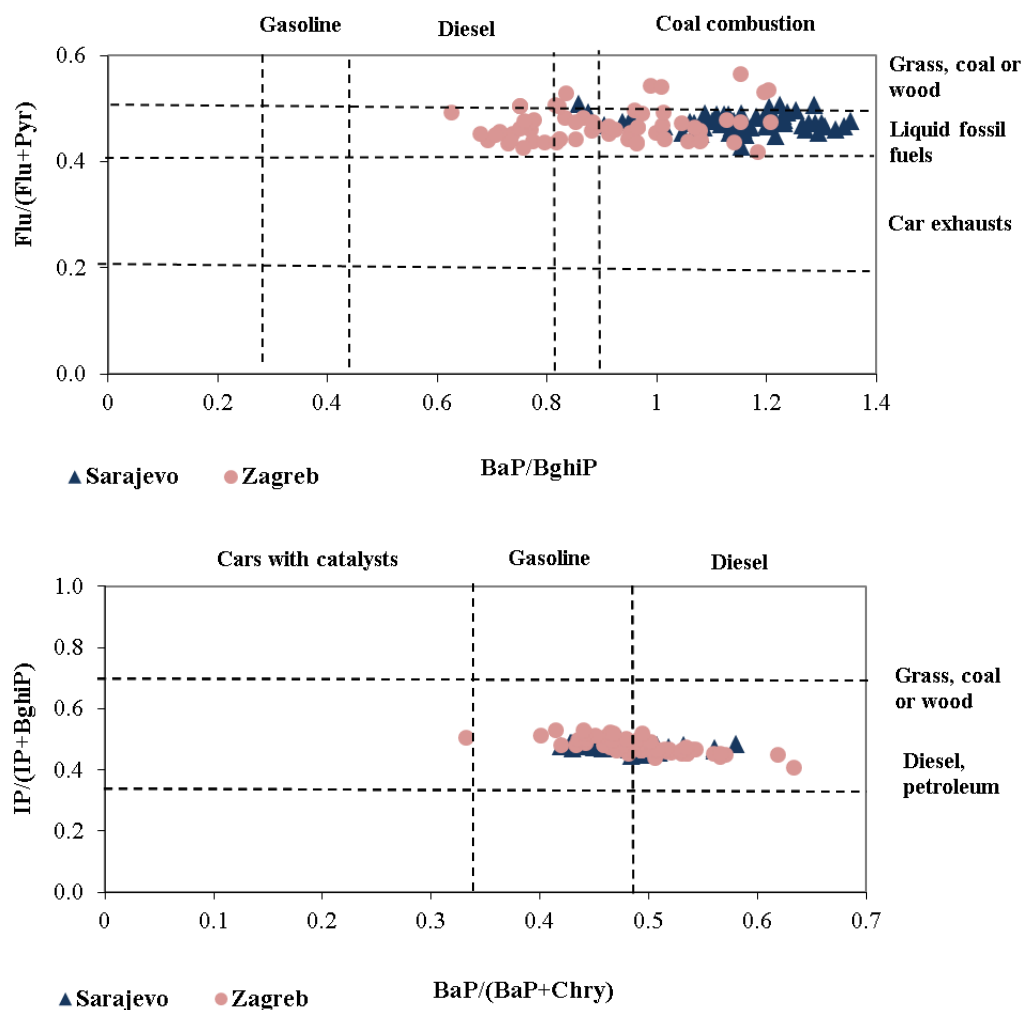


Figure 3. PAH diagnostic ratios in Sarajevo and Zagreb

3.2. PAH diagnostic ratios

Ratios of certain PAHs are specific for some combustion processes and they can be an effective tool to quickly assess potential pollution sources. Many authors used different PAH diagnostic ratios to determine the sources of PAH pollution (Yunker et al., 2002; Zhang et al., 2004; Fu et al., 2010; Tobiszewski and Namieśnik 2012; Agudelo-Castañeda and Teixeira 2014). In this paper, the ratios Flu/(Flu+Pyr), Ind/(Ind+Pyr), BaP/BghiP and BaP/(BaP+Chry) were calculated for each day and compared with literature values. According to Yunker et al. (2002) and Zhang et al. (2004), a Flu/(Flu+Pyr) ratio lower than 0.4 is characteristic for car exhausts, whereas a ratio between 0.4 and 0.5

is specific for liquid fossil fuel combustion. IP/(IP+BghiP) ratio between 0.35 and 0.7 is characteristic for petroleum and diesel, while higher values indicate grass, wood or coal combustion (Agudelo-Castañeda and Teixeira 2014; Yunker et al., 2002). BaP/(BaP+Chry) ratio lower than 0.33 is specific for cars with catalysts, between 0.33 and 0.46 for gasoline combustion and lower than 0.7 for diesel combustion (Ravindra et al., 2008). Finally, a BaP/BghiP ratio between 0.3 and 0.45 is characteristic for gasoline, between 0.45 and 0.8 for diesel and between 0.9 and 6.6 for coal combustion (Fu et al., 2010; Agudelo-Castañeda and Teixeira 2014). PAH diagnostic ratios for Sarajevo and Zagreb are presented in Figure 3. The results show that combustion of gasoline and diesel was the source of PAHs at both locations (traffic), as was the combustion of other liquid fossil fuels (petroleum, crude oil) which can be related not only with traffic but with household heating as well. Wood burning was occasionally indicated as a source in Zagreb, while in Sarajevo the contribution of coal combustion was more evident.

3.3. Carcinogenic potency of PAHs

Carcinogenic potency of PAHs was estimated on the basis of toxic equivalency factors (TEFs) from the literature. There are several TEF schemes proposed by different authors (Clement, 1988; Nisbet and LaGoy 1992; Larsen and Larsen 1998; Boström et al., 2002). The most used TEFs are those proposed by Nisbet and LaGoy (1992), but modified with lower DahA value (1.0 instead of 5.0 originally proposed by authors) and those TEFs were applied in this study as well (Table 1).

Table 1. Toxic equivalency factors (TEF) used in this study (modified from Nisbet and LaGoy (1992))

PAH	Flu	Pyr	BaA	Chry	BbF	BkF	BaP	DahA	BghiP	IP
TEF	0.001	0.001	0.100	0.010	0.100	0.100	1.000	1.000	0.010	0.100

For assessing the risk of PAHs in ambient air, the carcinogenic potencies of the individual PAHs are expressed relative to the potency of BaP. BaP equivalents (BaP_{eq}) were calculated by multiplying mass concentration of individual PAH with its respective toxic equivalency factor. To estimate the carcinogenicity of the PAH mixture, total carcinogenic potency (TCP) was calculated by summing up the BaP_{eq} of each measured PAH. The calculation was carried out according to the equation (1):

$$TCP = \sum BaP_{eq}(PAH) = \sum TEF(PAH) \cdot \gamma(PAH) \quad (1)$$

TCP - total carcinogenic potency

TEF - toxic equivalency factor of particular PAH

γ – mass concentration of particular PAH

Relative potency factor (RPF) was determined as the ratio between the TCP to the mass concentration of BaP, according to the equation (2):

$$RPF = \frac{TCP}{\gamma(BaP)} \quad (2)$$

Table 2 presents the estimated TCP and RPF for Zagreb and Sarajevo. TCP was more than twice higher in Sarajevo compared to Zagreb, while RPF was similar at both locations.

Table 2. Total carcinogenic potency (TCP) and relative potency factor (RPF) in Sarajevo and Zagreb for the period 10 December 2017 – 27 February 2018

	TCP / ng m ⁻³	RPF
Sarajevo	10.053	1.452
Zagreb	4.506	1.449

The percentage contributions of the carcinogenic potency of individual PAHs to the total carcinogenic potency were calculated as well and are presented in Figure 4. BaP had the highest contribution to the total carcinogenic potency at both locations (69 % and 67 % in Sarajevo and Zagreb, respectively), followed by benzo(b)fluoranthene, dibenzo(a,h)anthracene and indeno(1,2,3-cd)pyrene. All other PAHs jointly contributed less than 10 % to the TCP.

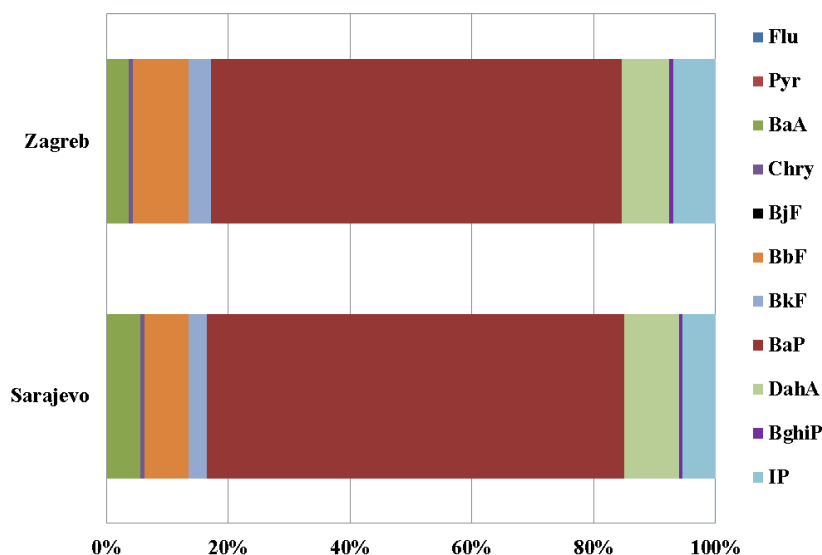


Figure 4. The contributions of individual PAHs to the total carcinogenic potency of the PAH mixtures in Sarajevo and Zagreb

4. Conclusion

Measurements of PAHs bounded to PM₁₀ particle fraction during winter 2017/2018 in Sarajevo and Zagreb showed significant differences in levels, contributions and carcinogenic potency. Although both capitals are located in southeastern Europe and are only 300 km of air distance apart, Sarajevo air is characterised by much higher concentrations of all PAHs, and by much higher contributions of fluoranthene and pyrene. Contributions of individual PAH and their diagnostic ratios indicated combustion of gasoline and diesel as a potential source of PAH (traffic) at both locations, as well as combustion of other liquid fossil fuels (petroleum, crude oil). Wood burning was occasionally indicated as a source in Zagreb, while in Sarajevo the contribution of wood and coal combustion was clearly evident. The total carcinogenic potency of PAH was estimated to be more than twice as high in Sarajevo as in Zagreb. BaP had the highest contribution to the total carcinogenic potency at both locations (69 and 67 %).

5. References

Agudelo-Castañeda, D.M., Teixeira, E.C., 2014. Seasonal changes, identification and source apportionment of PAH in PM₁₀. Atmos Environ 96, 186–200.



BHAS (Bosnia and Herzegovina Automobile and Motorcycle Club), 2019. Information on registered motor vehicles in Bosnia and Herzegovina in the period January-December 2018, <https://bihamk.ba/assets/files/tmHcjlkdVy-informacija-o-registrovanim-vozilima-u-2018-godinipdf.pdf>, accessed in 2019 (in Bosnian).

Boström, C., Gerde, P., Hanberg, A., Jernström, B., Johansson, C., Kyrklund, T., Rannug, A., Törnqvist, M., Victorin, K., Westerholm, R., 2002. Cancer risk assessment, indicators, and guidelines for polycyclic aromatic hydrocarbons in the ambient air. *Environ Health Perspect* 110, 451–488.

Clement, 1988. Comparative potency approach for estimating the cancer risk associated with exposure to mixture of polycyclic aromatic hydrocarbons (Interim Final Report). In Prepared for EPA under Contract 68-02-4403; ICF-Clement Associates: Fairfax, VA, USA.

De Pieri, S., Arruti, A., Huremovic, J., Sulejmanovic, J., Selovic, A., Đorđević, D., Fernández-Olmo, I., Gambaro, A., 2014. PAHs in the urban air of Sarajevo: levels, sources, day/night variation, and human inhalation risk. *Environ Monit Assess* 186, 1409–1419.

Fu, S., Yang, Z.Z., Li, K., Xu, X.B., 2010. Spatial characteristics and major sources of polycyclic aromatic hydrocarbons from soil and respirable particulate matter in a Mega-City, Chin. *Bull Environ Contam Toxicol* 85, 15–21.

Institute for Statistics of FBiH, First release, Year XI, Number: 14.2.1, Sarajevo 30.08.2019. (ISSN 1840-3478) <http://fzs.ba/wp-content/uploads/2019/08/14.2.1.pdf>, accessed 2019.

Jakovljević, I., Žužul, S., 2011. Policiklički aromatski ugljikovodici u zraku, *Arh Hig Rada Toksikol* 62, 357-370.

Jakovljević, I., Pehnc, G., Vadjjić, V., Šišović, A., Davila, S., Bešlić, I., 2015. Carcinogenic activity of polycyclic aromatic hydrocarbons bounded on particle fraction. *Environ. Sci Pollut Res* 22(20), 15931–15940.

Jakovljević, I., Pehnc, G., Vadić, V., Čačković, M., Tomašić, V., Doko Jelinić, J., 2018. Polycyclic aromatic hydrocarbons in PM₁₀, PM_{2.5} and PM₁ particle fraction in an urban area. *Air Qual Atmos Health* 11, 843-854.

Larsen, J.C., Larsen, P.B., 1998. Chemical carcinogens. In *Air Pollution and Health*; Hester, R.E., Harrison, R.M., Eds. The Royal Society of Chemistry: Cambridge, UK, pp. 33–56.

Nisbet, I.C.T., LaGoy, P.K., 1992. Toxic equivalency factors (TEFs) for polycyclic aromatic hydrocarbons (PAHs). *Regul Toxicol Pharm* 16, 290–300.

Pehnc, G., Jakovljević, I., 2018. Carcinogenic potency of airborne polycyclic aromatic hydrocarbons in relation to the particle fraction size. *Int J Environ Res Public Health* 15, 2485.

Ravindra, K., Sokhi, R., Grieken, R.V., 2008. Atmospheric polycyclic aromatic hydrocarbons: Source attribution, emission factors and regulation. *Atmos. Environ.* 42, 2895–2921.

Rogula-Kozłowska, W., Kozielska, B., Klejnowski, K., Szopa, S., 2013. Hazardous compounds in urban PM in the central part of Upper Silesia (Poland) in winter. *Arch Environ Prot* 39, 53–65.



18th World Clean Air Congress, 23-27 September 2019, Istanbul
organized by TUNCAP and IUAPPA

Šišović, A., Pehnc, G., Jakovljević, I., Šilović Hujić, M., Vadjjić, V., Bešlić, I., 2012. Polycyclic aromatic hydrocarbons at different crossroads in Zagreb, Croatia. *Bull Environ Contam Toxicol* 88, 438–442.

Tobiszewski, M., Namieśnik, J., 2012. PAH diagnostic ratios for the identification of pollution emission sources. *Environ. Pollut.* 162, 110-119.

Yunker, M.B., Macdonald, R.W., Vingarzan, R., Mitchell, R.H., Goyette, D., Sylvestre, S., 2002. PAHs in the Fraser River basin: a critical appraisal of PAH ratios as indicators of PAH source and composition. *Org Geochem* 33, 489–515.

Zhang, Z., Huang, J., Yu, G., Hong, H., 2004. Occurrence of PAHs, PCBs and organochlorine pesticides in the Tonghui River of Beijing, China. *Environ Pollut* 130, 249–261.

An integrated analysis of dust transport over Turkey

Efem Bilgic¹, Gizem Tuna Tuygun¹ and Orhan Gunduz²

¹Dokuz Eylul University The Graduate School of Natural and Applied Sciences, Izmir, Turkey

²Dokuz Eylul University Environmental Engineering Department, Izmir, Turkey

efem.bilgic@deu.edu.tr

Abstract. Dust storms are considered as meteorological hazards that occur when strong winds lift large amounts of sand, dust and other fine graded material from bare, dry ground into the atmosphere. Typically, highly concentrated dust originates from desert areas of Africa and Middle East and are transported long distances influencing air quality and human health in many countries in Europe, Asia and Africa. It is assumed that about 40% of aerosols in the troposphere are dust particles associated with wind erosion. Being situated on the crossroads of Africa, Asia and Europe, Turkey is one of the mostly affected countries from dust emissions originating from sub-Saharan region. Based on this premise, the fate and transport of a dust storm episode influencing Turkey is analyzed based on remotely-sensed observations of a number of satellites and a Lagrangian particle transport model - FLEXPART. First, episodes with high particulate matter concentrations are determined by analyzing ground-based monitoring station datasets. Later, a source term is assigned to the event by analyzing satellite imagery from the exact time period of the episode and a dust mass loading rate is obtained by using reanalysis data. Finally, the atmospheric dispersion of the emitted dust is estimated using the FLEXPART model. The meteorological data required by FLEXPART is supplied from NCEP/NCAR database. The simulation results are then statistically analyzed and validated by comparing with both the AERONET fine/coarse-mode aerosol optical depth (AOD) and PM₁₀ concentrations obtained from ground level monitoring stations in and around Turkey. Spatiotemporal distributions of the dust column density and aerosol optical depth are presented and cumulative dust depositions over Turkey are predicted.

Keywords: Dust storms, Particulate matter, MERRA, Atmospheric dispersion model, Source term.

1. Introduction

Atmospheric dust is emitted from arid and semi-arid regions in the world due to processes at the surface that lift the dust into the atmosphere where it interacts with radiation and water vapor during transport (WMO, 2017a). Dust storms have been historically considered as a natural phenomenon, but their occurrence and intensity have increased over the last years due to anthropogenic activities such as forest reduction, soil degradation and desertification (Sissakian et al., 2013). Atmospheric dust is subject to long-range transport of intercontinental scale, including North African dust plumes reaching over the Atlantic Ocean, summer dust plumes from the Arabian Peninsula reaching over the Arabian Sea and Indian Ocean and spring dust plumes from East Asia reaching over the Pacific Ocean. Research has now proven the fact that mineral dust aerosols influence the global climate system and cloud microphysics in multiple ways (Flores et al., 2017).

Mediterranean Region has high aerosol radiative forcing in comparison with the entire world, especially during summer months (Agacayak et al., 2015). Mineral dust transported from Saharan Desert to Europe is often a problem for the countries located on the coasts of the Mediterranean Sea. Millions of tons of dust are transported every year primarily from the Sahara Desert, Syria and Arabian Peninsula, which are in close vicinity of Turkey. Dust may cause 80% of PM₁₀ concentrations with seasonal peaks (Pey et al., 2013). Transported dust results in elevated particulate matter concentrations at monitoring sites (Salvador et al., 2013).

Previous studies showed that although Saharan dust transport can occur in every season, its highest impact is observed during March, April, May and October. It is also suggested that 70% of these events occur in the transition seasons where mineral dust episodes tend to continue up to 10 days. Dust transport is dominated by the cyclones during spring and by the Saharan depression and Libyan ridge during summer (Meloni et al., 2008; Kabatas et al., 2014; Agacayak et al., 2015; Flores et al., 2017). The studies mentioned thus far mostly focused on western and central North Africa and Sahara regions and effects on western part of Turkey. There are relatively fewer measurements and modeling studies focusing on the Arabian Peninsula.

Goudie and Middleton (2006) provided an extensive discussion of the causes of dust storms in the Middle East. Within this region, eastern Syria, northern Jordan, and western Iraq are considered to be the source for most of the fine dust particles (less than 50 µm in diameter) found in Arabian dust storms. The United Arab Emirates unified aerosol experiment (UAE2) focused on dust in the coastal and desert regions of the United Arab Emirates in August to September 2004 to evaluate the properties of dust particles that converge in the UAE region from numerous sources and their impact on the radiation budget (Reid et al., 2008). Kalenderski et al. (2013) simulated a winter dust event that occurred in January 2009 over the Arabian Peninsula and the Red Sea to study various dust related phenomena. Notaro et al. (2013) investigated the temporal and spatial characteristics of Saudi Arabian dust storms using trajectory analysis. Using MODIS data, they found that the highest aerosol optical depth (AOD) is achieved during dust storms that originate from the Rub Al Khali and Iraqi Deserts.

Dust particles in the air can be transported for long distances from the source regions and cause high levels of daily PM₁₀ concentrations. Dust may be added to the local pollution of anthropogenic origin and affect air quality. Forecasts of dust outbreaks and transport are critical for human health prevention (WMO, 2017b). Quantification of occurrence and intensity of desert dust transport on air quality PM₁₀ standards is important.

Based on this premise, this study focused on the movement of atmospheric dust originating from a dust storm in the Arabian Peninsula and proposed a systematic way to analyze its origination, transport and impact on Turkey. Since dust transport is a significant aerosol source for Turkey, this paper specifically analyzed the effects of a major dust episode, which occurred on 10–17 October of 2018 in the Arabian Peninsula, that reached Turkey in the following days. The source term characterization was achieved by remotely sensed data and a Lagrangian particle transport model (i.e. FLEXPART) was used to simulate the long ranged transport of the emitted dust. The results were then compared with the measured ground level measurements and a discussion on its potential impacts over Turkey was presented. The comparisons were made with monitored PM₁₀ concentrations from 5 different stations over Turkey and aerosol optical depth (AOD) values from AERONET sun/sky radiometer measurements.

2. Methodology

2.1. Episode and source determination

The first step in this analysis was determination of the long-range dust transport events and the selection of a number of periods from recent events. Once the event is selected, AQMS and AERONET data were examined during the related period and a period, in which most parts of Turkey was effected, was

accepted to be the simulation period for this study. Later, this period is further validated with MODIS-Terra retrieved AOD. Eventually, October 10-17 period of the year 2018 was selected as the extreme dust episode of concern for this study.

2.1.1. PM_{10} measurement dataset.

In Turkey, PM_{10} measurements are provided by Turkish Ministry of Environment and Urbanization National Air Quality Observation Network from a system of more than 200 stations. The monitoring network uses beta Gauge instruments, which allow an accurate estimation of the particulate mass under all conditions. Stations that are mainly affected by dust transport from Arabian Peninsula during the selected episode according to satellite observations, as shown in the following sections, were selected for verifying model results.

In this study, five different air quality monitoring stations (AQMS) that have PM_{10} measurements were analyzed from different regions, including two stations from Southeast Anatolia, two stations from Mediterranean, one station from Black Sea and one station from Eastern Anatolia region, over Turkey (Figure 1). The analysis of PM_{10} observations revealed that Kilis has the highest daily average PM_{10} concentration over the aforementioned duststorm episode ($467.8 \mu\text{g}/\text{m}^3$ on 16 October 2018), while lowest daily average PM_{10} concentrations were found in Sinop station located in Black Sea region. Air quality was beginning to deteriorate in Kilis, Adana and Sanliurfa after October 11, 2018 as seen in Figure 2, while air quality in Black Sea region started to be effected by dust transport after October 15, 2018. Eastern Anatolia region started to be effected by the same dust transport after October 14, 2018. Sanliurfa, Adana, Kilis and Erzurum stations showed similar concentration pattern on 15 October 2018.

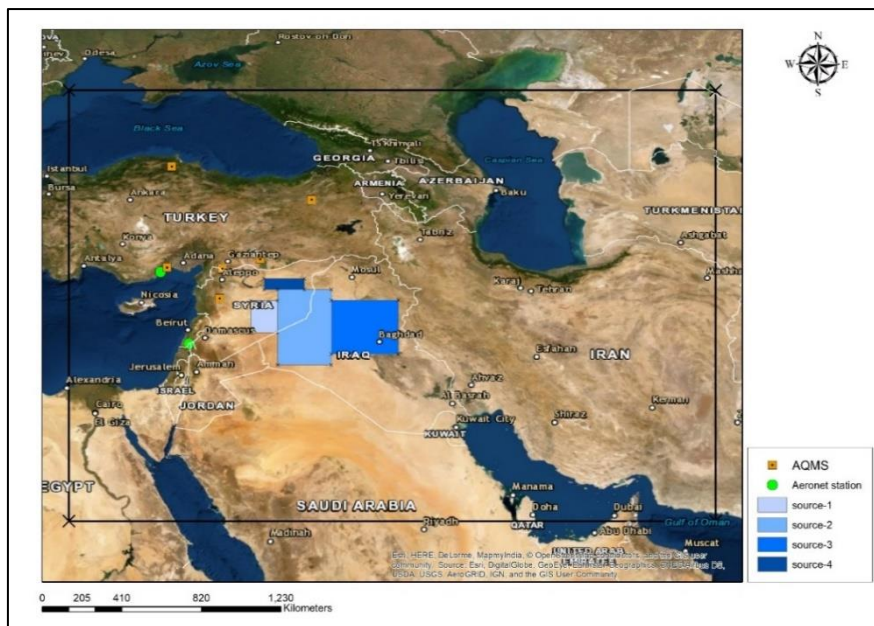


Figure 1. Location of monitoring stations and dust sources used in this study

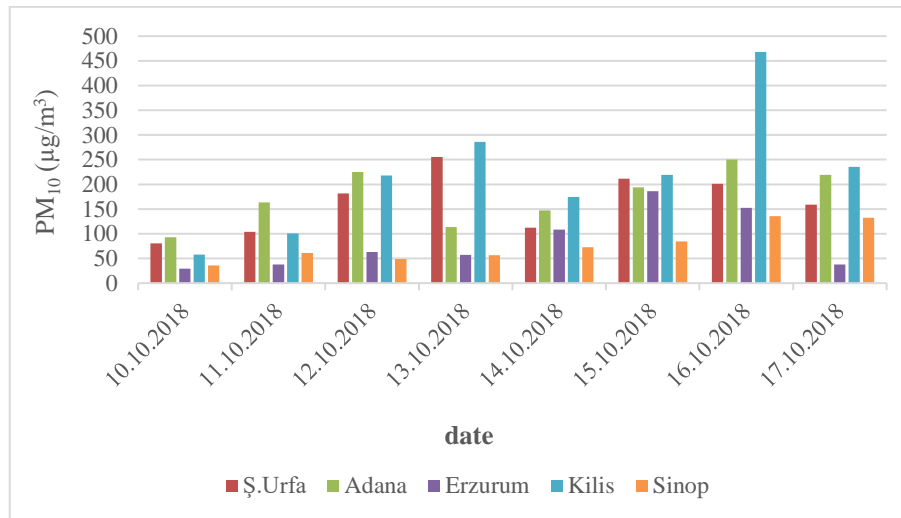


Figure 2. Daily average PM10 concentrations over 5 stations

2.1.2. AERONET aerosol optical depth measurements.

Aerosol optical depth is a measurement of light extinction caused by natural and anthropogenic aerosols suspended in the atmosphere such as desert dust, sea salt, smoke from biomass burning, and vehicle and industrial emissions. In this study, the ground based monitoring network, Aerosol Robotic Network (AERONET, Holben et al., 1998), was used to analyze the dusty days over the study area. Automatic sun-sky scanning spectral radiometers are used by this network to provide globally distributed near-real time observations of aerosol optical depth and aerosol size distributions. AERONET has more than 300 sites all over the world (Holben et al., 1998). In this study, Level 2 AERONET data (i.e., pre and post field calibrated, automatically cloud cleared and manually inspected) from Migal (33.236 N°, 35.578 E°) and IMS-METU-Erdemli (36.565 N°, 34.255 E°) stations was used to predict the dust storm period. Angstrom Exponent (AE) values were also obtained from the AOD measured at 440 and 870 nm since the combined use of the AOD and AE allows to distinguish between different aerosol types. The low average AE 444-870 value (<0.7) and high AOD values (>0.30) at these stations confirms the major influence of large dust particles (Chudnovsky et al., 2017). Figure 3 shows the temporal variation of AOD and AE for Migal station, which is closest AERONET station to dust sources used in this study. Figure 3 indicated that dust particles were dominant mainly on October 11, 2018. It also indicated that this region started to be effected by a strong dust storm after October 15, 2018 and dust particles remained dominant in the area till October 17, 2018 where lowest AE and highest AOD were recorded.

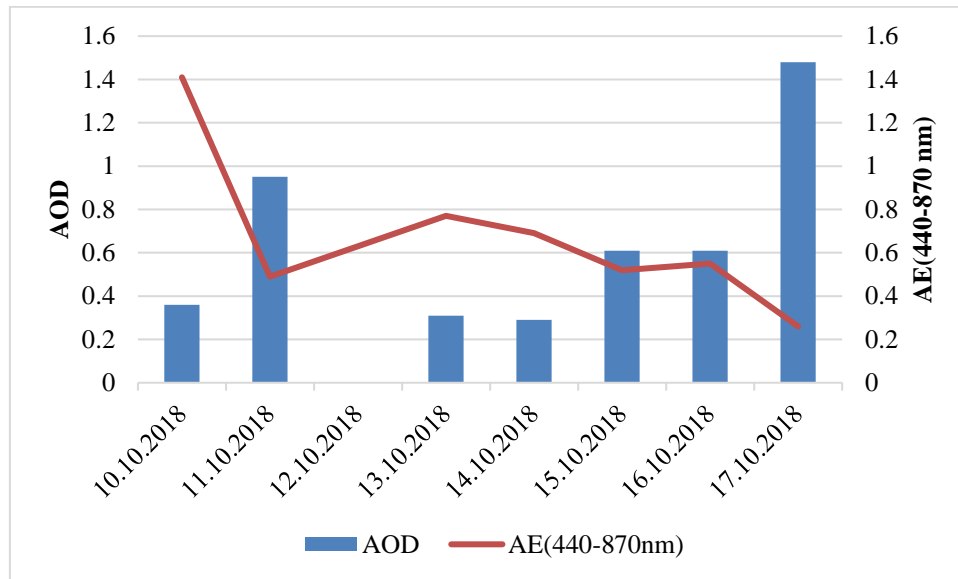


Figure 3. Temporal variation of AOD and AE for Migal AERONET station

2.1.3. Satellite observations from MODIS

MODIS Dark Target and Deep Blue combined AOD was used to describe the dust load over Arabian Peninsula. This data set has a quality assurance confidence (level 2 single pixel measurements) of 3 over land and >0 over ocean and has a maximum retrievable signal of 1.0 (Masuoka et al., 2010). Mahowald et al. (2017) indicated that during dust events, AOD can be used as a reliable tool to represent dust loading in the atmosphere. Accordingly, high AOD values observed in Syria and Iraq Deserts verified that a severe dust storm event has occurred from October 10 to 17, 2018 (Figure 4). The storm originated from the deserted lands of Syria and Iraq during this period. The storm started to move towards southern and southeastern parts of Turkey on October 15, 2018. It started to effect Cyprus island on October 16, 2018. The MODIS-retrieved AOD data can measure the global aerosol scattering or absorption effect and is often used to analyze variations in dust aerosol loading (Li et al., 2015). MODIS–Terra with Dark Target and Deep Blue algorithms were used in this study. Figure 4 shows high AODs (> 1.5) in the deserts located in Syria and Iraq after October 10, thereby implying the existence of dust plumes in these regions. Mainly, a strong dust storm started over Iraq deserts on October 15, 2018. A combination of MODIS and MERRA-2 reanalysis data revealed that dust aerosols were dominant in both deserts. Furthermore, high AODs were observed and gradually distributed towards south and then southeast Turkey after this storm. Variations in high dust loadings (Figure 5) showed strong agreement with those retrieved from the MODIS.

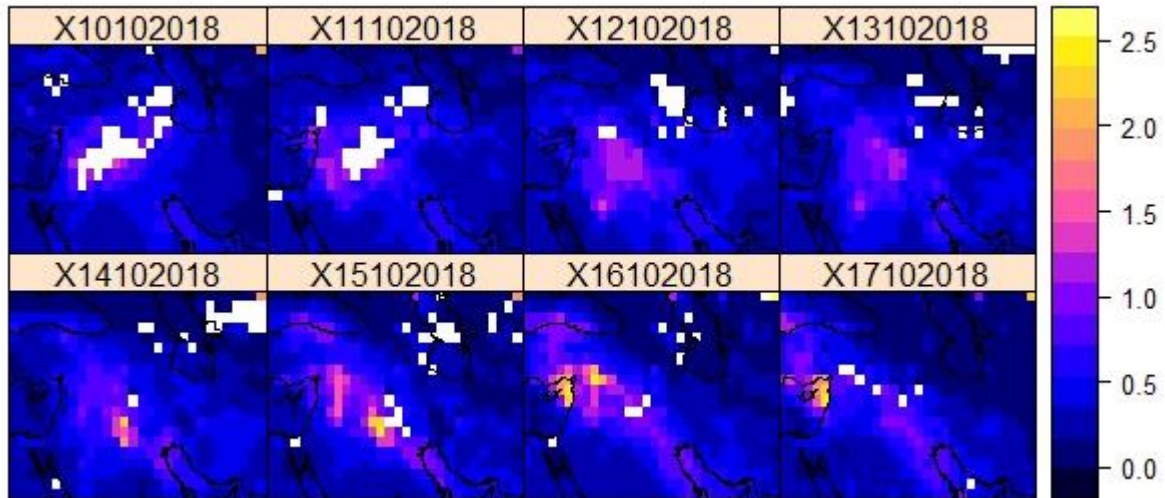


Figure 4. The variations in the MODIS-Terra retrieved AOD combining the DT and DB algorithms at 550 nm during October 10 – 17, 2018

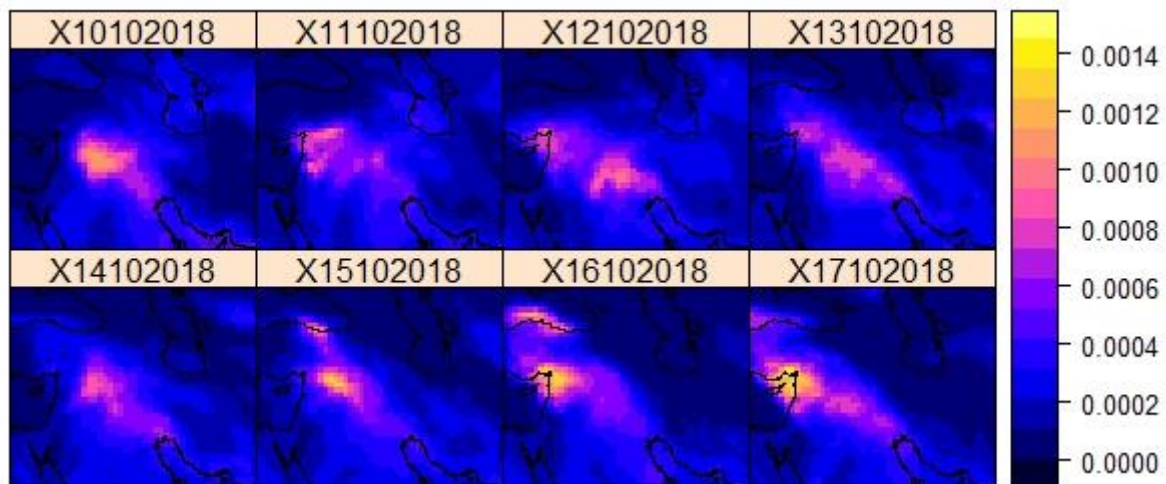


Figure 5. Spatiotemporal distribution of the dust column density ($\text{kg}/\text{m}^2\cdot\text{day}$) over the study region based on MERRA-2 during October 10–17, 2018

These results revealed that the dust plumes from the desert were gradually transported to upwind regions such as southeast and south Turkey and Cyprus and later even to inner and northern parts of Turkey from October 15 to 17, 2018. It should be noted, however, that MODIS can only provide the horizontal transport characteristics of dust aerosols during transport processes; and it cannot be used to determine the vertical distribution of the dust layer. In this study, before estimating the dust mass loading, the spatiotemporal distribution of the dust column density over study region was determined using MERRA-2 data. As presented in Figure 5, the spatial distribution of the dust column density showed some differences to that of the MODIS-retrieved AOD, likely due to the differences in data sources. Briefly, the AOD from MODIS was retrieved from the instantaneous observation of satellites, whereas the dust column density from MERRA-2 was obtained through a 24-hour averaged model simulation.

2.1.4. MERRA-2 reanalysis data.

MERRA-2 replaced the original MERRA by using an upgraded version of the Goddard Earth Observing System Model, Version 5 data assimilation system produced by the GMAO (Randles et al., 2016). It

places observations from NASA's Earth Observing System (EOS) satellites into climate contexts, thereby updating the MERRA system to include the most recent satellite data (Randles et al., 2016). By contrast, MERRA-2 performs aerosol and meteorological assimilations simultaneously. Furthermore, MERRA-2 incorporates AOD measurements from various Polar Operational Environmental Satellites of the National Oceanic and Atmospheric Administration (NOAA), as well as EOS platforms and ground-based observations from NASA (Randles et al., 2016), which provide considerably more accurate estimates of dust transport, emission, and deposition than do single models and observations (Buchard et al., 2016). It was found that the global annual mean dust emission and loadings were consistent with the multimodel AeroCom Phase I median emissions and loadings (Colarco et al., 2014). The dust loadings can be estimated using the following equation:

$$DL = D_{\text{mean}} \times S \quad (1)$$

where DL indicates dust loadings, D_{mean} is the estimated mean dust column density based on MERRA-2 for a certain area in East Asia, and S is the source area (Figure 1) for estimated dust loading.

MERRA-2 data were used to determine the release area and estimate the release amount of dust source in this study (Table 1). First, source data was estimated considering satellite and reanalysis data. This is a complicated procedure because satellite does not give clear information about the release starting point. Regarding big changes between sequential satellite and reanalysis data, release area and time were predicted. Then, release amounts were estimated for each source area using dust column density data with $0.625^\circ \times 0.5^\circ$ resolution obtained by MERRA-2. Because satellite data doesn't include only dust loading from source but also include loadings that originate from other grids, extracting release data from the satellite data is quite difficult. Thus, various runs were simulated and the source term that gives the best correlation with AQMSs was selected.

Table 1. Release amount and area obtained from MERRA-2 by dust sources

Source	Area (m ²)	Release Start Date	Release End Date	Total Release (ton)
Source 1	19182	10/10/2018	16/10/2018	98518
Source 2	89901	10/10/2018	16/10/2018	514598
Source 3	79313	10/10/2018	16/10/2018	392127
Source 4	9470	10/10/2018	16/10/2018	41649

2.2. Atmospheric dispersion model

A Lagrangian particle dispersion model, i.e. FLEXPART, was later used to estimate atmospheric transport of dust particles in the study. FLEXPART is a long-range transport model and considers a simple zero acceleration equation:

$$X(t+\Delta t) = X(t) + v(X,t)\Delta t \quad (2)$$

where X represent position of each particles at time t, and the equation estimate the new position of each particle after Δt time. v is wind velocity consist of three wind vector:

$$v = v' + v_t + v_m \quad (3)$$

v' is grid scale wind, v_t i turbulent wind fluctuations and v_m is meso-scale wind fluctuations. FLEXPART also calculates wet and dry deposition of each particle considering particle characteristics and meteorological conditions. FLEXPART uses three-dimensional meteorological fields in grib format for estimations and GFS data was used in this study (Saha et al., 2011). GFS data obtained by NOAA has



0.5 degree horizontal and 6-hourly temporal resolution. Also, this dataset includes 23 vertical atmospheric pressure level. The simulated ground level particle concentrations were later compared with the AQMSs. Further details on the model is provided in FLEXPART technical document (Stohl et al., 2005).

3. Results and discussion

Dust that originates from Syrian and Iraq deserts were determined by remotely sensed data and its transportation was then simulated using an atmospheric dispersion model and reanalysis data. Then, ground level model results were compared with air quality monitoring station data in Turkey. During simulations, four different area sources were determined following steps mentioned in section 2.1.4 (Figure 1). However, it must be noted that dust did not release constantly and did not originate from same areas during the simulations. Thus, repeated simulations were used by changing the release duration to obtain the best fits with measured data. As a result of this iterative procedure, the specific release defined in Table 1 was obtained and used in running the simulations.

FLEXPART simulations demonstrated that dust particles mainly moved toward north and west direction during the episode. Starting with midday October 10, 2018, dust particles entered Turkey through southeast Anatolia border with Syria. In the following day, the entire southeast Anatolia Region and a major portion of eastern Anatolia were affected by desert particles. Dust concentrations were relatively higher in the entire eastern and southeastern Anatolia regions, eastern Mediterranean and some parts of Central Anatolia on 12-13 October 2018. Model results demonstrated that Black Sea region was also affected after October 14, 2018. Finally, east parts of Turkey are significantly affected from desert dusts on October 15 and 16, 2018 (Figure 6).

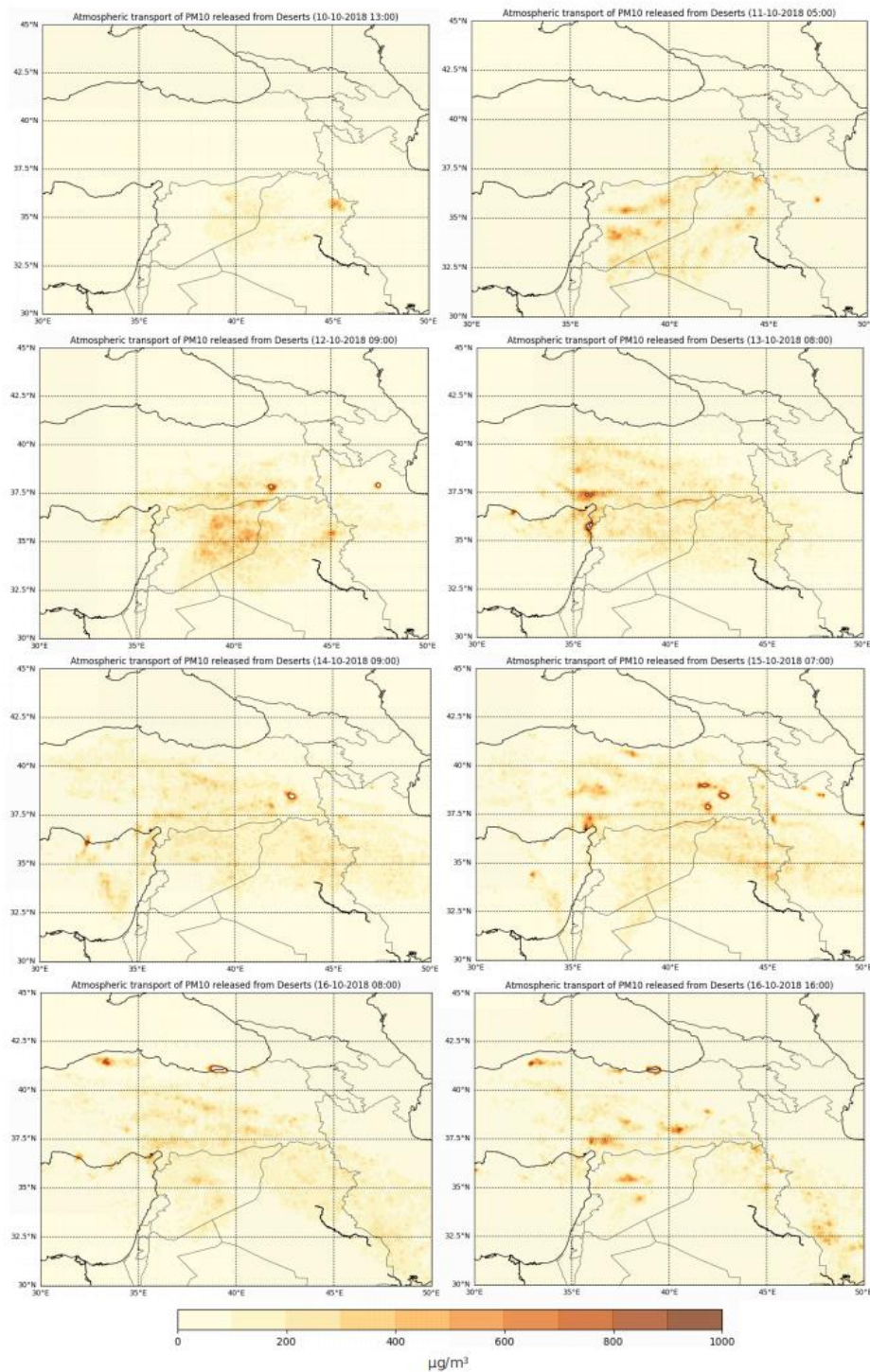


Figure 6. Atmospheric transport of particulate matters released from Syrian and Iraq deserts

When the result of simulations were compared with ground level measurements, it was seen that FLEXPART outputs gave over/under estimations in different parts of the simulation period as well as in different receptor locations. Hourly changes of the particle matter concentrations in the air gave a



fairly reasonable pattern for dust emissions and an acceptable agreement between simulated results and measurements for some stations and/or some time steps. First day, FLEXPART results and AQMSs measurements were relatively close to each other in the city of Sanliurfa. However, model gave underestimations at the end of the day. Although correlations between model simulations and ground level measurements was found again next day, model results showed underestimations again in October 13, 2018. Some correlation between model results and monitoring station measurements were found in the first day, in Kilis just as in Sanliurfa. However, model gave underestimated results especially in October 13 and 16, 2018. Erzurum AQMS gave lower values than model results at the end of October 13, 2018 and beginning of the October 15, 2018. On the other hand, model gave underestimated results at the end of October 15, 2018. Until October 15, model results were mostly lower than measurements except during October 14, 2018. After October 15, model results became higher than monitoring station data, but temporal variations of the concentrations showed a fairly similar pattern. Any correlations could not be found between AQMS measurements and model results in Adana. Early and late results were lower than monitor data and model gave overestimated values between 14th and 15th October of 2018 (Figure 7).

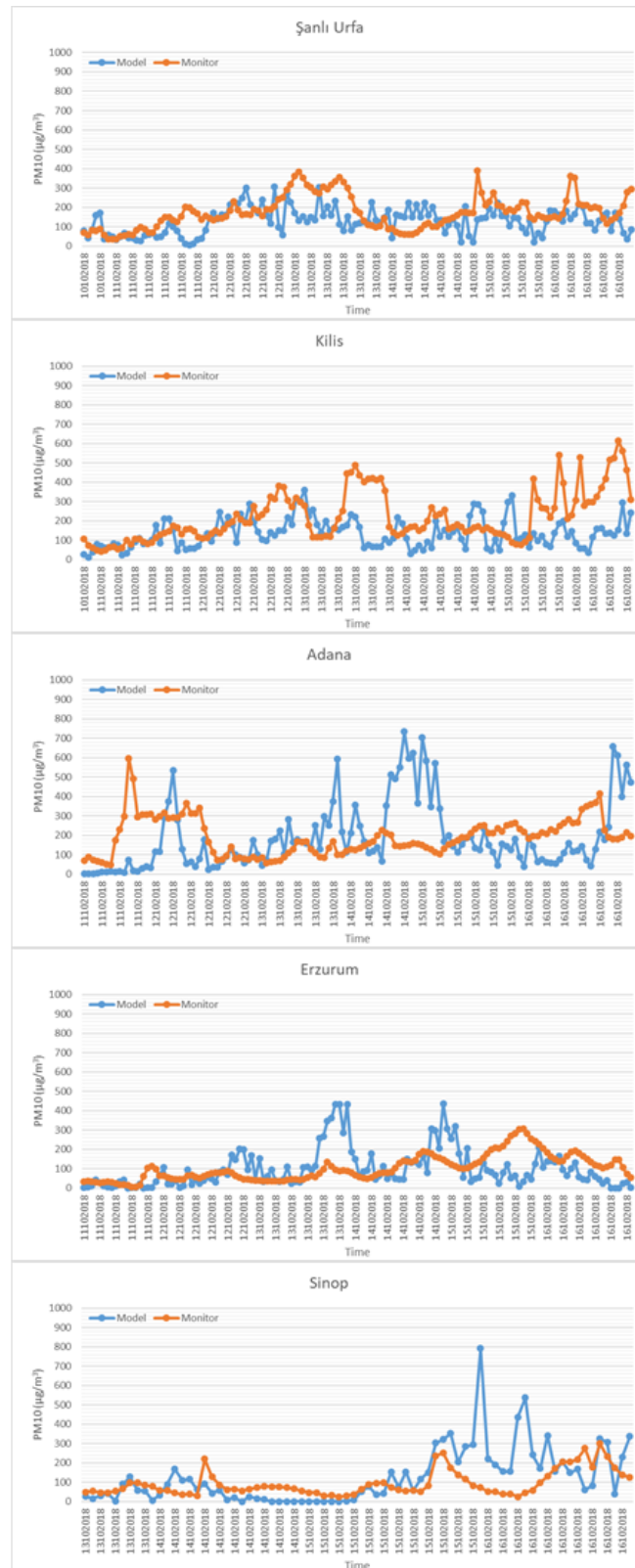


Figure 7. Comparisons between AQMS measurements and model results in some receptor points

The results are later compared with the AERONET station data sets. Figure 8 (upper panel) demonstrates the particle size distribution of the dust in terms of the AERONET level 2.0 product for the period between 13 and 15 October at Erdemli station. As we have already revealed from our analysis, columnar measurements do not refer to pure dust since the contamination of the column from local emissions maximizes within the PBL. However, from the temporal variation presented in the upper panel of Figure 8, it is clear that before the arrival of dust particles over Erdemli (Mersin), high fraction of fine mode AOD values at 500 nm (~ 0.6 - 0.7) were recorded on 10 October 2018, while during the 13-15 April 2018, the coarse mode AOD values were increased and highest PM₁₀ concentrations and coarse mode fraction were found on 14 October 2018.

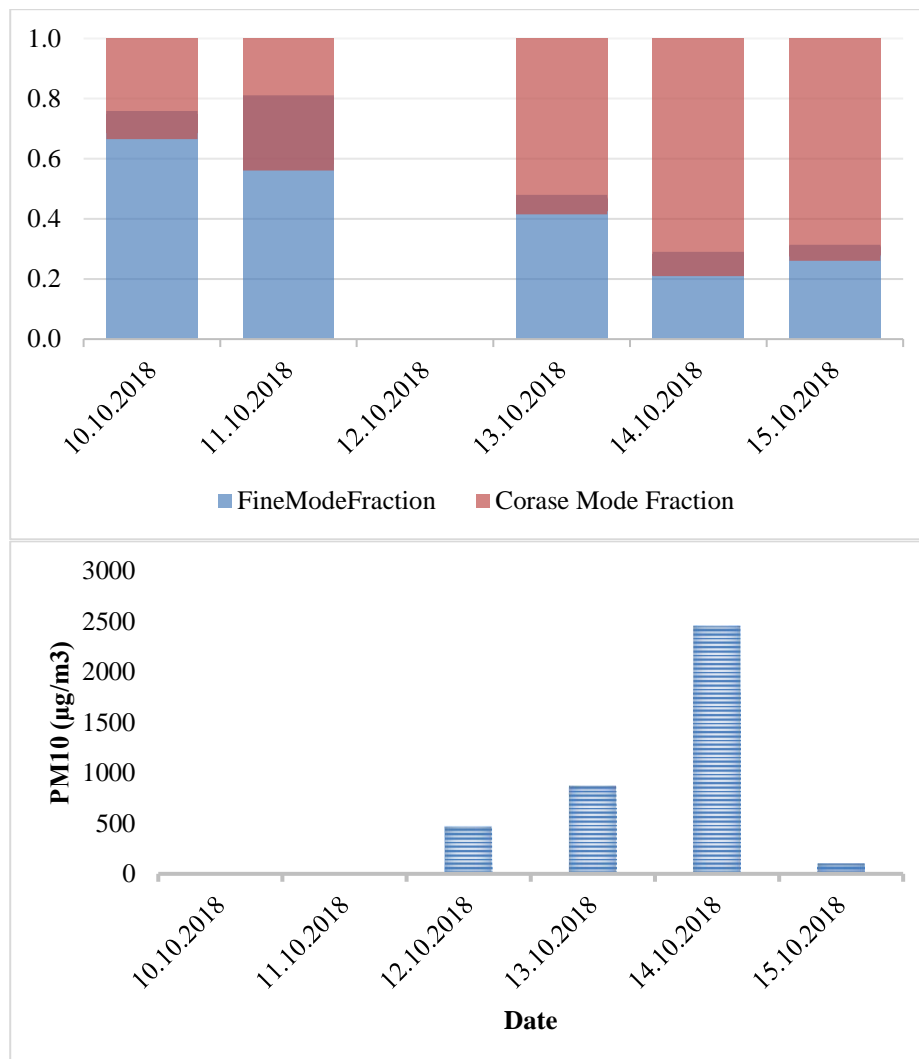


Figure 8. AERONET fine/coarse-mode aerosol optical depth (AOD) obtained over IMS-METU-Erdemli at 500 nm for the period between 10 and 15 October 2018, Temporal evolution of the PM₁₀ concentration (in $\mu\text{g}/\text{m}^3$) according to FLEXPART simulations (lower graph)

The respective coarse-mode particles inside the atmospheric column were on the order of 33.5–37.5% before the event, and remained around 71–72% during the event. This means that the coarse-mode particles dominated the dust storm period.

4. Conclusions

Atmospheric transport of dusts originating from deserts was simulated in this study by producing an approximate source term through satellite data. While the results captured the general temporal pattern, they over/under estimated ground level measurements at different time periods and receptor locations. The fairly parallel pattern in simulated and measured results as a function of time demonstrated that this approach can be used in modeling desert storm dust emissions. Although producing source term using satellite data is possible, this approach needs some improvements. The model results are expected to improve proven to work, better source term estimations can be made with more sophisticated use of remotely sensed data. In this regard, better estimates of wind direction and velocity are likely to reveal better source terms, which in turn will yield better simulations of ground level results.

MERRA data has a fairly high temporal resolution and finding source release times with MERRA datasets can be made. However, estimating the release amount is complicated as it has significantly lower vertical resolution (only one layer represents the entire atmosphere) and does not provide any particle size distribution. Such lack of data can be refined by using data from other satellites such as LIDAR. Furthermore, the measurement quality and location selection of AQMS are also crucial factors in the evaluation of model results. Inconsistencies between some model results and AQMS measurements can be caused by inaccuracies in automatic monitoring of particulate matter in these stations and/or poor calibration of the equipment. Increasing the number of PM₁₀ measurements for model validation could be a good option to better analyse the accuracy of the model.

5. References

- Agacayak, T., Kindap, T., Unal, A., Pozzoli, L., Mallet, M., Solmon, F., 2015. A case study for Saharan dust transport over Turkey via RegCM4.1 model. *Atmos. Res.* 153, 392-403.
- Buchard, V., da Silva, A.M., Randles, C.A., Colarco, P., Ferrare, R., Hair, J., Hostetler, C., Tackett, J., Winker, D., 2016. Evaluation of the surface PM_{2.5} in Version 1 of the NASA MERRA Aerosol Reanalysis over the United States. *Atmos. Environ.* 125, 100–111.
- Colarco, P.R., Nowotnick, E.P., Randles, C.A., Yi, B., Yang, P., Kim, K.M., Smith, J.A. and Bardeen, C.G., 2014. Impact of radiatively interactive dust aerosols in the NASA GEOS-5 climate model: Sensitivity to dust particle shape and refractive index. *J. Geophys. Res. Atmos.* 119, 753–786.
- Flores, R.M., Kaya, N., Eser, O., Saltan, S., 2017. The effect of mineral dust transport on PM₁₀ concentrations and physical properties in Istanbul during 2007–2014. *Atmos. Res.* 197, 342-355.
- Goudie, A. S. and Middleton, N. J.: *Desert Dust in the Global System*, Springer, Heidelberg, 2006.
- Holben, B. N., Eck, T. F., Slutsker, I., Tanré, D., Buis, J. P., Setzer, A., Vermote, E., Reagan, J. A., Kaufman, Y. J., Nakajima, T., Lavenue, F., Jankowiak, I., and Smirnov, A., 1998. AERONET-A federated instrument network and data archive for aerosol characterization, *Remote Sens. Environ.* 66, 1–16.
- Kabatas, B., Unal, A., Pierce, R.B., Kindapa, T., Pozzoli, L., 2014. The contribution of Saharan dust in PM₁₀ concentration levels in Anatolian Peninsula of Turkey. *Science of the Total Environment.* 488–489, 413–421.
- Kalenderski, S., Stenchikov, G., and Zhao, C., 1999. Modeling a typical winter-time dust event over the Arabian Peninsula and the Red Sea, *Atmos. Chem. Phys.* 13, 1999–2014.
- Li, R., Gong, J., Zhou, J., Sun, W. and Ibrahim, A.N., 2015. Multi-satellite observation of an intense dust event over southwestern China. *Aerosol Air Qual. Res.* 15, 263–270.



- Mahowald, N. M., Scanza, R., Brahney, J., Goodale, C. L., Hess, P. G., Moore, J. K., and Neff, J., 2017. Aerosol deposition impacts on land and ocean carbon cycles, *Current Climate Change Reports*. 3, 16–31.
- Masuoka, E., Roy, D., Wolfe, R., Morissette, J., Sinno, S., Teague, M., Saleous, N., Devadiga, S., Justice, C., and Nickeson, J.: MODIS Land Data Products: Generation, Quality Assurance and Validation, in: *Land Remote Sensing and Global Environmental Change*, edited by: Ramachandran, B., Justice, C., and Abrams, M., 2010. *Remote Sensing and Digital Image Processing*, Vol. 11, Springer, New York (NY), 509–531.
- Meloni, D., Sarra, A., Monteleone, F., Pace, G., Piacentino, S., Sferlazzo, D.M., 2008. Seasonal transport patterns of intense Saharan dust events at the Mediterranean island of Lampedusa. *Atmos. Res.* 88, 134–148.
- Notaro, M., Alkolibi, F., Fadda, E., and Bakhry, F., 2013. Trajectory analysis of Saudi Arabian dust storms, *J. Geophys. Res.-Atmos.* 118, 6028–6043.
- Pey J, Querol X, Alastuey A, Forastiere F, Stafoggia M., 2012. African dust outbreaks over the Mediterranean basin during 2001–2011: PM10 concentrations, phenomenology and trends, and its relation with synoptic and mesoscale meteorology. *Atmos. Chem. Phys. Discuss.* 12, 195–235.
- Randles, C.A., da Silva, A.M., Buchard, V., Darmenov, A., Colarco, P.R., Aquila, V., Bian, H., Nowotnick, E.P. Pan, X., Smirnov, A., Yu, H. and Govindaraju, R., 2016. The MERRA-2 Aerosol Assimilation. NASA Technical Report Series on Global Modeling and Data Assimilation. NASA/TM-2016-104606, 45, 143.
- Reid, J. S., Piketh, S. J., Walker, A. L., Burger, R. P., Ross, K. E., Westphal, D. L., Brientjes, R. T., Holben, B. H., Hsu, C., Jensen, T. L., Kahn, R. A., Kuciauskas, A. P., Mandoos, A. A., Mangoosh, A., Miller, S. D., Porter, J. N., Reid, E. A., and Tsay, S. C., 2008. An overview of UAE2 flight operations: observations of summertime atmospheric thermodynamic and aerosol profiles of the southern Arabian Gulf, *J. Geophys. Res.*, 113, D14213.
- Saha, S., Moorthi, S., Wu, X., Wang, J., Nadiga, S., Tripp, P., Behringer, D., Hou, Y., Chuang, H., Iredell, M., Ek, M., Meng, J., Yang, R., Mendez, M. P., van den Dool, H., Zhang, Q., Wang, W., Chen, M., and Becker, E., 2011. NCEP Climate Forecast System Version 2 (CFSv2) 6-hourly Products. Research Data Archive at the National Center for Atmospheric Research, Computational and Information Systems Laboratory. Dataset. <https://doi.org/10.5065/D61C1TXF>. Accessed in 11 August 2019.
- Salvador, P., Artíñano, B., Molero, F., Viana, M., Pey, J., Alastuey, A., Querol, X., 2013. African dust contribution to ambient aerosol levels across central Spain: characterization of long-range transport episodes of desert dust. *Atmos. Res.* 127, 117–129.
- Sissakian, V.K., Al-Ansari, N., Knutsson, S., 2013. Sand and dust storm events in Iraq. *Nat. Sci.* 05, 10–11.
- Stohl, A., Forster, C., Frank, A., Seibert, P., Wotawa, G., 2005. Technical note: The Lagrangian particle dispersion model FLEXPART version 6.2. *Atmos. Chem. Phys.* 5, 2461–2474.
- WMO, 2017a. World Meteorological Organization (WMO) Sand and Dust Storm Warning Advisory and Assessment System (SDS-WAS). https://www.wmo.int/pages/prog/arep/wwrp/new/SDS_WAS_background.html.
- WMO, 2017b. World Meteorological Organization (WMO) Sand and Dust Storm Warning Advisory and Assessment System (SDS-WAS): Health Aspects. https://www.wmo.int/pages/prog/arep/wwrp/new/SDS_WAS_background.html.

Spatial distribution of health risks associated with PM_{2.5} in Turkey and Iran using satellite and ground observations

Burcak Kaynak¹, Ezgi Akyuz² and Mehrdad Samavati¹

¹Istanbul Technical University, Environmental Engineering Dep., Istanbul, Turkey

²Istanbul Technical University, Eurasia Institute of Earth Sciences, Istanbul, Turkey

burcak.kaynak@itu.edu.tr

Abstract. PM_{2.5} originated from anthropogenic or natural sources is still a problem for both developing and developed countries worldwide and highly associated with health impacts. In this study, exposure, health effects, and mortality associated with PM_{2.5} have been calculated using satellite retrievals and ground observations for both Turkey and Iran. Satellite retrievals and ground observations, population data, concentration-response factors and baseline mortality rates are used as inputs for concentration-response estimation functions in this study. High resolution PM_{2.5} estimations (dust and sea-salt included and removed) developed from aerosol optical depth (AOD) data was used. A high resolution population dataset along with satellite derived PM_{2.5} were used. Health risk estimations from three different causes was calculated by applying the cause-specific mortality rates from WHO for Iran and for Turkey for the year of 2016. These are ischemic heart disease, lung cancer and all causes, which are attributable to PM_{2.5} pollution. According to satellite-derived PM_{2.5}, mortality estimations of 36967 in Turkey and 34491 in Iran were found by all causes using dust and sea salt removed satellite-based PM_{2.5} concentrations. Meanwhile, estimations of 30357 in Turkey and 30562 in Iran were found for provinces with PM_{2.5} measurements available from ground monitoring stations. Province based estimations were obtained with better spatially resolved PM_{2.5} concentrations. Calculations with ground observations was higher than with satellite-derived PM_{2.5}. for Turkey, but calculations with dust and sea salt included satellite-based PM_{2.5} was higher in Iran. Values estimated in this study were higher than found in global studies for both countries.

Keywords: PM_{2.5}, Health risk, Remote sensing.

1. Introduction

Air pollution and drought are serious issues for countries such as Turkey and Iran located in Middle East. Although some of the cities such as Iğdır in the eastern part of Turkey and Khuzestan in south-western part of Iran reported with high particulate matter (PM), these are not actually populated cities. Other sources such as dust events can also be responsible for PM levels in such regions. Increase in population and industrialization are not the only sources of PM. Climate change, governments' energy policies, such as new dam constructions in susceptible regions may contribute to PM pollution by reducing the water flow. Drought also contributes as a new source for particulate matter (PM).

Air pollution has a significant impact on human health and related health studies revealed the importance of monitoring and control of air pollution. In 2016, 4.1 million premature deaths are associated with the ambient PM which is reported as the sixth global burden of disease (GBD) risk factor. The World Health Organization (WHO) remarks that higher PM levels contributes to almost 800 000 premature deaths per year with a ranking of 13th leading mortality cause (Lim et al., 2012). Long-term PM exposure was resulted in a 24% and 76% increase in cardiovascular disease and cardiovascular mortality per 10- $\mu\text{g}/\text{m}^3$

increase in PM_{2.5} for a group of 65000 postmenopausal women with no previous heart disease over six years (Brook et al., 2010).

A global study previously was conducted to estimate the global exposure of ambient PM_{2.5} mass and trends using PM_{2.5} concentrations gathered from multiple satellite instrument and 210 ground based measurements (van Donkelaar et al., 2015). Cohen (2004) for the first time developed a human health function from Poisson regression model which estimates the premature death associated with air pollution. Later on, this function was also used by Anenberg et al. (2010) and Lelieveld et al. (2013). Tosun (2017) used AIRQ+ software to calculate the health effects of air pollution by PM, SO₂, NO_x, O₃, and CO's concentration data for Ankara, Adana, Diyarbakir, Izmir, Erzurum, Konya, Istanbul, and Samsun provinces. There are other studies conducted by Çapraz (2013) for Istanbul province, and Mercan (2016) for Thrace Region in Turkey. AIRQ+ software was used in assessments for Iranian cities such as Tehran (Naddafi et al., 2012). Also, the results showed that 282 deaths were originated only by lung cancer disease due to PM_{2.5} in 10 Iranian cities in 2016 (Hadei et al., 2017). Shahsavani et al. (2012) used an aerosol spectrometer to measure PM₁₀, PM_{2.5}, and PM₁ separately and estimated total mortality during five months of the study period (April-September) as 934 deaths attributed to PM₁₀ and 197 deaths attributed to PM_{2.5}.

The aim of this study is to estimate the health effects from exposure to ambient PM in premature death and mortality rates caused by all causes, ischemic heart disease (IHD), and lung cancer (LC). In this scope, the remote-sensing AOD derived PM_{2.5} with available ground PM_{2.5} measurements were investigated; premature death rate caused by ambient PM_{2.5} was estimated; the high-risk population by producing spatial distribution maps were prepared, PM_{2.5} concentrations and mortality rates in both countries were compared.

Researchers performed studies in Asian countries (HEI, 2004), European countries (WHO HRAPIE, 2013), and United States (Zanobetti and Schwartz, 2009) reporting effect estimates by all causes (Table 1). According to the studies summarized (Chen et al., 2011; Yang et al., 2012), the exposure-response coefficient was 0.0054 (95% CI: 0.0010–0.0096) based on the meta-analysis, which suggests a 0.54% rise in risk for each 10 µg/m³ PM_{2.5} concentration increase in China. The percentage increase in the mean number of deaths for a 10 µg/m³ increase was 1.23% (95% CI: 0.45–2.01) in Europe, and 0.98% (95% CI: 0.75–1.22) in US.

Table 1. Summary of studies for PM_{2.5} in Asian, European countries and United States

Study city/year	Effect estimate (%)		Adapted from
	of all-cause mortality	95% CI	
Gangzhou 2007-2008	0.90	(0.55,1.26)	Yang et al., (2012)
Shanghai 2004-2005	0.30	(0.06,0.54)	Chen et al., (2011)
Beijing 2007-2008	0.53	(0.37,0.69)	Chen et al., (2011)
Shanghai 2004-2008	0.47	(0.22,0.72)	Chen et al., (2011)
Shenyang 2006-2008	0.35	(0.17,0.53)	Chen et al., (2011)
9 French cities 2000-2004	1.59	(0.80, 2.38)	HRAPIA Project, (2013)
Vienne 2002-2004	2.57	(1.09, 4.04)	HRAPIA Project, (2013)
Czech Republic (coal basin) 1993-1994	0.57	(-0.20, 1.35)	HRAPIA Project, (2013)
Prague 2006-2006	0.40	(-0.80, 1.60)	HRAPIA Project, (2013)
Erfurt 1991-2002	-0.66	(-1.82, 0.50)	HRAPIA Project, (2013)
Barcelona 2003-2004	3.92	(2.27, 5.57)	HRAPIA Project, (2013)
Las Palmas de Gran Canaria 2001-2004	-0.91	(-4.08, 2.25)	HRAPIA Project, (2013)
Santa Cruz de Tenerife 2001-2004	-0.68	(-4.00, 2.63)	HRAPIA Project, (2013)
London 2000-2005	0.52	(-0.76, 1.80)	HRAPIA Project, (2013)
West Midlands 1994-1996	0.34	(-0.85, 1.53)	HRAPIA Project, (2013)
112 cities of U.S.*	0.98	(0.75, 1.22)	Zanobetti and Schwartz, (2009)

* The largest cities are Los Angeles, California; New York City, New York; and Chicago, Illinois.

2. Methodology

Turkey and Iran, both with approximately 83 million populations were selected for this study. In Turkey, PM_{2.5} and PM₁₀ are exceeding the standards determined by WHO and EPA and EU standards. European Environment Agency (EEA) reported that 97.2% of the urban population in Turkey is exposed to unhealthy levels of particulate matter (PM₁₀) (Gauss et al., 2016). On the other hand, Iran is among the countries susceptible to drought due to climate change (JahaneSabz, 2018). Dust events which are getting more and more frequent affect the southwest of Iran, resulting in PM concentrations up to 8600 µg/m³ (ISNA, 2018). Relationship between PM_{2.5} and health are investigated through exposure-response function, and premature mortality rates are estimated caused by the increase in PM pollution levels. The methodology in this study uses air quality measurements (ground and satellite-derived), high-resolution population datasets, and exposure-response functions obtained from the literature.

2.1. Datasets

PM_{2.5} concentrations from 48 air quality monitoring stations for 24 provinces were obtained from National Air Quality Network (NAQN) of Ministry of Environment and Urbanization (MoEU) for Turkey. Because PM_{2.5} measurements of Iran requested from Department of Environment Islamic Republic of Iran (DOE IR), but cannot be obtained, available annual PM_{2.5} concentrations from various air quality monitoring stations for 10 provinces reported in the literature were used (Hadei et al., 2017).

Satellite-derived PM_{2.5} dataset (V4.GL.02) of 2016 with 0.01°×0.01° resolution was used for calculations (van Donkelaar et al., 2016). Both dust and sea salt included, and removed (anthropogenic portion) versions were used (Figure 1). Significant dust events affect the satellite PM_{2.5} observations, especially central and eastern part of Turkey and northern parts of Iran reaching up to 30 µg/m³ (Figure 1).

High resolution dataset of Gridded Population of the World for 2015 (GPWv4) was used with 250×250 m² resolution (CIESIN, 2017). The spatial resolution was converted to the resolution of PM_{2.5} satellite dataset for performing the calculations on grid level. The results were then spatially joined with provinces and countries in investigation, and total values were calculated on province and country levels.

2.2. Health-risk calculations

The exposure-response function, which is based on Poisson regression model (Greenland, 1995), was used to estimate health effects of exposure by defining how much the mortality rate change caused by some unit increase in a pollutant's concentration. The function is based on parameters such as age, sex, season, smoking, education level, socio-economy level and source-apportionment of the pollutant (Kan et al., 2008). Premature death values caused by PM_{2.5} were calculated using Equation (1):

$$RR = e^{\beta\Delta X} \quad (1)$$

RR is the relative risk, β is the exposure-response function coefficient, ΔX is the concentration difference between the background pollutant concentration, X_0 (the lowest observed concentration for this study) (Pope et al., 2002) and observed pollutant concentration. β values were obtained from an epidemiological study performed in the United States (Table 2) (Krewski et al., 2009) due to lack of local cohort studies performed in Turkey and Iran.

Table 2. β coefficient and upper and lower bounds (Krewski et al., 2009)

	All causes (AC)	Ischemic heart diseases (IHD)	Lung cancer (LC)
Coefficient	0.00554	0.02167	0.01293
(Lower Bound- Upper Bound)	(0.00354-0.0076)	(0.01748-0.02585)	(0.00554-0.02029)

Attributable fraction (*AF*) which is the fraction of the mortality attributable to the risk factor was calculated using Equation (2) and excess mortality ($\Delta Mort$) caused by PM_{2.5} exposure was estimated using Equation (3):

$$AF = 1 - (e^{-\beta\Delta X}) \quad (2)$$

$$\Delta Mort = y_0(1 - e^{-\beta\Delta X})Pop \quad (3)$$

Pop is the population affected by the change in PM_{2.5} levels, y_0 is the baseline mortality rate, and $\Delta Mort$ is an estimation of the excess mortalities caused by PM_{2.5} exposure. Iran is in Eastern Mediterranean region and Turkey is in Europe in WHO region divisions, and thus they have different country-specific mortality values. Baseline mortality rates for Iran and Turkey were calculated using estimated death with cause-specific data from WHO for the year 2015 (WHO, 2015) as the ratio of by cause specific mortality over population and given in Table 3.

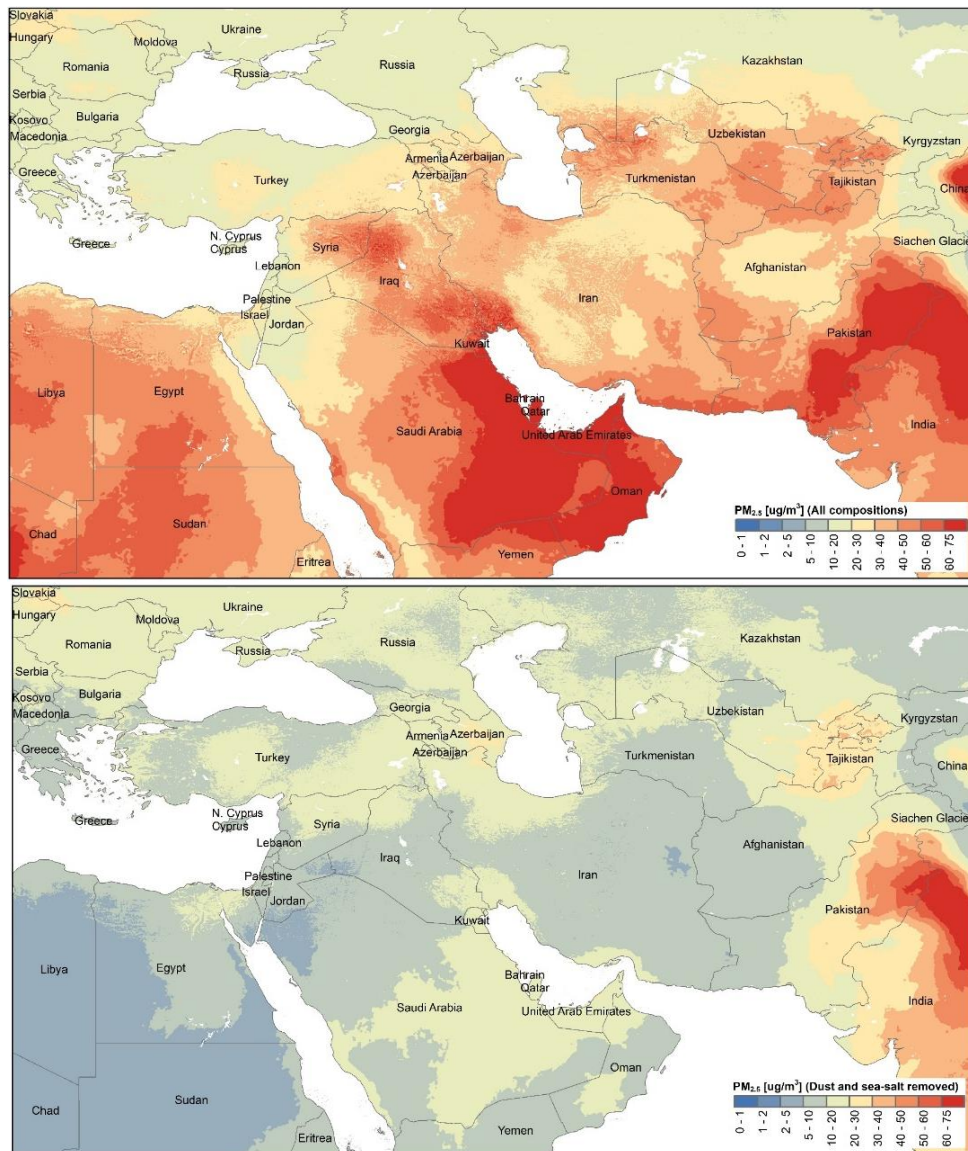


Figure 1. Annual satellite-derived PM_{2.5} retrievals of all compositions -dust and sea-salt included- (top), and anthropogenic origin -dust and sea salt removed- (bottom) for 2016

Table 3. Mortality values and calculated baseline mortality rates for specific causes (WHO, 2015)

Age Range	All Causes		Ischemic Heart Diseases		Lung Cancer	
	Iran	Turkey	Iran	Turkey	Iran	Turkey
30-49	43.6	45.9	7.7	8.6	0.34	3.1
50-59	32.2	34.2	9.4	6.5	0.5	5.6
60-69	45.9	57.1	14.6	12.2	0.7	6.9
+70	163.3	188.9	53.4	46.1	1.6	6.4
Total (≤30)	285.1	326.1	85.2	73.5	3.2	21.9
Baseline Mortality Rate, yr ⁻¹	0.010696	0.011003	0.003195	0.002481	0.000119	0.000738

3. Results and discussion

The effect of anthropogenic PM_{2.5} in mortality by all causes, ischemic heart diseases (IHD), and lung cancer (LC) was calculated separately using dust and sea salt removed satellite-derived PM_{2.5} for Turkey

(Figure 2) and Iran (Figure 3) for the year 2016. Mortality estimations for all compositions were also calculated using satellite-derived PM_{2.5}-dust and sea salt included- and available ground observations. The baseline mortality rates by all causes using WHO country-specific mortality causes were similar between Turkey and Iran. However, baseline mortality rates by LC was significantly different indicating six times higher rates in Turkey than Iran, and by IHD was 30% higher in Iran than Turkey.

3.1. Mortality estimations using satellite-derived PM_{2.5}-dust and sea-salt removed-

Mortality by all causes results indicated high-populated regions such as Istanbul and Ankara with higher estimations as expected (Figure 2, upper). A closer look at the four highest populated provinces in detail indicates differences on province levels mainly associated with population density. For Turkey, the most at-risk population by all causes are in Istanbul, Ankara, Izmir and Bursa when the total number of individual mortalities (>1800) was considered because of the high population of these provinces. However, Batman, Ankara, Osmaniye, Aksaray, Mersin, Iğdır and Ağrı provinces are at most risk when percent of the total population (>0.06%) in the province was considered.

Mortality estimates by IHD indicate almost 5200 individuals in Istanbul only, following with Ankara, Izmir and Bursa. The ranks of the provinces are similar to all causes with lower estimated. The lowest values estimated for LC because of the concentration-response coefficient being the lowest.

For Iran, Tehran population is the mostly affected by all causes (>6000) almost three times higher than the next highest (Figure 3, upper). The provinces of East Azerbaijan, Alborz, Khuzestan, Mazandaran, and Gilan when the total number of individual mortalities (>1800) was considered. However, Ardebil, Gilan, Quazvin and Mazandaran provinces are at most risk when percent of the total population (>0.06%) in the province was considered. Similar rankings are observed by IHD. LC mortality rate of Iran were estimated as significantly lower than of Turkey. A closer look indicates more sparse distribution in Iran than in Turkey except Tehran and its surrounding.

3.2. Mortality estimations using satellite-derived PM_{2.5}-dust and sea-salt included-

Ground observations include both anthropogenic and natural sources at the same time. Unless there is PM speciation measurements and a source apportionment study being performed, distinguishing the dust and sea-salt portion is not possible. Because of that reason, the mortality caused by all causes were also estimated using dust and sea-salt included satellite-derived PM_{2.5}. In Turkey, annual PM_{2.5} concentrations reached up to 64.8 µg/m³ when PM_{2.5} satellite retrievals were used with dust and sea-salt while the total mortalities by all causes increased more than 150%. This increase is more than 275% for Iran.

The importance of satellite-based PM_{2.5} considering dust and sea-salt in such health effect estimations, is higher for countries such as Iran which are experiencing dust events so often than Turkey. The results of Iran showed significant increase in mortalities. In provinces such as Khuzestan, which is the hotspot of dust events in Iran, mortalities increased almost 5 times and ranked as 2nd after Tehran when the total number of individual mortalities (>1800) were considered.

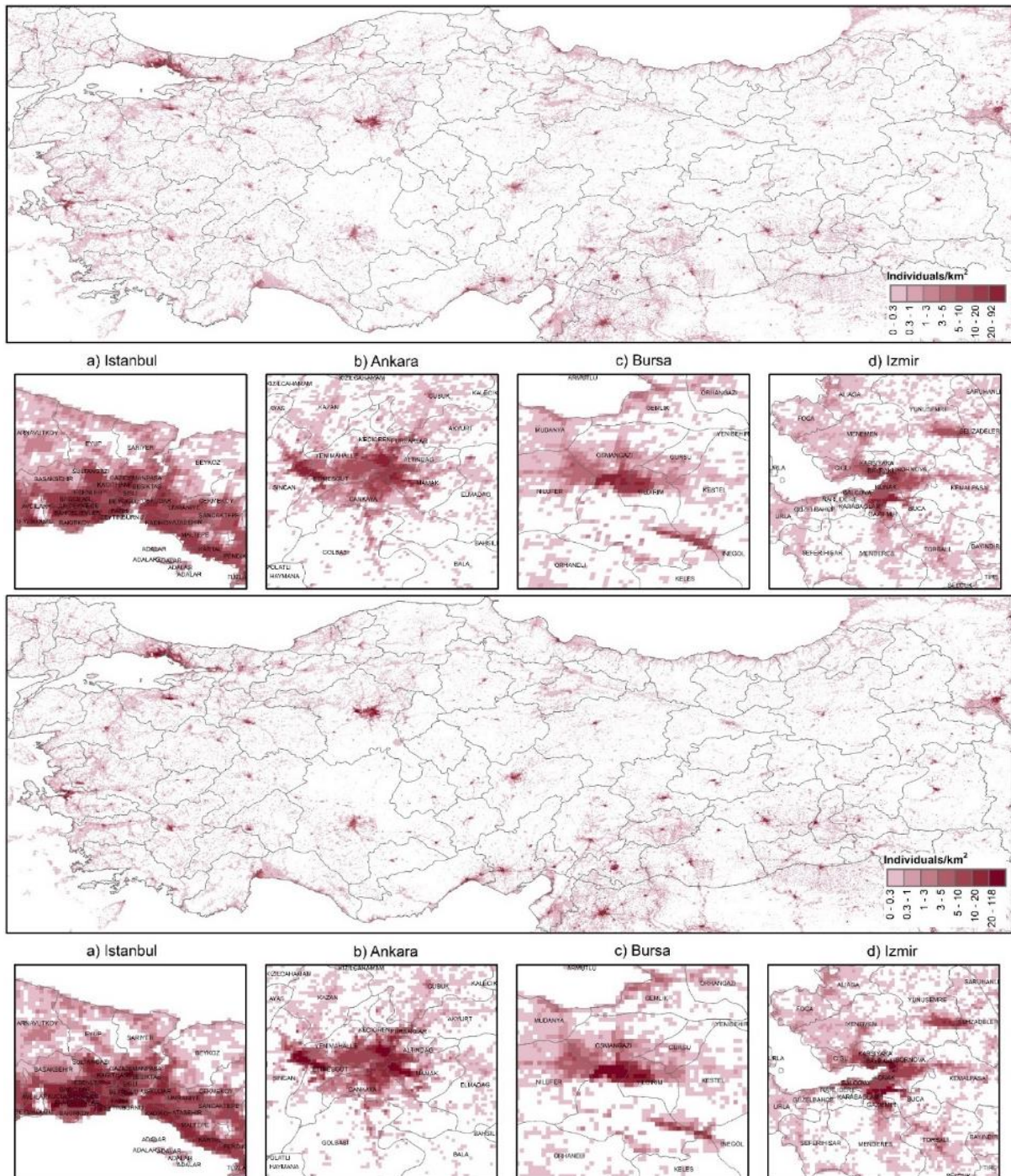


Figure 2. The spatial distribution of mortality associated with satellite-derived $PM_{2.5}$ by all causes (dust and sea-salt removed) (top) and (dust and sea-salt included) (bottom) in Turkey

3.3. Mortality estimations using ground-based $PM_{2.5}$

Annually averaged ground-based observations were used to estimate the mortalities associated with $PM_{2.5}$ exposure on province level. The spatial coverage is limited in this case to the provinces where $PM_{2.5}$ measurements are available for 2016. Ground observations are usually located in urban areas with higher level of pollution, so the lowest ground observations may not represent the background $PM_{2.5}$

and Artvin in Turkey. Especially, Erzurum, Erzincan, Edirne and Amasya the values were 5 times higher in ground observations. Total mortalities calculated using satellite-derived PM_{2.5} for these selected provinces were approximately half (41%-dust and sea salt removed, 56%-dust and sea salt included) of ground observations indicate in Turkey. The main reason for this result is the assumption of uniform exposure in the provinces. In small provinces, only one ground observation station information was used and spatial representability can be an issue due to location selection in that Province. The dust and sea salt contribution did not have a significant impact except Erzincan, Erzurum and Iğdır in Turkey.

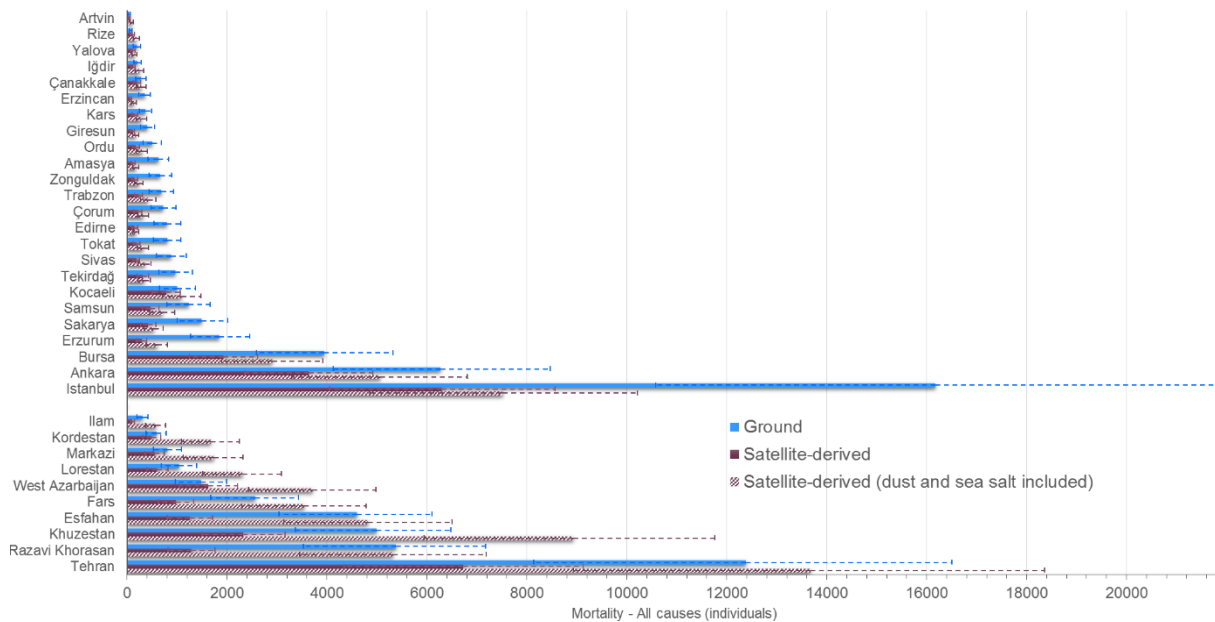


Figure 4. Mortalities associated with ground and satellite-derived PM_{2.5} observations by all causes for provinces in Turkey (top) and Iran (bottom)

The results were different in Iran. Estimations using dust and sea salt included satellite-derived estimations were higher than ground estimations for all provinces only Razavi Khorasan, Isfahan and Tehran with very similar estimations. Specifically, Kordestan, West Azarbaijan, Lorestan and Markazi were the provinces with dust and sea salt included satellite-derived estimations 2 times higher than with ground observations. Total mortalities calculated using satellite-derived PM_{2.5} for these selected provinces were approximately half (47%) when dust and sea salt removed, but higher (136%) when dust and sea salt included when compared to ground observations in Iran. The impact of dust and sea salt in satellite-derived estimations in provinces of Razavi Khorasan (>3 times) and Ilam (>4 times) were maximum indicating a very high contribution of natural sources in PM_{2.5} concentrations. Overall, dust and sea salt contribution had a significant impact in Iran in all provinces. Khuzestan and other western cities of Iran are affected by dust events which have sources based in Syria and Iraq (NASA, 2015). For IHD and LC, the estimations calculated with the same method were summarized in Table 3.

Top four most at risk population provinces of Turkey were found as the most populated provinces of the country as well. However, in Iran, populated provinces such as Razavi Khorasan or Esfahan are not among the top five results in satellite-derived estimations. This might be due to industry distribution patterns in Turkey and Iran, because the most industrialized provinces in Iran are not the most populated ones.

The calculated values were also compared with three relevant global studies (Table 4). Values estimated by ground observations were significantly higher considering the population under investigation and satellite-derived observations were higher than values reported in these studies for both countries.

Table 4. Summary of mortality estimations for all cases and comparison with previous estimates

Causes	Turkey		Iran		Reference
	Satellite	Ground ¹	Satellite	Ground ²	
All causes ³	58155 (37766-78474)	40583 (26493-54472)	95618 (62617-127937)	34153 (22527-45369)	This study
All causes	36967 (23848-50220)		34491 (22252-46853)		This study
Ischemic heart diseases	30240 (25076-35599)	30357 (25525-34774)	37368 (30732-43732)	30562 (26156-34428)	This study
Lung cancer	5591 (3516-8480)	5884 (2723-8574)	871 (387-1321)	776 (372-1095)	This study
All causes	36 500 (29300-43 800)		27 100 (24 400-29 900)		HEI (2019)
All causes	32 668 (27 197-38 289)		26 267 (22 583-30 064)		WHO (2016)
All causes	28 785		29 661		IHME (2016)

¹out of 35 024 768 individuals, living in reported provinces.

²out of 20 288 129 individuals, living in reported provinces.

³using dust and sea-salt included satellite-derived PM_{2.5}.

4. Conclusions

Both Turkey and Iran have serious concerns about PM_{2.5}. For this reason, PM_{2.5}-related mortalities were calculated using satellite-based and ground observations in this study. In 2016, approximately 35000 deaths by all causes were estimated to be associated with satellite-derived PM_{2.5} both in Turkey and Iran. Despite the similar population of the countries, there are differences in the estimated mortality for IHD and LC. The main reason for that difference is the differences in the baseline mortality rates in Turkey than Iran, especially in by LC. The other reason can be the spatial correlation of the PM_{2.5} pollution with high-density population areas, resulting in higher exposure. The contribution of dust and sea-salt affected Iran significantly when compared to Turkey.

Mortality estimation by ground observations was calculated only for provinces where PM_{2.5} measurements were available which corresponds to approximately 42% and 24% of the population in Turkey and Iran, respectively. It was a simpler approach using an average PM_{2.5} on province level and lacks the spatial resolution that satellite-based observation has. Another important difference is that natural sources of dust and sea-salt cannot be distinguished in ground observations.

The uncertainty and spatial representability of the datasets are important in assessment of these results. Uncertainties in the PM_{2.5} calculations from AOD which is complicated and requires variety of information needs to be considered. In addition, ground PM_{2.5} measurements are still very limited in both countries when compared to Europe and US and spatial representability is an issue for exposure calculations. Lastly, the exposure-response function coefficient used in this study is adapted from a study in US, due to changes in regions local studies for developing region specific coefficients are needed for better estimates.

5. References

- Anenberg, S.C., Horowitz, L.W., Tong, D.Q., West, J.J., 2010. An estimate of the global burden of anthropogenic ozone and fine particulate matter on premature human mortality using atmospheric modeling. *Env. Heal. Perspect* 118, 1189–1195. <https://doi.org/10.1289/ehp.0901220>.
- Brook, R.D., Rajagopalan, S., Pope 3rd, C.A., Brook, J.R., Bhatnagar, A., Diez-Roux, A. V, Holguin, F., Hong, Y., Luepker, R. V, Mittleman, M.A., Peters, A., Siscovick, D., Smith Jr., S.C., Whitsel, L., Kaufman, J.D., American Heart Association Council on, E., Prevention, C. on the K. in C.D., Council on Nutrition, P.A., Metabolism, 2010. Particulate matter air pollution and cardiovascular disease: An update to the scientific statement from the American Heart Association. *Circulation*. 121, 2331–2378.

<https://doi.org/10.1161/CIR.0b013e3181dbee1>.

Çapraz, O., 2013. Istanbul'da 2007-2012 yılları arasında hava kirliliğinin olumler üzerindeki etkilerinin modellenmesi.

Chen, R., Li, Y., Ma, Y., Pan, G., Zeng, G., Xu, X., Chen, B., Kan, H., 2011. Coarse particles and mortality in three Chinese cities: The China Air Pollution and Health Effects Study (CAPES). *Sci. Total Environ.* <https://doi.org/10.1016/j.scitotenv.2011.08.058>.

CIESIN, 2017. Gridded Population of the World, version 4 (GPWv4): national identifier grid revision 10 [WWW Document]. URL <http://sedac.ciesin.columbia.edu/data/set/gpw-v4-national-identifier-grid-rev10> (accessed 4.10.18).

Cohen, S., 2004. Social Relationships and Health. *Am. Psychol.*

Gauss, M., Nyíri, Á., Benedictow, A., Klein, H., 2016. Transboundary air pollution by main pollutants (S, N, O₃) and PM in 2014. EMEP.

Greenland, S., 1995. Dose-Response and Trend Analysis in Epidemiology: Alternatives to Categorical Analysis. *Epidemiology.* 6, 356–365.

Hadei, M., Hashemi Nazari, S.S., Yarahmadi, M., Kermani, M., Farhadi, M., Shahsavani, A., 2017. Estimation of Gender-Specific Lung Cancer Deaths due to Exposure to PM_{2.5} in 10 Cities of Iran During 2013 - 2016: A Modeling Approach. *Int. J. Cancer Manag.* 10. <https://doi.org/10.5812/ijcm.10235>

HEI, 2019. Data source: Global Burden of Disease Study 2017.

HEI, 2004. Health Effects of Outdoor Air Pollution in Developing Countries of Asia: A Literature Review. *Heal. Eff. Inst. Report* 15.

IHME, 2016. Global Burden of Disease Study.

ISNA, 2018. غلظت گرد و غبار ظهر امروز اهواز، بیش از 57 برابر حد مجاز. ISNA.

JahaneSabz, 2018. دنیای سبز تر | ایران چهارمین کشور در معرض خشکسالی جهان است.

Kan, H., London, S.J., Chen, G., Zhang, Y., Song, G., Zhao, N., Jiang, L., Chen, B., 2008. Season, sex, age, and education as modifiers of the effects of outdoor air pollution on daily mortality in Shanghai, China: The Public Health and Air Pollution in Asia (PAPA) Study. *Env. Heal. Perspect.* 116, 1183–1188. <https://doi.org/10.1289/ehp.10851>.

Krewski, D., Jerrett, M., Burnett, R.T., Ma, R., Hughes, E., Shi, Y., Turner, M.C., Pope III, C.A., Thurston, G., Calle, E.E., others, 2009. Extended follow-up and spatial analysis of the American Cancer Society study linking particulate air pollution and mortality. Health Effects Institute Boston, MA.

Lelieveld, J., Barlas, C., Giannadaki, D., Pozzer, A., 2013. Model calculated global, regional and megacity premature mortality due to air pollution. *Atmos. Chem. Phys.* 13, 7023–7037. <https://doi.org/10.5194/acp-13-7023-2013>.

Lim, S.S., Vos, T., Flaxman, A.D., Danaei, G., Shibuya, K., Adair-Rohani, H., Amann, M., Ezzati, M., et al., 2012. A comparative risk assessment of burden of disease and injury attributable to 67 risk factors and risk factor clusters in 21 regions, 1990–2010: A systematic analysis for the Global Burden of Disease Study 2010. *Lancet* 380, 2224–2260. [https://doi.org/10.1016/S0140-6736\(12\)61766-8](https://doi.org/10.1016/S0140-6736(12)61766-8).

Mercan, Y., 2016. Kırklareli'nde 2010-2014 yılları arasında kardiyovaskuler ve solunum sistemi hastalıkları nedeni ile acil polikliniklere başvuruların ve olumlerin hava kirliliği ve meteorolojik parametreler ile ilişkisi.

Naddafi, K., Hassanvand, M.S., Yunesian, M., Momeniha, F., Nabizadeh, R., Faridi, S., Gholampour, A., 2012. Health impact assessment of air pollution in megacity of Tehran, Iran. *Iranian J. Environ. Health Sci. Eng.* 9, 28.

NASA, 2015. Dust Marches Across Iraq and Iran [WWW Document]. URL



<https://earthobservatory.nasa.gov/NaturalHazards/view.php?id=86539>.

Pope, I.C., Burnett, R.T., Thun, M.J., et al., 2002. Lung cancer, cardiopulmonary mortality, and long-term exposure to fine particulate air pollution. *JAMA* 287, 1132–1141. <https://doi.org/10.1001/jama.287.9.1132>.

Shahsavani, A., Naddafi, K., Jafarzade Haghhighifard, N., Mesdaghinia, A., Yunesian, M., Nabizadeh, R., Arahami, M., Sowlat, M.H., Yarahmadi, M., Saki, H., Alimohamadi, M., Nazmara, S., Motevalian, S.A., Goudarzi, G., 2012. The evaluation of PM₁₀, PM_{2.5}, and PM₁ concentrations during the Middle Eastern Dust (MED) events in Ahvaz, Iran, from april through september 2010. *J. Arid Environ.* 77, 72–83. <https://doi.org/10.1016/j.jaridenv.2011.09.007>.

Tosun, E., 2017. The Evaluation Of Turkey's Air Quality Data Between 2009 and 2016. Hacettepe University.

van Donkelaar, A., Martin, R. V, Brauer, M., Boys, B.L., 2015. Use of satellite observations for long-term exposure assessment of global concentrations of fine particulate matter. *Env. Heal. Perspect* 123, 135–143. <https://doi.org/10.1289/ehp.1408646>.

van Donkelaar, A., Martin, R. V, Brauer, M., Hsu, N.C., Kahn, R.A., Levy, R.C., Lyapustin, A., Sayer, A.M., Winker, D.M., 2016. Global estimates of fine particulate matter using a combined geophysical-statistical method with information from satellites, models, and monitors. *Env. Sci Technol* 50, 3762–3772. <https://doi.org/10.1021/acs.est.5b05833>.

WHO, 2016. Ambient air pollution: A global assessment of exposure and burden of disease.

WHO, 2015. Mortality Database [WWW Document]. URL <http://apps.who.int/healthinfo/statistics/mortality/whodpms/> (accessed 1.9.19).

WHO HRAPIE, 2013. Health risks of air pollution in Europe – HRAPIE project. World Health Organ. <https://doi.org/10.1021/acs.est.5b05833>.

Yang, C., Peng, X., Huang, W., Chen, R., Xu, Z., Chen, B., Kan, H., 2012. A time-stratified case-crossover study of fine particulate matter air pollution and mortality in Guangzhou, China. *Int. Arch. Occup. Environ. Health.* <https://doi.org/10.1007/s00420-011-0707-7>.

Zanobetti, A., Schwartz, J., 2009. The effect of fine and coarse particulate air pollution on mortality: A national analysis. *Environ. Health Perspect.* <https://doi.org/10.1289/ehp.0800108>.

Acknowledgement

We would like to thank A. van Donkelaar, and R. V. Martin for Satellite-Derived PM_{2.5} Dataset and SEDAC for Gridded Population of the World (GPW) Dataset.

Long-term analysis of the columnar-surface aerosol relationship with planetary boundary layer height at southern coastal site of turkey

Gizem Tuna Tuygun and Tolga Elbir

Dokuz Eylul University, Department of Environmental Engineering, Izmir/TURKEY

gizem.tuna@deu.edu.tr

Abstract. Planetary Boundary Layer Height (PBLH) has been considered to be a key factor influencing the direct relationship between satellite-derived Aerosol Optical Depth (AOD) and ground-level Particulate Matter (PM). AOD is the column integral of the aerosol extinction coefficient in vertical distribution of the total atmosphere, while PM is the surface measurement. PBLH can account for much of the variability in near-surface air quality. Therefore, the relationship between PBLH and concentrations of surface pollutants, especially particulate matter (PM) should be investigated at different regions. In this study, the relationship between PM and the PBLH was investigated in a coastal site of Turkey. PM₁₀ concentrations were normalized with MODIS AOD to qualitatively account for background or transported aerosol that is not concentrated in the PBLH. To study the effect of PBLH on the PM vs AOD correlation the PBLH was categorized into three different height intervals; low (PBLH < 500 m), moderate (500 m < PBLH < 1000 m), and high (PBLH > 1000 m). AOD data from both MODIS Terra, and MODIS Aqua satellites was used to investigate correlation between PM₁₀ and AOD. The Collection 6.1 MODIS-Terra and Aqua Level-2 AOD products at 550 nm were used with a nominal spatial resolution of 3 km × 3 km. Satellite AOD data products were validated using AOD data from IMS-METU-Erdemli AERONET site located in the southeastern coast of Turkey. Both dataset indicated high correlation as 0.82 for Terra and 0.85 for Aqua. The region is highly effected from dust transport from central-eastern Sahara in summer, and the Middle East-Arabian peninsula in autumn. Hourly PM₁₀ concentrations were obtained from Mersin-Icel air quality monitoring station that is the nearest station to IMS-METU Erdemli. The PBLH was obtained from the Modern Era-Retrospective Reanalysis for Research and Applications (MERRA) reanalysis dataset to generate a PBLH climatology for 2008-2016. Clearly, after normalizing PM₁₀ by AOD, the spread of the scatter plots were significantly reduced, and the correlations became more significant for both product, especially for Terra (from -0.16 to -0.41). Based on the seasonal differences between PM₁₀ and AOD, PBLH was included in the analysis in order to understand its role in the relationship between AOD and PM₁₀. In this way, highest values of PBLH were usually obtained in summer (>2 km), although occasional high values were found in other seasons. The correlation of PM₁₀ and AOD markedly improves with PBLH (from -0.19 to 0.36, and from -0.95 to 0.33) mainly when PBLH is higher than 1 km for Terra and Aqua, respectively. The results indicated that the reasonable correlation between ground and columnar values was obtained when the mixing layer was thick for both satellite. PBLH higher than 1 km was generally observed in autumn and summer seasons in this region.

Keywords: MODIS, AOD, Planetary Boundary Layer Height, PM₁₀, Turkey

1. Introduction

Atmospheric aerosols are a complex mixture of organic and inorganic solid compounds with different sizes and chemical composition. The international scientific community (IPCC, 2013) acknowledges that aerosols greatly influence the energy budget of the atmosphere. They are also greater concern to public since they are much more visible than gaseous pollutants (Guo et al., 2009; Li et al., 2016). In fact, particulate matter (PM) has been identified as one of the pollution indicators more clearly related to human health.

Multiple factors contribute to the severe air pollution over Turkey. Strong emission due to rapid urbanization and industrialization is a primary cause. In addition, dust transport, meteorological conditions and diffusion within the planetary boundary layer (PBL) play important roles in the exchange between polluted and clean air. Among the meteorological parameters of importance, the PBL height (PBLH) can be related to the vertical mixing, affecting the dilution of pollutants emitted near the ground through various interactions and feedback mechanisms (Su et al., 2018).

Therefore, PBLH is a critical parameter affecting near-surface air quality, and it serves as a key input for chemistry transport models (Du et al., 2013; Luan et al., 2018). The PBLH can significantly impact aerosol vertical structure, as the bulk of locally generated pollutants tends to be concentrated within this layer. Turbulent mixing within the PBL can account for much of the variability in near-surface air quality. On the other hand, aerosols can have important feedbacks on PBLH, depending on the aerosol properties, especially their light absorption (e.g., black, organic, and brown carbon). In a recent comprehensive review, Li et al. (2017) present sample evidence of such interactions and characterize their determinant factors. There are various methods for identifying the PBLH. However, using ground-based observations to retrieve the PBLH suffers from poor spatial coverage and very limited sampling. Several studies have investigated the relationship between PBLH and surface pollutants in literature (Quan et al., 2013; Li et al., 2017; Segura et al., 2017; Su et al., 2017; Luan et al., 2018). Assessing the relationship between PM and the PBLH quantitatively over the region that is affected by dust transport is of particular interest. PBL turbulence is not the only factor affecting air quality, so there can be large seasonal and temporal differences in the interaction between the PBLH and PM. Therefore, PBLH–PM relationship remains uncertain, that warrants a further investigation.

Given the above-mentioned limitations, the current study presents a comprehensive and long-term exploration of the relationship between the PBLH and ground level PM over the region that is effected by dust transport in autumn and spring. Seasonal variations and correlations under different PBLH classifications were also considered. In the study, PM was normalized by MODIS Aerosol Optical Depth (AOD), a widely used parameter to represent the total-column aerosol amount, to qualitatively account for background or transported aerosol that is not concentrated in the PBLH. The relationships between PBLH and PM_{10}/AOD over the region were also determined.

2. Data and Method

Concentrations of particulate matters having diameter of 10 μm or less (PM_{10}), AOD data from AERONET and MODIS (Terra and Aqua satellites) and PBL heights for the period of 2008-2016 obtained from Modern Era-Retrospective Reanalysis for Research and Applications (MERRA) reanalysis dataset were used in a rural site (IMS-METU-Erdemli) at southern Mediterranean coast of Turkey. The rural IMS-METU-Erdemli atmospheric sampling site is located on the coastline of Eastern Mediterranean (EM), Erdemli, Turkey (36.57°N and 34.26°E). AEROSOL ROBOTIC NETWORK (AERONET) sun photometer has been operated at this site since December 1999. In the region, there is an ambient air quality monitoring station named Mersin-Icel located 35-km northeast from IMS-METU-Erdemli station (36.77 °N and 34.56°E) (Figure 1). It has been operated by the Ministry of Environment and Urbanization since 2008. PM_{10} concentrations were obtained from this station.

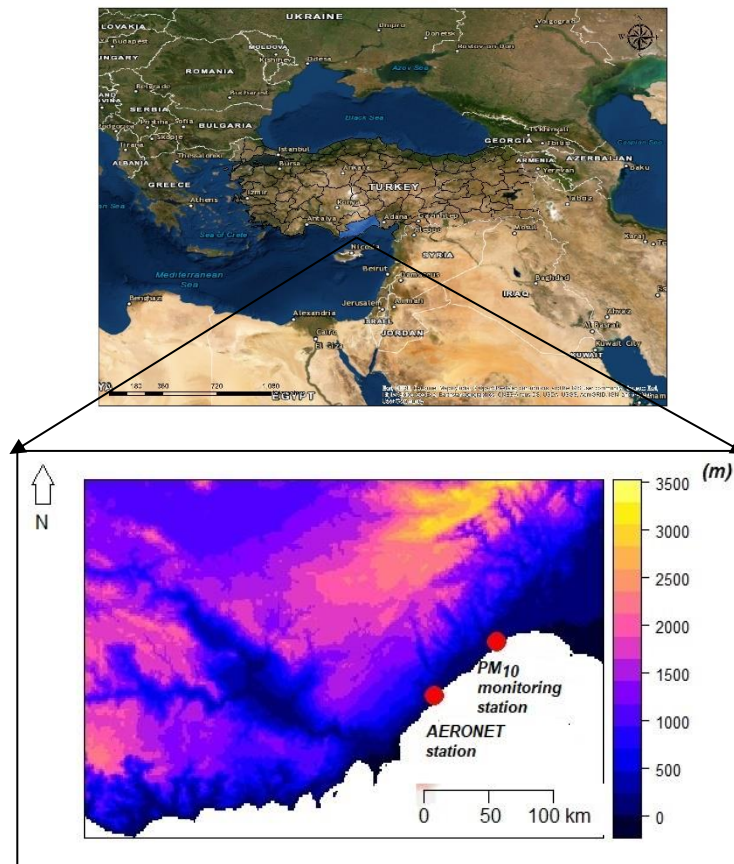


Figure 1. Location of the stations and topography over the region

The sites are surrounded by cultivated land and greenhouses, while the city of Mersin with a population of 800.000 has soda, chromium, and fertilizer producing industries and a thermic power plant (Koçak et al., 2012). The weather pattern of the Mediterranean region is climatically characterized by mild, relatively wet winters and hot, dry summers (Tutsak and Koçak, 2019). The temperature presents a strong seasonal cycle with a winter minimum and a summer maximum. The sampling site is located in a region having typical conditions of the Mediterranean climate.

2.1. Aerosol Optical Depth Measurements

Ground-based AOD measurements used in this paper were obtained from the Mersin-Erdemli AERONET station in Turkey. The equipment of CIMEL CE-318 sun photometer has been used in the station since 1999. The CIMEL CE318 measures the direct Sun radiance in eight spectral channels generally (340, 380, 440, 500, 675, 870, 936 and 1020 nm) and also the diffuse sky radiance in the solar almucantar at 440, 675, 870, and 1020 nm. Processed data are classified in three levels: level 1.0 refers to AOD data that has not been quality or cloud screened. Level 1.5 refers to AOD already cloud-screened (Smirnov et al., 2000) and pre-calibration applied. Finally, level 2.0 corresponds to ‘quality assured’ data, where pre and post-calibrations are also taken into account. AOD accuracy for level 1.5 and 2.0 data is about 0.01-0.02 in the visible and near infrared spectral regions (Eck et al., 1999). Version 3 (the last version) Level 2 AERONET AOD at 500 nm data was used in this work.

MODIS products used in this study were obtained from both Terra (MOD04_L2) and Aqua (MYD04_L2) satellites corresponding to Level 2 Collection 6.1 Dark Target algorithm with a pixel size of 3×3 km. The first MODIS instrument was launched at the end of 1999 on board the EOS Terra and the second one was in May 2002 on board the EOS Aqua. These instruments measure radiance in 36

visible, near-infrared, and infrared spectral bands from 0.415 to 14.235 μm . The aerosol retrieval uses seven spectral bands (0.47-2.13 μm) and two independent algorithms to retrieve aerosol parameters over land (Remer et al., 2005; Levy et al., 2009) and over ocean (Tanre et al., 1997; Levy et al., 2003). In this study, the values of both MOD04 and MYD04 AOD that were extracted at 550 nm (MODIS parameter name: Optical_Depth_Land_And_Ocean). The MODIS data was averaged within a 5 \times 5 pixel window around the AERONET station to match its AOD data and surface PM₁₀ data from the nearest air quality monitoring station. To account for the background pollution level, PM₁₀ was normalized with MODIS AOD to qualitatively account for background or transported aerosol that is not concentrated in the PBLH.

2.2. Planetary Boundary Layer Height (PBLH)

The PBLH data obtained from the Modern Era-Retrospective Reanalysis for Research and Applications (MERRA) reanalysis dataset with a spatial resolution of 2/3 $^{\circ}$ \times 1/2 $^{\circ}$ (longitude–latitude). The MERRA reanalysis data uses a new version of the Goddard Earth Observing System Data Assimilation System Version 5 (GEOS-5), that is a state-of-the-art system coupling a global atmospheric general circulation model (GEOS-5 AGCM) to NCEP's Grid-point Statistical Interpolation (GSI) analysis (Rienecker et al., 2011). Compared with other reanalysis products (e.g., ECMWF), MERRA PBLHs have advantages for analysis with higher temporal resolution (Su et al., 2018). Since the reanalysis data takes account of large-scale dynamical forcing, MERRA data was used to generate PBLH climatology over the study region.

3. Results

3.1. Long term climatological patterns of PBLH and surface PM₁₀ and MODIS AOD

Figure 2 shows the distribution of PM₁₀, AOD at 550 nm measured by MODIS-Terra and MODIS-Aqua and PBLH derived from MERRA-2 reanalysis data that pairs with Terra sensor for morning (10:30 LST) and Aqua sensor for afternoon (13:30 LST). Data was spatially and temporally collocated in hourly averages. Then, daily averages were obtained from hourly data pairs. Since different number of data pairs are available for Terra and Aqua, data pairs having same dates were used for analysis to obtain more reliable comparison. Both sensors showed consistent results despite of some differences due to the time differences between satellites. PM₁₀ concentrations were relatively higher for Terra (in the morning) with the mean of 62.99 $\mu\text{g}/\text{m}^3$, while PBLH was found relatively higher for Aqua (in the afternoon) with the mean of 2002 m.

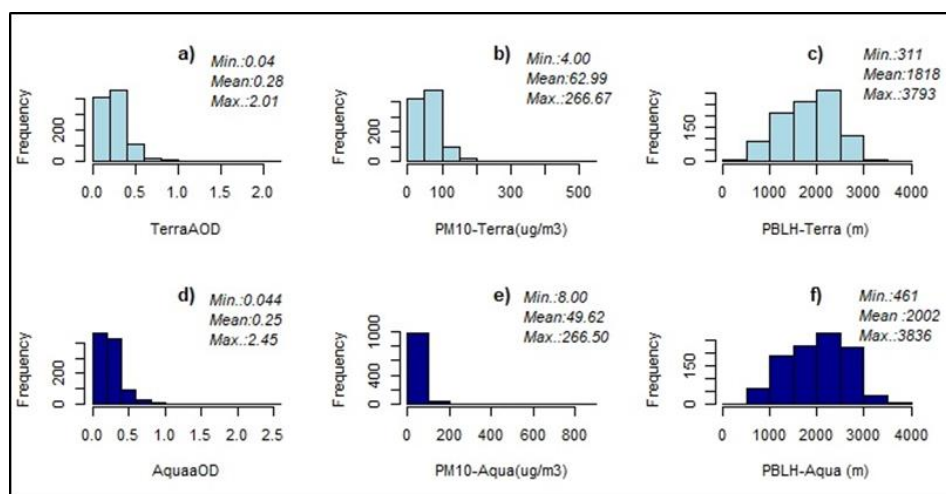


Figure 2. Descriptive statistics of AOD, PM₁₀ and PBLH for Terra (a,b,c) and Aqua (d,e,f) between 2008 and 2016 in Mersin-Icel

Seasonal MODIS AOD at 550 nm was obtained from the Terra (MOD) and Aqua (MYD) datasets for morning and afternoon, respectively (Figure 3). Morning and afternoon AOD shared the same seasonal patterns; however, the magnitude of the seasonal variation differed. This could be attributed to discrepancies in cloud cover and land-surface conditions between the locations of morning and afternoon AOD retrievals. MODIS AOD was higher in spring and summer followed by autumn and winter as seen in Figure 3.

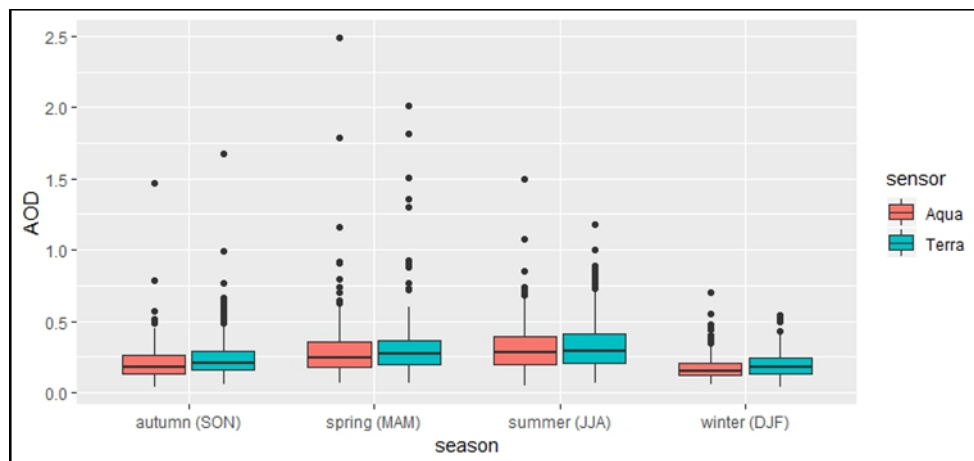


Figure 3. Seasonal distribution of MODIS AOD at Mersin-Icel station (Seasonal box and whisker plots showing the 10th, 25th, 50th, 75th and 90th percentile values of Terra and Aqua AOD. The black dots indicate outlier values).

Concentrations of the air pollutants were not constant through the year. The variation of concentrations indicated that the pollutants were not only originated from local sources, but also from external sources located in different regions. The seasonal variation of PM₁₀ was similar to that of MODIS AOD (Figure 4). Higher PM₁₀ concentrations were observed at all seasons, but, highest values were mainly observed in spring and autumn due to long-range dust transportation. The spring and autumn were highly effected by dust transport from central-Sahara and the Middle East-Arabian peninsula, respectively with higher PM₁₀ concentrations overwhelmingly above 150 µg/m³ during these seasons.

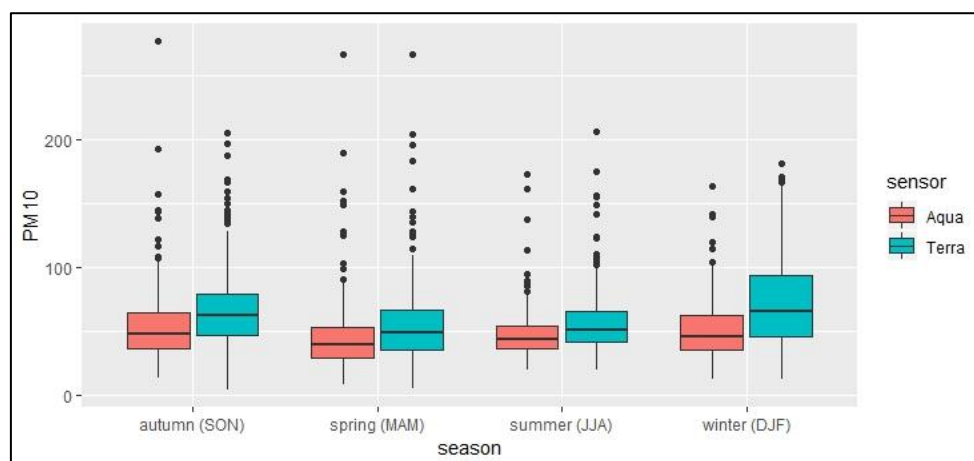


Figure 4. Seasonal distribution of PM₁₀ at Mersin-Icel station (Seasonal box and whisker plots showing the 10th, 25th, 50th, 75th and 90th percentile values of PM₁₀. The black dots indicate outlier values).

The climatology of the PBLH, especially its seasonal variability, is very important for air-pollution-related studies. The box plot in Figure 5 shows statistical characteristics of seasonal PBLH variation obtained by the MERRA-2 reanalysis. The MERRA-2 values were higher in spring and summer, while the peak values were lower in autumn and winter. PBLHs were mainly shallower in winter, when development of the PBLH was typically suppressed by the weaker solar radiation reaching the surface. Although occasional high values were also found in other seasons, mainly highest PBLHs were observed in summer. The PBLH pattern affects the PM-AOD seasonal interactions, as it determines the mixing capacity of the atmosphere and the relation between the values observed at ground and the columnar integration.

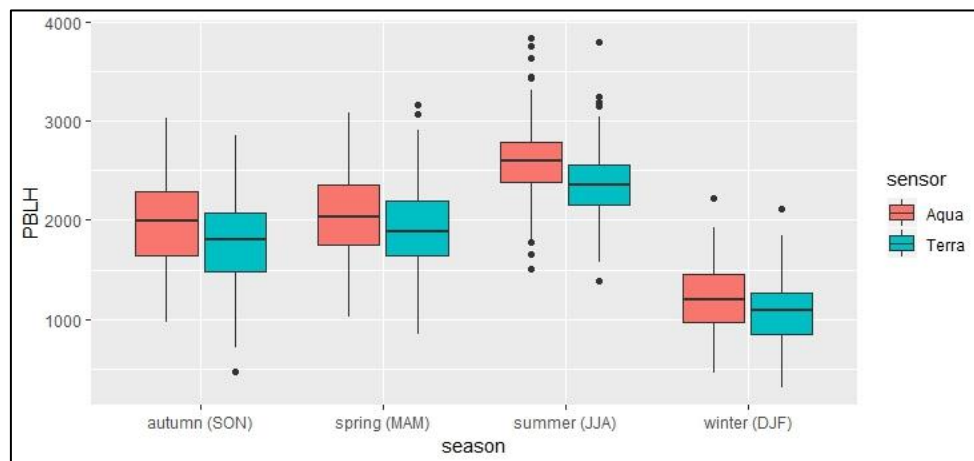


Figure 5. Seasonal distribution of PBLH at Mersin-Icel station (Seasonal box and whisker plots showing the 10th, 25th, 50th, 75th and 90th percentile values of PBLH. The black dots indicate outlier values).

3.2. Assessment of MODIS AOD and PM_{10} relationship under different PBLH

Figure 6 shows scatterplots and corresponding linear fittings of AOD MODIS Terra and Aqua vs PM_{10} data for daily averages. The resultant linear fitting slopes were $30 \mu\text{g}/\text{m}^3$ and $32 \mu\text{g}/\text{m}^3$ PM_{10} concentrations per AOD unit, and intercepts were $54.4 \mu\text{g}/\text{m}^3$ and $40.9 \mu\text{g}/\text{m}^3$ for Terra and Aqua, respectively. Correlation coefficients were low and very similar between both datasets. Correlation between PM_{10} and Aqua AOD was relatively higher (0.21).

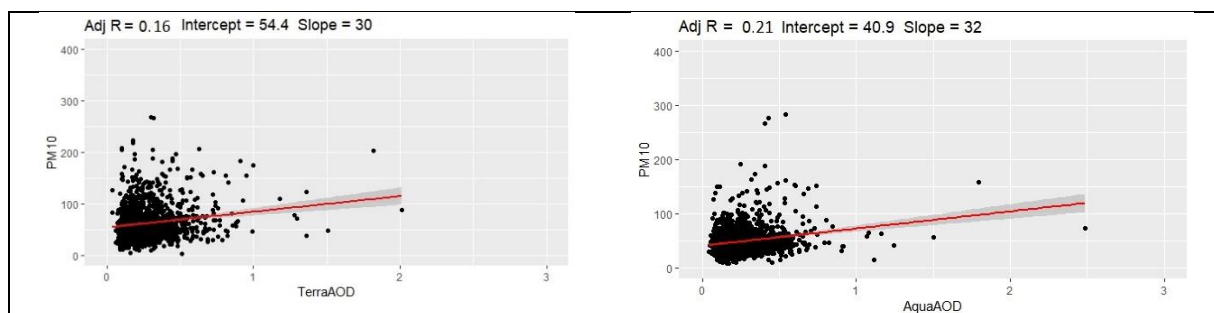


Figure 6. Scatterplots and corresponding linear fittings of AOD MODIS Terra and Aqua vs PM_{10} data for daily averages

Table 1 shows a summary of the linear fitting parameters obtained for PM_{10} vs AOD MODIS Terra and Aqua, segregated by seasons. Both data sets were best correlated in spring (0.36 for Terra and 0.30 for Aqua), while lower correlations were found in winter (0.17 for Terra and 0.24 for Aqua). However, there was no significant difference between seasons.

Table 1. Results of the seasonal linear fit obtained for PM₁₀ concentrations vs AOD measured by MODIS Terra and Aqua, including: slope (m), intercept (n), correlation coefficient (r), and total number of data (N).

	season	m	n	r	N
PM₁₀-AOD_{Terra}	winter	77.5	61.6	0.17	268
	spring	49.1	37.4	0.36	313
	summer	39.1	41.7	0.29	409
	autumn	75.5	49.5	0.29	380
PM₁₀-AOD_{Aqua}	winter	59.5	40.4	0.24	316
	spring	38.7	33.1	0.30	300
	summer	32.3	36.5	0.25	450
	autumn	73.1	37.6	0.29	367

In general, when the planetary boundary layer height is low the aerosols concentrate near the ground; when the planetary boundary layer height swells the aerosols disperse more easily and its concentration at ground decreases. Then, to study the effect of PBLH on the PM₁₀ vs AOD relation the data was firstly separated in three different height intervals (Segura et al., 2017). Three different classes were selected, depending on PBLH such as low ($H < 500$ m), medium ($500 \text{ m} < H < 1000$ m), and high ($H > 1000$ m). Mainly high PBLH (> 1000 m) was the significant class with some outliers of AOD for all seasons and the maximum AOD reached 2 for Terra and 2.5 for Aqua in spring. Also, the maximum PM₁₀ reached $300 \mu\text{g}/\text{m}^3$ for both product (Figure 7).

Results of the linear fit resulting from PM₁₀ vs AOD from MODIS Terra and Aqua, are shown in Table 2. In all cases, the slope (m), intercept (n) and correlation coefficient (r) improved with PBLH. The correlation significantly improved with PBLH (from 0.03 to 0.21) for Terra, especially at high PBLH (> 1000 m). For Aqua, the main improvement was found when PBLH was changing from low to medium PBLH ($500 \text{ m} < \text{PBLH} < 1000$ m). In any case, the results were significantly good for high PBLHs, it is pointing at a good correlation between ground and columnar values when the mixing layer was thick. The limited sample size suggested that the magnitude of correlations for PBLH lower than 500 m may not be so reliable as other PBLH classes.

Table 2. Results of the linear fit for PM₁₀ concentrations vs AOD measured by MODIS Terra, and MODIS Aqua under different PBLHs, including: slope (m), intercept (n), correlation coefficient (r), and total number of data (N).

	PBLH (m)	m	n	r	N
PM₁₀-AOD_{Terra}	< 500	-79.6	119.3	-0.06	12
	500-1000	7.3	72.7	0.03	141
	> 1000	37.3	50.4	0.21	1244
PM₁₀-AOD_{Aqua}	< 500	-98.1	59.9	-0.95	3
	500-1000	54.0	41.6	0.15	92
	> 1000	32.6	40.3	0.21	1338

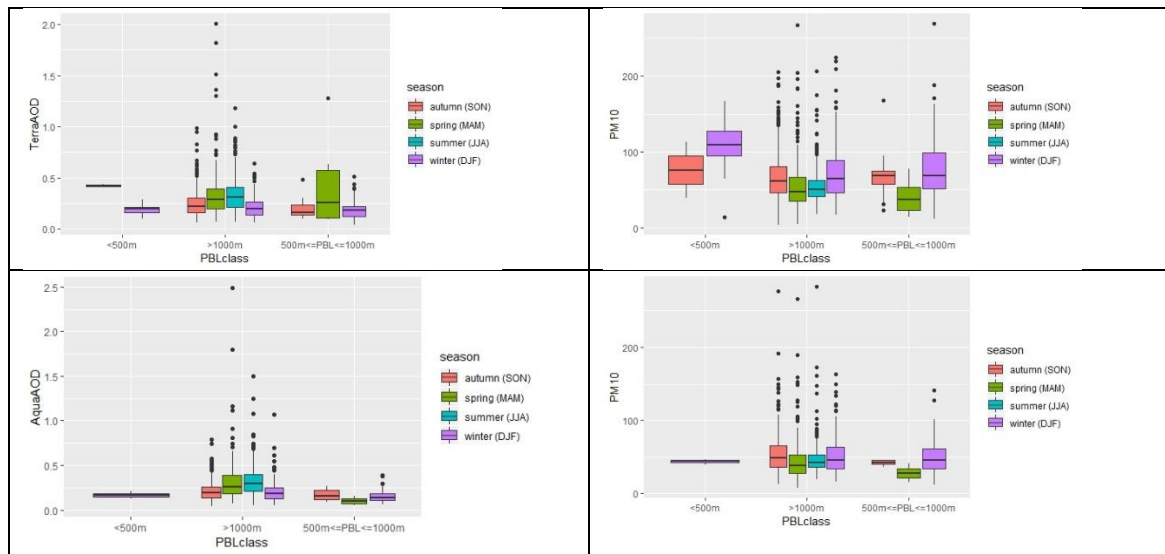


Figure 7. Seasonal pattern of AOD and PM₁₀ for different PBLH classes

3.3. Relationships between PM₁₀ and PBLH

The relationship over this region showed the most prominent seasonal differences between PM₁₀ and PBLH correlations (Table 3). Despite the overall negative correlations, the correlations between PBLH and PM₁₀ had large spreads and differences according to the season. Both regular linear regression was applied to characterize the PBLH–PM₁₀ relationship. Correlations were found significantly low. Relatively higher negative correlations between PM₁₀ and PBLH were found in summer (-0.17) for Terra and in spring (-0.18) for Aqua.

The monthly mean values of PM₁₀ and PBLH for Terra and Aqua are presented in Figure 8. For winter, the PBLH was generally low and PM₁₀ concentrations were high, and thus PBLH showed the most significant negative correlation with PM₁₀. Conversely, the PBLH was generally higher in summer, PM₁₀ concentrations were lower.

The relationship of PBLH–PM₁₀ is not always significant, nor are they always negative (Du et al., 2013). In addition to PBLH, PM is also affected by other factors, such as emissions, wind, synoptic patterns, and atmospheric stability. In some conditions (e.g., strong wind and low aerosol loading), PBLH does not play a dominant role in modulating surface pollutants, and this results in weak or uncorrelated relationships between PBLH and PM. Weak PBLH–PM correlations are a common feature over relatively clean regions. In this study, due to the importance of regional pollution levels, PM₁₀ was normalized by MODIS total-column uncorrelated relationships between PBLH and PM₁₀. Differences between correlations according to the season are given in Table 3. Most significant improvement was found in autumn for both product.

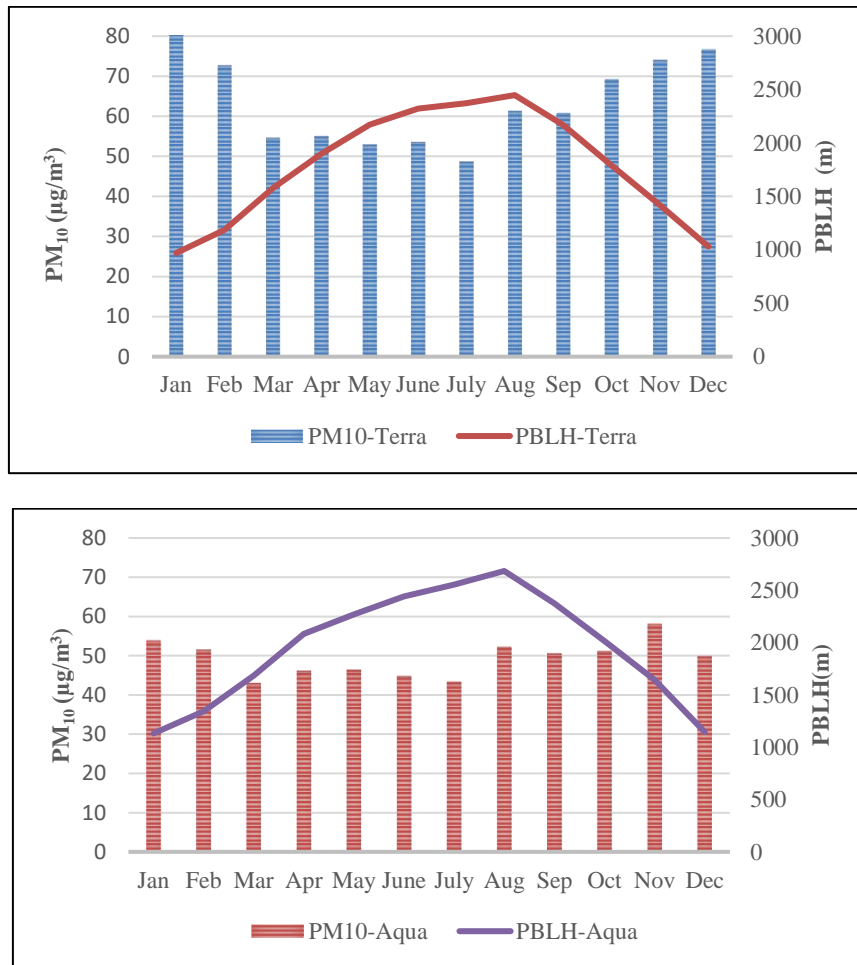


Figure 8. The monthly mean values of PM₁₀ and PBLH for 2008-2016

Table 3. Seasonal correlation coefficients between PM₁₀-PBL-AOD

Season	Terra		Aqua	
	PM ₁₀ -PBL	PM ₁₀ /AOD-PBL	PM ₁₀ -PBL	PM ₁₀ /AOD-PBL
autumn (SON)	-0.03	-0.22	-0.02	-0.15
spring (MAM)	-0.15	-0.02	-0.18	-0.04
summer (JJA)	-0.17	-0.09	-0.05	-0.05
winter (DJF)	-0.16	-0.24	-0.01	-0.20

Compared to previous PBLH-PM₁₀ correlations, the normalized PM₁₀ (PM₁₀/AOD) improved correlation significantly for both product, resulting in smaller differences between Terra and Aqua (Figure 9). Correlations increased -0.16 to 0.41 for Terra and -0.02 to -0.33 for Aqua. Most significant improvement was found in autumn for both product (Table 3). Winter had also great improvement (-0.01 to -0.20) for Aqua.

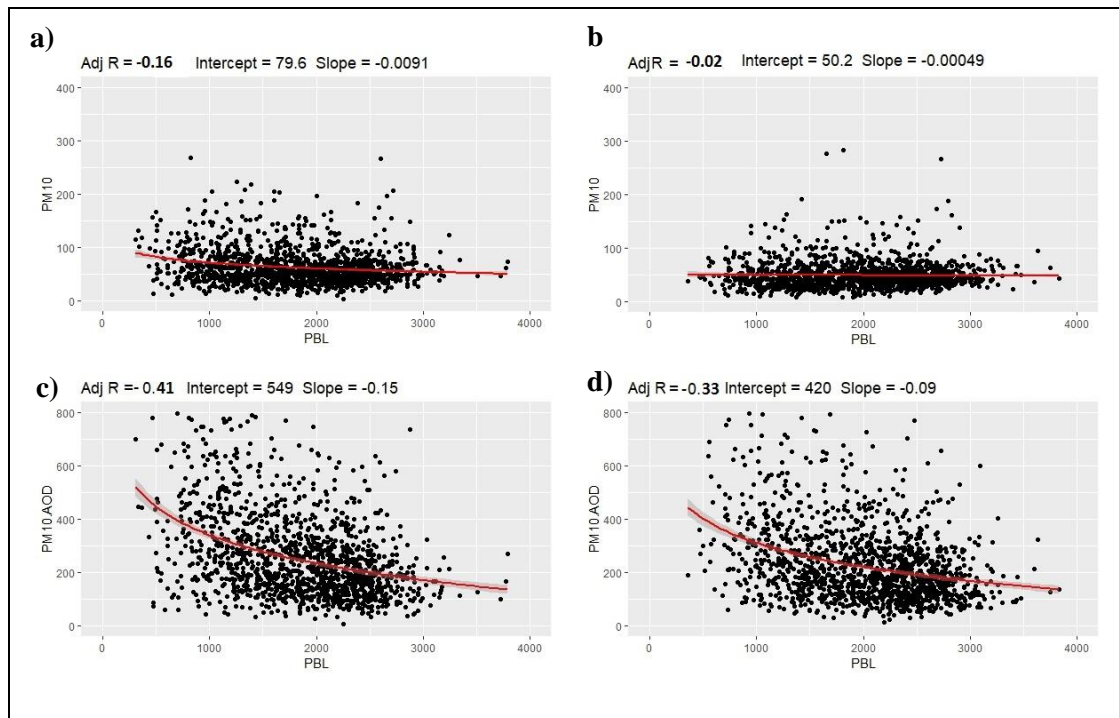


Figure 9. The relationship between PM_{10} -PBL (a,b) and PM_{10}/AOD -PBL (c,d) for Terra and Aqua, respectively

4. Conclusions

A multi-annual database (2008-2016) of surface PM_{10} concentrations, along with satellite columnar AOD at 550 nm were analyzed for Mersin-Icel site, located in the city center and southern coast of Turkey. The hourly PM_{10} concentrations were provided by Ministry of Environment and Urbanization. The satellite based AOD data was retrieved from MODIS Terra and Aqua sensors, maintained by NASA. Seasonal differences in PM -AOD relation were investigated. Highest correlations were observed in spring while lowest correlations were in winter. PBLH was used to understand its role in the seasonal relationship between AOD and PM_{10} . The PBLH was obtained from MERRA reanalysis dataset to generate a PBLH climatology for 2008-2016. In this way, highest values of PBLH were usually obtained in summer (>2 km), although occasional high values were found in other seasons. Correlation of PM_{10} -AOD was significantly improved with PBLH (from -0.19 to 0.36, and from -0.95 to 0.33) when PBLH was higher than 1 km for Terra and Aqua, respectively. The results indicated that the good correlation between ground and columnar values were obtained when the mixing layer was thick for both satellite.

After normalizing PM_{10} by AOD, the spread of the scatter plots were significantly reduced, and the correlations became more significant for Terra (from -0.16 to -0.41) and Aqua (from -0.02 to -0.33). The relationships between PBLH and PM_{10}/AOD over different regions are also expected to be significant for relating PM to remotely sensed AOD, since the way PBLH affects near-surface aerosol concentration. The feedback of absorbing aerosol is also a potential factor affecting the PBLH- PM relationships. The important feedback of absorbing aerosols may also contribute to the nonlinear relationship between PBLH and PM . This issue merits further analysis using comprehensive measurements from field experiments, from that integrated aerosol conditions and model simulations can account for aerosol radiative forcing while controlling for the other relevant variables.

Such information can help improve our understanding of the complex interactions between air pollution and boundary layer depth, and thus, can benefit policymaking aimed at mitigating air pollution at both local and regional scales. Our findings provide deeper insight and contribute to the quantitative understanding of aerosol–PBL interactions that could help in refining meteorological and atmospheric chemistry models. Further, this work may enhance surface pollution monitoring and forecasting capabilities.

5. References

- Boucher, O., Randall, D., Artaxo, P., Bretherton, C., Feingold, G., Forster, P., Kerminen, V. M., Kondo, Y., Liao, H., Lohmann, U., and Rasch, P., 2013. Clouds and aerosols, in: *Climate Change 2013: The Physical Science Basis. Contribution of Working Group I to the Fifth Assessment Report of the Intergovernmental Panel on Climate Change*, 571–657, Cambridge Univ. Press, Cambridge, UK and New York, NY, USA.
- Du, C., Liu, S., Yu, X., Li, X., Chen, C., Peng, Y., Dong, Y., Dong, Z., Wang, F., 2013. Urban Boundary Layer Height Characteristics and Relationship with Particulate Matter Mass Concentrations in Xi'an, Central China. *Aerosol Air Qual. Res.*, 13: 1598–1607.
- Eck, T., Holben, B.N., Reid, J.S., Dubovik, O., Smirnov, A., O'Neil, N.T., Slutsker, I., Kinne, S., 1999. Wavelength dependence of the optical depth of biomass burning urban and desert dust aerosols. *J. Geophys. Res.* 104, 31333–31349.
- Guo, J., Su, T., Li, Z., Miao, Y., Li, J., Liu, H., Xu, H., Cribb, M., and Zhai, P., 2017. Declining frequency of summertime local-scale precipitation over eastern China from 1970 to 2010 and its potential link to aerosols, *Geophys. Res. Lett.*, 44, 5700–5708.
- Guo, J. P., Zhang, X. Y., Che, H. Z., Gong, S. L., An, X., Cao, C. X., Guang, J., Zhang, H., Wang, Y. Q., Zhang, X. C., and Xue, M., 2009. Correlation between PM concentrations and aerosol optical depth in eastern China, *Atmos. Environ.*, 43, 5876–5886.
- Koçak, M., Theodosi, C., Zarmas, P., Séguret, M.J.M., Herut, B., Kallos, G., Mihalopoulos, N., Kubilay, N., Nimmo, M., 2012. Influence of mineral dust transport on the chemical composition and physical properties of the Eastern Mediterranean aerosol. *Atmos. Environ.* 57, 266–277.
- Levy, R.C., Remer, L. A., Tanre, D., Mattoo, S., and Kaufman, Y. J., 2009. Algorithm for Remote Sensing of Tropospheric Aerosol over Dark Targets from MODIS: Collections 005 and 051 (Revision 2. Product ID: MOD04/MYD05. MODIS website (http://modis-atmos.gsfc.nasa.gov/MOD04_L2/atbd.html).
- Levy, R.C., Remer, L.A., Tanre, D., Kaufman, Y.J., Ichoku, C., Holben, B.N., Livingston, J.M., Russell, P.B., Maring, H., 2003. Evaluation of the Moderate-Resolution Imaging Spectroradiometer (MODIS) retrievals of dust aerosol over the ocean during PRIDE. *J. Geophys. Res.* 108, 13.
- Li, Z., Guo, J., Ding, A., Liao, H., Liu, J., Sun, Y., and Zhu, B., 2017. Aerosol and boundary-layer interactions and impact on air quality, *Natl. Sci. Rev.*, 4, 810–833.
- Li, J., Li, C., Zhao, C., and Su, T., 2016. Changes in surface aerosol extinction trends over China during 1980–2013 inferred from quality-controlled visibility data, *Geophys. Res. Lett.*, 43, 8713–8719.
- Luan, T., Guo, X., Guo, L., Zhang, T., 2018. Quantifying the relationship between PM_{2.5} concentration, visibility and planetary boundary layer height for long-lasting haze and fog–haze mixed events in Beijing. *Atmos. Chem. Phys.*, 18, 203–225.
- Quan, J., Gao, Y., Zhanga, Q., Tieg, X., Caoc, J., Hane, S., Menga, J., Chena, P., Zhaoa, D., 2013. Evolution of planetary boundary layer under different weather conditions, and its impact on aerosol concentrations. *Particuology* 11, 34–40.



Pope, A., Burnett, R.T., Thun, M.J., Calle, E.E., Krewski, D., Ito, K., et al., 2002. Lung cancer, cardiopulmonary mortality, and long term exposure to fine particulate air pollution. *J. Am. Med. Assoc.* 287, 1132-1141.

Remer, L.A., Mattoo, S., Levy, R.C., Munchak, L.A., 2013. MODIS 3 km aerosol product: algorithm and global perspective. *Atmos. Meas. Tech.* 6, 1829-1844.

Rienecker, M. M., Suarez, M. J., Gelaro, R., Todling, R., Bacmeister, J., Liu, E., Bosilovich, M. G., Schubert, S. D., Takacs, L., Kim, G.-K., Bloom, S., Chen, J., Collins, D., Conaty, A., da Silva, A., Gu, W., Joiner, J., Koster, R. D., Lucchesi, R., Molod, A., Owens, T., Pawson, S., Pegion, P., Redder, C. R., Reichle, R., Robertson, F. R., Ruddick, A. G., Sienkiewicz, M., and Woollen, J., 2013. MERRA: NASA's Modern-Era retrospective analysis for research and applications, *J. Climate*, 24, 3624–3648.

Segura, S., Estelles, V., Utrillas, M.P., Martínez-Lozano, J.A., 2017. Long term analysis of the columnar and surface aerosol relationship at an urban European coastal site. *Atmos. Environ.* 167, 309-322.

Smirnov, A., Holben, B.N., Eck, T., Dubovik, O., Slutsker, I., 2000. Cloud-screening and quality control algorithms for the AERONET database. *Remote Sens. Environ.*, 73, 337-349.

Su, T., Li, Z., Kahn, R., 2018. Relationships between the planetary boundary layer height and surface pollutants derived from lidar observations over China: regional pattern and influencing factors. *Atmos. Chem. Phys.*, 18, 15921–15935.

Tanre, D., Kaufman, Y.J., Herman, M., Mattoo, S., 1997. Remote sensing of aerosol properties over oceans using the MODIS/EOS spectral radiances. *J. Geophys. Res.* 102, 16971-16988.

Tutsak, E., Koçak, M., 2019. Long-term measurements of aerosol optical and physical properties over the Eastern Mediterranean: Hygroscopic nature and source regions. *Atmos. Environ.*, 207, 1–15.

Acknowledgment

This study has been supported in part by the TUBITAK 2214/A Doctoral Research Scholarship Programme. We extend sincerest thanks to the AERONET, MODIS and MERRA-2 teams for their datasets.

Location optimization for future coal-fired power plants using geographical information system and dispersion model

Baris Saridikmen¹, Ezgi Akyuz² and Burcak Kaynak¹

¹Istanbul Technical University, Department of Environmental Eng., Istanbul, Turkey

²Istanbul Technical University, Eurasia Institute of Earth Sciences, Istanbul, Turkey

burcak.kaynak@itu.edu.tr

Abstract. Determination of existing pollution is not enough by itself to manage air quality of a region. It is also necessary to consider the possible future impacts from sources such as urbanization, energy and industry sector. Energy sector still uses fossil fuels, preferably coal as a national resource and continues to increase the installed capacity of coal-fired power plants in Turkey. In addition to technology, capacity, fuel type and quality, location of the power plant is strongly impacting its contribution to air pollution in a region because meteorology, geography and existing sources also strongly affect ambient pollution levels, their health and environmental impacts. The objective of this study is to determine the most suitable locations for coal-fired power plants using economic, environmental and geographical constraints compared to current practice where this selection is mostly done using economic constraints. Environmental and public health concerns are then investigated in environmental impact assessment reports. In this study, location selection is performed for Thrace region of Turkey. Three alternative locations (Corlu, M. Ereğlisi, Havsa) in addition to one proposed location (Cerkezkoş) for power plant were selected according to the assessment criteria and spatial processing. CALPUFF dispersion model was used to estimate SO₂ and PM₁₀ concentrations in the study domain covering Thrace Region for each alternative location. The most impacted air quality monitoring stations and contribution of SO₂ and PM₁₀ from all four cases were also calculated and assessed according to the current pollution levels. The annual and daily concentrations and their impact areas indicated all the alternative location were better than the proposed location. In addition, the population affected was found to be nine times higher than the closest alternative in the proposed case.

Keywords: Coal-fired power plants, Location optimization, SO₂, PM₁₀.

1. Introduction

Increasing population expectably lead to an increase in energy demand. The energy policies and the lack of high quality natural resources in Turkey necessitates all domestic resources to be used to satisfy the energy demand. Not only the industries but also fossil fuel power plants cause an increase in air pollution by releasing pollutants into the atmosphere. Thus, possible contributions of proposed plants to the atmosphere should be determined while satisfying the energy demand. Both PM and SO₂ are released from the stack as primary pollutants and may react in the atmosphere causing secondary pollutants. The main driver behind SO₂ pollution is the coal-fired power plants (CPPs) while the main resources of PM may be both anthropogenic (e.g. residential heating, industrial production) and natural (e.g. dust storms).

In Turkey, various types of power plants are operated for electricity production. According to Electricity Market Development Report (RoTEMRA, 2018) more than half (55.37%) of national installed power is from fossil fuels with natural gas 32.29%, lignite 11.36% and regular coal being 1.26%. In Thrace Peninsula, in Turkish electricity grid produced 19 544 GWh while consumed 32 341 GWh in 2016 and its consumption is expected to rise to 43 000 GWh in 2027. Thrace has limited access to Turkish

electricity grid since any power lines either has to go through the Bosphorus Strait which has a limited amount of space or through the Dardanelles Strait which because of its width has to be a subterranean/submarine line which is expensive and needs to be imported.

Previously, studies were carried out using different methodologies for selecting locations for power plants. Villacreses et al. (2017) have calculated the availability for wind farms in Ecuador to build a Geographical Information System (GIS) using multi-criteria decision-making (MCDM) methods and found that central Andes region of Ecuador is more efficient for wind farms. Cebi et al. (2016) proposed a fuzzy set theory and linguistic scales for a biomass plant in the Aegean Region. Kauria (2016) developed a global location optimization model for utility-scale solar power plants and pointed that Harare/Zimbabwe was more suitable than Helsinki/Finland and Denver/US. Aydın et al. (2013) developed a GIS-based site selection method for hybrid renewable energy systems in Turkey considering the acceptability for both wind and solar power. Khan (2018) has developed a location analysis methodology that can minimize the pollutant exposure to public while ensuring that the combined costs of electric transmission losses and coal logistics are minimized using a variety of distance calculations, picking the most suitable location alternatives and using a plume dispersion model (METI-LIS) to pick the best location in a small domain. Biberacher et al. (2015) observed that different layers on a GIS yields important results in energy planning where they studied bioenergy and power plant location optimization for Pakistan. Zheng et al. (2011) proposed a methodological framework for site optimization in designing a Regional Air Quality Monitoring Network (RAQMN) for regional air quality management. There is no study in the literature made for location optimization of thermal power plants in Turkey. However, Ozkurt et al. (2013) used CALPUFF dispersion model to characterize the air pollution in Canakkale by determining SO₂ and NO₂ contributions in Can and BayramiC districts. Vardar and Yumurtacı (2010) calculated the pollutant emissions of some lignite-fired power plants in Turkey using the coal content and suggested that all other CPPs have to be modernized with effective measurement and control equipment in order to improve the combustion efficiencies. Saylan et al. (2011) found that precipitation chemistry, which is a direct result of season-to-season air quality in the Thrace region, has changed.

The aim of this study is to assess the Thrace Region for a potential location for a CPP according to geographical, environmental and economic constraints. Three alternative locations were proposed and compared with one already proposed location in the region.

2. Methodology

2.1. Study domain

Thrace Region has Edirne, Kırklareli, and Tekirdag provinces with 1 802 315 population, also covers parts of Istanbul and Canakkale provinces with a total population over 2 million. Region is a peninsula, which is located in Europe, and providing energy to this region is a significant challenge due to this geographic characteristic. Therefore, coal-fired power plants (CPPs) along with other plants are being planned for the region. Natural gas and wind power plants are operated to supply the energy demand in the region. In this study, location optimisation for a coal-fired power plant for this region was aimed. A large study domain of 270×250 km² area was selected with a cell size of 2×2 km². There are 12 air quality monitoring stations (AQMSs) in three provinces, and 51 AQMSs in the whole study domain. Also, there are 33 meteorology stations which are operated in the study domain. The dominant wind direction is from north-northeast. However, the seasonal variation in wind speed and directions was significant. Wind profiles showed similarity for winter and spring with varying wind directions and summer and fall with a strong dominant wind direction of north-northeast. Terrain height in this region reaches up to 1 000 m in Yıldız Mountains in the northern parts, but generally region is composed of plains up to 300 m. The small settlements are spread throughout the region and the population is concentrated in districts of Corlu, Suleymanpasa and Cerkezkoç in Tekirdag, Luleburgaz in Kırklareli

and Merkez in Edirne. Within the region, there are 13 organized industrial zones and a free trade zone which is the fourth largest in Turkey.

2.2. Location selection

For the selection of the best site for a CPP, various factors need to be taken into account. By following a methodology considering these factors, three location alternatives to the proposed location given in Cerkezkoy EIA application (MGS, 2018) were identified (Figure 1).

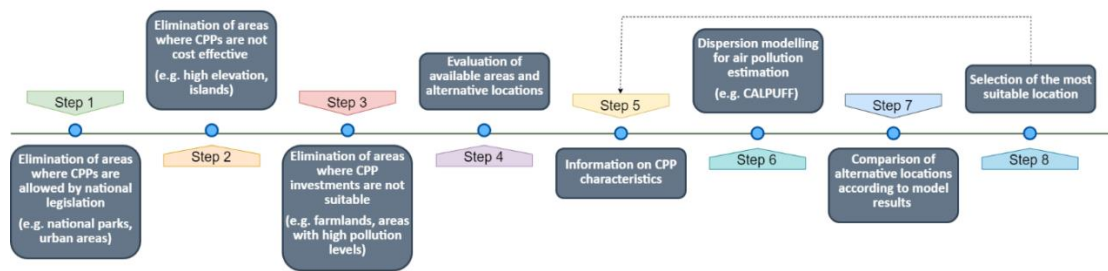


Figure 1. Methodology stages of location selection for CPPs

Selection is based on environmental, geographical, and economic criteria. Historical areas and natural reserves, agricultural areas, forests, high elevation and ruggedness of the terrain, existing air pollution level, precipitation, wind direction and population density can be considered as environmental and geographical factors. Proximity to roads, railroads, ports, coal reserves, ash-using industries, consumers and workforce can be taken into account as the economic factors. These factors should be evaluated depending on their positive and negative impact for the region.

Firstly, high resolution digital elevation map, population density, land cover (indicating urban settlements and forest and agricultural regions) datasets were intersected with the study domain in ArcGIS. Air pollution levels from ground monitoring stations were obtained.

Land use categories of CORINE Land Cover (CORINE, 2018) and terrain height information of SRTM Digital Elevation (SRTM, 2014) datasets were used. In the *first step*, 2 km around urban areas (such as urban fabric, industrial, commercial and transport units -ports and airports-) as well as 4 km in the direction of airport runways are eliminated. In *second step*, areas where a thermal power plant would not be cost effective, were excluded such as high altitude regions on north-western part of Thrace Region by the Yıldız Mountains. National boundaries of Turkey were roughly taken into consideration in terms of air pollutants dispersion according to the region's dominant wind direction. *Third step* involves the elimination of areas where a coal-fired power plant would not be suitable regarding economic concerns of the region and the country (such as farmlands). The forest areas are not preferred due to environmental concerns. Irrigated farmlands and forested areas were eliminated, but usable lands like arable lands and scrubs were qualified as suitable areas. Regions with high air pollution were specified using observations from National Air Quality Monitoring Network (MoEU, 2016) not to contribute to the current air pollution levels.

The possible contribution to air pollution of the CPP will be investigated within the study domain and in AQMSs with CALPUFF dispersion model. After this elimination, the selection of alternative locations within available regions were performed as the *fourth step*. For the *fifth step*, the final step before air dispersion modelling is the data collection regarding the CPP. This information includes the capacity of the plant, technology to be used, stack height, and any pollution control measures. These should be determined in order to have the least capital expense with acceptable (or profitable) operation expenses while satisfying the national regulations. Cerkezkoy CPP is a lignite-fired 990 MW (330 MW

three separate stacks) power plant project owned by EUAS (MGS, 2018). CPP is proposed to be located very close to Cerkezkoym province center, which was taken as the first case. Since there is no information on emissions in EIA application, a similar fuel and capacity CPP as Can-2 CPP in Canakkale province was used for emission and stack information for dispersion modeling (Table 1). Can-2 CPP is a single unit 330 MW lignite-fired power plant that was commissioned in August 2018 (EN-CEV, 2014). The stack height of Can-2 CPP (120 m) was increased to 150 m for safety because of the population density of Thrace Region.

Table 1. Emission and stack specifications of coal-fired power plant

Capacity (MWe)	Fuel type	Emissions (kg/hr)		Stack Information		Exit	Exit
		SO ₂	PM ₁₀	Height (m)	Diameter (m)	Velocity (m/s)	Temperature (°K)
3×330	Lignite	280	28	150	6.25	15	336

The first alternative location is close to another proposed CPP; Cebi which is an imported coal-fired power plant project with 350 MWe, but also satisfies the criteria explained above. It is approximately 5 km west of Marmara Ereğlisi district. Two more alternative locations were selected using the criteria; one in Tekirdag province (Corlu district, 15 km north of Corlu town center and the distance to E-80 highway is less than 1 km), second one in Edirne province (Havsa district, 15 km west of Havsa town center and 35 km southeast of Edirne urban center. It is 7 km away from D100 state road).

2.3. Dispersion modeling

CALPUFF, which is a multi-layer, multi-species, non-steady-state Lagrangian puff model (Aceituno, 1988) is listed as an alternative model for the other dispersion models by the U.S. Environmental Protection Agency (EPA). CALPUFF simulates the transport, transformation and removal of pollution with varying meteorological conditions. Better results on complex terrains and no limitation for the number of meteorology stations are the reasons for selection of this model in this study. Model have three modules: CALMET, CALPUFF and CALPOST, and also a pre-processor for the CALMET module.

Shuttle Radar Topography Mission (SRTM) DEM dataset was used in this study as an input for the pre-processor (SRTM, 2014) with 1 arc-second resolution (i.e. approximately 30 m). As land use dataset, a mostly used product of Copernicus Land Monitoring Service, CORINE Land Cover (CLC) was used (CORINE, 2018). Land cover data which is in raster format was spatially processed in ArcGIS to match CORINE land use classes with CALPUFF land use classes. Surface and upper meteorology measurements (TSMS, 2016) were provided from Turkish State Meteorological Service. 33 surface and 1 radiosonde meteorology station data were used to generate the required input files for CALMET. Terrain height, land use, AQMSs, and meteorology stations were shown in Figure 2 using the input files meteorological fields were generated by CALMET.

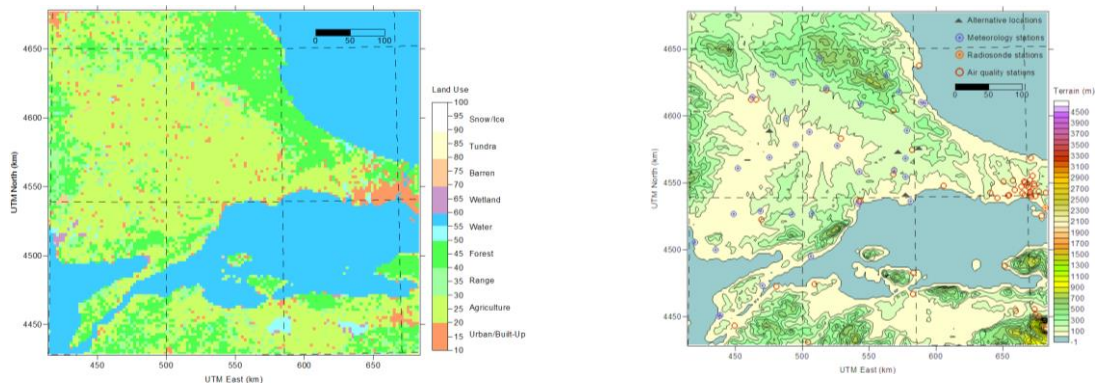


Figure 2. Land use (left) and terrain height (right) indicating meteorology and air quality stations

CALPUFF module was run to determine the atmospheric dispersion of PM₁₀ and SO₂ for all locations with dry and wet deposition. Module requires emission rates of pollutants to be tracked, stack height and diameter, exit temperature and exit velocity. The information of the CPP is given in Table 1. CALPOST, the post processing module, was used to obtain the hourly, daily, and annual averages of PM₁₀ and SO₂ concentrations and peak values.

3. Results and discussion

3.1. Air quality

Air quality in Thrace has issues with respect to SO₂ and PM₁₀ pollution. AQMSs which indicated high pollution and are located in Edirne, Kırklareli and Tekirdag provinces were taken into consideration. The average pollution levels, their compliance with Air Quality Assessment and Management Regulation and exceedances are given in Table 2.

Kesan MTHM exceeded the SO₂ and PM₁₀ hourly and daily limit values for the last three years with very high concentrations and high number of exceedances up to 200 days. Winter SO₂ limit value was exceeded almost in all stations all years except for the year of 2018. Annual SO₂ limit value was exceeded or slightly below the limit value, which results in exceedances in winter averages except for three stations in 2018.

PM₁₀ concentrations were observed significantly higher than daily limit value in all the stations with minimum of 55 days and a maximum of 181 days in the most recent year, 2018. Annual PM₁₀ concentrations exceeded the limit value for all stations except Cerkezkoy MTHM in 2018. The worst concentration is 94 µg/m³ in Tekirdag which is more than twice the limit value of 40 µg/m³.

Table 2. Pollutant concentrations in selected AQMSs and exceedances according to limit values

AQMS (year)	Hourly ¹	SO ₂ [*]			PM ₁₀ [*]		
		Daily ²	Annual ³	Winter ³	Daily ²	Annual ³	
Edirne	(2016)	2	0	24.80	36.78	122	46.27
	(2017)	6	2	27.07	42.45	99	45.68
	(2018)	3	0	9.55	15.09	92	44.40
Kesan MTHM	(2016)	2089	173	264.88	489.84	222	70.49
	(2017)	1443	184	165.40	293.71	218	71.61
	(2018)	1221	132	138.29	250.20	178	55.45
Tekirdag	(2016)	22	11	27.37	49.46	-	-
	(2017)	30	16	26.10	41.82	-	-
	(2018)	18	8	18.35	35.09	155	94.30
Kirkclareli	(2016)	21	5	18.82	32.78	293	73.87
	(2017)	10	2	17.22	28.06	205	60.76
	(2018)	0	0	12.73	19.80	181	53.53
Cerkezkoy MTHM	(2016)	1	57	24.05	31.82	260	71.04
	(2017)	1	31	18.38	28.08	207	57.55
	(2018)	0	25	12.56	18.75	55	34.01
Corlu MTHM	(2016)	-	-	-	-	92	40.77
	(2017)	-	-	-	-	107	41.67
	(2018)	1	0	18.43	25.72	87	40.49

¹ 350 µg/m³ more than 24 times (SO₂) should not be exceeded in a year.

² 125 µg/m³ more than 3 times (SO₂) and 50 µg/m³ more than 35 times (PM₁₀) should not be exceeded in a year.

³ 20 µg/m³ (SO₂) and 40 µg/m³ (PM₁₀) should not be exceeded in a year.

* Hourly and daily values are given as number of exceedances, yearly and winter (1 Oct-31 March) values are given as averages.

Last 10 years of available daily SO₂ and PM₁₀ concentrations in the selected AQMSs were also investigated with respect to annual and seasonal variation (Figure 3). Historically, the region has exceedances in both pollutants, especially in winter months. Although SO₂ pollution is observed to be decreased within the years in the stations, there are still exceedances. PM₁₀ concentrations shows a seasonal trend with maximum concentrations observed in winter, with very minor decrease within the years with significant exceedances. Considering the current level of SO₂ and PM₁₀ pollution, during the location selection of CPP, close proximity to Tekirdag, Kesan MTHM and Edirne MTHM stations were avoided.

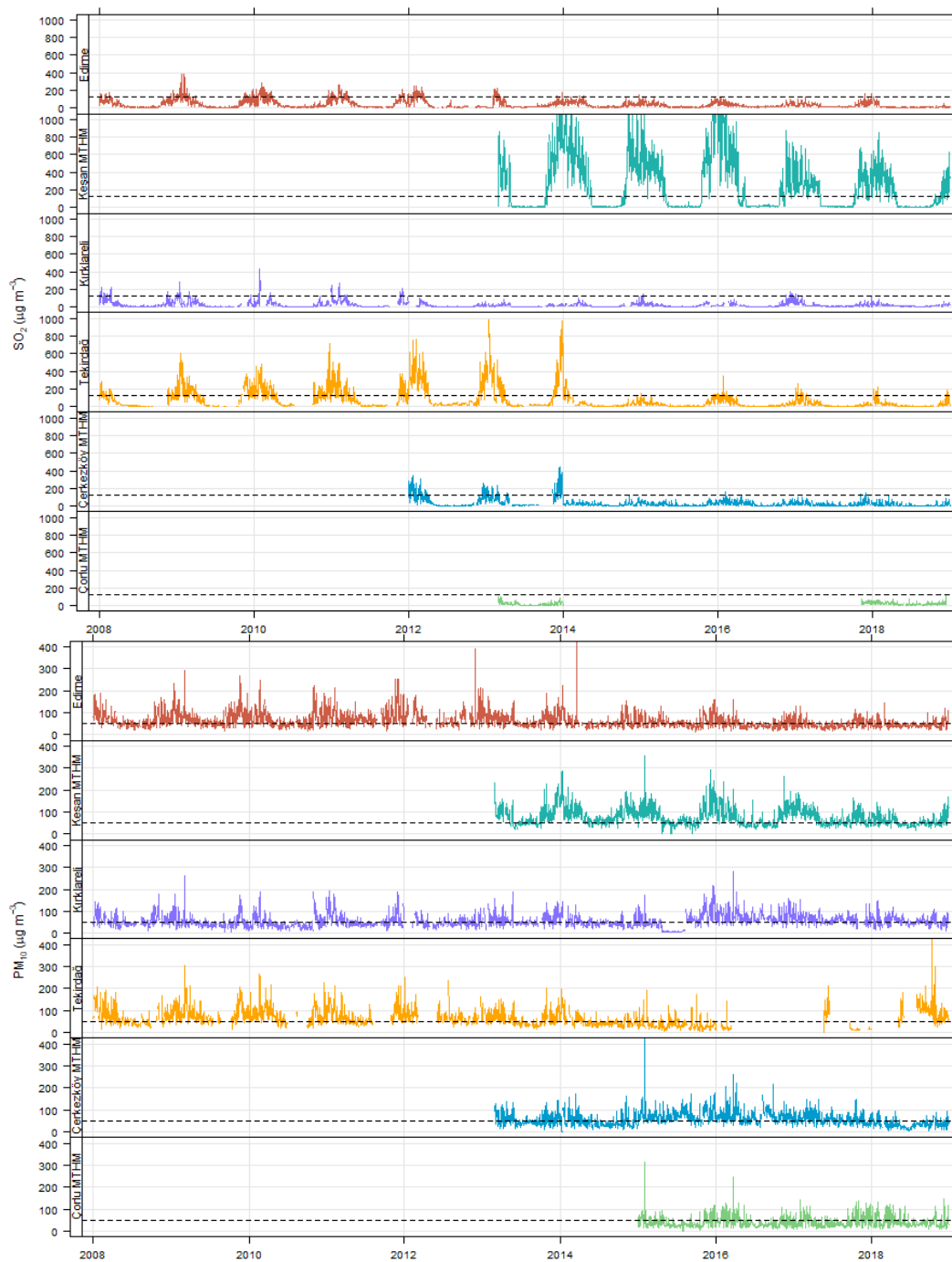


Figure 3. Daily PM₁₀ (up) and SO₂ (down) concentrations of AQMSs (dashed line indicates limit value)

3.2. Model results

Dispersion modelling using CALPUFF model was performed for one proposed and three alternative locations as four different cases. Concentration fields were calculated for the year of 2016. Annual average concentrations indicated the affected regions and concentration contributions for SO₂ (Figure 4). In Cerkezkoym and Corlu cases, SO₂ and PM₁₀ pollutions were transported mostly along with the dominant winds in northeast direction (Figure 4) which are in fall and summer months. The wind speeds were calmer with a fairly uniform wind direction in winter and spring. The affected regions were larger in Cerkezkoym case than Corlu even though the locations are close to each other. The pollution

distribution in Havsa case was mostly southward due to dominant wind direction, however the region affected was smaller and maximum annual impact ($2.62 \mu\text{g}/\text{m}^3$) (Table 3) was significantly lower than the previous two cases. In addition, the affected regions in Cerkezkoy and Corlu cases are densely populated areas compared to Havsa case. In M. Ereğlisi case, the pollution was spread over larger areas than other cases, due to varying wind directions, especially in winter and spring, however, the main transport was to southwest direction which is in line with the wind direction in fall and summer season. Maximum impact in M. Ereğlisi case was found to be similar to Havsa case. The impacted areas were usually over the Marmara Sea with minor population exposure.

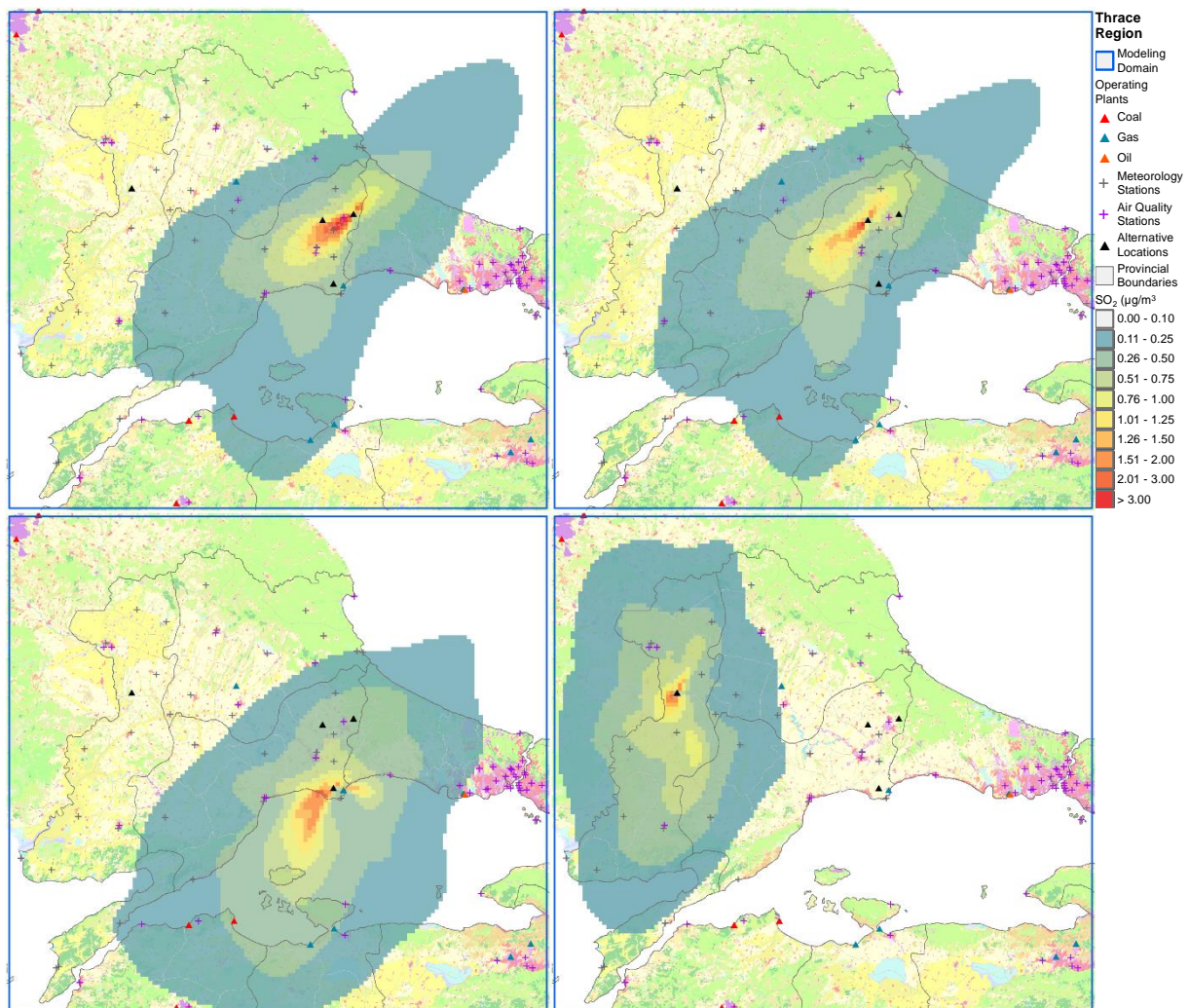


Figure 4. Annual SO_2 pollution distribution of alternative locations: Cerkezkoy (upper left), Corlu (upper right), Marmara Ereğlisi (lower left) and Havsa (lower right)

Maximum concentrations estimated by CALPUFF in the study domain were always significantly higher than the maximum concentrations estimated at AQMSs locations (Table 3). The three mostly affected AQMSs for each case were summarized with maximum domain concentrations.

Karaagac MTHM close to Edirne, Corlu OSB MTHM close to Corlu MTHM, Merkez MTHM close to Tekirdag stations were not included in air quality assessment because the data was limited. The impact at these stations would be similar to the close-by stations given in the assessment.

Table 3. Hourly, daily, and annual pollutant contributions of the CPP at selected AQMSs

	Cerkezkoy		Corlu		Marmara Ereglisi		Havsa	
SO ₂ (µg/m ³)	281.0	(Study Domain)	493.3	(Study Domain)	406.3	(Study Domain)	547.7	(Study Domain)
Hourly	160.3	(Cerkezkoy MTHM)	97.0	(Corlu OSB MTHM)	41.7	(Corlu MTHM)	34.2	(Karaagac MTHM)
	36.4	(Corlu MTHM)	70.6	(Cerkezkoy MTHM)	35.3	(Tekirdag)	30.5	(Edirne)
	25.6	(Corlu OSB MTHM)	65.1	(Corlu MTHM)	34.5	(Merkez MTHM)	13.3	(Luleburgaz MTHM)
SO ₂ (µg/m ³)	32.3	(Study Domain)	34.2	(Study Domain)	32.3	(Study Domain)	35.4	(Study Domain)
Daily	23.0	(Cerkezkoy MTHM)	6.4	(Corlu OSB MTHM)	6.1	(Corlu OSB MTHM)	6.3	(Edirne)
	9.3	(Corlu OSB MTHM)	5.7	(Cerkezkoy MTHM)	5.9	(Corlu MTHM)	5.4	(Karaagac MTHM)
	5.6	(Corlu MTHM)	5.3	(Corlu MTHM)	4.5	(Tekirdag)	2.2	(Kesan MTHM)
SO ₂ (µg/m ³)	4.13	(Study Domain)	4.21	(Study Domain)	2.64	(Study Domain)	2.62	(Study Domain)
Annual	2.12	(Cerkezkoy MTHM)	0.62	(Corlu OSB MTHM)	0.43	(Corlu MTHM)	0.43	(Kesan MTHM)
	1.19	(Corlu OSB MTHM)	0.58	(Cerkezkoy MTHM)	0.41	(Corlu OSB MTHM)	0.39	(Edirne)
	0.96	(Corlu MTHM)	0.56	(Corlu MTHM)	0.40	(Cerkezkoy MTHM)	0.39	(Karaagac MTHM)
PM ₁₀ (µg/m ³)	28.4	(Study Domain)	49.7	(Study Domain)	41.2	(Study Domain)	55.2	(Study Domain)
Hourly	16.0	(Cerkezkoy MTHM)	9.9	(Corlu OSB MTHM)	4.3	(Corlu MTHM)	3.5	(Karaagac MTHM)
	3.7	(Corlu MTHM)	7.1	(Cerkezkoy MTHM)	3.6	(Tekirdag)	3.1	(Edirne)
	2.6	(Corlu OSB MTHM)	6.5	(Corlu MTHM)	3.5	(Corlu OSB MTHM)	1.4	(Luleburgaz MTHM)
PM ₁₀ (µg/m ³)	3.4	(Study Domain)	3.5	(Study Domain)	3.3	(Study Domain)	3.6	(Study Domain)
Daily	2.3	(Cerkezkoy MTHM)	0.7	(Corlu OSB MTHM)	0.7	(Corlu OSB MTHM)	1.0	(Edirne)
	1.0	(Corlu OSB MTHM)	0.6	(Cerkezkoy MTHM)	0.7	(Corlu MTHM)	0.9	(Karaagac MTHM)
	0.6	(Corlu MTHM)	0.6	(Corlu MTHM)	0.5	(Tekirdag)	0.3	(Luleburgaz MTHM)
PM ₁₀ (µg/m ³)	0.42	(Study Domain)	0.43	(Study Domain)	0.27	(Study Domain)	0.27	(Study Domain)
Annual	0.22	(Cerkezkoy MTHM)	0.07	(Corlu OSB MTHM)	0.05	(Corlu MTHM)	0.05	(Kesan MTHM)
	0.13	(Corlu OSB MTHM)	0.07	(Cerkezkoy MTHM)	0.05	(Corlu OSB MTHM)	0.05	(Edirne)
	0.11	(Corlu MTHM)	0.06	(Corlu MTHM)	0.05	(Cerkezkoy MTHM)	0.05	(Karaagac MTHM)

Daily maximum concentrations observed in every grid were calculated for all four cases (Figure 5). M.Ereglisi affects Tekirdag urban center with SO₂ concentrations more than 20 µg/m³, Corlu MTHM station up to 5 µg/m³ (Figure 5, Table 3). Havsa maximum concentrations were observed usually within 6 km distance from the CPP, however the maximum concentrations above 35 µg/m³ were observed on the border of Greece. High concentrations were observed in Cerkezkoy case along urban and industrial development and results indicated these impacts can also be observed in Cerkezkoy and Corlu stations. Corlu case, even though in close proximity to Cerkezkoy case, the maximum daily concentrations were significantly smaller with moderate concentrations between 15-20 µg/m³. Even though Havsa case has the lowest concentrations in general, the stations mostly affected are Karaagac MTHM, Edirne and Kesan MTHM. These stations indicate significant pollution currently and due to this reason, even these small impacts may contribute to non-attainment in the region. M. Ereglisi case mainly indicates transport over the sea however Tekirdag station with severe PM₁₀ and moderate SO₂ problem was affected.

A total population of 260 489, 28 493, 25 854 and 975 was living in regions with more than 15 µg/m³ SO₂ contribution in Cerkezkoy (55 grids), Corlu (50 grids), M. Ereglisi (51 grids) and Havsa (25 grids) cases.

PM₁₀ pollution distribution results indicated very similar results with SO₂ but with lower magnitudes (Figure 6). The highest PM₁₀ contribution was found in Cerkezkoy case with more than 0.4 µg/m³ annual, 3.4 µg/m³ maximum daily concentrations. It was also the case with highest contribution to close-by AQMSs as well. All other cases have lower contributions with minimum values estimated in Havsa case.

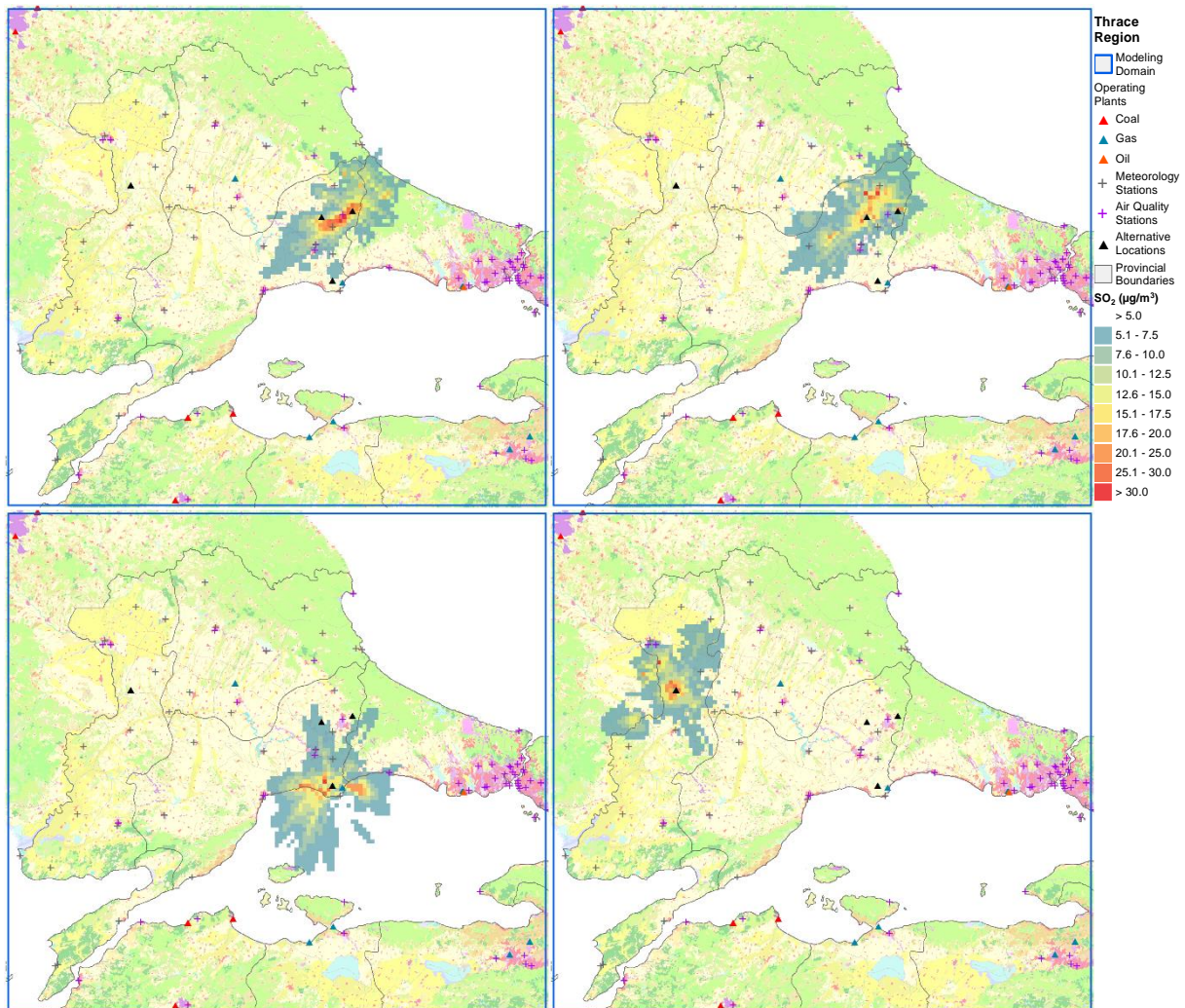


Figure 5. Daily maximum SO₂ pollution distribution of alternative locations: Cerkezkoy (upper left), Corlu (upper right), Marmara Ereğlisi (lower left) and Havsa (lower right)

4. Conclusions

Three alternative locations instead of a proposed location for a new CPP in Thrace Region were suggested in this study. CALPUFF dispersion model was used to simulate these four cases for the year of 2016. Highest concentrations of SO₂ and PM₁₀ over larger impact areas were simulated in Cerkezkoy case which is the proposed location. This case was also found to affect the highest population in the region compared to three alternatives.

Even though Corlu case is located very close to Cerkezkoy, Corlu case affected a smaller region with lower population density than Cerkezkoy. Resulting concentrations in Havsa and M. Ereğlisi cases were similar and lower than other two cases. However, they have moderate impact on some of the AQMSs which had significant exceedances. Proposed location resulted in the highest air pollution impact which indicates the necessity of the location selection methodology. The most suitable location for the CPP was found to be Havsa, considering the pollution contribution estimated by CALPUFF. However, M. Ereğlisi could also be a second alternative if economic factors such as transportation costs are taken into account.

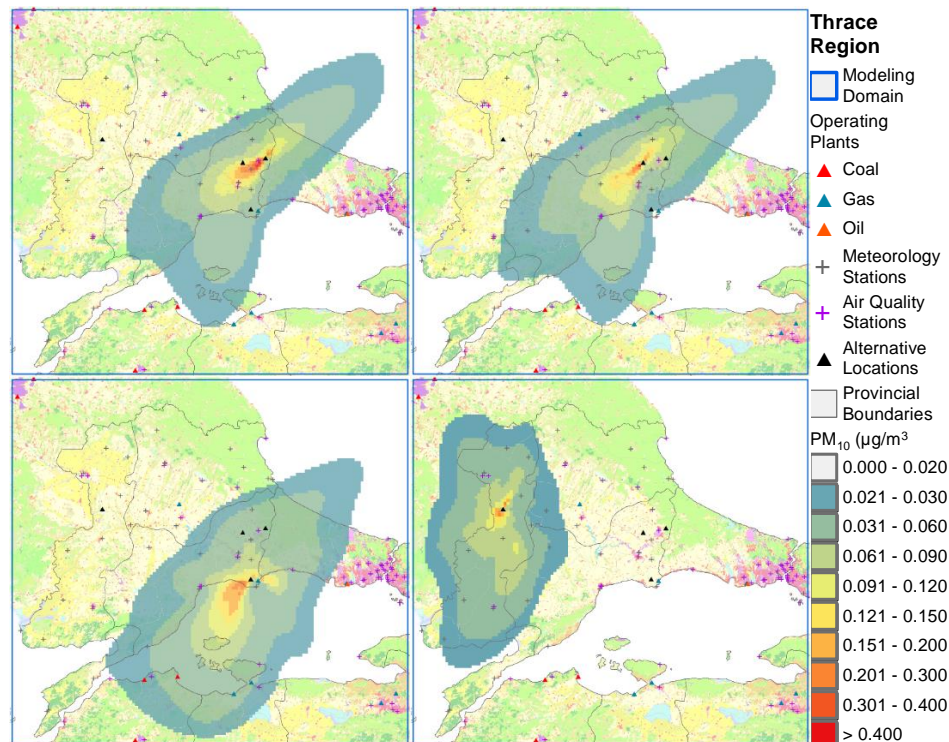


Figure 6. Annual PM₁₀ pollution distribution of alternative locations: Cerkezkoym (upper left), Corlu (upper right), Marmara Ereğlisi (lower left) and Havsa (lower right)

5. References

- Aceituno, P., 1988. CALPUFF Modeling System Version 6 User Instructions. Mon. Weather Rev. 116, 505–524.
- Aydin, N.Y., Kentel, E., Duzgun, H.S., 2013. GIS-based site selection methodology for hybrid renewable energy systems: A case study from western Turkey. Energy Convers. Manag. 70, 90–106.
- Biberacher, M., Tum, M., Gunther, K.P., Gadocha, S., Zeil, P., Jilani, R., Mansha, M., 2015. Availability assessment of bioenergy and power plant location optimization: A case study for Pakistan. Renew. Sustain. Energy Rev. 42, 700–711.
- Cebi, S., Ilbahar, E., Atasoy, A., 2016. A fuzzy information axiom based method to determine the optimal location for a biomass power plant: A case study in Aegean Region of Turkey. Energy. 116, 894–907.
- CORINE, 2018. CLC CORINE Land Use 2018 [WWW Document]. URL <https://land.copernicus.eu/pan-european/corine-land-cover/clc2018> (accessed 7.7.19).
- EN-CEV, 2014. Can-2 CPP Environmental Impact Assessment Report.
- Kauria, L., 2016. Developing a global location optimization model for utility-scale solar power plants.
- Khan, N., 2018. Location Optimization of a Coal Power Plant to Balance Coal Supply and Electric Transmission Costs Against Plant's Emission Exposure.
- MGS, 2018. Cerkezkoym CPP Environmental Impact Assessment Application.
- MoEU, 2016. National Air Quality Monitoring Network [WWW Document]. URL <https://www.havaizleme.gov.tr/> (accessed 7.20.19).
- Ozkurt, N., Sari, D., Akalin, N., Hilmioglu, B., 2013. Evaluation of the impact of SO₂ and NO₂ emissions on



the ambient air-quality in the Can-Bayramic region of northwest Turkey during 2007-2008. *Sci. Total Environ.* 456, 254–266. <https://doi.org/10.1016/j.scitotenv.2013.03.096>

RoTEMRA, 2018. Electricity market development report 2017. Ankara.

Saylan, L., Caldag, B., Bakanogulları, F., Toros, H., Yazgan, M., Sen, O., Ozkoca, Y., 2011. Spatial variation of the precipitation chemistry in the Thrace region of Turkey. *CLEAN--Soil, Air, Water.* 39, 491–501.

SRTM, 2014. NASA Shuttle Radar Topography Mission DEM [WWW Document]. URL <https://earthexplorer.usgs.gov/> (accessed 7.7.19).

TSMS, T.S.M.S., 2016. Surface and Radiosonde Meteorology Data [WWW Document]. URL <https://mgm.gov.tr/eng/forecast-cities.aspx>.

Vardar, N., Yumurtaci, Z., 2010. Emissions estimation for lignite-fired power plants in Turkey. *Energy Policy* 38, 243–252. <https://doi.org/10.1016/j.enpol.2009.09.011>.

Villacreses, G., Gaona, G., Martinez-Gómez, J., Jijón, D.J., 2017. Wind farms suitability location using geographical information system (GIS), based on multi-criteria decision making (MCDM) methods: The case of continental Ecuador. *Renew. Energy.* 109, 275–286.

Zheng, J., Feng, X., Liu, P., Zhong, L., Lai, S., 2011. Site location optimization of regional air quality monitoring network in china: methodology and case study. *J. Environ. Monit.* 13, 3185–3195.

Evaluation of hourly based precipitation chemistry in suburban site of Bolu

Hatice Karadeniz¹ and Serpil Yenisoğ Karakas²

¹Bolu Abant İzzet Baysal University, Scientific Industrial and Technological Application and Research Center (SITAC), Gököy, Bolu, 14030

²Bolu Abant İzzet Baysal University, Faculty of Art and Science, Chemistry Department, Gököy, Bolu, 14030

haticekaradeniz@ibu.edu.tr

Abstract. Precipitation chemistry is important for understanding atmospheric chemistry and transportation mechanism for a region. Therefore, 6-hour rain samples in rainy days were collected manually in the campus of Bolu Abant İzzet Baysal University between March 2019 and May 2019. Totally, 21 wet deposition samples were collected in 12 rainy days. The collected rain samples were analysed by ion chromatography for ions including Cl^- , NO_2^- , NO_3^- , PO_4^{3-} , SO_4^{2-} , Na^+ , Ca^{2+} , Mg^{2+} , K^+ , NH_4^+ . Volume weighted mean concentrations of ions each sample were also calculated for determination of air pollution levels and transportation of pollutants in the city atmosphere. The highest volume weighted mean concentration for anion and cation belonged to NO_3^- (5.11 mg L^{-1}) and Ca^{2+} (2.12 mg L^{-1}), respectively. The pH values of individual precipitation varied from 4.70 to 7.70. Acidic sample was affected by the air came from central Anatolia. Ammonium ion showed good correlations with NO_3^- and SO_4^{2-} . $(\text{NH}_4)_2\text{SO}_4$ and NH_4HSO_4 could be more predominant than NH_4NO_3 in the atmosphere according to the correlation coefficients. Rain out and wash out rain events were observed in two rain events. Percentage of rainout mechanism in March 12, 2019 was higher than April 13, 2019. The highest washout ratios were observed for nitrate ion in the sampling area.

Keywords: Rain, Water Soluble Inorganic Species, Rainout-Washout Mechanism, Correlation

1. Introduction

Rainwater is important precipitation events as a sink for determining the long- and short-term changes of pollutants like particulate matter and dissolved gases in the atmosphere (Al-Khasman, 2009; Akoto et al., 2011; Karşı et al., 2018). Composition of precipitation type are varied from site to site due to the difference of the local sources (Cao et al., 2009). It depends on the local emissions, pollutants transport, and drop size and the rainout (in-cloud scavenging), the washout (below-cloud scavenging) (Migliavacca et al., 2005). However, the measured species in the divided fractions of the same rain give information about local background of about the sampling area (Karşı et al., 2018). Moreover, it is important to understand the ionic composition of precipitation samples for understanding the acid precipitation events in the sampling site (Huang et al., 2009). The characteristics of major ions in rainwater in developed countries have been widely studied. These studies gave some information about the sources of the major ions and atmospheric quality of the sampling site (Meng et al., 2019). Moreda-Piñeiro et al. (2014) reported the results of samples collected in Spain during 2011–2012 and Cl^- , Na^+ and Mg^{2+} were linked to a marine origin; SO_4^{2-} and Ca^{2+} were derived from a crustal source; and NH_4^+ and NO_3^- were mainly attributed to agricultural activity. Fossil fuel combustion is source of sulfur and nitrogen oxides and these oxides are the precursors of major acidic ions (SO_4^{2-} and NO_3^-) in precipitation (Mouli et al., 2005; Das et al., 2005). Correlation of NH_4^+ with NO_3^- and SO_4^{2-} gives clue of sulfuric

acid and nitric reaction in the sampling site (Bridgman, 1994; Zhang et al., 2007). In Bolu, sequential sampling of four rainfall events (33 subsamples) were analyzed for major ions and pH by Karşı et al. (2018).

In this study, the results of time-based sequential rain samples in major ion compositions and washout, rainout identifications were investigated. The contributions of different sources were evaluated with correlation coefficients.

2. Experimental

2.1. Sampling site and sampling

Bolu is located at the Black Sea region of Turkey. The altitude of the city which is surrounded by high mountains is 730 m. Although the density of population and activities is not quite high, the main international highways (TEM and D-100), city traffic, domestic heating and air masses coming from the industrialized cities like İstanbul, Kocaeli Karabük, Russia and the European cities, to the city atmosphere are the main pollution sources (Karşı et al., 2018). The sampling was performed in the campus of Bolu Abant İzzet Baysal University between March 2019 and May 2019. Twenty-one samples were collected manually in 6 hours intervals in 12 rainy days and stored in +4°C until the analysis.

2.2. Analysis of samples

Samples were analysed for Cl^- , NO_2^- , NO_3^- , PO_4^{3-} , SO_4^{2-} , Na^+ , Ca^{2+} , Mg^{2+} , K^+ , NH_4^+ by using Dionex ICS-1100 model ion chromatography equipped with conductivity detector. An AS9-HC (Dionex, 250 mm x 4 mm) and CS12-HC (Dionex, 250 mm x 4 mm) column were used for the analysis of anions and cations, respectively. The separations of anions and cations was achieved by isocratic elution of 9 mM Na_2CO_3 and 10 mM $\text{CH}_3\text{SO}_3\text{H}$ with a 1.0 mL min^{-1} , respectively.

3. Result and discussion

3.1. General characteristics of data

Six anions (F^- , Cl^- , NO_2^- , NO_3^- , SO_4^{2-} , PO_4^{3-}) and five cations (Na^+ , NH_4^+ , K^+ , Mg^{2+} , Ca^{2+}) were quantitatively measured by IC. Hourly based volume of rain samples was changeable. Therefore, mass of ions was compared as μeq for total anion (Σ^-) and total cation (Σ^+). Figure 1 showed that the equivalent concentrations of total anions showed a significant anion deficiency (correlation coefficient, $r = 0.81$), with the ratio Σ^- / Σ^+ in the range of 0.582 ± 0.27 . It means that some anions like acetate, formate, carbonate etc. should be added to measurement because of the anion deficiency (Satsangi et al., 1998).

Table 1 showed that the VWM concentrations of major ions were in the order of $\text{NO}_3^- > \text{SO}_4^{2-} > \text{Ca}^{2+} > \text{Cl}^- > \text{Na}^+ > \text{NO}_2^- > \text{K}^+ > \text{NH}_4^+ > \text{Mg}^{2+}$. Among the anions, SO_4^{2-} , Cl^- , and NO_3^- were the dominant ones. Nitrate ion was the highest concentration anion due to the fact burning of fossil fuels, emission from vehicles in the sampling area (Russel et al., 1998). Calcium ion was the highest ion among the cations and Ca^{2+} was also strongly correlated with Mg^{2+} ($r = 0.926$). Therefore, it could derive from the soils (Mouli et al., 2005). Ammonium ion which should be from the human and animal excrements or agriculture activities. Phosphate ion was not detected in samples.

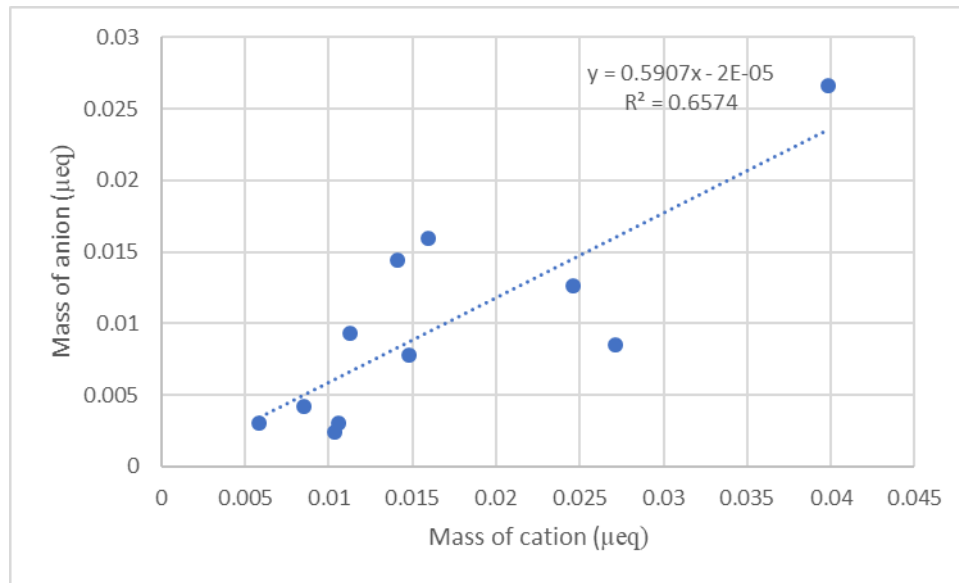


Figure 1. Plot of Σ^- versus Σ^+

Table 1. Statistical evaluations of data (mg L^{-1})

Ions	N	VWM	Arithmetic mean	Median	Min	Max
Na^+	21	0.715	3.47	1.20	0.0971	19.8
NH_4^+	19	0.105	0.159	0.118	0.0067	0.542
K^+	21	0.182	0.458	0.245	0.0437	2.01
Mg^{2+}	21	0.101	0.209	0.158	0.0131	0.676
Ca^{2+}	21	2.12	2.89	1.82	0.191	14.1
Cl^-	21	1.12	4.28	1.09	0.473	38.6
NO_2^-	21	0.470	0.274	0.0830	0.0568	2.36
NO_3^-	21	5.11	4.49	1.98	0.0852	44.6
SO_4^{2-}	21	3.71	4.96	2.96	0.634	18.3
pH	21	6.33	7.00	7.19	4.70	7.70

3.2. Variation of pH value

The temporal variations of pH for the rainwater samples are plotted in Figure 2. The pH values of individual precipitation varied from 4.70 to 7.70 with a volume weighted mean of 6.33. The rain samples having pH values less than 5.60 are considered as acid rain (Huang et al., 2008). The collected samples did not have acidic properties except for the sample collected in 17.03.2019 (pH:4.7) and this acidic sample was affected by the air came from Europe and Black Sea region (Figure 3). The sample had higher SO_4^{2-} , NO_3^- , NO_2^- concentrations than the other samples and sulfur and nitrogen oxides resulting from fossil fuel combustion is particularly important precursors of these acidic ions (Mouli et al., 2005; Das et al., 2005).

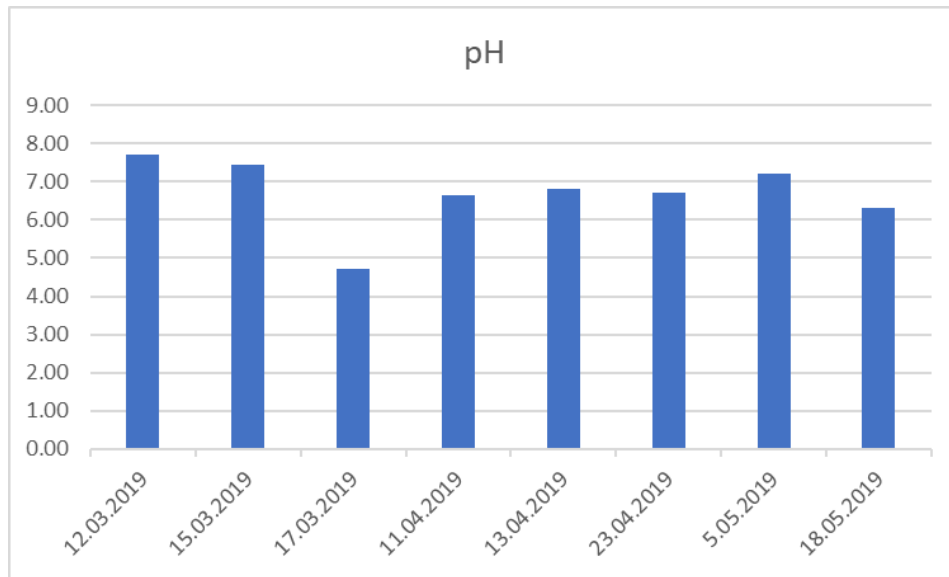


Figure 2. The temporal variations of pH for the rainwater samples

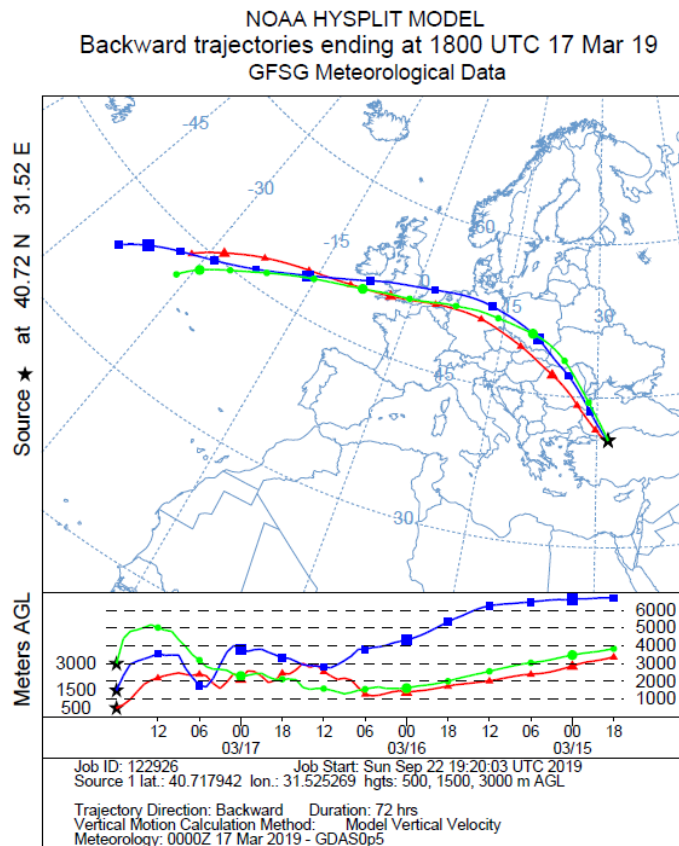


Figure 3. Air mass back trajectory terminating at Bolu for March 17, 2019

3.3. Correlation Analysis

Correlation analysis was performed to distinguish the possible common sources of ionic constituents. Correlations among ions in precipitation were calculated and listed in Table 2. Correlation coefficient between sulfate and nitrate were 0.758. Good correlations supported that these ions behave similarly in precipitation and have also similar emission sources (Zhang et al., 2007). Crustal origins cations Ca^{2+} , Mg^{2+} showed good correlations ($r=0.633$). Ammonium ion showed good correlations with NO_3^- and SO_4^{2-} . Ammonia generally found in the atmosphere as $(\text{NH}_4)_2\text{SO}_4$, NH_4HSO_4 , NH_4NO_3 in aerosols by reacting with sulfuric acid and nitric acid (Bridgman, 1994; Zhang et al., 2007). Correlation coefficient of NH_4^+ versus SO_4^{2-} ($r=0.747$) was higher than those of NH_4^+ versus NO_3^- ($r=0.619$) showing that $(\text{NH}_4)_2\text{SO}_4$ and NH_4HSO_4 could be more predominant than NH_4NO_3 in the atmosphere (Zhang et al., 2007; Cao et al., 2009). Correlation between Na^+ and Cl^- ($r=0.564$) was a sign of sea salt. Other correlations are observed between Ca^{2+} and NO_3^- , Na^+ and SO_4^{2-} , K^+ and SO_4^{2-} . These correlations may be observed because of the atmospheric chemical reactions of the acids of H_2SO_4 and HNO_3 .

Table 2. Correlation analysis ($p<0.05$)

	NH_4^+	Ca^{2+}	Cl^-	Mg^{2+}	NO_3^-	NO_2^-	K^+	Na^+	SO_4^{2-}
NH_4^+									
Ca^{2+}	0.2869								
Cl^-	0.3534	-0.0665							
Mg^{2+}	0.1642	0.633	0.1027						
NO_3^-	0.6195	0.866	-0.0344	0.2515					
NO_2^-	-0.1574	-0.0771	-0.1343	0.0467	-0.0722				
K^+	0.5275	0.3872	0.4668	0.6092	0.1441	-0.1618			
Na^+	0.2884	0.1862	0.5641	0.6409	-0.0777	-0.1497	0.7875		
SO_4^{2-}	0.747	0.1862	-0.0069	0.331	0.7573	-0.1375	0.426	0.1167	

3.4. Rainout and washout events of the ions

Washout and rainout ratios of two time-based fractional rain samples by using concentrations of ions in each rain event and shown in Figure 4. The lowest precipitation values of fractional samples were determined to understand rain out mechanism (Karşı et al., 2018). Five fractions in March 12, 2019 and four fractions in April 13, 2019 were collected. Maximum value for rainout to washout ratios was observed in April 13, 2019. However, percentage of rainout mechanism in March 12, 2019 was higher than in April 13, 2019. The highest washout ratio was observed for nitrate ion (97.2%) in April 13, 2019 and highest rain out ratio was observed for Na^+ (66.1%) in March 12, 2019.

Mass changes of anions and cations with fraction numbers were evaluated. Fractional differences of Na^+ and NH_4^+ were illustrated in Figure 5 and Figure 6 as an example. Hourly based samples showed the highest concentrations in the initial fractions (Figure 5). Ammonium, K^+ , NO_3^- , SO_4^{2-} ions increased after third fractions in March 12, 2019 (Figure 6). Micrometeorological changes at the sampling site affected the samples during sampling (Karşı et al., 2018).

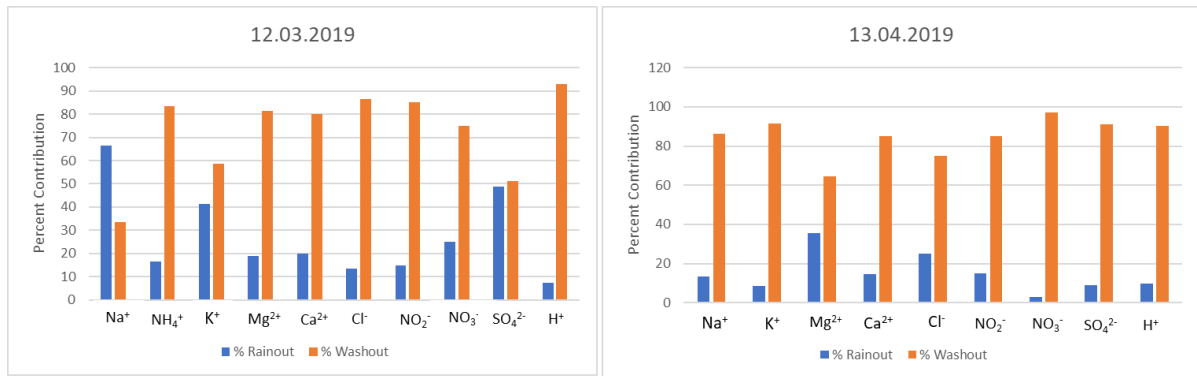


Figure 4. Percent contributions of rainout and washout processes to the total concentrations for samples collected in 12.03.2019-13.04.2019

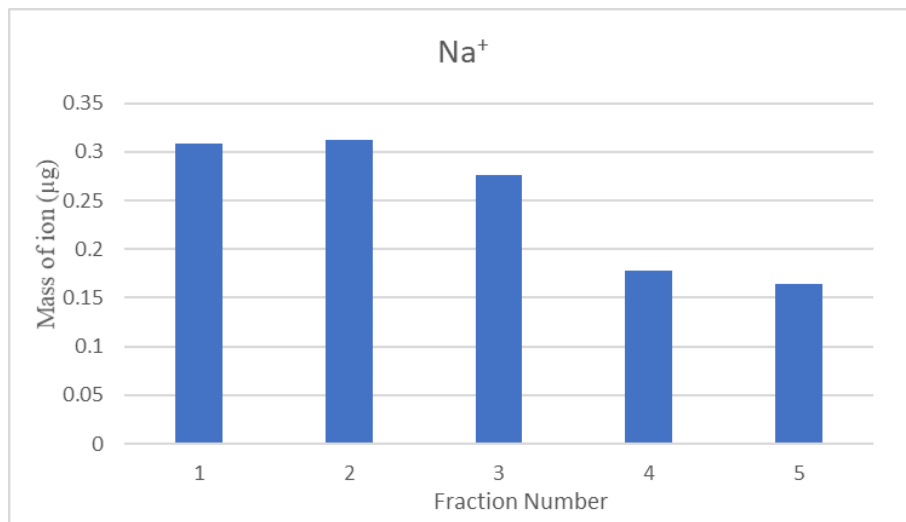


Figure 5. Mass changes of Na⁺ in each fraction

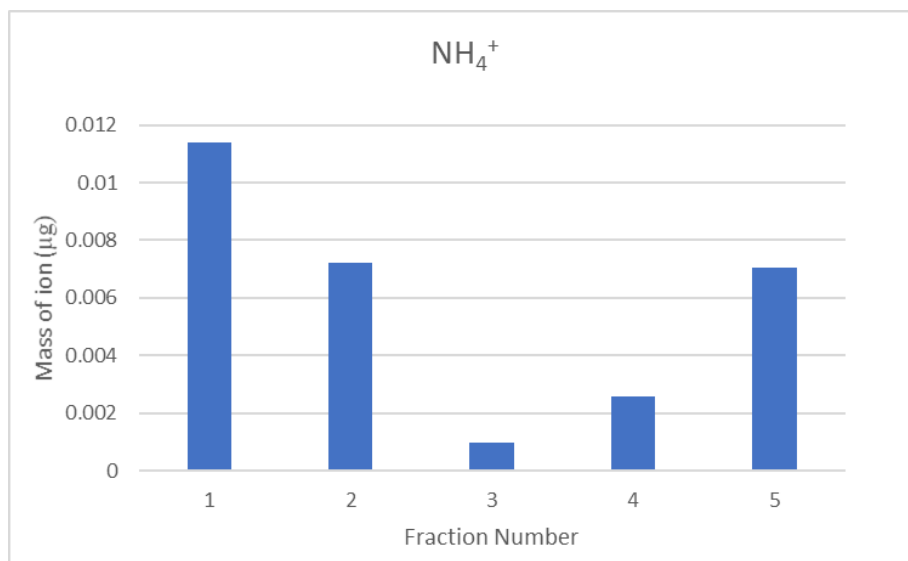


Figure 6. Mass changes of NH₄⁺ in each fraction



4. References

- Al-Khashman, O.A., 2009. Chemical characteristics of rainwater collected at a western site of Jordan. *Atmos. Res.* 91, 53–61.
- Akoto, O., Darko, G., Nkansah, M.A., 2011. Chemical composition of rainwater over a mining area in Ghana. *Int. J. Environ. Res.* 5, 847–854.
- Bridgman, H., 1994. *Global Air Pollution*. Wiley, London, p. 261.
- Cao, Y. Z., Wang, S., Zhang, G., Luo, J., & Lu, S., 2009. Chemical characteristics of wet precipitation at an urban site of Guangzhou, South China. *Atmos. Res.* 94, 462-469.
- Das, R., Das, S., Misra, V., 2005. Chemical composition of rainwater and dust fall at Bhubaneswar in the east coast of India. *Atmos. Environ.* 39, 5908–5916.
- Huang, K., Zhuang, G., Xu, C., Wang, Y., Tang, A., 2008. The chemistry of the severe acidic precipitation in Shanghai, China. *Atmos. Res.* 89, 149-160.
- Karşı, M. B. B., Yenisoy-Karakaş, S., Karakaş, D. 2018. Investigation of washout and rainout processes in sequential rain samples. *Atmos. Environ.*, 190, 53-64.
- Meng, Y., Zhao, Y., Li, R., Li, J., Cui, L., Kong, L., Fu, H., 2019. Characterization of inorganic ions in rainwater in the megacity of Shanghai: Spatiotemporal variations and source apportionment. *Atmos. Res.*, 222, 12-24.
- Migliavacca, D., Teixeiraa, E., Wiegand, F., Machado, A., Sanchez, J., 2005. Atmospheric precipitation and chemical composition of an urban site, Guaíba hydrographic basin, Brazil. *Atmos. Environ.* 39, 1829–1844.
- Moreda-Piñeiro, J., Alonso-Rodríguez, E., Moscoso-Pérez, C., Blanco-Heras, G., Turnes- Carou, I., López-Mahía, P., Muniategui-Lorenzo, S., Prada-Rodríguez, D., 2014. Influence of marine, terrestrial and anthropogenic sources on ionic and metallic composition of rainwater at a suburban site (northwest coast of Spain). *Atmos. Environ.* 88, 30–38.
- Mouli, P.C., Mohan, S.V., Reddy, S.J., 2005. Rainwater chemistry at a regional representative urban site: influence of terrestrial sources on ionic composition. *Atmos. Environ.* 39, 999–1008.
- Russell, K. M., Galloway, J. N., Macko, S. A., Moody, J. L., Scudlark, J. R., .1998. Sources of nitrogen in wet deposition to the Chesapeake Bay region. *Atmos. Environ.*, 32, 2453-2465.
- Satsangi, G. S., Lakhani, A., Khare, P., Singh, S. P., Kumari, K. M., Srivastava, S. S., 1998. Composition of rainwater at a semi-arid rural site in India. *Atmos. Environ.*, 32, 3783-3793.
- Zhang, M., Wang, S., Wu, F., Yuan, X., Zhang, Y., 2007. Chemical compositions of wet precipitation and anthropogenic influences at a developing urban site in south-eastern China. *Atmos. Res.*, 84, 311-322.

Acknowledgments

The authors are grateful to Prof. Dr. Duran Karakaş for his helps during calculation of data.

Effects of long-term exposure to PM_{2.5} air pollution on life expectancy of elderly population in Taiwan

Jing-Shiang Hwang and Tsuey-Hwa Hu

Institute of Statistical Science, Academia Sinica, Taipei, Taiwan

hwang@sinica.edu.tw

Abstract. Mortality is the most serious health effect of air pollution. Studies of modeling differences in life expectancy (LE) in time or space against changes in fine particulate matter (PM_{2.5}) concentrations in subnational areas have shown evidence that long-term exposure to PM_{2.5} reduced LE of the overall population. We used claims data of national health insurance to create study cohorts of residents aged 60 years and older living in 64 small areas in Taiwan where air quality monitoring stations are situated. The survival status of the elderly people was followed from 2001 to 2013. For each cohort, we created a reference population of subjects whose sex and age matched the study subjects, with the former's survival function generated from standard life tables. We modified an extrapolation algorithm to estimate the lifetime survival function of each cohort. We also proposed a measure of expected lifetime mean exposure to PM_{2.5} air pollution for each study cohort. Finally, we regressed the standardized life expectancy deviation of each study cohort, defined by LE difference between the cohort and the matched reference population, against expected lifetime mean exposure to PM_{2.5} of the cohort with adjustment of socioeconomic variables among the study cohorts to estimate the air pollution effects. Long-term exposure of the elderly population aged 60+ to a 10 µg/m³ increase in PM_{2.5} was strongly associated with reduction in life expectancy by 0.39 years (SE = 0.07 years). This study delivers strong evidence that elderly people's life expectancy is vulnerable to long-term exposure to PM_{2.5} air pollution.

Keywords: Air pollution health effects, Survival extrapolation, Expected years of life lost, Fine particulate matter.

1. Introduction

The effects of long-term exposure to ambient particulate matter (PM) air pollution on mortality have been well studied for health risk assessment (Dockery et al. 1993; Pope et al. 1995; Beelen et al. 2014). Since mortality is the most serious health effect of air pollution, the World Health Organization has started reporting the impact on mortality in terms of the number of premature deaths due to air pollution in recent years. However, studies have shown that the number of premature deaths is not meaningful for air pollution, whereas loss of life expectancy (LE) is an appropriate impact indicator that can be informative for environmental policy decisions (Rabl 2003; Brustugun 2014). The expected loss of LE, taking into account differences in age at death and risk of dying for different genders and ages is also more easily understood than the number of deaths from a risk communication perspective.

Many studies have reported loss of LE that can be attributed to ambient fine particulate matter (PM_{2.5}) using a comparative risk assessment approach and data from the Global Burden of Disease (GBD) project (Apte et al., 2018; Lancet Planet Health, 2019). The GBD approach was proposed mainly to compare loss of LE among countries or regions where population-weighted exposure can be calculated or estimated but may lack attributable relative risk estimates of the exposed populations. Currently, the relative risk estimates in these comparative risk assessment studies are based on information from a few studies such as the seminal American Cancer Society cohort studies (Krewski et al., 2009; Jerrett et al., 2009). Although models integrating relative risk estimates from multiple sources may increase accuracy of mortality estimates over a global range of exposure, these are indirect estimates with some degrees of uncertainty (Burnett et al., 2014).

Another approach for quantifying effects of long-term exposure to PM_{2.5} on LE of overall populations is modelling the relationship between the differences in LE and differences in PM_{2.5} exposure in time or space across selected areas. The difference-in-differences approach was first successfully demonstrated by evaluating the changes in LE associated with differential changes in PM_{2.5} air pollution among 211 county units in the U.S. during the 1980s and 1990s (Pope et al., 2009). A later analysis of 545 counties examining the changes from 2000 to 2007 generated similar results, although the estimated relationship was weaker (Correia et al., 2013). Recently, a clever regression discontinuity design based on distance from the Huai River in China was proposed to model the relationship between LE and air pollution exposure among areas with a spatial discontinuity for air pollution and LE (Chen et al., 2013; Ebenstein et al., 2017). The results suggested huge loss of LE for long-term exposure to high PM concentrations in China.

The findings of these studies provided strong evidence that sustained exposure to PM affected LE. However, there are some limitations to overcome. These analyses were conducted with cross-sectional data on mortality rates, air pollution concentrations and covariates to assess the general impact of air pollution across an overall population. Although older people are particularly vulnerable to air pollutants, these studies did not address the health impacts on the elderly population (Sandstrom, Wen 2012; He, 2016). The LE was calculated by taking the average of LE at birth or adjusted LE predicted using complicated models and annual mortality rates for a short time period for each study area. Another limitation of these study is that the sizes of study areas were too large. The uncertainty of exposure levels using averaged PM concentrations of a few local monitoring stations may be large, and this was ignored in the analysis. Furthermore, these studies did not collect mortality status of the individuals living in a study area.

To address the above issues, this study proposes a different design and alternative analytical approaches to quantify effects of long-term exposure to PM_{2.5} on loss of LE of the vulnerable elderly population. First, we used claims data of National Health Insurance (NHI) in Taiwan to create study cohorts of residents aged 60 years and older living or working in 64 small areas of rural townships and city districts where ambient air quality monitoring stations are situated. We extracted each individual's medical visit records during 1998 – 2013 in the claims database to select subjects into a study cohort and linked with the mortality registry to collect survival status of the subjects by the end of 2013. With the survival data, we modified an extrapolation method to estimate the lifetime survival function for each study cohort (Hwang et al. 2017). The survival function of a population of referents whose sex and age matched with subjects in the study cohort was generated from the standard life table of the general population. Second, similar to the standardized mortality ratio (SMR) used for comparison among subnational areas in a country, we proposed a statistic called standardized life expectancy deviation (SLED) of a study cohort, which is defined as the LE difference between the cohort and the sex- and age-matched reference population. Hence, like SMR, the defined SLED can be used for quantifying expected life years gained or lost for people living or working among the study areas with respect to the general population. Third, similar to the population-weighted exposure, we also proposed a measure of survival-weighted exposure to PM_{2.5} air pollution for each study cohort. Finally, we used weighted regression models to

estimate the association between SLED and survival-weighted exposure to PM_{2.5} with adjustment of influential socioeconomic, demographic and environmental variables among the 64 study cohorts and areas.

2. Methods

2.1. Data sources

The National Health Insurance program launched at the end of 1995 provides universal health care coverage to 99.6% of Taiwan's residents, and has service contracts with 93% of the country's hospitals and clinics in 2018 (<https://www.nhi.gov.tw>). The registry of beneficiaries includes a unique encrypted identifier, sex, date of birth, and insured payroll-related amount. The claims data contain diagnoses, prescriptions, and details of each outpatient visit or their inpatient care. Disease diagnoses are coded using the International Classification of Diseases, Ninth Revision (ICD9). The scale (academic medical center, metropolitan hospital, community hospital, or primary care clinic) and location of the de-identified health care facilities can be found in the registry for contracted medical facilities.

The Taiwan Air Quality Monitoring Network (TAQMN), established in 1993, consists of 76 monitoring stations including six traffic sites, three offshore sites and one in a national park, as well as 66 stations situated in populous urban and rural areas of the island used for informing the public about the ambient air quality. Open data consisting of hourly measurements of major pollutants and weather parameters are available for the public (<https://taqm.epa.gov.tw/taqm/en>). Socioeconomic and demographic variables at the city district and township level can be found at Taiwan government open data platform (<https://data.gov.tw/en>).

2.2. Study design

We selected 64 small study areas, shown in Figure 1, with a median size of 45 km² consisting of townships and city districts in Taiwan where ambient air quality monitoring stations of the TAQMN are situated and PM_{2.5} measurements have been available since 2006. Since ambient monitoring stations are usually located in the populous center of a study area, the PM_{2.5} concentrations measured at the monitoring station are presumed to represent air pollution exposure levels of subjects living or working in the area. For each study area, we created a study cohort of subjects who had lived or worked in the study area since January 1, 2001, and had been in the area to the end of 2013 or died during the follow-up. To create the cohort of a study area, we first identified subjects who visited a community hospital or primary care clinic located in the study area for minor treatment during 1998 – 2000, still survived by the end of 2000, and were aged 60 years and older. Minor treatment here refers to treatment with a medical fee of less than the 75th percentile of the fees for visits in primary clinics. The above criteria for selecting study subjects were to avoid including subjects from outside the study area. All the medical visits for each subject during the follow-up period were retrieved. An encrypted identifier for each subject was used to link the mortality registry to obtain the survival status of the subject during the follow-up. A subject's survival time was calculated as the period from the start date of follow-up to the death date if deceased; otherwise, to the date of her/his last medical visit, and treated as censored. The elderly people are presumably less likely to have moved away during the follow-up. But to ensure that the selected subjects in a study area were actually those who had been continuously exposed to the PM_{2.5} levels of the study area, we further excluded the identified subjects in an area during 1998 – 2000 who may not have really lived in the study area for a long time by retaining only the subjects who had visits to health facilities located within 10 km of the area center at least once in the last 3 years if she/he survived by the end of follow-up. For subjects who died during the follow-up, we retained subjects who had visits at local health facilities at least once in the last 3 years before death.

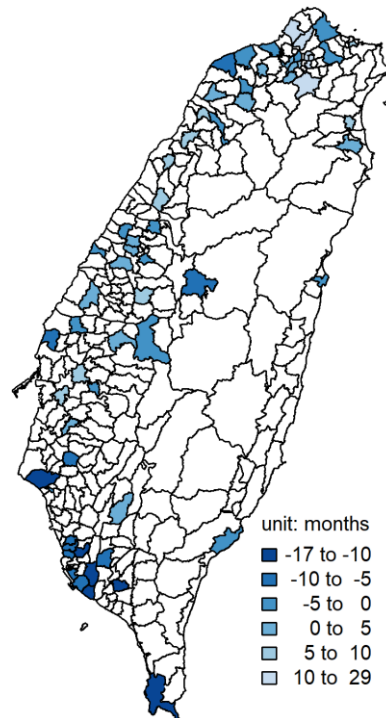


Figure 1. Map of the selected 64 study areas of city district and township in Taiwan. The area color in the map denotes estimated standardized life expectancy deviation for the study cohorts.

2.3. Standardized life expectancy deviation

In estimating the LE and SLED of a study cohort, we need to estimate the lifetime survival function of the cohort. With the survival data of a cohort, we can obtain an estimate of the survival function of the cohort, denoted by $S(t|\text{cohort})$, for time t up to the maximum follow-up. However, even though the study subjects aged 60+ had been followed for 13 years, a high proportion of the subjects had moved away or were alive by the end of follow-up. When the censoring rate is high, the commonly used parametric models may produce inaccurate long-term extrapolation of the survival curve of the cohort (Jackerson, 2017). In this study, we proposed to modify the rolling extrapolation method, which has been shown to be more accurate and robust than the popular parametric models in estimating the lifetime survival function of a cohort of patients with specific conditions (Hwang et al., 2017; Wu et al., 2018; Huang et al., 2019).

2.4. Survival extrapolation method

We describe briefly the rolling extrapolation algorithm proposed by Hwang et al. (2017) for estimating LE and SLED in the following four steps. First, we generated the survival function of a population of referents whose sex, age and start date of follow-up matched with the study subjects, denoted as $S(t|\text{general})$. If the survival function $S(t|\text{general})$ is larger than $S(t|\text{cohort})$, we call the generated general reference population a healthy reference population and set $S(t|\text{healthy}) = S(t|\text{general})$. Otherwise, we modify the generation procedures to simulate another set of survival times to obtain the survival function $S(t|\text{healthy})$.

Second, we define relative survival between the study cohort and the healthy reference population, denoted as $W(t) = S(t|\text{cohort})/S(t|\text{healthy})$. Instead of extrapolating $W(t)$ for estimating $S(t|\text{cohort})$ beyond the maximum follow-up, we extrapolate $\text{logit}[W(t)]$. The logit transformed

function would be approximately linear after some time of follow-up under some reasonable assumptions (Hwang et al., 2017).

Third, we take advantage of the approximate linearity property of $\text{logit}[W(t)]$ which is relatively easily modelled with a smooth function and extrapolated to the adjacent time point. Specifically, the best fitted restricted cubic splines model to the $\text{logit}[W(t)]$ during the observed period is used to extrapolate the curve one time point ahead. We treat the newly predicted value of $\text{logit}[W(t)]$ at the neighbouring time point as “observed” because such short-term prediction is often very accurate with the property of approximate linearity. We then roll the extrapolation procedures by updating the observation periods of same length one time point ahead and refitting the restricted cubic splines models for the updated observation periods to predict the value of $\text{logit}[W(t)]$ at the successive time point.

Fourth, when the $\text{logit}[W(t)]$ is completely extrapolated, we can back-transform it to obtain the complete $W(t)$ function, which is used with $S(t|\text{healthy})$ to calculate an estimate of the lifetime survival function $S(t|\text{cohort})$ of the study cohort. The life expectancies of the cohort LE_{cohort} and the matched general reference population LE_{general} are estimated by integrating extrapolated $S(t|\text{cohort})$ and $S(t|\text{general})$, respectively. The standard errors and 95% CIs of estimates of LE and SLED = $LE_{\text{cohort}} - LE_{\text{general}}$ can be obtained using bootstrap methods (Hwang et al., 2017). An R package “iSQoL2” is available for estimating LE and SLED (<http://sites.stat.sinica.edu.tw/isqol>).

2.5. Survival-weighted exposure

With the extrapolated survival function of a study cohort, we proposed using survival-weighted exposure to represent mean lifetime exposure levels of air pollution for the cohort in a study area. The expected lifetime cumulative exposure of the cohort can be presented by $\int_0^{\infty} S(t) \times C(t) dt$, where $S(t)$ is the extrapolated survival function of the cohort and $C(t)$ is the function of average concentration level of air pollution in the study area (Hwang and Wang, 1999, 2004). Hence, the expected lifetime exposure of the cohort can be presented by the survival-weighted exposure (SWE),

$$\text{SWE} = \int_0^{\infty} S(t) \times C(t) dt / \int_0^{\infty} S(t) dt = \int_0^{\infty} P(t) \times C(t) dt,$$

where $P(t) = S(t) / \int_0^{\infty} S(t) dt$ is a weight function.

2.6. Statistical analysis

Let Y_i and s_i be the estimate of standardized life expectancy deviation and standard error of the estimate for the i th study cohort. Denote SWE_i as the survival-weighted exposure to $\text{PM}_{2.5}$ for the cohort. The stepwise regression model is written as

$$Y_i = \beta_0 + \beta_1 \text{SWE}_i + \sum_{j=1}^p \gamma_j X_{ji} + \varepsilon_i,$$

where $\varepsilon_i \sim N(0, s_i^2 \sigma^2)$. We conducted standard stepwise selection procedures to identify influential covariates X_{ji} from the socioeconomic and area characteristic variables including population density, proportion of elderly population age 60+ during 1996 – 2000, death rates of cancers (ICD9:140-208) and chronic obstructive pulmonary disease (COPD; ICD9:490-493) of the elderly population in 1996 – 2000, gross consolidated income, insured payroll-related amount, proportion of agricultural workers, proportion of college graduates among those aged 15+, hospital beds per 1000 people, and annual 95th percentile of daily maximum wind speed of a study area.

3. Results

We summarize characteristic variables of the 64 study areas and cohorts in Table 1. The study areas had a median size of 45 km² and ranged from 2 km² to 247 km². The study areas covered a wide range of population density from the most densely populated city district of 26,562 people per km² in Taipei City to rural townships of 200 people per km². The median population density of the study areas was 2147 people/km². The largest study cohort consisted of 60,096 people, while the smallest cohort had 1116 people, and the median was 13,885 people. The average ages at beginning of follow-up ranged between 68.9 – 70.7 years old. Proportions of females were as low as 43% and as high as 61%.

Table 1. Summary characteristics of the 64 study cohorts and areas

Variable	Min	25%	50%	75%	Max
<i>Variable related to study cohort</i>					
Cohort size (people)	1116	8309	13885	22688	60096
Age at start date (years old)	68.9	69.6	69.9	70.2	70.7
Female of the cohort (%)	42.8	51.6	54.0	56.2	60.8
Insured payroll-related amount (in NT\$1000)	14.5	18.3	19.3	20.0	21.7
Censoring rate (%)	33.1	39.8	41.3	44.0	48.1
LE (year)	13.6	14.7	15.4	15.7	17.3
SLED (year)	-1.41	-0.41	-0.03	0.40	2.36
<i>Characteristic variable related to study area</i>					
Area size (km ²)	1.9	29.3	45.1	70.8	247.2
Population density (people/km ²) ^a	199	998	2147	5856	26562
Age 60+ (%) ^b	0.05	0.09	0.12	0.13	0.19
Agricultural workers (%) ^a	0.03	0.20	0.76	2.01	24.52
College graduates among age 15+ (%) ^c	10.3	17.0	21.4	24.7	49.6
Gross Consolidated Income (in NT\$1000) ^c	261	732	784	872	1672
Death from cancers among age 60+ (%) ^b	0.61	0.71	0.77	0.83	1.20
Death from COPD among age 60+ (%) ^b	0.03	0.05	0.06	0.08	0.15
Hospital beds (no. per 1000 people) ^c	0.0	2.0	6.3	10.6	43.2
Maximum wind speed (m/sec)	3.9	5.1	5.7	7.3	14.7
Survival-weighted exposure of PM _{2.5} (µg/m ³)	11.9	23.0	26.4	33.0	39.5

The data used for analysis come from different periods: ^a2010, ^b1996-2000, ^c2013.

To gain some insights into how the proposed survival extrapolation method worked, in Figure 2 we give plots of extrapolated logit[$W(t)$] curve, extrapolated survival curve and standardized life expectancy deviation for a cohort. The logit[$W(t)$] curve was approximately linear before the end of the maximum follow-up of 156 months and beyond. The estimate of LE was 13.8 (SE = 0.23) years and the SLED estimate was -1.4 (0.24) years for the cohort. Summarized in Table 1, the life expectancies of the 64 study cohorts of subjects age 60+ had a median of 15.4 years and ranged between 13.6 years and 17.3 years. The standardized life expectancy deviations were estimated with a median of -0.03 years and a range of -1.41 years to 2.36 years.

The hourly PM_{2.5} concentrations during 2006 – 2017 are available for the 64 study areas from the data service of TAQMN, while PM₁₀ are available long before year 2006. We aggregated the measurements to obtain monthly mean concentrations of PM_{2.5} during 2006 – 2017 and PM₁₀ during 2001 – 2017 for each study area. We used the fitted linear model of measured monthly levels of PM_{2.5} regressed against PM₁₀ during 2006 – 2017 to estimate monthly mean levels of PM_{2.5} from 2001 to 2005 for each study area, respectively. We then used a fitted ARIMA time series model to the monthly mean levels of PM_{2.5}

during 2006 – 2017 to predict the monthly mean levels beyond 2017 for each study area. Since there was a clear downward trend of PM_{2.5} air pollution in Taiwan, the model-predicted monthly mean levels were decreasing in all 64 areas. We set a lower bound of 10 µg/m³ annual level for the predicted monthly levels in an area if the area's annual mean concentration in 2017 is larger than 10 µg/m³; otherwise the lower bound was given by the annual mean concentration of the area in 2017. As an example, Figure 3 shows the estimated monthly average concentrations of PM_{2.5} and estimated survival function of the Linyuan township. The area under the product of the two functions shown in Figure 3 is the estimate of expected lifetime cumulative exposure of the township. With the monthly mean levels of PM_{2.5} and survival rates, we obtained estimates of SWE of PM_{2.5} which extended from 11.9 µg/m³ to 39.5 µg/m³ and had a median of 26.4 µg/m³ among the 64 study cohorts.

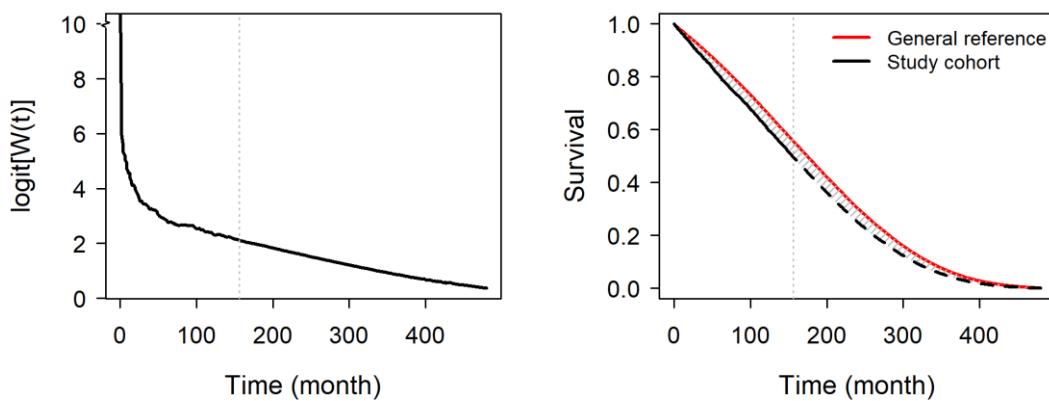


Figure 2. Extrapolated logit[W(t)] curve and survival function for the Linyuan township.

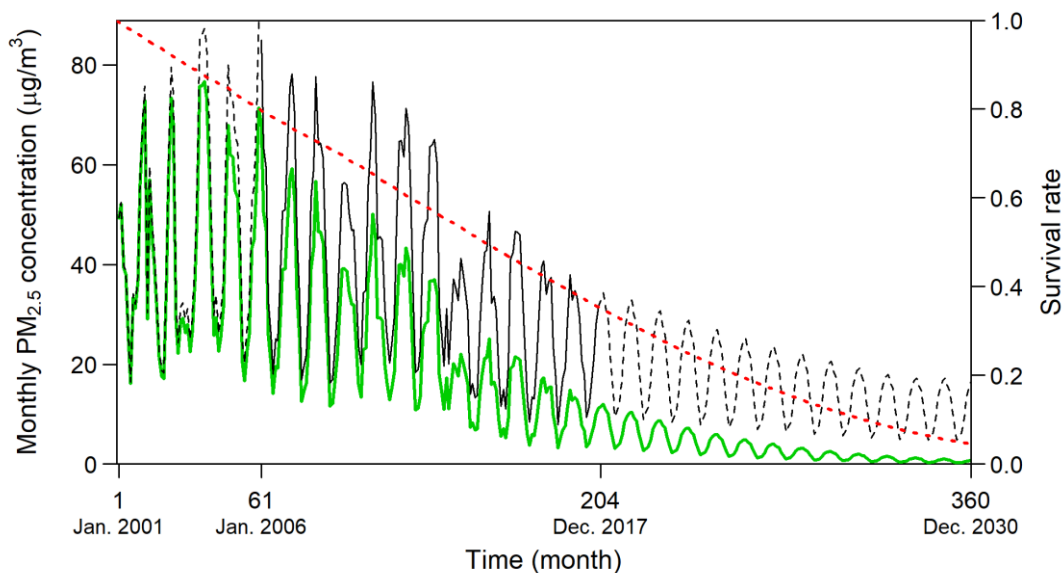


Figure 3. The estimated monthly PM_{2.5} concentrations and survival rates (red) for the Linyuan township. The bottom curve (green) is the product of the above two curves.

Figure 4 shows standardized life expectancy deviations plotted against survival-weighted exposure levels of PM_{2.5} among the 64 study cohorts. The simple regression model of SLED against SWE gave

the slope an estimate of -0.475, which indicates that life expectancies and PM_{2.5} exposures were negatively associated. But the plot also shows clear clustering for study areas in the northern, southern and eastern areas of Taiwan. The association between SLED and SWE was further estimated with adjustment of influential covariates through the stepwise regression model. Table 2 summarizes estimated regression coefficients for the association between the PM_{2.5} levels and life expectancies and for the effects of five selected covariates. When the effects of available influential socioeconomic and demographic covariates were controlled, the coefficient estimate of SWE was adjusted from -0.475 to -0.388. For comparison with previous studies, we report that a 10 µg/m³ increase in PM_{2.5} was significantly associated with an estimated mean loss of life expectancy of 3.88 months (SE = 0.67 months) or 0.32 (0.05) years for the elderly population of age 60 and older.

Table 2. Results of stepwise regression model with response variable of SLED (in months)

Variable	Estimate	S.E.	P-value
Insured payroll-related amount (log scale)	22.59	6.59	0.0023
Proportion of college graduates among 15+	62.97	7.85	0.0000
Proportion of age 60+	72.61	19.88	0.0006
Proportion of death from cancers among 60+	-1395	654	0.0372
Proportion of death from COPD among 60+	-9559	2761	0.0010
Survival-weighted exposure of PM _{2.5}	-0.39	0.07	0.0000

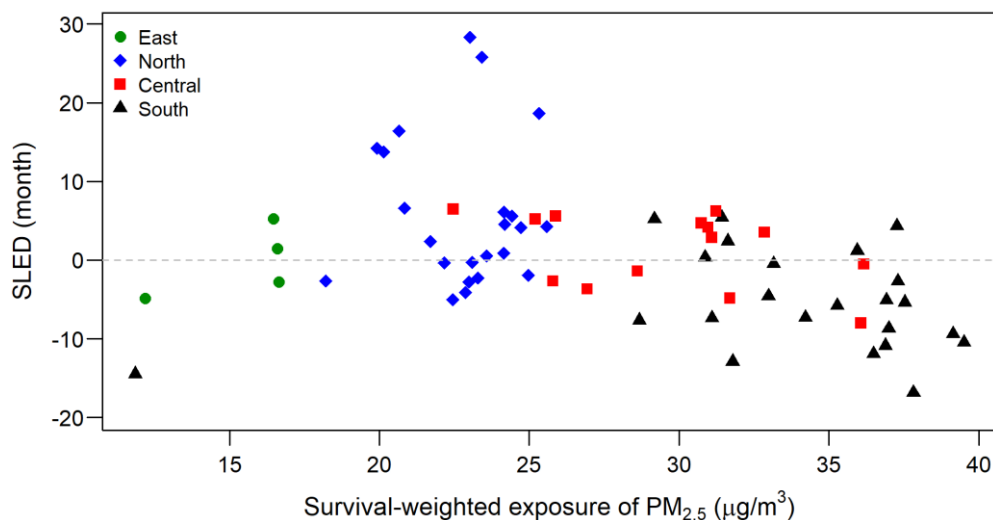


Figure 4. Standardized life expectancy deviations plotted versus survival-weighted exposure of PM_{2.5} levels for the cohorts in the 64 study areas which are marked with four different shapes to indicate cohorts located in eastern, northern, central and southern Taiwan.

4. Discussion

The comprehensive claims data of NHI and a wide range of PM_{2.5} levels during the past two decades in Taiwan provided us a great opportunity to propose a new study design and analytical approaches for examining the association between long-term exposure to PM_{2.5} and life expectancy. Although the association estimate in the model of SLED against the single variable of PM_{2.5} exposure was significant,

the adjusted R^2 was only 0.17. The stepwise regression model increased the adjusted R^2 to 0.79, indicating that the association estimate of $PM_{2.5}$ exposure was well adjusted by the five selected covariates shown in Table 2. We found that socioeconomic variables of college graduates among age 15+ in a study area and insured payroll-related amount of a cohort were positively associated with SLED of the cohort very significantly. Table 2 also shows that the higher the proportion of people aged 60+ during 1996 – 2000 in a study area, the more the life added to the cohort in the area since starting follow-up of January 1, 2001. In contrast, the more deaths there were from COPD or cancers of people aged 60+ during 1996 – 2000 in a study area, the more the life deducted from the cohort in the area. The residuals plot of the final model shows the original location clustering has disappeared, which indicates the confounding effects have been removed.

Even though the study cohorts of people aged 60+ were followed for 13 years, the censoring rates ranged between 33.1% – 48.1%, mainly due to moving away and loss of follow-up (Table 1). The accuracy of extrapolation of the survival function to end of life is critical for estimating LE. The popular approach of using a best fitted parametric survival model for long-term extrapolation may result in seriously biased estimates (Jackson et al., 2017; Hwang et al., 2017). The rolling extrapolation algorithm has been shown to be more accurate and robust in long-term survival extrapolation (Hwang et al., 2017).

Our analysis provides another solid piece of evidence that long-term exposure to $PM_{2.5}$ is significantly associated with loss of life expectancy, consistent with the findings of previous studies modelling differences in life expectancy against differences in PM exposure in either time or space (Pope et al. 2009; Correia et al., 2013; Wang et al., 2013; Ebenstein et al., 2017). Our result of a decrease of $10 \mu\text{g}/\text{m}^3$ in $PM_{2.5}$ was associated with an increase in mean life expectancy of 0.32 (0.05) years, which was close to the 0.35 (0.16) years from an analysis of 545 U.S. counties for the period from 2000 to 2007 (Correia et al., 2013). But our results were obtained from the elderly population aged 60+ with long-term exposure to a median $PM_{2.5}$ concentration of $26.4 \mu\text{g}/\text{m}^3$, while the U.S. study reported the impact of reduction of $PM_{2.5}$ with lower mean concentration of $13.2 \mu\text{g}/\text{m}^3$ in 2000 to a mean of $11.6 \mu\text{g}/\text{m}^3$ in 2007 on difference in life expectancy at birth of the overall population between the two years.

5. References

Beelen R, Raaschou-Nielsen O, Stafoggia M, et al. 2014. Effects of long-term exposure to air pollution on natural-cause mortality: An analysis of 22 European cohorts within the multicentre ESCAPE project. *Lancet*. 383, 785–95.

Brustugun OT, Moller B, Helland A 2014. Years of life lost as a measure of cancer burden on a national level. *Brit J Cancer*. 111, 1014–1120.

Burnett RT, Pope CA III, Ezzati M, Olives C, Lim SS, Mehta S, Shin HH, Singh G, Hubbell B, Brauer M, Anderson HR, Smith KR, Balmes JR, Bruce NG, Kan H, Laden F, Prüss-Ustün A, Turner MC, Gapstur SM, Diver WR, Cohen A 2014. An integrated risk function for estimating the global burden of disease attributable to ambient fine particulate matter exposure. *Environ Health Perspect*. 122, 397–403.

India State-Level Disease Burden Initiative Air Pollution Collaborators 2017. The impact of air pollution on deaths, disease burden, and life expectancy across the states of India: The Global Burden of Disease Study. *Lancet Planet Health*. 2018.

Correia AW, Pope CA III, Dockery DW, Wang Y, Ezzati M, Dominici F 2013. Effect of air pollution control on life expectancy in the United States: An analysis of 545 U.S. counties for the period from 2000 to 2007. *Epidemiology*. 24, 23–31.



- Dockery DW, Pope CA III, Xu X, Spengler JD, Ware JH, Fay ME, Ferris BG, Speizer FE 1993. An association between air pollution and mortality in six US cities. *New England J of Medicine*. 329, 1753-1759.
- Ebenstein A, Fan M, Greenstone M, He G, Zhou M 2017. New evidence on the impact of sustained exposure to air pollution on life expectancy from China's Huai River Policy. *PNAS*. 114,10384-10389.
- He T, Yang Z, Liu T, et al. 2016. Ambient air pollution and years of life lost in Ningbo, China. *Scientific Reports* 6. Article number: 22485.
- Huang CC, Lin CN, Chung CH, Hwang JS, Tsai ST, Wang JD 2019. Cost-effectiveness analysis of oral cancer screening in Taiwan. *Oral Oncology*. 89, 59-65.
- Hwang JS, Hu TH, Lee LJH, Wang JD 2017. Estimating lifetime medical costs from censored claims data. *Health Economics*. 26, e332–e344.
- Hwang JS, Wang JD 1999. Monte Carlo estimation of expected quality-adjusted survival for follow-up studies. *Statistics in Medicine*. 18, 1627-1640.
- Hwang JS, Wang JD 2004. Integrating health profile with survival for quality of life assessment. *Quality of Life Research*. 13, 1-10.
- Jackson, CJ, Stevens, J, Ren, S, Latimer N, Bojke L, Manca A, Sharples L 2017. Extrapolating survival from randomised trials using external data: a review of methods. *Medical Decision Making*. 37, 377-390.
- Jerrett M, Burnett RT, Pope CA III, Ito K, Thurston G, Krewski D, Shi Y, Calle E, Thun M 2009. Long-term ozone exposure and mortality. *New England J of Medicine*. 360, 1085–1095.
- Krewski D, Jerrett M, Burnett RT, Ma R, Hughes E, Shi Y, et al. 2009. Extended Follow-Up and Spatial Analysis of the American Cancer Society Study Linking Particulate Air Pollution and Mortality. HEI Research Report 140. Boston, MA: Health Effects Institute.
- Pope CA III, Ezzati M, Dockery DW 2009. Fine-particulate air pollution and life expectancy in the United States. *New England J of Medicine*. 360, 376–386.
- Pope CA III, Thun MJ, Namboodri MM, Dockery DW, Evans JS, Speizer FE, Heath CW 1995. Particulate air pollution as a predictor of mortality in a prospective study of US adults. *Amer. J. of Resp. Critical Care Med*. 151, 669-674.
- Rabl A 2003. Interpretation of air pollution mortality: number of deaths or years of life lost? *Journal of the Air & Waste Management Association*. 53, 41-50.
- Sandstrom T, Frew AJ, Svartengren M, Viegi G 2003. The need for a focus on air pollution research in the elderly, *Eur Respir J* . 21, 92S-95S.
- Wang C, Zhou X, Chen R, Duan X, Kuang X, Kan H 2013. Estimation of the effects of ambient air pollution on life expectancy of urban residents in China. *Atmospheric Environment*. 80, 347-351.
- Wen M, Gu D 2012. Air pollution shortens life expectancy and health expectancy for older adults: the case of China. *The Journals of Gerontology: Series A*. 67, 1219–1229.



18th World Clean Air Congress, 23-27 September 2019, Istanbul
organized by TUNCAP and IUAPPA

Wu TY, Chung CH, Lin CN, Hwang JS and Wand JD 2018. Lifetime risks, loss of life expectancy, and healthcare expenditures of 19 cancers in Taiwan. *Clinical Epidemiology*. 10, 581-591.

Acknowledgement

This study is supported by the Sustainability Science Research Program, Academia Sinica AS-SS-107-01.



Near-real time low-cost PM source apportionment using microscopic chemical imaging

Alan W. Gertler¹ and Danny Moshe²

¹Desert Research Institute, 2215 Raggio Parkway, Reno, Nevada, United States 89512

²GreenVision Systems, Ltd., 27 Habarzel St., Tel Aviv, Israel, 6971039

Alan.Gertler@dri.edu

Abstract. Elevated levels of particulate matter (PM) are a major cause of human mortality, with the greatest impacts occurring in the Eastern Mediterranean, South-East Asian, and Western Pacific regions. An important approach to address this issue is the use of PM source apportionment to develop, implement, and assess air quality improvement programs. However, there are a number of barriers limiting the routine application of source apportionment methods. These include: cost, the need for specialized laboratory facilities, and the time delay between sampling and reporting the source contributions. The first two barriers are especially problematic in low- and medium-income countries (LMICs), where budgets are lower and specialized laboratories with highly trained staff are not as common.

One potential solution for overcoming these barriers is the use of microscopic chemical imaging (MCI) for PM source apportionment. The MCI technology uses the fluorescence of individual particles collected on a Teflon substrate to identify the PM sources. Since this is a fluorescence-based approach that does not require further laboratory or data analyses, source contributions can be determined in near-real time and at a much lower cost.

To demonstrate the applicability of the MCI technology under a range of conditions and programmatic needs, a description of the method and its validation via comparison with the Chemical Mass Balance receptor modeling approach is presented, along with the results of three case studies. Issues addressed in the studies included quantifying fugitive emissions from a coal power plant (Hadera, northern Israel), monitoring with high temporal resolution in a polluted megacity (Shanghai), and assessing the contributions from both diesel- and gasoline-fueled motor vehicles (Tel Aviv). Based on the results of these studies, use of MCI could enable the routine application of source apportionment monitoring to aid with air quality management programs and improve our understanding of the health impacts of PM.

Keywords: PM, Source apportionment, Urban air quality, Ambient monitoring, Near-real time assessment, Particle fluorescence.

1. Introduction

The health impact of particulate matter (PM) is one of the major environmental threats we face today. The World Health Organization (WHO) reported that one-in-nine deaths worldwide in 2012 could be attributed to air pollution (WHO, 2016), with most of these deaths due to exposure to fine particulate matter (PM_{2.5}). Of the total burden, 3 million deaths were linked to ambient exposure, with the highest risk occurring in the Eastern Mediterranean, South-East Asian, and Western Pacific regions. Compounding this risk factor is these regions represent a large fraction of the world's population and include numerous mega-cities in China, Egypt, and India.

One of the key tools for determining and implementing strategies to reduce ambient PM levels is the application of source apportionment methods to determine the relative contributions of various sources to the observed PM concentrations. Watson et al. (2002) presented an extensive review of over 500 papers covering a range of source apportionment models (i.e., chemical mass balance, enrichment factor, factor analysis, etc.). They describe seven components that should be implemented in the application of receptor models for improving air quality including: chemically characterizing source emissions and ambient PM samples for major components followed by quantifying the source contributions.

In a similar vein, Viana et al. (2008) reviewed 20 years (1987-2007) of source apportionment papers focused on European measurements. In their review they described the sampling and analytical methods, limitations, and application/importance of the approach in a European context. Among the four research trends they identified was the use of receptor modeling in epidemiological and health studies. They point out that the epidemiological studies linking PM and health effects have used mass concentrations, as opposed to chemical or source data (e.g., the above referenced WHO, 2016 document was based solely on PM₁₀ and PM_{2.5} mass measurements). They go on to state: “during the last decade an increased pressure has emerged to uncover the specific PM constituents responsible for the observed health effects.” Addressing this need would require a significant increase in current PM chemical characterization and source apportionment studies. The development of a low-cost PM source apportionment technology that could be widely deployed would have the potential to provide input to aid with elucidating the impacts of specific emissions sources (e.g., cars, diesel vehicles, power plants, smelters, etc.) on human health.

Johnson et al. (2011) focused on the use of source apportionment techniques in developing countries. The motivation for the report was concern over a lack of source apportionment data in the developing world, especially given the importance of the information for implementing control strategies. They described 14 case studies in 18 cities in developing countries. Overall their report supported the importance and need for source apportionment as an air quality management tool, especially given the trends in rapid urban growth and the climate change co-benefits from controlling energy use and emissions.

A common conclusion of the Watson et al. (2002), Viana et al. (2008), and Johnson et al. (2011) reviews and the numerous references contained in those documents is the need for source apportionment in order to reduce ambient PM levels, improve air quality, and protect human health. Given this pressing need and the potential health benefits world-wide but particularly in developing countries, what are the barriers to more fully implementing source monitoring programs for PM source apportionment? Watson et al. (2002) allude to one of the barriers: cost.

A second barrier is the need for specialized laboratory capabilities for quantifying PM chemical composition with high precision and accuracy. Depending on the chemical species used for the source apportionment, laboratory analyses could include any combination of ion chromatography, automated wet chemical analysis, atomic absorption, x-ray fluorescence, thermal optical reflectance (for organic and elemental carbon), GC/mass spec, etc. While there are many laboratories worldwide capable of performing the analytical tasks, there is often a lack of adequate QA/QC procedures, especially in developing countries.

A third barrier is time. The implementation of traditional source apportionment approaches requires the collection of ambient samples followed by laboratory analyses, modeling, and reporting. The timeline for completion of these tasks could be as short as a few weeks but is generally on the order of months. This long time delay between sample collection and dissemination of the source apportionment results greatly limits the implementation of the technique to aid with controlling source contributions during air pollution episodes.

One potential method for overcoming the barriers of cost, the need for specialized laboratory facilities, and need for more timely information is the use of microscopic chemical imaging (MCI) for PM source apportionment (Gertler et al., 2014). In this paper we present additional method validation data and the results from a number of recent PM source apportionment studies performed using the MCI technique in order to demonstrate the capabilities and potential for implementation of the approach.

2. Description of MCI for PM source apportionment

In a previous paper Gertler et al. (2014) described the MCI technology, application for PM source apportionment, and validation of the method. Briefly, the technique employs chemical imaging coupled with adaptive learning algorithms to identify chemical species that are present on particles collected on either Teflon filters or a continuous roll of Teflon tape. Size segregated samples (e.g., PM_{2.5} or PM₁₀) can be collected for periods ranging between 1 to 24-hours, depending on the required time resolution and ambient loading. The samples are exposed to a UV source and particle-by-particle spectra for the wavelength region of 395-1000 nm are collected using an interferometer-based imaging spectrometer coupled to a fluorescence microscope with UV optics and an interferometer with wavelength accuracy down to 2 nm. Pixel-by-pixel spectral information is collected, along with particle size and morphology data, with quantification of pixels to 0.25 μm (equivalent to a particle of the same size). Typically, 15 to 20% of the particles on a filter are scanned. For the Hadera and Shanghai cases presented later, this was generally in the range of 5,000 to 10,000 particles per filter. For the Tel Aviv case, it was 1,500 to 2,000 particles per filter. The observed spectral (wavelength, peak intensity, and peak width) and morphological data for each particle is automatically compared with source-specific spectral and morphological data contained in the source library and a multi variance regression algorithm is used to identify the PM source of the individual particle. The source contribution estimates are then based upon the sum of the observed fluorescence intensities (i.e., measures of concentration) from the individual particles.

Figure 1 shows examples of spectral source profiles for emissions from the stack of a coal-fired power plant, fugitive emissions from post combustion coal waste piles, soil, diesel vehicle tailpipe, and spark ignition vehicle tailpipe source samples. The source samples were collected as part of previous source apportionment efforts (e.g., Abu-Allaban et al., 2007a) and originally used to develop chemically speciated CMB source profiles. The saved Teflon filters were scanned using the MCI instrument to develop the spectral profiles for use in the MCI source library. It should be noted that these are not “pure spectra” but are spectra representative of either a characteristic mixture of compounds produced during the combustion process or by the crystalline nature of source emissions (generally soils). The result is similar to the chemical fingerprints used in traditional source apportionment studies wherein a specific technology and fuel produces a unique mixture of chemicals emitted (relative concentrations of the various species) in this case the mixture of chemicals emitted yields a unique fluorescence spectrum.

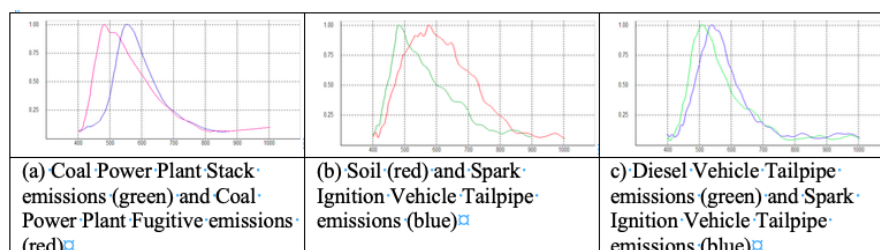


Figure 1. Examples of spectral profiles for selected source samples. Differences in peak maxima and width are used for the characterization of collected ambient particles. The y-axis represents normalized intensity and the x-axis is wavelength (nm)

This approach is similar to the CMB methodology; with the difference being spectral data is used in lieu of chemical speciation and concentration data. Since this is a fluorescence and imaging based approach that does not require any further laboratory or data analyses, source contributions can be determined in near-real time (i.e., within 30 minutes of taking a sample). As seen in these examples, there are marked differences among the spectra from the various sources, which enables source attribution of a collected ambient particle. To test the precision of the identification, repetitive scans were conducted on different sections of the same filter and resulted in source attribution results less than or equal to +/-10%.

One issue with the approach is particles must fluoresce to be linked to a specific source. Thus the method is easily applied to primary particle emissions from combustion sources (due to the presence of PAHs) and geological sources (due to their crystalline structure). Contributions from non-fluorescing particles, such as those from secondary sources (e.g., NH_4NO_3 and $(\text{NH}_4)_2\text{SO}_4$), can be estimated using the morphological data collected during the scanning process by comparing the volume of fluorescing vs. non-fluorescing particles. For the case studies described in the next section, the effort was focused on primary rather than the secondary contributions to the observed PM and so analysis of the non-fluorescing particles was not conducted.

Gertler et al (2014) described the validation of the approach using (1) comparison against saved images to test correct identification and (2) comparison against a more complete CMB analysis of samples collected in Cairo performed by Abu-Allaban et al. (2002). The results for the second comparison are presented in Figure 2 and show a good agreement, with a slope of 0.949 and R^2 of 0.726. Following on from this assessment, additional comparisons (Figure 2) were performed on filters collected as part of studies conducted in Hyderabad (Guttikunda et al., 2012) and Singapore (Gertler et al., 2012). Again, good agreement was obtained for the comparison with a slope of 0.825 and R^2 of 0.871 for the Hyderabad apportionments and 0.991 and 0.931 for the Singapore findings. It should be noted that inherent in this comparison is the assumption that the CMB is the “gold standard” for source apportionment. Different source apportionment methods will yield variations in predicted PM apportionment. Given this variability and uncertainty (likely on the order of 20%), the conclusion of comparability is warranted.

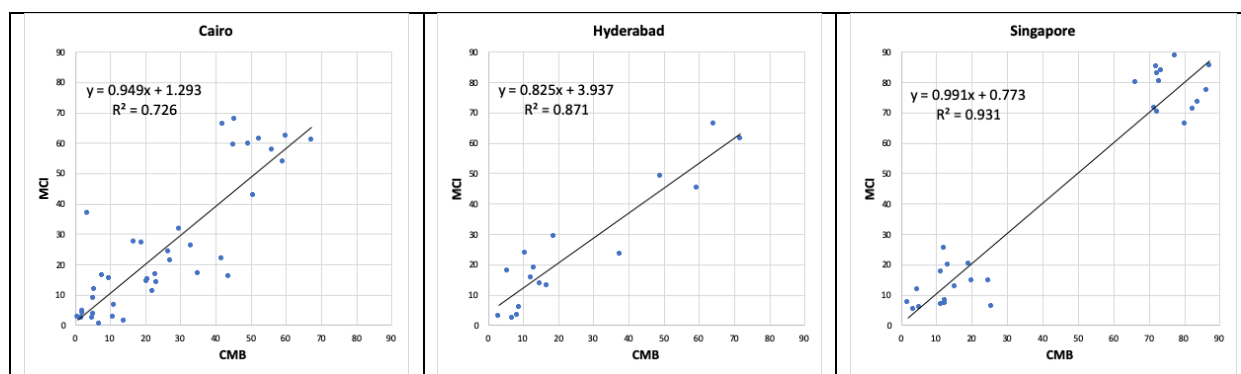


Figure 2. Comparison of source apportionment estimates obtained using the MCI method against those obtained using the CMB. Cairo result is from Gertler et al. (2014)

For either field or laboratory applications, the MCI instrument can be used in either a continuous or batch mode. For the continuous mode, the instrument is deployed at a field location, samples are collected on a continuous Teflon strip, and the source apportionment results are generated automatically on-site within 30 min. of completion of the sampling cycle. For the batch operation, samples are collected on Teflon filters using a standard filter sampling system (e.g., minivol sampler operating at 5 lpm) and shipped to a facility that has an MCI instrument for analysis. The advantage of the batch operation is it requires fewer MCI instruments, thus reducing the cost. The disadvantages are it requires

additional labor for filter collection/shipping and there is a delay in when the source apportionment information becomes available. Based on the current cost of the MCI system and assuming 500 cycles/instrument/year and an 8-year equipment depreciation rate, the cost for each reported source apportionment result would be less than \$80. The cost for the batch mode would be less, since fewer instruments are required. Based on our previous studies in developing countries using the laboratory-based CMB approach (e.g., Abu-Allaban et al., 2007a, Guttikunda et al., 2012, and Lowenthal et al., 2014), this cost is more than a factor of 10 less than this commonly applied laboratory-based source apportionment method.

3. Case studies using MCI for PM source apportionment

Recently the MCI technology for PM source apportionment was applied at a number of diverse locations to test the ability of the technique to assess source contributions under a range of conditions. In this section we describe the results of three recent studies:

- Hadera, Israel: PM₁₀ source apportionment to assess the impact of fugitive emissions on a local community.
- Shanghai: Enhanced temporal PM_{2.5} source apportionment as a proof of concept to evaluate variations in source contributions in a highly polluted environment.
- Tel Aviv, Israel: Monitoring diesel vs. gasoline mobile source PM_{2.5} contributions to aid with implementing and assessing plans to reduce diesel PM emissions.

In the sections that follow we detail the city-specific air quality issues, monitoring efforts, and results.

3.1. Hadera PM₁₀ source apportionment study

The city of Hadera is a major municipality (2016 population 91,707) located north of the Tel Aviv metropolitan region in Israel and east of the 2590 MW coal-fired Orot Rabin power plant. Previous environmental studies have observed elevated levels of pollutants inland from the plant, which are transported as far away as northern Jordan (Asaf et al., 2011). The prevailing winds tend to transport the emissions along an east-west axis and so there is a high likelihood of impact on Hadera and the nearby communities. In mid-2017 the local air quality control district (Eigud Arim Sharon Carmel, EASC) received complaints about fugitive emissions (wind blown particulate matter from the combusted coal waste piles) depositing on the community of Hephziba, which is located a few kilometers due east of the facility. To address the issue of the impact of the power plant on the local area, a PM source apportionment study was conducted to determine the relative contributions of various sources to the observed PM₁₀ concentrations during September/October 2017 (Moshe, 2017).

Samples were collected at two monitoring locations along the east-west axis extending from the power station inland towards Hadera. These included Hephziba, a small community that had voiced concerns about fugitive emissions impacts, and Pardes-Channa, a location further inland with a monitoring station operated by EASC. The sites were chosen to assess the impact of stack emissions from the power station and the change in the relative source contributions from any fugitive emissions. For the Hephziba location, samples were collected on Teflon filters using a minivol sampler fitted with a size-selective PM₁₀ inlet operating at a flow rate of 5 lpm. Samples were collected during the period of August 30 to October 16, 2017. Collection times varied from 12 to 24 hours, with the 12-hour samples ranging from midnight to noon and noon to midnight. The reason for the inconsistencies in sampling times was the restriction on changing filters during the Jewish Sabbath and High Holidays (Rosh Hashanah and Yom Kippur). At Pardes-Channa, samples were collected on a continuous Teflon strip fitted to a PM₁₀ inlet operating at 16.7 lpm. Samples were collected continuously during the period September 13 to October 14 for 12-hour intervals (midnight to noon and noon to midnight). Since the sampling system operated automatically, there was no restriction on the sampling periods and so a continuous record of 12-hour samples was collected at this location.

The source apportionment results (percent mass contributions from the primary emissions sources) for all periods are presented in Figures 2 and 3 for Hephziba and Pardes-Channa, respectively. Table 1 summarizes the average source contributions for the full monitoring periods and for the timeframe when sampling overlapped at the two locations (September 13 – October 3). The largest contribution at both locations was from mobile sources, with the next largest contribution coming from the power station. It is interesting to note that the results are quite similar for all measurement periods versus the overlap period. For the Hephziba monitoring site, located closest to the power plant and adjacent to a major highway, the mobile source contribution was 29.8% and the coal power plant contribution was 29.1%. In addition, the fugitive coal and coal residue emissions from waste piles adjacent to the power plant were estimated to contribute 11.5% to the observed PM₁₀. At the Pardes-Channa site, located further inland and in a more residential area, the mobile source contribution was 38.6%, coal power plant emissions averaged 19.3%, and the fugitive coal and coal residue contribution was 2.7%. Based on these results, we see a significantly greater contribution from fugitive emissions at the Hephziba location (11.5%) versus the Pardes-Channa location (2.7%). This implies a greater impact of fugitive emissions from the power station at the nearby location and supports the need to control fugitive emissions from the plant.

Table 1. Average PM₁₀ source contribution results (% mass by primary emission source) for all measurement periods and the period when samples were simultaneously collected at both locations (September 13 – October 3)

	Coal Power Plant & Industry	Fugitive Coal Emissions	Industry	Mobile Sources	Soil & Road Dust	Biomass, Cooking, Garbage Burning	Port Activities	Unident Sources
Pardes-Channa (all)	19.3	2.7	12.8	38.6	15.5	5.1	0.4	5.5
Pardes-Channa (overlap)	20.5	2.4	14.0	37.4	15.1	6.1	0.5	4.0
Hephziba (all)	29.1	11.5	9.3	29.8	6.5	4.7	1.4	7.7
Hephziba (overlap)	24.5	11.5	11.7	33.4	6.7	3.9	1.2	7.2

Given the number of highways near the monitoring sites, the large contribution from mobile sources at both locations is not surprising. However, what is unusual is the large contribution from the power station (~20%) at the more inland location. Clearly this has a major impact on ambient PM₁₀ both locally and in the region and raises questions regarding the adequacy of the PM emissions control technology at the facility.

One other source to note is the port activities contribution. This is due to emissions from ships delivering coal to the power station. While this is relatively small, 0.4% and 1.4% at Pardes-Channa and Hephziba respectively, it demonstrates the ability of the MCI technique to differentiate between various sources, along with the showing the decreasing contribution from sources along the coast as one moves further inland.

3.2. Shanghai PM_{2.5} source apportionment study

Shanghai is one of the most polluted cities in the world. In the WHO 2016 report, it was ranked as the seventh most polluted megacity, having an average PM_{2.5} level of 52 µg/m³ during the period of 2011-2015. Numerous studies have been conducted in Shanghai to determine the major sources contributing to ambient PM_{2.5}. For example, Wang et al. (2013) used the CMAQ model to assess potential sources and concluded traffic, industrial sources, and resuspended geological material dominated. Lü et al.

(2012) applied an SEM approach to characterize collected particles and found soot particles and fly ash to be the major sources. Wang et al. (2016) assessed the carbonaceous fraction and determined a greater contribution came from mobile sources than coal combustion.

Given the frequency of air pollution events in Shanghai, there is need for near-real-time PM source apportionment in order to implement short-term control strategies to reduce the potential health impacts. Based on this need, the primary objectives of the effort were to demonstrate the feasibility of the near real-time approach for PM_{2.5} source apportionment coupled with enhanced temporal resolution of the attribution results.

Monitoring was conducted at the SEMC (Shanghai Environmental Monitoring Center) site in Pudong. The area is located east of the Huangpu River across from the city center of Shanghai in Puxi and is characterized as a residential/business area. However, there are a number of nearby coal-fired power stations, along with close proximity to the port that could potentially impact the sampling location. Samples were collected on a continuous Teflon filter strip using a medium volume PM_{2.5} size selective inlet during the period of May 5 - 21, 2017. Sampling periods ranged from 4 hours to 12 hours. For the purpose of an initial assessment, the results were aggregated into 24-hour periods.

The 24-hour source apportionment results are presented in Figure 3. The largest source contribution for all but two of the dates was from mobile sources, with an average contribution of 30.7%. The second largest contribution was from industrial sources (non-coal fired) at 19.8%, followed by coal-fired sources at 18.7%. Significant contributions were observed for resuspended soil (9.8%), biomass burning and cooking (8.9%), and port activities (primarily emissions from ships, 5.6%).

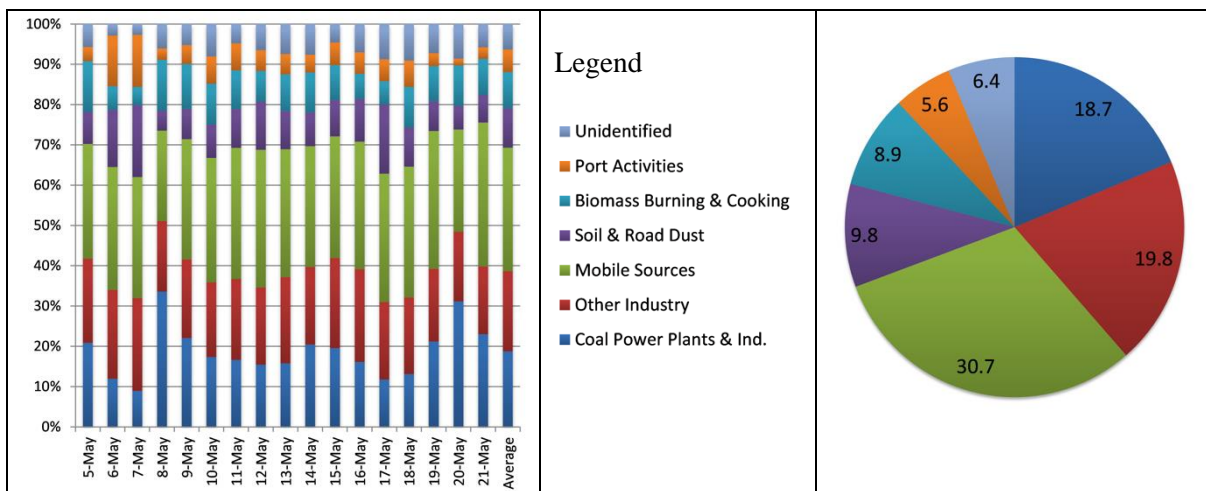


Figure 3. Stacked bar plots and average of 24-hour PM_{2.5} source contributions for Shanghai

These results are consistent with previous studies (Wang et al., 2013, Lu et al., 2012, and Wang et al., 2016), which highlighted the importance of mobile, coal-fired, industrial, and geological sources. What is unusual from this work is the potential impact from biomass burning/cooking and port activities.

Based on these findings, some approaches to improve air quality in Shanghai could include control strategies for biomass burning/cooking and port activities, in addition to existing strategies for mobile sources, coal and industrial sources, and geological sources.

3.3. Tel Aviv diesel vs. gasoline mobile source PM emissions.

Mobile sources are one of the major contributors to elevated levels of PM_{2.5} in urban areas (e.g., EEA, 2017, Abu-Allaban et al., 2007b). Due to their significantly higher PM emission rates, a large fraction of the mobile source contribution comes from the diesel sector (Gertler, 2005). Given the magnitude of

emissions from the diesel fraction of the fleet, there is a need to implement policies to reduce their emissions; however, a key aspect of any reduction strategy is to provide stakeholders and affected groups with sufficient data to justify and support any proposed approaches. Further, following the implementation of any policies it is important to monitor and assess the effectiveness of the approach. Like many urban areas Tel Aviv experiences elevated PM, with much of this attributed to mobile sources. The city is considering reducing the number and activity of diesel vehicles in order to improve air quality. As part of their efforts to develop an air quality improvement strategy, there is need to assess the relative contributions from diesel vs. gasoline vehicles. Due to the colinearity of many of the chemical marker species used in traditional source apportionment approaches, quantifying the diesel vs. gasoline contributions is challenging and often involves the use of additional markers such as PAHs (Chow et al., 2007). Addition of organic marker species increases the analytical complexity and cost of a source apportionment program. Moshe and Gertler (2018) highlighted the ability of the MCI approach to resolve the diesel vs. gasoline contributions using the source profiles shown in Figure 1. Based on that previous work, a demonstration-monitoring program was conducted in Tel Aviv to assess the relative contributions from diesel vs. gasoline motor vehicles.

Monitoring was conducted for a one-week period (August 5-11, 2018) using a continuous MCI system located at the Tel Aviv Municipal Environmental Department site on Dizengoff St., a major thoroughfare and bus route in central Tel Aviv. One unusual aspect of the public transit sector in Israel is buses do not operate in Tel Aviv during the Jewish Sabbath (Shabbat, Friday evening at sundown to Saturday evening at sundown). Thus there are significantly fewer diesel vehicles operating during this time frame; although private diesel-fueled transit vans and trucks continue to function during the period. To capture the change in the fleet mix over Shabbat, 24-hour samples were collected on an evening-to-evening schedule.

For the one-week monitoring study, the average estimated mobile source PM_{2.5} contribution for the weekday period was 57.5% (range of 52.5 to 62.6%), as opposed to 53.2% on Shabbat. During this period, the mobile source sector was the major source of PM_{2.5} on all days. The critical aspect of the effort was the ability to assess changes in the contributions from the gasoline vs. diesel sectors. Figure 4 compares the relative contributions from the different fuel types for the average weekday period vs. the Shabbat period when the municipal buses did not operate. For this limited monitoring study, the average diesel contribution to the total mobile source component during the weekday period was 84.1% (range of 79.5 to 89.4%) vs. 68.1% on Shabbat. The results are similar to those previously observed by Moshe and Gertler (2018) and highlight the potential impact on ambient PM levels of implementing controls on diesel emissions.

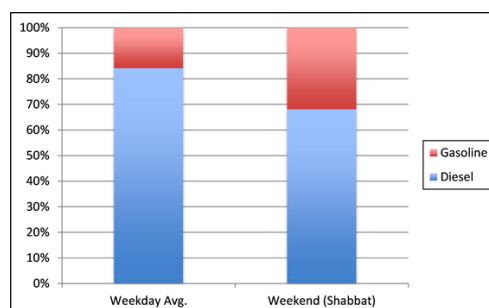


Figure 4. Comparison of mobile source emissions for weekday vs. weekend [on Saturday (Shabbat) buses do not operate]

4. Summary and conclusions

PM source apportionment is an important tool for developing, implementing, and assessing air quality improvement programs that are necessary to protect human health and welfare. The routine implementation of source apportionment monitoring can aid in improving our understanding of the specific sources contributing to the health effects. However, there are a number of barriers limiting our use of source apportionment programs. These include: cost, the need for specialized laboratory facilities, and the time delay between when samples are collected and the source apportionment results are reported. The first two barriers are especially problematic in LMICs, where budgets are lower and specialized laboratories with highly trained staff are not as common. To assess a potential solution to these issues, in this paper we described an individual particle fluorescence-based technique that has the potential to provide source apportionment results in near-real time, does not require specialized laboratory facilities, and costs significantly less per sample than current methods. The range of application of the MCI method was shown via three case studies conducted in Hadera (northern Israel), Shanghai, and Tel Aviv using to monitor and assess PM source contributions.

Major results from the case studies included:

- Hadera: Ability to monitor source contributions automatically in near-real time and over an extended period. Major contributors were mobile sources and a coal-fired power plant. The study confirmed the impact of fugitive emissions on a nearby community and quantified emissions from ships delivering coal to the facility.
- Shanghai: Monitored a large mixture of sources in a highly polluted environment. The largest contributor was mobile sources (30.7%) followed by industrial sources (non-coal fired, 19.8%) and coal-fired sources (18.7%). One unusual result was the finding that biomass burning and cooking contributed 8.9% of the PM.
- Tel Aviv: Primary focus was on diesel vs. gasoline vehicle contributions. The MCI technology was able to differentiate between diesel and gasoline sources. Mobile sources contributed the majority of the PM_{2.5}, with the diesel component being the largest fraction. During the period of reduced municipal transport, the diesel fraction of the mobile source contribution decreased from 84.1 to 68.1%.

Based on these results, the MCI approach enabled the estimation of PM source contributions over a range of conditions and concentrations. Deployment of this methodology could enable the routine application of source apportionment monitoring to aid with air quality management programs and improve our understanding of the health impacts of PM.

5. References

- Abu-Allaban, M., Lowenthal, D.H., Gertler, A.W., Labib, M., 2007a. Sources of PM₁₀ and PM_{2.5} in Cairo. *Environmental Monitoring and Assessment*. 133, 417-425.
- Abu-Allaban, M., Gillies, J.A., Gertler, A.W., Clayton, R., Proffitt, D., 2007b. Motor Vehicle Contributions to Ambient PM₁₀ and PM_{2.5} for Selected Urban Areas in the U.S., *Environmental Monitoring and Assessment*. 132, 155-163.
- Asaf, D., Peleg, M., Alsawair, J., Soleiman, A., Matveev, V., Tas, E., Gertler, A., Luria, M., 2011. Trans-Boundary Transport of Ozone from the Eastern Mediterranean Coast, *Atmos. Environ.* 45, 5595-5601.
- Chow, J.C., Watson, J.G., Lowenthal, D.H., Chen, L.-W.A., Zielinska, B., Mazzoleni, L.R., Magliano, K.L., 2007. Evaluation of Organic Markers for Chemical Mass Balance Source Apportionment at the Fresno Supersite. *Atmospheric Chemistry and Physics*. 7, 1741-2754.
- European Environment Agency, 2017. Air Quality in Europe – 2017 Report. EA Report No 13/2017.



- Gertler, A.W., 2005. Diesel vs. Gasoline Emissions: Does PM from Diesel or Gasoline Vehicles Dominate in the U.S.? *Atmospheric Environment*. 39, 2349-2355.
- Gertler, A.W., Moshe, D., Rudich, Y., 2012. Urban PM source apportionment mapping using microscopic chemical imaging. Presented at Air Quality Management at Urban, Regional and Global Scales, 4th International Symposium and IUAPPA Regional Conference, Istanbul, Turkey, September 10-13, 2012.
- Gertler, A.W., Moshe, D., Rudich, Y., 2014. Urban PM Source Apportionment Mapping Using Microscopic Chemical Imaging, *Sci. Tot. Environ.* 488-489, 456-460.
- Guttikunda, S.K., Kopakka, R.V., Dasari, P., Gertler, A.W., 2012. Receptor Model-Based Source Apportionment of Particulate Pollution in Hyderabad, India, *Environ. Monit. Assess.* 185, 5585-5593.
- Johnson, T.M., Guttikunda, S., Wells, G.J., Artaxo, P., Bond, T.C., Russell, A. G., Watson, J.G., West, J., 2011. Tools for Improving Air Quality Management: A Review of Top-down Source Apportionment Techniques and Their Application in Developing Countries, formal Report 339/11, published by The World Bank Group, Washington, DC, United States, 193 pages.
- Lowenthal, D.H., Gertler, A.W., Labib, M.W., 2014. Particulate Matter Source Apportionment in Cairo: Recent Measurements and Comparison with Previous Studies, *Int. J. Environ. Sci. Technol.* 11, 657-670.
- Lü, S., Zhang, R., Yao, Z., Yi, F., Ren, J., Wu, M., Feng, M., Wang, Q., 2012. Size Distribution of Chemical Elements and Their Source Apportionment in Ambient Coarse, Fine, and Ultrafine Particles in Shanghai Urban Summer Atmosphere. *J. Environ. Sci.* 24(5) 882–890.
- Moshe, D., 2017. On-line Near Real Time PM Source Apportionment of Particulate Matter at Two Eigud Arim Sharon Carmel Air Monitoring Stations. Final report prepared for Eigud Arim Sharon Carmel, Israel, November 2017, 25 pages.
- Moshe, D., Gertler, A.W., 2018. A Novel Approach for Implementing Control Strategies to Reduce the Impact of Traffic Emissions From Roads and Highways. *Proceedings of 7th Transport Research Arena TRA 2018, Vienna, Austria, April 16-19, 2018.*
- Viana, M., Kuhlbusch, T.A.J., Querola, X., Alastueya, A., Harrison, R.M., Hopke, P.K., Winiwarter, W., Vallius, M., Szidat, S., Prévôt, A.S.H., Hueglin, C., Bloemen, H., Wählin, P., Vecchi, R., Miranda, A.I., Kasper-Giebl, A., Maenhaut, W., Hitznerberger, R., 2008. Source Apportionment of Particulate Matter in Europe: A review of Methods and Results. *Aerosol Sci.* 39, 827–849.
- Wang, F., Guo, Z., Lin, T., Rose, N.L., 2016. Seasonal Variation of Carbonaceous Pollutants in PM_{2.5} at an Urban ‘Supersite’ in Shanghai, China. *Chemosphere*. 146, 238 – 244.
- Wang, Y., Li, L., Chen, C., Huang, C., Huang, H., Feng, J., Wang, S., Wang, H., Zhang, G., Zhou, M., Cheng, P., Wu, M., Sheng, G., Fu, J., Hu, Y., Russell, A.G., Wumaer, A., 2013. Source Apportionment of Fine particulate Matter During Autumn Haze Episodes in Shanghai, China. *J. Geophys. Res. Atmos.* 119, 1903–1914.
- Watson, J.G., Zhu, T., Chow, J.C., Engelbrecht, J., Fujita, E.M., Wilson, W.E., 2002. Receptor Modeling Application Framework for Particle Source Apportionment. *Chemosphere*. 49, 1093–1136.
- World Health Organization, 2016. *Ambient Air Pollution: A Global Assessment of Exposure and Burden of Disease*, published by the World Health Organization, Geneva, Switzerland, 131 pages.



18th World Clean Air Congress, 23-27 September 2019, Istanbul
organized by TUNCAP and IUAPPA

Acknowledgements

The authors would like to acknowledge the direct support received from Eigud Arim Sharon Carmel (EASC, Hadera), the Shanghai Environmental Monitoring Center, the Tel Aviv Municipal Environmental Department (TAMED), and the major in-kind contributions from GVS for developing the MCI methodology and performing the field measurements. In addition, we would like to thank Mr. Nir Sahar and Dr. Nurit Shaham-Waldmann of EASC and Dr. Michal Mendelevich (TAMED) for their assistance with the field measurement. Dr. Gertler would also like to thank the Lady Davis Fellowship Foundation at the Hebrew University and the Desert Research Institute for their support of his sabbatical during which many of the field studies reported in this paper were performed.

Analysis of NO₂ and SO₂ in Marmara Region

Seda Nur Suer and Ceyhan Kahya

İstanbul Technical University, Faculty of Aeronautics and Astronautics, Department of Meteorological Engineering, Istanbul, Turkey

suers@itu.edu.tr, ckahya@itu.edu.tr

Abstract. Living creatures must live in a healthy environment in order to lead a healthy life. This situation further increases the importance of air pollution. Air pollution is the amount of pollutants present in the atmosphere to reach the amount that will affect the living and the environment negatively. Air pollution has become a threat to human health and the environment, especially with the industrial revolution. In addition to industrial activities, increasing urbanization has led to an increase in the amount of pollutants released to the atmosphere. Air pollution has many natural and anthropogenic sources such as industry, heating, motor vehicle use. Besides, meteorological conditions such as temperature, humidity and precipitation can be observed. One of the important factors is also known as temperature reversal. As the result of an increase in temperature with an elevation, the pollutant particles on the earth do not distribute and create unhealthy conditions on the region. Nitrogen dioxide, the primary source of motor vehicles, is an indicator of the importance of vehicle emissions. The main source of sulfur dioxide (SO₂) is a gas produced by the combustion of industrial fuels and fuels used for heating purposes. Especially during the winter months, the values increase due to heating. With the increasing population and developing technology, efforts to reduce air pollution have started to increase. In this research, the relationship between NO₂ and SO₂ has been analyzed for Marmara Region. Three stations (Basaksehir, Kandilli and Sultanbeyli) from Istanbul, one station from Tekirdag and one station from Sakarya (Ozanlar) were chosen. For this purpose, NO₂ and SO₂ data measured between December 2012 and December 2018 were analyzed. As a result the healthiest station by means of NO₂ and SO₂ were found to be Kandilli, Istanbul. Especially during winter months, the highest value was found to be 341 µg/m³ in Tekirdag.

Keywords: NO₂, SO₂, Air Pollution, Marmara Region

1. Introduction

Since air is important for the survival of living things and for the continuity of natural processes, air pollution has an important place in living life. Air pollution can be defined as "the presence of pollutants in the atmosphere in concentration and time that will cause harmful effects in human health, plants, structures and materials (Wark and Warner, 1981). Today, increasing population, developments in industrial areas and urbanization, such as factors pollute the air and this situation directly and indirectly affects the human health negatively. While air pollution can occur as a result of natural events such as volcanic eruptions, wildfires, motor vehicle use can also occur for anthropogenic reasons such as fossil fuels consumed for warming purposes. In addition to these resources, it is important to analyze and evaluate the air quality of the pollutants in the environment, whether they are transported to the surrounding areas due to the effect of the duration, intensity, meteorological conditions. It is known that air pollution has negative effects not only on health but also on the environment. In this direction, stations are established and measurements are made so that the emissions of pollutants do not exceed the limit values and can be kept under control. The analysis aims to reduce these pollution values.

2. Study Area

The Marmara region is a region that shows rapid population growth throughout Turkey and industrial activities also increase at the same rate. This region is affected by natural resources such as Saharan transport, as well as air pollution problems due to many anthropogenic sources.

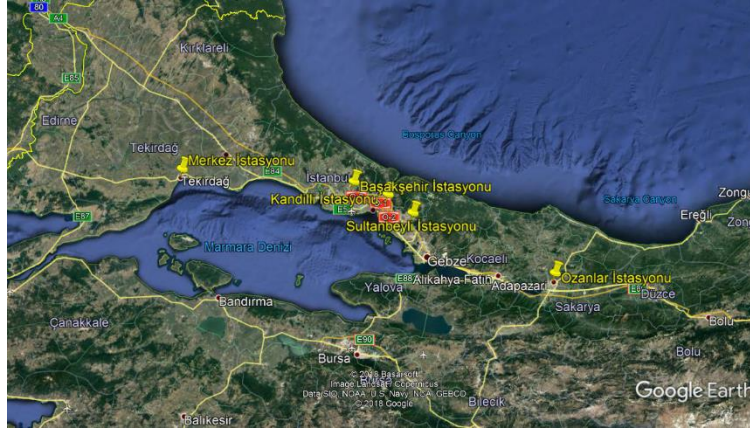


Figure 1. Analyzed stations of Marmara region

3. Data and Methodology

The developing industry and technology in the Marmara region has prepared the ground for population growth. The increase in air pollution has been observed in this region due to fuel consumption for heating, increase in motor vehicle use, fabrication and urbanization. The aim of this study is to compare the values of NO₂ and SO₂ in the Marmara region and evaluate them together with the sources they cause. In this study, the data of Basakşehir, Kandilli and Sultanbeyli stations in Istanbul Province, Ozanlar station in Sakarya province and Central Station in Tekirdag province were obtained from Air Quality Monitoring Stations conducted by the Ministry of Environment and Urban Planning. The December 2012 to December 2018 data from these stations cover the dates between December 2012 and December 2018. The data were downloaded daily and grouped seasonally and analyzed. The missing data is completed and arranged, and time series charts are drawn. In addition, the stations which were showed extreme increases are emphasized in this research as opposed to the stations that obtained results as expected.

4. Analysis

4.1. Balıkesir

Basakşehir is one of two organized industrial zones in Istanbul and is also affected by pollution emission due to the activities of Ikitelli Organized Industrial Zone. The air quality measurement station established here is an industrial type measurement station. There is no significant increase or decrease of NO₂ and SO₂ values in the 5-year period. The spring term average of NO₂ data is 38.68 µg/m³, SO₂ data is 9,06 µg/m³.

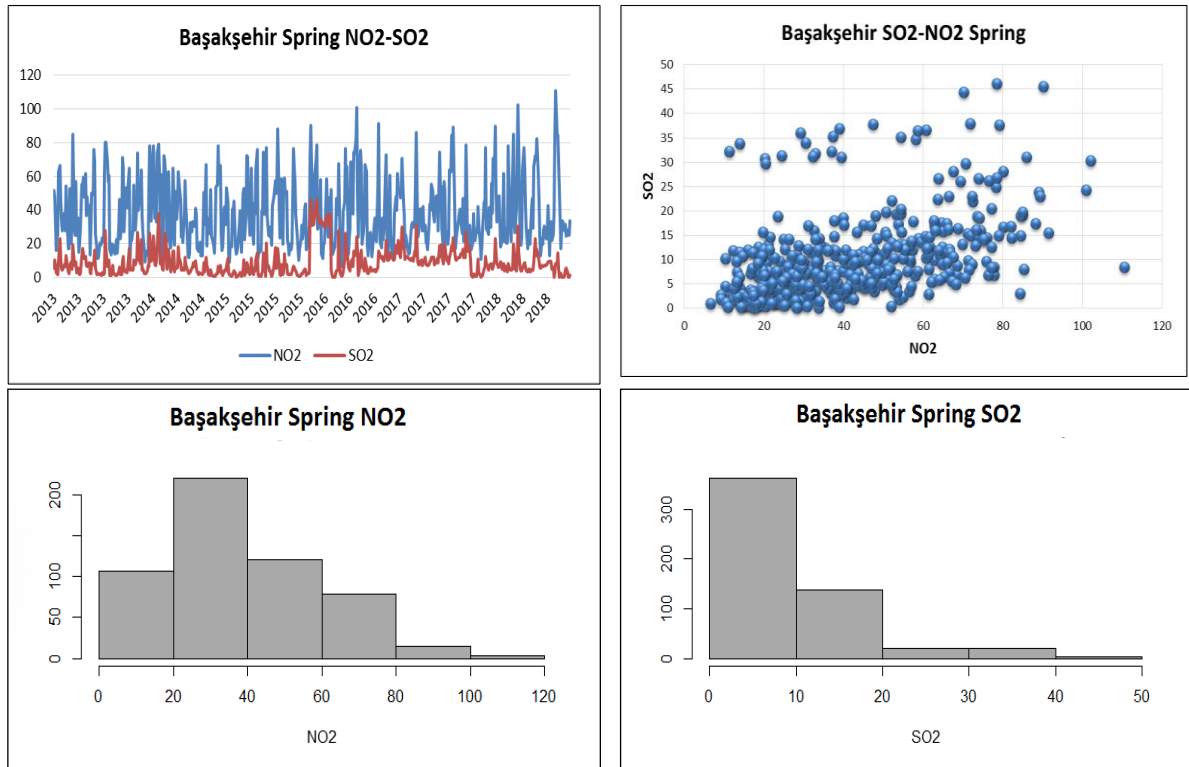


Figure 2. 2013-2018 Basaksehir Spring NO₂ & SO₂ Time Series and Histogram

The average 5-year NO₂ data was 22.43 µg/m³. The SO₂ data shows above-average increases, particularly from 2015. The Air Quality Assessment and management regulation of SO₂ defines an average of 20 µg/m³ per year for the ecosystem and a daily limit of 175 µg/m³ and 410 µg/m³ per hour for the protection of human health. None of the data in the chart exceeds these values, but the population of Basaksehir district has increased by about 100,000 thousand as of 2015. This sudden increase caused the warming and industrial activities of the region to increase as well. This increase has also increased SO₂ emissions far above average in 2018. As a result of these activities, the Ministry of Environment and Urban Planning and TOKI decided to make preparations to move the industrial sites for vented industry and production located in Basaksehir out of the city and as a result of this decision, the values began to decrease again towards their average levels.

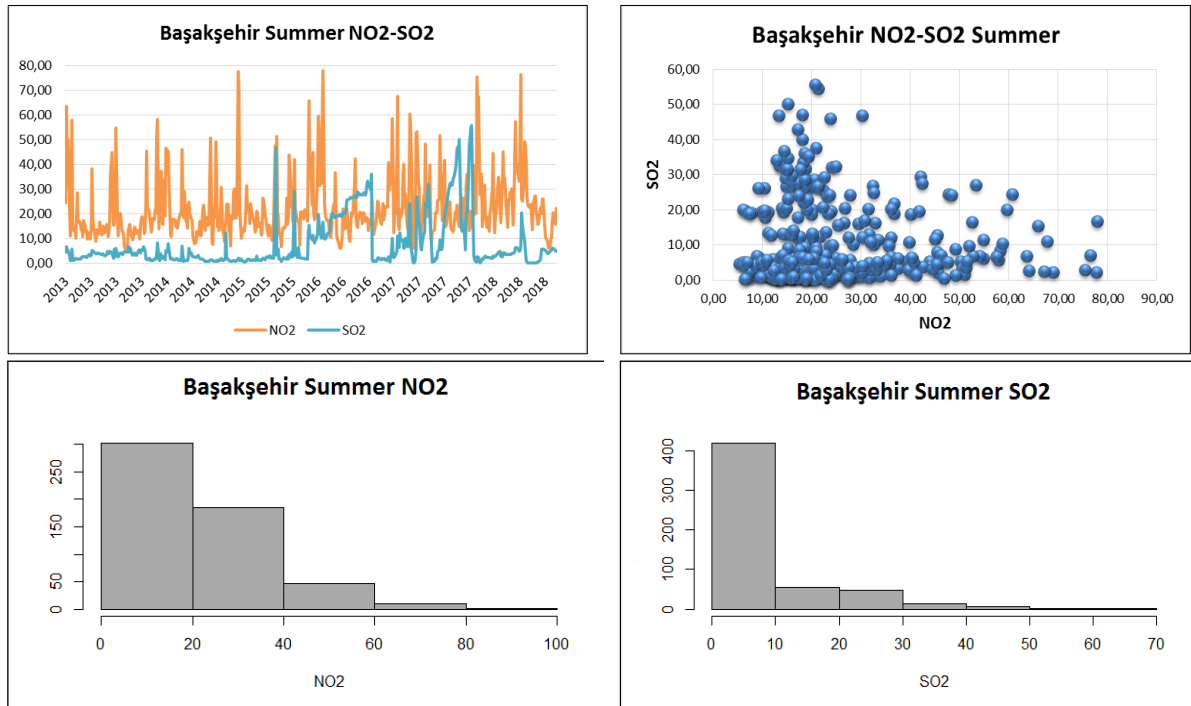


Figure 3. 2013-2018 Basakşehir Summer NO₂ & SO₂ Time Series and Histogram

The average of NO₂ data was calculated at 36.26 $\mu\text{g}/\text{m}^3$. Especially after 2015, there is an increase in SO₂ values at the beginning of the autumn months. The average of the data was calculated as 6.39 $\mu\text{g}/\text{m}^3$. The reason for the increase in values is that meteorological conditions are slowly starting to return to winter conditions, and this situation is starting to re-consume fossil fuels for warming.

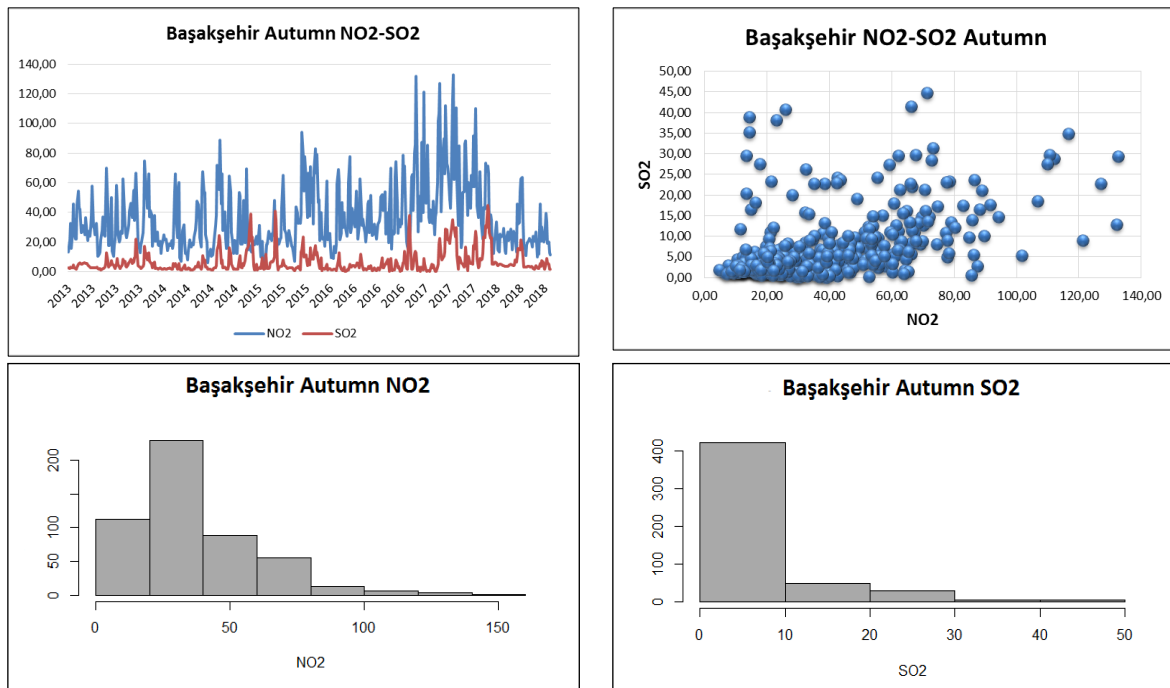


Figure 4. 2013-2018 Basakşehir Autumn NO₂ & SO₂ Time Series and Histogram

The average of NO₂ and SO₂ data were calculated as 33.45 µg/m³ and 10.79 µg/m³. A significant increase or decrease was not observed.

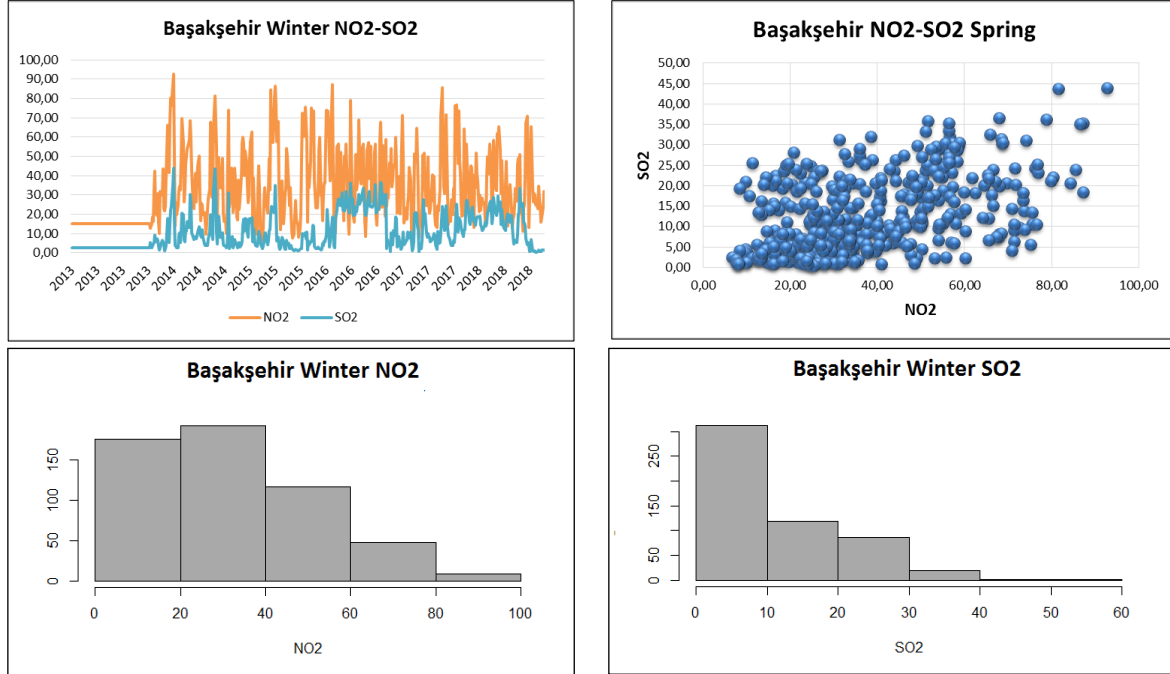


Figure 5. 2013-2018 Basakşehir Winter NO₂ & SO₂ Time Series and Histogram

4.2. Kandilli

Kandilli is a district of Üsküdar, Istanbul Province, and as population increases in Üsküdar, density increases in the old settlements located in the coastal area, while settlements spread inland. Since the main cause of air pollution in this region is settlements, the type of station established here is the traffic type station. A decrease in NO₂ values is seen in 2017. Since there is no news that will affect this decrease in the news calls made, it can be interpreted that vehicle usage may be decreased due to short-time population decrease in the area where the station is located. The 5-year average of NO₂ data is 46.16 µg/m³. A value of 89.01 µg/m³ was observed in the time series on March 12, 2016. When an investigation was conducted for this date, which had a maximum value of 5 years, it was concluded that a large amount of fire had been caused by the Nevruz celebrations, and that this level had not declined for some time due to the continuation of the celebrations.. The increase in SO₂ levels has therefore been. The average of SO₂ data is 18.31 µg/m³.

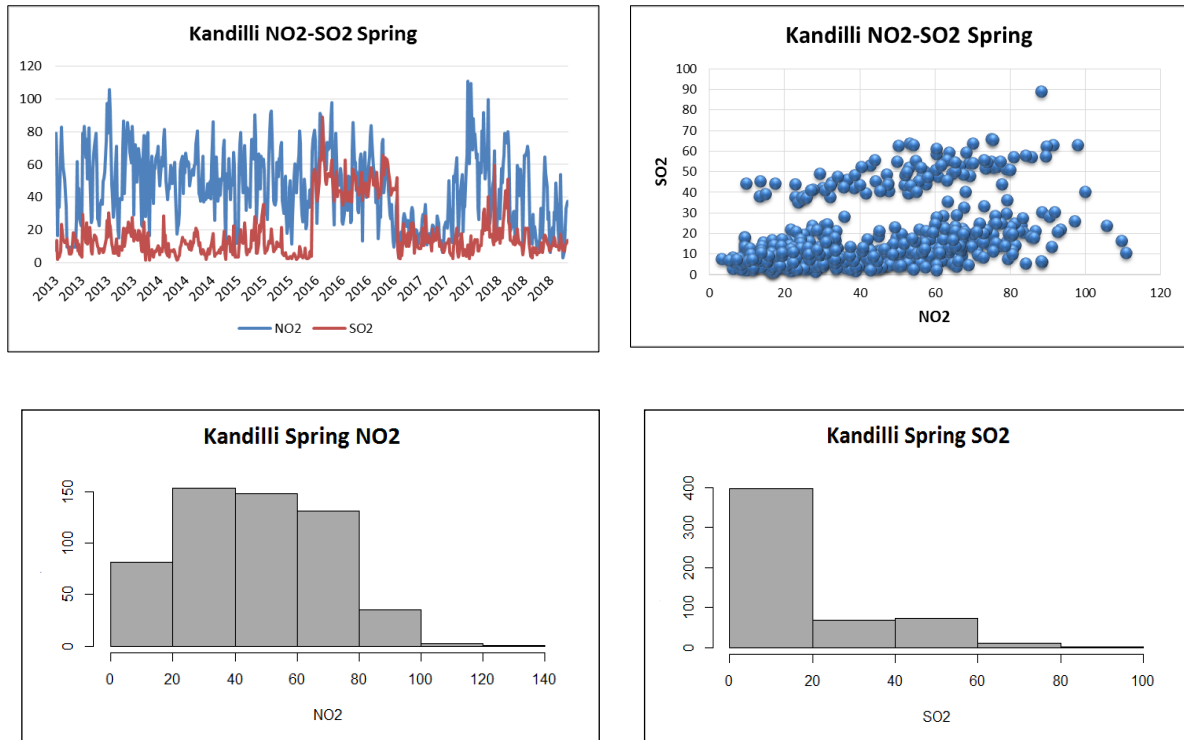


Figure 6. 2013-2018 Kandilli Spring NO₂ & SO₂ Time Series and Histogram

The average of NO₂ data for the years 2013-2018 at Kandilli station was calculated as 29.77 µg/m³. No significant increase or decrease is seen except for the 97.42 µg/m³ value measured on August 21, 2016. When the news was examined, the vehicles were diverted near the site of Kandilli station due to the new road routes designated for triathlon races on 21 August 2016. Vehicle density concentrated in the area has led to an increase in NO₂ and SO₂ levels at this date. When the skew-T chart of this date was examined, an enverzion layer lasting between 250mb-350mb was found throughout the day.

The average of NO₂ data for the years 2013-2018 at Kandilli station was calculated as 29.77 µg/m³. No significant increase or decrease is seen except for the 97.42 µg/m³ value measured on August 21, 2016. When the news was examined, the vehicles were diverted near the site of Kandilli station due to the new road routes designated for triathlon races on 21 August 2016. Vehicle density concentrated in the area has led to an increase in NO₂ and SO₂ levels at this date. When the skew-T chart of this date was examined, an enverzion layer lasting between 250mb-350mb was found throughout the day.

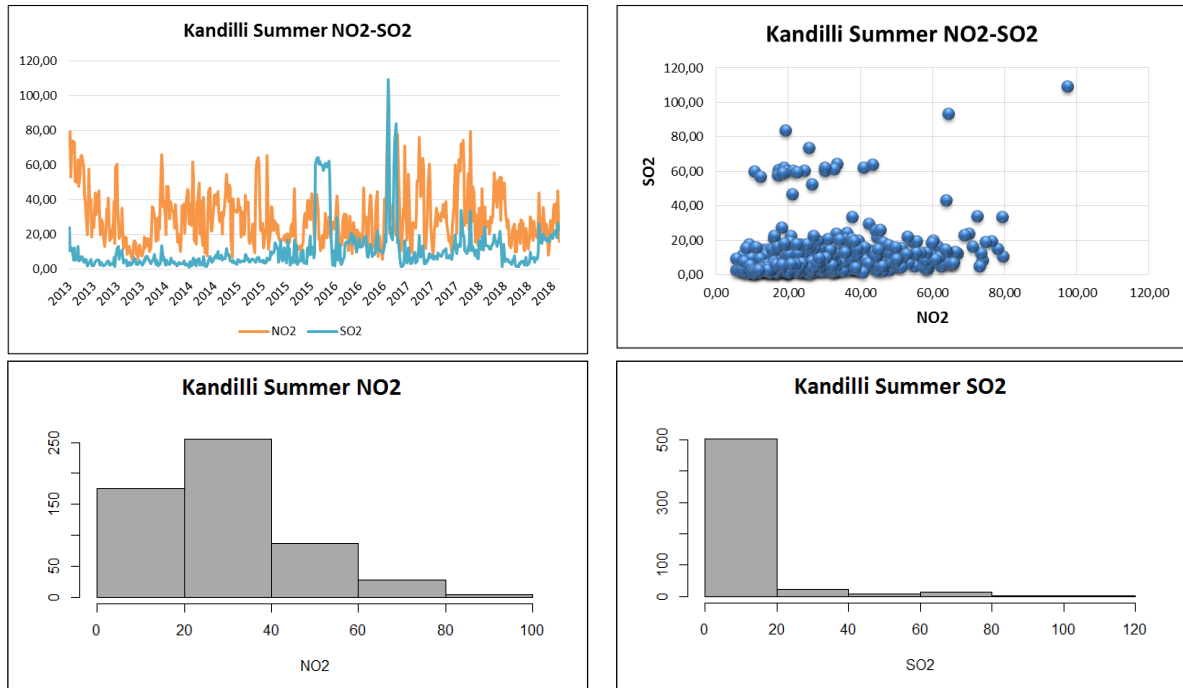


Figure 7. 2013-2018 Kandilli Summer NO₂ & SO₂ Time Series and Histogram

The NO₂ average for the 2013-2018 fall months of Kandilli station was calculated at 36.41 µg/m³. The 5-year average of SO₂ data was found to be 11.28 µg/m³. There has been an increase in averages over the summer season.

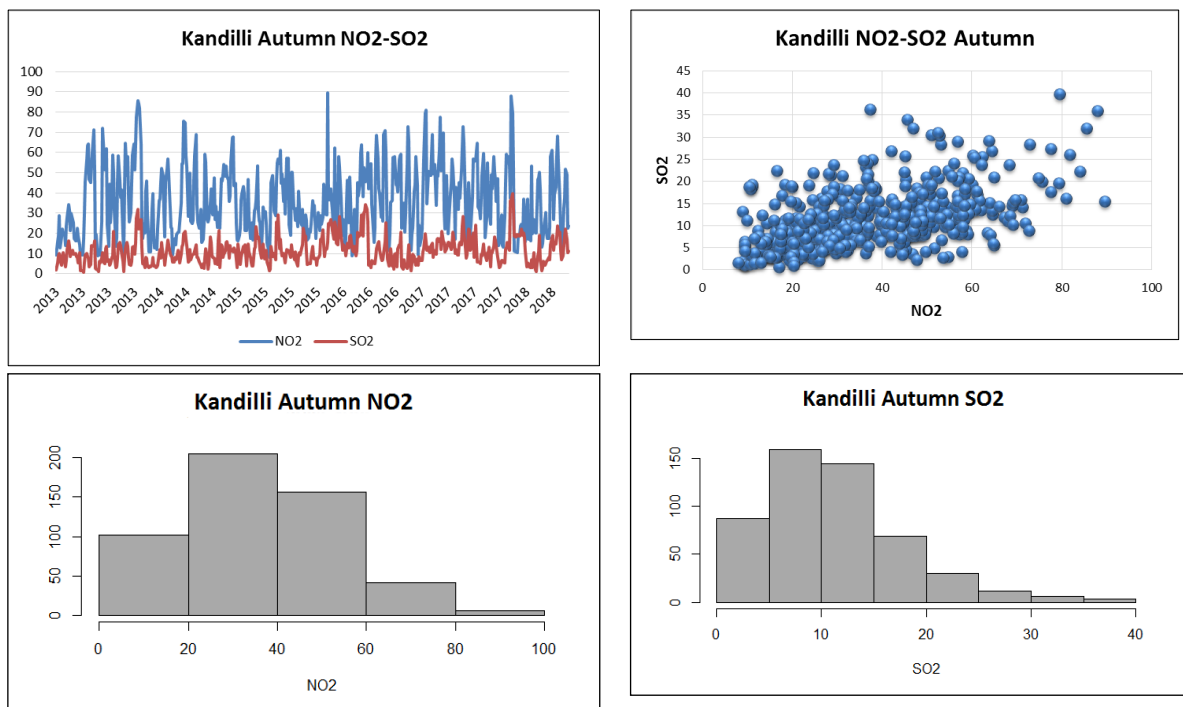


Figure 8. 2013-2018 Kandilli Autumn NO₂ & SO₂ Time Series and Histogram

The average of NO₂ data was calculated at 36.82 µg/m³. Increases in values vary depending on fossil fuel consumption. The average of the SO₂ data was calculated as 14,15 µg/m³. About 60% of the data

is below average. When the histogram is examined, it is observed that the data is concentrated at low values.

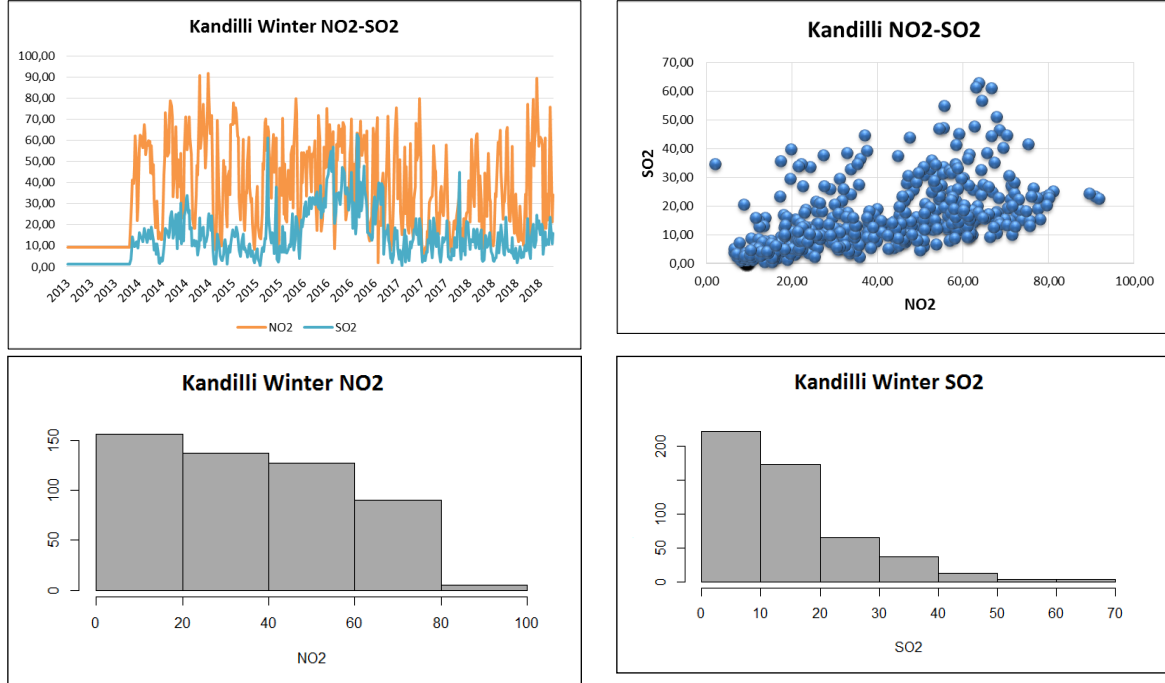


Figure 9. 2013-2018 Kandilli Winter NO₂ & SO₂ Time Series and Histogram

4.3. Sultanbeyli

Sultanbeyli district is connected to Istanbul and Trans European Motorway passes through the middle of the district. Sultanbeyli, which has a population of 309 thousand 347 people, has reached its present state as a result of rapid structuring activities, especially between 1985-1990 its population exceeded 80 thousand from 5 thousand. The mean of the 5-year NO₂ data was calculated as 6.21 $\mu\text{g}/\text{m}^3$. The average of SO₂ data was calculated at 5.54 $\mu\text{g}/\text{m}^3$. In 2014, the above-average value of 24.14 $\mu\text{g}/\text{m}^3$ is read. The reason for this increase is the consumption of fossil fuels due to the need for warming.

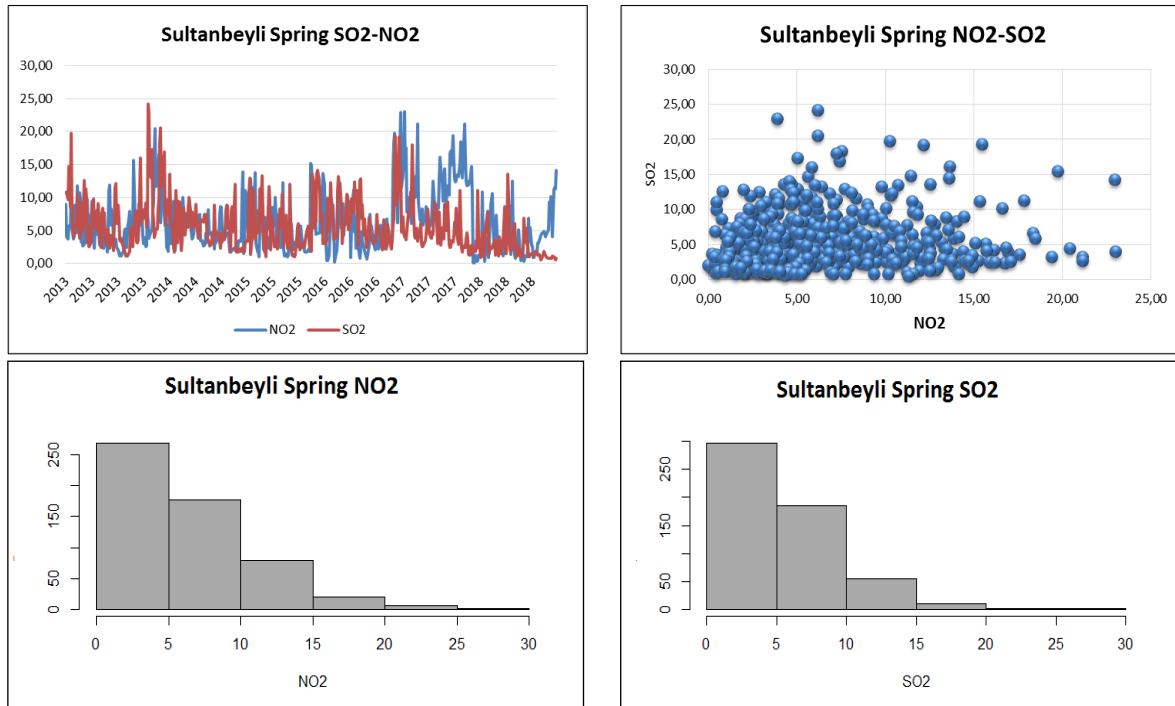


Figure 10. 2013-2018 Sultanbeyli Spring NO₂ & SO₂ Time Series and Histogram

The average of NO₂ data was calculated as 11.23 µg/m³. In general, the value increases at the beginning of the summer months and the value decreases towards the end of the summer months are seen. The average of 5-year SO₂ data was calculated at 2.85 µg/m³. In particular, a value of 9.71 µg/m³ was read, significantly above the average on June 14, 2014. When news surveys were conducted, it was concluded that a fire had broken out in Ataşehir and Kadıköy on the same day. In addition, skew-t diagrams of the same day are examined between 950-1000mb and 550-500 mb of enverzion layer is seen. Looking at the meteorological conditions at this date, especially between morning and noon in the region was affected by wind from the North was also seen. These results can be cited as the reason for the increase.

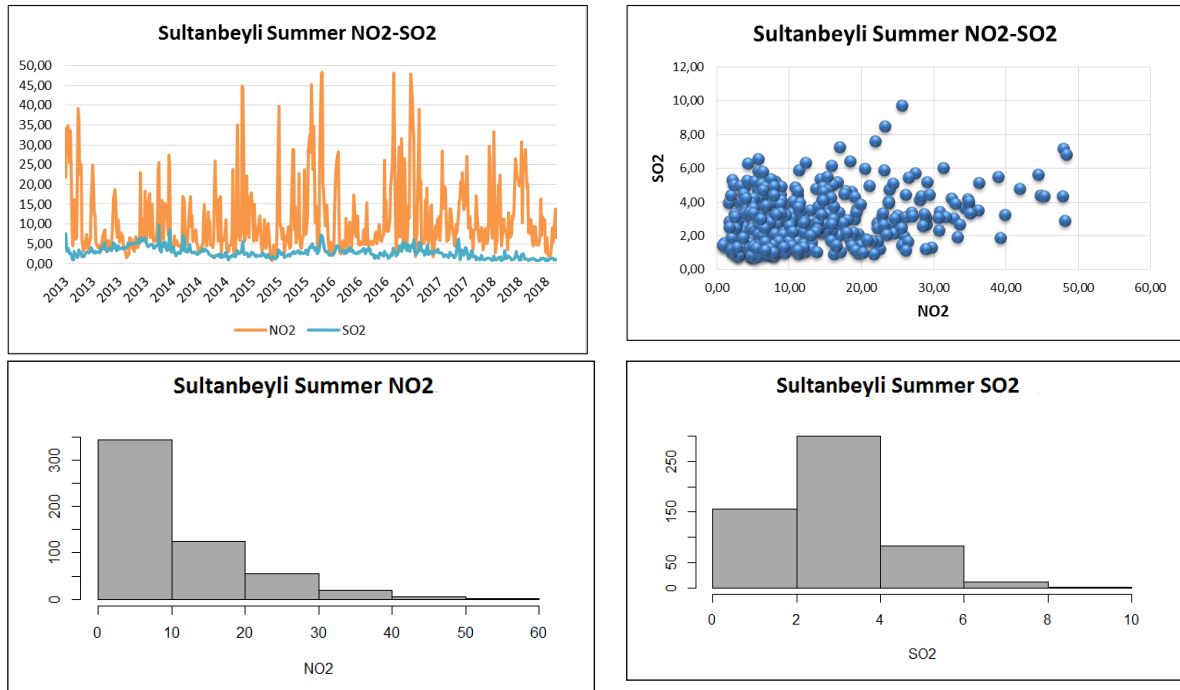


Figure 11. 2013-2018 Sultanbeyli Summer NO₂ & SO₂ Time Series and Histogram

The average of the NO₂ data was calculated as 23.95 µg/m³. About 58% of the data is below average. There is no significant increase or decrease in the time series. The average 5-year SO₂ data was measured at 4.29 µg/m³. The average has increased relative to the summer season. As meteorological conditions begin to return to cold weather, the increase created by warming in this parameter is observed.

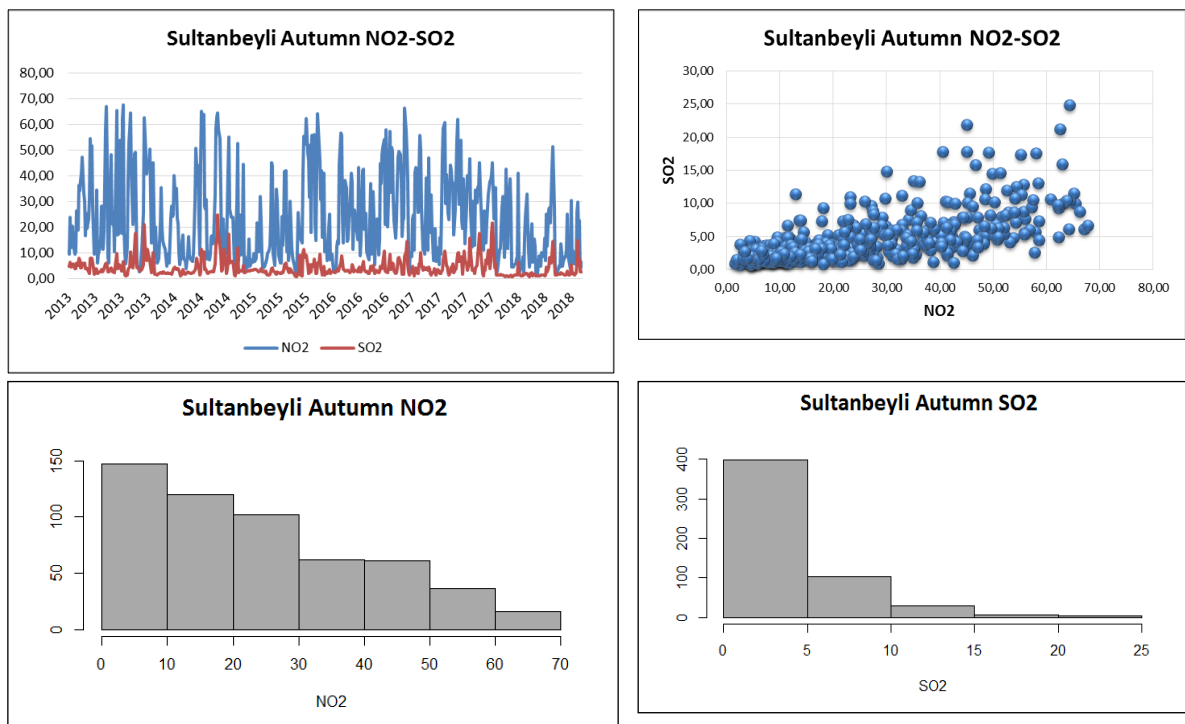


Figure 12. 2013-2018 Sultanbeyli Autumn NO₂ & SO₂ Time Series and Histogram

The average of NO₂ data was calculated as 10.71 µg/m³. The skew-t diagram of 57.78 µg/m³ observed on 29 December 2017 shows that at 00Z time the region was under the influence of an inversion layer between 950 mb and 1000 mb.

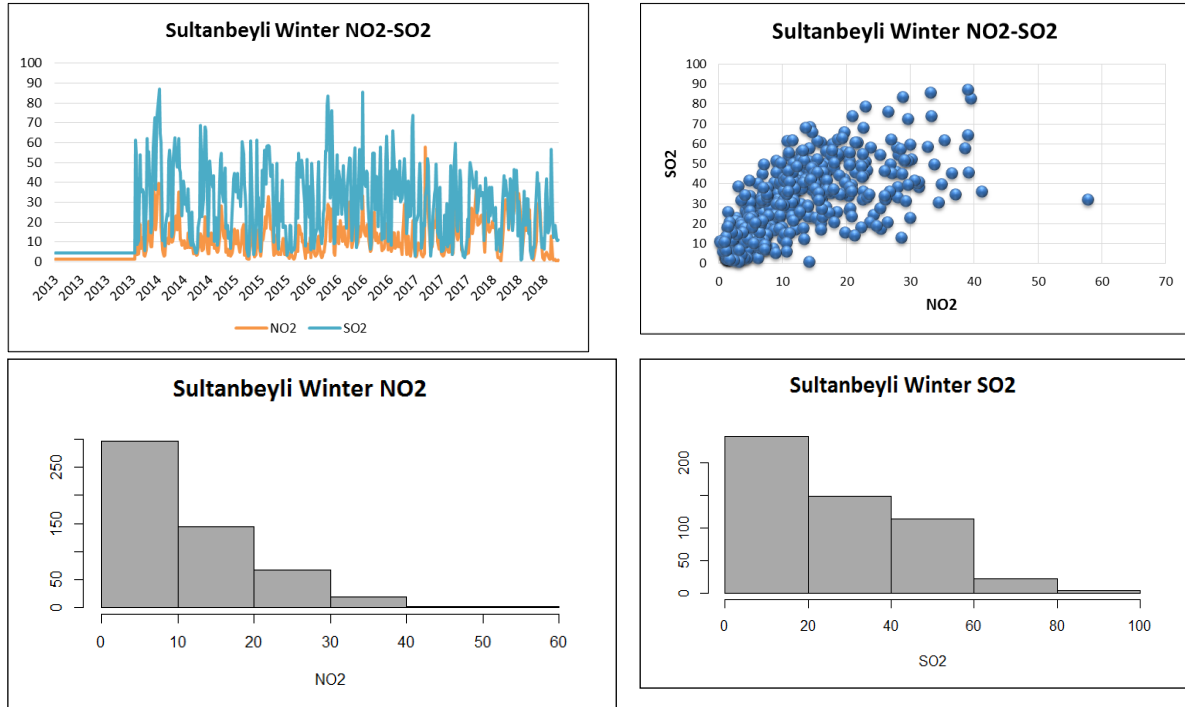


Figure 13. 2013-2018 Sultanbeyli Winter NO₂ & SO₂ Time Series and Histogram

4.4. Ozanlar

Ozanlar is a village in Adapazarı District of Sakarya province. Adapazarı is the most populated district of Sakarya province with a population of 239,284. The economy in Sakarya province is based on agriculture and industry. Especially in terms of the PM₁₀ parameter is considered as one of the most polluted provinces of Sakarya. The 5-year average of SO₂ data was calculated at 13.89 µg/m³ but in April 2016 and March 2018 values of 92.08 µg/m³, 102.82 µg/m³ and 91,13 µg/m³ were observed. In April March 2016, a fire broke out in a textile workshop and an amusement park, and in March 2018, a heavy fire broke out in a carpet workshop. No significant increase or decrease was observed except for these dates.

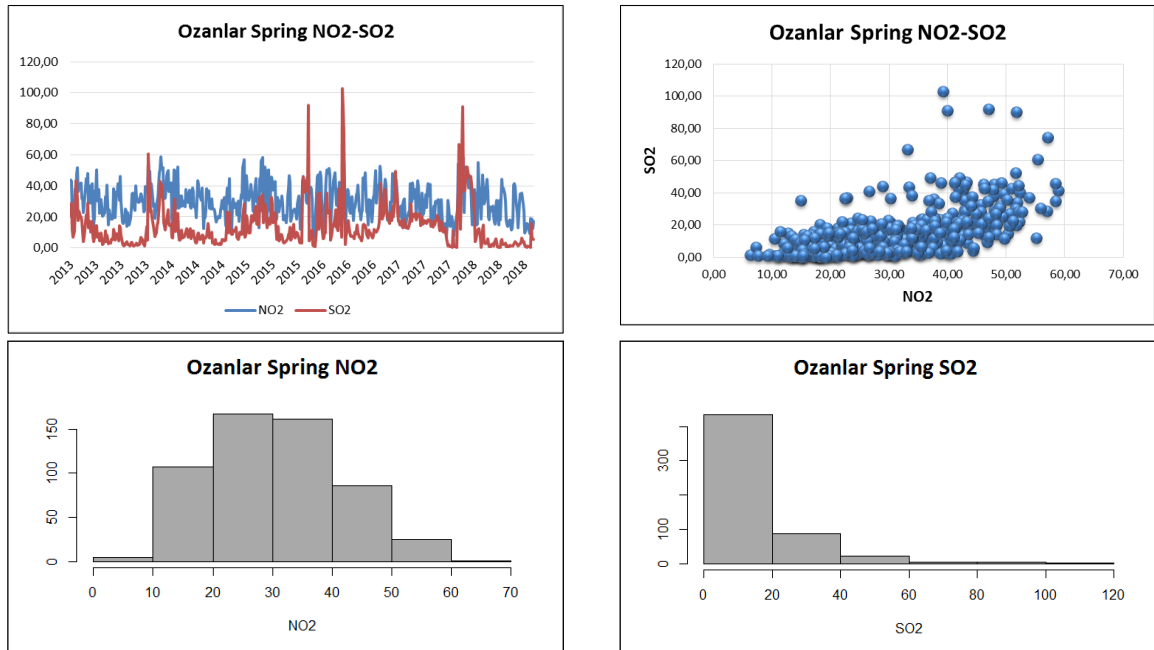


Figure 14. 2013-2018 Ozanlar Spring NO₂ & SO₂ Time Series and Histogram

The average of NO₂ and SO₂ data was calculated as 18.48 µg/m³ and 7.42 µg/m³.

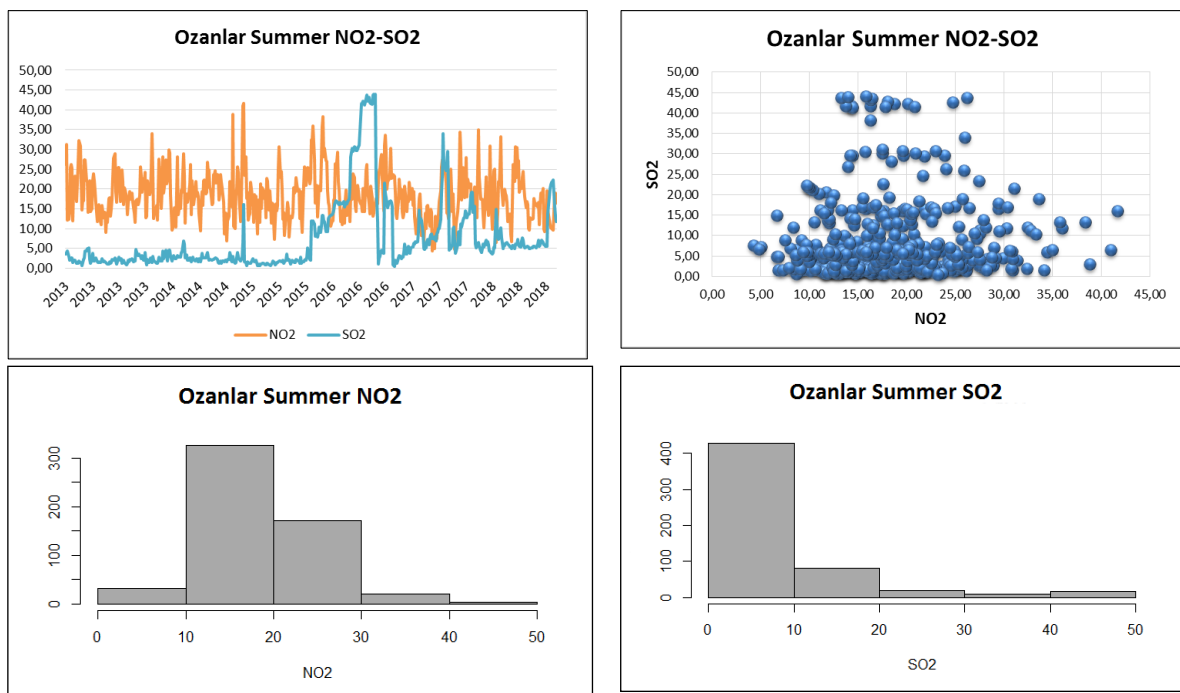


Figure 15. 2013-2018 Ozanlar Summer NO₂ & SO₂ Time Series and Histogram

The average of NO₂ data was calculated as 31.17 µg/m³. About 46% of the data is below average. The Histogram appears to be symmetrical. The average of SO₂ data was found to be 13.15 µg/m³. However, the time series read an above-average value of 73.41 µg/m³ on November 11, 2015. When the news investigation was conducted for this date, it was observed that there were fire incidents in Istanbul and Izmit provinces. The region of the bars remained under the influence of winds from the west on this

date. At the same time, the skew-t diagram of Istanbul, the closest point to this region, shows an enverzion base between 800 mb and 900 mb. The sudden increase in SO₂ levels on 11 November 2018 is due to this reason.

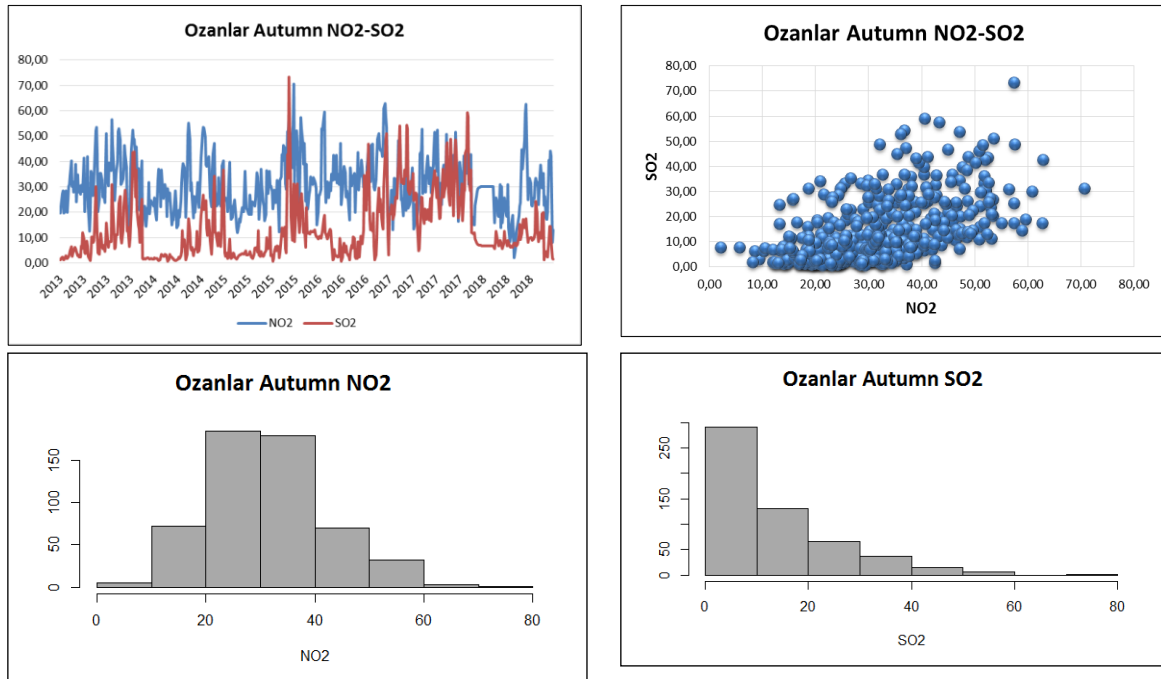


Figure 16. 2013-2018 Ozanlar Autumn NO₂ & SO₂ Time Series and Histogram

The average of NO₂ data for the winter months was 37.76 µg/m³. when the SO₂ data for the winter months of the station is examined, it is observed that there has been an increase in values especially at the beginning of the winter months. Parallel to the increase in fossil fuel consumption, emissions of SO₂ have also increased. The mean of the data set was calculated as 27.53 µg/m³.

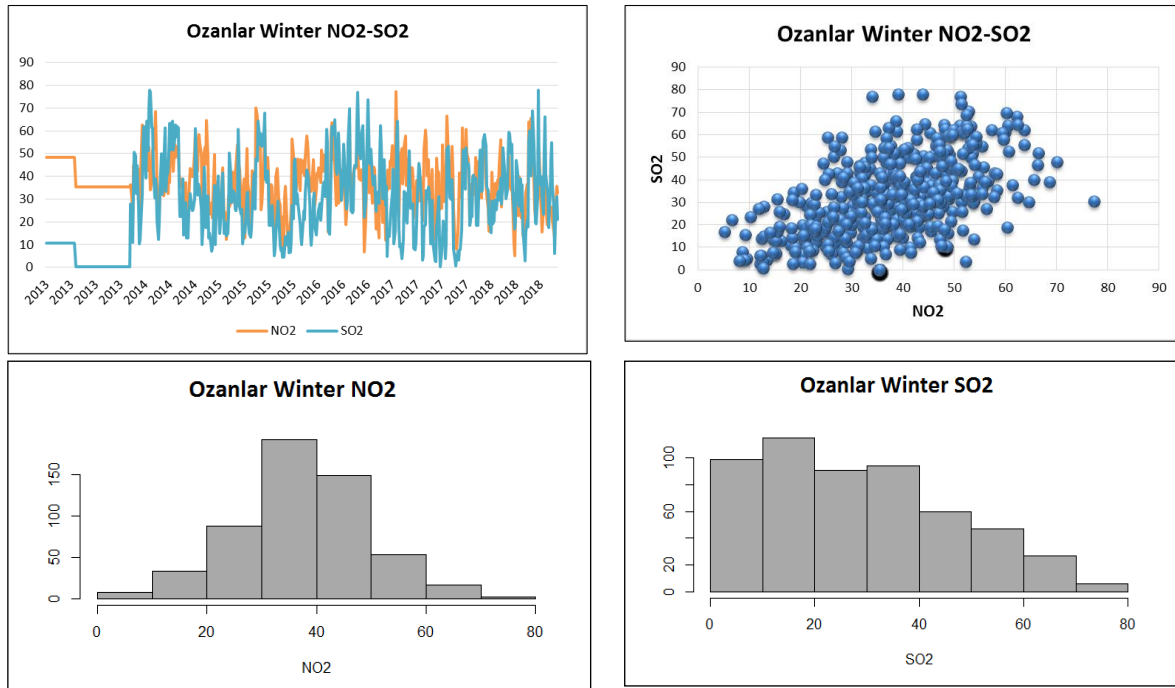


Figure 17. 2013-2018 Ozanlar Winter NO₂ & SO₂ Time Series and Histogram

4.5. Tekirdag

Tekirdag is one of the six provinces with two seashores in Turkey (Tekirdag Belediyesi, 2014). In Tekirdag there are 5 Chambers of Commerce and Industry, 11 Organized Industrial Zones and 1 European Free Zone in the districts of Central, Malkara, Corlu, Cerkezkoy and Hayrabolu (Albayrak et alç, 2013; Özmen and Seray, 2018). This station type is the traffic type station. In spring season, the NO₂ average was calculated as 50.01 µg/m³. The average of 5-year SO₂ data was calculated at 32.12 µg/m³. The fact that the values are at their highest values in the spring season of each year, especially in March, is due to the continued consumption of fossil fuels in the months that are the continuation of the winter season.

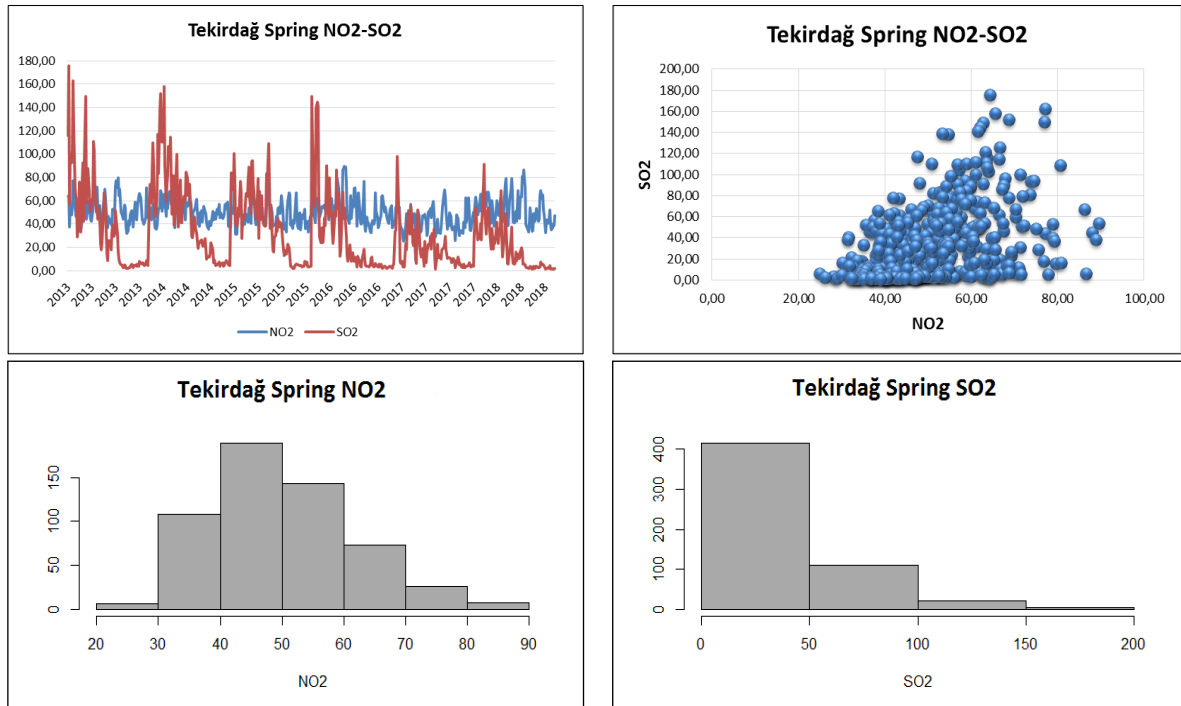


Figure 18. 2013-2018 Tekirdag Spring NO₂ & SO₂ Time Series and Histogram

The NO₂ average was calculated as 45.31 µg/m³. The average of SO₂ values between 2013-2018 was calculated as 3.26 µg/m³. About 62% of the data is above average. The majority of the data is above average, although it does not exceed 125 µg/m³, which is the limit value of the data. This is due to Tekirdag's industrial activities that have developed in recent years. Many areas used as farmland have increased compared to the previous periods of SO₂ due to being zoned for construction with developing industry and the expansion of industrial activities in these areas.

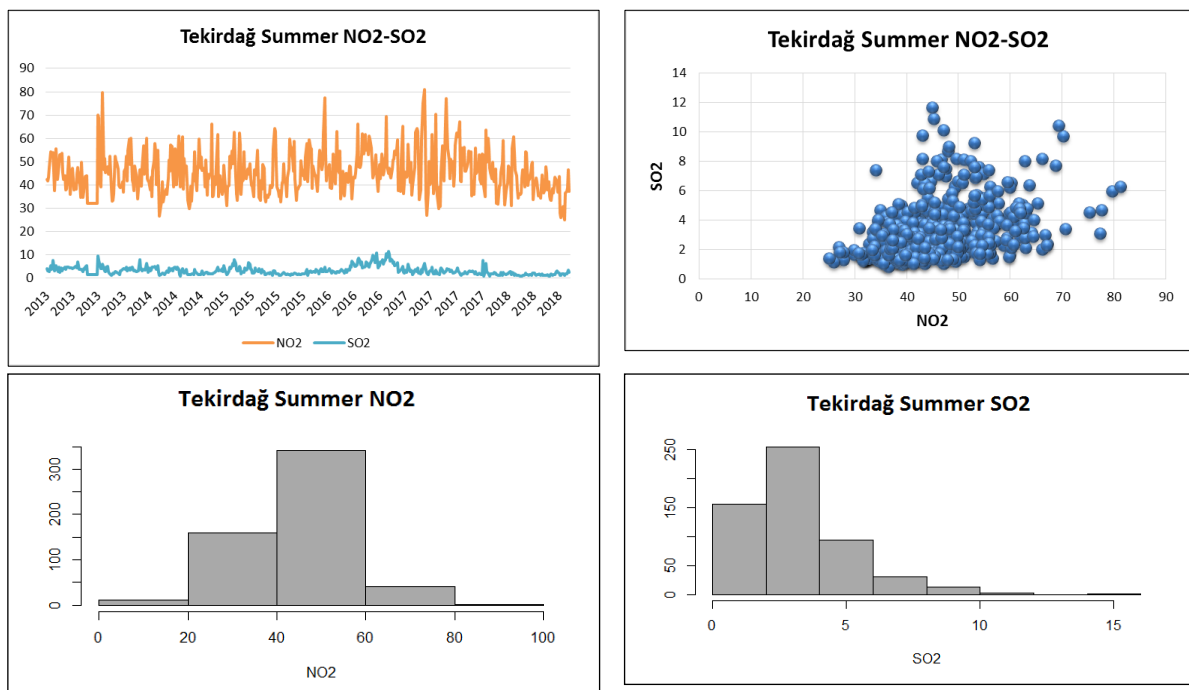


Figure 19. 2013-2018 Tekirdag Summer NO₂ & SO₂ Time Series and Histogram

The average of the NO₂ data was calculated as 43.21 µg/m³. The average of SO₂ data was calculated at 18.09 µg/m³, with about 74% of the data below average. According to EU limit conditions, the daily limit value for SO₂ is 125 µg/m³ and should not be exceeded 3 times a year. As of 1 January 2019, these conditions apply to Turkey and as shown in the time series chart, the limit value has been exceeded 7 times in the autumn season. This caused the region to become a threat to living things.

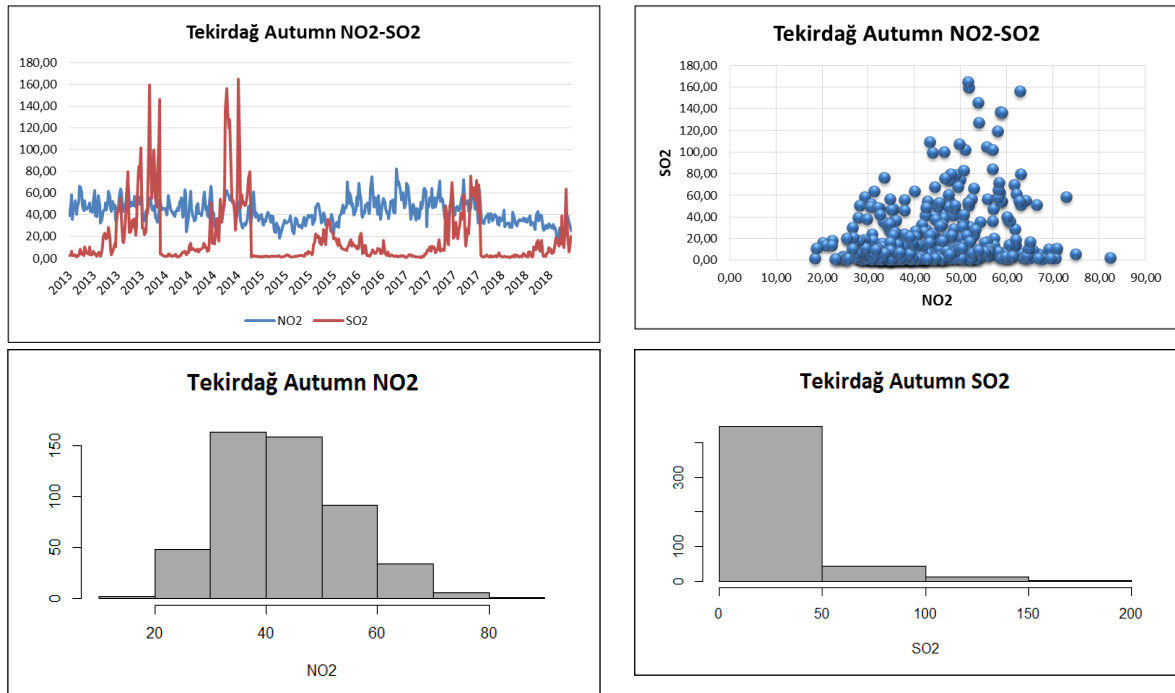


Figure 20. 2013-2018 Tekirdag Autumn NO₂ & SO₂ Time Series and Histogram

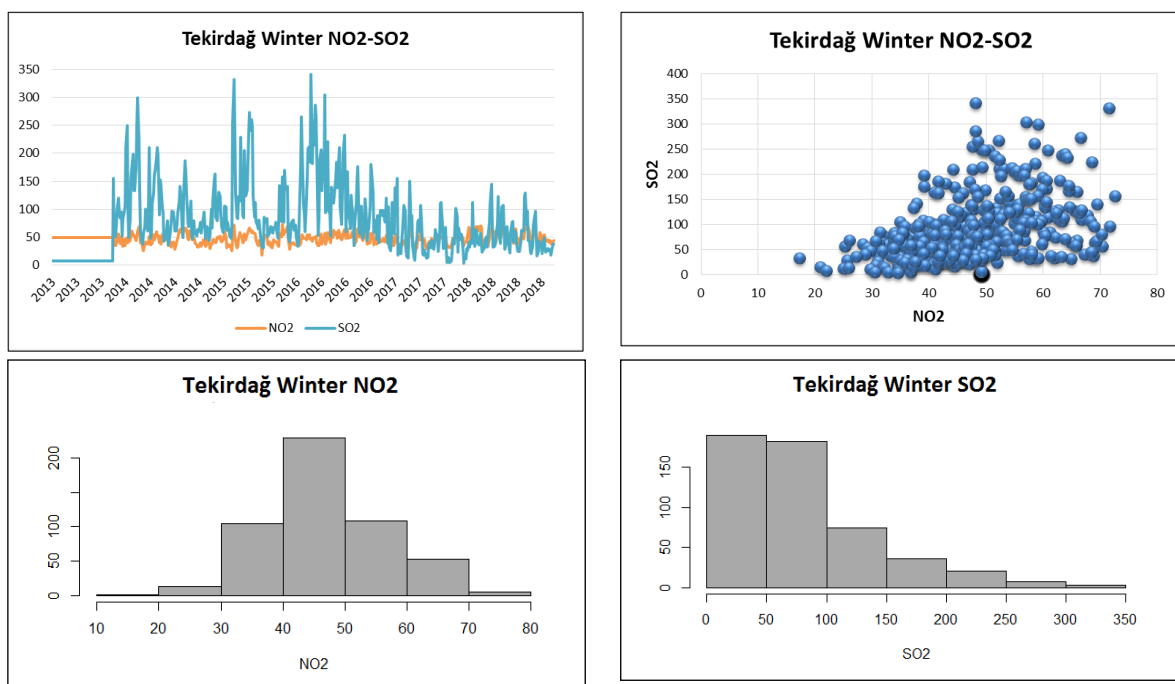


Figure 21. 2013-2018 Tekirdag Winter NO₂ & SO₂ Time Series and Histogram

The average of the NO₂ data was calculated as 47.40 µg/m³. The average of the data was calculated as 78.54 µg/m³ when the SO₂ changes of the last 5 years of the winter months were examined. As of 1 January 2019, the AB limit values are valid for the limit value of the SO₂ parameter in Turkey. Accordingly, SO₂ emission should not exceed 125 µg/m³ more than 3 times a year in 24-hour periods. Looking at the chart, as of February 2014, the concentration of SO₂ is above the limit value. The value of 341 µg/m³ was read, especially during the winter of 2016. Values have increased to levels that threaten living health. According to the Air Quality Index, this level is dangerous and people are warned to avoid all physical activity in the outdoor environment. To look at the source of this increase, the Tekirdag province Environment Situation Report of 2017 published by the Tekirdag Provincial Directorate of Environment and Urban Planning was examined. 3 of the 100 largest companies in Turkey and 15 of the 500 largest companies in Tekirdag are within the boundaries of the report described in metal goods and machinery manufacturing development, proximity to Istanbul, transportation, marketing opportunities played an important role in the development of the industry. In Tekirdag, there were 13 organized industrial zones and 1 free zone, and 1081 companies were registered to operate in organized industrial zones (Özmen and Zeray, 2018). Corlu Creek and its side tributaries, the largest tributary feeding the Ergene River, are exposed to pollution after intensive industrialization in Cerkezkooy and Corlu. These factors explain the high values measured at the station.

4.6. Correlation Analysis

The main factors in increasing NO₂ and SO₂ values are motor vehicle use and industrial activities. NO₂ values increase in areas where vehicle use is concentrated, while SO₂ values increase in areas where combustion events occur. If the correlation coefficients in a station do not experience a noticeable decrease or increase seasonally, then the values in that station are generally within a certain range during the analysis period.

Table 1. Correlation Analysis of 5 Stations

Season/Station	Basaksehir	Kandilli	Sultanbeyli	Ozanlar	Tekirdag
Spring	0.5213402	0.36861	0.13283	0.58431	0.44141
Summer	0.056841	0.17707	0.2667	0.03307	0.4008
Autumn	0.5045539	0.52864	0.66253	0.54156	0.25525
Winter	0.5872252	0.60933	0.72863	0.41873	0.37479

For example, when the seasonal variation of the Tekirdag Central Station correlation coefficients is examined, it is observed that the values are almost close to each other. The main reason for this is that Tekirdag province has continued its industrial activities throughout the year as one of the most prominent cities in Turkey with its factories and industrial facilities. This causes the values measured at Tekirdag Central Station to remain within a certain range. When seasonal periods are examined in more detail on a monthly basis, a significant decrease or increase may occur. During the day, a certain increase in daily data can be seen as a result of emissions being carried to the station area after a fire event in a nearby area due to weather conditions or the region being under the influence of an enverzion layer. When the summer season changes are examined, for example, when looking at Istanbul stations, there are differences between the summer season and the winter season correlation coefficients. The main reason for this is that due to the concentration of population due to tourism activities in Istanbul during the summer season, motor vehicle use is increasing and NO₂ values are increasing. But at the same time, as the need for warming has been reduced to a minimum, SO₂ values are declining. The correlation coefficient is lower as the difference between SO₂ and NO₂ increases due to these increases and decreases.

Table 2. Average, Maximum, Minimum and Exceed Days

Station	Season	NO ₂				SO ₂			
		Average	Maximum	Minimum	Exceed	Average	Maximum	Minimum	Exceed
Başakşehir	Spring	38,69	110,44	6,63	-	9,06	46,20	0,10	-
	Summer	22,43	81,48	5,33	-	7,80	65,69	0,03	-
	Autumn	36,26	149,01	4,84	3	6,39	44,77	0,06	-
	Winter	33,45	92,69	6,57	-	10,79	43,85	0,39	-
Kandilli	Spring	46,16	110,84	3,14	-	18,31	89,01	1,36	-
	Summer	29,68	97,42	5,58	-	10,85	109,60	1,28	-
	Autumn	36,41	94,07	8,00	-	11,29	39,83	0,71	-
	Winter	36,82	91,75	2,03	-	14,14	63,07	0,68	-
Sultanbeyli	Spring	6,21	22,97	0,01	-	5,54	24,14	0,53	-
	Summer	11,23	48,37	0,80	-	2,85	9,71	0,72	-
	Autumn	23,95	67,67	1,54	-	4,29	24,87	0,77	-
	Winter	10,72	57,78	0,15	-	26,33	87,10	1,03	-
Ozanlar	Spring	30,33	58,87	6,28	-	13,89	102,82	0,12	-
	Summer	18,48	48,81	4,30	-	7,42	44,04	0,44	-
	Autumn	31,17	70,57	2,18	-	13,15	73,41	0,66	-
	Winter	37,77	77,38	5,23	-	27,53	77,98	0,19	-
Tekirdağ	Spring	50,01	89,52	24,95	-	32,12	175,83	1,17	10
	Summer	45,31	81,12	9,36	-	3,26	14,13	0,84	-
	Autumn	43,21	82,36	18,51	-	18,09	165,22	0,89	7
	Winter	47,40	72,62	17,23	-	78,54	341,33	3,61	96

When data between 2013 and 2018 are analyzed, it is observed that during summer and winter season, there are days which exceeds the limit value of EU. Particularly summer, autumn, and winter season, industrial activities caused air more polluted enough to threat living beings.

5. Conclusion

In this study, NO₂ and SO₂ data of five stations belonging to Marmara region were analyzed. As a result of the examination of the data, it was observed that the parameters vary depending on many factors. Especially when looking at the Central Station of Tekirdag province, which has come to the fore with its industrialization, it was found that the SO₂ values gradually increased and reached levels that would threaten the living life and ecosystem by exceeding the boundary values. The data from 2013-2018 measured a value of 32.12 µg/m³ in the spring season, while increasing fossil fuel consumption in the winter season due to the need for warming was added, along with increased industrialization, a value of 78.54 µg/m³ was measured. The highest value in correlation analysis was 0.7286258 and Sultanbeyli station was observed during the winter season. The higher the correlation coefficient, the more closely the data measured at this station parallels each other. When looking at all the correlation coefficients calculated in general, it is seen that they are all calculated between 0 and +1. This indicates that the NO₂ and SO₂ parameters have a significant relationship with each other in all seasons and on all stations. In this respect, one of the parameters increased when the other increased, one decreased when the other decreased. According to the air quality index, the best region is Üsküdar, where Kandilli station is located. The following measures can be taken to reduce air pollution; filters can be installed in the chimneys of industrial plants, high-calorie coals can be used to heat homes, chimneys and stove pipes can be cleaned every year. In addition, the use of natural gas should be spread. Green areas should be increased and zoning plans should be reorganized and measures to reduce air pollution should be taken. Public transport should be preferred, not personal vehicles. Thermal insulation should be applied in residential construction. Renewable energy systems should be developed and their use should be expanded and fossil fuel consumption reduced. One of the most important measures is regular measurement and follow-up.



18th World Clean Air Congress, 23-27 September 2019, Istanbul
organized by TUNCAP and IUAPPA

6. References

Albayrak Ö., Tohumvu K.S., Ayhan Y., Gül B., Bülbül C., Akdemir E., 2013. Tekirdag İl Çevre Durum Raporu 2012, Tekirdag: Tekirdag Valiliği Çevre Ve Şehircilik İl Müdürlüğü.

Özmen E., Zeray A.C., 2018. Tekirdag'ın Çevre Durum Raporu: Ergene'nin Kirliliği Artarak Devam Ediyor, Demirören Haber Ajansı.

Tekirdag Belediyesi, 2014. <http://www.tekirdag.bel.tr/tekirdag/cografya>.

Wark K., Warner C. F., 1981. "Air Pollution Its Origin & Control" 2.Baskı, Harper & Row Publishers, New York.

Size-segregated particulate matter down to PM_{0.1} and carbon content during a haze episode in Sumatra Island, Indonesia

Muhammad Amin¹, Rahmi Mulia Putri¹, Suthida Piriyakarnsakul⁷, Andre Rizky², Aulia Ullah³, Worradorn Phairuang^{6,7}, Fumikazu Ikemori⁴, Mitsuhiro Hata⁵ and Masami Furuuchi^{5,6}

¹ Graduate School of Natural Science and Technology, Kanazawa University, Kanazawa, Ishikawa, 920-1192, Japan,

² Faculty of Science and Technology, Sultan Syarif Kasim Islamic State University, Pekanbaru, Riau, 28293, Indonesia,

³ Environmental Engineering Department, Engineering Faculty, Jambi University, Jambi, Jambi, 36364, Indonesia,

⁴ Nagoya City Institute for Environmental Science, Nagoya, 460-8508, Japan,

⁵ Faculty of Geoscience and Civil Engineering, Institute of Science and Engineering, Kanazawa University, Kanazawa, Ishikawa, 920-1192, Japan,

⁶ Faculty of Environmental Management, Prince of Songkla University, Hat Yai, Songkhla 90112, Thailand,

⁷ Air Pollution and Health Effect Research Center, Prince of Songkla University, Hat Yai, Songkhla, 90110 Thailand

mfuruch@staff.kanazawa-u.ac.jp

Abstract. Seasonal changes in size-segregated particulate matter (PM) down to PM_{0.1}, particles smaller than 0.1 μm , were monitored in three different cities in Sumatra Island, Indonesia in 2018. In order to identify possible emission sources, carbonaceous components in particles collected by a cascade air sampler that is capable of collecting PM_{0.1} particles were analyzed by the thermal/optical reflectance method following the IMPROVE-TOR protocol and attempts were then made to identify possible local emission sources based on the components in conjunction with the calculation of air mass movement from burned areas, or hot spots, as determined from satellite image data. The PM_{2.5} and PM₁₀ levels at all sites were below the NAQS for Indonesia, while those at sub-urban and urban sites exceeded the WHO guidelines for 24 hours. The PM_{0.1} levels in sub-urban and urban areas were similar to those in large cities in East Asia, such as Bangkok and Hanoi. The PM levels during the peatland fire period was much lower than data reported before 2016, indicating a drastic decrease in the number of hotspots. The influence of the peatland fires in the dry season was more significant in cities located on the east coast of Sumatra Island because of the larger number of hotspots and air mass trajectories along the coast. A clear increase in the OC/EC ratio in the dry season was observed, particularly in fine fractions as PM_{0.1}. Although detailed contributions of local sources were not clear, at the rural site, PM_{0.1} particles may have been affected by a local cement factory near the rural site in rainy season and local biomass burning in the dry season. The Py-OC/OC₄ ratio was found to be useful in terms of understanding the influence of biomass burning. Using Py-OC/OC₄, the levels of PM_{0.1} particles was found to be related to biomass burning.

Keywords: PM_{0.1}; Emission Sources; Carbonaceous Component; Smoke-Haze Sumatera-Island; Indonesia

1. Introduction

Air pollution is becoming a serious problem in Indonesia, especially by particulate matter (PM) emitted from biomass burning in forests and peatland fires (Levine, 1999; Heil and Goldammer, 2001; Heil et al., 2007; Koplitz et al., 2016; Kuwata et al., 2018). The average concentration of fine particles (PM_{2.5}), e.g., was reported to be 7817 µg/m³ during the forest fire period, corresponding to a level hundred times higher than daily standard for Indonesia (65 µg/m³) and three hundred times higher than the WHO standards (25 µg/m³) (Betha et al., 2013). Indonesia became a main contributor of emissions derived from forest fires in the Equatorial Asia region since the El Niño year in 1997 (Tacconi, 2002). Because of the meteorological characteristics over the South East Asian region, air pollution in Indonesia would not be expected to be a local problem but in reality, now a transboundary smoke-haze problem that affects neighboring countries as Singapore, Malaysia, Southern Thailand, Brunei and Philippines (Heil and Goldammer, 2001; Radojevic, 2003; Heil et al., 2007; Quah and Varkkey, 2013; Vadrevu et al., 2014; Sankaran, 2015).

An area that is highly contaminated by PM could result in adverse influences on the human health. This is particularly true in the case of fine and ultrafine particles that contain higher amounts or fractions of hazardous chemicals than in coarse particles and can penetrate deeply inside the lung (Pekkanen et al., 1999; Osunsanya et al., 1999). However, our understanding of the behavior and characteristics of ambient particles with aerodynamic diameters ≤0.1µm, or PM_{0.1} is still not sufficient, regarding chemicals including carbonaceous components (Kim et al., 2011a; Chen et al., 2013). This is especially true for the South East Asia region as Indonesia. Since PM_{0.1} was assumed to contain various harmful components and may lead to toxic effects for human health, the National Research Council blueprint for particulate matter (PM) of the US in 1998 singled out PM_{0.1} as the main research (U.S. National Research Council, 1998). A number of studies have now confirmed that PM_{0.1} particles has adverse effects on human health (Wichmann et al., 2000; Terzano et al., 2010), including the human brain (Calderón-Garcidueñas, 2008).

As so far reported, nearly 90 % of particles emitted from biomass burning are smaller than 1 µm, or, PM₁ and nearly 50 % of these are smaller than 0.1 µm, or, PM_{0.1} even in mass basis (Hata et al. 2014; Rogula-Kozłowska, 2016; Phairuang et al. 2019) reported that carbonaceous components in PM_{0.1} are sensitive to carbon-containing particles that are emitted during the burning of agricultural crops. The situation regarding PM in Indonesia may, therefore, be strongly influenced by fine and ultrafine particles that are emitted as the result of the burning of forests and peatlands. However, as of now, there is little information available concerning the characteristics of coarse and fine particles that are emitted along with PM_{0.1} particles in Indonesia.

In this study, in order to examine the present status and characteristics of airborne particulates in Indonesia, seasonal behaviors of size-segregated particulate matter (PM) down to the PM_{0.1} level were observed in three different cities in Sumatra Island, Indonesia in year 2018. Sumatra island was selected as a typical area with peatland fires during the dry season. The use of a cascade air sampler for collecting air samples that can collect size-segregated particulate matter down to PM_{0.1} was conducted both in rainy and dry seasons at three different locations in Sumatra island. These areas can be categorized as “rural”, “sub-urban” and “urban” and the influences of local emission sources as well as that for peatland fires are discussed. Carbonaceous components of size fractionated particles were analyzed by a thermal/optical method and possible local emission sources were discussed based on the components in conjunction with the calculation of air mass movement from burned areas, or hot spots, specified by satellite image data.

2. Methodology

2.1 Sampling sites

2.1.1 Padang city

A sampling site was located on 4th floor of Environmental Engineering Division, Faculty of Engineering, Andalas University (S 00° 54' 46.3" E 100° 27' 50.0"), Padang city, which is located in a west coast area of North Sumatra island and the capital city of the Pauh sub-district (See Figure 1). The total area of the district is around 14629 ha and consists of rice fields (1061 ha), gardens (364 ha), fields (219 ha), community forests (1927 ha), and non-cultivated wild fields (110 ha), fish ponds and state forests (10366 ha), roads, settlements and offices (582 ha) (BPS Padang city, 2018). The site is surrounded by forest and was located around 13 km from the city center so that it was categorized as a "rural" site, where the influence of emissions from traffic may not have been important. As an industrial emission source, that might possibly be affected by the weather, a large cement factory that uses coal as a fuel was located about 2.5 km south of the sampling site (Bachtiar et al., 2016). The climatic division of the Padang area is classified as a tropical rain forest climate and is one of Indonesia's wettest cities with frequent rainfall throughout the year.

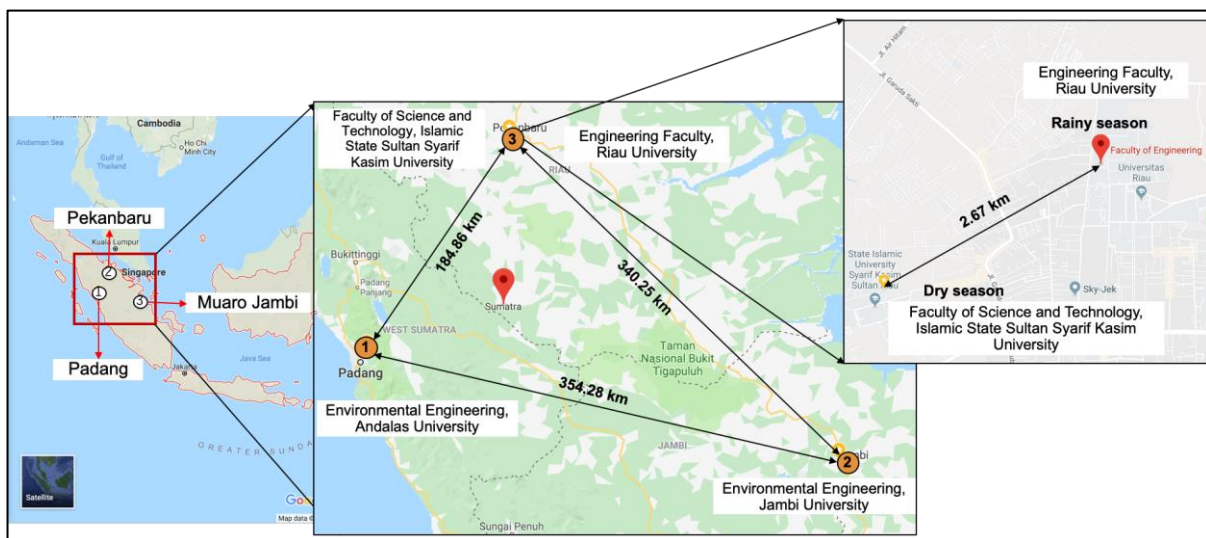


Figure 1. Locations of sampling sites in 3 different cities on Sumatra Island, Indonesia

2.1.2 Muaro Jambi Regency

A sampling site was located at the roof top of the Environmental Engineering building (3rd floor), Jambi University, Muaro Jambi (01° 40.437' in the South and 103° 34.566' in the East, 48 meters above sea level), which is located at the border of Mestong and the Jambi Luar Kota sub-district, Muaro Jambi on the east coast of Sumatra island (See Figure 1). The sub-district is sectioned by cross-provincial roads connecting the provinces of Jambi and South Sumatra with a large amount of daily traffic by trucks, cars and motorbikes. The land use of these sub-districts consists of agriculture, residential areas and industrial areas. According to the available data (BPS Muaro Jambi Regency, 2018), there are 157 industrial units consisting of 140 units of small industries and 17 units large/medium industries. Since the university was located at the periphery of an urban area, the sampling site was categorized as "sub-urban" site. The sub-urban site could be influenced by peatland fires in this area as has been reported (Abdul Halim et al., 2018; Muraleedharan et al., 2000; Nowak et al., 2018; Pentamwa and Oanh, 2008). Provincial roads that connect Jambi province and South Sumatera Province (~1.2 km away from the sub-urban site) could also be possible PM sources both in rainy and dry seasons, especially nanoparticles and fine particles.

The climate in Jambi is also classified as a tropical rain forest climate but is rather dry with a much smaller precipitation in the dry season than that in Padang.

2.1.3 Pekanbaru City

A sampling site was located on the roof top of the Engineering Faculty building, Riau University, Tampan sub-district, Pekanbaru City (01° 40.437' in the South and 103° 34.566' in the East, 48 meters above sea level) (BPS Pekanbaru City, 2018) (See Figure 1). The Tampan sub-district is located at the city center of Pekanbaru with land use dominated by settlements, hospitals, roads, offices, restaurants, industries and hotels (BPS, 2018). There are 119 units of small industries, 3 units of medium industries and 13 units of hotels (BPS Pekanbaru city, 2018). The university was surrounded by heavy traffic roads and was a distance of approximately 100 m from a cross-provincial road (Riau and West Sumatera Province). Since the sampling site was located in one of the busiest areas in the Pekanbaru city with a large influence of traffic, this site was categorized as an “urban” site. The urban site was also directly affected by the biomass burning activities during the dry season especially from peatland fires as the main sources of yearly air pollution in this region (Heil and Goldammer, 2001; Kusumaningtyas and Aldrian, 2016; Quah and Varkkey, 2013; Reddington et al., 2014) A volcanic eruption temporally affected the air pollution in the area (Hendrasto et al., 2012; Wahyuni Nurwihastuti et al., 2019). The climate in Pekanbaru is also classified as a tropical rain forest, similar to that in Jambi.

2.2 Sampling Methods

A cascade air sampler, termed here as an Ambient Nano Sampler (ANS), that was developed by Furuuchi et al. (2010) and can collect PM_{0.1}, PM₁, PM_{2.5}, PM₁₀, TSP at an air flow rate of 40 l/min was used as a common sampler. Quartz fibrous filters (QFF) (2500 QAT-UP, Pall Corp., USA) of Ø55 mm that had been pre-baked at 350 °C in an oven for 1 hour then conditioned at 21.5 ± 1.5 °C, and 35 ± 5 % RH in a PM_{2.5} weighing chamber (PWS-PM2.5, Tokyo Dylec Corp., Japan) for 48 hours before and after sampling were used to collect particles (>10, 2.5-10, 1.0-2.5, 0.5-1.0, and <0.1 µm). An inertial filter (IF) consisting of webbed stainless steel fibers (average fiber diameter d_f = 9.8 µm, Nippon Seisen Co. Ltd., felt type, SUS-316) plugged in a cartridge nozzle of Ø 5.25 mm (Otani et al., 2007; Furuuchi et al., 2010) was used for the separation of PM_{0.1} particles. Before assembling the inertial filter cartridge, the stainless steel web was cleaned with ethanol to reduce the blank value for carbon. Each prepared filter was wrapped in aluminum foil then kept in a plastic bag during transport to the sampling sites along with blank filters to verify possible contaminants during the filter transportation.

2.3 Sampling procedure

For a better understanding of the contribution of biomass burning during smoke-haze periods in Sumatra Island caused by forest and peatland fires as well as crop residue burning, the sampling period included both the rainy season as a background situation and a dry season corresponding to a haze-event in Indonesia. For logistical reasons, a sampling tour by a car using a same ANS was scheduled for the rainy season while a simultaneous sampling using 3 different ANSs at the three sites was conducted during the dry season. Based on the situation at each site, the sampler was installed in a suitable type of shelter. The sampling period and duration of sampling at each site are summarized in Table 1 along with information on the above three sampling sites. Meteorological information during the study period was obtained from the Meteorology, Climatology and Geophysical Agency (BMKG) of Indonesia (BMKG, 2019).

Table 1. Sampling period, duration and meteorological condition in Sumatera Island, Indonesia

Location	Season	Date	Total (n)	Temp (°C)	Humidity (%)	Precipitation (mm)	Sunlight (hour)
Padang (Rural)	Rainy	March 08 th -13 th	5	26.53	89.00	11.2	5.13
	Dry	August 17 th -29 th	8	26.53	89.00	7.5	5.13
Murao Jambi (Suburban)	Rainy	March 14 th -19 th	5	27.35	83.00	4.1	5.32
	Dry	August 17 th -24 th	8	27.86	78.30	0.4	4.46
Pekanbaru (Urban)	Rainy	March 20 th -25 th	5	27.28	80.33	10.0	5.72
	Dry	August 17 th -26 th	8	27.96	80.00	1.8	5.89

Sources: www.bmkg.go.id

2.4 Analysis of carbonaceous components

The thermal/optical analyses of carbonaceous components in particles collected on QFF were conducted on a square, punched filter sample (10 x 15 mm) using a carbon analyzer (Sunset Laboratory, Carbon Aerosol Analyzer), following the IMPROVE protocol (Chow et al., 2004; Han et al., 2007; Kim et al., 2011a, 2011b). Briefly, the OC fractions were determined at four temperature steps in 100% helium: OC1 at 120 °C, OC2 at 250 °C, OC3 at 450 °C, and OC4 at 550 °C. The EC fractions were determined at three temperature steps in a mixture of 2% oxygen and 98% helium: EC1 at 550 °C, EC2 at 700 °C, and EC3 at 800 °C. Prior to each set of carbon analyses, the TC value was calibrated by that of a reference chemical, sucrose (C₁₂H₂₂O₁₁) (196-00015, Sucrose, Wako Pure Chemical Industries, Ltd., Japan). OC was defined as OC1+OC2+OC3+OC4+Py-OC while EC defined as EC1+EC2+EC3-Py-OC, where Py-OC denotes the pyrolyzed fraction of organic carbon. Char-EC defined as EC1-Py-OC and soot-EC defined as EC2 + EC3 were also evaluated (Han et al., 2009). The repeatability of the analyses of the punched filter samples with deposition spots of ambient particles was preliminarily confirmed to be fairly good, with a CV less than 3.2% for OC and 7.9% for EC except 17.8% for EC in particles > 10 µm. The minimum detection limit (MDL) was evaluated as 0.2 µg·cm⁻² and 0.1 µg·cm⁻² respectively for OC and EC based on measured travel blanks of filters (n=5). Samples collected on IF (0.1–0.5 µm) were not analyzed since the thermal/optical method cannot be applied.

2.5 Backward trajectory and hotspots

Following the previous report (Tuti Budiwati, 2016), 72 hours backward trajectories of air parcels arriving at the monitoring sites in Padang, Jambi and Riau at a distance of 500 meters from the average ground level (AGL) were calculated using the Hybrid Single-Particle Lagrangian Integrated Trajectory Model version 4 (HYSPLIT4) (ALR, 2019), where the meteorological data from Global Data Assimilation System (GDAS) (resolution 0.5 degree from the NOAA were used (NOAA, 2019). Geographic locations of hotspots or active fires in Indonesia with a resolution of 1 km × 1 km that are available from Moderate Resolution Imaging Spectroradiometer (MODIS) satellite remote sensing imagery were used to specify possible areas corresponding to biomass burning (MODIS, 2019).

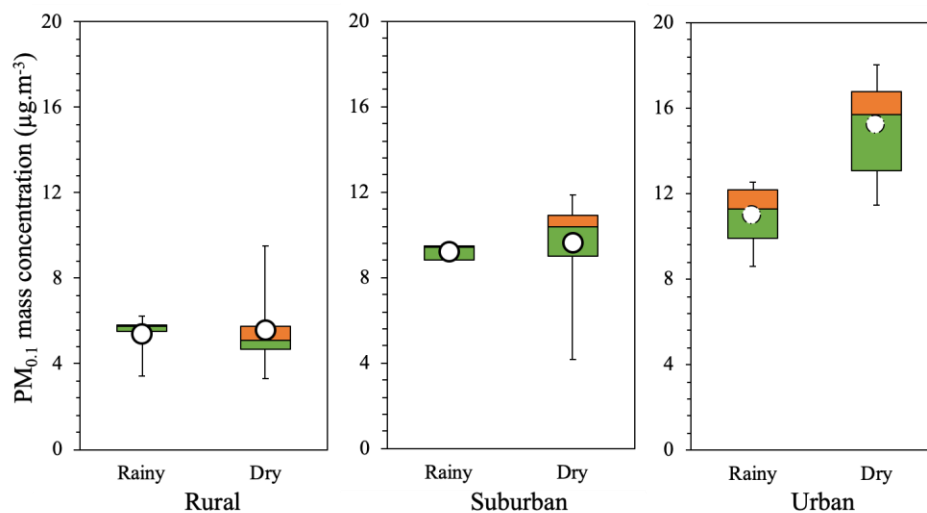
3. Results and Discussion

3.1 Status of PM concentration

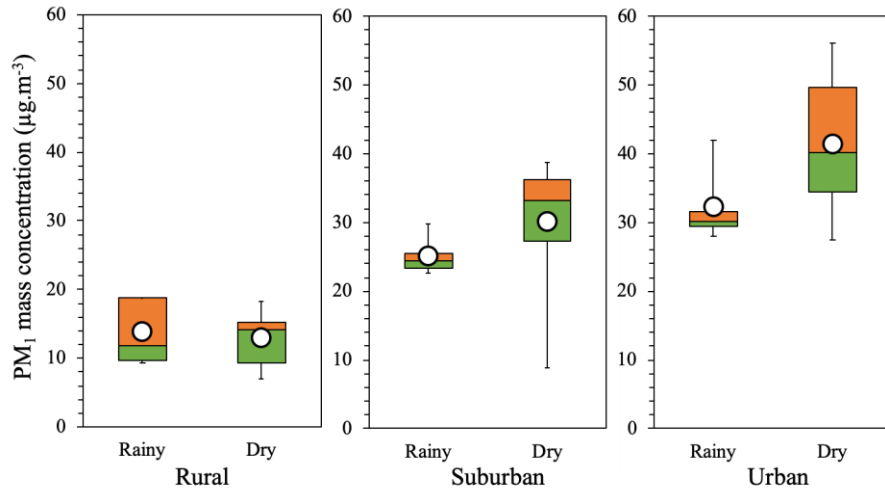
The average mass concentration of PMs at all sites during the rainy and dry seasons are shown in Figure 2(a-e), respectively for PM_{0.1}, PM₁, PM_{2.5}, PM₁₀ and TSP. The average PM₁₀ and PM_{2.5} values in rainy–dry seasons at the urban site (56.0–79.3 and 42.8–59.1 µg·m⁻³, respectively) were always larger than the

WHO guidelines for 24 hours (50 and 25 $\mu\text{g}\cdot\text{m}^{-3}$, respectively) and only the PM_{10} value (48.31 $\mu\text{g}\cdot\text{m}^{-3}$) was less than the guidelines at the sub-urban site while all of the guideline values were satisfied at the rural site. It should be noted that the values were within the National Air Quality Standards of Indonesia (150 and 65 $\mu\text{g}/\text{m}^3$ for PM_{10} and $\text{PM}_{2.5}$, respectively) at all sites. The $\text{PM}_{0.1}$ level in rainy season at sub-urban and urban sites (9.2–9.6 and 10.9–15.6 $\mu\text{g}\cdot\text{m}^{-3}$, respectively) was somewhat similar to those in other large cities in South East Asia (e.g., Bangkok (14.80 \pm 1.99 $\mu\text{g}\cdot\text{m}^{-3}$) (Phairuang et al., 2019) and Hanoi (6.06 \pm 2.71 $\mu\text{g}\cdot\text{m}^{-3}$) (Thuy et al., 2018)) while one at the rural site (5.36–5.57 $\mu\text{g}\cdot\text{m}^{-3}$) was about two times larger than that at a rural site in Kanazawa (2.7 $\mu\text{g}\cdot\text{m}^{-3}$), a local city in Japan (Zhao et al., 2016).

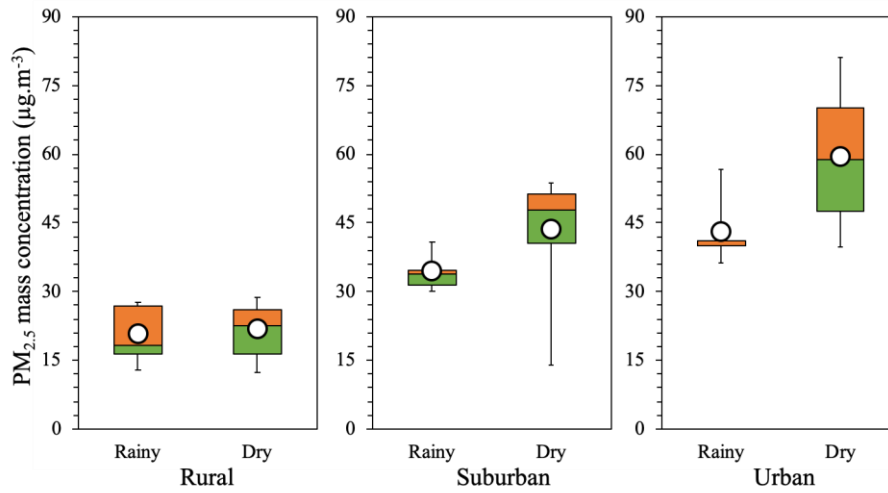
Compared with previous haze-episodes in Indonesia, however, the PM levels in the dry season from this study were much smaller than previously reported data. For example, the $\text{PM}_{2.5}$ level during a haze-episode in year 2012 in Central Kalimantan was up to 7817 $\mu\text{g}\cdot\text{m}^{-3}$ (Betha et al., 2013). During the massive peatland fires in Riau province in June 2013, the PM_{10} level reached unhealthy and hazardous levels in which the PM_{10} level ranged 360–600 $\mu\text{g}\cdot\text{m}^{-3}$ (Kusumaningtyas and Aldrian, 2016). In the most recent serious episode in 2015, the PM_{10} level in Pekanbaru city reached 600 $\mu\text{g}\cdot\text{m}^{-3}$ (Crippa et al., 2016). This may be explained by a drastic decrease in the frequency of peatland fires in year 2016 that was controlled by the Indonesian government (Aminingrum, 2017; Jikalahari., 2018; Saputra, 2019). Figure 3 shows the number of hotspots plotted as an indicator of peatland fires from 2009 to 2018 (ASMC, 2019). There was a periodic fluctuation in the number of hotspots such that increases from May, the beginning of the dry season, reached a peak in July or August then decreased drastically after September, the beginning of the rainy season. The difference in PM_{10} between 2015 and 2018 in Pekanbaru city of ~ 7 times could be reasonably explained by the difference in the peak number of hot spots of ~ 6 times similar to studies reporting a positive correlation between the number of hotspots and pollutant level (Anwar et al., 2010; Gaveau et al., 2014; Kusumaningtyas and Aldrian, 2016).



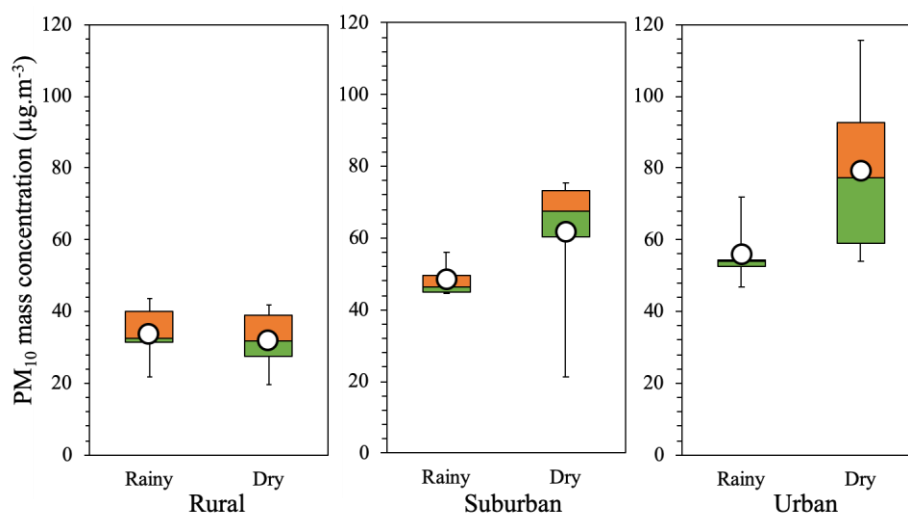
(a) $\text{PM}_{0.1}$



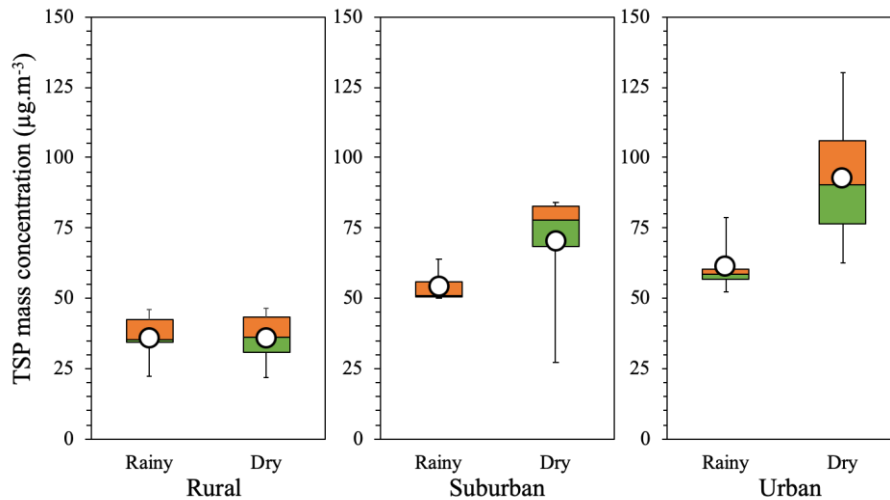
(b) PM₁



(c) PM_{2.5}



(d) PM₁₀



(e) TSP

Figure 2. Seasonal particle mass concentration in Sumatra Island, Indonesia: (a) PM_{0.1}, (b) PM₁, (c) PM_{2.5}, (d) PM₁₀ and (e) TSP.

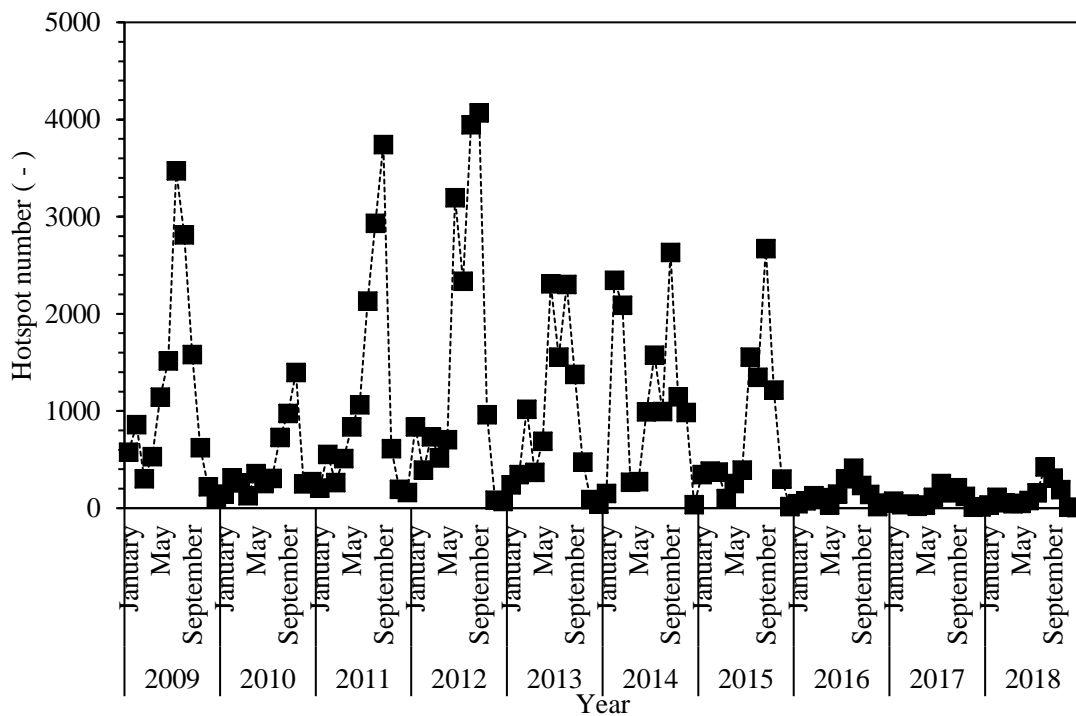


Figure 3. Numbers of yearly hotspots in Sumatra Island (2009-2018), Indonesia.

3.2 Possible influences of local emission sources

Regardless of the season, the PM concentration increased in the order of rural, suburban and urban sites since this would be related to an increase in the amount of pollutants emitted from local sources. Figures 4 and 5 respectively show the size distribution and mass fractions of each size of PMs collected at the studied sites. Size distributions at sub-urban and urban sites were similar with different levels of PM and there was a peak fraction of around 1 μm at which a large difference between those and the rural sites appears. In the dry season, at both the suburban and urban sites, the PM level increased similarly while each size fraction remained nearly constantly. To the contrary, a coarse fraction of $> 1 \mu\text{m}$

dominated the PM mass concentration at the rural site and almost no seasonal difference both in size distribution and PM level was detected, suggesting a different contribution or types of local emission sources. The influence of haze transport by air mass and meteorological conditions are also important parameters.

Figure 6(a–f) show air mass trajectories arriving at each sampling site plotted together with hot spots. The air mass approaching the studied sites in a rainy season was from the South China sea, indicating that the influence of peatland fires may not be so serious in this season, although a slight influence in long range transportation from the upper part of South East Asia cannot be excluded. Hence, differences in the chemical characteristics of PMs between sites in the rainy season should be mainly from local emissions, except for agricultural open burning and also from meteorological conditions. At the rural site, in both rainy and dry seasons, the air mass came from the ocean, or, from the South China sea and the Indian ocean, respectively. Since such an air mass route commonly generates a low particle level (Bousiotis et al., 2018) local emissions could also be discussed in the dry season at rural sites as shown later.

Regarding the possible influence of local emission sources, the level of carbonaceous components listed in Table 2 and the fraction of each component shown in Figure 7(a–e) provide important information. Although one possible reason for almost no seasonal difference in the PM level and particle size distribution at the rural site might be related to a small difference in the total number of rainy days between the rainy and dry seasons due to climate characteristic (BMKG, 2015), it is interesting to note that a larger fraction of diesel soot-like EC, particularly in PM_{0.1}, and an OC/EC ratio (1.27–2.81) smaller than those at other sites (1.36–4.78) was observed at the rural site in the rainy season when the influence of the local open burning of agricultural residues should not be important. As previously described in 2.1.1, this might be related to the influence of a large cement factory while taking into account a lowered importance of traffic emission comparing to other two sites. At sub-urban and urban sites, the tendencies at these sites were similar although a larger fraction of EC in the range of 0.5–1 μm, or a peak size range, was observed. char-EC/soot-EC and soot-EC/TC ratios, that can be attributed to biomass burning and diesel exhaust (Han et al., 2009, 2010), evaluated for peak size ranges (2.22 and 0.08 for the rural, 3.37 and 0.07 for the sub-urban, and 4.45 and 0.08 for the urban sites, respectively) were in the range of the rural and urban categories (Furuuchi et al., 2014). The char-EC/soot-EC ratio for PM_{0.1} was consistently less than unity, indicating it has diesel soot-like characteristics (Phairuang et al., 2019). However, probably because of mixed but similar contributions of emission sources in the corresponding areas, detailed information on the contributions of each source are not very clear, except for carbon. Since both sub-urban and urban sites are located in areas with busy traffic, the characteristics may be similar but with more influences from emission sources at the urban site.

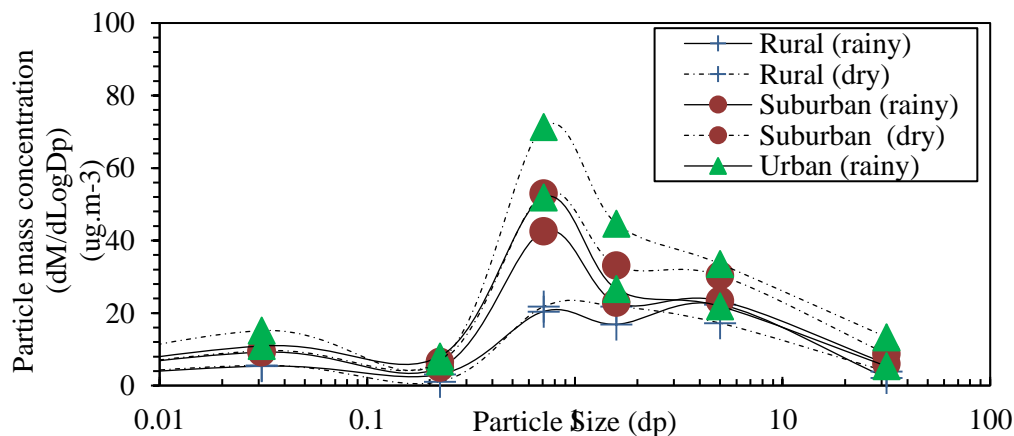


Figure 4. Particle size distribution observed at the study sites in Sumatra-Island.

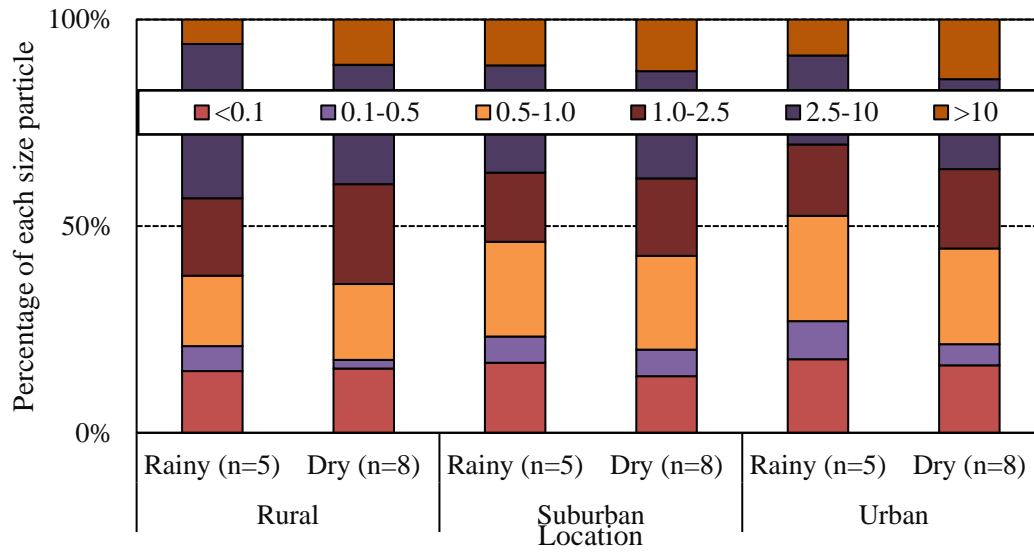
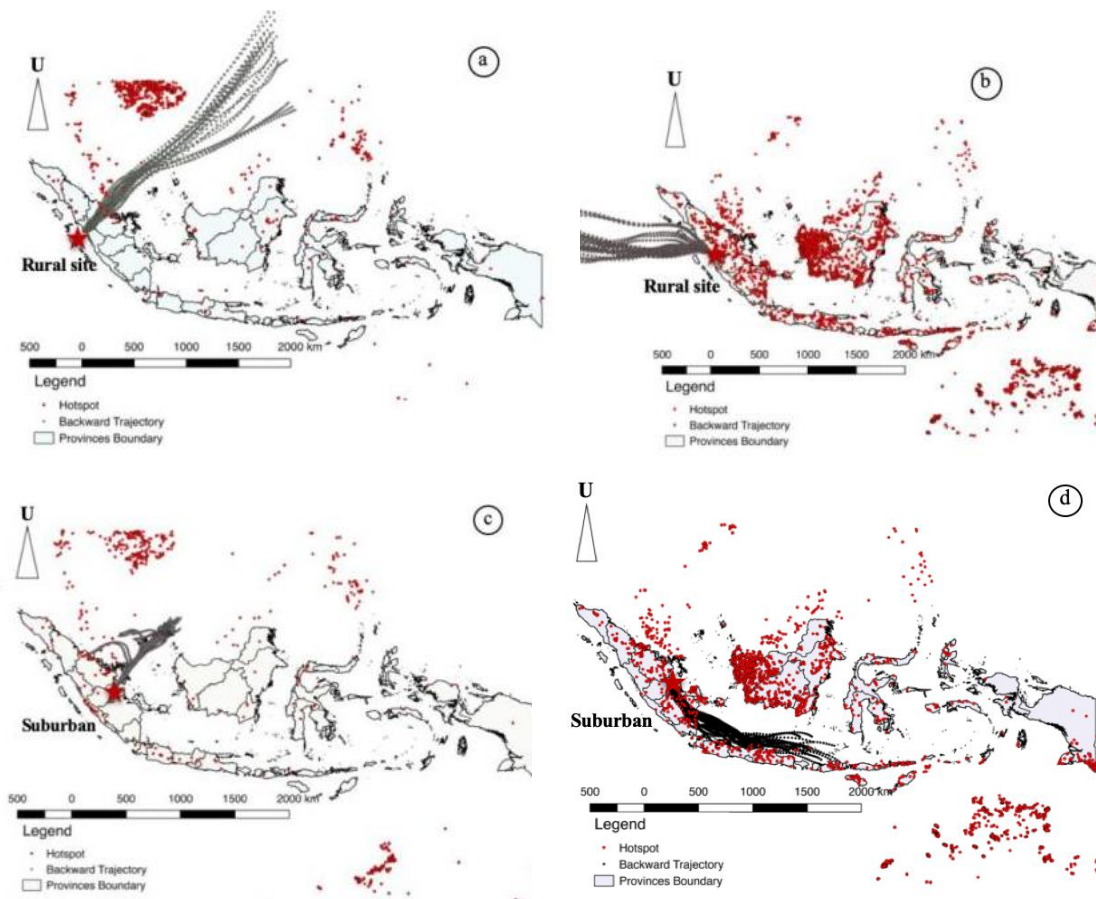


Figure 5. Size fraction of particles on mass basis observed at study sites in Sumatra Island



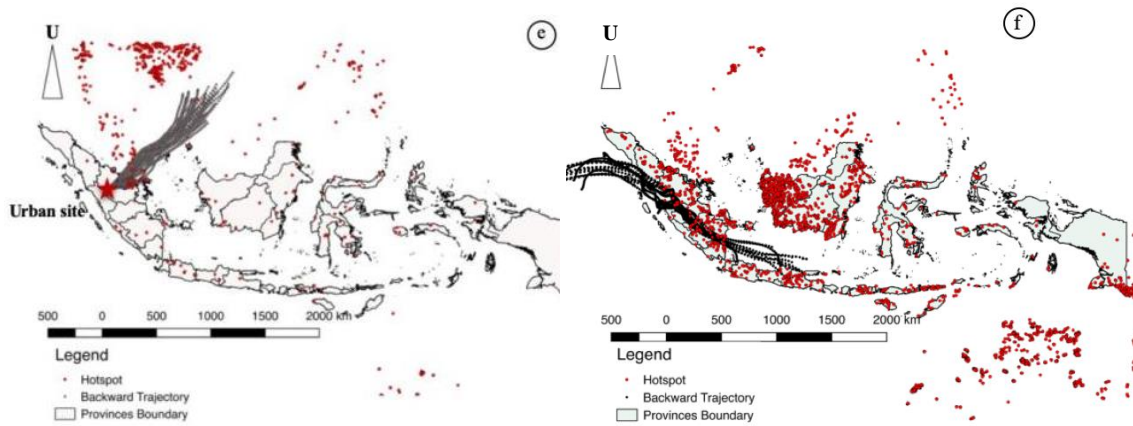
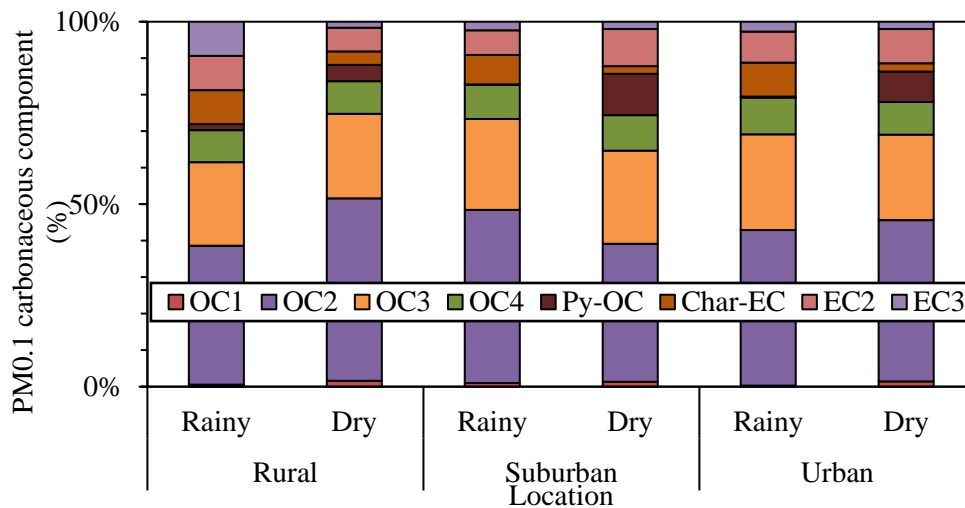
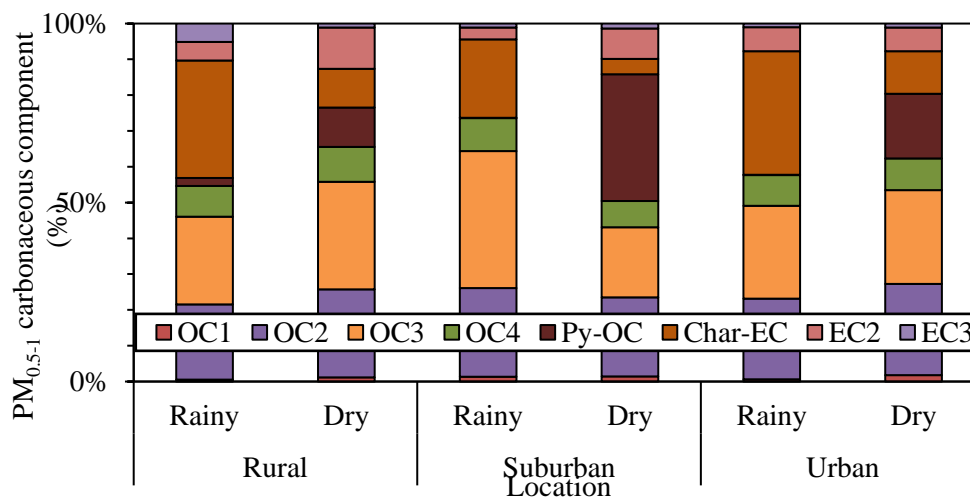


Figure 6. Seasonal air mass backward trajectory in Sumatra Island (a) rural (rainy season), (b) rural (dry season), (c) suburban (rainy season), (d) suburban (dry season), (e) urban (rainy season) and (f) urban (dry season).



(a)



(b)

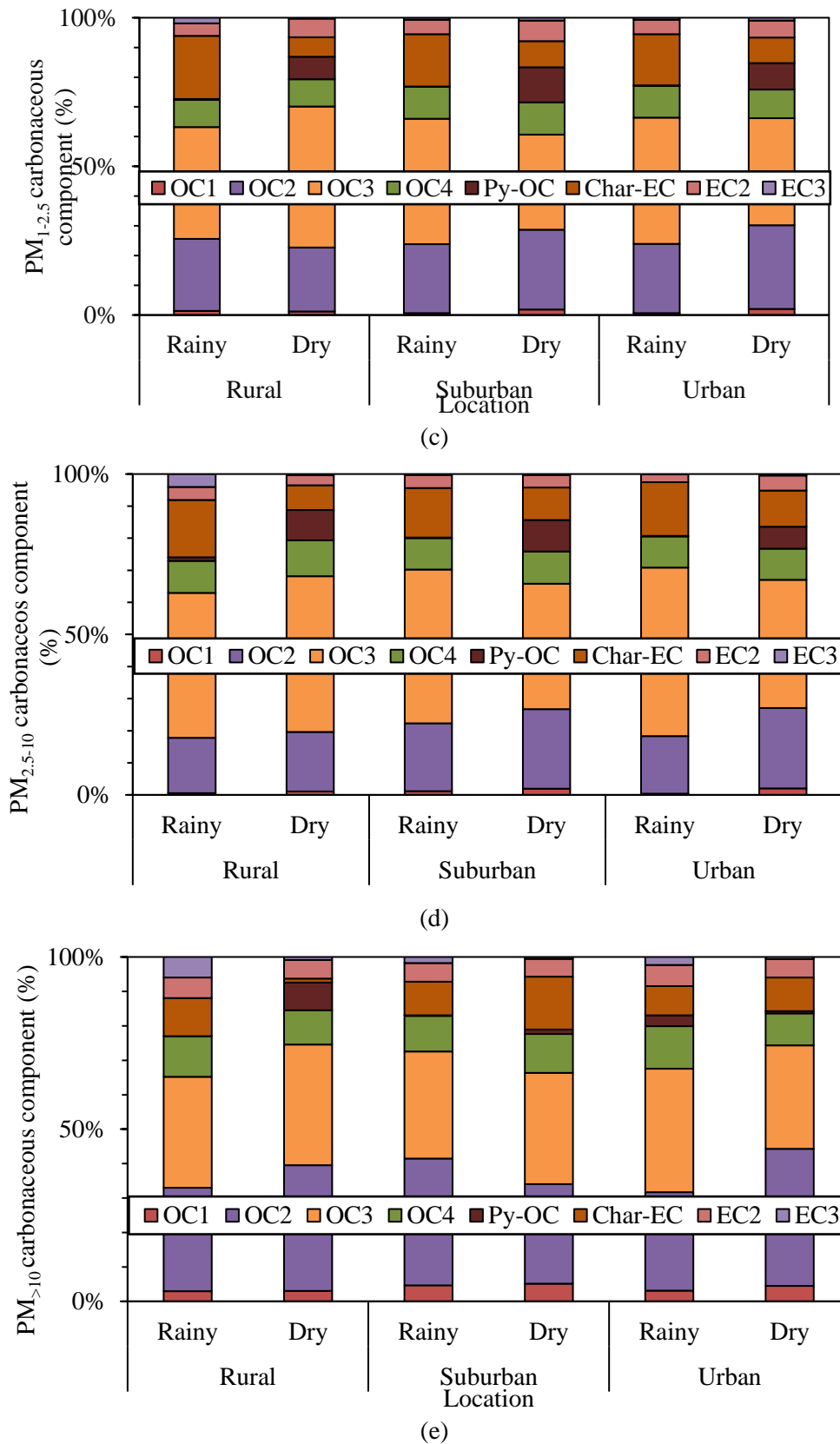


Figure 7. Fractions of carbonaceous components in (a) PM_{0.1}, (b) PM_{0.5-1}, (c) PM_{1-2.5}, (d) PM_{2.5-10} and (e) PM_{>10} in the rainy and dry seasons.

Table 2. Seasonal average concentrations of carbonaceous components in Sumatera Island
(a)

Location	Season	Size of PM	OC ($\mu\text{g}/\text{m}^3$)	EC ($\mu\text{g}/\text{m}^3$)	OC/EC (-)	Char-EC ($\mu\text{g}/\text{m}^3$)	Soot-EC ($\mu\text{g}/\text{m}^3$)	Char-EC/Soot-EC (-)
Rural	Rainy	<0.1	2.71	1.08	2.51	0.36	0.72	0.50
		0.5-1	1.84	1.45	1.27	1.11	0.35	3.19
		1-2.5	1.84	0.77	2.39	0.50	0.27	1.85
		2.5-10	1.68	0.60	2.81	0.41	0.19	2.22
		>10	0.22	0.06	3.35	0.03	0.03	0.93
	Dry	<0.1	1.49	0.21	7.08	0.07	0.14	0.46
		0.5-1	0.65	0.23	2.79	0.11	0.13	0.86
		1-2.5	0.94	0.15	6.05	0.08	0.08	1.00
		2.5-10	1.01	0.14	7.10	0.10	0.05	2.16
		>10	0.14	0.01	11.33	0.00	0.01	0.19
Suburban	Rainy	<0.1	2.67	0.56	4.81	0.26	0.29	0.89
		0.5-1	1.37	0.66	2.08	0.51	0.15	3.37
		1-2.5	1.71	0.44	3.92	0.33	0.10	3.21
		2.5-10	2.67	0.66	4.04	0.52	0.14	3.57
		>10	0.31	0.06	4.88	0.04	0.03	1.37
	Dry	<0.1	1.86	0.36	5.20	0.05	0.30	0.17
		0.5-1	1.24	0.35	3.56	0.11	0.24	0.43
		1-2.5	1.40	0.33	4.29	0.17	0.15	1.13
		2.5-10	1.25	0.24	5.28	0.17	0.07	2.42
		>10	0.21	0.06	3.69	0.04	0.02	2.68
Urban	Rainy	<0.1	2.34	0.60	3.87	0.27	0.33	0.83
		0.5-1	1.26	0.92	1.37	0.75	0.17	4.45
		1-2.5	1.45	0.43	3.40	0.32	0.10	3.09
		2.5-10	1.90	0.46	4.17	0.40	0.06	6.48
		>10	0.23	0.05	4.71	0.02	0.02	1.01
	Dry	<0.1	2.85	0.50	5.71	0.08	0.42	0.20
		0.5-1	2.33	0.73	3.18	0.44	0.29	1.52
		1-2.5	1.97	0.39	4.98	0.22	0.17	1.28
		2.5-10	1.77	0.38	4.67	0.26	0.12	2.17
		>10	0.29	0.06	5.31	0.03	0.02	1.64

(b)

Location	Season	Size of PM	TC ($\mu\text{g}/\text{m}^3$)	MC ($\mu\text{g}/\text{m}^3$)	TC/MC (%)	Soot-EC/TC (-)	Py-OC/OC4 (-)
Rural	Rainy	<0.1	3.79	5.36	70.64	0.19	0.19
		0.5-1	3.30	6.15	53.57	0.10	0.26
		1-2.5	2.61	6.73	38.77	0.10	0.04
		2.5-10	2.28	13.44	17.00	0.08	0.11
		>10	0.28	2.13	13.15	0.12	0.00049
	Dry	<0.1	1.70	5.57	30.44	0.08	0.49
		0.5-1	0.88	6.56	13.45	0.13	1.12
		1-2.5	1.09	8.69	12.57	0.07	0.83
		2.5-10	1.15	10.36	11.12	0.04	0.85
		>10	0.15	3.92	3.80	0.06	0.816
Suburban	Rainy	<0.1	3.22	9.20	35.04	0.09	0.01
		0.5-1	2.03	12.45	16.29	0.07	0.02
		1-2.5	2.14	9.09	23.58	0.05	0.01
		2.5-10	3.33	14.09	23.62	0.04	0.01
		>10	0.37	6.05	6.19	0.07	0.013

Location	Season	Size of PM	TC ($\mu\text{g}/\text{m}^3$)	MC ($\mu\text{g}/\text{m}^3$)	TC/MC (%)	Soot-EC/TC (-)	Py-OC/OC4 (-)
Urban	Dry	<0.1	2.21	9.61	23.05	0.12	1.15
		0.5-1	1.59	15.94	9.98	0.10	4.83
		1-2.5	1.73	13.18	13.11	0.08	1.09
		2.5-10	1.48	18.28	8.10	0.04	0.97
		>10	0.26	8.77	2.99	0.06	0.114
	Rainy	<0.1	2.94	10.92	26.97	0.11	0.02
		0.5-1	2.18	15.64	13.94	0.08	0.01
		1-2.5	1.88	10.61	17.70	0.06	0.01
		2.5-10	2.36	13.17	17.91	0.03	0.01
		>10	0.27	5.35	5.12	0.08	0.254
Urban	Dry	<0.1	3.35	15.16	22.13	0.11	0.93
		0.5-1	3.07	21.48	14.27	0.08	2.07
		1-2.5	2.36	17.79	13.27	0.07	0.92
		2.5-10	2.15	20.20	10.62	0.05	0.71
		>10	0.35	13.36	2.62	0.06	0.064

3.3 Influences of peat land fires and air mass transportation

As the air mass trajectory shown in Figure 6 describes, the air mass passing through peatland areas arrived at the study sites in the dry season except the rural site so that it should have a large influence particularly at the sub-urban and urban sites. The air mass arriving the sub-urban site in the dry season (See Figure 4(e)) moved through the South Sumatera Province that was covered with many hot spots corresponding to the burning of agricultural crop residue and peatland fires that emit a considerable amount of PMs (Permadi and Kim Oanh, 2013). Although the air mass movement to the urban site was not as simple as that to the sub-urban site, an important fraction of trajectories still moved through hot spot areas (See Figure 4(f)).

The OC, EC and OC/EC were increased at all locations in the dry season and fine and ultrafine fractions ($\text{PM}_{0.1}$ and $\text{PM}_{0.5-1}$) were found to contain a higher fraction of carbon (See Table 2). The OC/EC ratio was somewhat similar between the sites (5.20–7.08) in the dry season, indicating that biomass burning events in Sumatra Island was the main reason for the significant increase in the OC/EC ratio as so far reported (Fujii et al., 2015). An increase in the OC/EC ratio was very clear, particularly in $\text{PM}_{0.1}$: in the order of rainy–dry seasons, 2.51 ± 1.01 – 7.08 ± 2.22 at the rural, 4.81 ± 0.82 – 5.20 ± 1.04 at the suburban and 3.87 ± 0.48 – 5.71 ± 2.38 at urban sites. Compared to previous studies in the dry season, OC/EC values in this study were comparable with those reported by Hayasaka et al (2014) at urban and rural sites located in Central Kalimantan (3.88–14.75 in 2010–2012). The much lower values than those in the dry season in Riau province (36.4 ± 9.08 in 2012) (Fujii et al., 2015) may be explained by a larger difference in the emitted amount of PM and the conditions in the vicinity of the sampling site. The nearly no seasonal difference in $\text{PM}_{0.1}$ levels with a large difference in the OC/EC ratio may be related to a difference in the contribution from factories caused by changes in a small scale climate in the corresponding area, such as wind direction and the formation of thermal inversions (Bachtiar et al., 2016).

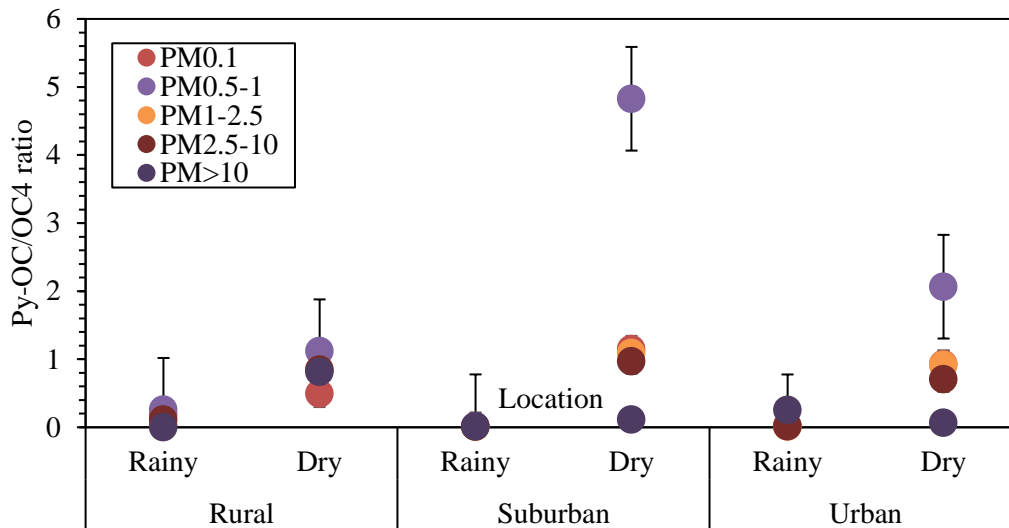


Figure 8. Seasonal Pyrolysis-OC (Py-OC)/OC4 ratio observed at the study sites in Sumatra-Island.

As seen from Fig.7, in the dry season, OC1, that was negligible in rainy season, and Py-OC increased in all size fractions of particles at all sites. This is particularly true for Py-OC in a core PM fraction (0.5–1 μ m) at the suburban site, indicating that biomass burning had a significant influence on the results. A ratio of Py-OC/OC4, a key parameter of the peatland fire suggested by Fujii et al. (2015), may also explain the above situation with the air mass movement as shown in Figure 8. The Py-OC/OC4 ratio increased in the dry season especially for fine and ultrafine fractions as PM_{0.1-0.5} and PM_{0.1}, and the largest peak appeared in a core fraction (0.5–1 μ m) at the sub-urban site. A reported behavior of PM_{0.1} that is originally of diesel soot-like characteristics but also sensitive to an influence of biomass burning (Phairuang et al., 2019) could be confirmed here by the Py-OC/OC4 ratio. A reason for why a clear influence of biomass burning in terms of the Pyr-OC/OC4 ratio was also found at the rural site, where the contribution of air mass transportation appears to be not very important both in rainy and dry seasons, might be attributed to open biomass burning in local communities.

4. Conclusion

Seasonal behaviors of size-segregated particulate matter (PM) in Sumatra Island, Indonesia were investigated based on air sampling at three different locations in the year 2018 by using a cascade air sampler that can collect size-segregated particulate matter down to PM_{0.1}. Carbonaceous components of size fractionated particles were analyzed by a thermal/optical method and possible local emission sources were discussed in conjunction with the movement of air masses over burned areas, or hot spots. The PM_{2.5} and PM₁₀ levels at all sites were below the NAQS for Indonesia while those at sub-urban and urban sites exceeded the WHO guidelines for a 24 hour period. PM_{0.1} levels in sub-urban and urban area were similar to those in large cities in East Asia. The present PM level was much lower than data reported prior to 2016 since the Indonesian government started controlling peatland fires in 2016. The influence of peatland fires in the dry season was significant in cities located on the east coast of Sumatra Island because of the larger number of hotspots and air mass trajectories along the coast. A clear increase in the OC/EC ratio in the dry season was found for fine fractions as PM_{0.1}. Although the detailed contribution of local sources remains unclear, at the rural site, it is possible that the PM_{0.1} level may have been affected by a local cement factory near the rural site in the rainy season and local biomass burning in the dry season. The Py-OC/OC4 ratio was found to be useful in discussing the influence of biomass burning. Using the Py-OC/OC4 ratio, PM_{0.1} was shown to be sensitive to biomass burning. These data will help in understanding the atmospheric aerosol and carbon components in Indonesia.



5. References

- Abdul Halim, N.D., Latif, M.T., Ahamad, F., Dominick, D., Chung, J.X., Juneng, L., Khan, M.F., 2018. The long-term assessment of air quality on an island in Malaysia. *Heliyon* 4.
- Air Resource Laboratory (ALR), 2019. The air resource laboratory (HYSPLIT 4). <http://ready.arl.noaa.gov/HYSPLIT.php>. (Accessed 10 August 2019).
- Aminingrum, 2017. Forest Fire Contest : The Case of Forest Fire Policy Design in Indonesia.
- Anwar, A., Juneng, L., Othman, M.R., Latif, M.T., 2010. Correlation between hotspots and air quality in Pekanbaru, Riau, Indonesia in 2006-2007. *Sains Malaysiana* 39, 169–174.
- Bachtiar, Vera Surtia & Ruslinda, Yenni & Wangsa, Dharma & Kurniawan, Ekho. (2016). Mapping of PM 10 Concentrations and Metal Source Identifications in Air Ambient at Surrounding Area of Padang Cement Factory. *Journal of Environmental Science and Technology*. 9. 390-398.
- Badan Meteorologi, Klimatologi, dan Geofisika (BMKG). 2015. Indonesia
- Badan Meteorologi, Klimatologi, dan Geofisika (BMKG). 2019. Indonesia
- Badan Pusat Statistik (BPS-Statistics of Muaro Jambi Regency).2018.Muaro Jambi in Figure. Muaro Jambi, Indonesia: BPS
- Badan Pusat Statistik (BPS-Statistics of Padang City).2018. Padang City in Figure. Padang, Indonesia: BPS
- Badan Pusat Statistik (BPS-Statistics of Pekanbaru City).2018. Pekanbaru City in Figure. Pekanbaru, Indonesia: BPS
- Betha, R., Pradani, M., Lestari, P., Joshi, U.M., Reid, J.S., Balasubramanian, R., 2013. Chemical speciation of trace metals emitted from Indonesian peat fires for health risk assessment. *Atmospheric Research* 122, 571–578.
- Blanco-Becerra, L.C., Gáfarro-Rojas, A.I., Rojas-Roa, N.Y., 2015. Influence of precipitation scavenging on the PM_{2.5}/PM₁₀ ratio at the Kennedy locality of Bogotá, Colombia. *Revista Facultad de Ingeniería* 2015, 58–65.
- BMKG, 2015. Meteorology, Climatology, and Geophysics Agency of Indonesia.
- Bousiotis, Dimitrios & Dall'osto, Manuel & Beddows, David & Pope, F. & Harrison, Roy. 2018. Analysis of New Particle Formation (NPF) Events at Nearby Rural, Urban Background and Urban Roadside Sites. *Atmospheric Chemistry and Physics Discussions*. 1-51. 10.5194/acp-2018-1057.
- Calderón-Garcidueñas, Lilian & Mora-Tiscareño, Antonieta & Ontiveros, Esperanza & Gomez-Garza, Gilberto & Barragan, Gerardo & Broadway, James & Chapman, Susan & Valencia-Salazar, Gildardo & Jewells, Valerie & Maronpot, Robert & Henríquez-Roldán, Carlos & Pérez-Guillé, Beatriz & Torres-Jardón, Ricardo & Herrit, Lou & Brooks, Diane & Osnaya, Norma & Monroy, Maria & González-Maciél, Angélica & Rafael, Reynoso & Engle, Randall. 2008. Air pollution, cognitive deficits and brain abnormalities: A pilot study with children and dogs. *Brain and Cognition*. 68. 117-127.
- Cao, G., Zhang, X., Zheng, F., 2006. Inventory of black carbon and organic carbon emissions from China. *Atmospheric Environment* 40, 6516–6527.

Cao, J.J., Wu, F., Chow, J.C., Lee, S.C., Li, Y., Chen, S.W., An, Z.S., Fung, K.K., Watson, J.G., Zhu, C.S., 2005. Characterization and source apportionment of atmospheric organic and elemental carbon during fall and winter of 2003 in Xi'an, China 3127–3137.

Chen, J., Li, C., Ristovski, Z., Milic, A., Gu, Y., Islam, M.S., Wang, S., Hao, J., Zhang, H., He, C., Guo, H., Fu, H., Miljevic, B., Morawska, L., Thai, P., Fat, Y., Pereira, G., Ding, A., Huang, X., Dumka, U.C., 2017. Science of the Total Environment A review of biomass burning : Emissions and impacts on air quality , health and climate in China. *Science of the Total Environment*, The 579, 1000–1034.

Chen, J., Yu, X., Sun, F., Lun, X., Fu, Y., Jia, G., Zhang, Z., Liu, X., Mo, L., Bi, H., 2015. The concentrations and reduction of airborne particulate matter (PM₁₀, PM_{2.5}, PM₁) at shelterbelt site in Beijing. *Atmosphere* 6, 650–676.

Chen, S.C., Hsu, S.C., Tsai, C.J., Chou, C.C.K., Lin, N.H., Lee, C. Te, Roam, G.D., Pui, D.Y.H., 2013. Dynamic variations of ultrafine, fine and coarse particles at the Lu-Lin background site in East Asia. *Atmospheric Environment* 78, 154–162.

Chen, Y., Xie, S., Luo, B., Zhai, C., 2017. Particulate pollution in urban Chongqing of southwest China: Historical trends of variation, chemical characteristics and source apportionment. *Science of the Total Environment* 584–585, 523–534.

Chow, J.C., Watson, J.G., Chen, L.W.A., Arnott, W.P., Moosmüller, H., Fung, K., 2004. Equivalence of elemental carbon by thermal/optical reflectance and transmittance with different temperature protocols. *Environmental Science and Technology* 38, 4414–4422.

Chow, J.C., Watson, J.G., Chen, L.W.A., Chang, M.C.O., Robinson, N.F., Trimble, D., Kohl, S., 2007. The IMPROVE_A temperature protocol for thermal/optical carbon analysis: Maintaining consistency with a long-term database. *Journal of the Air and Waste Management Association* 57, 1014–1023.

Crippa, P., Castruccio, S., Archer-Nicholls, S., Lebron, G.B., Kuwata, M., Thota, A., Sumin, S., Butt, E., Wiedinmyer, C., Spracklen, D. V., 2016. Population exposure to hazardous air quality due to the 2015 fires in Equatorial Asia. *Scientific Reports* 6, 1–9.

Fujii, Y., Kawamoto, H., Tohno, S., Oda, M., Iriana, W., Lestari, P., 2015. Characteristics of carbonaceous aerosols emitted from peatland fire in Riau, Sumatra, Indonesia (2): Identification of organic compounds. *Atmospheric Environment* 110, 1–7.

Furuuchi, M., Eryu, K., Nagura, M., Hata, M., Kato, T., Tajima, N., Sekiguchi, K., Ehara, K., Seto, T., Otani, Y., 2010. Development and performance evaluation of air sampler with inertial filter for nanoparticle sampling. *Aerosol and Air Quality Research* 10, 185–192.

Furuuchi, M Ryousuke Hosokawa, Mitsuhiko Hata, Hang Peou, Hu, Seingheng , Try Sophal , Posry Ung and Shinji Tsukawaki. 2015. Characteristics of Ambient Nanoparticulates and Emission Sources in Urban Area of Cambodia. *Proceedings of 9 th International Aerosol Conference (IAC)*, August 28 th -September 2 nd ,2014, Busan, Korea.

Gaveau, D.L.A., Salim, M.A., Hergoualc'H, K., Locatelli, B., Sloan, S., Wooster, M., Marlier, M.E., Molidena, E., Yaen, H., DeFries, R., Verchot, L., Murdiyarso, D., Nasi, R., Holmgren, P., Sheil, D., 2014. Major atmospheric emissions from peat fires in Southeast Asia during non-drought years: Evidence from the 2013 Sumatran fires. *Scientific Reports* 4, 1–7.



- Gugamsetty, B., Wei, H., Liu, C.N., Awasthi, A., Tsai, C.J., Roam, G.D., Wu, Y.C., Chen, C.F., 2012. Source Characterization and Apportionment of PM₁₀, PM_{2.5} and PM_{0.1} by Using Positive Matrix Factorization. *Aerosol and Air Quality Research* 12, 476–491.
- Han, Y., Cao, J., Chow, J.C., Watson, J.G., 2007. Evaluation of the thermal / optical reflectance method for discrimination between char- and soot-EC 69, 569–574.
- Han, Y.M., Lee, S.C., Cao, J.J., Ho, K.F., An, Z.S., 2009. Spatial distribution and seasonal variation of char-EC and soot-EC in the atmosphere over China. *Atmospheric Environment* 43, 6066–6073.
- Hata, Mitsuhiro & Chomanee, Jiraporn & Thongyen, Thunyapat & Bao, Linfa & Tekasakul, Surajit & Tekasakul, Perapong & Otani, Yoshio & Furuuchi, Masami. (2014). Characteristics of nanoparticles emitted from burning of biomass fuels. *Journal of Environmental Sciences*. 26. 10
- Hayasaka, H., Noguchi, I., Putra, E.I. ndr., Yulianti, N., Vadrevu, K., 2014. Peat-fire-related air pollution in Central Kalimantan, Indonesia. *Environmental pollution (Barking, Essex : 1987)* 195, 257–266.
- Heil, A., Goldammer, J.G., 2001. Smoke-haze pollution: a review of the 1997 episode in Southeast Asia. *Regional Environmental Change* 2, 24–37.
- Heil, A., Langmann, B., Aldrian, E., 2007. Indonesian peat and vegetation fire emissions: Study on factors influencing large-scale smoke haze pollution using a regional atmospheric chemistry model. *Mitigation and Adaptation Strategies for Global Change* 12, 113–133.
- Hendrasto, M. & Suro, & Budianto, A. & Kristianto, & Triastuty, Hetty & Haerani, N. & Basuki, A. & Suparman, Yasa & Primulyana, Sofyan & Prambada, Oktory & Loeqman, A. & Indrastuti, Novianti & Andreas, A.S. & Rosadi, U. & Adi, S. & Iguchi, Masato & Ohkura, Takahiro & Nakada, Setsuya & Yoshimoto, M.. 2012. Evaluation of volcanic activity at sinabung volcano, after more than 400 years of quiet. 7. 37-47.
- Jikalahari. Catatan Akhir Tahun 2018. 2018. Hutan Binasa, Banjir Melanda; Jikalahari: Pekanbaru, Riau,
- Kim, K.H., Sekiguchi, K., Furuuchi, M., Sakamoto, K., 2011a. Seasonal variation of carbonaceous and ionic components in ultrafine and fine particles in an urban area of Japan. *Atmospheric Environment* 45, 1581–1590.
- Kim, K.H., Sekiguchi, K., Kudo, S., Sakamoto, K., 2011b. Characteristics of atmospheric elemental carbon (char and soot) in ultrafine and fine particles in a roadside environment, Japan. *Aerosol and Air Quality Research* 11, 1–12.
- Kim, Y.J., Kim, K.W., Kim, S.D., Lee, B.K., Han, J.S., 2006. Fine particulate matter characteristics and its impact on visibility impairment at two urban sites in Korea: Seoul and Incheon. *Atmospheric Environment* 40, 593–605.
- Kopplitz, S.N., Mickley, L.J., Marlier, M.E., Buonocore, J.J., Kim, P.S., Liu, T., Sulprizio, M.P., DeFries, R.S., Jacob, D.J., Schwartz, J., Pongsiri, M., Myers, S.S., Myers, Kopplitz, S.N., Mickley, L.J., Marlier, M.E., Buonocore, J.J., Kim, P.S., Liu, T., Sulprizio, M.P., Fries, R.S. De, Jacob, D.J., Schwartz, J., Pongsiri, M., Samuel, S., 2016. Public health impacts of the severe haze in Equatorial Asia in September–October 2015: demonstration of a new framework for informing fire management strategies to reduce downwind smoke exposure. *Environmental Research Letters* 11, 94023.

- Kopplitz, S.N., Mickley, L.J., Marlier, M.E., Ponette-gonzález, A.G., Lisa, M., Pittman, A.M., Mead, M.I., Castruccio, S., Latif, M.T., Nadzir, M.S.M., Dominick, D., Thota, A., Crippa, P., 2015. Impact of the 2015 wildfires on Malaysian air quality and exposure : a comparative study of observed and modeled data OPEN ACCESS Impact of the 2015 wildfires on Malaysian air quality and exposure : a comparative study of observed and modeled data.
- Kumar, S., Aggarwal, S.G., Sarangi, B., Malherbe, J., Barre, J.P.G., Berail, S., Séby, F., Donard, O.F.X., 2018. Understanding the Influence of Open-waste Burning on Urban Aerosols using Metal Tracers and Lead Isotopic Composition 2433–2446.
- Kusumaningtyas, S.D.A., Aldrian, E., 2016. Impact of the June 2013 Riau province Sumatera smoke haze event on regional air pollution. *Environmental Research Letters* 11.
- Levine, J.S., 1999. The 1997 fires in Kalimantan and Sumatra, Indonesia: Gaseous and particulate emissions. *Geophysical Research Letters* 26, 815–818.
- Muraleedharan, T.R., Radojevic, M., Waugh, A., Caruana, A., 2000. Chemical characterisation of the haze in Brunei Darussalam during the 1998 episode. *Atmospheric Environment* 34, 2725–2731.
- Nowak, D.J., Hirabayashi, S., Doyle, M., McGovern, M., Pasher, J., 2018. Air pollution removal by urban forests in Canada and its effect on air quality and human health. *Urban Forestry and Urban Greening* 29, 40–48.
- Osunsanya, T., G. Prescott, A. Seaton, 2001: Acute respiratory effects of particles: mass or number? – *Occup. Environ. Medicine* 58, 154–159.
- Otani, Y., Eryu, K., Furuuchi, M., Tajima, N. and Tekasakul, P. (2007). Inertial classification of nanoparticles with fibrous filters. *Aerosol Air Qual. Res.* 7: 343–352.
- Otani, Yoshio & Eryu, Kazunobu & Furuuchi, Masami & Tajima, Naoko & Tekasakul, Perapong. 2007. Inertial Classification of Nanoparticles with Fibrous Filters. *Aerosol and Air Quality Research.* 7. 343-352.
- Pekkanen, J., Timonen, K.L., Ruuskanen, J., Reponen, A., Mirme., A. Effects of ultrafine and fine particles in urban air on peak expiratory flow among children with asthmatic symptoms. *Environ. Res.*, 74 (1997), pp. 24-33.
- Pentamwa, P., Oanh, N.T.K., 2008. Air quality in Southern Thailand during haze episode in relation to air mass trajectory. *Songklanakarin Journal of Science and Technology* 30, 539–546.
- Permadi, D.A., Kim Oanh, N.T., 2013. Assessment of biomass open burning emissions in Indonesia and potential climate forcing impact. *Atmospheric Environment* 78, 250–258.
- Phairuang, W., Hata, M., Furuuchi, M., 2017. Influence of agricultural activities, forest fires and agro-industries on air quality in Thailand. *Journal of Environmental Sciences (China)* 52, 85–97.
- Phairuang, W., Suwattiga, P., Chetiyankornkul, T., Hongtieab, S., Limpaseni, W., Ikemori, F., Hata, M., Furuuchi, M., 2019. The influence of the open burning of agricultural biomass and forest fires in Thailand on the carbonaceous components in size-fractionated particles. *Environmental Pollution*.
- Quah, E., Varkkey, H.M., 2013. The political economy of transboundary pollution: mitigation of forest fires and haze in Southeast Asia. *The Asian Community: Its Concepts and Prospects* 323–358.



- Radojevic, M., 2003. Chemistry of forest fires and regional haze with emphasis on Southeast Asia. *Pure and Applied Geophysics* 160, 157–187.
- Reddington, C.L., Yoshioka, M., Balasubramanian, R., Ridley, D., Toh, Y.Y., Arnold, S.R., Spracklen, D. V., 2014. Contribution of vegetation and peat fires to particulate air pollution in Southeast Asia. *Environmental Research Letters* 9.
- Rogula-Kozłowska, W. 2016. Size-segregated urban particulate matter: mass closure, chemical composition, and primary and secondary matter content, *Air Quality, Atmosphere & Health*. 9: 533-550
- Saputra, Erlis. 2019. Beyond Fires and Deforestation: Tackling Land Subsidence in Peatland Areas, a Case Study from Riau and Indonesia. *Land*. 8. 76.
- Sankaran, T.L.S.A.C., 2015. The Impact of Indonesian Forest Fires on Singaporean Pollution and Health 2015.
- Siao, W.S., Balasubramanian, R., Rianawati, E., Karthikeyan, S., Streets, D.G., 2007. Characterization and source apportionment of particulate matter $\leq 2.5 \mu\text{m}$ in Sumatra, Indonesia, during a recent peat fire episode. *Environmental Science and Technology* 41, 3488–3494.
- Tacconi, L., 2002. Fires in Indonesia: Causes, Costs and Policy Implications. Center for International Forestry Research (CIFOR) Bogor, Indonesia 96, 1283–1285. Tata, H.L., Narendra, B.H., 2018. Forest and land fires in Pelalawan District , Riau , Indonesia : Drivers , pressures , impacts and responses 19, 544–551.
- Terzano, C., Di Stefano, F., Conti, V., Graziani, E. and Petroianni, A. 2010. Air Pollution Ultrafine Particles: Toxicity beyond the Lung. *Eur. Rev. Med. Pharmacol. Sci.* 14: 809–821.
- Thuy, Nguyen & Dung, Nghiem & Sekiguchi, Kazuhiko & Ly, Bich Thuy & Hien, Nguyen & Yamaguchi, Ryosuke. (2018). Mass Concentrations and Carbonaceous Compositions of PM_{0.1}, PM_{2.5}, and PM₁₀ at Urban Locations of Hanoi, Vietnam. *Aerosol and Air Quality Research*. 18. 10.4209/aaqr.2017.11.0502.
- Vadrevu, K.P., Lasko, K., Giglio, L., Justice, C., 2014. Analysis of Southeast Asian pollution episode during June 2013 using satellite remote sensing datasets. *Environmental Pollution* 195, 245–256.
- Velasco, E., Rastan, S., 2015. Air quality in Singapore during the 2013 smoke-haze episode over the Strait of Malacca: Lessons learned. *Sustainable Cities and Society* 17, 122–131.
- Wahyuni Nurwihastuti, D., Juli Dwi Astuti, A., Yuniastuti, E., Bungana Beru Perangin-Angin, R., Simanungkalit, N.M., 2019. Volcanic hazard analysis of sinabung volcano eruption in karo north sumatra indonesia. *Journal of Physics: Conference Series* 1175, 12186.
- Wichmann, C., Serin, R., & Motiuk, L. (2000). Predicting suicide attempts among male offenders in federal penitentiaries (Research Report R-91). Ottawa, Ontario: Research Branch, Correctional Service of Canada.
- Zhao, Tianren & Hongtieab, Surapa & Hata, Mitsuhiro & Matsuki, Atsushi & Yoshikawa, Fumie & Furuuchi, Masami. (2016). Characteristics comparison of ambient Nano-particles in Asian cities.



18th World Clean Air Congress, 23-27 September 2019, Istanbul
organized by TUNCAP and IUAPPA

Acknowledgments

This study was supported by Indonesia Endowment Fund for Education (LPDP) scholarship, Ministry of Finance, Indonesia.

Conflicts of interest

There are no conflicts of interest to declare

Air pollution reduction with intelligent transportation systems: Dilovası scenario

Zübeyde Oztürk¹, Onur Alp Arslantaş¹, Hande Emanet Beba¹, Merve Yılmaz² and Hüseyin Toros³

¹Istanbul Technical University, Faculty of Civil Engineering, Department of Civil Engineering, Istanbul, Turkey

²Istanbul Technical University, Faculty of Aeronautics and Astronautics, Department of Meteorology Engineering, Istanbul, Turkey

³Istanbul Technical University, Faculty of Aeronautics and Astronautics, Department of Meteorology Engineering, Istanbul, Turkey

ozturkzu@itu.edu.tr

Abstract. Traffic management is one of the main application areas for ITS (Intelligent Transportation Systems). This management begins with the collection of movements and data affecting the route. Ultimately, the data will be used for information access systems. This study is one of the study areas of “Scenario for Reducing the Dilovası Air Pollution with the ITS Application” which is supported by TUBITAK within the COST (European Cooperation in Scientific and Technology) Program. Within the scope of “Scenario for Reducing Air Pollution with the Intelligent Transport System Application” work package, an alternative route design was made to TEM (Trans European Motorway). Air pollution from road traffic has the highest share in air pollution caused by transportation. Dilovası, which is designated as a sample region in this study, is a region where high industrialization and the main arteries connecting Istanbul metropolises to other cities pass through the city center, where air pollution is intense and the effects caused by this pollution are seen intensively. Transfer to north of vehicle traffic will reduce the air pollution caused by transport to the region. The variable values of air pollution make it possible to use the newly designed road as an alternative way. It is planned that the TEM will be closed and the alternative route will be mandatory if air pollution reaches the value that will affect human health. There are two air pollution measuring stations in the Dilovası region. These stations measure air pollution and produce standardized data. If the data received from the stations are evaluated as part of the ITS designed in the project and the values are not at the desired level, the decision to close the current route is given by the system. This decision must be forwarded to the drivers on the road approaching the area. Among the methods used are many applications such as variable message boards, radios, internet and smart phone systems. The aim is that drivers should turn to an alternative route and should be informed that the current route is closed. In addition, it is important to establish a working system based on meteorological conditions like air pollution in its application. For example, the prevailing wind in the region is known to blow from the north-northeast direction and carry pollution to the region. Therefore, it will be ensured that the emissions from the highway will be transported out of the region by an alternative route.

Keywords: Air pollution, Intelligent transportation systems, Traffic, Transportation

1. Introduction

The highway is a type of transportation that has an important impact on climate change as well as air pollution. The main purpose of this study is to provide a method to prevent the effect of road transport and emission pollution on smart transportation systems. Road transport, which is one of the stakeholders

of environmental pollution causing climate change, aims to provide a method to prevent the emission-related pollution impact by smart transportation systems. The National Action Plan Document on Climate Change states that the Road Sector is one of the sectors causing the highest greenhouse gas emissions among the Transportation sectors. It is emphasized that the share of urban transport in measured emissions is high. These data point to Intelligent Transportation Systems in many areas and in reducing greenhouse gas impacts on highways. Smart Transportation Systems not only facilitate transportation in many areas, but also a strategy to develop useful products and practices to prevent air pollution and reduce greenhouse emissions. Transportation, which has an important share in air pollution, causes environmental pollution during construction of transportation roads, production of motor vehicles, destruction of vehicles and operation of roads. This study is one of the research areas titled Dil Dilovası Air Pollution Mitigation Scenario with Intelligent Transportation System Application ((Project No: 117Y298) supported by TUBITAK within the scope of COST (European Cooperation in the Field of Scientific and Technical Research) Program. Within the scope of the Intelligent Transportation System Scenario for Air Pollution Reduction "work package, an alternative route design to TEM highway was designed. In this context, it is aimed to benefit from smart transportation systems in order to minimize air pollution during the operation of road transport. Dilovası was chosen as the sample section and an alternative road crossing search was made for the existing roads and it was suggested to use smart transportation system for the transportation of traffic.

2. Air Pollution and Transportation

Air pollution is defined as the presence of one or more of the pollutants together in the amount and time that will harm the health of living things in the atmosphere (Incecik,1994). Under normal conditions; 78.09% nitrogen, 20.95% oxygen, 0.093% argon, 0.03% carbon dioxide (Güler and Akin, 2015). Air pollution can be defined as the levels of pollutants such as Sulfur dioxide (SO₂), particulate matter (PM), nitrogen dioxide (NO₂) and ozone (O₃) that have negative effects on the environment and health. This pollution disrupts the natural processes in the atmosphere and adversely affects public health.

A large proportion of passenger and freight transport in Turkey is done by motorized road transport. The most important factor that causes air pollution is the type, efficiency and amount of energy that causes pollution. Although motor vehicles on the road consume energy and generate various wastes, the transportation sector has an important share in the sector in terms of energy consumption rate as shown in Figure 1. Of the fuels used by road vehicles, gasoline and diesel fuels derive the most harmful substances (Öztürk, 1994). All of these will cause the environmental impacts of the vehicles to be seen to a great extent on the roads and the region.

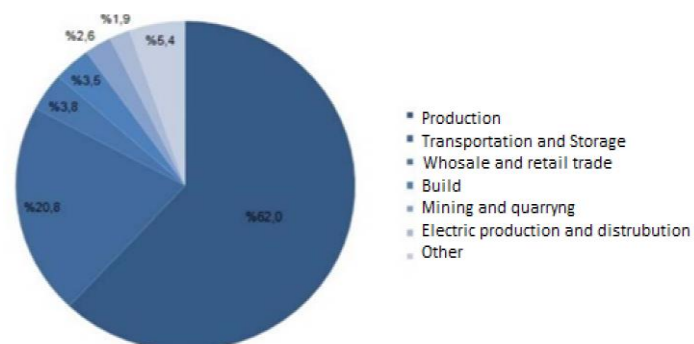


Figure 1. Distribution of final energy consumption by sector, 2017 (Öztürk, 1994).

The pollution caused by transportation is caused by greenhouse gas emissions. As shown in Figure 2, greenhouse gas emission values in our country have increased every year since 1990. Providing transportation in Turkey's overwhelmingly highways and principles of allowing the polluting road transport the main cause of environmental pollution due to transportation-related motor vehicle is road traffic.

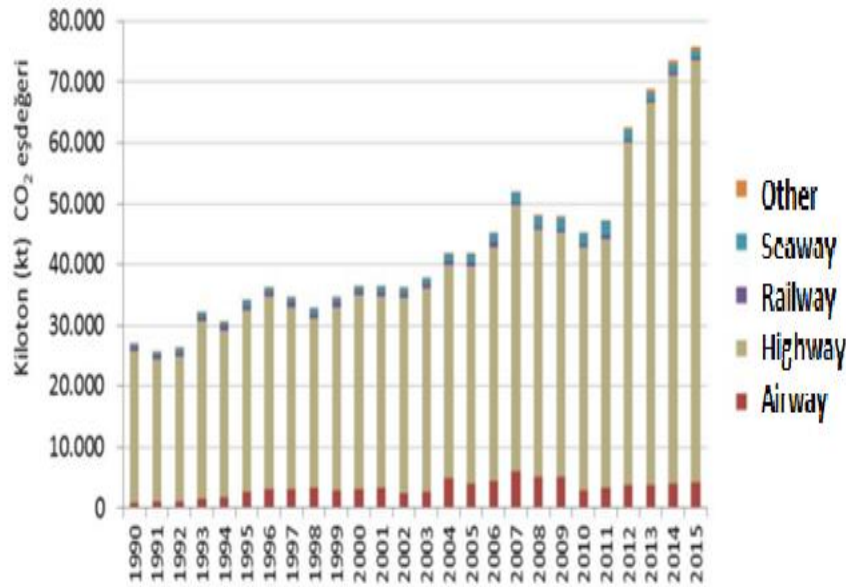


Figure 2. Greenhouse gas emissions by type of transport

3. Intelligent Transportation Systems

Transportation is a sector that is highly affected by technological developments. It is inevitable that transportation will renew, change and advance itself along with technological developments. Because transportation and life are in mutual interaction (Kumar et al., 2005). The benefits of technological advances should not be limited to the ease of construction of roads, stations and transport centers, but should be considered as a contribution to transport by many methods, such as sensors, microchips and various communication devices networks, which store data on the operation of complex transport networks (Kumar et al., 2005). In this axis, the presence of AUS, which includes high technology, traffic control and different transportation modes, aims to reduce the responsibility of people to think or make decisions by providing innovative services (Ezel, 2010).

Intelligent Transportation Systems (AUS) can be called as systems consisting of technologies such as electronic, data processing and wireless networks that provide security level and efficiency in the transportation network (UDHB, 2014). According to another view, AUS collects and processes traffic-related data and information and transfers them to the units and exchanges between the units using information and communication technologies (Shaheen and Finson, 2013).

With the increasing awareness of the AUS systems and the ease of providing solutions to the problems, a number of studies and applications have been made. For this reason, many institutions in many countries have attempted to establish AUS standards. The classification made by the ISO (international standards organization) shows that intelligent transportation systems are now divided into various service areas and service groups, as shown in Table 1.

Table 1. Service Areas and Classification of Intelligent Transportation System

Passenger Information
Traffic Management and Operations
In-Vehicle Systems
Public transport
Emergency
Personal safety related to road transport
Monitoring of weather and environmental conditions
Disaster response management and coordination
National Security

4. Region and Traffic Characteristics in the Study



Figure 3. Dilovası map-Google Earth Image

Dilovası is a settlement unit in Gebze which was separated from Gebze in 2008 and became a district. Dilovası, located in the industrialized East Marmara and Izmit Gulf, under the influence of the metropolitan area of Istanbul; It is a region where development is increasing with the power of industrialization. Rapid industrialization in this region has caused unplanned urbanization and infrastructure problems (Akbaş, 2013).

Dilovası district is located on D-100 highway and Istanbul Motorway (TEM) routes. These roads are intercity roads and are allowed to pass many classes of vehicles.



Figure 4. Dilovası region road view.

TEM (Trans European Motorway) is a route that starts from the borders of the Baltic Sea in Europe and passes through Central Europe to Edirne and reaches Istanbul and Ankara. In addition, in the east of our country, Tarsus reaches to the border gates of Habur and Cilvegözü in the Southeast and ends in Mersin. A certain section of the TEM Motorway passes through the Dilovası region and is one of the two main arteries in the Dilovası region (Figure 4). When the traffic volume on the TEM Highway is examined, according to the values obtained by the ratio of total traffic passing through a section of the road in both directions for a year in the Dilovası region, 28% of the traffic is composed of heavy vehicles and 72% is light vehicles (Table 2).

Table 2. Dilovası Region Highway Total Annual Average Daily Traffic (2017)

Section Name	Length-KM	Light Vehicle / Day	Heavy Vehicle / Day	Total Vehicle / Day
Gebze-Dilovası	6.2	58,232	22,143	80,375

4.1. Tem Motorway

TEM (Trans European Motorway) is a route that starts from the borders of the Baltic Sea in Europe and passes through Central Europe to Edirne and reaches Istanbul and Ankara. In addition, in the east of our country, Tarsus reaches to the border gates of Habur and Cilvegözü in the Southeast and ends in Mersin. A certain section of the TEM Motorway passes through the Dilovası region and is one of the two main arteries in the Dilovası region (Figure 4). When the traffic volume on the TEM Highway is examined, according to the values obtained by the ratio of total traffic passing through a section of the road in both directions for a year in the Dilovası region, 28% of the traffic is composed of heavy vehicles and 72% is light vehicles (Table 2).

Table 3. Dilovası Region Highway Total Annual Average Daily Traffic (2017)

Section Name	Length-KM	Light Vehicle / Day	Heavy Vehicle / Day	Total Vehicle / Day
Gebze-Dilovası	6.2	58,232	22,143	80,375

4.2. D100 Highway

D100 Highway is a State Road passing through Dilovası region. (Figure 4) The D100 highway is the name of the highway starting from the city center of Istanbul to a part of the Ankara road. Although it is a high standard road, it is not a highway. D100 When the traffic volume of the highway is analyzed, according to the values obtained by the ratio of total traffic passing through a section of the road in both directions for one year in the Dilovası region, 23% of the traffic is composed of heavy vehicles and 77% is light vehicles. (Table 4).

Table 4. Dilovası Region D100 Highway Total Annual Average Daily Traffic (2017)

KKNO	Slice	Length-KM	Count Type	Light Vehicle / Day	Heavy Vehicle / Day	Total Vehicle / Day
100-7	3	15	OTSS1	24,511	7,278	31,789

The first priority environmental problem of Kocaeli province where Dilovası district is also connected is air pollution (Tekeli, 1994). Two of the air quality monitoring stations established by the Ministry of Environment and Urbanization in Kocaeli province are located in Dilovası district. The data of these stations show that Dilovası's air is quite dirty compared to other provinces.

Table 5. Dilovası Region Station Data (Hava İzleme, 2018).

Station	Parameter	Min.Date	Max Date	Min Value	Med. Value	Max value	Total	Std.Dev.	Data Rate
0141001 Kocaeli - Dilovası - İMES OSB 1- (Kocaeli-Dilovası)	NO2	9.4.2018	9.4.2019	-56.18414	23.6077157	200.3137	171	25.3397261	98.9071038
0141001 Kocaeli - Dilovası - İMES OSB 1- (Kocaeli-Dilovası)	PM10	9.4.2018	9.4.2019	0	30.1247918	1584.422	163	41.2325581	98.9071038
0141001 Kocaeli - Dilovası - İMES OSB 1- (Kocaeli-Dilovası)	CO	9.4.2018	9.4.2019	-274.6292	598.760625	11108.85	172	374.246776	98.9071038
0141000 Kocaeli - Dilovası İMES 2- (Kocaeli-Dilovası)	PM10	9.4.2018	9.4.2019	0.0006105	28.7261502	416.454	172	28.0261962	100.546448
0141000 Kocaeli - Dilovası İMES 2- (Kocaeli-Dilovası)	CO	9.4.2018	9.4.2019	0	388.915512	4262.762	182	216.163927	100.546448
0141000 Kocaeli - Dilovası İMES 2- (Kocaeli-Dilovası)	NO2	9.4.2018	9.4.2019	0.3160028	15.7917153	156.3448	182	14.6333202	100.546448

5. Investigation of the Proposed Method in Dilovası Region

The process of designing the transition is an effort to connect the two points in the most appropriate way. This is an economic comparison between eligibility options sought in the effort (Hava İzleme, 2019). As a result of the investigation on Dilovası maps, a route of 9,169 km is designed and horizontal and vertical axis information is given.



Figure 5. Designed Route

5.1. Route Properties

5.1.2. Project Speed

The road designed in the project will form part of the Istanbul - Ankara motorway. Vehicles will never leave the highway through the toll booths; they will not enter or exit. Therefore, the project speed of 120



km / h used on such roads and Istanbul-Ankara Highway was deemed suitable for the design in order to ensure the standards from the highway intact.

5.1.3. Geometric Standards

When selecting geometric standards, the intervals determined by the General Directorate of Highways and ensuring the comfort of motorways; The minimum conditions required for the continuity of the current comfort level of the Istanbul-Ankara motorway were tried to be met.

5.1.4. Horizontal axis, profile, superelevation

KGM determined the minimum curve radius $R = 1000\text{m}$ according to the conditions. In the design of the road, an effort has been made not to go below this limit as a curve radius. Transition curves between the horizontal curves were not used. For maximum slope on the motorway, 4% value was considered appropriate at 120 km / h project speed. Considering the terrain conditions, Kocaeli-Istanbul direction of this slope route was applied as 6% for the first 3 km. Parabolic vertical curves were used between slopes in the profile. While placing the curves, it was considered that the conditions of visibility and adequate comfort could be established as criteria. In determining the geometric properties of curves, $K = 100$ value determined by General Directorate of Highways was provided. In order to provide drainage of surface water and to compensate for the effect of centrifugal force, circulation was applied. The minimum transverse slope is selected as roof in sections where the radius of curvature exceeds 5000 m and 2.5% is chosen as a roof.

5.1.5. Crosssections

The cross-section used along the Istanbul-Ankara highway was taken and a cross-section with 2 x 3 lanes was envisaged. The cross-section is separated from the center by a 5 m refuge in two separate platforms and consists of 3 traffic lanes measuring 3.75 m with banquetts of 1m inside and 3m wide on each platform. For filling cases, a width of 1 m is placed between the filling slope and the banquet. Guardrail shall be placed on this width. There is also a guardrail on both sides of the center median. Filling slopes take different slope slopes according to different heights

5.2. AUS Usage and Traffic Management

The first stage of event management design is the determination of air pollution. At this stage, T.C. The data provided by two Air Quality Measurement Stations installed by the Ministry of Environment and Urbanization will be evaluated. The system will evaluate according to the National Air Quality Index and will detect Air Pollution. The decision made by the system according to air pollution values can be in two ways: Blocking the current route and opening the current route to traffic. In line with these decisions, the road will be closed to traffic or opened. It is envisaged to apply a penalty system to the vehicles entering the route after the road is closed.

6. Evaluation

In this study, the reduction of the share of road traffic in the pollution by means of smart transportation systems applications within the TUBITAK COST Project was detailed and studies were carried out for Dilovası, which is the selected sample region in this regard. The situation of the Dilovası region and the usability of the intelligent transportation systems were examined. In the light of the data, the share of transportation on air pollution was found to be significant. Gases generated by road traffic, ie combustion of motor vehicles, constitute a large part of air pollution caused by transportation. In this study, it has been tried to reduce its share in air pollution and to dilute the air pollution in the determined region. The importance and future role of smart transportation systems has been recognized by the institutions which have a say on the highways of our country. All kinds of studies on smart transportation systems are remarkable. This project, which works together with AUS to reduce environmental pollution, is an example for both topics.

7. Results

Dilovası region is a residential area created by the industry, which was tried to be removed from Istanbul metropolis in the past. The main transportation arteries drawn by the industry and the settlement (Istanbul-Ankara Motorway and D100 Highway) increase the pollution in the region. Many studies and measures have been taken to prevent industrial air pollution in the region. This study is a special study carried out in the transportation area considering the presence of Istanbul-Ankara Motorway and D100 highway in the region. The new route is located in the north of Dilovası region, where the population affected by air pollution lives, and has been taken in a position to remove contamination contributions. The choice of this route was made compulsory in times of increasing air pollution and was released as an option at other times. The AUS drivers used at this point were provided with the same methods used in many AUS projects, and it was foreseen to place signs and illuminated signs on the roads. It has been found that air pollution from transport can be removed without compromising highway comfort and guiding drivers. The areas of use of intelligent transportation systems are generalized by ISO classifications. The examination of air and environmental conditions from these classes is considered as a classification covering air pollution. In addition, the assessment of the outputs of air pollution and the effect of traffic order according to these outputs made the system designed in the project under the heading of traffic management and operations.

8. References

- Akbaş, A., 2013. Türkiye'nin 2023 Akıllı Ulaşım Vizyonu ve Ulusal AUS Mimarisinin Geliştirilme Yöntemi Üzerine, %1 içinde Toplu Ulaşım Haftası Transist 6. Ulaşım Sempozyumu ve Fuarı Bildiriler Kitabı, İstanbul, İETT, Aralık 2013, pp. 416-424.
- Ezell, S., 2010. Intelligent Transportation Systems, The Information Technology & Innovation Foundation.
- Güler, Ç., Akın, L., 2015. Halk Sağlığı Temel Bilgiler, Hacettepe Üniversitesi Yayınları, pp. 670-748. Hava İzleme, 2018. www.havaizleme.gov.tr, Erişim Tarihi: 11.11.2018.
- Hava İzleme, 2019. https://www.havaizleme.gov.tr/STN/STN_Report/StationDataDownload, Erişim Tarihi: 09.04.2019.
- İncecik, S., 1994. Hava Kirliliği, İstanbul: İstanbul Teknik Üniversitesi.
- Kumar, M., Albert, S., K Deeter, D. A., 2005. Summary of Rural Intelligent Transportation Systems (ITS) Benefits as Applied to ODOT Region 1, Oregon Department of Transportation Region 1.
- Öztürk, Z., 1994. Otoyol ve Demiryolunun Önemli Çevre Etkilerinin İncelenmesi ve Değerlendirilmesi, İstanbul, İTÜ.
- Shaheen, S., Finson, R., 2013. Intelligent Transportation Systems, Reference Module in Earth Systems and Environmental Sciences, California.
- Tekeli, İ., 1994. Development of Istanbul Metropolitan Area, İstanbul: Kent Basımevi.
- UDHB (Ulusal Akıllı Ulaşım Sistemleri Strateji Belgesi), 2014. (2014-2023) ve Eki Eylem Planı (2014-2016), T.C. Ulaştırma Denizcilik ve Haberleşme Bakanlığı, Ankara.

Determination of greenhouse gas reduction potential for solid fuel based power plants in Turkey

Ece Gizem Cakmak^{1,2} and Hasancan Okutan²

¹TUBITAK Marmara Research Center, Environment and Cleaner Production Institute, Gebze, Kocaeli, Turkey

²Istanbul Technical University, Department of Chemical Engineering, Maslak, Istanbul, Turkey

gizem.cakmak@tubitak.gov.tr

Abstract. Climate change, as one of the most important problems faced by the human race in the present century, is triggered by the increasing use of fossil fuels, land use changes and various human activities generating greenhouse gases (GHG) such as carbon dioxide (CO₂), methane (CH₄) and nitrous oxide (N₂O). According to the latest IPCC (The Intergovernmental Panel on Climate Change) Special Report on the impacts of global warming, 1°C of global warming above pre-industrial levels are estimated to be caused by human activities and it is likely to reach 1.5°C between 2030 and 2052 if it continues to increase with the current rate. Under these circumstances, countries need to limit their greenhouse gas emissions in accordance with the provisions of the Paris Agreement. In this context Turkey provided its nationally determined contribution and committed to reduce its GHG emissions up to 21 percent from the business as usual level by 2030. However, as a developing country, Turkey needs to evaluate its domestic energy resources taking into account its energy policies in which lignite and biomass have been mainly targeted as national energy sources for a sustainable and secure energy supply chain. Therefore assessment of new investments to be made for the solid fuel based power generation plants will be important both in terms of environmental aspects and determination of the most suitable technologies that will increase the utilization of domestic energy resources and increase the contributions of Turkey on the mitigation of GHG emissions in global scale. Within the scope of this study, the current situation of the solid fuel based power generation plants operating in Turkey was determined and alternative clean coal technology scenarios for reducing the GHG emissions from these power plants were evaluated. For this purpose, a modelling tool known as TIMES (The Integrated MARKAL-EFOM System) which provides to the users an interface to analyse energy, economy and environment relation on a basis of technological development was used. Results were obtained for the business as usual scenario which assumes that current policies for the energy generation will remain same and for the alternative clean coal technologies scenario for the period of 2010-2050. Energy demand growth was projected based on national statistics on population, gross domestic products and recently licensed power plants.

Keywords: Emissions, Power generation, Climate change, Greenhouse gas, Solid fuels.

1. Introduction

Use of fossil fuels, land use changes and various human activities are considered as the main factors resulting climate change which is basically triggered with the accumulation of greenhouse gases such as carbon dioxide (CO₂), methane (CH₄) and nitrous oxide (N₂O) in the atmosphere. If the global warming process continues to increase with the current rate, extreme high temperatures, floods, severe drought events, forest fires and many related problems are expected for the main basins inclusively Turkey.

Around 37 % of greenhouse gas emissions worldwide are generated by the electricity and heat generation sector. In Turkey, total greenhouse gas emissions in 2017 was 526 Mton CO₂e and 70.9 % of this was corresponding to the energy production and consumption. In 2017, the total amount of emissions in electricity and heat generation plants was 155 Mton CO₂e, which is 29.4 % of the country's total emissions. GHG emissions from solid fuel-based power plants, which have a significant share in country's electricity generation sector, was 98 Mton CO₂e for 2017, covering 63.7 % of the electricity generation and heat sector. The trends for the greenhouse gas emissions from solid fuel-based power plants for 1990-2017 is given in Figure 1 (NIR, 2019).

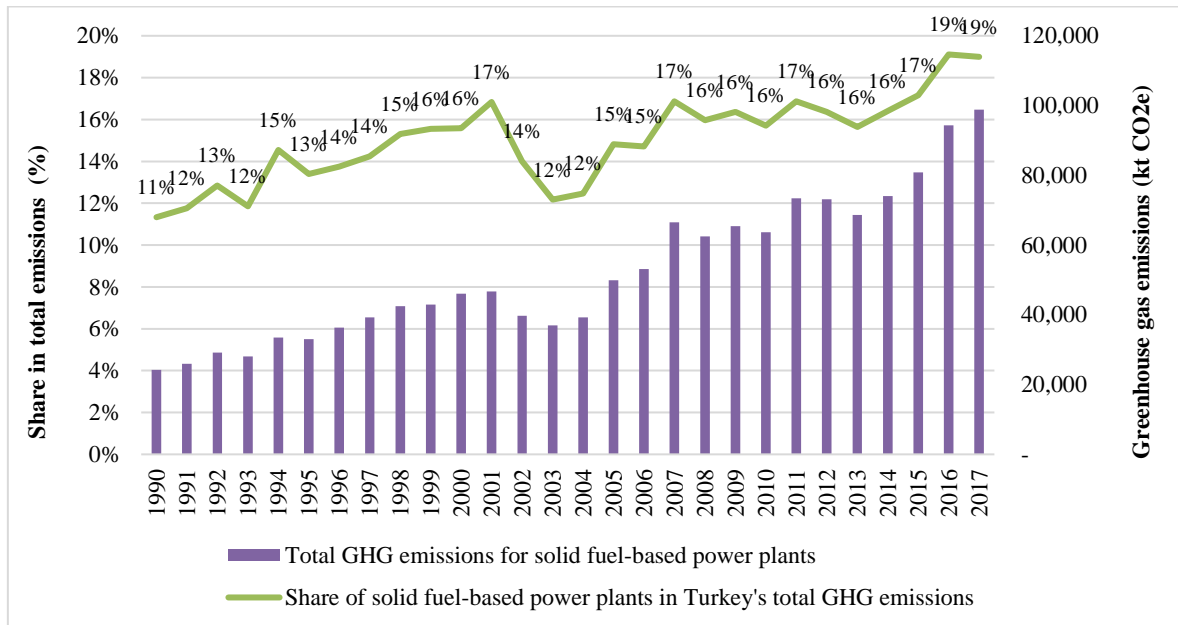


Figure 1. GHG emissions trends for the solid fuel-based power plants (NIR, 2019)

On the other hand, according to the distribution of world primary energy consumption in terms of resources for 2014, petroleum has the first place with a share of 31.3% and coal has the second place with a share of 28.6%. For the case of Turkey, it is seen that natural gas, which has a share of 48%, is followed by coal (16% of which is domestic source) with a share of 30% (MENR, 2017). On the other hand, looking closely to the installed capacity of power plants in terms of coal and biomass resources, it is seen that solid fuel power plants account for 22.06% of the installed power in 2016.

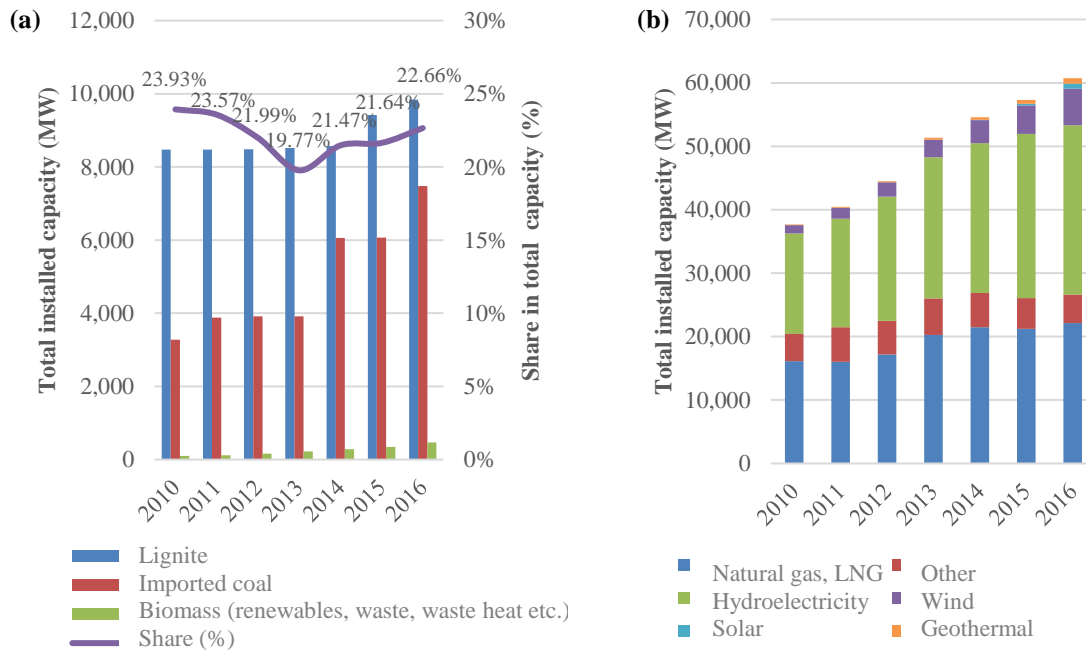


Figure 2. (a) Development of capacity for the solid fuel-based power plants, (b) Development of capacity for other sources (MENR, 2017)

2. Methodology

Within the scope of this study, capacity and technical perspectives for currently operating solid fuel-based power plants were determined and assessment on the greenhouse gas emission reduction potential was made within different scenarios.

2.1. Calculation of greenhouse gas emissions

Relevant IPCC 2006 guidelines and Turkey's National Greenhouse Gas Emission Inventory were taken into account as basis. Within the framework of the 2006 IPCC guideline, three different approaches have been proposed for the accounting of greenhouse gas emissions from combustion of fuels. In general, all of these approaches use the same formulation (see formula 1 below), which is also referred below as multiplication of the amount of fuel consumed with an emission factor. The main difference between those approaches is due to the determination of emission factor considering national and local factors (NIR, 2019; IPCC, 2006).

$$\text{Greenhouse gas emissions (kt CO}_2\text{)} = \text{Amount of fuel consumed (TJ)} \times \text{Emission factor (kt CO}_2\text{/TJ)} \quad (1)$$

Within the scope of the Turkey's National Greenhouse Gas Emission Inventory, the calculation was made based on both National Energy Balance Tables and inventory data on a plant basis compiled by the Ministry of Energy and Natural Resources. The difference on the results of these calculations was approximately 1.5 %, i.e. lower values obtained for the calculations using energy balance tables. Within the scope of this study, National Energy Balance Tables are used together with the average conversion coefficients and emission factors, which were determined in the National Greenhouse Gas Emission Inventory (NIR, 2019).

2.2. Determination of current infrastructure for the solid fuel-based power plants

Solid fuel-based power plants were classified under 4 sub-groups as hard coal, asphaltite, lignite and imported coal in accordance with the database of the Ministry of Energy and Natural Resources. For this purpose, data on several parameters such as, installed capacity and technology used in these plants have been collected mainly through public sources, i.e. official statistics and reports, scanning of web, and as a result of this study, a database has been established for solid fuel-based power plants. Relevant information have been summarized in Table 1.

Table 1. Capacity of solid fuel-based power plants according to the type of fuel and combustion technology (GW)

Type of fuel	Type of technology	2010	2015	2020	Planning
Lignite	Pulverized	3.03	5.84	8.66	5.63
	Fluidized bed	0.57	0.61	0.61	0.04
Imported coal & hard coal	Pulverized	7.75	7.75	8.08	0.70
	Fluidized bed	0.43	0.95	2.04	1.30

3.2. Modeling framework

Within the objectives of this study, a modelling tool known as TIMES (The Integrated MARKAL-EFOM System), which provides users an interface to analyse energy, economy and environment relations on a basis of technological development, was used. TIMES allows the interaction between supply and demand through price elasticity of demand and searches for a solution with the least total discounted cost over the whole period (ETSAP, 2016).

Model includes several technologies defined more detailed for the solid fuel-based power plants (i.e. lignite and imported coal) and aggregated for the renewable sources (i.e. hydroelectricity, solar, wind and biomass). Demand side was also included mainly according to the National Energy Balance Tables aggregated for industry, transportation and building stock. Demand projections was made mainly based on population projections prepared by the National Statistics Office for the period of 2019-2080.

In addition electricity consumption projections were prepared by the Ministry of Energy and Natural Resources were also taken account which resulted an increase from 300 TWh in 2018 to 613 TWh in 2039. On the other hand for solid fuel-based and biomass-based power plants, dataset for the power plants which were recently licenced but not yet in operation, was taken into account for the determination of near term total installed capacity values.

The model is calibrated to 2010 and 2015 data and the time horizon ends in 2050. Basically defined technologies are working for the transformation of fuels to the defined outputs depending on the technology in order to fulfil the total demand for the specified output. Efficiency parameters and cost of new technologies are determined based on EPA TIMES database and also several national and international studies and summarized in Table 2.

Table 2. Capital, fixed and variable costs, lifetime and efficiency of new technologies

Description of technology	Input	Lifetime (year)	Fixed cost (2000\$USm/G Wyr)	Variable cost (2000\$USm/PJ)	Capital cost (2000\$USm/GWyr)	Efficiency (%)
Pulverized combustion-Conventional	Lignite, hard coal	35	30,3	1,2	2001	0,33
Pulverized combustion-Supercritical	Lignite, hard coal	50	30,3	1,2	2335	0,38
Pulverized combustion-Ultra Supercritical	Lignite, hard coal	50	30,3	1,2	2557	0,42
Integrated gasification cycle	Lignite, hard coal	40	49,9	1,9	2891	0,39
Fluidized bed	Lignite, hard coal	50	27,9	1,1	2152	0,33
Biomass combustion	Biomass	35	84,4	1,6	1768	0,25
Biogas combustion-Anaerobic digestion	Biomass	25	83,3	1,6	2499	0,28

3. Results

Modeling framework was developed initially for the baseline/reference scenario in which several assumptions made in addition to the ones mentioned in Section 2 of this document. Mainly it was assumed that the current shares of energy sources will be maintained over the horizon and total generation of electricity will increase according to the demands defined individual demand technologies. Based on this energy consumption of power plants and greenhouse gas emissions calculated through model were presented in Figures 3 and 4. Total capacity installed over the horizon for the solid fuel-based power plants was also given in Table 3.

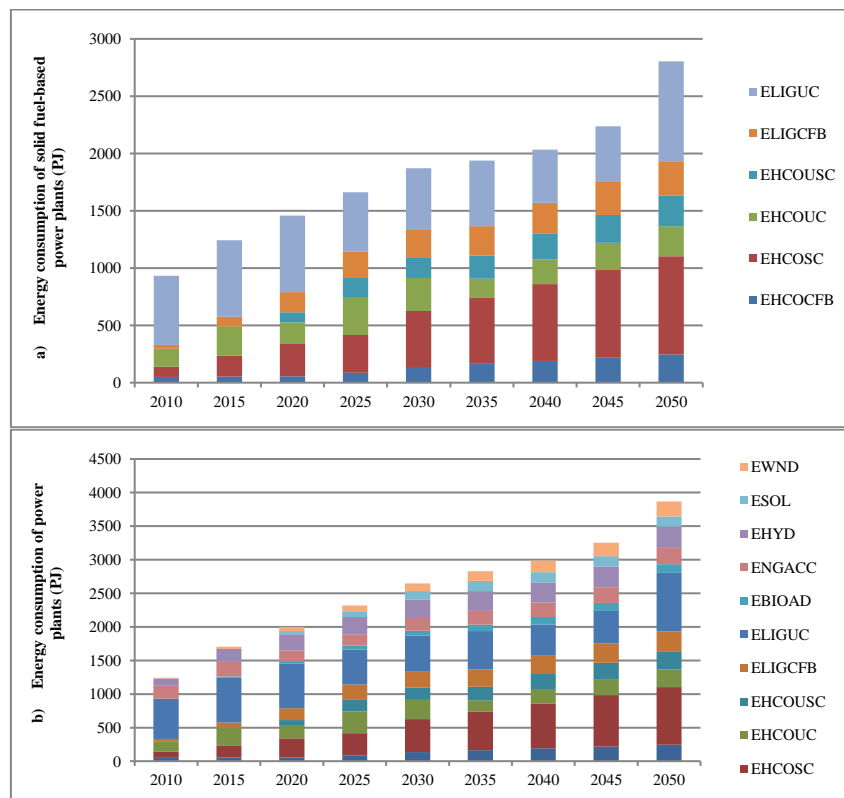


Figure 3. Development of energy consumption of (a) solid fuel-based power plants, (b) all power plants for the base scenario

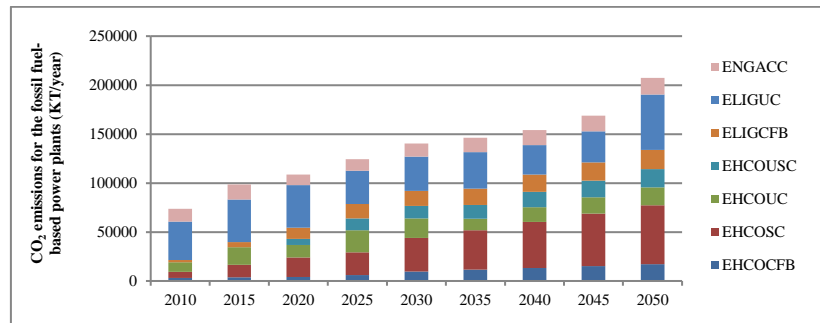


Figure 4. CO₂ emissions for the fossil fuel-based power plants for the base scenario

For the base scenario, total CO₂ emission calculated for the fossil fuel-based power plants on 2010 and 2015 are very close to the statistics published by TurkStat within latest National Greenhouse Gas Inventory (2019), which proves the appropriate operation of the modeling framework (NIR, 2019). On the other hand, capacity development of power plants seem to be in line with the current infrastructure and near term planning determined and published by Ministry of Energy and Natural Souces (MENR, 2017).

Table 3. Development of capacity for the power plants (GW) for the base scenario

Technology	2010	2015	2020	2025	2030	2035	2040	2045	2050
EHCOCFB	0,6	0,6	0,7	1,0	1,6	1,9	2,2	2,5	2,8
EHCOSC	1,2	2,4	3,8	4,4	6,5	7,7	9,0	10,2	11,5
EHCOCUC	1,8	3,0	3,5	4,0	6,0	7,0	9,0	10,0	11,0
EHCOSUC	0,0	0,0	1,3	2,6	2,7	3,0	3,3	3,6	3,9
ELIGCFB	0,4	1,0	2,0	2,6	2,8	3,0	3,2	3,3	3,5
ELIGUC	7,0	7,8	8,1	9,0	11,5	12,6	13,7	14,7	15,8
EBIOAD	0	0,2	0,313	0,6	0,7	0,9	1,1	1,2	1,3
ENGACC	16,1	21,2	25,8	30,6	35,4	40,2	44,9	49,7	54,5
EHYD	15,38	25,87	33,73	35,34	38,57	40,54	41,2	42,87	43
ESOL	0	0,248	6,19	11,34	16,49	21	21	21	21
EWND	1,32	4,503	8,4	12,3	16,11	19,95	23,7	27,5	31,3

Two alternative scenarios were obtained in which it was assumed that overall CO₂ emissions for the total system will be less than current situation, i.e. 5 % and 10 % less. Results for the total energy consumption of power plants and greenhouse gas emissions calculated through the model were presented in Figures 5 and 6.

Based on the scenario analysis, it was seen that some of the defined clean coal technologies (such as super critical combustion, fluidized bed combustion) are gaining importance within the model horizon in relation to their efficiency. However integrated gasification technology as another defined technology in the model both for lignite and hard coal, model doesn't invest through the modeling horizon which is assumed to be mainly related to the higher costs of the referred technology.

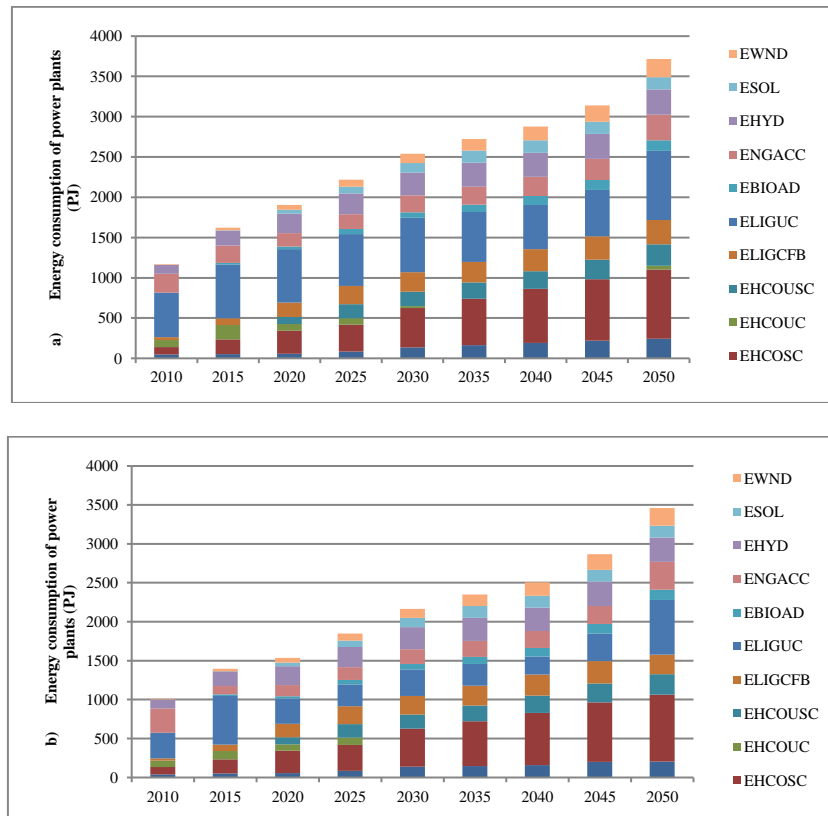


Figure 5. Development of energy consumption of all power plants (a) for 5% less GHG scenario and (b) for 10% less GHG scenario

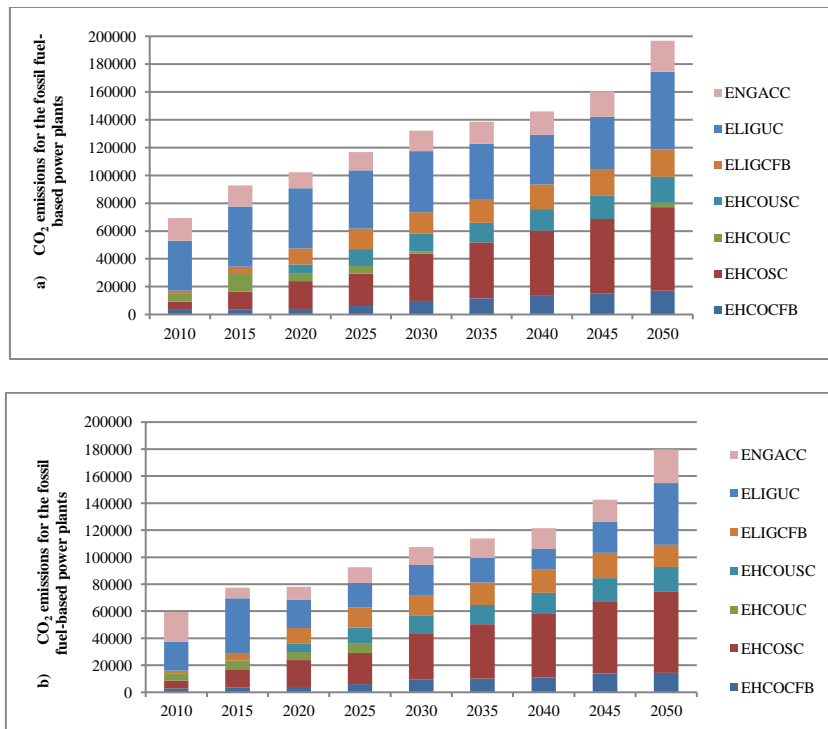


Figure 6. CO₂ emissions for the fossil fuel-based power plants (a) for 5% less GHG scenario and (b) for 10% less GHG scenario



4. Conclusions

The results obtained in this study have been determined by using the data obtained through statistics, and reports mainly published by the Ministry of Energy and Natural Resources. Various sources from internet and literature also made it possible to gather information and data on Information on the current infrastructure of the power plants. Therefore more detailed results would be obtained by increasing the level of detail of these datasets. Furthermore, it is possible to reduce uncertainties related to the modeling to a significant extent by defining individual plants within the modeling framework. On the other hand, in the evaluation of these technologies, various factors such as lifetime and costs of technologies, availability/efficiency of installed capacity have be taken into consideration. Similarly, it would be beneficial to carry out more detailed assessments that take into account national datasets, geographical conditions and differing conditions.

5. References

MENR (Ministry of Energy and Natural Resources), 2017, Turkey Electricity Demand Projection Report.

ETSAP (Energy Technology Systems Analysis Programme), 2016, Overview of TIMES Modelling Tool, International Energy Agency-Energy Technology Systems Analysis Program, <http://www.iea-etsap.org/web/Times.asp>, accessed in 2019.

IPCC (Intergovernmental Panel on Climate Change), 2006, Guidelines for National Greenhouse Gas Inventories-Volume 2-Energy-Chapter 2-Stationary Combustion.

NIR (National Inventory Report), 2019. Turkish Greenhouse Gas Inventory 1990-1017, EEA Technical Report No. 9/2009, Ankara.

TurkStat (Turkish Statistical Institute), 2013, Population Projections (2013-2079) <http://www.tuik.gov.tr/PreHaberBultenleri.do?id=15844>, accessed in 2019.

WB (World Bank), 2017, Global Economic Prospects, <http://data.worldbank.org/data-catalog/global-economic-prospects>, accessed in 2019.

Ambient air polybrominated diphenyl ether (PBDE) concentrations in Urla, İzmir, and back trajectory modelling

İlknur Ayır¹, Mesut Genisoglu¹, Aysun Sofuoğlu², Perihan B. Kurt-Karakuş³, Aşkın Birgül³ and Sait C. Sofuoğlu¹

¹Izmir Institute of Technology, Department of Environmental Engineering, Gulbahce, Urla, 35430, Izmir, Turkey

²Izmir Institute of Technology, Department of Chemical Engineering, Gulbahce, Urla, 35430, Izmir, Turkey

³Bursa Technical University, Faculty of Engineering, Department of Environmental Engineering, 16310 Yildirim, Bursa, Turkey

cemilsofuoğlu@iyte.edu.tr

Abstract. Polybrominated diphenyl ethers (PBDEs) are a class of halogenated compounds that have emerged as a major group of persistent organic pollutants. They have been used in various industrial and commercial applications due to their high boiling points, non-flammability, chemical stability, insulating properties, and chemical stability. Because of their persistence and long-range transport, PBDEs are measured at places with no local sources. In this study, particulate and gaseous phase samples were collected weekly for 24 h with a high-volume sampler between December-2018 and June-2019 in Urla (38.31N, 26.63E) with 101-mm microfiber quartz filters and polyurethane foam (PUF), respectively. Two 5-cm PUF plugs in series and XAD-2 in between were placed to eliminate breakthrough. Samples were stored until extraction at -20 °C. All samples were spiked with surrogate standards (PBDE-77, PBDE-181) prior to extraction. PUF plugs were extracted for 24 h with a 1:1 acetone-hexane. Filters were extracted in the solvent mixture by soaking overnight followed by keeping in an ultrasonic bath for 10 min. All sample extracts were concentrated using a rotary evaporator, and analyzed with a GC-MS for PBDE-17, -28, -47, -71, -66, -99, -100, -138, -153, -154, -183, -190, -209. QA/QC measures included blanks, determination of detection limits and recoveries. Lagrangian particle dispersion model HYSPLIT was used in backward mode to infer on the long-range source regions of PBDEs at the sampling location. Gas phase Σ_{14} PBDE concentrations ranged between 5.56 pg/m³ and 510 pg/m³ while particle phase Σ_{14} PBDEs varied between 118 pg/m³ and 376 pg/m³. PBDE -47, -183, -190 were found to be the dominant congeners in both of the phases, whereas PBDE -99, -28, -153, -154 were the congeners with relatively lower contribution. The 120-hr backward trajectories calculated for 20 samples showed that possible PBDE sources mainly lie in north and northeast of the sampling location.

Keywords: PBDEs, Flame retardants, Active sampling, Long range atmospheric transport, Back trajectory.

1. Introduction

Polybrominated diphenyl ethers (PBDEs) are brominated flame retardants that were used in household furnishings and electronics from the 1970s to early 2000s (Krol et al., 2012; Vuong et al., 2019). They were phased out of use in the U.S. in 2004 because of increasing concerns about their persistence and developmental toxicity (Vuong et al., 2019).

PBDEs consist of 209 congeners which contain diphenyl-ether skeleton and named according to the number and position of bromine atoms by the IUPAC system. Chemical structure of PBDEs is given in Fig. 1.

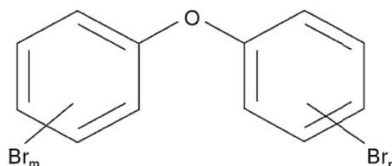


Figure 1. Chemical structure of polybrominated diphenyl ethers (PBDEs)

PBDEs have been used as additives in wide range of polymers, plastics, textiles, furniture electrical or electronic devices and automobile parts to prevent or retard the spread of fire. PBDEs are easily integrated into polymers during manufacture process (Talness et al., 2008). The polymeric materials in products can contain 5–25% PBDE by weight (Siddiqi et al., 2003). Due to their lack of binding sites, they can be released into environment by volatilization or dust formation when they cannot chemically bond on material surface. PBDEs are distributed into all environmental media depending on their physicochemical properties.

Highly brominated BDEs have created less concern because of their high K_{OW} and low vapor pressure resulting in less mobility and strong sorption to soil and sediments (Schenger et al., 2008). For example, penta BDEs are found mainly in the atmosphere and aqueous media, while higher brominated compounds such as BDE-209 tend to accumulate in soil and sediments (Yang et al., 2015). Environmental fate models can be used to characterize the behavior of these chemicals in the environment (Schenger et al., 2008). PBDEs, being persistent organic pollutants, are found in remote areas far away from their sources due to long-range transport. High volume active air sampling is a widely favoured technique to study their transport (Kurt-Karakus et al., 2018). In this study, high volume air sampling was conducted for PBDEs in gas and particulate phases at Izmir Institute of Technology, Urla, Turkey. Back-trajectory modeling was employed to infer on the source regions.

2. Material methods

2.1. Sampling

Modified GPS-11 (Thermo-Andersen Inc.) high volume sampler was used for the collection of gaseous and particulate samples. The diameter of quartz filter was 101 mm. The PUF was 5 cm thick sheet stock polyurethane type (density 0.222 g/cm³), fully fitted in the PUF cartridge. Two PUFs were placed in series to eliminate breakthrough and 10-gram XAD-2 placed between the PUFs. Samples were collected from December 2018 to June 2019 at a frequency of once in a week for 24 h at Urla sampling station at Izmir Institute of Technology campus. The samplers collected 150-160 m³ of air per sample. Samples were wrapped with aluminium foil and kept at -20 °C until extraction.

2.2. Sample extraction

PUF-XAD-2 cartridges were extracted with Soxhlet for 24 h with a mixture of 1:1 acetone:hexane. Quartz filters were extracted ultrasonically with 1:1 acetone: hexane. The extract volumes were reduced to 1 ml, solvent exchanged to isooctane, and concentrated using a rotary evaporator (BUCHI-Rotavapor-R210)

2.3. Instrumental analysis

Samples were analysed using a GC (Agilent 7890B) coupled with an MSD (Agilent 5977) operated on EI (electron impact)-selective ion monitoring (SIM) mode. Separation of congeners was performed on a capillary DB-5 column (15 m, 0.25 mm i.d., 0.1 μm film thickness).

2.4. Quality assurance / quality control

Prior to extraction, each sample was spiked with surrogate standards, 25 ng PBDEs (-77, -181) in order to determine the recovery efficiency. The mean method recovery efficiencies (%) of $^{13}\text{C}_{12}\text{PBDE-77}$ were found to be 78% and 95% for gas and particulate phases, respectively. Recovery for $^{13}\text{C}_{12}\text{PBDE-181}$ were found to be 84% for gas phase and 88% for particulate phase.

3. Results and discussion

Ambient air PBDE concentrations have been reported for many locations in the world. Reports are variable at different locations with differences in emissions strength, congeners, sampling methods (active or passive), and the atmospheric phase (particle, gas, or both). Gas phase $\Sigma 14\text{PBDE}$ concentrations varied between 50 pg/m^3 and 510 pg/m^3 in this study, while particle phase $\Sigma 14\text{PBDE}$ concentrations were found between 118 pg/m^3 and 376 pg/m^3 . The concentrations obtained in this study are in the range of values reported in the literature. They are less than those reported for industrial zones but similar to the other types of sites. BDE-190 and BDE-100 were the main contributors to the total concentrations. Figure 2 and Figure 3 show contribution of each congener in each sample for gas and particle phases, respectively. In general, BDE-28, -47, and -190 were the congeners with the highest detection frequencies.

Kurt-Karakus et al. (2018) reported an annual average gas + particle phase $\Sigma 14\text{PBDE}$ concentration of $191 \pm 329 \text{ pg}/\text{m}^3$ in a countrywide sampling campaign in Turkey. The mean values for urban and rural sites were $183 \pm 260 \text{ pg}/\text{m}^3$ and $200 \pm 387 \text{ pg}/\text{m}^3$, respectively. $\Sigma 7\text{PBDEs}$ concentrations ranged from 81 to 149 pg/m^3 and from 6 to 11 pg/m^3 at industrial and urban/suburban sites, respectively, in Izmir (Cetin and Odabasi, 2008). Lammel et al. (2015) reported a mean $\Sigma 7\text{PBDE}$ concentration of 8.5 pg/m^3 , while Besis et al. (2017) reported 197 pg/m^3 when BDE-209 is included at the Urla site. In Japanese cities, PBDE concentrations between 19 and 25 pg/m^3 were reported for Hokkaido (Takigami et al., 2009) and 4.5-65 pg/m^3 for Kyoto (Hayakawa et al., 2004). Muenhor et al. (2010) reported $\Sigma_{10}\text{PBDEs}$ at e-waste storage facilities in Thailand between 8 pg/m^3 and 150 pg/m^3 , while Vives et al. (2007) reported an average concentration of 106 pg/m^3 in the Lake Maggiore. Concentrations of $\Sigma_{10}\text{PBDE}$ were reported between 39 and 48 pg/m^3 in Toronto, Canada (Shoeib et al., 2004), while lower levels (3-30 pg/m^3) were reported later from the same region (Harner et al., 2006). Hoh and Hites (2005) reported an average $\Sigma_{26}\text{PBDE}$ concentration of 10035 pg/m^3 for Chicago, while a 50 pg/m^3 was reported for $\Sigma 7\text{PBDE}$ at a site close to Chicago by Strandberg et al. in 2001. Meanwhile, higher concentrations have been reported at industrial sites: between 1941 pg/m^3 in the city of Guangzhou (Chen et al., 2006) and 1450 pg/m^3 of $\Sigma_{15}\text{PBDEs}$ in the Pearl River Delta (Zhang et al., 2009 a, b) in China, and between 81 and 149 pg/m^3 in Aliğa, Turkey (Odabasi et al., 2008), about 60 km from the sampling site of this study .

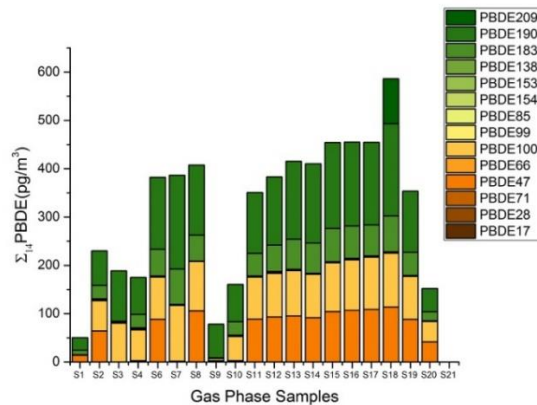


Figure 2. Σ_{14} PBDEs and main congeners in gas phase samples

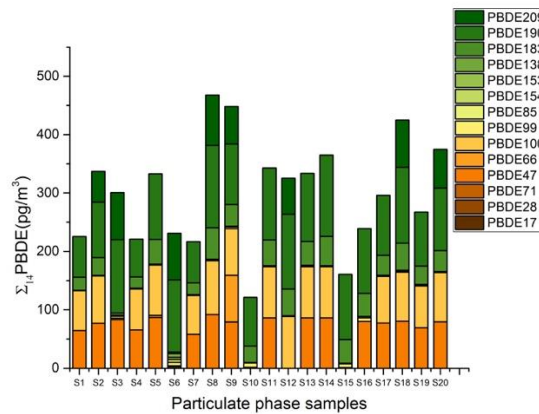


Figure 3. Σ_{14} PBDEs and main congeners in particle phase samples

3.1. Back trajectories

Meteorological datasets archived on the ARL server were used to drive the HYSPLIT4 model. GDAS data with a horizontal resolution of 1° which corresponds to $100 \text{ km} \times 100 \text{ km}$ and 23 vertical layers were used in order to determine the back trajectories. In this study, 120-h backward trajectories calculated for 20 samples showed that possible PBDE sources mainly lie in north and northeast of the sampling location. Figure 4 shows backward trajectories for a high-PBDE-concentration day at the sampling location indicate possible source regions in Russia.

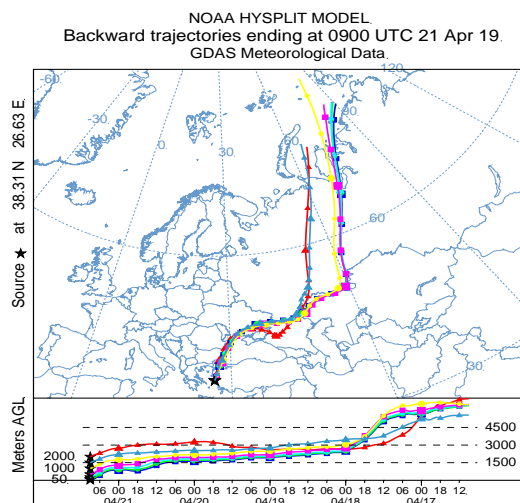


Figure 4. Backward trajectories for a high-concentration day at the sampling location

4. Conclusion

In this study gas and particulate phase samples were collected by active sampling method at a site in Urla, Turkey. Gas phase Σ_{14} PBDE concentrations ranged from 50 pg/m^3 to 510 pg/m^3 whereas the range was found to be 118 - 376 pg/m^3 for particulate phase. BDE-190 and -100 were the main contributors to the total concentrations, while BDE-28, -47, and -190 were the congeners with the highest detection frequencies. Back trajectory analysis indicated that possible PBDE source regions mainly lie in north and northeast of the sampling location.

5. References

- Besis, A., Lammel, G., Kukucka, P., Samara, C., Sofuoglu, A., Dumanoglu, Y., Eleftheriadis, K., Kouvarakis, G., Sofuoglu, S.C., Vassilatou, V., Voutsas, D., 2017. Polybrominated diphenyl ethers (PBDEs) in background air around the Aegean: implications for phase partitioning and size distribution. *Environmental Science & Pollution Research*. 24, 28102–28120.
- Cetin, B., Odabasi, M., 2008. Atmospheric concentrations and phase partitioning of polybrominated diphenyl ethers (PBDEs) in Izmir, Turkey. *Chemosphere*. 71(6), 1067-1078.
- Chen, L. G., Mai, B. X., Bi, X. H., Chen, S. J., Wang, X. M., Ran, Y., Zeng, E. Y., 2006. Concentration levels, compositional profiles, and gas-particle partitioning of polybrominated diphenyl ethers in the atmosphere of an urban city in South China. *Environmental Science & Technology*. 40(4), 1190-1196.
- Harner, T., Shoeib, M., Diamond, M., Ikononou, M., Stern, G., 2006. Passive sampler derived air concentrations of PBDEs along an urban–rural transect spatial and temporal trends. *Chemosphere*. 64(2), 262-267.
- Hayakawa, K., Takatsuki, H., Watanabe, I., Sakai, S. I., 2004. Polybrominated diphenyl ethers (PBDEs), polybrominated dibenzo-p-dioxins/dibenzofurans (PBDD/Fs) and monobromo-polychlorinated dibenzo-p-dioxins/dibenzofurans (MoBPXDD/Fs) in the atmosphere and bulk deposition in Kyoto, Japan. *Chemosphere*. 57(5), 343-356.
- Hoh, E., Hites, R. A., 2005. Brominated flame retardants in the atmosphere of the east-central United States. *Environmental Science & Technology*. 39(20), 7794-7802.
- Król, S., Zabiegała, B., Namieśnik, J., 2012. PBDEs in environmental samples: sampling and analysis.



Talanta. 93, 1-17.

Kurt-Karakus, P. B., Ugranli-Cicek, T., Sofuoglu, S. C., Celik, H., Gungormus, E., Gedik, K., Jones, K. C., 2018. The first countrywide monitoring of selected POPs: Polychlorinated biphenyls (PCBs), polybrominated diphenyl ethers (PBDEs) and selected organochlorine pesticides (OCPs) in the atmosphere of Turkey. *Atmospheric Environment*. 177, 154-165.

Lammel, G., Audy, O., Basis, A., Efstathiou, C., Eleftheriadis, K., Kohoutek, J., Rusina, T. P., 2015. Air and seawater pollution and air-sea gas exchange of persistent toxic substances in the Aegean Sea: spatial trends of PAHs, PCBs, OCPs and PBDEs. *Environmental Science and Pollution Research*. 22(15), 11301-11313.

Muenhor, D., Harrad, S., Ali, N., Covaci, A., 2010. Brominated flame retardants (BFRs) in air and dust from electronic waste storage facilities in Thailand. *Environment International*. 36(7), 690-698.

Shoeib, M., Harner, T., Ikononou, M., Kannan, K., 2004. Indoor and outdoor air concentrations and phase partitioning of perfluoroalkyl sulfonamides and polybrominated diphenyl ethers. *Environmental Science & Technology*. 38(5), 1313-1320.

Siddiqi, M. A., Laessig, R. H., Reed, K. D., 2003. Polybrominated diphenyl ethers (PBDEs): new pollutants-old diseases. *Clinical Medicine & Research*. 1(4), 281-290.

Strandberg, B., Dodder, N. G., Basu, I., Hites, R. A., 2001. Concentrations and spatial variations of polybrominated diphenyl ethers and other organohalogen compounds in Great Lakes air. *Environmental Science & Technology*. 35(6), 1078-1083.

Takigami, H., Suzuki, G., Hirai, Y., Sakai, S. I., 2009. Brominated flame retardants and other polyhalogenated compounds in indoor air and dust from two houses in Japan. *Chemosphere*. 76(2), 270-277.

Vuong, A. M., Braun, J. M., Wang, Z., Yolton, K., Xie, C., Sjodin, A., Chen, A., 2019. Exposure to polybrominated diphenyl ethers (PBDEs) during childhood and adiposity measures at age 8 years. *Environment International*. 123, 148-155.

Yang, S., Fu, Q., Teng, M., Yang, J., 2015. Polybrominated diphenyl ethers (PBDEs) in sediment and fish tissues from Lake Chaohu, central eastern China. *Archives of Environmental Protection*. 41(2), 12-20.

Zhang, B. Z., Guan, Y. F., Li, S. M., Zeng, E. Y., 2009a. Occurrence of polybrominated diphenyl ethers in air and precipitation of the Pearl River Delta, South China: annual washout ratios and depositional rates. *Environmental Science & Technology*, 43(24). 9142-9147.

Zhang, X., Diamond, M. L., Ibarra, C., Harrad, S., 2009b. Multimedia modelling of polybrominated diphenyl ether emissions and fate indoors. *Environmental Science & Technology*. 43(8), 2845-2850.

Acknowledgements

Financial support was provided by Turkish Scientific and Technological Research Council (TUBITAK) Grant#118Y254.

Indoor air gas-particulate partitioning of synthetic musk compounds

Esin Balcı¹, Mesut Genisoglu¹, Aysun Sofuoğlu² and Sait C. Sofuoğlu¹

¹Izmir Institute of Technology, Dept. of Environmental Engineering, Urla, Turkey

²Izmir Institute of Technology, Dept. of Chemical Engineering, Urla, Turkey

cemilsofuoglu@iyte.edu.tr

Abstract. In this study, partitioning of Synthetic Musk Compounds (SMCs) between gas and particle phases was investigated in an indoor environment. An SMC mixture was placed in a glass petri dish on top of a hotplate and left for volatilization for 1 h in an unoccupied room (L×W×H, 6.10×2.90×3.80 m). A ventilator was operated during the 1-h period at a low speed for a better mixing in the room of which windows were kept closed and the door was sealed. Then, samples were collected for the 0-4 h and for the 121-145 h (6th day) using XAD-2 sandwiched between two PUF plugs and glass-fiber filter for gas and PM₁₀ phases, respectively. The collected samples were analyzed using a GC-MS after the extraction, clean-up and concentrating. Experimental results demonstrated that SMC concentrations decreased over time, which could be described by second order kinetics. Six of the SMCs partitioned to PM₁₀ with at least 10% at beginning of the experiment, whereas it dropped to two compounds at the end, showing that SMCs may partition well between the two phases but they tend to be in the gas phase. logK_p values at the beginning of the experiment were calculated to be -0.94, -1.35, -1.05, -0.30, -0.42, -0.35, and 0.25 m³/μg for DPMI, ADBI, AHMI, ATII, HHCB, AHTN, and MK, respectively. However, at the end of the experiment, logK_p values could be calculated for only ADBI, HHCB, and AHTN to be -1.18, -1.82, -2.10 m³/μg, respectively, because concentrations of the remaining compounds were BDL in one or both of the phases.

Keywords: Synthetic musk compounds, Gas-particulate partitioning, Indoor environment.

1. Introduction

Synthetic Musk Compounds (SMCs) which are a group of Semi-Volatile Organic Compounds (SVOCs) have been produced in large quantities as a substitute of expensive and nonsustainable natural musk obtained from animals and fragrant plants (Salvador and Chisvert, 2007; Bester, 2009; Sofuoğlu et al., 2010; Lopez-Nogueroles et al., 2013). SMCs are widely used all over the world as fragrance in consumer products such as air fresheners, cleaning supplies, and personal care products (Walters et al., 2005; Salvador and Chisvert, 2007; Sofuoğlu et al., 2010; Lu et al., 2011; Lopez-Nogueroles et al., 2013; Chen et al., 2018; Wong et al., 2019). Concerns about the biological and environmental effects of SMCs have begun in 1980 for the first time, due to the fact that their presence in freshwater fish samples was shown in Japan, and then their occurrence have been investigated in all environmental media (Kannan et al., 2005; Salvador and Chisvert, 2007; Taylor et al., 2014). They have also been detected in biota (Draisci et al., 1998; Nakata et al., 2015) and in human biological samples including adipose tissue (Kannan et al., 2005; Schiavone et al., 2010), breast milk (Lignel et al., 2008), and blood (Hu et al., 2010).

SMCs can be divided into four major groups according to their chemical structure: nitro (NMs), polycyclic (PCMs), macrocyclic (MCMs), and alicyclic (ACMs) (Vallecillos et al., 2015; Wong et al., 2019). Nitro musks, which are alkylated nitrobenzene derivatives, exhibit similar physical and chemical

properties to persistent organic pollutants (POPs) having a wide range of transport ability, environmental resistance, and bioaccumulation capacity in ecosystems. They generally refer to the five most commercially relevant compounds; Musk Ketone (MK), Musk Ambrette (MA), Musk Moskene (MM), Musk Tibetene (MT), and Musk Xylene (MX). MM and MT are prohibited for use in cosmetics because they were shown to cause some skin problems and allergic reactions (Salvador and Chisvert, 2007; Winter, 2009). MA has been discontinued from use due to photosensitivity and neurotoxicity (Taylor et al., 2014; Sheppard, 2018). MX and MK were the most commonly used NMs in the sector. However, under the Regulation on Registration, Evaluation, Authorization and Restriction of Chemicals (REACH), MX was classified as a substance that is highly resistant and that has biological accumulation. In parallel with International Fragrance Association (IFRA), it was banned by European Commission due to its potential impact on the environment (International Fragrance Association, 2011). In addition, use of MK was limited in the US because of its bioaccumulative properties. NMs have largely been replaced by PCMs due to bans/restrictions in several countries. Compared with NMs, PCMs have such better properties as higher resistance to light and alkali environments. They include Galaxolide (HHCB), Tonalide (AHTN), Celestolide (ADBI), Phantolide (AHMI), Traseolide (ATII), Cashmeran (DPMI). From these compounds, AHTN and HHCB are the most commercially-used PCMs (95%) (Gatermann et al., 2002). Owing to this reason, both compounds were determined as high production volume chemicals by the US Environmental Protection Agency (USEPA) and added the Hazardous Substances Data Bank (HSDB®) and Toxicology Data Network (TOXNET®). Because the other two groups of SMCs (MCMs and ACMs) have been recently introduced in the market, they are not used as much as PCMs. With the exception of several studies that focused on MCM and ACM, many studies on SMCs usually target PCMs and NMs because these compounds have lipophilic structure, bioaccumulation capacity, volatility, and resistance to natural degradation. Thus, they can be found in water, sediments, indoor and outdoor air, and house dust. Although the levels and fate of SMCs in different matrices have been extensively studied, knowledge about their distribution in the indoor environment is very limited. Consumer products used in households constitute an important source of contamination for the indoor residential environment (Walters et al., 2005; Kubwabo et al., 2012). Therefore, exposure through indoor air which is one of the most human-exposure-relevant environments may be of critical importance (Kiyemet, 2009). They exist in both in the gas and particle phases due to their semi-volatile properties (Weschler and Nazaroff, 2008; Ozcan, 2013; Wei et al., 2016). In turn, the partitioning between the two phases is crucial for estimation of exposure through determination of total SMC concentration in indoor air. In this context, this study aimed to investigate partitioning of SMCs between gas and particulate phases experimentally in an indoor environment.

2. Materials and methods

2.1. Materials

The Musk-Mix 11 standard comprising DPMI, ADBI, AHMI, ATII, AHTN, and HHCB from PCMs, MA, MK, MX, MT from NMs was purchased from Neochema GmbH & Co.KG (Bodenheim, Germany). Gas chromatographic grade ethyl acetate, acetone, n-hexane, and dichloromethane (Suprasolv; Merck, Germany) were used for the clean-up, extraction, and GC-MS applications. After extraction of indoor air samples, Florisil (100–200 mesh; Sigma-Aldrich, USA) and anhydrous sodium sulfate (Fluka, Steinheim, Germany) were used. Florisil was preferred for cleaning pesticide residues, other chlorinated hydrocarbons and for separating nitrogen compounds from hydrocarbons and aromatic compounds from aliphatic-aromatic mixtures and similar applications for use with oils, fats and waxes (USEPA, 2007) while anhydrous sodium sulfate was used for the removal of any water residue.

2.2. Methods

Musk mixture prepared to contain ~46 µg from each of DPMI, ADBI, AHMI, ATII, AHTN, HHCB, MA, MK, MX, and MT was placed in a glass petri dish on top of a hotplate and left for volatilization through 1-h in an unoccupied room (L×W×H of 6.10×2.90×3.80 m). A ventilator was operated during

the 1-h period at a low speed for a better mixing in the room of which windows were kept closed and the door was sealed. The gas and particulate phase samples were collected with an active air sampling system consisted of a Harvard impactor (Air Diagnostics & Engineering Inc., Harrison, ME, USA), in which a 37-mm glass-fiber filter (1 μm pore) was placed in the impactor to capture PM with aerodynamic diameter $<10 \mu\text{m}$ at 10 L/min flow rate, Amberlite XAD₂ resin sandwiched between polyurethane foam (PUF) plugs (Supelco, Bellefonte, USA) in a glass holder followed to collect gas phase sample, connected to a vacuum pump (Air Diagnostics & Engineering Inc., SP-280). Schematic diagram of the active air sampling system is shown in Figure 1.

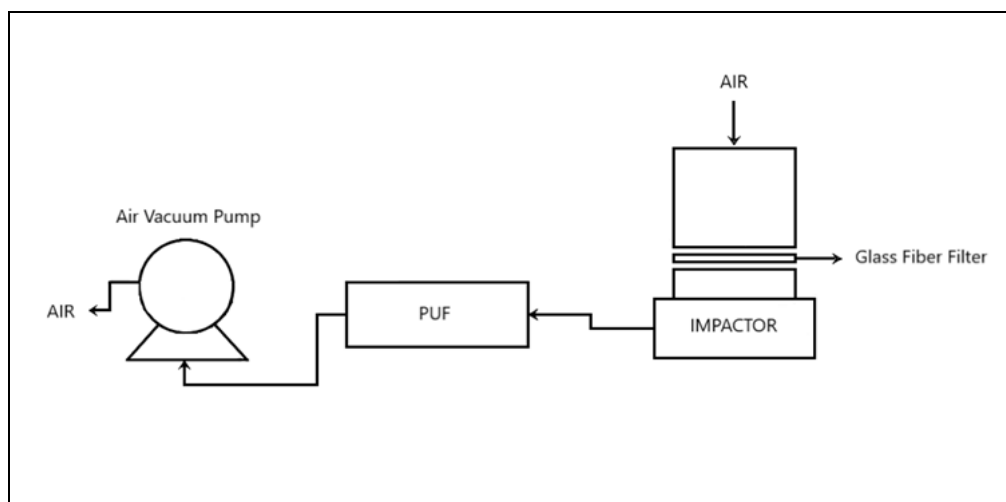


Figure 1. Air Sampling System

Five samples were collected in the first day of the experiment followed by samples collected at 2nd, 3rd, 4th, and 6th days. Here concentrations determined in the very 1st sample collected through the first 4-h period and the very last sample collected through the 121-145th hours are presented. Flow rate at the start of each sample was set to 10 L/min, and measured at the end to determine if the difference is $<10\%$ required to deem the sample acceptable.

In this study, before extraction procedure was implemented, 10 μL of fluoranthene-d10 surrogate standard solution (50 $\text{pg}/\mu\text{L}$ concentration) was added to the samples. After the each of gas and particulate samples were ultrasonically extracted for 30 min in acetone and hexane mixture (1:1 v/v), they were evaporated under nitrogen gas flow (100 mL/min) in order to reduce the volume to 5 mL (100 mL/min). Next, 10 mL of hexane was added three times to change the solvent to hexane, and then the sample was concentrated to 2 mL by evaporation. For clean-up of the sample, a chromatographic column prepared by placing a piece of glass wool, 0.75 g Florisil and 1 cm sodium anhydrous sulfate into a pasteur glass pipet was used. Prior to column chromatography, florisil and sodium anhydrous sulphate were activated in the oven at 650 $^{\circ}\text{C}$ and 450 $^{\circ}\text{C}$, respectively. Before florisil was placed in the column, its deactivation was performed by adding water. Firstly, the samples were passed through the column and discharged. After 4 mL of ethyl acetate was passed in the column, solvent phase samples were collected in a 40 mL amber vial. Volume of the samples was reduced to 1 mL under nitrogen gas flow. Then, solvent was changed into the hexane and the extracts were stored at -20 $^{\circ}\text{C}$ until GC-MS analysis. A GC-EI-MS, equipped with DB-5MS (30m \times 0.25mm \times 0.25 μm) capillary column and programmable-temperature-vaporizing injection, was used for separation and quantification of SMCs, operated in selective ion monitoring (SIM) mode.

The partitioning of SMCs between particle and gas phases can be characterized by the SMCs particle/gas partition coefficient (K_p) using Equation (1) (Weschler et al., 2008).

$$K_P = \left(\frac{C_P}{C_{PM10}} \right) / C_G \quad (1)$$

where, C_P (ng/m^3) is the SMC concentrations in the particulate matter, C_{PM10} ($\mu\text{g}/\text{m}^3$) is the PM_{10} concentration and C_G (ng/m^3) is the SMC concentrations in the gas phase.

3. Results and discussion

3.1. PCM concentrations in the gas and particulate phase

At the start of the experiment gas phase concentrations were determined as 8.55, 9.14, 7.88, 4.49, 41.4, and 9.30 ng/m^3 , respectively for DPMI, ADBI, AHMI, ATII, HHCB, and AHTN (Figure 2a). At the end of the experiment, gas phase concentrations were decreased to 0.18, 12.03, and 4.72 ng/m^3 for ADBI, HHCB, and AHTN, respectively, while the remaining compounds were below detection limit (BDL). At the start of the experiment, PM_{10} -bounded DPMI, ADBI, AHMI, ATII, HHCB, and AHTN concentrations were determined to be 1.79, 0.74, 1.28, 4.10, 28.8, and 7.55 ng/m^3 , respectively, whereas at the end, particle-phase DPMI, ADBI, HHCB, and AHTN were found as 0.28, 0.07, 1.07, and 0.22 ng/m^3 , respectively, and the others were BDL.

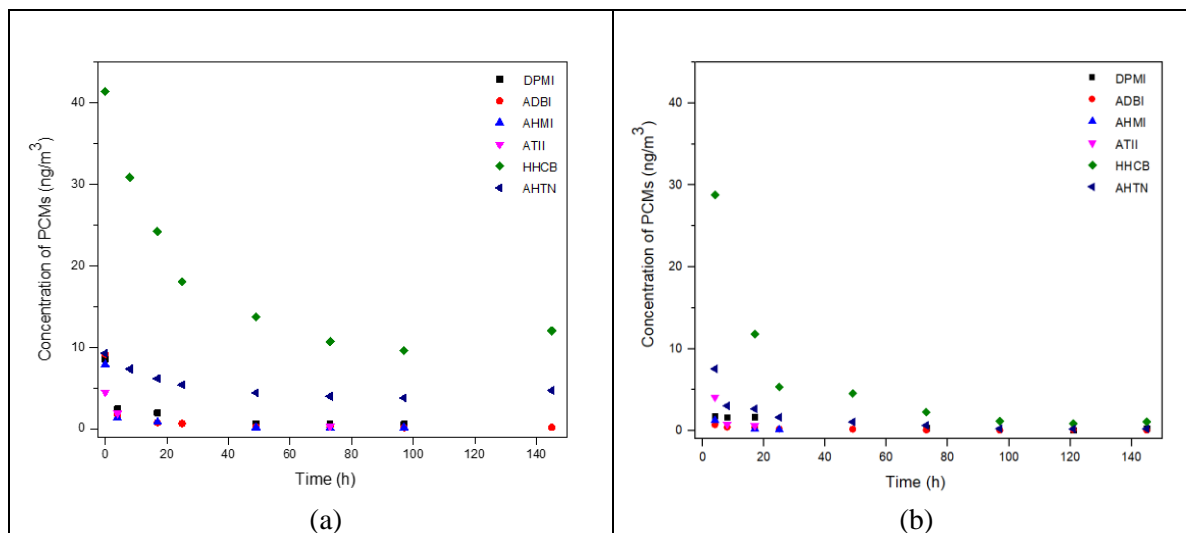


Figure 2. Concentrations of PCMs in the (a) gas and (b) particle phases during the experiment

It is known that SMCs may photochemically degrade under different light sources such as UV and sunlight. Wong et al. (2019) investigated SMC concentrations in urban and surrounding environments including air, soil, and surface water. Researchers reported half-lives of SMCs in air due to photodegradation. Half-lives of PCMs ranged from 0.1 to 1.4 days. AHTN and HHCB, with a half-life of 0.6 and 0.22 days, respectively, were found to be the highest concentration compounds in all media. Besides, in the OSPAR data (2004), the half-lives of AHTN and HHCB were reported as 0.83 and 0.41 days, respectively. In this study, PCM concentrations decrease in accordance with second order kinetics. Therefore, concentrations decreased at much higher rates compared to those reported by the above-mentioned literature. The difference indicates that the other processes such as sorption onto indoor surfaces in addition to PM are much more influential compared to photodegradation in outdoor air. The SMCs ranked as AHTN, HHCB, DPMI, AHMI, ADBI, and ATII in this study from high to low rates.

3.2. NM concentrations in the gas and particulate phases

At the beginning of the experiment, all of NMs were observed in the gas phase, as shown in Figure 3a. Their concentrations were determined to be 2.02, 9.20, 12.1, and 10.3 ng/m^3 , respectively for MK, MX, MA, and MT. At the end of the experiment, only MK and MX were detectable at 0.58 and 0.53 ng/m^3 ,

respectively. MA and MT were BDL before the end of the first day. As shown in Figure 3b, only MK could be found in the particle phase at the beginning, which also was BDL after 48 hours.

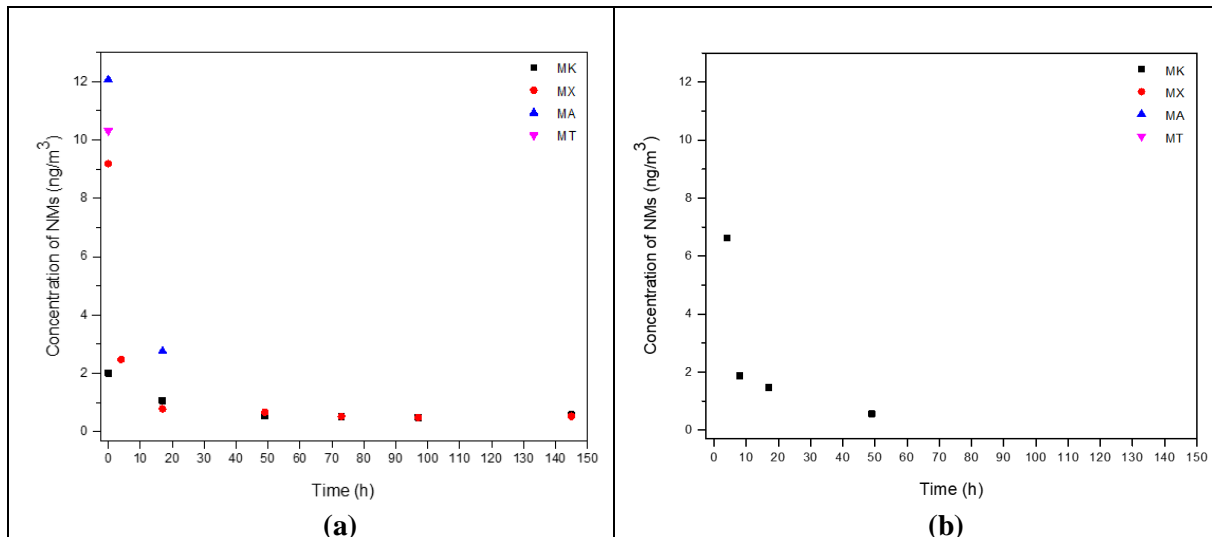


Figure 3. Concentrations of NMs in the (a) gas and (b) particle phases throughout the study

It is known that photodegradation occurs in ambient air. The half-life of MT associated with photodegradation in outdoor air was reported to range between 1.0 and 1.5 hr during summer, while it ranged from 6 to 10 hr in winter, and it was even longer (12.8 day) for MX (ECHA, 2008). Wong et al. (2019) reported photodegradation half-lives for NMs to be 7.1, 7.3, 8.3, and 13 days for MA, MT, MK, and MX, respectively, in ambient air. In this study, it was found that decrease in NM concentrations can be described by second order kinetics, therefore, due to mainly other processes than photodegradation. It may be related to the available indoor surfaces, i.e., cement-plastered walls, gypsum-board suspended ceiling, and office furniture for sorption in addition to the PM.

3.3. Gas/Particle Partitioning

In this study, unlike the start of the experiment, the SMCs were found to be at a higher proportion in the gas phase than the particle phase at end of the experiment. Chen et al. (2007) investigated presence and distribution of PCMs in a typical cosmetic plant in China, and reported that they were dominantly found in the gas phase. Sofuoglu et al. (2010) reported concentrations of SMCs in a primary school classroom and a women's sport center in both phases, of which concentrations in the gas phase were higher than particulate phase. A study carried out by Weinberg et al. (2011) focused on the presence of SMCs released from a wastewater treatment plant to air. Although, researchers observed all of SMCs in the gas phase, ATII, MX, and MT were not detected in the particle phase, while HHCB and AHTN were found in both phases. Nevertheless, the authors underlined that most of SMCs dominate in gas phase, with particle phase being <1% of the total musk concentration except for AHMI and ADBI in some samples.

As shown in Figure 4, DPMI, AHMI, ATII, HHCB, and AHTN of PCMs, and only MK of NMs were found in both of the phases in the first 4 h of the experiment, while MX, MA, and MT were all in the gas phase. Figure 5, on the other hand, shows that ADBI, HHCB, AHTN, MK, and MX were dominantly in the gas phase, while DPMI could not be detected in the gas phase at the 6th day. However, DPMI concentrations in the gas and PM phases at the 5th day were both detectable at 0.56 ng/m³ and 0.07 ng/m³, respectively. As a result, DPMI appears to partition to the particulate phase at the end of the experiment.

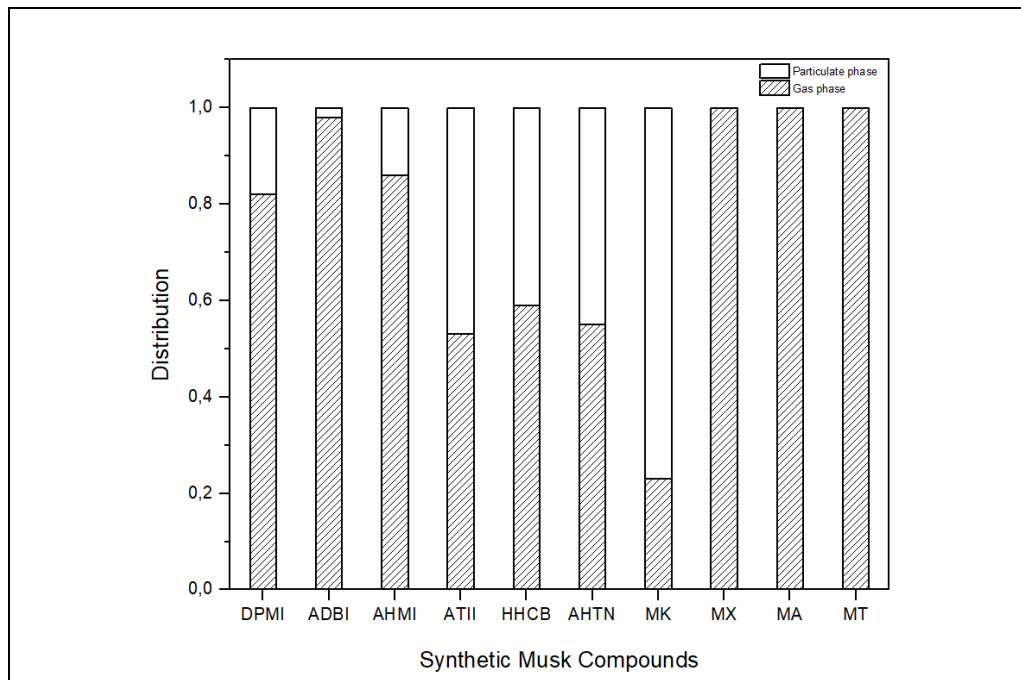


Figure 4. SMCs partitioning between the gas and particle phases during the first 4h

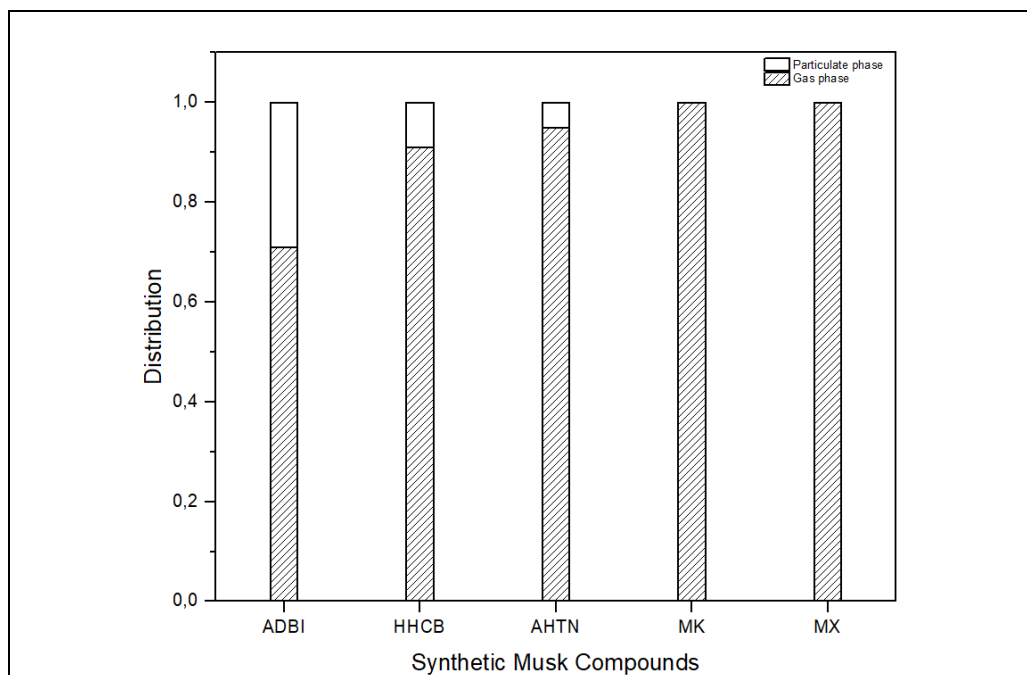


Figure 5. SMCs partitioning between the gas and particle phases during the 6th day

In this study, particle/gas partition coefficient (K_p) was calculated from Equation (1). According to the measurement results, the PM_{10} concentration varied from $5.95 \mu\text{g}/\text{m}^3$ to $33.7 \mu\text{g}/\text{m}^3$ during the experiment. $\log K_p$ values based on the measured SMC concentrations in this study were calculated to be -0.94, -1.35, -1.05, -0.30, -0.42, -0.35, and 0.25 $\text{m}^3/\mu\text{g}$ for DPMI, ADBI, AHMI, ATII, HHCB, AHTN, and MK, respectively, during the first 4 h of the experiment. However, $\log K_p$ values could be

calculated for only ADBI, HHCB, and AHTN at the end of the experiment to be -1.18, -1.82, and -2.10 m³/μg, respectively, due to the BDL compounds.

4. Conclusion

This experimental study conducted in indoor air demonstrated that SMCs are found highly in the gas phase compared to the particle phase. The decrease in SMC concentrations during the experiment could be described by second order kinetics. Six of the SMCs partitioned to PM₁₀ with at least 10% at the beginning of the experiment with logK_p values ranging between -0.94 and 0.25 m³/μg, whereas it dropped to two compounds at the end with logK_p values ranging from -2.10 to -1.18 m³/μg, showing that SMCs may partition well between the two phases but they tend to be in the gas phase.

5. References

- Bester, K., 2009. Analysis of musk fragrances in environmental samples. *Journal of Chromatography A*. 1216, 470-480.
- Chen, D., Zeng, X., Sheng, Y., Bi, X., Gui, H., Sheng, G., Fu, J., 2007. The concentrations and distribution of polycyclic musks in a typical cosmetic plant. *Chemosphere*. 66, 252-258.
- Chen, T.A., Chung, W.H., Ding, E.M.C., Ding, W.H., 2018. Ultrasound-assisted emulsification microextraction for rapid determination of unmetabolized synthetic polycyclic and nitroaromatic musks in human urine. *Journal of Chromatography B*. 1092, 440-446.
- Draisci, R., Marchiaava, C., Ferreti, E., Palleschi, L., Catellani, G., Anastasia, A., 1998. Evaluation of musk concentration of freshwater fish in Italy by accelerated solvent extraction and gas chromatography with mass spectrometric detection. *Journal of Chromatography*. 814, 187-197.
- ECHA, 2008. <https://echa.europa.eu/documents/10162/2109eaae-6394-4840-84de-55ad0a5d4797>, accessed in 2019.
- Gatermann, R., Biselli, S., Hühnerfuss, H., Rimkus, G.G., Franke, D., Hecker, M., Kallenborn, R., Karbe, L., König, W.A., 2002. Synthetic musk in the environment. Part 2: Enantioselective transformation of the polycyclic musk fragrances HHCB, AHTN, AHDI and ATII in freshwater fish. *Archives of Environmental Contamination and Technology*. 42, 447-452.
- Hu, Z., Shi, Y., Niu, H., Cai, Y., Jiang, G., Wu, Y., 2010. Occurrence of synthetic musk fragrances in human blood from 11 cities in China. *Environ. Toxicol. Chem.* 29, 1877-1882.
- International Fragrance Association, 2011. EU regulation follows fragrance industry's voluntary global ban. Press Release.
- Kannan, K., Reiner, J.L., Yun, S.H., Perrota, E.E., Tao, L., Johnson-Restrepo, B., Rodan, B., 2005. Polycyclic musk compounds in higher trophic level aquatic organisms and humans from the United States. *Chemosphere*. 61, 693-700.
- Kiyemet, N., 2009. Determination of synthetic musk compound levels in indoor air. Master of Science (MSc) Thesis, Izmir Institute of Technology. Izmir, Turkey, 50 pages.
- Kubwabo, C., Fun, X., Rasmussen, P.E., Wu, F., 2012. Determination of synthetic musk compounds in indoor dust by gas chromatography-ion trap mass spectrometry. *Anal. Bioanal. Chem.* 404, 467-477.
- Lignel, S., Darnerud, P.O., Aune, M., Cnattingius, S., Hajslova, J., Setkova, L., Glynn, A., 2008. Temporal trends of synthetic musk compounds in mother's milk and associations with personal use of perfumed products. *Environ. Sci. Technol.* 42, 6743-6748.



- Lopez-Nogueroles, M., Lordel-Madeleine, S., Chisvert, A., Salvador, A., Pichon, V., 2013. Development of a selective solid phase extraction method for nitromusk compounds in environmental waters using a molecularly imprinted sorbent. *Talanta*, 110, 128-134.
- Lu, Y., Yuan, T., Yun, S.H., Wang, W., Kannan, K., 2011. Occurrence of synthetic musks in indoor dust from China and Implications for Human Exposure. *Arch. Environ. Contam. Toxicol.* 60, 182-189.
- Nakata, H., Hinosaka, M., Yanagimoto, H., 2015. Macrocyclic-, polycyclic- and nitromusks in cosmetics, household commodities and indoor dusts collected from Japan: Implications for their human exposure. *Ecotoxicology and Environmental Safety*. 111, 248-255.
- OSPAR, 2004. <https://www.ospar.org/documents?d=6978>, accessed in 2019.
- Ozcan, C., 2013. Determination of gas-particle partitioning parameters and indoor air concentrations of synthetic musk compounds. Master of Science Thesis. Izmir Institute of Technology, Izmir, 59 pages.
- Salvador, A., Chisvert, A., 2007. *Analysis of Cosmetic Products*, Second ed. Elsevier Science, Cambridge.
- Schiavone, A., Kannan, K., Horii, Y., Focardii, S., Corsolini, S., 2010. Polybrominated diphenyl ethers, polychlorinated naphthalenes and polycyclic musk in human fat from Italy: comparison to polychlorinated biphenyls and organochlorine pesticides, *Environ. Pollut.* 158, 599-606.
- Sheppard C., 2018. *Advances in Marine Biology*, first ed. Academic Press, Cambridge.
- Sofuoglu, A., Kiyem, N., Kavcar, P., Sofuoglu, S.C., 2010. Polycyclic and nitromusk in indoor air: A primary school classroom and a women's sport center. *Indoor air*. 20, 515-522.
- Taylor, K.M., Weisskopf, M., Shine, J., 2014. Human exposure to nitro musks and the evaluation of their potential toxicity an overview. *Environmental Health*. 13, 14.
- U.S. Environmental Protection Agency (USEPA), 2007. Method 3620C-Florisil Cleanup.
- Vallecillos, L., Borrull, F., Pocurull, E., 2015. Recent approaches for the determination of synthetic musk fragrances in environmental samples. *Trends in Analytical Chemistry*. 72, 80-92.
- Walters, A., Santillo, D., Johnston, P., 2005. http://www.greenpeace.to/synthetic_musks_2005.pdf, accessed in 2019.
- Wei, W., Mandin, C., Blanchard, O., Mercier, F., Pelletier, M., Le Bot B., Glorennec, P., 2016. Temperature dependence of the particle/gas partition coefficient: An application to predict indoor gas-phase concentrations of semi-volatile organic compounds. *Science of Total Environment*. 563, 506-512.
- Weinberg, I., Dreyer, A., Ebinghaus, R., 2011. Wastewater treatment plant as sources of polyfluorinated compounds, polybrominated diphenyl ethers and musk fragrances to ambient air, *Environmental Pollution*, 159, 125-132.
- Weschler, C.J., Nazaroff W.W., 2008. Semivolatile organic compounds in indoor environments. *Atmospheric Environment*. 42, 9018-9040.
- Winter, R., 2009. *A Consumer's Dictionary of Cosmetics Ingredients*, seventh ed. Three Rivers Press, New York.
- Wong, F., Robson, M., Melymuk, L., Chubashini, S., Alexandrou, N., Shoeib, M., Luk, E., Helm, P., Diamond, M.L., Hung, H., 2019. Urban sources of synthetic musk compounds to the environment. *Environmental Science Processes Impacts*. 21, 74-88.



Air quality level, emission sources and control strategies in Bursa

Burak Çalışkan, Nihan Ozengin and S. Sıddık Cindoruk

Bursa Uludag University, Faculty of Engineering, Environmental Engineering Department, Nilufer, Bursa/Turkey

cindoruk@uludag.edu.tr

Abstract. In parallel with the rapidly increasing population and the number of motor vehicles, irregular urbanization, and unplanned industrialization, air pollution has reached dangerous levels in much cities. In recent years, high-quality fuels used especially in our big cities have removed air pollution from being an important environmental problem. Bursa is a good example in this aspect because air pollution, which is caused by intensive urbanization because of industrialization and excessive migration, has been a problem for Bursa for many years. This study was realized with the cooperation of Bursa Metropolitan Municipality Environmental Protection and Control Department, Bursa Uludag University Environmental Engineering Department and Bursa Governorship Provincial Directorate of Environment and Urbanization. In this study, in order to improve the air quality of Bursa, the main causes of air pollution were presented and their solutions were discussed in the workshop attended by the related institutions. In the scope of study; the measurement data obtained from air pollution monitoring stations were evaluated. The parameters of sulfur dioxide (SO₂), carbon monoxide (CO), nitrogen oxides (NO_x = NO + NO₂) and particulate matter (PM) measured between 2013-2018 were examined. Air pollutant resource groups that are active in the city of Bursa came to the fore as industry, transportation, heating and uncontrolled combustion activities respectively. A workshop was organized with the participation of stakeholders on air quality monitoring, measurement, control and evaluation. After presenting the measurement and calculation results previously obtained to the stakeholders, the opinions of the stakeholders were taken in the titles of resources, operational problems and solution suggestions. Opinions were evaluated using statistical methods (Pareto, SPSS) and prioritized. Especially the fact that the industry is located in the city and the transportation network of the city is inadequate has emerged as the main source of the air pollution problem. In order to solve this problem, it was emphasized that effective supervision should come to the forefront and new industrial facilities should not be established in the regions close to the city.

Keywords: Conventional air pollutants, Industrial emissions, Mobile sources, Air pollution prevention.

1. Introduction

Air pollution is a result of modern life In urban areas; The energy and mass residues required for transportation, heating and enlightenment fill air with intense gas and dust residues. The main source of energy required for activities such as transportation, heating, production and power supply is based on the combustion reaction. Especially combustion of petroleum, coal and gas fuels, which are called as fossil fuels, creates many combustion products (Katsouyanni, 2003; Tasdemir et al., 2005). However, many air pollutants are formed and released into the atmosphere depending on the rate of oxygen supply

and combustion temperature to the impurities in the fuel. In addition to combustion, it is possible to discharge pollutants into the atmosphere from various processes.

Distorted and unplanned urbanization, the continued development of industry and urbanization in Bursa, the inadequacy of infrastructure and roads, and in addition to the unconscious discharge of air pollutants into the atmosphere, the problem of air pollution has become a major problem. Increasing traffic density, industrial chimney inspections despite all goodwill studies can not be done effectively and can not be prevented use of dirty fuel air pollution in Bursa has increased to higher levels. When meteorological and topographic conditions of Bursa are added to this, a problem of air pollution that can be felt by all citizens has emerged especially in winter.

In this study, all the data required for determination of the level of determination of air pollution sources in Bursa and development of solution suggestions were collected and evaluated. Emission sources were classified and a solution workshop was organized with the participation of all relevant institutions and organizations. At the end of this workshop, the results obtained were subjected to prioritization analysis and recommendations were developed.

2. Determination of current air quality of Bursa

2.1. Measurement stations

In order to evaluate the air quality in Bursa, measurement results of air pollutant parameters were examined. In this context, the results of air quality parameters recorded in the last 5 years (2013-2018) from 6 stations of Marmara Clean Air Center (MCAC) of Ministry of Environment and Urbanization were obtained. These stations; Bursa Uludag University Campus, Kültürpark, Beyazit Street, Kestel, Inegol and Soganlı total 6 pieces (Figure 1).

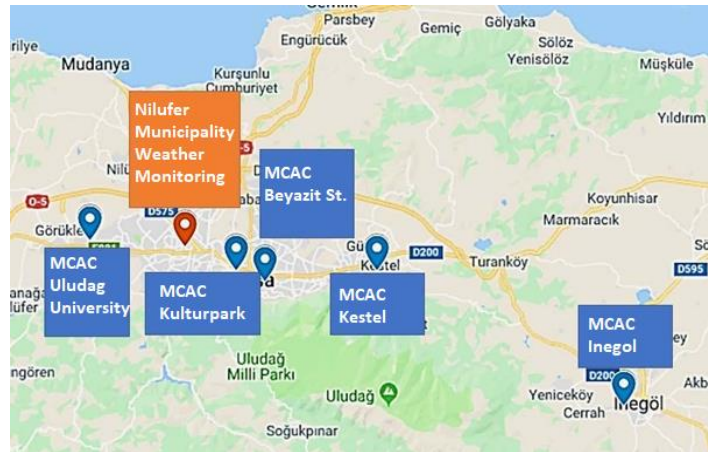


Figure 1. Map of MCAC Station locations

The stations where the measurements are made consist of a separate automatic measuring device for each pollutant. All measurements are performed with API brand devices. All devices record a 30-minute average of the measured data continuously every 3 minutes for 24 hours. In addition, meteorological data (pressure, humidity, temperature, wind speed and wind direction) are continuously measured.

3. Evaluation of annual data

3.1. PM concentrations

According to the time-dependent change of PM₁₀ concentrations measured at Bursa (Soganlı) station, the limit value for the annual average of 44 µg/m³ in Air Quality Assessment and Management Regulation (AQAMR) is exceeded for most of the time.

The mean PM₁₀ value for this region was 95.88 ± 66.5 µg/m³. This concentration was higher than the 24 hour limit of 60 µg/m³. The concentration of PM₁₀ measured at Beyazit Street station is 79.66±54.86 µg/m³ and is above the limit value. 3.7% of the measured PM₁₀ concentrations were recorded above 200 µg/m³. Excessive values in these results also indicate especially winter months.

Measurements obtained from the Kestel region include measurements made until 09/10/2017. The station has been inactive for a while on this date. The mean PM₁₀ concentration was 70.14±47.63 µg/m³ and was above the limit value. This is also reflected in the PM₁₀ concentration results. In Inegol district, the average annual value is 75.78±68.67 µg/m³ and is above the limit value. While 61% of the hourly data exceeded the limit value, 23% was recorded above the average value.

PM_{2.5} concentrations were measured on the University Campus. According to these values, 45% of the hourly data exceeded 25 µg/m³, which is the limit value given by the World Health Organization (WHO) (27.97±17.94 µg/m³). In the annual average, it is observed that the increase in the winter months affects the rate of exceeding the limit. In addition, due to the forested structure of the campus, it is thought that there is an increase in fine dust concentrations.

3.2. SO₂ concentrations

The annual average concentration on campus is 8.98±10.89 µg/m³ and is below the limit value. In 11% of the data, the limit value (20 µg/m³) was exceeded and the hourly limit value (150 µg/m³) was exceeded twice. It can be said that SO₂ is not a significant problem in this region. According to the 2.5-year data of hourly data of SO₂ pollutant in Soganlı, average value was recorded as 6.9±7.8 µg/m³. When evaluated together with PM₁₀, it can be said that the region is mostly affected by traffic pollution. The average value of the 5-year data measured at Beyazit Street was 12.76±14.10 µg/m³. This value is below the limit value. However, in some parts of the time, this value has been exceeded, but the hourly limit value (150 µg/m³) in the AQAMR has been exceeded only 5 times. It has been observed that the proportion of sulfur containing fuel types used in the region can be taken into consideration. The mean values measured at the Kestel station were found to be 26.99±39.73 µg/m³. 39% of the data is above 20 µg/m³, which is the limit value given for the protection of ecosystem. It was seen that 1.9% of the measured hourly data was above the hourly limit value (150 µg/m³), especially in winter. The annual average value of hourly data in Inegol district was determined as µg/m³. It was observed that the average value exceeded the annual limit value very little. However, it was determined that the limit value was exceeded in 29% of the data set. In the 1% of the data set, the hourly limit value (150 µg/m³) was exceeded. According to the measurement results, it is determined that there is not a very high excess in terms of SO₂ parameter in Inegol district.

It was seen that 1.9% of the measured hourly data was above the hourly limit value (150 µg/m³), especially in winter. The annual average value of hourly data in Inegol district was determined as 20.82 ± 31.03 µg/m³. It was observed that the average value exceeded the annual limit value very little. However, it was determined that the limit value was exceeded in 29% of the data set. In the 1% of the data set, the hourly limit value (150 µg/m³) was exceeded. According to the measurement results, it is determined that there is not a very high excess in terms of SO₂ parameter in Inegol district.

3.3. NO₂ concentrations

The 5-year average value of the hourly data measured at Bursa Uludag University Campus is 25.1 ± 19.9 $\mu\text{g}/\text{m}^3$, which is below the annual limit value (44 $\mu\text{g}/\text{m}^3$) given for 2018 in the AQAMR. While 16% of the measured hourly data set is recorded above the limit value, 39% is determined above the average value. The exceedances of the limit values have been realized especially in September-March periods and most of these exceedances are as of 2017.

The reason for this is that the location of the sampling station is moved closer to the vehicle traffic. When the NO concentrations expressing the proximity of the emission source were examined for the campus, the values that followed similar values between 2013-2016 increased after this date. In general, it can be said that there is no significant pollution in terms of NO₂ pollution in the campus. The average concentration in the Kulturpark is 41.16 ± 24.43 $\mu\text{g}/\text{m}^3$ and is below the limit value. While 41% of the hourly data set was above the limit value (44 $\mu\text{g}/\text{m}^3$), 45% was recorded above the average value. When the ratio of concentration exceeding the limit values and NO concentrations are evaluated together, it is considered that this pollution is mostly caused by vehicle traffic. The annual average value of NO₂ data recorded at Beyazit Avenue measuring point, which has a high traffic density and has a narrow street, was determined to be 69.75 ± 27.77 $\mu\text{g}/\text{m}^3$. It is above the limit of 44 $\mu\text{g}/\text{m}^3$ given to AQAMR for 2018. 80% of the measured hourly data set is recorded above the limit value. In addition, 45% of the data were measured above the average value. When the NO concentrations in this region were examined, it was found that the mean value was 63.86 ± 71.4 $\mu\text{g}/\text{m}^3$, indicating the proximity of the source from which NO_x compounds were discharged into the atmosphere. NO_x compounds, especially in the presence of hydrocarbon (HC) compounds and carcinogenic peroxyacetyl nitrate (PAN) compounds in sunny periods may cause the formation (Lee et al., 2013; Han et al., 2019). Since unburned HCs are also likely to be expelled from vehicles during peak traffic, this risk is particularly important for this area. As the traffic load around the Inegol measurement station was lower than the district center, NO₂ and NO concentrations at this point were recorded low. The average annual value obtained is 32.33 ± 22.85 $\mu\text{g}/\text{m}^3$ and is below the limit value. While 22% of the hourly data set exceeded the limit value, it was found that 38% was above the average value. High NO₂ concentrations in this region have been achieved with increasing emissions from heating, especially in winter.

3.4. CO-NO Concentrations

The CO concentration was measured only on Beyazit Street. When evaluated together with NO, it gives important information about the pollutant source. The annual average of all CO data was found to be 1.5 ± 1.3 mg/m^3 and well below the limit value (10 mg/m^3). However, as it is seen from hourly data, it is seen that CO concentration increases especially in winter period. NO concentrations show the same course. Until March 2015, NO concentrations gave a constant measurement result due to possible device failure and are not reliable. However, the NO release obtained after this date indicates increased concentrations during the winter months. As previously mentioned, the CO and NO parameters indicate incomplete combustion process emissions (Von Burg, 1999; Nastase et al., 2018). Since the measurement point represents the region where the traffic and domestic heating is intense, it shows that the need for increasing heating during winter and the traffic load are together. The most important issue for this region is that the increase in CO level is likely to increase HC. The risk of carcinogenic substances is higher in this region.

4. Evaluation of seasonal data

4.1. PM₁₀ concentrations

Seasonal variation of PM₁₀ concentration over the years is given in Figure 2. PM_{2.5} concentrations in Bursa Uludag University are almost same for 2014, 2016 and 2017; and are between 20 - 30 $\mu\text{g}/\text{m}^3$ in spring and summer and 30 - 40 $\mu\text{g}/\text{m}^3$ in autumn and winter seasons. When the results of the culture park were examined, it was seen that the average concentration varied between 50 - 80 $\mu\text{g}/\text{m}^3$. PM₁₀ concentrations in Beyazit Street also showed an upward trend in autumn and winter seasons. PM₁₀

concentrations measured in this region varied between 45-120 $\mu\text{g}/\text{m}^3$. It is seen that the limit values can be exceeded in almost all seasons in Beyazit Street which is known to be subject to heavy traffic load. PM_{10} concentrations measured in Kestel region showed significant differences between 82.65 – 134.42 $\mu\text{g}/\text{m}^3$ at seasonal level. The concentration of PM_{10} for Inegol was above the limit value in almost all seasons (45-80 $\mu\text{g}/\text{m}^3$). The widespread use of natural gas, the increase in human consciousness, albeit in part, and the fact that winters are not overwhelming due to global warming have been shown to cause this decline.

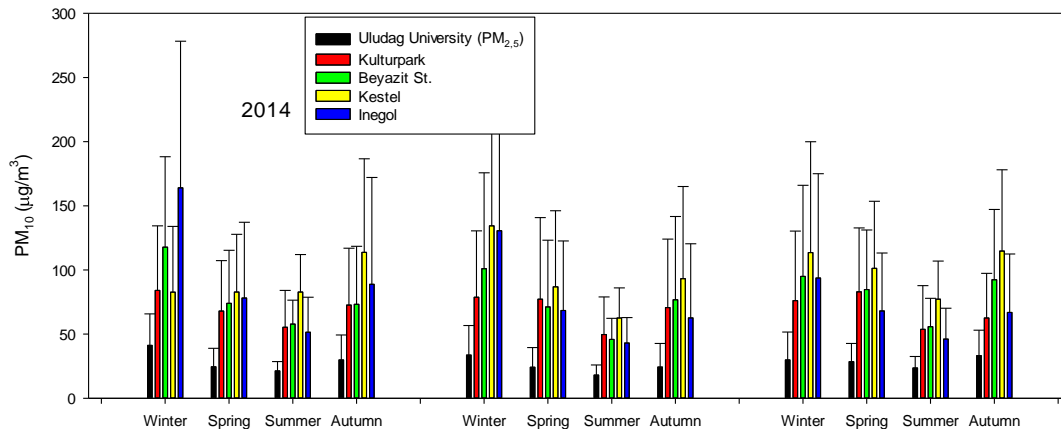


Figure 2. Seasonal variations of PM_{10} concentration

4.2. SO_2 concentrations

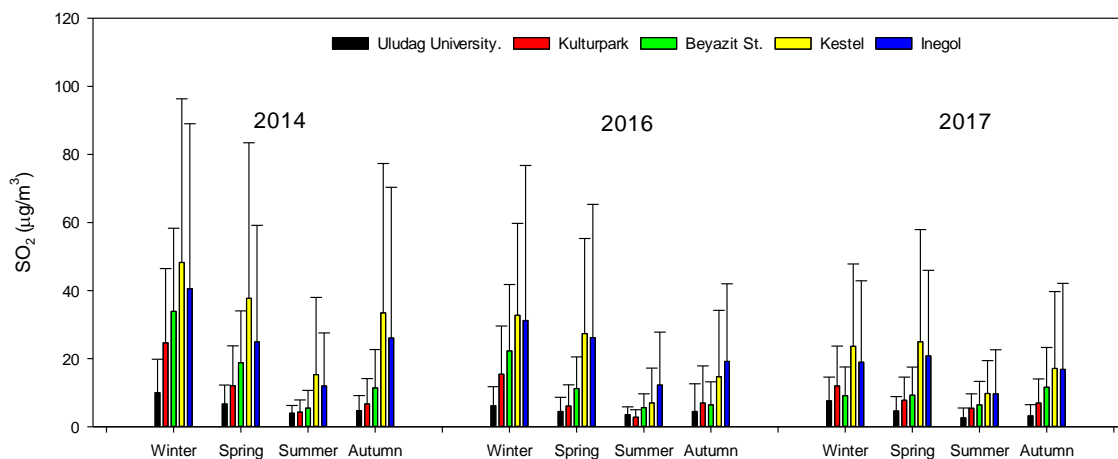


Figure 3. Seasonal variations of SO_2 concentration

The seasonal variation of sulfur dioxide concentration over the years is given in Figure 3. The seasonal results obtained at the Uludag University Campus have not changed significantly over the years, but despite this, there is a downward trend since 2014. The average SO_2 concentration in autumn, spring and summer was in the range of 2.5-6.0 $\mu\text{g}/\text{m}^3$ and in winter it varied in the range of 6-10 $\mu\text{g}/\text{m}^3$. There was no problem in terms of SO_2 in the campus. Seasonal SO_2 concentrations in the Kulturpark region showed a downward trend from 2014 to 2017. SO_2 seasonal average values recorded in summer and autumn seasons varied between 2.7-6.97 $\mu\text{g}/\text{m}^3$. Although there is a significant difference in the seasonal averages of SO_2 in Beyazit Street compared to summer and winter seasons, there has not been an

exceeding of the limit value. Moreover, seasonal values have been in a downward trend from 2014 to 2017. In the Kestel region, where higher seasonal averages were recorded in 2014, it was determined that the limit exceeded $48 \mu\text{g}/\text{m}^3$ in the winter season of 2014 and this value decreased to $23 \mu\text{g}/\text{m}^3$ until 2017. The seasonal release of SO_2 concentration at Inegol measurement point was lower than Kestel region. However, in terms of the location of the Inegol measurement point, the occurrence of these results was considered normal.

4.3. NO_2 concentrations

Changes in seasonal NO_2 concentration over the years are given in Figure 4.

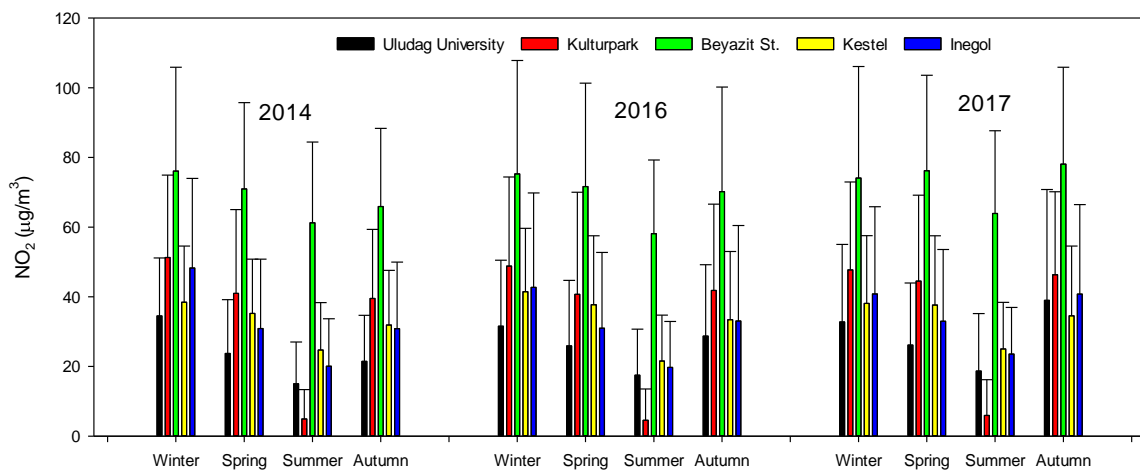


Figure 4. Seasonal variations of NO_2 concentration

Winter season values of NO_2 concentrations measured at Bursa Uludag University Campus decreased slightly between 2014 and 2016 and started to increase with 2017 and 2018. The reason for this increase was accepted as the sampling station being pulled closer to traffic. The seasonal change at the Kulturpark station was close to each other except in summer. The seasonal change at the Kulturpark station was close to each other except in summer. In the spring, autumn and winter seasons, both the warming and the traffic load were higher than in the summer, causing NO_2 concentrations to be 10 times higher than in the summer. However, it is seen that the limit value $44 \mu\text{g}/\text{m}^3$ has been slightly exceeded. On the other hand, NO_2 concentrations measured in Beyazit Street show that seasonal release is not very significant. The NO_2 value, which is around $60 \mu\text{g}/\text{m}^3$ in the summer, has changed in average at $70 \mu\text{g}/\text{m}^3$ in the other seasons. These values, which are above the limit value, have been affected by the combustion-related emissions, traffic and heating, for most of the year. The average NO_2 concentration in Kestel district varies between $23 \mu\text{g}/\text{m}^3$ and $38 \mu\text{g}/\text{m}^3$ for winter. It is seen that the limit value is not exceeded at the seasonal level in the measuring station. Seasonal NO_2 concentrations in Inegol district also showed seasonal release in other regions, especially parallel to Kestel. The Inegol measurement station is located in the southwest of the city and is partly away from the industrial zones and traffic. This situation is thought to have an effect on the results.

5. Hourly data assessment

It has been found that hourly $\text{PM}_{2.5}$ averages at Uludag University Campus are between $25\text{-}30 \mu\text{g}/\text{m}^3$ for most of the day and partially increased from 07-08 to 17-18 hours. The absence of a significant source of combustion other than vehicle traffic on campus led to a stable level of $\text{PM}_{2.5}$ concentrations. On the other hand, SO_2 emissions can be seen from the increase between 08 and 18 in the morning, especially when diesel vehicles cause more emissions between 2013 and 2014. Since Euro 6 engines have been

used since 2015, the values have decreased since then. However, after 2016, with the change of the sampling point in the campus, a partial increase has started again. Since NO₂ is a traffic pollutant in this region, maximum values were recorded between 07-09 and 17-22 in the morning when the vehicle density was high. The average hourly values of SO₂ concentrations in Kulturpark decreased over the years. For this reason, it is determined that there is no significant impact on SO₂ in the region and that it has increased slightly due to the effects of both heating and vehicle emissions between 8-17 hours when traffic is intensive. It has been observed that the number of vehicles has been increasing each year to the present day, especially contributing to the increase in NO₂ concentrations. Beyazit Street PM₁₀ concentration is observed to be above the limit value in almost all hours of the day in all years. In the Kestel region, it is observed that PM₁₀ concentrations change at a level above the limit value almost all hours of the day. The fact that hourly changes are close to each other shows that industrial effects continue in the evening and at night, besides the traffic source. In addition, heating and transportation activities were found to be effective on average. When SO₂ concentrations are examined, it is seen that there is no significant problem in limit value maintenance. It is seen that SO₂, which is estimated to be caused by heating and industrial emissions at night, is below 10 µg/m³. Although there is a slight increase due to the resumption of morning traffic and heating activities, the exceeding of the limit value is not significant. Inegol measurement station is located on the campus of the Vocational High School and is located at the end point of the city in a relatively south-west direction. Consequently, concentration levels should be examined in this context since it is located relatively far from the traffic and industrial load in the city. PM₁₀ concentrations are closer to the limit values from midnight to early morning. Towards noon and evening, it approaches the maximum values. After 2013 and 2014, there is a decrease in hourly average values in terms of PM₁₀ and it is not sufficient.

6. Source distribution of classical air pollutants in the city center

Natural gas usage amounts for industrial and heating purposes, coal consumption amounts used for industrial and heating purposes, fuel consumption amounts were obtained from Bursa Metropolitan Municipality and using these data, total pollution contribution values were determined by EMEP Corinair-2009 emission factors and their distribution was examined (Etiopie, 2009). Evaluations were made on the basis of 2016 data in which all data can be intersected jointly.

One of the most important sources of airborne particles is the use of coal for heating purposes with 67%. This is followed by emissions of diesel vehicles (19%) and coal consumption (9%), respectively. This distribution has been demonstrated only in terms of anthropogenic sources and the effect of sources that cannot be obtained such as uncontrolled combustion, fires, construction activities and mines could not be included. The effect of natural gas use on PM₁₀ concentration in the air was found to be 5%. It is seen that PM_{2.5} is the highest source of coal consumption for heating purposes with a rate of 82%. This is followed by coal consumed in industry (12%). The effect of heating and industrial use of natural gas on PM_{2.5} is 6%. It is determined that PM₁₀ pollutant arising from transportation is caused by the use of 54% fuel oil (rural diesel), 36% diesel and 10% gasoline. A similar situation was observed for PM_{2.5}.

Since sulfur is one of the main components of fossil fuels, fossil fuels are the major source of SO₂ in the air. This is the case with 81%. However, it should not be overlooked that petroleum products (such as oil, poor quality diesel) used in trucks and buses are also a significant source of SO₂. Therefore, it should be considered that the rate of 81%, which seems to belong to coal use, is lower and the rate of transportation is much higher. Clear clarification of this situation requires detailed research. The proportional distributions for each pollutant have been calculated by including the amount of gasoline, diesel and fuel oil consumed in Bursa since the data of the liquefied petroleum gas (LPG) cannot be provided. It has been determined that SO₂ resulting from transportation is caused by 39% gasoline (LPG), 38% fuel oil (rural diesel) and 23% diesel. In total, it is seen that 61% diesel fuels have the effect.

The most important source of NO_x (NO+NO₂), which is another important pollutant of combustion origin, is the natural gas (38%) used in industry, followed by transportation with 35%. The use of natural gas used for heating purposes (25%) and the consumption of coal used for heating purposes (2%) were determined as other pollutant sources. The contribution of NO_x to air pollution was determined to be 98% due to natural gas and transportation. It is seen that NO_x from transportation belongs to 69% fuel-oil (rural diesel), 18% gasoline (LPG) and 13% diesel. It has been determined that 82% of the NO_x given to the atmosphere from transportation in Bursa city center is caused by the use of diesel-derived fuel.

VOCs are another group of pollutants originating significantly from combustion, industrial processes, transportation, fuel stations and contaminated surfaces, but these organic pollutants are not measured by MCAC. Although there were no illegal evaporations from fuel stations, transportation was the highest resource group with 32%. Subsequently, coal used in heating (29%), natural gas used in industry (21%), natural gas used for heating (14%) and coal used in industry (4%) are followed. Although the health effects of these compounds are widely available in the literature, less information is produced about their atmospheric levels because their measurement is more difficult than other conventional air pollutants. (Bozkurt et al., 2018; Lamplugh et al., 2019; Zhang et al., 2019). The mass flow values (tonnes / year) of the VOCs given to the atmosphere were calculated based on the amount of fuel consumed in the vehicles. However, these values only include those resulting from fuel consumption and do not include leakage evaporation from fuel stations. According to this distribution, the share of gasoline (LPG) in transportation in terms of VOC emissions was 60% and the total amount of diesel derivatives was 40%.

It was determined that the biggest source for CO, which is more important in Bursa, especially in the days of lodos, is coal combustion for heating purposes (46%). This is followed by transportation (30%), natural gas used in industry (10%), coal used in industry and natural gas used for heating purposes (7%). It is determined that CO, which is released from the transportation to the atmosphere and poor combustion product, is caused by 83% gasoline engines (LPG) and 17% by diesel derivatives. Assuming that approximately 37.9% of gasoline vehicles are LPG (TÜİK, 2018) the contribution rate of gasoline will not be so high.

7. “Stakeholder workshop on determination of air pollution prevention strategies” in Bursa

After informing about the workshop implementation method, workshop tables were created and the views of the stakeholders on the questionnaires prepared earlier were collected according to the numbered rating system. The first part of the survey asked the scale, awareness and sources of the air pollution problem in Bursa. In the second part, it was asked to express their opinions on how these problems should be solved according to each source parameter. They were asked to answer the questionnaire in three scales, low, medium and high.

The importance of the sources of air pollution in Bursa was industry> transportation> dirty fuel usage> domestic heating> uncontrolled combustion. In particular, the pollution caused by industry and transportation has been observed to be caused mainly by legislation. It is stated that the limit values given in the legislation are not high enough for almost all pollutant sources and therefore this may be the case for some pollutants. Especially in transportation, industry, domestic heating and uncontrolled incineration, this deficiency was observed more. In the solution proposals, while improving public transport for transportation was the main focus, basic solutions such as flue gas inspections, method of measurement, use of zero waste approach for chimneys and use of alternative energy sources got the highest score. When evaluating the use of polluted fuels which are important for air pollutant sources, it is considered that all solution proposals are of primary importance, but fuels with high pollutant qualities should not be allowed. Among the solutions proposed for the control of uncontrolled combustion from air pollutant sources, the highest score is to prevent uncontrolled incineration for open

disposal and to prevent the burning of waste materials for heating purposes. Figure 5 shows the graphs of some survey questions and solution suggestions.

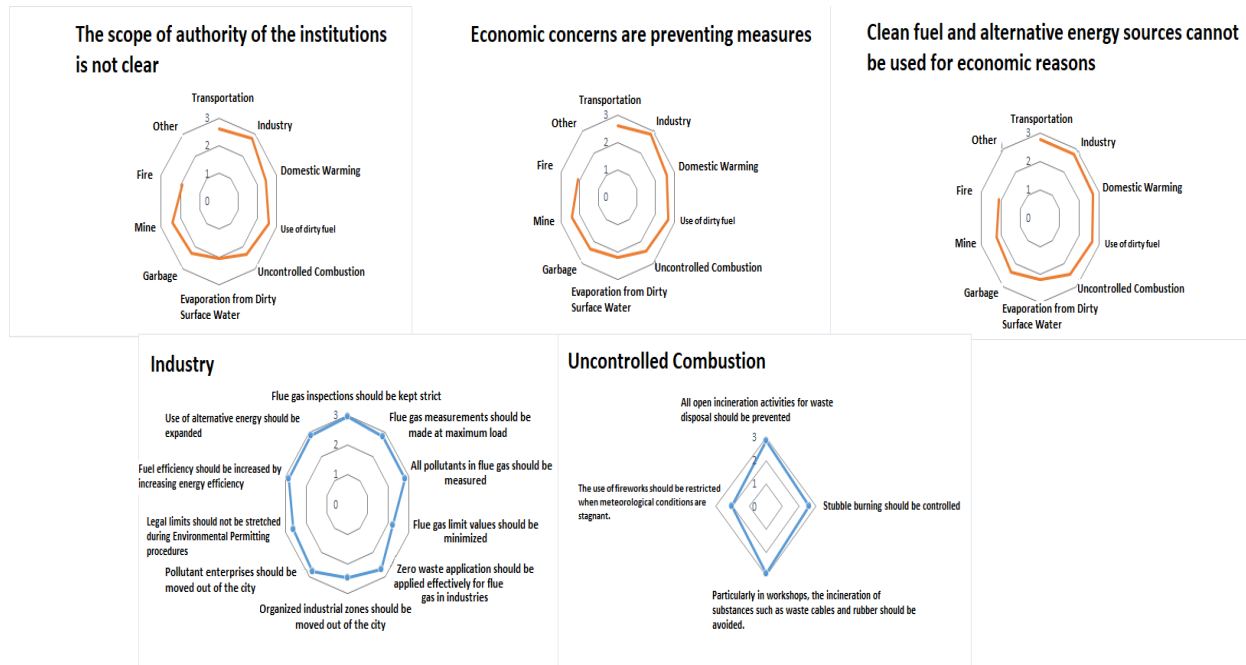


Figure 5. Graphical representation of answers to survey problems and solution suggestions

8. Results

In this study carried out in 6 different locations in Bursa, the conventional air pollutants such as PM₁₀, SO₂ and NO₂ were investigated and when the results of the measurements were evaluated, it was found that there are 3 basic air pollutant source groups in Bursa. While PM concentrations were mostly above the limit values in the regions, it was found that there was not much problem in terms of SO₂ concentrations. These are the main sources of heating, industry and transportation that contribute to the primal air pollution in Bursa. Although NO_x concentrations were found to be high in cold season, it did not show great seasonal changes in many regions. The intricate nature of industry and transport makes it difficult to distinguish the characterization of pollutant resources by sharp lines. However, when both the pollutant concentrations measured by MTHM in the air and the amount of fuel and fuel consumed are taken into consideration, it is seen that industry and transportation have emerged as an important air pollutant source for Bursa. For PM₁₀ and PM_{2.5} pollutants, coal consumption was found to be important.

According to the results obtained from the workshop, industrial emissions constitute the first of the air pollutant sources in Bursa. This is followed by traffic, the use of dirty fuel for heating activities, uncontrolled combustion and evaporation from dirty surfaces. Short, medium and long term solutions have been developed for all these problems. Increasing the flue gas and exhaust inspections, strictly prohibiting the use of highly polluting fuels and encouraging the use of natural gas are the most urgent actions to be taken in the short term. In the medium term, it is necessary to establish procedures for correct and reliable flue gas inspections and measurements, to improve public transport, to make necessary initiatives to implement zero waste approach as zero emissions, and not to use coal or other liquid fuels in urban areas. actions have been proposed. The long-term actions were to construct alternative roads, to move organized industrial zones out of the city, not to include the chimney industry in the city, to maximize the rate of alternative energy use, and to contain emission problems of treatment sludge drying beds.



9. References

- Bozkurt, Z., Uzmez, O.O., Dogeroglu, T., Artun, G., Gaga, E.O., 2018. Atmospheric concentrations of SO₂, NO₂, ozone and VOCs in Duzce, Turkey using passive air samplers: Sources, spatial and seasonal variations and health risk estimation. *Atmos. Pollut. Res.* 9, 1146-1156.
- Etiopie, G., 2009. EMEP/EEA air pollutant emission inventory guidebook 2009.
- Han, K., Lee, S., Yoon, Y., Lee, B., Song, C., 2019. A model investigation into the atmospheric NO_y chemistry in remote continental Asia. *Atmos. Environ.* 214, 116817.
- Katsouyanni, K., 2003. Ambient air pollution and health. *British medical bulletin.* 68, 143-156.
- Lamplugh, A., Harries, M., Xiang, F., Trinh, J., Hecobian, A., Montoya, L.D., 2019. Occupational exposure to volatile organic compounds and health risks in Colorado nail salons. *Environ. Pollut.* 249, 518-526.
- Lee, J.B., Yoon, J.S., Jung, K., Eom, S.W., Chae, Y.Z., Cho, S.J., Kim, S.D., Sohn, J.R., Kim, K.H., 2013. Peroxyacetyl nitrate (PAN) in the urban atmosphere. *Chemosphere.* 93, 1796-1803.
- Nastase, G., Serban, A., Nastase, A.F., Dragomir, G., Brezeanu, A.I., 2018. Air quality, primary air pollutants and ambient concentrations inventory for Romania. *Atmos. Environ.* 184, 292-303.
- Tasdemir, Y., Cindoruk, S.S., Esen, F., 2005. Monitoring of criteria air pollutants in Bursa, Turkey. *Environ Monit. Assess.* 110, 227-241.
- TÜİK, 2018. Trafik Kayıtlı Otomobillerin Yakıt Cinsine Göre Dağılımı İstatistikleri.
- Von Burg, D.R., 1999. Toxicology update. *Journal of Applied Toxicology: An International Forum Devoted to Research and Methods Emphasizing Direct Clinical, Industrial and Environmental Applications.* Wiley Online Library, pp. 379-386.
- Zhang, Y., Wei, C., Yan, B., 2019. Emission characteristics and associated health risk assessment of volatile organic compounds from a typical coking wastewater treatment plant. *Sci. Total. Environ.* 693, 133417.

Application of reduction scenarios on traffic related NO_x emissions in Trabzon, Turkey

Melike Nese Tezel^{1,2}, Deniz Sari¹, Nesimi Ozkurt¹ and S. Sinan Keskin²

¹ Environment and Cleaner Production Institute, TUBITAK Marmara Research Center, 41470 Kocaeli, Turkey

² Environmental Engineering Department, Marmara University, 34722, Istanbul, Turkey

nese.tezel@tubitak.gov.tr

Abstract. Short and long-term exposure to air pollution are known to be associated with many health problems such as respiratory diseases, lung cancer, and chronic heart diseases. Traffic related emissions are the main sources of certain air pollutants that affect large number of people in city centers. Due to the unfeasibility of exposure evaluations based on measurements, models are used to estimate human exposures in air pollution and health studies. Quantification of traffic related emissions and their dispersion modelling are the main requirements to determine human exposure. In this study, Trabzon city center which is located in the Eastern Black Sea region of Turkey was selected as the study area since high traffic intensity in this urbanized section is the dominant air pollution source. Moreover, air quality measurement stations are located very close to the road sections in city center, so that they provide mainly the road traffic related air pollutant concentrations. Traffic emission inventory in Trabzon was prepared to determine the concentrations of main traffic related pollutants (NO_x, SO₂, CO, PM and VOC). Among these, NO_x concentrations were calculated by using AERMOD dispersion model at the receptor points as the most representative air pollutant of road traffic emissions. Model results were compared to the station measurement data by using different statistical tools. Exposures of the population to traffic-related NO_x emissions were examined considering meteorological and topographic effects. Results indicated that 10% of the population in Trabzon city center was exposed to traffic-related NO_x concentrations higher than the regulatory limit value. In the scope of the clean air action plan, some scenarios that include decreasing the number of heavy vehicles in different fractions were modelled to observe the effects on the exposure levels of the population to traffic-related NO_x emissions.

Keywords: Road traffic, NO_x pollution, Modelling, Exposure

1. Introduction

In recent decades, there has been an extraordinary growth in terms of urbanization, vehicle numbers, and industrial activities, especially in developing countries. As a result of this increasing urbanization trend, ambient air quality has become the main environmental concern all over the world. The major sources of air pollutants can be classified as vehicular traffic, domestic, industrial, and thermal power plants (Mishra & Goyal, 2015). Especially the confined areas around busy roads are severely affected by air pollutants. Air pollution exposure is a major global risk factor for premature morbidity and mortality and has been linked to cardiovascular diseases, hypertension, and atherosclerosis (Brook et al., 2010; Foraster et al., 2011; Rao et al., 2014; Fuks et al., 2017). Urbanization cause changes in air quality by affecting local and regional climate with changing meteorological parameters. Widespread air quality measurements on correct locations are extremely important to present the problem (Kindap

et al., 2008). However, continuous air pollution monitoring is not feasible and applicable method for widespread use due to financial and practical limitations (Gibson et al., 2013). Because of these reasons, air quality modelling can be classified as a suitable way to understand the effects of urban air pollution. Detailed emission inventory studies should be carried out in order to use air quality models efficiently (Kindap et al., 2008).

Emission inventories are important data sets which show the amount of air pollutants from different sources in a specified geographical area. Inventory data contains pollutant type, amount of the emissions in a specific time (emission rate), source of emission, and position of the source. Emission inventories are primary inputs for air quality models together with meteorological conditions and topography. They give very important outputs for policy-makers by quantifying the impact of various sources (Markakis et al., 2012; Sari & Bayram, 2014). Dispersion modelling can be used to estimate the atmospheric concentrations of selected air pollutants at receptor sites if input data are available for emission source characteristics (type, point, line, volume, and area sources), terrain, land use, and meteorological conditions (Gibson et al., 2013; Sari & Bayram, 2014). There are many dispersion models developed and in use all around the World (Khan et al., 2018). Among these, the US-EPA has developed various models to simulate air quality in different scenarios.

In recent years, increasing population and unplanned urbanization accompanied by increases on industrialization, coal use for domestic heating, and motor vehicle numbers close to the city center have caused increasing air pollution in Trabzon, an Eastern Black Sea city in Turkey. Because of the topographical structure, wind movements are restricted and air pollutants are concentrated in the city center especially in stagnant atmospheric conditions (MoEU, 2016a). In this study, a traffic emission inventory in Trabzon was prepared to determine the concentrations of main pollutants (NO_x, SO₂, CO, PM and VOC). Calculated traffic related NO_x emission data were used in the AERMOD dispersion model to obtain NO_x concentrations at different sections of the Trabzon city center. Previous studies indicated that AERMOD shows high sensitivity to wind speed, wind direction, and surface roughness length (Laffoon et al., 2005) and it is the preferred model by US-EPA for regulatory compliance demonstration for simple and complex terrain in the near field (less than 50 km) (Rood, 2014). Therefore, considering the complex geographical structure of Trabzon and the selected domain (10x20 km), AERMOD View 7.3.0 modelling software was preferred to calculate the distribution of the traffic-related NO_x concentrations. AERMET and AERMAP pre-processor software were used to prepare hourly meteorological data and the geographic database for the study area, respectively. Model results were evaluated by comparison to the measurement data from the four air quality stations located nearby to the city center and operated by the Ministry of Environment and Urbanization. NO_x concentrations were calculated for selected discrete receptor points on regular grid systems in the study area and population exposure to NO_x was calculated. In the scope of the clean air action plan, some scenarios that include decreasing the number of heavy vehicles in different fractions were modelled to observe the effects on the exposure levels of the population to traffic-related NO_x emissions.

2. Materials and methods

2.1. Characteristics of the study area

Trabzon is one of the important cities in the Eastern Black Sea region in Turkey and is located between 40° 33' and 41° 07' N latitudes and 39° 07' and 40° 30' E longitudes. Trabzon occupies 0.6% of the country's territory with a greater metropolitan area of 4,685 km². The population living in the city center (Ortahisar province) corresponds to 41% of the total population in Trabzon. The city has a narrow flat land nearby the seashore and an elevated land structure and high slopes from coast to inland. Only 10% of the total area is flat and close to plain, 30% is mountainous. Trabzon has cool summers and warm winters with an average temperature of 14.4 °C. Rainfall happens in all seasons with an average depth of 891 mm. Because of the topographical structure, wind strength is weak and air pollutants are concentrated in the city center especially during the stagnant atmospheric conditions. There are frequent

cases of thermal inversion in the city center that prevents atmospheric mixing and causes polluted air to be trapped within the surface layer (MoEU, 2016b).

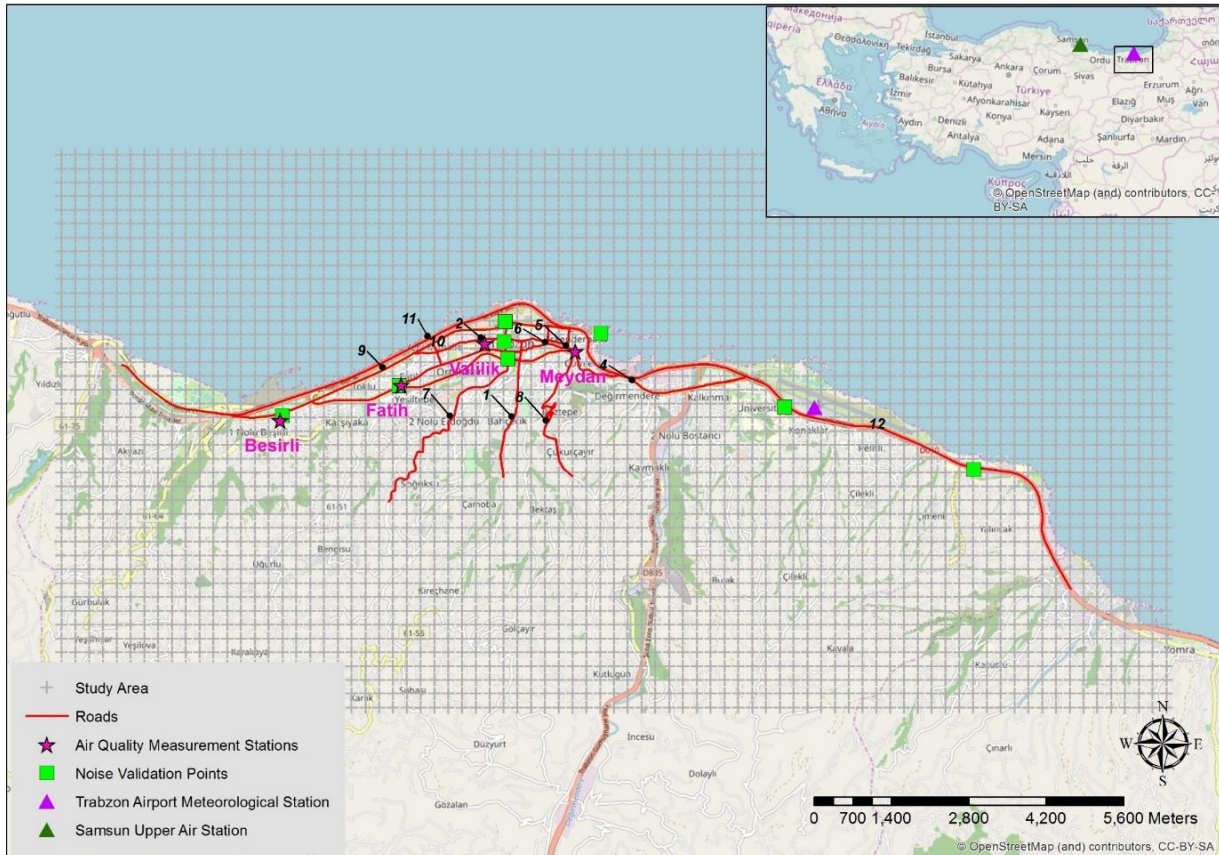


Figure 1. The study area

In this study, 12 road sections with 53 km total length were modelled. Heavy (light commercial cars, heavy-duty vehicles, and buses) and light (passenger cars, motorcycles, and mopeds) vehicle counts in these road sections were carried out by eye observations on an hourly basis for day, evening, and night time periods. To obtain the highest emission values, a day of the week with maximum traffic density was selected. Vehicle counts were performed within the busiest hours of three different periods [daytime (07:00-19:00), evening time (19:00-23:00), and night time (23:00-07:00)] on the selected day (TUBITAK, 2016). Road sections are shown in Figure 1 and vehicle counting data together with other characteristics of the studied roads are given in Table 1.

The main input variables for model included population and traffic data on road lines, city map/types of buildings, geographical database, and meteorological conditions. The geographical database was obtained from the “Shuttle Radar Topography Mission (SRTM) 90 m Digital Elevation Data” provided by the National Aeronautics and Space Administration (NASA) of the USA and Trabzon Municipality’s base map (NASA, 2015). Geometry and usage purposes of buildings (residential, school, hospital, or auxiliary building), number of flats and inhabitants per building are required information for preparing a building layer. City map/types of buildings were obtained from the Trabzon Municipality’s base map. In order to calculate the number of inhabitants per building, the population of districts in the study area was distributed to buildings according to their areas. The population of the Ortahisar district in 2014 were obtained from Turkish Statistical Institute’s Address-Based Population Registration System Database (TURKSTAT, 2014). In order to consider the effect of meteorological conditions on the NO_x concentration distributions, the hourly meteorological data for the study area were prepared by the

AERMET pre-processor software (AERMOD module) for the year 2016. Inputs of AERMET pre-processor were one-year surface meteorological data (cloud height, wind direction, wind speed, pressure, temperature, humidity, and cloudiness) obtained from Trabzon Airport Meteorological Station and upper air meteorological data obtained from Samsun Meteorological Station. Wind roses for daily average, daytime, evening time, and night time periods were prepared. It was observed that the daytime dominant wind direction was east while evening and night time dominant wind directions were south west.

Table 1. Hourly vehicle counts on the streets and highways (TUBITAK, 2016)

ID	Road Name (Length of road in km)	Annual average daily traffic (AADT) (Vehicle/day)	Hourly Vehicle Number (Heavy/Light)		
			Day (07:00-19:00)	Evening (19:00-23:00)	Night (23:00-07:00)
1	Sehit Refik Cesur Street (2.5)	11,428	163/367	122/319	94/319
2	Kahramanmaras Street (2.8)	11,672	334/370	269/323	47/60
3	Hasan Saka Street (0.4)	6,864	136/293	80/239	10/45
4	Yavuz Selim Boulevard(8.5)	20,340	235/910	274/1012	31/151
5	Gazipasa Street (0.3)	19,264	375/678	239/716	74/277
6	Cumhuriyet Street (0.3)	15,460	471/485	171/258	87/197
7	Senol Gunes Street (4.6)	27,336	590/1053	244/707	122/355
8	Taksim Street (3.4)	21,896	409/734	400/831	86/321
9	Sahil Yolu Street (6.5)	18,744	502/542	212/504	111/308
10	Inonu Street (3.4)	14,444	322/490	221/404	69/206
11	010-21 6 th section (11.8)	45,440	469/2244	302/1683	151/467
12	010-22 1 st section (8.6)	54,372	628/2636	240/2149	122/584

Besirli, Fatih, Valilik, and Meydan are the four districts with air quality monitoring stations operated by the Ministry of Environment and Urbanization (MoEU) in the city center of Trabzon. The hourly measurement results of the stations can be accessed instantly and retrospectively from the website of the MoEU (MoEU, 2017). Valilik and Meydan stations are located in areas where many roads with heavy traffic are concentrated. These stations are also located next to higher mountains compared to Besirli and Fatih stations, resulting in more closed and isolated ambient air environment from the other source regions. Boundaries of the study area and the geographical locations of the stations in the study area are given in Figure 1.

2.2. Air quality modelling

2.2.1. Emission inventory for the road traffic-related emissions

Emission inventories are essential data sets giving the number of air pollutants emitted from different sources in a specified geographical area (Sari & Bayram, 2014). One of the methods used for vehicle emissions is the multiplication of the distance taken by a specified vehicle type with the emission factor of the pollutant emitted by that vehicle (Faiz et al., 1996) and this approach was used in this study. The EMEP/EEA catalogue was preferred since it has a wide variety of calculation options with different complexities. Some of those options can be applied to countries with older vehicle fleets. Motor vehicle ages used in Trabzon are generally high and to obtain complete data about these vehicles is a difficult task. Therefore, emission factors in the mentioned catalogue were used directly without any country or technology specific details (Tier-1 approach). For this purpose, a report prepared by the Turkish Statistical Institute (TURKSTAT) was used to obtain the number of vehicles registered by their sizes and fuel types at the city center of Trabzon in 2015 (TURKSTAT, 2016). This report covers four main

vehicle types in use named as heavy duty vehicles (HDV), light commercial vehicles (LCV), private cars (PC), and motorcycles (two-wheel). Gasoline, diesel, and LPG are the main fuel types that are used in these vehicles. Percentages of the registered vehicle types were calculated and obtained values are presented in Table 2. Hourly average vehicle counts obtained for three time periods (day, evening, night) on the selected day were multiplied by these percentages to find the number of vehicles in each type, and the amounts of fuel types used by them were calculated for the 12 road sections included in this study.

Table 2. Percentages of vehicle types in Trabzon in 2015

Fuel	Heavy		Light	
	HDV***	LCV**	PC*	Two-wheel
Gasoline		1.20%	20.48%	5.77%
Diesel	19.26%	79.53%	41.66%	
LPG			32.09%	

(*) Passenger Cars, (**) Light Commercial Vehicles, (***) Heavy-Duty Vehicles

Air pollution caused by road traffic is evaluated under the name of line sources. According to the EMEP/EEA guidebook, the main pollutants from these sources are particulate matter (PM₁₀, PM_{2.5}), sulphur dioxide (SO₂), carbon monoxide (CO), non-methane volatile organic compounds (NMVOC), and nitrogen oxides (NO_x). Pollutant emissions in each road section were calculated for the three periods of the selected day by using formulas in Tier-1 approach. Tier 1 emission factors given in Table 4 (EMEP/EEA, 2016). The hourly average vehicle numbers, typical fuel consumption (g/km), length of the road sections (km), fuel consumption specific emission factor of pollutant (for specified vehicle category and fuel type) (g/kg) are the main inputs of the emission calculation. In addition to day, evening, and night periods, the hourly average emission value for the selected day was calculated according to the following formula;

$$\left(\text{Hourly average emission for a day} \right) = \frac{\left(\text{Daytime emissions} \times 12 \right) + \left(\text{Evening time emissions} \times 4 \right) + \left(\text{Nighttime emissions} \times 8 \right)}{24} \quad (1)$$

Table 3. Tier 1 mean emission factors (EMEP, 2016)

	(g/kg Fuel)	CO	NMVOC	NO _x	PM ₁₀	PM _{2.5}	SO ₂
PC	Gasoline	84.7	10.05	8.73	0.03	0.008	0.0056
	Diesel	3.33	0.7	12.96	1.1	0.275	0.0010
	LPG	84.7	13.64	15.2	0	0	
LCVs	Gasoline	152.3	14.59	13.22	0.02	0.005	0.0080
	Diesel	7.4	1.54	14.91	1.52	0.38	0.0013
HDVs	Diesel	7.58	1.92	33.37	0.94	0.235	0.0038
	CNG	5.7	0.26	13	0.02	0.005	
Two-wheel vehicles	Gasoline	497.7	131.4	6.64	2.2	0.55	

2.2.2. Dispersion model for the road traffic-related NO_x emissions

A traffic emission inventory in Trabzon was prepared to be used in AERMOD to determine the NO_x concentrations in various locations. NO_x concentrations were calculated for the receptor points in the 250x250m grid sizes in the study area. The meteorological data and wind fields were processed by AERMET meteorological module and results were used as input for AERMOD model. The geographic database was prepared by using the SRTM Data with AERMAP pre-processor software. AERMAP and AERMET results in conjunction with grid-wise on-road vehicular emission loads were used to calculate

the daily average, annual average, and the maximum NO_x concentrations in µg/m³ using the AERMOD modelling software in three separate runs. Calculated results were compared with measurement results obtained from the air quality measurement stations in the study area. Results were evaluated by the help of a geographic information system (GIS) software to determine the NO_x exposure levels of the population living in the study area.

2.2.3. Comparisons of model results with measurements

NO_x concentrations originated from the road traffic were calculated at the locations of the stations by the dispersion modelling software. Comparisons between model-calculated results and measurement results of air quality monitoring stations were performed by three different statistical methods: Index of Agreement (IOA), Factor of Two (FAC2), and Normalized Mean Square error (NMSE). IOA evaluates how the magnitudes of the observed values are related to the variances from the predicted values. IOA near “– 1.0” could mean that the model estimated deviations about the observed average value are poor estimates of the observed deviations; but, it also could mean that there is little observed variability. Therefore, when IOA approaches to the lower limit, comments should be made cautiously (Willmott et al., 2012). FAC2 method is defined as the percentage of prediction within a factor of 2 of the observed values, and these should be within 0.5 and 2.0 (Abril et al., 2016). NMSE method is a standardized measure of the overall error from the comparisons between observed and predicted values. A perfect data match would have zero error and NMSE values smaller than 1.5 indicate better performance (Abril et al., 2016).

2.3. Clean air action plans

Clean air action plans are prepared to reduce and control pollutant concentrations if one or more pollutants exceed the specified levels in the regulation. The characterization and assessment of air-quality are essential steps for the implementation of the “Clean Air Action Plan” as this is set by the Turkish Regulation on Ambient Air-Quality Assessment and Management (Ozkurt et al., 2013; Koksall et al., 2017). Ministry of Environment and Urbanization is responsible for coordinating the preparation of the clean air action plans for residential areas. Preparation and implementation of the plans includes close cooperation between local authorities and the provincial directorates/units of the related institutions. Short, medium, and long term measures are planned and implemented according to the air pollution sources and categories together with the attention on the specific conditions of the cities (Koksall et al., 2017). Some of the action plan examples are listed below:

- Reduction of urban traffic congestion (parking arrangements for motor vehicles and parking fees, no surface public parking allowed inside the city center, possession of bicycle rental areas in the city center, junction rearrangements),
- Integration of road and rail system (Koksall et al., 2017),
- Higher emission standards,
- Fuel quality enhancement,
- Elimination of carburetor equipped vehicles,
- New energy cars and motorcycles,
- Vehicle catalyst replacement,
- Utilization of diesel particulate filter and etc. (Mohammadiha et al., 2018),
- Banning or implementation of taxes for diesel cars entering the city centers (BI, 2019),

In this study, five scenarios were selected for the reduction of traffic-sourced NO_x emissions in Trabzon city center. According to the statement made by the competent authorities, a rail system construction is planned on the coastline of Trabzon in the near future. With this initiative, it is foreseen that the traffic density on the coastline will decrease. However, studies have shown that it is difficult to change a driver's transportation habit, even if free public transportation is available (BI, 2019). Therefore, it was assumed that there will be no change in the number of private cars with the construction of a railway

system in scenario 1. In the scope of this scenario, minibus and busses (approximately 15% of the heavy vehicles) on 010-21 6th and 010-22 1st road sections were eliminated.

The main step of the clean air action plans seems to be the banning cars from entering city centers. Fifteen major cities around the world are starting to take this action. In December 2018, Madrid began restricting access to gas-powered vehicles made prior to 2000 and diesel vehicles made prior to 2006. In 2020, none of the older diesel-powered cars will be allowed to enter the city center and hybrid vehicles with an "eco label" will be encouraged. Any car that's found in violation of the new rules will have to pay a fine of around \$100. Moreover, Brussels is applying \$400 fine on diesel vehicles that enter the low-emission zone of its city center. The city ultimately hopes to ban all diesel vehicles by 2030 (BI, 2019). In the scope of these applications, 10%, 20% reduction in the number of diesel-powered heavy vehicles, and 50% reduction in the number of diesel-powered heavy and light vehicles on all roads were selected as scenario 2, 3 and 5 respectively. These scenarios could be applicable by restricting the entry of diesel vehicles or encouraging zero emission cars within the city center.

According to the statement made by the Trabzon local government, the construction of the southern ring road is planned to reduce the density of the inter-city roads passing through the coastline. With the construction of this road, it is predicted that the number of heavy and light vehicles will decrease in the 6th section of 010-21 and the 1st section of 010-22 road as included in scenario 4. Vehicle count estimations were made with the help of the City Roads Traffic and Transportation Information Report prepared by the General Directorate of Highways of Turkey in 2014 (GDoH, 2014) and are presented in Table 4. These counts correspond to approximately 40% reduction in the number of AADT on these road sections.

Table 4. Estimated vehicle counts on 010-21 6th and 010-22 1st road sections in scenario 4

ID	Road Name (Length of road in km)	AADT	Hourly Vehicle Number (Heavy/Light)		
			Day (07:00-19:00)	Evening (19:00-23:00)	Night (23:00-07:00)
1	010-21 6 th section (11.8)	26,810	277/1324	178/923	89/276
2	010-22 1 st section (8.6)	32,079	371/1555	142/1268	72/345

Modeled scenarios in this study are summarized below;

- Scenario 1: Elimination of minibus and busses (approximately 15% of the heavy vehicles) on 010-21 6th and 010-22 1st road sections with the construction of a planned railway system
- Scenario 2: 10% reduction in the number of diesel-powered heavy vehicles on all roads
- Scenario 3: 20% reduction in the number of diesel-powered heavy vehicles on all roads
- Scenario 4: 40% reduction of AADT on 010-21 6th and 010-22 1st road sections with the planned construction of south ring road
- Scenario 5: 50% reduction in the number of diesel-powered heavy and light vehicles on all roads

3. Results and discussion

3.1. Emission inventory results

Air pollutants originating from road traffic are one of the most important factors influencing the air quality in the Trabzon city along with emissions from domestic heating and industry (MoEU, 2016a). Road traffic-sourced CO, NMVOC, NO_x, PM₁₀, PM_{2.5}, and SO₂ emissions were calculated by using the hourly vehicle counts for different time periods in a day (day, evening, night, and daily average), the type of the registered vehicles, and the emission factors. Results of those calculations are presented in Table 5 and Table 6. Results indicate that the maximum emission values were observed during daytime for most of the roads because of the higher traffic density. Even though evening time period (4 hours)

is shorter than daytime period (12 hours), hourly emission values in evening time are close to those of daytime since light vehicle counts in evening time is almost equal to daytime vehicle counts as presented in Table 1.

In Trabzon city center, almost 60% of the light vehicles consume LPG and gasoline with proportions of 32% and 26%, respectively (Table 2). As can be seen from Table 3, gasoline and LPG fueled engines emit much more CO, NMVOC, and SO₂ than diesel engines. On the other hand, emission factors of NO_x of HDV with diesel engines are 3 times higher than that gasoline engines. If it is considered that almost all heavy vehicles have diesel-fueled engines and the percentage of the heavy vehicle number is approximately one-third of the light vehicle number, NO_x and PM₁₀ emissions from road traffic are mainly caused by heavy vehicles in Trabzon city center. Diesel engines produce higher levels of PM and NO_x emissions compared to CO and HC emissions since excess air coefficient in diesel engines is higher than that of gasoline engines (MoNE, 2011).

Table 5. Calculated hourly average road traffic related emissions (daytime and evening) (g/h)

Road Name	Day (07:00-19:00)						Evening (19:00-23:00)					
	CO	NMVOC	NO _x	PM ₁₀	PM _{2.5}	SO ₂	CO	NMVOC	NO _x	PM ₁₀	PM _{2.5}	SO ₂
Sehit Refik Cesur	3956	706	1703	87	22	0.21	3389	603	1357	69	17	0.17
Kahramanmaras	4944	894	3114	165	41	0.36	4252	768	2560	135	34	0.30
Hasan Saka	508	91	223	11	3	0.03	402	71	151	8	2	0.02
Yavuz Selim	31,904	5657	10,755	530	133	1.34	35,588	6313	12230	605	151	1.52
Gazipasa	899	161	433	22	6	0.05	902	160	339	17	4	0.04
Cumhuriyet	704	128	462	25	6	0.05	351	63	186	10	2	0.02
Senol Gunes	21,449	3841	10,403	537	134	1.23	13,698	2436	5230	263	66	0.64
Taksim	11,043	1978	5340	276	69	0.63	12,287	2195	5509	282	71	0.66
Sahil Yolu	16,895	3057	10,798	571	143	1.24	14,047	2505	5889	299	75	0.71
Inonu	7539	1354	3983	207	52	0.47	6064	1086	2904	150	37	0.35
010-21 6 th section	107,908	19,099	33,548	1633	408	4.25	80,341	14,204	23,689	1142	286	3.03
010-22 1 st section	93,049	16,486	30,383	1491	373	3.81	73,509	12,963	18,906	888	222	2.48
TOTAL	300,799	53,451	111,146	5556	1389	13.68	244,831	43,366	78,951	3866	967	9.93

Table 6. Calculated hourly average road traffic related emissions (night and daily avg.) (g/h)

Road Name	Night (23:00-07:00)						Daily Average					
	CO	NMVOC	NO _x	PM ₁₀	PM _{2.5}	SO ₂	CO	NMVOC	NO _x	PM ₁₀	PM _{2.5}	SO ₂
Sehit Refik Cesur	3319	589	1182	59	15	0.15	3649	650	1472	74	19	0.18
Kahramanmaras	782	141	455	24	6	0.05	3441	622	2135	113	28	0.25
Hasan Saka	74	13	23	1	0	0.00	345	62	145	7	2	0.02
Yavuz Selim	5226	925	1614	78	20	0.20	23,625	4189	7954	392	98	0.99
Gazipasa	344	61	117	6	1	0.01	714	128	312	16	4	0.04
Cumhuriyet	255	45	109	6	1	0.01	496	89	299	16	4	0.03
Senol Gunes	6876	1223	2620	132	33	0.32	15,299	2734	6947	356	89	0.83
Taksim	4512	800	1544	76	19	0.19	9073	1621	4103	210	53	0.49
Sahil Yolu	8463	1506	3296	166	41	0.40	13,610	2448	7479	391	98	0.87
Inonu	2943	523	1109	56	14	0.14	5761	1032	2845	147	37	0.34
010-21 6 th section	23,090	4103	8561	428	107	1.05	75,041	13,284	23,576	1150	287	2.98
010-22 1 st section	20,467	3622	6362	310	77	0.81	65,598	11,611	20,463	997	249	2.59
TOTAL	76,348	13,552	26,993	1341	335	3.34	216,654	38,471	77,729	3869	967	9.61

3.2. Comparisons of measured and model predicted values

Calculation results of air pollution model were compared to measurement results from air quality measurement stations by three different statistical methods (IOA, FAC2, and NMSE). As presented in

detail in a recent study published by our group, comparisons between model calculated and meteorological station measurement data gave consistent results in general (Tezel et al., 2019). Measurement data gave statistically good results for both Valilik and Meydan districts. Valilik and Meydan stations are located in areas where many roads with heavy traffic are concentrated. As a result, road traffic seems to be the dominant source of NO_x for these stations as indicated by the close agreement between model and measurement data. Besirli and Fatih districts are more vulnerable to wind effects compared to Meydan and Valilik stations due to their topography. NO_x concentrations can be disturbed by southwest dominant wind and street canyon vortex at a stronger level. These factors could possibly play role on the disagreement between the measured and calculated NO_x concentrations in Besirli and Fatih districts. Therefore, it might be concluded that model results can be used satisfactorily for Valilik and Meydan districts to identify locations with critical NO_x exposure levels. The NO_x exposure levels calculated by the model for Fatih and Besirli districts should be considered as minimums since statistical analyses indicated some other significant sources for these districts.

3.3. Air quality modelling results

According to the Air Quality Assessment and Management Regulation issued by the Ministry of Environment and Urbanization in Turkey, the 1-hour average NO_x emissions at a receptor site cannot exceed 18 times the limit value in a year. The target for the limit value of NO_x emissions by 2024 is 200 µg/m³. The legal emission limit was 300 µg/m³ in 2014 when the directive was published. This limit is planned to be reduced 10 µg/m³ per year to reach the 2024 target (MoEU, 2008). Since this study was conducted using meteorological data from 2016, the limit value was accepted as 280 µg/m³. If the hourly average NO_x emission values for any receptor point exceed the limit value 19 times during a year, it is considered that there is a critical NO_x exposure at that point. In Figure 2, the distribution map shows the areas where the limit values were exceeded and critical exposure levels were reached. Results indicate that, 10.1% of the total population, 29 schools, and 19 hospital buildings are exposed to traffic related NO_x emissions above the threshold values during a year (Table 7).

Table 7. Traffic Related NO_x exposure results

Hourly Average NO _x Values at Receptors During a Year (µg/m ³)	Households	Population	School	Hospital
< 280	68,918	237,851	190	54
> 280	13,938	31,804	29	19

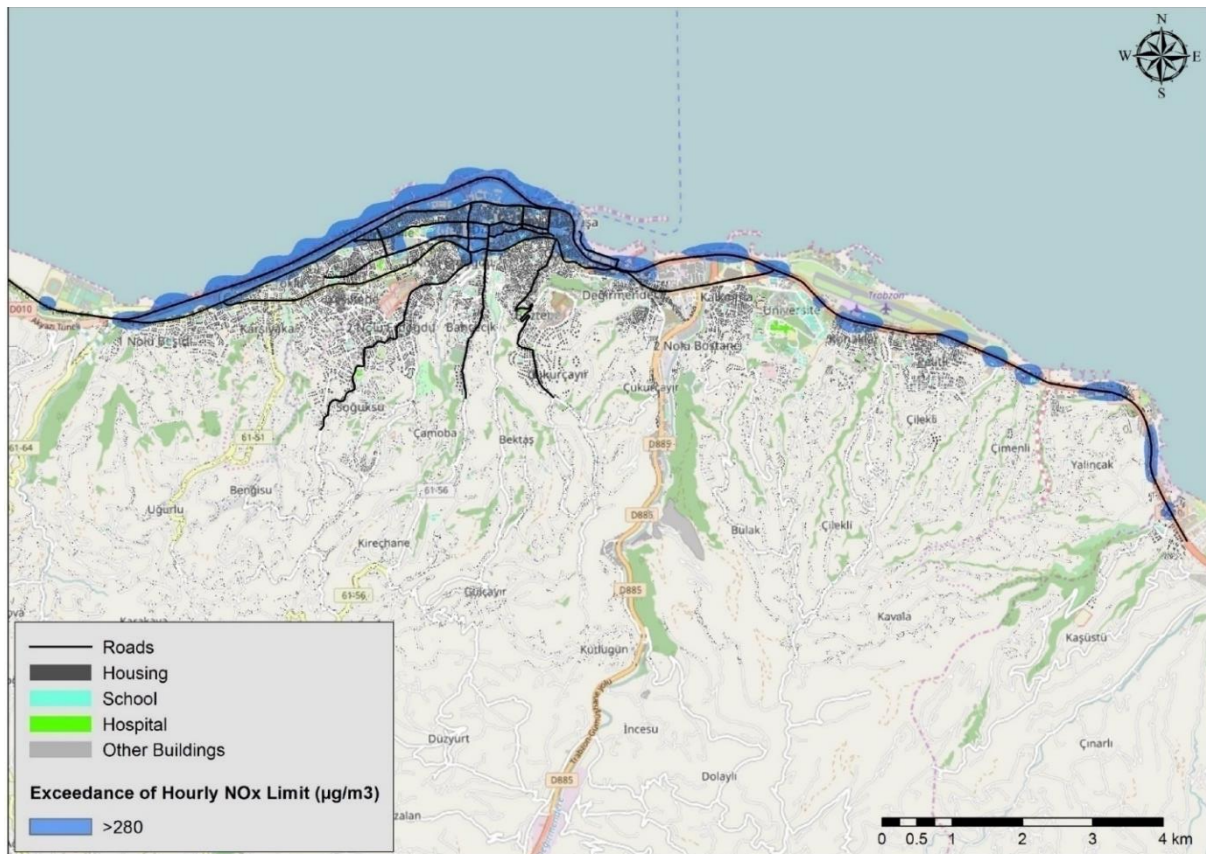


Figure 2. Exceedance of legal limit for traffic related NO_x in the city center of Trabzon

3.4. Results of selected scenarios for NO_x emission reduction

3.4.1. Hourly average road traffic related NO_x emissions

Five separate scenarios for NO_x emission reductions were applied and new emission values were calculated for every road section. Reductions on road traffic related hourly NO_x emissions in scenarios 1-5 are 3.43%, 4.96%, 10.05%, 23.23%, and 35.82%, respectively. As presented in Table 8, the most effective NO_x emission reduction scenario is 50% reduction in the number of heavy and light diesel-powered vehicles.

Table 8. Calculated daily average road traffic related NO_x emissions for different scenarios (g/h)

Road Name	Scenario 1	Scenario 2	Scenario 3	Scenario 4	Scenario 5
Sehit Refik Cesur	1472	1390	1304	1472	918
Kahramanmaras	2135	1980	1816	2135	1225
Hasan Saka	145	137	128	145	90
Yavuz Selim	7954	7591	7215	7954	5189
Gazipasa	312	294	274	312	191
Cumhuriyet	299	277	255	299	172
Senol Gunes	6947	6514	6080	6947	4222
Taksim	4103	3853	3592	4103	2496
Sahil Yolu	7479	6955	6431	7479	4380
Inonu	2845	2660	2470	2845	1700
010-21 6 th section	22,139	22,600	21,594	13,914	15,672
010-22 1 st section	19,230	19,622	18,760	12,069	13,630
TOTAL	75,059	73,873	69,917	59,673	49,883

Scenario 1: Construction of a railway system

Scenario 2: 10% reduction in the number of diesel-powered heavy vehicles

Scenario 3: 20% reduction in the number of diesel-powered heavy vehicles

Scenario 4: Construction of south ring road

Scenario 5: 50% reduction in the number of diesel-powered heavy and light vehicles

3.4.2. Traffic related NO_x exposures for different scenarios

Calculated NO_x emissions for every road section were entered as input to the model and five separate runs were performed. Model results were used to determine exposure to traffic related NO_x emissions above the threshold value during a year and results are presented in Table 9. Results indicate that 9.88%, 7.24%, 5.31%, 6.23%, and 0.05% of the total population are exposed to traffic related NO_x emissions above the threshold value in scenario 1 (railway construction), in scenario 2 (10% reduction in the number of diesel-powered heavy vehicles), in scenario 3 (20% reduction in the number of diesel-powered heavy vehicles), in scenario 4 (construction of south ring road), and in scenario 5 (50% reduction in the number of heavy and light diesel-powered vehicles), respectively. Scenario 5 is the most effective exposure reduction scenario for traffic related NO_x emissions. Model calculated reductions on NO_x exposure levels obtained from the selected scenarios are also presented as a color coded map in Figure.

Table 9. Exposure to traffic related NO_x above the threshold value under different scenarios

	Households	Residents	Schools	Hospitals	Effectuated Population Fraction
Scenario 1	13,729	31,043	27	11	9.88%
Scenario 2	11,156	22,756	16	9	7.24%
Scenario 3	8208	16,698	10	9	5.31%
Scenario 4	8879	19,575	15	9	6.23%
Scenario 5	41	144	0	0	0.05%

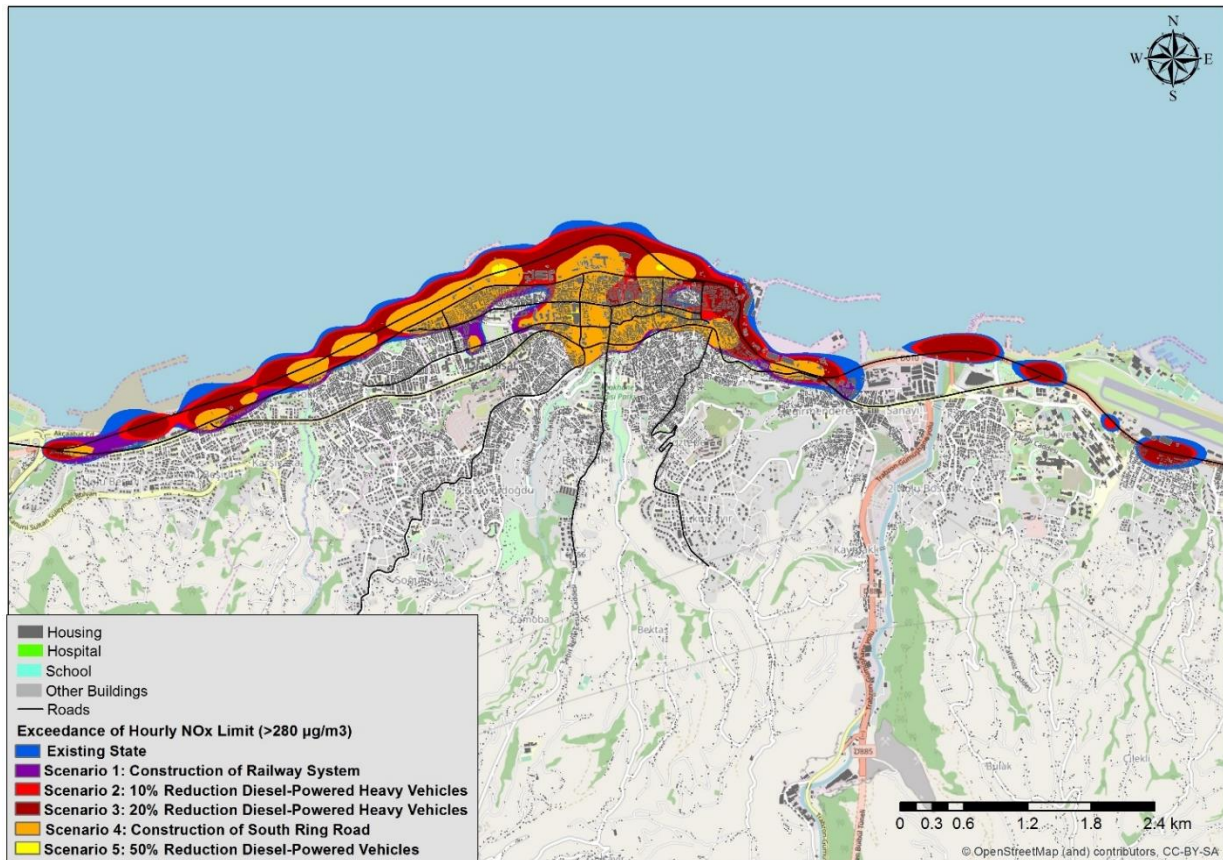


Figure 3. NO_x exposure reductions obtained through five different scenarios

4. Conclusion

In the scope of this study, road traffic-related emission inventories were prepared for the Trabzon city center. Among the related pollutants, NO_x was selected for modelling purpose due to the fact that it is more representative for road traffic emissions especially in city centers with high traffic density. Calculated NO_x inventories were used as input in the related model to obtain NO_x levels at different receptor grid points. Model results were compared to measurement results obtained from nearby meteorological stations using three different statistical tests. Among the four districts examined, two districts (Valilik and Meydan) in the city center showed good level of agreement between model and measurements indicating that traffic was the most dominant source of NO_x in these districts. Results for the other districts (Fatih and Besirli) indicated no agreement for NO_x pointing out some other significant NO_x sources in addition to the traffic.

Results indicated that 10% of the population in Trabzon city center was exposed to traffic-related NO_x concentrations higher than the regulatory limit. Results also indicated that the impact of heavy vehicles on these exposure levels was more significant than those of light vehicles. Accordingly, five different exposure reduction scenarios were selected and their impacts were examined. The results indicated that the measures represented by the scenarios 1 through 5 result in reductions in exposure levels by 1.2%, 27.6%, 46.9%, 37.7%, and 99.5%, respectively. According to these values, the most effective exposure reduction can be obtained by 50% reduction in the number of heavy and light diesel-powered vehicles.



5. References

- Abril, G. A., Diez, S. C., Pignata, M. L., & Britch, J. (2016). Particulate matter concentrations originating from industrial and urban sources: Validation of atmospheric dispersion modeling results. *Atmospheric Pollution Research*, 7(1), 180-189. Doi: <https://doi.org/10.1016/j.apr.2015.08.009>.
- BI. (2019). 15 major cities around the world that are starting to ban cars. *Business Insider*. Access Date: 04.09.2019, Retrieved from: <https://www.businessinsider.com/cities-going-car-free-ban-2018-12#madrid-banned-older-cars-from-its-city-center-1>.
- Brook, R. D., Rajagopalan, S., Pope, C. A., 3rd, Brook, J. R., Bhatnagar, A., Diez-Roux, A. V., Holguin, F., Hong, Y., Luepker, R. V., Mittleman, M. A., Peters, A., Siscovick, D., Smith, S. C., Jr., Whitsel, L., & Kaufman, J. D. (2010). Particulate matter air pollution and cardiovascular disease: An update to the scientific statement from the American Heart Association. *Circulation*, 121(21), 2331-2378. Doi: <https://doi.org/10.1161/CIR.0b013e3181d8e1>.
- EMEP/EEA. (2016). Air pollutant emission inventory guidebook - Road transport 2016 Air pollutant emission inventory guidebook 2016 - Road transport: European Environment Agency.
- Faiz, A., Weaver, C., & Walsh, M. (1996). *Air Pollution from Motor Vehicles*. Washington, D.C.: The World Bank.
- Foraster, M., Deltell, A., Basagana, X., Medina-Ramon, M., Aguilera, I., Bouso, L., Grau, M., Phuleria, H. C., Rivera, M., Slama, R., Sunyer, J., Targa, J., & Kunzli, N. (2011). Local determinants of road traffic noise levels versus determinants of air pollution levels in a Mediterranean city. *Environ Res*, 111(1), 177-183. Doi: <https://doi.org/10.1016/j.envres.2010.10.013>.
- Fuks, K. B., Weinmayr, G., Basagana, X., Gruzjeva, O., Hampel, R., Oftedal, B., Sorensen, M., Wolf, K., Aamodt, G., Aasvang, G. M., Aguilera, I., Becker, T., Beelen, R., Brunekreef, B., Caracciolo, B., Cyrus, J., Elosua, R., Eriksen, K. T., Foraster, M., Fratiglioni, L., Hilding, A., Houthuijs, D., Korek, M., Kunzli, N., Marrugat, J., Nieuwenhuijsen, M., Ostenson, C. G., Penell, J., Pershagen, G., Raaschou-Nielsen, O., Swart, W. J. R., Peters, A., & Hoffmann, B. (2017). Long-term exposure to ambient air pollution and traffic noise and incident hypertension in seven cohorts of the European study of cohorts for air pollution effects (ESCAPE). *European Heart Journal*, 38(13), 983-990. Doi: <https://doi.org/10.1093/eurheartj/ehw413>.
- Gibson, M. D., Kundu, S., & Satish, M. (2013). Dispersion model evaluation of PM_{2.5}, NO_x and SO₂ from point and major line sources in Nova Scotia, Canada using AERMOD Gaussian plume air dispersion model. *Atmospheric Pollution Research*, 4(2), 157-167. Doi: <https://doi.org/10.5094/apr.2013.016>.
- Khan, J., Ketzler, M., Kakosimos, K., Sørensen, M., & Jensen, S. S. (2018). Road traffic air and noise pollution exposure assessment – A review of tools and techniques. *Science of The Total Environment*, 634, 661-676. Doi: <https://doi.org/10.1016/j.scitotenv.2018.03.374>.
- Kindap, T., Unal, A., & KARACA, M. (2008). Air Pollution Problem and Solution Ways in Turkey. Paper presented at the National Symposium on Air Pollution and Control, Hatay, Turkey.
- Koksal, C. E., Yilmaz, A. G., & Gürtepe, İ. (2017). Clean Air Action Plans and Monitoring. Paper presented at the 7th National Air Pollution and Control Symposium, Antalya. <http://hkk2017.akdeniz.edu.tr/wp-content/uploads/2017/10/048.pdf>.



Laffoon, C., Rinaudo, J., Soule, R., & Bowie, T. (2005). Developing State-Wide Modeling Guidance for the Use of AERMOD – A Workgroup’s Experience, Louisiana Department of Environmental Quality; RTP Environmental Associates; Trinity Consultants; ENVIRON International Corporation.

Markakis, K., Im, U., Unal, A., Melas, D., Yenigun, O., & Incecik, S. (2012). Compilation of a GIS based high spatially and temporally resolved emission inventory for the greater Istanbul area. *Atmospheric Pollution Research*, 3(1), 112-125. Doi: <https://doi.org/10.5094/apr.2012.011>.

Mishra, D., & Goyal, P. (2015). Quantitative Assessment of the Emitted Criteria Pollutant in Delhi Urban Area. *Aerosol and Air Quality Research*, 15(4). Doi: 10.4209/aaqr.2014.05.0104.

Air Quality Assessment and Management Regulation (Hava Kalitesi Değerlendirme ve Yönetimi Yönetmeliği), (2008), Ministry of Environment and Urbanisation, Republic of Turkey 26898 Official Journal, 06.08.2008.

MoEU. (2016a). Trabzon City Environmental Status Report - 2015, Provincial Directorate of Environment and Urbanization, Ministry of Environment and Urbanisation, Republic of Turkey, Retrieved from: <http://www.csb.gov.tr/db/ced/eduardosya/Trabzon2015.pdf>.

MoEU. (2016b). Trabzon City Environmental Status Report - 2015 (Trabzon İli 2015 Yılı Çevre Durum Raporu). Ministry of Environment and Urbanization Website, Ministry of Environment and Urbanization, Republic of Turkey. Access Date: 12.05.2015, Retrieved from: <http://www.csb.gov.tr/db/ced/eduardosya/Trabzon2015.pdf>.

MoEU. (2017). National Air Quality Monitoring Network. Web site of the Ministry of Environment and Urbanisation Republic of Turkey, Ministry of Environment and Urbanisation Republic of Turkey. Access Date: 29.07.2017, Retrieved from: <https://www.havaizleme.gov.tr/>.

Mohammadiha, A., Malakooti, H., & Esfahanian, V. (2018). Development of reduction scenarios for criteria air pollutants emission in Tehran Traffic Sector, Iran. *Science of The Total Environment*, 622, 17-28. Doi: 10.1016/j.scitotenv.2017.11.312.

MoNE. (2011). Exhaust Emission Control, Ministry of National Education, Republic of Turkey, Retrieved from: http://megep.meb.gov.tr/mte_program_modul/moduller_pdf/Egzoz%20Emisyon%20Kontrol%C3%BC.pdf.

NASA. (2015). Shuttle Radar Topography Mission (SRTM) 90 m Digital Elevation Data. National Aeronautics and Space Administration (NASA), Access Date: 15.09.2015, Retrieved from: https://dds.cr.usgs.gov/srtm/version2_1/SRTM3/.

Ozkurt, N., Sari, D., Akalin, N., & Hilmioglu, B. (2013). Evaluation of the impact of SO₂ and NO₂ emissions on the ambient air-quality in the Can-Bayramic region of northwest Turkey during 2007-2008. *Sci Total Environ*, 456-457, 254-266. Doi: <https://doi.org/10.1016/j.scitotenv.2013.03.096>.

Rao, X. Q., Zhong, J. X., Maiseyeu, A., Gopalakrishnan, B., Villamena, F. A., Chen, L. C., Harkema, J. R., Sun, Q. H., & Rajagopalan, S. (2014). CD36-Dependent 7-Ketocholesterol Accumulation in Macrophages Mediates Progression of Atherosclerosis in Response to Chronic Air Pollution Exposure. *Circulation Research*, 115(9), 770-U766. Doi: <https://doi.org/10.1161/circresaha.115.304666>.



Rood, A. S. (2014). Performance evaluation of AERMOD, CALPUFF, and legacy air dispersion models using the Winter Validation Tracer Study dataset. *Atmospheric Environment*, 89, 707-720. Doi: <https://doi.org/10.1016/j.atmosenv.2014.02.054>

Sari, D., & Bayram, A. (2014). Quantification of emissions from domestic heating in residential areas of Izmir, Turkey and assessment of the impact on local/regional air-quality. *Sci Total Environ*, 488-489, 429-436. Doi: <https://doi.org/10.1016/j.scitotenv.2013.11.033>.

Tezel, M. N., Sari, D., Ozkurt, N., & Keskin, S. S. (2019). Combined NO_x and noise pollution from road traffic in Trabzon, Turkey. *Science of The Total Environment*, 696, 134044. Doi: <https://doi.org/10.1016/j.scitotenv.2019.134044>.

TUBITAK. (2016). Trabzon Metropolitan Municipality Strategic Noise Map Report (Trabzon Büyükşehir Belediyesi Stratejik Gürültü Haritaları Raporu), Ministry of Environment and Urbanisation. The Scientific and Technological Research Council of Turkey - Marmara Research Center .

TURKSTAT. (2014). Address-Based Population Registration System Results. Turkish Statistical Institute. Access Date: 11.03.2017, Retrieved from: <https://biruni.tuik.gov.tr/medas/?kn=95&locale=tr>
TURKSTAT. (2016). Registered motor vehicles, 2010 - 2015 (Trafığe Kayıtlı Araçlar, 2010-2015), Turkish Statistical Institute (Türk Standartları Enstitüsü),

Willmott, C. J., Robeson, S. M., & Matsuura, K. (2012). A refined index of model performance. *International Journal of Climatology*, 32(13), 2088-2094. Doi: <https://doi.org/10.1002/joc.2419>

Acknowledgements

The authors are thankful to TUBITAK Marmara Research Center; Environment and Cleaner Production Institute; Ministry of Environment and Urbanization for their support.

The authors have declared no conflict of interest.

Seasonal variations of organochlorine pesticides (OCPs) in air samples during day and night periods in Bursa, Turkey

Gizem Eker Sanlı and Yucel Tasdemir

Department of Environmental Engineering, Faculty of Engineering, Bursa Uludag University, 16059, Nilufer/Bursa, Turkey

tasdemir@uludag.edu.tr

Abstract. The aim of this study was to determine the seasonal variation of organochlorine pesticide (OCP) concentrations in Bursa, Turkey. The sampling region was a campus located nearly 20 km away from the city center and it was considered as a semi-rural site. Atmospheric concentrations of OCPs in the particulate and gas phase were measured separately during night and day time periods. Air samples were collected using a high volume air sampler (HVAS) and OCPs analyzed with a GC-ECD. The average of the total (gas + particulate) OCP concentration was calculated as 598.60 ± 194.20 pg/m³ and 65% of the total concentration was found to be in the gas phase. It was observed that OCPs with low molecular weights tended to stay in the gas phase. OCP values were relatively high in the summer months of June, July, and August. In these months, the OCP concentrations ranged between 63.71-799.06 pg/m³ in the particle phase and 173.79-798.99 pg/m³ in the gas phase. The maximum annual average gas phase OCP concentration was measured for Beta-HCH species as 176.01 pg/m³. In the particle phase, the maximum value was 66.96 pg/m³ and it was for Endosulfan-beta. OCP concentrations measured during the day and night time periods were found to be close to each other. There was no significant difference in particle phase OCP concentrations during day and night times. For some species (Alpha-Beta HVCH, Endrin, Endrin Aldehyde, etc.), night concentrations were high, while some species (Gamma HCH, Methoxychlor) reached higher levels during day times. The similar situation was observed for gas phase samples as well. The lack of a significant difference in OCP concentrations indicated that the impact of local resources was limited on diurnal variations.

Keywords: OCP, Semi-rural area, Particle-gas phase, Day-night time periods.

1. Introduction

Organochlorine pesticides (OCPs), which are an important member of pesticides, had been widely used worldwide for enhancing agricultural production and for controlling vector-borne diseases before the 1980s (Shunthirasingham et al., 2010). Many OCPs including dichlorodiphenyl trichloroethanes (DDTs) have been gradually phased out due to their properties. OCPs carry a serious health risk for living organisms and cause environmental problems; harmful, carcinogenic and organic pollutants that remain in nature for many years without degradation (Zhou et al., 2008). OCPs are generally applied directly to the soil or by sprinkling on crops. After their application, they spread to the atmosphere due to their physico-chemical properties. OCPs are subject to dispersion, chemical reactions, transportation over long distances, and removal by deposition in the atmosphere (Bozlaker et al., 2009; Harner et al., 1999, Cindoruk ve Tasdemir, 2014). OCPs can deposit onto soil, water and plant bodies depending on their atmospheric concentrations and meteorological conditions (ATSDR, 2005)

In some countries, isodrine and endrin have not been allowed to be used since 1972. The use of lindane is only permitted under special conditions. Organic pollutants such as HexachloroCycloHexanes (HCH) and DichloroDimethylTrichloroethan (DDT) are transported by air and water on a global scale due to their wide agricultural use (Kıstaubayeva, 2015). OCPs exhibit bioaccumulation in the food chain due to their vapor pressure, chemical solubility, durability, and these compounds can be transported over a very long distance (Bozlaker, 2008). High atmospheric concentrations were reported for OCP species although they were prohibited to be used. In recent years, OCP compounds have been studied around the world in different media (Bigot et al. 2017; Chen et al. 2017; Fang et al. 2017; Gioia et al. 2005; Wang et al. 2018; Wu et al. 2016). However, a limited number of studies about atmospheric concentrations and deposition fluxes of these pollutants have been carried out in Turkey (Sofuoglu et al., 2004; Bozlaker, 2008; Cindoruk, 2011; Cindoruk and Tasdemir, 2014).

OCPs do not have point sources. They enter the atmosphere through evaporation from previously contaminated soils, water bodies, and vegetation. Similar to other semi-volatile organic compounds, when OCPs are dispersed in the air, they partition between gas and particle phases (Cindoruk, 2011; Sanusi et al., 1999; Sauret et al., 2008). OCPs aimed to get an equilibrium between gas and particle phases depending on ambient air temperature, vapor pressures and molecular weights. OCP concentration and the phase (gas or particle) distribution in the atmosphere are the main factors affecting the atmospheric behavior (Tasdemir, Odabasi et al., 2004; Odabasi et al., 2008; Bozlaker et al., 2009).

The usage of hexachlorocyclohexane (HCH), Endrin, Heptachlor and DDT were banned in Turkey in accordance with promulgated regulation within the frame of Stockholm Convention 2001. Although OCPs were prohibited in Turkey in the 1980s, many studies have reported that their residues are still found in the human body and in breast milk (Seydaoglu et al. 2005; Mert and Bilgin 2006; Cok et al. 2011) as well as in urban air (Ozcan and Aydin 2009) and food products (Yavuz et al. 2010; Kalyoncu et al. 2009; Guler et al. 2010). Illegal uses, emissions from some industrial sources and air transportation from some other sites might be the reasons of OCP pollution in Turkey (Acara et al., 2006; Bozlaker et al., 2009).

The goal of this study was to determine (i) the levels and species of OCPs in a semi-rural site, (ii) the gas and particle phase distribution of OCPs, (iii) the OCP concentration variations during day and night time periods, and (iv) the seasonal variation of atmospheric OCP concentrations.

2. Materials and method

2.1. Sampling studies

Sample collection was performed at the Bursa Uludag University (40° 13'40.66" N – 8° 52'35.11 " E) which was classified as a semi-rural area (Figure 1). This campus located about 20 km away from the city center and in the vicinity of the Nilufer district. Sampling studies were conducted for one year. Air samples were collected with a high volume air sampler (HVAS- Thermo Andersen GPS 11 Model, USA). The HVAS had a filter and polyurethane foam (PUF) cartridge to hold particle and gas phase OCPs, respectively. The filter unit had a glass fiber filter with a diameter of 10.2 cm. After this unit, the PUF cartridge holds the gas phase OCP compounds. Two PUF were inserted into the glass cartridge having 5.5 cm diameter.

The samples collected between 08: 00-18: 00 were called as day time samples, and between 18:00-08:00 hours as night samples. Daily data were calculated using the results between 00:00-24:00. Daily data were used for the annual average calculations of the concentration values. Other calculations were made separately for day and night periods.

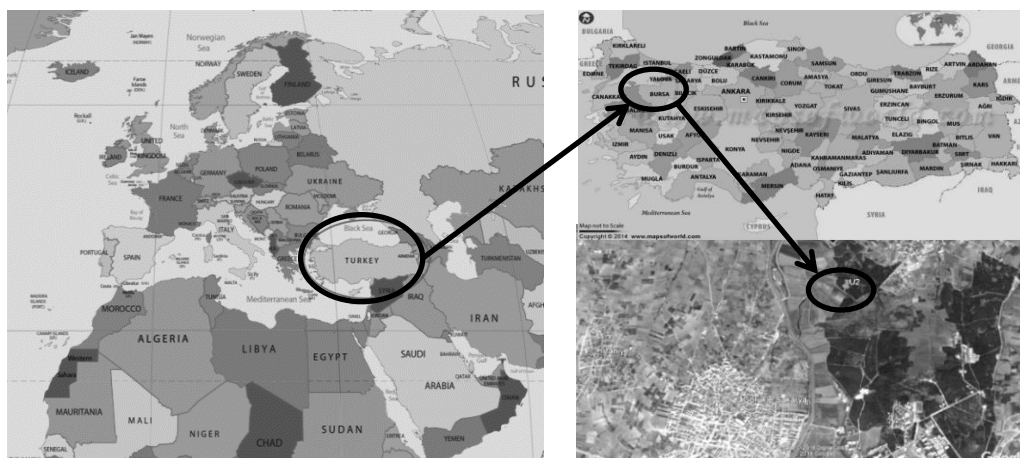


Figure 1. Sampling site

2.2. Analytical procedure and OCP determination

PUF cartridges were subjected to Soxhlet extraction with a 1:4 mixture of dichloromethane/petroleum ether (DCM/PE) for 24 hours. Filters were extracted in an ultrasonic bath for 30 minutes using 25 mL of DCM/PE (1:4) mixture. The extracts were passed through a sodium sulfate (Na_2SO_4) column to remove residual water. The volume of the dehydrated samples was reduced to 5 mL with a rotary evaporator (30 rpm). Fifteen mL of HEX was added to the sample and the volume was again reduced to 5 mL. A slow flow of nitrogen gas was then applied to the sample until the volume reduced to 2 mL. Samples were passed through a cleaning column containing 3 g silica (H_4SiO_4), 2 g alumina (Al_2O_3) and 2 g Na_2SO_4 , respectively (Tasdemir and Esen, 2007). Prior to this process, the column was cleaned to prevent possible contamination with 20 mL of DCM and 20 mL of PE, respectively. Two mL of sample and then 25 mL of PE was added to the column, the fraction formed by the complete passage of PE was removed and then 20 mL of DCM was added to the column to collect the OCP fraction (Cindoruk and Tasdemir, 2007; Cindoruk and Ozturk, 2016). The volume of the sample was gradually reduced to 5 mL with a rotary evaporator and then to 1 mL with gentle nitrogen gas. This sample was taken into 2 mL vials and stored at $-20\text{ }^\circ\text{C}$ until analysis (Cindoruk, 2011).

Gas chromatography (GC) analyses were conducted using an HP 7890A- μECD (Micro-Electron Capture Detector, Agilent, USA) instrument. The oven temperature was set to $80\text{ }^\circ\text{C}$ (1 min), with increases of $20\text{ }^\circ\text{C min}^{-1}$ to $240\text{ }^\circ\text{C}$ (5 min), followed by $5\text{ }^\circ\text{C min}^{-1}$ up to $270\text{ }^\circ\text{C}$, then $20\text{ }^\circ\text{C min}^{-1}$ up to $300\text{ }^\circ\text{C}$ (3.5 min). The inlet temperature was maintained at $250\text{ }^\circ\text{C}$, and the detector temperature was $320\text{ }^\circ\text{C}$. The carrying gas was high purity helium and the makeup gas was high purity nitrogen. HP5-MS, with dimensions of $30\text{ m}\times 0.32\text{ mm}\times 0.25\text{ }\mu\text{m}$, was used as a capillary column.

2.3. Quality assurance/quality control

The glassware used in the experimental studies was washed with water and then passed through pure water, methanol (MeOH), ACE/HEX (v/v; 1/1) and DCM, and dried at $105\text{ }^\circ\text{C}$. Glass fiber filters used in the HVAS were kept at $450\text{ }^\circ\text{C}$ for one night to remove organic impurities. The PUFs were cleaned with Soxhlet apparatus for 24 hours, respectively with pure water, MeOH, ACE/HEX (1/1, v/v) and DCM and dried at $60\text{ }^\circ\text{C}$. The filters and PUFs were kept in a refrigerator until the sample collection. The Na_2SO_4 , H_4SiO_4 and Al_2O_3 chemicals were stored at $450\text{ }^\circ\text{C}$ for 1 night before use.

External recovery standards were employed to determine the OCP recovery levels and the recovery values were over 75%. Therefore, the reported data were not recovery-corrected (Sofuoglu et al., 2004; Zheng et al., 2010; Cindoruk and Tasdemir, 2014). The IDL, the instrument detection limit, was calculated and they ranged from 0.04 pg (Heptachlor epoxide) to 0.15 pg (Methoxychlor) for each OCP

species. Blanks samples were prepared from PUF cartridges and filters to determine possible contamination during transport, storage and preparation of samples. The limit of detection (LOD) for each OCP was determined by adding three standard deviations to the average of the blanks (average + 3xSD). The values smaller than the LOD were not included in the calculation. The LOD values varied from 0.71 (alpha-HCH) to 2.13 ng (Endosulfan beta) for the filters, and from 1.19 (Endrin) to 1.87 ng (Gamma-HCH) for the PUF samples.

3. Results and discussion

3.1. OCP concentrations and their gas and particle distributions

Some researchers determined many different OCP species from the atmospheric samples around the world. It was noteworthy that many types of OCPs have been measured in the atmosphere even though some of them were prohibited. Evaporation, atmospheric transport and/or illegal use are thought to be the main reasons for atmospheric OCPs measured (Zhang et al., 2011).

HCH is an organochlorinated insecticide consisting of eight isomers. Of these, alpha-(α), beta-(β), gamma-(γ) and delta-(δ) isomers are of commercial importance (Bozlaker, 2008). In our study, the average concentration value of Beta-HCH in the gas phase was maximum (176.01 pg/m^3) (Figure 2). The presence of HCH isomers in recipient media has a more important potential problem than many other OCPs (DDT, endrin, aldrin, heptachlor, etc.). Their solubility in water is higher than other isomers, which causes them to be considered in the risk factor compounds. The HCH isomers can evaporate in significant amounts from water to air by evaporating with temperature rise. This characteristic can be effective in increasing the beta-HCH species at the average annual OCP concentrations in the gas phase. Most chemicals used as a water-based, acrylic-based liquid curing material that prevents water loss of fresh concrete by applying by roller or spray method on newly poured concrete surfaces contain Hexachlorocyclohexane (HCH). All internal and external field concretes including airport, road and bridge concrete, harbors, retaining walls, columns and beams, terrace roofs, etc. can be considered in this manner. The high Beta-HCH value may be due to the mixing and transport of the chemicals used for the purposes mentioned above. As a matter of fact, there were new settlements in close proximity of the sampling region. Another reason to obtain high Beta HCH concentration can be attributed to the spraying or dry particle methods of pesticide usage as emphasized by researchers (Sanusi et al., 1999; Gill and Sinfort, 2005). HCH compounds were found to be high in another study conducted in Izmir/Turkey (Sofuoglu et al., 2004). Furthermore, Cindoruk (2011) showed that Beta-HCH was the dominant compound in the gas phase for all sites in Bursa/Turkey.

The gas and particle phase concentration distributions of the OCP compounds are plotted in Figure 2. The maximum value at the average annual OCP gas phase concentrations was measured for the Beta-HCH species with 176.02 pg/m^3 . In the particle phase, the maximum value was 66.96 pg/m^3 and it belonged to Endosulfan-beta species. In another study conducted in Bursa (Cindoruk, 2011), particle phase OCP concentrations were measured in the range of $227.76\text{-}234.75 \text{ pg/m}^3$ and gas phase OCP concentrations were ranged between $861.88\text{-}917.92 \text{ pg/m}^3$. Similar results were obtained by Gioia et al. (2005) in New Jersey- USA. Researchers reported that gas phase OCP concentrations were higher than particle phase concentrations. (Gioia et al., 2005).

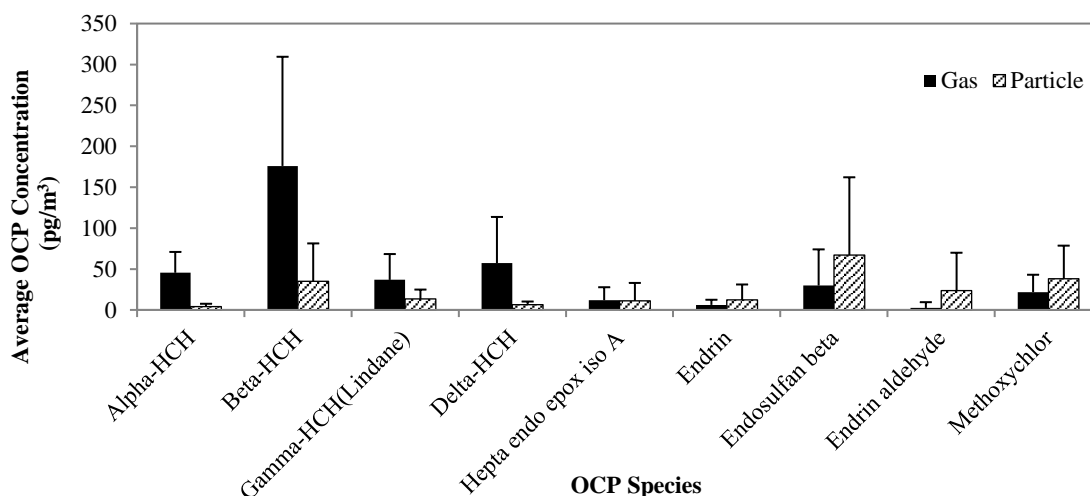


Figure 2. Annual average OCP concentrations in the gas and particle phases

Total OCP concentrations were relatively high in the months of June, July and August. In the summer season, the concentration values ranged between 63.71-799.066 pg/m³ in the particle phase and 173.79-798.99 pg/m³ in the gas phase. The reason for the high concentrations in these months could be the intensification of agricultural activities and the increase of pesticides applications (Gioia et al., 2005; Odabasi et al., 2008). Another reason would be the increase in the air temperature. When the temperature increases, atmospheric OCP concentrations increase as a result of evaporation from surfaces such as soil, water and plants. The lowest concentrations were measured in January. It was concluded that precipitation (snow, rain) occurring in this month may lead to increase in deposition of OCPs and decrease in an atmospheric concentration (Cao et al., 2007, Zhou, Zhu et al., 2008). In the study conducted by Cindoruk and Ozturk (2016) in Mudanya, high wet deposition fluxes were obtained in December and January. Also, researchers showed that total OCP deposition fluxes increased in these months in Bursa-Yavuzselim (Cindoruk and Tasdemir, 2014). Higher summertime OCP concentrations in the air were also reported by Cortes et al. (1999), Gioia et al. (2005), Odabasi et al. (2008), and Sun et al. (2006). Sofuoglu (2004) reported higher values of OCPs in spring at a suburban site of Izmir. At a coastal/urban site of Izmir, Odabasi et al. (2008) found generally higher atmospheric OCP concentrations in the summer and winter sampling periods.

3.2. Concentrations of OCPs in day and night time periods

Annual distribution of particle phase OCP concentrations are given in Figure 3. The highest average OCP concentration value for the particle phase belonged to Endosulfan-beta both for day and night sample period. The average concentration values for this compound was 66.33 pg/m³ at night and 63.60 pg/m³ at day periods (Figure 3). The minimum average OCP concentration value was determined for Alpha-HCH species for both in a day (2.98 pg/m³) and night (4.73 pg/m³) periods. The minimum day and night concentrations were found to be close to each other. There was no statistically significant difference in particle phase OCP concentrations during day and night periods. For some species (Alpha-Beta HCH, Endrin, Endrin Aldehyde, etc.), night concentrations were high while some species (Gamma HCH, Methoxychlor) reached bigger levels during day times. The similar case was observed for gas phase samples as well. The lack of a significant difference in OCP concentrations indicated that the impact of local resources was limited. There were limited studies about OCP concentrations during day and night time periods. Lammel et al. (2011) found that maxima of most OCPs were observed preferentially during the day-time. Researchers emphasized that concentration in air and the vertical concentration gradient of the HCH isomers varied with air temperature (day-time maxima).

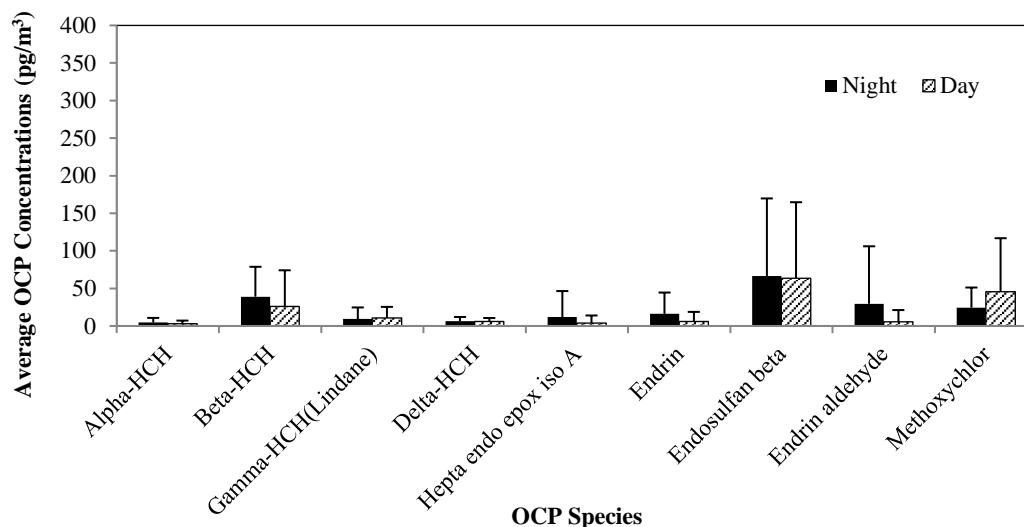


Figure 3. Annual distribution of particle phase OCP concentrations

Endosulfan active substances which were banned in 2006 in European Union countries have been used in our country for many years. In 2007, the General Directorate of Protection and Control prohibited the use of endosulfan active substances used in various stages of production, including cotton, cereals and vegetables. In the present study, particle phase Endosulfan beta concentration was high. This result may be explained by the common usage of this chemical in agricultural purposes located near the sampling site, which is the Bursa Uludag University Campus.

Figure 4 showed the annual distribution of gas phase OCPs. Compound-based concentrations were distributed over a wide range. The maximum average gas phase concentration was measured for Beta-HCH species. The values were 217.11 pg/m^3 and 140.78 pg/m^3 for the night and day periods, respectively (Figure 4). The lowest concentration was determined for Endrin aldehyde.

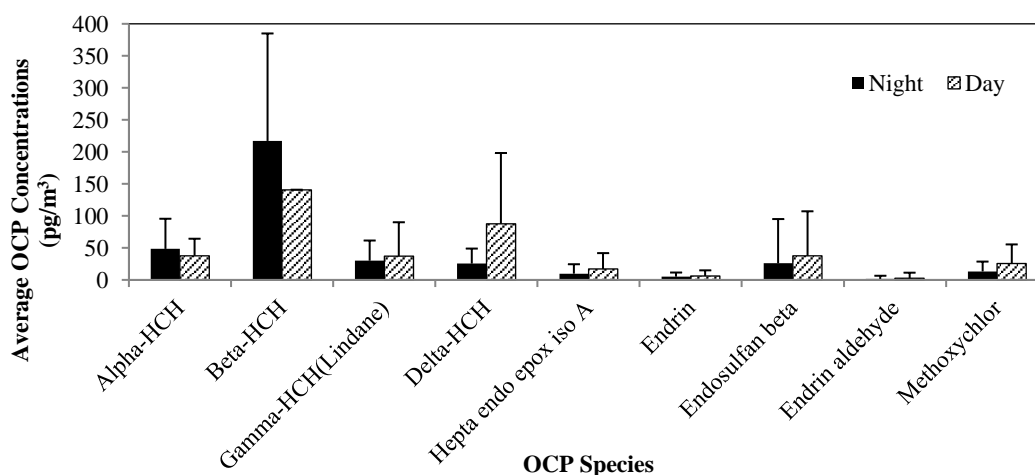


Figure 4. Annual distribution of gas phase OCP concentrations

Lammel et al. (2011) emphasized that dry deposition supposedly constituted an effective sink in the nocturnal boundary layer, but not during the day-time (sunny, well-mixed). They showed that day-time OCP concentrations were generally higher than night-time concentrations. Data of the present study and the data of the study conducted by Lammel et al. (2011) were partially compatible. In the present study,



daytime OCP concentrations were higher for some OCP species in both particle and gas phases than concentrations in the night time periods.

4. Conclusions

Despite the banning of most OCP compounds in Turkey, some OCP species can be still used for agricultural applications. There are limited studies about OCP concentration measurements in Turkey; therefore, this study was performed to measure air concentrations of OCPs in one of the big cities in Turkey. Bursa has over 2.5 million habitants and it has strong industrial and agricultural activities. The sampling was performed using an active sampler, an HVAS. Particle and gas phase OCP compounds were measured for day and night time periods. Our main findings can be summarized as follows:

- OCP concentrations levels were in line with the other measured values.
- Gas phase OCP concentrations were higher than particle phase concentrations.
- Beta HCH (gas phase) and Endosulfan beta (particle phase) species have been identified as dominant species. However, no statistically significant differences were found in concentrations during the day and night time periods.
- OCP concentrations in summer were higher than in other seasons.

The minimization of pesticide pollution in all environments will be ensured through the adoption of an integrated pest management approach in agriculture, protecting the environment and human health. The fact that OCPs have been used despite prohibitions for many years in agriculture is an indication that integrated pest management is not adequately adopted and implemented. Uncontrolled use of OCPs affects not only the area where they are used but also many different locations in remote areas where OCPs are not used. The results of the present study could be regarded as an early indication of the potential risks of OCP residues to agricultural production and highlight the need for further studies involving periodical monitoring and assessment and ultimately a full evaluation of the level of OCP contamination in Bursa-Turkey.

5. References

- Acara, A., Balli, B., Yeniova, M., Aksu, P., Duzgun, M., Dagli, S., 2006. Turkey's Persistent Organic Pollutants (POPs) on the Draft National Implementation Plan for the Stockholm Convention, UNIDO-POPs Project.
- ATSDR, 2005. Toxicological profile for alpha-, beta-, gamma-, and delta-hexachlorocyclohexane. U.S. Department of Health and Human Services, Public Health Service. Retrieved August, from <http://www.atsdr.cdc.gov/toxprofiles/tp43.pdf>.
- Bigot, M., Hawker, D.W., Cropp, R., Muir, D.C.G., Jensen, B., Bossi, R., Nash, S.M.B., 2017. Spring melt and the redistribution of organochlorine pesticides in the sea-ice environment: a comparative study between arctic and antarctic regions. *Environmental Science & Technology*. 51, 8944-8952.
- Bozlaker, A., 2008. A Study Of Semi-Volatile Toxic Organic Air Pollutants In Aliaga Heavy Industrial Region, Doktora Tezi, Dokuz Eylul Universitesi.
- Bozlaker, A., Muezzinoglu, A. Odabasi, M., 2009. Processes affecting the movement of organochlorine pesticides (OCPs) between soil and air in an industrial site in Turkey. *Chemosphere*. 77, 1168-1176.
- Cao, H., Liang, T., Tao, S., Zhang, C.S., 2007. Simulating the temporal changes of OCP pollution in Hangzhou, China. *Chemosphere*. 67, 1335-1345.

- Chen, L.G., Feng, Q.H., He, Q.S., Huang, Y.M., Zhang, Y., Jiang, G., Zhao, W., Gao, B., Lin, K., Xu, Z.C., 2017. Sources, atmospheric transport and deposition mechanism of organochlorine pesticides in soils of the Tibetan Plateau. *Science of the Total Environment*. 577, 405-412.
- Cindoruk, S. S. Tasdemir, Y., 2014. The investigation of atmospheric deposition distribution of organochlorine pesticides (OCPs) in Turkey. *Atmospheric Environment*. 87, 207-217.
- Cindoruk, S. S., Tasdemir, Y., 2007. Deposition of atmospheric particulate PCBs in suburban site of Turkey. *Atmospheric Research*. 85, 300-309.
- Cindoruk, S.S. Ozturk, E., 2016. Atmospheric deposition of organochlorine pesticides by precipitation in a coastal area. *Environmental Science And Pollution Research*. 23 24504-24513.
- Cindoruk, S.S., 2011. Atmospheric organochlorine pesticide (OCP) levels in a metropolitan city in Turkey, *Chemosphere*. 82, 78-87.
- Cok, I., Yelken, C., Durmaz, E., Uner, M., Sever, B., Satır, F., 2011. Polychlorinated biphenyl and organochlorine pesticide levels in human breast milk the Mediterranean city Antalya, Turkey. *Bull. Environ. Contam. Toxicol.* 86, 423-427.
- Cortes, D.R., Hoff, R.M., Brice, K.A., & Hites, R.A., 1999. Evidence of current pesticide use from temporal and clausius-clapeyron plots: a case study from the integrated atmospheric deposition network. *Environmental Science and Technology* 33, 2145-2150.
- Gill, Y., Sinfort, C., 2005. Emission of pesticides to the air during sprayer application: a bibliographic review. *Atmos. Environ.* 39, 5183-5193.
- Gioia, R., Offenbergl J.H., Gigliotti, C.L., Totten, L.A., Du, S. Eisenreich, S.J., 2005. Atmospheric concentrations and deposition of organochlorine pesticides in the US Mid-Atlantic region. *Atmospheric Environment*. 3, 2309-2322.
- Guler, G.O., Cakmak, Y.S., Dagli. Z., Aktumsek A, Ozparlak H., 2010. Organochlorine pesticide residues in wheat from Konya region, Turkey. *Food Chem. Toxicol.* 48:1218-1221.
- Harner, T., Wideman, J.L., Jantunen, L.M.M., Bidleman, T.F., Parkhurst, M.J., 1999. Residues of organochlorine pesticides in Alabama soils. *Environ. Pollut.* 106, 323-332.
- Kalyoncu, L., Agca, I., Aktumsek, A., 2009. Some organochlorine pesticide residues in fish species in Konya, Turkey. *Chemosphere*. 74, 885-889.
- Kıstaubayeva, A., 2015. PAH ve OCP Bileşiklerinin Toprak Ortamında Mekansal Dağılımının Belirlenmesi ve Hava Toprak Fazı Geçişlerinin Araştırılması, YÜksek Lisans Tezi, Yıldız Teknik Üniversitesi.
- Lammel, G.,Klanova, J., Eric, L., Ilic, P., Kohouteka, J., Kovacic, I., 2011. Sources of organochlorine pesticides in air in an urban Mediterranean environment: volatilisation from soil, *J. Environ. Monit.* 13, 3358-3364.
- Mert, E., Bilgin, N.G., 2006. Demographical, aetiological and clinical characteristics of poisoning in Mersin, Turkey. *Hum. Exp. Toxicol.* 25, 217-223.
- Odabasi, M., Cetin, B., Demircioglu, E., Sofuoglu, A., 2008. Air-Water exchange of polychlorinated biphenyls (PCBs) and organochlorine pesticides (OCPs) at a coastal site in Izmir Bay, Turkey. *Marine Chemistry*. 109, 115-129.
- Ozcan, S., Aydin, M.E., 2009. Polycyclic aromatic hydrocarbons, polychlorinated biphenyls and organochlorine pesticides in urban air of Konya, Turkey. *Atmos. Res.* 93,715-722.
- Sanusi, A., Millet, M., Mirabel, P., Wortham, H., 1999. Gas-particle partitioning of pesticides in atmospheric samples. *Atmos. Environ.* 33, 4941-4951.

- Sauret, N., Wortham, H., Putaud, J.P., Mirabel, P., 2008. Study of the effects of environmental parameters on the gas/particle partitioning of current pesticides in urban air. *Atmos. Environ.* 42, 544–553.
- Seydaoglu, G., Satar, S., Alparslan, N., 2005. Frequency and mortality risk factors of acute adult poisoning in Adana, Turkey 1997–2002. *Mt Sinai J. Med.* 72, 393–401.
- Shunthirasingham, C., Mmereki, B. T., Masamba, W., Oyiliagu, C. E., Lei, Y. D., Wania, F., 2010. Fate of pesticides in the arid subtropics, Botswana, Southern Africa. *Environmental Science and Technology*. 44, 8082–8088.
- Sofuoglu, A., Cetin, E., Bozacioglu, S.S., Sener, G.D., Odabasi, M., 2004. Short-term variation in ambient concentrations and gas/particle partitioning of organochlorine pesticides in Izmir, Turkey. *Atmos. Environ.* 38, 4483–4493
- Sun, P., Blanchard, P., Brice, K., Hites, R.A., 2006. Atmospheric organochlorine pesticide concentrations near the Great Lakes: Temporal and spatial trends. *Environmental Science and Technology*. 40, 6587–6593.
- Tasdemir, Y., Esen, F., 2007. Dry Deposition fluxes and deposition velocities of PAHs at an urban site in Turkey. *Atmospheric Environment*. 41, 1288–1301.
- Tasdemir, Y., Odabasi, M., Vardar, N., Sofuoglu, A., Murphye, T.J., Holsen, T.M., 2004. Dry deposition fluxes and velocities of polychlorinated biphenyls (PCB) associated with particles. *Atmospheric Environment*. 38, 2447–2456.
- Wang, Y.Z., Zhang, S.L., Cui, W.Y., Meng, X.Z., Tang, X.Q., 2018. Polycyclic aromatic hydrocarbons and organochlorine pesticides in surface water from the Yongding River basin, China: Seasonal distribution, source apportionment, and potential risk assessment. *Science of the Total Environment*. 618, 419–429.
- Wu, Y.L., Wang, X.H., Ya, M.L., Li, Y.Y., Hong, H.S., 2016. Distributions of organochlorine compounds in sediments from Jiulong river estuary and adjacent western Taiwan Strait: implications of transport, sources and inventories. *Environmental Pollution*. 219, 519–527.
- Yavuz, H., Guler, G.O., Aktumsek, A., Cakmak, Y.S., Ozparlak, H., 2010. Determination of some organochlorine pesticide residues in honeys from Konya, Turkey. *Environ. Monit. Assess.* 168, 277–283.
- Zhang, L., Huang, Y., Dong, L., Shi, S., Zhou, L., Zhang, T., Mi, F., Zeng, L., Shao, D., 2011. Levels, seasonal patterns, and potential sources of organochlorine pesticides in the urban atmosphere of Beijing, China. *Arch. Environ. Contam. Toxicol.* 61, 159–165.
- Zheng, X.Y., Chen, D.Z., Liu, X.D., Zhou, Q.F., Liu, Y., Yang, W., Jiang, G.B., 2010. Spatial and seasonal variations of organochlorine compounds in air on an urban–rural transect across Tianjin, China. *Chemosphere*. 78, 92–98.
- Zhou, R., Zhu, L., Chen, Y., 2008. Levels and source of organochlorine pesticides in surface waters of Qiantang River, China. *Environ. Monit. Assess.* 136, 277–287.

Acknowledgement

This study was financially supported by Uludag University (Project number: BAP 2007/28) and Technological Research Council of Turkey (TUBİTAK) project number 107Y165. We would like to thank Aslan Karademir and Manolya Gunindi for their valuable contribution.

Determination of fluxes and mass transfer coefficients of Polychlorinated Biphenyls (PCBs)

Ahmet Egemen Sakın and Yücel Tasdemir

Department of Environmental Engineering, Faculty of Engineering, Bursa Uludag University, 16059, Bursa, Turkey

tasdemir@uludag.edu.tr

Abstract. This study evaluates a modified water surface sampler (MWSS) to sample atmospheric polychlorinated biphenyls (PCBs). We collected 44 flux and ambient air samples using the MWSS and a high volume air sampler (HVAS), respectively. The average of the PCB fluxes of the dissolved phase obtained from the MWSS was 11.18 ± 13.44 ng/m²-day. Particle phase PCBs were also determined by attaching a filter to the sampler. The particle phase flux ratio was 10.92 % of the total. However, this value was lower than the particle phase ratio (15%) obtained by HVAS. This was mainly due to the collection apparatus attached to the MWSS. 4-CBs and lower chlorinated PCBs were dominant in the samples. We correlated homolog groups from both the MWSS and HVAS, and we found high correlation coefficient. These results indicated that both samplers collected similar atmospheric PCBs. Then, we calculated mass transfer coefficients. To calculate the MTCs, dissolved phase PCB fluxes were divided by gas phase PCB concentrations, which were collected using an HVAS. Average MTC was determined to be 0.13 ± 0.14 cm/s and this average value was in line previously reported MTCs for semivolatile organic compounds.

Keywords: Active sampling, Deposition, Air-water exchange, Sampling ratios, POPs.

1. Introduction

Polychlorinated biphenyls (PCBs), an important member of persistent organic pollutants (POPs), have been classified as carcinogenic materials by IARC because of their observed effects on animals (IARC, 1987). They have also been characterized as endocrine disruptor chemicals because of their impact on internal hormone receptors (IARC 1987; Lauby-Secretan et al., 2013). The scientific community is interested in PCBs not only because of their harmful effects and toxicities but also because of their ecological characteristics, such as persistence, bio-accumulation, and transportability over long distances. Moreover, according to the studies carried out by the World Health Organization, 1.2 million tons of PCBs were produced globally from 1929–1977. This large amount gives some indication as to why PCBs are a severe problem (WHO, 1993).

Atmospheric PCBs are transported over long distances where they are deposited on wet surfaces and terrestrial regions (Gunindi et al., 2010). Deposition on water surfaces and evaporation comprise a vital component of PCB transformation (Shahin et al., 2002). Dry deposition studies have been performed by using water as a collection surface for semi-volatile organic compounds (SVOCs) (Cindoruk et al., 2007). In previous studies, PAH, pesticides, sulfate, and nitrate levels have been measured in addition to PCBs by using water surface samplers (Zobrist et al., 1993; Odabasi et al., 2002; Tasdemir et al., 2006; Esen et al., 2010). In general, air-water exchange studies have been performed by using water surface samplers. To determine the flux between air and water, the two-film model was used by

considering concentration measurements from both phases (Schwarzenbach et al., 1993). Mass balance and two-film model approaches have been used to determine evaporation from water bodies for SVOCs (Hoff et al., 1996; Pirrone et al., 1995). When sampling pollutants, it is reasonable to use water because of its abundance. In addition, this approach allows us to understand the mechanisms for air-water transfer of pollutants, such as PCBs.

The air-water exchange is a function of Henry's law constant, the concentration gradient and the overall MTC. According to the two-film model, the net flux (F_g , ng/m²-d), which is the fugacity difference between air and water, can be represented as follows:

$$F_g = K_G \{C_g - C_w(H/RT)\} \quad (1)$$

where C_g and C_w are the ambient air and water concentrations of the contaminants (ng/m³), H is the Henry's law constant (L atm/mol), R is the universal gas constant (0.082 L-atm/mol-K), K_G is the gas phase overall MTC (m/d).

The objectives of this study can be summarized as follows: (i) evaluating a MWSS for sampling PCBs especially for gas phase PCBs, (ii) defining the dissolved and particle phase PCB levels, (iii) calculating the mass transfer coefficients for each PCB, and (iv) correlating the results depending on the seasonal and meteorological conditions.

2. Materials and Method

2.1 Sampling Program

A modified water surface sampler (MWSS) was operated simultaneously with a high volume air sampler (HVAS). The samples were collected at the Bursa Uludag University Campus (BUUC) between February 04, 2013, and November 15, 2013, to represent each season of the year. Throughout the sampling period, wind speed, wind direction, temperature, and atmospheric pressure were also measured.

2.2. Modified Water Surface Sampler (MWSS)

Atmospheric samples were collected using a modified water surface sampler (MWSS, Figure 1). The MWSS was composed of stainless steel and is 59.5 cm in diameter and 0.5 cm in depth. This volume, otherwise known as the sampling platform, was full of water. All of the connecting apparatus and tubes in the sampler were made of Teflon and glass.

Distilled water was introduced into the sampler from a hole in the middle where it remained for approximately 2–4 minutes. Then, it was collected from 4 spillways. The water collected in a reservoir first passed through the filter, which retained the particle phase. Then, it passed through a column composed of XAD-2 resin, whose height was approximately 30 cm. The cleaned water, whose organics were captured by the resin column, was pumped into the sampling platform again for re-circulation. Different types of WSSs were employed in previous studies for POP measurements (Tasdemir et al., 1997; Odabasi et al., 1999; Tasdemir et al., 2005; Tasdemir et al., 2005; Tasdemir et al., 2006; Cindoruk et al., 2007; Tasdemir et al., 2007; Tasdemir et al., 2007; Tasdemir et al., 2008). Our design differs from the previously used WSSs. For example, the upper surface or cover of the MWSS was used in this study and prevented the atmospheric deposition of particles. The MWSS cover had eight holes, 7 mm diameter, and walking-stick shaped tubes on the edge of the cover (Figure 1). Below the sampler, there was a similar number of holes with plain tubes with the same width (Figure 1). A chimney working logic was achieved by use of the pipes in the MWSS in order to have more air sampled.

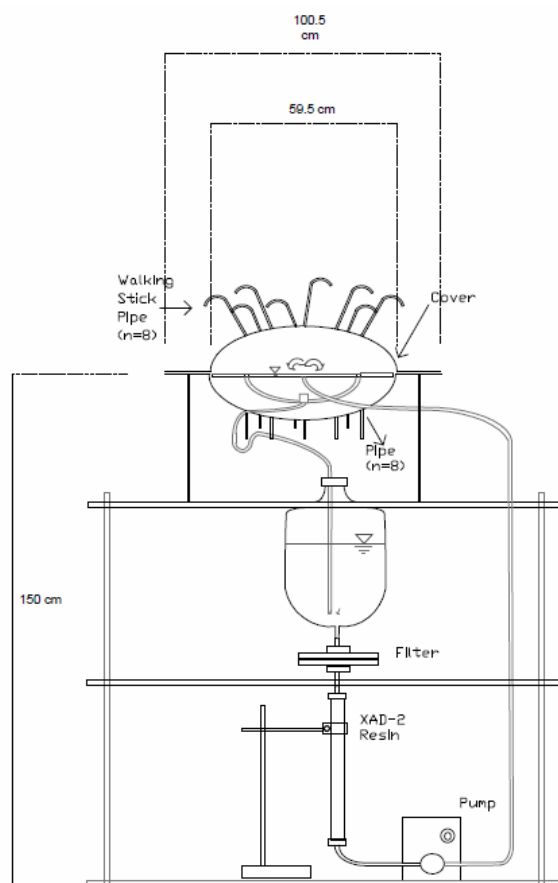


Figure 1. The MWSS Used in the Sampling

2.3. Analysis

Before sampling and analyzing, the equipment used in this study was washed with distilled water and then with methanol (MeOH) and dichloromethane (DCM). The filters were wrapped with aluminum foil and heated at 450 °C for 24 hours to remove any possible organic residues (Cindoruk et al., 2007). The PUF cartridges used in the HVAS and resin were extracted, first with distilled water, then with MeOH, and finally with acetone /hexane (ACE/HEX) (1/1, v/v) and DCM for 24 hours (Cindoruk et al., 2007). After cleaning, the filters and resin were kept in a deep freezer. The filters were wrapped with aluminum foil in reserved bags, and the resin was placed in capped glass jars.

The collected filter and resin samples were extracted twice in an ultrasonic bath with a 1/1 (v/v) mixture of ACE/HEX for 15 minutes each. The extract was reduced using a rotary evaporator. To calculate the extraction efficiency, a surrogate standard containing PCB #14, #65 and #166 was added into each sample at the start of the extraction (Cotham et al., 1995; Odabasi et al., 1999; Vardar et al., 2004; Cindoruk et al., 2007). The samples in the HEX were reduced to 2 mL using a gentle stream of nitrogen gas. Clean up procedure applied with a fractionation column containing 3 g of silicic acid with 3% water, 2 g of alumina with 6% water and 2 g of sodium sulfate (Cindoruk et al. 2008). Samples were washed with sulfuric acid to prevent any organic contamination (Cindoruk et al. 2010). Before analysis, PCB 204 was added to the samples that were prepared for GC analysis to correct the volume to that of the internal standard.

The samples were analyzed using an Agilent Tech. 7890A model gas chromatographer with an Agilent Tech. 7683B model injector. The program used during the analysis was as follows: 70 °C for 2 minutes,

with a 25° C /min increase until reaching 150 °C, followed by a 3 °C /min increase until reaching 200 °C, and an 8 °C/min increase until reaching 280 °C; hold at 280 °C for 8 mins, with a 10 °C/min increase until reaching 300 °C and stay at this temperature for 2 minutes. The inlet temperature was 250 °C, and the detector temperature was 320 °C. Helium gas with a 1.9 mL/min flow rate was used as the carrier gas, and high-purity nitrogen gas was used as the makeup gas. A DB5-MS capillary column (30 m. x 0.250 mm. x 0.25 µm) was employed.

2.4 Quality Assurance and Quality Control

Blank samples (n=8) were collected to determine and avoid any possible contamination during the transportation, preparation, and analysis of the collected samples. Blank samples were carried to the sampling point at the same conditions and subjected to the same analysis as the other samples. Using these samples, the LOD (limit of detection) was calculated (Odabasi et al., 1999). The samples were blank-corrected, and only values higher than the LOD were used in the calculations. At the start of the extraction, surrogate standards were added to the samples. The recovery values for PCB #14, #65 and #166 were 66.43±35.7%, 64.92±32.11% and 78.34±17.24% respectively. The levels of the losses that occurred during extraction and analysis were determined and calculated along with the results. Before the analysis with gas chromatography (GC), an internal standard was added to the samples order to reach exact volumes.

3. Results

3.1. Atmospheric PCB Concentrations

In this study, we analyzed 87 PCB congeners: PCB #4/10, #9/7, #6, #8/5, #18, #15/17, #16/32, #26, #31, #28, #21/53, #22, #45, #52, #47, #49/48, #44, #37/42, #71/41/64, #100, #74, #70/61, #66/95, #91, #56/60, #92, #84, #89/101, #119, #56/60, #92, #84, #89/101, #119, #83, #81/87, #86, #85, #77/110, #135/144, #114/149, #118, #123, #131, #153, #132/105, #163/138, #126, #128, #167, #174, #202/171/156, #172, #180, #200, #170/190, #169, #199, #207, #194, #205, and #206. The total (gas+particle phase) PCB concentrations measured with the HVAS changed in the range of 8 pg/m³ and 906 pg/m³, and their average was 346.53±249.0 ng/m³. The obtained results aligned with those of other studies (Cetin et al., 2007; Bozlaker et al., 2008; Hu et al., 2010; Barthel et al., 2012; Kaya et al., 2012; Li et al., 2012; Meire et al., 2012; Yenisoy-Karakas et al., 2012; Xu et al., 2013; Zhang et al., 2013; Kuzu et al., 2014). The sampling point had no PCB source; therefore, the changes in concentrations mainly came from either the meteorological conditions or transportation of PCBs. This site was also investigated in previous studies, which demonstrated a decrease in the PCB levels at this site (Cindoruk et al., 2007; Cindoruk et al., 2008; Cindoruk et al., 2010).

Upon review of the gas and particle phase concentrations, 85% of the total concentration consisted of gas-phase PCB concentrations. Moreover, this percentage value was similar to the ratios obtained in previous studies performed in the region (Cindoruk et al., 2008; Cindoruk et al., 2010). A review of the homolog group distribution indicated that 2-, 3-, and 4- CBs were dominant, similar to the results of previous studies (Cindoruk et al., 2007; Cindoruk et al., 2008).

3.2. Dissolved and Particulate Phase PCB Fluxes

The designed sampler had 16 tubes in total, eight on top and eight below, to allow air to enter the MWSS. These tubes and the cover were the main differences from previous WSSs. The diameter of each tube was 0.7 cm. Because the MWSS had 16 tubes, the total area of air exchange was approximately 6.15 cm². This clearance is very small compared with samplers composed of polyurethane foam (PUF), which had a clearance of about 150 cm². The goal of this study was to use the MWSS to sample only pollutants in the gas phase because the gap where the air entered into the sampler was much smaller than that of previously used samplers. Also, it was expected that the particulate intake would be low because the columns were only 0.7 cm in diameter. Moreover, the upper tubes were in the shape of a walking-stick,

which minimizes the particulate phase entrance. Therefore, only a XAD-2 resin column was used to capture dissolved phase PCBs in some samples. However, in other samples (04-06/02/2013, 06-08/02/2013, 08-11/13/2013, 11-13/02/2013, 13-15/02/2013, 15-18/02/2013, 18-20/02/2013, 20-22/02/2013, 22-25/02/2013, 03-05/08/2013, 05-08/05/2013, 08-10/05/2013, 10-13/05/2013, 15-17/07/2013, 17-19/07/2013, 08-11/11/2013), possible PCBs in the particle phase were also targeted for sampling by placing a filter holder in front of the resin column.

Dissolved and particle-phase fluxes were measured by using the MWSS in this study. The particle phase and dissolved phase were measured separately, and the maximum particle-phase flux was measured in the spring. Dissolved phase PCB fluxes were in the range of 0.54 ng/m²-day and 48.76 ng/m²-day and the average value was 11.18±13.44 ng/m²-day. Likewise, the particle phase changed between 0.44 ng/m²-day and 2.25 ng/m²-day and its average was 1.37±0.54 ng/m²-day. Total (particle + dissolved phase) PCB fluxes were shown in Figure 2.

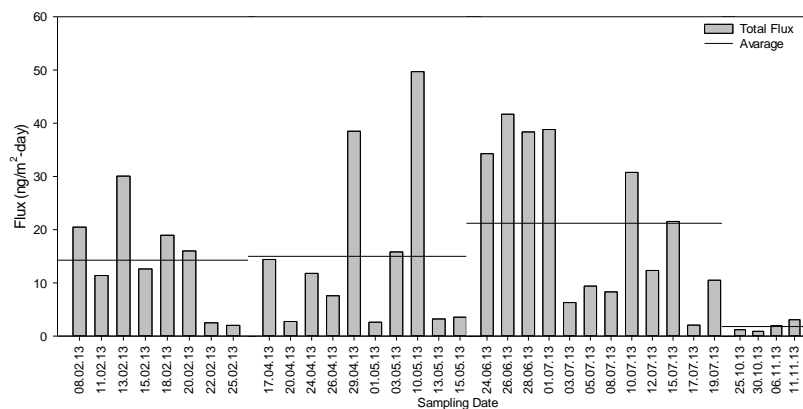


Figure 2. Time-Dependent Flux Variations

In a previous study, particle-phase PAHs were captured by placing a glass fiber filter (GFF) just before the XAD-2 resin column in the water surface sampler (Odabasi et al. 1999). In our study, dissolved phase fluxes and particle phases were sampled separately. We determined particulate phase PCBs by analyzing the filter in the MWSS, and the particulate PCB flux ratio was 10.92 % of the total. Even this ratio was smaller than that (15%) obtained by the HVAS, indicating that particulates were still entering the MWSS. This finding indicated that there are some uncertainties regarding the passive samplers which have been used PUF discs because of their higher air entrance.

Previous samplings by the MWSS in Bursa, Cindoruk, and Tasdemir (2007) reported that the ratio of the particle phase PCB flux to gas-phase PCB flux was 40%. In our sampling, we measured a ratio of particle-phase PCB flux to gas-phase PCB flux of 10.9 %. The main differences between the samplers were the cover and tubes. The previous MWSS had no cover and tubes, while our MWSS had cover and tubes. The results showed covering the sampler and pipes helped to keep the particle phase-out. In this study, MTCs were calculated to compare the two samplers. The previous MWSS had an average MTC of 0.6 ± 0.19 cm/s, and our MWSS had an average of only 0.12 ± 0.14 cm/s. Also, the flux values of the two samplers were compared. The previous MWSS and our MWSS had averages of 22.05±11.26 ng/day and 2.08±2.58 ng/day, respectively. These results indicated some differences in the collection properties of PCBs. When the top of the sampler was open and the air was transferred to water, dry deposition and gas-exchange were effective, especially when wind speeds were high. The wind effect and particulate entrance were minimized by covering the top of our sampler. The observed decrease in the MTC values, flux values and ratios of the particle phase showed that the cover had the desired effect.

The homolog group distribution is presented in Figure 3. When the homolog distributions were reviewed, it was determined that 2-, 3- and 4- CBs were 81.15% of the total flux. In the studies performed, the gas phase was the dominant phase, and the heavy congeners preferred to exist in the particle phase, which agreed with the previous results of measurements taken in the region (Cindoruk et al., 2008; Cindoruk et al., 2010).

3.3. Seasonal Changes

The seasonal changes of the PCB fluxes measured by the MWSS and the average temperature obtained in each season are shown in Figure 4. The derived fluxes increased when the average ambient temperatures rose. Interestingly, the values obtained in autumn were lower than those obtained in winter due to lower temperature. The regression coefficient between the seasonal average fluxes and the annual average temperatures was calculated as $r=0.99$. Such a high R-value indicated that atmospheric temperature was the predominant factor if there were no local PCB sources. No PCB source was available in the sampling region to the influence of the atmospheric concentrations. Therefore, the PCB fluxes were found to depend on the meteorological conditions, mainly atmospheric temperature.

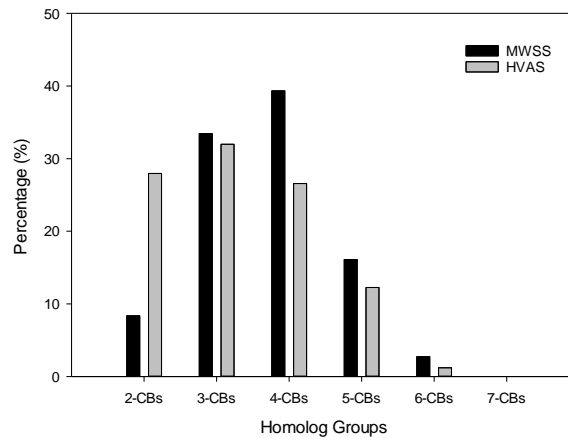


Figure 3. Homolog Group Distributions for the Fluxes and Ambient Air Concentrations

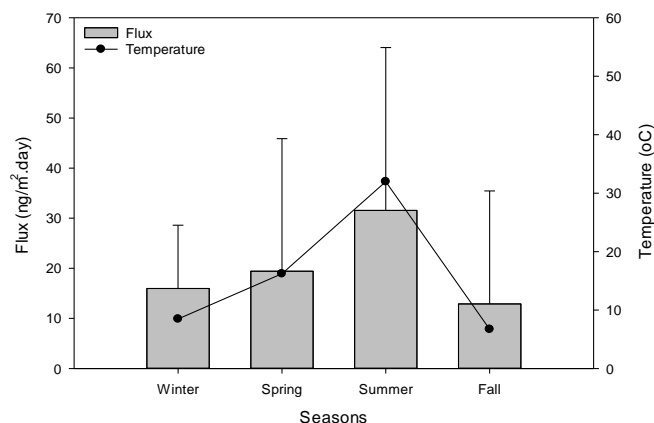


Figure 4. Seasonal Variation of the Flux Levels

3.4. Mass Transfer Coefficients

To calculate the mass transfer coefficients (MTCs), PCB flux measured directly using an MWSS, were divided by gas phase PCB concentrations, which were collected using an HVAS. Tasdemir et al. (Tasdemir et al., 2007) reported MTC values obtained with a modified water surface sampler (MWSS) as 0.60 ± 0.52 cm/s and 0.54 ± 0.47 cm/s. Our values were between 0.01 cm/s and 0.63 cm/s, and their average calculated as 0.13 ± 0.14 cm/s. These values were lower than the reported values. This difference could be related to minimizing the meteorological effects, especially wind speed, on the MWSS. When wind speed decreases, the air-water exchange rates also reduce. This reduction causes lower MTCs.

4. Conclusions

In this study, MWSS and HVASs were used simultaneously to collect atmospheric PCB samples. Average of the PCB concentrations measured with the HVAS was 346.53 ± 249.0 ng/m³. Gas-phase concentration was about 85% of the total and 2-, 3-, and 4- CBs were dominant species. Dissolved phase PCB fluxes were in the range of 0.54 ng/m²-day - 48.76 ng/m²-day, and particle-phase changed between 0.44 ng/m²-day - 2.25 ng/m²-day. Dissolved-phase mean flux was about 89% of the total flux including particulate and dissolved fluxes. 2-, 3- and 4- CBs were dominant homolog groups similar to the concentrations measured with HVAS. This result indicated that both samplers collect similar PCBs samples. A high correlation between the seasonal average fluxes and the seasonal average temperatures found. This result indicated that no PCB source was available in the sampling site and therefore, PCB concentrations were affected mainly by the atmospheric temperature. MTC values were calculated using the dissolved PCB fluxes and gas phase atmospheric PCB concentrations. The calculated mean MTC was 0.13 ± 0.14 cm/s and this was smaller than previously reported ones. This was probably due to the sampler design including cover and sticks on it.

5. References

- Chaemfa, C., J. L. Barber, et al. (2008): Field calibration of polyurethane foam (PUF) disk passive air samplers for PCBs and OC pesticides. *Environmental Pollution* 156(3): 1290-1297.
- Chaemfa, C., J. L. Barber, et al. (2009): Further studies on the uptake of persistent organic pollutants (POPs) by polyurethane foam disk passive air samplers. *Atmospheric Environment* 43(25): 3843-3849.
- Choi, S. D., S. Y. Baek, et al. (2008): Passive air sampling of polychlorinated biphenyls and organochlorine pesticides at the Korean Arctic and Antarctic research stations: Implications for long-range transport and local pollution. *Environmental Science & Technology* 42(19): 7125-7131.
- Cindoruk, S. S., F. Esen, et al. (2007): Concentration and gas/particle partitioning of polychlorinated biphenyls (PCBs) at an industrial site at Bursa, Turkey. *Atmospheric Research* 85(3-4): 338-350.
- Cindoruk, S. S. and Y. Tasdemir (2007): Characterization of gas/particle concentrations and partitioning of polychlorinated biphenyls (PCBs) measured in an urban site of Turkey. *Environmental Pollution* 148(1): 325-333.
- Cindoruk, S. S. and Y. Tasdemir (2010): Ambient Air Levels and Trends of Polychlorinated Biphenyls at Four Different Sites. *Archives of Environmental Contamination and Toxicology* 59(4): 542-554.
- Cotham, W. E. and T. F. Bidleman (1995): Polycyclic Aromatic-Hydrocarbons and Polychlorinated-Biphenyls in Air at an Urban and a Rural Site near Lake-Michigan. *Environmental Science & Technology* 29(11): 2782-2789.



- Esen, F., Y. Tasdemir, et al. (2010): Determination of mass transfer rates and deposition levels of polycyclic aromatic hydrocarbons (PAHs) using a modified water surface sampler. *Atmospheric Pollution Research* 1(3): 177-183.
- Gouin, T., T. Harner, et al. (2005): Passive and active air samplers as complementary methods for investigating persistent organic pollutants in the Great Lakes basin. *Environmental Science & Technology* 39(23): 9115-9122.
- Gouin, T., M. Shoeib, et al. (2008): Atmospheric concentrations of current-use pesticides across south-central Ontario using monthly-resolved passive air samplers. *Atmospheric Environment* 42(34): 8096-8104.
- Gunindi, M. and Y. Tasdemir (2010): Atmospheric polychlorinated biphenyl (PCB) inputs to a coastal city near the Marmara sea. *Marine Pollution Bulletin* 60(12): 2242-2250.
- Harner, T. and T. F. Bidleman (1997): Polychlorinated naphthalenes in urban air. *Atmospheric Environment* 31(23): 4009-4016.
- Harner, T., K. Pozo, et al. (2006): Global pilot study for persistent organic pollutants (POPs) using PUF disk passive air samplers. *Environmental Pollution* 144(2): 445-452.
- Harner, T., M. Shoeib, et al. (2004): Using passive air samplers to assess urban - Rural trends for persistent organic pollutants. 1. Polychlorinated biphenyls and organochlorine pesticides. *Environmental Science & Technology* 38(17): 4474-4483.
- IARC (1987): IARC MONOGRAPHS ON THE EVALUATION OF CARCINOGENIC RISKS TO HUMANS. Overall Evaluations of Carcinogenicity.
- Jaward, F. M., N. J. Farrar, et al. (2004): Passive air sampling of polycyclic aromatic hydrocarbons and polychlorinated naphthalenes across Europe. *Environmental Toxicology and Chemistry* 23(6): 1355-1364.
- Lauby-Secretan, B., D. Loomis, et al. (2013): Carcinogenicity of polychlorinated biphenyls and polybrominated biphenyls. *Lancet Oncology* 14(4): 287-288.
- Li, Q. L., Y. Xu, et al. (2012): Levels and spatial distribution of gaseous polychlorinated biphenyls and polychlorinated naphthalenes in the air over the northern South China Sea. *Atmospheric Environment* 56: 228-235.
- Li, Y. M., D. W. Geng, et al. (2012): Study of PCBs and PBDEs in King George Island, Antarctica, using PUF passive air sampling. *Atmospheric Environment* 51: 140-145.
- Motelay-Massei, A., T. Harner, et al. (2005): Using passive air samplers to assess urban-rural trends for persistent organic pollutants and polycyclic aromatic hydrocarbons. 2. Seasonal trends for PAHs, PCBs, and organochlorine pesticides. *Environmental Science & Technology* 39(15): 5763-5773.
- Odabasi, M. and H. O. Bagiroz (2002): Sulfate dry deposition fluxes and overall deposition velocities measured with a surrogate surface. *Science of the Total Environment* 297(1-3): 193-201.
- Odabasi, M., A. Sofuoglu, et al. (1999): Measurement of dry deposition and air-water exchange of polycyclic aromatic hydrocarbons with the water surface sampler. *Environmental Science & Technology* 33(3): 426-434.



- Persoon, C. and K. C. Hornbuckle (2009): Calculation of passive sampling rates from both native PCBs and deuration compounds in indoor and outdoor environments. *Chemosphere* 74(7): 917-923.
- Pozo, K., T. Harner, et al. (2004): Passive-sampler derived air concentrations of persistent organic pollutants on a north-south transect in Chile. *Environmental Science & Technology* 38(24): 6529-6537.
- Shahin, U. M., T. M. Holsen, et al. (2002): Dry deposition measured with a water surface sampler: a comparison to modeled results. *Atmospheric Environment* 36(20): 3267-3276.
- Tasdemir, Y. and F. Esen (2007): Dry deposition fluxes and deposition velocities of PAHs at an urban site in Turkey. *Atmospheric Environment* 41(6): 1288-1301.
- Tasdemir, Y. and F. Esen (2008): Deposition of polycyclic aromatic hydrocarbons (PAHs) and their mass transfer coefficients determined at a trafficked site. *Archives of Environmental Contamination and Toxicology* 55(2): 191-198.
- Tasdemir, Y. and H. Gunez (2006): Ambient concentration, dry deposition flux and overall deposition velocities of particulate sulfate measured at two sites. *Atmospheric Research* 81(3): 250-264.
- Tasdemir, Y. and H. Gunez (2006): Dry deposition of sulfur containing species to the water surface sampler at two sites. *Water Air and Soil Pollution* 175(1-4): 223-240.
- Tasdemir, Y. and T. M. Holsen (2005): Measurement of particle-phase dry polychlorinated biphenyls (PCBs) with deposition fluxes of a water surface sampler. *Atmospheric Environment* 39(10): 1845-1854.
- Tasdemir, Y. and T. M. Holsen (2006): Gas-phase deposition of polychlorinated biphenyls (PCBs) to a water surface sampler. *Journal of Environmental Science and Health Part a-Toxic/Hazardous Substances & Environmental Engineering* 41(10): 2071-2087.
- Tasdemir, Y., M. Odabasi, et al. (2005): Measurement of the vapor phase deposition of polychlorinated biphenyls (PCBs) using a water surface sampler. *Atmospheric Environment* 39(5): 885-897.
- Tasdemir, Y., M. Odabasi, et al. (2007): PCB mass transfer coefficients determined by application of a water surface sampler. *Chemosphere* 66(8): 1554-1560.
- Tasdemir, Y., M. Odabasi, et al. (2004): Dry deposition fluxes and velocities of polychlorinated biphenyls (PCBs) associated with particles. *Atmospheric Environment* 38(16): 2447-2456.
- Tasdemir, Y., M. Odabasi, et al. (1997): Development and evaluation of a water surface sampler to investigate the deposition of semivolatile organic compounds (SOCs). *Air Quality Management: At Urban, Regional and Global Scales*: 305-310.
- Tasdemir, Y., N. Vardar, et al. (2004): Concentrations and gas/particle partitioning of PCBs in Chicago. *Environmental Pollution* 131(1): 35-44.
- Vardar, N., Y. Tasdemir, et al. (2004): Characterization of atmospheric concentrations and partitioning of PAHs in the Chicago atmosphere. *Science of the Total Environment* 327(1-3): 163-174.
- Wania, F., L. Shen, et al. (2003): Development and calibration of a resin-based passive sampling system for monitoring persistent organic pollutants in the atmosphere. *Environmental Science & Technology* 37(7): 1352-1359.



18th World Clean Air Congress, 23-27 September 2019, Istanbul
organized by TUNCAP and IUAPPA

WHO (1993): Guidelines for Drinking-Water Quality - Second Edition - Volume 1 - Recommendations. World Health Organization Geneva 1993.

Zobrist, J., P. Wersin, et al. (1993): Dry Deposition Measurements Using Water as a Receptor - a Chemical Approach. *Water Air and Soil Pollution* 71(1-2): 111-130.

Dust and radon levels on the west coast of Namibia – what did we learn?

Hanlie Liebenberg-Enslin¹, Detlof von Oertzen² and Norwel Mwananawa³

¹ Airshed Planning Professionals (Pty) Ltd, PO Box 5260, Halfway House,

² VO Consulting, P.O. Box 8168, Swakopmund, Namibia,

³ Ministry of Mines and Energy, Private Bag 13297, Windhoek, Namibia

hanlie@airshed.co.za

detlof@voconsulting.net

Norwel.Mwananawa@mme.gov.na

Abstract. The study investigated the potential for adverse health impacts from exposures to inhalable atmospheric dust and radon concentrations in the main towns along Namibia's central-western coast. An ambient air quality monitoring network was established at the end of 2016 to measure and track the inhalable dust (specifically PM₁₀) and radon concentrations. Data collected between November 2016 and the end of December 2018 were assessed and some of the PM₁₀ samples were analysed for mineral and radionuclide content. In addition, emissions from man-made sources were quantified and simulated using a regional dispersion model. Episodic dust storms associated with easterly bergwinds are a common phenomenon during the winter months in the western part of Namibia. During such events, dust is transported over long distances westwards towards and well into the Atlantic Ocean. In view of the natural and man-made nature of atmospheric dust, the study differentiated between sources of natural dust and those arising as a result of man-made processes. It was found that PM₁₀ concentrations were, on average, higher at the coastal monitoring stations than at the stations located further inland, often exceeding the daily World Health Organisation (WHO) guideline value. Whilst high atmospheric dust concentrations were mostly associated with easterly bergwind conditions, sea salt was found to be a significant PM₁₀ contributor at the coastal stations. Modelled results, which only included emissions from man-made sources, indicated that these sources contribute very little to the total PM₁₀ concentrations measured at the coastal towns. The radiation exposure doses associated with the inhalation of atmospheric dust and radon concentrations were found to be well-below the world-wide average inhalation doses provided by the United Nations Scientific Committee on the Effects of Atomic Radiation (UNSCEAR).

Keywords: Inhalable particulate matter, Health impacts, Radiation exposure dose, Natural and man-made emissions, Air Quality Management, Namibia.

1. Introduction

The Erongo Region is located in the central western part of Namibia and is bounded by the Atlantic Ocean to the west and the escarpment to the east (approximately 180 km inland). The Region is drained in the central part by the deeply incised Swakop and Khan Rivers, with the Kuiseb River separating the stony desert from the Namib sand dunes in the south (Tyson and Seely, 1980).

The Region falls within the west coast arid zone of Southern Africa and is characterised by low rainfall with extreme temperature ranges and unique climatic factors influencing the natural environment and

biodiversity (Goudie, 2009). Easterly bergwinds occur when the leading edge of a coastal low¹ is associated with an offshore flow which leads to dynamic and adiabatic warming as air descends the escarpment. In winter, such bergwind conditions over Namibia bring strong easterly winds from the interior of the country when the Botswana anti-cyclone is positioned firmly over southern Africa. While associated with strong wind speeds and hot conditions, these winds are relatively short lived (Raison, 2017). Episodic dust storms associated with these bergwinds are a common phenomenon during the autumn and winter months. Associated dust is derived primarily from intermittent natural sources, giving rise to dust emissions only under conditions of high wind speeds. Anthropogenic sources of dust, such as unpaved roads and mining operations, continuously contribute to the atmospheric dust load in the Erongo Region.

High concentrations of particulates in the air pose a risk to human health and welfare. Various studies have found a link between increased morbidity and mortality, especially amongst children and the elderly, and dust storm events (Ginoux et al., 2004; Karanasiou et al., 2012; De Longueville et al., 2013). Modelled global fine particulate matter concentrations – specifically dust with an aerodynamic diameter of 2.5 µm – were found to cause premature mortality, resulting in a global per capita motility rate of 0.014% per year and an estimated 1.7% of the total cardiopulmonary and lung cancer deaths (Giannadaki et al., 2014).

In 2010, a Strategic Environmental Management Plan (SEMP) was developed for the Erongo Region and included a comprehensive air quality impact assessment where all sources contributing to air pollution in the region (i.e. mining operations, public roads, and natural exposed areas prone to wind erosion, as well as ambient atmospheric radon concentrations) were identified and quantified, with dispersion modelling conducted to determine the significance of their impacts (Liebenberg Enslin et al., 2010). As part of SEMF air quality update, the Namibian Ministry of Mines and Energy (MME) embarked on developing an overarching Air Quality Management Plan (AQMP) for the mines and industries within the Erongo Region. The Plan needed to set clear air quality objectives and strategies and implement an ambient monitoring network to measure particulate matter levels within the Region.

1.1. Monitoring Network

The baseline air quality characterization and radiation dose assessment needed to include recent and comprehensive data, focussing on particulate matter and radon. To achieve these objectives, an ambient monitoring network was established at the end of 2016, measuring fine particulate matter (PM)² and radon together with meteorological parameters. The aim of the monitoring network was to determine the current levels of PM and radon concentrations in locations where people reside. The ambient monitoring data was then used to identify the main contributing sources and to establish practicable ambient air quality guidelines.

Monitoring locations were chosen based on the most populated areas in the Region, i.e. the main towns, with the exception of Jakalswater which served as a background station. The towns included in the monitoring campaign included Swakopmund, Walvis Bay, Arandis and Henties Bay. The locations of the sites are shown in Figure 1, with the parameters recorded listed in Table 1.

¹ Coastal lows are shallow weather systems, with varying depth but will never extend to pressures lower than 850 hPa (1,524 m above sea level).

² Thoracic or inhalable particles – aerodynamic diameter of less than 10 µm, which is abbreviated PM₁₀, and respirable particles with an aerodynamic diameter of less than 2.5 µm, which is abbreviated PM_{2.5}.

Table 1. Monitoring stations and pollutants and parameters recorded

Monitoring Stations	PM ₁₀	PM _{2.5}	Wind Speed	Wind Direction	Temperature	Relative Humidity	Solar Radiation	Barometric Pressure	Rainfall	Radon
Swakopmund	X	X	X	X	X	X	X	X	X	X
Walvis Bay	X	X	X	X	X	X		X		X
Arandis	X		X	X	X	X	X	X	X	X
Henties Bay	X				X	X		X		
Jakalswater	X		X	X	X	X		X		

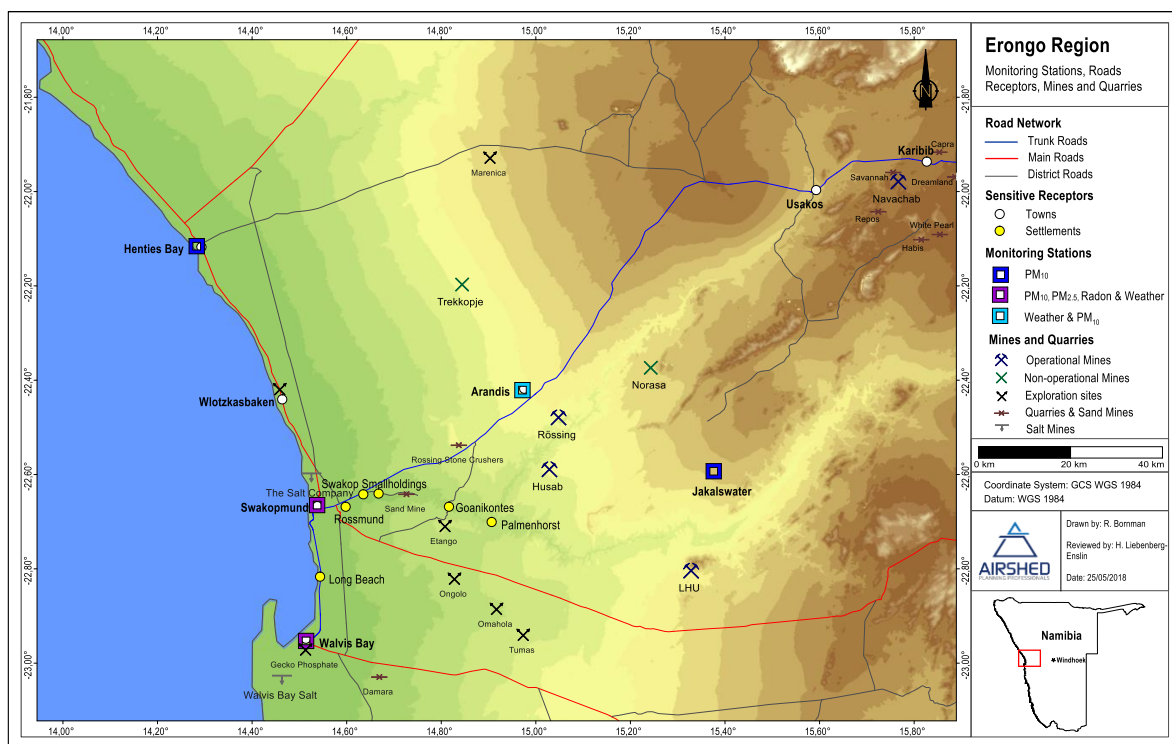


Figure 1. Ambient air quality monitoring stations, sensitive receptors, roads, mines and quarries

2. Status Quo of Air Quality in the Region

The baseline characterization included the assessment of ambient air quality data and dispersion modelling results. Whereas ambient monitoring data provides an indicator of the current state of the air at a given point, dispersion modelling was used to identify the main contributing sources in the region. For the dispersion modelling input, emission rates were quantified, and meteorological and topographical data processed.

2.1. Emissions Inventory

Sources of atmospheric pollution are either natural or man-made. Dust transported by strong winds is considered to originate naturally, where dust particles are lifted from exposed gravel plains and suspended under high-wind situations. Another natural source of particulates is the ocean, contributing both sea salts and organic matter. In addition, a wide range of man-made sources exist, including dust generated from vehicles travelling on roads (paved, treated and unpaved roads), vehicle exhaust

emissions, mining and mineral exploration operations (uranium, gold, stone quarries and sand mining), harbour emissions (ships, loading and unloading activities, use of mobile equipment and others), construction activities, fires, small boilers and incinerators.

All main man-made sources were quantified, i.e. all main public roads (paved, unpaved and salt/treated roads), the operational mines and quarries, and point sources (within the towns of Swakopmund and Walvis Bay, and at the mines in the Region). A number of sources, expected to be individually small contributors to the PM₁₀ and PM_{2.5} concentrations within the region, were identified but could not be accounted for due to insufficient information. Windblown dust emissions from the natural exposed surfaces and from mine sources (tailings storage facilities, waste rock dumps and stockpiles) were quantified.

Regional roads (paved, unpaved and salt/treated roads) were the main man-made contributing source to particulate emissions followed by mining and quarry operations. Particulate emissions from point sources were small contributors to the overall emissions. Windblown dust, although an intermittent source, resulted in the main emission source.

The contribution of all quantified source groups is illustrated in Figure 2, where reference to total suspended particulates is abbreviated TSP.

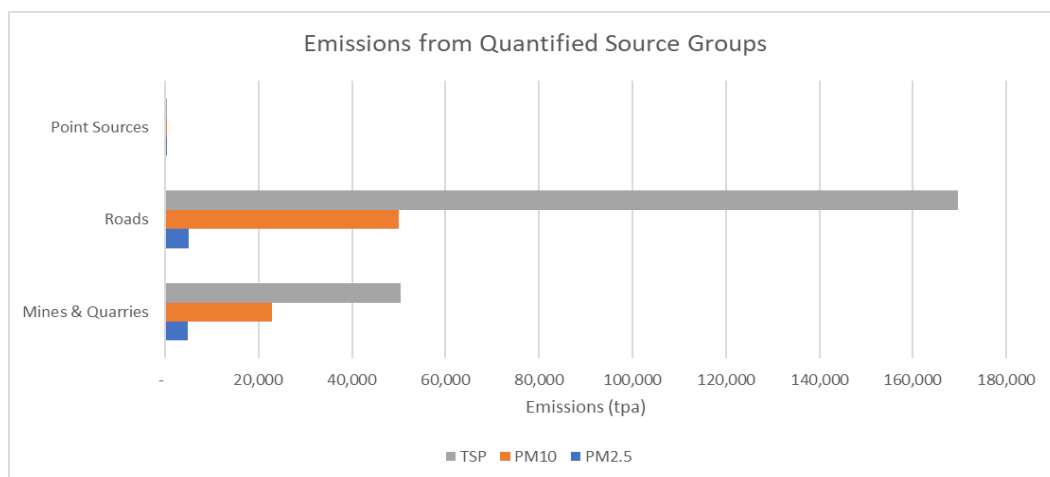


Figure 2. Main quantified source group contributions to particulate emissions in the Region, in tonnes per annum (tpa)

2.2. Measured Air Quality in the Region

Wind direction and wind speed determine the distribution and dilution of particulate matter and radon concentrations in the air.

Over the monitoring period of 26 months (i.e. from 1 November 2016 to 31 December 2018), the wind field varied significantly within the Region, with wind direction in the central part predominantly north-westerly and east-north-easterly and along the coast, north-westerly and south-westerly. On average, wind speeds were lower at the inland stations (Arandis and Jakalswater) compared to the coastal stations (Walvis Bay and Swakopmund). East-winds associated with bergwind conditions (taken when the wind direction was from the northeast to the southeast and when wind speeds exceeded 10 m/s) were observed between 0.4% of the time at Walvis Bay to 3% at Arandis. The monitored data indicated wind speeds to increase towards the coast under east-wind conditions, with wind speeds as high as 28 m/s recorded at the coast.

Measured PM₁₀ and PM_{2.5} concentrations at Swakopmund and Walvis Bay are shown in Figure 3, with PM₁₀ concentrations at Rössing Arandis Station and Jakalswater provided in Figure 4. In the absence of local air quality guidelines, reference was made to the World Health Organisation (WHO) Interim Target 3 (IT-3) (WHO, 2005) and the South African National Ambient Air Quality Standards (NAAQS) (South African Government Gazette, 2009).

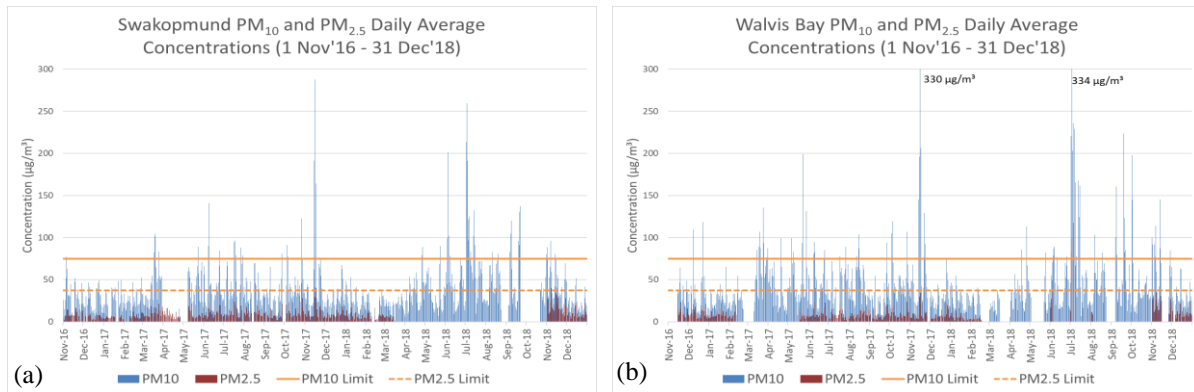


Figure 3. Daily average PM₁₀ and PM_{2.5} concentrations at (a) Swakopmund and (b) Walvis Bay for the period 1 November 2016 to 31 December 2018

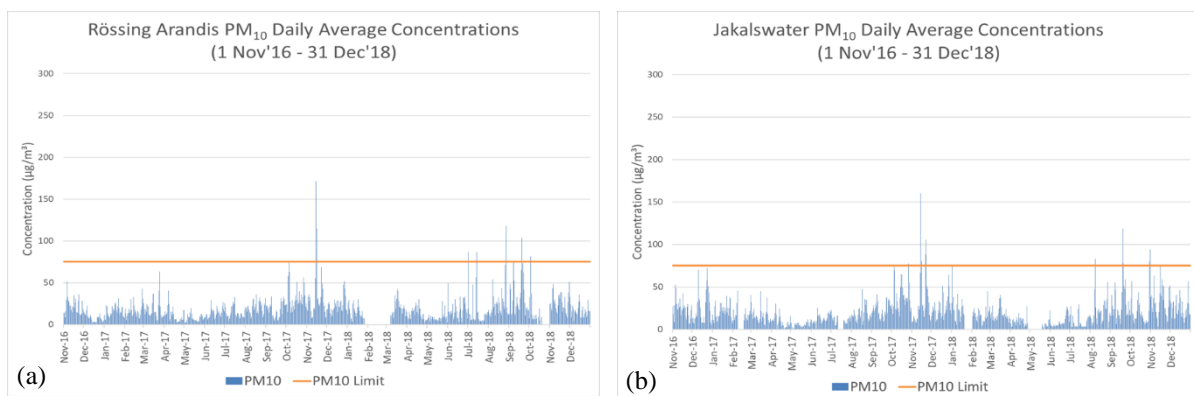


Figure 4. Daily average PM₁₀ concentrations at (a) Rössing Arandis Station and (b) Jakalswater for the period 1 November 2016 to 31 December 2018

The highest PM₁₀ concentrations recorded over the 26 months were during east-wind conditions and are reflected across all the stations, but with higher concentrations at Swakopmund and Walvis Bay. At Walvis Bay, high PM₁₀ concentrations were not only recorded when the wind was from the east-northeast, but also from the south-southwest due to the recirculation of PM₁₀ as a result of north-easterly/south-westerly wind conversion lines and cyclonic circulation associated with coastal troughs and coastal lows (Liebenberg-Enslin et al., 2017). Thus, the percentage contribution from east-wind conditions to high PM₁₀ concentrations at Walvis Bay is likely to be higher. At the inland stations Arandis (Rössing and Orano mines) and Jakalswater, the high PM₁₀ concentrations during east-wind were associated with lower wind speeds than at the coast.

The stations of Swakopmund and Walvis Bay also recorded high PM₁₀ concentrations outside of east-wind conditions, specifically when the wind was blowing from the southwest and west. At these two towns, there were clear contributions from the ocean (westerly sector) where the most likely source of PM₁₀ emissions are sea salts and organic matter. Formenti et al. (2018) reported the likelihood of sea salt dominating the PM_{2.5} measurements conducted in 2013 by the Henties Bay Aerosol Observatory

(HBAO). The contribution from sea salt was confirmed through chemical analyses; where the average sodium content in the PM₁₀ was 6.1% at Swakopmund and 4.5% at Walvis Bay. Henties Bay was the only station where no exceedances of the PM₁₀ limit were recorded and with the lowest period average concentration.

PM_{2.5} was only measured at Walvis Bay and Swakopmund for the period 1 November 2016 to 31 March 2018. Although the temporal variation in daily concentrations coincided with the PM₁₀ concentration trends (indicating similar source contributions), the PM_{2.5} concentrations were significantly lower and well below the interim concentration guideline. From the measured data over the 17-month period, PM_{2.5} does not seem to be a pollutant of concern at neither Swakopmund nor Walvis Bay.

2.3. Modelled Air Quality

Dispersion modelling was conducted to identify the main contributing sources to the measured PM₁₀ and PM_{2.5} concentrations. The model was run for a period between 1 November 2016 and 31 October 2018. The sources identified and quantified in the emissions inventory included: (i) regional roads (paved, unpaved and salt/treated); (ii) windblown dust from mine tailings storage facilities, waste rock dumps and stockpiles; (iii) mining and quarrying operations in the region; and (iv) point sources.

Windblown dust from exposed natural surfaces was quantified, but the model results were unrealistic in that it did not reflect a similar temporal variation as the emission rates i.e. emissions when wind speeds exceeded 10 m/s. The modelling concentrations also did not correlate with measured results, and these results were subsequently omitted from the dispersion modelling results.

The main contributing modelled source to PM₁₀ and PM_{2.5} emissions was vehicle entrainment from roads (paved, unpaved and salt/treated surfaces), followed by mining and quarry operations. The modelling results, where PM₁₀ concentrations were simulated at the various air quality sensitive receptors, indicated mining and quarrying operations to be the main contributing source to the central receptors of Arandis, Palmenhorst and Jakalswater, whereas the contribution from roads dominated at all other receptors. Simulated PM_{2.5} concentrations also indicated the main contribution to be from roads at most of the receptors, except for Arandis where the mining and quarry operations was the main contributing source group.

Not all sources could be accounted for in the dispersion model's emissions inventory and this was confirmed during the model validation. The model validation was based on comparisons between the modelled results and measured PM₁₀ concentrations at Jakalswater and Henties Bay. These two stations have the lowest uncertainty in terms of background sources (unaccounted sources). The model results show acceptable correlation with measured results at Jakalswater and Henties Bay even though the model generally under-predicted atmospheric PM concentrations. Estimated short-term (hourly or daily) background concentrations (not associated with the emissions included in the simulations) ranged from fairly insignificant levels of 6 µg/m³ and 8 µg/m³ at Jakalswater and Swakopmund, to significant levels of 17 µg/m³ and 29 µg/m³ at Henties Bay and Walvis Bay.

3. Public Radiation Dose

3.1. Ambient Radon Concentrations in Air

The annual average public exposure dose contributions from the inhalation of radon and its decay products, based on the long-term average radon concentrations determined as part of the study, amount to 0.1 mSv/a at Walvis Bay, 0.2 mSv/a at Swakopmund, and 0.4 mSv/a at the monitoring location in-between Arandis and Rössing.

The above-mentioned public exposure doses are far smaller than the world-wide average public exposures due to radon – i.e. 1.095 mSv/a – as suggested by UNSCEAR (2000). The findings confirm a well-known phenomenon that characterizes the average outdoor radon concentrations in most of the southern hemisphere. They are (amongst others) the result of higher average ambient temperatures in the southern hemisphere, a more effective mixing of radon in ambient air due to more substantial thermal forces in the atmosphere, and the height above ground level of the monitoring stations employed in the study.

3.2. Ambient Radioactive Dust in Air

Three batches of PM₁₀ dust samples were collected (some 60-day monitoring periods per batch) at the project's meteorological stations at Swakopmund, Walvis Bay, Henties Bay and Jakalswater between Apr/May and June 2018 (batch #1), between June and August 2018 (batch #2), and between August/September and October 2018. These were subjected to alpha spectrometric analyses at an accredited German laboratory (IAF Radioökologie GmbH, Radeberg), based on measurement uncertainties and decision thresholds as per the International Organization for Standardization (ISO 11929).

On assessment of the results of the radionuclide analyses it was decided that the results of sample batch #1 would not be further considered as the measured radionuclide activities indicated that the samples had likely been contaminated. In contrast, the second and third sample batches all exhibited radionuclide concentrations below the radionuclide-specific limit of detection of the alpha spectrometric analyses. This result provides a valuable upper limit for the radioactive atmospheric dust concentrations at the monitoring locations.

Assuming that the actual alpha activity per 60-day sample amounts to 2 mBqα per main radionuclide in the uranium decay series, the upper limit for the adult (infant) inhalation exposure dose amounts to 0.003 mSv/a (0.002 mSv/a). These doses are slightly below the inhalation dose due to atmospheric dust as provided by UNSCEAR (0.0058 mSv/a for adults and 0.005 mSv/a for infants) (UNSCEAR, 2000).

The findings provide further evidence that the exposure dose due to the inhalation of radioactive dust in ambient air in the main population centres in the Erongo Region does not constitute a public health risk, also noting that the contribution of this inhalation dose to the total public dose due to natural background radiation in the Erongo Region is very small indeed, and therefore insignificant.

4. Conclusions

4.1. Ambient Air Quality in the Region

Measured PM₁₀ concentrations over the 26 months at the four SEMP stations (Swakopmund, Walvis Bay, Henties Bay and Jakalswater) and two mining stations (the Rössing and Orano stations at Arandis) indicated elevated PM₁₀ concentrations at all the stations except at Henties Bay. PM_{2.5} concentrations were significantly lower and well below the interim concentration guideline, but showed similar temporal trends than PM₁₀ concentrations, thus confirming that the same sources contribute to the ambient atmospheric PM₁₀ and PM_{2.5} concentrations.

Modelled results indicated that vehicle entrainment from roads (paved, unpaved and salt/treated surfaces), followed by mining and quarry operations to be the main contributing sources of PM₁₀ and PM_{2.5} emissions, but the modelled impacts at the coastal receptors were very low. Here, monitored data and chemical analysis of the PM samples indicated natural windblown dust and sea salt to be the main contributing sources.

The measured and modelled results were used to recommend PM guidelines for the Erongo Region, with specific reference to the international WHO Interim Targets and the SA NAAQS. It can be argued that the contributions from natural sources, such as mineral windblown dust during east-wind conditions and from sea salts, should be excluded from air quality guidelines, as these sources cannot be controlled, and sea salt does not pose a health risk. Also, the contribution from man-made sources under east-wind conditions were found to be small when compared to natural PM concentrations in the air. It was therefore recommended to adopt the SA NAAQS limit for PM₁₀ and the WHO Interim Target 3 for PM_{2.5}, but with more allowable exceedance days due to east-wind conditions and the presence of sea salt.

4.2. Atmospheric Pathway Contribution to the Total Public Radiation Dose in the Erongo Region

The radiation-related public exposure doses due to the inhalation of radon, radon progeny and radioactive dust were quantified using real-time empirical results for ambient atmospheric radon concentrations, and radionuclide concentrations from selected PM₁₀ samples.

The atmospheric radon concentrations determined at Walvis Bay, in-between Arandis and Rössing, and at Swakopmund imply site-specific annual average public exposure doses of 0.1 mSv/a, 0.4 mSv/a and 0.2 mSv/a, respectively. These results, which are solely based on the data acquired as part of this study, imply a regional population-weighted exposure dose of less than 0.2 mSv/a due to radon. The regional population-weighted adult (infant) exposure dose due to the inhalation of ambient radioactive dust is below 0.003 mSv/a (0.002 mSv/a).

The contributions of both radon and ambient radioactive dust to the public exposure dose in the Erongo Region are below the world-wide average doses suggested by UNSCEAR and other international bodies (UNSCEAR, 2000).

The monitoring efforts undertaken as part of the study focused on the main population centres in the Erongo Region. This implies that the contributions of individual sources of radioactive atmospheric dust, for example those originating at the mines operating in the Erongo Region, could not be quantified to any degree of confidence, as these are best monitored in the immediate vicinity of such operational sites.

5. Recommendations

Mitigation and management of man-made sources in the Erongo Region should include Dust Management Plans that are to be established by all operational mines and quarries, with dust suppression to be applied at all mining, mineral exploration, milling and construction operations. These plans and mitigation measures should be reported annually to the authorities.

Further analysis of PM₁₀ dust samples are required to better quantify the actual contributions from sea salt and natural mineral dust to the measured concentrations in ambient air.

Monitoring will continue at all locations. Data will be regularly reported on a website which is accessible to the public.

6. References

De Longueville, F., Ozer, P., Doumbia, S. and Henry, S., 2013. Desert dust impacts on human health: an alarming worldwide reality and a need for studies in West Africa. *International Journal of Biometeorology*, 57, 1-19.



- Formenti, P., Pickett, S. J., Namwoonde, A., Klopper, D., Burger, R., Cazaunau, M., and Feron, A. (2018). Three years of measurements of light-absorbing aerosols over coastal Namibia: seasonality, origin, and transport. *Atmospheric Chemistry and Physics*, 17003-17016.
- Giannadaki, D., Pozzer, A. and Lelieveld, J., 2014. Modeled global effects of airborne desert dust on air quality and premature mortality. *Atmospheric Chemistry and Physics*, 14, 957-968.
- Ginoux, P., Prospero, J. M., Torres, O. and Chin, M., 2004. Long term simulation of global dust distribution with the GOCART model: correlation with North Atlantic Oscillation. *Environmental Modelling and Software*, 19, 113-128.
- Goudie, A. S., 2009. Dust storms: Recent developments. *Journal of Environmental Management*, 90, 89-94.
- Karanasiou, A., Moreno, N., Moreno, T., Viana, M., de Leeuw, F., Querol, X., 2012. Health effects from Sahara dust episodes in Europe: literature review and research gaps. *Environment International*, 15, 107-114.
- Liebenberg Enslin, H., Krause, N. and Breitenbach, N., (2010). Strategic Environmental Assessment for the Central Namib Uranium Rush Air Quality Specialist Report. Report APP/09/MME 02 Rev0 to the Ministry of Mines and Energy, Namibia.
- Raison, 2017. <http://www.raison.com.na>, accessed in September 2017.
- South African Government Gazette No. 32186, 2009. National Ambient Air Quality Standards. Pretoria: Department of Environmental Affairs and Tourism, Notice 12105
- Tyson, P.D., and Seely, M.K., 1980: Local winds over the Central Namib. *The South African Geographical Journal*, Vol. 62, No. 2, September 1980.
- United Nations Scientific Committee on the Effects of Atomic Radiation (UNSCEAR), (2000). Report of the United Nations Scientific Committee on the Effects of Atomic Radiation to the General Assembly.
- World Health Organization (WHO), (2005). WHO air quality guidelines global update 2005: Report on a Working Group meeting, 18-20 October. Bonn, Germany: World Health Organisation.

Acknowledgements

The authors acknowledge the Ministry of Mines and Energy, Geological Survey of Namibia and Federal Institute for Geosciences and Natural Resources for making the data available for use in this study.



Modeling of greenhouse gas emissions from the transportation sector in Istanbul

Tugba Dogan Guzel^{1,2} and Kadir Alp²

¹TUBITAK Marmara Research Center, Environment and Cleaner Production Institute, Gebze/Kocaeli

²Istanbul Technical University, Department of Environmental Engineering, Maslak/Istanbul

tugba.dogan@tubitak.gov.tr

Abstract. Climate change has become increasingly popular in recent years. In this context, important steps are also taken in international negotiations. Paris Agreement, which aims to limit greenhouse gas emissions and maintain the increase in the global average temperature below 2°C, entered into force in November 2016. The countries that have ratified the agreement should declare their contribution to reducing greenhouse gas emissions. Within this context, one of the most important components contributing to global greenhouse gas emissions is the transportation sector. The greenhouse gas emission from the transportation sector is 84.7 Mton CO₂eq., which accounts for 16% of the total greenhouse gas emissions throughout Turkey in 2017. With a rate of 93%, road transportation corresponds to the biggest share of greenhouse gas emissions from the transportation sector. In this study, greenhouse gas emissions were modeled from 2016 through 2055, in order to assess the impacts of the transportation sector on climate change in Istanbul, which is the most crowded city and has the highest number of vehicles in Turkey. For this purpose, the TIMES Model (The Integrated MARKAL-EFOM System) as a technology-rich and economic model was used. The transportation sector was considered in four subcategories as road transportation, railways, domestic aviation, and water-borne navigation. The results of the study were obtained for the reference scenario, which assumes that the existing plans and policies will continue. Furthermore, three alternative scenarios which are related to electric rail transportation, electric and hybrid cars and limiting CO₂ emissions.

Keywords: Climate change, Emission, Greenhouse gas, Transportation, TIMES model

1. Introduction

Climate change is one of the most important problems on a global scale in recent years. Due to the rapid increase in greenhouse gas emissions including carbon dioxide (CO₂), methane (CH₄) and dinitrogen monoxide (N₂O), which are released into atmosphere as a result of human activities such as industrialization, fossil fuel consumption, agricultural activities and energy production, a significant rise in the average temperature of the earth's surface has been observed. According to data of 2018 obtained from NASA (National Aeronautics and Space Administration), the average global temperature on Earth has increased by about 0.8°C since 1880 (NASA, 2018). In this respect, the Paris Agreement, which aims to limit greenhouse gas emissions and maintain the increase in the global average temperature below 2°C, entered into force in November 2016. The countries that have ratified the agreement should declare their contribution to reducing greenhouse gas emissions. Within this context, one of the most important components contributing to global greenhouse gas emissions is the transportation sector.

The transportation sector has an important share in terms of total energy demand and it is responsible for 25.5% of the total primary energy consumption in Turkey and road transport is the main reason of

consumption (GDEA, 2017). The number of motor vehicles in traffic is approximately 22 million and 4 million (18.3%) of this value is the number of vehicles in Istanbul which is the most populous city with the highest traffic density (TurkStat, 2018a). **Figure** shows the change in the number of motor vehicles in Istanbul (TurkStat, 2019b).

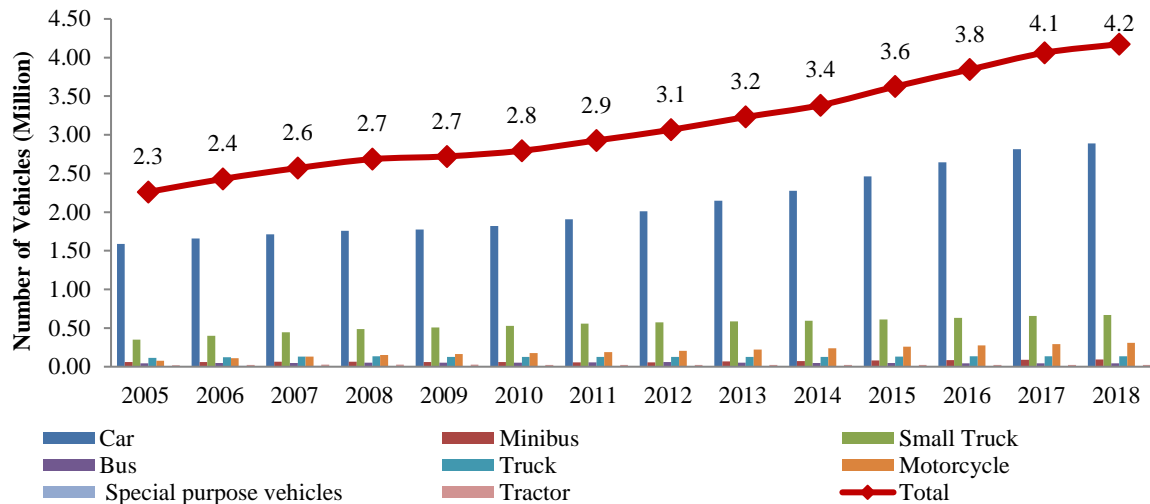


Figure 1. The number of vehicles in Istanbul

According to 2005 data, Istanbul population increased by 24%, while the total number of motor vehicles increased by 85%. In other words, approximately 185 motor vehicles fell to a thousand people in 2005, while this value increased to 277 in 2018 (TurkStat, 2018a; TurkStat, 2018b). Therefore, there has been a significant increase in greenhouse gas emissions from the transportation sector over the years (Figure 2).

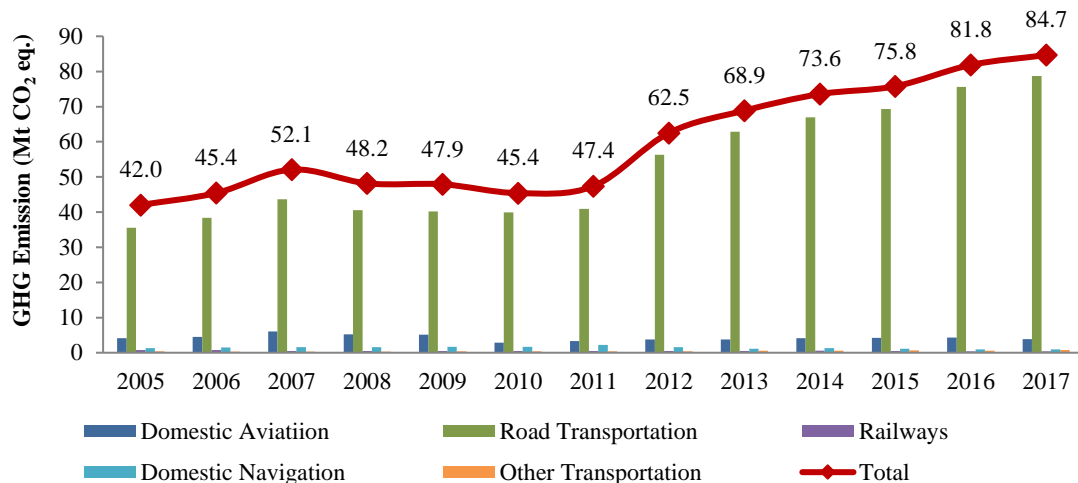


Figure 2. The GHG emission trend

The greenhouse gas emission from the transportation sector is 84.7 Mton CO₂eq, which accounts for 16% of the total greenhouse gas emissions throughout Turkey in 2017. With a rate of 93%, road transport corresponds to the biggest share of greenhouse gas emissions from the transportation sector. This value is followed by domestic aviation (4.5%), domestic water-borne navigation (1.1%) and railways (0.5%) in 2017. In 2017, total greenhouse gas emissions increased more than twice as compared to 2005 (NIR, 2019).

To summarize, the transportation sector is one of the key sectors that contribute to climate change. This study aims to model the greenhouse gas emissions for the period of 2016-2055, in order to assess the impacts of the transportation sector on climate change in Istanbul, which is the most crowded city and has the highest number of vehicles in Turkey. For this purpose, the TIMES Model was used as a technology-rich and economic model.

2. Methodology

2.1. TIMES Model

The TIMES (The Integrated MARKAL-EFOM System) model is an economic model that provides a technology-rich basis for analyzing dynamics in a local, national or multi-region energy system on a long term horizon. The model is generally applied for the analysis of the entire energy sector, but it can also be applied for a detailed examination of a single sector (Loulou et al., 2005). There are various studies on transportation sector using TIMES Model. In a study conducted for the Scandinavian transport sector, the role of transport modal shift for decarbonization in both freight and passenger transport was evaluated using the TIMES Model (Salvucci et al., 2019). In another study, carbon tax scenarios have been established with the TIMES Model to further analyze the transportation sector and provide transportation development paths for the US and Chinese energy system (Zhang et al., 2016).

Data such as end-use energy service demands, existing capacity, features of available future technologies are entered into the model by the user. The model aims to meet demand with a minimum global cost. One of the most important output is environmental emissions and the model is also suitable for the analysis of energy environmental policies (ETSAP, 2019).

2.2. Model structure for the transportation sector

In this study, 2016 was selected as a base year and TIMES Model was developed from 2016 to 2055 with the interval of the five-year period (2016, 2020, 2025...2055) for the transportation sector in Istanbul. The brief model structure is shown in Figure 3. The transportation sector was considered in four subcategories as road transportation, railways, aviation, and water-borne navigation. Fuels which are gasoline, diesel, LPG, CNG, jet fuel, fuel oil and electricity are energy carriers used by several demand technologies such as bus, car, airplane, and ship.

2.3. Demand projections and data input

All demand projections (Table 1) in the model are defined in the PJ unit. The data used in the model were compiled from the statistical data published by Turkish Statistical Institute (TurkStat), Istanbul Metropolitan Municipality, Ministry of Transport and Infrastructure, General Directorate of Energy Affairs, as well as reports and academic studies published on the internet. TurkStat data, National Greenhouse Gas Emission Inventory Report (NIR), Energy Balance Tables and Common Reporting Format (CRF) tables made significant contributions to the calculations. Some of the emission factors entered in the model are IPCC values and some of them are calculated from the results obtained from the studies conducted in our country. Energy extraction, energy conversion, and import technologies were also considered in the model, but emission factors are defined only for demand technologies. Therefore, the model does not include emissions from extraction and conversion processes. For demand processes, technology life, efficiency, investment cost, fixed operation and maintenance cost, residual capacity data included in the model. EPA technology data were used if country-specific data were not available.

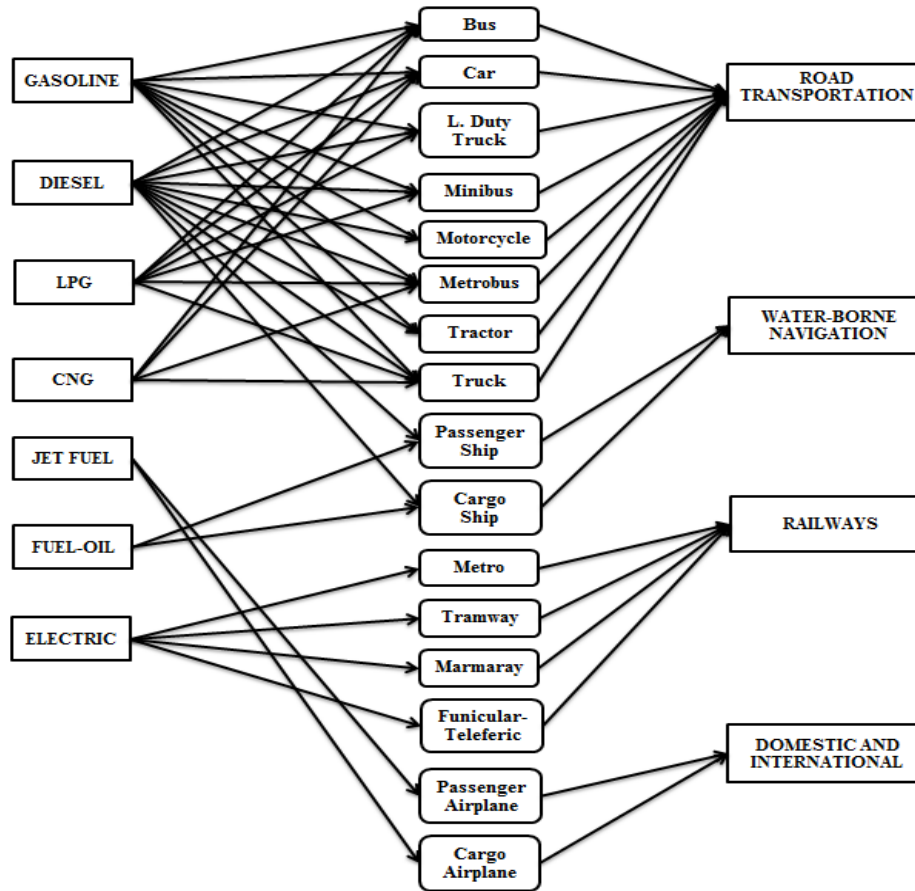


Figure 3. Brief structure of the transportation sector

Table 1. Demand service projections (PJ)

Transport Mode	2016	2020	2025	2030	2035	2040	2045	2050	2055
Domestic Aviation	31.6	27.6	29.4	30.9	32.2	33.2	34.1	34.7	35.2
International Aviation	110.4	111.0	118.3	124.3	129.4	133.6	136.9	139.5	141.3
Road Transportation	205.4	245.9	296.2	351.8	414.1	483.4	560.1	645.0	739.0
Railways	1.1	1.3	1.6	2.1	2.6	3.4	4.3	5.4	6.9
Water-Borne Navigation	6.4	6.5	6.8	7.2	7.5	7.9	8.3	8.7	9.2

2.4. Base year calibration

Calibration is performed in order to ensure that the model results are consistent with the statistical data for the base year and it is important to increase the reliability of the model. The statistical data obtained for the country total were taken into account in the model considering the ratio of data such as Istanbul population and number of vehicles to the country overall. For example; Since 22% of diesel vehicles are located in Istanbul, it is assumed that 22% of total diesel consumption is consumed in Istanbul.

2.5. Scenarios

In addition to the reference scenario, three alternative scenarios were run to analyze the change in greenhouse gas emissions:

- **Base/Reference Scenario (Base):** The reference scenario is the scenario in which current plans and policies are maintained, emission reduction measures are not taken, and the current subcategory demand rates continue in the future.
- **Scenario 1 (S1):** After 2016, all the electric railway transportation that has been made and planned to be made is included in the model. Moreover, with the increase in rail transport, the use of personal automobiles and motorcycles, buses and minibusses has been reduced.
- **Scenario 2 (S2):** Electric and hybrid vehicle technologies are included in the model for automobile demand, which contributes significantly to greenhouse gas emissions. The ratio of electric and hybrid vehicles in the total number of automobiles was taken as 3%, 8%, 24%, 43% and 54% for the years 2020, 2025, 2030, 2035 and 2040 respectively (TEHVA,2019). It has been accepted that it will continue at the same rate in the remaining years. Furthermore, it is assumed that the number of electric and hybrid vehicles is equal for each period and replaces diesel vehicles.
- **Scenario (S3):** Carbon dioxide emission, which constitutes almost all of the greenhouse gas emissions originating from the sector, was modeled by bringing the upper limit to years. Thus, it was determined which technology the model would turn to in order not to exceed the maximum emission.

Data used in scenario calculations are given in Table 2.

Table 2. Data used in scenarios

Scenario Assumptions	2016	2020	2025	2030	2035	2040	2045	2050	2055
Railway Length (km)	244	487	766	982	982	982	982	982	982
Ratio of Electric and Hybrid Cars (%)	-	3	8	24	43	54	54	54	54
CO ₂ Upper Limit (Mt)	25	25	30	40	40	40	50	50	50

3. Results and discussion

3.1. Fuel Consumption

The results of the study were obtained for the reference scenario, which assumes that the existing plans and policies will continue. Besides, the results were analyzed for 3 more scenarios with detailed information in section 3. Figure 4 shows fuel consumption results based on scenarios and transport mode. It can be clearly seen that the sub-sector with the highest fuel consumption is road transport. The share of railways and water-borne navigation in fuel consumption is very low. On the other hand, in scenario 3, which limits the emission of carbon dioxide, fuel consumption increased significantly compared to the reference scenario. Fuel consumption of scenario 3 is about 59% higher than the reference scenario. Since, in order to remain below the maximum CO₂ emission limit set for these years (50,000 kt CO₂), the model opted for road technologies that consume low-emission LPG fuel and reduced aircraft use. In addition, total fuel consumption decreased by 12.8% in scenario 2 and 4.7% in scenario 3 in 2055. According to the model results, the most advantageous scenarios was determined as scenario 1 based on railway transportation and scenario 2 with electric and hybrid car in use.

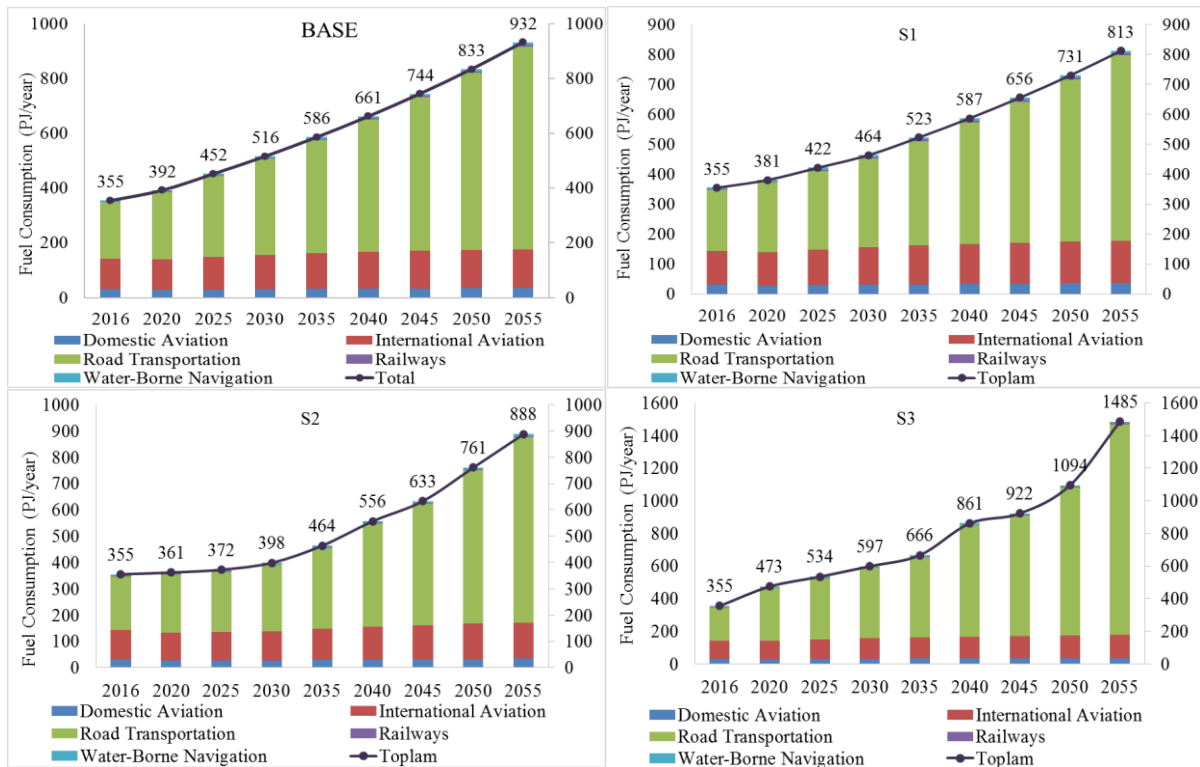


Figure 4. Fuel consumption of transport modes

Figure 5 shows the total fuel consumption trends of the scenarios. Public transportation vehicles such as Metro and Tramway have high capacity and can meet demand with lower cost and consumption. Thus, with the expansion of the railway network, total fuel consumption will decrease. In terms of fuel consumption, the use of electric and hybrid vehicles until 2040, and the use of rail systems in the following years, seems attractive. In fact, the main reason for this situation is the assumption that the ratio of the number of electric and hybrid vehicles within the total number of vehicles remains constant after 2040.

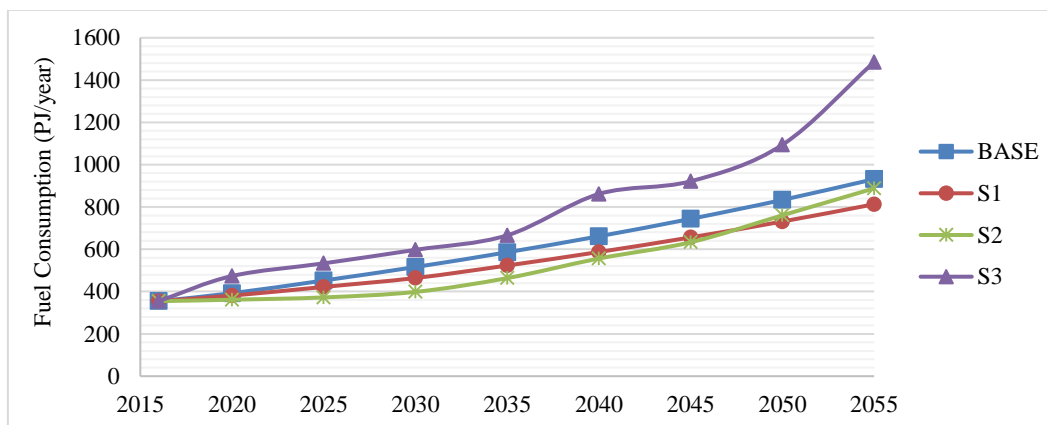


Figure 5. Total fuel consumption trends of scenarios

3.2. Greenhouse gas emissions

The model results refer only to emissions from combustion of fuels in vehicles. In the calculations, global warming potential is taken as 25 for CH₄ and 298 for N₂O (IPCC, 2007) and detailed emission outputs are given in Table 3. The share of CO₂ emissions in the total emissions is 98.8%. The emission

outputs of the scenarios including the technology details are given in Figure 6. Emissions are illustrated by including CH₄ and N₂O emissions in CO₂ equivalent.

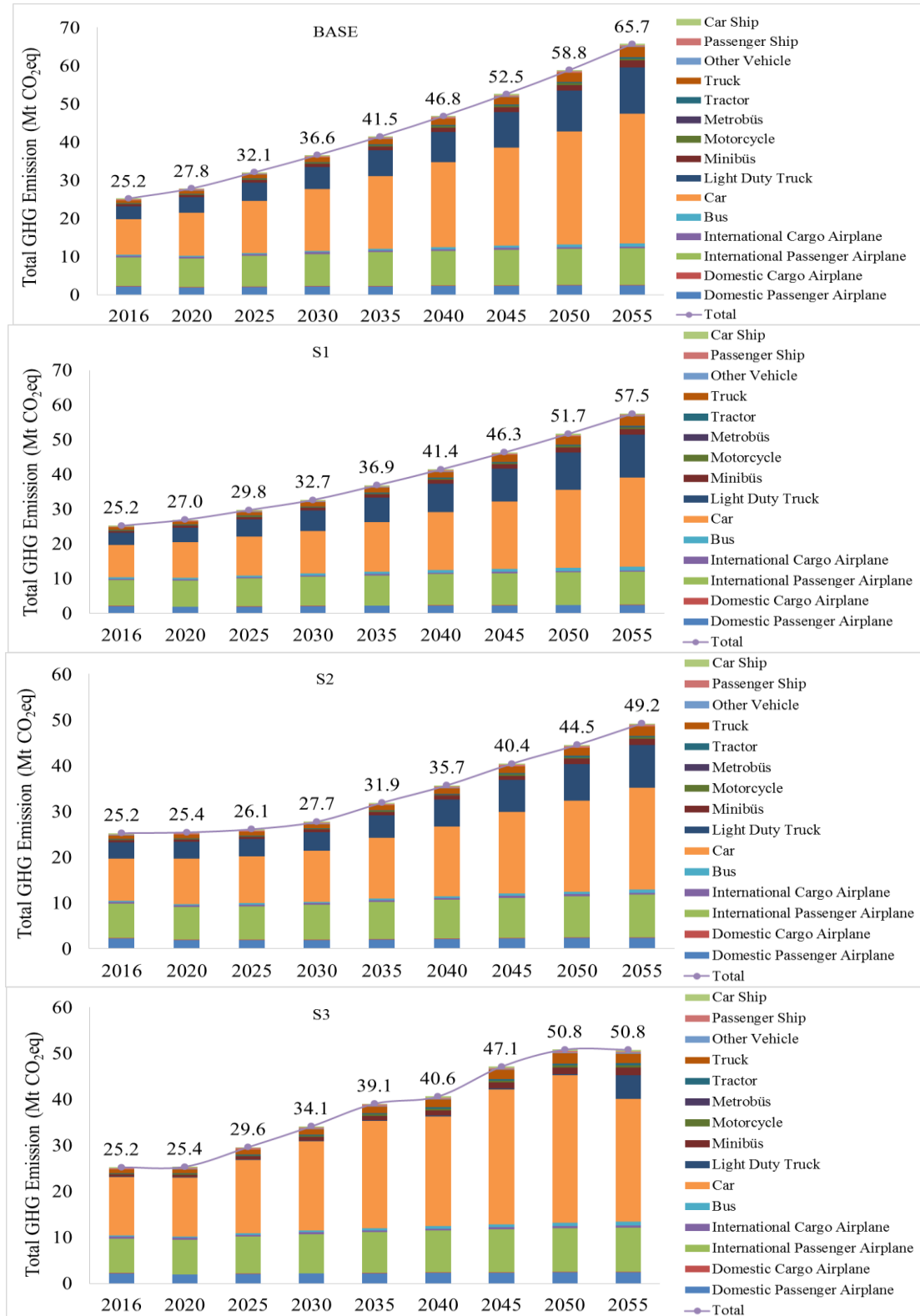


Figure 6. GHG emissions of technologies

The largest share of emissions is caused by automobiles. 58% (including international aviation) of the current emissions are caused by road transport. Domestic and international aviation also plays an important role in greenhouse gas emissions. As the amount of greenhouse gas emissions from rail transport is zero, there is no breakdown of railway vehicles in the graphs.

Table 3. GHG emission details (kt)

Secenario	2016	2020	2025	2030	2035	2040	2045	2050	2055	
Base	CH ₄	1.04	1.20	1.43	1.68	1.97	2.28	2.62	3.00	3.42
	N ₂ O	0.92	1.02	1.19	1.37	1.57	1.78	2.01	2.27	2.55
	CO ₂	24942	27486	31670	36109	40945	46188	51883	58074	64842
S1	CH ₄	1.04	1.19	1.38	1.59	1.85	2.14	2.46	2.82	3.21
	N ₂ O	0.92	1.01	1.15	1.30	1.48	1.68	1.90	2.14	2.41
	CO ₂	24942	26632	29379	32230	36379	40858	45707	50961	56694
S2	CH ₄	1.04	1.10	1.15	1.25	1.52	1.94	2.27	2.88	3.49
	N ₂ O	0.92	0.99	1.03	1.14	1.43	2.20	2.54	3.81	4.97
	CO ₂	24942	25078	25741	27362	31399	34976	39611	43308	47659
S3	CH ₄	1.04	2.23	2.47	2.72	3.00	4.82	4.90	6.33	15.71
	N ₂ O	0.92	1.02	1.19	1.37	1.57	1.77	2.01	2.26	1.36
	CO ₂	24942	25000	29198	33652	38537	40000	46413	50000	50000

Figure 7 shows the total GHG emissions trends of the scenarios. In contrast to fuel consumption, the lowest greenhouse gas emissions occurred in scenario 2. By using electric and hybrid vehicles instead of diesel vehicles, greenhouse gas emission savings will be 18.7% in 2025 and 25.1% in 2055. Moreover, with the increase in rail transport, emissions decreased by 7.2% in 2025 and 12.5% in 2055. In Scenario 3, the upper limits were already set and which technology the model would turn to without exceeding these limits was determined. It is concluded that scenario 2 is more advantageous in terms of greenhouse gas emissions.

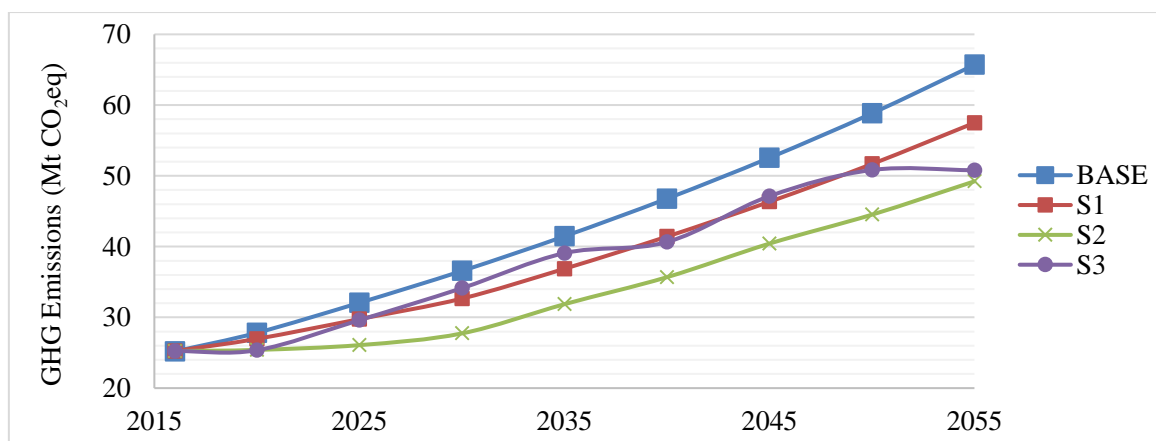


Figure 7. Total GHG emission trends of scenarios



4. Conclusion

Reducing greenhouse gas emissions from the transport sector is crucial to limiting global warming that causes climate change. In this study, the transportation sector for Istanbul has been examined and it has been investigated whether different scenarios affect greenhouse gas emission reduction. In particular, the effects of the increase in the rail transportation network and the widespread use of electric and hybrid vehicles, which have become current issues in the transportation sector in recent years, have been analyzed.

It is considered that there will be important reductions in greenhouse gas emissions if electric and hybrid vehicles continue to increase instead of diesel cars.

In terms of passenger capacity, rail systems provide a great advantage over motor vehicles. As a result of the expansion of the electric rail system vehicles, emission rates have been reduced by 12.5%. However, if individual vehicle users change their preferences in the direction of using public transport, higher greenhouse gas reduction results can be achieved with the same railway length.

Fuel consumption of scenario 3 is about 59% higher than the reference scenario. When the emission limitation was imposed on the model, there was a tendency towards vehicles with high amounts of LPG to keep the emission at the desired level. The use of LPG fuel, which has a lower emission factor than gasoline and diesel fuel, has increased and the necessity of reducing the use of aircraft has emerged. To summarize, both electric and hybrid vehicle use and the transition to rail mass transportation systems can be effective in reducing greenhouse gas emissions. Also, it is considered important to replace all transportation vehicles with efficient technologies and to switch to environmentally friendly fuels for more emission reduction.

5. References

- ETSAP (Energy Technology Systems Analysis Programme), 2019. <https://iea-etsap.org/index.php/etsap-tools/model-generators/times>, accessed in 2019.
- GDEA (General Directorate of Energy Affairs), 2017. <https://www.eigm.gov.tr/tr-TR/Denge-Tablolari/Denge-Tablolari>, accessed in 2019.
- IPCC (Intergovernmental Panel on Climate Change), 2007. *Climate Change 2007: The Physical Science Basis- Working Group I Contribution to the Fourth Assessment Report of the Intergovernmental Panel on Climate Change*, Cambridge, United Kingdom and New York, NY, USA, 996 pages
- Loulou, R., Remne, U., Kanudia, A., Lehtila, A., Goldstein, G., 2005. *Documentation for the TIMES Model-PART I*, 78 pages.
- NASA (The National Aeronautics and Space Administration), 2018. <https://climate.nasa.gov/vital-signs/global-temperature/>, accessed in 2019.
- NIR (National Inventory Report), 2019. *Turkish Greenhouse Gas Inventory 1990-1017*, EEA Technical Report No. 9/2009, Ankara, 567 pages.
- Salvucci, R., Gargiulo, M., Karlsson, K., 2019. The role of modal shift in decarbonizing the Scandinavian transport sector: Applying substitution elasticities in TIMES-Nordic. *Applied Energy* 253.
- TEHVA (Turkey Electric and Hybrid Vehicles Association), 2019. <http://tehad.org/2019/06/10/otomotiv-sektorunun-yol-haritasi/>, accessed in 2019.
- TurkStat (Turkish Statistical Institute), 2018a. http://www.tuik.gov.tr/PreTablo.do?alt_id=1027, accessed in 2019.



18th World Clean Air Congress, 23-27 September 2019, Istanbul
organized by TUNCAP and IUAPPA

TurkStat (Turkish Statistical Institute), 2018b. http://www.tuik.gov.tr/PreTablo.do?alt_id=1051, accessed in 2019.

Zhang, H., Chen, W., Huang, W., 2016. TIMES modelling of transport sector in China and USA: Comparisons from a decarbonization perspective. *Applied Energy*. 162, 1505-1514.



Impact on urban and regional air quality from unconventional energy production of shale gas in North Texas

Guo Quan Lim and Kuruvilla John

Department of Mechanical and Energy Engineering, University of North Texas, 3940 N Elm St, Denton, TX 76207

kuruvilla.john@unt.edu

Abstract. Shale gas production in the Barnett Shale, among the largest onshore natural gas fields in the U.S., experienced a significant boost in the early 2000s. The Dallas-Fort Worth (DFW) metroplex located adjacent to this energy production region, has consistently failed to comply with the U.S. Environmental Protection Agency's (EPA) National Ambient Air Quality Standards (NAAQS) for ozone. In this study, we conduct a long-term trend analysis on the measured concentrations of ozone, oxides of nitrogen (NO_x) and total non-methane organic compounds (TNMOC) from three ambient air quality monitoring sites in North Texas. The air quality data for Dallas Hinton (DAL), Fort Worth Northwest (FWNW) and Denton (DEN) was acquired from 2000 through 2018. At all three sites, the oxides of nitrogen (NO_x) has declined since 2000 (-3.87%/year at DAL, -2.69%/year at FWNW, and -1.21%/year at DEN), primarily due to decreased emissions from mobile and stationary sources in the region. However, since 2000, DEN saw an increase in TNMOC concentrations by about +9.97%/year, while these declined in DAL (-1.62 %/year) and FWNW (-0.63%/year). The dominant TNMOC species measured at all three sites were ethane, propane, and n-butane, typically associated with natural gas emissions. The isopentane/n-pentane ratios calculated for DAL (1.931) and FWNW (1.514) suggested a higher influence from vehicular emissions, while DEN (0.959) was heavily influenced by natural gas production activities. The ozone formation potential (OFP) were calculated for all measured TNMOC species. Species associated with traditional urban sources (1-butene, m/p-xylene, propylene and toluene) affected the calculated OFP in DAL and FWNW, while the species linked to natural gas operations (ethane, isopentane and propane) influenced the OFP in DEN. In order to reduce ground level ozone near DAL and FWNW, NO_x and reactive TNMOC species must be reduced, while a reduction in NO_x and all TNMOC species concentration will benefit DEN.

Keywords: Barnett Shale, Shale gas, Ozone, NO_x, TNMOC.

1. Introduction

Shale gas is a previously unavailable natural gas resource trapped under shale formations. Through advancements in hydraulic fracturing and horizontal drilling technologies (U.S. EPA, 2019), significantly harvesting shale gas is now possible, and the access to shale gas has increased the world's available natural gas resources (IEA, 2018). Environmental health controversies often surround shale gas extraction and production. The increased shale gas production activities around the U.S. are negatively affecting many local neighborhoods and communities. Contamination of water resources, ambient air pollution, light and noise pollution, and seismic activities are among the most prominent environmental issues caused by shale gas production (Manda et al., 2014; Centner & Petetin, 2015). In addition, extraction processes cause significant drain on water resources as 12 to 20 million liters of

water on average are required to produce a single horizontal well (Nicot & Scanlon, 2012). Commonly used hydraulic fracturing liquids also contain toxic and carcinogenic chemicals that can affect human health (Wang et al., 2014). Rapid development in the Marcellus Shale, a shale formation that underlies parts of Ohio, West Virginia, Pennsylvania and New York, caused an estimated \$7.2 million to \$32 million in air quality damages. Maintaining air quality standards proved to be difficult as the current air quality regulations largely do not factor in emissions from shale gas productions (Litovitz et al., 2013).

The Barnett Shale is an active shale gas region (SGR) in North Texas, located adjacent to the Dallas-Fort Worth (DFW) metroplex region. Shale gas production activities in the Barnett Shale went through unprecedented growth between 2000 and 2012. At its peak, the region was producing up to 5.8-million MMBtu of natural gas per day (Railroad Commissions of Texas, 2018). Alkane species related to oil and gas production emissions were the most abundant total non-methane organic carbon (TNMOC) group measured in DFW, and there was a higher concentration of TNMOC in less urbanized regions with high natural gas production volume than in highly urbanized regions (Lim et al., 2019). Ahmadi and John (2015) observed a decreased in measured ozone concentrations across the DFW metroplex region from 2000 to 2013; however, the mean concentrations of ozone measured in SGR were higher than the non-SGR by 8%. They also saw an additional 4% in reduction in the number of days where the daily maximum eight-hour ozone concentration exceeded 75 ppb in non-SGR.

In this paper, we describe a long-term study of ground-level ozone and its precursors, NO_x and TNMOC, from 2000 to 2018. A strong emphasis was placed on the impacts from the Barnett Shale activities as numerous past studies had observed substantial impact from the shale gas play on local and regional air quality (Rich et al., 2014; Ahmadi & John, 2015; Lim et al., 2019). With the increase in exploration for and extraction of unconventional energy sources on a global scale, the impact of unconventional shale gas emissions on air quality has become an increasingly important factor.

2. Study Region

DFW is one of the fastest-growing metropolitan regions in the U.S. an estimated population of 7,539,711 (U.S. Census Bureau, 2019). The metroplex region employs over 3.7-million people and the mining, logging, and construction sector showed the most substantial growth during the 2017 fiscal year at a +5.5% growth (U.S. BLS, 2018).

Air pollutant concentration data were retrieved from:

- **Dallas Hinton (DAL)** (32.82006N; -96.860117W) is a monitoring station located in a highly urbanized non-SGR in Dallas County. DAL is in the city of Dallas, one of the largest cities in the state of Texas. An estimated 1.7 million people live in the city of Dallas. The city of Dallas also saw a 12% growth in population between April 1, 2010, and July 1, 2017 (U.S. Census Bureau, 2019). In 2017, the daily vehicle miles travelled (DVMT) in the city of Dallas was 122.8-million miles per day (TxDOT, 2018).
- **Fort Worth Northwest (FWNW)** (32.805818N; -97.356568W), in Tarrant County, is a moderately urbanized SGR. FWNW is located just south of Fort Worth Meacham International Airport and is about 8-km north of downtown Fort Worth, a fastest-growing large cities within the U.S. There are an estimated 874,000 people that live in the city of Fort Worth, and the population grew by 17.3% from 2010 through 2017 (U.S. Census Bureau, 2019). In 2017, the DVMT in the city of Fort Worth was approximately 62.7-million miles per day (TxDOT, 2018), which was roughly half of Dallas'.
- **Denton Airport South (DEN)** (33.219069N; -97.1962836W) is in an exurban SGR located in Denton County. DEN is located 1-km north of the Denton Enterprise Airport and is just outside of the Denton city limit. The city of Denton has an estimated 136,000 inhabitants and saw a

17.1% growth in population since 2010 (U.S. Census Bureau, 2019). The city had a DVMT of 16.2-million miles per day in 2017 (TxDOT, 2018), which was the lowest among the three sites.

3. Methodology

Air pollutant concentration data was downloaded from the Texas Commissions on Environmental Quality (TCEQ) operated portal: Texas Air Monitoring Information System (TAMIS). Ozone, NO_x, and TNMOC concentrations collected from 2000 through 2018, were used in this study. Ozone and NO_x concentrations were available in hourly updated values at all three sites. TNMOC concentrations were available as daily averaged values updated every sixth day. FWNW started collecting TNMOC samples in November 2003. TNMOC concentrations were collected using steel SUMMA canisters and were analysed using gas chromatograph-mass spectrometers (Ethridge, et al., 2015).

The R programming language, an open-source statistical computing language (R Core Team, 2018), was used to organize data, analyse trends, and aid in visualization. R was implemented to perform the Mann-Kendall's (MK) test, the Kruskal-Wallis (KW) test, and the Dunn's test. The MK test determines if the trend experienced by the group was significant (Pohlert, 2018). The KW test was performed to identify if there were at least one significant difference in mean value within the group (McBean & Rover, 1998). Finally, Dunn's test was used to determine whether a specific mean value was significant from the rest (Dinno, 2017). The alpha for all three tests were set to 0.05.

4. Results and discussions

4.1. Ozone

Ozone is a secondary pollutant produced by the photochemical reactions in the atmosphere between NO_x and TNMOC. Exposure to elevated concentrations of ozone can cause respiratory system inflammation, lung infections, and triggers asthma attacks; especially in young children, older adults, and those with existing lung issues are especially at risk from ozone pollution (U.S. EPA, 2018). The NAAQS ozone design value is the annual fourth-highest daily maximum 8-hour ozone concentration averaged over three years. The ozone design value must be under 80-, 75-, and 70-ppb to obtain ozone attainment status under the 1997, 2008, and 2015 revisions, respectively (U.S. EPA, 2016). Nine of the thirteen counties that made up the DFW metroplex had consistently failed to comply with the U.S. Environmental Protection Agency's (EPA) ozone National Ambient Air Quality Standards (NAAQS) under the Clean Air Act (TCEQ, 2018).

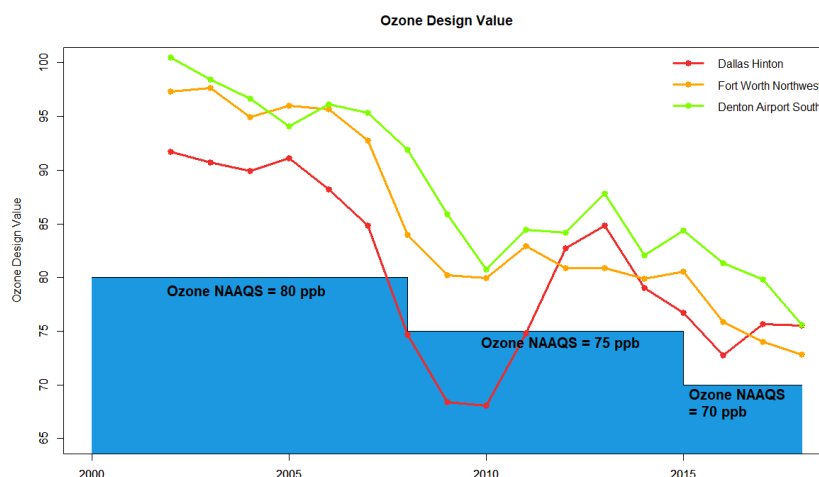


Figure 1. Ozone design value for DAL, FWNW, and DEN; and the NAAQS.

While the ozone design values in 2018 were lower than in 2002, the most substantial reduction occurred before 2010. Figure 1 shows the ozone design value for DAL, FWNW, and DEN alongside the U.S. EPA's ozone NAAQS design values. FWNW and DEN were never in attainment throughout the study period, whereas DAL was briefly attainment the NAAQS for ozone during 2008 through 2011. Aside from 2005, the ozone design value at DEN was consistently higher than the two urbanized sites. DAL's ozone design value dropped from 91.7 ppb in 2002 to 75.6 ppb in 2018, a rate of -1 ± 1.17 ppb/year or $-1.03\%/year$. FWNW saw a -1.53 ± 0.69 ppb/year or $-1.57\%/year$ decline in the ozone design value from 97.3 ppb to 72.8 ppb. DEN's ozone design value dropped from 100 ppb to 75.6 ppb, which was a -1.53 ± 0.78 ppb/year or $-1.67\%/year$ decrease on average. Using the MK test, we determined the downward trends experienced at all three sites across the 18-year monitoring period were all significant with P-values of 0.001976 at DAL, 0.001886 at FWNW, and 0.01096 at DEN.

In addition to ozone design values, mean concentration of ozone and number of high ozone days were also used in this study as measure of ambient ozone pollution. For this study, any day with observed eight-hour averaged daily maximum ozone concentration greater than 70 ppb was considered a high ozone day. Between 2000 and 2018, the mean concentration of ozone measured at DAL, FWNW, and DEN were 26 ± 0.044 ppb, 26.92 ± 0.045 ppb, and 29.61 ± 0.046 ppb, respectively. The total number of high ozone days were 345 in DAL, 416 in FWNW, and 582 in DEN. Despite its location in the least urbanized site of the three, DEN had the highest ozone design value, mean concentration of ozone, and number of high ozone days. This observation strongly indicates a factor outside of the conventional urban emission sources contributing to ozone formation, particularly at DEN, an exurban site.

4.2. Oxides of nitrogen (NO_x)

Conventional urban anthropogenic sources of NO_x , a precursor to the ozone formation, includes gasoline vehicle exhaust, commercial and industrial solvent uses, and power plant emissions (Watson et al., 2001; Barletta et al., 2002). Between 2000 and 2018, the mean NO_x concentration measured at DAL, FWNW, and DEN were 20.853 ± 0.0814 ppb, 15.852 ± 0.0579 ppb, and 9.094 ± 0.028 ppb, respectively. While the mean and 90th-percentile NO_x concentrations at DAL and FWNW had decreased consistently since 2000, DEN's concentration saw an increase from 2002 to 2005, and then followed by a decline post-2006, as shown in Figure 2. Between 2000 and 2018, the NO_x concentration decreased by -0.878 ± 0.612 ppb/year ($-3.87\%/year$) at DAL, -0.461 ± 0.374 ppb/year ($-2.69\%/year$) at FWNW, and -0.231 ± 0.353 ppb/year ($-1.21\%/year$) at DEN. Using the MK test, the downward trends observed at the three sites were statistically extremely significant, where the P-values for all three sites were <0.00001 .

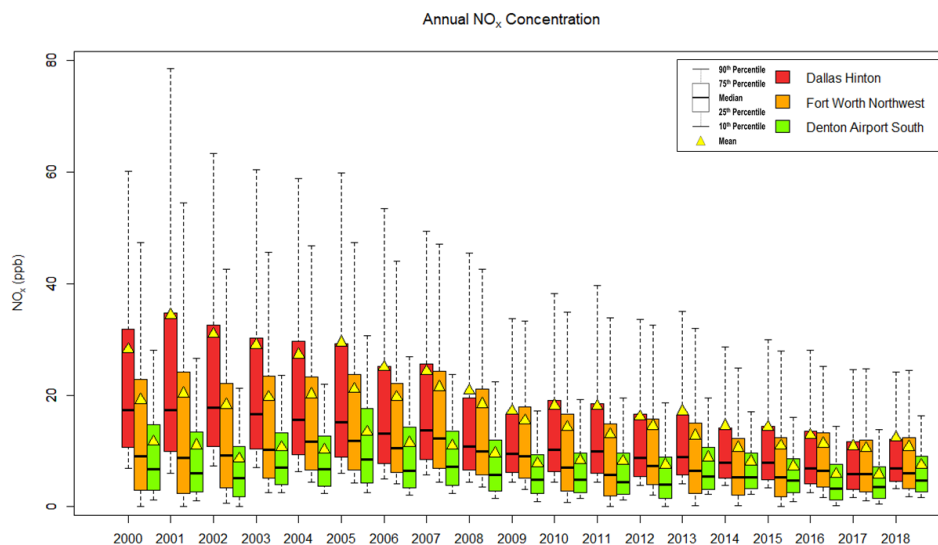


Figure 2. Oxides of nitrogen (NO_x) box whiskers plot (ppb).

The decline in NO_x concentration was likely the result of improvement as a result of better emission control technologies and the implementation of effective emission regulation policies, which resulted in urban air emission curbing (Wang et al., 2012; Zhang et al., 2014). Heavy-duty off-road trucks are commonly used to bring materials to and from the gas wells, and these trucks emit NO_x, particulate matter, and TNMOC (Roy et al., 2014). Thus, we suspect the increase in measured NO_x concentrations at DEN from 2002 to 2005 were likely caused by elevated truck traffic during the development phase.

4.3. Total non-methane organic carbon (TNMOC)

TNMOC are precursor species for the formation of ground-level ozone and can be emitted from either biogenic or anthropogenic sources. In a typical urban region, TNMOC can be emitted from vehicular exhaust emissions, fossil fuel combustion, power plant emissions, industrial and domestic solvent use, oil and gas production facilities, and fugitive emission leaking from pipelines and storage tanks of fuels.

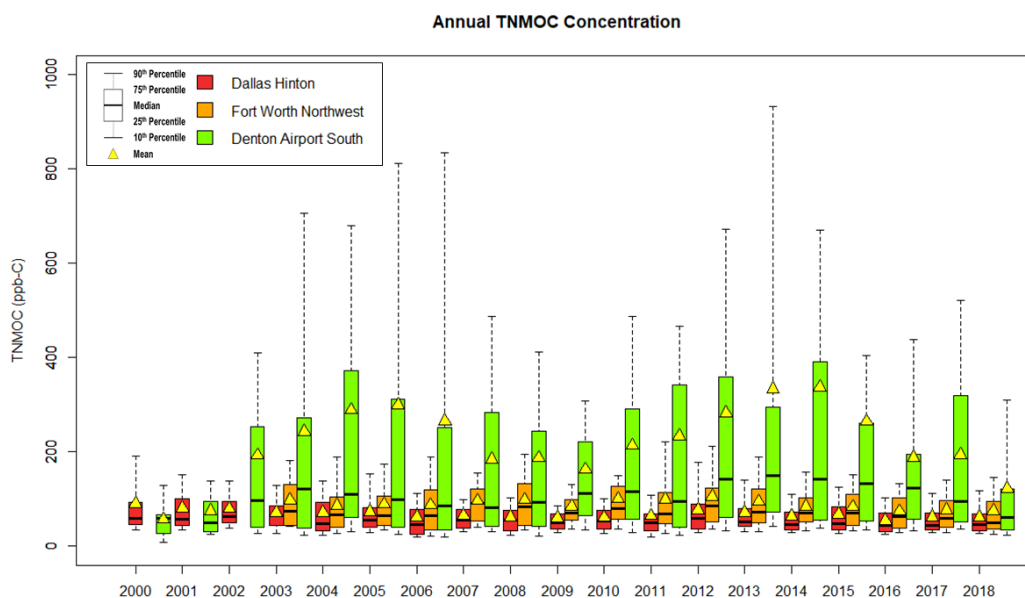


Figure 3. Total non-methane organic carbon (TNMOC) box whiskers plot (ppb-C).

DEN had a significantly larger mean TNMOC concentration compared to DAL and FWNW despite its location and being the least urbanized region among the three. The mean concentration of TNMOC measured at DAL, FWNW, and DEN during the study period was 67.4 ± 1.51 ppb-C, 89.31 ± 2.12 ppb-C, and 220.69 ± 10.36 ppb-C, respectively. DEN was also the only one of the three sites that showed an increase in measured TNMOC concentrations from 2000 through 2018, whereas the TNMOC concentrations in DAL and FWNW had decreased, as shown in Figure 3. Between 2000 and 2018, DAL's mean TNMOC concentration decreased by -1.57 ppb-C/year (-1.62 %/year), which was a significant downward trend according to the MK test with a P-value <0.00001 . From 2004 to 2018, the mean concentration of TNMOC at FWNW experienced a slight decrease of -0.81 ppb-C/year (-0.63 %/year). Despite the relatively low rate of decrease, this was still significant according to the MK test, with a P-value of 0.04579. Between 2000 and 2018, the measured mean TNMOC concentration increased at the rate of $+3.59$ ppb-C/year ($+9.97$ %/year). The upward trend shown by the TNMOC concentration measured at DEN was a significant trend as the MK test P-value was 0.0002937.

The TNMOC concentration measured in DEN was 3.3 times larger than DAL and 2.5 times larger than FWNW. DEN was also the only one of the three sites to have shown an increase in measured TNMOC concentration between 2000 and 2018. The decrease in measured NO_x concentrations at all three sites was an indication of decreased emission from vehicular exhaust and other combustion related sources.

Also, the TNMOC concentrations measured at FWNW, located within the shale gas region, were higher than DAL, despite having approximately half the population size and traffic volume. Thus, we suspected that enhanced shale gas activities in DEN was responsible for the elevated TNMOC concentrations observed. We also theorize that FWNW was affected by both conventional urban sources and unconventional shale gas sources, but on a smaller degree as compared to DEN, possibly due to more stringent local regulations.

4.3.1. Impacts of natural gas production on TNMOC concentrations

Ethane, propane, and n-butane are emissions species from oil and gas production activities; whereas acetylene, ethylene, and propylene are more commonly associated with fossil fuel burning and vehicular exhaust emissions (Liao et al., 2015). According to Baker et al. (2008), the typical concentrations of propane in U.S. cities during summertime is between the range of 0.87 ppb-C to 10.53 ppb-C. The mean concentrations of propane measured during summertime at DAL and FWNW were 6.283 ± 0.167 ppb-C and 8.02 ± 0.307 ppb-C, respectively, and were both within the range observed in other major U.S. cities. The mean propane concentration measured in DEN during summertime was 26.028 ± 2.62 ppb-C, which was much higher than the typical urban propane concentrations. The mean concentration of propane measured during summertime at DEN more closely resembled concentrations measured at other oil and gas regions, where it fell between the concentrations measured at Colorado's Northern Front Range metropolitan area (24 ppb-C) (Abeleira et al., 2017), and the Marcellus Shale (39 ppb-C) (Swarthout et al., 2015).

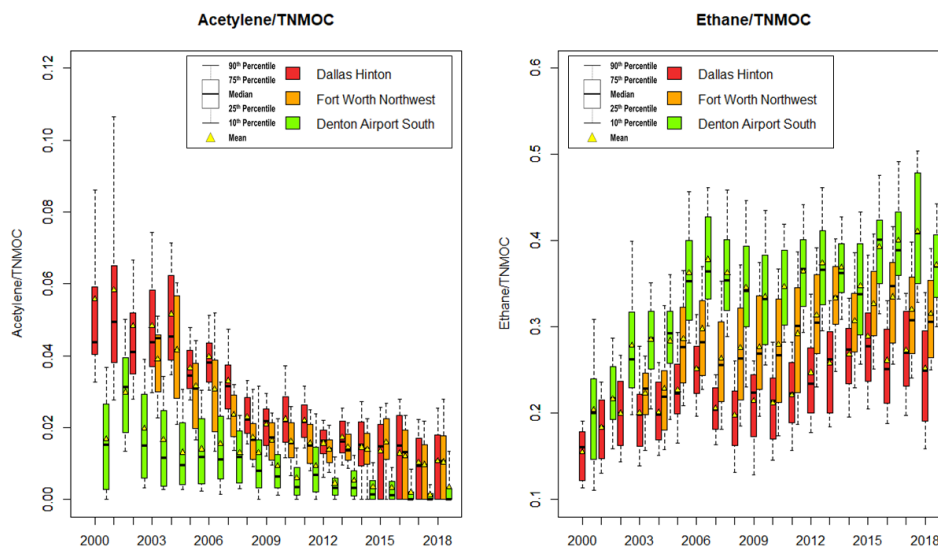


Figure 4. Acetylene/TNMOC ratio and ethane/TNMOC ratio box whiskers plot.

The annual acetylene-to-TNMOC (acetylene/TNMOC) ratio and the ethane-to-TNMOC (ethane/TNMOC) ratios were calculated to identify the changes in the composition of both species measured. The mean acetylene/TNMOC ratio calculated for DAL, FWNW, and DEN were 0.028 ± 0.0007 , 0.019 ± 0.0004 , and 0.01 ± 0.0004 , respectively; whereas the mean ethane/TNMOC ratio was 0.229 ± 0.002 at DAL, 0.296 ± 0.003 at FWNW, and 0.342 ± 0.003 at DEN. As shown in Figure 4, all three sites saw a decreased in the acetylene/TNMOC ratio decreased and an increase in the ethane/TNMOC ratio. This indicated that the impact from gasoline-powered vehicular exhaust and other combustion related sources in DFW was in decline, whereas the impact from unconventional oil and gas emissions had increased.

Oil and gas production-related emissions can be differentiated from gasoline-powered vehicular emissions through isopentane to n-pentane (isopentane/n-pentane) ratios. Regions with higher vehicle emissions have isopentane/n-pentane ratios greater than one, whereas regions with higher natural gas emissions have isopentane/n-pentane ratio under one and closer to 0.9 (Swarthout et al., 2015). DAL and FWNW had isopentane/n-pentane ratios higher than one, at 1.931 and 1.514, respectively; whereas DEN's ratio was lower than one, at 0.959. This suggested that there were stronger impacts from gasoline vehicle sources at DAL and FWNW, while DEN had a stronger impact from natural gas sources.

4.3.2. Ozone formation potential (OFP) of TNMOC

Calculating the ozone formation potential (OFP) of each TNMOC species is a crucial step in the development of ozone control strategies (Liu et al., 2016; Li et al., 2017; Zhu et al., 2018). The maximum incremental reactivity (MIR) value used in this study was based on Carter's (2009) report. The OFP of TNMOC species at DAL, FWNW, and DEN were 35.28 ± 0.87 ppb, 35.98 ± 0.82 ppb, and 50.38 ± 2.04 ppb, respectively. The species that generated the highest OFP of TNMOC at DAL were ethylene (30.64%), propylene (12.19%), ethane (5.66%), 1-butene (5.65%), m/p-xylene (5.62%), and n-butane (5.43%). At FWNW, the species that generated the highest OFP of TNMOC were ethylene (26.93%), ethane (10.17%), propylene (9.79%), propane (7.01%), n-butane (12.88%), and 1-butene (6.21%). Whereas, ethane (20.57%), propane (15.32%), n-butane (16.16%), ethylene (10.38%), isobutane (8.53%), and isopentane (6.2%) were the species with the highest OFP of TNMOC at DEN.

At DAL, the OFP of the alkane, alkene, alkyne, aromatics, and diene TNMOC species were 9.63 ± 0.23 ppb, 18.1 ± 0.53 ppb, 1.03 ± 0.03 ppb, 5.3 ± 0.15 ppb, and 2.15 ± 0.07 ppb, respectively. The OFP of TNMOC at FWNW was 13.8 ± 0.34 ppb from alkanes, 16.8 ± 0.43 ppb from alkenes, 0.82 ± 0.02 ppb from alkynes, 3.99 ± 0.13 ppb from aromatics, and 1.16 ± 0.04 ppb from dienes. Alkanes were the largest contributors to the OFP of TNMOC in DEN at 38.6 ± 1.89 ppb, followed by alkene (8.43 ± 0.25 ppb), aromatics (2.84 ± 0.23 ppb), diene (1.06 ± 0.05 ppb), and alkyne (0.55 ± 0.01 ppb). Between 2000 and 2018, the OFPs of TNMOC at DAL and FWNW were in constant decrease but the OFP of TNMOC at DEN largely followed the TNMOC concentration trend. DAL and FWNW's OFP of TNMOC decreased by -2.24 ± 0.98 ppb/year ($-4.57\%/year$) and -1.94 ± 1.23 ppb/year ($-4.14\%/year$), respectively; while DEN's saw an increase of 0.02 ± 2.6 ppb/year ($+2.7\%/year$).

Despite a relatively lower reactivity and MIR, alkanes were responsible for 26.59% of total OFP at DAL, 37.74% of total OFP at FWNW, and 74.99% of total OFP at DEN. Alkanes were the largest group in terms of measured concentrations at all three monitoring stations, which was 79.67% at DAL, 87.79% at FWNW, and 96.95% at DEN. Elevated alkane emissions from natural gas production activities were responsible for the increased in OFP of TNMOC at DEN. Alkane emissions from oil and gas productions were also shown to had contributed to more than half of TNMOC reactivity in other oil and gas regions (Swarthout et al., 2013; Abeleira et al., 2017).

4.4. TNMOC-NO_x-Ozone relationships

The mean concentrations of TNMOC measured at DAL during high ozone days (daily maximum eight-hour ozone > 70 ppb) was 57 ± 2.86 ppb-C, which was 15.6% smaller than the concentrations measured during non-high ozone days at 67.52 ± 1.59 ppb-C. However, the mean concentrations of reactive TNMOC species (species with MIR >2) was slightly larger during high ozone days, which were 12.8 ± 0.123 ppb-C and 12.4 ± 0.114 ppb-C on high and non-high ozone days, respectively. While the mean concentration of reactive TNMOC was only 3.2% larger during high ozone days, the mean concentration of DAL's isoprene, a highly reactive biogenic species, was almost three times larger during high ozone days. Isoprene concentrations play a critical role in ozone generation, where Chameides et al. (1988) stated that inclusion of isoprene and other biogenic species into a photochemical model increased the need for the reduction of anthropogenic TNMOC from 30% to 70% to meet NAAQS prescribed ozone design value. The NO_x concentrations on high ozone days (21.86 ± 1.43 ppb) were 6.3% higher than the concentrations measured during non-high ozone days (20.57 ± 0.67 ppb).

While the difference between high (90.87 ± 7.18 ppb-C) and non-high ozone day (89.29 ± 2.23 ppb-C) mean TNMOC concentrations measured at FWNW were minor (1.8%), the mean concentration of reactive TNMOC species was 47.6% larger on high ozone days (15.2 ± 0.61 ppb-C versus 10.3 ± 0.094 ppb-C). There was also a 50.6% difference in the mean concentrations of NO_x measured during high (22.32 ± 1.82 ppb) and non-high ozone days (14.82 ± 0.46 ppb).

TNMOC concentrations at DEN was significantly larger (33.9%) during high ozone days, the mean concentrations measured during high and non-high ozone days were 242.66 ± 26.12 ppb-C and 181.17 ± 8.72 ppb-C, respectively. However, the difference in the mean concentration of reactive TNMOC species was only 2.9% due to most of the TNMOC species that made up DEN's concentrations were not reactive. During high ozone days, the reactive TNMOC species had a mean of 7.1 ± 0.08 ppb-C, whereas the non-high ozone days mean concentrations were 6.9 ± 0.08 ppb-C. While the majority of TNMOC concentrations measured at DEN were non-reactive, previous studies have shown that elevated concentrations of non-reactive alkanes species can also lead to increase in ozone concentration (Katzenstein, et al., 2003). The mean NO_x concentration measured during high ozone days were 24.5% higher than the mean NO_x concentration measured during no-high ozone days (10.83 ± 0.46 ppb versus 8.71 ± 0.23 ppb).

High NO_x concentrations were the driving force behind the high ozone days at all three monitoring sites. During high ozone days, an elevated concentration of reactive TNMOC species was measured in DAL and FWNW while non-reactive TNMOC species were measured in DEN. Thus, we believe regulating reactive TNMOC species emissions, in addition to the continuation of NO_x reduction efforts, will be beneficial in reducing ozone generation at DAL and FWNW. The efforts to reduce the number of high ozone days in DEN will be closely linked to regulating non-reactive TNMOC species, which are largely fugitive emissions from oil and gas play, alongside the further continuation of the NO_x reduction efforts.

5. Conclusion

An argument can be made for spatially varying emission control strategy within a single urban airshed based on the predominance of precursor emission. Since 2000, we had observed a decrease in emission from vehicular exhaust and other combustion related emission as evident from the constant decrease in NO_x concentrations. Despite the decrease in conventional urban source emissions, the ozone design values were still consistently failing to achieve ozone attainment under the NAAQS. However, since 2013, the ozone design values at all three sites began to decrease, this also coincided with the decrease in the measured TNMOC concentrations and overall natural gas production volume in the Barnett Shale. We have strong evidence that the unconventional emissions from the Barnett Shale were a major influence on the TNMOC concentrations measured in DEN, and to a smaller degree, in FWNW. DEN, the least urbanized of the three sites, had the largest pool of measured TNMOC, which was 3.5 and 2.2 times larger than the concentrations at DAL and FWNW, respectively. DEN was also the only site among the three to see an increase in the mean TNMOC concentration between 2000 and 2018. Ethane was the hydrocarbon species with the highest measured concentrations at all three sites, and it was among the TNMOC species that generated the highest OFP despite a relatively low MIR value. From 2000 to 2018, the OFP of TNMOC species at DAL and FWNW decreased while the OFP of TNMOC at DEN, which was heavily influenced by natural gas related alkane species, had increased. We believe DAL and FWNW would benefit from a reduction in NO_x and reactive TNMOC species, whereas the ozone generation in DEN can be controlled via a reduction in both NO_x and TNMOC species associated with the shale gas operations.



6. References

- Abeleira, A., Pollack, I. B., Sive, B., Zhou, Y., Fischer, E. V., Farmer, D. F., 2017. Source characterization of volatile organic compounds in the Colorado Northern Front Range Metropolitan Area during spring and summer 2015. *Journal of Geophysical Research: Atmosphere*, 122, 3595-3613.
- Ahmadi, M., John, K., 2015. Statistical evaluation of the impact of shale gas activities on ozone pollution in North Texas. *Science of The Total Environment*, 536, 457-467.
- Baker, A. K., Beyersdorf, A. J., Doezema, L. A., Katzenstein, A., Meinardi, S., Simpson, I. J., Blake, D. R., Rowland, F. S., 2008. Measurements of nonmethane hydrocarbons in 28 United States cities. *Atmospheric Environment*, 42, 170-182.
- Barletta, B., Meinardi, S., Simpson, I. J., Khwaja, H. A., Blake, D. R., Rowland, F. S., 2002. Mixing ratios of volatile organic compounds (VOCs) in the atmosphere of Karachi, Pakistan. *Atmospheric Environment*, 36, 3429-3443.
- Carter, W. P., 2009. Updated maximum increment reactivity scale and hydrocarbon bin reactivities for regulatory applications. Riverside, CA: College of Engineering Centre for Environmental Research and Technology, University of California.
- Centner, T. J., Petetin, L., 2015. Permitting program with best management practices for shale gas wells to safeguard public health. *Journal of Environmental Management*, 163, 174-183.
- Chameides, W., Lindsay, R., Richardson, J., Kiang, C., 1988. The role of biogenic hydrocarbons in urban photochemical smog: Atlanta as a case study. *Science*, 241, 1473-1475.
- Dinno, A., 2017. Package 'dunn.test'. <https://cran.r-project.org/web/packages/dunn.test/dunn.test.pdf>, accessed on May 20, 2019.
- Ethridge, S., Bredfeldt, T., Sheedy, K., Shirley, S., Lopez, G., Honeycutt, M., 2015. The Barnett Shale: From problem formulation to risk management. *Journal of Unconventional Oil and Gas Resources*, 11, 95-110.
- IEA., 2018. *World Energy Outlook 2018*. Paris: International Energy Agency.
- Katzenstein, A.S., Doezema, L.A., Simpson, I. J., Blake, D.R., F. Sherwood Rowland, 2003. Extensive regional atmospheric hydrocarbon pollution in the southwestern United States. *PNAS*, 100, 11975-11979. doi: 10.1073/pnas.1635258100
- Li, B., Ho, S. S., Xue, Y., Huang, Y., Wang, L., Cheng, Y., Dai, W., Zhong, H., Cao, J., Lee, S., 2017. Characterizations of volatile organic compounds (VOCs) from vehicular emissions at roadside environment: The first comprehensive study in North-western China. *Atmospheric Environment*, 161, 1-12.
- Liao, J., Wang, T., Jiang, Z., Zhuang, B., Xie, M., Yin, C., Wang, X., Zhu, J., Fu, Y., Zhang, Y., 2015. WRF/Chem modeling of the impacts of urban expansion on regional climate and air pollutants in Yangtze River Delta, China. *Atmospheric Environment*, 106, 204-214.
- Lim, G. Q., Matin, M., John, K., 2019. Spatial and temporal characteristics of ambient atmospheric hydrocarbons in an active shale gas region in North Texas. *Science of The Total Environment*, 656, 347-363.
- Litovitz, A., Curtright, A., Abramzon, S., Burger, N., Samaras, C., 2013. Estimation of regional air-quality damages from Marcellus Shale natural gas extraction in Pennsylvania. *Environmental Research Letters*, 14-17.
- Liu, B., Liang, D., Yang, J., Dai, Q., Bi, X., Feng, Y., Yuan, J., Xiao, Z., Zhang, Y., Xu, H., 2016. Characterization and source apportionment of volatile organic compounds based on 1-year of observational data in Tianjin, China. *Environmental Pollution*, 218, 757-769.



- Manda, A. K., Heath, J. L., Klein, W. A., Griffin, M. T., Montz, B. E., 2014. Evolution of multi-well pad development and influence of well pads on environmental violations and wastewater volumes in the Marcellus shale (USA). *Journal of Environmental Management*, 142, 36-45.
- McBean, E., Rover, F., 1998. *Statistical procedures for analysis of environmental monitoring data and risk assessment*. New Jersey: Prentice Hall.
- Nicot, J.-P., Scanlon, B. R., 2012. Water use for shale-gas production in Texas, U.S. *Environmental Science, and Technology*, 46, 3580-3586.
- Pohlert, T., 2018. Trend: Non-parametric trend tests and change-point detection. <https://CRAN.R-project.org/package=trend>, accessed on May 20, 2019.
- R Core Team, 2018. *R: A language and environment for statistical computing*. Vienna, Austria: R Foundation for Statistical Computing. Retrieved from <https://www.r-project.org/>
- Railroad Commissions of Texas, 2018. Barnett Shale Information. <http://www.rrc.state.tx.us/oil-gas/major-oil-and-gas-formations/barnett-shale-information/>, accessed in September 24, 2018.
- Rich, A., Grover, J. P., Sattler, M. L., 2014. An exploratory study of air emissions associated with shale gas development and production in the Barnett Shale. *Journal of the Air & Waste Management Association*, 64(1), 61-72.
- Roy, A. A., Adams, P.J., Robinson, A. L., 2014. Air pollutant emissions from the development, production, and processing of Marcellus Shale natural gas. *Journal of the Air & Waste Management Association*, 64(1), 19-37, doi: 10.1080/10962247.2013.826151
- Swarthout, R. F., Russo, R. S., Zhou, Y., Hart, A. H., Sive, B. C., 2013. Volatile organic compound distributions during NACHTT campaign at the Boulder Atmospheric Observatory: Influence of urban and natural gas sources. *Journal of Geophysical Research: Atmosphere*, 118, 10614-10637.
- Swarthout, R. F., Russo, R. S., Zhou, Y., Miller, B. M., Mitchell, B., Horsman, E., Lipsky, E., McCabe, TCEQ, 2018. Dallas-Fort Worth: Current attainment status. <https://www.tceq.texas.gov/airquality/sip/dfw/DFW-status>, accessed on September 24, 2018.
- TxDOT, 2018. Roadway Inventory Annual Reports 2017. <http://www.txdot.gov/inside-txdot/division/finance/discos.html>, accessed on September 24, 2018.
- U.S. BLS., 2018. Dallas-Fort Worth Area Economic Summary. https://www.bls.gov/regions/southwest/summary/blssummary_dallasfortworth.pdf, accessed on August 23, 2018.
- U.S. Census Bureau, 2019. Quickfacts - Denton city, Texas; Fort Worth City, Texas; Dallas city, Texas. <https://www.census.gov/quickfacts/fact/table/dentoncacitytexas,fortworthcitytexas,dallascitytexas/PST045217>, accessed on August 23, 2018.
- U.S. EPA., 2016. NAAQS Table. <https://www.epa.gov/criteria-air-pollutants/naaqs-table>, accessed on August 20, 2018.
- U.S. EPA, 2018. Health Effects of Ozone Pollution. <https://www.epa.gov/ground-level-ozone-pollution/health-effects-ozone-pollution>, accessed on May 20, 2019.
- U.S. EPA., 2019. Unconventional Oil and Natural Gas Development. <https://www.epa.gov/uog>, accessed on May 15, 2019.
- Wang, Q., Chen, X., Jha, A. N., Rogers, H., 2014. Natural gas from shale formation – The evolution, evidences, and challenges of shale gas revolution in the United States. *Renewable and Sustainable Energy Reviews*, 30, 1-28.



Wang, Y., Ren, X., Ji, D., Zhang, J., Sun, J., Wu, F., 2012. Characterization of volatile organic compounds in the urban area of Beijing from 2000 to 2007. *Journal of Environmental Sciences*, 24(1), 95-101.

Watson, J. G., Chow, J. C., Fujita, E. M., 2001. Review of volatile organic compounds source apportionment by chemical mass balance. *Atmospheric Environment*, 35, 1567-1584.

Zhang, Q., Yuan, B., Shao, M., Wang, X., Lu, S., Lu, K., Wang, M., Chen, L., Chang, C., Liu, S., 2014. Variations of ground-level O₃ and its precursors in Beijing in summertime between 2005 and 2011. *Atmospheric Chemistry and Physics*, 14, 6089-6101.

Zhu, H., Wang, H., Jing, S., Wang, Y., Cheng, T., Tao, S., Lou, S., Qiao, L., Li, L., Chen, J., 2018. Characteristics and sources of atmospheric volatile organic compounds (VOCs) along the mid-lower Yangtze River in China. *Atmospheric Environment*, 190, 232-240.

Acknowledgments

The authors would like to acknowledge the Texas Commission on Environmental Quality (TCEQ) for providing the ambient air monitoring and pollutant concentration data and making it publicly available through the TAMIS (<http://www17.tceq.texas.gov/tamis/index.cfm>). We also want to acknowledge the Railroad Commissions of Texas (RRC) for providing UGD production data through their online portal (<https://www.rrc.state.tx.us/about-us/resource-center/research/online-research-queries/>). The findings and opinions expressed in this study are of the authors only and do not represent the views of their employer nor of any of the agencies mentioned above that were instrumental in providing the relevant data.

Modeling of PM₁₀ emissions from motor vehicles in Zonguldak, Turkey

Ozgur Zeydan and Elif Ozturk

Zonguldak Bulent Ecevit University, Department of Environmental Engineering,
67100, Zonguldak, Turkey

ozgurzeydan@yahoo.com

Abstract. Motor vehicles still use fossil fuels in developing countries like Turkey. Motor vehicle emissions are one of the main contributors of air pollution in cities. This pollution can cause a serious threat to human health. Therefore, prevention or reduction of motor vehicle emissions is in the concern of scientists. The aim of this study is the modeling of particulate matter (PM₁₀) emissions from motor vehicles in the city center of Zonguldak, Turkey. As a study area, portion of D010 State Road is selected. The numbers of vehicles are counted in three different sections of this road. Automobiles are classified as gasoline, diesel or LPG cars according to the data of Turkish Statistical Institute. The emission factors are selected from the latest version of EMEP/EEA Emission Inventory Guidebook in order to calculate the amount of motor vehicle emissions. After that, air quality modeling is performed by using CALRoads View software which can run CAL3QHCR (California Line Source for Queuing & Hot Spot Calculations Refined) model. CAL3QHCR can model traffic emissions by considering signalization of the road. Two different scenarios are applied in air quality modeling: (1) current flow of traffic with queuing at red lights and (2) optimization of traffic by the help of green wave. It is assumed that, applying green wave could prevent queuing at traffic lights and traffic will flow freely which reduce idle emissions. In the former scenario, maximum hourly PM₁₀ concentration is found as 292.1 µg m⁻³, while in the latter scenario maximum hourly PM₁₀ concentration is calculated as 29.1 µg m⁻³. So it is proved that with the aid of signal optimization, the motor vehicle related air pollution could be reduced in cities.

Keywords: Motor vehicles, PM₁₀ emissions, Air quality modeling, CAL3QHCR, Signal optimization.

1. Introduction

Motor vehicles still use fossil fuels in developing countries like Turkey. According to the Turkish Statistical Institute, only 0.1% of the vehicles in Turkey use electric or hybrid motors (TUİK, 2018). Rest of the vehicles depend on fossil fuels like gasoline, diesel or liquefied petroleum gas (LPG). Variety of emissions are released from these vehicles including carbon dioxide (CO₂), carbon monoxide (CO), nitrogen oxides (NO_x), volatile organic compounds (VOCs) and particulate matter (PM) (Uherek et al., 2010). Motor vehicle emissions are one of the main contributors of air pollution in cities (Al-jeelani, 2013). This pollution can cause a serious threat to human health (Forehead and Huynh, 2018). Also, these emissions affect atmospheric structure and climate (Uherek et al., 2010). Therefore, prevention or reduction of motor vehicle emissions is in the concern of scientists.

In order to reduce or minimize motor vehicle emissions, several methods have been applied including motor technology improvement, using alternative fuels and traffic optimization (Akay and Akgungor,

2008; Uherek et al., 2010; Woodcock et al., 2009). Air quality modeling is necessary to determine the effects of emission reduction strategies. Several Gaussian based line source models (ADMS-Roads, APRAC, CALINE, CAL3QHC, CAL3QHCR, HIWAY, M-GFLSM, R-Line) can be applied to predict pollutant concentrations near roads (Forehead and Huynh, 2018; Gokhale and Raokhande, 2008; Greco et al., 2007; Mishra and Padmanabhamutry, 2003; Nagendra and Khare, 2002; Sharma et al., 2007). Among these models, CAL3QHC and CAL3QHCR are widely used by researchers to forecast CO, NO_x and PM concentrations from motor vehicle emissions (Abdul-Wahab, 2004; Chart-asa et al., 2013; Demirarslan and Cetin Dogruparmak, 2018; Gokhale and Raokhande, 2008; Mishra and Padmanabhamutry, 2003; Zhou and Sperling, 2001).

In this study, air quality modeling is performed to determine the effectiveness of green wave strategy in the D010 State Road in Zonguldak, Turkey. Particulate matter (PM₁₀ - particle diameter is less than or equal to 10 µm) emissions released from motor vehicles have been modelled by using CAL3QHCR model for 2 different scenarios: (1) queuing at intersections during red light and free flow of traffic by assuming the signal optimization at intersections by green wave technology. Study area and fleet information are given in Materials & Methods section. Also, emission inventory and CAL3QHCR model are described in the same chapter. Results of inventory and findings of modeling study are given in Results and Discussion part. There exist a brief conclusion at the end of the paper.

2. Materials and methods

2.1. Study area and vehicle counts

Zonguldak Province is located at the Black Sea shore of Turkey. Modeling area lies between Zonguldak city center and Kozlu County. A portion of "D010 State Road" is selected for modeling. The road starts from the roundabout at the Zonguldak city center and ends at the entrance of tunnel at Degirmenagzı region in Kozlu. The total distance of this road is 7.05 km. Figure 1 represents the selected road and roundabouts with signalization. There exist 6 roundabouts; however, the numbers of vehicles are counted at three different roundabouts. Counting locations are Zonguldak 100. Yıl Bus Terminal, Esas 67 Burda Shopping Mall and Kozlu Park Shopping Mall. These points are represented with numbers 2, 3 and 5 in Figure 1 respectively. There exist a truck garage at point 1. Intersection 4 is located near fuel stations on the Zonguldak and Kozlu border. Intersection 6 is the entrance to Fatih Sitesi district of Kozlu. Since air quality model allows inputting emissions for different directions of the road, the numbers of vehicles are determined for two different directions which are also shown in Figure 1. The number of vehicles are counted in March 2019 during both weekdays and weekend. It is assumed that total number of vehicles remains the same for other months. The time period of counting was between 07:00 and 19:00.

The numbers of vehicle that pass through modeling road are listed in Table 1. As seen from this table, passenger cars constitute the major portion and followed by minibuses and light commercial trucks. It was not possible to distinguish the passenger cars according to the fuel type during the vehicle count. Therefore, automobiles are classified as gasoline, diesel or liquefied petroleum gas (LPG) cars according to the data of Turkish Statistical Institute. In Turkey, 24.9% of passenger cars use gasoline, 36.8% of passenger cars use diesel and 37.9% of passenger cars use LPG as a fuel in 2018. The fuel type is unknown for 0.3% of passenger cars (TUIK, 2018).



Figure 1. Study area

Table 1. Vehicle counts

	100. Yıl Bus Terminal		Esas 67 Burda Shopping Mall		Kozlu Park Shopping Mall	
	Direction 1	Direction 2	Direction 1	Direction 2	Direction 1	Direction 2
Gasoline Cars	1914	1837	1577	1422	1996	1572
Diesel Cars	2825	2711	2328	2099	2496	2321
LPG Cars	2909	2792	2397	2161	3034	2389
Light Commercial Trucks	785	697	638	536	953	649
Buses	51	103	83	88	70	45
Trucks	148	198	203	181	179	151
Minibuses	811	756	495	450	837	657
Heavy Duty Vehicles	81	67	75	67	85	58
Motorcycles	113	100	52	46	64	56
Total	9637	9261	7848	7050	9714	7898

2.2. Emission inventory

One of the input of air quality models is an emission inventory. Emission inventory can be defined as the list of pollutants released from certain activities for a given area and for a limited of time. Emission amounts of motor vehicles can be determined simply by Equation (1).

$$E = EF \times M \times N \quad (1)$$

where,

E: Emission amount (ton year⁻¹)

EF: Emission factor (g km⁻¹)

M: Distance travelled by each vehicle (km)

N: Number of vehicles

If site specific emission factors does not exist, emission factors databases could be helpful. In this study, emission factors are selected from the latest version of EMEP/EEA Emission Inventory Guidebook 2016 published by European Environment Agency (EEA, 2016). Tier 2 Method is chosen. In this method, there exist several sub-categories for each vehicle category. For example, there are 4 sub-categories (mini, small, medium and large-SUV-executive) for gasoline fuelled vehicles. For this reason, the average values of Tier 2 emissions factors of sub-categories are calculated and used in this study. Only Euro 4 or later emission standard is considered for the selection of emission factors. PM₁₀ emission factors, used in this study, are listed in Table 2 according to the vehicle type.

Table 2. PM₁₀ emission factors

Vehicle Type	Average PM ₁₀ EF (g km ⁻¹)
Gasoline Cars	0.001
Diesel Cars	0.002
LPG Cars	-
Light Commercial Trucks	0.001
Buses	0.041
Trucks	0.019
Minibuses	0.001
Heavy Duty Vehicles	0.019
Motorcycles	0.003

2.3. Air quality modeling

In this study, CAL3QHCR (California Line Source for Queuing & Hot Spot Calculations Refined) line source model is used for dispersion modelling. CAL3QHCR is based on California Line Source Dispersion Model (CALINE) which can predict pollutants (CO, NO₂ and PM) concentrations near roadways. CAL3QHC is the improved version of CALINE and can be used to predict pollutant concentrations near roadways from both moving and idling vehicles. This model also calculates length of queues formed by idling vehicles at signalized intersections by considering signalization (Gokhale and Raokhande, 2008; Mishra and Padmanabhamutry, 2003). CAL3QHCR is refined version of CAL3QHC and uses yearly 1-hour meteorological data. Other input parameters of this model are lane geometry, receptor locations, traffic flow count and emission amounts (Mishra and Padmanabhamutry, 2003; Zhou and Sperling, 2001). All these models are based on steady-state Gaussian formulation (Chart-asa et al., 2013). Air quality modeling is performed by using CALRoads View software that can run CAL3QHCR line model. Two different scenarios are applied in air quality modeling: (1) current flow of traffic with queuing at red lights and (2) optimization of traffic by the help of green wave (free flow condition at intersections). Green wave signalization calculations are beyond the scope of this study, therefore in 2nd scenario, only green wave is assumed and modeling is performed consequently. Hourly 1-year meteorological data of the year 2018 is obtained from Turkish State Meteorological Service and is used in modeling.

3. Results and discussion

3.1. Inventory results

Since vehicles counts are performed in 3 different locations, road is divided into 3 pieces for emission calculations. The lengths of these parts are 1.77, 2.92 and 2.36 km among the direction 1. Then, PM₁₀ emission are calculated by using Equation (1) and represented in Table 3. As seen from this table, diesel car's emissions have the highest contribution to total vehicle related particulate emissions. Total PM₁₀ emission is 96.7 kg year⁻¹ in the study area.

Table 3. PM₁₀ emission inventory results (tons year⁻¹)

	100. Yıl Bus Terminal		Esas 67 Burda Shopping Mall		Kozlu Park Shopping Mall	
	Direction 1	Direction 2	Direction 1	Direction 2	Direction 1	Direction 2
	Gasoline Cars	0.002	0.002	0.002	0.002	0.002
Diesel Cars	0.004	0.004	0.010	0.005	0.005	0.004
Light Commercial Trucks	0.001	0.0005	0.001	0.001	0.001	0.001
Buses	0.001	0.003	0.004	0.004	0.002	0.002
Trucks	0.002	0.002	0.004	0.004	0.003	0.003
Minibuses	0.001	0.0005	0.001	0.0005	0.001	0.001
Heavy Duty Vehicles	0.001	0.001	0.002	0.001	0.001	0.001
Motorcycles	0.0002	0.0002	0.0002	0.0002	0.0002	0.0002
Total	0.0122	0.0132	0.0242	0.0177	0.0152	0.0142

3.2. Modeling results

CAL3QHCR model has been run for 2 different scenarios: current traffic flow which involves queuing at red lights and green wave scenario. In the former scenario, maximum hourly PM₁₀ concentration is predicted as 292.1 µg m⁻³ (X= 398219.1, Y=4589795.0). On the other hand, maximum hourly PM₁₀ concentration is found as 29.1 µg m⁻³ (X= 393594.5, Y=4586906.5) in the latter scenario. As Zhou and Sperling (2001) mentioned that hotspot emissions occur as a result of queuing activities of vehicles. Assumption of applying green wave technology at intersections could reduce the maximum particulate matter concentration up to one tenth of the former case. Figure 2 shows the pollution distribution maps at the intersection points. In scenario 1, intersections 1 and 2 is the most polluted locations. Roundabouts 3, 5 and 6 are the other polluted regions where particulate matter concentration exceeds 220 µg m⁻³. Even for the scenario 1, point 4 is the least polluted location. For green wave scenario, particulate matter concentrations sharply decreased below 29 µg m⁻³. This is an expected result since vehicle emissions are at maximum during idle phase. Another recent work at the study area stated that signal improvement at one intersection (the Bus Terminal intersection) would lead to 45%, 54%, 57% and 42% reductions in CO₂, CO, HC and NO_x emission amounts (Demirel Bayik et al., 2018). Similarly, Akay and Akgungor (2008) mentioned that green wave scenario reduced emissions in five streets of Kırıkkale city (Turkey) by 74% in general. Therefore, it can be concluded that preventing queues at red lights and allowing traffic to flow continuously at constant speed (cruise phase) minimizes motor vehicle emissions improves air quality of the cities. The benefits of green wave is not limited with air quality improvement. Mitigation of health impacts and reduction in fuel use are the other co-benefits of continuous traffic flow.

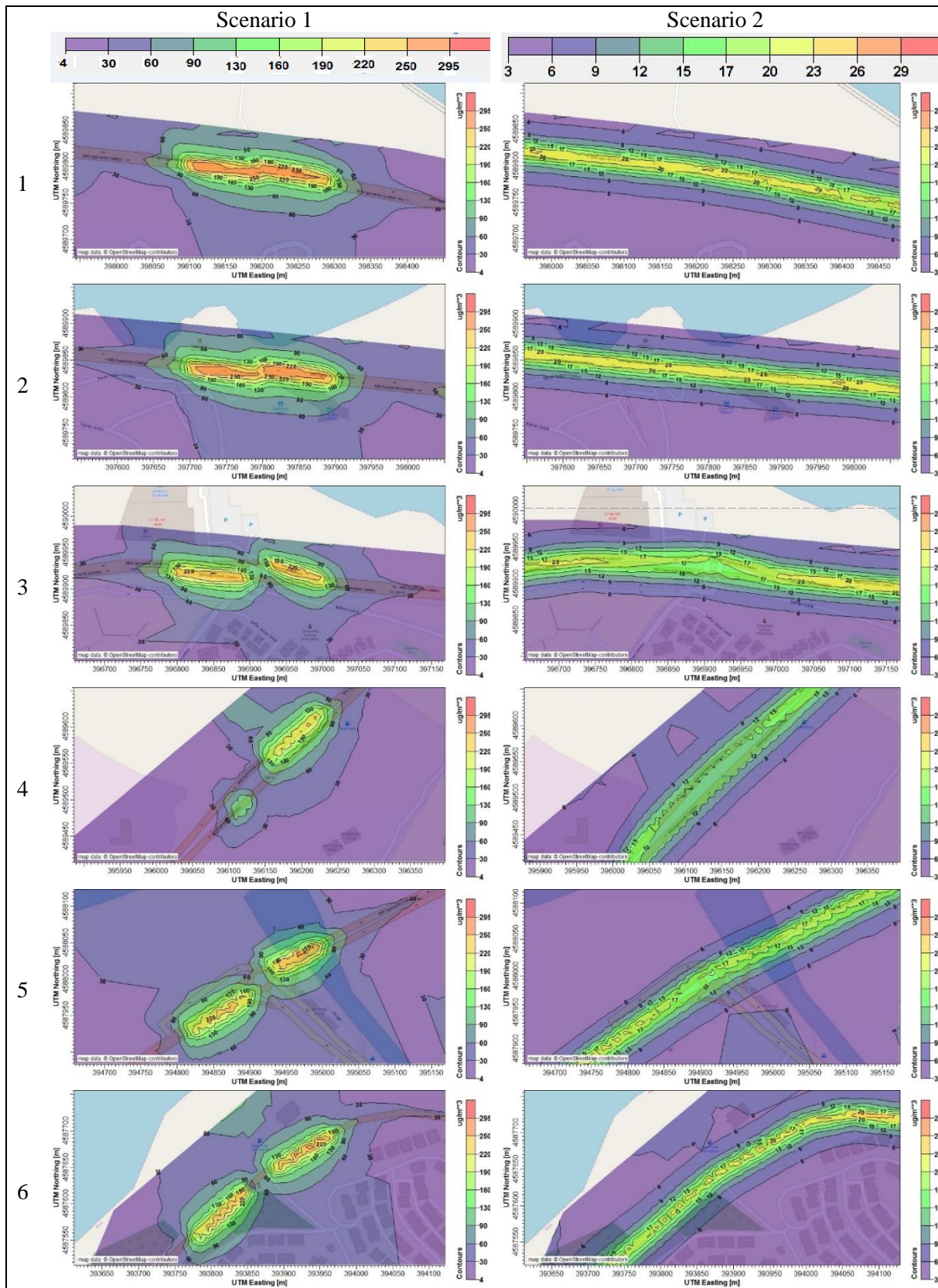


Figure 2. Modeling results at intersections

4. Conclusion

Motor vehicle emissions create air pollution problem in cities. Hotspot emissions occur generally as a result of idling activities of vehicles at intersection points. In this study, particulate matter emissions in one of the main roads in Zonguldak city has been determined by vehicle counting and emission inventory method. The total PM₁₀ emission was 96.7 kg year⁻¹ in the study area. After that, calculated emissions have been modelled by using CAL3QHCR to predict concentration of particulate matter. The maximum concentration was 292.1 µg m⁻³ for the 1st scenario while it was decreased to 29.1 µg m⁻³ for the 2nd scenario. So, it is proved that with the aid of signal optimization at intersections, the motor vehicle related air pollution could be reduced in cities.

5. References

- Abdul-Wahab, S.A., 2004. An application and evaluation of the CAL3QHC model for predicting carbon monoxide concentrations from motor vehicles near a roadway intersection in Muscat, Oman. *Environ. Manage.* 34, 372–382. doi:10.1007/s00267-004-0146-2
- Akay, M.E., Akgungor, A.P., 2008. Modeling of Traffic Signals Synchronisation Effect for Vehicle Emission Reduction. *J. Polytech.* 11, 51–56.
- Al-jeelani, H.A., 2013. The Impact of Traffic Emission on Air Quality in an Urban Environment. *J. Environ. Prot. (Irvine., Calif).* 4, 205–217. doi:10.4236/jep.2013.42025.
- Chart-asa, C., Sexton, K.G., Gibson, J.M., 2013. Traffic Impacts on Fine Particulate Matter Air Pollution at the Urban Project Scale: A Quantitative Assessment. *J. Environ. Prot. (Irvine., Calif).* 04, 49–62. doi:10.4236/jep.2013.412a1006.
- Demirarslan, K.O., Cetin Dogruparmak, S., 2018. Dispersion Modeling of Traffic Emissions originated from Mining: The Case of Artvin. *J. Nat. Hazards Environ.* 90, 11–21. doi:10.21324/dacd.420274.
- Demirel Bayik, G., Polat Alpan, M., Zeydan, O., Tanis, M., Bayik, C., 2018. Vehicle Emissions at Intersections Before and After Signal Improvement : Zonguldak Example. *Int. J. Adv. Mech. Civ. Eng.* 5, 33–37.
- EEA, 2016. EMEP/EEA air pollutant emission inventory guidebook 2016.
- Forehead, H., Huynh, N., 2018. Review of modelling air pollution from traffic at street-level - The state of the science. *Environ. Pollut.* 241, 775–786. doi:10.1016/j.envpol.2018.06.019.
- Gokhale, S., Raokhande, N., 2008. Performance evaluation of air quality models for predicting PM₁₀ and PM_{2.5} concentrations at urban traffic intersection during winter period. *Sci. Total Environ.* 394, 9–24. doi:10.1016/j.scitotenv.2008.01.020.
- Greco, S.L., Wilson, A.M., Hanna, S.R., Levy, J.I., 2007. Factors influencing mobile source particulate matter emissions-to-exposure relationships in the Boston urban area. *Environ. Sci. Technol.* 41, 7675–7682. doi:10.1021/es062213f.
- Mishra, V.K., Padmanabhamutry, B., 2003. Performance evaluation of CALINE3, CAL3QHC and PART5 in predicting lead concentration in the atmosphere over Delhi. *Atmos. Environ.* 37, 3077–3089. doi:10.1016/S1352-2310(03)00272-3.
- Nagendra, S.M.S., Khare, M., 2002. Line source emission modelling. *Atmos. Environ.* 36, 2083–2098. doi:10.1016/S1352-2310(02)00177-2.
- Sharma, N., Chaudhry, K.K., Chalapati Rao, C. V., 2007. Vehicular pollution prediction modelling : a review of highway dispersion models. *Transp. Rev. A Transnatl. Transdiscipl. J.* 24, 409–435.
- TUİK, 2018. Distribution of cars registered to the traffic according to fuel type [WWW Document]. URL http://www.tuik.gov.tr/PreIstatistikTablo.do?istab_id=1582, accessed in 9.20.19.



Uherek, E., Halenka, T., Borken-Kleefeld, J., Balkanski, Y., Berntsen, T., Borrego, C., Gauss, M., Hoor, P., Juda-Rezler, K., Lelieveld, J., Melas, D., Rypdal, K., Schmid, S., 2010. Transport impacts on atmosphere and climate: Land transport. *Atmos. Environ.* 44, 4772–4816. doi:10.1016/j.atmosenv.2010.01.002.

Woodcock, J., Edwards, P., Tonne, C., Armstrong, B.G., Ashiru, O., Banister, D., Beevers, S., Chalabi, Z., Chowdhury, Z., Cohen, A., Franco, O.H., Haines, A., Hickman, R., Lindsay, G., Mittal, I., Mohan, D., Tiwari, G., Woodward, A., Roberts, I., 2009. Public health benefits of strategies to reduce greenhouse-gas emissions: urban land transport. *Lancet* 374, 1930–1943. doi:10.1016/S0140-6736(09)61714-1.

Zhou, H., Sperling, D., 2001. Traffic emission pollution sampling and analysis on urban streets with high-rising buildings. *Transp. Res. Part D Transp. Environ.* 6, 269–281. doi:10.1016/S1361-9209(00)00029-8.

Acknowledgments

This project is funded by Zonguldak Bulent Ecevit University Scientific Research Fund (2018-77047330-02).

Estimating particulate matter (PM) concentrations from a meteorological index for data-scarce regions: a pilot study

Anzel de Lange¹, Rebecca M. Garland^{1,2} and Liesl L. Dyson¹

¹Department of Geography, Geoinformatics and Meteorology, University of Pretoria (UP), Hatfield, 0028, South Africa

²Council for Scientific and Industrial Research (CSIR), Climate Studies, Modelling and Environmental Health Research Group, Pretoria, 0001, South Africa

anzel.delange@up.ac.za

Abstract. In regions where air quality data are scarce or access thereto is limited, a comprehensive understanding of air pollution is hindered by a lack of emission data and ambient air pollution measurements. Therefore, in this pilot study, we assess the feasibility of estimating particulate matter (PM) mass concentrations from a meteorological index. Measured PM concentrations from air quality monitoring stations (2013–2016) situated in and around South African air pollution priority areas were analysed. Simulated meteorological parameters were used to calculate the newly-developed Air Dispersion Potential (ADP) index, which describes the meteorological potential for pollution dispersion in the atmosphere. For most conditions, there exists weak ($r=0.1-0.29$) to moderate ($r=0.30-0.49$) correlations between the ADP index and PM classes. At the three stations with adequate data availability, it was found that the ADP index was relatively successful in predicting conditions of high PM concentrations. An investigation of the effect of meteorological conditions on the diurnal variation of PM concentrations led to both the quantification of this effect, and the realization that at these diverse sites, up to 29% of variation in hourly PM concentrations can be explained by variations in meteorology. The application of the index in this way can play an important role in air quality management by quantifying the impacts of meteorological drivers on PM peaks.

Keywords: Air pollution, South Africa, particulate matter, air dispersion potential (ADP), meteorological parameters.

1. Introduction

A comprehensive understanding of air pollution in SA, and other developing countries, is hindered by the lack of emission and measured air pollution concentration data. It is improbable for air quality to improve in countries where these types of data are scarce (Fajersztajn et al., 2014). In SA, there is no default government emission inventory, emission factors and activity data are difficult to attain, and available datasets often contain large uncertainties (Garland et al., 2017; Naidoo et al., 2014). Only recently has the government developed a system for the reporting and tracking of annual emissions from regulated industrial sources (i.e. National Atmospheric Emissions Inventory System). Air quality modelling in SA is further complicated by the diverse and numerous emission sources contributing to the air pollution problem. These include emissions from sources as diverse as industry, vehicles, biomass burning, biogenic, domestic fuel use, waste burning, and wind-blown dust.

While there are some measurements of air quality in South Africa, in general, monitoring is limited. There is a countrywide network of air quality monitoring stations, however, making use of ground-based measured air pollution concentration data from compliance monitoring stations for research purposes in

SA is challenging. This is due in part to issues such as limited spatial and temporal coverage, and varying degrees of data quality. Many developing countries face large uncertainties in emissions and a lack of observational data, but still require an understanding of air quality in order to combat their pollution problems. Meteorological science is an important tool in the field of air pollution research. This is especially true when access to good quality air pollutant concentration and emission data are limited.

This pilot study investigates the possibility of using an index, calculated from simulated meteorological data, to estimate PM concentrations in SA, a region where emission data are not freely available and ambient PM data are limited. Defining a relationship between meteorological parameters and PM concentrations in SA could lead to the possibility of using these simulated meteorological parameters as a proxy for pollutant concentrations, or as a method to characterize variation in PM concentrations. The development of an index based on only simulated meteorological parameters has many benefits for countries lacking the capacity to forecast air pollution or the infrastructure to measure pollutant concentrations. Pollutant concentration forecasts can be vital in health and early warning systems for high-risk groups. Thus, a multi-parameter index is proposed and its performance in air quality hotspots in SA is assessed as a case study.

2. Air dispersion potential

In this paper, we present Air Dispersion Potential (ADP), a comprehensive and contemporary representation of the characteristics of air pollution dispersion. ADP is a joint probability distribution that considers the combined effect of relevant dynamic, thermodynamic, and turbulence processes that determine the conditions of air pollutant dispersion in the atmosphere. The ADP calculation is used to determine the potential for air to disperse pollutants based on three meteorological parameters; atmospheric stability in the form of Monin-Obukhov Length (MOL) and Mixing Height (MH), both measured in metres (m), as well as WS, which is measured in metre per second (ms^{-1}). The ADP index (Equation 1) is calculated per hour:

$$P(\text{ADP})=P(|V|)P(H)P(L) \quad (1)$$

where $|V|$ is wind velocity, $P(L)$ the appropriate atmospheric stability information, and $P(H)$ the mixing height (Swart, 2016). The unit of the ADP is m^3s^{-1} and its value describes how many cubic meters per second (ventilation rate) are passing through a certain point and thus, what the conditions are for the pollutants to diffuse.

The intervals for WS, MH, and MOL are quantified by proxy for very unfavourable, unfavourable, moderate, favourable, and very favourable for pollution dispersion (Table 1).

Table 1. Wind Speed (WS), Mixing Height (MH) and Monin-Obukhov Length (MOL) intervals, as well as resultant ADP value ranges

Meteorological parameter	Very unfavourable	Unfavourable	Moderate	Favourable	Very favourable
WS	0 to 0.2 m s^{-1}	0.3 to 1.5 m s^{-1}	1.6 to 3.3 m s^{-1}	3.4 to 5.4 m s^{-1}	> 5.4 m s^{-1}
MH	0 to 200 m	> 200 to 400 m	> 400 to 500 m	> 500 to 800 m	> 800 m
MOL	10 to 200 m	200 to 500 m	> 500 or < -500 m	-200 to -500 m	-50 to -200 m
ADP	20	> 20 to 40	> 40 to 60	> 60 to < 80	>= 80

3. Data and methodology

3.1. Study region

All the air quality monitoring stations investigated are located in South Africa's industrialized regions (Figure 1). Their location in, or in close proximity to residential and rural areas, mines and power stations, make for elevated pollution. Five air quality monitoring stations were chosen for this study based on their location (near or in the declared priority areas), site classification, types of pollutants monitored, and availability of data.

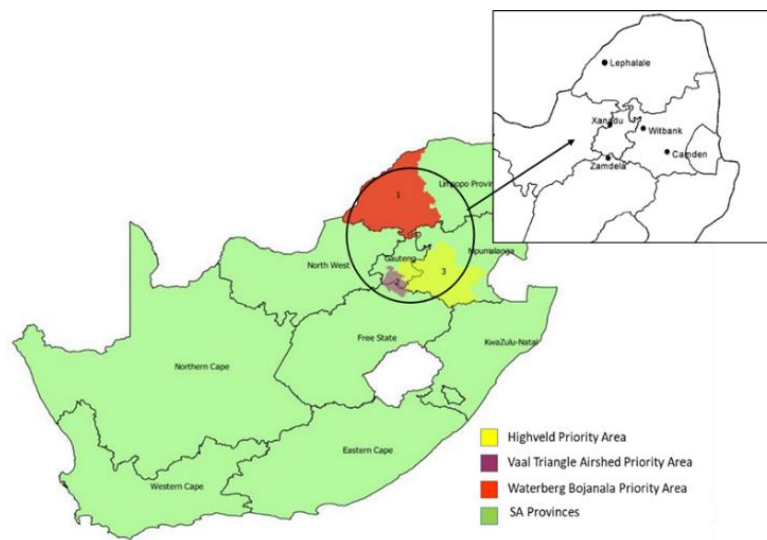


Figure 1. South African Air Quality Priority Areas; the insert shows the locations of five sites chosen for this study (Adapted from SAAQIS, 2018)

3.2. Measured hourly PM concentrations

The South African Air Quality Information System (SAAQIS) website provides researchers and stakeholders with air quality and some meteorological data at locations throughout the country. Hourly PM concentration and wind-speed data for five ambient air pollution measurement stations were obtained for the period 2013 to 2016 from SAAQIS. The hourly WS data were used for the verification of simulated WS produced by the meteorological model, while PM concentrations are used to investigate its relationship with the ADP index.

Data Quality Control (QC) includes the removal of unrealistic values, negative values, and, repeated values; repeated values were identified as periods where more than two hourly values in a row were exactly the same (US EPA, 2017; Zahumensky, 2004). The availability of hourly PM concentration data after the QC procedure for each site was as follows: Xanadu (38.77%), Lephalale (94.03%), Camden (65.76%), Zamdela (66.34%), and Witbank (82.73%).

3.3. The air pollution model (TAPM)

The Air Pollution Model (TAPM), developed by the Australian CSIRO Atmospheric Research Division, is a prognostic air pollution model that also simulates meteorology (Hurley, 2008). The meteorological component of TAPM was used to simulate hourly meteorological parameters, for the period 2013 to 2016, as required for the calculation of the ADP index. The model simulations were set up to run with four nested grids of 27 km, 9 km, 3 km and 1 km resolution. The grids were chosen in this way so that a resolution of 1 km could be achieved for the inner grid. Meteorological parameters were simulated for specific station locations. Therefore, the model output was at the location of the observational stations,

and it was not necessary to adopt any interpolation scheme (other than those used by TAPM) to extract the simulated meteorology.

3.4. Evaluation of relationships and ADP index performance

In order to statistically investigate the relationship between PM concentrations and the ADP index, both variables are classed according to predetermined intervals. Categories used for PM concentrations are site specific and based on 20th percentiles of the actual measured pollutant-concentration data after quality correction. Very favourable ADP and very low PM concentrations were allocated classifications of 5, while very unfavourable ADP and very high concentrations of PM were classed as 1 (Table 2). This process assists in establishing a relationship between the two variables.

Visually examining the bivariate data with the use of a scatterplot (not shown) was the first step to find a relationship. Thereafter, the classed data were ranked and the Spearman rank correlation coefficient (r) was calculated in order to statistically measure the degree of relationship between the two variables (Wilks, 2011). The strength of the absolute value of the Spearman rank correlation coefficient is classified as follows: Small/weak: $r=0.1$ to 0.29 ; medium/moderate: $r=0.30$ to 0.49 ; and large/strong: $r=0.50$ to 1.0 (Cohen, 1988).

Table 2. Description of all PM concentration and ADP classifications. Class combination used to assess ADP's performance as predictor are underlined

		PM concentration classes				
		1	2	3	4	5
ADP classes	1	<u>ADP very unfavourable, PM concentrations very high (CLASS 1)</u>	ADP very unfavourable, PM concentrations high	ADP very unfavourable, PM concentrations moderate	ADP very unfavourable, PM concentrations low	ADP very unfavourable, PM concentrations very low
	2	ADP unfavourable, PM concentrations very high	<u>ADP unfavourable, PM concentrations high (CLASS 2)</u>	ADP unfavourable, PM concentrations moderate	ADP unfavourable, PM concentrations low	ADP unfavourable, PM concentrations very low
	3	ADP moderate, PM concentrations very high	ADP moderate, PM concentrations high	<u>ADP moderate, PM concentrations moderate (CLASS 3)</u>	ADP moderate, PM concentrations low	ADP moderate, PM concentrations very low
	4	ADP favourable, PM concentrations very high	ADP favourable, PM concentrations high	ADP favourable, PM concentrations moderate	<u>ADP favourable, PM concentrations low (CLASS 4)</u>	ADP favourable, PM concentrations very low
	5	ADP very favourable, PM concentrations very high	ADP very favourable, PM concentrations high	ADP very favourable, PM concentrations moderate	ADP very favourable, PM concentrations low	<u>ADP very favourable, PM concentrations very low (CLASS 5)</u>

Contingency tables were used to verify categorical forecasts and to show the joint distribution of forecast and observations in various categories (Jolliffe and Stephenson, 2012). In order to calculate statistics from contingency tables, all data was classified as hits (event forecasted and observed); misses (event not forecasted, but observed); false alarms (event forecasted, but not observed); and correct negatives (event forecasted not to occur and was not observed). When evaluating the ADP index performance, we considered statistics calculated from a multi-category contingency table as described in Table 3.

3.5. Quantifying the effect of meteorology on diurnal PM variation

We consider known patterns in emissions and meteorology (diurnal and weekday/weekday variation) to attempt to estimate the effects of emissions and meteorological conditions on PM concentration levels. We attempt to quantify the impact of meteorological drivers, like the changing PBL, on PM peaks. Diurnal variations of PM concentrations were examined in order to identify the optimum period of study at each site. Thereafter, the Coefficient of Determination (R^2) was calculated during the relevant hours. Wilks (2011) defines R^2 as the “proportion of variation in the predictand that is described or accounted for by the regression”. Based on the preceding information, the effect of change in meteorological conditions (represented by the ADP index) on PM concentrations is quantified as a percentage (%) deduced from the R^2 statistic.

Table 3. Description, equation and ranges for the chosen categorical statistics, which include; POD (Probability of Detection), SR (Success Ratio), and FAR (False Alarm Ratio) (Adapted from CAWCR, 2015; Done et al., 2004)

Statistic	Description	Equation	Range	Perfect score
POD	POD (hit rate) gives an indication of the observed events in classes that were correctly forecasted. POD does not consider false alarms.	$POD=H/(H+M)$	0 to 1	1
SR	SR gives an indication of the forecasted events in classes that were correctly observed. SR does not consider misses.	$SR=H/(H+FA)$	0 to 1	1
FAR	FAR is an indication of the predicted events that did not occur.	$FAR=FA/(FA+CN)$	0 to 1	0

4. Results

4.1. Identifying relationships

The distribution of PM_{10} , $PM_{2.5}$ and PM_1 per ADP class was investigated. The dominant ADP class for all observations is Class 2, this may be interpreted as meaning that most of the hours with PM observations experienced unfavourable conditions for pollution dispersion. The dominant class combination is PM Class 1 (high pollutant concentration) and ADP Class 2 (unfavourable conditions). Very unfavourable ADP conditions (Class 1) occur the least.

In order to investigate the strength of the relationship between ADP and PM classes, correlations between the two datasets were calculated (Table 4). The entire period, summer (DJF), and winter (JJA) are investigated to identify the conditions under which ADP and PM classes show the strongest correlation.

Table 4. Correlations (r) between ADP and PM classes for the entire period, summer and winter. The underlined values show correlations of moderate strength (0.30–0.49)

Station name	Period		Summer (DJF)			Winter (JJA)			
	PM_{10}	$PM_{2.5}$	PM_1	PM_{10}	$PM_{2.5}$	PM_1	PM_{10}	$PM_{2.5}$	PM_1
Xanadu	0.13	0.22		0.07	0.14		<u>0.31</u>	<u>0.48</u>	
Lephalale	0.22	0.22		0.08	0.08		<u>0.34</u>	<u>0.38</u>	
Camden	0.18	<u>0.31</u>		0.20	0.24		0.11	<u>0.46</u>	
Zamdela	0.22	0.24		0.21	0.20		0.25	<u>0.32</u>	
Witbank	0.10	<u>0.36</u>	<u>0.46</u>	-0.02	<u>0.30</u>	<u>0.41</u>	0.07	<u>0.41</u>	<u>0.48</u>

Although the correlations between ADP and PM classes vary only from weak (0.1–0.29) to moderate (0.30–0.49) strength, most are at least positive. This means that higher classes (more favourable) ADP

are related to higher classes (lower concentrations) of PM. All correlation coefficients in Table 4 have calculated p-values less than 0.05; this means that the observed differences between PM concentration and ADP index classes are unlikely to be due to chance.

Xanadu and Lephalale have relatively good correlations in the winter for both PM₁₀ and PM_{2.5}, and very weak correlations in the summer. At Zamdela, correlations are between 0.20 and 0.32 for all cases. For all sites, except PM₁₀ at Camden, the correlation between ADP and PM classes is stronger in the winter. In most of the cases considered, coarse particulates show a weaker relationship between their PM classes and ADP, and fine particulate show more promising results with medium-strength relationships, especially during winter. It is well documented that higher concentrations of PM_{2.5} and PM₁₀ are associated with stable atmospheric conditions, low wind speeds, and the occurrence of inversion layers (Czernecki et al., 2017; Di Virgilio et al., 2018; Perrino et al., 2008; Xu et al., 2018). The results suggest that, because PM_{2.5} presents stronger correlations with the ADP index than PM₁₀, it is influenced by these meteorological variables to a larger extent. Additionally, at higher wind speeds, PM₁₀ concentrations in some areas may increase due increased wind-blown dust. This influences the relationship between PM₁₀ and WS classes, because larger WS could lead to higher PM₁₀ concentrations.

Wet deposition plays an important role in the removal of PM, especially fine particulates, from the atmosphere (Wu et al., 2018). The process of wet deposition might negatively affect the correlations between the ADP index and PM concentration classes as rainfall is not considered in the ADP index. The study region is situated in the austral summer rainfall region of SA (Tyson and Preston-Whyte, 2000). Therefore, the process of wet deposition may explain some of the weaker correlations in Table 4 during summer.

4.2. Forecast performance

Data contained in multi-category contingency tables are used to assess the performance of ADP as a predictor in the different classes. Plotted in Figure 2 are POD, SR and FAR for Zamdela, Lephalale and Witbank. POD and SR are plotted together with the FAR, in order to assess the performance of ADP as a forecasting tool. Lephalale in winter produces a high SR score in Class 1. This means that a relatively large fraction of Class 1 PM events forecasted by ADP were observed correctly. However, this score may be misleading because of the small fraction (<1%) of events forecasted in Class 1. FAR is also at its lowest level (0.5) in Class 1. In contrast to Class 1, Class 2 has a high POD score, which translates to Class 2 having many PM-observed events that were correctly forecasted by ADP, for both summer and winter.

In both summer and winter, Zamdela has a relatively high FAR for all classes, never dropping below 0.6. The best performing class with respect to POD is Class 2, whereas Class 5 has the highest score for SR. POD for the forecasts in Class 1, in both seasons, are close to zero. The fact that POD scores in Class 1 are close to zero means that there were very little forecasts for very unfavourable ADP for Zamdela. Witbank has relatively high SR for Class 1 in winter, and POD is the highest in Class 2 for both summer and winter.

The poor performance of ADP forecasts in Class 1 are due to very few hours (less than 1%) being classed as having very unfavourable conditions for ADP. In future research, it would be worthwhile to reconsider the MOL, MH and WS intervals used in the ADP calculation in order to improve ADP forecasts, and decrease false alarms, in Class 1.

4.3. Effect of meteorology on diurnal PM variation

In this section, we consider known patterns in emissions and meteorology (diurnal and weekday/weekend variation) to estimate the effects of emissions and meteorological conditions on PM concentration levels. There is no significant difference in the strengths of weekday and weekend correlations between ADP and PM (not shown). Therefore, we can conclude that the weekday/weekend

variances in emissions are not driving the relationship between ADP and PM for the sites considered here.

The next aspect to consider the diurnal variation of PM concentrations. Meteorological conditions (represented by the ADP index) have an effect on the morning decrease and afternoon increase of PM concentrations. This effect was calculated for Lephalele, Zamdela and Witbank, in both summer and winter periods. Lephalele results are presented in detail in Figure 3, while all sites are summarized in Table 6. PM concentration levels at Lephalele follow the typical diurnal variation, with two PM peaks (morning and evening) and a minimum at noon, as expected (Mdluli, 2008; Hersey et al., 2015). The percentages displayed on Figure 3 are based on the R^2 statistic (Coefficient of Determination) and display the proportion of variation in PM that is accounted for by ADP. The afternoon increase in PM concentrations is largely affected by the onset of unfavourable conditions for pollution dispersion in the evening, especially during winter (29% PM_{10} , 24% $PM_{2.5}$).

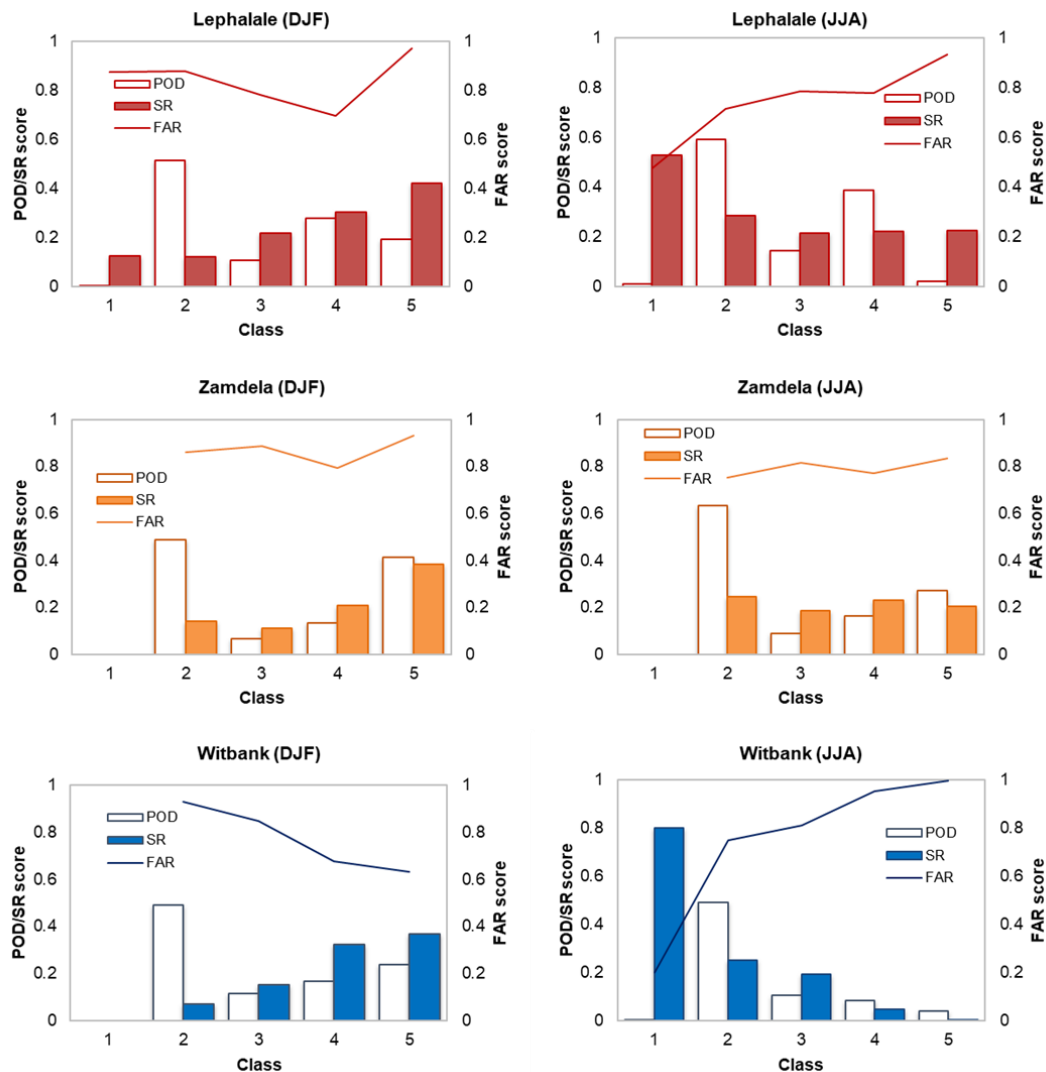


Figure 2. Probability of detection (POD), success ratio (SR), and False Alarm Ratio (FAR) scores for Zamdela, Lephalele and Witbank in both the winter (JJA) and the summer (DJF) for PM_{10} . High POD and SR scores (close to 1) indicate better performance, whereas lower FAR scores (close to 0) indicate a better forecast with less false alarms. Classes 1 to 5 on the x-axis refer to the class combinations, as described in Table 4. $PM_{2.5}$ graphs (not shown) exhibit very similar patterns for all sites

Zamdela PM concentrations have a morning and afternoon peak in winter and summer. At this site, afternoon PM increases are influenced more by the change in meteorological conditions, than PM decreases in the mornings (Table 6). Witbank PM₁₀ concentrations are less dependent on changes in meteorological conditions than PM_{2.5}. Considering PM₁₀ in winter, only 10% of the morning decrease and 13% of the afternoon increase in concentrations is attributed to change in ADP, compared to 27% and 26% for PM_{2.5}. This is also true during the summer months, when PM_{2.5} is more dependent on change in meteorological conditions than PM₁₀.

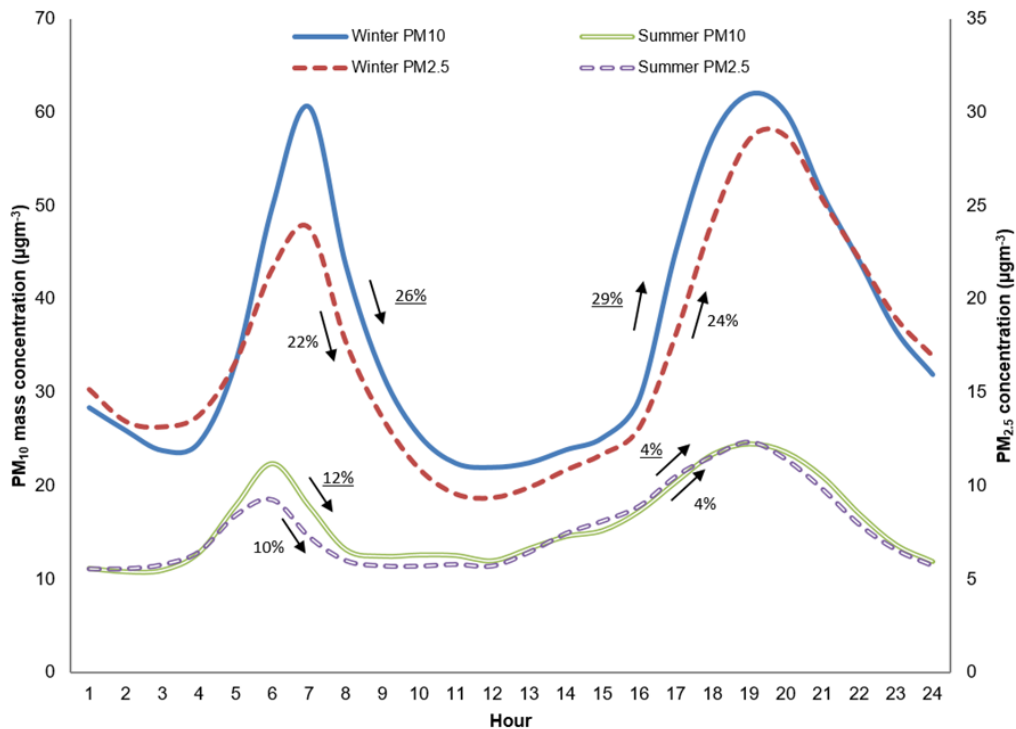


Figure 3. Diurnal variation of PM₁₀ and PM_{2.5} concentrations (μgm^{-3}) at Lephalale for both winter and summer. Arrows and percentages (PM₁₀ underlined) indicate the direction and amount of change in PM concentrations attributed to the change in meteorological conditions (i.e. ADP)

PM concentrations levels are affected by meteorological conditions studied to a different degree at each site, but there are some common threads. In general, meteorological conditions have a stronger influence on the diurnal variation of PM concentrations in the winter as compared to the summer, and the afternoon increase in PM concentrations is influenced more by a change in the meteorological conditions than the morning decrease.

Table 6. Percentage change in PM concentrations attributed to the change in meteorological conditions for all sites investigated

	PM ₁₀				PM _{2.5}			
	Winter		Summer		Winter		Summer	
	PM decrease	PM increase	PM decrease	PM increase	PM decrease	PM increase	PM decrease	PM increase
Zamdela	6%	24%	4%	13%	12%	22%	6%	11%
Lephalale	26%	29%	12%	4%	22%	24%	10%	4%
Witbank	10%	13%	0.3%	1%	27%	26%	9%	9%

The onset of “bad” meteorology (unfavourable conditions) in the afternoon has a significant effect on PM concentrations at most sites, especially in the winter. “Good” meteorology, associated with the mixed layer, influences the decrease in PM concentrations, but to a lesser extent than unfavourable conditions, in most cases. Diurnal variation in PM concentrations, at the sites investigated, is dominated by variability of emissions rather than meteorological conditions contained in the ADP index.

Here we investigated the PM concentration slopes that should be highly influenced by the variables contained in the ADP index. The remaining two slopes (PM increase in the morning and PM decrease in the evening) should not be affected by these meteorological parameters to the same extent. Therefore, when R^2 for the remaining slopes were calculated, all results were less than those presented in Table 6. On average across all sites, the influence of change in ADP on morning PM increase was 2.7%, and on evening PM decrease, only 1.3%.

5. Discussion and conclusions

There exists a relationship between PM classes and ADP; PM concentration classes are positively correlated with ADP classes under all circumstances investigated. Due to the inverse relationship between meteorological parameters such as WS, MH, MOL and pollutants in the atmosphere, this result is expected. PM_{10} has a weaker relationship with ADP, and $PM_{2.5}$ performs best in most cases. Correlation coefficients vary from weak to moderate. On average, the degree of relationships in summer is weaker than in winter. A possible explanation for this phenomenon is the fact that all sites investigated are situated in the summer rainfall region of SA.

The forecast performance was assessed (using SR, POD and FAR); all sites produced very similar results for PM_{10} and $PM_{2.5}$. A combination of POD and SR scores indicated that, for all cases, ADP predictions work best in the frequently occurring Class 2. Class 2 represents unfavourable ADP and high PM concentrations. Since there are serious health risks associated with high concentrations of particulate pollution, this is a significant result. Non-meteorological influences contribute to weak correlations, POD scores, and SR scores.

The ADP index, as used in this pilot study, is not sufficient to estimate PM concentration at the sites considered because of relatively weak correlations, and low SR and POD scores. The ADP index may be applied elsewhere, but further research and optimization of the index for South African conditions is recommended first. MOL, MH and WS intervals need to be re-evaluated in order to find the ideal thresholds for use in SA. In future research, precipitation could be included in the index to account for the effect that rainfall has on ADP index performance. Although this might add value to the index, accurately forecasting hourly precipitation is not a trivial task, especially due to the spatial heterogeneity of rainfall over the study region. Further research could therefore include the index being tested at appropriate background sites. The forecast capabilities of the ADP index may also be significantly improved by a complete dataset of good quality PM concentration data from a well-maintained monitoring station.

The typical morning decrease in PM concentrations (coincides with the formation of the mixed layer), and afternoon increase of PM concentrations (coincides with the formation of the stable boundary layer) is influenced, to a degree, by the meteorological variables contained in the ADP calculation. Using the R^2 statistic to describe this influence has led to the quantification of the influence of “good” (favourable) and “bad” (unfavourable) meteorological conditions on PM concentrations. These findings allowed us to quantify the impact that these meteorological variables (i.e. ADP) have on the diurnal cycle of the PM. The application of this index in this way can play an important role in air quality management when quantifying the impacts of drivers of PM peak concentrations.

It was found that each site is affected differently by meteorological factors, but in general, ADP has a stronger effect on the diurnal variation of PM concentrations in the winter. The afternoon increase in PM concentrations is also influenced more by meteorology than the morning decrease. For both PM₁₀ and PM_{2.5}, ADP accounted for more than 20% of the afternoon increase in PM levels at 2 of the 3 sites studied in the winter. This is an important result for air quality management in the area, as it quantifies, for the first time to our knowledge, the role that meteorology plays in this diurnal cycle across these sites, and highlights the large role that emissions play in the diurnal cycle.

6. References

- Cohen, J., 1988. Statistical power analysis for the Behavioral Sciences, second ed., Lawrence Erlbaum Associates, New Jersey.
- Collaboration for Australian Weather and Climate Research (CAWCR), 2015. <http://www.cawcr.gov.au/projects/verification/>, accessed in June 2018.
- Czernecki, B., Pórolniczak, M., Kolendowicz, L. Marosz, M., Kendzierski, S., Pilgaj, N., 2017. Influence of the atmospheric conditions on PM₁₀ concentrations in Poznań, Poland. *J. Atmos. Chem.* 74, 115-139.
- Di Virgilio, G., Hart, M.A., Jiang, N., 2018. Meteorological controls on atmospheric particulate pollution during hazard reduction burns. *Atmos. Chem. Phys.*, 18, 6585-6599.
- Done, J., Davis, C., Weisman, M., 2004. The next generation of NWP: Explicit forecasts of convection using the weather research and forecasting (WRF) model. *Atmos. Sci. Lett.* 5, 110-117.
- Fajersztajn, L., Veras, M., Barrozo, L., Saldiva, P., 2014. Air monitoring coverage in low-income countries: An observational study. *Lancet.* 384, S14.
- Garland, R.M., Naidoo M., Sibiyi, B., Oosthuizen, R., 2017. Air quality indicators from the Environmental Performance Index: Potential use and limitations in South Africa. *Clean Air J.* 27, 33-41.
- Hersey, S.P., Garland, R.M., Crosbie, E., Shingler, T., Sorooshian, A., Piketh, S., Burger, R., 2015. An overview of regional and local characteristics of aerosols in South Africa using satellite, ground, and modeling data. *Atmos. Chem. Phys.* 15, 4259-4278.
- Hurley, P., 2008. TAPM V4. Part 1: Technical description. CSIRO Marine and Atmospheric Research Paper No. 25. ISBN: 978-1-921424-71-7.
- Jolliffe, I., Stephenson, D., 2012. Forecast verification: A practitioner's guide in atmospheric science, second ed. John Wiley & Sons, New Jersey. ISBN: 978-0-470-66071-3.
- Mdluli, T., 2008. The societal dimensions of domestic coal combustion: People's perceptions and indoor aerosol monitoring. Ph.D. Thesis. University of the Witwatersrand, Johannesburg, South Africa, 170 pages.
- Naidoo, S., Piketh, S., Curtis, C., 2014. Quantification of emissions generated from domestic burning activities from townships in Johannesburg. *Clean Air J.* 2, 34-41.
- Perrino, C., Catrambone, M., Pietrodangelo, A., 2008. Influence of atmospheric stability on the mass concentration and chemical composition of atmospheric particles: A case study in Rome, Italy. *Environ. Int.* 34, 621-628.
- South African Air Quality Information System (SAAQIS), 2018. <http://www.saaqis.org.za/Default.aspx>, accessed in February 2018.
- Swart, A., 2016. Assessment of the baseline meteorological and air quality conditions over Uubvlei, Oranjemund, Namibia. M.Sc. Dissertation, University of Pretoria, Pretoria, South Africa, 94 pages.



Tyson, P.D., Preston-Whyte, R.A., 2000. The weather and climate of Southern Africa. Oxford University Press Southern Africa, Cape Town, South Africa. ISBN: 978-0-195-71806-5.

US EPA (United States Environmental Protection Agency), 2017. QA Handbook for air pollution measurement systems: Volume II: Ambient air quality monitoring program. EPA-454/B-17-001.

Wilks, D., 2011. Empirical distributions and exploratory data analysis. Statistical Methods in the Atmospheric Sciences, third ed. International Geophysics Series, Volume 100, Academic Press.

Wu, Y., Liu, J., Zhai, J., Cong, L., Wang, Y., Ma, W., 2018. Comparison of dry and wet deposition of particulate matter in near-surface waters during summer. PLOS ONE 13, e0199241.

Xu, Y., Xue, W., Lei, Y., Yang, Z., Cheng, S., Ren, Z., Huang, Q., 2018. Impact of Meteorological Conditions on PM_{2.5} Pollution in China during Winter. Atmosphere. 9. 429.

Zahumensky, I., 2004. Guidelines on quality control procedures for data from automatic weather stations. WMO-No. 955. Geneva, Switzerland.

Acknowledgements

The authors acknowledge South African Department of Environmental Affairs, ESKOM and The South African Weather Service (SAWS) for the use of their PM and meteorological data, and SAWS for providing pollutant concentration and some meteorological data for all investigated sites through SAAQIS. This work was supported by SASOL through the Laboratory for Atmospheric Studies (LAS) at the University of Pretoria. The authors extend appreciation to the late Professor George Djolov without whom this research would not have been possible.

Experimental investigation of co-combustion of biocoal with Soma lignite in a 30 kWth circulating fluidized bed

Babak Keivani¹, Hayati Olgun¹ and Aysel T. Atimtay²

¹Ege University, Solar Energy Institute, 35100 Bornova, Izmir, Turkey

²Middle East Technical University, Department of Environmental Engineering, 06800 Ankara, Turkey

ayselatimtay@gmail.com

Abstract. This work covers co-combustion of biocoal obtained from red pine with Soma lignite in a 30 kW-thermal capacity circulating fluidized bed combustor (CFBC) system in air and oxygen-enriched atmosphere. The combustor was of 108 mm inside diameter and 6 m height. The combustion temperature was held at 850+50°C. Oxygen enriched combustion tests were carried out at different ratios of lignite and biocoal mixtures. Biocoal was produced from red pine wood chips under 300°C and 30 min conditions by a screw type torrefaction system. Biocoal share in the fuel mixture was increased up to 50% by wt. It was found that the fuel mixtures up to 50% by wt. of biocoal were combusted effectively in the system. The oxygen concentration in the oxidant was varied between 21 and 28% by vol. for the oxygen-enriched combustion experiments. Flue gas emissions were measured by Gasmeter DX-400 flue gas analyser. The results showed that biocoal can be a good additive fuel to lignite coal and oxygen-enriched co-combustion is an option for reducing flue gas emissions of SO₂, CO and N₂O. Particularly high oxygen concentrations reduced CO emissions. Also high level of biocoal addition significantly reduced SO₂ emissions. In contrast, NO_x emissions increased with high oxygen concentrations and high levels of biocoal addition.

Keywords: Biomass, Torrefaction, Biocoal, Oxygen enriched combustion, Circulating fluidised bed combustion.

1. Introduction

The total recoverable and usable biomass energy potential of Turkey was estimated as 17 million tonnes of oil equivalent (mtoe) (Saracoglu, 2015). It is estimated by General Directorate of Forestry (GDF) that the annual sustainable forest residue potential is approximately 5 to 7 million tons. The maximum production potentials of fire wood, forest residues and shrubs vegetation are in the Mediterranean Region of Turkey (Saracoglu, 2015). Therefore, the conversion of these forest residues to combustible solid fuels is crucial for Turkey's sustainable energy production. However, this potential cannot be used effectively for the energy demand of the country with conventional combustion technologies. Especially the transportation of these forest residues to energy conversion centers is a problem. On the other hand, Turkey is a rich country in lignite resources. Turkey's proved recoverable lignite reserves were 14.76 billion tonnes in 2015. The calorific values of these lignites are usually medium to low, ranging from 1000 to 5000 kcal/kg. The distribution of heating values is 1 % over 4001 kcal/kg, 4 % between 3001-4000 kcal/kg, 22 % between 2001-3000 kcal/kg, 70 % between 1001-2000 kcal/kg and 3 % below 1000 kcal/kg (Ersoy, 2015). These lignites generally have high sulphur and ash contents. Turkey imports 72% of its total primary energy demand. This demand increases every year because Turkey's development rate is about 4-5 %/year which requires large amount of energy. Therefore, it will be wise to use lignite

and biomass sources together in clean energy production with a suitable combustion technology. A suitable technology for burning low calorie, high ash and high sulphur fuels with biomass can be co-firing in fluidized bed or in pulverized combustion (Varol et al., 2014; Atimtay et al., 2017). One of the advantages of co-firing is to use an existing plant to burn two fuels together which may be more economical and more environmentally friendly. Biomass co-firing has the potential to reduce emissions from coal-fuelled power plants. Contribution of biomass to emission reduction in co-firing with coal is limited due to its different structure and due to transportation difficulties. However, it is possible to increase this contribution by torrefaction of biomass and by obtaining biocoal which is similar to lignite coal. Generally, biomass has low volumetric energy density, high moisture content and hydrophilic nature that leads to higher costs in transportation, storage and processing. Using woody biomass directly as a fuel for combustion/co-combustion systems is challenging due to its fuel properties as compared to lignites. Therefore, the use of biomass together with coal in power plants is limited. One way to increase the use of woody biomass in energy systems is to turn biomass into biocoal by torrefaction. Torrefaction, which is a thermal pre-treatment process, is a viable technology that significantly alters the physical and chemical composition of the biomass (Tumuluru et al., 2011). Torrefaction is defined as heating biomass slowly in an inert environment in a temperature range of 200–300°C. This process improves the physical, chemical and biochemical composition of the biomass, making it to perform better for co-firing and gasification purposes.

Increase of fossil fuel consumption in the world leads to increase of CO₂ emissions. Recent CO₂ concentration in the atmosphere has reached to 414 ppm (NASA 2019). Co-combustion of biomass with lignite in existing coal power plants has a potential to reduce CO₂ emissions. Additionally, biomass causes lower SO₂ and N₂O emissions due to low sulphur and nitrogen content.

Oxy-fuel combustion has an emerging carbon capture and storage (CCS) technology for new and existing power plants where the fuel is burned in a mixture of oxygen and recycled flue gas (RFG) instead of air. This produces a flue gas consisting mainly of carbon dioxide and water vapour. One of the applications of oxy-fuel combustion is Oxygen Enriched Combustion (OEC) where combustion takes place in increased oxygen concentration. Pure oxygen is added to the combustion air and thus oxygen concentration is increased in the oxidant stream.

In this study, biocoal produced in a pilot continuous torrefaction system up to 5 kg/h biomass capacity was used for co-combustion. Operating conditions of the torrefaction system were optimized according to the characteristics of Turkish lignites. Detailed information about this system is given elsewhere (Olgun and et al., 2016). This work covers co-combustion of biocoal obtained from red pine with Soma lignite in a 30 kW-thermal capacity circulating fluidized bed combustor (CFBC) system under air and oxygen-enriched atmosphere. In the experiments, the lignite coal was burned alone as well as in a mix with biocoal obtained from red wood pine. The biocoal portion in the fuel mix was increased up to 50% by wt starting with Soma lignite only.

2. Materials and methods

2.1. Fuel and bed material

In this study, Soma lignite and biocoal was used as fuels. Biocoal was produced from red pine wood chips in a laboratory scale 5 kg/h screw type “continuous torrefaction system” which was installed in Ege University. Fuel analyses were performed according to the ASTM procedures given in Table 1. Proximate analysis was performed with a LECO TGA 701 Thermogravimetric Analyser. LECO AC350 bomb calorimeter was used to measure the higher heating value of the fuels. Ultimate analysis was performed with LECO Truspec CHN-S device (Atimtay et al., 2017; Engin and Atakul, 2016). Ultimate, proximate analysis and heating values of the fuels are given in Table 2.

Table 1. Standards used for analysis of the raw biomass and the different biocoals prepared in this study

Ultimate Analysis	Standard Used	Proximate Analysis	Standard Used
C	ASTM D 5373-14	Moisture	ASTM D 7582-12
H	ASTM D 5373-14	Ash	ASTM E 1755-01
N	ASTM D 5373-14	Volatile Matters	ASTM D 7582-12
S	ASTM D 4239-14	Fixed Carbon	ASTM D 3172-13
Ash	ASTM E 1755-01		
Moisture	ASTM D 7582-12	HHV	ASTM D 5865-13
O	ASTM D 3176-09	HGI	ASTM D5003

Table 2. Fuel analysis

	Soma lignite (S)	Red pine biomass (BIO)	Biocoal from redpine (BC)
Moisture (wt%)	5.14	9.81	0.79
Volatile Matter, VM (wt%)	32.78	73.76	39.22
Ash (wt%)	40.49	0.89	1.50
Fixed Carbon, FC (wt%)	21.60	15.54	58.49
C (wt%)	42.40	44.93	68.9
H (wt%)	1.84	5.88	5.78
N (wt%)	0.84	0.32	0.63
S (wt%)	0.73	0.03	0.08
O (wt%) (by difference)	11.51	47.94	23.04
LHV* (kcal/kg) Original (wt%)	2515	3816	5356
Dry (wt%)	3221	4447	5619
HHV (kcal/kg) Original (wt%)	2743	4188	5628
Dry (wt%)	3375	4776	5879
HGI	64	23	104

(LHV*: Lower Heating Value, HHV: Higher Heating Value, HGI: Hardgrove Grindability Index)

It can be seen from the tables that the heating value the biocoal is higher than Soma lignite. The bed inert material was silica sand (99.5% SiO₂) with an average particle size of 0.34 mm, a particle density of 2.4 g/cm³, and a bulk density of 1.7 g/cm³. Between 4.5 and 4.75 kg of silica sand was used as bed material during experiments. The test matrix for OEC is given in Table 3.

Table 3. Test matrix for OEC combustion

Fuels (Soma lignite: S; Biocoal:BC), (% by wt.)	O ₂ ratio in air (% by vol.)
S	21, 23, 26, 28
90 % S + 10 % BC	21, 23, 26, 28
80 % S + 20 % BC	21, 23, 26, 28
70 % S + 30 % BC	21, 23, 26, 28
50 % S + 50 % BC	21, 23, 26, 28

2.2. Experimental system and procedure

The pilot scale CFBC system consists of fuel feeder, combustor reactor, cyclones, down comer, ash removal and collection port, FD fans and ID fan, air and combustor heaters, chimney (Varol et al., 2014; Kayahan et al., 2016) (Figure 1). The combustor reactor is made of 300 AISI 310 stainless steel pipe of 108 mm inner diameter and 6 m height. There are 6 electrical air heaters on air duct and 8 electrical air heaters on the combustor column. Air is fed into the system by an air blower (FD fan) with a head

pressure of 200 mbar. Fuel is fed by screw feeders. Fuel feeding rate is controlled by a frequency controller. Oxygen flow rate is controlled by mass flow controller (MFC). Temperature, pressure and flow rates through the system are measured and controlled by SIEMENS Win CC SCADA system. The oxygen concentration in the inlet stream is analysed by ABB Magnos 206 paramagnetic online oxygen analyser and flue gas at the outlet is analysed by GASMET DX 4000 FTIR. The measured flue gas components are CO₂ (0-100%, ±1%), O₂ (0-25%, ±1%), H₂O (0-25% ± 1%), NO_x (0-1000 ppm), N₂O (0-500 ppm), HCN (0-1000 ppm), SO₂ (0-2000 ppm), CO (0-10000 ppm).

The experimental procedure is explained below. Initially, all electrical heaters (combustor column heaters and air duct heaters) are switched on. Empty combustor is heated by hot air until the temperature at the lower region reaches 250°C (Figure 2). After the bed material (silica sand) is loaded, the temperature decreases down to 120-150°C (Figure 2). When the bed temperature reaches again to 280-300°C, which generally takes about 5-6 h, fuel feeding is started. Since the fuel is cold, temperature in the bed decreases at the first moments of fuel feeding (Figure 2). In twenty to fourteen minutes ignition occurs and temperature starts to rise (Figure 2). At around 780°C, the combustor column heaters are turned off while the air duct heaters remain online. 8-10 h is required from the start of the fuel feeding to reach steady state operation when air is used.

All fuels were combusted in air atmosphere first, and then the combustion mode was switched to OEC. Mode change was performed very slowly by increasing O₂ concentration at small steps to the target value to prevent rapid temperature rise and hot spot formation. A typical temperature profile during combustion experiments is shown in Figure 2. Each experiment took approximately 14-18 h long. Bed pressure drop was continuously monitored during the experiment. Temperatures during the tests were kept between 800 and 900°C which is typical for CFB combustion. O₂ concentration of the combustion air was increased from 21% (atmospheric condition) to 28% by volume. Oxygen enrichment was achieved by adding pure oxygen into primary air line with a mass flow controller. During combustion tests, biocoal in the fuel blends was set to 0%, 20%, 30%, 50% by wt. In Figure 2 the rapid temperature decreases are seen caused by the feeding system blockage or closing.

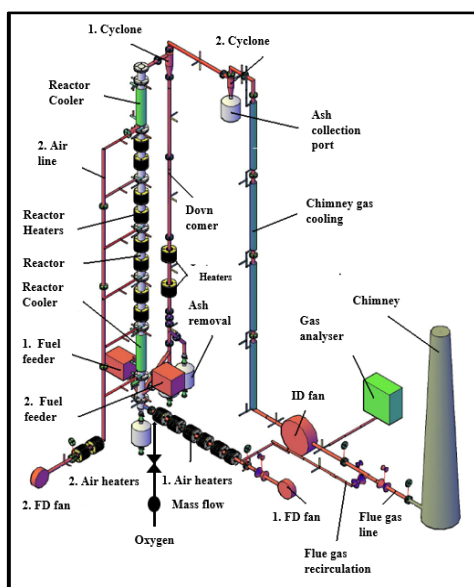


Figure 1. The pilot scale circulating

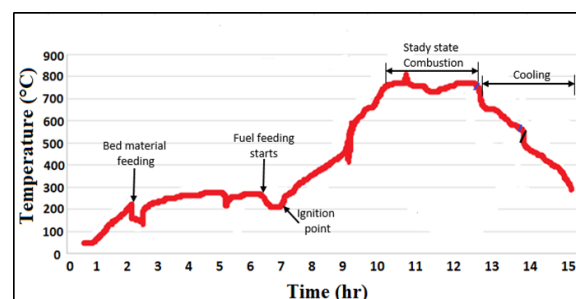


Figure 2. Temperature profile during combustion experiment fluidized bed combustion system (CFBC)

3. Results and discussion

3.1. Temperature profiles

The oxygen enriched combustion tests were first carried out with Soma lignite alone. Then mixtures of biocoal and lignite were prepared according to the required fuel composition shown in Table 2. The average bed temperature was affected by the oxygen concentration in the primary air. As the oxygen concentration increased, the average bed temperature increased in the experiments. With an oxygen concentration of 21%, the average bed temperature varied between 710-750°C, while it increased to 875°C at 28% oxygen concentration with Soma (Figure 3). By adding a limited amount of biocoal to Soma lignite, LHV of the mixture increases because LHV of biocoal is higher than LHV of Soma lignite. As shown in Figure 3, the bed temperature decreased slightly for the mixture of Soma lignite mixed with 20% biocoal at 21 and 23 % oxygen concentration.

However, as the content of biocoal in the fuel mixture increases more than 20% by wt., the average temperature of the bed gradually decreases because the biocoal has a slightly higher volatile content than Soma lignites (Figure 3).

On the other hand, when 50% biomass is added to lignite (Figures 3), the bed temperature is lower at all O₂ concentrations compared to lignite burning. This indicates that, there is a limit for biocoal contribution for better combustion. Taking into account that the maximum biomass contribution in the commercial co-combustion application is between 10% and 15%, this result shows us that we can add more biochar than biomass.

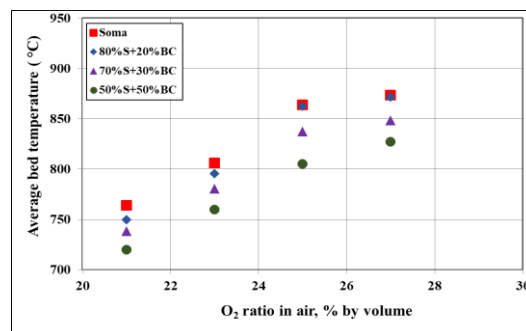


Figure 3. Effect of O₂ concentration on the average bed temperature for Soma lignite

Changes of temperature along the combustor height are given in Figure 4 for Soma lignite for oxygen enriched experiments. As the oxygen concentration increased in the combustion air, temperatures in the dense bed (300-320 mm) and in the freeboard (1252-2248 mm) increased for all cases. Additionally, the volatile content of coal has a tendency to evaporate and burn in the freeboard which results in increasing freeboard temperature. A peak temperature was observed in the freeboard due to combustion of volatile matter in the freeboard rather than in the bed. Higher the volatile matter content of the fuel burned in the combustor, the higher is the maximum temperature reached in the freeboard. This is clearly seen in Figure 4.

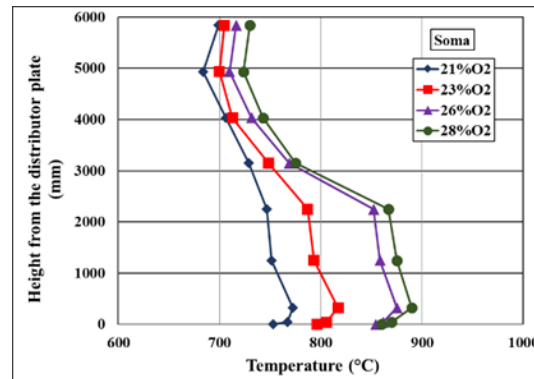


Figure 4. Effect of O₂ concentration on temperature distribution in the combustor with Soma lignite alone

Changes of temperature along the combustor height are given in Figure 5 for mixtures of Soma lignite with biocoal for oxygen enriched experiments. The peak temperature observed in the freeboard for Soma lignite is 810°C. On top of this if biocoal is added to lignite, maximum temperatures (about 900°C) in the freeboard is observed until 2000-2200 mm height, then the temperature starts to decrease as height increases due to decrease in combustion of volatile matter.

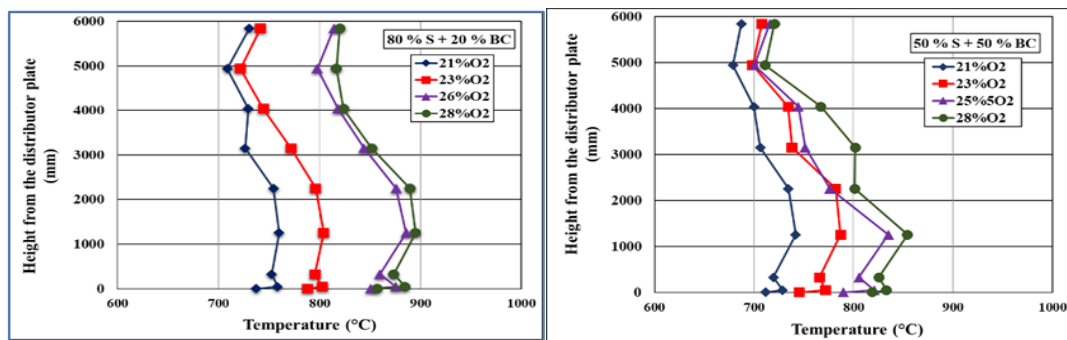


Figure 5. Effect of O₂ concentration on temperature distribution in the combustor with Soma lignite mixtures with biocoal

3.2. Emissions

Change in emissions of major pollutants (CO, NO, and SO₂) during combustion in oxygen enriched primary air are presented in this section. Concentration of each pollutant in the flue gas is based on 6 vol% O₂ in flue gas and is expressed in mg/Nm³ (on dry basis) at normal temperature (273°K) and pressure (1 atm). The measured ppm data were corrected for oxygen enriched cases and converted to mg/MJ.

3.2.1. CO emissions.

Better combustion in oxygen enriched air is indicated by the decreased in CO emission data. CO concentrations with respect to O₂ ratio in air are given in Figure 6 for all cases studied. For the combustion of Soma lignite alone in normal air (21% by vol. O₂), CO concentration was found to be 520 mg/MJ. As the oxygen concentration in the combustion air increased, better combustion occurred and CO emission decreased to 295 mg/MJ for Soma lignite, for air containing 27% by vol. O₂. The highest concentrations of CO was found in the combustion of 50%/50% by wt. biocoal and coal mixture. There are two possible reasons for this: (i) higher volatile content of fuel mixture obtained by the addition of biocoal increases volatile matter (hydrocarbon concentration) in the freeboard, which limits the oxidation of CO. OH and HO₂ radicals may react easier with hydrocarbons than CO, (ii) CO escapes

from the reactor unburnt. A possible remedy for decreasing CO emission from the combustor can be injection of secondary air into the freeboard, thus increasing the oxidation of CO and also by increasing the turbulence in the freeboard of the combustor.

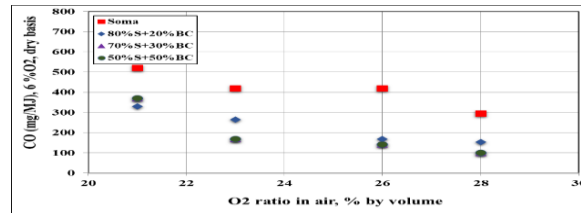


Figure 6. Effect of O₂ concentration on CO emissions for Soma lignite

As the oxygen concentration in the combustion air increased, better combustion occurred and CO emission decreased to 295 mg/MJ with 28% O₂ by vol. in air (Fig. 6). Even if 50% by wt. biocoal is added to the Soma lignite, it does not create any adverse situation in the combustion system and in the emissions. 50% by wt. biocoal addition has lowered the CO emission value down to 100 mg/MJ with 28% O₂ in air. This can be attributed to metal oxide contents of Soma lignite ash. As can be seen from ash analysis of Soma lignite in Table 5, Soma lignite ash is rich in silica, alumina and CaO. These oxides may act as catalyst for the oxidation of CO in the combustor.

3.2.2. CO₂ emissions.

Figure 7 shows the CO₂ concentration change with increase in O₂ concentration for all combustion tests. Oxygen enrichment supports better combustion; therefore, oxygen enrichment increases CO₂ concentration in all cases. Biocoal addition to lignites seems to have an increasing synergetic effect on combustion as the oxygen enrichment and biomass portion in the fuel mix increases. As the share of biocoal in the fuel blends increased, the CO₂ concentrations for Soma lignite increased. The addition of biocoal to Soma lignites increases the synergic effect on combustion as the oxygen enrichment and biocoal fraction of the mixture increases. The synergistic effect can be attributed to the high alkaline and the earth alkaline metal oxide content of the biomass.

Table 5. Ash composition of Soma lignite, % by wt. (dry basis)

Coal	Al ₂ O ₃	BaO	CaO	Fe ₂ O ₃	K ₂ O	MgO	MnO	Na ₂ O	P ₂ O ₅	SO ₃	SiO ₂	SrO	TiO ₂	V ₂ O ₅
Soma	22.24	0.12	19.37	5.85	1.95	2.08	0.07	0.24	0.25	6.79	39.51	0.05	1.14	0.14

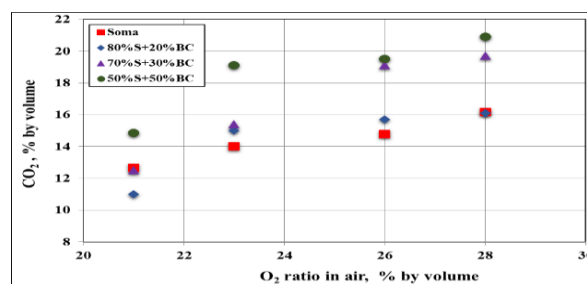


Figure 7. Effect of O₂ concentration on flue gas CO₂ concentration Soma lignite

The combustion efficiency was calculated from the following relationship (Patumsawad and Cliffe, 2002):

$$\eta_{CE} = 100x \frac{\% \text{ CO}_2 \text{ in flue gas}}{(\% \text{ CO}_2 + \text{CO}) \text{ in flue gas}} \quad (1)$$

This efficiency calculation procedure is based on knowledge of the flue gas composition and assumes that there are no carbon losses, and the carbon composition presented in the feed is converted completely to carbon monoxide and carbon dioxide. Actually this was the case. Figure 8 shows combustion efficiency variation with O₂ concentration for Soma lignite and its biocoal mixtures. If the carbon balance is made on the system, it shows that all the carbon in the fuel is converted to CO or CO₂.

This shows that the assumption of “no carbon left unburned in the ash” in calculating the combustion efficiency is justified. The combustion efficiency has reached to about 99% and efficiency showed a slight increase to 99.6% as the oxygen concentration in air increased. As the biocoal is added to Orhaneli lignite, the combustion efficiency increased to 99.5% for the additions of 20 and 30% biocoal to the fuel mix. However, for 50% addition of biocoal, the combustion efficiency decreases to lower levels in Soma lignite alone especially at lower O₂ concentration. This can be explained by the lower average bed temperature.

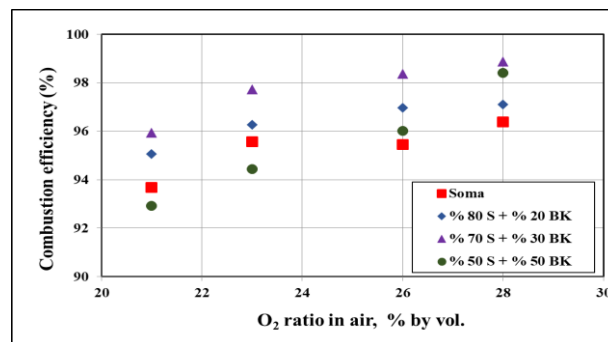


Figure 8. Effect of O₂ concentration on combustion efficiencies in Soma lignite

3.2.3. NO_x emissions

The mechanism of NO_x (NO and NO₂) formation during combustion is very complex. Depending on the temperature, stoichiometric ratio and type of nitrogenous species present in the combustion zone, mechanism of nitrogen oxides formation changes. Usually the type of flame determines the conditions of the predominant mechanism of NO_x formation. NO constitutes most of the NO_x emissions during combustion (>90%). Temperatures in oxygen enriched atmosphere is also far below the thermal NO_x formation temperature 1000 °C. Romeo et al. (2011) showed that the thermal NO_x is negligible at CFB Oxyfuel tests (Romeo, 2011). Thermal-NO_x formation does not seem to be the reason for NO emissions in circulating fluidized bed combustion because of lower operating temperatures (800-900°C) (Romeo, 2011). Possible NO_x formation pathway at the studied conditions is conversion of fuel-N to NO. Temperature effect on fuel-NO_x formation is not clear in the literature. Khan et al. (2008) reports that fluidized bed operation temperatures are suitable for the highest fuel NO_x conversion rates (Khan, 2008). On the other hand Miller and Bowman (1989), claims that fuel-N to NO_x conversion poorly depends on temperature.

Change in NO_x emissions with respect to O₂ concentration is shown in Figure 9. Maximum temperature observed in the furnace was 750 °C and 871 °C. By looking at the increase of NO_x emissions in small temperature intervals, it is reasonable to think that temperature has no significant effect on fuel-N to NO conversion between 760 °C and 890 °C.

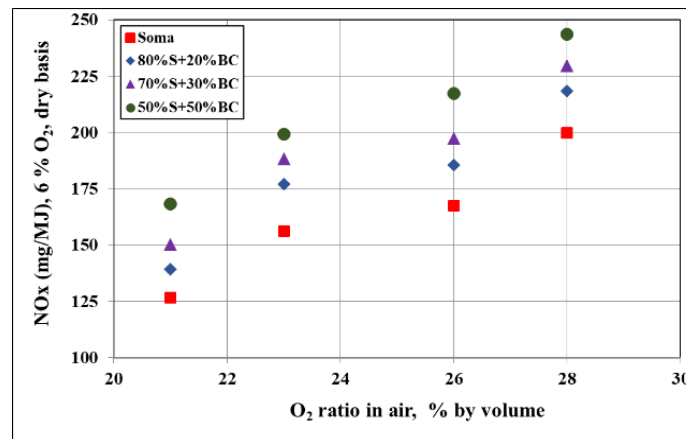


Figure 9. Effect of O₂ concentration on NO_x emission in Soma lignite

NO_x emissions from combustion of Soma lignites alone rose from 127 mg/MJ to 200 mg/MJ, with increase of O₂ concentration (Figure 9). It is seen that increasing O₂ concentration from 21% to 27% by vol. in oxidizer atmosphere results in slight increase of NO_x emissions for Soma lignite. This may be due to increase in OH radicals as a result of higher O₂ concentration in the combustor and this enhances the NO_x formation (Duan et al., 2015).

Effect of biocoal addition on NO_x formation is also shown in Figures 9 for Soma lignite. NO_x emissions for all fuel mixes were higher than that of the parent lignite. Results show that increasing biocoal share in fuel blend results in higher NO_x emission. Although the nitrogen content of biocoal (0.63 % by wt.) is lower than the nitrogen content in lignite (0.84% by wt. in volatile content. Moreover, biocoal has higher H/N ratio (9.17) than lignite (2.19 for Soma). Fuels having higher H/N ratio are expected to generate higher NH₃ which increases the NO formation.

3.2.4. SO₂ emissions

Combustion of the Soma lignite alone does not produce any measurable SO₂ emissions because of very low S content (0.73% by wt.). Therefore, SO₂ emissions for Soma), nitrogen conversion of fuel-N in biocoal is higher than that in the lignite due to higher Soma lignite is not given here.

4. Conclusions

Oxygen enrichment decreased the CO formation and increased CO₂ concentration in all cases due to better combustion. As the share of the biocoal in the fuel mixture increased, emission of CO for the Soma lignite decreased. The highest CO emission was obtained with Soma lignite alone, while the CO emission decreased as the biocoal additive increased. As the oxygen content increased along with the addition of biocoal, Soma showed a faster increase in CO₂ concentration. The addition of biocoal to Soma lignite increased the synergic effect on combustion. The synergistic effect can be attributed to the high alkaline and the earth alkaline metal oxide content of the biocoal. Impact is more prominent on Soma lignite. Enriching oxygen concentration in air with O₂ up to 27%, increased NO_x emissions by promoting Fuel-N conversion in the temperature range of this study. Higher biocoal share in the fuel blend caused lower SO₂ emissions primarily due to the low S content of biocoal.

Further work should be done for commercial applications. Energy and exergy analyzes should be done in torrefaction and CFB systems. A model should be developed for scale up. More research is needed for heat transfer in an oxygen enriched combustion environment to evaluate the retrofitting option of OEC technology to existing power plants.



5. References

- Atimtay A.T., Kayahan U., Unlu A., Engin B., Varol M., Olgun H., Atakul H., 2017. Co-firing of pine chips with Turkish lignites in 750 kWth circulating fluidized bed combustion system. *Bioresource Technology*. 224, 601–610.
- Duan, L., Duan, Y., Zhao, C., and Anthony, E.J., 2015. NO emission during co-firing coal and biomass in an oxy-fuel circulating fluidized bed combustor, *Fuel*. 150, 8–13.
- Ersoy M., Role of coal in Turkey, Workshop on best practices in production of electricity from coal, 29 October 2015, Genova, https://www.unece.org/.../se/.../8_M.Ersoy_TURKEY.pdf
- Khan, A.A., De Jong, W., Jansens, P.J., and Spliethoff, H., 2008. Biomass combustion in fluidized bed boilers : Potential problems and remedies. *Fuel Process. Technol.* 90, 21–50.
- Miller, J.A., Bowman, G.T., 1989. Mechanism and modeling of nitrogen chemistry in combustion. *Prog Energy Combust. Sci.* 15, 287-338.
- NASA, Global Climate Change, <https://climate.nasa.gov/vital-signs/carbon-dioxide/>
- Olgun, H., Keivani, B., Gultekin, S., Kabadayi, A., Experimental study on torrefaction of pine wood in a continuous screw conveyor, 6th International Symposium On Energy from Biomass and Waste, 14-17 November 2016, Venice.
- Patumsawad, S., Cliffe, K.R., 2002. Experimental study on fluidised bed combustion of high moisture municipal solid waste. *Energy Conversion and Management*. 43, 2329–2340.
- Romeo, L.M., Díez, L.I., Guedea, I., Bolea, I., Lupiáñez, C., González, A., Pallarés, J., and Teruel, E., 2011. Design and operation assessment of an oxyfuel fluidized bed combustor. *Exp. Therm. Fluid Sci.* 35(3), 477–484.
- Saracoglu, N. Energy production from forest residues in Turkey. 3rd International Symposium and Innovative Technologies in Engineering and Science, Valencia, Spain. ISITES 2015.
- Tumuluru J.S., Sosanj S., Hess J.R., Wright C.T., Boardman R.D., 2011. A review on biomass torrefaction process and product properties for energy applications. *Industrial Biotechnology*. 384-401.
- Varol M., Atimtay A.T., Olgun H., Atakul H., 2014. Emission characteristics of co-combustion of a low calorie and high sulfur–lignite coal and woodchips in a circulating fluidized bed combustor: Part 1, Effect of excess air ratio. *Fuel*. 117, 792–800.

Acknowledgements

The financial support for this work by TUBITAK-ARDEB 1003 program (Project Code: 213M527) is greatly appreciated. The Authors thank in particular the staff of the Chemistry Department of Ege University, Izmir, Turkey for the collaboration and help in the analysis.

Integrated air quality assessment of Konya in terms of meteorology, topography and emission sources

Mete Tayanc¹, Ismail Sezen², Ezgi Akyuz², Burcak Kaynak³, Metin Baykara²
and Alper Unal²

¹Marmara University, Department of Environmental Eng., Istanbul, Turkey

²Istanbul Technical University, Eurasia Inst Earth Sci, Istanbul, Turkey

³Istanbul Technical University, Department of Environmental Eng., Istanbul, Turkey

mtayanc@marmara.edu.tr

Abstract. Considering an integrated approach to assess all of the measured pollutants in a diurnal, monthly, seasonal and annual time scales and understanding the mechanisms hiding under low air quality conditions is essential for tackling the future air pollution issues. Konya, located on central Anatolia, is the largest province of Turkey having a surface area of 40,838 m² and has different industrial activities including the production of cement, sugar, machinery, chemicals, textile, food, packing material, electronic equipment and paper. Lack of recent detailed studies is limiting our information on underlying air pollution problems of Konya and obscuring policy makers to develop applicable mitigation measures. In this study, we used hourly monitored air quality data of CO, NO, NO₂, NO_x, PM₁₀, PM_{2.5}, and SO₂ from 5 stations of Konya and investigated temporal and spatial variability for the 2008-2018 period via statistical analysis. Air quality data of Konya is subjected to quality control and the periods that have large missing data gaps or no data at all are eliminated from the study. Upon analysis, largest problem is found to be the PM₁₀, together with the highest 2008-2018 periodic mean value of PM₁₀ as 70.5 µg/m³ in Karatay Belediye, followed by 67.4 µg/m³ in Meram, 58.7 µg/m³ in Selcuklu, 48.2 µg/m³ in Erenkoy Belediye and 43.7 µg/m³ in Selcuklu Belediye. In the legislation, 24 hour limit of PM₁₀ is given as 50 µg/m³ for the protection of human health and this limit should not be exceeded more than 35 times in a year. It is found that the limit value is violated in all of the stations, mainly during winter and autumn. High positive correlations exist among the stations and the highest correlation is the one between Selcuklu Belediye and Karatay Belediye with the Pearson correlation coefficient, $r=0.77$ and adjusted R^2 , $aR^2=0.59$ value. Generally, long-term data showed decreasing trends in PM₁₀ levels. Diurnal variability is found to be more pronounced than the weekly variability. For almost all of the pollutants, except for photochemical pollutants like O₃, a prominent result is the nighttime and morning rush hours high pollutant levels. This condition is related with the emissions and meteorology. Prevailing stable atmospheric conditions during night generate stagnant and low wind speed conditions, especially during winter, leading to high pollutant values. On the other hand, photochemistry is the leading process in the high O₃ values during noon and early afternoon.

Keywords: Integrated air quality assessment, Konya, Meteorology, Emission sources.

1. Introduction

Konya is the largest province of Turkey having a surface land and lake area of 40,814 m² and covers approximately 5% of the country territory. The land surface area of the province is 38,873 m² and the majority of its territory is located as the high plains of Central Anatolia. Average altitude of the province is 1,016 m. Figure 1 show the topography and settlement maps of Konya. As it can be seen from the figure Konya City is located on a plain surrounded by high hills on the western side and agricultural low

lands on the east. Topography begins to rise up from Meram district towards west, towards Beyşehir Lake generating peaks exceeding 1750 m. There are five monitoring stations at Konya: Selçuklu, Selçuklu Belediye, Meram, Karatay Belediye and Erenköy Belediye (Yeni Sille Belediye). As seen in this figure, the stations are mainly located at urban areas.

Konya province has the 7th place according to the ranking of population done in 2018 with respect to Address Based Population Registration System (Adrese Dayalı Nüfus Kayıt Sistemi - ADNKS) (Turkish Statistical Institute, 2018) with a population of 2,205,609 constituting 2.69% of the Turkey's population. Population density (number of people in km²) is 56.74. Population of Selçuklu, Meram and Karatay district Centers within the boundaries of Konya Metropolitan Municipality constitutes the 54% of the population of Konya with a population over one million. Akşehir, Beyşehir, Cumra, Ereğli, Iğın, Kulu and Seydişehir districts are other places with populations over 50,000.

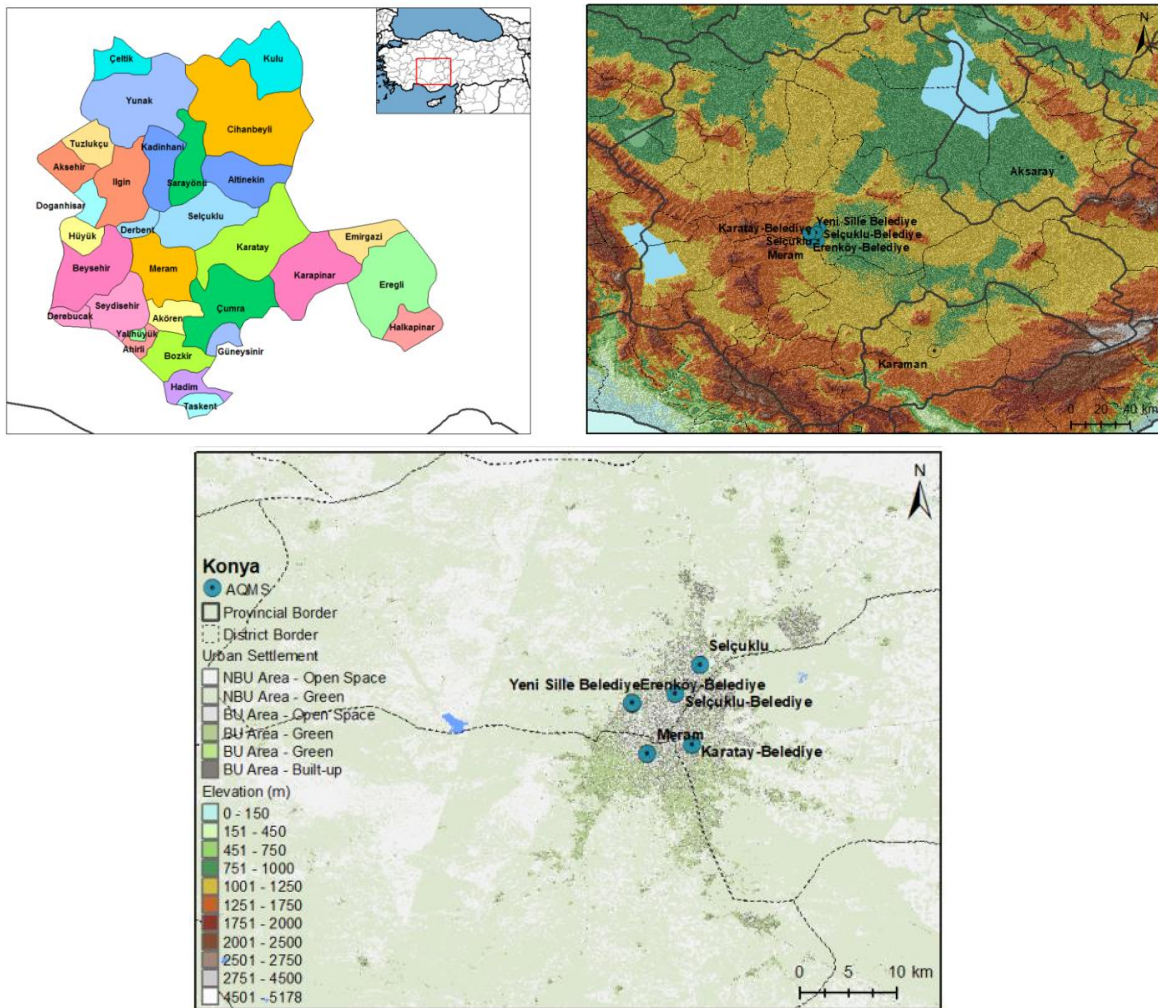


Figure 1. Konya geographical location and districts (top left), topographical map (top right) and settlement map (bottom) together with air quality monitoring stations (AQMS)

2. Climate and emission sources

2.1. Climate

Konya has a continental type Mediterranean climate with hot summers and cold winters. According to Turkish State Meteorological Service (TSMS, 2019) July average temperature climb up to 23.5 °C (Table 1). Average of maximum temperatures exceed 30 °C during summer months. The highest temperature recorded in Konya was 40.6 °C on 30 July 2000. During winter, January average temperature drop below 0 °C. Average of minimum temperatures can sometimes be lower than -4 °C. The lowest temperature recorded was -28.2 °C on 6 January 1942. Due to Konya's high altitude and its dry summers, nightly temperatures in the summer months are cool. Precipitation levels are low with an average annual total of 322.4 mm and precipitation can be observed throughout the year. Wettest month is May and driest is August with monthly totals as 43.5 mm and 4.9 mm, in order. Dominant wind direction is northerly; north and north westerly wind constitutes 58% of the cases.

Table 1. Climatological summary of Konya in the period 1929-2018

	Jan	Feb	Mar	Apr	May	Jun	Jul	Aug	Sep	Oct	Nov	Dec	Annual
Avg. Temp. (°C)	-0.2	1.4	5.6	11.1	15.8	20.1	23.5	23.2	18.5	12.5	6.3	1.7	11.6
Avg. Max. Temp. (°C)	4.6	7.0	11.8	17.5	22.3	26.6	30.1	30.2	26.0	20.0	13.0	6.6	18.0
Avg. Min. Temp. (°C)	-4.2	-3.3	-0.2	4.3	8.6	12.6	15.8	15.6	10.9	5.9	0.8	-2.4	5.4
Mean Daily Sunshine Hours	3.3	4.7	5.9	7.1	8.9	10.6	11.6	11.2	9.5	7.2	5.3	3.2	88.5
Mean Prec. Days	9.9	8.4	8.8	9.0	10.6	6.6	2.2	1.5	3.1	6.1	6.6	10.0	82.8
Avg. Mon. Tot. Prec. (mm)	37.6	28.5	28.9	31.9	43.6	25.5	6.3	4.6	12.3	30.0	32.0	42.1	323.3
Record High Temp. (°C)	17.6	23.8	28.9	31.5	34.4	37.2	40.6	39.0	36.1	31.6	25.4	21.8	40.6
Record Low Temp. (°C)	-28.2	-26.5	-16.4	-8.6	-1.2	1.8	6.0	5.3	-3.0	-8.4	-20.0	-26.0	-28.2

2.2. Air pollution emission sources in Konya

Konya is established on one of the oldest civilized regions, Catalhoyuk (appr. 7000 BC) of Anatolia and has always been an important agriculture, science, trade and industry center through Silk Road due to its location as a passage between East and West. Konya has always been played crucial role during the time of Silk Road, that's why named as the capital of Selcuk Empire for more than hundred years. Hence Konya became a powerful and wealthy province in the Ottoman Empire and Republic of Turkey times through industry, agriculture and trade.

According to Konya Sanayi Odası (<http://www.kso.org.tr/sayfa/en/industry-1>), Konya has different industrial activities including the production of cement, sugar, machinery, chemicals, textile, food, packing material, electronic equipment and paper. Industries are mainly located in organized industrial zones mainly located on the northern regions of the City.

Within the boundaries of Konya province there are 705 organizations that already got emission permission (Kunt and Dursun, 2016). According to the authors, there are 167 industrial organizations with high pollutant qualifications in the city center and the number of vehicles in traffic was counted as 593,089 in the year of 2014. Konya Clean Air Action Plan (2013-2019) (<https://webdosya.csb.gov.tr/db/konya/icerikbelge/icerikbelge1500.pdf>) declared that 88,899 out of 265,489 residential buildings are using natural gas for heating purposes in the city corresponding to 34% of the total, and the remaining 176,590 buildings depend on coal. Report expresses 3 main sources of air pollution in the city: residential heating, industrial emissions and traffic. High levels of air pollution in a city not only depends on the emissions but also on topography and meteorology.

3. Results

Air quality data of Konya province in the period of 2008-2018 is subjected to quality control and the periods that have large missing data gaps or no data at all are eliminated from the study. There are 5 active air pollution measurement stations in Konya that passed the quality check for the air pollution analyses: Selcuklu Belediye, Karatay Belediye, Erenkoy Belediye (newly called as Yeni Sille Belediye), Selcuklu and Meram. Generally, Selcuklu Belediye and Karatay Belediye stations have high quality pollution data since the early 2016 (2015 for PM₁₀). Selcuklu and Meram have only PM₁₀ measurements and the reliable PM₁₀ data of these stations extends back to 2008. Contrary, Erenkoy Belediye has reliable observation data only in 2018. Periods belonging to the early phases of measurements had large percentages of missing data resulted in the elimination of those periods.

3.1. Violation of the limit values

Table 2 provides exceedance analysis for Konya between 2008 and 2018. According to Hava Kalitesi Degerlendirme ve Yonetimi Yonetmeligi maximum daily 8 hour average of CO is 10 mg/m³. No hourly limit value for CO is provided. Allowable shorter time period limit values are always larger than those having longer time periods. In this respect, it can be reliably said that there is no violation of the CO limit value in any station of Konya.

According to the legislation, 250 µg/m³ hourly limit value of NO₂ should not be exceeded 18 times in a year to protect human health. NO₂ hourly limit was exceeded in 2017 and 2018 by 494 and 456 hours, that are almost 27 and 25 times greater in period than the 18 hours yearly limit for NO₂. On the other hand, yearly NO₂ limit (50 µg/m³) was exceeded in 2017 with an annual concentration of 83.6 µg/m³.

In terms of NO_x, it can be said that the yearly limit value of 30 µg/m³ has been violated since 2016 with annual concentrations several times of the limit; 130.1, 190.7 and 643.4 µg/m³ from 2016 to 2018. For O₃, daily 8h limit value of 120 µg/m³ was exceeded 7 times in 2016, 4 times in 2017 and again 7 times in 2018.

PM₁₀ daily and yearly limits were exceeded throughout the measurement period with very high number of exceedances and concentrations. Number of days having concentrations higher than the limit is larger than 150 days in any given measurement year, climbing up to 275 days in 2008. Associated with this, annual concentrations have been higher than the 40 µg/m³ limit value, with a maximum of 99 µg/m³ in 2008. This is an indicator that Konya has serious PM₁₀ issues especially during autumn and winter.

Hourly SO₂ concentrations did not exceed 350 µg/m³ at any time. But yearly limit of SO₂, that is 20 µg/m³, were violated in 2011, 2012 and 2017 with values 23, 20.3 and 26.3 µg/m³, respectively. Winter-time violation is more pronounced though, with violations in 2010, 2011, 2013, 2014, 2016 and 2017. Exceedances during 2011 and 2016 have values close to the twice of the limit value, 36 and 39.8 µg/m³, in order.

Table 2. Violation of the limit values in Konya

Pollutant	Period	Limit	Exc.	2008	2009	2010	2011	2012	2013	2014	2015	2016	2017	2018
CO	Max. Daily 8h	10000	1	-	-	-	-	-	-	-	0	0	0	0
NO ₂	Hourly	250	18	-	-	-	-	-	-	-	0	6	494	456
	Yearly	50	1	-	-	-	-	-	-	-	-	48.5	83.6	-
NO _x	Yearly	30	1	-	-	-	-	-	-	-	-	130.1	190.7	643.4
O ₃	Max. Daily 8h	120	1	-	-	-	-	-	-	-	0	7	4	7
	Yearly	50	35	275	219	222	184	224	176	206	218	169	241	186
PM ₁₀	Daily	50	1	99	84.3	75.5	69.8	72.2	63.1	60.4	58.5	56.3	83.3	58.3
	Yearly	40	1	99	84.3	75.5	69.8	72.2	63.1	60.4	58.5	56.3	83.3	58.3
SO ₂	Hourly	350	24	0	0	0	0	0	0	0	0	0	0	0
	Daily	125	3	0	0	0	4	0	0	0	0	0	5	0
	Yearly	20	1	15.6	13.8	16.3	23	20.3	12.1	13.6	10.2	15.7	26.3	13.6
	Winter	20	1	16.7	14.8	25.1	36	-	25.9	21.3	13.2	39.8	30.1	-

* Except *Winter* and *Yearly*, all values presented are number of exceedances. *Winter* and *Yearly* are given as average values in ($\mu\text{g}/\text{m}^3$).

3.2. NO_x analysis

Violation of the limit values in Konya show that the primary pollutant of interest is PM₁₀ and to a secondary importance level, NO_x and O₃. Thus, in the scope of this article, we gave special emphasis on the analyses of these pollutants and the evaluation of the results via topography and meteorology. 3 active air pollution measurement stations in Konya measure NO, NO₂ and NO_x: Selcuklu Belediye, Karatay Belediye and Erenkoy Belediye. Selcuklu Belediye and Karatay Belediye stations have high quality NO_x data since the early 2016. On the other hand, Erenkoy Belediye has reliable NO_x observation only in 2018, thus it is mostly kept out of the analysis. Figures 2 - 4 show the statistics, time variations and trend figures of the hourly NO_x measurements in the Konya province. It can be seen from the figures that the highest mean values of NO_x is found as 240.8 $\mu\text{g}/\text{m}^3$ in Selcuklu Belediye and 180.3 $\mu\text{g}/\text{m}^3$ in Karatay Belediye urban stations. Those high values of NO_x in urban stations can be the indicator of the intensity of photochemical activity over the City. Lowest mean value belongs to Erenkoy Belediye, with a value of 40.3 $\mu\text{g}/\text{m}^3$.

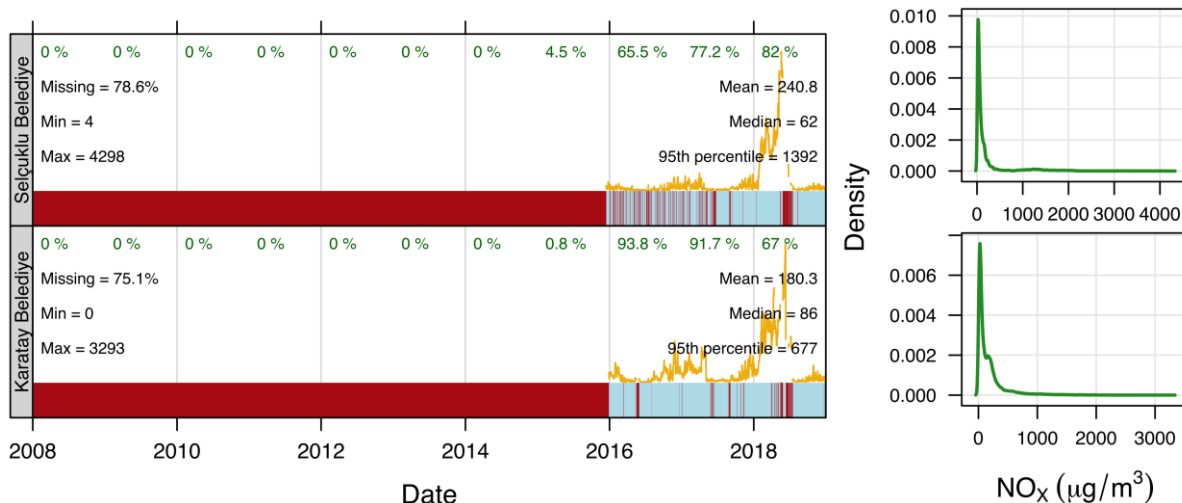


Figure 2. Hourly NO_x statistics in Konya

According to Hava Kalitesi Degerlendirme ve Yonetimi Yonetmeligi, annual limit of 30 $\mu\text{g}/\text{m}^3$ level of NO_x has been applied to protect human health. Since there is no hourly limit expressed in the legislation, comparisons of measurements with the limit the value was not done. Erenkoy (Yeni Sille) Belediye is located at a suburban region in the northwest of Konya City with many parks and green areas around. Dominant north and north westerly winds at Konya turns this location into an upwind or background position in the majority of the observation cases. A careful investigation of the density plots on the right

hand side of Figure 2 show that the annual limit value $30 \mu\text{g}/\text{m}^3$ was rarely exceeded in Konya. 95th percentile data belonging to the stations are 1392, 677, $131 \mu\text{g}/\text{m}^3$, in order, meaning that during 95% of the hourly cases NO_x concentrations were below those values.

Seasonal plots (Figure 3) of NO_x illustrate that winter and spring has high concentrations in the urban locations, Selçuklu Belediye and Karatay Belediye. It is intuitively clear in the plots that Selçuklu Belediye has the highest NO_x concentrations during the winter and spring seasons, mainly influenced by the emissions from traffic and heating, and photochemical reactions may exacerbate the problem. For Selçuklu Belediye, during weekdays of winter, Monday, Tuesday and Wednesday NO_x averages are slightly higher than those of Thursday and Friday, as it is for CO, NO and NO_2 . Interestingly, during winter and spring, when there are high concentrations of NO_x at Selçuklu Belediye, weekend levels are found to be larger than those of weekdays. However, this condition cannot be seen at Karatay Belediye.

Morning rush hours peak NO_x values generated mainly by the traffic is clearly visible in the figure. Emissions, photochemistry and meteorology play an important role in the hourly variation of NO_x . Emissions during morning traffic is acting as precursors of photochemical reactions that produce O_3 , aldehydes and PANs. Thus, a sharp decrease in NO_x levels after the rush hours during morning is expected owing to photochemical reactions, especially during spring and autumn seasons when solar radiation intensity is higher than the winter. But photochemical activity does not exist during evening and night, thus NO_x levels remain high for long time periods.

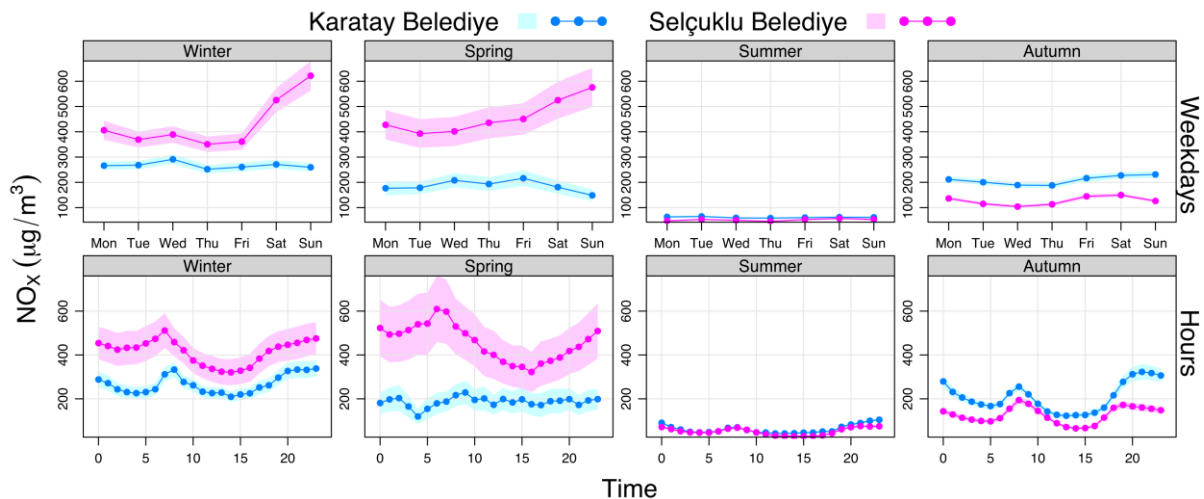


Figure 3. Hourly NO_x variability during daytime and daily NO_x variability during week belonging to each season

In all of the seasons and almost for all of the stations a prominent result is the high night time NO_x levels. This condition is directly related with the meteorology and chemistry. Prevailing stable atmospheric conditions during night generate stagnant and low wind speed conditions. A scientific result of this is the generation of low boundary layer height or mixing height, trapping the pollutants close to the surface. Low wind speeds or calm conditions exacerbate the problem by decreasing the pollutant transport in the horizontal leading to high NO_x values. Contrary, during noon and early afternoon, during sunny days, differential warming up of the surfaces by sun generate unstable atmosphere associated with higher boundary layer altitudes and moderate to strong mountain - valley breezes. This situation leads to the transport of pollutants in the horizontal as well as in the vertical generating considerably lower levels of pollution. Reactions of NO and NO_2 with the hydrocarbons is a quick process during daytime producing photochemical pollutants. So, these reactions can be responsible in the sharp decrease of NO_x concentrations after 8.00, 9.00 am.

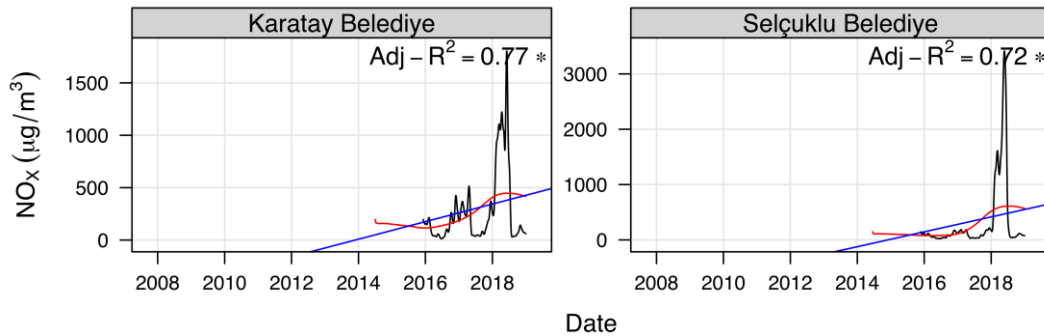


Figure 4. Trends of NO_x during the measurement period

It can be seen in Figure 4 that the urban stations of Konya have increasing NO_x trends with considerably large Adj-R² values, 0.77 for Karatay Belediye and 0.72 for Selçuklu Belediye. Since Erenkoy belediye only has data in 2018, trend established to it is not reliable. This feature of NO_x, together with those of NO and NO₂, should be taken into account because NO_x is an important contributor of photochemical smog.

3.3. O₃ analysis

As is NO_x measurements O₃ is also measured at 3 stations in Konya: Selçuklu Belediye, Karatay Belediye and Erenkoy Belediye. Selçuklu Belediye and Karatay Belediye stations have high quality O₃ data since the early 2016. On the other hand, Erenkoy Belediye has O₃ measurement only in 2018, thus it is generally kept out of the analysis. Figures 5-7 show the statistics, time variations and trend figures of the hourly O₃ measurements in the Konya province. It can be seen from Figure 5 that the highest mean values of O₃ is found as 34.6 µg/m³ in Karatay Belediye and 27.1 µg/m³ in Selçuklu Belediye urban stations. Lowest mean value belongs to Erenkoy Belediye, with a value of 24.8 µg/m³.

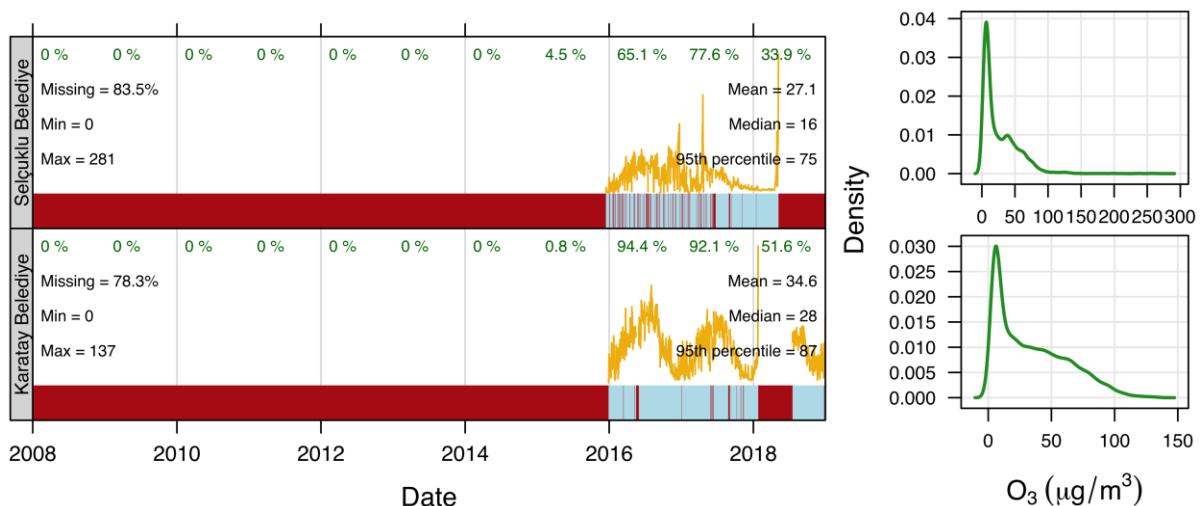


Figure 5. Hourly O₃ statistics in Konya

According to Hava Kalitesi Değerlendirme ve Yönetimi Yönetmeliği, 180 µg/m³ one hour average limit value is established as a *notice threshold* and 240 µg/m³ one hour average limit value is established as a *warning threshold*. 95th percentile data belonging to the stations are 75, 87 and 65.9 µg/m³, in order. Thus, it is obvious that 95th percentile values are much lower than the hourly limit values. Density figures also show that the violation of 180 µg/m³ limit value is not a much pronounced case.

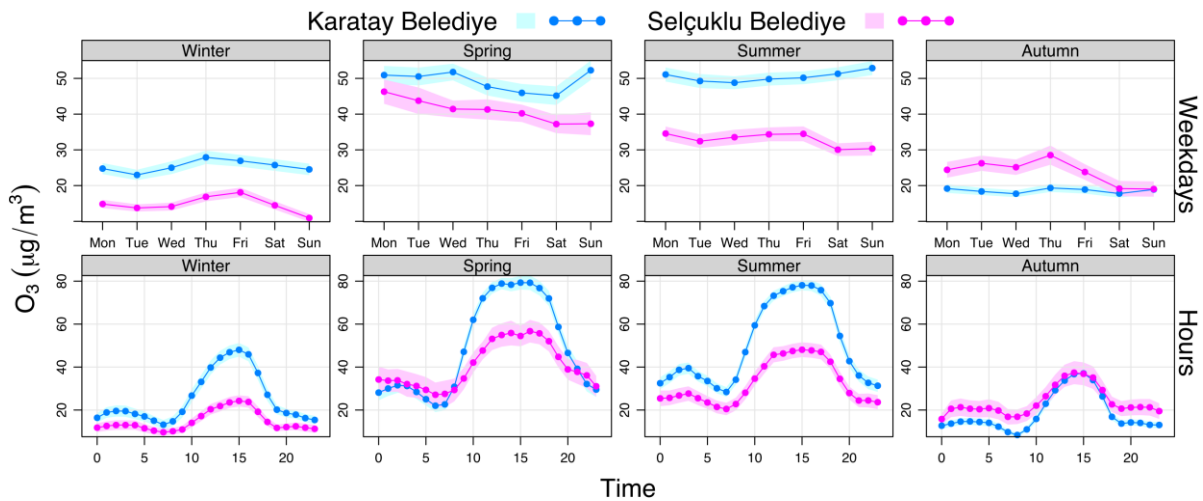


Figure 6. Diurnal and weekly variability of O_3 during the seasons

Time series (Figure 6) of O_3 illustrate that during spring and summer high concentrations of O_3 exist in Karatay Belediye followed by Selçuklu Belediye. Variability of O_3 values during the days of the week is not well established. Diurnal figures show that the maximum O_3 levels are always around noon time or early afternoon, owing to the sequence of photochemical reactions. The presence of the secondary pollutant O_3 in a region can be an indicator of the presence of other photochemical pollutants like aldehydes and PANs that some types can be hazardous.

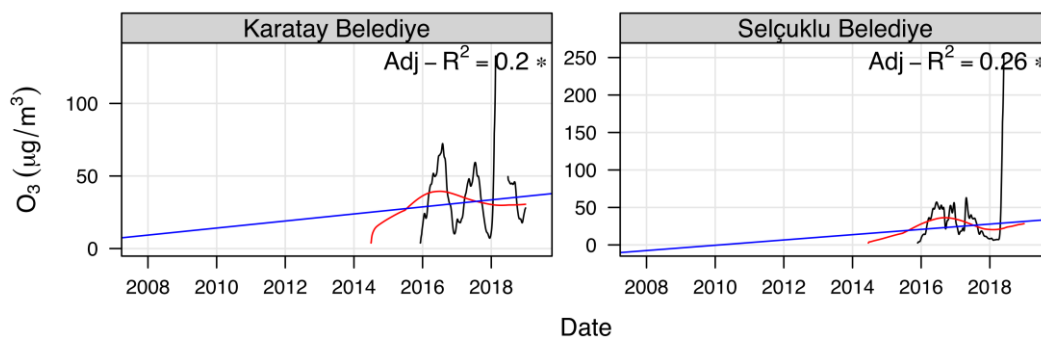


Figure 7. Trends of O_3 during the measurement period

It can be seen in Figure 7 that the urban stations of Konya have increasing O_3 trends, like NO_x trends, with Adj- R^2 values 0.26 for Selçuklu Belediye and 0.2 for Karatay Belediye. This feature of O_3 , together with those of NO , NO_2 and NO_x should be taken into account because violation of the limit values can occur in the near future.

3.4. PM_{10} analysis

5 active PM_{10} measurement stations exist in Konya: Selçuklu Belediye, Karatay Belediye, Erenkoy Belediye, Selçuklu and Meram. Selçuklu Belediye and Karatay Belediye stations have PM_{10} data since the middle of 2014. Contrary, Erenkoy Belediye has measurements only in 2018, thus it is mostly eliminated in the analysis. On the other hand, Selçuklu and Meram PM_{10} data is more or less continuous through the 2008-2018 period. Figures 8-10 show the statistics, temporal variations, pair plots and trends of the hourly PM_{10} measurements in the Konya province. It can be seen from Figure 8 that the highest mean values of PM_{10} is found as $70.5 \mu\text{g}/\text{m}^3$ in Karatay Belediye followed by $67.4 \mu\text{g}/\text{m}^3$ in Meram, $58.7 \mu\text{g}/\text{m}^3$ in Selçuklu, $48.2 \mu\text{g}/\text{m}^3$ in Erenkoy Belediye and $43.7 \mu\text{g}/\text{m}^3$ in Selçuklu Belediye.

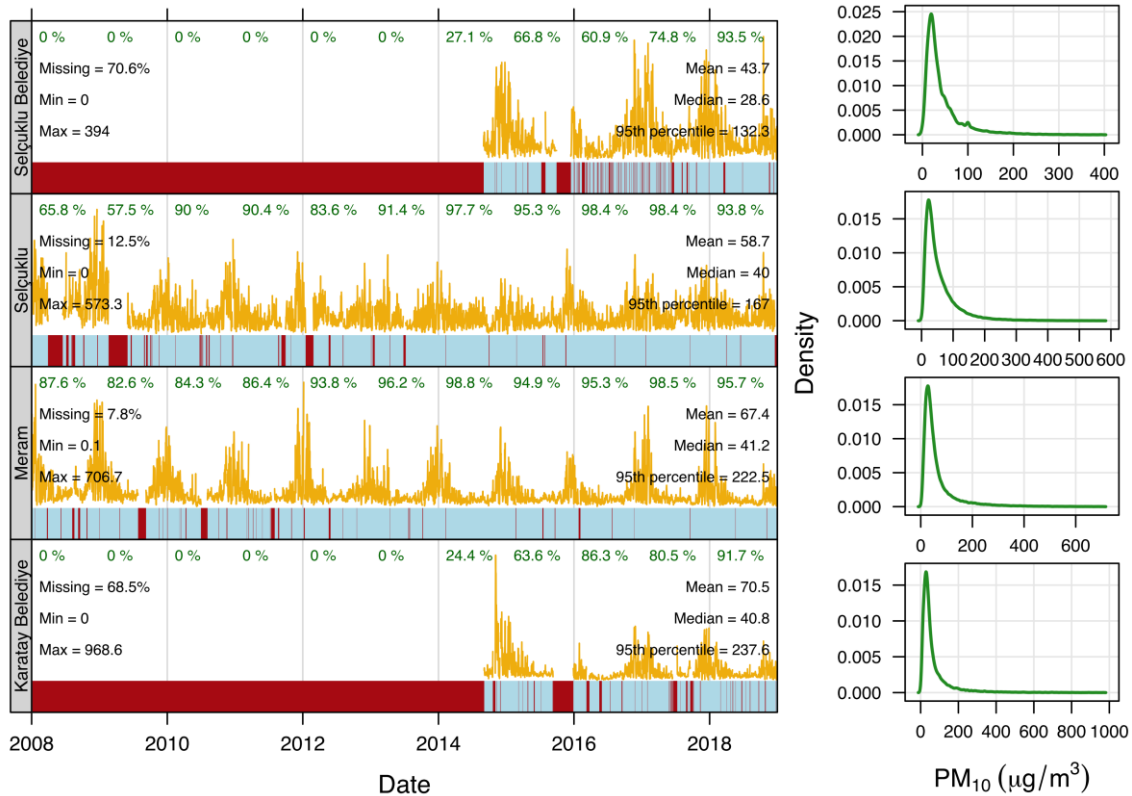


Figure 8. Hourly PM₁₀ statistics in Konya

In Hava Kalitesi Değerlendirme ve Yönetimi Yönetmeliği, 24 hour limit of PM₁₀ is given as 50 µg/m³ for the protection of human health and this limit should not be exceeded more than 35 times in a year. One can see in Figure 9 that the daily limit value is mainly violated during winter and autumn in all of the stations. 95th percentile data belonging to the stations are 132.3, 237.6, 111, 167 and 222.5 µg/m³, in the order given in the Figure 8. Karatay Belediye and Meram districts have the highest percentiles. It is obvious that 95th percentile values are much higher than the daily limit values. Density figures also show that the violation of 50 µg/m³ limit value is very frequent. Thus, it should be expressed that PM₁₀ pollution is a serious problem during winter and autumn in the Konya province.

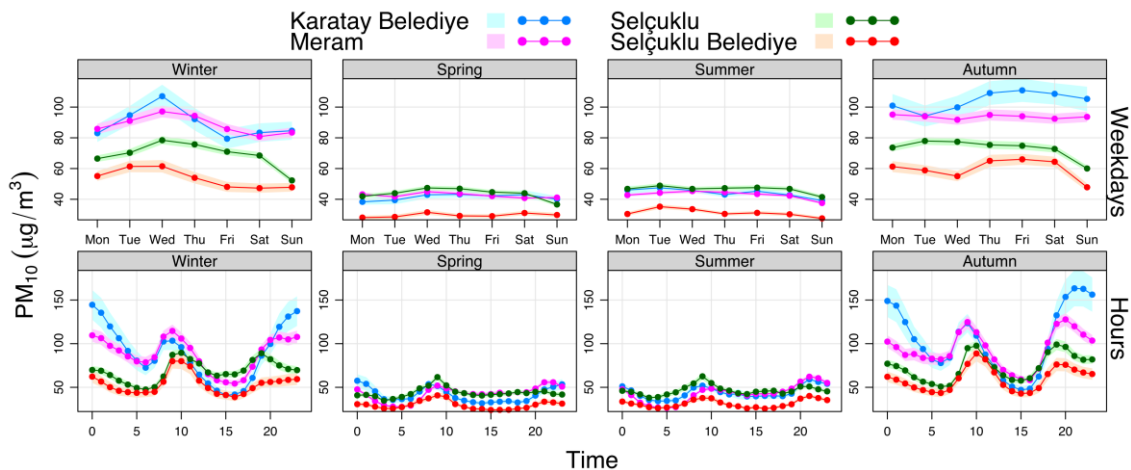


Figure 9. Diurnal and weekly variability of PM₁₀ during the seasons

Seasonal plots (Figure 9) of PM₁₀ illustrate that during winter and autumn day very high concentrations of PM₁₀ exist in all of the locations, threatening human health. Karatay Belediye and Meram districts have the highest values, associated with a weekly variability in the values. Diurnal variability is more pronounced than the weekly variability. High values exist during the morning rush hours and during night. Primary particles and secondary particles that form from the volatile chemicals in the atmosphere can be responsible from this high levels of PM₁₀ pollution. In all of the seasons and for all of the stations a prominent result is the high night time and morning rush hours PM₁₀ levels. This condition is related with the emissions, meteorology and chemistry. Prevailing stable atmospheric conditions during night generate stagnant and low wind speed conditions, especially during winter. A result of this is the generation of low mixing heights trapping the pollutants close to the surface. Low wind speeds or calm conditions exacerbate the problem by decreasing the pollutant transport in the horizontal leading to high PM₁₀ values. Contrary, during noon and early afternoon of sunny days, differential warming up of the surfaces by sun generate unstable atmosphere associated with higher boundary layer altitudes and moderate to strong mountain - valley breezes in the Konya area. This situation leads to the transport of pollutants in the horizontal as well as in the vertical generating considerably lower levels of pollution.

Pairs figure (Figure 10) shows that PM₁₀ data highly obey the log-normal distribution. It can be stated that high positive correlations exist among the stations and the highest correlation is the one between Selçuklu Belediye and Karatay Belediye with the Pearson correlation coefficient, $r=0.77$ and adjusted R^2 , $aR^2=0.59$ value.

Figure 11 show the trend plots of the stations. Generally, long-term measurements show considerable decreasing trends in PM₁₀ levels with adjusted- R^2 values 0.86 for Meram and 0.39 for Selçuklu. This decrease in the concentrations with respect to years can be a result of clean air action plans and mitigation measures that have been applied in the province to reduce pollutant emissions (KCAAP, 2019).

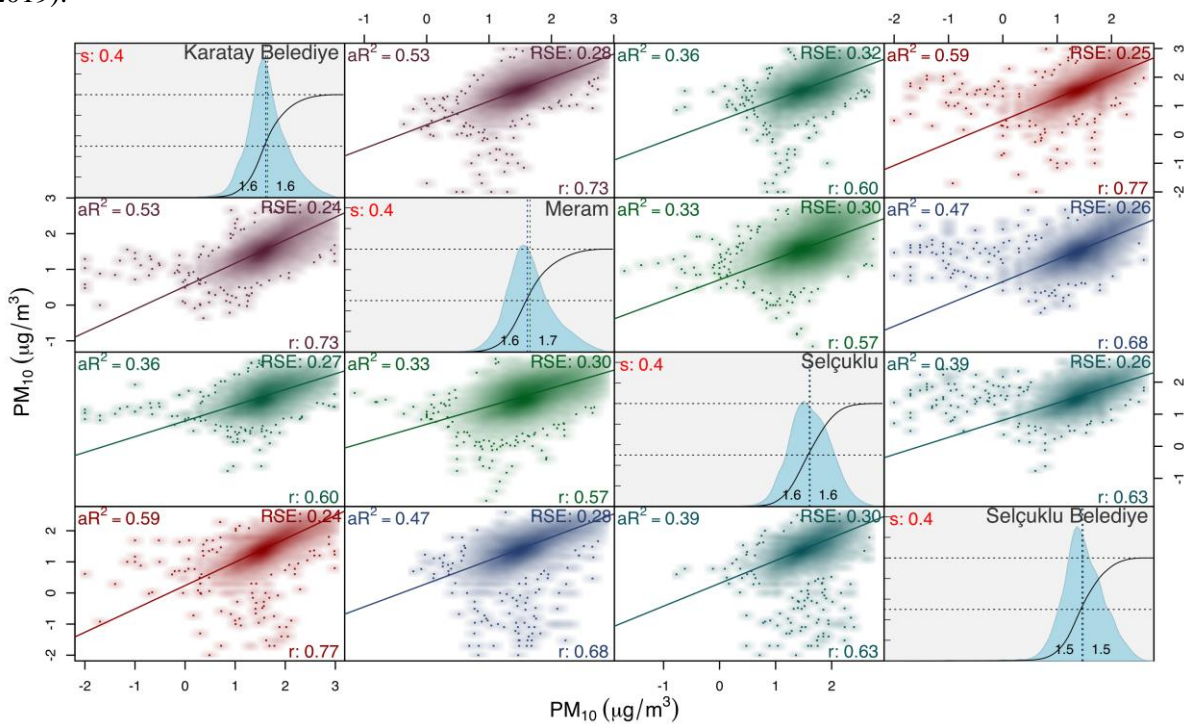


Figure 10. Hourly PM₁₀ pairs plots

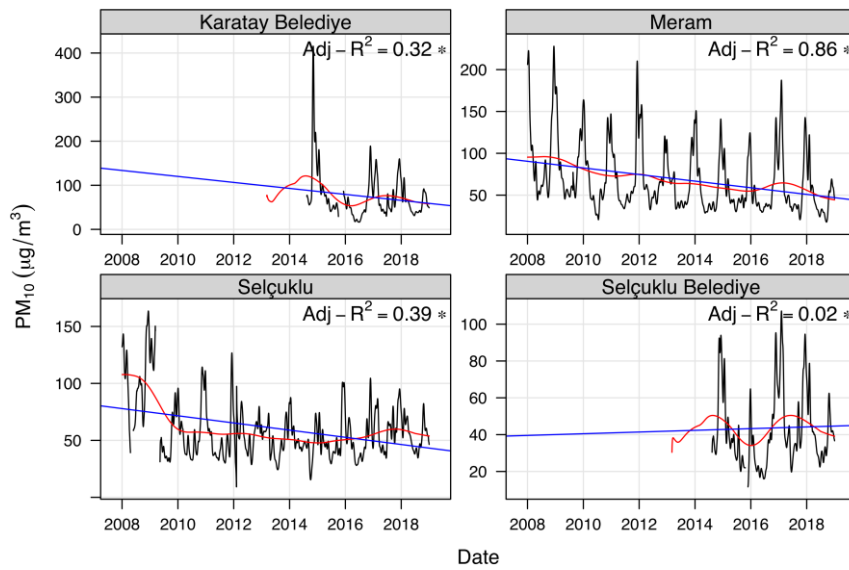


Figure 11. Trends of PM₁₀ during the measurement period

3.5. Case study: episodic analysis

Period of January 29, 2018 – February 5, 2018 was characterized as having PM₁₀ concentrations much higher than the daily limit value of 50 µg/m³ and was chosen for the episode analysis. During this one week episode, PM₁₀ concentrations climbed above 500 µg/m³ several times and reached to a peak value of 714 µg/m³. PM₁₀ variability during the period is illustrated in Figure 12a. In order to study this episode in terms of meteorology, atmospheric transportation mechanisms in the vertical and horizontal are considered. Figure 12b provide atmospheric sounding image obtained for Ankara (WMO no: 17130) at 00Z January 30, 2018. Vertical temperature profile is the dark solid curve on the right. It is clear that the temperature is increasing with height from surface to an approximate altitude of 3 km, showing the presence of a strong persistent inversion, trapping the emitted pollutants at the surface. On the other hand, reanalysis of sea level pressure (SLP) together with 500 mb geopotential height map belonging to 30th of January 2018, when the maximum PM₁₀ concentration was recorded (714 µg/m³), is generated and presented in Figure 12c. White contours show sea level isobars. If one focus on middle Anatolia, the presence of a strong high pressure system with SLP larger than 1030 mb can be seen. Isobars are located far away from each other, generating low pressure gradient force and in turn low wind speeds or calm conditions. This typical atmospheric condition together with topography of the region generated high PM₁₀ levels owing to low wind speeds and inversions, limiting the horizontal and vertical transportation, dispersion and dilution.

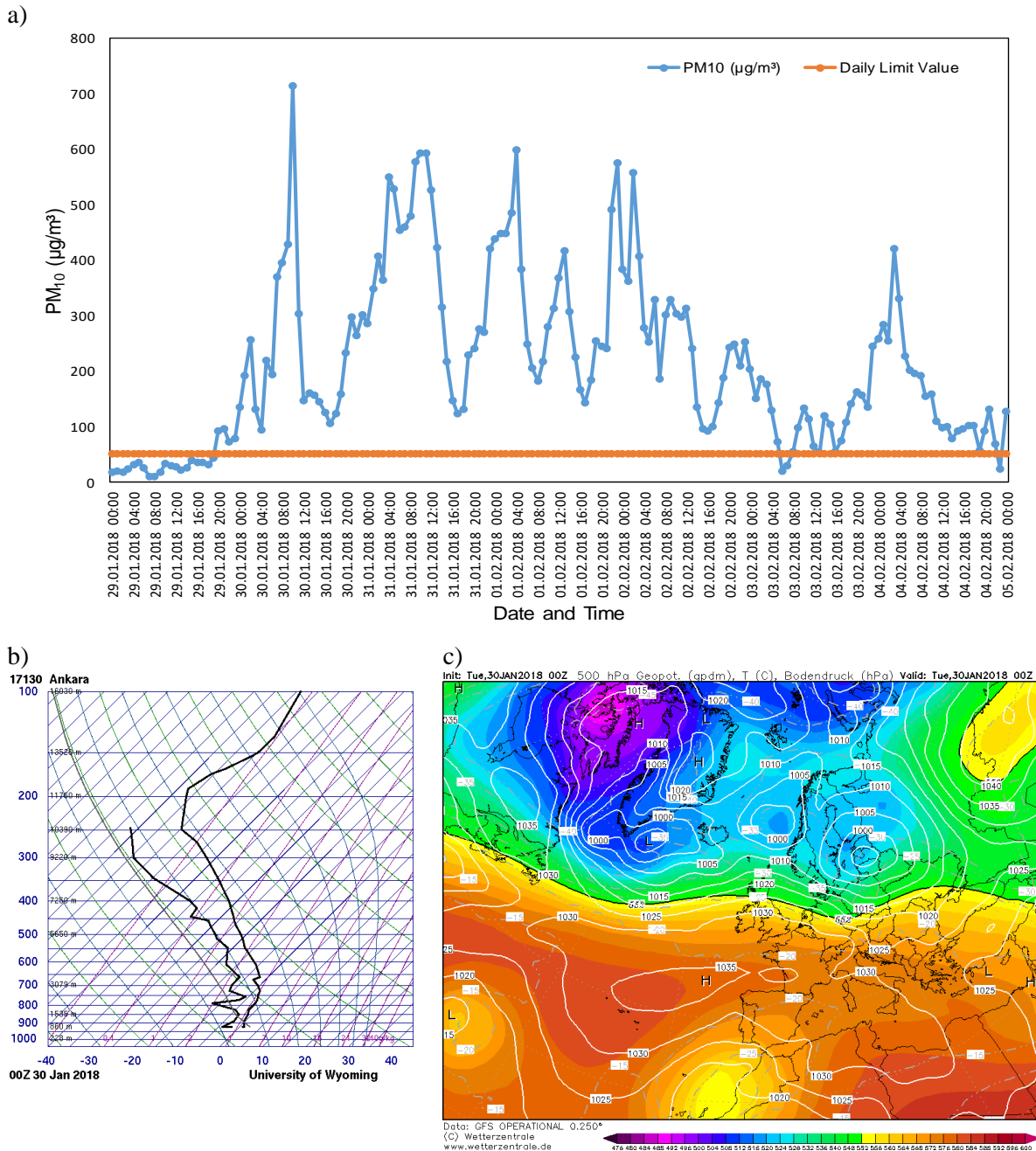


Figure 12. a) PM_{10} at Meram station during 29.01.2018- 05.02.2018 episode, b) Skew-T diagram obtained from radiosonde at Ankara, credit: University of Wyoming, c) Surface SLP and geopotential height at 500 mb level, credit: wetterzentrale.de

4. Conclusions

Hourly monitored air quality data of CO, NO, NO₂, NO_x, PM₁₀, PM_{2.5}, and SO₂ from 5 stations at Konya is subjected to various analyses, temporal and spatial variability of pollution in the 2008-2018 period is studied in terms of meteorology and topography. It is found that the worst problem belongs to PM₁₀ pollution, where PM₁₀ daily and yearly limits were exceeded throughout the measurement period with very high number of exceedances and concentrations. Number of days having concentrations higher



than the limit is larger than 150 days in any given measurement year, climbing up to 275 days in 2008. Seasonal analysis of PM₁₀ illustrate that during winter and autumn days very high concentrations of PM₁₀ exist in Konya, especially in Karatay Belediye and Meram districts. Case study done for the 29.01.2018- 05.02.2018 episode showed the importance of meteorology and topography on the high levels of pollution. Emission sources are mainly certain industries, traffic and residential heating. Limitation of the pollutant transportation and dilution in the horizontal and vertical atmosphere by meteorological conditions and the location of the Konya on a plain surrounded by high hills is believed to be the main reasons of having low air quality in the region.

5. References

Konya Sanayi Odası (<http://www.kso.org.tr/sayfa/en/industry--1>), accessed in 2019.
KCAAP (Konya Clean Air Action Plan (2013-2019)).

<https://webdosya.csb.gov.tr/db/konya/icerikbelge/icerikbelge1500.pdf>, accessed in 2019.

Kunt F. and Dursun S., 2016. Air pollution modelling of Konya City center by using artificial intelligence methods. Wulfenia Journal. No.11, volume 23.

TSMS (Turkish State Meteorological Service), 2019. <https://www.mgm.gov.tr/veridegerlendirme/il-ve-ilceler-istatistik.aspx?m=KONYA>, accessed in 2019.

Turkish Statistical Institute, 2018. <https://biruni.tuik.gov.tr/ilgosterge/?locale=tr>, accessed in 2019.

Acknowledgments

This study has been co-funded by the European Union and the Republic of Turkey with the project 'Technical Assistance for Improving Air Quality and Raising Public Awareness in Cities in Turkey - CITYAIR (in line with CAFE Directive)' and Contract N° TR2017 ESOP MI A3 01/SER/01.

Analysis of surface ozone levels in the forest and vegetation areas in Northwest Anatolia

Deniz Sari¹, Selahattin Incecik² and Nesimi Ozkurt³

^{1,3}TUBITAK Marmara Research Center, Environment and Cleaner Production Institute, 41470 Kocaeli, Turkey

²Istanbul Technical University, Istanbul, Department of the Meteorology, Istanbul, Turkey

deniz.sari@tubitak.gov.tr

Abstract. Surface ozone, which is one of the significant critical pollutants in the 21st century, threatens to human health, forest and vegetation in rural and urban areas. The primary purpose of this study is to understand the atmospheric conditions that lead to the ozone episodes in the north-western side of the Biga Peninsula, which covers by the mountainous and forested area. Ozone concentrations were measured with passive samplers and monitoring stations for three years to identify and characterise the ozone episodes that occur in the study area. WRF meteorological model was run for these episodes to describe the atmospheric conditions. Meteorological model results were tested with observed meteorological data from four stations using different statistical techniques. The influences of the meteorological parameters on ozone levels were also examined by wind speed and ambient temperature. In order to analyze the long-range transport sources contributing to the high ozone levels in the region, backward trajectories were computed using the HYSPLIT model for these episodes. The WRF outputs were served as input for HYSPLIT. This analysis was completed with 3-day backward air mass trajectories to assess the contribution of long-range transport of away contributors, resulting in the following main routes: Istanbul, Eastern Europe, and Western Russia. Additionally, an air quality model was used to understand the sources of high ozone concentration in the region for these periods. The results show that mountainous areas have higher cumulative exposure to ozone than suburban locations.

Keywords: Biga Peninsula, HYSPLIT, WRF, Surface ozone, Air quality models.

1. Introduction

Surface ozone in the troposphere is a toxic air pollutant, a greenhouse gas and a principal constituent of photochemical smog. Its elevated concentrations can cause severe damage to human health and the natural ecosystem. Most of the human health impacts associated with the respiratory system and lung irritation. Exactly, agricultural productions and trees are threatened by surface ozone in rural areas. Its damages on the ecosystem were found on sensitive plant species and reduced the yield of crops.

Moreover, surface ozone is essential greenhouse gas with radiative forcing, which can have an impact on climate change by enhancing the greenhouse effect. Surface ozone is a secondary pollutant formed under intense solar radiation driven chemical reactions involving ozone precursors like nitrogen oxides (NO_x), carbon monoxide (CO), and non-methane volatile organic compounds (NMVOCs). Ozone concentrations are generally more significant in rural areas than in large urban centers due to the destruction processes by the rapid chemical interactions between ozone and nitric oxide. These precursors result from both human activities and biogenic sources. Biogenic from plants and trees emissions like as isoprene and monoterpenes can be an essential source of VOCs on hot days. According to EU Directive 1-h standard levels for surface ozone is 120 µg/m³ at maximum 8-hr daily average and not exceeding 25 days in a calendar year.

Atmospheric conditions also have a role in the formation of ozone as well as its dispersion, transport, and accumulation at the surface. Numerous studies have indicated that intense solar irradiation, high temperature, anticyclonic pressure conditions, and inert atmosphere are suitable for photochemical production and accumulation of ozone (e.g., Thompson et al., 2001; Vukovich and Sherwell, 2003; Duenas et al., 2002).

Besides, *surface ozone* in rural areas can be strongly influenced by transported long-range emissions from distant urban areas. Emissions from polluted areas may cause too high ozone levels and its precursors in surrounding areas by long-range transportation. Due to the impacts of atmospheric conditions on ozone levels and the nonlinear relationships between ozone and its precursors, it is generally challenging to recognize the sources of ozone at a particular location (Tong et al., 2018).

The numerous studies have been performed on the surface ozone and its precursors over the past several decades in the worldwide. However, a more significant part of the studies was conducted in urban areas. The only a small part of the ozone studies was carried out for rural areas. This situation is similar to the studies performed in Turkey. For example, Im et al. (2013) examined the elevated ozone levels at an island in Istanbul by using HYSPLIT model. Kasparoglu et al. (2015) examined the back trajectories and showed the impacts of European air pollutants on the ozone levels in Şile province of Istanbul. Sari et al. (2016) investigated the surface ozone levels in the forest and vegetation areas of the Biga Peninsula, Turkey and showed the transported air pollutants to the area using back trajectories. Kasparoglu et al. (2018) examined the elevated ozone and its precursors over the Marmara region at the northwest of Turkey. They showed the impacts of transport of air pollutants over the urban and rural areas in Marmara region. The back trajectories from Eastern Europe and Ukraine support the results by findings of Freiwan and Incecik (2006).

Biga Peninsula which is situated at the northwest part of Anatolia consists of the hilly and mountainous mass. Mount Ida which is up to 1774 m, located on the south of the region. Forest and farmland areas cover nearly 80% while the urban settlement locates about 1% of the peninsula. While there is no busy road traffics, three thermal power plants, ceramic factories, and small industries sited in the study area. The climate of the Peninsula is typically Mediterranean, hot and dry in summer and cold and wet in winter.

In this study, in order to identify the reasons of elevated ozone concentrations, ozone measurements from the rural and semi-urban areas in the Biga Peninsula of Turkey during the three years of its record (2013-2015) have been analyzed. The trend of surface ozone concentrations in the study region generally reach the maximum levels during July–August and minimum values in October–December periods. The mountainous areas have higher cumulative exposure to surface ozone than the rural and urban areas in the region. The annual average of surface ozone concentrations was measured in the range of 48–117 $\mu\text{g}/\text{m}^3$ while monthly average ozone concentrations were between 78 and 187 $\mu\text{g}/\text{m}^3$ for summer periods (June, July, and August) in the region. Moreover, the maximum ozone concentration monitored at around 16:00–17:00 in rural; 15:00–16:00 in suburban sites respectively while the minimum ozone concentration is obtained during the morning hours (07:00–08:00 LST in rural; 04:00–05:00 LST in local site), respectively (Sari et al., 2016).

2. Material and methods

2.1. Study area

The Biga Peninsula is located in between 39°27'30" - 40°27'30"N and 26°02'48" - 27°30'00"E. The study area which is in Marmara Region of Turkey, covered with agricultural areas, forest areas, and the limited settlement areas. Forest and farmland areas cover nearly 80% of the study area. There are rich flora and fauna diversity in the region. Olive, Calabrian Pine (*Pinus brutia*) and Black Pine (*Pinus nigra*)

are the dominant tree species in the area (Kantarci, 2001). There is no busy road traffic in the peninsula. There are three thermal power plants (TPP) established in the peninsula, two of them at the north of coastal area (2 x600MW supercritical TPP located at the 30 km away from the Biga district), and a 320MW TPP is at the 26 km south of the Can area in addition to a ceramic factories and small industries. Although the climate of the region present typically Mediterranean climate, the northwest side of the peninsula is under the influence of “Marmara climate: hot and dry in summer, and cold and rainy in winter” which is a mixture of the Black Sea and Mediterranean climate (Kantarci, 2011). The highest average sunshine duration is above 12 hours/day in summer while it was the lowest in winter as nearly 3 hours/day. The mean maximum summer temperature is above 30 °C, and the mean annual air temperature is nearly 17 °C. The annual mean relative humidity is close to 70%. Biga receives maximum rainfall in winter with nearly 80mm while about 5mm in summer. In the study area, the prevailing wind speed and direction is nearly 5 m/s and NE in summer.

2.2. Monitoring ozone levels

The surface ozone data over the three years (2013-2015) consists of total ten passive samplers and two continuous air quality stations while the meteorological data came from the meteorological stations in the region (Figure 1). The eight of the passive sampling points were situated in residential areas while PS5 and PS10 points were located over the mountains in the peninsula. The measurements of total accumulated pollutant concentrations were measured at each month for three years at every site using diffusion tubes. Passive samplers are useful for mountainous and remote areas, secure of handling, low cost, and reliable in monitoring the air pollutants for a specific time (Gibson et al.,2009).

The online monitoring stations are established by the Marmara Clean Air Center in 2012, are located in Can (83m asl) and Lapseki (12 m asl) which are small residential areas in the Peninsula. API 400E photometric ozone analyzer is used for measurement of ozone concentrations at Lapseki and Can stations.

The daily maximum 8-h ozone concentrations reaching 120 $\mu\text{g}/\text{m}^3$ or above (which is the 8-h European standard threshold) and hourly limit (180 $\mu\text{g}/\text{m}^3$) are considered when ozone episodes were selected in the period.

2.3. Modelling

The WRF model which generates atmospheric fields at a high resolution, is used for a long-range of applications from meters to thousands of kilometers. The meteorological model uses fully compressible, non-hydrostatic equations, terrain-following vertical coordinates, and staggered horizontal grids (Skamarock et al., 2008). WRF has numerous opportunities for spatial discretization, diffusion, nesting to downscale, boundary conditions, and parameterization schemes for sub-grid scale physical processes. The physics of the model involve in microphysics, cumulus convection, planetary boundary layer turbulence, land surface, and longwave/shortwave radiation.

The WRF simulations for all episodes is run using a set of 9, 3, and 1 km horizontal resolution and one-way nested grids (Figure 2). A total of 30 vertical levels from the surface to the 100hPa are considered in the model. The outermost domain (D01) covers the most areas of East Europe and Russia, with the horizontal grids of 287×273 and the grid spacing of 9km. The nested domain (D02) covers the Balkans and the western side of Turkey, with the horizontal grids of 346×298 and the grid spacing of 3 km while D03 which is the most exceptional domain covers the Northwestern part of Anatolia including Biga Peninsula, with the grid system of 526×448 and 1km resolution.

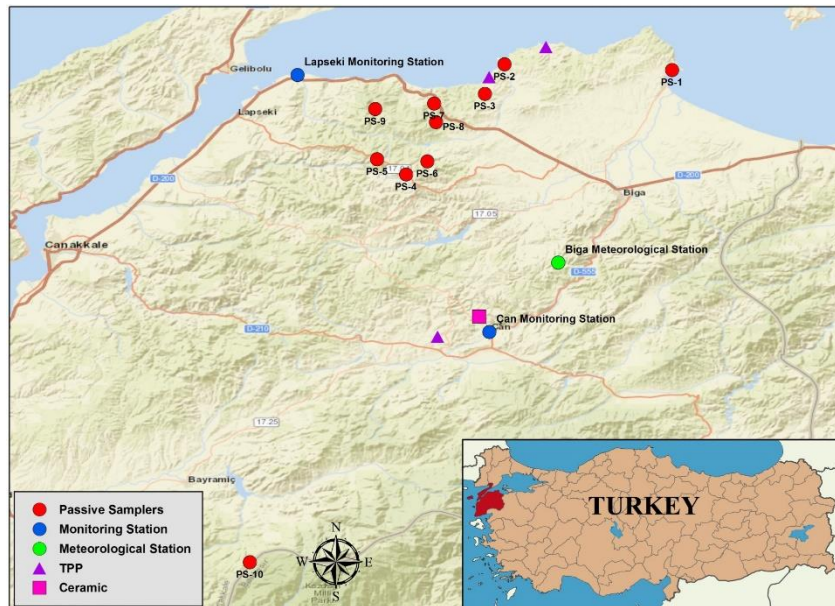


Figure 1. A map of the study region

The initial meteorological fields and boundary conditions were adopted from National Centers for Environmental Prediction Final Analyses data which has 1-degree horizontal resolution. The boundary conditions are forced every six hours.

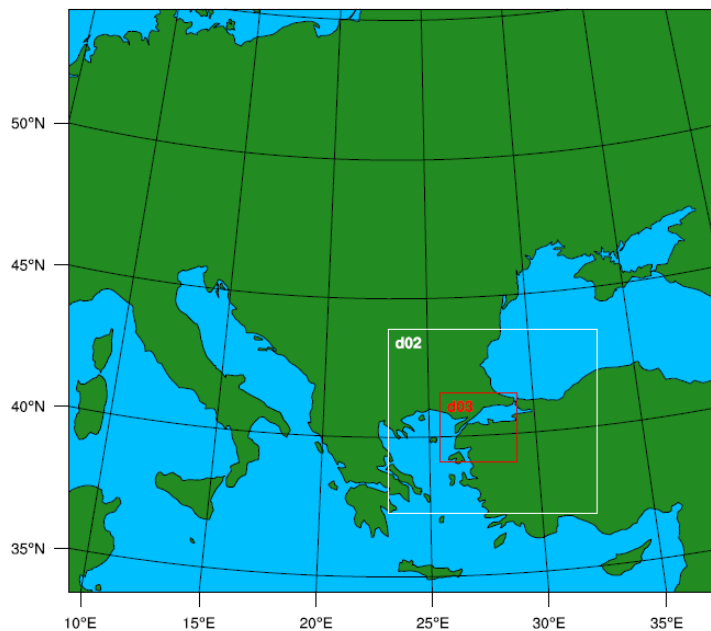


Figure 2. WRF model domain

Since model performances depend on many factors, there is no established direct technique to determine whether a model is good or incompatible. The main factors which are inputs, model parameters and the algorithm of the model, affect the model performance. Aim to make sure that the modeling results are applicable; the model performance should be evaluated. The estimations produced via models have been validated with computing different statistical methods. Model results were tested with observed

meteorological data from four meteorology stations by using different statistical techniques. These techniques are the index of agreement (d), correlation (r), mean absolute error (MAE) and the mean squared error (MSE). The closeness of the values of “d” and “r” to 1 indicates that a good model is selected and run, in other words, the significance of modeling results (Nunnari et al., 2004). Willmott (1981) stated that very different statistical parameters could be applied in comparing the model outputs with the measurement results. He observed that only the correlation coefficient is insufficient in data analysis and recommended MSE and d techniques as an alternative for such comparisons.

The Hybrid Single-Particle Lagrangian Integrated Trajectory (HYSPLIT) model which has been developed at the NOAA Air Resources Laboratory (ARL), is a useful tool for the study of long-range transport of air mass (Camalier et al., 2007). In this study, HYSPLIT 4 model was performed to follow the long-range transport sources leading to the high ozone levels in the region. Generally, HYSPLIT run by using the Global Data Assimilation System (GDAS) meteorological dataset. However, HYSPLIT model was integrated with meteorological outputs produced with the WRF model to use backward trajectory analysis in this study. HYSPLIT model is coupled with the WRF model to identify the ozone and its precursor transportation in this study.

In the presented study, HYSPLIT 4 model was used to compute the trajectory of a single pollutant particle. The transportation of a pollutant is obtained by assuming either puff or particle dispersion. The puffs enlarge until they exceed the size of the grid horizontally and vertically. Then they split into numerous new puffs and share the amount of pollution. According to particle dispersion, a fixed number of fundamental particles are advected about the domain by the mean wind field and turbulent components. (Yerramilli et al., 2012; Draxler and Hess, 1998).

The backward trajectories for a 72-h period were plotted at 3-h intervals starting from the study area to identify probable sources. It is expected that using meteorological files from outputs of WRF model with higher spatial resolution in the computation of back trajectories give better results.

3. Results and Discussion

3.1. Characteristics of ozone episodes

Episode periods are a few days up to 2-3 weeks with high concentrations of air pollutants, characterized by exceedances of the thresholds set to protect human health. In this study, the daily maximum 8-h ozone concentrations reaching $120 \mu\text{g}/\text{m}^3$ or above (which is the 8-h European standard threshold) are considered and selected five different ozone episodes in 2013 and 2015. The time series of the daily 8 hours mean ozone concentrations in episodes are shown in Figure 3.

Hourly average ozone level, amount of day when maximum daily 8 hours mean larger than $120 \mu\text{g}/\text{m}^3$ and amount of hour which is then $180 \mu\text{g}/\text{m}^3$ for each episode are given in Table 1. Ozone concentration is dependent on emissions of precursors and the amount and intensity of sunlight. So, ozone episodes will mainly occur during periods of warm sunny weather.

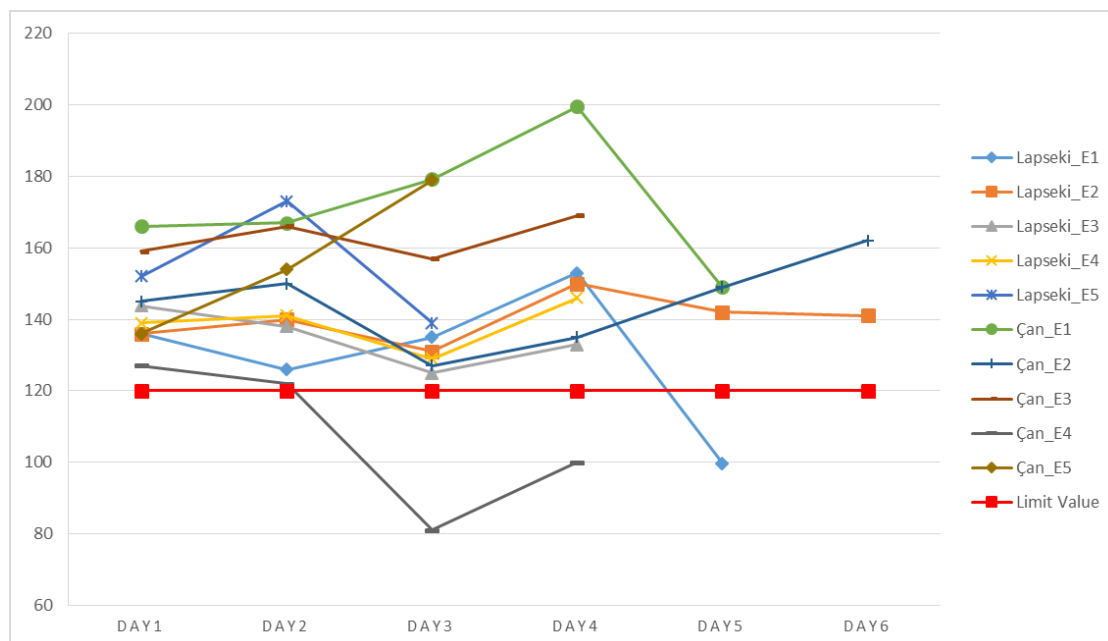


Figure 3. Time series of the daily 8 hours mean ozone concentrations in episodes in the Biga Peninsula ($\mu\text{g}/\text{m}^3$)

Table 1. Ozon levels in the five episodes

AQ Stations	E1- (22-26/06/13)			E2- (09-14/08/13)			E3- (10-13/08/14)			E4- (01-04/09/14)			E5- (27-29/07/15)		
	Av	T-1	T-2	Av	T-1	T-2	Av	T-1	T-2	Av	T-1	T-2	Av	T-1	T-2
Lapseki (rural)	99.7	4	-	117	6	-	91.6	4	-	99.3	4	-	109	3	2
Çan (semi urban)	131	5	8	97.7	6	2	99.1	4	3	68.1	2	-	94.7	3	5

Av.: Hourly average ozone level in episode $\mu\text{g}/\text{m}^3$

T1: Amount of day when maximum daily 8 hours mean larger than $120 \mu\text{g}/\text{m}^3$

T2: Amount of hour which is then $180 \mu\text{g}/\text{m}^3$

3.2. Meteorological conditions in the ozone episodes

Meteorological conditions play a crucial role in the transportation and dispersion of air mass. The main meteorological parameters as temperature, pressure, relative humidity, wind speed, and direction are considered in order to evaluate the influence on ozone concentrations. High ozone levels were shown to be mainly associated with sufficient sunshine duration, high temperature and pressure, and low wind speed in a day.

Light winds cause worse dispersion and to increase concentrations of ozone and its precursors. However, during periods of moderate wind speeds long-range transport may affect the areas and may produce high ozone concentrations.

The low wind speeds associated with high-pressure systems allow for the accumulation of ozone and its precursors. Besides, the clear skies in high-pressure systems may increase the solar radiation at the surface, which is suitable for photochemical processes in ozone production.

According to results of the WRF meteorological model, high-pressure systems and low wind speed prevail for first episode in the region (Figure 4).

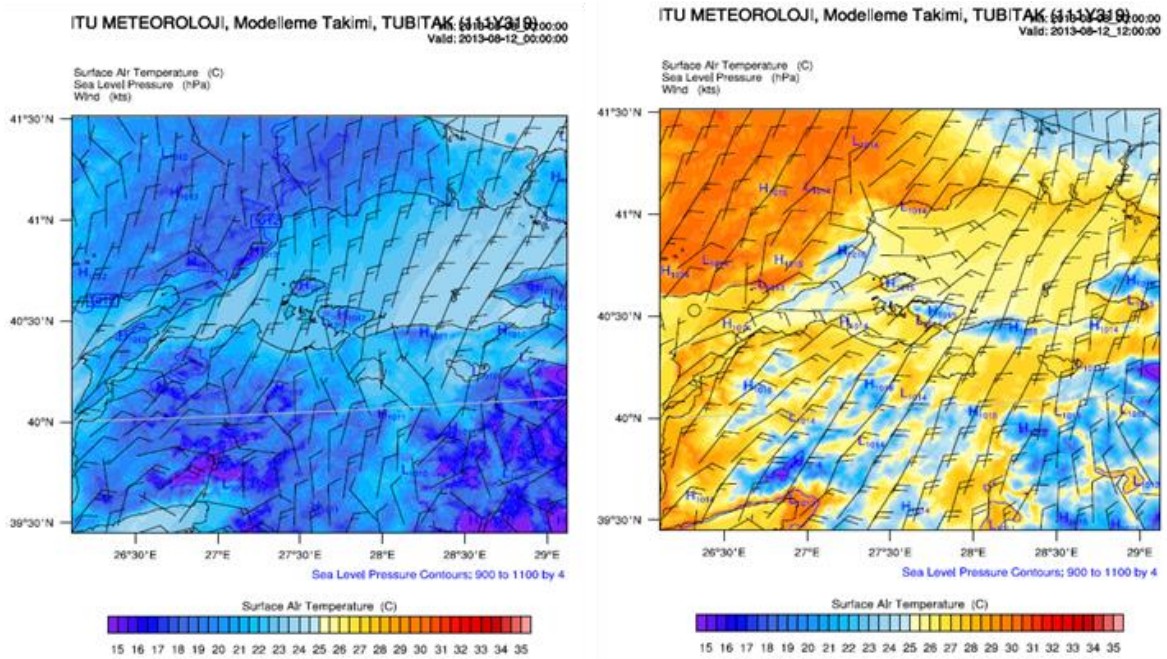


Figure 4. WRF outputs for 1st episode

During the second episode (Figure 5) and the third episode (Figure 6) periods, the high-pressure system prevails in the region, while wind speeds are light levels.

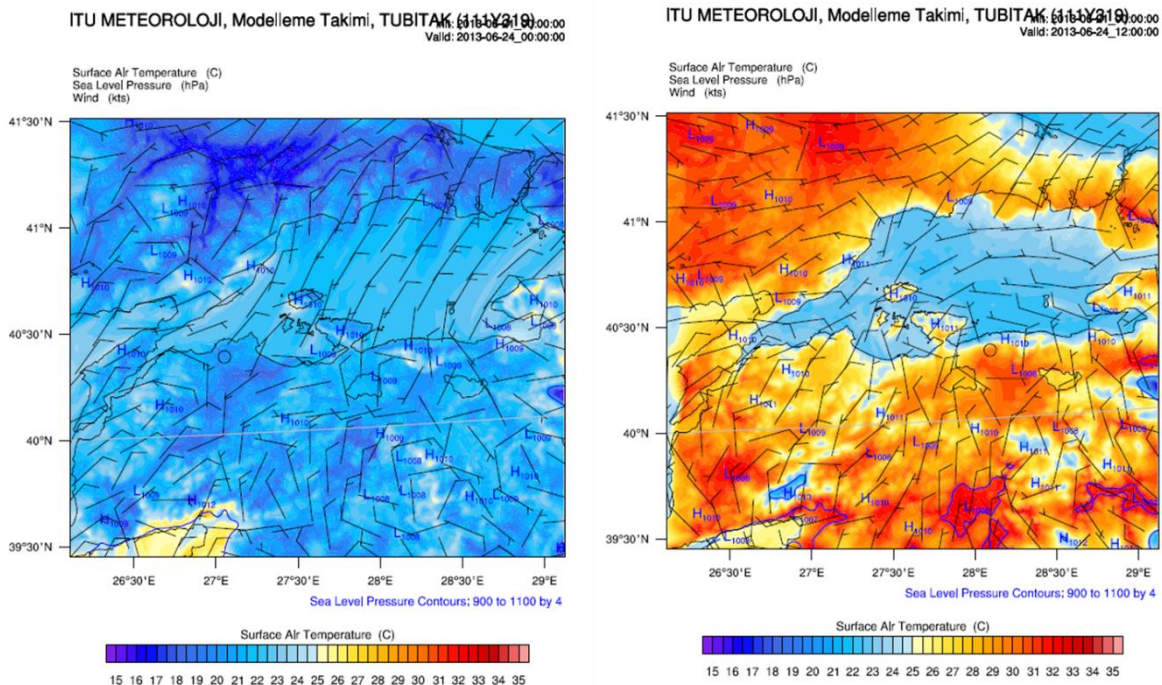


Figure 5. WRF outputs for 2nd episode

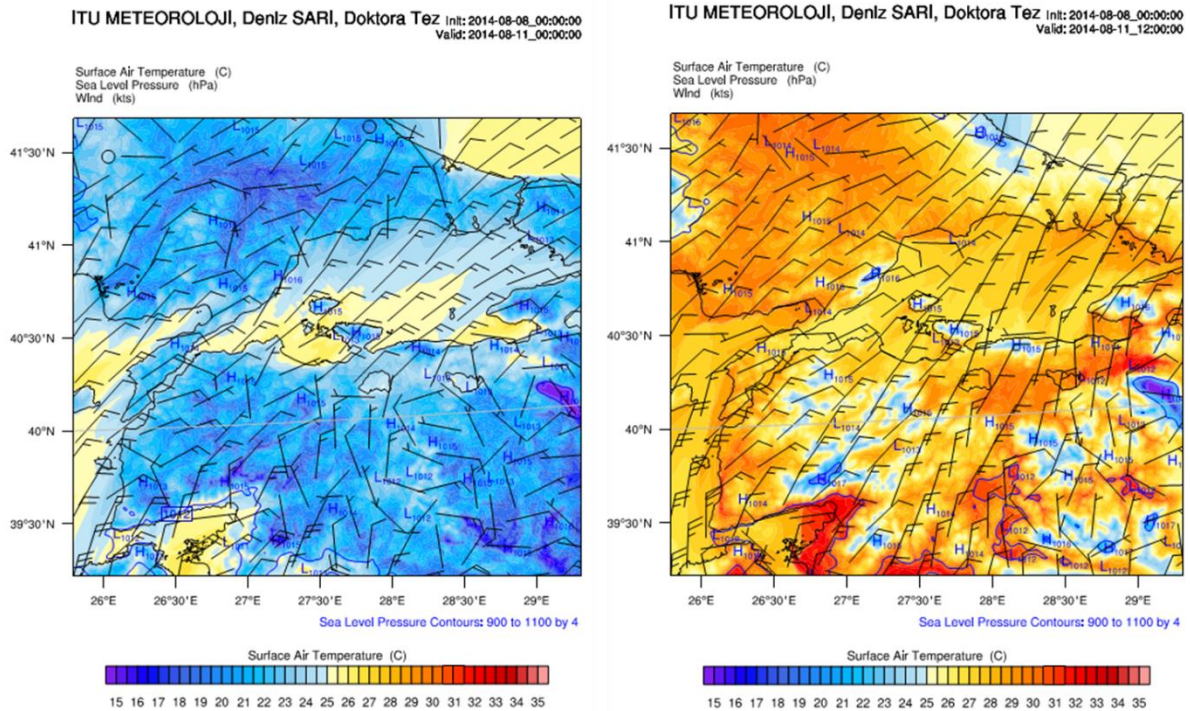


Figure 6. WRF outputs for 3rd episode

According to the WRF model outputs, the high-pressure systems and light winds are observed in the region during the fourth episode (Figure 7) and the fifth episode (Figure 8).

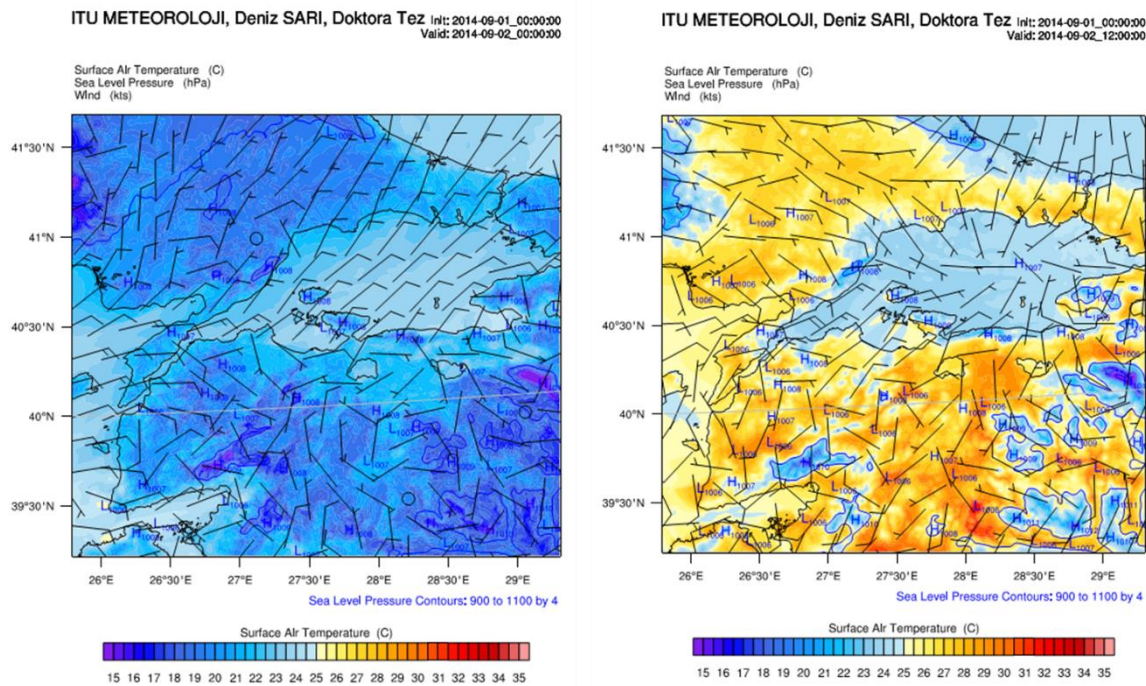


Figure 7. WRF outputs for 4th episode

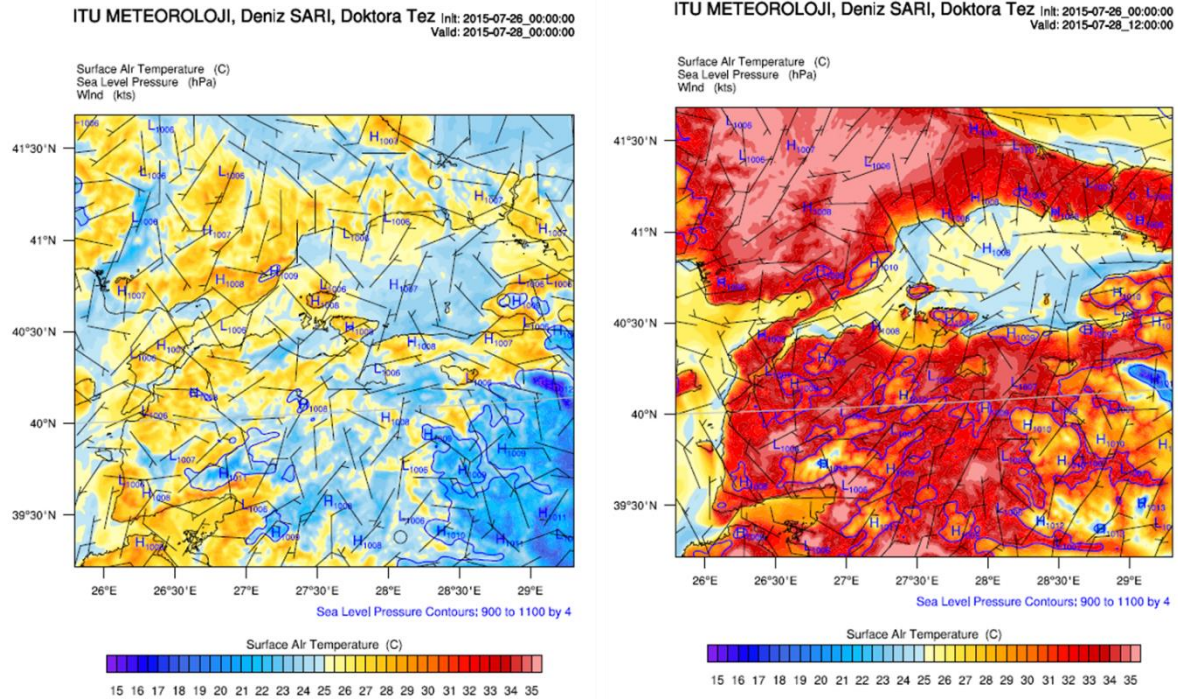


Figure 8. WRF outputs for 5th episode

3.3. Validation

Validation of models is essential to evaluate the quality of model results. Validation operations are generally performed predictions and observation for a specific period. Although there are many different validation techniques, the relationship between predictions and observations is mainly examined. The existence of the same meteorological conditions, the same geographical basis and the evaluation of the points at the same coordinates are of great importance during the model verification process.

The model outputs were compared with the meteorological measurements during the five episodes to validate the WRF model predictions. Biga, Canakkale, Bursa and Tekirdag Meteorological stations were chosen for the most suitable representation of the region in terms of climate. The location of the stations is given in Figure 9. Temperature, relative humidity, wind speed, and pressure data from four different meteorological stations for five episodes were used. In order to evaluate the model performance, four statistical metrics are used: correlation, index of agreement, mean absolute error and root mean square error.

The results indicate that the prediction of the temperature and wind speed is quite successful. The values of relative humidity were examined was calculated close to observation in all stations except Tekirdag station. When the predictions of pressure values and the observations are compared, it is determined that very close results are obtained for Canakkale and Tekirdag. However, the differences in the Biga and Bursa stations were significant, and there was a very low consistency between the results for atmospheric pressure. Wind direction (u and v components) error values for all stations were not high values, and it was observed that the model estimations were close to the measurement results. The results of statistical analyses for model validation were given in Table 2.

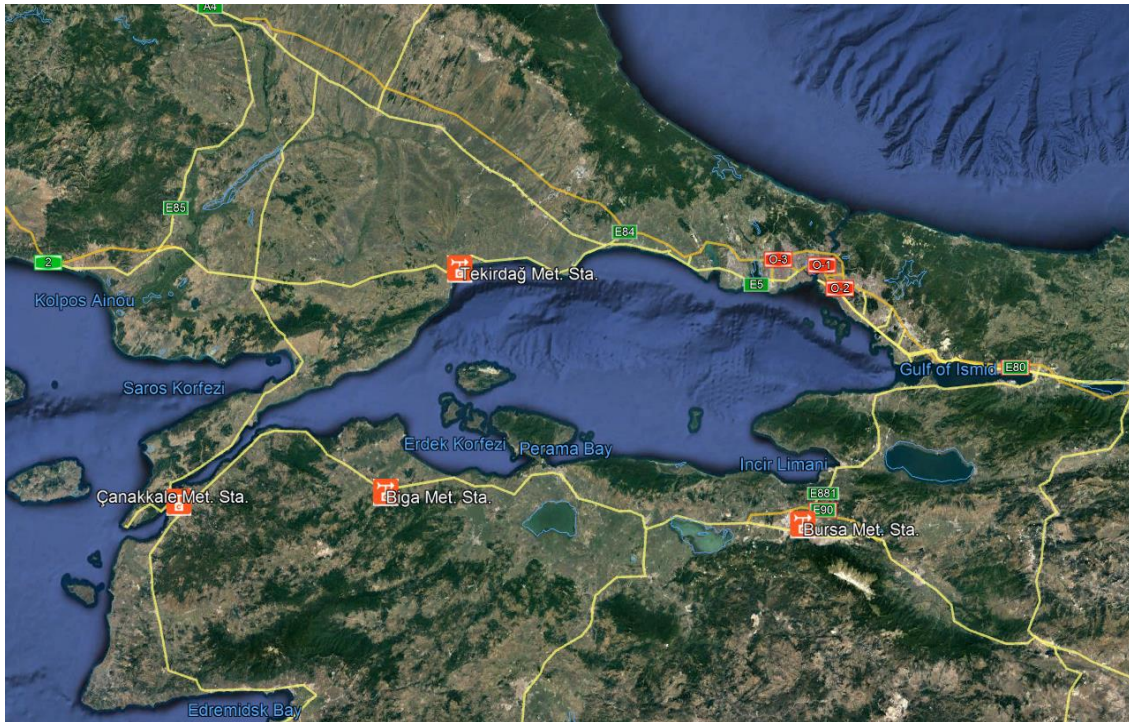


Figure 9. The locations of meteorological stations

Table 2. The results of statistical analyses for model validation

Meteorological Parameter	Meteorology Stations	Episode 1				Episode 2				Episode 3				Episode 4				Episode 5			
		d	r	MAE	MSE	d	r	MAE	MSE	d	r	MAE	MSE	d	r	MAE	MSE	d	r	MAE	MSE
Temperature	Biga	0.9	0.9	2.3	2.6	0.8	1.0	2.6	2.8	0.9	0.9	1.9	2.3	0.9	0.9	1.1	1.4	0.9	0.9	2.4	2.9
	Çanakkale	0.9	0.9	2.1	2.4	0.8	0.9	3.0	3.5	0.9	0.9	2.0	2.5	1.0	0.9	1.5	0.9	0.9	0.9	2.0	2.5
	Tekirdağ	0.6	0.8	4.6	4.9	0.4	0.8	6.7	6.9	0.6	0.8	4.8	5.2	0.7	0.7	2.9	3.3	0.7	0.8	2.9	3.4
	Bursa	0.9	0.9	2.8	3.2	0.9	0.9	3.4	3.7	0.8	0.9	3.3	3.7	0.8	0.9	2.9	3.2	1.0	0.9	1.9	2.6
Relative Humidity	Biga	0.8	0.9	14.1	15.8	0.8	0.9	16.9	18.7	0.9	0.9	11.7	13.0	0.8	0.7	9.7	11.3	0.8	0.7	11.3	13.8
	Çanakkale	0.8	0.7	10.9	13.5	0.8	0.6	12.4	15.0	0.9	0.8	8.2	10.5	0.8	0.7	8.7	11.7	0.5	0.6	22.0	24.8
	Tekirdağ	0.5	0.5	17.7	20.2	0.5	0.3	26.3	30.2	0.6	0.5	13.6	15.8	0.4	0.1	14.6	17.7	0.4	0.3	23.0	25.7
Wind Speed	Biga	1.0	0.7	1.7	2.1	1.0	0.7	1.6	2.1	1.0	0.6	1.3	1.6	1.0	0.6	1.3	1.6	1.0	0.6	1.1	1.4
	Çanakkale	0.9	0.6	2.0	2.5	1.0	0.5	1.6	2.0	0.9	0.5	1.4	1.8	0.9	0.3	1.2	1.7	0.8	0.3	1.5	2.0
	Tekirdağ	0.9	0.5	1.4	1.8	0.9	0.4	4.0	4.4	0.7	0.2	3.7	4.0	0.8	0.1	2.1	2.5	0.9	0.3	1.4	1.7
	Bursa	0.9	0.6	1.2	1.4	0.9	0.6	1.6	2.0	0.9	0.6	1.1	1.3	0.8	0.4	1.9	2.3	0.9	0.4	1.3	1.7
Pressure	Biga	0.5	1.0	6.8	6.9	0.4	1.0	7.2	7.3	0.3	0.9	7.4	7.5	0.3	0.9	6.3	6.3	0.2	0.9	7.1	7.2
	Çanakkale	0.9	1.0	1.0	1.1	1.0	1.0	1.0	1.2	1.0	1.0	0.4	0.5	0.8	0.7	0.8	1.0	0.9	0.9	0.6	0.7
	Tekirdağ	1.0	1.0	0.8	0.9	1.0	0.9	0.9	1.2	0.8	0.9	1.2	1.3	0.8	0.7	0.7	0.9	0.4	0.4	1.8	2.0
u- wind component	Bursa	0.3	0.9	12.4	12.5	0.3	0.9	13.8	13.8	0.2	0.8	13.4	13.4	0.1	0.7	12.0	12.0	0.1	0.8	11.9	11.9
	Biga	0.7	0.6	1.9	2.3	0.7	0.6	1.7	2.1	0.6	0.4	1.9	2.2	0.4	0.0	1.9	2.4	0.9	0.9	0.7	0.9
	Çanakkale	0.5	0.3	1.7	2.3	0.6	0.3	1.1	1.4	0.5	0.2	1.1	1.5	0.6	0.5	1.7	2.2	0.6	0.4	1.6	2.1
	Tekirdağ	0.6	0.8	4.6	4.9	0.5	0.2	3.2	3.6	0.3	0.0	3.2	3.6	0.3	-0.3	2.4	2.8	0.6	0.4	1.9	2.4
v- wind component	Bursa	0.5	0.4	2.2	2.7	0.5	0.4	1.7	2.2	0.5	0.3	1.8	2.3	0.3	0.1	3.4	3.9	0.5	0.2	2.1	2.6
	Biga	0.8	0.6	1.4	1.9	0.8	0.6	1.3	1.6	0.8	0.7	1.3	1.7	0.8	0.7	1.3	1.8	0.9	0.9	0.7	0.9
	Çanakkale	0.5	0.4	3.3	3.9	0.6	0.6	2.6	3.0	0.6	0.5	2.2	2.6	0.4	0.0	2.2	2.7	0.3	-0.2	2.2	3.1
	Tekirdağ	0.5	0.3	2.3	2.8	0.5	0.2	4.1	4.9	0.3	-0.4	4.4	4.9	0.4	0.1	2.9	3.4	0.6	0.5	1.5	1.8
Bursa	0.4	0.1	1.9	2.5	0.5	0.3	2.0	2.4	0.1	-0.4	2.0	2.5	0.5	0.1	1.6	1.9	0.3	-0.3	1.9	2.5	

3.4. LRT of Ozone and Its Precursors

In this study, HYSPLIT 4 model was performed to follow the long-range transport sources leading to the high ozone levels for five episodes in the region. HYSPLIT model was integrated with outputs of WRF meteorology model.

The HYSPLIT model was used to compute hourly 3D backward trajectories at 500m above ground level (AGL). 500m AGL for model runs was selected to show the well-mixed conditions in the atmospheric boundary layer and likely to affect the surface air quality in the region. Seventy-two hours period may be right to capture the long-range transport of air mass since most pollutants deposit within a couple of days (Im et al., 2013). The HYSPLIT back trajectory analysis driven by the WRF simulated fields with 1 km resolution is shown in Figure 10.

This analysis was completed with 3-day backward air pollutant trajectories to calculate the contribution of long-range transport of the contributors, resulting in the following main routes: İstanbul, Eastern Europe, and Western Russia. Most episodes were caused by local photochemical production and pollutant accumulation, and transport of pollutants from the highly polluted regions could significantly influence the air quality in the site, especially from İstanbul (Figure 10).

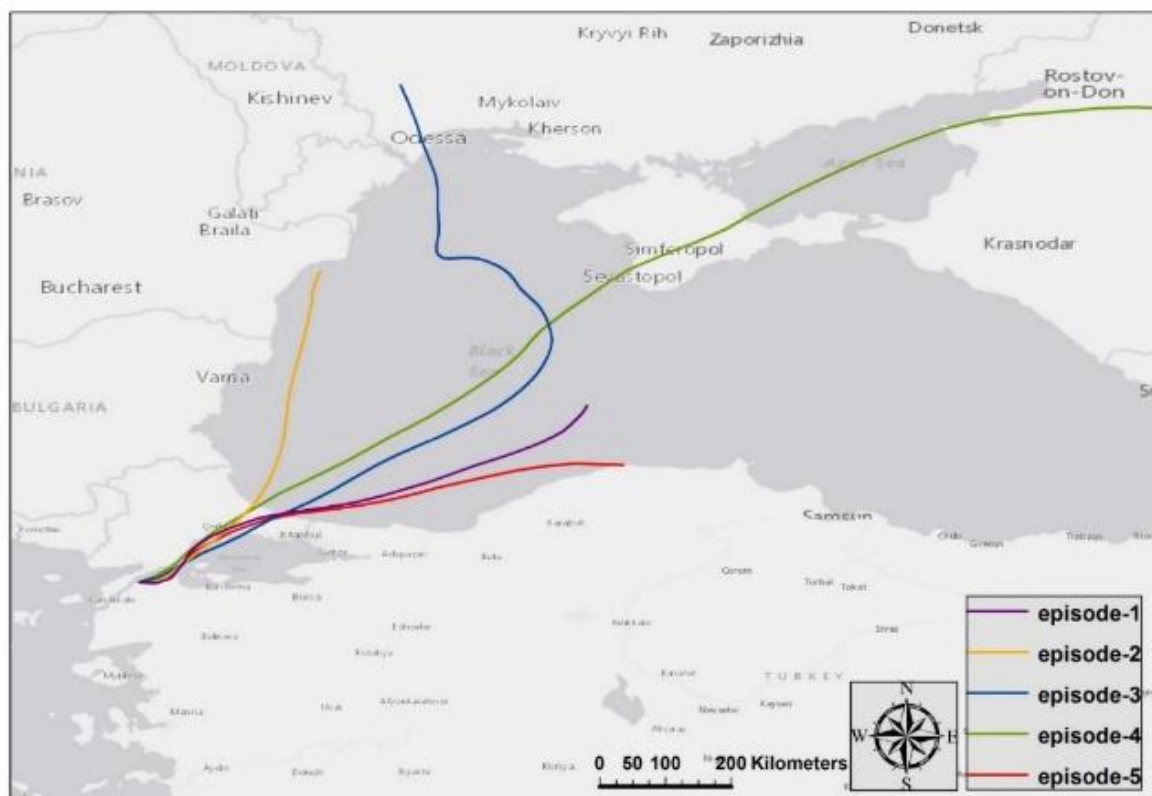


Figure 10. Outputs of HYSPLIT back trajectory analysis

4. Conclusions

In this study, ozone measurements from forest and vegetation areas in the Biga Peninsula of Turkey from 2013 to 2015 have been analyzed in order to identify the reasons of high ozone concentrations. The daily maximum 8-h ozone concentrations which reach $120 \mu\text{g}/\text{m}^3$ or above are considered and selected five different ozone episodes during three years. The WRF model is used to generate meteorological fields at high resolution over the Biga Peninsula region for these five episodes. The model outputs were

compared with the meteorological measurements during all episodes to validate the predictions. The results of validation showed that the temperature, wind speed, and direction were the most reliable parameters which were produced via modeling. According to result, meteorological conditions and synoptic weather patterns leading to low wind speeds were associated with high ozone levels in the study region.

Then the HYSPLIT4 driven by the WRF simulations is used to identify the possible emission source locations and transportation routes. The results from the five different ozone episodes selected between 2013 and 2015 indicate that İstanbul, Eastern Europe, and Western Russia are possible source locations affecting the elevated ozone in Biga Peninsula. Ozone episodes were caused by local photochemical production, pollutant accumulation, and transport of emissions from the highly polluted regions especially from the north including İstanbul.

5. References

- Camalier, L., Cox, W., Dolwick, P., 2007. The effects of meteorology on ozone in urban areas and their use in assessing ozone trends. *Atmospheric Environment*. 41, 7127-7137.
- Draxler, R.R., Hess, G.D., 1998. An Overview of the HYSPLIT_4 Modelling System for Trajectories, Dispersion, and Deposition. *Australian Meteorological Magazine*. 47, 295-308.
- Duenas, C., Fernandez, M.C., Canete, S., Carretero, J., Liger, E., 2002. Assessment of ozone variations and meteorological effects in an urban area in the Mediterranean Coast. *The Science of the Total Environment*. 299, 97-113.
- Freiwan, M., Incecik, S., 2006. Modeling European air pollutants transport to the eastern Mediterranean region, *ITU Dergisi*. 5, 255-266.
- Gibson, M. D., Guernsey, J.R., Beauchamp, S., Waugh, D., Heal, M. R., Brook, J. R., Maher, R., Gagnon, G. A., McPherson, J. P., Brydeng, B., Gouldh, R., Terashimaa, M., 2009. Quantifying the Spatial and Temporal Variation of Ground-Level Ozone in the Rural Annapolis Valley, Nova Scotia, Canada Using Nitrite-Impregnated Passive Samplers, *Journal of the Air & Waste Management Association*. 59, 3, 310-320.
- Im, U., Incecik, S., Guler, M., Tek, A., Topcu, S., Unal, Y.S., Yenigun, O., Kindap, T., Odman, M.T., Tayanc, M., 2013. Analysis of surface ozone and nitrogen oxides at urban, semi-rural and rural sites in İstanbul, Turkey. *Science of The Total Environment*. 443, 920-931.
- Kantarci, D., 2001. The Effect of Air Pollution on Forests in Biga Peninsula, *Journal of Environmental Protection and Ecology (JEPE)*. 4, 806-818.
- Kantarci, D., 2011. Vertical climate zones in Biga peninsula: The impact of climate change and air pollution on forests, *Procedia Social and Behavioral Sciences*. 19, 797-810.
- Kasparoglu, S., Incecik S., Topcu S., 2018. Spatial and temporal variation of O₃, NO and NO₂ concentrations at rural and urban sites in Marmara region of Turkey. *Atmospheric Pollution Research*. 9, 1009-1020.
- Kasparoglu, S., Incecik, S., Ozer, B., 2015. Variations in O₃ and NO_x at Coastal Suburban, and Urban Sites in İstanbul, The 5th International WeBIOPATR Workshop & Conference Particulate Matter: Research & Management Belgrade, Serbia 14th-16th October, 2015.
- Nunnari, G., Dorling, S., Schlink, U., Cawley, G., Foxall, R., Chatterton, T., 2004. Modelling SO₂ concentration at a point with statistical approaches. *Environmental Modelling & Software*. 19, 887-905.
- Sari, D., Incecik, S., Ozkurt, N., 2016. Surface ozone levels in the forest and vegetation areas of the Biga Peninsula, Turkey, *Science of The Total Environment*. 571, 1284-1297.



- Skamarock, W., Klemp, J., 2018. A time-split nonhydrostatic atmospheric model for weather research and forecasting applications. *Journal of Computational Physics*. 227, 3465-3485.
- Thompson, M., Reynolds, J., Cox, L., Guttorp, P., Sampson, P., 2001. A review of statistical methods for the meteorological adjustment of tropospheric ozone. *Atmospheric Environment*. 35, 617-630.
- Tong, L., Zhang, J., Xu, H., Xiao, H., He, M., Zhang, H., 2018. Contribution of Regional Transport to Surface Ozone at an Island Site of Eastern China, *Aerosol and Air Quality Research*. 18, 3009–3024.
- Vukovich, F., Sherwell, J., 2003. An examination of the relationship between certain meteorological parameters and surface ozone variations in the Baltimore–Washington corridor, *Atmospheric Environment*. 37, 971-981.
- Willmott, C.J., 1981. On the validation of models. *Physical Geography*. 2, 184-194.
- Yerramilli, A., Dodla, V., Challa, V., Myles, L., Pendergrass, W., Vogel, C., Dasari, H., Tuluri, F., Baham, J., Hughes, R., Patrick, C., Young, J., Swanier, S., Hardy, M., 2012. An integrated WRF/HYSPLIT modeling approach for the assessment of PM_{2.5} source regions over the Mississippi Gulf Coast region. *Air Qual. Atmos. Health*. 5, 401-412.



Success of volatile organic compounds (VOCs) emission reduction and challenges for oil and gas sector in Thailand

**Vichuda Tipsunave¹, Wasin Pinprateep¹, Ekkapat Mahasurachaikul²
Nathasith Chiarawatchai¹ and Chanansiri Panpanit¹**

¹ PTT Public Company Limited Sustainability Strategy Department
Bangkok-Thailand

² PTT Public Company Limited Safety, Security, Health, and Environment
Management Department Bangkok-Thailand

Vichuda.t@pttplc.com, Wasin.p@pttplc.com

Abstract. The majority of Volatile Organic Compounds (VOCs) is concentrated in Rayong Province, Thailand, which can contribute to an adverse health effects. PTT Public Company Limited (PTT), an integrated oil and gas company and subsidiaries which operate several facilities in Rayong, decided to develop VOCs inventory guideline by itself to identify major sources of VOCs and to determine VOCs reduction potentials. PTT integrated guidelines and regulations from USEPA and Thailand as well as PTT's experience in the industry. This resulted in VOCs inventory comprising six sources non-methane VOCs: flares, fugitives, loading and unloading, storage tank, combustion, and waste water treatment plant. Accordingly, PTT categorized into two business activities namely upstream and downstream for effective management. VOCs reduction potentials and management were examined for each source by analysing API standards, USEPA regulations and guideline, and local guidelines such as Bay Area Air Quality Management District. PTT successfully established VOCs inventory and expanded to fully cover upstream and downstream. For example, VOCs from flares was calculated by flare volume, heating value and emission factors. Fugitives VOCs was calculated from emission factors or from monitoring equipment in accordance with USEPA Method 21. Based on the 2018 inventory, majority of emission was from flares in the upstream business, followed by fugitives, and loading and unloading activities in downstream business respectively. VOCs reduction potentials have been determined and implemented such as flare utilization in production process for VOCs from flares and a Smart Leak Detection and Repair for VOCs from fugitives. Other mitigations are improving combustion efficiency, modifying liquid fuel transfer equipment, and covering of wastewater treatment plant. In terms of management, PTT recognized impact to surrounding communities and therefore integrated VOCs response program in emergency management plan. After continuous implementation and management, PTT successfully reduce approximately 15% Upstream VOCs in 2018 compared to 2017. The VOCs response program has been widely utilized in surrounding area to monitor and control environmental problems in collaboration with communities.

Keywords: Health effects, Oil and gas industry, Thailand, VOCs Maximum

1. Background

In Thailand, there is a growing concern regarding adverse health effects of Volatile Organic Compounds (VOCs). Majority of VOCs is concentrated in Rayong Province (Figure1.) in which it has been announced as pollution controlled area according to Rayong administrative court order. As oil and gas sector is considered as one of major sources of VOCs, PTT Public Company Limited (PTT), the biggest energy company in Thailand and operator of several facilities in Rayong, is obliged to account and mitigate VOCs to environmental impacts. Regulation and guidelines involving VOCs were developed, yet remain challenging for industries to quantify and manage emission. As a result, PTT decides to develop VOCs inventory guideline by itself to identify major sources of VOCs and to determine VOCs reduction potentials. (Figure2.)



Figure 1. Rayong Province Thailand

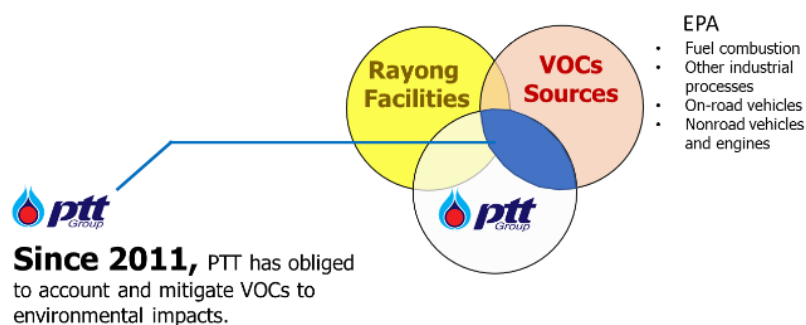


Figure 2. Scope of VOCs management

2. Methodology

PTT has integrated guidelines and regulations from USEPA and Thailand, along with PTT's experience in the industry. The inventory comprises of six sources non-methane VOCs emission inventory: flares, fugitives, loading and unloading, storage tank, combustion, and waste water treatment plant (Table 1.) as well as categorized into two business activities namely upstream and downstream for effective

management. Accordingly, VOCs reduction potentials and management were examined for each source by analysing API standards, USEPA regulations and guideline, and local guidelines such as Bay Area Air Quality Management District.

Table 1. VOCs inventory evaluation method

VOCs inventory evaluation method		Reference
Flares	<ul style="list-style-type: none"> Flare volume x heating value x emission factors 	(4), (8), (9)
Fugitives	<ul style="list-style-type: none"> USEPA Method 21 / Alternative Work Practice to Detect Leaks from Equipment Calculation by Average Emission Factors Approach 	(1), (2), (3), (4), (5), (7), (9)
Loading & unloading	<ul style="list-style-type: none"> Loading loss calculation 	(4), (6), (9)
Storage tank	<ul style="list-style-type: none"> Tank 4 Program 	(4), (6), (9)
Combustion	<ul style="list-style-type: none"> Fuel volume x emission factors 	(4), (6), (9)
Wastewater treatment plant	<ul style="list-style-type: none"> Water 9 Program 	(4), (6), (9)

3. Result

PTT successfully established VOCs inventory and expanded to fully cover upstream and downstream that was in compliance with Thailand's regulation. For example, VOCs from flares was calculated by flare volume, heating value and emission factors. Fugitives VOCs was calculated from emission factors or from monitoring equipment in accordance with USEPA Method 21. Loading and unloading activities VOCs was calculated from loading loss. Tank 4 Program and Water 9.0 Program were used for Storage tank VOCs and Wastewater treatment plant VOCs calculation respectively. In addition, Combustion VOCs was determined from fuel consumption and emission factors.

Based on the 2018 inventory, majority of emission was from flares in the upstream business, followed by fugitives, and loading and unloading activities in downstream business respectively. (Figure 3. & Figure 4.)

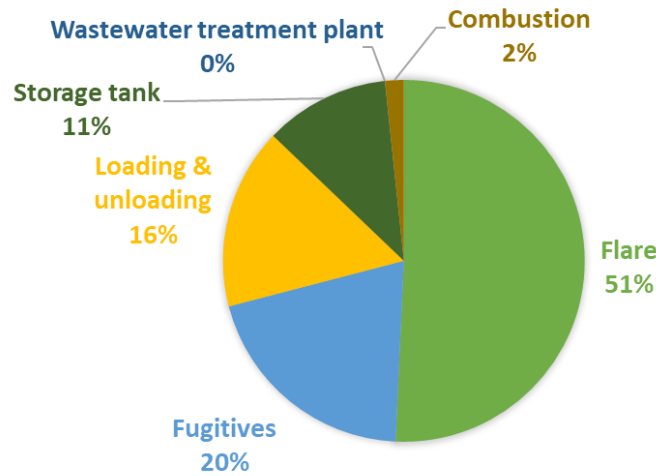


Figure 3. VOCs inventory 2018

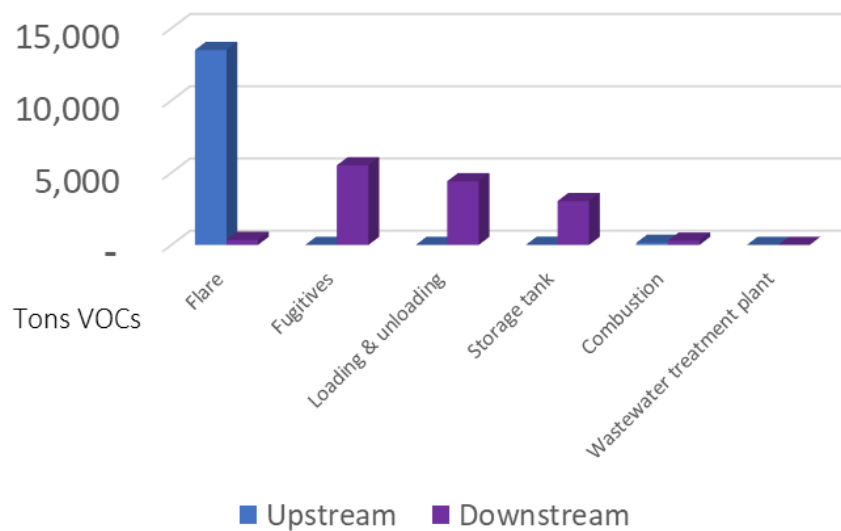


Figure 4. Upstream & Downstream VOCs inventory 2018

Focusing on major sources, VOCs reduction potentials have been determined and implemented such as flare utilization in production process for VOCs from flares, A Smart Leak Detection and Repair for fugitives VOCs. Other mitigations are improving combustion efficiency, modifying liquid fuel transfer equipment, and covering of wastewater treatment plant. (Table 2.) In terms of management, PTT recognized impact to surrounding communities and therefore integrated VOCs response program in emergency management plan.

Table 2. VOCs inventory & reduction potentials

	Reduction potentials	Reference
Flares	Flare utilization	(10)
Fugitives	A Smart Leak Detection and Repair	(1), (2), (3), (4), (5), (7), (9)
Loading & unloading	Modifying liquid fuel transfer equipment	(4), (6), (9)
Storage tank	Well maintenance, Vapor recovery unit	(4), (6), (9)
Combustion	Improving combustion efficiency	(4), (6), (9)
Wastewater treatment plant	Covering of wastewater treatment plant	(4), (6), (9)

4. Conclusion

After continuous implementation and management, PTT successfully reduce approximately 15% Upstream VOCs in 2018 compared to 2017. (Figure 5.) For Downstream, VOCs decrease around 2.4 % mostly from Fugitives reduction. (Figure 6.) The VOCs response program has been widely utilized in surrounding area to monitor and control environmental problems in collaboration with communities.

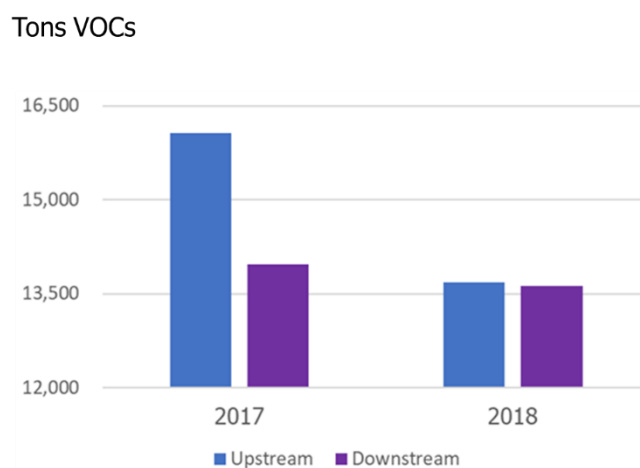


Figure 5. Upstream & Downstream VOCs reduction

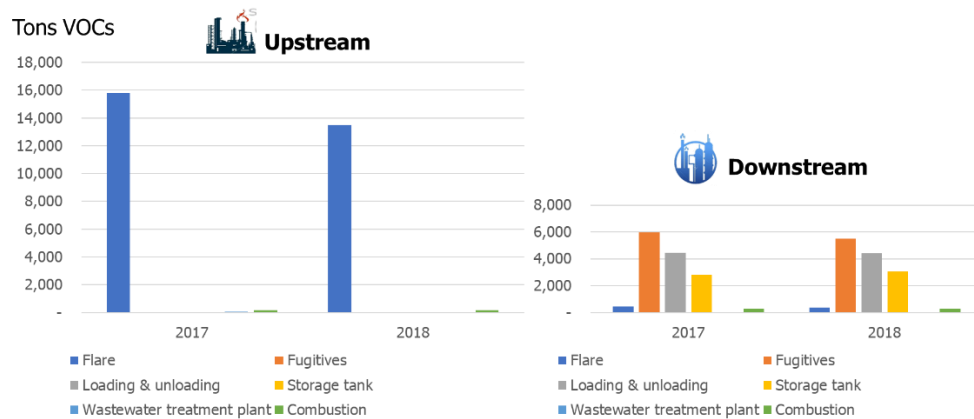


Figure 6. Upstream & Downstream VOCs reduction for each source

5. References

BAAQMD (Bay Area Air Quality Management District), 2006. <http://www.baaqmd.gov/plans-and-climate/emission-tracking-and-monitoring/flare-minimization-plans>, accessed in 2006.

Department of Industrial Works Thailand, 2010. Announcement of the department of industrial works regarding the determination of types or types of factories that required to submit emission inventory report.

Department of Industrial Works Thailand, 2013. Announcement of the department of industrial works on the report of the measurement of fugitive volatile organic compounds from equipment.

Ministry of Industry Thailand, 2012. Notification of the ministry of industry regarding the rules, regulations and procedures for monitoring and controlling fugitive volatile organic compounds from industrial equipment.

Suadee, W., 2015. Volatile organic compounds (VOCs) emission inventory and control guideline, Thailand.

U.S. Environmental Protection Agency, 1995. Air Chief 12, Emission Monitoring and Analysis.

U.S. Environmental Protection Agency, 1995. Compilation of Air Pollutant Emission Factors, Volume I: Stationary Point and Area Sources.

U.S. Environmental Protection Agency, 1995. EPA-453/R-95-017, Protocol for Equipment Leak Emission Estimates.

U.S. Environmental Protection Agency, 2015. Emissions Estimation Protocol for Petroleum Refineries - Version 3.0.

Water Technology and Industrial Environment Bureau, Department of Industrial Works Thailand, 2010. VOCs inventory from industrial sources.

Acknowledgments

Authors wishing to acknowledge PTT and subsidiaries working team all over upstream and downstream business for continuous implementation and management on VOCs mitigation.

A study of metallic composition in the daily PM_{2.5} samples at Kirklareli, Turkey

Halil N. Oruc¹, Huseyin Ozdemir¹, Rosa M. Flores², Ismail Sezen¹, Bulent Akkoyunlu³, Goksel Demir⁴, Alper Unal¹ and Mete Tayanc²

¹Istanbul Technical University, Eurasia Institute of Earth Science, Istanbul, Turkey

²Marmara University, Department of Environmental Engineering, Istanbul, Turkey

³Marmara University, Department of Physics, Istanbul, Turkey

⁴University of Health Sciences, Department of Occupational Health and Safety, Istanbul, Turkey

n.haliloruc@gmail.com

Abstract. Ambient fine particulate matter, PM_{2.5}, can be highly correlated with anthropogenic sources including agricultural activities, industrial processes, fossil fuel combustion, construction and demolition activities. To study fine particulates and their sources in the atmosphere of Thrace Region of Turkey, daily PM_{2.5} samples were collected at two stations in Kirklareli; one urban and one rural (background) station. A low-volume sampler equipped with 47-mm Teflon filters was used to obtain samples for a 216 days time period extending from 20th of March 2018 to 21st of October 2018, representing the spring, summer and fall seasons. Elemental concentrations of Na, K, Ca, V, Mn, Fe, Ni, Zn, Sr, Sn, Si, Mg, Al, Cr, Cu, Pb, B, and As in PM_{2.5} samples belonging to the rural and urban stations were determined by an ICP-MS instrument. Statistical techniques such as correlation, linear regression, and trend tests were used to analyse the PM_{2.5} data. Observed PM_{2.5} values were investigated together with the PM₁₀ data obtained from the same stations, to get information about the temporal variability of PM_{2.5} and the violation of the limit values. Urban and rural PM_{2.5} concentrations were found to range from 4.32 to 86.92 µg/m³ and from 3.55 to 68.86 µg/m³, and mean values were found to be 27.58 and 18.77 µg/m³, in order. EU legislation expresses for PM_{2.5} that a 24 h mean concentration of 25 µg/m³ not to be exceeded more than 35 times during a calendar year and this condition was found to be violated in both, the urban station (101 days out of 207 days) and in the rural station (42 days out of 198 days). Metal concentrations ranged as Na (2.75 – 1642.3 ng/m³), K (43.15 – 929.43 ng/m³), Fe (92.85– 2616.48 ng/m³), Si (61.2 – 4587 ng/m³) for the urban station and Na (0.01 – 1002 ng/m³), K (2 – 543 ng/m³), Fe (6 – 1516 ng/m³), Si (1 – 2845 ng/m³) for the rural station. Al, generally used for identifying whether the sources are natural or anthropogenic, was chosen as a reference element in the Enrichment Factor (EF) analysis. Results showed that the EF values of metals are considerably close to both stations. According to the EF analysis, six metals (Ca, K, Fe, Sr, Si, Mg) out of 18 metals are found to be natural in both of the stations, showing the impact of human-induced emissions. In addition, the only difference between the two stations is that the source of the Cr element in the rural station is natural.

Keywords: Heavy metals, Fine particulate matter, Elemental composition.

1. Introduction

Particulate matter (PM) can be primary and secondary and can be highly correlated with the anthropogenic sources including agricultural activities, industrial processes, fossil fuel combustion, construction and demolition activities. PM has been categorized in terms of diameter size since 1990 and studies have mainly focused on PM₁₀ (aerodynamic diameter < 10 µm). While sources of PM₁₀ are generally natural, such as sea spray, and dust originated from soil and desert, PM_{2.5} (aerodynamic

diameter < 2.5 μm) is mainly generated from anthropogenic processes such as combustion and condensation. $\text{PM}_{2.5}$ is physically formed by the condensation of hot steam released from the exhaust or furnace (Whitby and Sverdrup, 1980).

$\text{PM}_{2.5}$, which has a lower inertial force than PM_{10} , passes easily through the nose and throat where it is inhaled and may affect the lungs at a higher rate (Chen et al., 2018). The health effects of $\text{PM}_{2.5}$, which have been noticed in recent years, have led to more studies to be conducted about this topic. When the chemical contents of the bulk (wet + dry) deposition samples collected at rural and urban areas in Kırklareli were compared, it was found that the rural samples were more acidic than the city center (Oruc, 2012). This shows that the sulphur dioxide and nitrogen oxides in air pollution over a city can be converted into acidic agents such as sulphate and nitrate over the period of suspension or transport. It is clear that atmospheric pollution in cities threaten life as well as soil and water quality.

The composition of particulate matter is very important as the constituents may cause severe health effects. The World Health Organization (WHO, 2007) stated that heavy metals such as Cd, Pb, and Hg, are mainly spread to nature as a result of various industrial activities. Also, transboundary air pollution can affect even very remote areas due to the persistence of metals and global atmospheric transport potential. In areas characterized by low local emissions, particularly in rural and semi-rural areas, several publications have demonstrated that mass concentrations of PM_{10} are significantly affected by long-range transport. (Mahowald et al., 2009; Tecer et al., 2008; Karaca, 2008).

Accumulated road dust was examined in a heavy metal study carried out by Pal et al. (2011). The results showed that Pb, Zn, and Cu were found on the side of the pavement, and Cd, Cu and Pb were found at 1 m distance from the pavement. Consequently it is stated that these metals are caused by traffic. It is particularly mentioned in the article that it is quite surprising that Pb, which has been banned from gasoline for more than 10 years, is high on the roadside. In another road dust examination by Swietlik et al. (2013) It is emphasized that the elements Cr, Cu, Ni, Pb, and Zn are traffic-related and it was concluded that Cu and Zn were measured at an 'excessive level'. In addition, Pb, Cu, and Cd are reported to be caused by vehicle-borne emissions (Na and Cocker 2009; Pacyna and Pacyna 2001).

Ergenekon and Ulutaş (2014) conducted heavy metal content analysis of airborne particles in the industrialized Gebze region and conducted source determination using principal component analysis (PCA). In the PCA process, it was found that the first group is mainly composed of Cr (0.92) and Fe (0.95), and medium-level Cd (0.58) and Mn (0.42) and it is stated that the particles having this content are industrial production plants and soil originated. The second factor contents Cu (0.76), Pb (0.62), Cd (0.59), and Mn (0.69) was reported to be traffic-borne.

Onat et al. (2013) conducted an elemental characterization study and a resource determination study with PCA for $\text{PM}_{2.5}$ and PM_{10} , at Istanbul Kültür University, located just south of the D100 highway, which is heavily traffic-intensive. It is concluded that $\text{PM}_{2.5}$ is dominated by certain anthropogenic sources with high factor values of S, Cr, Zn, Cu and K elements found in $\text{PM}_{2.5}$. The high factor values of Mg, Al, Ba and Si in $\text{PM}_{2.5}$ are classified as terra-originated.

The aim of this study is to determine the concentrations and composition of $\text{PM}_{2.5}$ samples collected at Kırklareli which is a less studied region of Marmara Region. Additionally, possible sources of measured elements in the $\text{PM}_{2.5}$ samples is studied via Enrichment Factor (EF) and Hybrid Single-Particle Lagrangian Integrated Trajectory (HYSPLIT) reverse trajectory receptor modeling methods. The results were evaluated with statistical approaches such as linear regression and trend test.

2. Methodology

2.1. Study area and measurement periods

In Kırklareli province, particulate matter sampling was carried out in urban (41.73 ° N and 27.23 ° E) and rural (41.79 ° N, 27.14 ° E) areas (Figure 1). The central station is located on the former rectorate of Kırklareli University and the rural station is on the Kayali Campus of Kırklareli University. Industry in Kırklareli is mostly concentrated around the D-100 highway and especially in Luleburgaz. (Kırklareli Directorate of Environment and Urbanization, 2011). Furthermore, the industrial zone of Kırklareli is located in the southeast of the city (Figure 1).

Kırklareli is a gateway from Turkey to the Balkans. Some studies show that the region is under the influence of long range pollution transports from the north and the northwest (Niemi et al., 2009; Tecer et al., 2008; Karaca et al., 2008). Furthermore, it has been shown that medium range dust transport to Kırklareli comes from Kocaeli and Istanbul (Sungur and Ozcan, 2015). In this study, daily PM_{2.5} measurements were performed in Kırklareli city and countryside between March 20 and October 21, 2018. In the 216-day period, 207 and 192 measurements were performed in urban and rural stations, respectively. Number of days detected heavy metals out of the 216 days are shown in Table 2.

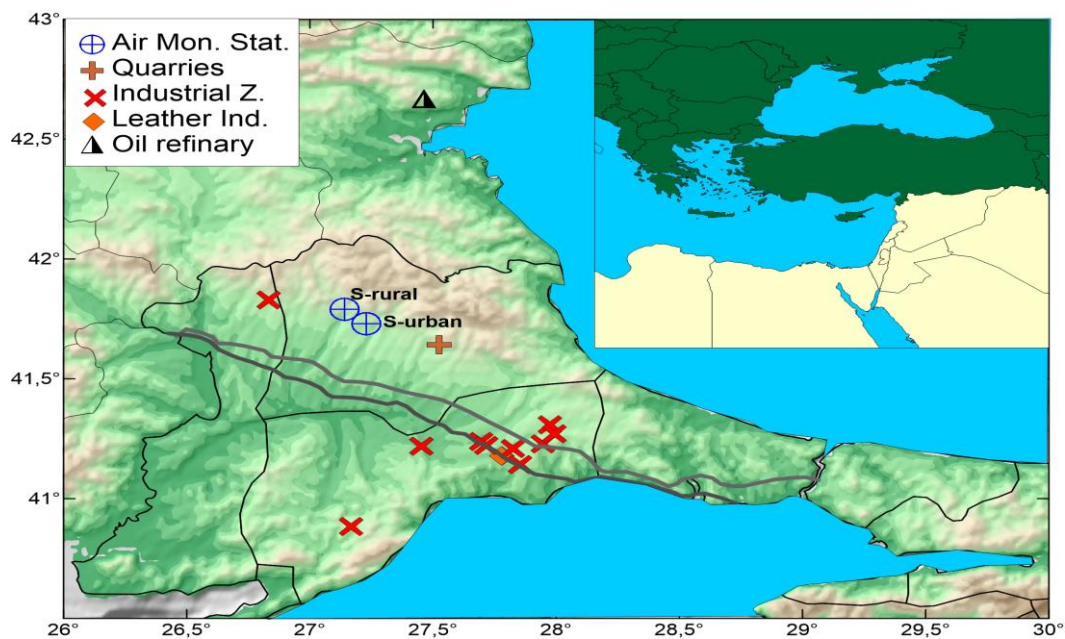


Figure 1. Kırklareli urban and rural sampling stations

2.2. Measurement processes

2.2.1. PM concentration measurement.

Data quality control procedures (QA/QC) have been applied according to EPA 40 CFR PART 50 standard to minimize contamination during sampling, transferring, conditioning, storage, analysis, and use of blank filters. Teflon filter was used for PM_{2.5} measurements (D = 46.2 mm, pore size = 2 µm). The filter was placed in the measuring chamber with a clean plastic forceps and stored in a Petri dish at the end sampling. The system was operated for 24 ± 1 hours. Air quality stations are properly fixed to the ground to minimize air leakage. In addition, the station is surrounded by wires to protect the station from external influences.

The flow rate of the device is set to be 16.7 liters/minute. The effect of moisture on the sample is inevitable and the moisture accumulated on the filter was minimized according to the filter conditioning

procedure. For this purpose, conditioning environment temperature range of the filter is kept between 15 - 30 °C and the humidity range was kept between 20-45%. Each filter was conditioned in the desiccator for 24 hours. The same precision balance (Ohaus Adventurer Pro - AV264) was used to obtain net weight before and after measurement. The total volume was calculated in µg/m³ using flow rate and operation time. The reference method of EPA 40 CFR PART 5 was used to calculate the mass concentration of PM_{2.5} by sampling for 24 hours.

2.2.2. Heavy metal concentration measurement.

In this study, 43 elements were measured with special focus and emphasis established on Na, K, Ca, V, Mn, Fe, Ni, Zn, Sr, Sn, Mg, Al, Cr, Cu, Pb, Sb, B and Si. EPA-3015H-EMP500 method was used for heavy metal extraction. To perform the extraction, filters were placed in microwave Teflon tubes and digested in a microwave oven (CEMMARS5) with 5 ml of sulfuric acid (H₂SO₄) and 5 ml of perchloric acid (HClO₄). The filters were heated to 210 °C for 15 minutes and allowed to stand at this temperature for 20 minutes. The resulting mixture was poured into 50 ml falcon tubes and completed with up to 25 ml of ultrapure water.

Heavy metal analysis was conducted between 27.03.2018-31.05.2018. Samples were analysed on Agilent Technologies model 7700 series ASX-500 Inductively Coupled Plasma-Mass Spectrometer device (ICP-MS) (Yildiz Technical University central laboratory chemistry department). ICP-OES device was used for silicon element analysis. Atomic collision cells were used in order to prevent any external contamination. The heavy metal results from the ICP-MS device were calculated in µg/m³ by Equation 1 as follows:

$$\frac{\text{Sampling Concentration} \left(\frac{\text{ng}}{\text{ml}}\right) \times \text{Dilution Amount (mL)}}{\text{Sampling Volume (m}^3\text{)}} \quad (1)$$

2.3. Statistical analysis methods

Correlation, box plot, and time series graphs were generated and linear regression analysis was performed for the measurements of PM_{2.5} concentrations between 27.03.2018 and 31.05.2018 in the rural and urban stations. EF was done for the determination of the sources of the heavy metals. Besides, HYSPLIT reversal trajectory model was used to detect the possible long-range transport cases.

2.3.1. Enrichment factor (EF).

The rate used to differentiate the sources of chemical components in precipitation and particulate matter is the enrichment factor. (Vermette et al., 1988, Ahmed et al., 1990, Singer et al., 1993, Akkoyunlu and Tayanc, 2003). EF was calculated by Equation 2. In this study, Al was selected as the reference element. The concentration of reference earth elements was based on local enrichment factors in the heavy metal study conducted by Coskun et al. (2006) done at the Thrace region.

$$EF = \frac{1}{N} \sum \frac{X(\text{aerosol})}{Al(\text{aerosol})} \div \frac{X(\text{soil})}{Al(\text{soil})} \quad (2)$$

$X(\text{aerosol})$: sample concentration of ion, $Al(\text{aerosol})$: sample concentration of Al,

$X(\text{soil})$: concentration of ion in soil, $Al(\text{soil})$: concentration of Al in soil

2.4. HYSPLIT backward trajectory model

HYSPLIT is a transport and dispersion model provided by the National Oceanic Atmospheric Administration (NOAA). The model was run on March 27, April 1-2, 2018 with 100m, 500m and 1500m heights. In the model, Global Forecast System (GFS) data was used at 0.25 ° resolution.

3. Results

PM_{2.5} measurements were performed between 20 March and 21 October 2018. Measurements were started daily at 08:00 and continued for 24 ± 1 hour. 207 and 198 days out of 216 days were collected for urban and rural stations due to excavation, device maintenance, and public holidays. General characteristic of dataset is shown in Table 1. The dataset has a very wide range. This shows that fine fraction PM values are highly affected by emission sources. PM_{2.5} concentrations of rural and urban sites reached to 86 and 68 $\mu\text{g}/\text{m}^3$, respectively. The annual mean and median values of the data set appear to be quite similar. Statistically, it can be said that PM_{2.5} values show a symmetrical distribution. On the other hand, EU legislation express for PM_{2.5} that a 24 h mean concentration of 25 $\mu\text{g}/\text{m}^3$ not to be exceeded more than 35 times during a calendar year. For both stations, the PM_{2.5} concentration exceeding this critical value is quite high. Especially for the urban station, which exceeds the critical value of 101 days over 207 days.

Figure 2 shows the temporal change of the measuring stations. The maximum values of urban and rural PM_{2.5} are between 27 March and 1 April. On March 27, long range dust transport appears from the Sahara desert and through North Africa (Figure 4a, 4c). The concentration trend between the two stations is similar during the study period. High oscillation of the PM_{2.5} concentrations was observed from May 1 to May 25. This can be due to the change in frequency of PM_{2.5} concentration coming from emission sources. March 27 - 31 is used as a selected episode in terms of PM_{2.5} concentrations. High concentrations are observed in the spring season (March 20 – 30 May) compared to the summer (June, July, August) and fall (September, October) period, while the trend in the summer and fall period is similar. In the spring season, concentrations of PM_{2.5} can appear to be dominated by long and medium range transports (Figure 4). The red - line represents the limit value (25 $\mu\text{g}/\text{m}^3$) determined by the EU. PM_{2.5} concentrations are above the limit for most days, while rural concentrations are below the red-line, with lower concentrations in summer period.

Table 1. General overview of PM_{2.5} dataset and comparison for EU legislation for urban and rural sites between 20th of March 2018 to 21st of October 2018 ($\mu\text{g}/\text{m}^3$)

Monitoring Station	Urban	Rural
Number of daily exceeded 25 $\mu\text{g}/\text{m}^3$ and their ratios in per cent	101 (207) 48%	42 (198) 22%
Annual mean value of PM _{2.5} ($\mu\text{g}/\text{m}^3$)	27.58	18.77
Annual median value of PM _{2.5} ($\mu\text{g}/\text{m}^3$)	24.54	16.67
Range of PM _{2.5} ($\mu\text{g}/\text{m}^3$)	4.31 - 86.92	3.55 - 68.86

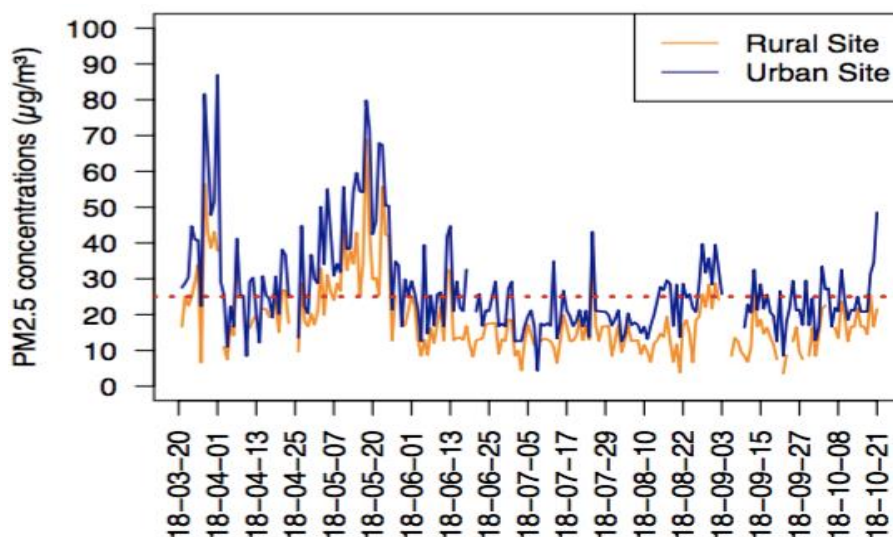


Figure 2. Temporal distribution of the PM_{2.5} concentrations in Kirklareli urban and rural sites

Heavy metals were measured in both urban and rural stations in 207 and 198 days, respectively. The heavy metals that could be detected are shown in Table 2. Strontium was the least detected element on both sides, while Si could be detected in almost all days. The Relative Standard Deviation (RSD) values of the detectable elements were high due to wide variations in the data set, similarly to PM_{2.5}. These high ranges can be associated to daily changes in the frequency of anthropogenic and natural sources that affect metal concentrations.

For both stations, it appears that the elements of soil origin (Al, Ca, Fe, K, Mg, Si) dominate the dataset. Soil origin silicon element seems to have the highest average value in the dataset. The concentrations of soil-borne elements in the urban station were higher than in rural stations. The reason for this may be the road and infrastructure works in the Kirklareli center. It is not surprising that the average values of Al, K metals and the number of detected days appear to be quite close to each other, given their main source.

Anthropogenic origin metals were observed to be relatively low compared to those of crustal origin. The low concentration of lead (Pb), which is known to be caused by traffic, can be associated with a low traffic density and vehicles starting to use unleaded fuel. Although the concentration of vanadium (V) was low, it was detected for most of the measurement days (Table 2). This indicates that the emission source V affects the sampling stations. The main source of the element V is oil combustion (EPA, 2010). Considering the prevailing wind direction affecting the Thrace region, the main source of Vanadium is the oil refining industries in Bulgaria and the contributions of the industries in Istanbul - Kocaeli with low probability. Arsenic (As) and Boron (B) sources are usually caused by coal combustion (EPA, 2010). Measured dates do not include winter season. Therefore, it can be said that the detected element B originates from local influences. There are a large number of medium-sized organized industrial zones around Kirklareli (Figure 1). Heavy metals originating from industry such as Ni, Cu, as are affected by these industrial fringes.

Table 2. Statistical summary of the detected metal concentrations at two sites of Kirklareli (ng/m³)

Elements	Urban (ng/m ³)					Rural (ng/m ³)				
	N	Mean ± RSD	Median	Min	Max	N	Mean ± RSD	Median	Min	Max
Al	139	285.95 ± 90.20	243.13	17.2	1843.1	132	160.1 ± 62.25	155.00	2.00	675.00
As	115	0.55 ± 118.64	0.38	0.03	5.12	102	0.13 ± 128.86	0.47	0.00	0.92
B	127	9.31 ± 56.42	8.24	0.35	36.73	104	4.98 ± 76.74	7.05	0.10	18.00
Ca	134	400.34 ± 61.7	354.30	9.90	1431	146	262.58 ± 79.95	153.50	7.00	1410.00
Cr	140	6.98 ± 75.98	6.26	0.30	34.21	126	1.52 ± 110.32	0.85	0.10	7.30
Cu	123	5.41 ± 50.25	4.95	0.96	13.01	101	1.12 ± 137.98	4.65	0.10	9.30
Fe	148	526.46 ± 60.57	426.66	92.9	2616.5	150	171.17 ± 89.35	182.50	6.00	1516.00
K	130	302.58 ± 53.08	284.86	43.2	929.43	131	141.83 ± 54.46	90.50	2.00	543.00
Mg	157	34.56 ± 296.47	11.26	0.20	981.78	150	7.46 ± 136.05	3.50	0.10	65.50
Mn	121	28.29 ± 139.98	17.42	1.08	393.54	133	10.18 ± 126.87	2.75	0.30	93.80
Na	149	297.05 ± 89.5	243.20	2.75	1642.3	144	86.09 ± 180.07	150.00	0.01	1002.00
Ni	101	10.01 ± 109.03	7.53	0.32	64.50	93	1.96 ± 128.76	1.80	0.10	9.70
Pb	114	5.31 ± 112.62	4.12	0.19	49.32	93	0.82 ± 144.16	0.33	0.02	6.39
Si	184	1110.68 ± 64.48	1056.07	61.2	4587	177	550.49 ± 87.2	913.50	1.00	2845.00
Sn	127	2.60 ± 329.43	0.97	0.12	87.5	97	0.47 ± 150.42	0.40	0.01	6.24
Sr	90	1.34 ± 124.33	0.84	0.04	8.53	91	0.75 ± 172.39	1.30	0.02	8.75
V	150	3.31 ± 80.77	2.66	0.17	14.98	142	0.79 ± 155.41	0.75	0.01	8.04
Zn	125	38.65 ± 78.09	29.97	1.44	205.12	118	9.21 ± 129.74	4.90	1.10	63.10

When the correlation graphs between the concentration changes of the detected heavy metals in the urban and rural areas are examined, it is seen that there is a significant relationship between the correlations of the heavy metals (Si, Na, Mg, Al) with each other (Figure 3). This high correlation represents the similarity of soil content in urban and rural areas. For the element K, while the rural values are mostly below 0.1 µg / m³, the uncertainty between the two datasets increases as the urban station has a wider range. Due to this uncertainty, the adjusted R² value in urban and rural stations was low (R²=0.03). This indicates that the K concentration in the urban station has a local source. On the other hand, after about 0.2 µg / m³ at the rural station, a linear increase is seen at both stations. The enrichment factor analysis of Fe shows that the source of Fe can be anthropogenic for urban while it is soil for rural. (Table 5). In this case, the correlation between the two stations can be expected to be low. There is no significant relationship between the two stations for Sr, and Ni. The reason for the low R² value is the daily processes of the industries in the Kirklareli center.

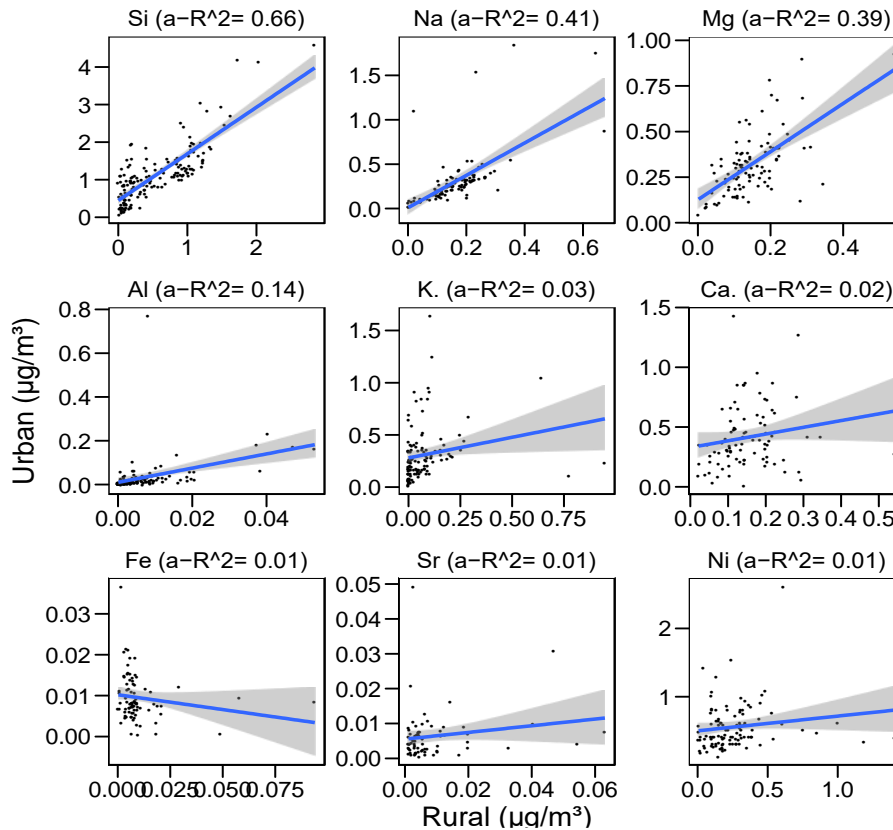


Figure 3. Correlation plots of urban and rural stations of each element with adjusted R^2 values ($\mu\text{g}/\text{m}^3$)

3.1. Comparison with other studies

Trace elements of this study were compared with seven studies which are separated as urban and rural areas. Arithmetic mean values ($\mu\text{g}/\text{m}^3$) are shown in Table 3. This study was compared with totally 10 regions, which are shown in Table 3. As expected, heavy metal concentrations in our work and in the compared urban areas in Table 3 are higher than concentrations observed in rural stations.

Hueglin, C. et al. (2005) studied on three places of Switzerland, which are Bern, Zurich-Kaserne and Chaumont. Sample numbers are 79, 79, and 78, respectively. In their study, $\text{PM}_{2.5}$ samples were collected and analyzed by using ICP-MS. Salvador, P. et al. (2007) studied on Bemantes, Spain. This place is a rural area and close to the urban site. $\text{PM}_{2.5}$ samples were collected and analyzed by using XRF. Amasra station was located 20 km east of the city and in the Black Sea Region. Sample type was PM_{10} in study. Instrumental Neutron Activation Analysis (INAA) and Atomic Absorption Spectrometry (AAS) were used to determine heavy metals.

Five different urban area studies were compared with Kirklareli urban station heavy metal values (Table 4b). Aliaga station values (Al, Cr, Mn, Ni, Pb, Sn, Sr, V, Ca, Fe, K, Mg, Zn) are very high. The reason for this situation is that there are industries with high pollution load such as oil refinery, iron and steel factory, and natural gas power plant around the stations. On the University Campus in Helva, the concentrations of Cu and Na are noticeably high. Similarly, Na and Ca concentrations are high values measured for Tirupati. Boron (B), which is emitted from coal burning, was measured in only one station. Concentrations measured in Kirklareli are higher than in Aliaga region. In addition, in Kirklareli, Mn, Sn, Al and Fe concentration values are the second highest station after Aliaga region. The urban values of the study have the lowest values for the soil source elements Sr and Zn. Since Silicon (Si) is not measured in urban areas, no comparison can be made.

Table 3. Author names, study areas and used instruments of compared studies

Author	Location	Station Type	Instrument
	Switzerland, Bern	Urban	ICP-MS
Hueglin, C. et al.	Switzerland, Zurich-Kaserne	Urban	ICP-MS
	Switzerland, Chaumont	Rural	ICP-MS
Salvador, P. et al.	Spain, Bemantes	Rural	XRF
Dogan, G.	Turkey, Amasra	Rural	INAA, AAS
Munzur, B	Turkey, Izmir, Candarli	Rural	EDXRF
Campa, A. M. S. et al.	Spain, Helva, University Campus	Urban	ICP-OES
	Spain, Helva, Nerva	Rural	ICP-OES
Mouli, P. C. et al.	India, Trupati	Urban	IC
Kara et al.	Aliaga region	Urban	ICP-MS
This study	Kirklareli	Rural	ICP-MS
	Kirklareli	Urban	ICP-MS

Table 4. Comparison of elements (ng/m³) measured in this study and those measured in other a) rural and b) urban areas

a) Rural	Al	As	Ca	Cr	Cu	Fe	K	Mg	Mn	Na	Ni	Pb	Sn	V	Zn	
Switzerland, Chaumont	34	0.16	46		6	26	68	10	0.8	68	1.3	4.7		0.8		
Spain, Bemantes		0.3	106	1	9	63	118	46	3	316	4	7	1	4	17	
Turkey, Amasra	900	1.15	270	0.87		200	135	110	8.68	300	1.13	12		2.1	10.4	
Turkey, İzmir, Candarli	239.9		504	1.5		265	160	77	11		1.1	0.5				
Spain, Helva. Nerva		1.26	710	2.12	5.09	480	310	230	9.3	850	1.3	3.9	0.5	2.8	27.3	
Turkey, Kirklareli,	160.1	0.13	262	1.52	1.12	171	141.8	7	10.18	86.09	1.96	0.8	0.5	0.7	9.21	
b) Urban	Al	As	Ca	Cr	Cu	Fe	K	Mg	Mn	Na	Ni	Pb	Sn	Sr	V	Zn
Switzerland, Bern	26	0.4	106		8.7	204	186	13	4.4	84	1.3	30			1.6	
Switzerland, Zurich-Kaserne	48	0.47	54		6.1	124	223	17	3.5	96	3.1	21			1.1	
Spain, Helva. University Campus		5.4	690	2.34	61.7	430	310	230	5.47	1320	2.65	12.2	1.6	2.85	4.2	46.6
India, Trupati			1470				420	190		3370						
Aliaga region	1198	4.24	2241	33.3	39.8	1832	604	508	75.5	918	12.4	175	4.9	7.39	15.6	929
Turkey, Kirklareli, Urban	286	0.6	400	6.9	5.4	527	303	35	28	297	10	5.3	2.6	1.34	3.3	38.7

Five different rural studies were compared with Kirklareli rural station (Table 4a). Since there is no other study of boron element, it could not be compared. As, Cr, Sr, Zn, Ca, Fe, K, Na, Mg concentrations are highest in Nerva. The elements Sn, V, and Mn are of industrial origin. Kirklareli rural has the lowest concentration values with Sn, Sr, V, Zn, Si and Mg elements. Although the rural station in Amasra is 20 km away from the city, it has the highest concentration of Al and Pb elements. It is thought that as a cause there are thermal power plants that are active about 35 km.

3.2. HYSPLIT backward trajectory studies

The episode date of the study was determined as 27 March 2018. Air mass backward trajectories were obtained from 1 to 2 April 2018 to further support episodes identified as dust transport. HYSPLIT trajectories (Figure 4a, 4b) show the important dust transport episode on March 27. This episode lasted for a few days from the end of March until the first few days of April. Since the air masses emerge directly from the Sahara Desert at high altitudes (i.e., 3000-1500 m), it has made a significant contribution to the surface PM₁₀ concentration in Kirklareli. Figure 4c shows HYSPLIT trajectory analysis for the episode period. In the backward 96-hour orbit, it is seen that the air masses coming to Kirklareli follow an upward route from Europe to North Africa. This is thought to cause dust transport.

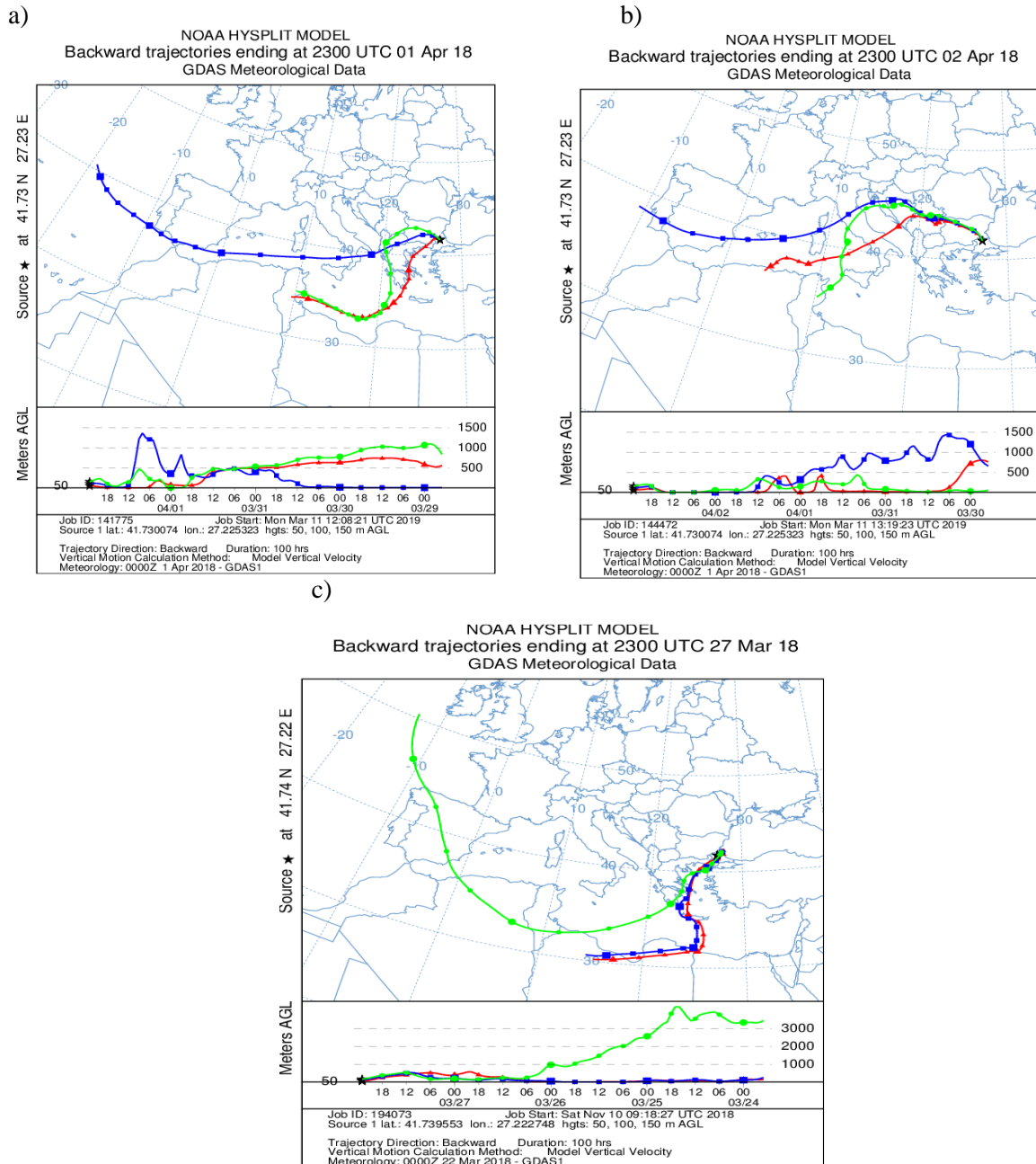


Figure 4. HYSPLIT trajectory analyses. a) and b) are analysis for 1 and 2 April 2018, respectively. c) is HYSPLIT 96-hour trajectory analyses for 27 March 2018

3.3. Enrichment factors analysis

The soil values for Si and Mg in this study were derived from Mason's (1996) study. For the similarity of local soil characterization, other elements were obtained the Coskun et. al. (2006) study. In this study Al was used as reference element for enrichment factor, because the source of Al is considered to be crustal. The enrichment levels of the elements are determined according to the enrichment factor results, which are shown in Table 5 by separating the urban and the rural. It is assumed that there is no enrichment in elements with EFs up to 10. The elements with EF between 10 and 100 are moderately enriched elements and the elements with EF more than 100 are highly enriched elements (Gharaibeh et. al, 2008). Highly enriched element means that source is different than soil. EF values of 15 elements are

shown in the Table 5. For both urban and rural areas, the sources of Cu, Ni, Zn, As and V are different from the soil. Cu>Ni>Zn>As>V Following this sequence, the anthropogenic properties of the elements are increased. While, the source of Ca, K, and Fe is soil, Pb, Na, Mn is low correlated with soil. According to the EF analysis, the source of Cr for the rural is soil, despite for the urban soil is can be natural source of Cr. Furthermore, soil may be the source of iron in the city, while it is the source in the countryside.

Table 5. Enrichment factors of the species according to the reference element (Al)

Elements	Urban	Rural
Cu	564.72	517.84
Ni	398.79	361.71
Zn	210.01	189.45
As	191.52	176.03
V	141.31	133.03
Fe	51.32	4.76
Pb	30.23	28.06
Na	19.11	18.14
Mn	18.37	17.03
Cr	10.21	9.40
Ca	7.77	7.03
K	6.66	6.04
Sr	3.56	3.19
Si*	1.76	1.58
Mg*	0.38	0.35

4. Conclusions

In Kirklareli, the concentration and content of particulate matter in the fine fraction was analysed for spring, summer, and autumn seasons of 2018. The temporal variation of PM_{2.5} concentrations is found to be similar for both stations. Especially between episode dates (27 - 30 March), PM_{2.5} concentrations reached their maximum levels. This is explained by the fact that dust transport which come from the Sahara Desert, North Africa, with the long-range transport dominates other emission sources.

As a result of the measurements, crustal originated elements were found to be the highest for Kirklareli. Si, Al, Ca, Mg concentrations in urban and rural areas were significantly correlated due to the soil origination. Al and Fe concentrations were found to be low owing to the structure of the soil and the lack of industrial density that may generate Al and Fe emissions around stations. Mn element is higher than those found in other studies (except for Aliaga region) and highly related with the amount of Mn from soil. Urban station is close to the Kirklareli bus terminal, suggesting that the Mn values were effected from the traffic related emissions. Concentrations of soil-borne metals in the Thrace region are described by Coşkun et al. (2006). In this study, Al and Fe elements were found to be 600 mg / kg and 26900 mg / kg, in order. When the relationship between values was examined, it can be seen that the difference in concentration between Fe and Mn is significant. The mean Pb value was lower than the limit value established by the EU (0.5 µg / m³). This is related to factors such as low industrial activity around the station and the use of unleaded gasoline in vehicles.

The soil-borne elements were found to be higher in the urban than the rural area. This can be explained by the loss of agglomerated form of the particles in the soil structure owing to anthropogenic activities such as construction works, infrastructure works, stone and cement factories, and increased possibility of more easily forming windblown dust. According to the results of the enrichment factor analysis, the sources of Ca, K, Sr, Si and Mg elements in the urban and Cr, Ca, K, Sr, Fe, Si and Mg elements in the

rural was obtained as soil. In this study, it is remarkable that the enrichment factor values of Mn and Na elements are higher than expected.

Future work includes the study of heavy metals in winter of 2018-2019. When the winter season data is obtained, it is believed that a more complete results set will emerge including the metal concentrations caused by residential heating. Further studies can also be used to integrate meteorological and physical air quality models in order to more precisely define the accuracy of measurement data and the sources of chemical constituents.

5. References

- Ahmed, A. F. M., Singh, P. R., Elmubarak, A. H., 1990. Chemistry of atmospheric precipitation at the western Arabian Gulf coast. *Atmospheric Environment*. 24A, 2927-2934.
- Akkoyunlu, B. O., Tayanc, M., 2003. Analyses of wet and bulk deposition in four different regions of Istanbul, Turkey. *Atmospheric Environment*. 37, 3571-79.
- Aldabe, J., Elustondo, D., Santamaria, C., Lasheras, E., Pandolli, M., Querol, X., Santamaria, J.M., Alastuey, A., 2011. Chemical characterization and source apportionment of PM_{2.5} and PM₁₀ at rural, urban and traffic sites in Navarra (North of Spain). *Atmospheric Research*. 102, 191-205.
- Begum, A., Mustafa, A. I., Amin, M. N., Chowdhury, T. R., Quraishi, S. B., Banu, N., 2013. Levels of heavy metals in tissues of shingi fish (*Heteropneustes fossilis*) from Buriganga River Bangladesh. *Environ Monit Assess*. 185, 5461-5469.
- Beuck, H., Quass, U., Klemm, O., Kuhlbusch, T. A. J., 2011. Assessment of sea salt and mineral dust contributions to PM₁₀ in NW Germany using tracer models and positive matrix factorization, *Atmos. Environ*. 45, 5813-5821.
- Bosco, M. L., Varrica, D., Dongarrà, G., 2005. Case study: Inorganic pollutants associated with particulate matter from an area near a petrochemical plant. *Environmental Research*. 99, 18-30.
- Bozlaker, A., Spada, N. J., Fraser, M. P., Chellam, S., 2013. Elemental characterization of PM_{2.5} and PM₁₀ Emitted from light duty vehicles in the Washburn Tunnel of Houston, Texas: release of rhodium, palladium, and platinum. *Environ. Sci. Technol*. 48, 54-62.
- Campa, A. M. S., Rodas, D. S., Castanedo, Y. G., Rosa, J. D., 2015. Geochemical anomalies of toxic elements and arsenic speciation in airborne particles from Cu mining and smelting activities: Influence on air quality. *J. Hazard Mater*. 291,18-27.
- Chen, W. -H., Wang, C. -W, Kumar, G., Rousset, P., Hsieh, T. -H., 2018. Effect of torrefaction pretreatment on the pyrolysis of rubber wood sawdust analyzed by Py-GC/MS. *Bioresource Technology*. 259, 469-473.
- Coskun, M., Steinnes, E., Frontasyeva, M. V., Sjobakk, T. E., Demkina, S., 2006. Heavy metal pollution of surface soil in the Thrace region, Turkey. *Environ. Monit. Assess*. 119, 545-556.
- Dogan, G., 2005. Comparison of the rural atmosphere aerosol compositions at different parts of Turkey. M.S. Thesis, Department of Environmental Engineering, Middle East Technical University, Ankara, Turkey.
- Ergenekon, P., Ulutaş, K., 2014. Heavy Metal Content of Total Suspended Air Particles in the Heavily Industrialized Town of Gebze, Turkey. *Bulletin of Environmental Contamination and Toxicology*. 92, 90-95.
- EU WHO, 2007. <http://www.euro.who.int/en/publications/abstracts/health-risks-of-heavy-metals-from-long-range-transboundary-air-pollution-2007>, accessed in August 2019.

- Gharaibeh, A. A., El-Rjoob, A.-W. O., Harb, M. K., 2010. Determination of selected heavy metals in air samples from the northern part of Jordan. *Environ. Monit. and Assess.* 160, 425-429.
- Gianini, M. F. D., Fischer, A., Gehrig, R., Ulrich, A., Wichser, A., Piot, C., Besombes, J.-L., Hueglin, C., 2012. Comparative source apportionment of PM₁₀ in Switzerland for 2008/2009 and 1998/1999 by Positive Matrix Factorisation. *Atmos. Environ.* 54, 149-158.
- Hueglin, C., Gehrig, R., Baltensperger, U., Gysel, M., Monn, C., Vonmont, H., 2005. Chemical characterisation of PM_{2.5}, PM₁₀ and coarse particles at urban, near-city and rural sites in Switzerland. *Atmospheric Environment*. 39, 637-651.
- Kara, M., Hopke, P. K., Dumanoglu, Y., Altiok, H., Elbir, T., Odabasi, M., Bayram, A., 2015. Characterization of PM Using Multiple Site Data in a Heavily Industrialized Region of Turkey. *Aerosol and Air Quality Research*. 15, 11-27.
- Karaca, F., 2008. Büyükçekmece havza atmosferindeki PM_{2.5} ve PM₁₀ partikül gruplarındaki metallerin istatistik dağılım özelliklerinin incelenmesi. *Ekoloji*. 68, 33-42.
- Karanasiou, A. A., Siskos, P. A., Eleftheriadis, K., 2009. Assessment of source apportionment by Positive Matrix Factorization analysis on fine and coarse urban aerosol size fractions. *Atmospheric Environment*. 43, 3385-3395.
- Kim, E., Hopke, P. K., Edgerton, E. S., 2003. Source identification of Atlanta aerosol by positive matrix factorization. *Journal of the Air & Waste Management Association*. 53, 731-739.
- Kim, E., Hopke, P. K., Edgerton, E. S., 2003. Source identification of Atlanta aerosol by positive matrix factorization. *Journal of the Air & Waste Management Association*. 53, 731-739.
- Kocak, M., Mihalopoulos, N., Kubilay, N., 2009. Origin and source regions of PM₁₀ in the Eastern Mediterranean atmosphere. *Atmospheric Research*. 92, 464-74.
- Lee, J. H., Hopke, P. K., 2006. Apportioning sources of PM_{2.5} in St. Louis, MO using speciation trends network data. *Atmospheric Environment*. 40, 360-377.
- Liu, W., Hopke, P. K., Vancuren, R. A., 2003. Origins of fine aerosol mass in the western United States using positive matrix factorization. *Journal of Geophysical Research*. 108.
- Mahowald, N. M., Engelstaedter, S., Luo, C., Sealy, A., Artaxo, P., Benitez-Nelson, C., Bonnet, S., Chen, Y., Chuang, P.Y., Cohen, D.D., Dulac, F., Herut, B., Johansen, A. M., Kubilay, N., Losno, R., Maenhaut, W., Paytan, A., Prospero, J. M., Shank, L. M., Siefert, R. L., 2009. Atmospheric Iron Deposition: Global Distribution, Variability, ve Human Perturbations. *Annual Review of Marine Science*. 245-278.
- Mason, B., 1996. *Principles of Geochemistry*, third ed. Wiley, New York.
- Mazzei, V., Longo, G., Brundo, M.V., Sinatra, F., Copat, C., Conti, G.O., Ferrante, M., 2008. Bioaccumulation of cadmium and lead and its effects on hepatopancreasmorphology in three terrestrial isopod crustacean species. *Ecotoxicol. Environ. Saf.* 110, 269-279.
- Moreno, J. L., Garcia, C., Landi, L., Falchini, L., Pietramellara, G., Nannipieri, P., 2001. The ecological dose value (ED 50) for assessing Cd toxicity on ATP content and DHA and urease activities of soil. *Soil Biol. Biochem.* 33,483-489.
- Mouli, P. C., Mohan, S. V., Reddy S. J., 2006. Chemical Composition of Atmospheric Aerosol (PM₁₀) at a Semi-Arid Urban Site: Influence of Terrestrial Sources. *Environ. Monit. Assess.* 117, 291-305.
- Munzur, B., 2008. Chemical composition of the atmospheric particles in the Aegean region. G.S. Thesis, Graduate School of Natural and Applied Sciences, Middle East Technical University, Ankara, Turkey.

- Na, K., Cocker III, D.R., 2009. Characterization and source identification of trace elements in PM_{2.5} from Mira Loma, Southern California. *Atmos. Res.* 93, 793-800.
- Niemi, M., Sibakov, M., Niemela, S., 1983. Antibiotic resistance among different species of fecal coliforms isolated from water samples. *Applied Environ. Microbiol.* 45, 79-83.
- Onat, B., Şahin, Ü. A., Bayat, C., 2013. Assessment of particulate matter in the urban atmosphere: Size distribution, metal composition and source characterization using principal component analysis. *Journal of Environmental Monitoring.* 14, 1400.
- Oruc I., 2012. Kırklareli'de Yaş, Bulk ve Kuru Birikim Kompozisyonunun İncelenmesi, Ph.D. Thesis, Graduate School of Natural and Applied Sciences, University of Trakya, Edirne, Turkey.
- Paatero, P., 1999. The multilinear engine - A table-driven, least squares program for solving multilinear problems, including the n-way parallel factor analysis model. *Journal of Graphical Statistics.* 8, 854-888.
- Pacyna, J. M., Pacyna, E. G., 2001. An assessment of global and regional emissions of trace metals to the atmosphere from anthropogenic sources worldwide. *Environmental Reviews.* 9, 269-298.
- Pal, S. K., Wallis, S.G., Arthur, S., 2011. Assessment of heavy metals emission from traffic on road surfaces. *Central Eur. J. Chem.* 9, 314-319.
- Pekney, N.J., Davidson, C.I., Robinson, A., Zhou, L., Hopke, P., Eatough, D., Rogge, W.F., 2006. Major source categories for PM_{2.5} in Pittsburgh using PMF and UNMIX. *Aerosol Sci. Technol.* 40, 910-924.
- Reff, A., Elberly, S., Bhave, P. V., 2007. Receptor Modelling of Ambient Particulate Matter Data Using Positive Matrix Factorization: Review of Existing Methods. *Journal of Air and Waste Management Association.* 57, 146-154.
- Salvador, P., Artúñano, B., Querol, X., Alastuey, A., Costoya, M., 2007. Characterisation of local and external contributions of atmospheric particulate matter at a background coastal site. *Atmospheric Environment.* 41, 1-17.
- Santoso, M., Hopke, P. K., Hidayat, A., Diah, D. L., 2008. Sources identification of the atmospheric aerosol at urban and suburban sites in Indonesia by positive matrix factorization. *Sci. Total Environ.* 2, 29-237.
- Singer, A., Shamay, Y., Fried, M., 1993. Acid rain on Mt. Carmel, Israel. *Atmospheric Environment.* 27, 2287-2293.
- Sungur A., Ozcan H., 2015 .Chemometric and geochemical study of the heavy metal accumulation in the soils of a salt marsh area (Kavak Delta, NW Turkey). *Journal of Soils and Sediments.* 15, 323-331.
- Swietlik, R., Strzelecka, M., Trojanowska M., 2013. Evaluation of Traffic-Related Heavy Metals Emissions Using Noise Barrier Road Dust Analysis. *Polish Journal of Environmental Studies.* 2, 561-567.
- Tecer, L. H., Alagha, O., Karaca, F., Tuncel, G., Eldes, N., 2008. Particulate Matter (PM_{2.5}, PM_{10-2.5}, and PM₁₀) and Children's Hospital Admissions for Asthma and Respiratory Diseases: A Bidirectional Case-Crossover Study. *Journal of Toxicology and Environmental Health. Part A: Current Issues.* 71, 512-520.
- Tecer, L.H., Alagha, O., Karaca, F., Tuncel, G., Eldes, N., 2008. Particulate Matter (PM_{2.5}, PM_{10-2.5}, and PM₁₀) and Children's Hospital Admissions for Asthma and Respiratory Diseases: A Bidirectional Case-Crossover Study. *Journal of Toxicology and Environmental Health, Part A: Current Issues.* 71, 512-520.
- U.S.EPA., 2010. <http://epa.gov/ttnatw01/hlthef/hapindex.html>, accessed in April 2019.



Vermette, S.J., Drake, J.J., Landsberger, S., 1988. Intra-urban precipitation quality: Hamilton, Canada. *Water, Air, and Soil Pollution*. 38, 37-53.

Viana, M., Kullbusch, T. A. J., Querol, X., Alastuey, A., Harrison, R. M., Hopke, P. K., Winiwarter, W., Vallius, A., Szidat, S., Prevot, A. S. H., Heuglin, C., Bloemen, H., Wahlin, P., Vecchi, R., Miranda, A.I., Kasper-Giebl, A., Maenhaut, W., Hitzenberger, R., 2008. Source apportionment of particulate matter in Europe: A review of methods and results. *Journal of Aerosol Science*. 39, 827-849.

Wang, S. L., Xu, X. R., Sun, Y. X., Liu, J. L., Li, H. B., 2013. Heavy metal pollution in coastal areas of South China: a review. *Mar. Pollut. Bull.* 76, 7-15.

Whitby, K. T., Sverdrup, G. M., 1980. California aerosols: their physical and chemical characteristics. *Environmental Science and Technology*. 9, 477-517.

Xie, Y. L., Hopke, P. K., Paatero, P., Barrie, L. A., Li, S. M., 1999. Identification of source nature and seasonal variations of arctic aerosol by positive matrix factorization. *Journal of the Atmospheric Sciences*. 56, 249-260.

Zhao, W., Hopke, P.K., 2006. Source Investigation for PM_{2.5} in Indianapolis. *Aerosol Science and Technology*. 40, 898-909.

Zhou, Q., Zhang, J., Fu, J., Shi, J., Jiang, G. B., 2009. An appealing tool for assessment of metal pollution in the aquatic ecosystem. *Anal Chim Acta*. 606, 135-150.

Acknowledgments

This study has been financially supported by TUBITAK 116Y163, Marmara University BAPKO FEN-A-131217-0668 and FEN-C-DRP-200318-0115 projects.

Seasonality of PM_{2.5} and its organic fraction in a traffic site in Besiktas, Istanbul

Rosa M. Flores¹, Elif Mertoglu¹, Huseyin Ozdemir², Bulent Akkoyunlu³,
Alper Unal⁴ and Mete Tayanc¹

¹Marmara University, Department of Environmental Eng., Istanbul, Turkey

²Istanbul Technical University, Maslak, 34469, Istanbul, Turkey

³Marmara University, Department of Physics, Istanbul, Turkey

⁴Istanbul Technical University, Eurasia Institute of Earth Sciences, Maslak, 34469, Istanbul, Turkey

rflores@marmara.edu.tr

Abstract. In this work, PM_{2.5} samples were collected on selected days during four seasons in spring-fall 2017 and winter 2018. Daily and hourly PM_{2.5} concentrations were determined with the gravimetric method and also obtained from the Air Quality Monitoring Network of Istanbul. Organic carbon (OC) and elemental carbon (EC) concentrations were determined with a thermo-optical carbon analyzer. The 24-h US-EPA air quality standard of 35 µg m⁻³ was exceeded 13, 25, 41, 42, and 57% in Catladikapi, Silivri, Kagithane, Umraniye, and Besiktas, respectively. These exceedances occur during the fall and winter and are due to a combination of emissions from fuel combustion for residential heating, traffic and industry and poor air dispersion due to weak atmospheric motion and low mixing heights. Average OC concentrations ranged in 6.62-7.32 µg m⁻³ during spring and summer and 13.76-14.1 µg m⁻³ during fall and winter. The OC concentrations observed in this work during the summer and winter are 2-4× and 3-6× higher than concentrations observed in USA and Europe, respectively. The EC concentrations on the other hand, do not show considerable seasonal variation with values between 2.16-3.26 µg m⁻³. These concentrations are much higher in Besiktas with values 7× and 9× higher than USA and Europe, in order. These results could be helpful for future implementation of strategies to reduce emissions from combustion sources in order to comply with air quality standards.

Keywords: Organic carbon, Elemental carbon, PM_{2.5}, Istanbul.

1. Introduction

According to the World Health Organization, air pollution is the world's largest environmental health risk, with an estimated value of 5.5 to 7 million of premature deaths. The link between exposure to fine particulate and adverse health effects has been well documented, however, uncertainties still remain regarding health impacts of PM according to size, composition, and number concentration. Organic aerosol (OA) is of special interest due to the fact that it may constitute a large fraction of fine PM. In addition, OA may be of both, primary and secondary origin, therefore it may be composed of thousands of individual organic species. Recently, it has been found that particles emitted by combustion sources are more relevant to human health. For this reason, it has been recommended to decrease the exposure to PM_{2.5} and related chemical components. Particularly, elemental carbon (EC) has been suggested as an additional health indicator.

Organic carbon (OC) can be both emitted directly and be a tracer for primary organic carbon (POC) or formed in the atmosphere and be a tracer for secondary organic carbon (SOC). Elemental carbon is a

tracer for carbon fuel-based combustion processes, particularly for diesel emissions. POC can show atmospheric aging processes of organic aerosol and can be a good parameter used for development of air quality control policies.

In Turkey, OC/EC measurements have been scarcely studied. In order to understand seasonal variation in the abundance of organic aerosol, in this work, PM_{2.5} samples were collected on selected days between May 2017 and January 2018 with a low volume sampler of OC/EC. PM_{2.5} concentrations were determined with the gravimetric method and also obtained from the Air Quality Network in Istanbul.

2. Sampling, analysis, and data collection

The sampling site is located in the touristic/residential area of Besiktas, Istanbul, at approximately 4-5 m above sea level and 10-15 m from the road. PM_{2.5} samples were collected on 47 mm quartz fiber filters using a Zambelli low volume sampler at a flow rate of 1 m³ h⁻¹. PM_{2.5} concentrations were determined with the gravimetric method by subtracting the initial mass of the filter sample from the final mass and next divided by the volume of the air passed through it. Before sampling, filters were pre-conditioned by placing them into a desiccator at room temperature for 24 hours to obtain a constant humidity. After the conditioning process, filters were weighted using an analytical balance with 10⁻⁴ g precision. Following a careful analysis of meteorological forecast models and trying to find possible future episodes in the predictions, sampling dates were determined as follows: spring: May 3-9, 2017, summer: July 6-12, 2017, fall: October 20-26, 2017, and winter: January 4-10, 2018. Hourly and daily-averaged PM_{2.5} concentrations were also obtained from the Air Quality Monitoring Network in Istanbul for four sampling sites: Catladikapi, Kagithane, Silivri, and Umraniye. Hourly and daily PM_{2.5} concentrations were compared to limit values in the regulations to understand their impact on human health and overall air quality.

Organic carbon (OC) and elemental carbon (EC) concentrations were determined in the daily PM_{2.5} samples with a Sunset thermo-optical carbon analyzer according to the recommended method NIOSH 870 as follows: (1) Organic carbon temperature ramps at 310, 475, 615, and 870°C in a 100% helium atmosphere and (2) Elemental carbon temperature ramps at 550, 625, 700, 775, 850, and 870°C in a 2% oxygen atmosphere (Andreae and Gelencsér, 2006). Organic compounds and soot carbon are oxidized to CO₂ during combustion and converted to CH₄. The total area under the ramp curves of OC and EC are calculated and converted to concentrations using a calibration standard of sucrose solution (Flores et al., in review). The standard deviation of these analyses in triplicate ranged 1.1-7.5% with an average of 4.0%. Standard deviations of 20% have been reported in the literature (Chow et al., 2008).

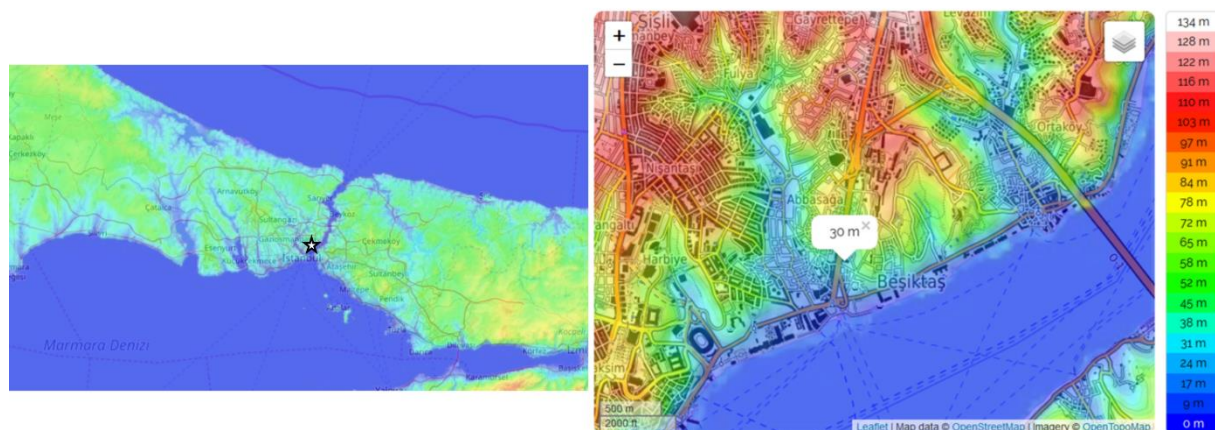


Figure 1. Location of the sampling site (white icon) and topography (altitude, m.a.g.l) of the place

3. Results

3.1. $PM_{2.5}$ concentrations

$PM_{2.5}$ concentrations were obtained from the Turkish Council of Environment and Urbanization. Daily average concentrations of $PM_{2.5}$ for Catladikapi, Kagithane, Silivri, and Umraniye are shown in Table 1 for sampling campaigns spring, summer, and fall 2017, and winter 2018. Additionally, in our sampling station (Besiktas) we collected daily $PM_{2.5}$ samples and calculated $PM_{2.5}$ concentrations with the gravimetric method. $PM_{2.5}$ concentrations at Besiktas sampling station are also given in Table 1.

Data for Catladikapi was only available for spring and summer 2017. However, concentrations show high correlation with other stations ($r=0.77-0.84$), thus similar trends due to variations in meteorology are expected. Data for Umraniye station is unavailable on 25-26 October 2017. However, Umraniye station appears to follow similar concentrations and behaviour as Kagithane with Pearson correlation coefficient of 0.84. Kagithane and Umraniye have populations of approximately 400,000 and 700,000, respectively. Lower population of 150,000 live in Silivri, thus lower concentrations of $PM_{2.5}$ are expected during the winter. The 24-h air quality standards established by World Health Organization (WHO) and United States Environmental Protection agency (US-EPA) are 25 and 35 $\mu\text{g m}^{-3}$, respectively. $PM_{2.5}$ daily averages have not been established in the European Union and Turkey. Standards for yearly averages have been established as 10, 12, and 25 $\mu\text{g m}^{-3}$ according to WHO, EPA, and EU, respectively. During the study period, the 24-h WHO air quality standard of 25 $\mu\text{g m}^{-3}$ was exceeded 33.3, 46.4, and 46.2% of the time in Catladikapi, Silivri, and Umraniye, respectively. Concentrations in Besiktas and Kagithane station exceeded the WHO air quality standard 74.0% and 77.8% of the time, respectively. Concentrations were mostly exceeded during the fall and winter at all sampling stations, except for Besiktas and Kagithane, which also show 85.7% exceedance during the spring (Table 1). Both stations are in close proximity to busy roads, thus continuous emissions from heavy traffic are expected to contribute to high $PM_{2.5}$ concentrations at all times. In addition, contributions from desert dust transport have been found important during spring (Flores et al., 2017).

The 24-h US-EPA air quality standard of 35 $\mu\text{g m}^{-3}$ was exceeded 13.3, 25.0, 40.7, and 42.3% of the time during the study period in Catladikapi, Silivri, Kagithane, and Umraniye, respectively. The number of exceedances in Catladikapi is underestimated due to lack of data availability during fall and winter. Similarly to WHO regulation, Besiktas station had the highest exceedance (55.6%) of the US-EPA standard compared to other stations. These exceedances on the EPA air quality standard occur during the fall and winter and are due to increased emissions from residential heating and very poor dispersion conditions with poor atmospheric motion and low mixing heights. Higher daily $PM_{2.5}$ concentrations have been also observed in our sampling station in Besiktas during the spring and summer seasons (Table 1). During the spring, concentrations in Besiktas are between 20% and two times greater than those recorded in Kagithane. On the other hand, during winter, concentrations in Besiktas are between 24% and 3.5 times less than those recorded in Kagithane. During summer, concentrations in Besiktas and Kagithane are comparable. In Besiktas, the WHO and EPA air quality standards were exceeded 74.0 and 55.6% of the time during the complete sampling campaign, respectively (Table 1). Although lower concentrations are observed during spring and summer, the WHO and EPA air quality standards are still exceeded 71.4 and 43% of the time. To decrease $PM_{2.5}$ concentrations in order to comply with the regulations, particularly in Besiktas and Kagithane requires strict measurements of traffic control. In addition, other important stations such as Catladikapi requires continuous monitoring and more reliable data availability.

Table 1. Daily average PM_{2.5} concentrations in µg m⁻³

Date	Besiktas (this work)	Catladikapi	Kagithane	Silivri	Umraniye
spring 2017					
03/05/17	40.31	30.56	27.58	18.04	20.92
04/05/17	2.57	38.35	29.29	22.00	23.88
05/05/17	50.07	33.60	28.83	23.23	22.33
06/05/17	71.97	30.29	31.63	28.35	24.88
07/05/17	36.56	20.60	30.46	18.87	17.04
08/05/17	40.42	23.06	22.79	12.86	15.21
09/05/17	31.37	20.53	32.58	16.92	16.92
% Exceedance WHO	85.7	57.1	85.7	14.3	0.0
% Exceedance US-EPA	71.4	14.3	0.0	0.0	0.0
summer 2017					
6/7/2017	116.59	9.44	12.85	11.30	10.21
7/7/2017	22.71	15.31	18.83	14.58	12.13
8/7/2017	21.32	8.13	20.08	12.78	9.25
9/7/2017	28.31	22.00	27.04	18.75	11.79
10/7/2017	27.17*	16.14	25.04	14.64	15.21
11/7/2017	20.53	12.86	19.92	10.15	11.25
12/7/2017	25.14	18.62	18.42	17.75	10.79
% Exceedance WHO	57.1	0.0	28.6	0.0	0.0
% Exceedance US-EPA	14.3	0.0	0.0	0.0	0.0
fall 2017					
20/10/2017	55.16	42.95	62.50	45.17	51.42
21/10/2017	215.87	--	94.88	82.33	75.76
22/10/2017	*	--	72.63	62.09	54.15
23/10/2017	63.53*	--	42.58	32.91	36.77
24/10/2017	37.91	--	59.42	25.88	52.09
25/10/2017	13.18	--	30.00	30.00	--
26/10/2017	22.27	--	--	18.30	--
% Exceedance WHO	66.7	--	100	85.7	100
% Exceedance US-EPA	66.7	--	83.3	42.9	100
winter 2018					
5/01/2018	76.60	--	29.50	27.11	30.53
6/01/2018	50.00	--	97.42	47.57	53.83
7/01/2018	35.66	--	71.29	49.83	44.08
8/01/2018	42.01	--	60.67	60.95	45.60
9/01/2018	23.03	--	79.79	47.58	59.50
10/01/2018	29.00	--	35.83	24.42	36.08
11/01/2018	43.51	--	56.00	34.00	62.00
% Exceedance WHO	85.7	--	100	85.7	100
% Exceedance US-EPA	71.4	--	85.7	57.1	85.7

Note 1. WHO 24-h air quality guideline is 25 µg m⁻³

Note 2. USA-EPA daily air quality standard is 35 µg m⁻³

*Due to technical issues, the sample was collected for only 19, 2, and 14 hours

Figure 2 shows the distribution of hourly concentrations in Catladikapi, Kagithane, Silivri, and Umraniye during (a) spring 2017, (b) summer 2017, (c) fall 2017, and (d) winter 2018 for dates specified in Table 1. During the studied period, there is a clear difference in hourly PM_{2.5} concentrations observed in fall-winter compared to spring and summer in all sampling stations. Maximum hourly concentrations

of $\sim 100\text{-}200 \mu\text{g m}^{-3}$ can be observed during the fall and winter (Fig. 2c, 2d). On the contrary, all hourly concentrations recorded during the spring and summer are below $60 \mu\text{g m}^{-3}$ (Fig. 2a, 2b), except during the spring in Kagithane ($91 \mu\text{g m}^{-3}$). This is consistent with observed low temperatures during the winter and the use of low quality of fuels for residential heating combined with poor dispersion of air pollutants due to low mixing heights, lack of vertical dispersion of contaminants, and low wind speeds during the winter, compared to the spring and summer. Although low correlations between $\text{PM}_{2.5}$ measured in this work and other criteria pollutants were obtained ($R^2 = 0.38\text{-}0.55$), concentrations follow similar trend during the sampling campaign as can be observed in Table 1. Analyzing trends and magnitudes of hourly concentration is useful for source apportionment and evaluation of air quality control strategies. In addition, epidemiological studies may be combined with hourly $\text{PM}_{2.5}$ concentrations for establishment of new air quality standards. For these reasons, monitoring of fine particulate matter at high time resolution of 1 h or less should be continuously and routinely performed.

Similarly to the European Commission, the National Environment Protection Council (NEPC) of Australia has established the air quality standard of $25 \mu\text{g m}^{-3}$ as 24 h average (NEPC, 2015). Although no standard has been established for hourly $\text{PM}_{2.5}$ concentrations, NEPC has recommended a value of $40 \mu\text{g m}^{-3}$ as an indicator of poor air quality that is unhealthy for everybody (EPA, 2018). In this work, less than 5% of the hourly $\text{PM}_{2.5}$ concentrations exceeded the recommended value of $40 \mu\text{g m}^{-3}$ during the spring and summer, except for Catladikapi and Kagithane with 12.9 and 12.4%, respectively. On the other hand, poor and very poor air quality were observed during the fall and winter at all stations, except Silivri, with over 50% of the hourly $\text{PM}_{2.5}$ concentrations exceeding $40 \mu\text{g m}^{-3}$. Although lower $\text{PM}_{2.5}$ concentrations were observed in Silivri, 32.9 and 39.5% of the data exceeded the threshold value during the fall and winter, respectively. Although Silivri has the lowest population density (200 km^{-2}) of the studied sampling sites ($15,338\text{-}25,679 \text{ km}^{-2}$), average concentrations and their distributions are comparable to the other sampling sites (e.g., Umraniye) and high concentrations are particularly observed during the fall and winter (Fig 2c, 2d). This shows the importance of implementing and supporting high quality fuel use for residential heating, especially during the cold season.

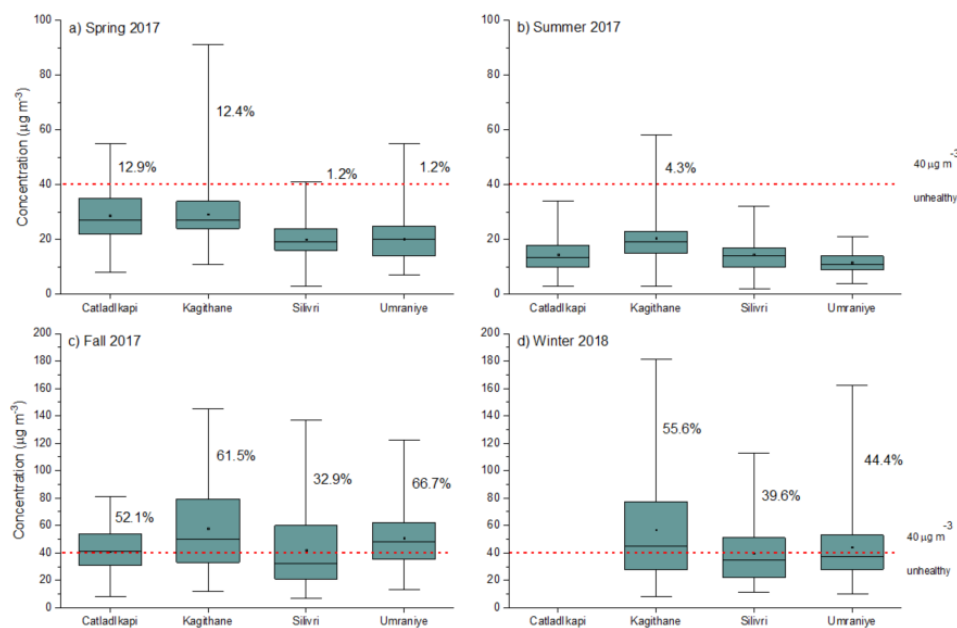


Figure 2. Distribution of hourly $\text{PM}_{2.5}$ concentrations in Istanbul in (a) spring 2017, (b) summer 2017, (c) fall 2017, and (d) winter 2018. The dates correspond to Table 1. The boxes indicate 25 and 75 percentiles, and the bars indicate minimum and maximum values. Mean (dot) and median (line) of the data are shown inside the boxes. $40 \mu\text{g m}^{-3}$ is used as indicator for unhealthy air quality

3.2. OC and EC concentrations

In this work, daily PM_{2.5} samples were collected and analyzed for OC and EC concentrations with a thermo-optical Sunset Laboratory carbon analyzer. Figure 3 shows seasonal variability of OC, EC, TC, and PM_{2.5} in Besiktas station. In addition, Table 2 shows OC/EC and OC/TC ratios and wind speed (WS) during the same study period. In order to make PM_{2.5} concentrations comparable to OC, EC, and TC, we used a concentration factor of 0.25.

The annual average OC and EC concentrations of PM_{2.5} samples analyzed in this study were found as 10.45 and 2.83 $\mu\text{g m}^{-3}$, respectively. Average OC concentrations ranged between 6.62-7.32 $\mu\text{g m}^{-3}$ during spring and summer, and over twice as much during the fall and winter with a range of 13.76-14.1 $\mu\text{g m}^{-3}$ (Table 2). OC concentrations had significant correlation with wind speed ($r=-0.48$) and wind direction ($r=0.53$) indicating that OC concentrations increase with atmospheric stability (i.e., low wind speed) and in addition to local sources, OC may be also be transported from nearby areas. During the summer, high OC and EC concentration of 17.42 and 4.64 $\mu\text{g m}^{-3}$ were observed on 6/7/17 which coincided with high daily average wind speed of 5.14 m s^{-1} (Table 2) and maximum hourly wind speed of nearly 9.0 m s^{-1} . On this day, high PM_{2.5} concentrations were also observed. An additional combustion activity near the sampling site may have been responsible for high concentrations of PM_{2.5} and organic aerosol, and were possibly transported with high wind speed from N direction. EC concentrations on the other hand, do not show considerable seasonal variation with the average values between 2.16-3.26 $\mu\text{g m}^{-3}$ during all four seasons (Table 2). Contrary to OC, EC had lower correlation coefficients with wind speed ($r=0.22$) and wind direction ($r=0.19$). Since the sampling site is located near a road with heavy traffic, continuous emissions from vehicle exhaust (i.e., EC) are expected. The contributions of OC to TC was on average 76.46% with the highest contribution during the winter (83.46%), indicating that although OC was the predominant carbon contributor, EC also had a significant contribution to organic aerosol at this particular traffic sampling site. The contribution of OC to PM_{2.5} was on average 33.18% (Table 2) and was more significant during the winter season (41.96%), indicating that emissions from fossil fuel combustion for residential heating is an important source of fine particulate matter during the winter. On the other hand, lowest OC contribution of 20.7% was observed during the spring, indicating that other sources of PM_{2.5} such as mineral dust transport and inorganic aerosol are predominant.

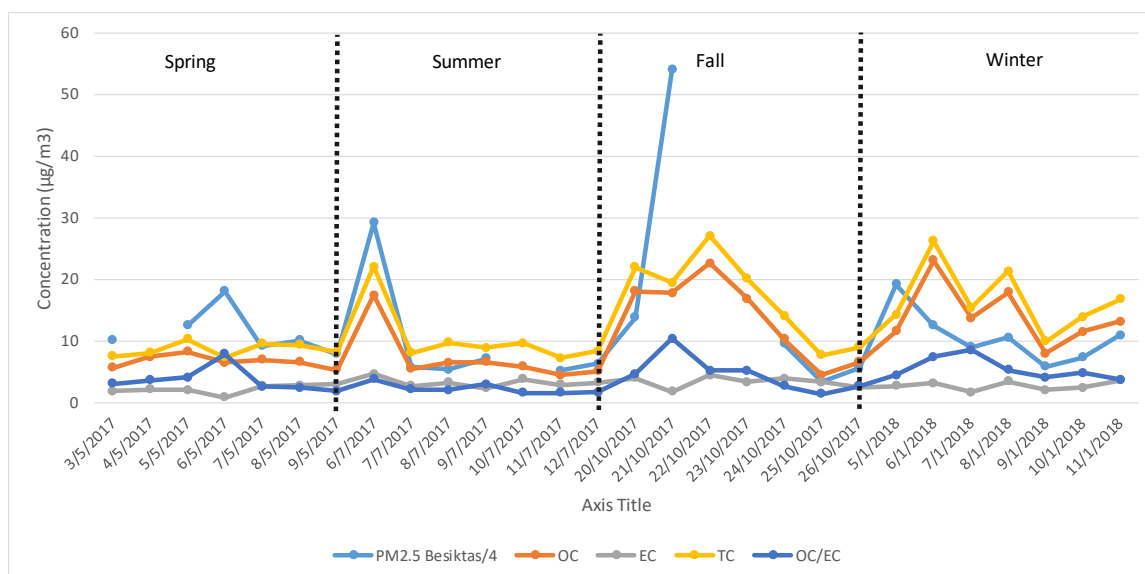


Figure 3. Average daily concentrations of OC, EC, TC, and PM_{2.5} ($\mu\text{g m}^{-3}$) in Besiktas

The OC concentrations observed in this work during the summer and winter are nearly 2-4 times and 3-6 times higher than concentrations observed in USA and Europe, respectively (Figure 4). A much higher

ratio was observed for EC concentrations in Besiktas, which were 7-9 times higher than concentrations observed in US and EU. Higher EC concentrations observed in Europe than in USA could reflect the higher use of diesel vehicles. In Besiktas, the traffic is mainly light-duty vehicles that could use both gasoline or diesel and continuous emissions from diesel-operated public transportation. Another important factor can be given as the elevation of the road; slope is considerably steep in Besiktas, forcing accelerating vehicles going upway to emit more pollutants as can be seen in Fig. 1.

High average EC concentrations have been also reported in Korea and Beijing with 7.3 and $8.7 \mu\text{g m}^{-3}$, respectively (He et al., 2001; Park et al., 2002). In Turkey, OC and EC concentrations have been investigated by Theodosi et al. (2010) and Öztürk and Keles (2016) in Istanbul and Bolu, respectively. Average annual and wintertime OC concentrations were obtained as 6.6 and $59.9 \mu\text{g m}^{-3}$ in Istanbul and Bolu, respectively. OC concentrations in our work were 58% higher than Theodosi et al. (2010) but 4 times lower than Öztürk and Keles (2016). The great variation in the reported concentration is due to the contribution of different sources in each of the sampling sites. The lowest OC concentrations obtained by Theodosi et al. (2010) were obtained at the top of a building away from direct sources, our sampling site receives direct emissions from vehicle exhaust, and the very high concentrations obtained by Öztürk and Keles (2016) during the wintertime were due to biomass burning for residential heating. Annual average EC concentration obtained in this work ($2.83 \mu\text{g m}^{-3}$) is comparable to Theodosi et al. ($2.92 \mu\text{g m}^{-3}$) but 2 times lower than Öztürk and Keles ($5.62 \mu\text{g m}^{-3}$). This shows the importance of continuous monitoring of organic aerosol at various sampling sites in order to reliably evaluate contributions from different sources.

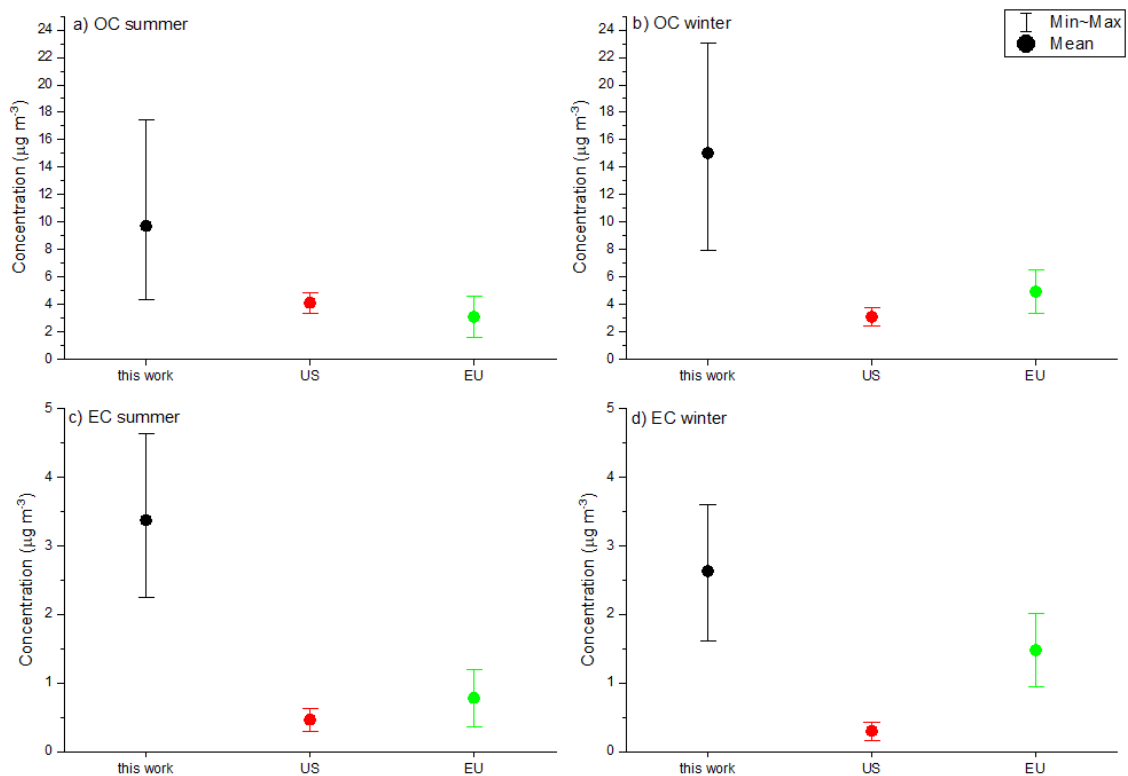


Figure 4. Comparison of OC and EC concentrations ($\mu\text{g m}^{-3}$) obtained in this work with other studies in the US and EU. Adapted from Weijers et al. (2013)

Table 2. Average daily concentrations of OC, EC, TC, and PM_{2.5} ($\mu\text{g m}^{-3}$)

Date	OC	EC	TC	OC/EC	OC/TC	%PM _{2.5}	WS m s ⁻¹
spring 2017							
3/5/2017	5.62	1.84	7.46	3.05	0.75	18.52	3.42
4/5/2017	7.41	2.06	8.03	3.59	0.92	-	3.70
5/5/2017	8.18	2.05	10.22	4.00	0.80	20.42	2.31
6/5/2017	6.43	0.82	7.32	7.81	0.88	10.17	1.52
7/5/2017	6.89	2.65	9.54	2.60	0.72	26.10	1.85
8/5/2017	6.55	2.76	9.32	2.37	0.70	23.05	1.30
9/5/2017	5.23	2.92	8.14	1.79	0.64	25.96	3.41
Average	6.62	2.16	8.58	3.60	0.77	20.70	2.50
summer 2017							
6/7/2017	17.42	4.64	22.05	3.76	0.79	18.91	5.14
7/7/2017	5.45	2.62	8.07	2.08	0.68	35.53	3.08
8/7/2017	6.49	3.23	9.72	2.01	0.67	45.59	3.26
9/7/2017	6.57	2.25	8.82	2.92	0.75	31.16	1.14
10/7/2017	5.84	3.74	9.58	1.56	0.61		4.75
11/7/2017	4.37	2.86	7.23	1.53	0.60	35.21	4.24
12/7/2017	5.08	3.20	8.28	1.59	0.61	32.93	3.04
Average	7.32	3.22	10.54	2.21	0.67	33.22	3.52
fall 2017							
20/10/2017	18.05	3.90	21.95	4.62	0.82	39.80	0.56
21/10/2017	17.74	1.72	19.46	10.34	0.91	9.01	0.86
22/10/2017	22.59	4.39	26.98	5.14	0.84		2.32
23/10/2017	16.81	3.28	20.08	5.13	0.84		1.89
24/10/2017	10.25	3.82	14.07	2.68	0.73	37.11	1.25
25/10/2017	4.38	3.27	7.65	1.34	0.57	58.07	3.54
26/10/2017	6.53	2.42	8.95	2.69	0.73	40.19	3.59
Average	13.76	3.26	17.02	4.56	0.78	36.84	2.00
winter 2018							
5/1/2018	11.57	2.62	14.19	4.42	0.82	18.53	2.20
6/1/2018	23.03	3.14	26.17	7.35	0.88	52.33	0.63
7/1/2018	13.70	1.61	15.31	8.49	0.89	42.94	0.80
8/1/2018	17.85	3.42	21.27	5.22	0.84	50.62	0.46
9/1/2018	7.91	1.97	9.88	4.01	0.80	42.89	2.34
10/1/2018	11.48	2.41	13.89	4.76	0.83	47.91	0.74
11/1/2018	13.16	3.59	16.75	3.67	0.79	38.49	1.31
Average	14.10	2.68	16.78	5.42	0.83	41.96	1.21
Overall average	10.45	2.83	13.23	3.95	0.76	33.18	2.31

OC/EC ratios are helpful for estimating sources of organic aerosol. OC/EC ratios lower than 1 indicate high EC concentrations and therefore emissions from diesel vehicles. Increasing OC/EC ratios are indicators of increasing emissions of OC and can be separated into sections. OC/EC ratios of 2.2-5.2 indicate emissions from light duty gasoline vehicles, residential wood combustion, and typical PM_{2.5}

concentrations. OC/EC ratios ranging between 12.7-14.5 are indicators of emissions from natural gas home appliances, paved road dust, and forest fires. A very high OC/EC ratio such as 67.6 indicates emissions from meat charbroiling (Table 3).

In this work, the average ratio during the four seasons was found to be 3.95. The lowest average ratios were observed during spring and summer with 3.6 and 2.21, respectively. The highest average ratios were observed during the fall and winter with the values of 4.56 and 5.42, respectively. The highest OC/EC ratios during the complete sampling dates ranged in 7.81-10.34. These high ratios were due to low EC concentrations rather than high OC concentrations. This could be due to low traffic emissions. According to Table 5, the OC/EC ratios observed in Besiktas appear to be a combination of light-duty gasoline and diesel vehicles and possibly shipping emissions during the summer and residential burning during the winter. The lowest OC/EC ratios of 1.34-1.56 were mostly due to a decrease in OC concentrations, however, EC concentrations were also slightly increased. The lowest OC/EC ratios also coincide with precipitation events.

Table 3. Ratios of OC to EC in emissions by different sources (Na et al., 2004)

Emission source	OC/EC ratio	Emission source	OC/EC ratio
Tunnel	0.76	Forest fire	6, 14.5
Heavy-duty diesel vehicles	0.8	Natural gas home appliances	12.7
Light-duty gasoline vehicles	2.2	Paved road dust	13.1
Ship emissions	2-3, 7	Meat charbroiling	67.6
Residential wood combustion	4.15		
Ambient PM _{2.5}	5.2±2.7		

4. Conclusions

In this work, seasonal variations of OC and EC were investigated in daily PM_{2.5} samples in the traffic site at the Besiktas district of Istanbul. Hourly and daily PM_{2.5} concentrations were also evaluated in terms of air quality standards and recommended thresholds in order to understand impacts on human health and overall air quality. Overall, both WHO and US-EPA standards of 25 and 35 µg m⁻³ were exceeded in all stations with the majority observed in Besiktas station with 74.0 and 55.6% of the data higher than the established threshold. Most of the exceedances occurred during the fall and winter period. OC and EC concentrations were over twice as high during the fall and winter, indicating the necessity of supporting the future use of high quality fossil fuels for residential heating and implementation of the traffic control strategies. As expected, the highest contribution of OC to PM_{2.5} was observed during the winter (41.96%) due to biomass burning. The lowest contribution was observed during the spring, indicating that natural and anthropogenic sources of inorganic fine aerosol may be more important. The OC concentrations observed in this work are nearly 2-6 times higher than concentrations observed in other studies in the USA and Europe. A much higher ratio was observed for EC concentrations in Besiktas, which were 7-9 times higher than concentrations observed in US and EU. Problems in the measurements and missing data gaps can generate quality issues in the overall data set, bringing uncertainties to the analysis. The results show that continuous and long-term observation of particle concentrations and their organic and elementary carbon constituents, and in turn, improved data availability of urban stations like Besiktas, Kagithane, and Catladikapi are necessary in order to have more reliable analysis for the aerosol trends. The results in this work may be further used for the evaluation and establishment of air quality control strategies.

5. References

- Andreae, M.O., Gelencsér, A., 2006. Black carbon or brown carbon? The nature of light-absorbing carbonaceous aerosols. *Atmos. Chem. Phys.* 6, 3131-3148.
- Chow, J.C., Doraiswamy, P., Watson, J.G., Chen, L.-W.A., Ho, S.S.H., Sodeman, D.A., 2008. Advances in integrated and continuous measurements for particle mass and chemical composition. *J. Air Waste Manage. Assoc.* 58, 141-163.
- EPA, V., 2018. PM_{2.5} particles in air. Available at <https://www.epa.vic.gov.au/your-environment/air/air-pollution/pm25-particles-in-air>, accessed on 27 February 2019.
- Flores, R., Mertoglu, E., Ozdemir, H., B, A., Unal, A., Tayanc, M., in review. Description of diurnal and seasonal variations of high-time resolved PM_{2.5}, OC, and EC concentrations at an urban traffic site in review.
- Flores, R.M., Kaya, N., Eser, Ö., Saltan, S., 2017. The effect of mineral dust transport on PM₁₀ concentrations and physical properties in Istanbul during 2007–2014. *Atmospheric Research.* 197, 342-355.
- He, K., Yang, F., Ma, Y., Zhang, Q., Yao, X., Chan, C.K., Cadle, S., Chan, T., Mulawa, P., 2001. The characteristics of PM_{2.5} in Beijing, China. *Atmos. Environ.* 35, 4959-4970.
- Na, K., Sawant, A.A., Song, C., Cocker, D.R., 2004. Primary and secondary carbonaceous species in the atmosphere of Western Riverside County, California. *Atmos. Environ.* 38, 1345-1355.
- NEPC, 2015. National Environment Protection (Ambient Air Quality) Measure. available at <https://www.legislation.gov.au/Series/F2007B01142>.
- Öztürk, F., Keles, M., 2016. Wintertime chemical compositions of coarse and fine fractions of particulate matter in Bolu, Turkey. *Environmental Science and Pollution Research.* 23, 14157-14172.
- Park, S.S., Kim, Y.J., Fung, K., 2002. PM_{2.5} carbon measurements in two urban areas: Seoul and Kwangju, Korea. *Atmos. Environ.* 36, 1287-1297.
- Theodosi, C., Im, U., Bougiatioti, A., Zarnpas, P., Yenigun, O., Mihalopoulos, N., 2010. Aerosol chemical composition over Istanbul. *Sci. Total Environ.* 408, 2482-2491.
- Weijers, E.P., Rocca, S., Verheggen, B., 2013. Carbonaceous aerosol: where is it coming from? ECN.

Acknowledgements

The authors would like to thank the Scientific and Technological Research Council of Turkey (TÜBİTAK) through project No. 115Y625. The authors thank Aysegul Pursa for her invaluable assistance, IETT-Besiktas for use of their facilities, and Ministry of Environment and Urbanization and Department of Transportation (Trafik Müdürlüğü) for data provided. Meteorological data was obtained from Weather Underground.

Dispersion modeling and air quality measurements to evaluate the odor impact of a wastewater treatment plant in İzmir

Faruk Dinçer¹, Fatih Kemal Dinçer¹, Deniz Sari¹, Özcan Ceylan¹ and Özgen Ercan¹

¹TUBITAK Marmara Research Center, Environment and Cleaner Production Institute
Barış Mah. Dr. Zeki Acar Cad. No:1 Gebze KOCAELİ / TURKEY

faruk.dincer@tubitak.gov.tr

Abstract. Municipal wastewater treatment plants (WTP) are potential sources of offensive odors that can create annoyance in the communities. Therefore, odors have been rated as the primary concern of the public relative to the implementation of wastewater treatment facilities. In this study, dispersion modeling and air quality measurements were used to quantify the potential odor impact around a Wastewater Treatment Plant in İzmir. AERMOD atmospheric dispersion model was used to predict odor levels in OU m⁻³ around the treatment plant. Odor measurement results of the wastewater treatment plant units that are considered as area odor sources were used for odor modeling. Air quality measurements of H₂S and NH₃, which are two main odorous compounds emit from wastewater treatment plants, were also conducted by using passive sampling methodology in the surroundings of the plant to evaluate the odor impact of the plant. Both odor emission and air quality measurements were conducted in the period of July-August 2018 for evaluation of odor impact, and consequent application of dispersion model. The air quality measurements of the pollutants which exceeds the odor threshold values do not create annoying odor impact on residential areas. The dispersion modeling demonstrates that the odor concentrations exceed 10 OU m⁻³ concentration levels that can be measured olfactometrically also do not create an odor impact on local residents.

Keywords: Wastewater treatment plants, Odor, Air quality, Dispersion modeling

1. Introduction

Odor emissions from wastewater treatment plants (WTPs) are becoming an important source of environmental annoyance. In recent years, public concern over odors originating from wastewater collection, transfer and treatment operations has increased. It is well known that odorous gases lead to air pollution, affect the quality of life and may cause health symptoms such as insomnia, loss of appetite and the development of irrational behavior (Brennan, 1993; Gostelow et al., 2001). Assessment of the odor levels together with air quality levels of odorous pollutants are necessary for odor control projects (Dincer and Muezzinoglu, 2007).

Odor measurements are carried out with sensory measurements that employ the human nose as detector. In this method, panelists test the odorous air at predetermined dilutions. These panelists are carefully selected to have average sensing capability in accordance with the EN13725:2003 standard (CEN, 2003), which is the method followed throughout. By using this method, the strength of odor perception as perceived by the panelists is measured, and the results are used as the odor concentration of the stimulant in OU/m³ (Dinçer and Muezzinoğlu, 2007).

Atmospheric dispersion modeling has been applied for the assessment of odor impacts in several cases using mainly Gaussian models such as the industrial source complex model (McIntyre 2000; Henshaw et al. 2006), AERMOD (USEPA, 2003) and the CALPUFF model (Yu et al. 2009). Dispersion modeling can effectively be used in order to estimate the dispersion of odors using available emission data and to correlate with complaints and, secondly, to estimate the maximum odor emissions which can be permitted from a site in order to prevent odor complaints (McIntyre 2000).

The main odorous compounds released into the atmosphere from WTPs include sulfur-containing substances such as hydrogen sulfur, dimethyl sulfur, dimethyl disulfur, and mercaptans together with nitrogen containing substances such as ammonia, amines, indole and skatole (Easter et al. 2005; Nicell and Henshaw 2007). Odor emissions may also contain many other odorants including volatile organic compounds such as organic acids, aldehydes and ketones (Dinçer and Müezzinoğlu, 2007). All of these substances are the products of anaerobic decay, and hence wastewater, which is allowed to become septic, has a strong potential to become odorous. Although various odorous compounds may be present, the most significant is the hydrogen sulfur (H₂S; Gostelow and Parsons 2000).

This work presents a methodology to evaluate the odor impacts of a WTP by using odor and air quality measurements together with the use of dispersion modeling. In order to achieve the aim of the study; (1) odor emission measurements of the WTP units are done, (2) the AERMOD dispersion model is used to evaluate odor impacts of the WTP and (3) air quality measurements of H₂S and NH₃ are conducted around the WTP domain.

2. Materials and methods

2.1. Description of the WTP

Izmir WTP serving 3.6 million population equivalents, has been in operation since 2001 and presently treats 7m³/s urban (mixed domestic and pretreated industrial) wastewater (Dinçer and Müezzinoğlu, 2008). All units are open to the atmosphere and the treatment method is extended aeration using surface aerators in carousel-type basins. Odor samples were collected from different treatment units of this WTP; fine screen, aerated grit chamber, primary sedimentation tank, sludge storage tank, aeration tank, final sedimentation tank and sludge cake storage area. Sampling was carried out on July 06, 2018, which coincides with the mid of the warm and dry season in this Mediterranean region. The ambient air temperature during sampling was 36 °C. Samples were collected between 09:30 a.m. and 13:00 p.m. The flow diagram of the WTP is given in Figure 1 together with the odor sampling points.

2.2. Odor measurements

Three samples were collected from each sampling point from the headspaces of the tanks by using a special sampling hood (with a surface area of 1 m²) located onto the surface of the water. The design of this hood and the sampling procedure were in accordance with the recommendations described in the European Standard EN 13725 (CEN, 2003). Air samples were drawn into 5-liter Nalophan bags using a special sampler working with the lung principle. These bags are impermeable to water and organics, absolutely odorant taste-free and are used only once. Samples were transported to the laboratory and analyzed within 30 hours.

The odor concentrations of the samples were measured by dynamic olfactometry, which measures the odor concentration in terms of dilutions required to reduce an odorous compound until its threshold concentration. These tests were carried out inside an odor-free, clean laboratory with selected and trained panelists. Each sample was diluted in the olfactometer (Olfasense TO8, Kiel, Germany) several times, differing from each other by a dilution factor of two and presented to the panelists three times. This method employs a “yes/no” technique and determines the number of times a sample must be diluted until the threshold of detection by 50% of the panelists is obtained.

In this study, AERMET meteorological model and AERMOD were carried out in seven different 10x10 km areas with the WTP being at the center with 50x50 m gridding. Elevation data of the study area were obtained from NASA's Radar Shuttle Radar Topographic Mission (SRTM) 90m Digital Elevation Data" file on the Consortium for Spatial Information (CGIAR-CSI) website.

2.4. Meteorological data

Meteorological data (wind direction and velocity, temperature, cloudiness, cloud height, pressure, relative humidity data from) were gathered during a period of 1 year from the study area using two meteorological stations (the base year of 2017). Pressure, measurement altitude, temperature, wind direction and wind speed values for radiosonde data from İzmir meteorological station belonging to the same period were also used. The wind roses of İzmir Adnan Menderes Airport and Çiğli Airport Meteorological Station, which are located close to the facilities, are given in Figure 2. AERMET results are used as input for the AERMOD dispersion model.

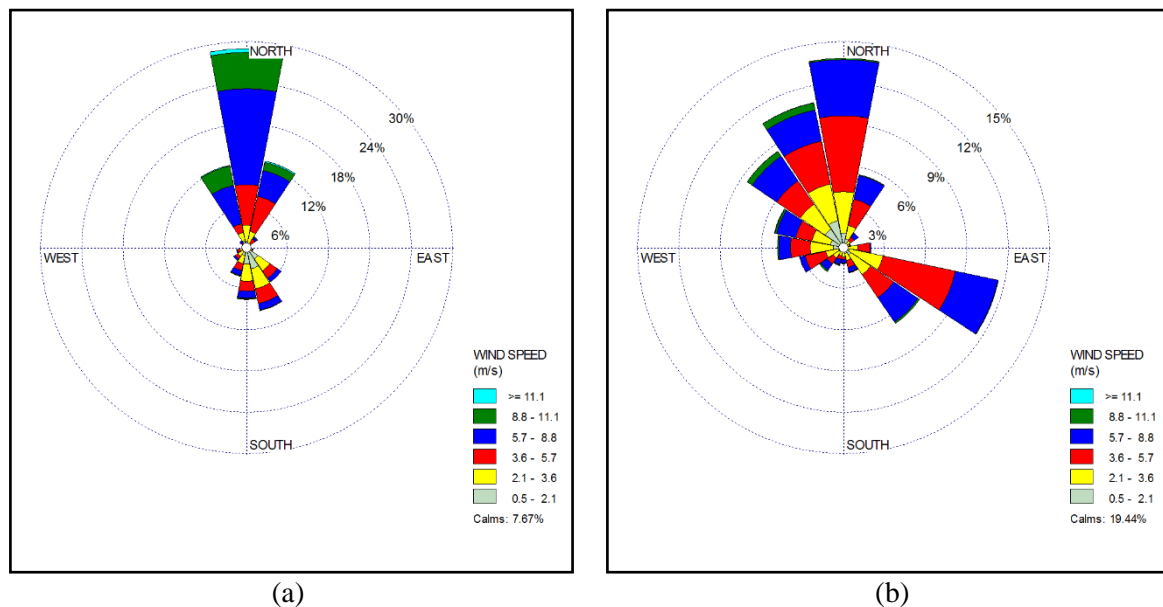


Figure 2. The wind roses of İzmir Adnan Menderes Airport (a) and Çiğli Airport (b) meteorological stations

2.5. Air quality measurements

H₂S and NH₃ were measured using diffusive samplers. Diffusive samplers are a special kind of passive samplers, which are capable of sampling gas or vapor pollutants from the atmosphere at a rate controlled by physical processes such as molecular diffusion through a static air layer or penetration through a membrane (Berlin et al., 1986).

Measurements were conducted at eleven sampling points including, urban, suburban, rural and industrial sampling locations (Figure 3) in the period of July-August 2018. For these pollutants, absorbent solutions were used to collect the pollutant of interest such as zinc acetate for H₂S and sulfuric acid for NH₃. H₂S passive samplers that were made of black acrylic tubes (71 mm in length and 11.0 mm internal diameter) fitted with black thermoplastic rubber caps and NH₃ passive samplers that were made of fluorinated ethylene polymer tubes (35.5 mm in length and 11.0 mm internal diameter) fitted with yellow and white thermoplastic rubber caps were purchased commercially and used as received.

All diffusive samplers used in the field were purchased from Gradko Environmental Ltd. (UK). The analyses were performed using UV/visible spectrophotometry for H₂S and ion chromatography for NH₃.

Limit of detection and overall method of uncertainty values were provided in the analysis reports $0.0.31 \pm 17.4\% \mu\text{g}$ for H_2S and $0.11 \pm 9.6\% \mu\text{g}$ NH_4^+ for NH_3 .



Figure 3. Location of H_2S and NH_3 sampling points

3. Results and discussions

3.1. Odor measurement results

The results of olfactometric measurements (odor concentrations and odor emission rates) are given together in Table 1. Olfactometric concentrations varied between 131-16384 OU m^{-3} with a geometric mean value of 2553 OU m^{-3} .

Table 1. Odor concentrations and odor emission rates of sampling points

Sampling Point	Odor concentration (OU m ⁻³)	Odor emission rate (OU (m ² sec ⁻¹) ⁻¹)
Fine screen	16384	1049
Aerated grit chamber	12040	771
Primary sedimentation tank	3866	247
Sludge storage tank	13004	832
Aeration tank	199	12.7
Final sedimentation tank	131	8.38
Sludge cake storage area	2734	175

For most regulations and atmospheric dispersion calculations, the odor emission rate i.e. odor units per time (q_{od} , OU h⁻¹ or OU sec⁻¹) is widely used. For an odor source with an outward and usually forced airflow (also known as active sources like aeration tanks, biofilters), the odor emission rate is the product of the odor concentration (C_{ou} , OU m⁻³) and the volumetric flow rate (Q_{air} , m³ h⁻¹). For passive sources like WTPs units, sludge thickeners and lagoons, odor emission is facilitated by natural flow of ambient air, and is often quantified by the area-related odor emission rate, given as OU (m² h⁻¹)⁻¹. The odor emission rate is then calculated by multiplying the areal odor emission rate with the total area of the odor source.

In Turkey, odor emission is regulated by “Regulation on Control of Odor Emissions (Official Gazette, 19.07.2013, No:28712)”. Any facility that has odor emission should be measuring its odor emissions if there is a complaint about the facility. There are limit values for odor concentrations of odor sources (either point or area sources). These limit values are 1,000 OU m⁻³ and 10,000 OU m⁻³. If a source has an odor concentration below 1,000 OU m⁻³, no further action is necessary for that source and facility. If a source has an odor concentration between 1,000 OU m⁻³ - 10,000 OU m⁻³, the facility must be done odor control or additional odor control measures and must report the measurement results to the Ministry of Environment and Urbanization. If a source has an odor concentration above 10,000 OU m⁻³, after administrative penalty application, the facility must done odor control or additional odor control measures also and must report the measurement results to the Ministry of Environment and Urbanization.

The odor concentrations of fine screen, aerated grit chamber and sludge storage tank are above the limit value of 10,000 OU m⁻³. Primary sedimentation tank and sludge cake storage area results are between 1,000 OU m⁻³ - 10,000 OU m⁻³. Based on upper information, odor control measures should be taken at these sources.

3.2. Modeling results

AERMOD model is used to perform a study of the odor pollution distribution that may be caused due to the odor emissions from the İzmir WTP to the population living in the surrounding area. Odor emission rates that are given in Table 1 are used for model calculations.

The maximum odor concentration values obtained by running the model according to the grid system coordinates in the model study area determined for İzmir WWTP are given in Table 2. Odor pollution maps showing daily and annual maximum values calculated for each grid peak within the study area are given in Figure 4 and Figure 5. The maximum values remain within the WTP site.

Table 2. Odor concentration levels from İzmir WTP

Time Period	Coordinates		Concentration (OU m ⁻³)
	X	Y	
Daily	500258	4258470	11534
Annual	500258	4258470	1551

Olfactometric measurements cannot be made on samples below 10 OU m⁻³ odor concentrations. For these instances either atmospheric dispersion models or field techniques based on semiquantitative statistical evaluations around the odor sources are used to prepare odor maps in field investigations around odorous facilities (VDI, 1993). In this study, model results discussions are made for the 10 OU m⁻³ ambient odor concentration levels which above the limit of human perception (Elbir et al., 2007).

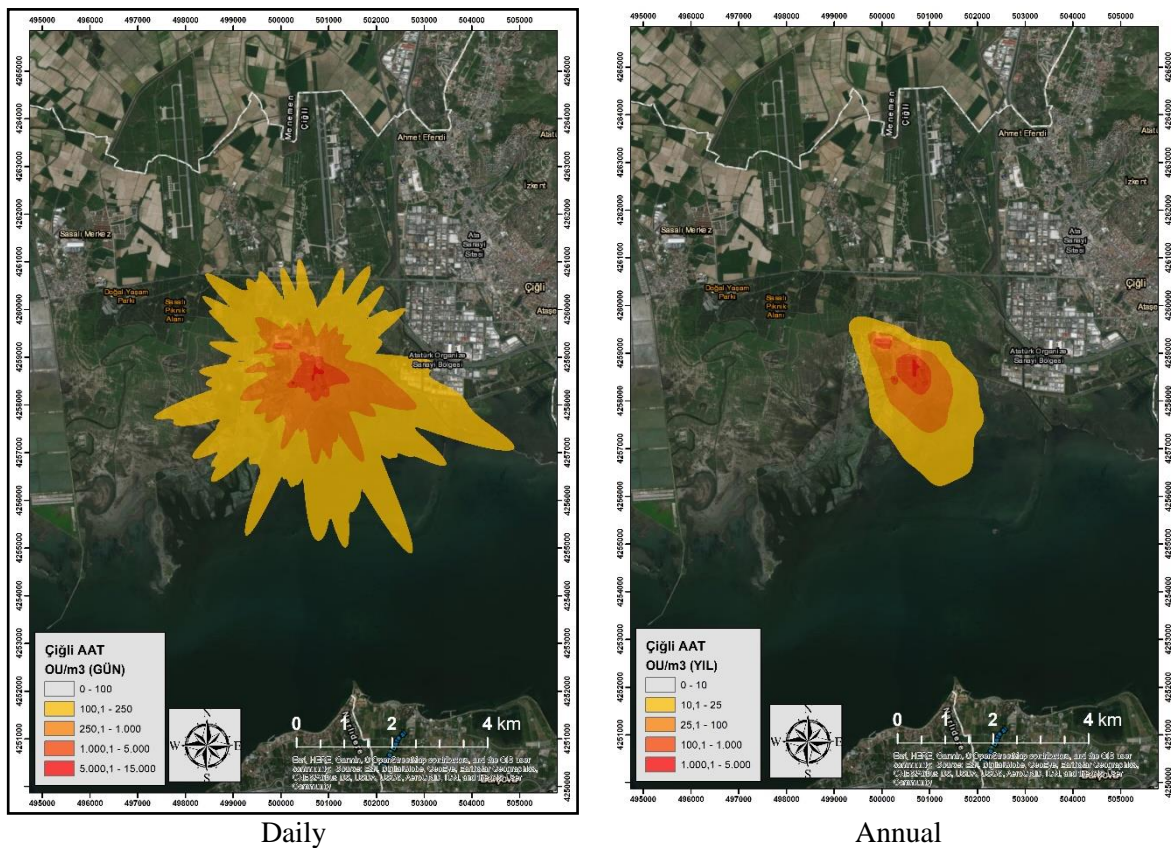


Figure 4. Odor pollution maps of İzmir WTP

As it can be seen from Figure 4, daily maximum odor concentrations do not create an odor impact on local residents, but annoying odor impact can be seen on industrial locations, while annual maximum odor concentrations do not create an odor impact both on local residents and industrial locations.

3.3. Air quality measurement results

The measured values of H₂S and NH₃ at all sampling points between July-August 2018 period are given in Table 3. H₂S concentrations varied between 0.08 to 52.05 µg m⁻³, while NH₃ concentrations varied between 13.73 to 286.33 µg m⁻³.

Maximum H₂S concentration (52.05 µg m⁻³) was measured at SP-1 point which is the entrance of the İzmir WTP. Maximum NH₃ concentration (52.05 µg m⁻³) was measured at SP-11 which is the sludge storage of the WTP.

The lowest odor threshold concentration value for hydrogen sulfide is given by EA (2007) as 0.71 µg m⁻³. The hydrogen sulfur odor in the ambient air can be recognized if its concentration reaches above this value. The hydrogen sulfur concentrations obtained in this study were evaluated based on the threshold concentration value.

The lowest odor threshold concentration value for ammonia is given by Ruth (1986) as 26.6 µg m⁻³. The ammonia odor in the ambient air can be recognized if its concentration reaches above this value. Ammonia concentrations measured in this study are evaluated based on odor threshold concentration value.

Table 3. Air quality measurement results of H₂S and NH₃

Sampling Point	Coordinates		Measurement results (µg m ⁻³) (06.07.2018-08.08.2018 period)	
	N	E	H ₂ S	NH ₃
SP-1	38° 28.619	27° 00.572	52.05	66.26
SP-2	38° 28.722	27° 00.525	21.39	66.09
SP-3	38° 28.637	27° 00.829	10.23	24.91
SP-4	38° 28.335	27° 02.056	4.22	23.18
SP-5	38° 28.411	27° 03.440	2.02	15.67
SP-6	38° 29.651	27° 01.492	1.02	14.23
SP-7	38° 29.621	26° 59.692	0.08	15.07
SP-8	38° 29.646	27° 00.591	0.17	13.73
SP-9	38° 31.063	27° 01.877	0.44	15.67
SP-10	38° 29.344	27° 03.148	0.53	14.77
SP-11	38° 29.118	27° 00.280	0.60	286.33

H₂S concentrations of SP-1 to SP-6 sampling points are above the odor threshold concentration value. SP-1 and SP-2 are located in the WTP site, where SP-3 is very near to the WTP. These three sampling points are affected by the WTP. SP-4 and SP-5 are located near an industrial organized district, while SP-6 is located at a wastewater pumping station. These three sampling points are affected by these sources.

In this study based on H₂S findings, urban (SP-10), suburban (SP-9) and rural (SP-7, SP-8) sampling points are not affected by the İzmir WTP. H₂S concentrations found at that sampling points are much lower than the concentrations reported by Kourtidis et al. (2008). Kourtidis et al. (2008) reported H₂S concentrations for the city of Thessaloniki in an urban sampling point with a mean value of 12 µg m⁻³ during the summer months of 2008.

NH₃ concentrations of SP-1, SP-2 and SP-11 are above the odor threshold concentration value. Both of these three sampling locations are located in the WTP site so are affected by the WTP. The NH₃ concentrations of the other sampling point are below the odor threshold value.

NH₃ concentrations found at urban and suburban sampling locations are higher than the concentrations reported by Reche et al. (2012). Reche et al. (2012) reported NH₃ concentrations of Barcelona city with a mean value of 10.6 µg m⁻³ during July 2011 and 3.9 µg m⁻³ during January 2011. The NH₃ concentrations of rural sampling points are also higher than previous studies. Meng et al. (2010) reported NH₃ concentrations with a mean value of 4.5 µg m⁻³ in rural areas of China.

4. Conclusions

Odor emissions from the İzmir WTP have a potential for complaints in the neighborhood. The minimization and abatement of unpleasant odor emissions are becoming two of the major challenges for WTPs worldwide. This study focused on assessment/management of odor emissions, the application of air dispersion modeling via AERMOD and air quality measurements of two odorous gases emitting from İzmir WTP. Application of AERMOD dispersion model from different sources and concentration levels revealed important information related to odor emissions from the WTP. Based on these odor emission values odor modeling studies demonstrate that the odor concentrations exceed 10 OU m⁻³ concentration levels that can be measured olfactometrically do not create an odor impact on local residents. Air quality measurements of H₂S and NH₃ which not exceeds the odor threshold values do not create annoying odor impact on residential areas also.

Although the modeling and air quality measurement results showed that residential areas are not affected by İzmir WTP, the odor concentrations of WTP units are above the limit values and need to be purified by using odor treatment applications in order to meet the Regulations and for better air quality for WTP's staff. Seasonal odor measurements together with modeling applications should be done afterwards.

5. References

- Berlin, R., Brown, R. H., Saunders, K. J. (Eds.), 1986. Diffusive Sampling: An Alternative Approach to Workplace Air Monitoring. London, UK: Royal Society of Chemistry.
- Brennan, B., 1993. Odour nuisance. *Water Waste Treat.* 36, 30-33.
- CEN (Comite Europe en de Normalisation), 2003. Air quality – Determination of odor concentration by dynamic olfactometry, European Standard EN 13725, Brussels, 74 pages.
- Dinçer, F., Müezzinoğlu, A., 2007. Odor determination at wastewater collection systems; olfactometry versus H₂S analyses. *CLEAN - Soil, Air, Water* 35(6), 565-570.
- Easter, C., Quigley, C., Burrowes, P., Witherspoon, J., Apgar, D., 2005. Odor and air emissions control using biotechnology for both collection and wastewater treatment systems. *Chem. Eng. J.* 113(2-3), 93-104.
- Elbir, T., Dinçer, F., Aysen Müezzinoğlu, A., 2007. Evaluation of measured and predicted odor concentrations around a meat packaging and rendering plant. *Environ. Eng. Sci.* 24(3), 313-320.
- Environment Agency (EA), 2007. Review of odour character and thresholds, Report No: SC030170/SR2, ISBN: 978-1-84432-719-5, Bristol, UK.



- Fileni, L., Matteucci, G., Passerini, G., Rizza, U., 2018. Analysis of air pollutant emissions in a wastewater treatment plant using dispersion models, in: Casares, J., Passerini, G., Barnes, J., Longhurst, J., Perillo G. (Eds.), WIT Transactions on Ecology and Environment, Air Pollution XXVI, Vol 230, doi: 10.2495/AIR180211, Southampton, pp. 219-230.
- Gostelow, P., Parsons, S.A., 2000. Sewage treatment works odour measurement. *Water Sci. Technol.* 41 (6), 33-40.
- Gostelow, P., Parsons, S.A., Stuetz, M., 2001. Odour measurements for sewage treatment works. *Water Res.* 35, 579-597.
- Henshaw, P., Nicell, J.A., Sikdar, A., 2006. Parameters for the assessment of odor impacts on communities. *Atmos. Environ.* 40(6), 1016-1029.
- Kourtidis, K., Kelesis, A., Petrakakis, M., 2008. Hydrogen sulfide (H₂S) in urban ambient air. *Atmos. Environ.* 42, 7476-7482.
- McIntyre, A., 2000. Application of dispersion modeling to odour assessment: a practical tool or a complex trap. *Water Sci. Technol.* 41(6), 81-88.
- Meng, Z.-Y., Lin, W.L., Jiang, X.M., Yan, P., Wang, Y., Zhang, Y.M., Yu, X.L., Jia, X.F., 2011. Characteristics of atmospheric ammonia over Beijing, China. *Atmos. Chem. Phys.* 11, 3041-3070.
- Nicell, J., Henshaw, P., 2007. Odor impact assessments based on dose-response relationships and spatial analyses of population response. *Water Pract.* 1(2), 1-14.
- Reche, C., Viana, M., Pandolfi, M., Alastuey, A., Moreno, T., Amato, F., Ripoll, A., Querol, X., 2012. Urban NH₃ levels and sources in a Mediterranean environment. *Atmos. Environ.* 57, 153-164.
- Ruth, J.H., 1986. Odor thresholds and irritation levels of several chemical substances: A review. *Am. Ind. Hyg. Assoc. J.* 47, A142-A151.
- US Environmental Protection Agency, 2004. AERMOD: Description of the model formulation. EPA-454/R-03-004. North Carolina: US Environmental Protection Agency, Research Triangle Park.
- Verein Deutscher Ingenieure (VDI), 1993. Determination of Odorants in Ambient Air by Field Inspections, VDI-Kommission Reinhaltung der Luft (KRdL). Düsseldorf, Germany.
- Yu, Z., Guo, H., Xing, Y., Lague, C., 2009. Setting acceptable odour criteria using steady-state and annual hourly weather data. *Biosyst. Eng.* 103(3), 329-337.

Determination of PM₁₀ and deposited dust dispersion on the settlement areas from Aksa Goynuk coal (lignite) fueled thermal power plant

Ozgen Ercan, Faruk Dincer, Deniz Sari, Ozcan Ceylan and Fatih Kemal Dincer

TUBITAK Marmara Research Center, Environment and Cleaner Production Institute
Baris Mah. Dr. Zeki Acar Cad. No:1 Gebze, Kocaeli, Turkey

ozgen.ercan@tubitak.gov.tr

Abstract. With the growing population and rapidly developing industrialization in Turkey, energy demand is also increasing. The majority of the energy is produced using imported products, which increase the current account deficit in Turkey. The use of coal from domestic sources is encouraged for economic reasons. One of the coal (lignite) fueled thermal power plants established for this purpose is operating in the province of Bolu. In order to determine the environmental effect of the plant on the settlement areas in the area, air quality monitoring studies have been conducted. In the study, the periodic PM₁₀ and deposited dust parameters have been monitored monthly at four sampling points between 2013-2019, including before and after installation of the plant. As a result of the study; the mean PM₁₀ measurement were obtained as 36.48±0.73; 37.61±0.75; 42.70±0.85 and 38.72±0.77 µg m⁻³ for four points. Meanwhile, the mean values of the deposited dust were found as 70.81±2.12; 35.55±1.07; 79.50±2.39 and 29.38±0.88 mg m⁻² day⁻¹. Despite the providing current limit values of the dust parameter for the power plant where the electrostatic precipitator (ESP) filter and flue gas desulfurization (FGD) systems are applied, it is observed that the dust emissions from activities such as coal extraction, crushing, sieving and ash storage in the area show different cases depending on meteorological conditions.

Keywords: Thermal power plant, Particulate matter, Deposited dust, Dispersion of emissions.

1. Introduction

Coal provides around 40% of the world's electricity, more than any other source (PGT, 2019). The energy required for human life is provided from various sources from centuries to the present. The first of these is the sun offered by nature free of charge, while other sources refer to fossil fuels, which are adversely affecting the health of living beings during extraction and energy production. Due to the limited amount of fossil fuels in nature and the adverse health effects that may occur during the process, the trend towards renewable energy systems is increasing rapidly. The distribution of energy production resources in our country is given in Figure 1.

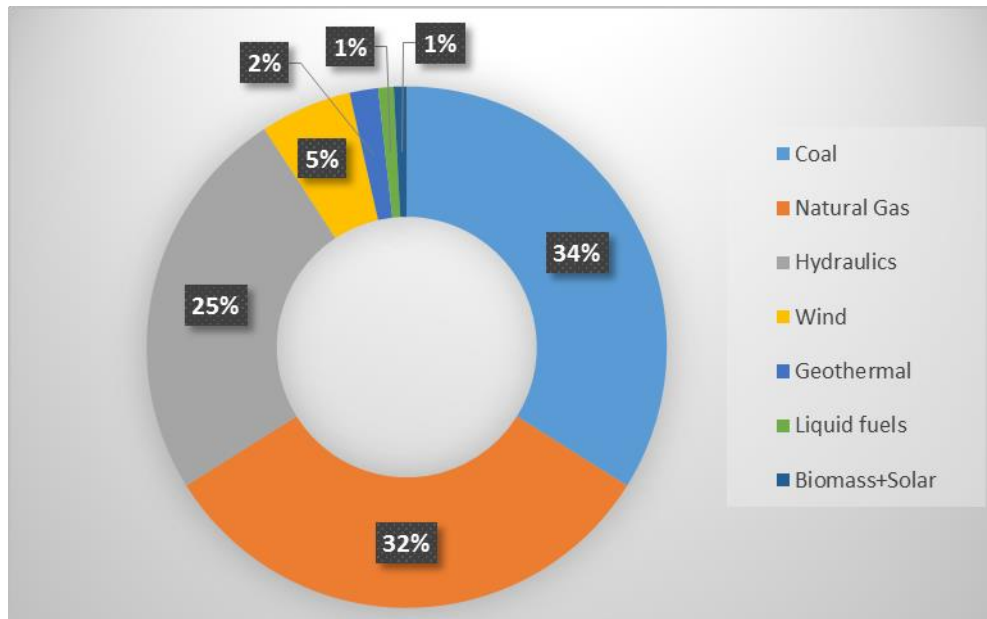


Figure 1. Distribution of electricity generation in Turkey by the end of 2016 (EUAS, 2016)

When the energy production policies of Turkey are examined, it is seen that the diversity in renewable energy resource is increased, and the nuclear power plant is established, and energy production planning is carried out for the country. Also, planning is being made for the use of the existing coal resources in our country with clean technologies. For this purpose, coal reserves are transferred to the private sector, and the establishment of coal-fired thermal power plants, and therefore the use of domestic resources in the production of electric energy are among the priorities (ENRM, 2016).

If the necessary and adequate prevention cannot be taken with the increase in the number of coal-fired thermal power plants, regional air pollution that affects human health and the ecosystem in the region can be significant (Zao et al., 2008). When the emissions from thermal power plants are examined; SO_2 , NO_x , and dust emissions are released into the atmosphere as the primary pollutants. SO_2 and NO_x pollutants in the atmosphere have many adverse effects on human health and cause acid rain, smoke, and turbidity. In addition to the emissions of dust released as a combustion product of coal, these pollutants can also be combined in the atmosphere to form dust emissions that can cause severe respiratory and cardiovascular effects and premature death (EPA, 2014; IEEE, 2010; Sardar et al., 2006).

Control technologies have been applied for the pollutants emitted from the chimneys of thermal power plants. These include an electrostatic dust trap and bag filter, where a 99% reduction in dust emissions is achieved, a flue gas desulfurization system (FGD) where SO_2 emissions can be reduced by 90% and a catalytic reduction (SCR) system with a 90% reduction for NO_x emissions.

The aim of this study is to determine the impact of dust emissions from the pre- and post-installation of the coal-fired power plant which is installed in Goynuk District of Bolu Province, from coal operating sites and rust dump sites in the region.

2. Materials and methods

2.1. Sampling points

Sampling points were selected according to the dispersion modeling result in the Environmental Impact Assessment (EIA) Report and environmental activities in the region. The coordinate information and location plan in the region of this sampling points are given Table 1 and Figure 2, respectively. Also,

Demirhanlar sampling point was chosen as a control point since it is outside of the power plant impact area.

Table 1. Coordinates of sampling points

Number	Sampling Point	Coordination
1	Bolucekova	40° 15.860' N; 30° 48.530' E
2	Catak	40° 12.992' N; 30° 49.681' E
3	Aksa Misafirhane	40° 14.997' N; 30° 45.297' E
4	Demirhanlar	40° 14.616' N; 30° 52.423' E

When Figure 2 is examined, a coal-fired thermal power plant is the main activity in the region. In addition, there are panels A and B, prepared for the extraction of coal in the region for the operation of the thermal power plant, rust casting areas where the soil and low quality parts were taken off from coal are discharged. The temporary ash storage area where the ashes formed after the operation are stored in the power plant and limestone operation area for use in operation.

The seasonal wind roses determined by using data from Bolu Central Station, which is closest to the power plant are given in Figure 3. When sampling points, activity areas are given in Figure 2, and seasonal wind roses given in Figure 3 are examined together, it is seen that Bolucekova sampling point is the most affected region in almost all seasonal periods. It shows that dust emissions from the activities in the region can be transported from the south-west direction to the north-west direction where Bolucekova sampling point is in autumn, winter and spring seasons, and from the south-east direction to the Misafirhane sampling point in the summer season. Also, the most severe wind was obtained spring, winter, autumn and summer periods, respectively.

2.2. Analytical method

Monthly deposited dust sampling between July 2013-July 2019 and daily PM₁₀ sampling every three months in July 2013-August 2019 was carried out at four different locations including before and after installation of the power plant. Deposited dust and PM₁₀ parameters were measured using according to TS 2341 and EN 12341 methods.

The filters conditioned before and after sampling were weighed and used in the field as specified in the relevant standard for PM₁₀, the gravimetric analysis results were divided by the amount of air drawn, and the results were calculated as $\mu\text{g m}^{-3}$. Deposited dust results were calculated as $\text{mg m}^{-2} \text{day}^{-1}$ that kept in the field for about one month with a particular surface area, the sampled part is conditioned after filtering in the laboratory, and the gravimetric weighing (mg) value is divided by the surface area (m^2) and sampling time (day).

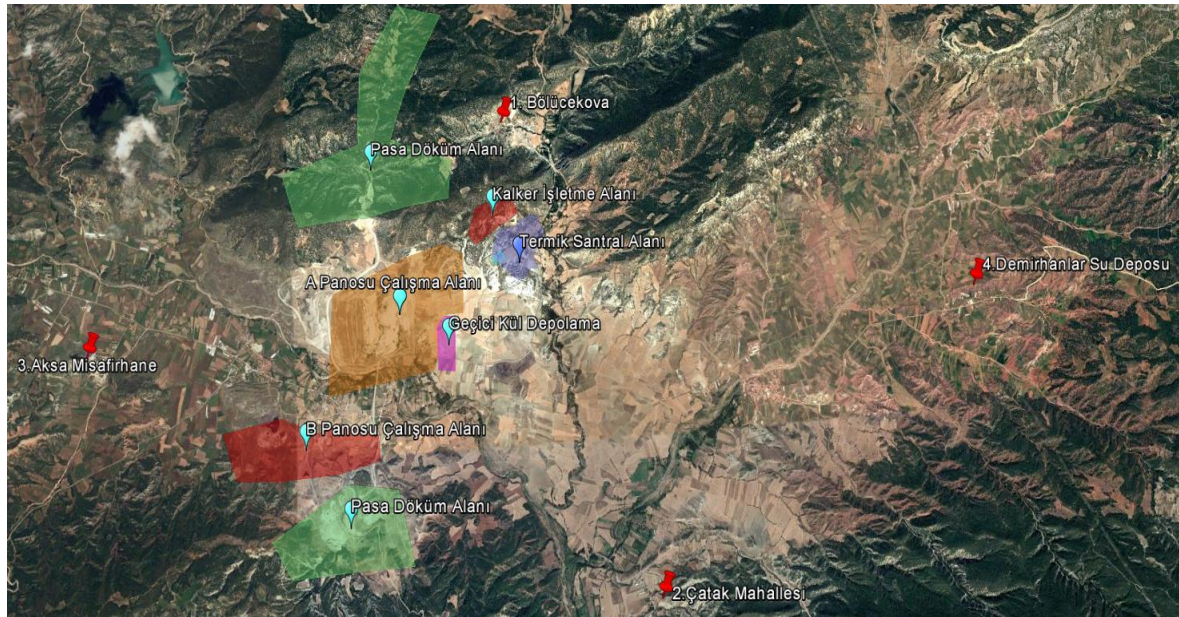


Figure 2. Sampling points with activity around power plant

3. Results

3.1. Spatial and temporal changes of PM_{10} concentrations

The results of the gravimetric analysis of PM_{10} samples at all sampling points including before and after installation and the average results are given in figure 4 and Table 2, respectively. When Figure 4 is examined, periodically different values were obtained at all points due to the reduction of PM_{10} concentrations in air and dust emissions from the ground, especially during periods of reduced activity and precipitation in the region. However, the values of 102.6 in Bolucekova, 103.7 and 166.2 in Misafirhane and 102.7 and 111.6 $\mu g m^{-3}$ in Demirhanlar sampling points, which were determined during the whole period, that caused from the partial time activities specific to those days in the region. Although the first unit of the thermal power plant started its operations in April 2015 and the second unit in February 2016, high values were generally determined especially in summer due to construction and other coal extraction materials in the region and activities related to their transportation.

Within the scope of the Regulation on Air Quality Assessment and Management (AQAMR, 2008), daily limit values starting from 100 $\mu g m^{-3}$ in 2013 and gradually decreasing and 50 $\mu g m^{-3}$ for 2019 were determined. Although it does not seem to provide limit values from time to time at some points during the whole period, the values obtained include only daily values. Since sequential continuous measurement results are needed to compare with the limit values in the regulation, the obtained daily values every three months are not compared with the regulation limit values.

As given Table 2, 36.5; 37.6; 42.7 and 38.7 $\mu g m^{-3}$ average values of sampling points were close to each other. Also, obtained mean values of before installation as 27.9; 29.8; 20.7 and 26.9 $\mu g m^{-3}$ were very close all sampling points. Otherwise, higher values after installation were obtained as 40.5; 41.3; 53.1 and 44.3 $\mu g m^{-3}$ compared before installation all points. It clearly shows that the effect of activities in the region on PM_{10} . When the statistical data of the measurements are examined, it is seen that the high standard deviation values at each point result from the significant differences between PM_{10} values as a result of the activities in the region at different places and at different times.

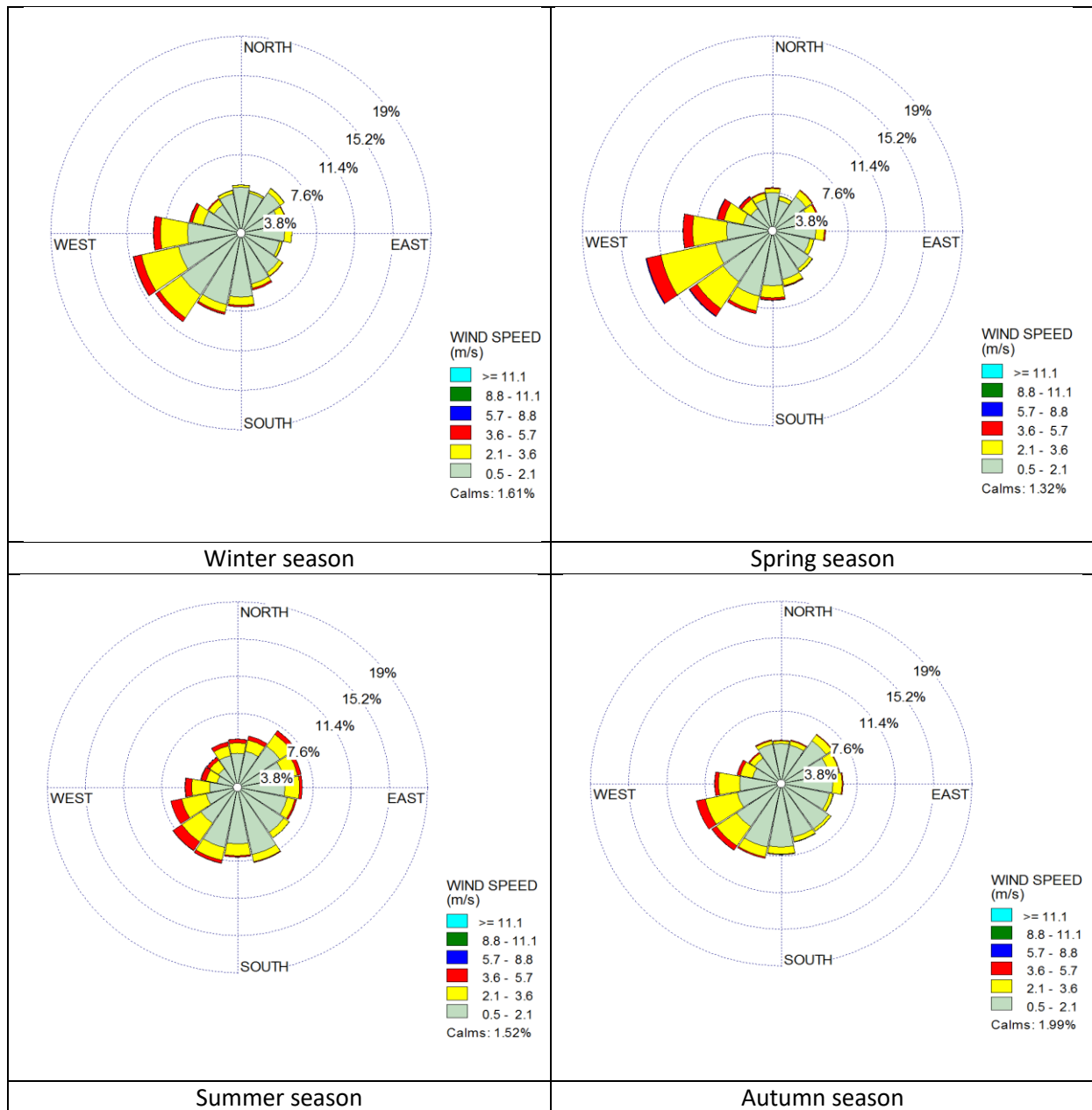


Figure 3. Seasonal wind roses of the nearest Bolu station

Table 2. Changes of PM₁₀ values before and after installation of power plant

	Sampling points ($\mu\text{g m}^{-3}$)			
	Bolucekova	Catak	Misafirhane	Demirhanlar
Sample Number	25	25	25	25
Mean values of before power plant installation	27.9	29.8	20.7	26.9
Mean values of after power plant installation	40.5	41.3	53.1	44.3
Mean values of all periods	36.5	37.6	42.7	38.7
Maximum values	102.6	66.9	166.2	111.6
Minimum values	2.3	13.2	1.9	2.4
Standard deviation	19.6	15.5	26.1	25.6

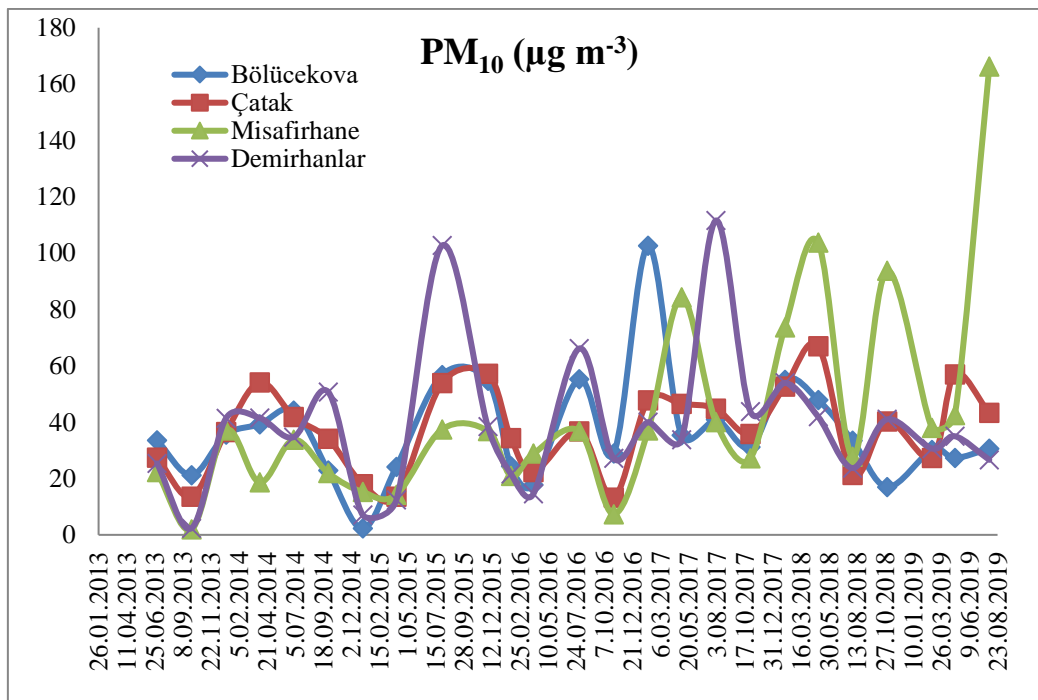


Figure 4. Temporal distribution of PM₁₀ results

3.2. Spatial and temporal changes of deposited dust concentrations

The temporal variation of deposited dust results at all points in the region is given in Figure 5. Table 3 shows the average values of the deposited dust values during the measurement period by years, and Table 4 shows the average values before and after the installation. When Figure 5 is examined, close values were determined at all sampling points, while high values were found from time to time in Bolucekova 2013-2016 period and Misafirhane point in 2017-2019 period. These results mainly show that the activities of the region have changed periodically.

The highest deposited dust concentrations were obtained 474.6 $\text{mg m}^{-2}\text{day}^{-1}$ and Bolucekova in November 2016, 442.7 $\text{mg m}^{-2}\text{day}^{-1}$ and April 2019 at Misafirhane. Before installation of power plant obtained values of 174.2 $\text{mg m}^{-2}\text{day}^{-1}$ at Misafirhane point in July 2013 and 227.0 $\text{mg m}^{-2}\text{day}^{-1}$ at the Bolucekova point in September 2013 show that the infrastructure (worker shelter, etc.) and power plant

construction activities in the region affect these result. Furthermore, the values of 301.0 and 382.7 mg m⁻² day⁻¹ obtained in May and August 2015 at Bolucekova point and 474.6 mg m⁻² day⁻¹ in November 2016, respectively, indicate that infrastructure activities may be performed in that region.

When the annual averages of the deposited dust values in Table 3 are examined, higher values were determined in Bolucekova in 2013, 2014, 2015, 2016 and 2017 compared to other points and it is considered that the facilities infrastructure and construction activities and these activities are close to Bolucekova. Also, higher values were obtained in Misafirhane points in 2018 and 2019 compared to other points. Especially in 2018 and 2019, intensive activities and storage area activities in Misafirhane region caused high results.

Besides, the results of deposited dust compared to the 210 mg m⁻² day⁻¹ limit value that given Regulation of Industrial Air Pollution Control (RIAPC, 2009) and covering the years 2014-2019, only Misafirhane mean value was obtained above the limit value in 2019.

Table 3. Annual averages of deposited dust values

Year	Sampling Points			
	Bolucekova (mg m ⁻² day ⁻¹)	Catak (mg m ⁻² day ⁻¹)	Misafirhane (mg m ⁻² day ⁻¹)	Demirhanlar (mg m ⁻² day ⁻¹)
2013	101.2	44.8	76.3	44.4
2014	42.2	29.5	24.4	28.0
2015	90.3	24.9	15.6	21.7
2016	75.2	28.8	28.9	22.4
2017	54.8	31.1	48.3	22.8
2018	84.4	58.6	163.0	44.8
2019	61.4	37.0	282.7	31.0

The mean values of deposited dust at each sampling point in Table 4 are given before and after installation of the power plant. The values of 70.8; 35.6; 79.5 and 29.4 mg m⁻² day⁻¹ were obtained at Bolucekova, Catak, Misafirhane, and Demirhanlar sampling points, respectively. Before the installation of power plant for Bolucekova, Catak, Misafirhane, and Demirhanlar, 53.9; 29.8; 35.4 and 29.4 mg m⁻² day⁻¹ values were determined, while after the installation of power plant covering after April 2015, 77.7; 37.9; 97.7 and 29.3 mg m⁻² day⁻¹ values were measured.

Table 4. Changes of deposited dust values before and after installation of power plant

	Sampling points ($\text{mg m}^{-2} \text{day}^{-1}$)			
	Boluçekova	Catak	Misafirhane	Demirhanlar
Sample Number	72	72	72	72
Mean values of before power plant installation	53.9	29.8	35.4	29.4
Mean values of after power plant installation	77.7	37.9	97.7	29.3
Mean values of all periods	70.8	35.6	79.5	29.4
Maximum values	474.6	151.2	442.7	91.0
Minimum values	10.7	1.7	0.5	2.1
Standard deviation	78.7	28.5	104.4	23.4

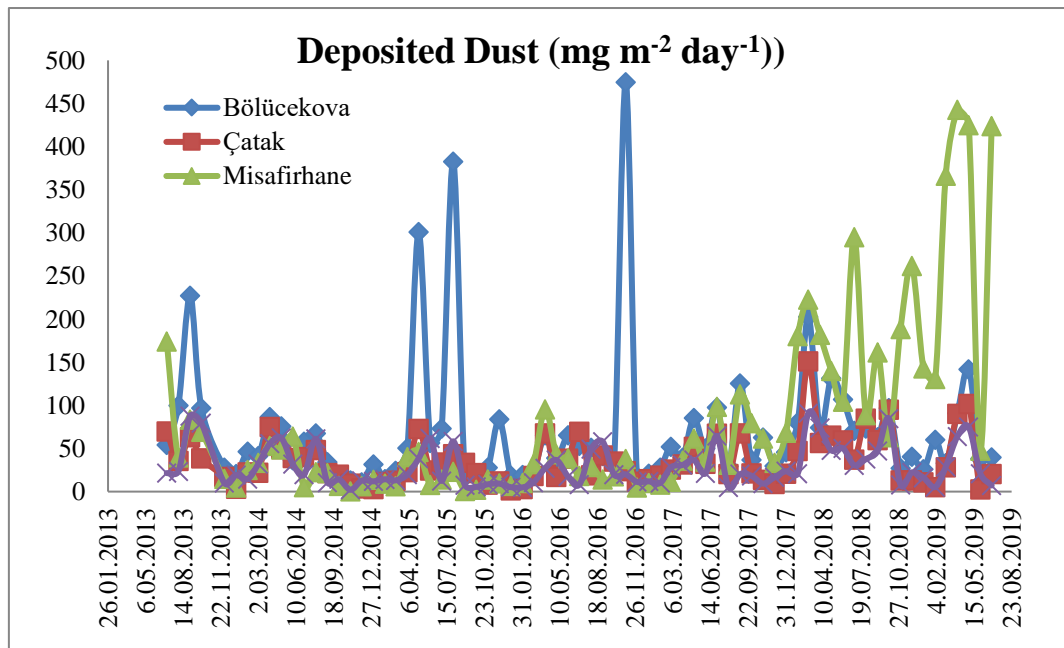


Figure 5. Temporal distribution of deposited dust results

4. Conclusions

The PM_{10} results indicate that all sampling points are affected by the industrial activities carried out in the region for both times (before and after installation of the power plant) at the same rate. On the other hand, Boluçekova sampling point is the most affected by deposited dust emissions before the power installation, while Misafirhane is the most affected after the power installation. The emissions sources are panel a coal operation area (from 2006) and rust casting area A (from 2013) in before installation time. In addition, industrial activities were carried out near the Misafirhane sampling point. Although the necessary measures have been taken to reduce the emissions from the stacks in the thermal power plant activity areas, other sources of non-flue emissions such as coal extraction, ash storage, dumpsite, limestone operation can cause major problems in the region. Only the maximum possible measures must be taken to prevent such emissions while carrying out these activities. For this purpose, coal storage areas should be covered to take into account the prevailing wind direction as much as possible, control



of these areas with automatic spraying-irrigation systems, taking necessary precautions in vehicles during filling-transporting-unloading activities will help prevent non-flue dust emissions in the region to reach residential areas.

5. References

- AQAMR, 2008. Air Quality Assessment and Management Regulation (Hava Kalitesi Değerlendirme ve Yönetimi Yönetmeliği), 26898 Official Journal, 06.08.2008.
- ENRM, 2016. Activity Report 2016, Energy and Natural Resources Minister.
- EPA, 2014. Reference News release: US Settlement with Michigan Utility to reduce emissions at its coal-fired power plants, fund projects to benefit Environment and communities.
- EUAS, 2016. Sector Report 2016.
- IEEE, 2010. Particulate matter emissions from a coal-fired power plant.
- PGT, 2019. Power Generation Technologies, Coal-fired power plants, 33-70.
- RIAPC, 2009, Regulation of Industrial Air Pollution Control (8. Sanayi Kaynaklı Hava Kirliliğinin Kontrolü Yönetmeliği), Ministry of Environment and Urbanisation, Republic of Turkey 27277 Official Journal.
- Sardar, S.B., Geller, M.D., Sioutas, C., Solomon, P.A. 2006. Development and evaluation of a high-volume dichotomous sampler for chemical speciation of coarse and fine particles. *Journal of Aerosol Science*. 37, 11, 1455-1466.
- Zhao, Y; Wang, S; Duan, L; Lei, Y; Cao, P; Hao, J, 2008. Primary air pollutant emissions of coal-fired power plants in China: Current status and future prediction. *Atmospheric Environment*, 42, 8442-8452.

Indoor air VOC levels associated with the use of bleach containing toilet-bowl cleaners and the effect of ventilation

Ilknur Ayri¹, Mesut Genisoglu¹, Handan Gaygisiz², Aysun Sofuoglu³ and Sait C. Sofuoglu¹

¹ Izmir Institute of Technology, Department of Environmental Engineering, Gulbahce, Urla, 35430, Izmir, Turkey

²Izmir Institute of Technology, Environmental Research Center, Gulbahce, Urla, 35430, Izmir, Turkey

³Izmir Institute of Technology, Department of Chemical Engineering, Gulbahce, Urla, 35430, Izmir, Turkey

cemilsofuglu@iyte.edu.tr

Abstract. Household cleaning products are sources of volatile organic compounds (VOCs). Bleach (NaOCl) containing products are a special case because reactions occur between chloride and their organic content such as surfactants, perfumes, etc. generating VOCs, mainly chloroform and carbon tetrachloride during shelf life in the product. Moreover, reactions with organic matter in water could result in their generation during use. Ventilation rate in toilets/bathrooms may be the determining factor along with emission rates if the generated VOCs would reach health threatening indoor air concentrations. Some types of drop-in or hanging toilet-bowl cleaners that contain bleach as a disinfectant and deodorant are such products. In this study; we purchased these products from supermarkets to determine potential chloroform and carbon tetrachloride emission. Experiments were conducted in 20-mL head-space vials by placing 1 g of sample. Solid-phase micro extraction with polydimethylsiloxane fiber was used for adsorption of VOCs from the headspace, and analyzed using GC-MS. Concentrations determined for 1 gram of sample (in 2 mL water for water contact samples) in the headspace vials were upscaled to actual product weights in 1.6 m³, 8.9 m³, and 18 m³ room volumes and for ventilation rates of 0.5 h⁻¹, 25.2 m³/h, 54 m³/h, and 72 m³/h for lifetimes specific to each product. Then, modelled their indoor air concentrations with various ventilation rates, during use to determine occupant exposure concentrations in various sized toilet/bathrooms. The estimated bathroom indoor air concentrations reach levels that may result in above acceptable health risks associated with use of some toilet-bowl cleaners. The use of certain products may produce carcinogenic risks above the acceptable risk level exceeding one-in-a-hundred thousand, with insufficient ventilation.

Keywords: Indoor air quality, Carbon tetrachloride, Chloroform, Emission, Ventilation, Toilet cleaning products.

1. Introduction

Contemporary people spend majority of their time indoors. Therefore, exposure to pollutants in indoor environments increases, and leads to adverse health effects (Shi et al., 2018). Volatile organic compounds (VOCs) and semi-VOCs are among the most common pollutants detected in indoor air and dust samples worldwide (Kishi et al., 2018). Cleaning is an important human activity that aims to promote hygiene, aesthetics, and material protection. In the United States, three million people with a total working population of 128 million are employed in various cleaner positions (Nazaroff et al., 2004).

Although cleanliness has undeniable benefits, there are health risks associated with the use of some cleaning products. Concerns are related to the fact that these products contain volatile organic compounds (VOCs) that contribute to urban or regional photochemical smog and may form reactions to support their formation in addition to having chronic-toxic and/or carcinogenic effects (Ly-Verdú, 2004; Odabasi et al., 2014).

Studies conducted by Odabasi (Odabasi, 2008) and Odabasi et al. (Odabasi et al., 2014) have shown that the use of chlorine bleach-containing household products result in significant indoor halogenated VOC concentrations. Many household cleaning products such as bleaches, mildew stain removers, toilet cleaners, cleaning sprays, gels, and scouring powders contain sodium hypochlorite (NaOCl, ~5%) as a disinfectant. Bleach can react with organic matters, generating VOCs (Odabasi, 2008).

Exposure to these substances is associated with many health effects. Symptoms like eye, nose, throat, and skin irritation, headache, dizziness, nausea, and effects on liver, kidney, and nervous system are among the health effects of VOCs (Odabasi, 2008). In order to alleviate these health effects, the exposure to these substances must be reduced by removing them from the indoor air.

Ventilation is an efficient method of reducing indoor air pollutant concentrations, and considered an important component of a healthy house. Ventilation is the means by which fresh air enters and circulates into the building, and the contaminated or old air is removed or diluted. The main purpose of ventilation is to create the most suitable conditions for the people living or working, considering health, comfort and productivity in terms of indoor air quality and thermal comfort. Specifically, indoor air concentration of a pollutant with a certain emission rate depends on the ventilation rate (Dimitroulopoulou, 2012). Residential bathroom exhaust is used to remove moisture, and eliminate odors emanating from bathrooms, lavatories, toilets, and other rooms containing similar sources of contaminants (Yin et al., 2016). As the ventilation rate increases, the concentration of the pollutants are reduced (Dimitroulopoulou, 2012). In relation, there is evidence that low air exchange rates may adversely affect human health (Hou et al., 2018).

Household cleaning products are sources of VOCs (Odabasi et al., 2014; Odabasi, 2008). While these products are used intermittently, automatic toilet-bowl cleaners may be continuous sources, especially if they contain bleach. The aim of this study is to estimate toilet/bathroom indoor air chloroform and carbon tetrachloride concentrations due to the use of automatic toilet-bowl cleaners, to determine the effect of ventilation, and to estimate associated cancer risk levels.

2. Material and Methods

2.1. Experimental

Various toilet-bowl cleaners were purchased from Turkey, Europe, and USA. All products contained hypochlorite as disinfectant. The experiments were conducted in 20-mL headspace vials with septum-lined caps. One gram of a sample was placed in two vials, one with 2 mL water and one without water. All the experiments were run in duplicate. Solid phase microextraction (SPME with polydimethylsiloxane fiber) was used for adsorption of VOCs from the headspace for analysis using GC/MS. After samples were kept at room temperature for 30 minutes, the fiber was injected. It was kept in for 30 minutes before it was injected into a GC (Agilent 6890N) equipped with a mass selective detector (Agilent 5973N MSD). The chromatographic column was HP5-MS (30 m, 0.25 mm, 0.25 μ m) and the carrier gas was helium at 1 mL min⁻¹ flow rate. Injection mode was splitless. The inlet temperature was 40 °C. Oven temperature program was: hold for 5 min at 40 °C, ramp to 230 at 5 °C min⁻¹, hold 5 min. Ionization mode of the MS was electron impact (EI).

2.2. Modeling

Indoor air concentrations of chloroform and carbon tetrachloride were modeled for the use of automatic toilet-bowl cleaners in toilets and bathrooms. The measured headspace concentrations were converted to toilet/bathroom indoor air concentrations. Emissions that may occur due to the use of these products in various room volumes and the concentrations that may remain in the rooms at various ventilation rates were estimated by modeling.

Different indoor air chloroform and carbon tetrachloride concentrations in various room volumes were estimated using Eq 1. Concentrations determined for 1 gram of sample (in 2 mL water for water contact samples) in the headspace vials were upscaled to actual product weights in 1.6 m³, 8.9 m³, and 18 m³ room volumes (Mui et al., 2017) and for ventilation rates of 0.5 h⁻¹, 25.2 m³/h, 54 m³/h, and 72 m³/h (Ye et al., 2017) for lifetimes specific to each product (Liang et al., 2013). In order to calculate indoor air concentration assumptions of complete mixing, constant ventilation and emission rates, and zero outdoor concentration were made.

$$V (dC_{in}(t))/dt = Q (C_{out} - C_{in}(t)) \quad (1)$$

where, V is volume of the room (m³), t is time (h), $C_{in}(t)$ is indoor VOC concentration at time t (mg/m³), Q is ventilation rate (m³/h), C_{out} is outdoor VOC concentration (mg/m³), and E is the emission rate of toilet-bowl cleaners (mg/h) obtained from the headspace experiments.

3. Results and Discussion

3.1. Concentrations and Effect of Ventilation Rate

The use Fig. 1, Fig. 2, and Fig. 3 depict variation in chloroform and carbon tetrachloride concentrations with increasing ventilation rate. Use of the products in small volume toilets results in higher exposures. The estimated indoor air concentration levels are lower than those reported in the literature (Odabasi, 2008; Zhou et al., 2011; Odabasi et al., 2014) probably because the reported concentrations are generally a result of cumulative effect of various emission sources indoors. In this study, Q1-Q3 range for the chloroform concentrations for drop-in and hanging automatic toilet-bowl cleaning products was <0.1 – 20 µg/m³, Q1-Q3 for carbon tetrachloride was <0.001 – 10 µg/m³, while the 95th percentile values reached two orders of magnitude higher levels. The mainly lower concentrations obtained in this study are probably due to the small weights of the considered products that last for long periods of time in use such as 45 to 357 days, in contrast to the larger sizes of household cleaning products used in all areas of the house that would result in higher formation during shelf life and during use (Odabasi, 2008; Odabasi et al., 2014). The high levels of 95th percentile values, however, may indicate variability in products in terms of potential to emit chloroform and carbon tetrachloride.

Odabasi (2008) has examined the formation of VOCs resulting from the use of bleach-containing cleaning products in bathroom, toilet, and hallways. It was reported that chloroform and carbon tetrachloride concentrations increased due to the use of these products. During application of these products, chloroform concentrations were reported to vary from 2.9 µg/m³ to 24.6 µg/m³, whereas the range was 0.25 µg/m³ to 459 µg/m³ for carbon tetrachloride. Later, Odabasi et al. (2014) have investigated formation of halogenated VOCs resulting from the use of various bleach-containing cleaning products: plain, fragranced, and surfactant added. It was reported that chloroform and carbon tetrachloride concentrations were higher for higher organic-content products, i.e. fragrance and surfactant added ones. The highest chloroform concentration was reported to be 154×10³ µg/m³, while the lowest concentration was reported to be 80 µg/m³. For carbon tetrachloride, these concentrations were reported to range from 169×10³ µg/m³ to 10 µg/m³.

The highest chloroform concentration of 218 $\mu\text{g}/\text{m}^3$ estimated in the lowest room volume of 1.6 $\mu\text{g}/\text{m}^3$ with the lowest ventilation rate of 0.5 h^{-1} , decreased to 188 $\mu\text{g}/\text{m}^3$ with the highest ventilation rate of 72 m^3/h . The corresponding carbon tetrachloride concentrations were $1.12 \times 10^3 \mu\text{g}/\text{m}^3$ and $96.8 \mu\text{g}/\text{m}^3$.

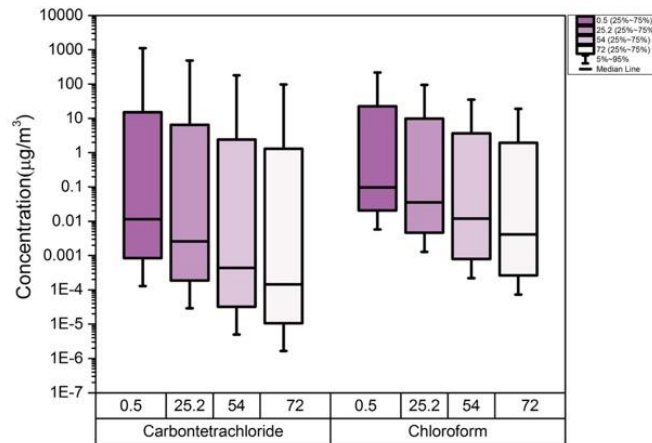


Figure 1. Chloroform and carbon tetrachloride concentrations in 1.6 m^3 bathroom/toilet with different ventilation rates.

In bathroom/toilet volumes of 8.9 m^3 and 18 m^3 , the highest chloroform concentrations were 40.2 $\mu\text{g}/\text{m}^3$ and 19.9 $\mu\text{g}/\text{m}^3$, and the concentrations of carbon tetrachloride were 207 $\mu\text{g}/\text{m}^3$ and 102 $\mu\text{g}/\text{m}^3$, respectively. Using the maximum ventilation rate of 72 m^3/h , the 45 % and 67 % of chloroform and carbon tetrachloride concentrations in the room is removed.

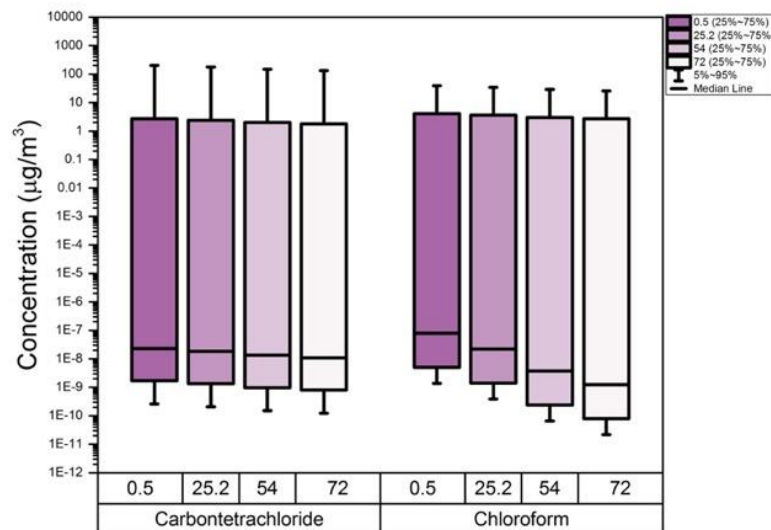


Figure 2. Chloroform and carbon tetrachloride concentration in 8.9 m^3 bathroom/toilet with different ventilation rates.

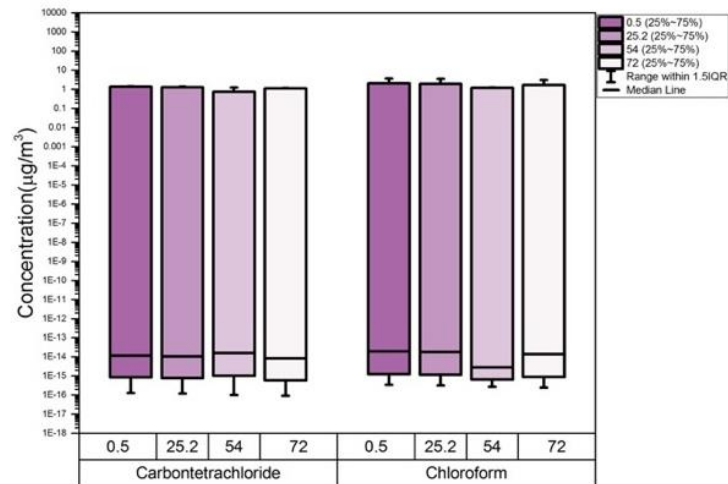


Figure 3. Chloroform and carbon tetrachloride concentration in 18 m³ bathroom/toilet with different ventilation rates.

3.2. Carcinogenic risks for inhalation exposure

In this study, cancer risk assessment for inhalation exposure was conducted for the indoor environment for three different room volumes and four different ventilation rates. Inhalation exposure was estimated using Equation 2. Carcinogenic risk value was estimated using Equation 3.

$$CDI = (C \times IR \times ET \times EF \times ED) / (BW \times AT) \quad (2)$$

$$Risk = CDI \times SF \quad (3)$$

where C is VOC indoor air concentration (mg/m³); IR is inhalation rate (m³/h), ET is exposure time (h/day), EF exposure frequency (days/year), ED is exposure duration (years), BW is body weight (kg), and AT average lifetime.

SF is a toxicological risk factor ((mg/kg/day)⁻¹) published in Integrated Risk Information System of the US Environmental Protection Agency. Activity level for toilet use was considered as sedentary passive, and corresponding mean and 95th percentile IR, ET, EF, and BW values were taken from Exposure Factors Handbook (Moya et al., 2011). ED and AT were considered equal to lifetime, canceling each other out.

Risk levels in this study are calculated as mean and 95th percentile values. According to the obtained values, the lowest risk value was obtained in the largest room volume and the highest ventilation rate, while the highest value was obtained in the lowest volume and the lowest ventilation rate. The lowest and highest mean and 95th percentile risk values in all products are given in Table 1.

Carbon tetrachloride levels exceeded 0.17 µg/m³ several orders of magnitude, which corresponds to de Minimis carcinogenic risk level of 10⁻⁶. Chloroform levels, also, exceeded 0.4 µg/m³ a few orders of magnitude, which corresponds to 10⁻⁵ carcinogenic risk in all room sizes and ventilation rates for the highest-emitting product, while they all stayed below 0.04 µg/m³ that corresponds to 10⁻⁶ for the lowest-emission product.

Table 1. The lowest - highest mean and 95th percentage risk values for chloroform (CF) and carbon tetrachloride (CTC).

VOC	Bathroom volume (m ³)	Ventilation Rate (m ³ /h)	Risk Mean	Risk 95 th Percentile
CF	18	72	4.97×10^{-7}	8.35×10^{-7}
CTC	18	72	2.26×10^{-5}	3.26×10^{-5}
CF	1.6	0.8	6.70×10^{-6}	1.14×10^{-5}
CTC	1.6	0.8	3.08×10^{-4}	4.45×10^{-4}

4. Conclusion

In this study, toilet/bathroom indoor air concentrations of chloroform and carbon tetrachloride that would occur as a result of the use of automatic toilet-bowl cleaners were investigated. Using mathematical modeling, the concentrations were calculated for 0.5 h⁻¹, 25.2 m³/h, 54 m³/h, and 72 m³/h ventilation rates, and 1.6 m³, 8.9 m³, and 18 m³ room volumes. More than 60% of chloroform and carbon tetrachloride were removed at the highest ventilation rate in the highest volume. Carcinogenic risk assessment showed that the risks range from below acceptable risk level of one-in-a-million to >10⁻⁵ for chloroform and >10⁻⁴ for carbon tetrachloride. Consequently, with insufficient ventilation, the use of certain products may produce considerable carcinogenic risks.

5. References

- Dimitroulopoulou, C., 2012. Ventilation in European dwellings: A review. *Building and Environment*, 47, 109-125.
- Hou, J., Zhang, Y., Sun, Y., Wang, P., Zhang, Q., Kong, X., & Sundell, J., 2018. Air change rates at night in northeast Chinese homes. *Building and Environment*, 132, 273-281.
- Kishi, R., Ketema, R. M., Bamai, Y. A., Araki, A., Kawai, T., Tsuboi, T., & Saito, T., 2018. Indoor environmental pollutants and their association with sick house syndrome among adults and children in elementary school. *Building and Environment*, 136, 293-301.
- Liang, W., & Yang, X., 2013. Indoor formaldehyde in real buildings: Emission source identification, overall emission rate estimation, concentration increase and decay patterns. *Building and Environment*, 69, 114-120.
- Ly-Verdú, S., Esteve-Turrillas, F. A., Pastor, A., & de la Guardia, M., 2010. Determination of volatile organic compounds in contaminated air using semipermeable membrane devices. *Talanta*, 80, 2041-2048.
- Moya, J., Phillips, L., Schuda, L., Wood, P., Diaz, A., Lee, R., & Chapman, K., 2011. Exposure factors handbook: 2011 edition. US Environmental Protection Agency.
- Mui, K. W., Wong, L. T., Yu, H. C., Cheung, C. T., & Li, N., 2017. Exhaust ventilation performance in residential washrooms for bioaerosol particle removal after water closet flushing. *Building Services Engineering Research and Technology*, 38, 32-46.
- Nazaroff, W. W., & Weschler, C. J., 2004. Cleaning products and air fresheners: exposure to primary and secondary air pollutants. *Atmospheric Environment*, 38, 2841-2865.
- Odabasi, M., 2008. Halogenated volatile organic compounds from the use of chlorine-bleach-containing household products. *Environmental Science & Technology*, 42, 1445-1451.



Odabasi, M., Elbir, T., Dumanoglu, Y., & Sofuoglu, S.C., 2014. Halogenated volatile organic compounds in chlorine-bleach-containing household products and implications for their use. *Atmospheric Environment*, 92, 376-383.

Shi, Y., & Li, X., 2018. A study on variation laws of infiltration rate with mechanical ventilation rate in a room. *Building and Environment*, 143, 269-279.

Ye, W., Zhang, X., Gao, J., Cao, G., Zhou, X., & Su, X., 2017. Indoor air pollutants, ventilation rate determinants and potential control strategies in Chinese dwellings: A literature review. *Science of the Total Environment*, 586, 696-729.

Yin, P., Pate, M. B., & Sweeney, J. F., 2016. The impact of operating pressure on residential bathroom exhaust fan performance. *Journal of Building Engineering*, 6, 163-172.

Zhou, J., You, Y., Bai, Z., Hu, Y., Zhang, J., & Zhang, N., 2011. Health risk assessment of personal inhalation exposure to volatile organic compounds in Tianjin, China. *Science of the Total Environment*, 409, 452-459.

Acknowledgments

We thank IYTE Research Fund (Grant #2016-IYTE-34 and #2017-IYTE-06) for financial support. We also thank Dr. Figen Korel, Dr. Mustafa Odabasi, Dr. Yetkin Dumanoglu for help in analytical work. Finally, we thank Mr. Sencer Sofuoglu, Dr. Guleda Engin, Ms. Burcak Ucock for their contribution in obtaining the abroad product samples.

Black carbon evaluation in an urban side of Istanbul atmosphere during spring and summer seasons

S. Levent Kuzu¹, Elif Yavuz¹, Ezgi Akyuz², Arslan Saral¹, Bulent Akkoyunlu³ and Huseyin Ozdemir⁴

¹Yildiz Technical University, Civil Engineering Faculty, Environmental Engineering Department, 34220, Davutpasa-Esenler, Istanbul, Turkey

²Istanbul Technical University, Eurasia Institute of Earth Sciences, Istanbul

³Department of Physics, Marmara University, 34722, Goztepe, İstanbul, Turkey

⁴Atmospheric Modeling Section, Department of Environmental Science, Aarhus University, Frederiksborgvej 399, Roskilde, Denmark

skuzu@yildiz.edu.tr

Abstract. This study was carried out at Yildiz Technical University Davutpasa Campus where is located between crowded districts of Istanbul. Main sources around the campus are Central Coach Station of Istanbul, residential buildings, small scale industrial facilities, and O-1 and O-2 highway connection. The objective of the study is to relate black carbon levels with conventional air pollutant parameters. Furthermore, determine potential sources using meteorological parameters. We monitored black carbon continuously by an aethalometer at rooftop of the Civil Engineering Faculty, typically 10 m above ground-level. Meteorological data are recorded by a Davis Vantage Pro-2 automatic weather station on the same building. Conventional ambient parameters are NO, NO₂, SO₂, PM_{2.5}, and PM₁₀. These parameters are gathered from monitoring station which is approximately 900 m away from black carbon sampling station. The station is operated by Istanbul Metropolitan Municipality. The average black carbon concentration was 2121±938 ng/m³. Spring concentration was 2217±940 ng/m³, whilst summer concentration was 1936±923 ng/m³. Less average concentration and variability was observed during summer season. The reason is attributed to decreased anthropogenic activities and increased boundary layer height. Correlation between black carbon concentrations and conventional parameters were investigated. Pearson correlation coefficients suggested that there was strong correlation (over 0.6) between BC and PM₁₀, PM_{2.5}, and NO₂. The correlation with the remaining parameters were moderate (between 0.3 and 0.6). The correlation of black carbon with PM_{2.5} was slightly higher than PM₁₀. Association of black carbon with meteorological parameters showed possible source regions and transportation patterns. Elevated black carbon concentrations were observed when the wind blew from north direction. Although studies with black carbon measurements are scarce in Istanbul, we discussed the study outcomes with the available data for Istanbul. The black carbon concentrations of this study are considerably lower than in previous studies. Temporal and spatial differences caused such concentration differences. This study fills a gap for a location that is relatively away from traffic sources when compared to relevant studies in Istanbul.

Keywords: Black carbon, Conventional pollutants, Meteorological data, Correlation.

1. Introduction

During the last two decades, urban air pollution has been recognized as one of the world's major environmental issues, particularly in megacities (Yusuf and Resosudarmo, 2009). Recently, air pollution

from megacities has attracted substantial scientific interest owing to their potential impact on regional and global climate (Duh et al., 2008; Favez et al., 2008).

Istanbul is the largest city of Turkey, with a population exceeding 15 million inhabitants (TUIK, 2018). Air pollution has been one of the main environmental problems in Istanbul where the formation and transport of pollutants are heavily influenced by the local meteorological and topographic characteristics (Tayanc, 2000). Increased levels of air pollutants in this area are the result of the rapid and uncontrolled growth in urbanization, industrialization, transportation and high concentrations of pollutants from domestic heating, industrial and road traffic activities (Tayanc, 2000). Historical pollutants have been mainly PM, SO₂, and NO_x in Istanbul (Akkoyunlu, Erturk, 2002). However, levels of air pollution have decreased substantially in recent years owing to fuel shift in domestic heating (Akkoyunlu, Erturk, 2002). Nowadays, main issue in atmospheric composition in crowded cities are PM and NO_x (Kuzu, 2019; Kumar, 2015).

Atmospheric aerosol particles play an important role in a number of environmental topics, such as the radiation transfer of the Earth's atmosphere and the hydrological cycle, as well as air quality, and thus have a substantial impact on the biosphere, including human health (Pope and Dockery, 2006; Andreae and Ramanathan, 2013). Atmospheric aerosol, especially in urban areas, contains a significant fraction of carbonaceous material. Atmospheric particulate carbon is comprised of a complex mixture of substances containing carbon atoms, usually being classified in two main fractions, black carbon (BC) and organic carbon (OC). Black carbon, also known as elemental carbon, has a graphitic-like structure and is black. The distinction between BC and EC is made by the measurement method used. Whereas EC is measured through thermal methods, BC is measured through optical techniques (Hitzenberger et al., 2006).

Carbonaceous aerosols constituting of organic carbon (OC) and elemental carbon (EC) contributes about 20–70% of the aerosol mass loading over urban regions (Ram and Sarin, 2011; Aswini et al., 2019). As organic aerosol (OA) makes up 20-90 % of the total submicron particulate mass in the atmosphere (Kanakidou et al., 2005).

Black carbon is a global environmental problem that has negative implications for both human health and our climate. Inhalation of black carbon is associated with health problems including respiratory and cardiovascular disease, cancer, and even birth defects. Black carbon also contributes to climate change causing changes in patterns of rain and clouds. Black carbon aerosol (BC), a by-product of incomplete combustion carbonaceous matter (e.g. biomass and fossil fuel) is recognized as the third most important global warming agent after CO₂ and CH₄ (IPCC, 2013). For the period 1750–2011 based on emitted compounds (gases, aerosols or aerosol precursors), emissions of BC have a positive radiative forcing through aerosol–radiation interactions and BC on snow (IPCC, 2013). After a few days of staying and transporting in the atmosphere, BC generally deposits into soils and stores in the soil carbon pool for thousands of years (Gao et al., 2008; Lehndorff et al., 2014).

There are two studies which presents the measured BC aerosol concentrations in Istanbul in the open literature. The first study was carried out by Ozdemir et al. (2014), in which the spatial and temporal variability of BC levels in Istanbul was evaluated and its relationship with specific traffic conditions were investigated. In that study, highly time-resolved BC measurements was performed and indicated higher BC concentrations at the sites affected by heavy traffic than the urban background site. Generally high BC concentrations were observed during daytime and lower concentrations during the night-time, with differences in the timing and the intensity of morning and evening peaks.

The second study was carried out by Onat et al. (2019). Their study shows the measured results of personal exposures to UFP, BC, and PM_{2.5} in different transportation modes and routes, and the relationship between these exposures and meteorological factors. The pollutant concentrations in the

traffic environment is changeable. Travellers are exposed to these pollutants in different amounts during their commutes according to travel mode and route characteristics. The lowest and highest pollutant concentrations were measured in the car with windows closed and the car with windows open, respectively. They demonstrate that the pollutant concentrations measured at the stations were significantly correlated with in-vehicle concentrations for buses, metrobuses, and light rail. The ventilation within the vehicles affected pollutant concentrations, and the lowest pollutant concentrations were in the car with windows closed and the A/C on. For road transport, using the expressway decreased the per-kilometer pollutant exposure in dense traffic. Statistically significant correlations were detected between meteorological factors and pollutant concentrations. The seasonal statistically correlation results indicated that the relation between the meteorological variables and in-vehicle pollutant concentrations were variable with the seasonal differences.

In this study, we aimed to determine temporal BC levels at an urban area with a little traffic contribution. The characteristics of the study area is different from previous studies. We evaluated BC concentrations along with conventional parameters and meteorological datas in order to allocate their possible sources.

2. Material and methods

2.1. Measurement site description

Istanbul was Turkey's most populous city with 15 million people, accounting for 18.6 percent of the total population (TUIK, 2018). Yildiz Technical University Davutpasa Campus is located in Esenler district of Istanbul, Turkey and has an approximately 1,000,000 m² total area. Main sources around the campus are Central Coach Station of Istanbul, residential buildings, small scale industrial facilities, and O-1 and O-2 highway connection.

Samples of black carbon has been collected at rooftop of the Civil Engineering Faculty, typically 10 m above ground-level. Meteorological data are recorded by a Davis Vantage Pro-2 automatic weather station on the same building. Conventional ambient parameters (NO, NO₂, SO₂, PM_{2.5}, and PM₁₀) are gathered from monitoring station which is operated by Istanbul Metropolitan Municipality. The station is approximately 900 m away from black carbon sampling station (Figure 1).

2.2. Sampling

The Aethalometer™ is the foremost instrument for the real-time measurement of optically-absorbing 'Black' or 'Elemental' carbon aerosol particles. Aethalometers provide fully automatic, unattended operation. The sample is collected as a spot on a roll of quartz fibre filter tape. 'BC' is defined by 'blackness', an optical measurement. The Aethalometer uses a continuous filtration and optical measurement method to give a continuous readout of real-time data. We set the time base to 5 minutes for the desired data rate. The data is written to diskette; transmitted by the COM port; and produced as an analogue voltage. Sampling is optimal at air flow rates from 2 to 6 standard liters per minute.

The Aethalometer has a optical head unit which holds the filter in the passing air stream, while illuminating it from above and determining the intensity of light transmitted by means of photo detectors mounted below. The optical head contains the aerosol inlet, the optical source assembly, the light guides for the photo detectors, and the filter tape support.

The two photo detectors are mounted on the main circuit board together with all electronic components for power, control and for data conversion from analogue to digital signals. This board is powered by a supply that can operate from any line input voltage without switching.

The aethalometer offer the option of two sizes of aerosol collecting spot: the "High Sensitivity" inlet, with a circular sample collecting spot of area 0.5 cm², and the "Extended Range" inlet, with a rounded-

rectangular sample collecting spot of area 1.67 cm². The 'Extended Range' ('ER') inlet is recommended for general use in urban areas or other locations of moderate to high aerosol concentration, where time resolutions of 5 minutes are acceptable.

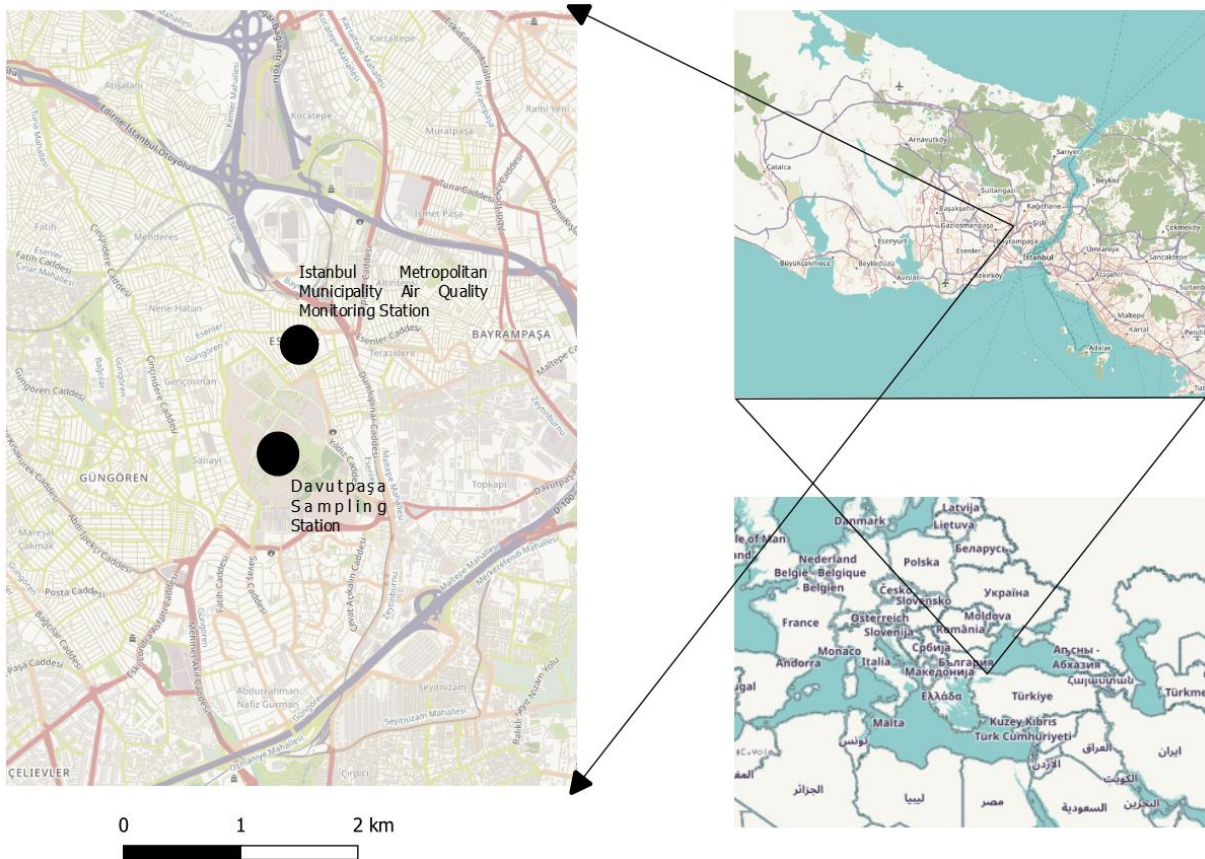


Figure 1. Location of the monitoring stations

The tape feeder has been specially designed to handle the quartz fibre material that is optimal for the black carbon measurement. It draws the 25-mm. wide tape from a supply spool mounted on the left side of the instrument. Each roll contains 15 meters length of tape, sufficient for approximately 1500 aerosol collection spots.

The front panel door covers the tape spools and optical head, the inner chassis panel with the data disk drive and control switches: the outer surface of the door holds the display screen and control keypad.

2.3. Calculations

The conditional probability function (CPF) is used as a result of correlating the changing wind directions of the point source additives with the pollutant concentration data (Wang et al., 2011). Equation 1 is used to calculate with this methodology.

$$CPF_{\Delta\theta} = \frac{m_{\Delta\theta}}{n_{\Delta\theta}} \quad (1)$$

In this equation; $m_{\Delta\theta}$ is the number of winds blowing from $\Delta\theta$ direction which have higher values than the selected criteria, $n_{\Delta\theta}$ is the total number of winds blowing from the direction written in subscript. In this study, we used a Davis Vantage Pro2 station that measures wind directions with 22.5°. Therefore,

calculations are performed on 16 different wind directions. The frequencies of the directions which are thought to be the means of transporting the pollutants are clarified in this way. Calm winds were omitted during the calculation. The upper 25% was chosen as the threshold value.

3. Results and discussion

3.1. Ambient concentrations

All air pollutant concentrations acquired during the study term is given in Figure 2. The values include NO, NO₂, NO_x, PM₁₀, PM_{2.5}, SO₂, BC concentrations between May 1, 2019 and July 15, 2019.

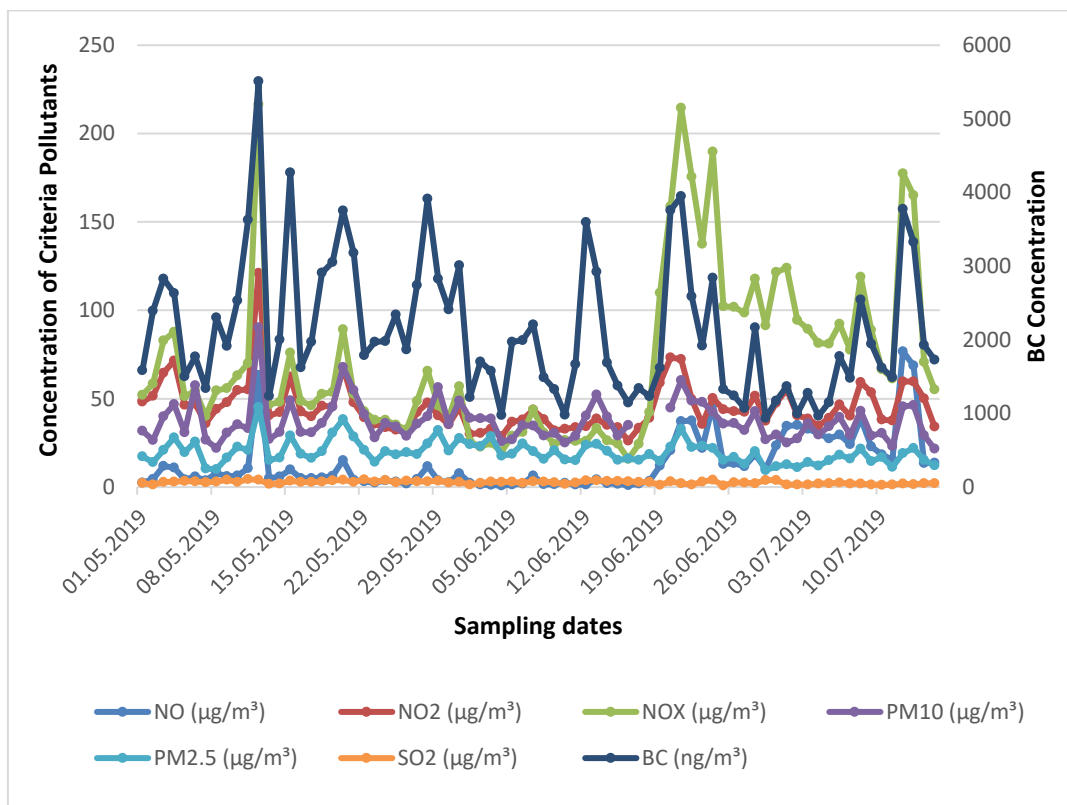


Figure 2. Ambient concentrations

The average PM₁₀ and PM_{2.5} concentrations were 37.2 and 19.7 µg/m³, respectively. PM_{2.5} constituted 53% of particles less than 10 µm. The common range for PM_{2.5}/PM₁₀ was reported to be between 0.4 and 0.8 (Pateraki et al, 2012). In another study, which was conducted at Davutpasa Campus the PM_{2.5}/PM₁₀ ratio was determined to be 0.75 (Kuzu and Saral, 2017). This outcome pointed out that the monitoring station in Esenler is more prone to resuspension of road dust than Davutpasa station. PM₁₀ concentrations exceeded the daily threshold limit, which is 50 µg/m³, 6 times during the spring sampling period, while only once during summer sampling period. The average BC concentration was 2121 ng/m³. It was 2217 ng/m³ during spring, whilst 1936 ng/m³ during summer sampling period. The average NO₂ and SO₂ concentrations were 45 and 2.7 µg/m³, respectively. Although average NO₂ concentration remained slightly lower than the threshold limit, the average SO₂ was notably lower than the threshold value.

3.2. Evaluation of air pollutants

In order to demonstrate the dependencies of various pollutants, a correlation was executed. We divided our data as spring and summer in order to differentiate the seasonal effects on BC concentrations. The Pearson's correlation coefficients are shown in Table 1 and Table 2 for spring and summer, respectively.

Table 1. Correlation of different pollutants during spring sampling

	NO	NO ₂	NO _x	PM ₁₀	PM _{2.5}	SO ₂	BC
NO	1						
NO ₂	0.913152	1					
NO _x	0.919424	0.957309	1				
PM ₁₀	0.708512	0.691667	0.659254	1			
PM _{2.5}	0.589068	0.587723	0.512301	0.918334	1		
SO ₂	0.253318	0.225066	0.167391	0.42701	0.411406	1	
BC	0.689265	0.732514	0.698208	0.708721	0.691681	0.466237	1

Table 2. Correlation of different pollutants during summer sampling

	NO	NO ₂	NO _x	PM ₁₀	PM _{2.5}	SO ₂	BC
NO	1						
NO ₂	0.581548	1					
NO _x	0.674706	0.73477	1				
PM ₁₀	0.522141	0.63451	0.836706	1			
PM _{2.5}	0.435828	0.670666	0.773902	0.932393	1		
SO ₂	-0.11313	-0.0824	0.210283	0.070136	0.012804	1	
BC	0.712466	0.801945	0.792333	0.774699	0.825615	-0.04957	1

The Pearson's correlation showed that the highest correlation was between BC and NO₂ during spring, whilst between BC and PM_{2.5} during summer. The weakest correlation was with SO₂ at both seasons. Even, a negative relation was observed between BC and SO₂ during summer. But it was not significant. Therefore, we can point out that SO₂ and BC does not seem to originate from the same source. based on the Pearson numbers, it is not easy to differentiate the strength of BC between PM_{2.5} and PM₁₀. Both have similar relations with BC. On the other hand, NO₂ has a more strong correlation than NO.

In order to determine geographical location of possible sources, we executed conditional probability function, namely CPF. The CPF plots are shown in Figure 3. Almost all species exhibited similar patterns. The north direction carried the most contaminated air masses for each of the measured pollutants. Central Coach Station of Istanbul and residential areas are present to the north direction of the monitoring sites. There was a little difference for NO_x from WNW direction. The winds from WNW did not carry elevated NO_x concentrations as with other remaining pollutants. Residential areas are present at that direction.

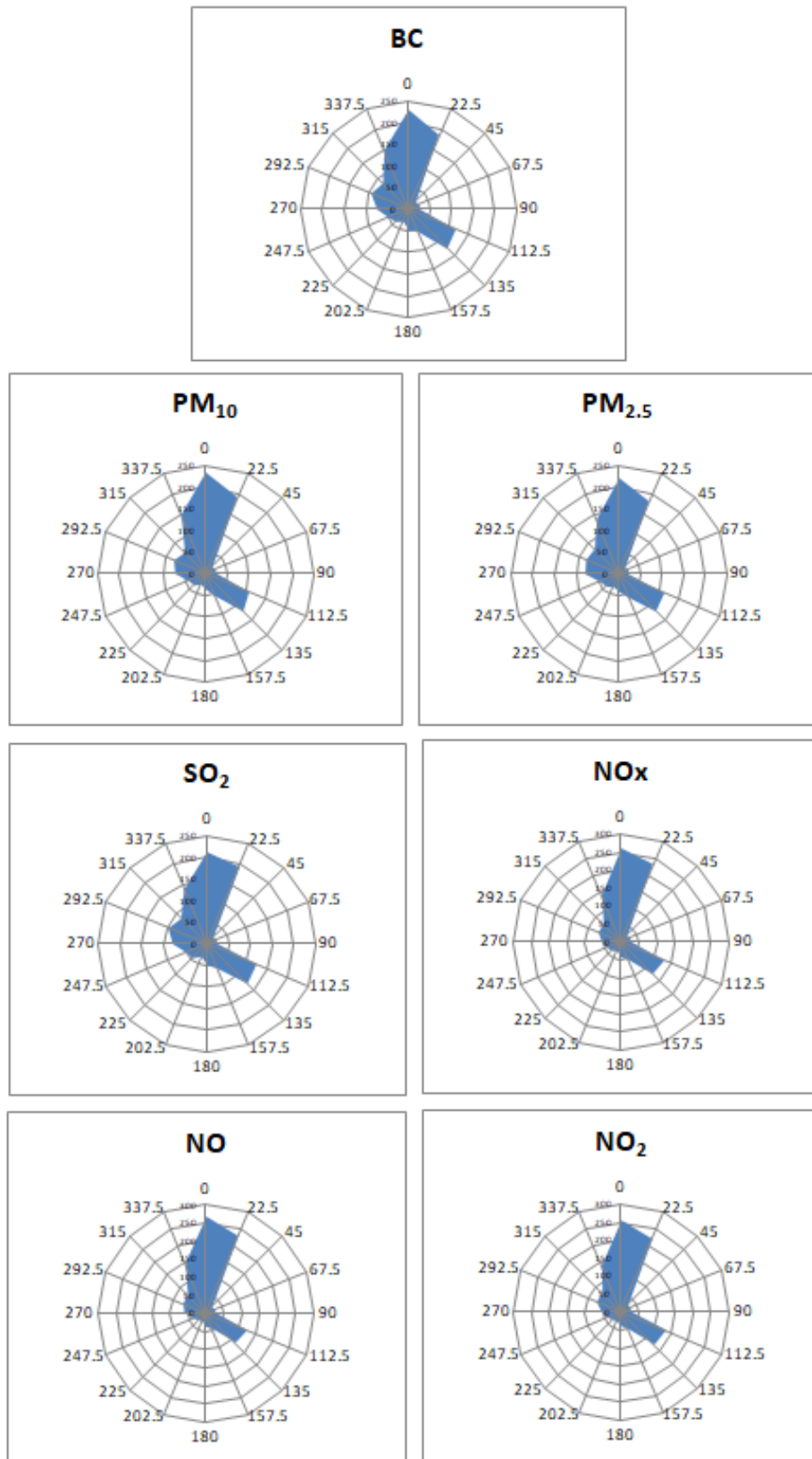


Figure 3. Conditional probability function of all measured species

4. Conclusion

In this study, BC concentrations were measured during summer and spring in an urban site of Istanbul. The average black carbon concentration was 2121 ± 938 ng/m³. Spring concentration was 2217 ± 940 ng/m³, whilst summer concentration was 1936 ± 923 ng/m³. Results of this study documented lower concentrations than previous studies in Istanbul. It is attributed to relatively being far from congested traffic, although traffic is still an important source for the sampling stations. But BC sampling station is present on a campus with higher vegetation cover than any urban side of Istanbul. This factor seemed to prevent achieving high BC concentrations. Although CPF results showed possible source regions for each pollutant, it did not serve accurate results to show the actual source. The authors propose using further detailed investigation methods in order to locate possible BC sources. Also, the temporal extent of the data needs to be extended.

5. References

- Akkoyunlu, A., Erturk, F. 2002. Evaluation of air pollution trends in Istanbul. *International journal of environment and pollution*. 18, 388-398.
- Andreae, M. O., Ramanathan, V., 2013. Climate's dark forcings. *Science*, 340, 280-281.
- Aswini, A. R., Hegde, P., Nair, P. R., Aryasree, S., 2019. Seasonal changes in carbonaceous aerosols over a tropical coastal location in response to meteorological processes. *Science of The Total Environment*. 656, 1261-1279.
- Duh, J. D., Shandas, V., Chang, H., George, L. A., 2008. Rates of urbanisation and the resiliency of air and water quality. *Science of the total environment*. 400, 238-256.
- Favez, O., Sciare, J., Cachier, H., Alfaro, S. C., Abdelwahab, M. M., 2008. Significant formation of water-insoluble secondary organic aerosols in semi-arid urban environment. *Geophysical Research Letters*. 35, 15.
- Gao, C., Liu, H., Cong, J., Han, D., Zhao, W., Lin, Q., Wang, G., 2018. Historical sources of black carbon identified by PAHs and $\delta^{13}C$ in Sanjiang Plain of Northeastern China. *Atmospheric environment*. 181, 61-69.
- Hitzenberger, R., Petzold, A., Bauer, H., Ctyroky, P., Pouresmaeil, P., Laskus, L., Puxbaum, H., 2006. Intercomparison of thermal and optical measurement methods for elemental carbon and black carbon at an urban location. *Environmental science & technology*. 40(20), 6377-6383.
- Stocker, T. F., Qin, D., Plattner, G. K., Tignor, M., Allen, S. K., Boschung, J., Nauels, A., Xia, Y., Bex, V., Midgley, P. M., 2013. *Climate change 2013: The physical science basis*.
- Kanakidou, M., Seinfeld, J. H., Pandis, S. N., Barnes, I., Dentener, F. J., Facchini, M. C., Van Dingenen, R., Ervens, B., Nenes, A., Nielsen, C.J., Swietlicki, E., Putaud, P., Balkanski, Y., Fuzzi, S., Horth, J., Moortgart, K., Winterhalter, R., Myhre, C.E.L., Tsigaridis, K., Vignati, E., Stephanou, E.G., Wilson, J., 2005. Organic aerosol and global climate modelling: a review. *Atmospheric Chemistry and Physics*. 5, 1053-1123.
- Kumar, P., Khare, M., Harrison, R. M., Bloss, W. J., Lewis, A., Coe, H., Morawska, L., 2015. New directions: air pollution challenges for developing megacities like Delhi. *Atmospheric Environment*. 122, 657-661.
- Kuzu, S. L., Saral, A., 2017. The effects of meteorological conditions on aerosol size distribution in Istanbul. *Air Quality, Atmosphere and Health*. 10, 1029-1038.
- Kuzu, S. L., 2019. Source identification of combustion-related air pollution during an episode and afterwards in winter-time in Istanbul. *Environmental Science and Pollution Research*. 26, 16815-16824.



- Lehndorff, E., Roth, P. J., Cao, Z. H., Amelung, W., 2014. Black carbon accrual during 2000 years of paddy-rice and non-paddy cropping in the Yangtze River Delta, China. *Global change biology*.20, 1968-1978.
- Onat, B., Sahin, U. A., Uzun, B., Akın, O., Ozkaya, F., Ayvaz, C., 2019. Determinants of exposure to ultrafine particulate matter, black carbon, and PM_{2.5} in common travel modes in Istanbul. *Atmospheric Environment*. 206, 258-270.
- Ozdemir, H., Pozzoli, L., Kindap, T., Demir, G., Mertoglu, B., Mihalopoulos, N., Theodosi, C., Kanakidou, M., Im, U., Unal, A., 2014. Spatial and temporal analysis of black carbon aerosols in Istanbul megacity. *Science of the Total Environment*. 473, 451-458.
- Pateraki, S., Asimakopoulos, D.N., Flocas, H.A., Maggos, T., Vasilakos, C., 2012. The role of meteorology on different sized aerosol fractions (PM₁₀, PM_{2.5}, PM_{2.5-10}). *Science of the Total Environment*. 419, 124-135.
- Pope III, C. A., Dockery, D. W., 2006. Health effects of fine particulate air pollution: lines that connect. *Journal of the air & waste management association*. 56, 709-742.
- Ram, K., Sarin, M. M., 2011. Day–night variability of EC, OC, WSOC and inorganic ions in urban environment of Indo-Gangetic Plain: implications to secondary aerosol formation. *Atmospheric Environment*. 45, 460-468.
- Tayanc, M., 2000. An assessment of spatial and temporal variation of sulfur dioxide levels over Istanbul, Turkey. *Environmental pollution*. 107, 61-69.
- TUIK, 2018. Turkish Statistical Institution. Annual population census, <http://www.tuik.gov.tr>, accessed in June 2019.
- Wang, G., Hopke, P. K., Turner, J. R., 2011. Using highly time resolved fine particulate compositions to find particle sources in St. Louis, MO. *Atmospheric Pollution Research*. 2, 219-230.
- Yusuf, A. A., Resosudarmo, B. P., 2009. Does clean air matter in developing countries' megacities? A hedonic price analysis of the Jakarta housing market, Indonesia. *Ecological Economics*. 68, 1398-1407.

Acknowledgements

This work was supported by Research Fund of the Yildiz Technical University with Project Number: FBA-2019-3599 and Research Fund of the Marmara University with Project Number: FEN-C-YLP-130319-0066.

Wintertime urban air pollution in Macedonia – composition and source contribution of air particulate matter

Dejan Mirakovski, Blazo Boev, Ivan Boev, Marija Hadzi Nikolova, Afrodita Zendelska and Tena Shijakova

AMBICON – FTNS, University “Goce Delcev”, 2000 Stip, Republic of North Macedonia

dejan.mirakovski@ugd.edu.mk

Abstract. High air pollution episodes in most urban areas in Macedonia fill the headlines in recent years, reinforcing public perception that polluted air is by far most important environmental and health problem that urban population face nowadays. Ambient pollutants concentrations often reach dramatic levels triggering warnings and action plans that are mostly based on personal exposure reduction and hopes for changes in weather conditions, thus leaving public disappointed and confused. Recent studies show that traffic, domestic heating, natural dust and industrial activities are the main sources of PM contributing to urban pollution in European cities. However, there are significant differences between sources and the components of urban AP in different cities. While domestic heating (biomass burning) dominates the contributions to PM in Eastern Europe and in many developing countries, sea salt is the most important (natural) source of PM₁₀ in north-western Europe. Therefore, detailed characterization (determination of size, form and chemical composition) of suspended air particulates is of crucial importance for definition of possible adverse health effects, sources allocation and applicable control measures.

During the last two years (2018-2019), AMBICON team has collected and analysed suspended particulate matters from specific urban zones throughout the country. Samples were taken according to standard gravimetric method (EN 12341:2014) using a low volume sampler and 47 mm PTFE filters. Chemical composition was determined using Fluorescent X-ray Spectrometer (Shimadzu EDX-900HS) according to EPA/625/R-96/010a. Seasonal and diurnal variation were obtained from MOEPP Air Quality Portal, as much as from AMBICON independent monitoring network with in house developed ambient particulate monitors.

The results demonstrate clear domination of biomass burning as primary contributor with much smaller contribution of traffic, industrial and crustal matter sources.

Keywords: Particulates, Concentration, Patterns, PMF, Contribution.

1. Introduction

Nine out of ten people are exposed to air pollution every day, establishing air pollution as the greatest environmental risk to health, that kills 7 million people prematurely every year from diseases such as cancer, stroke, heart and lung disease (WHO, 2019). Although the pollution sources significantly differ between the regions, around 90% of these deaths are in low- and middle-income countries, with high volumes of emissions from industry, transport, agriculture, and often most important dirty cookstoves and fuels in homes (WHO, 2019). And small, landlocked Macedonia is well fitted in this grim picture, as the largest urban areas are often high on the various pollution list, while capitol Skopje was pointed



as most polluted capital city in Europe (UNEP, 2018) with PM₁₀ annual mean of about 69 µg/m³ for 2016 (WHO, 2018).

What is even worse, this is not a new problem, and first research efforts, published more than a decade ago indicated high air pollution problem, locating heavy traffic (Dimitrovski and Bojkovska, 2002) and domestic heating and industry (Stafilov et al., 2003) as a main pollution source. As pollution patterns clearly shows some changes through a virtual elimination for some of the pollutants like Pb, and reduction for some SO₂, NO₂ and some metals like Cd, Fe and Mn, reflecting changes in source profiles like introduction of leadless gasoline and low sulfuric fuel, shifts from heavy oil to LNG in city heating plants, as much as upgrade of largest industrial plants with appropriate control equipment, particulate levels keep the trends showing same pattern throughout the last decade (Mirakovski et al. 2018).

High particulates spikes, especially during the winter season, often reach hazardous levels thought the country urban areas, thus filling the headlines in recent years and reinforcing public perception that polluted air is by far most important environmental and health problem that urban population face nowadays. Confusing and partial data from different sources, slow warnings and inefficient action plans mostly based on personal exposure reduction and hopes for changes in weather conditions, leaving public disappointed and even more confused.

Ambient particulates or suspended particulate matter are common name for heterogenous mixture of solid and liquid particles which composition, biological and physical properties vary from location to location and changes over time, greatly due to temporal-spatial variations in emissions, varying proximity to sources, meteorological variables, and local topographies (Cho et al, 2018). Based on their size, these particles are divided into two major categories. Particles designated as PM_{2.5} (fine particles) have a diameter of less than or equal to 2.5 micrometres (µm), while particles with a diameter between 2.5 µm and 10 µm are designated as PM₁₀ (coarse) particulates. Depending on the atmospheric conditions those particles can remain airborne for long periods and invade the indoor air environment. Majority of particulate mass is comprised of different forms of carbonaceous substances, sulphates, ammonium, nitrate, and various ions. Manganese, copper, zinc, cadmium, chromium, iron, nickel, potassium, calcium, vanadium, barium, arsenic, selenium and strontium are the most commonly found metals in the pollution sources (Magnani et al 2016). Chemical composition of PM is important determinant in its health outcomes (Kundu and Stone, 2014). Also, chemical composition of particulates at the point of impact or receptor, can be used to evaluate the contamination and pollutant sources contributions through a receptor modelling (some of commonly referred factor analysis methods).

Therefore, detailed characterization (determination of size, form and composition) of air particulates is of crucial importance for definition of possible adverse health effects, sources allocation and applicable control measures.

Traying to shed a light on the problem, during the last two years (2018-2019), we have collected and analysed suspended particulate matters and concentration data from several urban zones throughout the country. Samples were taken in Skopje, according to standard gravimetric method (EN 12341:2014) using a low volume sampler and 47 mm PTFE filters. Chemical composition was determined using Fluorescent X-ray Spectrometer (Shimadzu EDX-900HS) according to EPA/625/R-96/010a method. Seasonal and diurnal variation were obtained with real time monitoring during the sampling campaigns, as much as from UGD AMBICON independent monitoring network in cities out of Skopje. Positive matrix factorisation was used to identify major PM₁₀ contribution sources in Skopje.

2. Materials and methods

2.1. Sampling

Ambient air monitoring was performed at two locations in Skopje, one road side at Boulevard “Ilindenska” and one background location at “Aminta the III” (Figure 1). The road side (RS) sampling point was located within the Skopje City Hall courtyard, about 2 meters from the road edge and background sampling (BS) point was located about 600 m to the east within Ministry of Agriculture courtyard.

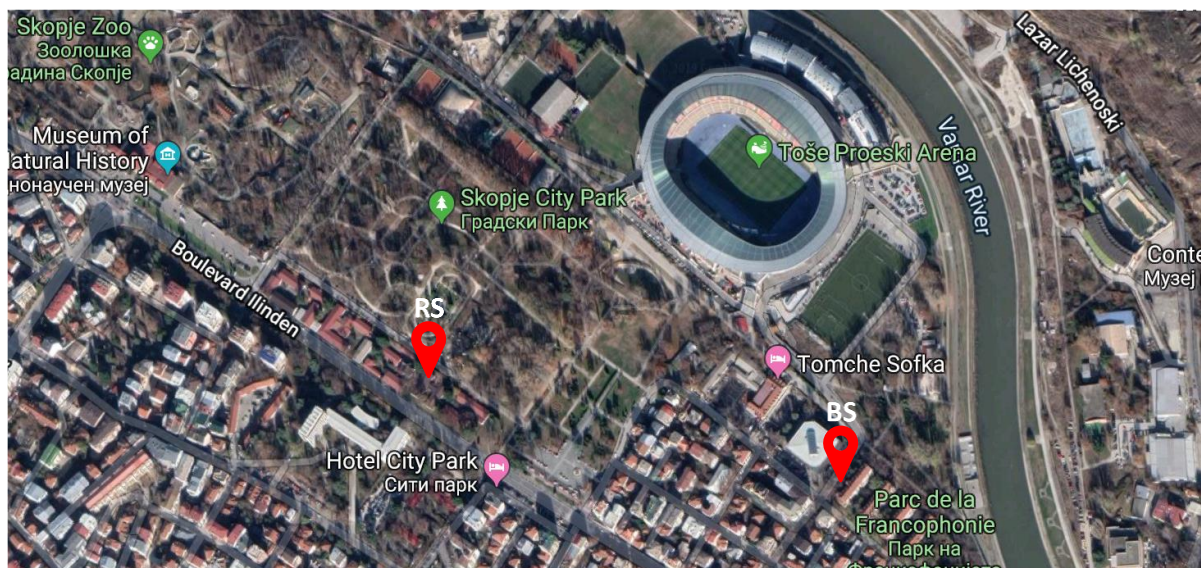


Figure 1. Sampling locations

Both locations were equipped with sequential dust sampling system PNS 16T-3.1 (Comde Derenda, Germany) with 16 filter cassettes for continuous collection of particulate matter and Air Pointers (MLU Recordum, Austria) for real time monitoring of PM₁₀, PM_{2.5}, NO₂ and CO using compliance or equivalent methods.

Sampling was performed at 2.2 meters height, continuously during 14 consecutive days in each season starting from November 8 - 21.2018, January 18-31.2019, May 6-27.2019 and July 13-27.2019. Particulate (PM₁₀) samples were collected on 47 mm PTFE filters and handled and measured gravimetrically fully in line with recommendation given in EN 12341:2014 Ambient air - Standard gravimetric measurement method for the determination of the PM₁₀ or PM_{2.5} mass concentration of suspended particulate matter.

2.2. Elemental analysis

Elemental composition was measured by the energy dispersive X-ray fluorescence (EDXRF) using Fluorescent X-ray Spectrometer (Shimadzu EDX-900HS, Japan) for determination of Na, Cl, K, Ca, Mn, Fe, Ni, Cu, Zn, As, Cd, Pb and Si fully in line with EPA/625/R-96/010a, Method IO-3.3 Determination of Metals in Ambient Particulate Matter Using X-Ray Fluorescence (XRF) Spectroscopy. Black Carbon was analysed using OT21 Transmissometer with dual wavelength light source; 880nm providing the quantitative measurement of Black Carbon in PM, and a 370nm for qualitative assessment of certain aromatic organic compounds.

2.3. Source contribution calculation

Source contribution/apportionment of PM₁₀ mass by Positive Matrix factorisation was performed using the EPA PMF version 5.0.14.21735 program in accordance with the user's guide (EPA, 2014). Positive

Matrix Factorization (PMF) is a receptor model, developed by Dr. Pentti Paatero (Department of Physics, University of Helsinki) in the middle of the 1990s (Paatero and Tapper, 1994), in order to develop a new method for the analysis of multivariate data that resolved some limitations of the PCA (Camero, 2009). One of the main positive aspects is the use of known experimental uncertainties as input data which allow individual treatment of matrix elements and can accommodate missing or below-detection-limit data that are a common feature of environmental monitoring (Song et al., 2001). PMF results have a quantitative nature and therefore it is possible to obtain the composition of the sources determined by the model (Paatero, 2004). Concentration and uncertainty data matrices were compiled as recommended in PMF 5.0 Fundamentals and User Guide (EPA, 2014). In total 20 base runs were performed, using 4 factors and base random seed with 0 % extra modelling uncertainty. Using the calculated signal to noise (S/N) ratios as recommended, Cl and Cd were categorized as “Bad” and excluded from the analysis. Na and As were included as “Weak” while the K, Ca, Mn, Fe, Ni, Cu, Zn, Pb, Si and EC were categorized as “Strong”.

3. Results and discussion

3.1. Particulates concentration

Data collected confirm more or less well-known fact that high pollution episodes occur almost exclusively during the heating seasons, in periods with stable atmospheric conditions, as the deep valleys express strong temperature inversion (normal decrease of air temperature with height is switched to increase) that prevent normal circulation in the atmosphere, creating some times prolonged periods with weak winds and leading to accumulation of emitted substances near the ground surface. And this is common for most of the country urban areas including Skopje, Prilep, Kavadarci, Strumica, Tetovo and so on (Figure 2). Most of the urban areas does manifest PM₁₀ yearly average above the TLV of 40 µg/m³, like Skopje agglomeration (53.6 µg/m³), Bitola (44 µg/m³), Kumanovo (52 µg/m³), Tetovo (49 µg/m³), Kicevo (43 µg/m³) and Kavadarci (55 µg/m³), but values out of the heating seasons are mostly well within the TLV's (MOEPP, 2019).

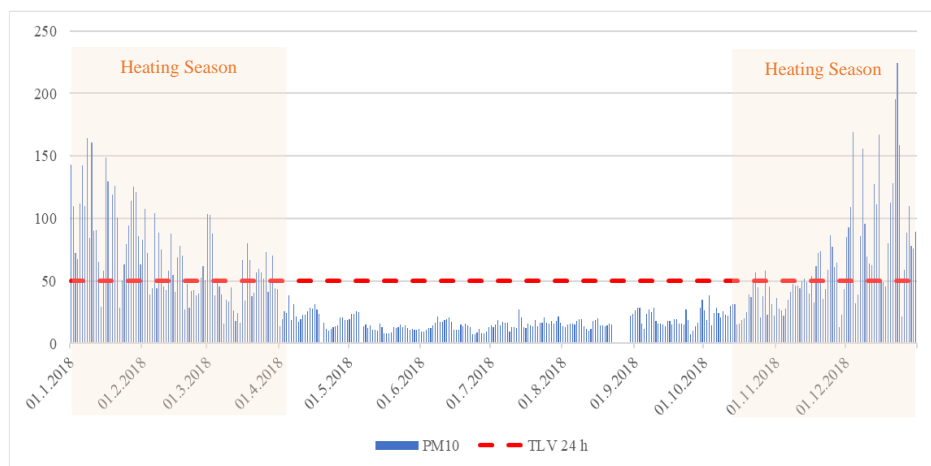


Figure 2. PM₁₀ daily averages for Kavadarci Center (UGD.AMBICON Monitoring Network)

Distinct diurnal cycles are also common for most the cities covered with the monitoring systems. During the high pollution episodes, they all exhibit bimodal pattern, with two peaks in morning and late evening (Figure 4). Such patterns are driven with natural changes in boundary layer height, but are also in direct conjunction with patterns of home heating usage, which also peaks in the morning and evening hours. And if the periods of stagnant atmosphere are prolonged for several consecutive days, the pattern persist with the maximums increased each consecutive day (Figure 3).

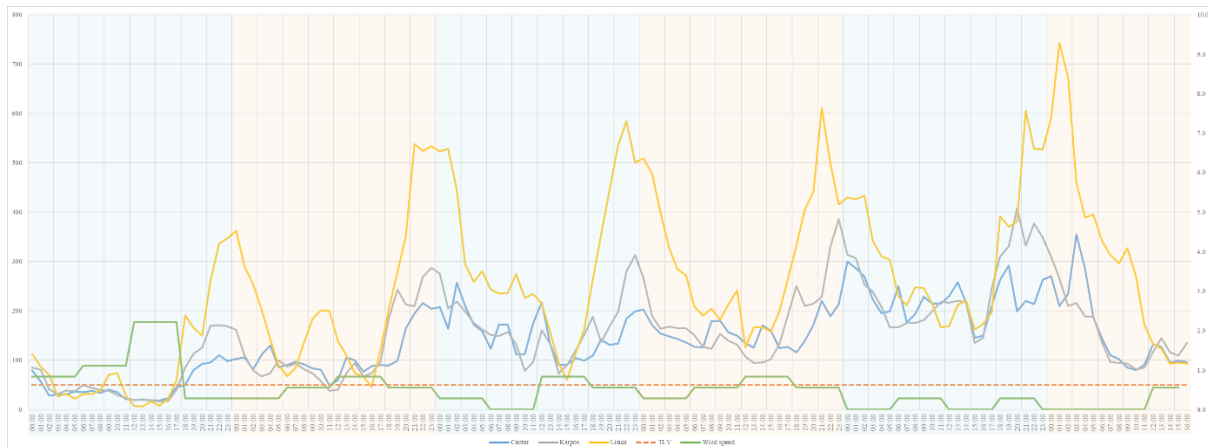


Figure 3. PM₁₀ Diurnal patterns for Skopje agglomeration 04-09.01.2018 (Mirakovski, 2018)

Similar diurnal patterns are reported elsewhere, for regions where domestic wood combustion for home heating is known to be a significant contributor to PM₁₀ concentrations during the winter (Ancelet et. al., 2014, Trompeter et. al., 2010).

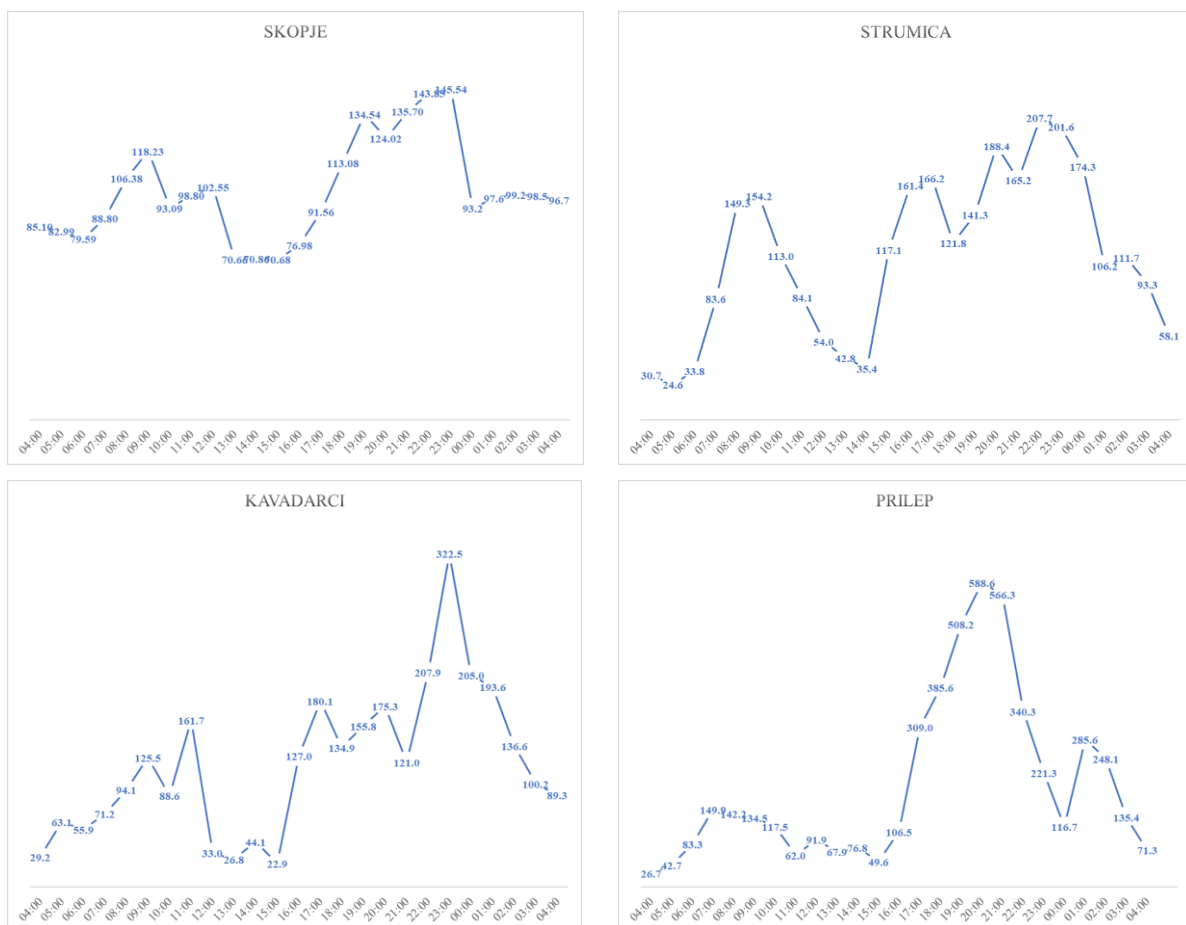


Figure 4. PM₁₀ diurnal patterns in Skopje, Strumica, Kavadarci and Prilep (16.01.2019 - UGD.AMBICON)

In addition, there is a correlation between particulates concentration (PM₁₀) and carbon monoxide (CO), which can be used as tracer for pollutants from combustion related sources (Sahu and Lal, 2013). Data obtained during our measurement campaign, shows excellent correlation during the heating season (autumn/winter) with Pearson coefficient value $r = 0.88$, and no correlation between the same during the spring/summer season ($r = -0.12$). Knowing CO emission inventory for Skopje agglomeration where domestic heating participate with 59%, industry with 16 % and traffic with 25 % (MOEPP, 2019) it could be safely concluded that domestic wood combustion contributes to significant part of winter time air pollution and actually drive pollution patterns explained above. And assuming the similar conditions in other cities mentioned above like Strumica or Prilep, where industry and traffic have even lower contributions, domestic wood combustion could be the single important source of pollution.

3.2. Source contribution

As the composition of the particulate matters at background and road side locations monitored in Skopje, does not differ significantly, especially during the heating season, Positive Matrix Factorization was performed on background data, as more representative for wider city area. Statistical description of the input data including average, maximum, and median concentrations of species used for source apportionment, as well as standard deviations, average uncertainties and limits of detection are given below (Table 1). As only 54 valid samples were available, stretched over a 12-month period, PMF exercise should be seen as indication for dominant sources and cannot replace full scale source apportionment study.

Table 1. PMF input data (54 samples)

	Unit	Average	Maximum	Median	Standard Deviation	Average Uncertainty	Detection limit
PM ₁₀	µg/m ³	52	187	36	36	3	3.0
PM _{2.5}	µg/m ³	36	174	14	38	2	3.0
EC (PM ₁₀)	ng/m ³	15034	43550	10712	9548	752	100
Na (PM ₁₀)	ng/m ³	76	624	25	114	30	39
Cl (PM ₁₀)	ng/m ³	94	763	90	92	141	181
K (PM ₁₀)	ng/m ³	477	2216	216	535	108	108
Ca (PM ₁₀)	ng/m ³	1232	2911	1214	757	212	118
Mn (PM ₁₀)	ng/m ³	26.1	204.5	6.9	44.6	4.4	5.1
Fe (PM ₁₀)	ng/m ³	707	1513	677	338	71	73
Ni (PM ₁₀)	ng/m ³	14.0	75.2	5.8	16.8	1.6	1.6
Cu (PM ₁₀)	ng/m ³	17.9	195.9	8.1	30.1	4.1	5.1
Zn (PM ₁₀)	ng/m ³	34.6	401.4	0.9	90.1	6.1	1.9
As (PM ₁₀)	ng/m ³	0.09	1.17	0.01	0.23	0.03	0.20
Cd (PM ₁₀)	ng/m ³	0.50	0.50	0.50	0.00	0.83	1.00
Pb (PM ₁₀)	ng/m ³	18.6	139.8	2.6	29.0	4.2	5.2
Si (PM ₁₀)	ng/m ³	176	658	109	164	61	118

As large numbers of species usually encountered in particulate matters were not quantified, including often dominant water-soluble ions (NH₄⁺, SO₄²⁻ and NO₃⁻), reconstructed masses determined using the elemental data accounted for only 28.4 % of the PM₁₀ mass. Performing multiple PMF runs to elemental data give optimal solution with 4 factors, identified as biomass burning (high EC content, K, Na and Si), industrial (Ni, Si, Na, Cu, As), traffic (Zn, Pb, Cu, EC) and crustal (Si, Ca, Fe, K) (Figure 5). Some of the elements have contribution in several sources, as some processes, like resuspending road dust or common combustion sources, contribute to a mixed source profiles (Ca, Na and K in traffic and crustal matter or EC in traffic and biomass burning).

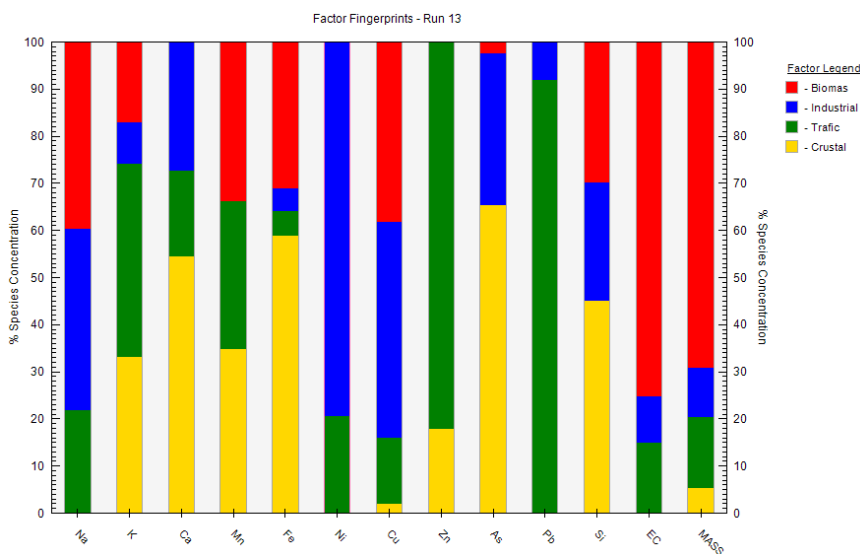


Figure 5. Factor fingerprints

The first factor, characterized as biomass burning has by far highest contribution to PM₁₀ mass reaching 69.2 %, while traffic, industrial and crustal matters contribute 15.2 %, 10.4 % and 5.3 % respectively (Figure 6).

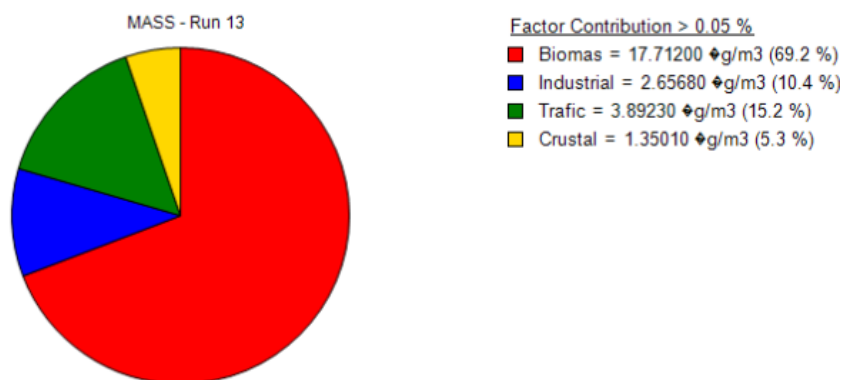


Figure 6. Factor contributions to PM₁₀ mass

Such high contribution from biomass burning is not surprising, having in mind Skopje agglomeration emission inventory for reference 2014, where domestic heating participates with 91%, in total PM₁₀ emissions, while industry, energy production, traffic, waste management, agriculture and construction have altogether with about 9 % (FMI & MOEPP, 2015). Adding the temporal distribution of this emissions to the picture, with biomass burning narrowed to in less than six months, this could be easily determined as the only significant source, that should be somehow altered in order to reduce frequent wintertime pollution episodes.

4. Conclusions

We have aimed to indicate sources that contribute to high particulate concentration during wintertime pollution episodes, by sampling and analyzing suspended particulate matters and concentration data in Skopje and several urban zones throughout the country during the last two years (2018-2019).

Concentration data collected confirm that most of the urban areas manifest PM₁₀ yearly average above the TLV of 40 µg/m³, like Skopje agglomeration (53.6 µg/m³), Bitola (44 µg/m³), Kumanovo (52 µg/m³), Tetovo (49 µg/m³), Kicevo (43 µg/m³) and Kavadarci (55 µg/m³), but values out of the heating seasons are mostly well within the TLV's. Distinct diurnal cycles are also common for most the cities covered with the monitoring systems, and they all exhibit bimodal pattern, with two peaks in morning and late evening. Such patterns are driven with natural changes in boundary layer height, but are also in direct conjunction with patterns of home heating usage, which also peaks in the morning and evening hours. In addition, there is an excellent correlation between carbon monoxide (as tracer for combustion related sources) and particulate concentration during the heating season (autumn/winter) with Pearson coefficient value $r = 0.88$, and no correlation during the spring/summer season ($r = -0.12$).

Positive Matrix Factorization was performed on background data, as more representative for wider city area, identifying 4 factors as biomass burning (high EC content, K, Na and Si), industrial (Ni, Si, Na, Cu, As), traffic (Zn, Pb, Cu, EC) and crustal (Si, Ca, Fe, K). The first factor, characterized as biomass burning have by far highest contribution to PM₁₀ mass reaching 69.2 %, while traffic, industrial and crustal matters contribute 15.2 %, 10.4 % and 5.3 % respectively (Figure 6).

All this strongly indicate biomass burning as the only significant source, that should be somehow altered in order to reduce frequent wintertime pollution episodes.

5. References

- Ancelet T., Davy P.K., Trompeter W.J., A. Markwitz, D.C. Weatherburn, 2014. Particulate matter sources on an hourly timescale in a rural community during the winter. *Journal of the Air & Waste Management Association*. 64:5, 501-508
- Air quality improvement plan for Skopje agglomeration, 2016. Finish Meteorological Institute and Ministry of Environmental Planning, Macedonia, Skopje, pages 116.
- Annual Report on quality of environment, 2018. Ministry of Environmental Protection and Physical Planning, Republic of North Macedonia, Skopje, pages 132.
- Cho CC, Hsieh WY, Tsai CH, Chen CY, Chang HF, Lin CS., 2018. In Vitro and In Vivo Experimental Studies of PM_{2.5} on Disease Progression. *Int J Environ Res Public Health*. 5(7):1380.
- Comero S., Capitani L., Gawlik B.M., 2009. Positive Matrix Factorisation (PMF) An introduction to the chemometric evaluation of environmental monitoring data using PMF, JRC, European Communities.
- Dimitrovski M., Bojkovska R., 2002. Influence of traffic on the air pollution ins Skopje, *J. Environ. Protection and Ecology*. 3, 593 - 601.
- Gary Norris, Rachele Duvall, Steve Brown, Song Bai, 2014. EPA Positive Matrix Factorization (PMF) 5.0 Fundamentals and User Guide, US EPA.
- Magnani ND, Muresan XM, Belmonte G, Cervellati F, Sticozzi C, Pecorelli A, Miracco C, Marchini T, Evelson P, Valacchi G., 2016. Skin Damage Mechanisms Related to Airborne Particulate Matter Exposure. *Toxicol Sci*. 149, 1, 227-36.
- Mirakovski D, Hadzi-Nikolova M., Boev I., Sijakova T., Doneva N., Zendelska A., Sources of urban air pollution in Macedonia – behind high pollution episodes. *Book of Abstracts. GREDIT Conference. March 22-25, 2018, Skopje, Macedonia*, pp. 35-36.
- Paatero P., Tapper U., 1993. Analysis of different modes of factor analysis as least squares fit problems. *Chemometrics and Intelligent Laboratory System*. 18, 183–194.
- Paatero P., 2004. User's guide for positive matrix factorization programs PMF2 and PMF3, Part1: tutorial. University of Helsinki, Helsinki, Finland.



Sahu, L.K., Varun Sheel, Kajino, M., Nedelec, P., 2013. Variability in Tropospheric Carbon Monoxide over an Urban Site in Southeast Asia. *Atmos. Environ.* 68, 243–255.

Song, X.H., Polissar, A.V., Hopke, P.K., 2001. Sources of fine particle composition in the northeastern US. *Atmos. Environ.* 35, 5277–5286.

Stafilov T., Bojkovska R., Hirao M., 2003. Air pollution monitoring system in Republic of Macedonia. *J. Environ. Protection and Ecology.* 4, 518 - 524.

Trompetter, W.J., Davy, P.K., Markwitz, A. 2010. Influence of environmental conditions on carbonaceous particle concentrations within New Zealand. *J. Aerosol Sci.* 41, 134–142.

UNEP, 2019. <https://www.unenvironment.org/news-and-stories/story/most-polluted-capital-europe-you-didnt-even-know-about>, accessed in September 2019.

WHO, 2018. Global Ambient Air Quality Database <https://www.who.int/airpollution/data/cities/en/>, accessed in September 2019.

WHO, 2019. Ten threats to global health in 2019. <https://www.who.int/emergencies/ten-threats-to-global-health-in-2019>, accessed in September 2019.

Acknowledgments

Authors wish to acknowledge assistance from City of Skopje and Farmahem Environmental Laboratory for their support and participation in sampling and data collection process.

Assessment of the levels of trace elements and ions in rainwater samples in Pamukkale, Denizli, Turkey

Sibel Cukurluoglu

Pamukkale University, Faculty of Engineering, Department of Environmental Engineering, Kinikli Campus, Pamukkale, Denizli, Turkey

scukurluoglu@pau.edu.tr

Abstract. The sources of trace elements and ions in rainwater samples were investigated in Pamukkale, Denizli, Turkey. The rainwater samples were collected from December 2011 to November 2012. Zn, Al, Fe, Cr, Ni, Mn, Cd, Pb, Cu, Li, Sr, Co, Ba, Ti, Ca⁺², Mg⁺², K⁺, NH₄⁺, Na⁺, Cl⁻, F⁻, NO₃⁻, and SO₄⁻² concentrations were determined using inductively coupled plasma optical emission spectrometry and ion chromatography. Zn, Al, and Fe account for 29.6%, 12.9% and 7.8% of the volume weighted mean total trace element concentration, respectively. The daily volume weighted mean concentrations of Ca⁺², SO₄⁻², and K⁺ contributed 63.6% to the total ion concentration. The value of volume weighted mean pH was 6.94±0.86. The results of principal component analysis indicated that the wet deposition was a three-component system (mixed, local, and anthropogenic components) for trace elements, while the ion-containing precipitation was a two-component system (mixed and local components). Wet deposition may be important for the travertines in Pamukkale due to high concentrations of trace elements and ions.

Keywords: Wet deposition, Trace elements, Ions, Factor analysis, Pamukkale.

1. Introduction

Transport of elements sourced from industrial or urban sources related to atmospheric deposition. The atmosphere is a significant pathway for the movement and redistribution of trace elements, which are present within the ecosystem at trace levels (Tahir and Khan, 2008).

Local natural sources such as sea spray, soil-derived windblown dust, suspended road dust; anthropogenic sources such as coal-combustion, vehicle exhausts, agricultural production, biomass burning; and long-range transport of soil dust and gaseous pollutants may affected the chemical composition of wet deposition (Xing et al., 2017).

Several factors such as differences of sources, precipitation amounts, and air mass directions are effective on air pollutant concentrations in precipitation. Pollutant concentrations may vary temporally and spatially (Koulousaris et al., 2009).

Trace element composition in precipitation has been determined in Pamukkale, Denizli, Turkey by Cukurluoglu (2017). In addition, Cukurluoglu (2018) investigated the acidification/neutralization effect of ions in rainwater samples. Acidic rain may adversely affect the travertine. Therefore, it is of great importance for Pamukkale travertine. Within the scope of these researches, the following data determined in Pamukkale, Denizli between December 2011 and November 2012 were presented in this study:

- the concentrations of Sr, Zn, Pb, Cd, Ni, Ba, Fe, Mn, Cr, Ti, Al, Li, Cu, and Co in rainwater samples
- the concentrations of F⁻, Cl⁻, NO₃⁻, SO₄⁻², NH₄⁺, Na⁺, K⁺, Mg⁺², and Ca⁺² in rainwater samples
- pH and electrical conductivity values of rainwater samples
- the possible sources of trace elements and ions determined using factor analysis

2. Materials and methods

2.1. Sampling

Wet deposition sampling was carried out at Pamukkale University Kinikli Campus, Pamukkale, Denizli, Turkey. Denizli is located at the Aegean Region, western part of Turkey. It has many industrial factories such as textile, chemical, plastic, metal, electricity etc. The weather is hot in summers, and cold in winters. It is rainy and warm in springs and autumns.

The rainwater samples were collected manually. The sampler is made of polyethylene material. It has a diameter of 24 cm. It was located approximately 1 m high from the ground level. Forty-five rainwater samples were collected during the sampling period. The three samples among them were rejected because of the insufficient amounts ($h < 0.1$ mm).

The materials used during sampling and analysis were washed with 1:1 HNO₃. Then they were rinsed with tap water and deionized water and finally dried. The same processes were replicated using 1:1 HCl (U.S.EPA, 2007). Blanks of laboratory and field were collected along with the rainwater samples.

2.2. Analysis

After the sampling, the samples were brought to the Research Laboratory of Environmental Engineering Department of Pamukkale University. The samples were filtered using Sartorius 0.45 μ m cellulose acetate filter. The filtrates were stored at 4 °C in a refrigerator until the analysis. They were acidified to pH 2 by ultra-pure concentrated nitric acid for trace element analysis.

F⁻, Cl⁻, NO₃⁻, SO₄⁻² and NH₄⁺ were determined using ion chromatography (IC, Dionex ICS-1000). Sr, Zn, Pb, Cd, Ni, Ba, Fe, Mn, Cr, Ti, Al, Li, Cu, Co, Na⁺, K⁺, Mg⁺², and Ca⁺² were measured using inductively coupled plasma optical emission spectrometry (ICP-OES, Optima 2100 DV).

pH and electrical conductivity were measured using a WTW pH 720 pH meter and a WTW Cond 730 conductivity meter, respectively.

2.3. Quality control

The limits of detection (LOD) values were calculated for trace elements and ions. LOD is defined as the mean blank mass plus three standard deviations (Odabasi et al., 1999).

LOD values ranged from 0.0002 (Cu) to 0.002 mg (Zn) for the trace elements in rainwater samples in this study. LOD values range with 0.003 for NH₄⁺ and 0.053 mg for SO₄⁻² for the ions. The amounts of trace elements and ions in precipitation samples were substantially higher than LODs.

2.4. Statistical analysis

Statistical relations were investigated using SPSS (Statistical Package for the Social Sciences) 16.0 software. The relations were determined at the $p < 0.01$ level.

Possible sources of trace elements and ions in rainwater samples were investigated using principal component analysis (PCA). PCA is a multivariate statistical method (Tripathee et al., 2014). It uses orthogonal transformations to convert a set of observations for variables (Zhang et al., 2014).

3. Results

3.1. pH and electrical conductivity values of rainwater samples

The minimum pH value of the rainwater samples was 4.66, while the maximum pH was 7.94. The value of volume weighted mean pH was 6.94 ± 0.86 . The pH value of rainwater in Pamukkale, Denizli, Turkey was not acidic, on an average. The minimum and maximum electrical conductivities of the precipitation samples were 8.3 and $218.0 \mu\text{S cm}^{-1}$, respectively. The average value of conductivity was determined as $72.4 \pm 59.1 \mu\text{S cm}^{-1}$.

3.2. Concentrations of trace elements in rainwater samples

The order of volume weighted mean (VWM) trace element concentrations was determined as $\text{Zn} > \text{Al} > \text{Fe} > \text{Mn} > \text{Cu} > \text{Ba} > \text{Ti} > \text{Sr} > \text{Cd} > \text{Li} > \text{Co} > \text{Pb} > \text{Cr} > \text{Ni}$ (Figure 1). Zn, Al, and Fe account for 29.6%, 12.9% and 7.8% of the VWM total trace element concentration, respectively. The minimum daily total concentration of the trace elements was determined as $162.5 \mu\text{g L}^{-1}$ on May 20, 2012. The maximum daily total concentration of the trace elements was measured as $1056.5 \mu\text{g L}^{-1}$ on January 1, 2012.

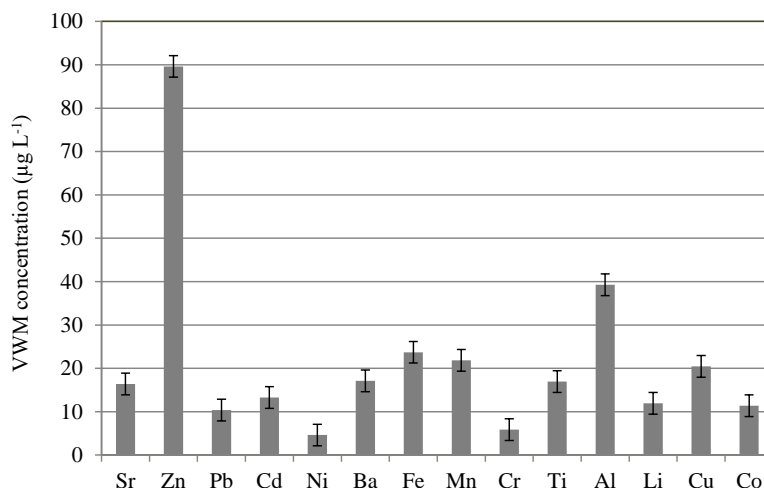


Figure 1. Volume weighted mean concentrations of trace elements

The daily trace element concentrations measured in Mexico by Baez et al. (2007), USA by Song and Gao (2009), and Korea by Kim et al. (2012) were lower than those observed in Pamukkale, Denizli, Turkey. Fe concentrations in Greece (Koulousaris et al., 2009), South Africa (Gichuki and Mason, 2013), and Nepal (Tripathee et al., 2014) were significantly higher than the Fe concentrations in Denizli. The high Al concentrations were observed in South Africa by Gichuki and Mason (2013), Spain by Moreda-Piñeiro et al. (2014), Nepal by Tripathee et al. (2014), and Tibet by Guo et al. (2015). The very high Pb, Cu, and Cd concentrations were determined in Jordan by Al-Khashman (2009). Connan et al. (2013) concluded that the concentrations of heavy metals in precipitations in the Bay of the Seine in the northwest of France were low because of the site was protected from important anthropogenic influences.

The high concentrations of Al and Fe were observed at the several sites in Turkey (Gülsoy et al. 1999, Okay et al. 2002, Akkoyunlu and Tayanc 2003, Başak and Alagha 2004, Saylan et al. 2002, Özsoy and Örnektekin, 2009 and Şaylan et al. 2009). The concentrations of Ni, Cr, Pb, Sr, Mn, and Zn measured in Denizli, Turkey were close to the concentrations in Mersin, Turkey (Özsoy and Örnektekin, 2009). The concentrations of Co, Cd, Ba, and Cu in Denizli precipitation were higher than the values in Mersin. The concentrations of Cu, Fe, and Al determined in Istanbul by Uygur et al. (2010) were higher than the

concentrations in Denizli, while Ni, Cr, Pb, and Co concentrations observed in Istanbul were lower than the concentrations in Denizli.

3.3. Concentrations of ions in rainwater samples

The order of VWM concentrations of ions was $F^- < NH_4^+ < NO_3^- < Na^+ < Cl^- < Mg^{+2} < K^+ < SO_4^{-2} < Ca^{+2}$ (Figure 2). The daily VWM concentrations of Ca^{+2} , SO_4^{-2} , and K^+ contributed 63.6% to the total ion concentration. The minimum and maximum daily total concentrations of the ions were measured as $100.5 \mu\text{eq L}^{-1}$ on April 10, 2012, and $2,612.1 \mu\text{eq L}^{-1}$ on January 1, 2012, respectively.

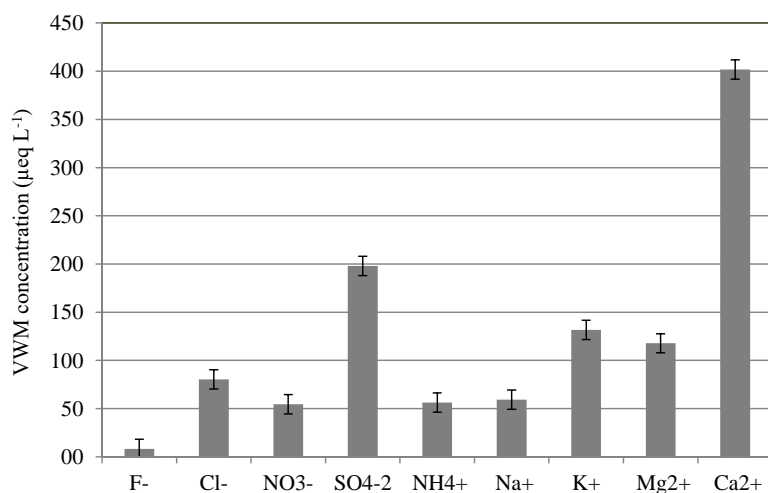


Figure 2. Volume weighted mean concentrations of ions

The total VWM concentration of all ions was determined as $625.7 \mu\text{eq L}^{-1}$. This value is higher than the value of $130.9 \mu\text{eq L}^{-1}$ observed in Lijiang, China (Zhang et al., 2014), while it is lower than the value of $922.6 \mu\text{eq L}^{-1}$ reported for Istanbul, Turkey (Okay et al., 2002). The concentration of K^+ in rainwater samples in Pamukkale, Denizli was higher than the values reported for the other regions in the world. The ion concentrations determined in China by Zhang et al. (2014) were significantly lower than the ion levels observed in Denizli. The concentrations of NH_4^+ in rainwater in Mexico were higher than the concentrations in Pamukkale, Denizli (Báez et al., 2007). F^- , Cl^- , SO_4^{-2} , Na^+ , and Ca^{+2} concentrations were determined high levels in Istanbul (Okay et al., 2002). The concentrations of the ions in Ankara precipitation were lower than the concentrations in Denizli except NH_4^+ (Topçu et al., 2002).

3.4. Relation between the concentrations of trace elements and ions and precipitation heights

Average precipitation height was determined as 13.8 mm day^{-1} during the sampling period. The minimum daily precipitation height was 1 mm day^{-1} , while the maximum height was 121 mm day^{-1} . The daily total concentrations of trace elements and ions in wet deposition samples decreased exponentially as the daily precipitation heights increased. These statistical relations were low levels. The both below-cloud raindrop scavenging effect and in-cloud processes may be affecting the composition of wet deposition in Pamukkale, Denizli.

3.5. Factor analysis for trace elements

Principal component analysis was used to investigate the possible sources of trace elements and ions in rainwater samples in Pamukkale, Denizli, Turkey. The loadings having a greater value than 0.50 were shown in the table. The varimax rotation was applied on significant factors with an initial eigenvalue >1 .

The results of PCA indicated that the wet deposition was a three-component system for trace elements. These systems consist of a mixed component (crustal and anthropogenic), a local pollution component, and an anthropogenic component. The mixed, local, and anthropogenic components explain 58.9, 18.2 and 9.4% of the total variance, respectively (Table 1).

Factor 1 is a mix of the crustal materials and anthropogenic activities. Cd, Cu, Co, Fe, Mn, Li, and Al have the high loading effects for this factor, while Ti, Pb, and Ba are moderately effect. The concentrations of Al and Fe may be related to the terrigenous particles. Ti has great amount in local soil. Cd and Cu originated from using of fertilizers and fungicides and mining. In addition, facilities of metallic and metallurgical can be sources of Cu. Cd, Pb, and Ba may have originated from the plastic industry. Industries of battery, paint, electricity, and textile may be sources of Mn, Li, Cd, Pb, and Ba.

Factor 2 is associated with the local anthropogenic pollution sources. There are industrial facilities close to the sampling area. Fossil fuel combustion and steel factories may be sources of Ni and Cr. Ni and Sr may be caused by glass factories. Metal facilities can be sources of Cr and Ti.

Factor 3 may be associated with anthropogenic sources. It includes Zn and Pb. Vehicle exhausts can be sources of these elements. Zn and Pb may have been originated from contaminated soil particles.

Table 1. Factor loading matrix for trace elements in wet deposition

Trace Element	Component		
	Factor 1	Factor 2	Factor 3
Cd	0.969		
Cu	0.965		
Co	0.965		
Fe	0.956		
Mn	0.919		
Li	0.890		
Al	0.884		
Ti	0.685	0.662	
Pb	0.627		0.619
Ba	0.620		
Ni		0.957	
Cr		0.928	
Sr		0.678	
Zn			0.900

Lynam et al. (2015) determined moderate to high enrichment in wet deposition samples in Illinois, USA. They concluded that anthropogenic sources contributed to deposition of many trace elements. The significant amounts of Al, Fe, Mn, Cr, and Ni were found in the northern Aegean atmosphere due to the storm in the Sahara Desert. In addition, it was stated that anthropogenic sources could affected some amounts of Cr and Ni in precipitation on the southeastern coast of the island of Lesbos, Greece (Koulousaris et al., 2009). Song and Gao (2009) concluded that anthropogenic sources at metropolitan Newark, New Jersey, USA were important on precipitation. They stated that Pb, V, Cr, and Ni were moderately enriched. It has been identified that most of the Fe, Co, and Al were sourced from crust sources, while Zn, Sb, Cu, and Cd were highly enriched.

3.6. Factor analysis for ions

The ion-containing precipitation was a two-component system according to the PCA analysis. These are a mixed component (crustal and anthropogenic), and a local pollution component. The mixed and local pollution components explain 53.5 and 19.1% of the total variance, respectively (Table 2).

Factor 1 is associated with a mix of the crustal materials and anthropogenic sources. It was high loading for NO_3^- , SO_4^{2-} , Mg^{+2} , and F^- and moderate loading for NH_4^+ , Ca^{+2} , and Na^+ . Fossil fuel combustion can cause the emissions of NO_3^- and SO_4^{2-} . Mg^{+2} , Ca^{+2} , and Na^+ may be originated from crustal source. The terrestrial particulates in the Denizli atmosphere may be the reason of high concentrations of Mg^{+2} and Ca^{+2} . Industries of plastic and chemical can be sources of F^- . NH_4^+ may have originated from agricultural activities.

Factor 2 is related to the local anthropogenic pollution source. Cl^- and K^+ have high loading effect, while Na^+ has moderate effect. Facilities of chemical, plastic, and textile can be sources of Cl^- . In addition, Cl^- , K^+ , and Na^+ may be sourced from glass industry.

Table 2. Factor loading matrix for ions in wet deposition

Ion	Component	
	Factor 1	Factor 2
NO_3^-	0.838	
SO_4^{2-}	0.830	
Mg^{+2}	0.820	
F^-	0.818	
NH_4^+	0.702	
Ca^{+2}	0.654	
Na^+	0.564	0.671
Cl^-		0.905
K^+		0.892

4. Conclusion

The sources of trace elements and ions in rainwater samples in Pamukkale, Denizli, Turkey were investigated between December 2011 and November 2012. The major trace elements in wet deposition samples were Zn, Al, Fe, and Mn in this study. The most abundant anion and cation were determined as SO_4^{2-} and Ca^{+2} , respectively.

The differences of pollutants, regions, meteorological conditions, soil characteristics may be affected the variability of the concentrations of trace elements and ions in rainwater samples. Long-range atmospheric transport of trace elements and ions could be affected the composition of precipitation (Al-Khashman, 2009).

This study showed that the concentrations of trace elements and ions in rainwater samples could reach high levels. This may be important for travertines in Pamukkale. Therefore, detailed investigation of wet deposition would be appropriate.

5. References

- Akkoyunlu, B.O., Tayanc, M., 2003. Analyses of wet and bulk deposition in four different regions of Istanbul, Turkey. *Atmos. Environ.* 37, 3571-3579.
- Al-Khashman, O.A., 2009. Chemical characteristics of rainwater collected at a western site of Jordan. *Atmos. Res.* 91, 53-61.
- Báez, A., Belmont, R., García, R., Padilla, H., Torres, M.C., 2007. Chemical composition of rainwater collected at a southwest site of Mexico City, Mexico. *Atmos. Res.* 86, 61-75.
- Başak, B., Alagha, O., 2004. The chemical composition of rainwater over Büyükçekmece Lake, Istanbul. *Atmos. Res.* 71, 275-288.

- Connan, O., Maro, D., Hébert, D., Roupsard, P., Goujon, R., Letellier, B., LeCavelier, S., 2013. Wet and dry deposition of particles associated metals (Cd, Pb, Zn, Ni, Hg) in a rural wetland site, Marais Vernier, France. *Atmos. Environ.* 67, 394-403.
- Cukurluoglu, S., 2017. Sources of trace elements in wet deposition in Pamukkale, Denizli, western Turkey. *Environ. Forensics.* 18, 1, 83-99.
- Cukurluoglu, S., 2018. Acidification/neutralization effect of ions in wet deposition samples in Pamukkale, Denizli, western Turkey. *Fresen. Environ. Bull.* 27, 11, 7291-7305.
- Gichuki, S.W., Mason, R.P., 2013. Mercury and metals in South African precipitation. *Atmos. Environ.* 79, 286-298.
- Guo, J., Kang, S., Huang, J., Zhang, Q., Tripathee, L., Sillanpää, M., 2015. Seasonal variations of trace elements in precipitation at the largest city in Tibet, Lhasa. *Atmos. Res.* 153, 87-97.
- Gülsoy, G., Tayanç, M., Ertürk, F., 1999. Chemical analyses of the major ions in the precipitation of Istanbul, Turkey. *Environ. Pollut.* 105(2), 273-280.
- Kim, J.E., Han, Y.J., Kim, P.R., Holsen, T.M., 2012. Factors influencing atmospheric wet deposition of trace elements in rural Korea. *Atmos. Res.* 116, 185-194.
- Koulousaris, M., Aloupi, M., Angelidis, M.O., 2009. Total metal concentrations in atmospheric precipitation from the northern Aegean Sea. *Water Air Soil Poll.* 201, 389-403.
- Lynam, M.M., Dvonch, J.T., Hall, N.L., Morishita, M., Barres, J.A., 2015. Trace elements and major ions in atmospheric wet and dry deposition across central Illinois, USA. *Air Qual. Atmos. Health.* 8, 135-147.
- Odabasi, M., Sofuoglu, A., Vardar, N., Tasdemir, Y., Holsen, T.M., 1999. Measurement of dry deposition and air-water exchange of polycyclic hydrocarbons with the water surface sampler. *Environ. Sci. Technol.* 33, 426-434.
- Okay, C., Akkoyunlu, B.O., Tayanç, M., 2002. Composition of wet deposition in Kaynarca, Turkey. *Environ. Pollut.* 118, 401-410.
- Özsoy, T., Örnektekin, S., 2009. Trace elements in urban and suburban rainfall, Mersin, Northeastern Mediterranean. *Atmos. Res.* 94, 203-219.
- Saylan, L., Toros, H., Sen, O., 2002. Temporal variability of the precipitation chemistry in the forest area of Istanbul, Turkey. *Int. J. Environ. Pollut.* 18(5), 508-516.
- Song, F., Gao, Y., 2009. Chemical characteristics of precipitation at metropolitan Newark in the US East Coast. *Atmos. Environ.* 43, 4903-4913.
- Şaylan, L., Toros, H., Şen, O., 2009. Back trajectory analysis of precipitation chemistry in the urban and forest areas of Istanbul, Turkey. *Clean-Soil Air Water.* 37(2), 132-135.
- Tahir, S.N.A., Khan, S., 2008. Measurement of atmospheric dry deposition flux and resultant deposition velocity of inorganic pollutants in the provincial capital of Punjab, Pakistan. *Environ. Forensics.* 9, 290-294.
- Topçu, S., Incecik, S., Atımtay, A.T., 2002. Chemical composition of rainwater at EMEP station in Ankara, Turkey. *Atmos. Res.* 65, 77-92.
- Tripathee, L., Kang, S., Huang, J., Sharma, C.M., Sillanpää, M., Guo, J., Paudyal, R., 2014. Concentrations of trace elements in wet deposition over the central Himalayas, Nepal. *Atmos. Environ.* 95, 231-238.
- U.S. Environmental Protection Agency, 2007. Inorganic Analytes. EPA Wastes, Hazardous wastes. Test methods, SW846, Ch. 3, Rev. 4. Washington, DC, 1-28.



18th World Clean Air Congress, 23-27 September 2019, Istanbul
organized by TUNCAP and IUAPPA

Uygun, N., Karaca, F., Alagha, O., 2010. Prediction of sources of metal pollution in rainwater in Istanbul, Turkey using factor analysis and long range transport models. *Atmos. Res.* 95, 55-64.

Xing, J., Song, J., Yuan, H., Li, X., Li, N. Duan, L., Qu, B., Wang, Q., Kang, X., 2017. Chemical characteristics, deposition fluxes and source apportionment of precipitation components in the Jiaozhou Bay, North China. *Atmos. Res.* 190, 10-20.

Zhang, N., Cao, J., He, Y., Xiao, S., 2014. Chemical composition of rainwater at Lijiang on the southeast Tibetan Plateau: Influences from various air mass sources. *J. Atmos. Chem.* 71, 157-174.

Acknowledgments

This research was financially supported by the Scientific Research Projects Fund of Pamukkale University, through the project number BAP-2011BSP022. The congress participation was provided by the Scientific Research Projects Fund of Pamukkale University with project number 2019KRM004-153.

An improved high pressure CO₂ capture technology for oxy-fuel combustion

Hande Cukurlu, Yasemen Kuddusi, Baris Oktay, Hasancan Okutan and Husnu Atakul

Istanbul Technical University, Department of Chemical Engineering

okutan@itu.edu.tr

Abstract. The fossil-fuel based power generation sector is facing important challenges to develop energy efficient solutions while reducing the greenhouse gas (GHG) emissions (mainly CO₂). For decreasing GHG emissions, several approaches have been evaluated and reviewed for capturing CO₂ in the utility industry namely Carbon Capture and Storage Technologies (CCS) including pre-combustion, oxy-fuel combustion and post-combustion. As a promising CCS technology, oxy-fuel combustion can be used in existing and new power plants. In oxy-fuel combustion, the fossil fuel, bio-fuel or biomass is combusted with pure oxygen using recycled flue gas stream that is highly enriched in CO₂ to control the combustion temperature and to ensure proper heat transfer. In the oxy-fuel combustion system, a high concentration of CO₂ (80-90%, dry basis) in the flue gas makes it easy and economical to capture it with the flue gas compression train. The aim of this work is to develop a novel large-scale experimental set-up for separation CO₂ from flue gas of oxy-fuel combustion by liquefaction method, which is based on compression. Experimental setup installed in the laboratory consists of five main units: Simulating flue gas composition, separation of water from highly enriched CO₂ simulated flue gas, CO₂ capture and storage, PLC system and gas chromatography system. Owing to newly developed large scale, experimental setup liquefaction of CO₂ has been successfully carried out at the temperatures between -10 and 0 °C and pressures between 35 to 80 bars. The results show that as the temperature decrease the operable pressure range increases. Meaning, based on desired CO₂ specifications operating conditions can be set. As the results of experiments and thermodynamic simulations show while pressure increasing at the constant temperature purity of liquid CO₂ decrease while the amount of liquid CO₂ increase. Thus, it is possible to get high yield of CO₂ using high pressures at the temperatures between -10 and 0 °C.

Keywords: Carbondioxide capture and storage, Oxy-fuel combustion, Flue gas.

1. Introduction

The energy demand of the earth is increasing due to the growing numbers of people. This demand is mainly answered by the use of fossil fuels. The use of fossil fuels as energy sources results increased amounts of greenhouse gases (GHGs) deposited in the atmosphere. As a result, the effect of this deposition over global climate change is an increasingly troubling matter. The largest part of the GHG emissions are made of carbon dioxide (CO₂) (Rubin and de Coninck, 2005).

It has been predicted by the International Energy Agency that population of the earth will be over 9 billion and the energy demand is expected to rise by 30% (International Energy Agency, 2017). Fossil fuels are expected to play a major role in meeting the demand in 2040 as well. The share of fossil fuels for energy generation in GHG's are approximately 30%. In addition, it has been pointed out that the

amount of carbon dioxide concentration in the atmosphere is the most prominent sources of global warming and climate change (Elias et al., 2018). It has been stated that the concentration of carbon dioxide in the atmosphere is 400 ppm. Based on the predicted increase of the fossil fuel use, it is expected that the CO₂ concentration will be 500 ppm in the year 2050 and 800 ppm in 2100 (Wennersten et al., 2015). Furthermore, in order to prevent melting of ice caps, which is one of the main indicators of global warming, CO₂ concentrations should be held at 350-550 ppm (Hansen et al, 2008). Some of the major actions to reduce CO₂ emissions are (Leung et al., 2014):

- Increasing the energy efficiency
- The increased dependency to low CO₂ emission sources such as natural gas, nuclear energy and hydrogen
- Widespread use renewable energy
- Carbon capture and storage (CCS) technologies

Based on a scenario for the year 2050, by the International Energy Agency (IEA), CCS technologies may reduce the CO₂ concentrations between 14-17% (International Energy Agency, 2013).

CCS technologies can be defined as the separation, capture and transportation of compressed CO₂ in the flue gas of any process and storage of CO₂ (Wennersten et al., 2015). CCS technologies are reviewed in two categories as commercial ones (or close to commercialization) and at the research phase. Major types of CCS technologies are:

- Pre-combustion CO₂ capture
- Post-combustion CO₂ capture
- Oxy-fuel (oxy-combustion)

The principal of pre-combustion CCS is gasification, which is the processing of solid fuels under oxygen lacking conditions to produce carbon monoxide (CO), hydrogen (H₂) and CO₂. The CO in the product of gasification is converted into CO₂ by water gas shift reaction and separated by physical solvents. Remaining H₂ is used to produce electricity in gas turbines (Å & Chalmers, 2015). However, the reliability of gasification processes are relatively lower than combustion processes, which means the probability of failures are higher and process requires high maintenance.

In post-combustion methods, the flue gas from a combustion process is passed through CO₂ separation unit before releasing into the atmosphere. It is possible to capture 90% of the CO₂ in the flue gases. Even though there are many alternatives to separate CO₂ from the flue gas, the most common method is amine scrubbing. In this method, CO₂ in the flue gas is adsorbed in the amine solvents such as monoethanolamine (MEA) and diethanolamine (DEA) and it is required for CO₂ to be desorbed and solvents to be regenerated in order to be reused. However, the disadvantages of this method are the cost and handling of chemical solvents, lower overall plant efficiency and regeneration process' CO₂ emissions.

The concept of oxy-combustion is based on oxygen-enriched air as oxidizer instead of air. To provide pure oxygen (O₂) to the system, nitrogen (N₂) is separated from the air by separation methods. The pure O₂ stream is mixed with recycled flue gas in order to prevent excessive flame temperatures and adverse effects of lack of N₂ in heat transfer. The main purpose is to obtain a flue gas that consists mostly CO₂, O₂ and water vapour. Which eliminates the need for separation of CO₂ from the flue gas. Same with air-fired plants, heated flue gas is used to produce superheated steam in order to generate electricity in the steam turbines and sent into flue gas cooling, compression and capture to separate CO₂ from the flue gas without any chemical process.

Oxy-fuel (or oxy-combustion) first emerged as a method to obtain high flame temperatures for glass, metal and cement industry to increase efficiency in 1970's (Baukal, 1998). Abraham et al., proposed that oxy-fuel could be used in the control of CO₂ emissions and increasing the efficiency of oil extraction (Abrahams et al., 1982). Oxy-fuel is first proposed as a way to produce electricity with CCS efficiently in 2000's. The attention to this subject is increasing as the newer pilot and demonstration scale oxy-fuel power plants built. The success of such plants will promote the utilization of oxy-fuel in commercial scale plants (Wall et al., 2009). The advantages of oxy-fuel can be listed as (Rubin et al., 2007):

- Possibility of obtaining inert nitrogen free flue gas therefore, the capture of CO₂ without additional chemical processes.
- Lower NO_x emissions compared to air combustion due to flue gas recycling prevention of NO_x producing reaction mechanisms.
- Due to lower flow rate of flue gas, the possibility of using smaller combustion equipment.
- Applicability to existing power plants.

So far, the pilot and demo scale trials of oxy-fuel combustion were in the atmospheric boiler pressure conditions. It is proposed that the increased boiler pressures in oxy-fuel combustion may increase the overall plant efficiency and prevent air leakages. High-pressure oxy-fuel (HiPrOx) or pressurized oxy-fuel concept is under research and compared with atmospheric conditions in terms of efficiency and parasitic load (the reduction of electrical output by the addition of CCS).

Hong et al, investigated the effect of boiler pressures in an oxy-fuel plant utilizing coal-water slurry as fuel source, in terms of efficiency and emissions in a simulation. This study concluded that the increased parasitic load by the pressurization of boiler by producing high-pressure oxygen in the air separation unit (ASU) is lower than the increase of output energy. Compression work in the CO₂ capture and compression stage is also less than atmospheric conditions (Hong et al., 2009).

In conclusion, the advantages of pressurized oxy-fuel over atmospheric oxy-fuel are:

- Prevention of air leakages into the system and possible nitrogen dilution of the flue gas
- Increased convective heat transfer efficiency
- Availability of flue gas vapour condensation due to increased pressure
- Prevention of steam bleeding from turbines due to increased thermal efficiency
- Smaller equipment sizes
- Less compression requirement due to increased pressure of the flue gas (Hong et al, 2009)

This study is aimed at low temperature and high-pressure CO₂ separation and capture from the flue gas produced by combustion of the mixtures of Turkish coals, biocoals and biomass in a bubbling fluidized bed boiler under high-pressure boiler conditions. Based on the literature work that has been done on this subject it is found that cryogenic conditions are favourable for efficient CO₂ capture and separation process.

Cryogenic CCS depends on separation of carbon dioxide from the flue gas by means of compression and liquefaction under low temperatures. Cryogenic distillation and separation processes have been used to produce high purity carbon dioxide commercially. Temperatures below -73,3°C are considered cryogenic region (Olajire et al., 2010). Process involves the separation due to phase changing conditions of carbon dioxide in the flue gas. Based on these conditions liquid or solid carbon dioxide can be separated from flue gas. Additionally the process can be operated at high-pressure conditions that can condense the water vapour in the flue gas (Schussler et al., 1989; Aaron et al., 2005).

One of the most important issues in cryogenic CCS is the required amount of compression for liquefaction, purification and transportation of carbon dioxide. Thus, the design and operating conditions

of cryogenic CCS unit is dependent on required carbon dioxide product specifications (Besong et al., 2013).

Based on these observations, this project aims to come up with an alternative to the cryogenic conditions in CCS with higher pressures and temperatures. For this purpose, ChemSep and CHEMCAD simulation programs are used to determine the experiment matrices and evaluation of experimental results. The mentioned simulation parameters and results are explained further in the second section of this paper.

2. Experimental

2.1. Setup

CO₂ separation and capture experiments are carried out in the setup shown in Figure 1 below. It is possible to operate the setup temperatures between 263 to 288K and pressures up to 150 bar.

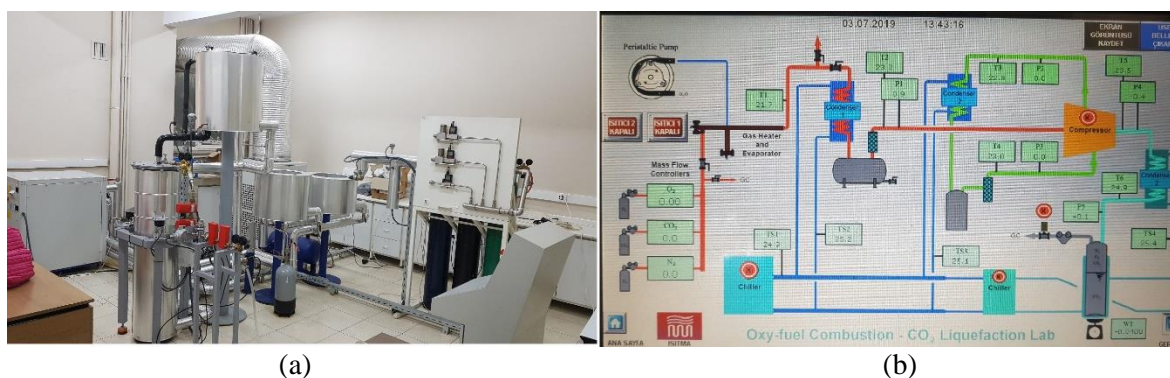


Figure 1. Laboratory scale CCS experiment setup (a) and process flow diagram (b)

Experimental setup installed in the laboratory consists of five main units: Flue gas simulating unit, separation of water from highly enriched CO₂ simulated flue gas, CO₂ capture and storage, PLC system and gas chromatography system.

Flue gas simulating unit consists pure gas cylinders, mass flow controllers (MFC), water evaporator and peristaltic pump. Flow of pure gases are adjusted to simulate the flue gas from an oxy-fuel combustion boiler and fed into mixing line. Water is fed in liquid form into the evaporator to add vapour to the flue gas if required. Compressor and three condensers working in conjunction with two chiller units pressurize and cool down the simulation gas to the desired conditions. Vapour in the stream is condensed and stored in two knockout drums in the system. Dry simulation gas is pressurized in 40L, liquid CO₂ collecting drum with cooling jacket around. The weight of the CO₂ collection drum is measured with 3 load cells and read through connected screen and PLC unit. The weight data is used in the calculations of liquefaction efficiency. Gas phase of the accumulated vapour-liquid mixture is evacuated into a line with gas chromatograph (GC) connected to it. GC is used to measure the composition of the vapour phase, collected in the drum. Liquid phase of the drum can be calculated by equations of state of choice based on the gas phase composition data. Entire system is controlled through programmable logic controller (PLC) that have 14 sensors that can measure variables such as temperature, pressure, flowrate and weight.

Owing to newly developed large scale, experimental setup liquefaction of CO₂ has been successfully carried out at the temperatures between -10 and 0 °C and pressures between 35 to 80 bars. The results show that as the temperature decrease the operable pressure range increases. Meaning, based on desired CO₂ specifications operating conditions can be set. As the results of experiments and thermodynamic

simulations show while pressure increasing at the constant temperature purity of liquid CO₂ decrease while the amount of liquid CO₂ increase. Thus, it is possible to get high yield of CO₂ using high pressures at the temperatures between -10 and 0 °C.

2.2. Materials

In order to simulate the flue gas that has been purified from particulate matter, sulphur and nitrogen based emissions, CO₂, N₂ and O₂ gases with 99, 99 % purity is used. Vapour can be added to the system in liquid phase and evaporated. Carrier gas of GC is selected as helium. To prevent the freezing of coolant of chillers, water-ethylene glycol mixture is used.

2.3. Methods

Simulation data sets are collected to investigate the phase behaviour of the simulation gas, which is a three-component mixture. ChemSep version 7.41 is used. System is designed as a flash separator and Peng-Robinson equation of state is selected to calculate phase behaviour. The obtained simulation data sets are limited to filter out undesired values. Limit values are selected to have a minimum liquefaction of 50% rate in CO₂ and purity of 90%. Based on these limitations, experiment matrices are developed. The composition of simulation gas is selected as follows: 85% CO₂, 8% N₂ and 7% O₂. Experiments are carried out 263K, 268K, and 273K set points and pressure range is 40-80 bar.

In order to reach the desired temperature values, two chiller units are started at the beginning of the experimental procedure. Temperature of the coolants around condenser and tank jackets are observed through the PLC unit. Flowrate of simulation gases are set accordingly to flue gas compositions, in the flue gas simulation unit. Compressor turned on to start the gas flow into the system. Simulation gases first passes through three condenser units for cooling down. Compressor pressurizes the gases in the liquid CO₂ collection drum. Based on the pressure reading from the drum, sampling solenoid valves are operated for GC analysis. The drum is stationed on load cells to measure out weight of the collected gases.

Liquid phase compositions are calculated through thermodynamic simulation programs that utilize equations of states whereas vapour phase compositions are experimentally determined. Quantitative analysis is made with mass and component balances. These balances are given below.

Overall Mass Balance:

$$F = L + V \quad (1)$$

Component Mass Balance:

$$x_{bi} * F = x_{si} * L + y_{gi} * V \quad (2)$$

In these formulas, F: total mass of the fed simulation gas (kg), L= mass amount of the liquid phase accumulated in the drum (kg), V: mass amount of the vapour phase accumulated in the drum (kg), x: liquid phase weight fraction, y: gas phase weight fraction, b: feed stream, g: vapour phase, s: liquid phase and i: component.

Liquefied gas efficiency is calculated with the equation below.

$$Liquefaction\ efficiency(\%) = \left(\frac{m_{liq}}{m_{feed}} \right) * 100 \quad (3)$$

In this equation, m_{liq} is the liquefied mass of gas (kg); m_{feed} is total mass of the feed gas (kg). This equation can be solved for CO₂ amounts to give the compression efficiency. However, it should be noted that single phase, liquid region conditions yield 100% in this equation even though purity is lower than desired. The evaluation of this efficiency should be done in conjunction with the CO₂ purity of the liquid phase.

3. Results

Experimental results are visualized in the figures 2 to 5.

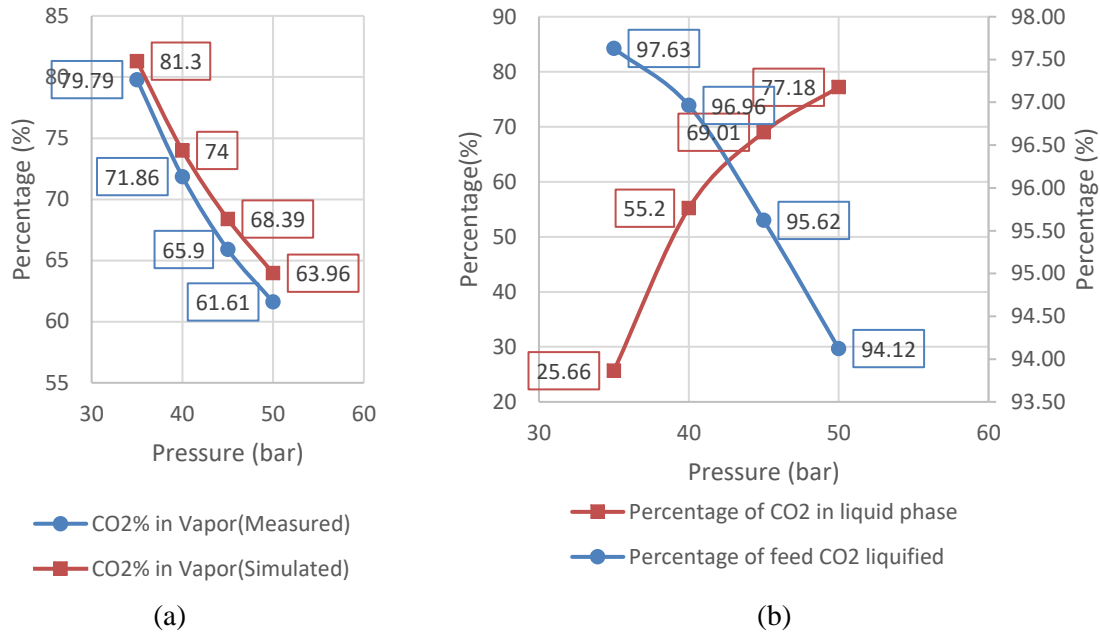


Figure 2. Experiment results for 263K. (a)Vapor phase CO₂ percentages as measured and simulated, (b)Liquid phase CO₂ purity against liquefaction efficiency

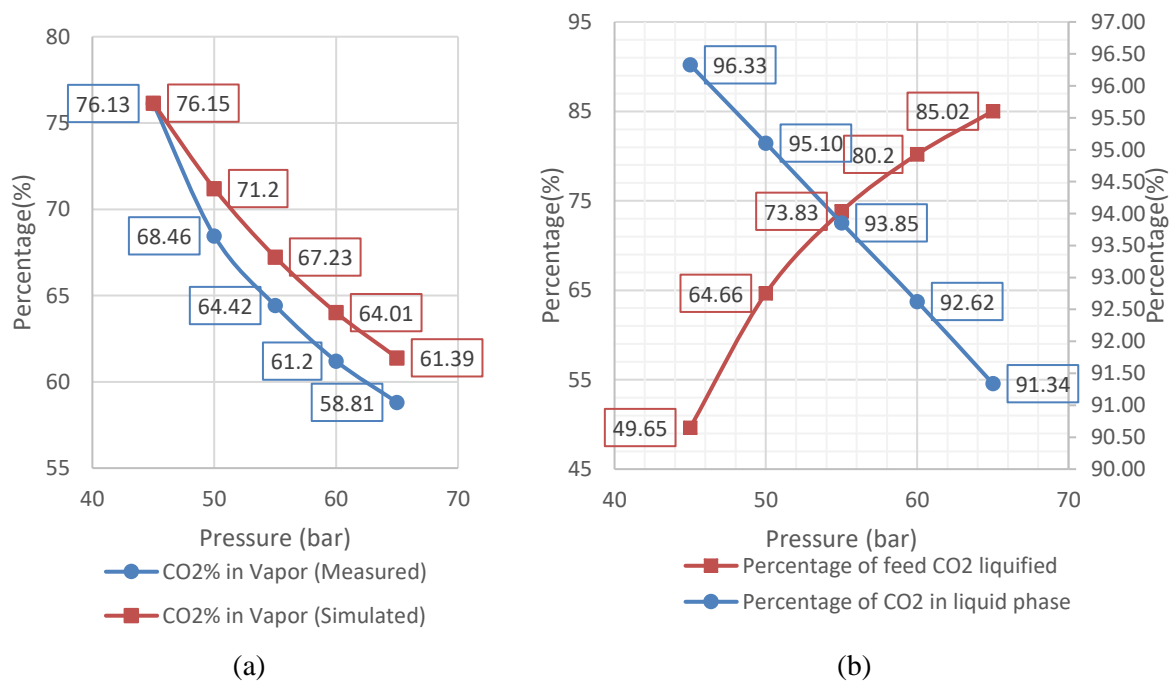


Figure 3. Experiment results for 268K. (a)Vapor phase CO₂ percentages as measured and simulated, (b)Liquid phase CO₂ purity against liquefaction efficiency

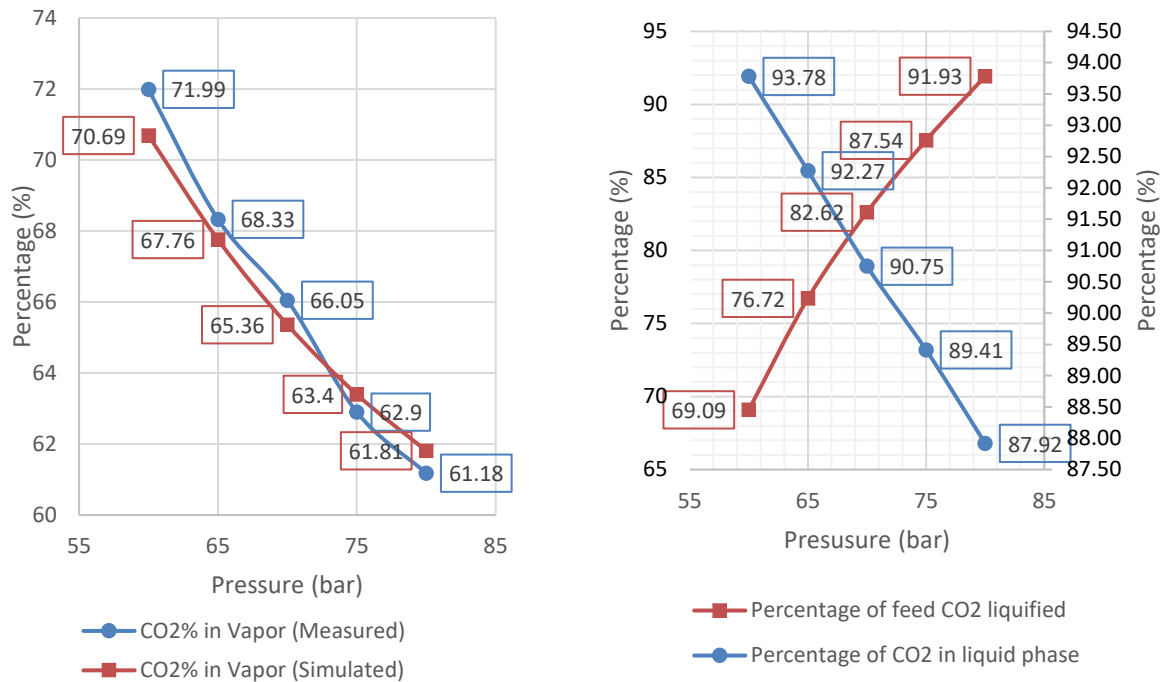


Figure 4. Experiment results for 273K. (a)Vapor phase CO₂ percentages as measured and simulated, (b)Liquid phase CO₂ purity against liquefaction efficiency

Based on the graphics above, it is observed that available pressure range, for the specified purity and minimum liquid flowrate limits, is decreasing as temperature increases. These results show compatibility with the simulation results stated in section 2.3. Thus, it is concluded that lower temperatures are favorable for larger operating pressure ranges. It is clear that, at constant temperatures, increasing pressure results in higher liquefaction flowrates. However, as the flowrate increases, impurities such as O₂ and N₂ condense as well, resulting lower CO₂ purity. With this in mind, calculation of the efficiency is done with the flowrate values that have minimum CO₂ purity of 90%. These efficiency values are compared against pressure with three different temperatures in figure 5.

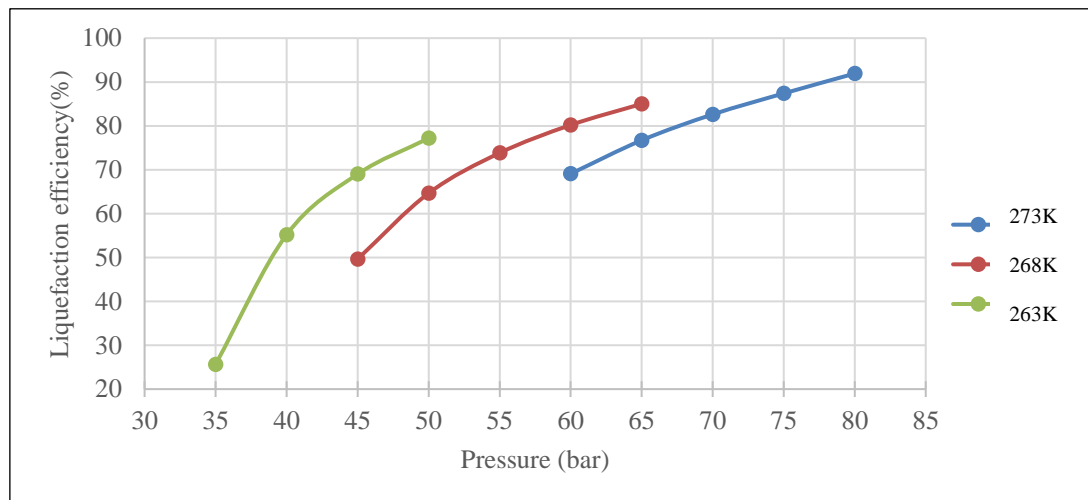


Figure 5. Comparison of CO₂ capture efficiencies in different temperatures with variable pressure

It can be concluded from figure 5 that CO₂ liquefaction efficiency is inversely proportional with temperature at constant pressure. Investigation of desired high-pressure values for efficient CO₂ capture and separation in oxy-fuel and high pressure oxy-fuel combustion is the next step of this study.

4. References

- Aaron, D., Tsouris, C., 2005. Separation of CO₂ from flue gas: a review. *Separation Science and Technology*. 40(1-3), 321–348.
- Abraham, B. M., Asbury, G., Lynch, E. P., Teotia, A. P. S., 1982. Coal-oxygen process provides CO₂ for enhanced recovery. *Oil Gas Journal*. 80, 11, 68–70.
- Besong, M. T., Maroto-Valer, M. M., Finn, A. J., 2013. Study of design parameters affecting the performance of CO₂ purification units in oxy-fuel combustion. *International Journal of Greenhouse Gas Control*. 12, 441–449.
- Charles, E., Baukal, 1982. *Oxygen Enhanced Combustion*. Allentown Pennsylvania: CRC Press.
- Rubin, E., de Coninck, H., 2005. *IPCC Special Report on Carbon Dioxide Capture and Storage*. Cambridge University Press, *Cost Curves for CO₂ Storage, Part 2*, Cambridge.
- Leung, D. Y. C., Caramanna, G., Maroto-valer, M. M., 2014. An overview of current status of carbon dioxide capture and storage technologies. *Renewable Sustainable Energy Reviews*. 39, 426–443.
- International Energy Agency, 2017. Chapter 1: Introduction and scope, *World Energy Outlook 2017*, 33–61, 2017.
- International Energy Agency, 2013. *Technology Roadmap Carbon capture and storage*, Paris.
- Lasek, J. A., Głód, K., Janusz, M., Kazalski, K., Zuwała, J., 2012. Pressurized oxy-fuel combustion: A study of selected parameters. *Energy and Fuels*. 26, 6492–6500.
- Andries, J., Becht, J.G.M., 1996. Pressurized fluidized bed gasification of coal using flue gas recirculation and oxygen injection. *Energy Conversion and Management*. 37, 855–860.
- J. G. Á, Chalmers, H., 2008. Carbon capture and storage. *Energy Policy*. 36, 4317–4322.
- Hansen, J., Sato, M., Kharecha, P., Beerling, D., Masson-delmotte, V., Pagani, M., Raymo, M., Royer, D.L., Zachos, J.C., 2008. Target Atmospheric CO₂: Where Should Humanity Aim? *The Open Atmospheric Science Journal*. 2, 217–231.



Hong, J., Chaudhry, G., Brisson, J.G., Field, R., Gazzino, M., Ghoniem, A.F., 2009. Analysis of oxy-fuel combustion power cycle utilizing a pressurized coal combustor. *Energy*. 34, 9, 1332–1340.

Rubin, M.B., Edward S., Rao, A., Berkenpas, B., 2007. *Oxygen-based Combustion Systems (Oxyfuels) with Carbon Capture and Storage (CCS)*, Pittsburgh.

Olajire, A. A., 2010. CO₂ capture and separation technologies for end-of-pipe applications—a review. *Energy*. 35(6), 2610–2628.

Soundararajan, R., Gundersen, T., 2013. Coal based power plants using oxy-combustion for CO₂ capture: Pressurized coal combustion to reduce capture penalty. *Applied Thermal Engineering*. 61, 1, 15–122.

Wennersten, R., Sun, Q., Li, H., 2015. The future potential for Carbon Capture and Storage in climate change mitigation - An overview from perspectives of technology, economy and risk. *Journal of Cleaner Production*. 103, 724-736.

Schussler, U., Kummel, R., 1989. Carbon dioxide removal from fossil fuel power plants by refrigeration under pressure. In *Energy Conversion Engineering Conference, 1989. IECEC-89.*, Proceedings of the 24th Intersociety, pp. 1789–1794, IEEE.

Wall, T., Liu, Y., Spero, C., Elliott, L., Khare, S., Rathnam, R., Zeenathal, F., Moghtaderi, B., Buhre, B., Sheng, C., Gupta, R., Yamada, T., Makino, K., Yu, J., 2009. An overview on oxyfuel coal combustion-State of the art research and technology development. *Chemical Engineering Research and Design*. 87, 1003–1016.

Acknowledgements

The works presented in this paper have been performed in the frame of “The Development of Pressurized Combustion Technologies for Coal, Biofuel An Biocoals Under Oxygen-Rich Conditions” project and supported by TUBITAK ARDEB under the contract number 216M358.

Non-ignorable pollution source: airborne microplastics

Emine Can-Guven

Department of Environmental Engineering, Faculty of Civil Engineering, Yıldız
Technical University, Istanbul, Turkey

ecguven@yildiz.edu.tr

Abstract. Plastics have become an indispensable part of our daily lives and their production is increasing day by day due to their widespread use. As a result, global plastic pollution has become a noteworthy issue. Plastics are grouped into macroplastics (> 25 mm), mesoplastics (5-25 mm), microplastics (MPs) (<5 mm) and nanoplastics (<100 nm) according to their size. In the environment, MPs are resulted from primary sources (plastic pellets) and secondary sources through the breakdown of large plastics. MP pollution has been investigated in different environmental media besides atmospheric transport and exposure of MPs has become one of the notable subjects. In this study, literature studies on MP presence and distribution in atmospheric environment were reviewed. Due to their small size, there is an exposure to MPs through inhalation, which raises various potential health effects. It was also determined that MPs could serve as a vector for particulate matter and other pollutants in the air. Natural source fiber particles were mainly detected in the studies that investigated MP pollution in the air. The presence of MPs in air is important not only because of health effects but also being a source to other environmental media in terms of atmospheric deposition. The number of studies investigating MP pollution in the atmosphere is limited. Thus, detailed and comprehensive studies on determining MP concentrations in the air as well as their health effects are required.

Keywords: Atmospheric fallout, Fibers, Indoor air, Inhalation, Outdoor air.

1. Introduction

Commercial production of plastics, which are widely used, started in the 1950s and is estimated to reach 350 million tons in 2017 (PlasticsEurope, 2018). The most commonly produced plastics are polypropylene (PP), polyethylene (PE), polyvinyl chloride (PVC), polyurethane (PUR), polyethylene terephthalate (PET) and polystyrene (PS) (PlasticsEurope, 2018). Due to the increasing world population, plastic production and usage increases and the resulting plastic pollution gains importance. It is estimated that 60-99 million tons of plastic waste is generated in 2015 and this amount is estimated to be 155-265 million tons/year in 2060 (Lebreton and Andrady, 2019). The light weight of plastic particles allows long distance transport and is detected even in Arctic and Antarctic waters, which are considered to be away from pollution sources (Waller et al., 2017). They are also expressed as resistant to degradation and biodegradation (Li et al., 2018). Plastics, which have many uses, are grouped according to their size as macroplastics (> 25 mm), mesoplastics (5-25 mm), microplastics (<5 mm) and nanoplastics (<100 nm) (Stock et al., 2019).

Studies on plastic pollution started in the 1970s, but microplastics (MPs) were first demonstrated by Thompson et al. (2004). MPs that attract attention due to the increase in plastic pollution have been the subject of many studies and the presence and distribution of them were investigated in many environmental mediums such as sea water (Wang et al., 2016), fresh water sources (Lin et al., 2018), drinking water (Mintenig et al., 2019), wastewater (Raju et al., 2018), soil (Rillig, 2012), sludge (Talvitie

et al., 2017), sediment (Lots et al., 2017) and sea sand (Yu et al., 2016). In addition, MPs were detected in aquatic organisms such as fish (Lusher et al., 2013), whale (Lusher et al., 2015), mussels (Qu et al., 2018) and sea turtles (Caron et al., 2018). MPs, which are commonly detected in environmental mediums, are capable of adsorbing hydrophobic organic pollutants such as polyaromatic hydrocarbons, organochlorinated pesticides, polychlorinated biphenyls, and heavy metals such as cadmium, zinc, nickel and lead due to their hydrophobic properties (Wright and Kelly, 2017). Therefore, MPs are considered as vector pollutants for priority pollutants (Wright and Kelly, 2017) and persistent organic pollutants (Bakir et al., 2014) which were banned due to their health effects.

Atmospheric environment is an important pathway in the transport of pollutants as well as one of the main areas that humans are exposed to various pollutants. Among these pollutants MPs should be evaluated at all points. Although MPs have been investigated in various environmental compartments, there are limited number of studies on the occurrence and fate of MPs in atmospheric environment. In this study, literature studies on MP presence and distribution in atmospheric environment were reviewed.

2. Microplastics

Plastic, name of a class of materials, is used in various fields to express the properties and attitude of materials. This term is also used to define a class of materials called polymers which are large molecules having commonly long chain-like molecular structure. Polymers that can be softened by heating and given a shape are mainly referred to plastic materials (GESAMP, 2015). The studies on plastics gone back to 1990s; however microplastic term was first mentioned in a study conducted by Thompson et al. (2004). They are defined as small plastic materials which have a size of lower than 5 mm at the first international research workshop on the occurrence, effects and fate of microplastic marine debris in 2008 (Arthur et al., 2008). The production of most common polymers and resources of microplastics are shown in Figure 1.

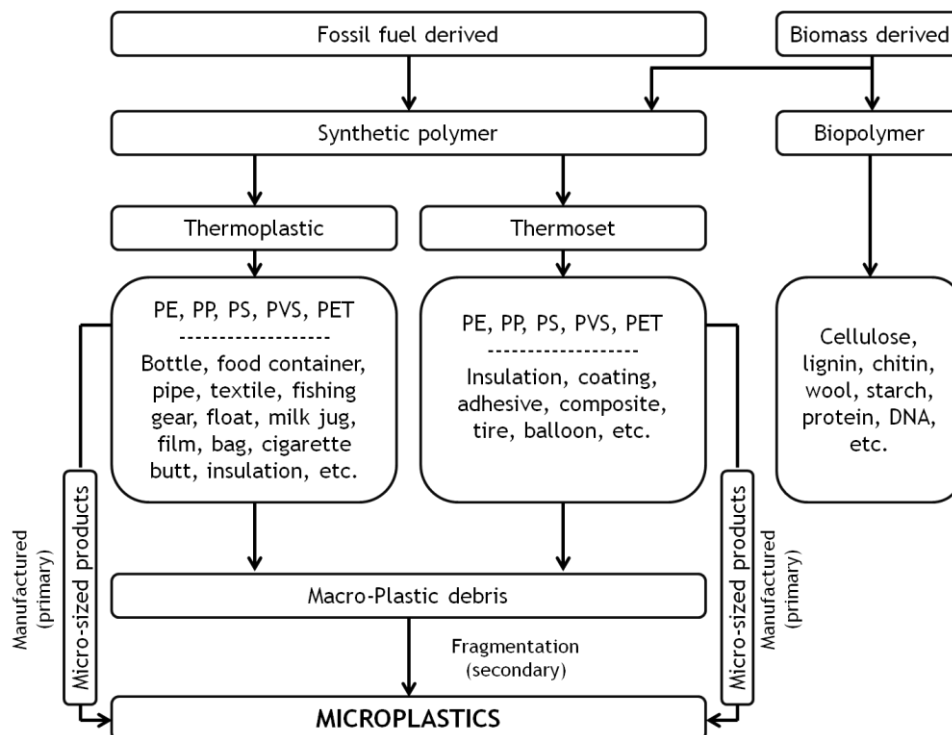


Figure 1. Production and sources of microplastics (GESAMP, 2015)

Though many different types of plastics are produced the most common ones are polypropylene (PP), polyethylene (PE), polyvinyl chloride (PVC), polyurethane (PUR), polyethylene terephthalate (PET) and polystyrene (PS) (PlasticsEurope, 2018). Plastics are generally synthesized from fossil fuels while biomass may be used as an alternative source (GESAMP, 2015). MP sources in the environment are referred to as direct sources (pellets) and secondary sources resulting from the disintegration of large plastics (Rezania et al., 2018). Primary MP pollution may arise from plastic production and/or recycling processes (Rezania et al., 2018) as well as daily activities such as using of personal care products (face wash gels, toothpastes, shower gels) (Conkle et al., 2018) and washing machines (Salvador Cesa et al., 2017). Secondary MP pollution is caused by mechanical, photolysis, thermal decomposition, thermo-oxidation and biodegradation processes of plastics found in marine litter, sanitary landfills, industrial or agricultural sources (Rezania et al., 2018).

Human exposure to MPs detected in environmental compartments may be caused by food (especially seafood), direct ingestion by mouth especially by children with dust particles found in the indoor environment (Gasperi et al., 2017). Studies have shown that MPs are present in nutrition products used for human consumption such as seafood (Rochman et al., 2015; Dehaut et al., 2016), drinking water (Kosuth et al., 2017), salt (Karami et al., 2017), sugar and honey (Liebezeit and Liebezeit, 2013). Exposure to MPs in such a widespread area is inevitable (Rist et al., 2018). The presence of microplastics in the atmospheric environment leads to inhalation exposure (Wright and Kelly, 2017). In a study conducted outdoor air in China, it was reported that 21 particles of MPs are inhaled daily (Liu et al., 2019). Once enter the human body, MPs may reach to the lungs and cause various health problems including inflammations as well as cancer (Pauly et al., 1998).

Airborne microplastics

Although MP pollution has been investigated in various environmental compartments, there are limited number of studies on the occurrence and fate of MPs in atmospheric environment (Table 1). In a study investigating the presence of MPs in indoor air, outdoor air and offices in urban and semi-rural areas, synthetic fibers were detected in house dust and indoor air (Dris et al., 2017). In another study in which atmospheric MP deposition was examined, it was determined that fibers were settled as dry or wet deposition from atmosphere (Dris et al., 2016). In another study in which atmospheric MP deposition was examined, MPs type of PE, PP and PS were determined, with fibers being dense (Cai et al., 2017). In the studies investigating atmospheric deposition in England (Stanton et al., 2019) and China (Liu et al., 2019) natural origin and synthetic fibers were found to be common in the air environment. In an indoor study, textile-borne microfibers were detected in house dust (Sundt et al., 2014). In addition to indoor dusts, dusts found in outdoor air also contain MPs and are a potential source of exposure (Dehghani et al., 2017). Besides the studies carried out in urban environments, MPs are also detected in areas that are thought to be away from pollution sources (Allen et al., 2019) indicating that MPs are transported by air. MP fibers and particles were also detected in the outdoor air at the intercity terminal in Sakarya, Turkey and soil and outdoor air on the university campus, but MP species were not identified (Kaya et al., 2018).

It is predicted that MPs entering the human body through inhalation may pose a health risk, cause acute and/or chronic inflammations and may have consequences leading to cancer (Pauly et al., 1998). In addition, it is stated that exposure to MPs in the air, especially in working environments, may cause chronic irritation, inflammation and cancer in individuals (Prata, 2018). In studies investigating the health effects of MPs, it is stated that air exposure is too important that could not be ignored (Gasperi et al., 2017; Wright and Kelly, 2017). However, the lack of airborne studies restricts the full assessment of the health effects of MPs.

Table 1. Researches on airborne microplastics

Study area	Properties of study area	Sample type	Results	Reference
Paris, France	Urban and sub-urban	Atmospheric fallout	<ul style="list-style-type: none"> • 2- 355 particles/m²/day • 29% synthetic fibers • 3-10 ton/year fibers deposited 	(Dris et al., 2016)
Paris, France	2 private apartments and one office	Indoor air	<ul style="list-style-type: none"> • 1.0-60.0 fibers/m³ • Deposition rate: 1586 and 11,130 fibers/day/m² 	(Dris et al., 2017)
Paris, France	Out of the apartments and office	Outdoor air	<ul style="list-style-type: none"> • 0.3-1.5 fibers/m³ • 67% natural material, primarily cellulosic • 33% fibers contain petrochemicals with polypropylene being predominant 	(Dris et al., 2017)
Dongguan, China	City center	Atmospheric fallout	<ul style="list-style-type: none"> • PE, PP, and PS were identified • Fiber, foam, fragment, film were found, and fiber was the dominant • The concentrations of non-fibrous microplastics and fibers:175-313 particles/m²/day 	(Cai et al., 2017)
Sakarya, Turkey	Intercity terminal	Outdoor air	<ul style="list-style-type: none"> • 9057-30,793 fibers and fragments in 30 min sampling 	(Kaya et al., 2018)
Trent catchment, UK	River catchment area	Outdoor air	<ul style="list-style-type: none"> • Natural textile fibers represented 93.8% of the textile fiber quantified 	(Stanton et al., 2019)
Shanghai, China	Municipal districts	Outdoor air	<ul style="list-style-type: none"> • 67% microfibers, 30% fragments, 3% granules • Textile clothes are likely major source 	(Liu et al., 2019)
French Pyrenees	Remote area	Atmospheric deposition	<ul style="list-style-type: none"> • 249 fragments, 73 films and 44 fibers per square meter 	(Allen et al., 2019)

3. Conclusions

Global plastic pollution is increasing in parallel with plastic production and usage. Microplastics have gain importance as a part of plastic pollution due to their physicochemical properties. In this study, literature studies on atmospheric microplastic pollution were evaluated and the main outcomes are as follows:

- There are limited studies on atmospheric microplastics.
- There is not a unique expression of the results thus comparison of studies is not possible. Therefore standard expressions of the results are needed.
- There is not a standard sampling and analysis procedure for airborne MPs. Thus, a standard analysis protocol should be presented.
- Dominance of natural fibers was indicated in some studies.
- More studies including indoor and outdoor air should be conducted especially covering urban areas to assess human exposure.

4. References

- Allen, S., Allen, D., Phoenix, V.R., Le Roux, G., Durántez Jiménez, P., Simonneau, A., Binet, S., Galop, D., 2019. Atmospheric transport and deposition of microplastics in a remote mountain catchment. *Nat. Geosci.* 12, 339.
- Arthur, C., Baker, J., Bamford, H., 2008. International research workshop on the occurrence, effects, and fate of microplastic marine debris, in: *Conference Proceedings*. Sept. pp. 9–11.
- Bakir, A., Rowland, S.J., Thompson, R.C., 2014. Transport of persistent organic pollutants by microplastics in estuarine conditions. *Estuar. Coast. Shelf Sci.* 140, 14–21.
- Cai, L., Wang, J., Peng, J., Tan, Z., Zhan, Z., Tan, X., Chen, Q., 2017. Characteristic of microplastics in the atmospheric fallout from Dongguan city, China: preliminary research and first evidence. *Environ. Sci. Pollut. Res.* 24, 24928–24935.
- Caron, A.G.M., Thomas, C.R., Berry, K.L.E., Motti, C.A., Ariel, E., Brodie, J.E., 2018. Ingestion of microplastic debris by green sea turtles (*Chelonia mydas*) in the Great Barrier Reef: Validation of a sequential extraction protocol. *Mar. Pollut. Bull.* 127, 743–751.
- Conkle, J.L., Báez Del Valle, C.D., Turner, J.W., 2018. Are we underestimating microplastic contamination in aquatic environments? *Environ. Manage.* 61, 1-8.
- Dehaut, A., Cassone, A.-L., Frère, L., Hermabessiere, L., Himber, C., Rinnert, E., Rivière, G., Lambert, C., Soudant, P., Huvet, A., others, 2016. Microplastics in seafood: benchmark protocol for their extraction and characterization. *Environ. Pollut.* 215, 223–233.
- Dehghani, S., Moore, F., Akhbarizadeh, R., 2017. Microplastic pollution in deposited urban dust, Tehran metropolis, Iran. *Environ. Sci. Pollut. Res.* 24, 20360–20371.
- Dris, R., Gasperi, J., Mirande, C., Mandin, C., Guerrouache, M., Langlois, V., Tassin, B., 2017. A first overview of textile fibers, including microplastics, in indoor and outdoor environments. *Environ. Pollut.* 221, 453–458.
- Dris, R., Gasperi, J., Saad, M., Mirande, C., Tassin, B., 2016. Synthetic fibers in atmospheric fallout: A source of microplastics in the environment? *Mar. Pollut. Bull.* 104, 290–293.
- Gasperi, J., Wright, S.L., Dris, R., Collard, F., Mandin, C., Guerrouache, M., Langlois, V., Kelly, F.J., Tassin, B., 2017. Microplastics in air: Are we breathing it in? *Curr. Opin. Environ. Sci. Heal.* 1, 1–5.
- GESAMP (Joint Group of Experts on the Scientific Aspects of Marine Environmental Protection), 2015. Sources, fate and effects of microplastics in the marine environment: a global assessment. *J. Ser. GESAMP Reports Stud.* 90, UK, 96 pages.
- Karami, A., Golieskardi, A., Choo, C.K., Larat, V., Galloway, T.S., Salamatinia, B., 2017. The presence of microplastics in commercial salts from different countries. *Sci. Rep.* 7, 46173.
- Kaya, A.T., Yurtsever, M., Çiftçi Bayraktar, S., 2018. Ubiquitous exposure to microfiber pollution in the air. *Eur. Phys. J. Plus.* 133, 488.
- Kosuth, M., Wattenberg, E. V, Mason, S.A., Tyree, C., Morrison, D., 2017. Synthetic polymer contamination in global drinking water. https://orbmedia.org/stories/Invisibles_plastics/multimedia, Accessed in September 2019.
- Lebreton, L., Andrady, A., 2019. Future scenarios of global plastic waste generation and disposal. *Palgrave Commun.* 5, 6.
- Li, J., Liu, H., Paul Chen, J., 2018. Microplastics in freshwater systems: A review on occurrence, environmental effects, and methods for microplastics detection. *Water Res.* 137, 362–374.
- Liebezeit, G., Liebezeit, E., 2013. Non-pollen particulates in honey and sugar. *Food Addit. Contam. Part*

A 30, 2136–2140.

Lin, L., Zuo, L.Z., Peng, J.P., Cai, L.Q., Fok, L., Yan, Y., Li, H.X., Xu, X.R., 2018. Occurrence and distribution of microplastics in an urban river: A case study in the Pearl River along Guangzhou City, China. *Sci. Total Environ.* 644, 375–381.

Liu, K., Wang, X., Fang, T., Xu, P., Zhu, L., Li, D., 2019. Source and potential risk assessment of suspended atmospheric microplastics in Shanghai. *Sci. Total Environ.* 675, 462–471.

Lots, F.A.E., Behrens, P., Vijver, M.G., Horton, A.A., Bosker, T., 2017. A large-scale investigation of microplastic contamination: Abundance and characteristics of microplastics in European beach sediment. *Mar. Pollut. Bull.* 123, 219–226.

Lusher, A.L., Hernandez-Milian, G., O'Brien, J., Berrow, S., O'Connor, I., Officer, R., 2015. Microplastic and macroplastic ingestion by a deep diving, oceanic cetacean: The True's beaked whale *Mesoplodon mirus*. *Environ. Pollut.* 199, 185–191.

Lusher, A.L., McHugh, M., Thompson, R.C., 2013. Occurrence of microplastics in the gastrointestinal tract of pelagic and demersal fish from the English Channel. *Mar. Pollut. Bull.* 67, 94–99.

Mintenig, S.M., Löder, M.G.J., Primpke, S., Gerdt, G., 2019. Low numbers of microplastics detected in drinking water from ground water sources. *Sci. Total Environ.* 648, 631–635.

Pauly, J.L., Stegmeier, S.J., Allaart, H.A., Cheney, R.T., Zhang, P.J., Mayer, A.G., Streck, R.J., 1998. Inhaled cellulosic and plastic fibers found in human lung tissue. *Cancer Epidemiol. Biomarkers Prev.* 7, 419–428.

PlasticsEurope, 2018. *Plastics - the Facts 2018* An analysis of European plastics production, demand and waste data, 60 pages.

Prata, J.C., 2018. Airborne microplastics: Consequences to human health? *Environ. Pollut.* 234, 115–126.

Qu, X., Su, L., Li, H., Liang, M., Shi, H., 2018. Assessing the relationship between the abundance and properties of microplastics in water and in mussels. *Sci. Total Environ.* 621, 679–686.

Raju, S., Carbery, M., Kuttykattil, A., Senathirajah, K., Subashchandrabose, S.R., Evans, G., Thavamani, P., 2018. Transport and fate of microplastics in wastewater treatment plants: implications to environmental health. *Rev. Environ. Sci. Biotechnol.* 17, 637–653.

Rezania, S., Park, J., Md Din, M.F., Mat Taib, S., Talaiekhosani, A., Kumar Yadav, K., Kamyab, H., 2018. Microplastics pollution in different aquatic environments and biota: A review of recent studies. *Mar. Pollut. Bull.* 133, 191–208.

Rillig, M.C., 2012. Microplastic in terrestrial ecosystems and the soil? *Environ. Sci. Technol.* 46, 6453–6454.

Rist, S., Carney Almroth, B., Hartmann, N.B., Karlsson, T.M., 2018. A critical perspective on early communications concerning human health aspects of microplastics. *Sci. Total Environ.* 626, 720–726.

Rochman, C.M., Tahir, A., Williams, S.L., Baxa, D. V., Lam, R., Miller, J.T., Teh, F.-C., Werorilangi, S., Teh, S.J., 2015. Anthropogenic debris in seafood: Plastic debris and fibers from textiles in fish and bivalves sold for human consumption. *Sci. Rep.* 5, 14340.

Salvador Cesa, F., Turra, A., Baruque-Ramos, J., 2017. Synthetic fibers as microplastics in the marine environment: A review from textile perspective with a focus on domestic washings. *Sci. Total Environ.* 598, 1116–1129.

Stanton, T., Johnson, M., Nathanail, P., MacNaughtan, W., Gomes, R.L., 2019. Freshwater and airborne textile fibre populations are dominated by 'natural', not microplastic, fibres. *Sci. Total Environ.* 666,



377–389.

Stock, F., Kochleus, C., Bänsch-Baltruschat, B., Brennholt, N., Reifferscheid, G., 2019. Sampling techniques and preparation methods for microplastic analyses in the aquatic environment – A review. *TrAC - Trends Anal. Chem.* 113, 84–92.

Sundt, P., Schulze, P.-E., Syversen, F., 2014. Sources of microplastic-pollution to the marine environment. *Mepex Nor. Environ. Agency*, 108 pages.

Talvitie, J., Mikola, A., Setälä, O., Heinonen, M., Koistinen, A., 2017. How well is microlitter purified from wastewater? – A detailed study on the stepwise removal of microlitter in a tertiary level wastewater treatment plant. *Water Res.* 109, 164–172.

Thompson, R.C., Olson, Y., Mitchell, R.P., Davis, A., Rowland, S.J., John, A.W.G., McGonigle, D., Russell, A.E., 2004. Lost at sea: where is all the plastic? *Science.* 304, 838.

Waller, C.L., Griffiths, H.J., Waluda, C.M., Thorpe, S.E., Loaiza, I., Moreno, B., Pacherres, C.O., Hughes, K.A., 2017. Microplastics in the Antarctic marine system: An emerging area of research. *Sci. Total Environ.* 598, 220–227.

Wang, J., Tan, Z., Peng, J., Qiu, Q., Li, M., 2016. The behaviors of microplastics in the marine environment. *Mar. Environ. Res.* 113, 7–17.

Wright, S.L., Kelly, F.J., 2017. Plastic and human health: a micro issue? *Environ. Sci. Technol.* 51, 6634–6647.

Yu, X., Peng, J., Wang, J., Wang, K., Bao, S., 2016. Occurrence of microplastics in the beach sand of the Chinese inner sea: The Bohai Sea. *Environ. Pollut.* 214, 722–730.

Long-term airborne monitoring of lead pollution by lichen *Flavoparmelia caperata* in Ramsar region, north of Iran

Ahmad Jahangiri¹, Amin Dalvand¹ and Reza Ghasemi²

¹Dept of Earth Sciences, University of Tabriz, Tabriz, Iran

²Geological Survey and Mineral Explorations of Iran, Tehran, Iran

A_jahangiri@tabrizu.ac.ir

Abstract. Epiphytic lichens have been widely used as biomonitors of metal deposition at a country level. The purpose of this study was to investigate the changes in the amount of Pb contamination in Ramsar city, in north of Iran. The lead content for three consecutive years (2013, 2014 and 2015) is determined with using Epiphytic lichen *Flavoparmelia caperata* (L.) Hale. In order to analyze of Pb contents we used the ICP-OES device and a total of 28 samples were taken separately each year and analyzed. The results of the thallus analysis of lichens showed that the mean concentrations of Pb for 2013, 2014, and 2015 were 3.18, 2.45 and 1.80 mg / kg (dry weight) respectively. In addition, the review and comparison of GIS maps for lead contamination revealed a gradual decrease from 2013 to 2015 for the contents of this element. This could be due to the reduction of lead access levels in polluting sources such as vehicle fuel, due to the laws in force in the country (reduced leaded petrol consumption). Also, comparison of lead values from the analysis revealed a very low level of contamination of the element for the study area, which indicates the optimal air quality in the studied area relative to this element. This study, which is based on the integration of ArcGIS and thallus analysis data, indicates that epiphytic lichens are valuable biological monitoring in the assessment of air pollution and mapping the environmental pollution levels map to heavy metals.

Keywords: Lichens, Biomonitor, Lead, Pollution, Air quality.

1. Introduction

Environmental pollution with heavy metals is a global hazardous that is related to human activities such as mining, smelting, energy and fuel production, power transmission, intensive agriculture, sludge dumping, melting operations, and vehicle emissions (Koz, et al., 2010). All the heavy metals at high concentrations have strong toxic effects and are regarded as environmental pollutants (Nedelkoska and Doran, 2000). Many of heavy metals may have detrimental effects to the human health. For instance lead (Pb) is the most significant toxin of the heavy metals, and the inorganic forms are absorbed through ingestion by food and water, and inhalation (Ferner, 2001). Lead is known to cause neurological disorders, anemia, kidney damage, miscarriage, lower sperm count, hepatotoxicity in higher concentration (ATSDR, 2007; 2008), and acute and chronic damage to the central nervous system (CNS) and peripheral nervous system (PNS) (Ogwuegbu and Muhanga, 2005). It affects children by leading to the poor development of the grey matter of the brain, thereby resulting in poor intelligence quotient (IQ) (Udedi, 2003). Therefore, long-term monitoring such as metals is needed in evaluating the quality of environment and in assessment the increase or decrease of contaminants in the vicinity of urban regions.

The use of biomonitors to evaluate environmental contamination has advantages, as they are easier to sample, allow a long-term monitoring with a large number of sampling sites, and also the simultaneous determination of several pollutants within the same matrix (Wolterbeek, 2002). Lichens are valuable

biomonitors of atmospheric pollution and are widely used for monitoring air pollution, either as bioindicators of air quality or as bioaccumulators of atmospheric deposition (Nimis et al., 1993; Garty, 1993; Purvis et al., 2008; Mendil et al., 2009; Loppi et al., 2004; Dalvand, et al., 2016). Lichens have played prominent roles in air pollution studies and have been defined as 'permanent control systems' for air pollution assessment (Garty, 1993; Sloof, 1995; Pignata et al., 2007; Conti, 2008). In addition, lichens as biomonitors have several advantages over conventional air sampling techniques such as easy sampling, low cost and the possibility of monitoring extensive areas, in any season, which make them useful for spatial and temporal evaluation of the pollutant accumulation in the environment (Conti and Cecchetti, 2001; Loppi et al., 2003; Scerbo et al., 2003). They can also be used for developing predictions in connection with human health (Cislaghi and Nimis, 1997).

The purpose of this study, which was carried out for the first time in Iran, was long-term monitoring to determine the annual air quality of Ramsar region of Iran, using the epiphytic lichen *Flavoparmelia caperata* (L.) Hale and GIS (Global Information System). In general, this research is based on the evaluation of lead values in lichen thalli collected from the studied area and mapping lead concentration with ArcGIS (10.2) software during the three year (2013 – 2015).

2. Materials and methods

2.1. Description of studied area

The study area is located between latitude '34°36' to 38°36' north and longitude '21°50' to '46°50' east. Ramsar has a mild and humid climate and is located at an altitude of 20 meters above sea level on the margin of the Caspian Sea and in the northern slopes of the middle Alborz mountains. The average annual temperature, precipitation and relative humidity are 16.16 mm, 1200 mm and 83%, respectively. In addition, the region has four types of dominant winds with northern, eastern, northwest, and southwest directions (data from the Islamic Republic of Iran Meteorological Organization). Due to natural attractions (climate and vegetation) and the presence of abundant spa springs, Ramsar is considered one of the most visited tourist destinations in Iran, which attracts many tourists from both the interior and the exterior.

The epiphytic lichen *Flavoparmelia caperata* (L.) Hale. was chosen for this study because of its one of the most abundant species in our studied area and is often used as a biomonitor including by another research group (e.g: Bargagli, et al., 2002; Loppi, et al., 2004; Baptista et al., 2008; Godinho, et al., 2008; Koz et al., 2010; Paoli, et al., 2012). The sampling was carried out in august month for each year (2013 – 2015), and thalli of the foliose lichen *F. caperata* were collected for lead analysis at 28 sampling station during the three year (Figure 1).

Only the peripheral part of the thalli (up to 5mm from lobe tips) was selected for the analysis, in *F. caperata* this part roughly corresponds to 1 year age and can be easily separated from the bark, being distinguishable by a paler color and absence of rhizinae. (Paoli, et al., 2012). Therefore, at each sampling station, only this parts were carefully collected from 10-15 thalli growing on bark of 5-10 trees (chiefly Orange (*Citrus Sinensis*)) between 100 and 200 cm from ground.

In laboratory, each sample was carefully cleaned under a binocular microscope with a plastic tweezers to remove foreign matter such as bark pieces, moss samples, soil particles and etc. (Yenisoy-Karakas and Tuncel, 2004; Paoli, et al., 2012). Samples were not washed, because the washing process may unpredictably alter their chemical composition (Bettinelli et al., 1996).

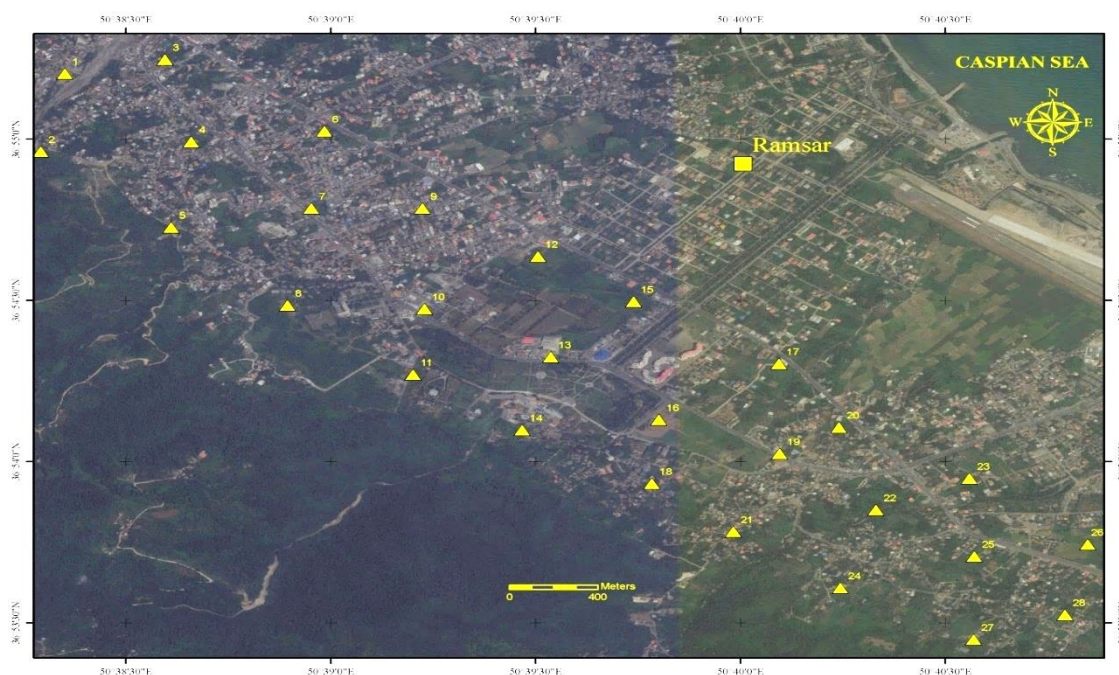


Figure 1. Location of 28 sampling station in studied area (Ramsar)

2.2. Analytical methods

Determinations were carried out using a Perkin Elmer Model Optima 2000 DV spectrometer (Perkin Elmer, USA) ICP-OES. Samples were dried in an oven at 40°C till constant weight was achieved. The dried samples were then grounded with a Mixer Grinder and sieved through a 100 microns mesh. All the samples were originally stored in closed plastics bags until analysis. For the wet digestion a mixture of HNO₃/H₂O₂ was used in this study. For this procedure, the temperature was maintained at 120°C for 2 h during digestion of 1.0 g of plant sample with 16 mL of 6:2 HNO₃/H₂O₂ mixtures on the hot plate. After cooling, 10 mL of distilled water was added on the sample and mixed. The residue was filtered through filter paper and then the sample was diluted to 50 mL with distilled water. Metal contents of final solution were determined by ICP-OES (Marin et al., 2011). Analytical quality was checked by analyzing the Standard Reference Material (SRM) IAEA-336. Also, the Detection Limit of lead in plant samples was 0.1 mg/kg.

Table 1. The lead concentrations and its ranges in lichens *Flavoparmelia caperata* (mg/kg d.w), collected from Ramsar region during 5 years (2013-2017).

Samples	(2013) Pb*	(2014) Pb	(2015) Pb
1	2.68	1.75	1.13
2	1.46	0.91	0.36
3	2.43	1.96	1.14
4	1.72	0.83	0.38
5	1.31	1.05	0.56
6	2.52	1.81	1.10
7	1.94	1.43	0.81
8	1.65	1.04	0.85
9	2.88	2.25	1.68
10	2.38	1.92	1.32
11	1.79	1.35	0.98
12	2.75	2.18	1.74
13	3.93	3.05	2.48
14	3.61	3.21	2.41
15	4.94	3.56	3.15
16	3.84	3.25	2.53
17	5.66	4.71	3.36
18	3.42	3.11	2.52
19	3.57	2.73	1.92
20	5.22	4.58	3.24
21	3.41	2.91	2.08
22	3.72	2.13	1.81
23	4.83	4.05	3.26
24	3.35	2.75	2.02
25	3.51	1.95	1.56
26	4.62	3.81	3.06
27	2.83	2.18	1.84
28	3.12	2.14	1.32
Range	1.31-5.66	0.83- 4.71	0.36-3.36
Average	3.18	2.45	1.80

3. Results and Discussion

Based on the results of the analysis (Table 1), the mean concentrations of Pb for 2013, 2014, and 2015 were obtained 3.18, 2.45 and 1.80 mg / kg (d.w) respectively. Comparison of the results shows a gradual decrease for the mean concentration of lead from 2013 to 2015 (Figure 2). In addition, the mapping of Pb contamination for 2013, 2014, and 2015, as shown in Fig. 2 is arranged using ArcGIS (10.2), which makes the comparison which displays a gradual decrease from 2013 to 2015 for lead contamination levels. Lead is an unnecessary and toxic element for plants (Muhammad et al., 2008). The limit for this element in plants and air is 2 µg/g (WHO, 1996) and 2-1 µg/m³ (Siegel, 2002). In general, their comparison with Bargagli and Nimis (2002) (Table 2), Pb contamination, was very low. In other words, all lead values were obtained are less than 10.

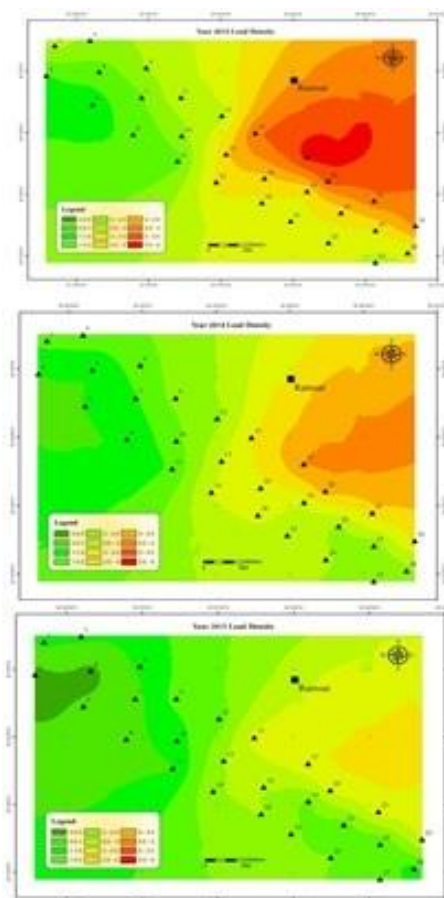


Figure 3. The distribution map of lead concentration in lichen samples for 2013 to 2015.

With regarding of extensive forest cover in the Ramsar area and the lack of notable mining and industrial activity, lead pollution is attributed to automobile fuel consumption. Lead in leaded gasoline and its concentration can be mainly related to traffic activity (Aslan et al., 2013). The lead to gasoline is released through vehicles in the environment and plants (ATSDR, 2008). Contamination of Pb in tourist areas could result in the transport of vehicles due to the high traffic volume of tourists in these areas (Loppi and Printzos, 2003).

Table 2. Comparison of the results of the F.L. caperata Tale elemental analysis with Bargagli and Nimis (2002), which is based on the concentration of the trace elements in mg / kg of dry weight of the sample.

Air Pollution	Pb
Very low	10>
Low	25
Moderate	55
High	95
Very high	95<

4. Conclusion

The results showed that the level of Pb contamination in all samples is very low, which indicates the optimal air quality in the studied areas relative to the contamination of the target element.

Given the fact that the replacement of leaded gasoline with unleaded gasoline in Iran was carried out from 2002 (Bahrami et al., 2007), the low concentration of lead in samples could be due to the gradual reduction of fuel use containing lead or other sources of potential lead contamination in the region. Therefore, one of the most probable sources of lead in samples can be due to the attraction of tourism (natural and spring springs) of Ramsar and the annual traffic of vehicles, where the rainfall and humidity of the region, its particles even in small amounts, continuously leaks out. It is suggested that the study area be evaluated in order to assess the process of reducing or increasing the pollution of lead and other airborne contaminants in future years using *F. caparata* lichen. The present study, which was carried out for the first time in the country, showed that epiphytic lichens are valuable biomonitors for assessing the degree of contamination and the trend of long-term changes in lead in the air and for a specific area.

5. References

Aslan, A., Gurbuz, H., Yazici, K., Cicek, A., Turan, M., Ercisli, S., 2013. Evaluation of lichens as bioindicators of metal pollution. *J. Elem. s.* 353-369.

ATSDR (Agency for toxic Substances and Disease Registry), (2007). Toxicological Profile for Lead. Agency for Toxic Substances and Disease Registry. U.S. Department of Health and Human services, Public Health Service, Atlanta, GA, United States.

Agency for Toxic Substances and Disease Registry(ATSDR), 2008. Division of Toxicology, Clifton Road, NE, Atlanta, GA, available at: <http://www.atsdr.cdc.gov/toxprofiles/>.

Bahrami, A., Joneidi Jafari, A., Ahmadi, H., Mahjub, H., 2007. Comparison of benzene exposure in drivers and petrol stations workers by urinary trans-muconic acid in west of Iran. *Industrial health* 45, 396-401.

Baptista, M.S., Vasconcelos, M.T., Cabral, J.P., Freitas, M.C., Pacheco. A.M.G., 2008. Copper, nickel and lead in lichen and tree bark transplants over different periods of time. *Environmental Pollution* 151, 408-413.

Bargagli, R., and Nimis, P.L., 2002. Guidelines for the use of epiphytic lichens as biomonitors of atmospheric deposition of trace elements. In: Nimis, P.L., Scheidegger, C., Wolseley, P.A. (Eds.), *Monitoring with Lichens-Monitoring Lichens*. Kluwer Academic Publishers, pp. 295-299.

Bargagli R, Monaci F, Borghini F, Bravi F, Agnorelli C., 2002. Mosses and lichens as biomonitors of trace metals. A comparison study on *Hypnum cupressiforme* and *Parmelia caperata* in a former mining district in Italy. *Environ Pollut*; 116, 279-87.

Bettinelli, M., Spezia, S., Bizzarri, G., 1996. Trace element determination in lichens by ICP-MS. *Atomic Spectroscopy* 17, 133-141.

Boamponsem, L.K., Adam, J.I., Dampare, S.B., Nyarko, B.J.B., Essumang, D.K., 2010. Assessment of atmospheric heavy metal deposition in the Tarkwa gold mining area of Ghana using epiphytic lichens. *Nuclear Instruments and Methods in Physics Research B* 268, 1492-1501.

Budka, D., Mesjasz-Przybyłowicz, J., Przybyłowicz, W.J., 2004. Environmental pollution monitoring using lichens as bioindicators: a micro-PIXE study. *Radiation Physics and Chemistry* 71, 783-784.

Carreras, H.A., Wannaz, E.D., Pignata, M.L., 2009. Assessment of human health risk related to metals by the use of biomonitors in the province of Cordoba, Argentina *Environ. Pollut.* 157, 117.



- Cislaggi, C. and Nimis, P. I., 1997. Lichens, air pollutions and lung cancer, *Nature*, 387, 463.
- Clair, S.B.St., Clair, L.L.St., Mangelson, N.F., Weber, D.J., 2002. Influence of growth form on the accumulation of airborne copper by lichens. *Atmospheric Environment* 36, 5637–5644.
- Conti ME, Cecchetti G., 2002. Biological monitoring: lichens as bioindicators of air pollution assessment – a review. *Environ Pollut*, 114:471–92.
- Dalvand, A., Jahangiri, A., Iranmanesh, J., 2016. Introduce lichen *Lepraria incana* as biomonitor of Cesium-137 from Ramsar, northern Iran, *Journal of Environmental Radioactivity*, 160, 36-41.
- Ferner DJ (2001). Toxicity, heavy metals. *eMed. J.* 2(5): 1.
- Han, J.H., and Choi, J-H., 2010. Broad Energy HPGe Gamma Spectrometry for Dose Rate Estimation for Trapped Charge Dating. *Journal of Analytical Science & Technology* 1 (2), 98 -108.
- Conti, M.E. and Cecchetti, G., 2001. Biological monitoring: lichens as bioindicators of airpollution assessment eareview. *Environ. Pollut.* 114: 471-492.
- Garty, J. 1993. Lichens as biomonitors for heavy metal pollution. p. In B. Markert (ed.) *Plants as biomonitors*. VCH, Weinheim, Germany.
- Garty, J., 2001. Biomonitoring atmospheric heavy metals with lichens: theory and application. *Crit. Rev. Plant Sci.* 20, 309–371.
- Ghio, A.J., 2004. Biological effects of Utah Valley ambient air particles in humans: a review. *Journal of Aerosol Medicine* 17, 157-164.
- Godinho, M.R., Wolterbeek, H.Th., Verburg, T., Freitas, M.C., 2009. Bioaccumulation behavior of transplants of the lichen *Flavoparmelia caperata* in relation to total deposition at a polluted location in Portugal. *Environmental Pollution* 151, 318-325.
- Koz, B., Celik N., Cevik, U., 2010. Biomonitoring of heavy metals by epiphytic lichen species in Black Sea region of Turkey. *Ecological Indicators* 10, 762–765.
- Loppi, S., Frati, L., Paoli, L., Bigagli, V., Rossetti, C., Bruscoli, C., Corsini., A., 2004. Biodiversity of epiphytic lichens and heavy metal contents of *Flavoparmelia caperata* thalli as indicators of temporal variations of air pollution in the town of Montecatini Terme (central Italy). *Science of the Total Environment* 326, 113–122.
- Loppi, S., and Pirintsos, S.A., 2003. Epiphytic lichens as sentinels for heavy metal pollution at forest ecosystems (central Italy). *Environmental Pollution* 121, 327–332.
- Marin, S., Lacrimioara., S., Cecilia., R., 2011. Evaluation of performance parameters for trace elements analysis in perennial plants using ICP-OES technique. *J. Plant Develop* (1), 87-93.
- Muhammad, F., Farooq, A., Umar, R., 2008. Appraisal of heavy metal contents in different vegetables grown in the vicinity of an industrial area. *Pak. J. Bot.* 40(5), 2099-2106.
- Nedelkoska TV, and Doran PM. 2000. Characteristics of heavy metal uptake by plants species with potential for phytoremediation and phytomining. *Minerals Engineering* 13: 549–561.



Nimis, P.L., M. Castello, and M. Perotti. 1993. Lichens as bioindicators environments of heavy metal pollution: A case study at La Spezia (N. Italy). p. the environment. Int. Conf., Vol. II, Geneva. Sept. 1989. CEP 265–284. In B. Markert (ed.) Plants as biomonitors, indicators for heavy metals in the terrestrial environment. VCH, weinheim Germany.

Ogwuegbu MOC, Muhanga W 2005. Investigation of Lead Concentration in the Blood of People in the Copperbelt Province of Zambia, J. Environ. (1): 66 – 75.

Paoli, L., Corsini, A., Bigagli, V., Vannini, J., Bruscoli, C., Loppi S., 2012. Long-term biological monitoring of environmental quality around a solid waste landfill assessed with lichens. Environmental Pollution 161,70-75.

Pirintsos, S.A., and Loppi, S., 2008. Biomonitoring atmospheric pollution: the challenge of times in environmental policy on air quality. Environmental Pollution 151, 269-271.

Peralta-Videa, J.R., Lopez, M.L., Narayan, M., Saupe, G., Gardea-Torresdey, J., 2009. The biochemistry of environmental heavy metal uptake by plants: Implications for the food chain. The International Journal of Biochemistry & Cell Biology 41, 1665–1677.

Purvis, O.W., Dubbin, W., Chimonides, P.D.J., Jones, G.C., Read, H., 2008. The multielement content of the lichen *Parmelia sulcata*, soil, and oak bark in relation to acidification and climate. Sci. Total Environ. 390, 558–568.

Siegel, F.R., 2002. Environmental Geochemistry of Potentially Toxic Metals. Springer press. Berlin, 218pp.

Szczepaniak, K., and Biziuk, M., 2003. Aspects of the biomonitoring studies using mosses and lichens as indicators of metal pollution. Environmental Research, 93:221-230.

Udedi SS (2003). From Guinea Worm Scourge to Metal Toxicity in Ebonyi State, Chemistry in Nigeria as the New Millennium Unfolds, 2(2): 13–14.

Yenisoy-Karakaş, S. and Tuncel, S.G., 2004. Geographic patterns of elemental deposition in the Aegean region of Turkey indicated by the lichen, *Xanthoria parietina* (L.) Th. Fr. Science of the Total Environment 329, 43–60.

Acknowledgment

Authors are thankful from Mrs. Sara Sadat Kazemi, in the Herbarium for Herbaceous Plant of Iran for helping in recognizing lichen samples as well as the work of Mrs. Elahe Abolhassani, in the analysis of the Laboratory of Geology and Exploration Iran, sincerely appreciate.

Forecasting of PM₁₀ concentrations in Istanbul using backpropagation neural network

Elif Palaz and Tolga Elbir

Dokuz Eylul University, Department of Environmental Engineering,
Tinaztepe Campus, Buca 35390, Izmir, Turkey

elifpalaz@yahoo.com.tr

Abstract. This study aims to predict urban air quality levels at an urban site in the city of Istanbul by an artificial neural network (ANN). PM₁₀ concentrations were predicted using hourly concentrations of other five air pollutants, i.e., SO₂, NO, NO₂, CO and O₃. Additionally, several meteorological parameters such as temperature, relative humidity, pressure, wind speed and wind direction were also used as hourly inputs of ANN. All data was obtained from Ministry of Environment and Urbanization for the period between March 2016 and April 2018. “MATLAB - Neural Network Toolbox” was used for development of the air quality prediction model. Levenberg Marquardt and Bayesian Regularization were used as the learning network model. Backpropagation Learning Algorithm was preferred since it provides fast convergence and stability in training of the model. The model was established based on 8656x11 data sets. Model data was separated into three subsets; %70 for training set, %10 for validation set and %20 for testing set. The best results were achieved when numbers of neurons were 42 and 70 for both methods. These models produced R² of 0.74 and 0.81 indicating reasonable correlations between the targets and predicted outputs.

Keywords: Artificial neural network, Air quality forecasting, Particulate matter, Prediction.

1. Introduction

Particulate matter with an aerodynamic diameter <10 μm (PM₁₀) is primarily generated by power generation, industry and transportation since it induces serious health consequences for the exposed population all over the world (Antanasijević et al., 2013). Many studies indicated that high PM₁₀ concentrations may play a role in respiratory diseases such as asthma, coughing and painful breathing, chronic bronchitis, and decreased lung functions (Lu et al., 2015; Phosri et al., 2019). They affect the cardiovascular system and other internal organs by ingestion. Chen et al. (2018) found that exposures to PM₁, PM_{2.5} and PM₁₀ during the first three years of life significantly increased the risk of autism spectrum disorder (ASD).

Several studies have been carried out for air quality forecast using statistical models, or deterministic models that have mainly used meteorological fields and pollution dispersion. While the deterministic models are usually complex and complicated, the statistical models are simpler but also have some disadvantages. Artificial neural network (ANN) which is one of the deep learning methods belongs to the category of statistical models (Moustris et al., 2013; Pawul and Śliwka, 2016). ANN is gradually developing as a promising technique for forecasting non-linear time series information like meteorological and air quality data (Athira et al., 2018). ANNs that are inspired by biological neurons can be powerful tools for forecasting and obtaining real time information on particulate matter (De Gennaro et al., 2013).

In recent years, many studies have been done to model PM₁₀ concentrations by analysing meteorological data in order to forecast PM₁₀ levels by using ANN or other machine learning techniques (Moustris et al., 2013; Pawul and Śliwka, 2016). Most neural network models have been successfully used in prediction of PM₁₀ levels with the value of R² changing from 0.60 to 0.98 (Tecer, 2007; Hrust et al., 2009; De Gennaro et al., 2013; Chellali et al., 2016)

This paper presents the preliminary results on prediction of hourly PM₁₀ concentrations using the air pollutants (SO₂, NO, NO₂, CO and O₃) and meteorological parameters (temperature, relative humidity, pressure, wind speed and wind direction) in an urban site of Istanbul by an artificial neural network (ANN). The dataset covered the period of 2016-2018. Models based on back-propagation neural network were trained, validated and tested using the collected data. It has been attempted to achieve more accurate values for PM₁₀ concentration using the different network architectures and different training algorithms (Levenberg–Marquardt (LM) and Bayesian regularization (BR)) by MATLAB software.

2. Material and methods

2.1. Study area

There are 26 urban monitoring stations in Istanbul operated by the Ministry of Environment and Urbanization. The stations are typically located 1.5–2.0 m above the ground level (Karaca and Camci, 2010). Among these stations, Aksaray station located at 41°00'52" °N, 28°57'16" °E was selected since it is at one of the three districts in Istanbul where air pollution has been observed highly (TTD, 2017). Daily PM₁₀ concentrations were above the threshold values of National and EU Directives in 71 days and 120 days in 2018, respectively. Annual average PM₁₀ concentration was 52.4 µg/m³ in 2018 (TCCSB, 2019). The map of the study area is given in Figure 1.

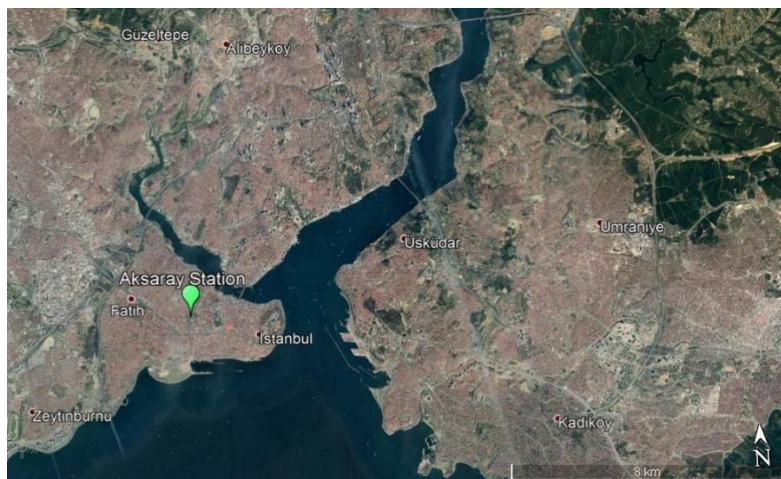


Figure 1. The map of the site

2.2. Development of ANN models

ANN is a deep learning method which has the capacity to learn, memorize and create relationships among the air quality and meteorological data. ANN is made up by simple processing units, the neurons, which are connected in a network by a large number of weighted links where the acquired knowledge is stored, and over which signals or information can pass. Multilayer perceptron ANN and nonlinear activation function are used for air quality forecast. Sigmoid function was used in the study as activation function as follows:

$$\sin(x) = \frac{1}{1 + e^x} \quad (1)$$

One of the main advantages of ANN is ability to model complex nonlinear relationships between input and output variables (Muhammadhassani et al., 2012). Multilayer artificial neural network is divided into three type layers: the input layer, the hidden layers, and the output layer. The input layer is where the data is entered to the network, the data is processed in the hidden layers, and the predicted output is obtained at the output layer. The neurons in the layers are interconnected by links called weights (Sekar et al., 2016).

In this study, input layer contains the 10 inputs such as the pollutants of SO₂, NO, NO₂, CO, O₃ and several meteorological parameters (temperature, relative humidity, pressure, wind speed and wind direction) to the network. The architecture of the ANN model used in forecasting the hourly concentrations of PM₁₀ is shown in Figure 2.

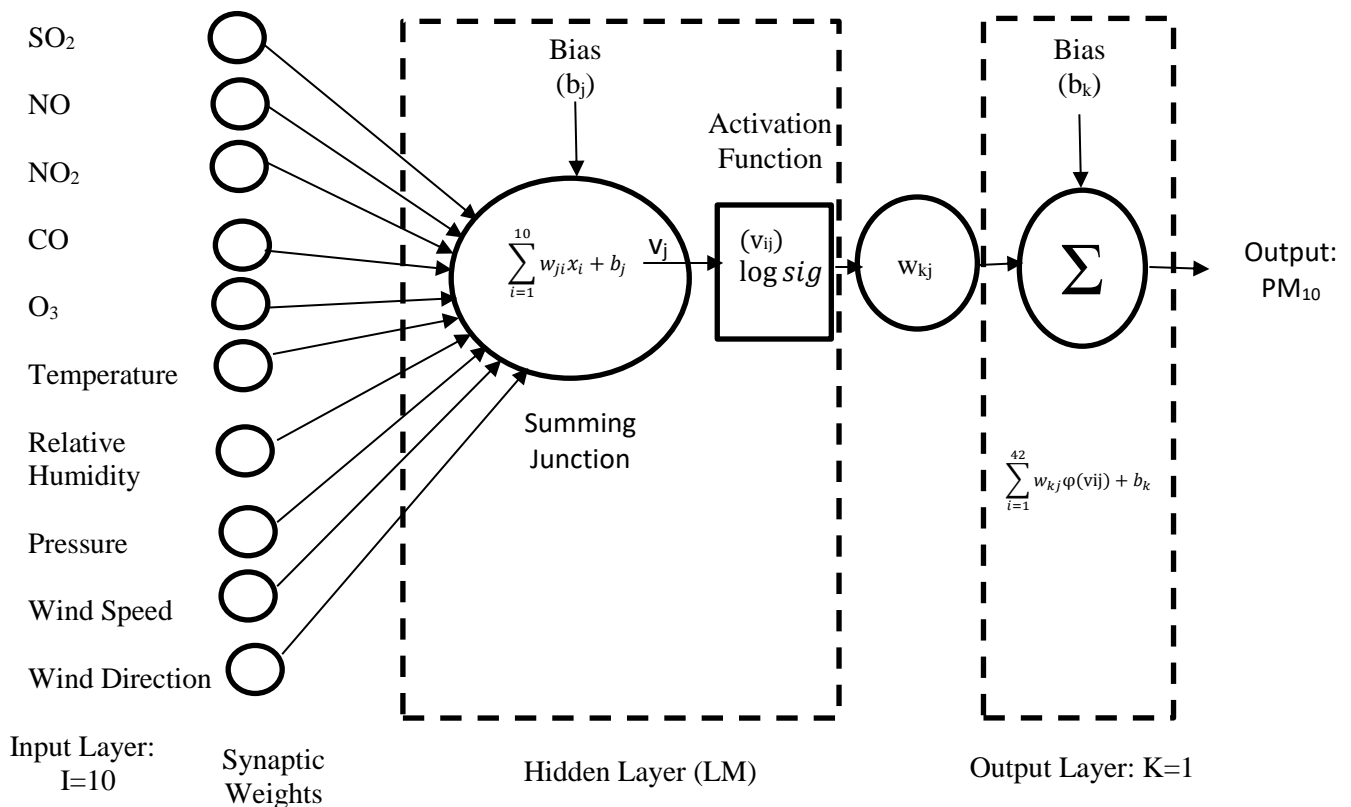


Figure 2. The architecture of the MLP type of neural network (10-42-1) in this study

Connection weights are updated using either supervised or unsupervised learning during the training (Inal, 2010). After determination of the network type, the appropriate training algorithm was selected as a multi-layer perceptron type of back-propagation neural network.

Back-propagation is the most commonly used supervised training algorithm in the multilayer feed-forward networks. In back-propagation networks, information is processed in the forward direction from the input layer to the hidden layer and then to the output layer (Sofuoglu et al., 2006). Different

forecasting algorithms have produced different results because performance of algorithms changes according to the data sets, network types, weight types, search types etc. For example, Levenberg-Marquardt (LM) algorithm can only be used with small networks because its memory requirements are proportional to the square of number of weights so it can only work with a few hundred weights (Kizilaslan and Karlik, 2008).

Training in ANNs consists of three elements: one of this is “weights between neurons that define the relative importance of the inputs”, second is an activation function that controls the generation of the output from a neuron, and last is the learning laws that describe how the adjustments of the weights are made during training. During training, a neuron receives inputs from a previous layer, weighs each input with a prearranged value, and combines these weighted inputs (Sofuoglu et al., 2006).

In this study, ANN-based models were developed to predict ambient PM₁₀ concentrations in Istanbul. “MATLAB (R2019a) - Neural Network Toolbox” was used for development of the air quality prediction model. It was used LM and BR models as training algorithms that based on Backpropagation (BP) neural network. In the BP training, learning rate (η) and momentum rate (μ) used to ‘speed up’ or ‘slow down’ the converge of error (Khare and Negendra, 2007). BP algorithm adjust the values of the weight matrices in the opposite direction of the gradient of the squared error function. However, in practice, the algorithm tends to converge very slowly, thus requiring high computational effort. To avoid the inconvenience, several optimization methods were incorporated to the BP algorithm to reduce its convergence time and mitigate the computational effort required (Da Silva et al., 2017). According to previous studies, LM and BR are the most common algorithms with success predictions for this reason (Elmas, 2003; Khare and Negendra, 2007; Sekar et al. 2016; Pawul and Śliwka, 2016). The Levenberg–Marquardt (LM) algorithm developed by Kenneth Levenberg and Donald Marquardt is suitable for ANNs dealing with moderate-sized problems (Jazayeri et al., 2016). LM algorithm is presented as Eq. 2 and 3 (Sharmer et al. 2000).

$$H = J^T J + \mu I \quad (2)$$

$$w_{k+1} = (w_k - J_k^t J_k + \mu I)^{-1} J_k e_k \quad (3)$$

where,

J: Jacobian matrix (matrix of first derivatives with respect to weight vector)

μ : Combination coefficient and,

I: Identity matrix

LM and BR are able to obtain lower mean squared errors (MSE) and higher squared-R values than any other algorithms for functioning approximation problems (Demuth and Beale, 2000). Backpropagation algorithms (especially LM) were preferred in this study since they provide fast convergence and stability in training of the models (Burney et al., 2008). The model was established based on input data set of 8656 x 10 parameters and output data set of 8656 x 1 parameters. Model data was partitioned into separate subsets; 70% for training set, 10% for validation set and 20% for testing set for all models.

Ambient air quality and meteorology data were obtained from Ministry of Environment and Urbanization for the period between March 2016 and April 2018. The data set covered all hourly meteorological parameters and PM₁₀, SO₂, NO, NO₂, CO and O₃ concentrations in $\mu\text{g}/\text{m}^3$. Before modelling, some pre-processing operations were thus applied on data set such as excluding rows with any missing data preserving hourly time index. Ambient Data Reduction and Audit Procedures (IDEM,

2017) were applied to all data for validation. Data set included missing data for some parameters on different days. A filter was then applied to exclude those days for pollutants or meteorological parameters (Nejadkoorki and Baroutian, 2012). R Programming was used for filtration the procedure criteria. Valid dataset contains 8656 hourly average samples collected from the monitoring site. The samples are further divided into three subsets, namely training (6059 groups), evaluation (866 groups) and a test set (1751 groups). The following network parameters were investigated during the development of the best network for the prediction of PM₁₀ concentrations: number of neurons in a hidden layer (varied from 5 to 80 in each hidden layer) and training algorithm (LM or BR).

All dataset were normalized to obtain similar impact of all inputs in ANN models. The normalization equation can be given as in

$$NI_{ij} = \frac{I(i,j) - \min(j)}{\max(j) - \min(j)} \quad (4)$$

In Eq. 4, I represents the input value, NI is the standardized value, i is the number of patterns and j indicates the measured value of variables (Keskin and Terzi, 2006).

2.3. Performance of models

The quality and reliability of the developed models were evaluated via several statistical indexes. Among the classical statistical criteria, the determination coefficient (R²), the mean squared errors (MSE), the root mean square error (RMSE) were used. The formulas of these indices are given in Table 1.

Table 1. Statistical performance Indices used in the study

Indices	Formulas
R ²	$\frac{\sum_{i=1}^N (A_i - P_i)^2}{\sum_{i=1}^N (A_i - \bar{A}_i)^2}$
MSE	$\frac{\sum_{i=1}^N (A_i - P_i)^2}{N}$
RMSE	$\sqrt{\frac{\sum_{i=1}^N (A_i - P_i)^2}{N}}$

3. Results and discussion

The results of the Scatter plots by using Levenberg-Marquardt algorithm models for training, validation, testing data, and all data sets are presented in Figure 3, respectively.

Selecting the number of hidden neurons for ANN is a significant stage as wrong selection can lead to either underfitting or overfitting issues, which can indeed adversely affect the overall efficiency of the model (Balram et al., 2019). Table 2 shows that “R”, “MSE” and “RMSE” values for different number of neurons in hidden layer. In the present study, the best results were achieved when hidden layer was 42 neurons. The model was evaluated using the “R” value for regression analysis of training, validation, test, and all data are 0.88, 0.82, 0.78, and 0.86, respectively.

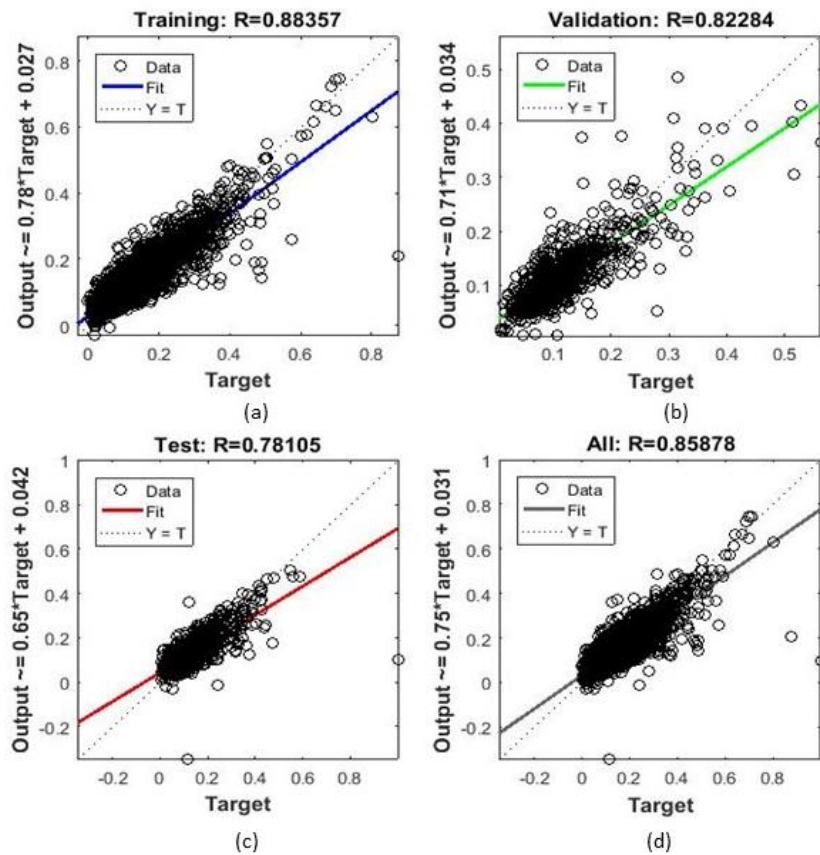


Figure 3. Scatter plots of observed versus predicted PM₁₀ concentrations for LM: (a) training data; (b) validation data; (c) testing data; (d) all data

Table 2. Evaluation of forecasting accuracy for LM

Number of Neuron in Hidden Layer	Training set data completeness	Validation set data completeness	Testing set data completeness	R-Train	R-Test	R-All	RMSE (µg/m ³)
5				0.82	0.75	0.80	19.45
10				0.81	0.81	0.81	19.88
15				0.83	0.80	0.82	18.59
20				0.85	0.80	0.84	17.73
25				0.83	0.83	0.83	19.45
30				0.87	0.81	0.85	16.87
35	70%	10%	20%	0.86	0.83	0.85	17.73
40				0.86	0.80	0.84	17.30
41				0.87	0.83	0.85	16.87
42				0.88	0.78	0.86	16.44
46				0.88	0.82	0.86	16.44
50				0.87	0.77	0.84	16.87

LM model used in this study provided a quite satisfactory accuracy, showing a correlation of 0.74 between the forecast values and the monitoring values. The similar results were obtained in previous studies in which PM₁₀ prediction was evaluated based on Backpropagation Algorithms (Tecer, 2007; Díaz-Robles et al., 2008; Zhang et al., 2013; Park et al., 2018). RMSE value was 16.44 µg/m³ when the number of hidden neurons was fixed at 42. The smaller values of RMSE denote the better model performance (Taspinar, 2015). Díaz-Robles et al. (2008) and Park et al. (2018) reported that BP produced R² was 0.74 (0.67~0.80), RMSE was 19.41~29.59 to predict PM₁₀ concentration.

BR learning algorithm was applied to same data set. The results of the scatter plots by using BR for training, testing data, and all sets are presented in Figure 4, respectively.

Optimum number of hidden layer was 70 for the model. The evaluation of forecasting accuracy for hourly PM₁₀ concentrations using BR is shown in Table 3.

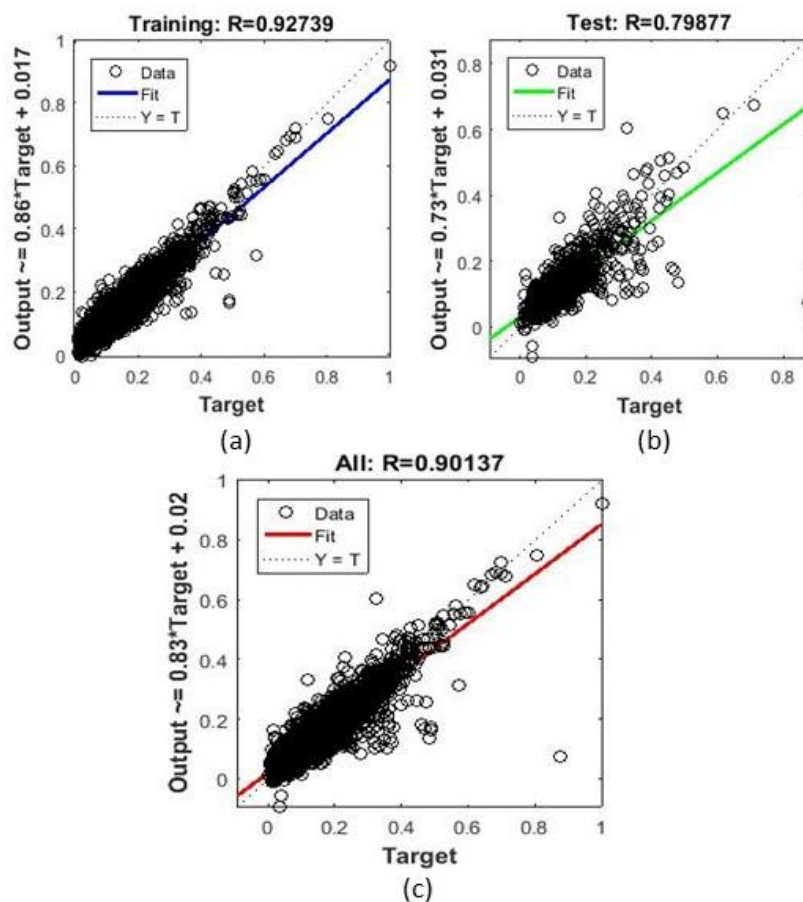


Figure 4. Scatter plots of observed versus predicted PM₁₀ concentrations for BR: (a) training data; (b) testing data; (c) all data

Table 3: Evaluation of forecasting accuracy for BR

Number of Neuron in Hidden Layer	Training set data completeness	Validation set data completeness	Testing set data completeness	R-Train	R-Test	R-All	RMSE ($\mu\text{g}/\text{m}^3$)
10				0.83	0.80	0.83	19.01
15				0.85	0.81	0.84	18.59
20				0.86	0.83	0.85	17.30
25				0.88	0.80	0.86	16.44
30				0.88	0.82	0.87	16.44
35				0.88	0.83	0.87	16.02
40				0.89	0.82	0.88	16.02
45				0.89	0.80	0.86	15.16
50	70%	10%	20%	0.90	0.80	0.87	14.73
55				0.91	0.82	0.89	14.73
60				0.91	0.83	0.89	14.73
65				0.92	0.81	0.90	13.87
70				0.93	0.80	0.90	13.01
75				0.92	0.77	0.89	13.01
80				0.91	0.83	0.89	14.30

The optimum BR architecture was found to be 1-hidden layer with 70 neurons (10-70-1). RMSE value was $13 \mu\text{g}/\text{m}^3$ when the number of hidden neurons was fixed at 70. In previous studies reported that R and RMSE value were 0.05-0.98 and $12\text{-}32 \mu\text{g}/\text{m}^3$, respectively (Hooyberghs et al., 2005; Stadlober et al., 2008; Zandi et al., 2013; Chellali et al., 2016).

Zandi et al. (2013) predicted maximum PM_{10} concentrations for the next day using the meteorological parameters in Timaru, New Zealand. The dataset was divided into training (70%), validation (15%), and test sets (15%) randomly. The Levenberg–Marquardt optimization and Bayesian Regularization training algorithms were applied to update the training weights and bias values. In this study, BR outperformed the LM algorithm as they found in the paper. BR does not require that a validation data set be separated out of the training data set. It uses all of the data. This advantage is especially noticeable when the size of the data set is small (Demuth and Beale, 2000). But the data set used in the study is large. Additionally, BR algorithm typically require longer training times than LM algorithm. So, it is impractical when it is compared with LM.

4. Conclusions

This paper presents the findings of a preliminary study focused on comparative analysis of LM and BR training algorithm for forecasting of PM_{10} concentrations in Istanbul. The results of the performed analysis showed that proposed ANN model had a significant forecasting accuracy. LM produced R^2 of 0.74 (RMSE: $16.4 \mu\text{g}/\text{m}^3$) which indicate good correlation between the targets and predicted outputs. Additionally, BR produces R^2 of 0.81 (RMSE: $13 \mu\text{g}/\text{m}^3$) for the same all data set. For instance, results of the study indicated that LM algorithm creates outputs quickly than BR, but BR obtained more reliable forecast results. The knowledge of reliable forecasts of occurrence of high air pollution levels would allow to undertake preventive actions (Pawul and Śliwka, 2016). The above findings were validated through a series of case studies, where the performance of the ANN models was evaluated for air quality

prediction. A new ANN architecture can be developed as alternative models based on back propagation algorithms in order to simultaneously predict hourly PM₁₀ concentrations in Istanbul. However, it could be identified the number of hours during the next day where PM₁₀ concentration will be above the threshold value ($[PM_{10}] \geq 50 \mu\text{g}/\text{m}^3$) according to the European Union Directive 2008/50/EC.

5. References

- Antanasijević, D. Z., Pocajt, V. V., Povrenović, D. S., Ristić, M. D., Perić-Grujić, A. A., 2013. PM₁₀ emission forecasting using artificial neural networks and genetic algorithm input variable optimization. *Science of the Total Environment*. 443, 511-519.
- Athira, V., Geetha, P., Vinayakumar, R., Soman, K. P., 2018. DeepAirNet: Applying recurrent networks for air quality prediction. *Procedia computer science*. 132, 1394-1403.
- Balram, D., Lian, K. Y., Sebastian, N., 2019. Air quality warning system based on a localized PM_{2.5} soft sensor using a novel approach of Bayesian regularized neural network via forward feature selection. *Ecotoxicology and environmental safety*. 182, 109386.
- Burney, S.M.A., Jilani, T. A., Ardil, C., 2008. Levenberg-Marquardt algorithm for Karachi stock exchange share rates forecasting. *World Acad. Sci. Eng. Technol.* 2(4), 171–176.
- Chen, G., Jin, Z., Li, S., Jin, X., Tong, S., Liu, S., Guo, Y., 2018. Early life exposure to particulate matter air pollution (PM₁, PM_{2.5} and PM₁₀) and autism in Shanghai, China: A case-control study. *Environment international*. 121, 1121-1127.
- Chellali, M. R., Abderrahim, H., Hamou, A., Nebatti, A., Janovec, J., 2016. Artificial neural network models for prediction of daily fine particulate matter concentrations in Algiers. *Environmental Science and Pollution Research*. 23(14), 14008-14017.
- Cetin E., 2003. *Yapay Sinir Ağları (Kuram, Mimari, Eğitim, Uygulama)*. Seckin Yayınları, 69-71.
- Da Silva, I. N., Spatti, D. H., Flauzino, R. A., Liboni, L. H. B., dos Reis Alves, S. F., 2017. *Artificial neural networks*. Cham: Springer International Publishing.
- De Gennaro, G., Trizio, L., Di Gilio, A., Pey, J., Pérez, N., Cusack, M., Querol, X., 2013. Neural network model for the prediction of PM₁₀ daily concentrations in two sites in the Western Mediterranean. *Science of the Total Environment*. 463, 875-883.
- Demuth, H., Beale, M., 2000. *Neural Network Toolbox User's Guide Version 4*; The Math Works Inc.: Natick. MA, USA, 5–22.
- Díaz-Robles, L. A., Ortega, J. C., Fu, J. S., Reed, G. D., Chow, J. C., Watson, J. G., Moncada-Herrera, J. A., 2008. A hybrid ARIMA and artificial neural networks model to forecast particulate matter in urban areas: The case of Temuco, Chile. *Atmospheric Environment*. 42(35), 8331-8340.
- Hrust, L., Klaić, Z. B., Križan, J., Antonić, O., Hercog, P., 2009. Neural network forecasting of air pollutants hourly concentrations using optimised temporal averages of meteorological variables and pollutant concentrations. *Atmospheric Environment*. 43(35), 5588-5596.
- Jazayeri, K., Jazayeri, M., Uysal, S., 2016. Comparative analysis of Levenberg-Marquardt and Bayesian regularization backpropagation algorithms in photovoltaic power estimation using artificial neural network. In *Industrial Conference on Data Mining*. Springer, Cham, pp. 80-95.
- IDEM, 2017. *Ambient Data Reduction and Audit Procedures*, Chapter 12. https://www.in.gov/idem/airquality/files/qa_manual_chap_12.pdf , accessed in September 2019.
- Inal, F., 2010. Artificial neural network prediction of tropospheric ozone concentrations in Istanbul, Turkey. *Clean–Soil, Air, Water*. 38(10), 897-908.

- Karaca, F., Camci, F., 2010. Distant source contributions to PM₁₀ profile evaluated by SOM based cluster analysis of air mass trajectory sets. *Atmospheric Environment*. 44(7), 892-899.
- Keskin, M.E., Terzi, O., 2006. Artificial Neural Network Models of Daily Pan Evaporation, *Journal of Hydrologic Engineering*. 11(1).
- Khare, M., Nagendra, S.S., 2006. Artificial neural networks in vehicular pollution modelling, Vol.41, Springer.
- Kizilaslan, R., Karlik, B., 2008. Comparison neural networks models for short term forecasting of natural gas consumption in Istanbul. In 2008 First International Conference on the Applications of Digital Information and Web Technologies (ICADIWT). IEEE. pp. 448-453.
- Lu, F., Xu, D., Cheng, Y., Dong, S., Guo, C., Jiang, X., Zheng, X., 2015. Systematic review and meta-analysis of the adverse health effects of ambient PM_{2.5} and PM₁₀ pollution in the Chinese population. *Environmental research*. 136, 196-204.
- Moustris, K. P., Larissi, I. K., Nastos, P. T., Koukouletsos, K. V., Paliatsos, A. G., 2013. Development and application of artificial neural network modeling in forecasting PM₁₀ levels in a Mediterranean city. *Water, Air, Soil Pollution*, 224(8), 1634.
- Mohammadhassani, J., Khalilarya, S., Solimanpur, M., Dadvand, A., 2012. Prediction of NO_x emissions from a direct injection diesel engine using artificial neural network. *Modelling and Simulation in Engineering*. 2012, 12.
- Nejadkoorki, F., Baroutian, S., 2012. Forecasting extreme PM₁₀ concentrations using artificial neural networks. *International Journal of Environmental Research*, 6(1), 277-28.
- Park, S., Kim, M., Kim, M., Namgung, H. G., Kim, K. T., Cho, K. H., Kwon, S. B., 2018. Predicting PM₁₀ concentration in Seoul metropolitan subway stations using artificial neural network (ANN). *Journal of hazardous materials*. 341, 75-82.
- Pawul, M., Śliwka, M., 2016. Application of artificial neural networks for prediction of air pollution levels in environmental monitoring. *Journal of Ecological Engineering*. 17(4).
- Phosri, A., Ueda, K., Phung, V. L. H., Tawatsupa, B., Honda, A., Takano, H., 2019. Effects of ambient air pollution on daily hospital admissions for respiratory and cardiovascular diseases in Bangkok, Thailand. *Science of the total environment*. 651, 1144-1153.
- Sekar, C., Ojha, C. S. P., Gurjar, B. R., Goyal, M. K., 2015. Modeling and prediction of hourly ambient ozone (O₃) and oxides of nitrogen (NO_x) concentrations using artificial neural network and decision tree algorithms for an urban intersection in India. *Journal of Hazardous, Toxic, and Radioactive Waste*. 20(4), A4015001.
- Sofuoglu, S. C., Sofuoglu, A., Birgili, S., Tayfur, G., 2006. Forecasting ambient air SO₂ concentrations using artificial neural networks. *Energy Sources, Part B*. 1(2), 127-136.
- TCCSB, 2019. T.C. Çevre ve Şehircilik Bakanlığı, Ulusal Hava Kalite İzleme Ağı. havaizleme.gov.tr, accessed in May 2019.
- Tecer, L. H., 2007. Prediction of SO₂ and PM Concentrations in a Coastal Mining Area (Zonguldak, Turkey) Using an Artificial Neural Network. *Polish Journal of Environmental Studies*. 16(4).
- TTD, 2017. Turk Toraks derneği Guz Sempozyumu Hava Kirliligi ve Akciger Sagligi Raporu <https://www.toraks.org.tr/subNews.aspx?sub=203¬ice=4311>, accessed in September 2019.
- Zhang, H., Liu, Y., Shi, R., Yao, Q., 2013. Evaluation of PM₁₀ forecasting based on the artificial neural network model and intake fraction in an urban area: A case study in Taiyuan City, China. *Journal of the Air & Waste Management Association*. 63(7), 755-763.



18th World Clean Air Congress, 23-27 September 2019, Istanbul
organized by TUNCAP and IUAPPA

Acknowledgments

The study was supported by Council of Higher Education under its Ph.D. scholarship program of 100/2000.

Microbial study of airborne microorganisms in indoor air of hospital in Northern Algeria

Amina Djadi^{1,2}, F. Benadda³, Farid Agouillal¹, Amel Kaced⁴, Abdelkader Lemou¹, Nabila Ait Ouakli¹, Nabila Cherifi¹ and Riad Ladji¹

¹Unité de Recherche en Analyses et Développement Technologique en Environnement, Centre de Recherche Scientifique et Technique en Analyses Physico-chimiques, Bousmail, Algeria

²Research Unit: Materials, Processes and Environment, University M'Hamed Bougara, Frantz Fanon City, Boumerdes 35000 Algeria.

³Laboratoire central, Unite microbiologie, Hospital el Kettar

⁴Centre de Recherche Scientifique et Technique en Analyses Physico-chimiques, Bousmail, Algeria

rladji@hotmail.com

Abstract. The hospital is a highly sensitive environment; it produces care and causes contamination of different compartments of the environment (air, water and soil). The control of internal pollution in a hospital environment is indispensable, because it's the first contact with patients, so it should not cause further infection or illness for the sick, especially when it comes to suppressed host immunity defenses. It is with this objective that we started this study which deals with the microbiological analysis of bioaerosols (BAs) in the indoor air of the medical emergencies of Blida hospital. We studied four operating theaters, two preoperative rooms and a resuscitation room. Sampling of indoor air was made by passive technique and the bacterial identification was done by two techniques, the Analytical Profile Index (API) system and Matrix Assisted Laser Desorption/Ionization Time of Flight Mass Spectrometry (MALDI-TOF MS). The highest contamination for bacteria is 2645 (CFU/m³) noted in postoperative 2, the lowest is observed in the traumatology block which is 191 (CFU/m³). Fungal contamination is highest in neurosurgery block 103 (CFU/m³); the lowest is in poste-operative 1 which is 6 (CFU/m³). Gram-positive cocci are the most predominant bacteria in the indoor air of medical emergencies. These bacteria can cause infections therefore increase the risk of contracting a nosocomial infection in the hospital. This study shows the importance of daily indoor air control of hospitals mainly operating theaters primarily that the patient's body is in direct contact with air. In order to reduce nosocomial infections and to create an Algerian standard that limits the rate of BAs in hospitals.

Keywords: Bioaerosols, Passive sampling, Bacterial identification, MALDI-TOF MS, API.

1. Introduction

Bio-aerosols are the present particles in the air originating from living organisms, microorganisms, and other biological materials (Martinez-Herrera et al., 2016), which include bacteria, viruses, fungi, endotoxins, β glucans, mycotoxins and allergens (Prussin and Marr, 2015, Ghosh et al., 2015, Viegas et al., 2017, Karimpour Roshan et al., 2019). It has been studied in a professional environment (Douglas et al., 2017, Yildiz et al., 2017, Necib and Boughediri, 2016) in schools and universities (Canha et al., 2015, , medical environment (Ghasemian et al., 2017, Asif et al., 2018, Okten et al., 2012), homes (Meharzi et al., 2017), sports Hall (Ramos et al., 2015) and hammam (Benammar et al., 2017).

Most of these studies attract attention to the harmful effect on health of these BAs, they may provoke infectious diseases, respiratory diseases and Cancer (Kim et al., 2017, Asif et al., 2018). The risk of getting an infection is even higher in healthcare departments where patients are more susceptible because of their health conditions, or in operating theatres because of tissue exposure to air, it has been demonstrated that periprosthetic infection rates correlate with the number of airborne bacteria within the wound (Napoli et al., 2012).

The purpose of this study is to evaluate the quantity of BAs in medical emergencies of the hospital of Blida, to identify the dominant bacteria, to be a focus for attention to the importance and the obligation of monitoring BAs in the indoor air hospital and raise awareness among health practitioners to reduce their rates in the environment, especially in operating theaters.

2. Materials and methods

2.1. Study area

The study was carried out in the medical emergency building at the hospital Frantz Fanon. The hospital is located at the center of wilaya of Blida, situated in the west of Algiers. Built in 1933, with a total area of 35 hectares and a total current capacity of 1613 beds, formerly psychiatric facility.

The sampling was realized at 3 operating rooms, post-operative room, resuscitation room and septic block. In each operating room, there is a central air conditioner, an air extractor that works once or twice a week and a sterile block that is started every 48 hours with a sterilization time of 4 hours, and after each humeno-depressive/ immunosuppressed patient. The table 1 summarizes the specialty of operating room and the average of surgery by day with the number of person present during surgery. For the septic room, the sterile block is started after each patient. The frequency of cleaning surfaces in operating theaters is after each surgery. It should be noted that sometimes the sterile block and ventilation does not work, in this case we increase the cleaning frequencies.

Table 1. Specialty of operating room and the average of surgery by day with the number of person present during surgery

Operating room	Average of surgery by day	Average of person present during surgery
General surgery block (L1)	4	8
Neurosurgery block (L2)	2	4
Traumatology block (L3)	7	8

2.2. Sampling procedure

The measurement of bacteria and fungi at different operating room were made by passive air sampling technique. The monitoring of both bacteria and fungi is made with Petri dishes (9 cm diameter) containing culture media at 1 m above the floor and at the center of the room. We have used nutrient agar and Sabouraud agar for bacteria and fungi respectively. The time of exposure for both is 1h. After exposure the sampling were taken to the laboratory and incubated at 37°C for 3 days for bacteria and at 25°C for 5 days for fungi. The determination of CFU / m³ is made by the equation reported by Hayleeyesus et al., 2014.

We have used two methods for identification of bacteria, API system and MALDI-TOF MS.

2.3. Laboratory method for bacterial identification

After incubation, Petri dishes, present colonies with different aspects and colors. Each colony is isolated on cooked blood agar until complete purification of the colony. Gram stain, oxidase and catalase are

performed on each pure colony. Most colonies come in the form of Gram-positive cocci. So a seeding on Chapman medium is carried out followed by identification by API system and by MALDI-TOF MS.

2.4. Bacterial identification by Analytical Profile Index (API)

After sample preparation, colonies were emulsified into the API Medium to achieve a homogeneous bacterial suspension of a 0.5 McFarland standard. A sterile syringe was used to distribute the bacterial suspension into the tubes and the cups are filled with specific reagents. The incubation of strips is realized at 37°C for 24 hours. The strips were read and the 7-digit numerical profile is obtained. The interpretation of results was performed with the analytical profile index by looking up the numerical profile in the list of profiles.

2.5. Bacterial identification by MALDI-TOF MS

For the identification of bacteria by Matrix Assisted Laser Desorption/Ionization Time of Flight Mass Spectrometry (MALDI-TOF MS) we have used The MALDI-TOF MS Microflex LT mass spectrometer (Bruker Daltonik, Germany) with FlexControl software (version 3.4) and biotyper software. We have used the direct transfer method and extended direct transfer method for identification of bacteria. The extended method is used as second plan if no peaks are found with the direct method, so we realize one or more subculture of some colonies for the crystallization of their proteins.

The direct method consist to smear biological material, fresh single colony from nutrient agar on the steel target plate and overlay the material with 1 µL of matrix solution [4-hydroxy-a-cyanocinnamic acid (HCCA)], within 1 hour and dry at room temperature then the target was transferred to the MALDI-TOF MS for analysis.

For extended method, fresh colony was smeared on the target overlaid with 1 µL of 70 % formic acid dried at room temperature, even its dry 1 µL of HCCA matrix is added, a second air-dried is necessary before introducing the sample for analysis by MALDI-TOF MS. Both methods are realized according to the manufacturer's instructions. Data acquisition is done in linear mode detector set 2558 v monitor 2555 v, with mass range [1986-20137] Da. UV is the source of Laser with a frequency of 60 hz and the number of shots is 40; high voltage and positive polarity.

The bacterial test standard (BTS) is Escherichia coli ATCC 25922 THL in dehydrated form. The interpretation of the identification score is based on the scale recommended by the manufacturer, highly probable species identification [2.300-3.000]; secure genus identification, probable species identification [2.000-2.299]; probable genus identification [1.700-1.999]; not reliable identification [0.000-1.699].

2.6. Statistical analysis

Data were analyzed using Statistical Package for Social Sciences (SPSS) version 20. One way ANOVA test was conducted to assess the statistical distribution and to obtain the min/max values, mean and the mean standard error of bacterial and fungal concentration recorded in the seventh locations of the investigated hospital during three days. Also the likelihood of statistically significant differences (*P-value*) between the concentrations of bacteria and fungi measured at different sampling locations and the linearity was determined between the concentrations of bacteria and fungi results.

3. Results and discussion

Airborne microorganisms was performed in the medical emergencies of the hospital of Blida, sampling was performed on 4 operating theaters (General surgery block (L1), Neurosurgery block (L2), Traumatology block (L3) and septic block (L7)), two operating posts (post-operative 1 (L4) and post-operative 2 (L6)) and a resuscitation room (L6). Both bacterial and fungal samples were taking in three consecutive days (D1, D2 and D3).

The results of the research into the concentration distribution, arithmetic mean and standard error of bacteria and fungi BAs present in the investigated locations are presented in Table 2 to Table 4 and in Figure 1.

Table 2. Number of bacterial CFU/m³ air at different sampling of the three days

Sampling day	Sampling location						
	L1	L2	L3	L4	L5	L6	L7
D1	896	485	632	1411	1852	338	441
D2	529	367	558	647	1911	440	485
D3	514	338	191	970	2645	544	529

L1:General surgery block; **L2:**Neurosurgery block; **L3:**Traumatology block; **L4:**Post-operative 1; **L5:**Post-operative 2; **L6:**Resuscitation room; **L7:**Septic block.
D1:16.01.2018; **D2:**17.01.2018; **D3:**18.01.2018.

Table 3. Number of fungi CFU/m³ air at different sampling of the three days

Sampling day	Sampling location						
	L1	L2	L3	L4	L5	L6	L7
D1	73	15	15	73	73	147	103
D2	59	103	29	59	59	44	44
D3	59	44	29	6	29	44	59

L1:General surgery block; **L2:**Neurosurgery block; **L3:**Traumatology block; **L4:**Post-operative 1; **L5:**Post-operative 2; **L6:**Resuscitation room; **L7:**Septic block.
D1:16.01.18; **D2:**17.01.18; **D3:**18.01.18.

The concentrations of bacteria and fungi BAs in the indoor environment of the medical emergency, estimated with the passive air sampling method, ranged between 191-2645 and 6-147 CFU/m³ respectively.

The highest concentration for bacteria is 2645 (CFU/m³) noted in postoperative 2 (L5) in the third day (D3), the lowest is observed in the traumatology block (L3) in D3 which is 191 (CFU/m³) (Table 5).

Fungal concentration is highest in Resuscitation Room (L6) in (D1) which is 147 (CFU/m³), while the lowest is in Poste-operative 1 (L4) in (D3) which is 6 (CFU/m³) (table 4).

Except the bacterial concentration of 460±136 CFU/m³ in the Traumatology block (L3; $P=0.077$) which seems not significant difference, the concentrations of bacteria measured in all the 6 other locations were significantly different to each other (P range from 0.002 to 0.045), the six locations can be ordered according to the highest bacteria concentration as L5, L4, L1, L7, L6 and L2 (2136±255, 1009±221, 646±125, 485±25, 447±59 and 397±45 CFU/m³ respectively).

The concentrations of fungi measured in location 2, 4, 5, 6 and 7 record not significant difference to each other ($P=0.054$ to 0.172), except General surgery block (Location 1) and Traumatology block (Location 3) which were significantly different to each other (64±5 CFU/m³, $P=0.005$ and 24±5 CFU/m³, $P=0.035$ respectively).

Table 4. Statistical distribution of bacteria and fungi (CFU/m³ air) according to the sampling day (D1 to D3) and the location (L1 to L7)

Distribution		Valid N	Min	Max	Mean	Mean Standard Error		
Per Day	General	Bacteria	21	191	2645	796	138	
		Fungal	21	6	147	55	7	
	D1	Bacteria	7	338	1852	865	214	
		Fungal	7	15	147	71	18	
	D2	Bacteria	7	367	1911	705	204	
		Fungal	7	29	103	57	9	
	D3	Bacteria	7	191	2645	819	317	
		Fungal	7	6	59	39	7	
	Per Location	L1	Bacteria	3	514	896	646	125
			Fungal	3	59	73	64	5
L2		Bacteria	3	338	485	397	45	
		Fungal	3	15	103	54	26	
L3		Bacteria	3	191	632	460	136	
		Fungal	3	15	29	24	5	
L4		Bacteria	3	647	1411	1009	221	
		Fungal	3	6	73	46	20	
L5		Bacteria	3	1852	2645	2136	255	
		Fungal	3	29	73	54	13	
L6		Bacteria	3	338	544	447	59	
		Fungal	3	44	147	78	34	
L7		Bacteria	3	441	529	485	25	
		Fungal	3	44	103	69	18	

L1:General surgery block; **L2:**Neurosurgery block; **L3:**Traumatology block; **L4:**Post-operative 1; **L5:**Post-operative 2; **L6:**Resuscitation room; **L7:**Septic block.
D1:16.01.18; **D2:**17.01.18;**D3:** 18.01.18.

The recovered samples during the three days show significant differences in both average bacterial and fungal concentrations, as recorded in Table 5 and Figure 2-(b).

The bacteria concentration of the first day was the highest (865±214 UFC/m³), in the third day, 819±317 UFC/m³ bacteria were collected; finally, the second day was characterized by a bacteria concentration of 705±204 UFC/m³.

However, the fungi concentration of the first day was the highest (71±18 UFC/m³), in the second day, 57±9 UFC/m³ fungi were collected; finally, the third day was characterized by a fungi concentration of 39±7 UFC/m³.

Contamination in the operating theaters (L1, L2, L3) remains significant compared to the literature (WHO, 1999, Cabo Verde et al., 2015, Napoli et al., 2012, Hoseinzadeh et al., 2013). This high rate may be due to the fact that it is operating theaters of medical emergencies, so at any time there may be surgery. As shown in Table 1, the number of present in different operating theaters varied between 2 to 8, as reported by many authors (Cabo Verde et al., 2015, Setlhare et al., 2014, Hayleeyesus et al., 2014, Heo et al., 2016, WHO, 1999), the variation of concentration of BAs depends on the number of present in the room and the human activity like coughing, sneezing, walking, washing and talking. In view of the urgency, the frequency of cleaning and sterilization of the blocks is not always respected. As reported

by (Asif et al., 2018 and Dehghani et al., 2018), the disinfection and sterilization directly influences the concentration of bacteria and fungi in the indoor air, the difference is significant before and after.

The postoperative 1 and 2 has too high a contamination, it may be relative to the number of beds in the room (average 10 beds) for postoperative 2 and one beds for postoperative 1, the latter is reserved for the sensitive patient, so the number of presents is relatively high in the room if it takes into consideration the number of practitioners practicing in the room. It is important to note that the room is busy all the time which increases the number of BAs in the air. The postoperative 1 which is relatively isolated (it is a small room in the great hall), presents a high contamination it is due to the cross-contamination, that is to say the passage of the pollution of the room 2 to Room 1, under the effect of the draft, the opening of the door, and the passage of people.

The scatter plots of bacteria versus fungi concentration, shows negative linear associations ($P=0.625$) with regression coefficient R^2 of 0.013 (n=21) as presented in Figure 3. This indicates that there is a very low and no significant correlation between the presence of bacteria and fungi in the seven investigated locations during the three days.

The identification of isolated bacteria in the different medical emergency departments was carried out by two techniques API system and MALDI-TOF MS, both techniques give similar results. The identification score for MALDI-TOF MS varies between 1.722 and 2.216, which gives genus identification for the values included in the interval [1.700-1.999] and species identification for the values included in the interval [2.000-2.299]. Those results are presented in Table 5.

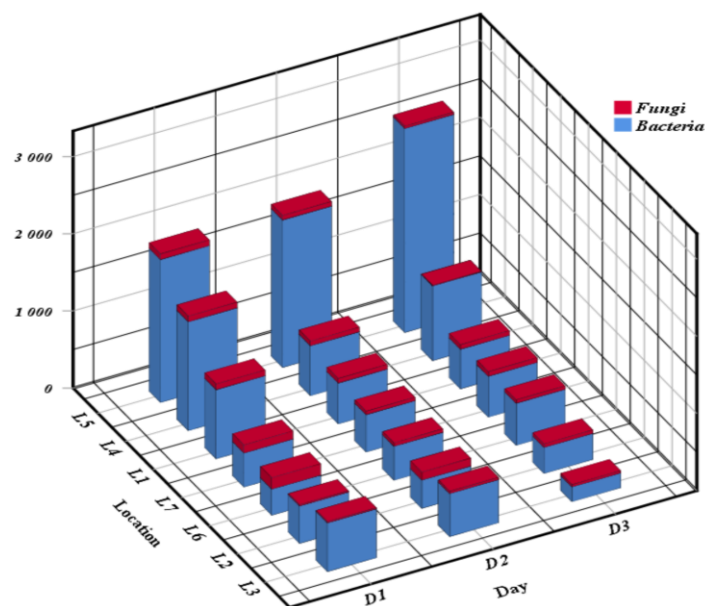


Figure 1. The range distribution in the 7 locations of the medical emergencies during the three days

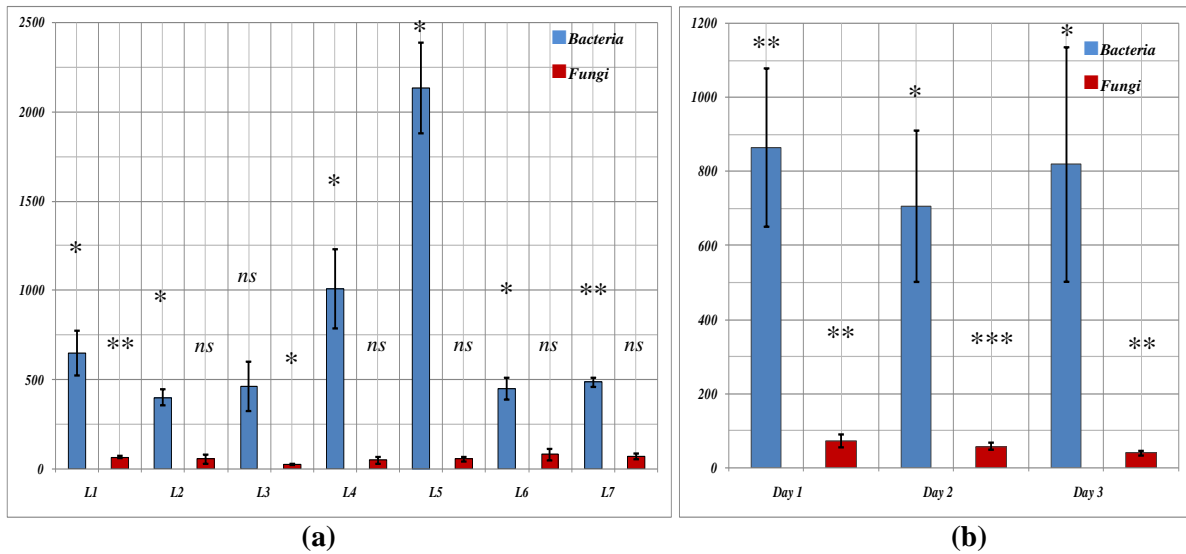


Figure 2. The mean distribution of bacterial and fungal concentration (UFC/m³) in the medical emergencies. (a) according the 7 locations (b) according the three days.
ns: not significant difference; *Significant difference; **Highly Significant difference; ***Very Highly Significant difference. L1:General surgery block; L2:Neurosurgery block; L3:Traumatology block; L4:Post-operative 1; L5:Post-operative 2; L6:Resuscitation room; L7:Septic block.
D1:16.01.18; D2: 17.01.18; D3: 18.01.18.

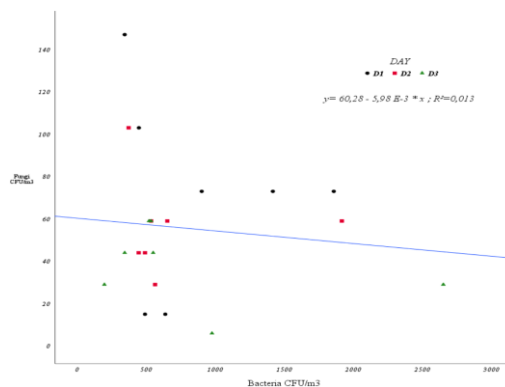


Figure 3. Scatter plots of fungal against bacteria concentration (CFU/m³) at the medical emergency

All the bacteria identified are Gram-positive cocci. We identified staphylococci with different wars (*Staphylococcus xylosus*, *Staphylococcus warneri*, *Staphylococcus lentus*, *Staphylococcus cohnii cohnii*, *Staphylococcus sciuri*, *Staphylococcus hominis*, *Staphylococcus auricularis*, and *Staphylococcus haemolyticus*). Micrococcus including *Micrococcus luteus*, Kocuria including *Kocuria marina sp*, *Kocuria rosea*, and *Kocuria varians*, an *Arthrobacter oxydans* and *Cellulomonas sp cellulomonas microbacterium*. The presence of these bacteria in the air comes from several origins, from the environment (including building, soil, alkaline waste water, dust, water, and air) and exterior of human and animals. These bacteria have a harmful effect on the health of the human; they can cause irritation, meningitis, prosthetic joint infections, skin infection and food poisoning (Asif et al., 2018, Kim et al., 2017, Pati, 2018).

Table 5. Identification of airborne bacteria in medical emergency by MALDI-TOF MS and API

Sampling site	MALDI-TOF MS identification	API system identification
General surgery block (L1)	<i>Staphylococcus xylosus</i> DSM 6179 DSM (1.796)	<i>Staphylococcus xylosus</i>
	<i>Kocuria marina</i> DSM 16420T DSM (2.005)	<i>Staphylococcus warneri</i> <i>Kocuria marina</i> sp
	<i>Kocuria rosea</i> IMET 11363T HKJ (2.216)	<i>Staphylococcus lentus</i> <i>Micrococcus</i> spp
Neurosurgery block (L2)	<i>Kocuria rosea</i> DSM 11630 DSM (1.9)	<i>Kocuria varians</i> <i>Staphylococcus cohnii cohnii</i>
Traumatology block(L3)	<i>Staphylococcus hominis</i> 18 ESL (1.933)	<i>Staphylococcus sciuri</i>
	<i>Micrococcus luteus</i> 59 PIM (1.707)	<i>Micrococcus</i> spp
	<i>Arthrobacter oxydans</i> IMET 10684T HKJ (1.952)	<i>Kocuria rosea</i>
Post-operative 1 (L4)	<i>Staphylococcus hominis</i> 18 ESL (2.055)	<i>Staphylococcus hominis</i> <i>Staphylococcus cohnii cohnii</i>
	<i>Kocuria rosea</i> IMET 11363T HKJ (1.84)	<i>Micrococcus</i> spp <i>Kocuria rosea</i> <i>Cellulomonas</i> sp <i>Cellulomonas microbacterium</i>
Post-operative 2 (L5)	<i>Staphylococcus xylosus</i> DSM 20266T DSM (1.722)	<i>Staphylococcus cohnii cohnii</i> <i>Staphylococcus hominis</i>
	<i>Staphylococcus haemolyticus</i> 10024 CHB (1.909)	<i>Micrococcus</i> spp <i>Staphylococcus sciuri</i>
	<i>Micrococcus luteus</i> IMET 11249 HKJ (1.733)	
Resuscitation room (L6)	<i>Kocuria rosea</i> B331 UFL (1.933)	<i>Staphylococcus cohnii cohnii</i> <i>Kocuria varians</i> <i>Kocuria rosea</i>
Septic block (L7)	<i>Staphylococcus haemolyticus</i> DSM 20264 DSM (2.107)	<i>Staphylococcus auricularis</i> <i>Staphylococcus cohnii cohnii</i> <i>Micrococcus</i> spp

4. Conclusion

This study allowed us to highlight the importance of studying and monitoring the microbiological quality of internal air in hospitals. These microbiological agents in suspension in the air can be pathogenic for the human, they can cause infections and increase the risk of nosocomial infections. The risk is even greater when it comes to operating theaters where bioaerosol is in direct contact with the patient's cellular tissue, and when it is an immunosuppressed patient.

The results of this study show that BAs concentrations in operating theaters and other rooms exceed the thresholds set by WHO and other international standards. Gram-positive cocci are the dominant bacteria in the hospital's internal emergency medical air.

It is recommended to consider the points that favor the persistence in the air of these BAs, in order to reduce their concentration in the indoor air, such as installation and maintenance of air handling and

ventilation systems, disinfection and sterilization, humidity, the specific coating of the walls, floors, ceilings and worktop laboratory of the biological room, good hygienic practices, awareness of hospital practitioners and the creation of Algerian regulations that limit the rate of BAs and their periodic control in hospitals.

5. References

- Agabou, A., Abdeldjalil M.C., Bensegueni, A., Semouma, S., 2013. Spatial variability of airborne bacteria in the municipal slaughterhouse of constantine – Algeria. *Journal of Microbiology, Biotechnology and Food Sciences*. 2 (6), 2419-2422.
- Ait Ziane, M., Lounis-Mokrani, Z., Allab, M., 2014. Exposure to indoor radon and natural gamma radiation in some workplaces at Algiers, Algeria. *Radiation Protection Dosimetry*. 160(1-3), 128–133.
- Asif, A., Zeeshan, M., Hashmi, I., Zahid, U., Bhatti, M. F., 2018. Microbial quality assessment of indoor air in a large hospital building during winter and spring seasons. *Building and Environment*. 135, 68–73.
- Benammar, L., Menasria, T., Chergui, A., Benfiala, S., Ayachi, A., 2017. Indoor fungal contamination of traditional public baths (Hammams). *International Biodeterioration & Biodegradation*. 117, 115–122.
- Cabo Verde, S., Almeida, S. M., Matos, J., Guerreiro, D., Meneses, M., Faria, T., Viegas, C., 2015. Microbiological assessment of indoor air quality at different hospital sites. *Research in Microbiology*. 166(7), 557–563.
- Canha, N., Almeida, S. M., Freitas, M. do C., Wolterbeek, H. T., 2015. Assessment of bioaerosols in urban and rural primary schools using passive and active sampling methodologies. *Archives of Environmental Protection*. 41(4), 11–22.
- David, M.Z., Daum, R.S., 2010. Community-Associated Methicillin-Resistant *Staphylococcus aureus*: Epidemiology and Clinical Consequences of an Emerging Epidemic. *Clinical Microbiology Reviews*. July 2010, 616–687.
- Ghasemian, A., Khodaparast, S., Savaheli F., Nojoomi M, 2017 Types and Levels of Bioaerosols in Healthcare and Community Indoor Settings in Iran. *Avicenna J Clin Microb Infec*. 4(1):e41036.
- Ghosh, B., Lal, H., Srivastava, A., 2015. Review of bioaerosols in indoor environment with special reference to sampling, analysis and control mechanisms. *Environment International*. 85, 254–272.
- Hayleeyesus, S. F., Manaye, A. M., 2014. Microbiological Quality of Indoor Air in University Libraries. *Asian Pacific Journal of Tropical Biomedicine*. 4, S312–S317.
- Heo, K. J., Lim, C. E., Kim, H. B., Lee, B. U., 2017. Effects of human activities on concentrations of culturable bioaerosols in indoor air environments. *Journal of Aerosol Science*. 104, 58–65.
- Karimpour Roshan, S., Godini, H., Nikmanesh, B., Bakhshi, H., Charsizadeh, A., 2019. Study on the relationship between the concentration and type of fungal bio-aerosols at indoor and outdoor air in the Children's Medical Center, Tehran, Iran. *Environmental Monitoring and Assessment*. 191:48.
- Khedidji, S., Balducci, C., Ladji, R., Cecinato, A., Perilli, M., Yassaa, N., 2017. Chemical composition of particulate organic matter at industrial, university and forest areas located in Bouira province, Algeria. *Atmospheric Pollution Research*. 8(3), 474–482.
- Khedidji, S., Ladji, R., Yassaa, N., 2013. A wintertime study of polycyclic aromatic hydrocarbons (PAHs) in indoor and outdoor air in a big student residence in Algiers, Algeria. *Environmental Science and Pollution Research*. 20(7), 4906–4919.
- Kim, K.-H., Kabir, E., Jahan, S. A., 2018. Airborne bioaerosols and their impact on human health. *Journal of Environmental Sciences*. 67, 23–35.



- Martínez-Herrera, E. O., Frías De-León, M. G., Duarte-Escalante, E., Calderón-Ezquerro, M. d. C., Jiménez-Martínez, M. d. C., Acosta-Altamirano, G., et al., 2016. Fungal diversity and *Aspergillus* species in hospital environments. *Annals of Agricultural and Environmental Medicine*. 23(2), 264–269.
- Meharzi, S., Mansouri, R., Chekchaki, N., Bouchair, N., Belgharssa, A., Tridon, A., Messarah, M., Amel Boumendjel, A., 2017. Indoor Aeroallergens in Asthmatic Pediatric Population in Annaba (Algeria), *Aerosol and Air Quality Research*. 17, 2482–2490.
- Napoli, C., Marcotrigiano, V., Montagna, M.T., 2012 Air sampling procedures to evaluate microbial contamination: a comparison between active and passive methods in operating theatres, *BMC Public Health* 2012, 12:594, <http://www.biomedcentral.com/1471-2458/12/594>.
- Necib, A., Boughediri, L., 2016. Airborne pollen in the El-Hadjar town (Algeria NE). *Aerobiologia*. 32(2), 277-288.
- Okten, S., Asan, A., 2011. Airborne fungi and bacteria in indoor and outdoor environment of the Pediatric Unit of Edirne Government Hospital. *Environmental Monitoring and Assessment*. 184(3), 1739–1751.
- Pati, P., 2018. Review on Common Microbiological Contamination Found in Hospital Air, *Journal of Microbiology and Pathology*. 2(1), 103.
- Prussin, A. J., Marr, L. C., 2015. Sources of airborne microorganisms in the built environment. *Microbiome*. 3(1).
- Ramos, C. A., Viegas, C., Verde, S. C., Wolterbeek, H. T., Almeida, S. M., 2016. Characterizing the fungal and bacterial microflora and concentrations in fitness centres. *Indoor and Built Environment*. 25(6), 872–882.
- Viegas, C., Faria, T., Pacifico, C., Dos Santos, M., Monteiro, A., Lança, C., Cabo Verde, S., 2017. Microbiota and Particulate Matter Assessment in Portuguese Optical Shops Providing Contact Lens Services. *Healthcare*. 5(2), 24.
- WHO, Indoor air quality: biological contaminants, 1990. WHO- Regional Publications. European Series, World Health Organization, Copenhagen, p. 11031.
- Yildiz, Ş., Enç, V., Kara, M., Tabak, Y., Emine Acet, E., 2017. Assessment of the potential risks of airborne microbial contamination in solid recovered fuel plants: a case study in Istanbul, *Environmental Engineering and Management Journal*. 16(7), 1415-1421.

Genotoxicity of polycyclic aromatic hydrocarbons (PAHs) in size segregated PM samples collected from a thermal power plant area

Eftade Odaman Gaga¹, Pelin Ertürk Arı^{2,1}, Gonca Cakmak³, Akif Arı^{2,1},
Roel Schins⁴, Mustafa Odabasi⁵, Yetkin Dumanoglu⁵ and Sema Burgaz³

¹Department of Environmental Engineering, Anadolu University, 26090, Eskişehir, Turkey,

²Department of Environmental Engineering, Abant İzzet Baysal University, 14030, Bolu, Turkey,

³Department of Toxicology, Faculty of Pharmacy, Gazi University, 06330, Ankara, Turkey,

⁴IUF-Leibniz Research Institute for Environmental Medicine, Duesseldorf, Germany,

⁵Department of Environmental Engineering, Faculty of Engineering, Dokuz Eylul University, Izmir, Turkey

egaga@anadolu.edu.tr

Abstract. Particulate matter (PM) is of great concern because of its adverse health effects including cardiovascular and respiratory diseases. Exposure to atmospheric PM is also associated with an increased risk of cancer. The size and chemical composition of PM are important parameters in particulate toxicology. The composition of the PM varies greatly and depends on many factors. It has been shown in previous studies that fine particles might be more toxic because of having large surface area, absorbing high concentrations of toxic air pollutants and easily depositing into lungs compared to coarse particles. Polycyclic aromatic hydrocarbons (PAHs) are a group of persistent organic pollutants with two or more benzene rings. 16 PAHs have been listed as priority pollutants by the United States Environmental Protection Agency (USEPA) due to their persistence, bioaccumulation, and toxicities. PAHs can exist both in particle and gas phases. Kütahya is one of the highly polluted cities in Turkey based on PM concentrations measured at fixed monitoring stations operated by Ministry of Urbanization and Environment (MUE). Three thermal power plants with a total of 1175MW thermal capacity are being operated in the region. A project was initiated in Kütahya to investigate health effects of air pollution in the region including genotoxicity of the particulate matter. Daily size segregated PM samples were collected by 5 stage high volume slotted cascade impactor from two different (urban and rural) locations in Kütahya during summer and winter seasons. Size distribution and chemical composition of the PM samples including PAHs were determined. In vitro genotoxicity of the samples was evaluated together with concentrations of PAHs measured in different size fractions. Most of the PAHs were accumulated on submicron PM, and the concentrations were shifted in smaller sizes for winter samples for both stations. The maximum DNA damage was observed in urban station winter PM_{2.1-1.3} µm size particles.

Keywords: Size-segregated PM, PAHs, Genotoxicity

1. Introduction

Air pollution is one of the important environmental problems in urban environments. Activities such as fossil fuel combustion for residential heating and traffic increase the concentrations of air pollutants especially in developing countries.

Atmospheric particulate matter (PM) is associated with many adverse health effects including cardiovascular and respiratory diseases. Many epidemiological studies have shown that exposure to PM increases lung cancer and mortality (Pope et al., 2002; Knaapen et al., 2004; Pope et al., 2004).

PAHs are a common group of organic pollutants formed from two or more fused aromatic rings. PAHs have been listed as priority pollutants by the USEPA due to their widespread distribution, bioaccumulation, toxicity, and carcinogenicity (EPA, 2014). They produced by incomplete combustion of organic material and released into the atmosphere as a result of various anthropogenic activities such as various industrial processes, coal combustion for power generation, vehicular emissions, coke production, and utilizing coal and biomass for space heating. (Baek et al., 1991; Li et al., 2003; Giri et al., 2013; Wu et al., 2018).

Although many studies indicate that the adverse health effects of respirable particles are linked with inflammation and oxidative damage, other studies have points out that genotoxic and cytotoxic effects of combustion aerosols are mainly related by PAHs, which are an important part of ambient organic aerosol (Topinka et al., 2013). The relative abundance of the organic fraction in ambient aerosol mass varies with particle size. Therefore, the levels of toxic and carcinogenic PAHs and their adverse health effects also vary with PM size (Duan et al., 2005; Shen et al., 2019).

The present study aimed to quantify the size-segregated PAH content and the genotoxicity of the aerosols collected from urban and rural sites of Kütahya, a thermal power plant affected city of Turkey.

2. Materials and Methods

2.1. Study area and sampling

Kütahya city is located in the mid-west region of Turkey at an altitude of 970 m above sea level. Other than thermal power plants, there are a variety of industrial activities including integrated nitrogen production plant, sugar factories, magnesite plant, mining, automotive manufacturing facilities, wood manufacturing plants and ceramics industries taking place in the region. Size segregated PM samples were collected for 10 days periods in summer and winter seasons in 2015, by a high volume air sampler (Thermo, USA) and 5 stage impactor system (TISCH model TE-235, USA) (Fig.1). The impactor system consists of 5 stages and a back-up stage for size cutting. Polytetrafluoroethylene (PTFE) filters were used to collect particles on impactor plates. The aerodynamic cut off diameters are 0.69, 1.3, 2.1, 4.2, and 10.2 μm).



Figure 1. Sampling sites

2.2. Determination of PAHs

PAHs concentrations were determined by ultrasonic extraction of filters by petroleum ether and dichloromethane (4/1 by volume) followed by gas chromatography-mass spectrometry (GC-MS) analysis.

2.3. Extraction of filters for Comet assay

For Comet Assay, extraction and the lyophilization of the PM samples from the one slot (1x10 cm) filters were carried out according to Wessels et al. (2010). Filters were placed in the polypropylene tubes and then 10 mL ultrapure water was added to the tubes. Vortex, ultrasonication, and hand stirring were respectively carried out for 5 min each. After the ultrasonication each suspension was freeze-dried.

2.4. Cell culture conditions and Comet Assay

Following 24hr incubation (37°C and 5% CO₂) of A549 cells (15000 cells well⁻¹) in 96 well plates, 100 µg mL⁻¹ PM suspensions were used in duplicate for 24 h incubation. At the end of the culture, cells were trypsinized and suspended with low serum-containing complete medium. The cell suspensions were mixed with low melting agarose at 37°C and dropped on the high melting agarose coated slides. Following the solidification of the suspensions, overnight lysing has been carried out. The electrophoresis was carried out at 25V and 300mA for 15 min in the electrophoresis buffer after 20min unwinding in the electrophoresis buffer. The slides were neutralized and stained with 20µg mL⁻¹ ethidium bromide. Each slide was evaluated under fluorescence microscope for quantification of the DNA damage in 50 cells with the use of Perceptive Software (COMET III). In total 100 cells were evaluated for each treatment.

3. Results and Discussion

Size segregated PM mass concentrations measured in urban and rural stations in summer and winter days are summarized in Fig.2. Total PM mass concentrations of all fractions were 60.1 ± 10.6 and 114.2 ± 40.4 µg m⁻³ for urban samples, in summer and winter seasons, respectively. Total PM concentrations in rural station in summer and winter samples were measured as 45.9 ± 16.8 and 46.4 ± 7.7 µg m⁻³. Percent contribution of fine particles to total PM (total of three cascade stages; <0.69, 0.69-1.3 and 1.3-2.1 µm) varied between $68.1\% \pm 4.9\%$ (urban summer samples) and $85.2 \pm 5.2\%$ (rural winter samples). A high abundance of fine PM to the total mass indicates dominance of combustion aerosols to PM mass budget in sampling area (Liu et al., 2014; Achilleos et al., 2016; Guo et al., 2017; Ruan et al., 2018). Atmospheric concentrations of PM are affected by combustion activities, and crustal conditions such as soil humidity and soil resuspension by wind action (Clements et al., 2014; Dimitriou and Kassomenos, 2014). It has been known that especially in urban atmospheres; traffic, road dust, industry and space heating emissions contribute significantly to atmospheric fine PM concentrations (Calvo et al., 2013; Bressi et al., 2014; Choi et al., 2015).

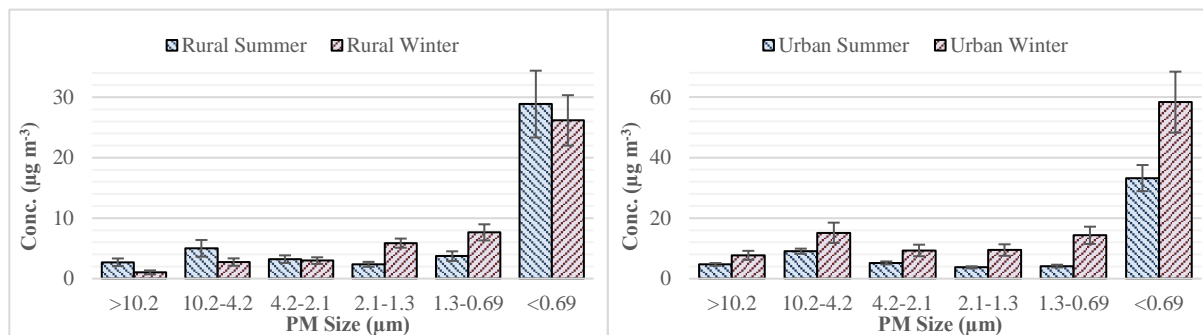


Figure 2. Size-segregated PM concentrations measured in urban and rural stations

Size-segregated PAH concentrations are summarized in Table 1. Most of the PAHs were accumulated on submicron PM, and the concentrations were shifted in smaller sizes for winter samples for both stations. Percent contribution of PAHs in fine mode is higher than coarse mode due to the combustion particles.

Table 1. Size segregated average concentrations of PAHs.

Size (μm)	> 10.2	4.2 – 10.2	2.1 – 4.2	1.3 – 2.1	0.69 – 1.3	< 0.69
Conc. (ng m^{-3})	Avg \pm Std.Dev	Avg \pm Std.Dev	Avg \pm Std.Dev	Avg \pm Std.Dev	Avg \pm Std.Dev	Avg \pm Std.Dev
Urban Summer	2.9 \pm 1.3	3.2 \pm 1.9	3.3 \pm 1.9	3.2 \pm 1.5	3.6 \pm 1.5	40.9 \pm 49.3
Urban Winter	5.2 \pm 1.9	6.7 \pm 1.4	6.8 \pm 4.2	23.1 \pm 27.9	53.0 \pm 27.9	295.6 \pm 145.2
Rural Summer	3.9 \pm 5.4	3.9 \pm 7.3	3.9 \pm 6.8	4.3 \pm 6.9	3.7 \pm 6.1	16.5 \pm 21.4
Rural Winter	3.8 \pm 1.9	2.0 \pm 2.4	2.7 \pm 2.2	2.8 \pm 0.7	7.2 \pm 2.4	38.3 \pm 13.2

A significant increase in the total concentration of PM-bound PAHs as the sum of 6 cascade stages in urban site samples in the winter period. Total average PAH concentrations were 390.4 \pm 209.1 ng m^{-3} at urban and 56.7 \pm 22.8 ng m^{-3} at the rural site in winter period whereas the total concentrations were 56.1 \pm 57.4 and 36.2 \pm 53.9 ng m^{-3} at urban and rural sites, respectively. The most abundant species were Phe, Flt, Pyr, Chr and BaA at both two sites.

Percent DNA damage evaluation of 100 $\mu\text{g mL}^{-1}$ concentration of PM_{4.1-2.1}, PM_{2.1-1.3}, PM_{1.3-0.69} and PM_{<0.69} μm collected in urban and rural stations in Kütahya is presented in Fig.3 as the tail intensity ratio to the control cells. The maximum DNA damage was observed in urban station winter PM_{2.1-1.3} μm size particles. Despite the differences in the tail intensity within the sampling points, season and PM sizes, there was not a significant difference between the samples by the 95% statistical confidence level by ANOVA-Dunnet T3 tests.

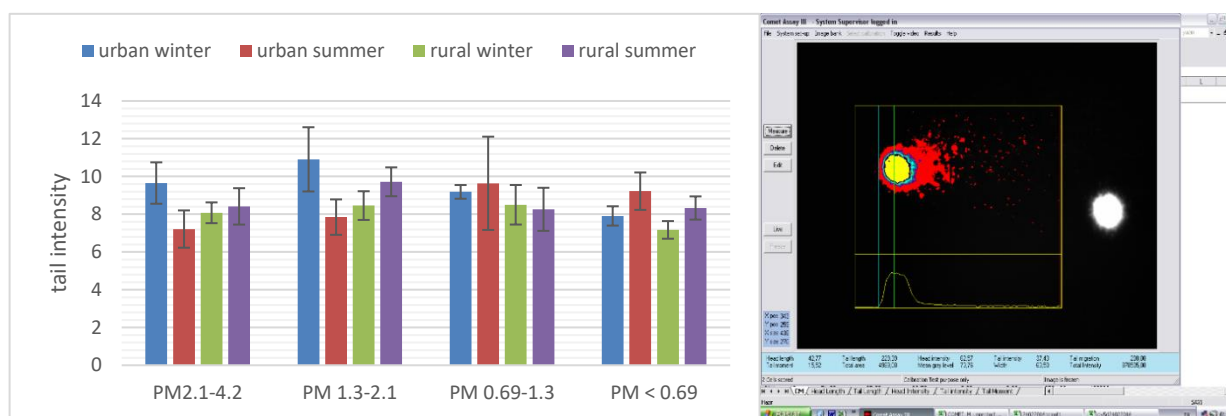


Figure 3. Urban and rural samples tail intensity and fluorescence appearance of damaged A549 cells.

The highest ratio of the tail intensity to the control samples was observed in the winter samples collected from urban site, followed by the rural site summer samples on PM size of 1.3 to 2.1 μm particles. Measuring the tail intensity to explain the DNA damage of ambient particles is a common approach, although the PAH concentrations alone would not be enough to make certain conclusions on the carcinogenicity of the particles. Heavy metals, oxidative potential and also other toxic and carcinogenic species such as nitro- or oxy- derivatives of PAHs should also be evaluated to understand mutagenicity of the aerosol samples.

4. References

- Achilleos, S., Wolfson, J.M., Ferguson, S.T., Kang, C.M., Hadjimitsis, D.G., et al. 2016. Spatial variability of fine and coarse particle composition and sources in Cyprus Atmos.Res. 169, 255-270
- Baek, S.O., Field, R.A., Goldstone, M.E., Kirk, P.W., Lester, J.N., Perry, R., 1991. A review of atmospheric polycyclic aromatic hydrocarbons: Sources, fate and behaviour. Water Air Soil Poll. 60, 279-300.
- Bressi, M., Sciare, J., Ghersi, V., Mihalopoulos, N., Petit, J.E., Nicolas, J.B., Moukhtar, S., Rosso, A., Feron, A., Bonnaire, N., Poulakis, E., Theodosi, C., 2014. Sources and geographical origins of fine aerosols in Paris (France). Atmos.Chem. Phys. 14, 8813-8839.
- Calvo, A.I., Alves, C., Castro, A., Pont, V., Vicente, A.M., Fraile, R., 2013. Research on aerosol sources and chemical composition: Past, current and emerging issues. Atmos. Res. 120-121, 1-28.
- Choi, J.K., Ban, S.J., Kim, Y.P., Kim, Y.H., Yi, S.M., Zoh, K.D., 2015. Molecular marker characterization and source appointment of particulate matter and its organic aerosols. Chemosphere 134, 482-491.
- Clements, N., Eav, J., Xie, M., Hannigan, M.P., Miller, S.L., Navidi, W., Peel, J.L., Schauer, J.J., Shafer, M.M., Milford, J.B., 2014. Concentrations and source insights for trace elements in fine and coarse particulate matter. Atmos. Environ. 89, 373-381.
- Dimitriou, K., Kassomenos, P., 2014. Indicators reflecting local and transboundary sources of PM_{2.5} and PM COARSE in Rome – Impacts in air quality. Atmos. Environ. 96, 154-162.
- Duan, J., Bi, X., Tan, J., Sheng, G., Fu, J., 2005. The differences of the size distribution of polycyclic aromatic hydrocarbons (PAHs) between urban and rural sites of Guangzhou, China. Atmos. Res. 78, 190-203.
- Giri, B., Patel, K.S., Jaiswal, N.K., Sharma, S., Ambade, B., Wang, W., Simonich, S.L.M., Simoneit, B.R.T., 2013. Composition and sources of organic tracers in aerosol particles of industrial central India. Atmos. Res. 120-121, 312-324.
- Guo, Y., Zhang, J., Zhao, Y., Wang, S., Cheng, J., Zheng, C., 2017. Chemical agglomeration of fine particles in coal combustion flue gas: Experimental evaluation. Fuel 203, 557-569.
- Knaapen, A.M., Borm, P.J.A., Albrecht, C., Schins, R.P., 2004. Inhaled particles and lung cancer. Part A: Mechanisms. Int. J. Cancer 109, 799-809
- Li, C.T., Lin, Y.C., Lee, W.J., Tsai, P.J., 2003. Emission of polycyclic aromatic hydrocarbons and their carcinogenic potencies from cooking sources to the urban atmosphere. Environ. Health Persp. 111, 483-487.
- Liu, Z.R., Hu, B., Liu, Q., Sun, Y., Wang, Y.S., 2014. Source apportionment of urban fine particle number concentration during summertime in Beijing. Atmos. Environ. 96, 359-369.
- Pope, C.A.III., Burnett, R.T., Thun, M.J., Calle, E.E., Krewski, D., Ito, K., 2002. Lung cancer, cardiopulmonary mortality, and long-term exposure to fine particulate air pollution. JAMA, J. Am. Med. Assoc. 287, 1132-1141.



Pope, C.A.III., Hansen, M.L., Long, R.W., Nielsen, K.R., Eatough, N.L., Wilson, W.E., Eatough, D.J., 2004. Ambient particulate air pollution, heart rate variability, and blood markers of inflammation in a panel of elderly subjects. *Environ. Health Persp.* 112, 339-345.

Ruan, R., Tan, H., Wang, X., Li, Y., Li, S., Hu, Z., Wei, B., Yang, T., 2018. Characteristics of fine particulate matter formation during combustion of lignite riched in AAEM (alkali and alkaline earth metals) and sulphur. *Fuel* 211, 206-213.

Shen, R., Wang, Y., Gao, W., Cong, X., Cheng, L., Li, X., 2019. Size-segregated particulate matter bound polycyclic aromatic hydrocarbons (PAHs) over China: Size distribution, characteristics and health risk assessment. *Sci. Total Environ.* 685, 116-123.

Topinka, J., Milcova, A., Schmučerová, J., Krouzek, J., Hovorka, J., 2013. Ultrafine particles are not major carriers of carcinogenic PAHs and their genotoxicity in size-segregated aerosols. *Mutat. Res-Gen. Tox. En.* 754, 1-6.

United States Environmental Protection Agency – EPA. (2014). Priority Pollutant List. <http://www.epa.gov/sites/production/files/2015-09/documents/priority-pollutant-list-epa.pdf>.

Wessels, A., Birmili, W., Albrecht, C., Hellack, B., Jermann, E., Wick, G., Harrison, R.M., Schins, R.P.F., 2010. Oxidant Generation and Toxicity of Size-Fractionated Ambient Particles in Human Lung Epithelial Cells. *Environ. Sci. Technol.* 44, 3539-3545.

Wu, X., Vu, T.V., Shi, Z., Harrison, R.M., Liu, D., Cen, K., 2018. Characterization and source apportionment of carbonaceous PM_{2.5} particles in China - A review. *Atmos. Environ.* 189, 187-212

Acknowledgments

This work was supported by the Scientific and Technological Research Council of Turkey under the grant of 112Y305 and The Committee of Scientific Research Projects of Anadolu University under the grants of 1306F272 and 1508F606.

Assessment of PM_{2.5} concentrations in indoor and outdoor environments of different workplaces

Fatma Nur Eraslan, Ozlem Ozden Uzmez and Eftade O. Gaga

Eskisehir Technical University, Faculty of Engineering, Department of Environmental Engineering, 26555 Eskisehir, Turkey

oozden@eskisehir.edu.tr

Abstract. This study provides information about indoor-outdoor PM_{2.5} mass concentrations, indoor/outdoor ratios (I/O) of PM_{2.5} for seven different workplaces; photocopier, bakery, restaurant, hairdresser, dry cleaner, market and hotel in Eskisehir, Turkey. Simultaneous measurements of both indoor and outdoor concentrations were performed. One-hour measurements were performed during the busy and less active hours of each workplace at both weekday and weekend periods. Indoor measurement results of the busy hours were higher than those obtained during less-active hours during both weekdays and weekend periods at all workplaces. According to the weekday results, the maximum PM_{2.5} concentration (average 1123.92 µg/m³) was measured at the hairdresser while the minimum concentration was measured at the hotel (27.20 µg/m³) during busy hours. The minimum concentration was obtained at the hotel (3.58 µg/m³) and the maximum concentration was measured at the hairdresser (average 1037.50 µg/m³) during the less-active hours of weekday measurements. According to the weekend results, the maximum concentration (3076.00 µg/m³) was measured at the hairdresser while the minimum concentration was measured at the hotel (77.13 µg/m³) during busy hours similar to weekday results. During less-active hours of the weekend, the minimum concentration was obtained in the grocery store (59.80 µg/m³) and the maximum concentration was measured at the hairdresser (2575.17 µg/m³). When I/O ratios were evaluated, the ratios obtained from hairdresser (I/O=7.26-72.34) and restaurant (I/O=1.60-17.32) were > 1 at all sampling periods. In the dry cleaner, except weekday busy hour (I/O=0.90), all I/O ratios were > 1 (I/O=1.09-3.27) while the ratios obtained during weekday and weekend busy hours at the bakery were > 1 (weekday I/O=1.84, weekend I/O=2.19). In general, PM_{2.5} concentrations varied due to several factors such as presence of strong indoor sources, activity density, ventilation effect, building's location, traffic density around the building etc.

Keywords: PM_{2.5}, Indoor and outdoor air measurement, Workplaces.

1. Introduction

The term of particulate matter 2.5 (PM_{2.5}), generally refers to the respirable fraction of fine particles that have aerodynamic diameter less than 2.5 micrometers (USEPA, 2008). Particularly fine fractions of particulate matter can have a greater impact on deeper regions of the respiratory system, including trachea and bronchi. Therefore, fine fractions of particulate matter are very important for human health and studies have generally focused on fine fractions of particulate matter (Massey et al., 2016; Berico et al., 1997; Ando et al., 1996).

Personal exposure to PM_{2.5} is influenced by different microenvironments where people spend most of their daily time. In these microenvironments, various activities take place which may constitute resources. For this reason, the effect of indoor air pollutants on human health is of great significance. In general, the particles are known to have two sources, indoor and outdoor activities. Indoor PM

concentration results from a variety of indoor activities, such as cooking, cleaning, walking and especially smoking (Fromme et al., 2007). Indoor air pollution in different microenvironments such as residences, schools, offices, hospitals, vehicles and workplaces have been investigated in previous studies (Massey et al., 2016; Jung et al., 2015; Li et al., 2015; Kulshrestha et al., 2014; Saraga et al., 2014; Brown et al., 2012; Pekey et al., 2010; Lee et al., 2001; Lee et al., 2002). The indoor air in different working environments can become very polluted due to the type of activities, resources, and equipment used in that workplace. Workplace air has a significant impact on employees' health. Therefore, the removal of particulate contaminants has become a necessity to be taken into consideration (Massey et al., 2016).

The purpose of this study is to provide information about indoor-outdoor PM_{2.5} mass concentrations, indoor/outdoor ratios (I/O) of PM_{2.5} for seven different workplaces in Eskişehir, Turkey. Since penetration of outdoor air is another source of indoor air pollution, simultaneous indoor and outdoor measurements were performed in each workplace.

2. Materials and methods

2.1. Locations and characteristics of the workplaces

In this study, indoor and outdoor PM_{2.5} mass concentrations were measured in seven different workplaces in Eskişehir, Turkey. These workplaces are photocopy store, bakery, restaurant, hairdresser, dry cleaner, grocery store and hotel (Figure 1). The locations of the workplaces are shown in Figure 1. All the workplaces except for the hotel are located in the city center. Specific characteristics of each workplace are given in Table 1. Also, a questionnaire was used to record some information about the activities and possible sources (cigarette smoke, candles or cooking, etc.) for each workplace.

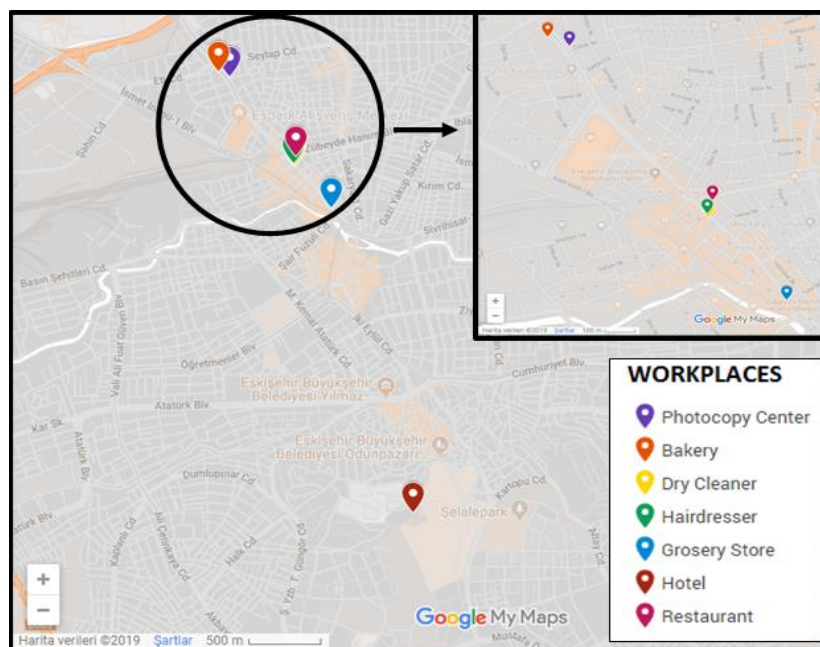


Figure 1. The locations of the workplaces

Table 1. Specific characteristics of the workplaces

Workplace	Equipment Used	Ventilation Type	Frequency of Cleaning	The Location of The Workplace
Restaurant	Barbecue	Exhauster on barbecue and natural ventilation	Every morning	On the street
Bakery	Furnace for bread	Portable fan and natural ventilation	Every morning	On the street
Photocopy	Three photocopy machines, three poster machines	Air conditioning and fan	Every morning and evening	On the street
Hairdresser	Sterilizing tools, hair dryer, curling iron	Air conditioning and natural ventilation	Every morning	On the street
Dry Cleaner	Two tumble dryers, iron, a dry-cleaning machine, eight washing machines, sewing machine	Aspirator and natural ventilation	Every morning and evening	On the street
Grocery Store	-	Natural ventilation	Every morning	On pedestrian street
Hotel	-	Ceiling fan, exhauster and air conditioning	Continuous	Far away from traffic

2.2. Sampling program

Measurement studies were conducted between 13 January - 23 February 2019 in Eskisehir, Turkey. Before sampling, interviews with each workplace were conducted. In these interviews, some important information such as the busy and less-active hours of the workplace, activities carried out in the workplace were noted. Indoor and outdoor concentrations were measured simultaneously during the less active and busy hours in each workplace. 1-hour measurements were performed during weekday and weekend periods in each workplace to investigate the relationship between weekday-weekend intensity and pollution levels in the workplaces. In total, four samples from each workplace were collected. Indoor and outdoor temperatures were also noted during the measurements.

2.3. Sampling method

Two DustTrak II aerosol monitors (Model 8530, TSI Inc.) were used to measure PM_{2.5} concentrations in both indoor and outdoor air (Figure 2). The results of the two monitors were compared to test the performance of each monitor before the measurement studies and the measurement results were very close to each other ($R^2=0.99$). The recording interval of the aerosol monitor was set to 1 minute and the monitor recorded 60 data for 1 hour. The aerosol concentration capacity of each monitor is in the range of 0.001 to 400 mg/m³.



Figure 2. DustTrak II aerosol monitors during measurement studies (left: indoor, right: outdoor)

3. Results

3.1. Indoor PM_{2.5} concentrations

According to the weekday results (Figure 3), the greatest exposure during busy hours was observed at the hairdresser (average $1123.92 \pm 343.53 \mu\text{g}/\text{m}^3$) that was approximately forty-one times higher than the concentration measured at the hotel where the minimum concentration was measured (average $27.20 \pm 2.43 \mu\text{g}/\text{m}^3$). In addition, indoor PM_{2.5} concentrations were higher than outdoor concentrations in restaurant, bakery and hairdresser during the weekday busy hours. The minimum concentration was obtained at the hotel (average $3.58 \pm 0.76 \mu\text{g}/\text{m}^3$) and the maximum concentration was measured at the hairdresser (average $1037.50 \pm 859.16 \mu\text{g}/\text{m}^3$) during the less active hours of weekday measurements.

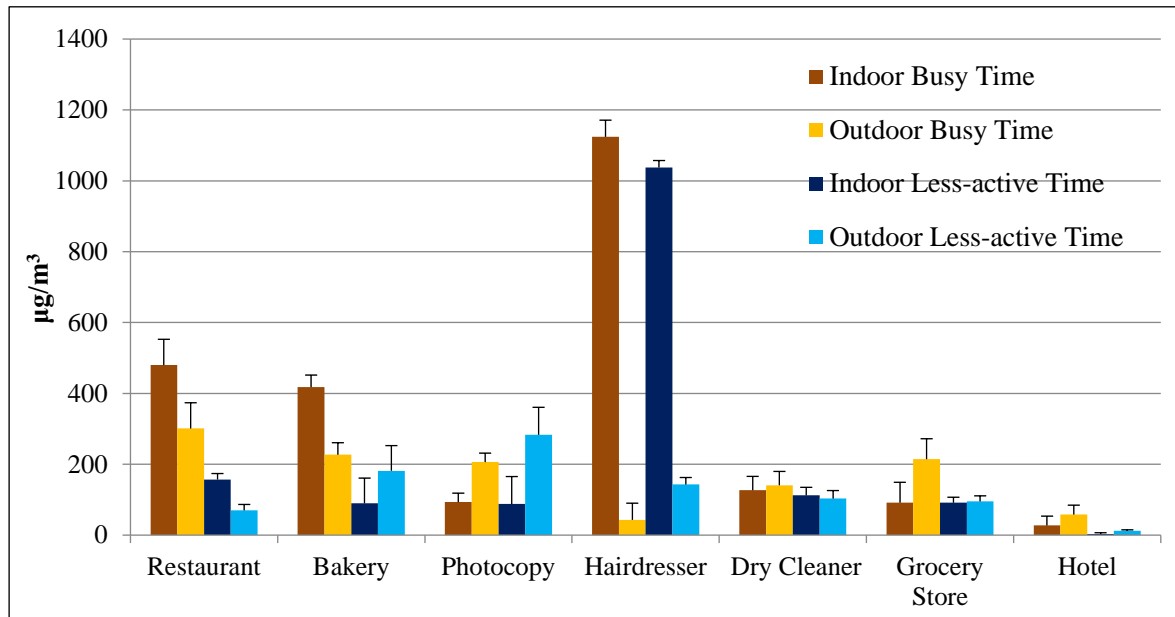


Figure 3. Weekday indoor - outdoor average PM_{2.5} concentrations

According to the weekend results (Figure 4), the maximum concentration (average $3076.00 \pm 1345.48 \mu\text{g}/\text{m}^3$) was measured at the hairdresser while the minimum concentration was measured at the hotel (average $77.13 \pm 7.92 \mu\text{g}/\text{m}^3$) during busy hours similar to weekday results. Indoor PM_{2.5} concentrations were higher than outdoor concentrations in restaurant, bakery, dry cleaner and hairdresser during the busy hours at the weekend. During less active hours of the weekend, the minimum concentration was obtained in the market (average $59.80 \pm 5.86 \mu\text{g}/\text{m}^3$) and the maximum concentration was measured at the hairdresser (average $2575.17 \pm 160.8 \mu\text{g}/\text{m}^3$). Measurement results obtained from restaurant, dry cleaner and hairdresser on both weekdays and weekends during less active hours showed that indoor PM_{2.5} concentrations were higher than outdoor concentrations.

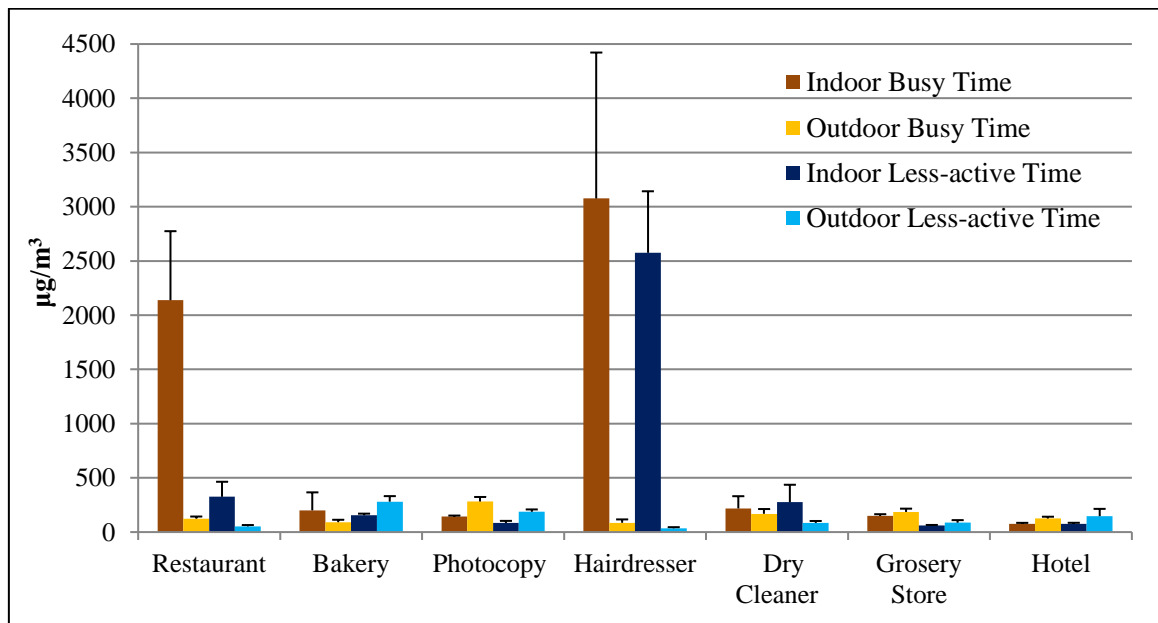


Figure 4. Weekend indoor - outdoor average PM_{2.5} concentrations

3.2. Indoor/Outdoor concentration ratios

Indoor/outdoor concentration ratios were also calculated for each workplace. When Indoor/Outdoor ratios were evaluated (Table 2), the ratios obtained from hairdresser (I/O=7.26-72.34) and restaurant (I/O=1.60-17.32) were > 1 at all sampling periods. In the dry cleaner, except weekday busy hour (I/O=0.90), all the I/O ratios were > 1 (I/O=1.09-3.27) while the ratios obtained during weekday and weekend busy hours at the bakery were > 1 (weekday I/O=1.84, weekend I/O=2.19). The ratios greater than 1 indicates the effect of workplace activities on indoor PM_{2.5} concentrations.

Table 2. Indoor/Outdoor PM_{2.5} ratios obtained in each workplace in weekday and weekend periods

Workplace	Weekday I/O		Weekend I/O	
	Busy time	Less-active time	Busy time	Less-active time
Restaurant	1.60 ± 0.46	2.25 ± 0.85	17.32 ± 7.19	6.15 ± 2.71
Bakery	1.84 ± 0.72	0.50 ± 0.16	2.19 ± 1.71	0.55 ± 0.10
Photocopier	0.45 ± 0.05	0.31 ± 0.09	0.51 ± 0.06	0.45 ± 0.11
Hairdresser	26.21 ± 347.97	7.26 ± 5.26	35.82 ± 18.02	72.34 ± 22.72
Dry Cleaner	0.90 ± 0.42	1.09 ± 0.65	1.30 ± 0.69	3.27 ± 1.75
Grocery Store	0.43 ± 0.15	0.96 ± 0.11	0.81 ± 0.15	0.69 ± 0.20
Hotel	0.47 ± 0.12	0.30 ± 0.14	0.62 ± 0.12	0.51 ± 0.25

Some statistical analyses were carried out using SPSS at 95% confidence level. Busy and less-active concentrations were compared for all workplaces and the results obtained for the restaurant and the photocopier were statistically significant. In other workplaces, non-significant results were obtained since the activity was higher than expected at less active times. The difference between indoor and outdoor concentrations was statistically significant in all of the workplaces except dry cleaner. Also, there was a statistically significance between the weekday and weekend results in all workplaces.

4. Discussion

In this study, indoor-outdoor PM_{2.5} mass concentrations, indoor/outdoor ratios (I/O) of PM_{2.5} were determined for seven different workplaces; photocopier, bakery, restaurant, hairdresser, dry cleaner, market and hotel in Eskisehir, Turkey. It was determined that there is a direct relationship between the intensity of indoor activities and PM_{2.5} concentrations.

Quite high PM_{2.5} mass concentrations have been obtained in the hairdresser, restaurant and bakery depending on the activities and type of the used equipments. Hair dryers that are used continuously in the hairdressers can be important sources of these high levels obtained in this workplace. In the restaurant, coal combustion is the most important source for particulate matter concentrations. Also, cooking style directly affects the results. (Lee et al., 2002). Higher outdoor concentrations in some workplaces than indoor concentrations were due to the high traffic density during the sampling period. As a result, the highest PM_{2.5} concentrations were obtained at the hairdresser in each period. The studies in the literature found that the use of hair appliances such as hair dryers and curling irons could increase indoor PM levels (Wu et al., 2012) and the results of this study are compatible with the literature studies.

In general, measurement results showed that PM_{2.5} concentrations varied due to several factors such as presence of strong indoor sources, activities, ventilation effect, building's location, traffic density around the building etc. (Lee et al., 2002; Wu et al., 2012; Saraga et al., 2014).

5. References

- Ando, M., Katagiri, K., Tamura, K., Yamamoto, S., Matsumoto, M., Li, Y. F., Liang, C. K., 1996. Indoor and outdoor air pollution in Tokyo and Beijing supercities. *Atmospheric Environment*. 30(5), 695-702.
- Berico, M., Luciani, A., Formignani, M., 1997. Atmospheric aerosol in an urban area—measurements of TSP and PM₁₀ standards and pulmonary deposition assessments. *Atmospheric Environment*. 31(21), 3659-3665.
- Brown, K. W., Sarnat, J. A., Koutrakis, P., 2012. Concentrations of PM_{2.5} mass and components in residential and non-residential indoor microenvironments: The Sources and Composition of Particulate Exposures study. *Journal of Exposure Science and Environmental Epidemiology*. 22(2), 161.
- Fromme, H., Twardella, D., Dietrich, S., Heitmann, D., Schierl, R., Liebl, B., Rüdén, H., 2007. Particulate matter in the indoor air of classrooms—exploratory results from Munich and surrounding area. *Atmospheric Environment*. 41(4), 854-866.
- Jung, C. C., Wu, P. C., Tseng, C. H., Su, H. J., 2015. Indoor air quality varies with ventilation types and working areas in hospitals. *Building and Environment*. 85, 190-195.
- Kulshrestha, A., Massey, D. D., Masih, J., Taneja, A., 2014. Source characterization of trace elements in indoor environments at urban, rural and roadside sites in a semi arid region of India. *Aerosol Air Qual. Res.* 14, 1738-1751.
- Lee, S. C., Li, W. M., Chan, L. Y., 2001. Indoor air quality at restaurants with different styles of cooking in metropolitan Hong Kong. *Science of the Total Environment*. 279(1-3), 181-193.
- Lee, S. C., Guo, H., Li, W. M., Chan, L. Y., 2002. Inter-comparison of air pollutant concentrations in different indoor environments in Hong Kong. *Atmospheric Environment*. 36(12), 1929-1940.
- Li, Y. C., Shu, M., Ho, S. S. H., Wang, C., Cao, J. J., Wang, G. H., Zhao, X. Q., 2015. Characteristics of PM_{2.5} emitted from different cooking activities in China. *Atmospheric Research*. 166, 83-91.
- Massey, D. D., Habil, M., Taneja, A., 2016. Particles in different indoor microenvironments-its implications on occupants. *Building and Environment*. 106, 237-244
- Pekey, B., Bozkurt, Z. B., Pekey, H., Doğan, G., Zararsız, A., Efe, N., Tuncel, G., 2010. Indoor/outdoor concentrations and elemental composition of PM₁₀/PM_{2.5} in urban/industrial areas of Kocaeli City, Turkey. *Indoor Air*. 20(2), 112-125.
- Saraga, D. E., Volanis, L., Maggos, T., Vasilakos, C., Bairachtari, K., Helmis, C. G., 2014. Workplace personal exposure to respirable PM fraction: a study in sixteen indoor environments. *Atmospheric Pollution Research*. 5(3), 431-437.
- USEPA., 14.11.2008. <http://www.epa.gov/ttn/chief/ap42/index.html>, accessed in August 2019.
- Wu, X., Apte, M. G., Bennett, D. H., 2012. Indoor particle levels in small-and medium-sized commercial buildings in California. *Environmental Science & Technology*. 46(22), 12355-12363.

Acknowledgments

The authors wish to thank workplace owners and employees for their care and understanding throughout the study.

Waterborne transport in Venice lagoon: a problem of sustainability

Eliana Pecorari¹, Giancarlo Rampazzo¹, Antonio Ferrari², Giovanni Giuponi² and Gianluca Cuzzolin²

¹Department of Environmental Science, Informatics and Statistics, University Ca' Foscari Venice, Via Torino, 155 30172 Venezia Mestre, Italy

²ACTV S.p.A. –Isola Nova del Tronchetto, 32 – 30135 Venezia

eliana.pecorari@unive.it

Abstract. Human activities in urban areas strongly affect air quality. In order to characterize the impact of the main air pollutants sources, emission inventories are requested by legislation. However, in water cities, where marine and inland water emissions from ships and small boats must be controlled, have largely been exempt from this duty. Research and development efforts have focused on characterizing main problems and offering suitable abatement solutions recently requested by new regulations. Despite this, some specific scenarios could not easily be considered because of their peculiarity. Venice, as a water town in its historical part, is a very distinctive case where transport is supplied by marine systems. The Venice Public Transport Company (ACTV) has been suggested to adopt electrical engines for the abatement of the main pollutants, however, Venice peculiarity forces another hybrid solution. Moreover, changing completely the ACTV fleet requires high costs not completely justified by the emission quantification. A real estimate of the maintenance costs and disposal must be evaluated for both the traditional vessel and the hybrid one. In order to better investigate on the impact of these vehicles, ACTV in collaboration with Ca' Foscari University, has developed an emission factor model: Water Bus Emission Factor Model (WATERBUS). This model permit to better quantify actual and future emission scenarios, helping in decision making. In the current situation diesel engines ensure a good air quality impact in Venice area. Future possible scenarios calculated with the WATERBUS model show a further improvement of the situation. Ten scenarios will be presented in order to test several possibilities in terms of public waterborne transport emission impact.

Keywords: Waterborne transport, Small boats emissions, Environmental impact of transportation, Management of transportation.

1. Introduction

Air quality emissions from waterborne transport draw attention to the engine type choice especially today that electric propulsion represents the new frontier in marine system technology. Recently, regulations have been updated (Swedish Maritime Administration, 1994; Skjølsvik et al., 2000; ENTEC, 2002; IMO-MARPOL, 2017; Durán-Grados et al., 2018; Moreno-Gutiérrez et al, 2019); Environment Protection Committee (MEPC) under the remit of International Marine Organization (IMO) has addressed environmental issues, including the prevention of pollution and management of marine environment from the ship-source pollution such as particulate matters (PM), nitrogen oxides (NO_x), sulfur oxides (SO_x) and greenhouse gases (GHGs) (MEPC, 2008; Skjølsvik et al., 2000; IMO, 2017). All these legislations will be applied also in water cities, like Venice historical part, where public transport is supplied by small vessels that substitute bus in normal cities.

Venice case is a very peculiar one due to the delicate ecosystem, the Venice Lagoon, sited in a complex urban and industrial site where several anthropogenic emission sources causes high level of air pollution (Rampazzo et al., 2008a). The historical part, in the centre of the lagoon, suffers from emissions from artistic glass factories settled in Murano island (Rampazzo et al., 2008b), cruise ships and small boats, and commercial and cruise dock operations. Moreover, local pollution is aggravated by secondary regional factors and the low-lying nature of area (Pecorari et al., 2013a; Squizzato et al., 2012; Carnevale et al., 2010).

In this context, clarifying the emission aspect from the public transport is very important in order to minimize its impact in the Venice air quality context.

With this aim, the Department of Environmental Sciences, Informatics and Statistics, Ca Foscari University, and ACTV S.p.A. decided to create a new project dedicated to study the real impact of the naval fleet emission in Venice lagoon. A specific emission factor model: Water Bus Emission Factor Model (WATERBUS) has been developed to calculate ACTV fleet emission estimate (Pecorari et al., 2013b). This model has been used to calculate ACTV fleet emissions starting from real consumptions data and real boat and lines characteristics in order to create the most realistic emission inventory. The model has been used to calculate the annual amount and every year annual emission inventory is calculated for the ACTV fleet. Current situation shows a not big impact respect to the Venice emission context, especially after 53 engines renewal that reduced emission by nearly 30-50% (considering main exhausts and particulate matter). However, in the next year a more restrictive legislation will be imposed. The existing legislation that has been used as a reference is the IMO 1 and IMO 2 and the EU Directive IWW stage IIIA. At the moment, ACTV is not obliged to respect any emission limits. New motorizations will have to comply the European regulation IWP, stage V (EC, 2014; EC, 2016).

Consequently, a change is in order. Could, the change of the engine type, be sufficient to further reduce the emissions? Could be enough to change the old engines with the more recent diesel types? Which choice could be the most economic? Is an economic choice the best solutions in a so complex systems like Venice where also touristic and social impact must be considered? In this paper, ten possible scenarios will be discussed compared to the current situation in order to answer to these questions.

2. Methodology

2.1. Venice as a water town and the public transport

The city of Venice is located between the Adriatic Sea and the Po Valley, an area acknowledged to be the most highly industrialized area in Italy. The whole study area covers almost 2500 km², and is composed of dry land, water and intertidal mud flats, and both salt and artificial marshes. Venice is affected by various sources of emissions extending over the principal parts of the city: the historical centre, and the mainland areas (Venezia Mestre and Marghera). The center is located in the middle of a lagoon and is affected by emissions from artistic glass-making factories on the island of Murano, shipping traffic, and both commercial and industrial dock operations. Other emission sources are located on the mainland: an urban zone, with all types of related emission sources; the industrial zone of Porto Marghera, which comprises chemical and metallurgical works, oil refineries, and coal power plants; heavy traffic roads and a motorway, one of the a major through-routes for heavy vehicles in Italy (Rossini et al., 2001; ARPAV, 2006; Rampazzo et al., 2008a; Rampazzo et al., 2008b).

In this context, waterborne public transport is provided by AVM Holding (AVM) since 2012, through its subsidiary company ACTV S.p.A.

2.2. The WATERBUS model

The WATERBUS model (Figure 1) was developed as a collaboration between Dep. DAIS, Ca Foscari University and ACTV S.p.A., main exhausts (NO_x, CO, HC) and PM emissions. It has been created using a bottom-up approach to evaluate the emission from the ACTV fleet. It has been specifically designed to better represents the fleet characteristics. As previously explained, this is due to the impossibility of applying the general guidelines or emission factors diffused for other type of waterborne emission sources (EMEP CORINAIR, 2009; INEMAR-ARPAV, 2013). The estimate was calculated from the data provided by ACTV and included: i) boats characteristics, ii) fuel consumptions for each boat; iii) engine types used, iv) line routes and v) the annual time table and the seasonal traffic change. Waterbus model concept has been described in Pecorari et al. (2013b) but has been developed and improved. It has been introduced a better characterization of the engines and of the consumption of each engine and of each vessel.

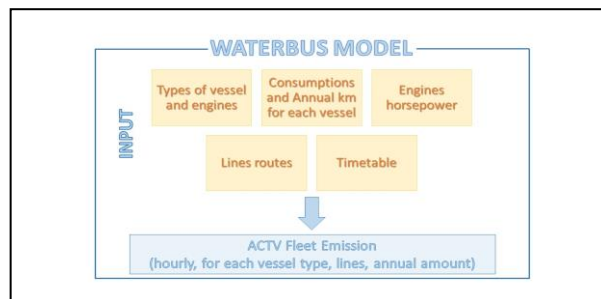


Figure 1. WATERBUS model: main elements

2.3. ACTV fleet: passengers, consumptions and emission estimate

The ACTV waterborne fleet is composed of 152 naval units (Figure 2) and approximately a hundred pontoon boarding points. In detail, the types of craft in the fleet are: ferry boats (NT), motor vessels (large) (MN), motorvessels (MB FOR), “vaporetto” (MB) and motorboats (MS). All craft are registered with RINA (the Italian Shipping Register), which certifies their state of structural efficiency, their safety and the quality of maintenance. Changes in passengers’ number, annual kilometres and consumptions estimate will be analysed for the following years: from 2012 to 2018. Annual emission estimates (NO_x, HC, CO and PM) will be shown and commented for three reference years: i) 2012, the first fleet configuration with old engines; ii) 2015, after the renewal of 53 boat’s engines; iii) 2018, the current situation. Descriptions of the main emission will refer to the annual total amount, values for vessel type and differentiations among the several lines in the Venice lagoon.

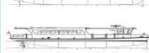
The Fleet						
Type	Dimensions [m]	Tonnage [ton]	Passenger flow	Crew	N° Boats	
 Ferry-boats	40-55	200-700	350-1000	6	7	
 Motorvessels (large)	33-38	170-290	800-1300	5*	7	
 Motorvessels	21-27	65-130	230-330-400	2	19	
 "Vaporetto"	21	24-25	200-220	2	62	
 Motorboat	19-23	20-25	150-190	2	50	
 Motorboats single pilot	8-10	4-5	20	1	8	

Figure 2. ACTV fleet characterization

2.4. Scenario's emission analysis

Changes in the fleet will characterize coming years. Looking to an increasing demand for tourism and to future imposing emission limits, the fleet will see variations. In order to test the best solution from emission point of view, ten scenarios will be evaluated in terms of emission changes. Table 1 shows the several scenarios in terms of the type of changes, number and type of vessels and lines involved. In some scenarios some hybrid-diesel engines will substitute the present diesel engine (*refitting hybrid-diesel*); in others some vessel will be changed with new ones (*new*); in others some engines will be changed with more recent diesel engine (*refitting*). The tenth scenario is the sum of all the previous possibilities. As regards emission factors, not all engines have been chosen or designed yet. As a consequence, data from European regulation IWP, stage V, for three different mechanical power: (stage V < 130 kW; stage V < 300 kW; stage V > 300 kW), (EC, 2014; EC, 2016) has been used as a reference. These data represent the maximum emissions values that could be produced by new engines. As a consequence, this estimate is clearly not completely comparable to the previous one. However, in terms of predicting changes in emissions, the order of magnitude and possible percentages could be approached. Moreover, the precautionary values allow to assure a safe emission estimate. Pollutants considered refer to the main exhausts (NO_x, HC and CO) and particulate (PM). No value has been calculated for CO₂ because it is not covered by the IWP regulation.

Table 1. Ten scenarios discussed to evaluate future emission changes for the ACTV fleet

Scenario n°	Number of vessels that will be changed	Changes	Lines
1	35	Hybrid-diesel refitting	L1; L2
2	5	New traditional "vaporetto" (MB)	L1; L2
3	7	New traditional motorvessels (MB FOR)	L14; L15
4	1	New traditional ferry boats (NT)	L11
5	10	New Hybrid-Diesel "vaporetto" (MB)	L1; L2
6	5	New Hybrid-Diesel motorvessels (MB FOR)	L14; L15
7	1	New ferry boat (NT)	L17
8	1	Refitting Marco Polo ferry boat (NT)	L17
9	1	Refitting Pellestrina ferry boat (NT)	L11
10	66	Sum of the previous scenarios	Previous all

3. Results and discussion

3.1. Current ACTV fleet "numbers"

ACTV fleet travels regular routes generally characterized by the same hours, kilometers and consumptions per years. Figure 3 shows the distribution of these parameters from 2012 to 2018. A tendency of decrease characterizes year 2015 and, only for kilometres variable, 2014. Changes are generally due to logistic aspect and tourism reason, however during 2013-2015 the fleet renewal has been completed affecting also the number and type of vessel circulating. After 2015 the general increase reflects the trend towards future expectations.

Consumption changes respect to the vessel type, due to the engine installed, but also to the type of route line boats must travel. The biggest average fuel consumptions order of magnitude, in one year, is consumed by the ferry boats (NT), 280000 kg and by motor vessels (MB for), 90000 kg and then by ferry boats, (NT), 80000 kg and lastly by vaporetto (MB) and motorboats (MS), nearly 30000 kg. However, considering the total amount in one year, MB and MS contribute similarly (26 and 24% respectively) and more than the others: MB for: 22%; NT: 21% and MN:6%. This is due to the type of

routes that MB and MS vessels travel. The highest impact is represented by vaporetto that travels mainly lines L1 and L2, that are characterized by the highest number of navigation hours (37% of the total amount in one year). This clearly affects emission distribution among the different vessels and lines as it will be described further.

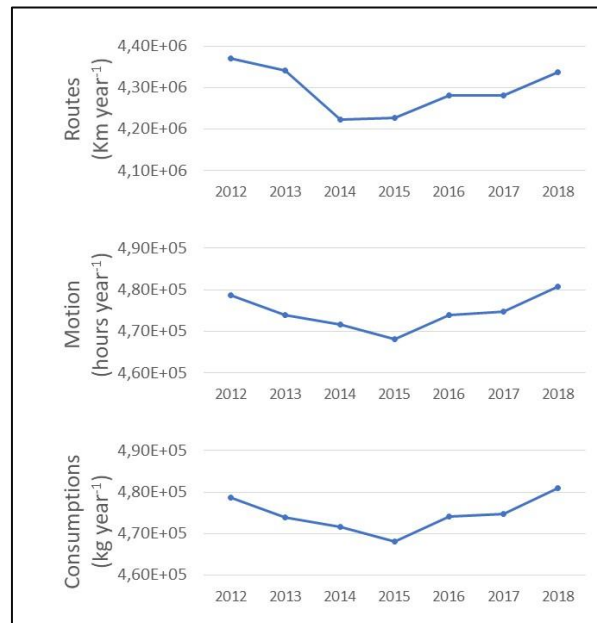


Figure 3. ACTV annual passengers' number, hours of motion and consumptions for the following years: from 2012 to 2018

3.2. ACTV fleet emissions distributions

Annual emission estimate has been reported here for three years as a reference: 2012, 2015 and 2018 as previously explained. After the first high decrease between 2012 and 2015 (Figure 4), due to the engine's renewal, a general tendency of small variations characterizes the following years. Variations can be positive or negative, but the order of magnitude is constant at the moment.

Evaluating difference between 2012 and 2018, percentages change in relation to the pollutant considered. Highest decrease have been reached for CO (nearly 50%) and subsequently for NO_x, PM and HC decrease by nearly 20% (Table 2).

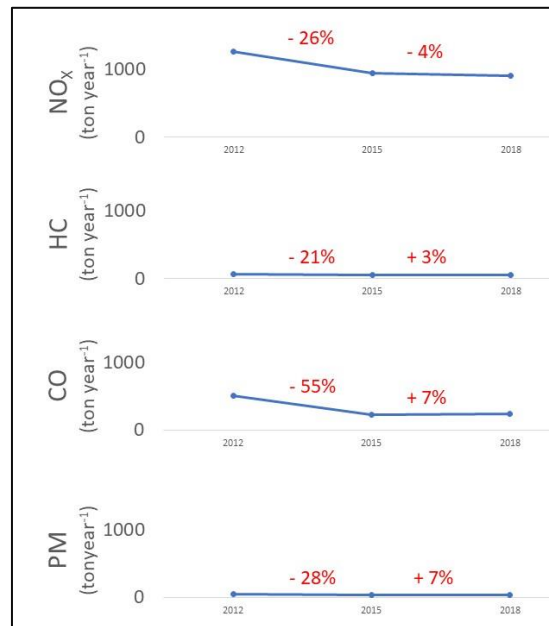


Figure 4. ACTV annual emission for years 2012, 2015 and 2018 and relative percentages decrease

Table 2. ACTV annual fleet emissions in 2012 and 2018 and relative percentage decreases for (NO_x, HC, CO and PM)

	2012 fleet emissions (ton year ⁻¹)	2018 fleet emissions (ton year ⁻¹)	Decrease (%)*
NO _x	1270	903	29
HC	67	54	19
CO	511	244	52
PM	44	34	23

*from 2012 to 2018

3.2.1. Emission distribution respect to the vessel type and among the several lines.

Great importance must be given to emissions distribution among the several lines and to the type of vessel used. As fuel consumption changes due to this fact, also emissions variation is affected by which lines are travelled and by which vessels is navigating. Lines 1 and 2 are the busiest not just for the position, but also for touristic reason. Despite a decrease characterize these lines' emission from 2012 to 2018, highest values are still related to them (Figure 5). Several lines reveal an increase in 2018 probably due to logistic reasons: this is very clear for Line 12. This is due mainly to the type of vessels involved according to the emission distribution for MB for boat type and NT that generally navigate in these lines (Figure 6).

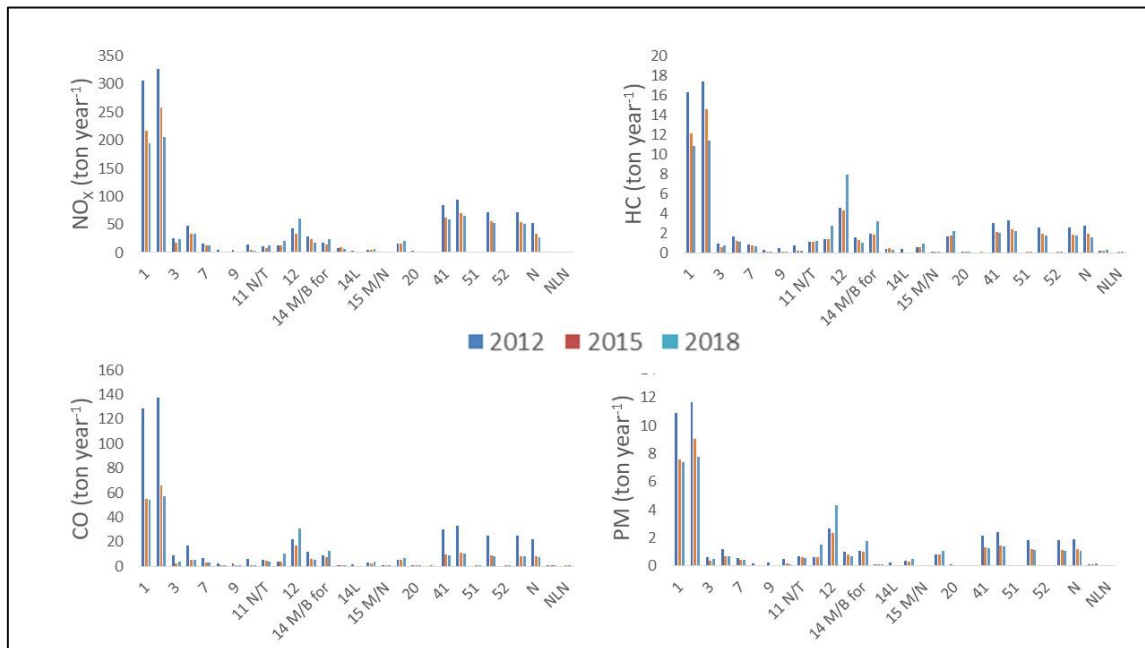


Figure 5. ACTV fleet emission distribution among the different lines for years 2012, 2015 and 2018

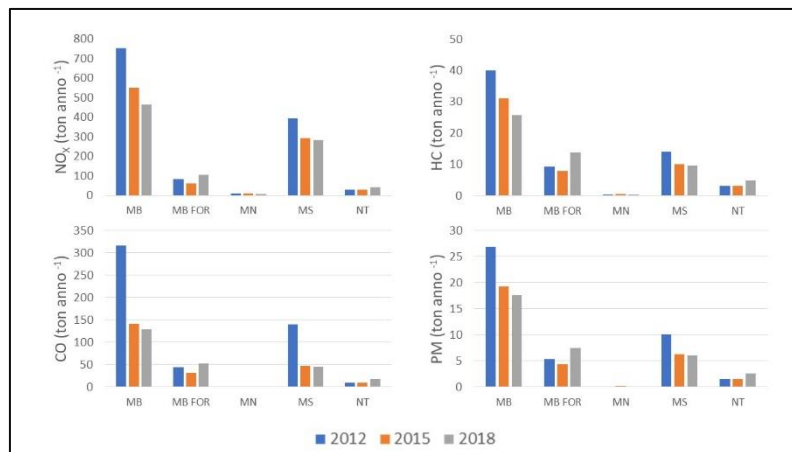


Figure 6. ACTV fleet emission distribution among the different vessels' type for years 2012, 2015 and 2018

3.3. Possible future scenarios

Future scenarios, where new engines or new vessels can substitute obsolete vehicles, show improvements at different levels respect to the pollutant considered (Figure 7). Obviously, scenario X is the most effective. However, due to economic reasons, maybe it is not necessarily the most sustainable. Changes require high investments and, in this case, public investment. Moreover, hybrid-diesel engines require higher equipment and maintenance costs respect to diesel ones. Except the first and the tenth scenario, percentage decreases are not so high to justify this choice. However, a change must be done in the future for both technical reason and future regulations. In terms of sustainability, this can help to reach out to public opinion that is strongly affected by alarmism and a perception that is strongly deviated by an impressive communication.

Considering the best solution, trying to join economic and environmental benefits, an important role is played by management. As previously shown, emissions change in relation to the vessel type and to the lines considered. Evaluating the different lines and looking at the possible changes in these scenarios, high decrease can be reached. As an example, lines 1 and 2 that are the most impacting can have the highest decrease with the first scenario characterized by new hybrid-diesel engine for NO_x, HC and PM. This could be very effective especially in correspondence of waterbus stops where the use of electric power generator could allow to avoid the most impacting maneuvers and the visible black smoke that causes people alarmism. CO scenarios suggest different solutions. However, this substance seems to be less impacting than the others that require more attention, especially considering the future importance of abating NO_x emissions.

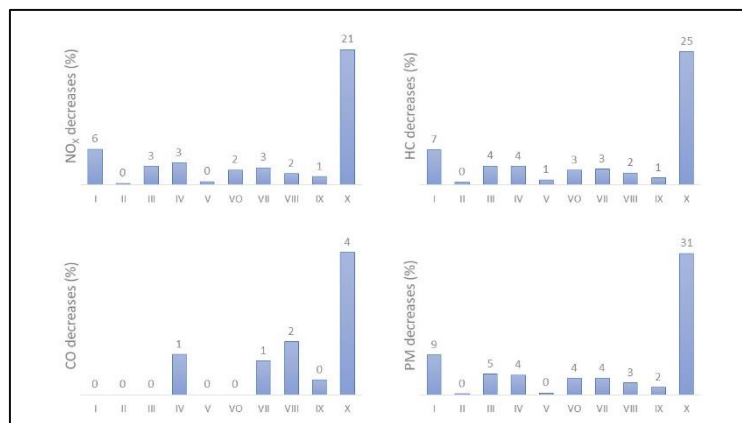


Figure 7. Percentages decreases for several pollutants (NO_x, HC, CO and PM) for each scenario

4. Conclusions

Waterborne transport emission estimate for reality like Venice could represent a great challenge in terms of sustainability. Difficulties due to infrastructures, public money and opinion always affect perception of what really is the problem and the possible solution. The creation of a specific emission model, WATERBUS model, permitted to better evaluate the impact in the Venice context and to propose possible future solutions. From study results, an important element arises: engine choice is important, but the integration with an appropriate management could bring to a more efficient and sustainable solution.

5. References

- ARPAV, 2006. Annual report on ambient air quality – ARIA 2006. (Environmental Agency of Veneto-ARPAV – Environmental Council Causes and Effects of Heavy Metal Pollution Office and Department of the Venice Province).
- Carnevale C, Pisoni E, Volta M., 2010. A non-linear analysis to detect the origin of PM₁₀ concentrations in Northern Italy. *Sci. Total. Environ.* 409:182-191.
- Durán-Grados V., Mejías J., Musina L., Moreno-Gutiérrez J., 2018. The influence of the waterjet propulsion system on the ships' energy consumption and emissions inventories. *Sci. Total Environ.* 631–632, 496-509.
- EMEP CORINAIR (Joint EMEP/CORINAIR Emission Inventory Guidebook, third ed.), October 2002 <http://www.eea.europa.eu/publications/EMEPCORINAIR5> [Updated 2016].



ENTEC, 2002. Final Report. Quantification of Ship Emissions. https://ec.europa.eu/environment/air/pdf/chapter2_ship_emissions.pdf.

European Commission (EC), 2014. Proposal for a regulation of the European Parliament and of the Council on requirements relating to emission limits and type approval for internal combustion engines for non-road mobile machinery. Retrieved from <http://eur-lex.europa.eu/legal-content/EN/TXT/?uri=CELEX:52014PC0581>.

European Commission (EC), 2016. Regulation (EU) 2016/1628 of the European Parliament and of the Council of 14 September 2016 on requirements relating to gaseous and particulate pollutant emission limits and type-approval for internal combustion engines for non-road mobile machinery, amending Regulations (EU) No 1024/2012 and (EU) No 167/2013, and amending and repealing Directive 97/68/EC. <https://eur-lex.europa.eu/legal-content/EN/TXT/?uri=CELEX%3A32016R1628>.

IMO, 2017. Marine Environment Protection Committee (MEPC) 71st Session.

IMO-MARPOL Annex VI and NTC 2008 with guidelines for implementation, 2017 ed., CPI Group (UK) Ltd., London. ISBN 978-92-801-1658-8, 2017.

INEMAR-ARPAV, 2013. Disaggregated emission inventory 2013. (<http://www.arpa.veneto.it/temi-ambientali/aria/emissioni-di-inquinanti/inventario-emissioni>).

Moreno-Gutiérrez J., Pájaro-Velázquez E., Amado-Sánchez Y., Rodríguez-Moreno R., Calderay-Cayetano F., Durán-Gradosa V., 2019. Comparative analysis between different methods for calculating on-board ship's emissions and energy consumption based on operational data. *Science of The Total Environment*. 650, Part 1. <https://doi.org/10.1016/j.scitotenv.2018.09.045>.

Pecorari E., Squizzato S., Ferrari A., Cuzzolin G., Rampazzo G. 2013. WATERBUS: A model to estimate boats' emissions in "water cities". *Transportation Research Part D: Transport and Environment*. 23, 73-80. (ISSN 1361-9209), doi:10.1016/j.trd.2013.04.003

Rampazzo, G., Masiol, M., Visin, F., Rampado, E., Pavoni, B., 2008a. Geochemical characterization of PM₁₀ emitted by glass factories in Murano, Venice (Italy). *Chemosphere*. 71:2068–2075.

Rampazzo G, Masiol M, Visin F, Pavoni B., 2008b. Gaseous and PM₁₀-bound pollutants monitored in three environmental conditions in the Venice area (Italy). *Water Air Soil Poll*. 195:161–176.

Rossini, P., De Lazzari, A., Guerzoni, S., Molinaroli, E., Rampazzo, G., Zancanaro, A., 2001. Atmospheric input of organic pollutant to the Venice lagoon. *Annali di Chimica – Rome* 91, 491–501.

Squizzato S, Masiol M, Innocente E, Pecorari E, Rampazzo G, Pavoni B., 2012. A procedure to assess local and long-range transport contributions to PM_{2.5} and secondary inorganic aerosol. *J. Aerosol Sci*. 46:64-76.

Skjolsvik KO, Andersen AB, Corbett JJ, Skjelvik JM, 2000. Study on Greenhouse Gas Emissions from Ships, Report to the International Maritime Organization, produced by MARINTEK, Det Norske Veritas (DNV), Centre for Economic Analysis (ECON) and Carnegie Mellon. MT Report Mtoo A23-038, Trondheim Norway, February 15.

Swedish Maritime Administration, 1994. Air pollution and control measures for the marine sector (in Swedish). Report 45-9371263, SjöKfartsverket, NorrkoKping, Sweden.

Acknowledgments

The authors want to acknowledge ACTV S.p.A. to support this work by technical and financial help.

Linkage among ambient air quality measurements, air quality models, and respiratory symptoms and diseases in different locations of Canakkale, Turkey

Sibel Mentese^{1,*}, Nihal Arzu Mirici², Tolga Elbir³, Gizem Tuna Tuygun³,
Coskun Bakar⁴, Sibel Oymak⁴ and Musserref Tatman Otkun⁵

¹ Faculty of Engineering, Environmental Engineering Department, Canakkale Onsekiz Mart University, Terzioglu Campus, Canakkale, Turkey

² Faculty of Medicine, Respiratory Diseases Department, Canakkale Onsekiz Mart University, Canakkale, Turkey

³ Faculty of Engineering, Environmental Engineering Department, Dokuz Eylul University, Tinaztepe Campus, Izmir, Turkey

⁴ Faculty of Medicine, Public Health Department, Canakkale Onsekiz Mart University, Canakkale, Turkey

⁵ Faculty of Medicine, Medical Microbiology Department, Canakkale Onsekiz Mart University, Canakkale, Turkey

sibelm@comu.edu.tr

Abstract. In Turkey, few epidemiological studies are available investigating the association between air pollution and health. Once the mortality rates due to the diseases in Canakkale was considered from 2007, relatively high death numbers from the respiratory system disorders were seen in Can town than Lapseki and Central towns of Canakkale city, Turkey. The aim of this cohort-type study is to examine the relationships between ambient air quality, respiratory diseases, and decreases in pulmonary function over a year in three different towns in Canakkale and also to estimate the of source contributors of ambient air pollution. In the first stage of the study, a detailed questionnaire was completed and pulmonary function test (PFT) was performed twice in a year. Ambient levels of particulate matter, SO₂, NO₂, and ozone were gathered from air quality monitoring stations in those three regions. Moreover, air quality measurement (VOCs, bioaerosols, CO₂, etc.) and modelling studies were carried by AERMOD program. Three air pollution sources, namely, industry, domestic heating, and traffic, were taken into account to find the contribution of the sources on CO, PM₁₀, SO₂, and NO_x emissions. According to the results, the most polluted area was Can, while Central town and Lapseki were the least polluted areas. Domestic heating was found to be the major source contributor of SO₂ emissions (exceeded the national limit), while NO_x emissions were originated from traffic and industry in Canakkale. In the present study, ambient air quality was worse in Can (industrialized region), which influenced PFT scores and the prognostics for chronic respiratory diseases. Also, the highest frequency of obstructive disorders was occurred in one of the village in Can town. The findings of this study showed that air quality monitoring, modeling, and medical follow-ups should be considered for future investment plans in this region related to human and environmental health needs.

Keywords: Air pollutants, Air quality modelling, Canakkale, Pulmonary function, Respiratory symptoms.

1. Introduction

Routes of exposure to air pollution are inhalation, ingestion, and dermal contact, while inhalation is the main route. Health effects of the air pollutants can be acute, chronic (not including cancer), and cancer. Epidemiological/animal model data indicate that primarily affected systems from the air pollution are the cardiovascular system and the respiratory system (WHO, 2014). Generally, monitoring of air pollution on human beings' health is accomplished by mortality and morbidity ratios (hospital admissions). Also, susceptibility factors, such as age, nutritional status, and predisposing conditions cause variability on the exposure degree and perception of air quality. Another critical point is difficulties on the estimation of a dose-response linkage of a certain air pollutant. Because, individuals expose to different composition of air pollutants, the dose, and time of exposure and the fact that individuals are usually exposed to pollutant mixtures other than to single substances.

According to Turkish Health Statistics, cardiovascular diseases rank first, cancer ranks second, and chronic respiratory diseases rank third among leading causes of death in Turkey. At national level, respiratory diseases are responsible for 10% of total deaths. Respiratory system diseases are the leading cause of hospitalization which accounted for 12.7% of all hospital admissions in 2014 (Basara et al., 2015). According to IARC data, lung cancer has the highest incidence and mortality compared to any other types of cancer in Turkey (IARC, 2016). These health indicators show the role of respiratory diseases in burden of disease and among the causes of mortality. Although the role of cigarette smoking in the etiologies of these diseases is known, it cannot be neglected that exposure to air pollution in some regions of our country pose a risk in this regard. Few epidemiological studies are available investigating the association between air pollution and health in Turkey. Once the mortality rates due to the diseases in Canakkale was considered from 2007, relatively high deaths numbers from the respiratory system disorders were seen in Can town than Lapseki and Central towns of Canakkale city, Turkey.

Emission inventory is a compilation of all air pollution quantities entering in the atmosphere from all sources in a geographical area for a time period and important for air quality (AQ) management strategies. AQ dispersion models (*e.g.* Gaussian, numerical, statistical, or physical) are useful tools for determining potential concentration impacts from proposed as well as existing sources. AQ models are useful tools to estimate potential source contributors of the air pollutants together with the real-time measurements. AERMOD model is a Gaussian model, used to calculate gaseous or particle pollutants emitted from the source(s) at different coordinates (US EPA, 2004).

The aim of this cohort-type study is to examine the relationships between ambient AQ, respiratory diseases, and decreases in pulmonary function over a year in three different towns in Canakkale and also to estimate the source contributors of ambient air pollution by AQ modelling.

2. Materials and Methods

2.1. Study design

Three different towns were selected here, which are Canakkale Central town (urban), Lapseki town center (rural), and Can town (industrial and rural; including downtown and 3 villages). In the first stage of the study, a detailed questionnaire was completed by the participants by face-to-face interviews and pulmonary function test (PFT) was performed twice in a year. Ambient levels of particulate matter, SO₂, NO₂, and ozone were gathered from air quality monitoring stations located in the centers of the three regions. Furthermore, monthly ambient AQ measurements of selected pollutants and parameters were carried out for VOCs, TBC, TMC, PM, CO₂, ozone, T, RH, etc. Moreover, air quality modelling studies were carried by AERMOD program. Three air pollution sources, namely, industry, domestic heating, and traffic, were taken into account to find the contribution of the sources on CO, PM₁₀, SO₂, and NO_x emissions.

2.2. Questionnaire and Pulmonary Function Test (PFT)

In the first stage of the study, a detailed questionnaire was completed by the participants by face-to-face interviews and pulmonary function test (PFT) was performed twice in a year. The questionnaire consisted of 47 questions, including descriptive information such as socio-demographic characteristics, health conditions, status of disease, respiratory complaints, and locations and characteristics of their homes. Written informed permission was obtained from the participants.

2.3. Air Quality Monitoring and Measurement

Monthly measurements of ambient air pollutants such as VOCs, TBC, TMC, PM, CO, CO₂, ozone, T, RH, etc. were conducted as prescribed in Mentese et al. (2015).

2.4. Air Pollution Inventory and Air Quality Modelling

Data gathered from national AQ monitoring stations in the city (Central, Lapseki & Can Towns) and related meteorological measurement stations in the city was used as input of the model. Ambient levels of particulate matter, SO₂, NO₂, and ozone were gathered from those air quality monitoring stations. AQ modelling studies were carried by AERMOD program (US EPA, 2004). Three air pollution sources, namely, industry, domestic heating, and traffic (both road and marine), were taken into account to find the contribution of the sources on CO, PM₁₀, SO₂, and NO_x emissions. Pollutant concentrations were calculated by AERMOD. Moreover, AERMET (Meteorological pre-processor) and AERMAP (topographical pre-processor) were used as input to AERMOD. Upper layer data was gathered from Göztepe station, Istanbul. Pollution sources within the defined grid system of the model, including a total of 339 segments as small area sources are as follows: 7 stacks as point sources from different industrial plants, an open-pit coal mine as an area source, 70 polygons as area source covering all residential areas of towns of Canakkale province, 89 roads, 194 ferry routes and 56 transit ship passage routes (see Figure 1).



Figure 1. The grid system of the modelling study.

3. Results and Discussion

Levels of ambient air pollutants at the study site in 2013 and 2014 are given in Table 1. The highest SO₂ levels were observed in Çan throughout the study. The maximum SO₂ concentration in Çan was as high as 977 µg/m³, while the maximum SO₂ levels in other regions were lower than 70 µg/m³. PM₁₀ levels in Central and Çan towns and PM_{2.5} levels in Lapseki were measured in terms of particulate Matter. The particle level (PM₁₀) was found to be higher in Çan than any other region. Average PM₁₀ level in Central town was close to PM_{2.5} levels found in Lapseki. Levels of NO₂ and ozone were measured in Lapseki and Çan. NO₂ levels were found to be higher in Çan than those measured in Lapseki. Ozone levels were

found to be higher in Lapseki than those measured in Çan. Lapseki is located closer to Center than Çan, and it is characterized as rural, densely forested, and agricultural land.

Table 1. Levels of ambient air pollutants at the study site in 2013 and 2014.

Parameter	2013			2014		
	Center	Lapseki	Çan	Center	Lapseki	Çan
PM ₁₀	18	-	58	23	-	71
PM _{2.5}	-	19	-	-	21	-
NO ₂	-	11	19	-	11	23
SO ₂	13	7	66	12	8	134
O ₃	-	86	73	-	63	50

Table 2 shows the Spearman Rank correlations based on the seasonal average values of the ambient AQ measurement results at Central Town for a year. Except for PM₁₀ and SO₂ measured at the Center, other outdoor air quality parameters (TBC, TMC, TVOC, NO_x and ozone) showed seasonal changes; these seasonal changes indicated higher levels in summer and lower in winter ($p < 0.05$). The relationships between outdoor pollutants measured at the Center are summarized as follows: positive relationships between bacterial and fungal levels; TVOC and PM₁₀; PM₁₀ and ozone; NO_x and SO₂; bacteria level and ozone; while negative relationships between fungal level and PM₁₀; fungal level and ozone; and TVOC and NO_x ($p < 0.05$).

Table 2. Spearman rank correlations among the ambient air pollutants and season - Central Town^a

Parameter	TBC	TMC	TVOC	PM ₁₀	SO ₂	Ozone	T	RH	NO _x	Season
TBC	1	-	-	-	-	-	-	-	-	-
TMC	0.28**	1	-	-	-	-	-	-	-	-
TVOC	0.10	-0.14	1	-	-	-	-	-	-	-
PM ₁₀	0.06	-0.26**	0.30**	1	-	-	-	-	-	-
SO ₂	-0.03	0.03	-0.06	0.03	1	-	-	-	-	-
Ozone	0.28*	-0.40**	0.06	0.50**	-0.01	1	-	-	-	-
T	0.41**	0.05	0.33**	0.20*	-0.28**	0.43**	1	-	-	-
RH	-0.51**	-0.06	-0.23**	-0.24**	0.13	-0.41**	-0.82**	1	-	-
NO _x	-0.08	0.08	-0.28*	0.05	0.19*	-0.01	-0.21*	0.05	1	-
Season	-0.60**	-0.20*	-0.18**	-0.08	0.04	-0.61**	-0.74**	0.62**	0.26**	1

^a Season was coded according to TVOC, total PM, and CO₂ emission profiles of the study sites, where: summer: 1, spring: 2, fall: 3, and winter: 4; * $p < 0.05$ and ** $p < 0.01$, $n = 184$.

According to Table 3, all ambient AQ parameters (PM_{2.5}, SO₂, TBC, TMC, TVOC, NO_x and ozone) measured in Lapseki showed seasonal changes; PM_{2.5}, SO₂ and NO_x levels were higher in winter, while TBC, TMC, TVOC, and ozone levels were higher in summer ($p < 0.05$). The relationship between air pollutants measured in Lapseki is summarized as follows: positive relationships between bacteria and fungal levels; TVOC and ozone levels; fungal levels and TVOC and ozone levels; PM_{2.5} and SO₂ and NO_x levels; TVOC and SO₂, while negative relationships were found between PM_{2.5} and TBC and TVOC; NO_x and TBC; TMC and ozone levels; and SO₂ and TBC, TMC and ozone levels ($p < 0.05$).

Table 3. Spearman rank correlations among the ambient air pollutants and season - Lapseki^a

Parameter	TBC	TMC	TVOC	PM _{2.5}	SO ₂	Ozone	NO _x	T	RH	Season
TBC	1	-	-	-	-	-	-	-	-	-
TMC	0.34**	1	-	-	-	-	-	-	-	-
TVOC	0.33**	0.26**	1	-	-	-	-	-	-	-
PM _{2.5}	-0.22**	-0.14	-0.45**	1	-	-	-	-	-	-
SO ₂	-0.20*	-0.36**	0.26**	0.26**	1	-	-	-	-	-
Ozone	0.24**	0.43**	-0.17	-0.17	-0.48**	1	-	-	-	-
NO _x	-0.20*	-0.36**	0.25**	0.25**	0.72**	-0.55**	1	-	-	-
T	0.45**	0.42**	-0.30**	-0.31**	-0.51**	0.63**	-0.47**	1	-	-
RH	-0.37**	-0.42**	0.23**	0.24	0.48**	-0.65**	0.42**	-0.72**	1	-
Season	-0.34**	-0.26**	-0.30**	0.23*	0.60**	-0.58**	0.57**	-0.80**	0.67**	1

^a Season was coded according to TVOC, total PM, and CO₂ emission profiles of the study sites, where: summer: 1, spring: 2, fall: 3, and winter: 4; * $p < 0.05$ and ** $p < 0.01$; n = 144

According to Table 4, all ambient AQ parameters (PM₁₀, SO₂, TBC, TMC, NO_x, and ozone), except for TVOC measured in Çan showed seasonal changes and PM₁₀, SO₂ and NO_x levels were higher in Çan as in Lapseki in winter, whereas TBC, TMC, and ozone levels were higher in summer ($p < 0.01$). The relationships between the outdoor air pollutants measured in Çan are summarized as follows: positive relationships between ozone and bacterial/fungal levels; NO_x levels and PM₁₀ and SO₂; PM₁₀ and SO₂; TVOC and NO_x, whereas negative relationships between TMC and TVOC, PM₁₀, SO₂, and NO_x; SO₂ and ozone and bacterial/fungal levels; and ozone levels and PM₁₀ and NO_x levels ($p < 0.05$).

Table 4. Spearman rank correlations among the ambient air pollutants and season - Çan^a

Parameter	TBC	TMC	TVOC	PM ₁₀	SO ₂	Ozone	NO _x	T	RH	Season
TBC	1	-	-	-	-	-	-	-	-	-
TMC	0.43**	1	-	-	-	-	-	-	-	-
TVOC	0.04	-0.21*	1	-	-	-	-	-	-	-
PM ₁₀	-0.10	-0.38**	0.12	1	-	-	-	-	-	-
SO ₂	-0.28**	-0.53**	0.10	0.71**	1	-	-	-	-	-
Ozone	0.30**	0.47**	-0.16	-0.72**	-0.87**	1	-	-	-	-
NO _x	-0.08	-0.42**	0.26**	0.76**	0.76**	-0.79**	1	-	-	-
T	0.34**	0.47**	-0.08	-0.53**	-0.77**	0.84**	-0.61**	1	-	-
RH	-0.01	-0.38**	0.22**	0.61**	0.61**	-0.64**	0.70**	-0.65**	1	-
Season	-0.48**	-0.50**	0.10	0.51**	0.78**	-0.84**	0.55**	-0.79**	0.44**	1

^a Season was coded according to TVOC, total PM, and CO₂ emission profiles of the study sites, where: summer: 1, spring: 2, fall: 3, and winter: 4; * $p < 0.05$ and ** $p < 0.01$, n = 156.

According to the results, the most polluted area was Can, while Central town and Lapseki were the least polluted areas. Domestic heating was found to be the major source contributor of SO₂ emissions (exceeded the national limit), while NO_x emissions were originated from traffic and industry in Canakkale city (see Figure 2). Although no limit exceedances were calculated for PM₁₀ and CO emissions throughout the city, PM₁₀ measurement levels were above the national limit in Can town. The risk of pulmonary function decline throughout a year calculated as 2.1 times higher in Can and 1.6 times

higher for smoker participants in all regions. In the present study, ambient AQ was worse in Çan (industrialized region), which influenced PFT scores and the prognostics for chronic respiratory diseases. Also, the highest frequency of obstructive disorders (24.6%) was occurred in one of the village in Çan town. The findings of this study showed that AQ monitoring, modelling, and medical follow-ups should be considered for future investment plans in this region related to human and environmental health needs.

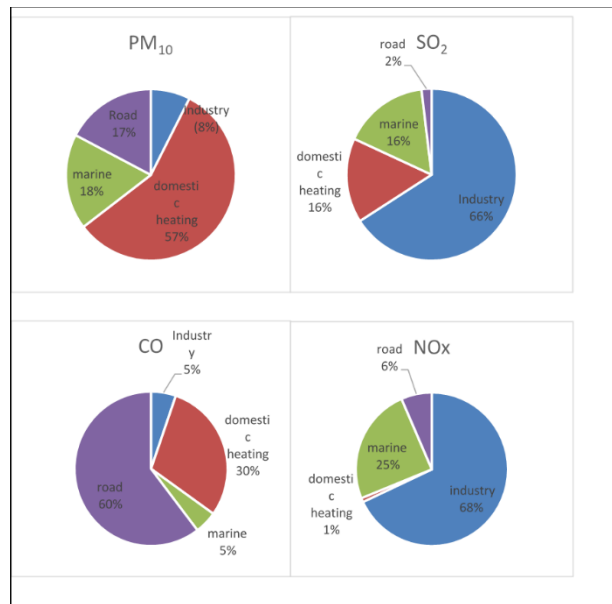


Figure 2. Contribution of pollutant sources to total emissions

4. References

- Basara, B.B.,Guler, C.,Yentur, G.K. 2015. The Ministry of Health of Turkey, health statistics yearbook 2014. General Directorate of Health Research, Ministry of Health, Ankara
- International Agency for Research on Cancer (IARC) (2016) Cancer Today, population Fact Sheets: Turkey. <https://gco.iarc.fr/today/>
- Menteşe S., Mirici N.A., Otkun M.T., Bakar C., Palaz E., Taşdibi D., et al., 2015. Association between respiratory health and indoor air pollution exposure in Canakkale, Turkey. *Building and Environment*, 93:72-83.
- US EPA (US Environmental Protection Agency), 2004. User's Guide for The AMS/EPA Regulatory Model – AERMOD, North Carolina, pp.216.
- World Health Organization (WHO), 2014. Media Centre. Ambient (outdoor) air quality and health, Fact sheet No: 313. <http://www.who.int/mediacentre/factsheets/fs313/en/>

Acknowledgments

This study was supported by TUBITAK. Project no: 112Y059.

A long-term multi-parametric indoor air quality (IAQ) monitoring study on respiratory diseases and sick building syndrome (SBS) linkages

Sibel Mentese^{1,*}, Elif Palaz^{1,2}, Deniz Tasdibi Mumcuoglu¹, Osman Cotuker¹, Nihal Arzu Mirici³, Coskun Bakar⁴, Sibel Oymak⁴, Muserref Tatman Otkun⁵ and Tolga Elbir²

¹ Department of Environmental Engineering, Canakkale Onsekiz Mart University, Turkey

² Faculty of Engineering, Environmental Engineering Department, Dokuz Eylül University, Tinaztepe Campus, Izmir, Turkey

³ Faculty of Medicine, Respiratory Diseases Department, Canakkale Onsekiz Mart University, Canakkale, Turkey

⁴ Faculty of Medicine, Public Health Department, Canakkale Onsekiz Mart University, Canakkale, Turkey

⁵ Faculty of Medicine, Medical Microbiology Department, Canakkale Onsekiz Mart University, Canakkale, Turkey

sibelm@comu.edu.tr

Abstract. Indoor air pollution can cause several respiratory diseases and symptoms. The sick building syndrome (SBS) is a situation related to indoor air pollution in which the occupants of a building experience health or comfort related effects that appear to be associated directly to the time spent in the “sick” building. It is called as syndrome, since no specific illness or cause can be identified. The SBS covers various nonspecific symptoms such as headache, dizziness, nausea, skin, eye, nose or throat irritation, difficulty in concentration, fatigue, etc., that occur among the occupants of a building. In this study, indoor air quality (IAQ) of 121 homes located in 3 different towns of Canakkale, Turkey was monitored throughout a year. Particulate matter, Volatile organic compounds (VOCs), bioaerosols, ozone, and CO₂ measurements, together with air temperature and humidity monitoring of those houses. Also, occurrence of SBS symptoms and other health or specifically respiratory health related data were gathered from the occupants’ questionnaire. Moreover, respiratory functions of the occupants were measured on a monthly basis by Spirometry. According to the results of this study, the highest indoor air pollutant levels were observed in Can town and the lowest levels were observed in Central town. The predominant SBS symptoms varied seasonally and spatially among the study sites. Correlations were found among the occurrence of SBS symptoms, measured indoor pollutants, and comfort parameters ($p < 0.05$). Also, daily ventilation amount of the houses was negatively correlated with CO₂ levels ($p < 0.05$), which used to be an indicator of adequacy of ventilation or fresh air intake. Also, high levels of indoor air pollutants were linked with increase of respiratory symptoms of the occupants ($p < 0.05$). Performing more studies from the health and IAQ points of view improve public awareness of indoor environmental comfort.

Keywords: Canakkale, Indoor air quality, Respiratory function Respiratory health, Sick building syndrome.

1. Introduction

The scope of sick building syndrome (SBS) indicates unspecified, combined, adverse health effects due to poor indoor air quality (IAQ). The sick building syndrome, which remains as symptom as the factors

that have not been fully confirmed yet, is one of the most noticeable subjects recently. People who spend a long period of time in the buildings with poor IAQ may be affected by various symptoms and even diseases, depending on the intensity of the source of pollutants. These buildings, which cause problems, are called “sick building”. Sick Building Syndrome (SBS) is thought to cause personal symptoms in a wide spectrum with exposure to indoor environmental source(s); while the exact cause of the symptoms is unidentified. The causes of SBS may be due to a single factor or a combination of multiple factors. These factors are roughly: insufficient ventilation, humidity, light, temperature; chemical pollutants from indoor sources; chemical pollutants and biological pollutants from external sources (WHO, 1989). The symptoms and complaints identified by WHO in this context are:

1. irritation of the eyes, nose and throat,
2. neurotoxic or general health problems,
3. skin irritation,
4. nonspecific hypersensitivity reactions,
5. odors and taste sensation.

In another study conducted in Çanakkale, the relationship between bacterial levels in indoor air and SBS symptoms was investigated (Mentese and Tasdibi, 2016). Accordingly, it was found that the frequencies of SBS symptoms vary seasonally and factors such as time spent at home and amount of daily cigarettes consumed increase the risk of SBS symptoms. Another study found a positive correlation between SBS symptom frequency and bacterial levels (Harrison et al., 1992). Other studies have also identified associations between exposure to bioaerosols and SBS and other hypersensitivity reactions (ACGIH, 1989; Carrer et al., 2001; Douwes et al., 2003).

Since the perception and public awareness of IAQ in Turkey is quite recent, studies conducted on this issue are limited so far. The aims of this study were (i) to investigate the variations of indoor air pollutants' levels in 121 homes located in 3 different towns of Canakkale city with no known complaints throughout a year; (ii) to compare outdoor air pollutants' levels with corresponding indoor levels, (iii) to find the links between several environmental factors and SBS occurrences; and (iv) to estimate the variation of SBS symptoms among the occupants. The results of this study will help to increase public awareness of the importance of providing better IAQ in developing countries such as Turkey.

2. Materials and methods

2.1. Sampling sites

Figure 1 shows the sampling locations on a map. This study was conducted in 121 homes located in 3 different towns of Canakkale city, namely, Center (n = 46), Lapseki (n = 36), and Can towns (n = 39). Central and Lapseki towns are close to Dardanelles strait, while Can town has no seashore. Central town represents an urban site; Lapseki represents a rural site; and Can represents a semi-urban and industrial site (*i.e.*, open-pit coal mines, a lignite-based power plant, and a ceramic factory). Among these three sites, Can has a bowl-shaped topography, posing a disadvantage to the majority of the local people who live at the lowest altitudes of the town by frequently observed temperature inversion episodes (Mentese and Yarıntepe, 2012).

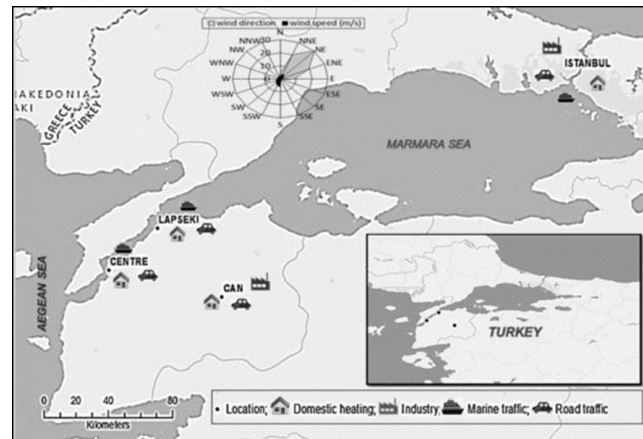


Figure 1. Sampling Locations: Center, Lapseki, and Can Towns

2.2. Sampling and analysis methods

Particulate matter, Volatile organic compounds (VOCs), bioaerosols, ozone, and CO₂ measurements, together with thermal comfort parameters such as air temperature and humidity were monitored in the indoor environments of those houses. Indoor CO₂, temperature, and relative humidity levels were measured with real time instrument. VOCs were collected by active sampling in adsorbent tubes and analysed by Gas Chromatography. Details regarding the sampling and analysing methods can be found in Mentese et al. (2015). Bioaerosols were sampled on selective culture media and enumeration was done under the light microscope. Also, occurrence of SBS symptoms and other health or specifically respiratory health related data were gathered from the occupants' questionnaire on a seasonal basis. Moreover, respiratory function of the occupants was measured by Spirometry on a monthly basis. Respiratory function of the participants was assessed by FEV₁/FVC ratio. Here, FEV₁ indicates the forced expiratory volume in 1 second (*i.e.*, the max amount of air that you can forcefully exhale in 1 second) and FVC indicates forced vital capacity (*i.e.*, the amount of air which can be forcibly exhaled from the lungs after taking the deepest breath possible).

2.3. SBS Questionnaire

To estimate the relationship between IAQ and SBS occurrences, a questionnaire was applied to all occupants in each sampling season. The participants were asked to complete the SBS-related part of the questionnaire if they were not diagnosed by the doctor that could cause the symptoms used to describe the SBS. 20% of the participants in Center; 11% in Lapseki, and 26% in Can had a disease diagnosed by the doctor that causes a symptom similar to any of the symptoms of SBS. These participants did not fill in the relevant part of the questionnaire regarding the frequency of SBS symptoms. SBS symptoms in the questionnaire include headache, fatigue, eye irritation, tickly throat, sneezing, coughing, dry skin, chest tightness, dizziness, difficulty in concentration, and influenza/cold. Since 11 SBS symptoms were taken into account in this study, the SBS score ranged from 0 (none of the SBS symptom was occurred) to 11 (all SBS symptoms were occurred).

3. Results and Discussion

Annual median levels of TVOC, TMC, TBC, Particle count, TVOC, Benzene, CO₂, Temperature (°C), and RH (%) at three sampling locations are given in Table 1. Briefly, the highest levels of both TBC and TMC were observed at Çan, Lapseki, and Center, in descending order and median levels of both TBC and TMC were below 10³ CFU/m³. Median levels of annual TVOC levels were found to be close at the sampling sites (around 500 – 550 µg/m³). The highest levels of benzene, CO₂, and particle counts were found in Çan, Lapseki, and Center, in a descending order. Both indoor temperature and RH values

were close at the three locations. Indoor-to-outdoor (I/O) ratios were found to be >1, indicating the burden of indoor emissions than outdoor sources (see Table 2).

Table 1. Annual median levels of TVOC, TMC, TBC, Particle count, TVOC, Benzene, CO₂, Temperature, and RH at three sampling locations

Parameter	Center	Lapseki	Çan
TBC (CFU/m ³)	319	595	711
TMC (CFU/m ³)	399	675	793
TVOC (µg/m ³)	508.8	528.2	548.1
Benzene (µg/m ³)	2.1	5.1	6.0
Particle count (#/cm ³)	111	154	174
CO ₂ (ppm)	689	745	790
Temperature (°C)	23.5	23	22.5
RH (%)	50.2	51.3	52.5

Table 2. Annual average I/O ratios of TVOC, TMC, TBC, TVOC and, Benzene Levels at three sampling locations

Parameter	Center	Lapseki	Çan
TBC	9.3	11.5	10.7
TMC	1.1	1.5	1.7
TVOC	60.0	109.5	64.6
Benzene	3.2	6.4	7.3

In this comprehensive study conducted in Çanakkale province (namely *Canakkale HealthAir Study*), it was determined that the SBS was mostly observed in Çan according to the scores of SBS symptoms which were used to define the SBS. SBS symptoms showed seasonal and spatial changes according to the observed symptom type. In general, the SBS symptoms were found to be widespread among the participants and some of the symptoms had seasonal variations, whereas some of the SBS symptoms were observed in the participants throughout the year. Seasonal and spatial changes of SBS symptoms according to the type of observed symptoms were also investigated (see Table 3). The most common symptoms in the Center were fatigue and cold, flu-like symptoms in autumn; fatigue in the winter and spring, and difficulty in concentration in the summer. The most common SBS symptoms in Lapseki were fatigue in autumn, coughing in winter, cold, flu-like symptoms in spring, and difficulty in concentration in summer. The most common symptoms of SBS in Çan were fatigue in autumn, difficulty in concentration in winter and summer and cold, flu-like symptoms in spring.

Table 3. Seasonal observation frequencies of the most frequent 3 SBS Symptoms at the sampling Locations (%)

Location	Season	SBS Symptom (observation frequency, %)		
		1. symptom	2. symptom	3. symptom
Center	F	fatigue (50%)	cold, flu-like symptoms (50%)	thickly throat (49%)
	W	fatigue (72%)	difficulty in concentration(63%)	cold, flu-like symptoms (61%)
	Spr.	fatigue (66%)	difficulty in concentration(63%)	cold, flu-like symptoms (51%)
	S	difficulty in concentration(51%)	fatigue (41%)	thickly throat (33%)
Lapseki	F	fatigue (65%)	cold, flu-like symptoms (52%)	difficulty in concentration(47%)
	W	difficulty in concentration(59%)	cold, flu-like symptoms (56%)	fatigue (50%)
	Spr.	cold, flu-like symptoms (71%)	difficulty in concentration (61%)	fatigue (43%)
	S	difficulty in concentration(61%)	fatigue (54%)	headache (36%)
Çan	F	fatigue (72%)	difficulty in concentration (66%)	eye irritation (47%)
	W	difficulty in concentration 73%)	cold, flu-like symptoms (64%)	fatigue (46%)
	Spr.	cold, flu-like symptoms (68%)	difficulty in concentration(66%)	fatigue (48%)
	S	difficulty in concentration(56%)	fatigue (48%)	thickly throat (32%)

Table 4 presents the seasonal and temporal change frequency of SBS symptom score. The highest percentage of participants with no SBS symptoms was observed in summer (20.0%) and least percentage in winter (4.7%). Also, half of the participants had > 4 SBS symptoms in autumn; > 3 SBS symptoms in winter and spring; and > 2 SBS symptoms in summer. All of the SBS symptoms were not observed in any of the participants living in the Center. The highest percentage of participants with no SBS symptoms in Lapseki was observed in winter (14.3%) and summer (14.3%), while the least percentage was in autumn (9.1%). Also, half of the participants had an average of > 4 SBS symptoms in autumn, winter and spring and 3 symptoms in summer. Moreover, none of the participants in Lapseki had all or 10 symptoms of SBS. The percentage of participants with no SBS symptoms in Çan was highest in autumn (11.8%) and least in winter (5.9%). Also, half of the participants had an average of 5 symptoms in autumn, > 4 symptoms in winter and spring and > 3 symptoms in summer. All SBS symptoms were observed in the summer in 4% of the participants in Çan. As can be seen from Table 4, the highest frequencies of SBS symptoms according to symptom scores were mostly observed in Çan.

Table 4. Seasonal and temporal change of SBS symptom score frequency (%)

SBS Symptom Score*	Center				Lapseki				Çan			
	F	W	Spr.	S	F	W	Spr.	S	F	W	Spr.	S
0	15.4	4.7	2.9	20	9.1	14.3	10	14.3	11.8	5.9	8.7	8.0
1	10.3	2.3	5.7	17.5	9.1	5.7	6.7	10.7	8.8	14.7	8.7	16.0
2	12.8	18.6	11.4	22.5	6.1	8.6	20	17.9	8.8	8.8	21.8	28.0
3	10.3	11.6	31.4	12.5	3.0	5.7	10	21.4	5.9	11.8	4.4	4.0
4	7.7	20.9	14.3	7.5	21.2	22.9	16.7	3.6	8.8	8.8	13.1	16.0
5	12.8	16.3	11.4	12.5	21.2	11.4	13.3	7.2	17.7	14.7	21.8	8.0
6	10.3	7.0	5.7	7.5	18.2	8.6	10	14.3	8.8	8.8	13.1	12.0
7	15.4	11.6	8.6	-	9.1	8.6	6.7	3.6	11.8	14.7	4.4	4.0
8	2.6	2.3	8.6	-	-	8.6	6.7	3.6	8.8	5.9	-	-
9	-	2.3	-	-	3.0	5.7	-	3.6	5.9	5.9	4.4	-
10	2.6	2.3	-	-	-	-	-	-	2.9	-	-	-
11	-	-	-	-	-	-	-	-	-	-	-	4.0

* SBS score ranged from 0 (none of the SBS symptom was occurred) to 11 (all SBS symptoms were occurred).

Table 5 shows the Spearman rank correlation results for the Center. According to this; the symptoms of SBS are directly proportional to the total PM and CO₂ levels in the indoor environment and inversely proportional to the indoor temperature ($p < 0.05$). There was a negative correlation between respiratory performance (FEV₁/FVC) and indoor CO₂ level ($p < 0.05$). In addition, daily ventilation duration was positively correlated with bacterial level and temperature and negatively correlated with CO₂ level and relative humidity ($p < 0.01$). The CO₂ level in the indoor air is considered as an important indicator of whether ventilation is sufficient (Mentese, 2009; Heudorf et al., 2009).

Table 5. Correlations among SBS symptoms, IAQ, respiratory function (FEV₁/FVC percentage), and personal habits in Central Town

Parameter	Time spent at home (h/d)	SBS symptom score	%(FEV ₁ /FVC)	Home ventilation duration (h/d)
Total particle count	0.09	0.15*	0.01	-0.05
TBC	0.01	-0.09	-0.01	0.15*
TMC	-0.01	-0.03	0.14	-0.08
CO ₂	0.04	0.16*	-0.16*	-0.38**
TVOC	-0.02	-0.01	-0.02	-0.11
Temperature	-0.08	-0.16*	0.02	0.41**
Δt (in-out)	-0.21	0.18*	-0.07	0.43**
RH	0.32*	0.03	0.04	-0.21**
Ozone	-0.03	0.05	-0.09	-0.05
Home ventilation duration (h/d)	-0.11	-0.09	0.02	1

(N = 184; * $p < 0.05$; ** $p < 0.01$)

Table 6 shows the results of Spearman rank correlation for Lapseki. According to this; no statistically significant correlation was found between SBS symptoms and IAQ parameters ($p > 0.05$). It was found that CO₂ level decreased with daily time spent indoors ($p < 0.05$). As the daily ventilation duration increased, the bacteria level and temperature inside the home changed positively; total PM, CO₂, TVOC and ozone levels were found to change negatively ($p < 0.01$). It is observed that the levels of these pollutants in the indoor air are reduced by means of ventilation.

Table 6. Correlations among SBS symptoms, IAQ, respiratory function (FEV₁/FVC percentage), and personal habits in Lapseki Town

Parameter	Time spent at home (h/d)	SBS symptom score	%(FEV ₁ /FVC)	Home ventilation duration (h/d)
Total particle count	-0.01	0.1	0.01	-0.54**
TBC	-0.07	-0.13	0.16	0.18*
TMC	-0.01	0.14	0.16	-0.03
CO ₂	-0.22*	0.13	-0.07	-0.35**
TVOC	-0.11	0.12	0.07	-0.28**
Temperature	0.1	-0.07	0.08	0.37**
Δt (in-out)	0.06	0.05	-0.02	-0.40**
RH	-0.16	-0.02	0.17	0.13
Ozone	0.11	0.05	-0.18	-0.37**
Home ventilation duration (h/d)	-0.02	-0.02	-0.02	1

(N = 144; * $p < 0.05$; ** $p < 0.01$)

Spearman rank correlation results for Çan are given in Table 7. According to this; the symptoms of SBS were directly proportional to the total PM levels in the indoor environment and inversely proportional with the indoor temperature and TVOC levels ($p < 0.05$). There was a negative correlation between the respiratory performance (FEV₁/FVC) of the participants and the level of bacteria in the indoor environment and an inverse relationship with the daily ventilation duration ($p < 0.05$). In addition, daily ventilation duration was positively correlated with temperature, while total PM, relative humidity, CO₂, TVOC and ozone were negatively correlated ($p < 0.01$), indicating that the level of pollutants is decreased by ventilation.

Table 7. Correlations among SBS symptoms, IAQ, respiratory function (FEV₁/FVC percentage), and personal habits in Çan Town

Parameter	Time spent at home (h/d)	SBS symptom score	%(FEV ₁ /FVC)	Home ventilation duration (h/d)
Total particle count	-0.01	0.27**	-0.09	-0.40**
TBC	-0.10	-0.07	-0.26**	0.10
TMC	0.01	-0.01	-0.15	0.03
CO ₂	0.07	0.10	-0.08	-0.35**
TVOC	0.02	-0.20*	-0.03	-0.22**
Temperature	-0.01	-0.23**	0.02	0.38**
Δt (in-out)	-0.01	0.18*	-0.12	-0.46**
RH	0.09	0.01	0.07	0.05
Ozone	0.03	0.02	-0.01	-0.32**
Home ventilation duration (h/d)	-0.05	-0.03	0.17*	1

(N= 156; * $p < 0.05$; ** $p < 0.01$)

According to the results of this study results:

- IAQ parameters showed spatial distribution and, in general, the highest pollutant levels were observed in Can town and the lowest levels were observed in Central town.
- The predominant SBS symptoms varied seasonally and spatially among the study sites.
- Correlations were found among the occurrence of SBS symptoms, measured indoor pollutants, and comfort parameters ($p < 0.05$).
- Daily ventilation amount of the houses was negatively correlated with CO₂ levels ($p < 0.05$), which used to be an indicator of adequacy of ventilation or fresh air intake.
- Also, high levels of indoor air pollutants were linked with increase of respiratory symptoms of the occupants ($p < 0.05$).

Overall, performing more studies from the health and IAQ points of view improve public awareness of indoor environmental comfort.

4. References

- ACGIH, 1989. "American Conference of Governmental Industrial Hygienists Guidelines for The Assessment About Aerosols in the Indoor Environment. ACGIH, Cincinnati, Ohio.
- Carrer, P., M. Maroni, D. Alcini, D. Cavallo. 2001. Allergens in indoor air: environmental assessment and health effects. *The Science of the Total Environment*, 270(1-3), 33-42.
- Douwes, J., Thorne, P., Pearce, N., Heederik, D. 2003. Bioaerosol Health Effects and Exposure Assessment: Progress and Prospects. *Annals of Occupational Hygiene* 47(3), 187-200.
- Harrison, J.C., Pickering, E., Faragher, P., Austwick, S. 1992. Little, and L. Lawton: An investigation of the relationship between microbial and particulate indoor air pollution and the sick building syndrome. *Respiratory Medicine* 86(3), 225-235.



18th World Clean Air Congress, 23-27 September 2019, Istanbul
organized by TUNCAP and IUAPPA

Heudorf, U., Neitzert, V., Spark, J. 2009. "Particulate matter and carbon dioxide in classrooms - The impact of cleaning and ventilation". *International Journal of Hygiene and Environmental Health*, 212(1), 45-55.

Menteş S., Mirici N.A., Otkun M.T., Bakar C., Palaz E., Taşdibi D., et al., 2015. Association between respiratory health and indoor air pollution exposure in Canakkale, Turkey, *Build Environ*, 93, 72-83.

Mentese, S. 2009. Investigation of Indoor Air Quality and Determination of Their Sources. Hacettepe University, Institute of Science, Ph.D. thesis.

Mentese, S., Tasdibi, D. 2016. Airborne bacteria levels in indoor urban environments: The influence of season and prevalence of sick building syndrome (SBS). *Indoor and Built Environment*, 25, 563-580

Mentese, S., Yarimtepe, C.C. 2012. Comparative determination of ambient air quality of Canakkale city according to the pollution sources. *Hava Kirliligi Arastirmalari Dergisi* 1, 66-74.

WHO, 1989. Housing: Sick Building Syndrome, Local Authorities, Health and Environment Briefing Pamphlet Series, no:2.

Acknowledgments

This study was supported by TUBITAK. Project no: 112Y059.

Comparison of BTEX exposure of commuters due to on-road traffic around Canakkale and Kilitbahir Harbors

Bahar Akca and Sibel Mentese

Department of Environmental Engineering, Canakkale Onsekiz Mart University,
Turkey

sibelm@comu.edu.tr

Abstract. A recent report published by World Health Organization indicates the importance of air pollution in terms of its carcinogenic effect on human health. Volatile organic compounds (VOCs) have considerable influence particularly on atmospheric chemistry, compared to other air pollutants. On the other hand, anthropogenic VOCs emissions in urban environments have shown increasing trend. The major source of VOCs is vehicle exhaust emissions both in the rural and urban air. Benzene, Toluene, Ethylbenzene, and Xylenes (BTEX) are the most common VOCs observed in vehicle exhaust air composition. The aims of this study were finding the daily, week/weekend, and spatial variations of BTEX compounds at the study sites. This study was conducted in main roadway routes from downtown of Canakkale city to Canakkale harbour and on the roadways of Kilitbahir Harbours. Both on-road traffic and automobiles that passed Dardanelles strait by ferry boats are thought to be the main potential sources of BTEX at the study site. Composite personal VOCs samples were collected from two routes starting either from Canakkale Harbour or Kilitbahir Harbours to both commuting directions. Air samples were collected and analyzed according to US EPA TO17 Method. VOCs samples were taken in different time periods of the day and also different days of the week. Levels of total VOCs and BTEX compounds were found to be higher around Central Harbour road than Kilitbahir Harbour roads ($p < 0.05$). No statistically significant difference was found for BTEX levels between weekdays and weekend days ($p > 0.05$). Also, BTEX levels did not vary between the days of the week ($p > 0.05$). This study showed that on-road traffic around Canakkale and Kilitbahir harbours have important and constant contributions on organic air pollutant levels, independent from the day, showing the average personal BTEX exposure of people commuting on those roads on a daily basis.

Keywords: Canakkale Harbor, Kilitbahir Harbor, Air pollutants, Organic air pollutants, BTEX.

1. Introduction

Air pollution is of a great concern worldwide and was shown a causative agent of cancer on human health by WHO (2014). Among the air pollutants, volatile organic compounds (VOCs), emitted mostly from anthropogenic sources, have considerable influence particularly on atmospheric chemistry. Even though, natural sources of VOCs are available too, anthropogenic VOCs emissions in urban environments have an increasing trend (Singh and Zimmerman, 1992). The major source of VOCs is vehicle exhaust emissions both in the rural and urban air (Kansal, 2009). VOCs cover a large group of organic compounds, and the frequently observed subgroups are aromatic hydrocarbons, paraffins, and olefins (Mentese, 2009). The type of VOC and its level are dependent on the characteristics of the source. VOC levels may show a seasonal distribution; for example, VOC levels were measured to be 3 times higher in the winter than in the summer (Gilli et al., 1990; Shields et al., 1996; Rehwagen et al., 2003). Basically, there are 3 important features of VOCs that make them important: *i*) there are many potential



sources available both in urban and rural environments, *ii*)their reactivity & triggering effect of the chain reactions, *iii*)their (potential or known) carcinogenicity (e.g. Benzene is a known human carcinogen).

Traffic is one of the major anthropogenic sources which is responsible from urban air pollution problems. Benzene, Toluene, Xylenes, and Ethylbenzene (BTEX) are the most common organic air pollutants observed in vehicle exhaust air composition. Also, Benzene has been classified as human carcinogen. Kilitbahir and Canakkale Harbours are one of the busiest harbours of Turkey due to increased number of scheduled passenger and vehicle ferry boats passing across the Dardanelles strait. The Dardanelles Strait is one of the major transit locations in the world for national and international maritime transport. Especially the traffic density of the Dardanelles has a contribution on air pollution caused by ships. As an annual average, 50 000 ships are passing through Dardanelles strait (Ministry of Transport and Infrastructure, 2015). Potential contribution of ship emissions on air pollution of Canakkale, in addition to road traffic, was first pointed out by Mentese and Yarımtepe (2012). No study has been conducted here so far to find the contribution of organic compounds around the Canakkale harbours.

In this study, air samples were collected from the major roads of Kilitbahir and Canakkale harbours to find exposure levels of drivers and passengers using the ferries by BTEX compounds. The aims of this study were finding the daily, week/weekend, and spatial variations of BTEX compounds at the study sites. For this aim, composite personal air samples with air sampling pump were collected from Kilitbahir and Canakkale Harbours roadways.

2. Materials and methods

This study was conducted in main roadway routes from downtown of Canakkale city to Canakkale harbor and from both directions to two Kilitbahir harbours where traffic load is high during the rush hours and holiday seasons. Canakkale harbour is located at the Asian continent, while Kilitbahir is located at the European continent of the country, split by Dardanelles strait. There are two main sources of road traffic in the selected route where the first one is due to local people who are commuting on these main roads, while the second source is due to the high number of automobiles that are aiming to load their automobiles into the ferries at Canakkale harbour. Composite personal VOCs samples were collected from a route starting approximately 1 km from Kilitbahir Harbours to both directions (length of total road is approximately 2 – 2.5 km) and from Canakkale Harbor to downtown main road directions. There have been considerable number of automobiles on the road commuting to both directions, particularly during the tourism season. VOC samples were collected in different days of the week during the summer season.

2.1. Sampling sites

The main sampling routes around Kilitbahir and Canakkale Harbours is given in Figure 1 and from to downtown main road directions (see Figure 2). In Kilitbahir, there are two harbours which stand alongside each other (distance between them is approximately 600 m).

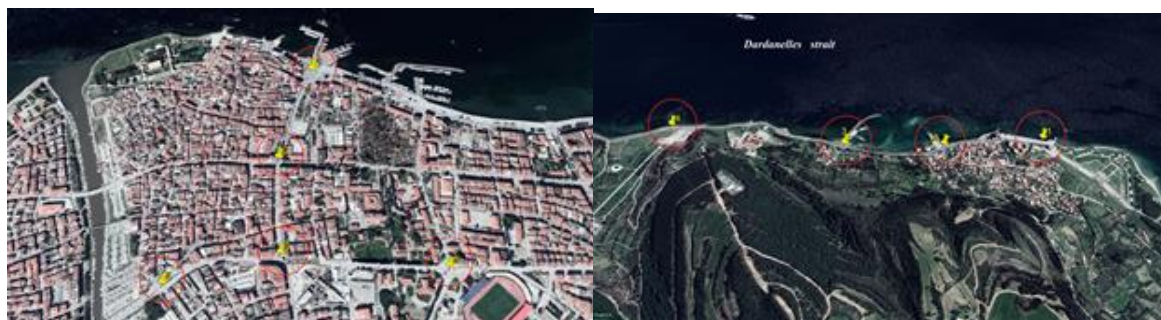


Figure 1. The routes of composite personal air sampling around Kilitbahir Harbours Roads (distance from point 1 to 4) and at Canakkale center to Harbour (distance from point 1 to 5), from left to right.

2.2. Sampling and analysis techniques

VOC samples were collected from point 1 to 4 at Kilitbahir harbors and from point 1 to 5 at Canakkale harbor by personal active sampling principle during a 15 min - walking duration at a nose level. Those roads are used by the vehicles whose passengers consist of local people commuting on a daily basis and the vehicles passing the Dardanelles strait by the vehicle ferries to reach somewhere else (i.e. to İstanbul direction or Anatolia). Thus, the composite samples will accurately reflect the VOCs emissions exposed by the commuters who use those harbors.

VOCs samples were taken in different time periods of the day and also different days of the week. VOCs samples were collected in principle to active personal sampling procedure by a person who carried a low-flow air sampling pump at a nose level that was attached to sampling tube for a 15-min walkway on the study route. Air samples then analyzed according to US EPA TO17 Method (US EPA, 1999). Briefly, air samples were collected in selective sorbents including stainless steel thermal desorber tubes and analyzed by Gas Chromatography Flame Ionization Detector followed by Thermal Desorber (Mentese et al., 2015). Concentrations of total concentrations of volatile organic compounds (TVOC) and BTEX were calculated according the 7-points calibration of the VOC standard solutions ($r^2 > 0.99$).

3. Results and Discussion

Figure 2 shows the average BTEX levels measured throughout the main roads to Kilitbahir and Canakkale harbors. Accordingly, BTEX levels were found to be almost 2-folds higher around Canakkale harbor than Kilitbahir harbors. Benzene level did not exceed the national limit value ($5 \mu\text{g}/\text{m}^3$ annually), but it was found to be close the limit value around Canakkale Harbor. Since there are two harbors located in Kilitbahir, it was thought that the burden of the traffic in terms of VOCs were shared in Kilitbahir by two harbors, but contrarily, VOCs accumulated around Canakkale harbor.

Figure 3 shows distributions of BTEX levels during the week days and weekend days around both Canakkale and Kilitbahir harbor roads. According to the ANOVA results, no statistically significant differences were found between the concentrations of each BTEX compound and week or weekend days ($p > 0.05$).

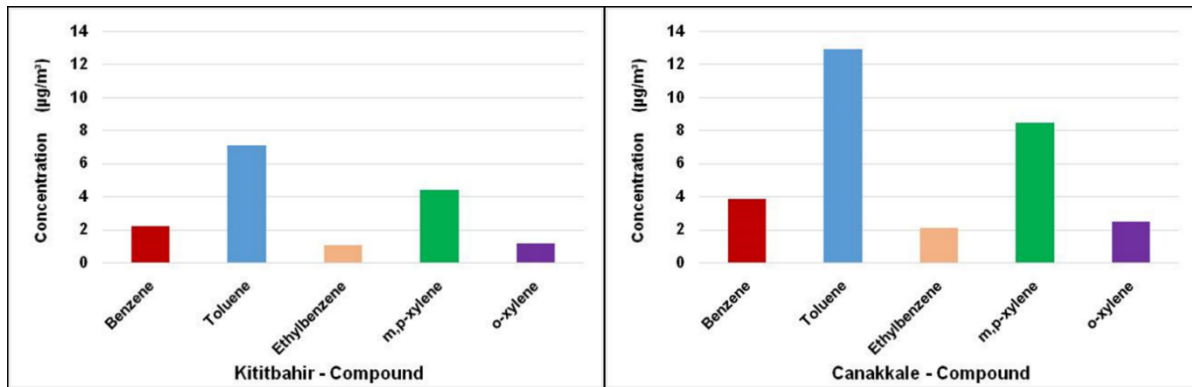


Figure 2. BTEX Levels measured around Kilitbahir and Canakkale harbors (from left to right).

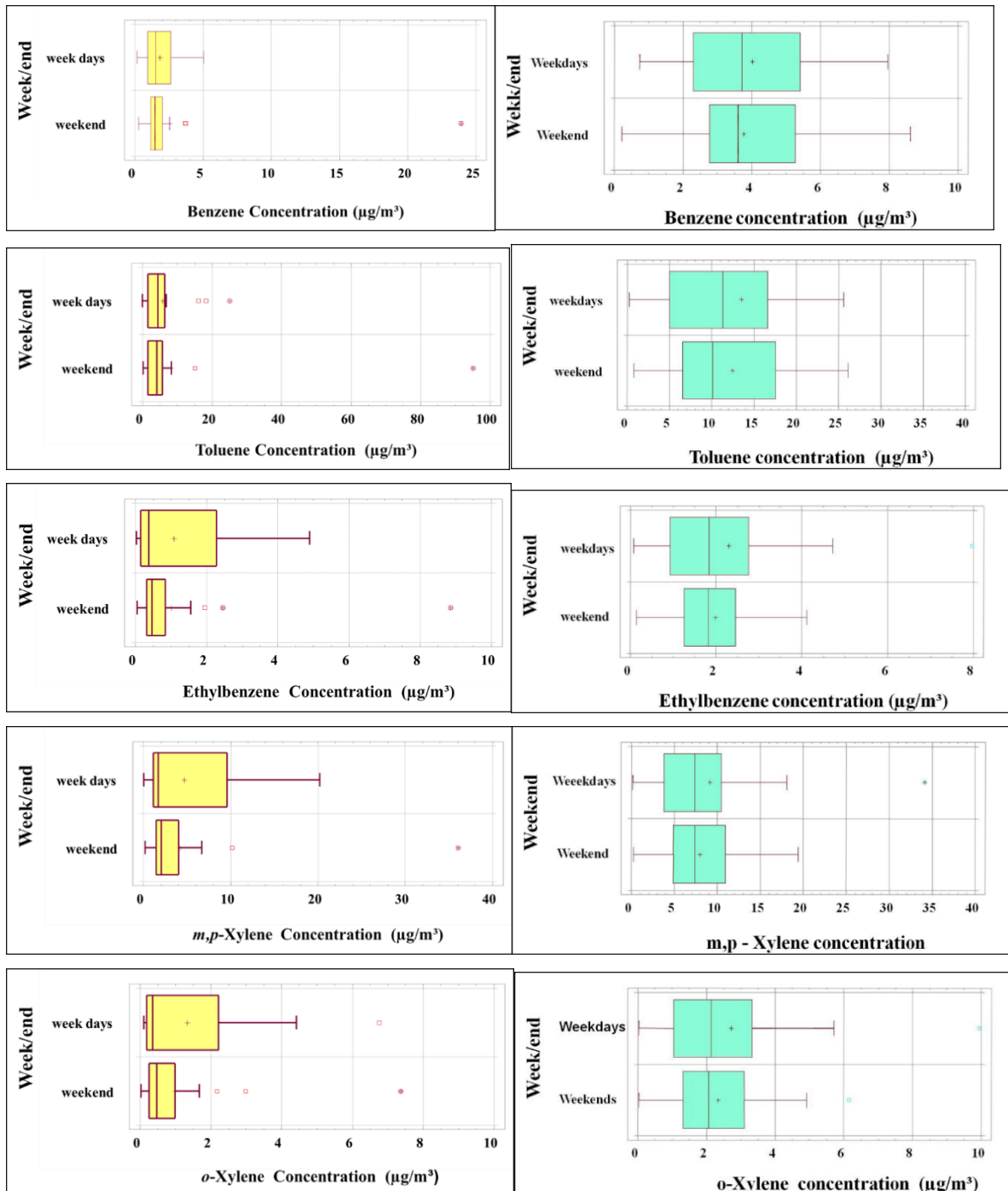


Figure 3. BTEX Concentrations during the week and weekend days throughout the main roads to Kilitbahir (yellow boxes, left-hand side) and Canakkale (blue boxes, right-hand side) harbors

Overall, both Canakkale and Kilitbahir harbors and the roads used to reach those harbors have considerable traffic. This study showed the average VOCs exposure of people commuting on those roads on a daily basis. Levels of total VOCs and BTEX compounds were found to be higher around Central Harbor roads than Kilitbahir Harbor roads ($p < 0.05$). Average levels of TVOC were around $87 \mu\text{g}/\text{m}^3$ around Kilitbahir and $120 \mu\text{g}/\text{m}^3$ around Canakkale harbor roads. Among the organic air pollutants, Toluene was the most frequent organic air pollutant. TVOC levels were found to be different in



weekends and weekdays ($p < 0.001$), but no statistically significant difference was found for BTEX levels between weekdays and weekend days ($p > 0.05$). Also, BTEX levels did not vary between the days of the week ($p > 0.05$). TVOC levels varied diurnally, and reached at its maximum level around noon.

This study showed that on-road traffic around Canakkale and Kilitbahir harbors have important and constant contributions on organic air pollutant levels, independent from the day, showing the average personal BTEX exposure of people commuting on those roads on a daily basis. Since this study has been the first study conducted in Canakkale roadways, it is expected that the results will enlighten the decision makers in terms of traffic regulations on these routes.

4. References

Gilli, G., Bono, R., Scursatone, E. 1990. Volatile Halogenated Hydrocarbons in Urban Atmosphere and in Human Blood, *Arch Environ. Health*, 45, 101-6.

Kansal, A. 2009. Sources and reactivity of NMHCs and VOCs in the atmosphere: A review. *J Haz Mat*, 166(1), 17-26.

Menteşe S., Mirici N.A., Otkun M.T., Bakar C., Palaz E., Taşdibi D., et al., 2015. Association between respiratory health and indoor air pollution exposure in Canakkale, Turkey, *Build Environ*, 93, 72-83.

Mentese, S. 2009. Investigation of Indoor Air Quality and Determination of Their Sources. Hacettepe University, Institute of Science, Ph.D. thesis.

Mentese, S., Yarimtepe, C.C. 2012. Comparative determination of ambient air quality of Canakkale city according to the pollution sources. *Hava Kirliligi Arastirmalari Dergisi* 1, 66-74

Ministry of Transport and Infrastructure of Turkish Republic. Marine Trade Statistics of 2015. http://www.ubak.gov.tr/BLSM_WIYS/DTGM/tr/Kitaplar/20161116_165220_64032_1_64480.pdf (access: 01.03.2019)

Rehwagen, M., Schlink, U., Herbarth, O. 2003. Seasonal Cycle of VOCs in Apartments, *Indoor Air*, 13, 283-91.

Shields, H.C., Fleischer, D.M., Weschler, C.J. 1996. Comparisons Among VOCs Measured in Three Types of U.S. Commercial Buildings with Different Occupant Densities, *Indoor Air*, 6, 2-17.

Singh, H.B. and Zimmerman, P. 1992. Atmospheric distributions and sources of nonmethane hydrocarbons. In: J.O. Nriagu, Editor, *Gaseous Pollutants: Characterisation and Cycling*, Wiley, New York p. 235.

US EPA, 1999. Compendium Method for the Determination of Organic Compounds in Ambient Air TO-17, EPA/625/R-96010b.

World Health Organization (WHO). 2014. Media Centre. Ambient (outdoor) air quality and health, Fact sheet No: 313. <http://www.who.int/mediacentre/factsheets/fs313/en/> (Access date: 13 June 2016).

Acknowledgments

This study was supported by Canakkale Onsekiz Mart University Scientific Research Unit, Project no: FYL-2018-2499. The researchers are also thankful to Ali Caglar and siblings of Bahar Akça for their help during the field studies.

Bibliometric analysis on use of mosses in air pollution studies and possibility of use of mosses for passive monitoring of PM₁₀

Bihter Olgun¹, Feyza Bingol¹, Cansu Mısırlıoğlu¹, Selcen Dogan², Ayca Erdem¹, Cigdem Moral¹ and Guray Dogan¹

¹Department of Environmental Engineering, Akdeniz University, 07058 Antalya, Turkey

²Department of Agricultural Biotechnology, Akdeniz University, 07058 Antalya, Turkey

gdogan@akdeniz.edu.tr

Abstract. Mosses are living organisms with no roots and use the ambient atmosphere to grow. It is known that there are about 15000 species of mosses. Mosses are resistant organisms and have been frequently used as bio-tracer in air pollution sampling studies in different parts of the world. The use of mosses as bio-tracers is a method used to determine the levels of total atmospheric pollutant deposition. Analysis of pollutant content in mosses is known as technical passive bio-monitoring and was first used in the late 1960s. This method was then developed and standardized using species specific to the areas studied. This study will be composed of two parts. In the first part, more than 1500 publications on moss use in air pollution studies between 1999 and 2019 were examined. For selection of publications; the “Web of Science” database, “moss” and “air pollution” keywords were used. 852 articles related to the sampling of air pollution by mosses were found. 460 studies, which are fully relevant, were examined. Approximately in 70% of the studies, *Hypnum cupressiforme*, *Pleurozium schreberi* and *Sphagnum species* were used. Most of the studies were conducted in either urban or rural atmospheres (68%). However, one fourth of the studies were conducted in industrial areas. It is shown that mosses were used more common in Europe than other parts of the world. Most of the studies were used to determine heavy metal distribution. On the second part of the study, possibility of use of moss for metals attached on PM₁₀ will be discussed for long term monitoring (monthly) of air pollution. The preliminary analysis for the conditioning of mosses and preliminary results will be discussed. At the same time, the use of mosses in PM₁₀-bound heavy metal sampling was investigated.

Keywords: Air pollution, Moss, Bibliometric analysis, Passive air sampling, PM₁₀.

1. Introduction

Bryophytes is a division of plants covering liverworts, hornworts and mosses. The Bryophytes comprise the second most diverse phylum of land plants. There are approximately 15000 moss species in the world. Mosses are multicellular and photosynthetic and there is no real root, leaf and body (Goffinet et al., 2008). The mosses can live on the northern and southern slopes, in the humid climates of both temperate and tropical regions, in the forest ecosystem, in soil, on stones and rocks in nature, completely in water, in the trunks and branches of dead and living trees (Schofield, 2001). Mosses, because of their resistance to pollution and climate variation, have been frequently used as bio-tracer in air pollution sampling studies in different parts of the world for about 50 years.

The urban atmosphere is subjected to large inputs of anthropogenic contaminants produced by both stationary sources such as power plants, industries and residential heating and mobile sources related to traffic. The use of sampling devices is a practical method for monitoring direct atmospheric deposition and deposition of heavy metals and other elements in the surface environment. However, studies on atmospheric contamination are often limited by the high cost of this method and the difficulty of extensive monitoring of time and space. Therefore, the use of organisms that act as bio-tracer for the sampling of air pollution has become widespread (Anicic et al., 2009). Many studies have proved the ability of moss to absorb and accumulate atmospheric pollutants in tissue.

Analysis of pollutant content in moss is known as technical passive bio-monitoring and was first introduced in the late 1968s. Then, the method was developed and standardized using species specific to the investigated areas.

In this study, more than 1500 publications on moss use in air pollution studies between 1999 and 2019 were examined. For publication selection; “Web of Science” database was used. For selection of publications; “moss” and “air pollution” keywords were used. Of the 852 studies on the sampling of air pollution with moss, 460 studies have been selected and examined that are fully relevant to the study topic. In the bibliometric study, the moss species used in the studies, the distribution of the species, and the types of pollutants sampled and the variation of the studies from year to year were determined. In the second part of the study, the use of mosses in PM10-bound heavy metal sampling was investigated.

2. Bibliometric analysis

Many species of moss were used in studies conducted between 1990 and 2019 for monitoring air pollution. Approximately 20 species of moss were used in studies. Approximately in 70% of the studies, *Hypnum cupressiforme*, *Pleurozium schreberi* and *Sphagnum* species were used. The species and distributions of moss used in the studies are shown in Figure 1 and Figure 2, respectively. The most commonly used species were *Hypnum cupressiforme* (25%), *Pleurozium schreberi* (22%), *Sphagnum* (21%), *Hylocomium splendens* (18%) and *Pseudoscleropodium purum* (14%), respectively.

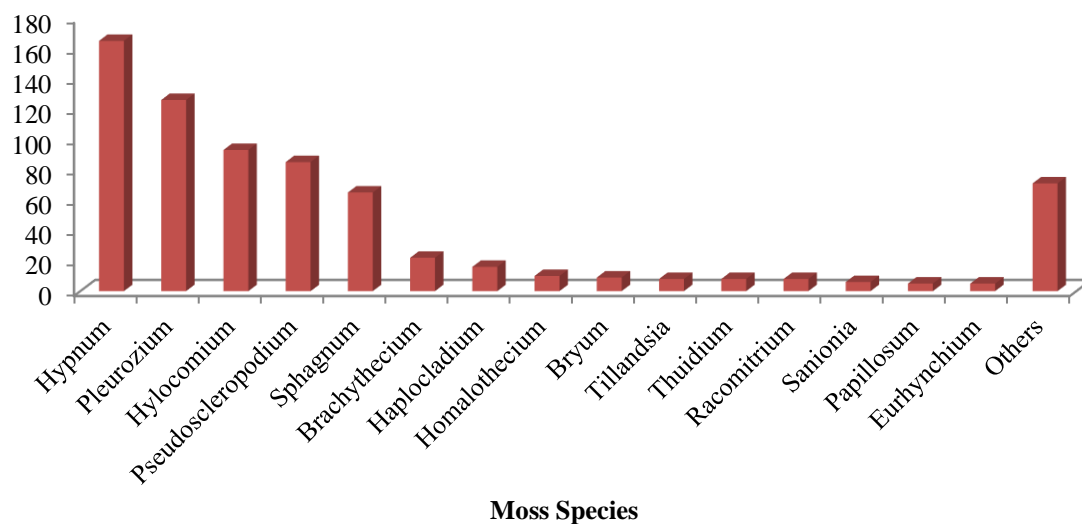


Figure 1. The species of moss used in the studies

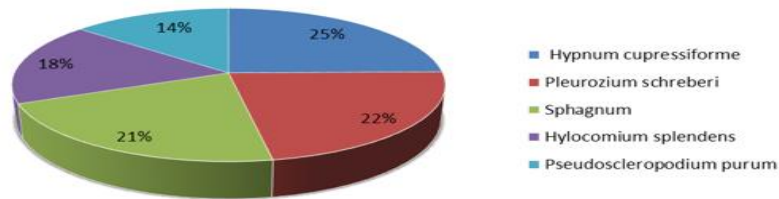


Figure 2. Distributions of moss species used in the studies

The published articles show that most of the studies are concentrated in urban areas. 208 studies were conducted in urban areas, 132 studies in rural areas, 100 studies in industrial areas and 20 studies in other areas. Figure 3 shows the distribution of the areas where the studies were conducted.

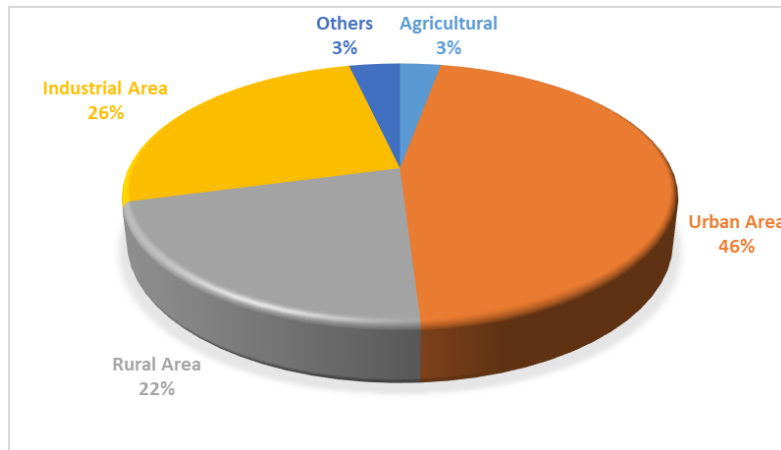


Figure 3. Distributions of publications by area

A 20-year working group was examined. When the distribution of publications by years is examined, it is seen that increase from year to year. It is seen that the most publications in this field have been made in the last 5 years. The distribution of publications by years is shown in Figure 4.

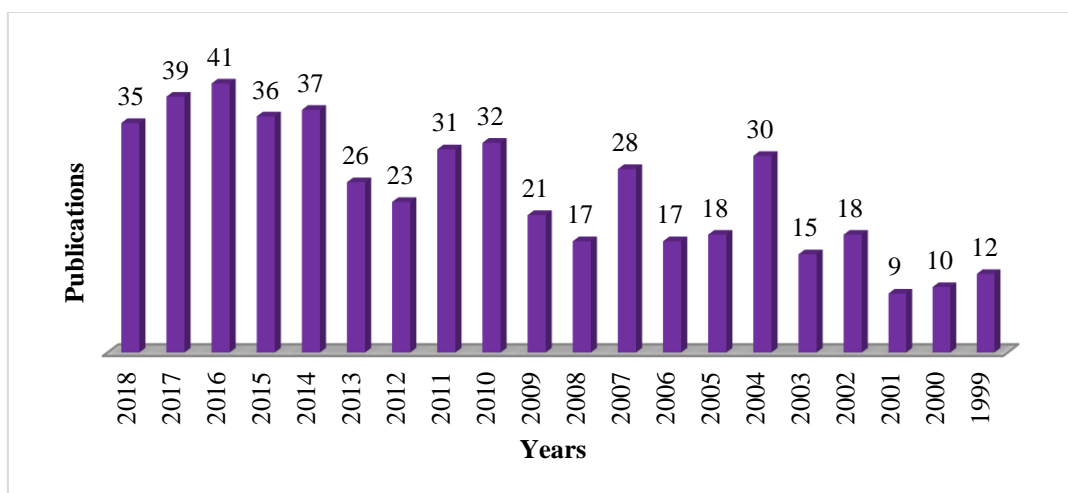


Figure 4. Distribution of publications by years

In many countries, moss species have been used to monitoring air pollution. The use of moss in the biomonitoring of air pollution has been concentrated in Spain, Poland, Italy and China. The distribution of the studies carried out in this field by countries is shown in Figure 5.

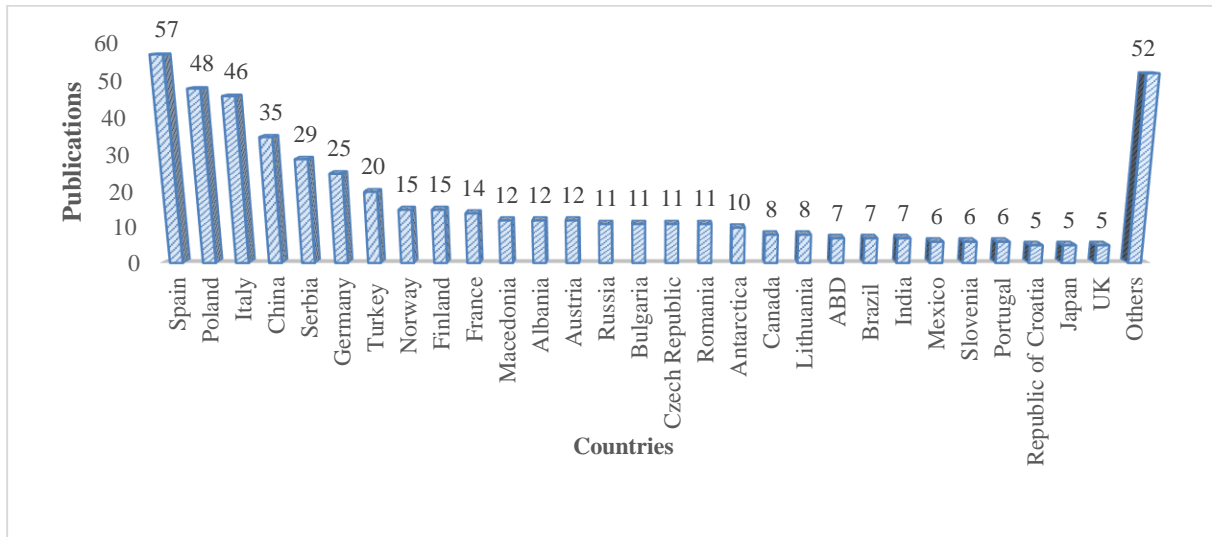


Figure 5. Distribution of the studies carried out in this field by countries

In the studies, various types of pollutants have been studied on mosses. The most common type of pollutant examined is heavy metal with 76%. This is because mosses are sensitive to heavy metals and are therefore considered as an indicator of pollution (Vukovic et al, 2015). The distribution of pollutant species investigated on mosses in the publications is shown in Figure 6.

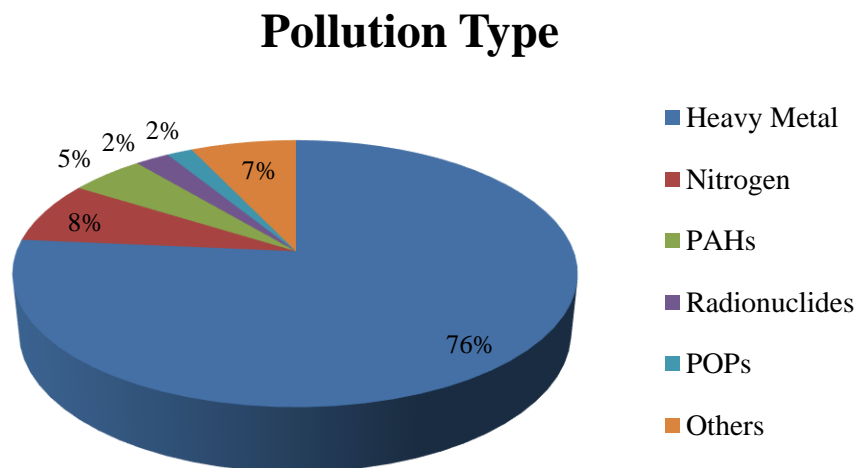


Figure 6. Distribution of pollutant in the publications

When the pollution types in the publications are examined, it is seen that the most pollution is caused by heavy metals. The most common pollutants in the heavy metals category are Fe, Pb and Zn (Fe>Pb>Zn). According to the results of the studies, iron is the most dominant type of pollutant. Sources of pollutants come from iron and steel mills, power plants, mining sites. Motor vehicles are among the

main causes of air pollution. Since the 1920s, the rate of lead in air pollution has increased rapidly due to the addition of lead composition to gasoline to improve the efficiency of engines (Anonymous 1).

3. Use of moss for metals attached on PM₁₀

In the literature, mosses are used as bio-monitor on the monitoring of heavy metals in the majority of studies. This results shows that the use of mosses for metal monitoring in the atmosphere is a suitable method. In many studies in the literature, mosses have been used for the monitoring metals attached on PM₁₀. In the literature, the studies carried out in this context over the web of science database have been examined. For selection of publications; the “Web of Science” database, “moss”, “biomonitoring”, “PM₁₀”, “heavy metal” and “air” keywords were used. Between 2007 and 2018, 14 publications have been reviewed in the literature. *Hypnum cupressiforme* was used as the moss type in 6 of 14 studies. In all of the studies, moss species used for sampling were collected from nature and a moss culture grown in laboratory environment was not used. In the studies, sampling times with mosses ranged from 1.5 months to 24 months. In studies on the retention of PM₁₀-bound metals on moss, the particles retained on the moss have proven to have the dimensions observed in PM₁₀ samples. At the same time, Not only particulate matters were adsorbed onto moss surfaces but they were also intercepted by the nylon filaments of the bags. (Adamo et al, 2008). In all studies, for pollutants, also instrumental monitoring was performed while bio-monitoring with land moss. In comparison biomonitoring data with instrumental monitoring data, similar order of abundances of the most elements in PM₁₀ and moss samples was found (Vukovic et al, 2014).

In our study, performance of adsorption capacities of mosses as bio-indicators with respect to PM₁₀ and PM_{2.5} samplers will be determined. To do this, a sampling station will be planted at a location near by Akdeniz University Department of Environmental Engineering and these two sampling approaches will be tested simultaneously. PM_{2.5} and PM_{2.5-10} sampling will be carried out on daily basis and moss sampling duration will be on monthly basis. The mosses will be placed on specially generated samplers. All samples then will be analyzed for 55 elements including arsenic, cadmium, nickel and lead. The moss sampler used is shown in Figure 7.



Figure 7. Moss sampler



4. References

- Anonymous 1. Dergi Park Akademik <http://dergipark.gov.tr/download/article-file/395152> Last access date: 09.01.2019.
- Adamo, P., Giordano, S., Naimo, D., Bargagli, R. 2008. Geochemical properties of airborne particulate matter (PM10) collected by automatic device and biomonitors in a Mediterranean urban environment. *Atmospheric Environment*. 42(2), 346-357.
- Anicic, M., Tasic, M., Frontasyeva, M. V., Tomasevic, M., Rajsic, S., Mijic, Z., Popovic, A. 2009. Active moss biomonitoring of trace elements with *Sphagnum girgensohnii* moss bags in relation to atmospheric bulk deposition in Belgrade, Serbia. *Environ. Pollut.* 157(2), 673-679.
- Goffinet, B., Buck, W, R., Shaw, A,J., 2008. Morphology, Anatomy, and Classification Of The Bryophyta. *Bryophyte Biology*, Second Edition, Cambridge University Press.
- Schofield, W.B., 2001. Introduction to Bryology, The Blackburn Press, New Jersey.
- Vukovic, G., Urosevic, M. A., Razumenic, I., Kuzmanoski, M., Pergal, M., Skrivanj, S., Popovic, A., 2014. Air quality in urban parking garages (PM10, major and trace elements, PAHs): Instrumental measurements vs. active moss biomonitoring. *Atmospheric Environment*. 85, 31-40.
- Vukovic, G., Urosevic, M. A., Pergal, M., Jankovic, M., Goryainova, Z., Tomasevic, M., Popovic, A. 2015. Residential heating contribution to level of air pollutants (PAHs, major, trace, and rare earth elements): a moss bag case study. *Environmental Science and Pollution Research*. 22(23), 18956-18966.

Acknowledgments

This work has been supported by The Scientific and Technological Research Council of Turkey with grant number 117Y026. The authors also would like to thank Prof. Dr. Gurdal TUNCEL and Prof. Dr. Gulen GULLU for their valuable comments on PM sampler optimization.

Gene-environment interaction: the evaluation of chromosomal damage among urban traffic policemen exposed to benzene in relation to *NQO1*, *GSTT1*, and *GSTM1* polymorphisms

Noor Fatimah Mohamad Fandi¹, Juliana Jalaludin^{1,2*}, Suhaili Abu Bakar³
and Mohd Talib Latif⁴

¹Department of Environmental and Occupational Health, Faculty of Medicine and Health Sciences, Universiti Putra Malaysia, 43400 Serdang, Selangor, Malaysia.

²Department of Occupational Health and Safety, Faculty of Public Health, Universitas Airlangga, 60115 Surabaya, East Java, Indonesia.

³Department of Biomedical Sciences, Faculty of Medicine and Health Sciences, Universiti Putra Malaysia, 43400 Serdang, Selangor, Malaysia.

⁴School of Environmental and Natural Resource Science, Faculty Science and Technology, Universiti Kebangsaan Malaysia, 43600 Bangi, Selangor, Malaysia.

juliana@upm.edu.my

Abstract. An urban air toxic of benzene at the ambient level has the ability to cause chronic health effects. Other than the nature of benzene carcinogenicity itself in resulting adverse health effects, the factor of genetic polymorphisms is necessary to be considered when assessing the health risk to benzene exposure. Aim of this study to evaluate the influence of benzene exposure and genetic polymorphisms of *NQO1*, *GSTT1*, and *GSTM1* in inducing chromosomal damage. *NQO1*, *GSTT1*, and *GSTM1* genes were chosen as their roles in genetic susceptibility for detoxification of benzene toxicity. This study found the geometric mean of benzene level among 107 urban traffic policemen was 20.42 $\mu\text{g}/\text{m}^3$ compared to only 7.59 $\mu\text{g}/\text{m}^3$ in a total of 100 office workers. Chromosomal damage was measured via micronuclei (MN) assay in traffic policemen had shown 1.8-fold higher than the comparative group ($p < 0.001$), accentuate the genotoxic effect potentially associated with benzene exposure. No significant association found between all studied genes with markers of effect, chromosomal damage (MN frequency). Carcinogenicity of benzene might have a major role in inducing the chromosomal damage rather than genetic polymorphisms factors among the studied groups. Multivariate analyse has confirmed the influence of benzene levels on MN frequency occurrence, apart from the environmental tobacco smoke and duration previous employment after factors of age and smoking habits controlled in study groups. A more comprehensive study necessary to assure the combination role of benzene and other involvement of genetic polymorphisms such as DNA-repair genes which might be responsible for benzene genotoxicity.

Keywords: Benzene; Chromosomal damage; *NQO1*, *GSTT1*, and *GSTM1* polymorphisms; Urban traffic policemen; Klang Valley

1. Introduction

Traffic police personnel have been recognized as one of the vulnerable professional groups who chronically exposed to multiple pollutants with carcinogenic and mutagenic effects. The traffic policemen are responsible for the daily task in directing the traffic and enforcement duty. This scenario poses a health threat to traffic police officers who work in high-traffic roads. In roads and urban areas, the vehicles emission is a primary source with light-duty vehicles (LDV) and heavy-duty vehicles

(HDV) emitted various of hazardous pollutants (Schmid et al., 2001). Among of these hazardous pollutants, benzene compound is well-identified generated from the motorcycle exhaust (Tsai et al., 2018). LDV user appears to be ongoing to grow as a matter of fact number of vehicles in Malaysia was increasing by years (RTVM, 2017). The most common of unleaded gasoline in Malaysia was Research Octane Number (RON) 95 and 97 of the EURO 2 standard in which RON 95 mostly preferable. The benzene content in EURO 2 standard can be added up to five percent by volume and this value still higher comparable to other European countries (Bahadar et al., 2014) and far away to achieve recommended maximum of 0.6% by Environmental Protection Agency (USEPA, 2007).

Therefore, the public health concern due to exposure to benzene has gained considerable attention as this benzene is ubiquitously released into the environment. Toxicity of benzene has sufficient evidence confirmed its ability to cause carcinogenic in human (USEPA, 2007). Capability of benzene to induce bone marrow as its target organ was proven leading to hematotoxin, anaemia, acute myeloid, and leukaemia (ATSDR, 2007; Glass et al., 2013). At ambient level, lifelong exposure to one $\mu\text{g}/\text{m}^3$ environmental benzene concentration is predicted to cause the risk of leukaemia to grow in six individual per million (WHO, 2000). Elsewhere, exposure to benzene was linked to genotoxic effects such as DNA damage, at ppb or ambient level (Sørensen et al., 2003; Maffei et al., 2005; Fracasso et al., 2010; Angelini et al., 2011).

Interestingly, the factors of genetic polymorphisms in human susceptibility to benzene must not be negligible apart from the nature of benzene carcinogenicity itself to acquire health risk such as DNA damage. The sign health effect at the cellular level is probably influence by both interaction, environmental factor of benzene exposure and genetic susceptibility (Chanvaivit et al., 2007; Carrieri et al., 2012) or so called “gene-environment interaction. The enzymes had claimed to be connected to the benzene metabolic pathways were *NQO1*, *GSTT1*, and *GSTM1* (Dougherty et al., 2008). Enzyme encoded for TT, CC and CT are conclusively defined have deficient, active and moderate in *NQO1* activity respectively (Kuehl et al., 1995; Siegel et al., 1999; Siegel et al., 2001). *NQO1* was believed to protect DNA damage against oxidative stress, natural and exogenous quinones (Autrup, 2000; Ross, 2000) as its function to reduce the highly toxic to less quinones by maintaining these quinones in reduced forms (Smith, 1999). Individuals carrying null *GSTT1* or *GSTM1* genes have restricted ability to metabolise carcinogens, which makes the individual more susceptible to cancer risk (Rebbeck, 1997).

At the present, the interaction of environmental exposure to benzene and interindividual variation in human involving enzymes activities were may found to be connected with marker of exposure and/or effects (Angelini et al., 2011; Mansi et al., 2012; Mitri et al., 2015) but still unclear to made for the final conclusion due to fluctuation results obtained (Dougherty et al., 2008). Therefore, this study aims to extend the knowledge by examining the influence of exposure levels to benzene and detoxifying genes of *NQO1*, *GSTT1*, and *GSTM1* polymorphisms on the marker of effects; MN frequency-indicator for the chromosomal damage among Malaysian male occupational group of traffic police personnel.

2. Materials and Methods

2.1. Study site

Klang Valley is regarded as Malaysia's economized centre with fast industrial and commercial growth, densely populated (DOS, 2010) and Malaysia's heavy-duty vehicle traffic region. The conurbation of population growth estimated to be reached 10.37 million population in Kuala Lumpur and the state of Selangor in 2020 (Second Physical Nation Plan, 2010) with a highly developed road network. As recorded, the Klang Valley region was covered with approximately 8.3 and 7.4 million LDVs and population, respectively, in the year 2017 (RTVM, 2017). Figure 1 shows the studied areas within Klang Valley region.

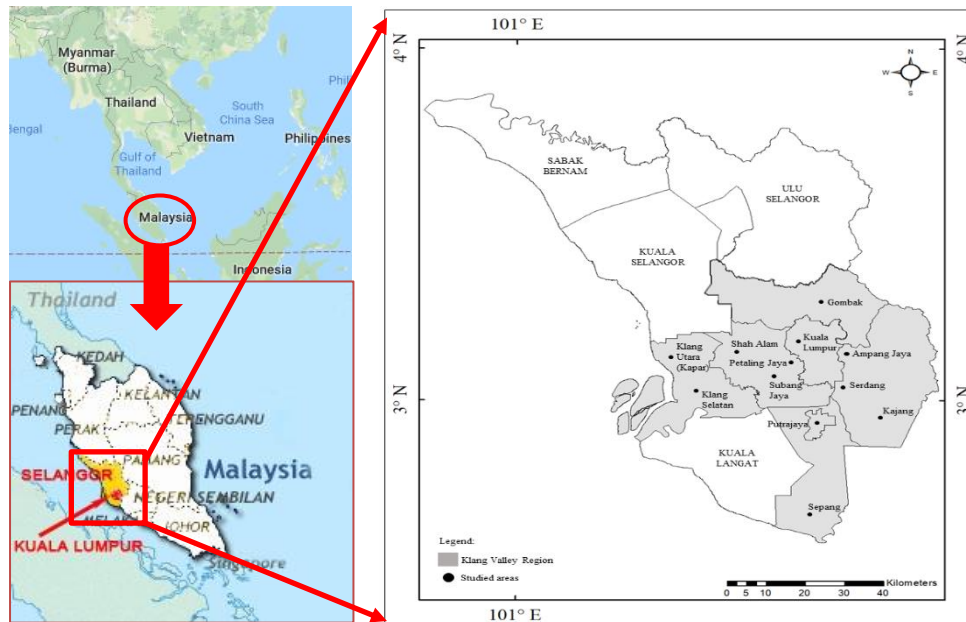


Figure 1. Studied areas within the Klang Valley region

2.2. Study subjects, personal air monitoring and biological samples collection

The two groups under this study were made of 107 outdoor traffic policemen as high exposure group and 100 of office workers as the comparative group who work in the city within the Klang Valley region. All subjects recruited were men, healthy, had worked equal or more than six months, and volunteered to participate with age ranged of 20-59 years old. Prior to the study conducted, the approval from the Ethics Committee for Research Involving Human Subject, Universiti Putra Malaysia had obtained. The subjects were briefly explained in the study information and informed consent was given before their participation was allowed. A structured questionnaire was distributed to assess the demographic information such as age, years of employment, smoking status, drinking behaviour, and undergone x-ray within six months. All subjects were monitored along their eight-working hour. The personal air samples to benzene exposure were measure by equipped the low air personal sampler attached with the sorbent tube within the subjects' breathing zone areas. The biological samples (buccal epithelial cells and blood samples) were collected simultaneously with personal air monitoring of benzene from August 2017 to January 2018.

2.3. Air Benzene Samples Analysis

All sample tubes were analysed for benzene based on the established method USEPA TO-17 (1999) for the determination of VOCs in ambient air using active sampling onto sorbent tubes. Briefly, samples in the sorbent tube were directly analysed via thermal desorption (TD) (Unity-2 and Ultra-TD sampler) (Markes International, UK) followed by an Agilent 6890N Gas Chromatograph (GC) equipped with a Mass Spectrometry (MS) Selective Detector (Agilent 5975C inert MSD). A DB-624 (J&W Scientific, USA) capillary column (60m length, 0.32 mm i.d, 1.80 μ m film thickness) was used for the benzene separation. Details of the set-up parameters for the TD-GCMS method are explained by Hamid et al. (2019). Calibration curve linearity for benzene was 0.9961 with limit of detection (LOD) of benzene was 0.22 μ g/m³.

2.4. MN Assay

Exfoliated buccal cells were collected using cytology brush by swabbing both the inner cheeks of subjects. The swab was dipped into 1.5 ml microcentrifuge tube containing 1 mL phosphate buffer saline

(PBS) 0.1 M for storage at -20°C before analysis. Duplicate slides for each subject were set up using well-standardized procedure in performing MN assay (Fleck et al., 2014). The Feulgen reaction was performed by hydrolysis of cells into 5N HCL for 30 minutes and followed by immersion process using Schiff reagent for 90-180 minutes. The criteria for MN scoring were as previously described by Fenech (1993) using 100x magnification. The calculation of MN per 1000 cells was presented formulated by Montero et al. (2006).

2.5. Genotyping

Genomic DNA was isolated from the whole blood using DNA extraction kits as followed recommended procedure by the manufacturer (Qiagen). *NQO1* genotypes were determined by the PCR-RFLP assay as described by Ergen et al. (2007). *GSTT1* and *GSTM1* genes were determined using multiplex polymerase chain reaction (PCR) method and primers used as described in the previous study with some modifications (Cheng et al., 2013; Matic et al., 2013; Sireesha et al., 2012; Uddin et al., 2014). The *GSTT1* and *GSTM1*'s amplification protocol consisted initial denaturation at 94°C for 5 min, denaturation at 94°C for 90 s, annealing 62°C for 60 s, extension at 72°C for 60 s, final annealing at 72°C for 5 min, and final extension at 72°C for 10 min for a total of 35 cycles. The amplification protocol used for *NQO1* was at 95°C and 5 min for initial denaturation, 95°C and 30 s for denaturation, 60°C and 30 s for annealing, 72°C and 30 s for extension and final extension at 72°C for 7 min with a total of 30 cycles. Restriction Enzyme Length Polymerase (RFLP) was performed by used the restriction enzyme of *HinfI* to cut the primer of interest gene. Verification of studied genes' fragments used 2% of agarose gel for *NQO1* gene and 3% for *GSTT1* and *GSTM1* genes respectively and run under electrophoresis prior visualized under UV light further. Human globin was used as an internal control for *GSTT1* and *GSTM1* genes (Cheng et al., 2013; Peterlin et al., 2014). The genotypes of the results were confirmed by repeat the analysis of 10% of the samples.

2.6. Statistical Analysis

The differences in demographic data between high-exposed and comparative groups were using Chi-Square. The normal distribution of benzene levels data was obtained after log transformation. Independent t-test was used for comparison benzene levels and MN frequency in study groups. Differences in MN frequency according to *NQO1*, *GSTT1*, and *GSTM1* were tested by multifactorial ANOVA and student's t-test. A stepwise method multivariable linear regression calculated the contribution of the significant variables simultaneously towards increasing MN frequency by controlling for the confounding factors (age and smoking status).

3. Results and Discussion

Table 1. Demographic data among respondents

Individual characteristics	Outdoor traffic policemen (N=107) n (%)	Office workers (N=100) n (%)	χ^2	<i>p</i> -value ^a
Age (years)				
20-39 (adult)	86 (80.4)	71 (71.0)	2.479	0.115
40-60 (middle age)	21 (19.6)	29 (29.0)		
Employment duration (years)				
0.5 - <4	37 (34.6)	24 (24.0)		
4-10	40 (37.4)	42 (42.0)		
>10	30 (28.0)	34 (34.0)		
Previous Job				
Outdoor/Industries	73 (68.2)	45 (45.0)	10.375	0.001**
Indoor/Administrative/Jobless	34 (31.8)	55 (55.0)		
Previous employment duration (years)				
Jobless	26 (24.3)	33 (33.0)	8.191	0.085
≤5	57 (53.3)	58 (58.0)		
6-10	13 (12.1)	6 (6.0)		
11-20	9 (8.4)	3 (3.0)		
>20	2 (1.9)	0 (0.0)		

^a Chi-Square test; ** Significant at $p < 0.01$

3.1. Demographic data

The number of drinkers was too small (a total of three respondents in both groups) which the statistical test has been negligible. Over 50% of respondents in both groups were moderate smokers (10-20 cigarettes per day) and majority have smoked for 11-20 years (represent 38.9% and 40.5% in traffic policemen and office workers respectively) (data are not shown). No significant difference was observed in age, current and previous employment duration, smoking habit, duration and category of smoking between both study groups ($p > 0.05$) exception for the type of previous job (Table 1); means these factors were well-controlled in this study.

3.2. Exposure levels to benzene and MN frequency

Table 2. Comparison personal benzene exposure level ($\mu\text{g}/\text{m}^3$) between outdoor traffic policemen and office workers

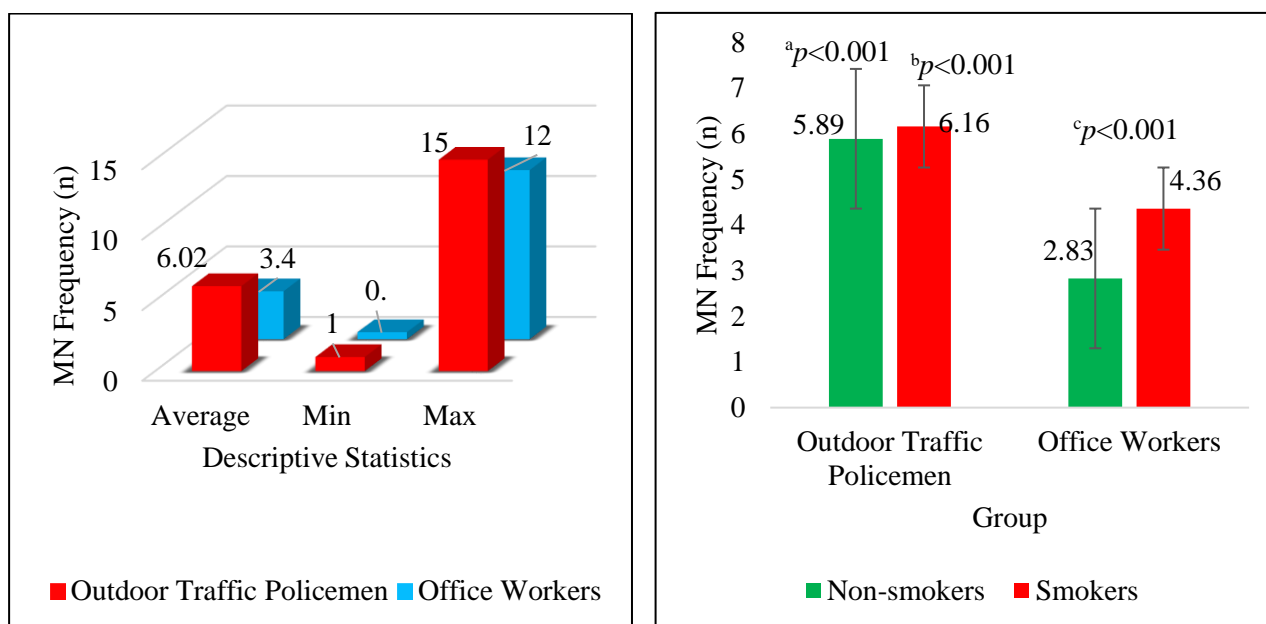
Compound	Group	GM	SD	Median	IQR	Min	Max	<i>t</i> statistic	<i>p</i> -value ^a
Log Benzene ($\mu\text{g}/\text{m}^3$) (TWA-8h)	Outdoor traffic policemen (n=107)	20.42 AM:24.78	1.88	19.95	2.57	3.39	85.11	11.008	<0.001***
	Office workers (n=100)	7.59 AM:9.00	1.94	9.18	4.79	0.95	28.84		

GM: Geometric mean; AM: Arithmetic mean; SD: Standard Deviation; ^a Independent t-test; ***Significant at $p < 0.001$

Table 2 shows the geometric mean and median benzene level exposed by the outdoor traffic policemen were 2.7 and 2.2-fold higher than the office workers with $p < 0.001$. This finding was in agreement with previous works by Angelini et al. (2011), Aryasiri et al. (2010), Crebelli et al. (2001), and Tomei et al. (2003). The present finding demonstrated the high-risk nature of the work in traffic police officers who were subjected to benzene carcinogenic than the office employees. Direct emissions while controlling the flows of traffic and carrying out enforcement duties daily, placed them at risk for their health. Even though, the geometric mean of individual benzene in both groups was lower than established benzene occupational limit ($1.6 \text{ mg}/\text{m}^3$) for TWA eight hours by current regulatory standard which applied at most by industrial sector (Malaysia OSHA 1994); however, this comparison seems ineffectively operate for the ambient environment.

If subdivided into smoking status, no significant difference in benzene levels was observed for smokers and non-smokers among similar profession in both groups. Documented GM (median) values in traffic policemen were $20.30 (17.10) \mu\text{g}/\text{m}^3$ for smokers and $20.49 (21.04) \mu\text{g}/\text{m}^3$ in non-smokers respectively. Meanwhile, smoking and non-smoking office workers showed exposure levels to benzene at GM (median) of $7.83 (9.18) \mu\text{g}/\text{m}^3$ and $7.44 (9.03) \mu\text{g}/\text{m}^3$, respectively. The present study was designed by only measured outdoor duty of the traffic policemen in which they were forbidden to smoke while performing their duty on the roads. Meanwhile, no difference between smokers and non-smokers in the office group explained as such they are not allowed to smoke in the air-conditioned building. These results indicating both, smokers and non-smokers in traffic policemen exposed to the almost similar level of benzene during their outdoor duty and smoking activity did not influence the level of benzene measured.

Outdoor traffic policemen had a higher exposure to benzene than office employees suggest that their outdoor duties were risky, particularly in urban regions such as Klang Valley. Klang Valley is one of Malaysia's metropolitan areas that suffered from unhealthy air from on-roads emissions, manufacturing sectors, forest fires and development of urbanization (Abdullah, Samah, and Jun, 2012). Motor vehicles were the most significant variables in the deterioration of air quality in Klang Valley regions; as a matter of fact, the private cars were increased from 91% to 93% in the years 2014 and 2017 (RTVM, 2014, 2017). This scenario had increased the utilization of aromatic-content fuels types which then leading to benzene level in the environment. The aromatic fuel content had increased the concentration of benzene in the atmosphere to 19.3 percent (Wu et al., 2007). In Urban areas of Malaysia, the vehicles emission/exhaust and gasoline evaporation contributed to a total of 94 percent for BTEX emission Malaysia (Hosaini et al., 2017).



^a Significantly difference from non-smoking office worker ($t=6.566, p<0.001$); ^b Significantly difference from smoking office worker ($t=6.563, p<0.001$); ^c Significantly difference from non-smokers and smokers in office workers ($t=3.929, p<0.001$)

Figure 2. The differences of MN frequency (per 1000 cells) between studied groups and subdivided into smoking status

Figure 2 demonstrates that outdoor police officers had an average frequency of 6.02 MN (per 1000 cells), 1.8 times greater than office employees with an average MN of 3.40. The outcome showed a substantial distinction between these two groups in MN frequency (per 1000 cells) with $p<0.001$. This finding indicates that even at a magnitude far below the defined threshold limit values (TLV), benzene could have a genotoxic impact. This finding is consistent with prior work carried out among traffic police staff by Angelini et al. (2011) and Maffei et al. (2005). Maffei et al. (2005) found MN in the average of 6.94 in smokers and 7.12 in non-smokers with benzene level at mean \pm SD of $24.32\pm 14.38 \mu\text{g}/\text{m}^3$ in both subgroups. Meanwhile, the median value for MN and benzene monitored were reported at 7.0 and $19.33 \mu\text{g}/\text{m}^3$, respectively by Angelini et al. (2011).

The smokers subgroup demonstrated a significantly higher in MN frequency (average of 4.36) than non-smokers subgroup (average of 2.83) with $t=3.929$ and $p<0.001$ in the office workers. Interestingly, for the outdoor traffic policemen, an opposite result was observed between smokers and non-smokers subgroup ($t=0.523, p=0.602$). However, MN frequency was significantly higher in non-smoking outdoor traffic policemen than non-smoking office workers ($p<0.001$). The identical trend with significant result also documented among smokers between outdoor traffic policemen and office workers ($p<0.001$). Considering in single group of office workers, MN frequency was significantly higher in smokers compared to the non-smokers demonstrated the smoking habit had heightened the MN levels. However, smoking habits did not substantially modify the occurrence of chromosomal damage in the group of outdoor traffic policemen. This finding was consistent with other previous studies that failed to link the influence of cigarette on the MN occurrence (Maffei et al., 2005; Angelini et al., 2011) but not in the cases found by Bindhya et al. (2010) and Mrdjanovic' et al. (2014).

3.3. MN frequency according to studied genes

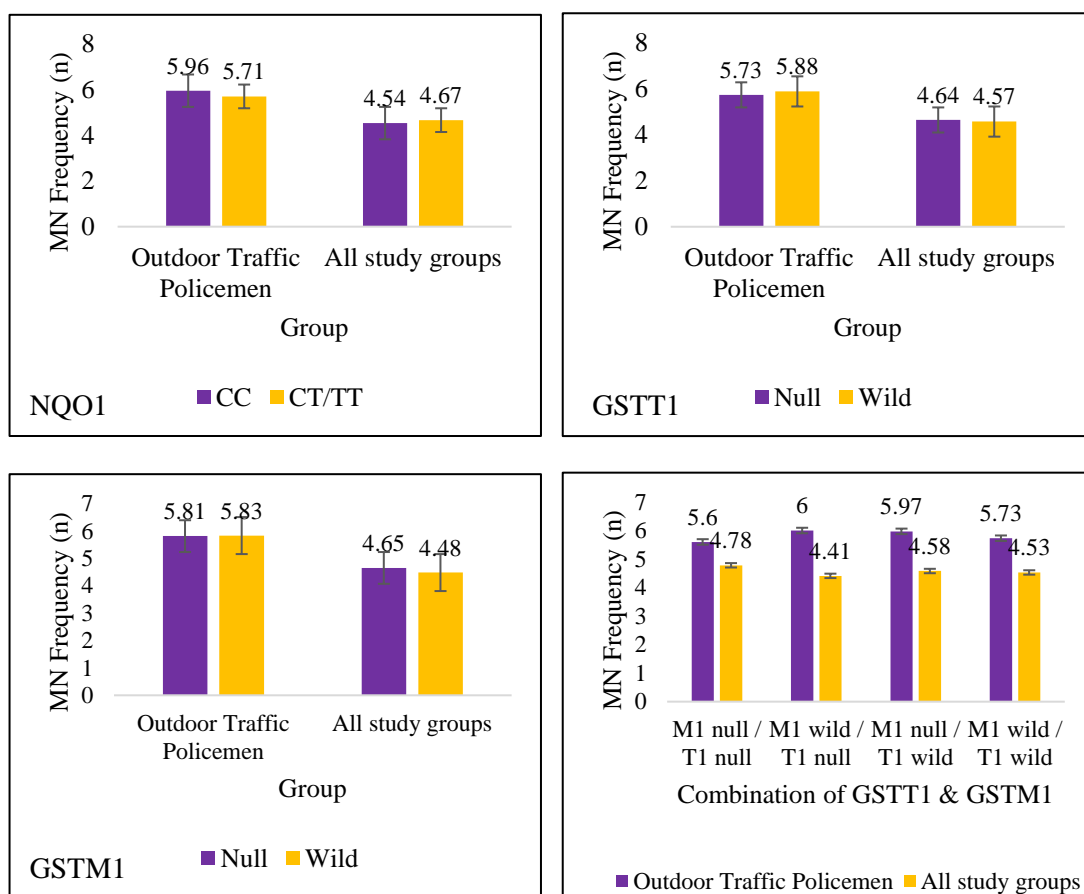


Figure 3. MN Frequency according to *NQO1*, *GSTT1*, and *GSTM1* genotypes

Results showed that all detoxifying genes studied did not influence the frequency of MN (Figure 3). These results were consistent with prior works observed by Zhang et al. (2014) but with greater benzene exposure levels than the present study had (ranging from 2.6 to 57.0 mg/m³). Taking into account for the low-level of benzene exposure (ranging from 13.46 to 31.41 µg/m³), Angelini et al. (2011) discovered no significant influence of *GSTT1* null and *NQO1* variant except for individuals with *GSTM1* null (males only) which showed increment in MN values among Italian police officers. Opposite to these present findings, Kim et al., (2008) reported that the petroleum refinery workers who carry *NQO1-TT* had higher MN frequencies than those with *NQO1-CC* or *NQO1-CT*. This was agreed as *NQO1-TT* genotypes have a complete absence of enzymatic activity (Siegel et al., 1999).

The results of the present study may be explained by other roles of genes polymorphism along with the phases of benzene metabolic pathways such as DNA-repair genes. For instance, Chanvaivit et al. (2007) had reported on the laboratory workers whose *XRCC1* 399Arg/Arg (homozygous wild) genotype exhibited a lower incidence of dicentric and deletions than those from workers who carried the 399Gln genotype (variant type). Elsewhere, Kim et al. (2008) reported the benzene-exposed workers carrying combination of *MPO* G/G (homozygous variant) and *XRCC1* Arg/Gln (heterozygous variant) or Gln/Gln genotype (homozygous variant) is less efficient in repairing the DNA damage induced by benzene as this homozygous or heterozygous variant of genes were suggested to have poor or no any enzymatic activities. *XRCC1* plays an important role in base-excision repair (Chanvaivit et al., 2007) and essential to hold up the protein attached to repairing enzymes (Kubota and Horiuchi, 2003). Ruchirawat et al. (2010) agreed that the decline in DNA repair capacity could enhance the damage in

DNA or chromosome level and leading to cancer development. The larger sample size probably provided a robust result in examining the gene-environment interaction for exposure at the ppb level.

3.4. Predictors for MN frequency

Table 3. Predictors for MN frequency

Model ¹	MN/1000 cells					
Overall	B	β	95 CI	t-value	p-value †	R ²
Constant	3.308		2.168, 4.448	5.722	<0.001***	0.209
ETS	-2.060	-0.296	-2.937, -1.183	-4.631	<0.001***	
Duration previous employment (years)	0.100	0.214	0.052, 0.192	3.678	<0.001***	
Log benzene level	1.206	0.159	0.249, 2.163	2.485	0.014*	
Adjusted R²=0.197, F=17.659						
After controlling smoking status, number cigarettes/day, and smoking duration						

¹ Multiple Linear Regression Model Stepwise Method; *Significant at $p<0.05$; ***Significant at $p<0.001$; Reference: (ETS: 0=Yes, 1=No); † Controlling for age and smoking

A stepwise method multivariable linear regression calculated the contribution of the significant variables simultaneously towards increasing MN frequency by controlling for the confounding factors (age and smoking status) as shown in Table 3. Result showed MN frequency had been influence by environmental tobacco smoke (ETS), duration previous employment, and benzene levels. This impossible to conclude the benzene has induced the chromosomal damage alone as other genotoxic pollutants encounter in urban air probably took a role. However, this study was supplemented with personal monitoring of benzene data suggested that the influence of ambient benzene in inducing MN frequency occurrence was undeniable.

4. Conclusion

This study has contributed an extensive knowledge of gene-environment interaction, particularly in Malaysian male occupational group who chronically exposed to the ambient benzene from traffic emission. The formation of more micronucleated cells in outdoor police officers than comparative groups announced a rise in the incidence of chromosomal damage among them. Multivariate analyses had confirmed the exposure to benzene had elevated the MN frequency, apart from the ETS and employment duration factors after age and smoking were statistically controlled. This study had provided a comprehensive understanding of the alone exposure to benzene arises from working activity could induce chromosomal damage without a combination of individual carries "mutant" (variant or null) alleles. Therefore, safety and health management strategies in managing air pollutants in traffic policemen should aim to prevent the cancer risk in the future.

5. References

Abdullah, A. M., Armi Abu Samah, M., and Yee Jun, T., 2012. An overview of the air pollution trend in Klang Valley, Malaysia. *Open Environmental Sciences*. 6(1).

Agency for Toxic Substances and Disease Registry (ATSDR), 2007. Toxicological Profile for Benzene, US Department of Health and Human Services, Atlanta, GA.

American Conference of Governmental Industrial Hygienists (ACGIH), 2006. Threshold limit values and biological exposure indices. Cincinnati, Occupational Health, United States of American.

Angelini, S., Kumar, R., Bermejo, J. L., Maffei, F., Barbieri, A., Graziosi, F., Carbonea, F., Fortia, and Hrelia, P., 2011. Exposure to low environmental levels of benzene: evaluation of micronucleus frequencies and S-phenylmercapturic acid excretion in relation to polymorphisms in genes encoding metabolic enzymes. *Mutation Research/Genetic Toxicology and Environmental Mutagenesis*. 719(1), 7-13.

Arayasiri, M., Mahidol, C., Navasumrit, P., Autrup, H., & Ruchirawat, M., 2010. Biomonitoring of benzene and 1, 3-butadiene exposure and early biological effects in traffic policemen. *Science of the Total Environment*. 408(20), 4855-4862.

Autrup, H., 2000. Genetic polymorphisms in human xenobiotic metabolising enzymes as susceptibility factors in toxic response. *Mutation Research*. 464, 65–76.

Bahadar, H., Mostafalou, S., and Abdollahi, M., 2014. Current understandings and perspectives on non-cancer health effects of benzene: A global concern. *Toxicology and Applied Pharmacology*. 276(2), 83-94.

Bindhya, S., Balachandar, V., Sudha, S., Devi, S. M., Varsha, P., Kandasamy, K., ... and Sasikala, K., 2010. Assessment of occupational cytogenetic risk, among petrol station workers. *Bulletin of Environmental Contamination and Toxicology*. 85(2), 121-124.

Carrieri, M., Bartolucci, G. B., Scapellato, M. L., Spatari, G., Sapienza, D., Soleo, L., ... & Trevisan, A., 2012. Influence of glutathione S-transferases polymorphisms on biological monitoring of exposure to low doses of benzene. *Toxicology Letters*. 213(1), 63-68.

Chanvaivit, S., Navasumrit, P., Hunsonti, P., Autrup, H., and Ruchirawat, M., 2007. Exposure assessment of benzene in Thai workers, DNA-repair capacity and influence of genetic polymorphisms. *Mutation Research/Genetic Toxicology and Environmental Mutagenesis*. 626(1), 79-87.

Chen, R., Ren, S., Meng, T., Aguilar, J., and Sun, Y., 2013. Impact of glutathione-S-transferases (GST) polymorphisms and hypermethylation of relevant genes on risk of prostate cancer biochemical recurrence: a meta-analysis. *PloS one*. 8(9), e74775

Crebelli, R., Tomei, F., Zijno, A., Ghittori, S., Imbriani, M., Gamberale, D., Martini, A., and Carere, A., 2001. Exposure to benzene in urban workers: environmental and biological monitoring of traffic police in Rome. *Occupational and Environmental Medicine*. 58(3), 165-171.

Department of Statistics (DOS), 2010. Population Statistic 2010. Department of Statistics, Malaysia.

Dougherty, D., Garte, S., Barchowsky, A., Zmuda, J., & Taioli, E., 2008. NQO1, MPO, CYP2E1, GSTT1 and GSTM1 polymorphisms and biological effects of benzene exposure—a literature review. *Toxicology letters*, 182(1-3), 7-17.

Ergen, H. A., Gormus, U., Narter, F., Zeybek, U., Bulgurcuoglu, S., and Isbir, T., 2007. Investigation of NAD (P) H: quinone oxidoreductase 1 (NQO1) C609T polymorphism in prostate cancer. *Anticancer research*. 27(6B), 4107-4110.

Fenech, M., 1993. The cytokinesis-block micronucleus technique: a detailed description of the method and its application to genotoxicity studies in human populations. *Mutation. Research*. 285, 35–44.



Fleck, A. D. S., Vieira, M., Amantéa, S. L., and Rhoden, C. R., 2014. A comparison of the human buccal cell assay and the pollen abortion assay in assessing genotoxicity in an urban-rural gradient. *International Journal of Environmental Research and Public Health*. 11(9), 8825-8838.

Fracasso, M. E., Doria, D., Bartolucci, G. B., Carrieri, M., Lovreglio, P., Ballini, A., ... and Manno, M., 2010. Low air levels of benzene: correlation between biomarkers of exposure and genotoxic effects. *Toxicology letters*. 192(1), 22-28.

Hosaini, P. N., Khan, M. F., Mustafa, N. I. H., Amil, N., Mohamad, N., Jaafar, S. A., ... & Latif, M. T., 2017. Concentration and source apportionment of volatile organic compounds (VOCs) in the ambient air of Kuala Lumpur, Malaysia. *Natural Hazards*. 85(1): 437-452.

Glass, D.C., Gray, C.N., Jolley, D.J., Gibbons, C., Sim, M.R., Fritschi, L., et al., 2003. Leukemia risk associated with low-level benzene exposure. *Epidemiology*. 14, 569-77.

Hamid, H.H.A., Latif, M.T., Nadzir, M.S.M., Uning, R., Khan, M.F., and Kannan, N., 2019. Ambient BTEX levels over urban, suburban and rural areas in Malaysia. *Air Quality, Atmosphere and Health*. 1-11.

Kim, Y. J., Choi, J. Y., Paek, D., and Chung, H. W., 2008. Association of the NQO1, MPO, and XRCC1 polymorphisms and chromosome damage among workers at a petroleum refinery. *Journal of Toxicology and Environmental Health, Part A*. 71(5), 333-341.

Kubota, Y., and Horiuchi, S., 2003. Independent roles of XRCC1's two BRCT motifs in recovery from methylation damage. *DNA Repair*. 2(4), 407-415.

Kuehl, B., L., Paterson, J., W., Peacock, J., W., Paterson, M., C., Rauth, A., M., 1995. Presence of a heterozygous substitution and its relationship to DT-diaphorase activity. *Br J Cancer*. 72(3), 555-561.

Lin, Y. S., Vermeulen, R., Tsai, C. H., Waidyanatha, S., Lan, Q., Rothman, N., Smith, M.T., Zhang, L., Shen, M., Li, G., Yin, S., Kim, S., and Rappaport, S.M., 2007. Albumin adducts of electrophilic benzene metabolites in benzene-exposed and control workers. *Environmental Health Perspectives*. 28-34.

Maffei, F., Hrelia, P., Angelini, S., Carbone, F., Forti, G. C., Barbieri, A., and Violante, F. S., 2005. Effects of environmental benzene: micronucleus frequencies and haematological values in traffic police working in an urban area. *Mutation Research/Genetic Toxicology and Environmental Mutagenesis*. 583(1), 1-11.

Malaysia Occupational Safety and Health Act, 1994. Act 514. Laws of Malaysia.

Mansi, A., Bruni, R., Capone, P., Paci, E., Pignini, D., Simeoni, C., ... and Tranfo, G., 2012. Low occupational exposure to benzene in a petrochemical plant: modulating effect of genetic polymorphisms and smoking habit on the urinary t, t-MA/S-PMA ratio. *Toxicology Letters*. 213(1), 57-62.

Matic, M., Pekmezovic, T., Djukic, T., Mimic-Oka, J., Dragicevic, D., Krivic, B., Suvakov, S., Savic-Radojevic, A., Pljesa-Ercegovac, M., Tulic, C., Coric, V., and Simic, T., 2013. GSTA1, GSTM1, GSTP1, and GSTT1 polymorphisms and susceptibility to smoking-related bladder cancer: a case-control study. In *Urologic Oncology: Seminars and Original Investigations*. 1(7), 1184-1192.

Mitri, S., Fonseca, A., Otero, U., Tabalipa, M., Moreira, J., & Sarcinelli, P., 2015. Metabolic polymorphisms and clinical findings related to benzene poisoning detected in exposed brazilian gas-station workers. *International journal of environmental research and public health*. 12(7): 8434-8447.



- Montero, R., Serrano, L., Araujo, A., Dávila, V., Ponce, J., Camacho, R., Morales, E., and Méndez, A., 2006. Increased cytogenetic damage in a zone in transition from agricultural to industrial use: comprehensive analysis of the micronucleus test in peripheral blood lymphocytes. *Mutagenesis*. 21(5), 335-342.
- Mrdjanović, J., Šolajić, S., Dimitrijević, S., Đan, I., Nikolić, I., and Jurišić, V., 2014. Assessment of micronuclei and sister chromatid exchange frequency in the petroleum industry workers in province of Vojvodina, Republic of Serbia. *Food and Chemical Toxicology*. 69: 63-68.
- Petrovič, D., and Peterlin, B., 2014. GSTM1-null and GSTT1-null genotypes are associated with essential arterial hypertension in patients with type 2 diabetes. *Clinical biochemistry*, 47(7-8), 574-577.
- Perera, F. P. (1996). Molecular epidemiology: insights into cancer susceptibility, risk assessment, and prevention. *Journal of the National Cancer Institute*. 88(8), 496-509.
- Rebbeck T., R., 1997. Molecular epidemiology of the human glutathione S transferase genotypes GSTM1 and GSTT1 in cancer susceptibility. *Cancer Epidemiol Biomarkers Prev*. 6, 733-743.
- Road Traffic Volume Malaysia, 2014. Kuala Lumpur: Highway Planning Division, Ministry of Works Malaysia.
- Road Traffic Volume Malaysia, 2017. Kuala Lumpur: Highway Planning Division, Ministry of Works Malaysia.
- Ross, D., Kepa, J. K., Winski, S. L., Beall, H. D., Anwar, A., & Siegel, D., 2000. NAD (P) H: quinone oxidoreductase 1 (NQO1): chemoprotection, bioactivation, gene regulation and genetic polymorphisms. *Chemico-Biological Interactions*. 129(1-2): 77-97.
- Ruchirawat, M., Navasumrit, P., Settachan, D., Tuntaviroon, J., Buthbumrung, N., and Sharma, S., 2005. Measurement of genotoxic air pollutant exposures in street vendors and school children in and near Bangkok. *Toxicology and Applied Pharmacology*. 206(2), 207-214.
- Schmid, H., Pucher, E., Ellinger, R., Biebl, P., and Puxbaum, H., 2001. Decadal reductions of traffic emissions on a transit route in Austria—results of the Tauerntunnel experiment 1997. *Atmospheric Environment*, 35(21), 3585-3593.
- Siegel, D., McGuinness, S.M., Winski, S., L., Ross, D., 1999. Genotype- phenotype relationship in studies of a polymorphism in NAD(P)H:quinone oxidoreductase 1. *Pharmacogenetics*. 9, 113-21.
- Siegel, D., Anwar, A., Winski, S., L., Kepa, J., K., Zolman, K., L., Ross, D., 2001. Rapid polyubiquitination and proteasomal degradation of a mutant form of NAD(P)H:quinone oxidoreductase 1. *Mol Pharmacol*. 59(2), 263–268.
- Sireesha, R., Laxmi, S. B., Mamata, M., Reddy, P. Y., Goud, P. U., Rao, P. V., Reddy, G.P., and Padma, T., 2012. Total activity of glutathione-S-transferase (GST) and polymorphisms of GSTM1 and GSTT1 genes conferring risk for the development of age-related cataracts. *Experimental Eye Research*. 98: 67-74.
- Smith, M., T., 1999. Benzene, NQO1, and genetic susceptibility to cancer. *Proceedings of the National Academy of Sciences*. 96(14), 7624-7626.
- Sørensen, M., Skov, H., Autrup, H., Hertel, O., and Loft, S., 2003. Urban benzene exposure and oxidative DNA damage: influence of genetic polymorphisms in metabolism genes. *Science of the Total Environment*. 309(1), 69-80.



Tomei, F., Ghittori, S., Imbriani, M., Pavanello, S., Carere, A., Marcon, F., Martini, A., Baccolo, T.P., Tomao, E., Zijno, A., and Crebelli, R., 2001. Environmental and biological monitoring of traffic wardens from the city of Rome. *Occupational Medicine*. 51(3), 198-203.

Tsai, J.H., Yao, Y.C., Huang, P.H., and Chiang, H.L., 2018. Fuel economy and volatile organic compound exhaust emission for motorcycles with various running mileages. *Aerosol. Air. Qual. Res.* 18, 3056-3067.

Uddin, M. M. N., Ahmed, M. U., Islam, M. S., Islam, M. S., Sayeed, M. S. B., Kabir, Y., and Hasnat, A., 2014. Genetic polymorphisms of GSTM1, GSTP1 and GSTT1 genes and lung cancer susceptibility in the Bangladeshi population. *Asian Pacific Journal of Tropical Biomedicine*. 4(12), 982-989.

U.S. Environmental Protection Agency, 2007. Reference concentration for unit inhalation exposure (RfC), IRIS summary. Integrated Risk Information System.

U.S. Environmental Protection Agency, 1999. EPA Compendium Method TO-17. Determination of volatile organic compounds (VOCs) in ambient air using active sampling onto sorbent tubes. EPA 625/R-96/010b. Office of Research and Development, Cincinnati.

World Health Organization (WHO), 2000. Benzene. In: *Air quality guidelines for Europe*, 2nd ed. Copenhagen, World Health Organization Regional Office for Europe. Retrieved at <http://apps.who.int/iris/bitstream/10665/107335/1/E71922.pdf>. (December 2017).

Acknowledgments

This work was supported by the Fundamental Research Grant Scheme 2016-2019 (Project code: 04-01-16-1808FR) funded by Malaysia Ministry of Education and special thanks to participation of traffic policemen in Klang Valley region with support of Bukit Aman Traffic Chief including volunteered group of office workers. We are grateful for Faculty Science Technology, Universiti Kebangsaan Malaysia for their greatest contribution in facilities for BTEX air samples analysis and Malaysia Department of Occupational Safety and Health for sampling instruments aided.

Sustainable cement sector strategies to control emissions and combat climate change

Canan Derinoz Gencil¹, M. Emre Erguclu² and Yasin Yigit³

¹Director of the Environment and Climate Change Department of the Turkish Cement Manufacturers' Association

²Chair of Turkish Cement Manufacturers' Association Task Force on Environmental Legislation

³Chair of Turkish Cement Manufacturers' Association Task Force on Alternative Fuels and Alternative Raw Materials

canand@tcma.org.tr

Abstract. The cement sector is a leading industry of Turkey as well as being the first biggest producer in Europe and 4th biggest producer in the World. The sector continues contribution to Turkey's economy by producing approximately 71 million tons of clinker and 75 million tons of cement annually in 2018 with a total of 74 facilities, 55 of which are integrated and 19 are grinding. Turkish cement sector is a leading industry, growing economically while considering all environmental responsibilities. The sector has great awareness and experience related to local air pollution control and global emissions such as the greenhouse gases. The sector has been making environmental investments since early 1990's. Up to day, all kiln stacks were equipped with dust abatement units, majority of them being baghouse filters those are more efficient than the electrostatic precipitators. Reduction systems for nitrogen oxide emissions were installed in many facilities to achieve the reduced local emission limits. As per the on-going European Union acquis, the sector follows and tries to apply the Best Available Techniques of the European Union Regulation. This paper reviews the level of environmental investments to control local air pollutants and CO₂ emission that have global affect. Cement production comprises approximately 5-7% of the global greenhouse gas emissions. Greenhouse gas emissions due to cement production can be classified as direct emissions (from decarbonisation and fuel) and indirect emissions (such as electric power consumption). The strategy of the cement sector in a low carbon economy requires implementation of the following pathways: increasing energy efficiency, increasing the use of alternative fuels, reducing the clinker/cement ratio, installing waste heat recovery units and using new and innovative technologies (e.g. Carbon capture, storage and use).

Keywords: Cement, Greenhouse gases, Alternative fuels, Energy efficiency, Sustainable development

1. Introduction

Turkish cement industry traces its history back over more than a century to 1911, when it had a capacity of just 20,000 t/yr in the then-capital İstanbul. By the end of 2018, the Turkish cement industry had a total of 55 integrated cement plants and 19 cement grinding facilities employing around 19,000 people. Today the industry has a combined clinker capacity of 90 million tonnes. The industry produced 71 million tons of clinker and 75 million tons of cement in 2018.

Turkish cement industry has been one of the major cement and clinker exporters in the world since 1970. At the end of 2018, export figures were realized as 6.1 million tons of clinker and 7.6 million tons of cement. Today, Turkish Cement Sector is a leader in production and exporting in Europe and the 4th largest producer and 3rd largest exporter of the World.



Turkey's cement consumption per capita is around 850 kg. The general expectation is that consumption will reach to 1,000-1,100 kg/per capita level, sustain these levels for a while and then decrease gradually to 500 kg/per capita levels. Turkey's maximum population is forecasted as 100 million and our consumption is expected to be around 100 million tons.

Turkish Cement Manufacturers' Association (TÇMB) established in 1957 is the common voice of the Turkish cement sector. It represents more than 95% of the cement production. TÇMB provides common solutions to its members for their research and development activities, analysis, quality control, training services and makes common initiatives for legal and administrative regulations.

2. Cement Production

Cement is a fine, soft, powdery substance, mainly used to bind fine sand and coarse aggregates together in concrete. Cement is a hydraulic binder that hardens when water is added. (CEMBUREAU, 2017)

The cement-making process can be divided into two basic steps (CEMBUREAU, 2017):

- The main element of cement is clinker. Clinker is made in a kiln, where the gas of 2,000°C heats the raw materials to 1,450°C. Main raw materials are limestone (calcium carbonate) and other materials. This process is known as calcination. During calcination, calcium carbonate (limestone) is transformed into calcium oxide (lime), which then reacts with the other constituents from the raw material to form new minerals, collectively called clinker. This near-molten material is rapidly cooled to a temperature of 100 - 200°C.
- Clinker is then ground with gypsum and other materials to produce the grey powder known as cement.

Primary fuels used to produce clinker are coal, petroleum coke and lignite. Cement sector in the world and our country replace the primary fuels and raw materials with the wastes conforming to acceptance criteria. Wastes with calorific value are used instead of conventional fuels. Wastes with mineral value are used for lime, which is the cement raw material, and other minerals.

3. Sustainability and Environmental Legislation

The guiding principle of the Turkish cement sector is environmental, economic and social sustainability. Cement sector has led the Turkish industry to comply with all regulations for more than 25 years. In 1993 and then in 2004, "Environmental Declarations" were signed between the TÇMB and the Ministry of Environment. Due signing these declarations, cement industry voluntarily agreed to reduce emissions below the regulatory limit values. Then, sector started necessary investments for emission control, improved its processes and completed all environmental permits. Cement sector was the first sector that completed the environmental permitting processes.

Currently, cement factories have all permits and licenses as per the national environmental legislation, the major one being the "Environmental Permit". It is secured due fulfilling requirements of the umbrella regulation called "Regulation on the Permits and Licenses Required As Per the Environmental Law". Cement factories have "Environmental Measurements" performed to obtain the environmental permits from the Ministry. These measurements are repeated at the periods provided in the Regulations and control measurements continue in the main stacks by means of the continuous measurement devices after the permit is obtained. Calibrations of the continuous measurement devices are also repeated at the frequencies provided in the legislation. All environmental measurements of the sector are performed by the "independent accredited laboratories" authorized by the Ministry of Environment and Urbanization.

Alternative fuel use, which was 88 thousand tons in 2008, reached about 1 million tons in 2018. This figure corresponds to approximately 6% thermal substitution ratio. At the cement factories in the European Union countries, about 44% (in some facilities almost 100%) of the thermal power is obtained from the wastes. In 2018 wastes used as alternative raw materials are about 1.5 million tonnes. This means cement sector recovered total 2.5 million tons of waste as alternative fuel and alternative raw material in year 2018.

Cement factories in our country are distributed throughout the country and approximately 35 of 55 factories have licenses for using the wastes as alternative fuel. Cement plants using wastes as alternative fuels fulfil a series of permitting procedures like trial burns, waste characterisation and securing licences. As per the “Regulation on Waste Incineration”, the accredited laboratories, which are authorized by the Ministry of Environment and Urbanization carry out periodical measurements.

4. Achievements in Local Air Pollution Control

Local air emissions relevant to cement manufacturing are, particulate matter (PM), Nitrogen oxides (NO_x), Sulfur oxides (SO₂) and heavy metals emissions. Cement plants using waste as alternative fuels should also control and monitor Total Organic Compounds (TOC) including Volatile Organic Compounds (VOC), Hydrogen Chloride (HCl), Hydrogen Fluoride (HF), polychlorinated dibenzo-p-dioxins and dibenzofurans (PCDD and PCDF), Carbon Monoxide (CO) and Carbon Dioxide (CO₂). (EC-JRC, 2013).

As CO₂ emissions have global affects, this topic is covered in the next section. The next section will also cover low carbon pathways and the achievements in this pathway; i.e. energy efficiency, alternative fuel use and blended cements.

4.1 Control of Dust Emissions

The main sources of dust emissions are; raw material preparation process (raw mills), grinding and drying units, the clinker burning process (kilns and clinker coolers), the fuel preparation and cement grinding unit (mills), raw material conveyors and elevators, storage for raw materials and cement, storage of fuels (petroleum coke, hard coal, lignite) and dispatch of cement (loading). Diffuse dust emissions sources are; storage and handling of materials and solid fuels, e.g. from open storage and also from road surfaces because of road transport. (EC-JRC, 2013)

Turkish cement sector follows the best available techniques to control dust emissions. Modern electrostatic precipitators (ESP) and baghouse filters are used to control dust emissions. Diffuse emissions are controlled by closed conveyor systems, paved and regularly cleaned roads are established and water sprays are used if necessary. Wherever possible, closed storage systems are built.

As seen in Table 1, dust emission limits for Turkish cement plants are close to the BAT-AELs (Best Available Techniques Associated Emission Levels) of the European Union Legislation. For the plants incinerating waste emission limit values are the same.

Table 1. Comparison of Particulate Matter Limit Values for Turkey and the EU

	Plants not incinerating waste		Plants incinerating waste	
	Turkey ⁽¹⁾	BAT-AEL ⁽²⁾	Turkey ⁽³⁾	Limit Value ⁽⁴⁾
Particulate Matter	50	<10-20	30	30

(1) Regulation 2009
(2) CIM 2013/163/EU
(3) Regulation 2010
(4) Directive 2010/75/EU

As mentioned above, all point sources of dust are controlled with baghouse filters (also called fabric filters) or electrostatic precipitators (ESP). The main issue of concern is the kiln stacks. Fabric filters have higher dust abatement capacities than the ESPs. In the scope of the environmental investments, Turkish cement plants out phased the ESPs and established more efficient baghouse filters at the kiln stacks. Fabric filter investments provided emission levels far lower than the legal limits in a number of facilities.

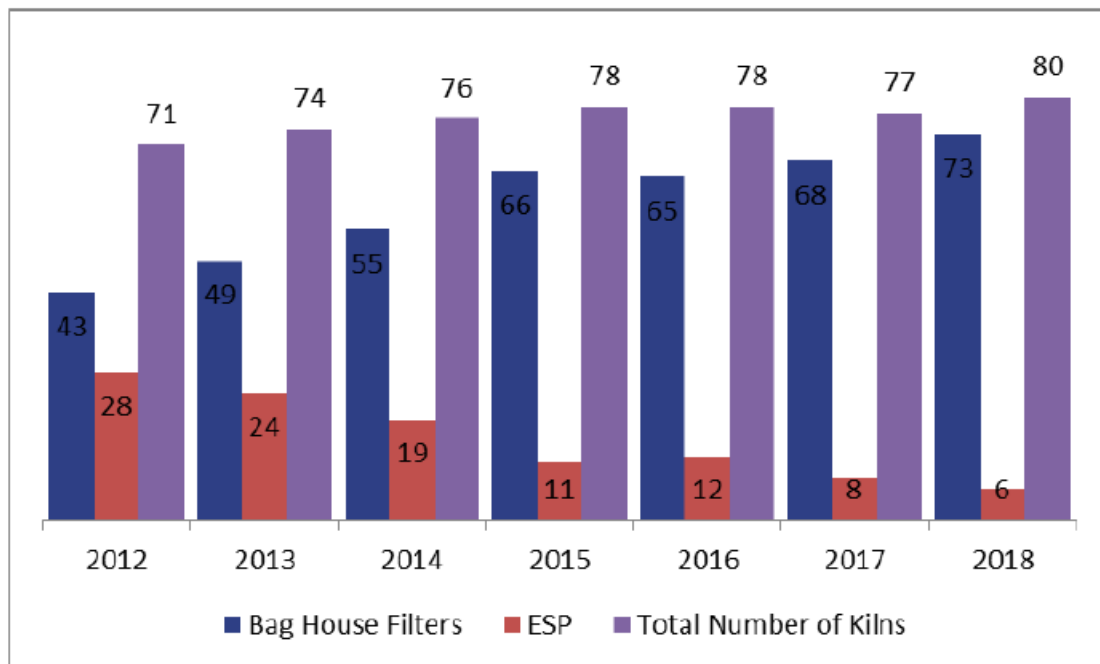


Figure 1. Dust Control Equipment (TCMA, 2019)

Figure 1 represents the total number of dust control equipment installed in the last 7 years. As seen in Figure 1, 43 of 71 kiln stacks were equipped with baghouse filters in 2012 whereas 73 of 80 stacks were equipped with baghouse filters in 2018. These figures mention that the ratio of plants equipped with baghouse filters at the kiln stacks increased from 60 % to 91 % in the last 7 years.

4.2 Control of NO_x Emissions

Nitrogen oxides (NO_x) emissions are result of clinker burning process at high temperature. These oxides are concern related to air pollution. Two main sources of NO_x production are; thermal NO_x and fuel NO_x.

Thermal NO_x are formed when part of the combustion air in the kiln reacts with oxygen to form oxides of nitrogen. This is the major mechanism of NO_x formation in the kiln. Fuel NO_x are formed when compounds containing nitrogen, chemically bound in the fuel, react with oxygen in the air to form various oxides of nitrogen. (EC-JRC, 2013)

Best available techniques to control NO_x emissions are; primary techniques (flame cooling, low NO_x burners, mid-kiln firing, process optimisation), staged combustion (conventional or waste fuels), Selective non-catalytic reduction (SNCR) and Selective catalytic reduction (SCR). (CIM 2013/163/EU) Turkish cement sector applies appropriate techniques to lower NO_x emissions. Reduction systems for nitrogen oxide (SNCR), have been installed in many facilities to achieve the nitrogen oxide emission limits reduced as of 2018.

Table 2 compares NO_x emission limits for Turkish cement plants with those mentioned as the BAT-AELs (Best Available Techniques Associated Emission Levels) of the EU and emission limits for plants incinerating waste. For the time being, NO_x limits in Turkey are higher than those in the EU except new plants incinerating waste.

Table 2. Comparison of NO_x Limit Values for Turkey and the EU

	Plants not incinerating waste		Plants incinerating waste	
	Turkey ⁽¹⁾	BAT-AEL ⁽²⁾	Turkey ⁽³⁾	Limit Value ⁽⁴⁾
NO _x	800	200-450	800 500 (new plants)	500

(1) Regulation 2009
(2) CIM 2013/163/EU
(3) Regulation 2010
(4) Directive 2010/75/EU

Turkish government carries out studies to adopt BAT-AELs as limit values in Turkey. TÇMB and sector representatives closely follow the developments.

It is of vital importance to establish rules that pay attention to the costs, reflect the realities of our country and do not go beyond the requirements of the EU legislation. For example in the coming years, it is important to take account of the additional operating costs to be incurred due to possible implementation of 200-450 mg/Nm₃ range for NO_x in our country and import/logistic problems to be faced under the circumstances of our country.

Turkey is an importer of ammonia, which is a consumable in NO_x removal plants. During the operation, logistics problems are faced in addition to the procurement costs of the ammonia. Ammonia production facilities are located in Marmara and Mediterranean Regions. It will be required to transport from distances above 1000 km to the facilities located in such regions as Black Sea and Eastern Anatolia.

Figure 2 represents the total number of NO_x control equipment installed in the last 7 years. As seen in Figure 2, 25 of the 80 stacks were equipped with SNCR systems up to year 2018.

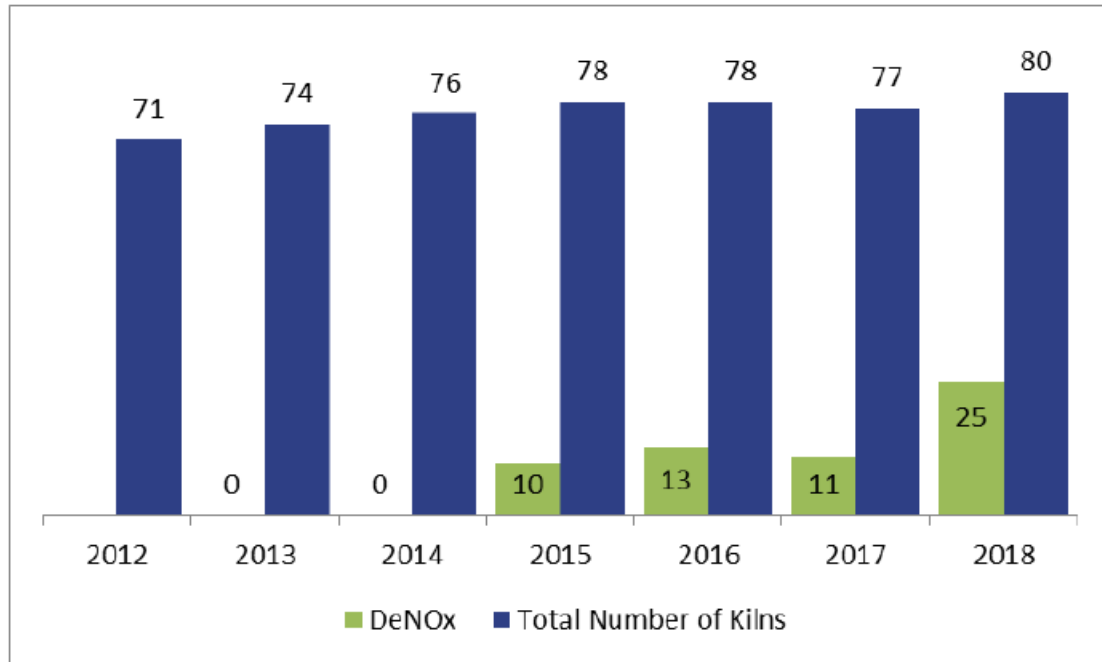


Figure 2. NO_x Control Equipment (TCMA, 2019)

5. Low Carbon Economy Pathway

Cement production comprises approximately 5-7% of the global greenhouse gas emissions. Greenhouse gas emissions due to cement production can be classified as direct and indirect emissions. Direct emissions are those controlled by the facility (emissions from decarbonisation and fuel). Indirect emissions are those, which are the result of the activities at the facility but result from other facilities (such as electric power consumption). (CSI,2011)

Turkish cement sector follows the advances regarding the international climate change conventions, which are signed by our country/to which our country is a party to limit the global warming;

- United Nations Framework Convention on Climate Change
- Kyoto Protocol
- Paris Agreement

TÇMB, Representative of the cement sector, follows the Climate Change Conferences on-site, which are organized annually within the scope of the United National Framework Convention on Climate Change and makes sectorial presentations from time to time. Advances at these conferences are shared with the members in the form of meetings and visual materials.

Turkish cement sector carries out studies/makes investments to implement the following leverages for the reduction/control of the greenhouse gases;

- To increase energy efficiency
- To use alternative fuels (especially biomass wastes)
- To reduce clinker/cement ratio (to increase the use of blended cement)
- To use new and innovative technologies (e.g. Carbon capture, storage and use)

Cement factories in our country implement greenhouse gas monitoring, reporting and verification process annually as per the legislation.

5.1 Increasing the Energy Efficiency

In cement clinker production, thermal (fuel) energy is required for chemical/mineralogical reactions of the clinker burning process and for raw material drying and preheating. The latter depends on the moisture content of the raw material. Enthalpy required for drying is higher for high moisture content raw materials. (EC-JRC, 2013)

The best available technique (BAT) for clinker production energy demand is “Dry process with multistage preheating and pre-calcination which is 2,900-3,300 MJ/tonne clinker (693-789 kcal/kg.clinker). (CIM 2013/163/EU)

Figure 3 shows the achievements in the specific heat demand of the Turkish cement sector and compares the figures with the BAT and EU average. As seen in Figure 3, specific heat demand of the Turkish cement sector decreased in the last 10 years. It is also seen that the yearly average values are lower than those of the EU-average.

Turkish cement sector increased its clinker production capacity for more than 2 times in the last 10 years. This means, new and modern dry kilns with pre-calciners were established and in the last 10 years which explains the difference between the EU-average value.

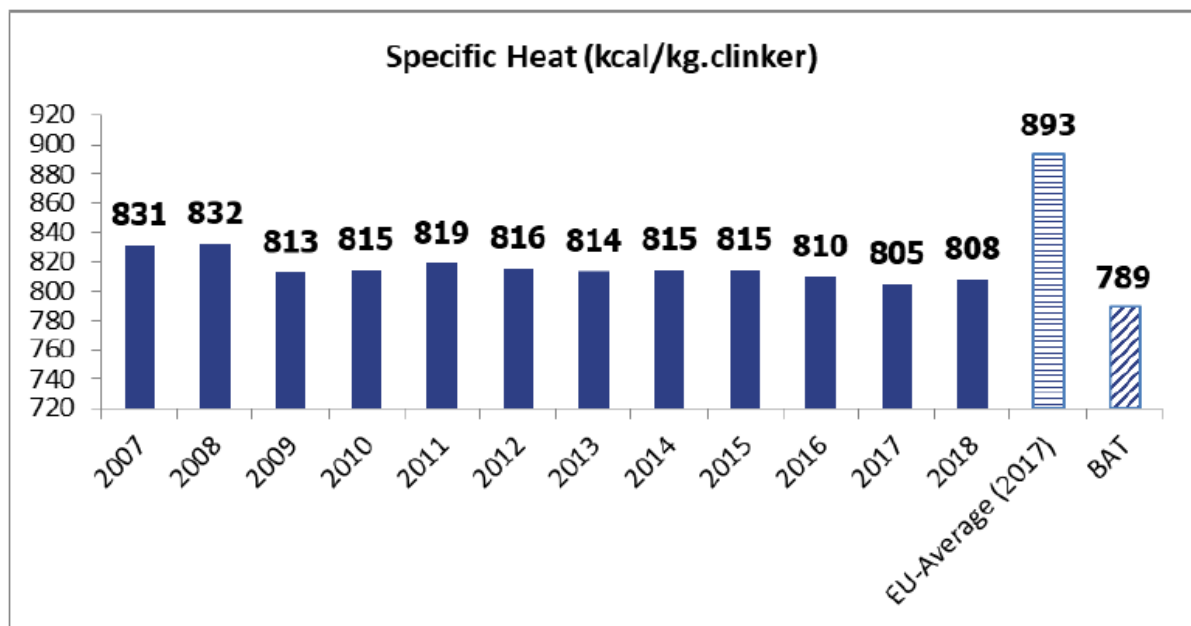


Figure 3. Achievements in the Specific Heat Consumption (TCMA,2019; MENR, 2019; GNR,2019; CIM 2013/163/EU)

In cement production, electrical energy is mostly required for the mills (finish grinding and raw grinding) and the exhaust fans (kiln/raw mill and cement mill). (EC-JRC, 2013)

Figure 4 shows the achievements in the specific power consumption of the Turkish cement sector and compares the figures with the BAT and EU average. As seen in Figure 4, specific power consumption of the Turkish cement sector decreased over the last 10 years. It is also seen that the average values are lower than those of the EU-average and even below the best available techniques. These achievements are also attributable to the modernization period of the Turkish cement sector in the last 10 years.

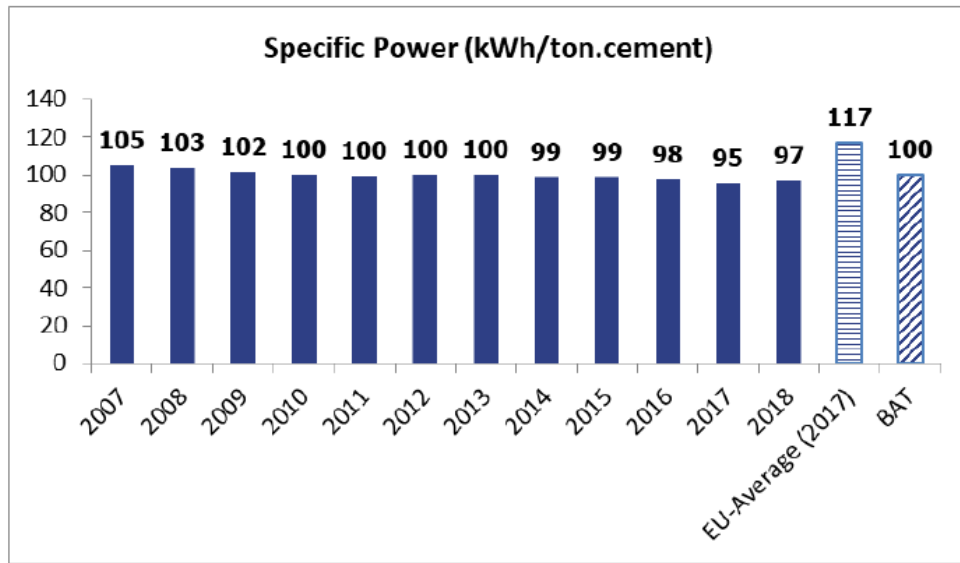


Figure 4. Achievements in the Specific Power Consumption (TCMA,2019; MENR, 2019; GNR,2019; CIM 2013/163/EU)

5.2 Increasing the Use of Alternative Fuels

Alternative fuels generally consist of industrial wastes, textile, wooden wastes, oil and petroleum wastes, pre-treated municipal solid wastes and dried municipal wastewater treatment sludge. Alternative raw materials can be grouped as mine wastes, heat-treated wastes and construction wastes.

Primary fossil fuels such as coal, petroleum coke, lignite and natural raw materials such as limestone, marn, clay are consumed less during alternative fuel and alternative raw material use. Thus, the need for the extraction of raw materials will be reduced leading to improving the environmental footprint of such activities.

Figure 5 shows the thermal substitution rate of alternative fuel and compares the values with the EU average. As seen, there are 10 fold increase in the last 10 years whereas there is much way the catch up with the EU average.

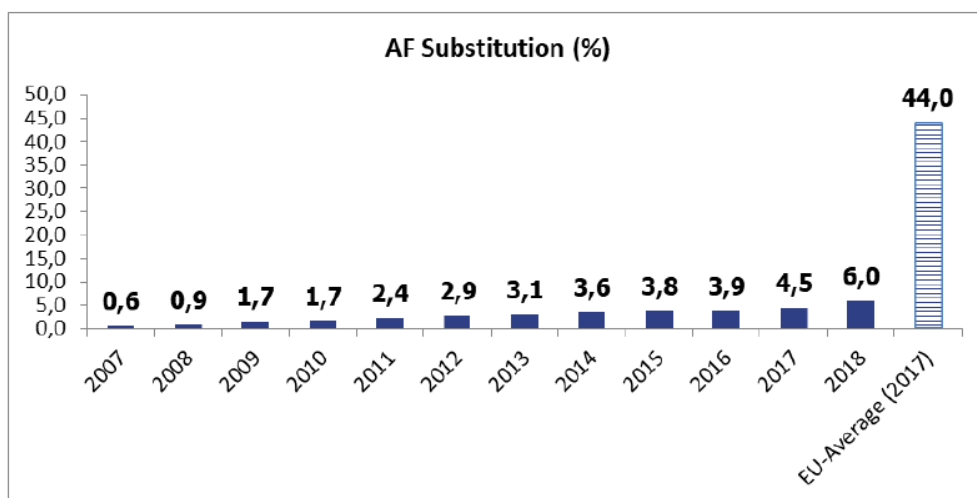


Figure 5. Alternative Fuel Substitution Rate

Using “Waste-derived fuel” produced by pre-treating municipal solid waste is a major key to increase the thermal substitution rate to that of EU average.

“Waste-derived fuel” can be produced by processing municipal solid wastes at the pre-treatment plants with biological drying systems to be installed at municipal solid waste sites. These plants can be established by the municipalities or private sector. Recoverable/recyclable materials are first sorted out. Then, organic content and non-recoverable plastic, paper, cardboard, textile are biologically dried and used as alternative fuel in the cement sector. Revenue can be generated from the sales of recoverable materials and sales of the fuel produced.

About 33 million tons/year of municipal solid waste are generated in Turkey and there is a potential to produce minimum 7 million tons alternative fuel. With the use of these alternative fuels in the cement sector;

- Saving on foreign currency can be achieved by preventing import of about 3 million tons of coal and it will be possible to decrease current deficit,
- An annual reduction of 1.7 million tons in greenhouse gases, which cause climate change, can be possible,
- The amount of waste to be transferred to the municipal landfills are reduced,
- Operating cost of the municipal storage area is reduced.

TÇMB continues dissemination activities related to energy recovery from treated municipal wastes in the cement kilns. Topics covered are technical issues and financial models as well as bottlenecks in terms of legislation and their solution opportunities.

The bottlenecks are mainly due to legislation and financial issues. As there are renewable energy incentives in Turkey, given to power production but not to process energy production (i.e. cement clinker production) from biomass waste, municipalities prefer to built and operate waste to energy plants instead of waste derived fuel plants.

5.3 Reducing clinker/cement ratio

In order to produce Portland cement, clinker is ground with additives (i.e gypsum and anhydrite). Blended cements are produced by using other constituents, such as granulated blast furnace (GBF) slag, fly ash, natural or artificial pozzolanas and limestone, or inert fillers. Grinding plants may be at separate locations from clinker production plants. (EC-JRC, 2013)

The criteria to use other constituents to produce blended cement are: availability, properties, and prices of the materials, the intended application of the cement, national standards and market acceptance.

In Turkey portland cement and blended cements are produced and certified as per the standard EN 197-1 (Cement- Part1: Composition, specification, conformity criteria for common cements).

Figure 6 shows the clinker/cement ratio of the cements in Turkey (TÇMB calculations) and compares the values with the EU average. As seen in the figure, the ratio is higher than the EU average. It is related to the barriers in Turkey.

These barriers can be summarized as below:

- Availability of granulated blast furnace (GBF) slag is limited to local steel production as import of GBF is prohibited. All GBF produced is used by the cement producers and the ready mix concrete producers.
- High portion of the GBF slag and fly ash is used by the ready mix concrete sector instead of the cement production.
- Governmental bids require use of high clinker cements and there are no alternatives for blended cements.

- Most of the plants are not close to the thermal power plants producing fly ash. Thus, transport costs of the fly ash to cement plants are not economically feasible.

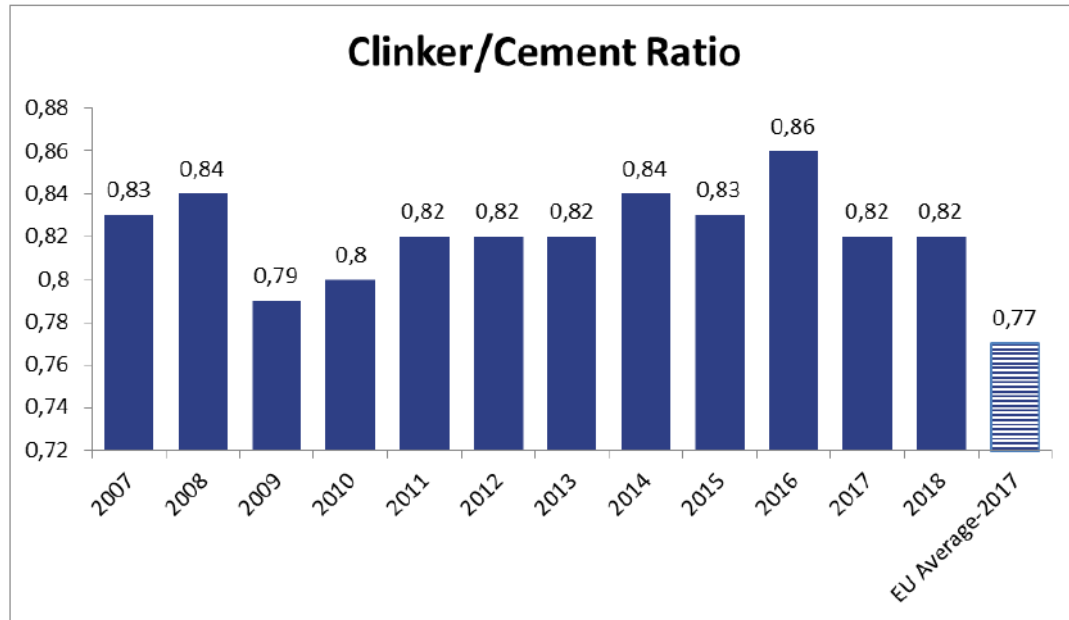


Figure 6. Clinker/Cement Ratio (TCMA, 2019)

5.4 Waste Heat Recovery

Waste heat recovery from the kiln and clinker cooler for power generation is possible in cement plants. In principle, it is applicable to all cement kilns if sufficient excess heat is available and appropriate process parameters can be met. Local conditions and cost aspects have to be considered. (EC-JRC, 2013). In Turkey, for the time being, 23 lines at 14 plants are in operation, producing 129 MW power.

5.5 Innovative Technologies

Innovative technologies in the cement manufacture to catch up low carbon pathway are new binding materials, Carbon Capture and Storage (CCS) and Carbon Capture and Use (CCU). (CEMBUREAU, 2017.)

Joint innovative projects can be summarized as below (CEMBUREAU, 2017a):

- CEMCAP- Carbon capture
- ECO-Binder- Innovative binder
- European Cement Research Academy (ECRA)- Carbon capture
- Low Emissions Intensity Lime And Cement (LEILAC) -Carbon capture
- NANOCEM- Clinker substitution, Concrete innovation

There are also company specific projects such as (CEMBUREAU, 2017a)

- Celitement- Innovative binder
- CEMEX- Carbon capture, Carbon reuse
- Cement Manufacturers Ireland (CMI)- Clinker substitution
- HeidelbergCement-Carbon reuse
- Lafarge/Aether-Clinker substitution



- LafargeHolcim & Solidia Technologies-Innovative binder
- Vereinigung der Österreichischen Zementindustrie (VÖZ)-Concrete Innovation

In Turkey, it is known that there are certain projects and TCMA will follow the details of the projects as soon as they are publicly available.

6. References

CEMBUREAU (The European Cement Association), 2017. <https://cembureau.eu/>, accessed in 2019.

CEMBUREAU (The European Cement Association), 2017 (a), Innovation in the Cement Industry.

CIM 2013/163/EU, Commission Implementing Decision of 26 March 2013 establishing the best available techniques (BAT) conclusions under Directive 2010/75/EU of the European Parliament and of the Council on industrial emissions for the production of cement, lime and magnesium oxide.

CSI (Cement Sustainability Initiative), 2011, The Cement CO₂ and Energy Protocol, 77 pages.

Directive 2010/75/EU, Directive 2010/75/EU of The European Parliament and of the Council of 24 November 2010 on industrial emissions (integrated pollution prevention and control) (Recast).

EC-JRC (European Commission Joint Research Centre), 2013, Best Available Techniques (BAT) Reference Document for the Production of Cement, Lime and Magnesium Oxide, Spain, 475 pages.

GNR, "Getting the Numbers Right" or "GCCA in NumbeRs", 2019, <https://gccassociation.org/gnr/>, accessed in 2019.

MENR, Ministry of Energy and Natural Resources, 2019, Benchmark Study for Turkish cement Sector.

Regulation 2009, Regulation for Control of Industrial Air Pollution, Turkish Air Pollution Regulation, Official Gazette of Turkey, Dated 03.07.2009, with Reference 27277.

Regulation 2010, Regulation Related to Incineration of Waste, Official Gazette of Turkey, Dated 06.10.2010 with Reference 27721

TCMA, 2019, Turkish Cement Manufacturers' Association Statistics.

Metal emissions characterization of piston engine aircraft in general aviation

Soner Ozenc Ilhan¹, Eftade O. Gaga¹, Gurkan Acikel², Duran Calisir², Mustafa Odabasi³, Akif Ari⁴, Gulzade Artun¹, Emre Can¹ and Enis T. Turgut⁵

¹Department of Environmental Engineering, Eskisehir Technical University, Eskisehir, 26555, Turkey

²Aircraft Maintenance Centre, Eskisehir Technical University, Eskisehir, 26555, Turkey

³Department of Environmental Engineering, Dokuz Eylul University, İzmir, 35390, Turkey

⁴Department of Environmental Engineering, Abant İzzet Baysal University, Bolu, 14280, Turkey

⁵Aircraft Airframe and Powerplant Department, Eskisehir Technical University, Eskisehir, 26555, Turkey

sonerozencilhan@eskisehir.edu.tr

Abstract. There have been numerous studies regarding air pollution caused by aviation activity. However, since these studies have generally focused on aircraft using jet engines, many research areas concerning the environmental impact of general aviation aircraft remain uncovered. However, there is a need to understand the emissions created by general aviation. For instance, unlike the fuel used in jet aircraft, Jet A1, AVGAS fuel contains a significant amount of lead (Pb). Therefore, to improve the current knowledge of the emissions created by general aviation, metal emissions of a typical piston-engine aircraft fuelled by AVGAS 100LL were identified.

Emission tests were carried out in 2018, during the operation of an engine under two fuel mixture ratios and six engine speeds. A total of thirty particulate matter (PM) samples were collected. All of the measurements were performed from the exhaust duct of the engine considering the on-wing principle. Samples were collected on 47mm Whatman PTFE (polytetrafluoroethylene) filters using a low volume vacuum pump. The sampling duration for each engine run was set to five minutes with a flow rate of exhaust gases flow at 20 L min⁻¹. Following the emission tests, all of the filter papers were analyzed using triple quadrupole ICP-MS (ICP-QQQ-MS) after a microwave acid digestion procedure.

The results of the analyses show Pb to be a major element, with concentrations ranging between 772 µg/m³ and 11139 µg/m³, relative to engine speed and mixture type. This is also evident from the fact that there is a significant amount of Pb as tetraethyl lead in AVGAS fuel. The relationship between other elements (e.g., Na, Al, S, Sn, In, Mg) and engine parameters were also investigated and discussed.

Keywords: Piston engine aircraft, AVGAS, Particulate matter, Lead

1. Introduction

The civil aviation sector has been growing rapidly in recent years. Every year, air traffic increases by roughly 5% (Delhaye et al., 2017; Masiol and Harrison et al., 2014). This increase of air traffic has a negative impact on regional air quality. Over the last two decades, the emissions of commercial gas turbine aircraft, in particular, have been investigated (Delhaye et al., 2017; Vander Wal et al., 2016; Yu et al., 2017; Kinsey, et al., 2011; Lobo, et al., 2015). However, there has been little focus on the emissions of piston engine aircraft used in general aviation (FOCA, 2007; Yacovitch et al., 2016; Merkisz et al., 2010). Currently, the Civil Aviation Organization (ICAO) is measuring carbon monoxide (CO), hydrocarbons (HC), nitrogen oxides (NO_x) and smoke amounts in turbojet and turbofan aircraft engines with engine outputs of more than 26.7 kN. However, this does not cover the emissions of piston engine aircraft used in general aviation.

General aviation is defined as all civil air operations, apart from scheduled and non-scheduled air transport operations (ICAO, 2009; Yu et al., 2017). It includes a host of air vehicles from motorized parachutes to private jets. Turboprop and turbofan engines aircraft, civilian helicopters and private jets are mostly operated in general aviation. However, piston engine aircraft dominate the general aviation fleet (Yu et al., 2017). In recent years, approximately 50% of the total number of general aviation aircraft is piston engine aircraft (GAMA, 2018).

Emissions of fine particulate matter (PM) from aviation activities are important because of their impact on local air quality, human health and global climate change (Kinsey et al., 2011). Due to differences in the combustion processes between piston engines and the jet engines, as well as differences in fuels used, it can be assumed that the toxic emissions of a piston engine aircraft will be greater than those of a jet engine (Merkisz et al., 2010). For this reason, particulate emissions of piston engine aircraft using AVGAS fuel with lead content are even more significant. Therefore, in this study, metal characterization of PM₁₀ emissions of piston engine aircraft was performed and emissions factors were calculated and are presented.

2. Material and method

2.1. Study area and sampling system

This study was conducted at the Aircraft Maintenance Centre on the campus of Eskisehir Technical University. The university campus is located to the north of the city of Eskisehir in Turkey. The location of the university campus is shown in Figure 1. The campus has an airport, aircraft maintenance centre and civil aviation faculty. The Faculty of Civil Aviation has a pilot training department. This pilot training department has several piston and turboprop engine training aircraft at the airport and an aircraft maintenance centre for flight training purposes. In this study, a piston-engine aircraft (SOCATA TB-20) powered by a single Lycoming IO-540-C4D5D engine was used for emission testing. The same aircraft was used throughout all of the tests cycles and sampling was carried out in the aircraft parking position. PM₁₀ samples were collected using a Zambelli 6000 Iso Plus PM sampler from the exhaust duct of the engine. The PM sampler was equipped with a PM emission probe of 5-mm-diameter PM₁₀ cyclone head and nozzle.

2.2. Experimental procedure

In this study, three different tests were conducted on three different dates. The tests were carried out on the 18 July, 24 July, and 27 July, 2018. The tests were carried out on both full rich (FR) and best power (BP) fuel mixture operations. The test cycle included six different engine speed points starting at idle (800 rpm) and ending with 2000 rpm with an interval of 250 rpm. Table 1 provides a summary of the test cycle. The pump was operated for five minutes at a constant flow rate of 20 L/min for given engine speeds. An impinger system was also included in the sampling system, according to EPA methods 5 and

17. The samples were collected on 47mm Whatman PTFE filters. After each test cycle, the filters were stored and the probe was washed with acetone. These procedures were applied for all engine speeds. When the tests were carried out with two fuel mixtures (24 and 27 July), the first test was carried out with the full rich fuel mixture, followed by the test with the best power fuel mixture. The filters were conditioned for 24 hours in a desiccator prior to and after sampling. After the sampling, the conditioned filters were weighed and mass concentrations were determined. The filters were analyzed using triple quadrupole ICP-MS (ICP-QQQ-MS) after microwave acid digestion. Nitric and hydrochloric acids were used for the acid digestion. In addition, oil and fuel samples were taken during the tests.



Figure 1. The location of the university campus

Table 1. Summary of the test cycle

Engine Speed (RPM)	Saples Date	Fuel Mixture Condition	Analyse Of ICP-MS	Calculation Of Emission Factors	Number Of Samples
800	18.07.2018	FR	✓	✓	6
1000					
1250	24.07.2018	FR+BP	✓	✓	12
1500					
1750			✓	✓	
2000	27.08.2018	FR+BP			12

2.3. Calculation of emissions factors

In this study, certain parameters, assumptions and equations are used to calculate the emission factors. These parameters, assumptions and equations are as follows:

- Pressure at cylinder inlet: MAP (display information)
- Cylinder compression ratio: 15:1 (fixed)
- Temperature at cylinder output: EGT (display information)
- Temperature at cylinder inlet: Atmospheric temperature (measured)
- Total engine volume: 8849 cc = 0.008849 m³ (constant)
- Engine speed: RPM (display information)

As a first step, the air mass in the cylinders should be measured. However, there was no equipment to measure air mass in the research group. Therefore, the ideal gas equation was used to determine the air mass (m_1 , kg) in the cylinders and the following theoretical calculation was carried out:

$$m_1 = \frac{P_1 \times V_1}{R \times T_1} \quad (1)$$

- P_1 = Cylinder inlet pressure (MAP, in Hg) (1 in Hg = 3386.39 Pa)
- V_1 = Total cylinder (x4) volume = 0.008849 m³
- R = Universal gas constant: 287 J/kg.K
- T_1 = Ambient temperature: e.g. 288 K.

As a second step RPM should be taken into account in order to find the air mass (\dot{m}_1) drawn into the engine per second or the air mass ($\dot{m}_2 = \dot{m}_1 + \text{FF}$) discharged from the exhaust in one second. Since the engine is four-cycle, each cycle is equal to two revolutions: for example, 1000 RPM is 16.67 (=1000/60) cycles per second. This is the intake of air to the cylinders 8.33 (=16.67/2) times a second or the exhaust air output from the cylinders 8.33 times a second. In this case, the amount of output exhaust air is calculated by multiplying the sum of air mass and fuel flow calculated for four cylinders by 8.33. This value represents the total output air mass from the exhaust in one second. The post-combustion pressure (P_2), the compression ratio reached $15 \times P_1$. Since the temperature (T_2) of the exhaust gas is known by the EGT parameter, the volumetric flow rate of the exhaust gas per second can be found using the following equation:

$$\dot{V}_2 = \frac{\dot{m}_2 \times R \times T_2}{15 \times P_2} \quad (2)$$

Using the calculated volumetric flow rate and actual sample volume (V_d), the mass flow rate of the PMs and only the X element for a given phase i of the flight, is calculated using the following formulas:

$$ER_i = \frac{(\dot{V}_2 \times PM_m)_i}{V_d} \quad (3)$$

$$ER_{x,i} = \frac{(\dot{V}_2 \times PM_{m,x})_i}{V_d} \quad (4)$$

Finally, using the following formulas, the emissions factor of the PMs and only the element X for a given i phase of flight is calculated:

For the element:

$$ER_{x,i} = \left(\frac{ER_x}{FF} \right)_i \quad (5)$$

For the total PM:

$$ER_i = \left(\frac{ER}{FF} \right)_i \quad (6)$$

3. Results

In this study, tests were carried out using two different fuel mixtures (Figure 2). According to the fuel flow (FF) data recorded during the tests, it can be seen that the fuel flow increased with increasing speed and that different fuel mixture conditions lines separated. However, the results for the same fuel mixture conditions at different dates compromised each other with no correlation between fuel flow and emission factor. In the full-rich mixture, the fuel consumption rate was between 7 L/h and 37 L/h, while in the best-power fuel mixture it was between 5 L/h and 25 L/h. The fuel flow data for the tests are shown in Figure 2. In addition, the results of the lubricating oil and aircraft fuel analyses are given in Table 2.

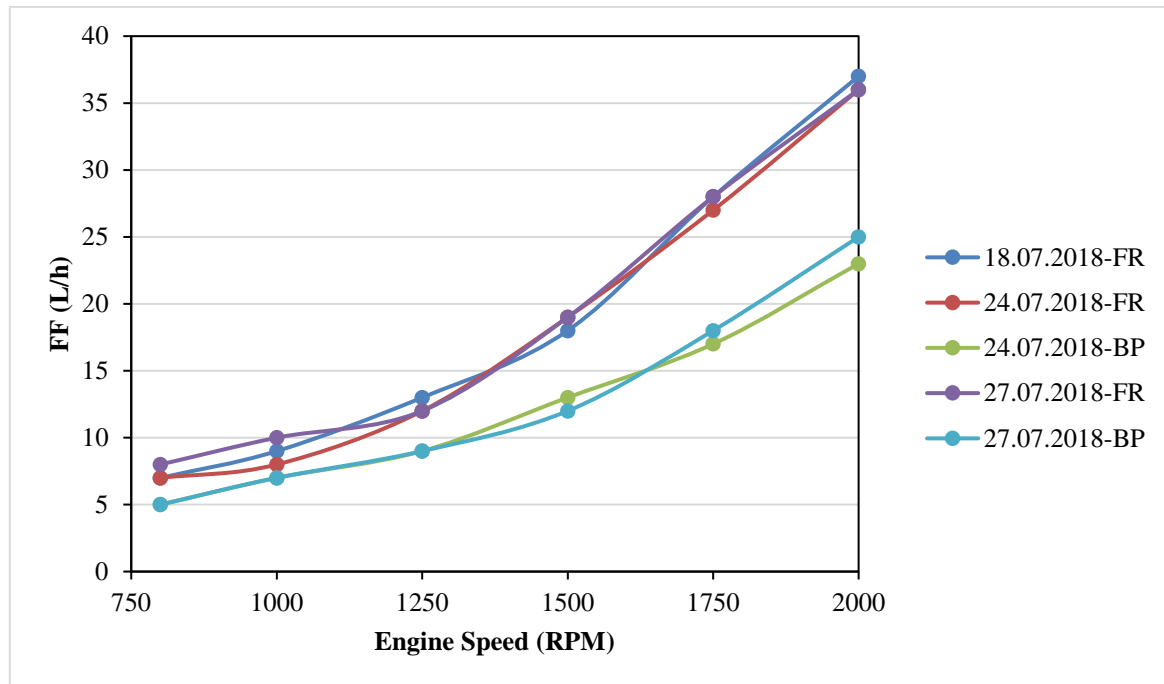


Figure 2. Fuel flow results

Table 2. Lubricating oil and aircraft fuel results

	Na ($\mu\text{g/L}$)	Mg ($\mu\text{g/L}$)	Al ($\mu\text{g/L}$)	Ca ($\mu\text{g/L}$)	Pb ($\mu\text{g/L}$)
OIL	379.2	775.2	184.9	1114.4	2049.3
FUEL	626.3	55.8	64.5	279.3	13267

The filters were conditioned for 24 hours in a desiccator and weighed after sampling and the mass concentrations were calculated by taking the difference between post and pre-weights. The results of the average mass concentration are shown in Figure 3. Mass concentrations are consistent at low engine speeds for different fuel mixtures. However, as engine speed increases, the difference between the fuel mixtures increases. The average mass concentrations for the full-rich fuel mixture were $32436 \mu\text{g/m}^3$ and $34455 \mu\text{g/m}^3$. The average mass concentrations for the best-power fuel mixture were $30248 \mu\text{g/m}^3$ and $54230 \mu\text{g/m}^3$.

Metal concentrations of the PM samples were determined and the results are given in Table 3. The average lead concentration for the full-rich fuel mixture was between $1407 \mu\text{g/m}^3$ and $5121 \mu\text{g/m}^3$. The average mass concentration for the best-power fuel mixture was between $1015 \mu\text{g/m}^3$ and $6685 \mu\text{g/m}^3$. Among other elements, magnesium has the minimum concentration ($5.18 \mu\text{g/m}^3$) with aluminum having the maximum concentration ($24.45 \mu\text{g/m}^3$).

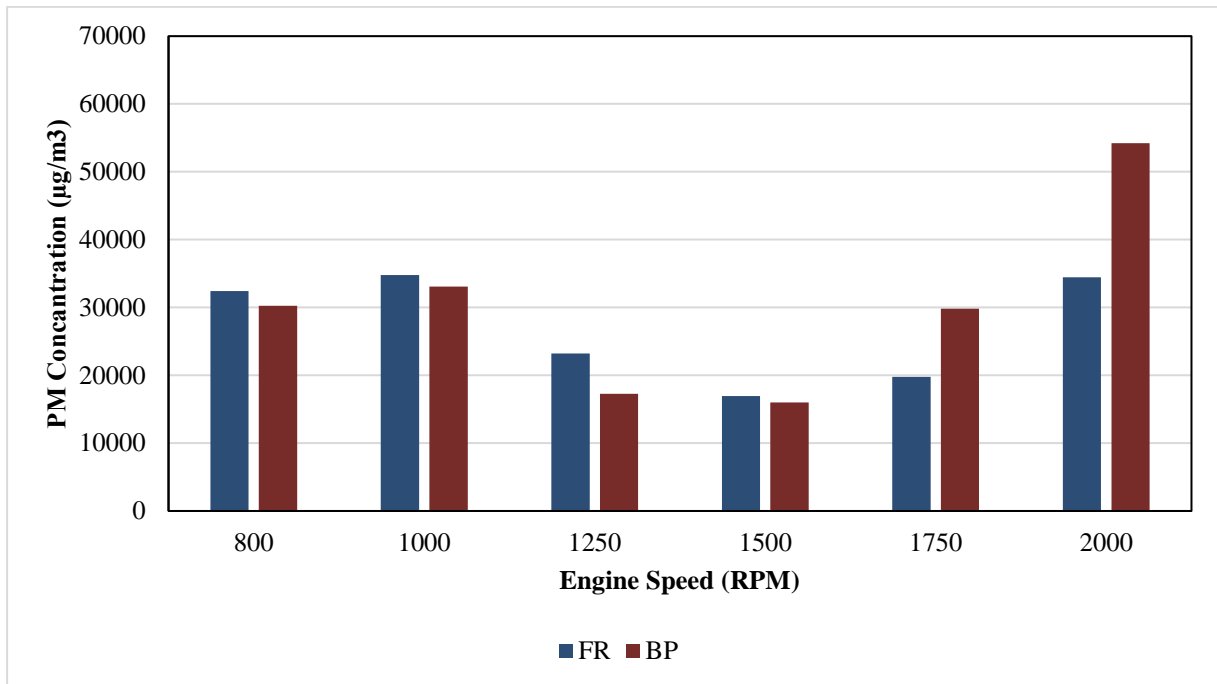


Figure 3. Average mass concentration results

Table 3. Average metal concentration results

FUEL MIXTURE	ENGINE SPEED (RPM)	Pb µg/m ³	Na µg/m ³	Mg µg/m ³	Al µg/m ³	S µg/m ³	Ca µg/m ³	In µg/m ³	Sn µg/m ³
FR	800	1472.2	62.6	8.8	35.5	54.8	29.4	12.3	13.0
	1000	2217.2	59.9	6.3	38.4	37.0	33.9	9.5	12.6
	1250	2186.9	80.8	8.9	44.0	41.3	76.2	11.8	13.3
	1500	1406.8	69.4	9.0	43.1	35.2	79.7	12.0	13.8
	1750	3668.0	65.4	6.1	42.3	15.9	52.4	11.3	13.4
	2000	5121.0	64.3	5.2	40.4	10.2	32.9	11.7	13.3
BP	800	1015.4	89.2	9.4	38.9	91.1	31.6	9.5	11.5
	1000	1664.9	75.6	10.3	224.5	14.6	82.3	11.5	13.7
	1250	2462.6	68.8	6.5	43.5	34.1	30.3	12.8	14.5
	1500	1772.1	53.2	6.4	33.9	12.7	26.5	10.5	12.1
	1750	4095.1	55.3	5.2	34.5	9.9	34.6	9.2	10.4
	2000	6684.9	55.5	5.4	43.0	35.2	25.7	10.4	11.1

Emissions factors were determined for PM mass and metal concentrations. Average mass emissions factor results are shown in Figure 4. Figure 4 shows that the mass curve of the emissions factor is U-shaped. The U-shaped curve of the mass emissions factor has been observed in previous emissions measurements of various gas turbine aircraft engines (Kinsey at al., Yu at al.). The average metal emissions factor results are given in Table 4. The highest metal emissions factor is calculated for lead (52.66 mg/kg fuel). The lowest metal emissions factor is magnesium (0.02 mg/kg fuel).

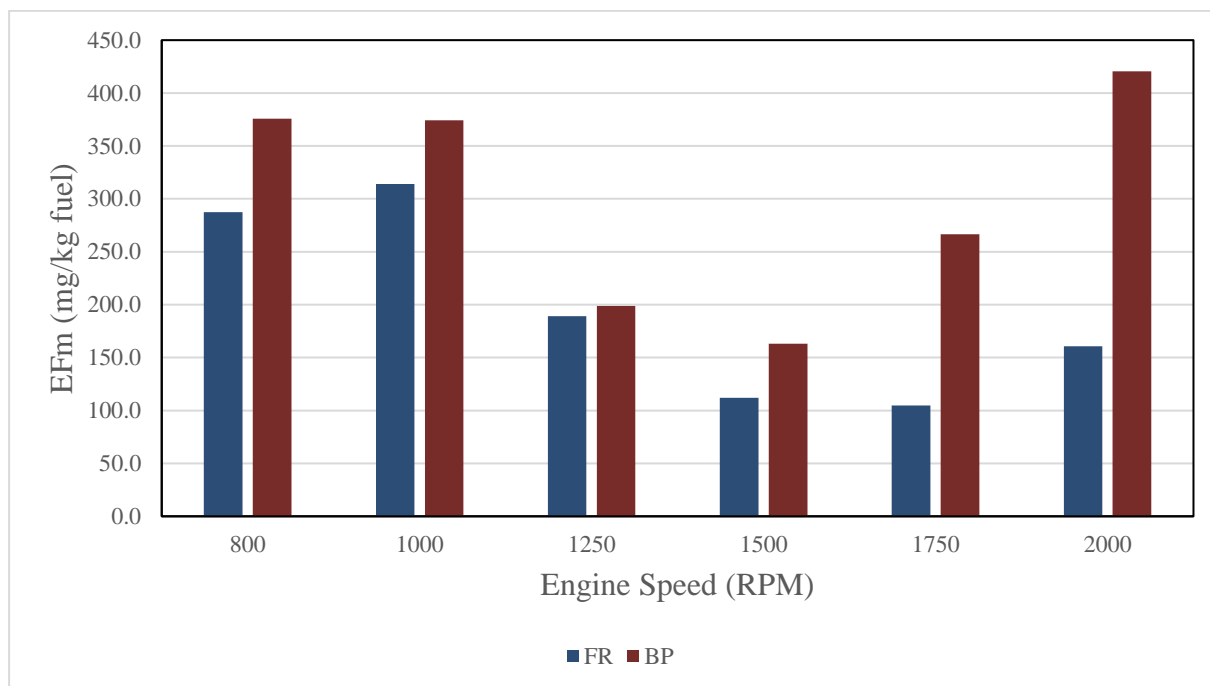


Figure 4. Average mass emissions factor results

Table 4. Average metal emissions factor results

FUEL MIXTURE	ENGINE SPEED (RPM)	Pb mg/kg Fuel	Na mg/kg Fuel	Mg mg/kg Fuel	Al mg/kg Fuel	S mg/kg Fuel	Ca mg/kg Fuel	In mg/kg Fuel	Sn mg/kg Fuel
FR	800	13.0	0.55	0.08	0.32	0.49	0.26	0.11	0.11
	1000	20.0	0.54	0.06	0.35	0.34	0.30	0.09	0.11
	1250	17.7	0.66	0.07	0.36	0.34	0.60	0.10	0.11
	1500	9.3	0.46	0.06	0.28	0.23	0.53	0.08	0.09
	1750	19.5	0.34	0.03	0.22	0.08	0.28	0.06	0.07
	2000	23.8	0.30	0.02	0.19	0.05	0.15	0.05	0.06
BP	800	12.6	1.08	0.12	0.48	1.10	0.39	0.12	0.14
	1000	19.0	0.86	0.12	2.52	0.17	0.93	0.13	0.16
	1250	28.3	0.79	0.07	0.50	0.40	0.35	0.15	0.17
	1500	17.7	0.54	0.06	0.35	0.13	0.26	0.11	0.12
	1750	36.6	0.50	0.05	0.31	0.09	0.31	0.08	0.09
	2000	52.7	0.43	0.04	0.33	0.28	0.20	0.08	0.09

4. Conclusion

Metal emissions of piston engine aircraft and emissions factors have been determined. Measurements were carried out with a TB-20 piston engine aircraft at the aircraft maintenance centre. The tests were carried out on three different days using two different fuel mixtures. The effect of fuel flow on emissions and fuel consumption were investigated. According to the fuel flow data, fuel flows increase at high engine speeds. However, no significant relationship was observed between fuel flow and emissions.

A U-shaped PM profile of mass emissions was observed with varying power, which is consistent with the literature (Kinsey et al., 2011; Yu et al., 2017). According to the metal results, lead is the major element in PM₁₀ originated from fuel composition. Other metals, such as sodium, calcium and



magnesium, arise from lubricating oil. Aluminum arises from mechanical wear (Vander Wal et al., 2016). There was no observable correlation between metal emissions and engine speed. However, the results of test performed under the best-power fuel mixture show that the metal lead was compatible with engine speed.

5. References

- Delhaye, D., Ouf, F. X., Ferry, D., Ortega, I. K., Penanhoat, O., Peillon, S., Salm, F., Vancessel, X., Focsa, C., Irimiea, C., Harivel, N., Perez, B., Quinton, E., Yon, J., Gaffie, D., 2017. The MERMOSE project: Characterization of particulate matter emissions of a commercial aircraft engine. *Journal of Aerosol Science*. 105, 48-63.
- GAMA (General Aviation Manufacturers Association), 2018. GAMA Annual Report 2018, Washington DC, 59 pages.
- Kinsey, J. S., Hays, M. D., Dong, Y., Williams, D. C., Logan, R., 2011. Chemical characterization of the fine particle emissions from commercial aircraft engines during the aircraft particle emissions experiment (APEX) 1 to 3. *Environmental Science & Technology*. 45(8), 3415-3421.
- Lobo, P., Hagen, D. E., Whitefield, P. D., Raper, D., 2015. PM emissions measurements of in-service commercial aircraft engines during the Delta-Atlanta Hartsfield Study. *Atmospheric Environment*. 104, 237-245.
- Masiol, M., Harrison, R., M., 2014. Aircraft engine exhaust emissions and other airport-related contributions to ambient air pollution: A review. *Atmospheric Environment*. 95, 409-455.
- Merkisz, J., Markowski, J., Pielecha, J., Babiak, M., 2010. Emission measurements of the AI-14RA aviation engine in stationary test and under real operating conditions of PZL-104 'Wilga' plane. *SAE International Journal of Fuels and Lubricants*. 3(2), 507-520.
- Rindlisbacher, T., 2007. Aircraft Piston Engine Emissions Summary Report. Switzerland: Federal Department of the Environment, Transport, Energy and Communications DETEC Federal Office of Civil Aviation FOCA Aviation Policy and Strategy Environmental Affairs.
- Vander Wal, R. L., B, Bryg, V., M., Huang, C. H., 2016. Chemistry characterization of jet aircraft engine particulate matter by XPS: Results from APEX III. *Atmospheric Environment*. 140, 623-629.
- Yacovitch, T. I., Yu, Z., Herndon, S. C., Miake-Lye, R., Liscinsky, D., Knighton, W. B., Kenney, M., Schoonard, C., and Pringle, P., 2016. *Exhaust Emissions from In-Use General Aviation Aircraft*, National Academies Press, Washington, D.C.
- Yu, Z., Liscinsky, D. S., Fortner, E. C., Yacovitch, T. I., Croteau, P., Herndon, S. C., Miake-Lye, R. C., 2017. Evaluation of PM emissions from two in-service gas turbine general aviation aircraft engines. *Atmospheric environment*. 160, 9-18.

Acknowledgments

This study was supported by the Scientific and Technological Research Council of Turkey (project number 115Y611).

Spatial and temporal variation of AERONET aerosol optical depth over Turkey and its surrounding

Esra Ozdemir, Gizem Tuna Tuygun, Fehmican Unsalan and Tolga Elbir

Dokuz Eylul University, Department of Environmental Engineering,
Tinaztepe Campus, Buca 35390, Izmir, Turkey

esraozdmrr@hotmail.com

Abstract. Aerosol Optical Depth (AOD) is defined as the measurement of light extinction by aerosol in the atmospheric column above the surface of earth and utilized to depict aerosol optical properties. The AERONET is a network of ground-based sun photometers, providing globally distributed observations of spectral AOD in the range of 0.34–1.06 μm , with a high temporal resolution (~ 15 min). This study aims to determine the spatial and temporal distribution of the selected aerosol parameters: the total aerosol optical depth (AOD_t) provided at a wavelength of 500 nm and Angstrom Exponent (AE) obtained from the AOD measured at 440 and 870 nm since the combined use of the AOD and AE allows to distinguish between different aerosol types. Daily average AERONET V3 Level 2.0, cloud-screened and quality assured AOD data at 10 sites in the Eastern Europe: Turkey, Ukraine, Romania, Bulgaria, Greece and Southern Cyprus were used for analysis. The seasonal variation of AOD in the region showed that the maximum AOD values occurred in spring and summer since hygroscopic growth at high relative humidity increases AOD, while low values were observed in winter that were characterized by precipitation. Significant monthly fluctuations of AOD and AE were found at all sites. The large particles (sea spray and dust) were dominant for $\text{AE} < 0.7$, while small particles (mainly smoke and urban aerosols) were dominant for $\text{AE} > 1.5$. Between these two thresholds, the aerosol is a mixture of fine and coarse fractions. The values of AOD (500 nm) higher than 0.3 and AE (440–870 nm) values lower than 0.7 refer to long-range transport of desert dust. Annual average AOD ranged from 0.18 to 0.27 over the region. At rural sites located in Turkey (IMS-METU-Erdemli) and Greece (Xanthi), this value was found relatively higher. The low average $\text{AE}_{440-870}$ value (< 0.7) and high AOD values (> 0.30) at these sites confirmed the major influence of large dust particles in spring months. It was also found that Forth-Crete (Greece) site was significantly affected by large dust particles. Correlation between AOD and AE at this site showed that consecutive peaks resulted from the great number of desert dust events. On the other hand, the AOD at urban sites was dominated by fine mode particles. The Angstrom Exponent ($\text{AE}_{444-870}$) above 1.5 was observed in urban sites such as Athens-NOA, Thessaloniki, and Sevastopol.

Keywords: Aerosol optical depth (AOD), AERONET, Angstrom exponent, Turkey.

1. Introduction

Aerosols or airborne particulate matters from both natural and anthropogenic emission sources have substantial influences on climate, environment and human health (You et al., 2016). Increased concentrations of atmospheric aerosols, especially those originated from biomass burning, fossil-fuel combustion, industrial emissions, etc. have become the main climate issue over the world (Bellouin, 2015; Zhang et al., 2016; Banerjee et al., 2018; Rupakheti et al., 2019).

Aerosols interact both directly and indirectly with the Earth's radiation budget and climate (NASA, 2017). As a direct effect, the aerosols absorb and/or scatter sunlight directly back into space. As an

indirect effect, aerosols in the lower atmosphere can modify the size of cloud particles, changing how the clouds reflect and absorb sunlight, thereby affecting the Earth's energy budget (NASA, 2017). Due to their various sources, high spatio-temporal variability and complex optical properties, aerosols remain as one of the largest uncertainties in the Earth's climate system. Therefore, aerosol properties are crucial aspects to be investigated in order to understand their influence on radiation budget, climate, air quality, ecosystems and human health (Kloog et al., 2015). As a result, the global impact of aerosols on the Earth's climate is difficult to quantify because there are no comprehensive and reliable measurements in most parts of the world (Hansen et al., 1997; Tripathi et al., 2005; Kaskaoutis et al., 2007; Kaskaoutis and Kambezidis, 2008; Russell et al., 2010).

In order to determine the absorption and scattering quantities, a parameter called Aerosol Optical Depth (AOD) is continuously monitored in the atmosphere with the help of satellites from space and special equipment from ground level. AOD is a dimensionless parameter that indicates the degree to which radiation transmission is inhibited by the absorption or scattering of sunlight through aerosols in the atmosphere. In other words, AOD is briefly defined as the reduction of electromagnetic energy at a specific wavelength due to aerosols in the atmosphere (Ghotbi et al., 2016).

There are many studies in literature on aerosol classification (Kaskaoutis and Kambezidis, 2006; Toledano et al., 2007; Zhao et al., 2013; Mallet et al., 2013; Tan et al., 2015; Tutsak and Kocak, 2019). These studies show that the aerosol optical depth and particle sizes differ temporally and spatially. Temporal and spatial changes cause aerosols to have different properties. The main reasons for this difference are the presence of pollutant sources emitting dust to the atmosphere, cloud density in the atmosphere, albedo, and other meteorological and topographical factors. Mallet et al. (2013) showed that aerosols can be transported from local sources (from urban industry) and from long-range sources such as desert dust. Tan et al. (2015) investigated aerosol characteristics over two regions under different environmental conditions in terms of different aerosol sources. They found that distribution of dominant aerosol types were completely different at different geographical locations. Tutsak and Kocak (2019) had a work in Mersin-Erdemli site between the years of 2000 and 2014. This study showed that elevated AOD values with low $AE_{440-870}$ were observed in spring owing to sporadic mineral dust transport from the North Africa and the Middle East. High AOD at 440 nm and $AE_{440-870}$ were characterized in summer because of high gas-to-particle conversion, sluggish air masses and absence of rain. In another study conducted in Spain, AOD value was found to be higher in summer (Toledano et al., 2007).

The aim of this study is to investigate the spatial and temporal variation of aerosol optical depth (AOD) and Angstrom Exponent (AE) measured by sun photometers at AERONET stations in Turkey and its surrounding. Aerosol types were classified using AOD and AE thresholds. Four classes of aerosol were identified namely maritime, desert dust, biomass burning and mixed-type. Dusty days were clearly determined over the region. Finally, particle volume size distribution (PVSD) data for dusty days was also examined for the sites which are mostly affected by dust transport.

2. Material and method

The AERONET (Aerosol RObotic NETwork) program is a federation of ground-based remote sensing aerosol networks established by NASA and LOA-PHOTONS (CNRS), and is greatly expanded by collaborators from national agencies, institutes, universities, individual scientists, and partners. The program provides a long-term, continuous and readily accessible public domain database of aerosol optical, micro-physical and radiative properties for aerosol research and characterization, validation of satellite retrievals, and synergism with other databases (AERONET, 2019). The network imposes standardization of instruments, calibration, processing and distribution. It performs AOD measurement with the help of sun photometers and takes measurements and records every 15 minutes at 340, 380, 440, 500, 675, 870, 940 and 1020 nm (AERONET, 2019). Except for 940 nm (used for retrieving WV), these measurements are then applied to calculate AOD, with an accuracy of ~ 0.01 for the wavelengths

longer than 440 nm and ~ 0.02 for shorter wavelengths (Eck et al., 1999). The Angstrom Exponent ($AE_{440-870}$) is defined by the logarithms of AOD and wavelength (see Equation (1)) and it is calculated for the all wavelengths varying from 440 to 870 nm employing a lean fit between AOD and wavelength (λ) (Holben et al., 1991; Holben et al., 2001). The value approaching zero denotes dominance of coarse particles whereas; the value larger than 1 implies the dominance of fine aerosol (Kaufman et al., 1994; Eck et al., 1999).

$$AE = -d \ln[AOD(\lambda)]/d \ln(\lambda) \quad (1)$$

The instrument also performs hourly sky radiance measurements in almucantar geometry at 440, 675, 870 and 1020 nm. These sky radiance measurements in conjunction with corresponding direct sun measurements are then used in inversion algorithms to derive particle volume size distribution (PVSD) (Dubovik and King, 2000; Dubovik et al., 2006). The retrieval error in PVSD is estimated to vary from 15% to 35% for the intermediate particle volume size range ($0.1 \leq r \leq 0.7 \mu\text{m}$). However, the error in PVSD for small ($0.05 \leq r \leq 0.1 \mu\text{m}$) and large ($7 \leq r \leq 15 \mu\text{m}$) particle volume size interval may reach up to 80%.

Six AERONET sites are available in Turkey. The main site of the country, IMS-METU-ERDEMLI is located at a southern coastal site. IMS-METU-ERDEMLI has been continuously operated between 2004 and 2017. The other five national sites (Tubitak_Uzay-Ankara, Haymana-Ankara, Tuz_Golu, Tuz Golu-2, Tuz Golu-3) have been used within the scope of several specific researches for short time periods. One of them, Tubitak-Uzay site has more data compared to other stations and has been operated only for 2009-2012. In this study, due to the insufficient number of AERONET sites in Turkey, the other sites from neighbouring countries are also considered to determine aerosol types in and around Turkey.

Daily averaged aerosol optical and microphysical properties (Level 2.0, Version 3 AERONET) have been obtained for all sites in this study. The missing values were not only resulted from quality control procedure but also occurred due to technical malfunction of the sun photometer instruments. However, particle volume size distribution was examined at Mersin-Erdemli and Forth-Crete sites for dusty days.

The data in Turkish sites were obtained on daily basis from the web site of <https://aeronet.gsfc.nasa.gov/>. Several sites from the neighbouring countries of Turkey such as Athens-NOA (Greece), Bucharest (Romania), Cut-Tepak (Cyprus), Eforie (Romania), Forth-Crete (Greece), Sevastopol (Ukraine), Thessaloniki (Greece) and Xanthi (Greece) were also used in this study. Figure 1 shows the geographical locations of the selected sites. The coordinates of sites, period of data, number of days and site characteristics are also reported in Table 1.

The temporal and spatial variations of AOD and AE data in AERONET sites were studied. Statistical analysis and graphical plots were performed with R programming language.

In this study, aerosol types were also classified in terms of AOD_{500} and $AE_{440-870}$ values proposed by Smirnov et al. (2002, 2003). Smirnov et al. (2002, 2003) suggested that maritime aerosol should have a threshold of $AOD < 0.15$ and $AE < 1.0$, biomass burning aerosols are located at threshold of $AOD > 0.4$ associated with $AE > 1.5$, and $AOD > 0.3$ with $AE < 0.7$ is indicative of dust particles. The threshold of AOD and AE that does not belong to any of the above groups are characterized as mixed-type aerosols. Also, dusty days were clearly detected by the sun photometers over the study region and particle volume size distribution (PVSD) data for dusty days were examined for the sites that were mostly affected by dust transport.



Figure 1. Location of the AERONET sites

Table 1. Brief information of the sites used in this study.

	Latitude (N°)	Longitude (E°)	Period	Number of Days	Site Characteristics
Athens-NOA	37.972	23.718	2008-2018	1502	Urban
Bucharest	44.450	26.525	2007-2016	1323	Urban
Cut-Tepak	34.674	33.042	2010-2017	929	Urban
Eforie	44.075	28.632	2009-2018	1193	Urban Coastal
Forth-Crete	35.332	25.282	2003-2017	2751	Coastal
Mersin-Erdemli	36.565	34.255	2004-2017	2600	Rural
Sevastopol	44.615	33.517	2006-2013	1736	Urban Coastal
Thessaloniki	40.630	22.960	2005-2017	2064	Urban Coastal
Tubitak-Uzay	39.891	32.778	2009-2012	467	Urban
Xanthi	41.146	24.918	2008-2015	714	Rural

3. Results

3.1. The spatial and temporal variations of AOD and AE

Tables 2 and 3 illustrate statistical summary of AOD and AE at ten AERONET sites. The mean AOD₅₀₀ value ranged from 0.18 to 0.27 at all stations. The highest AOD value was obtained as 1.63 in Mersin-Erdemli during spring. The lowest AOD value was obtained as 0.015 in Sevastopol during winter. The increase in AOD values in summer and spring, and decrease in winter and autumn were observed due to meteorology. The mean AE₄₄₀₋₈₇₀ value ranged from 1.12 to 1.55 at all stations. The lowest AE value was measured 0.038 in Forth-Crete during spring. Forth-Crete site was significantly affected by large dust particles.

Table 2. Statistics of AOD for ten sites

Sites	Mean	STD	Min	Max	Median
Athens-NOA	0.191	0.103	0.024	0.737	0.171
Bucharest	0.249	0.140	0.038	1.070	0.226
Cut-Tepak	0.186	0.109	0.035	0.986	0.157
Eforie	0.194	0.104	0.032	1.141	0.175
Forth-Crete	0.188	0.104	0.028	0.950	0.167
Mersin-Erdemli	0.261	0.151	0.023	1.631	0.227
Sevastopol	0.194	0.102	0.015	0.773	0.177
Thessaloniki	0.234	0.141	0.016	1.061	0.207
Tubitak-Uzay	0.203	0.092	0.042	0.846	0.192
Xanthi	0.274	0.144	0.029	1.348	0.256

Table 3. Statistics of AE for ten sites

Sites	Mean	STD	Min	Max	Median
Athens-NOA	1.352	0.454	0.043	2.671	1.444
Bucharest	1.517	0.323	0.047	2.315	1.591
Cut-Tepak	1.162	0.432	0.084	2.031	1.254
Eforie	1.444	0.314	0.166	1.983	1.507
Forth-Crete	1.117	0.486	0.038	2.735	1.189
Mersin-Erdemli	1.248	0.343	0.069	2.176	1.316
Sevastopol	1.450	0.331	0.067	2.324	1.507
Thessaloniki	1.548	0.336	0.132	2.631	1.611
Tubitak-Uzay	1.373	0.359	0.138	2.176	1.470
Xanthi	1.410	0.341	0.152	2.061	1.460

Figures 2 and 3 show the seasonal variations of the AOD and AE at ten sites. Figure 2 shows that the seasonal AOD averages in Mersin-Erdemli site are higher than other nine sites with the maximum AOD at 500 nm of 0.36 in summer and the minimum of 0.17 in winter. The seasonal average of AOD in Forth-Crete is the lowest with the maximum AOD₅₀₀ of 0.2 in summer and the minimum of 0.13 in winter.

The seasonal variation of AOD in the region showed that the maximum AOD values occurred in summer since hygroscopic growth at high relative humidity increases AOD, while low values were observed in winter that were characterized by precipitation. It was found that AOD increased in winter at Bucharest and Tubitak-Uzay sites, since the coal burning in residential areas were available in winter. The autumn had also a lower AOD value than other seasons. Cold weather, strong winds and high pressure may cause this situation.

Figure 3 shows the seasonal variations of AE at ten sites. The largest AE was observed at Thessaloniki site followed by Bucharest and Sevastopol sites. Since these sites are located in city centres, the AE value was higher. The presence of anthropogenic sources caused small particles to increase. The AE at Forth-Crete was the lowest. Generally, the AE at ten sites was higher in summer and lower in spring. The seasonal variations of AOD could most likely be related to weather patterns.

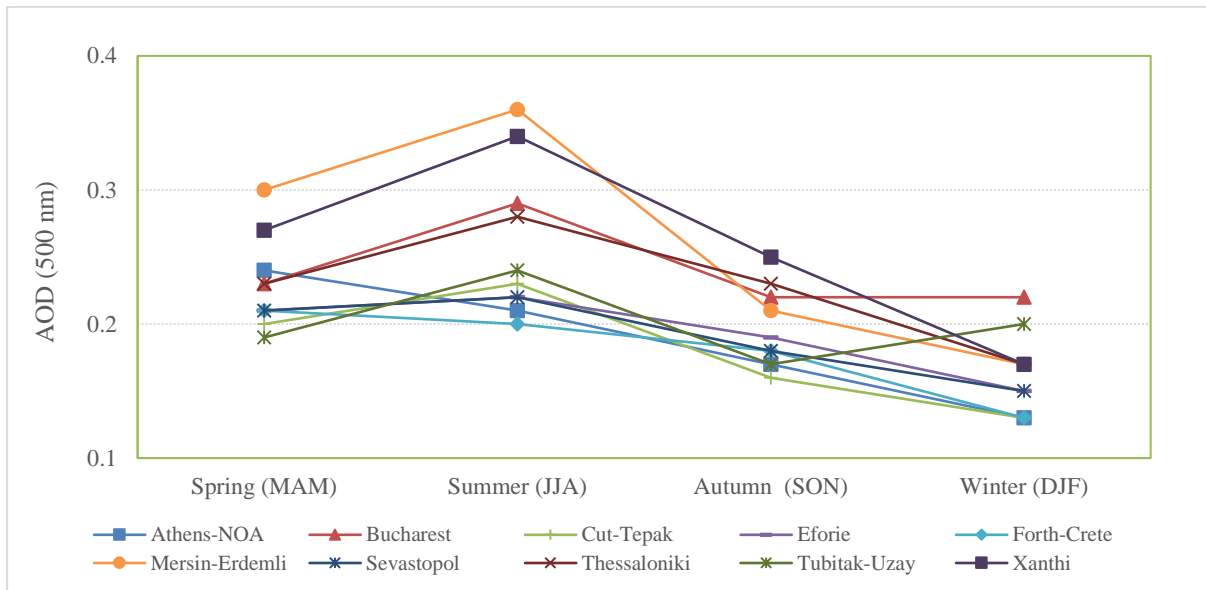


Figure 2. Seasonal variations of AOD₅₀₀ at ten sites

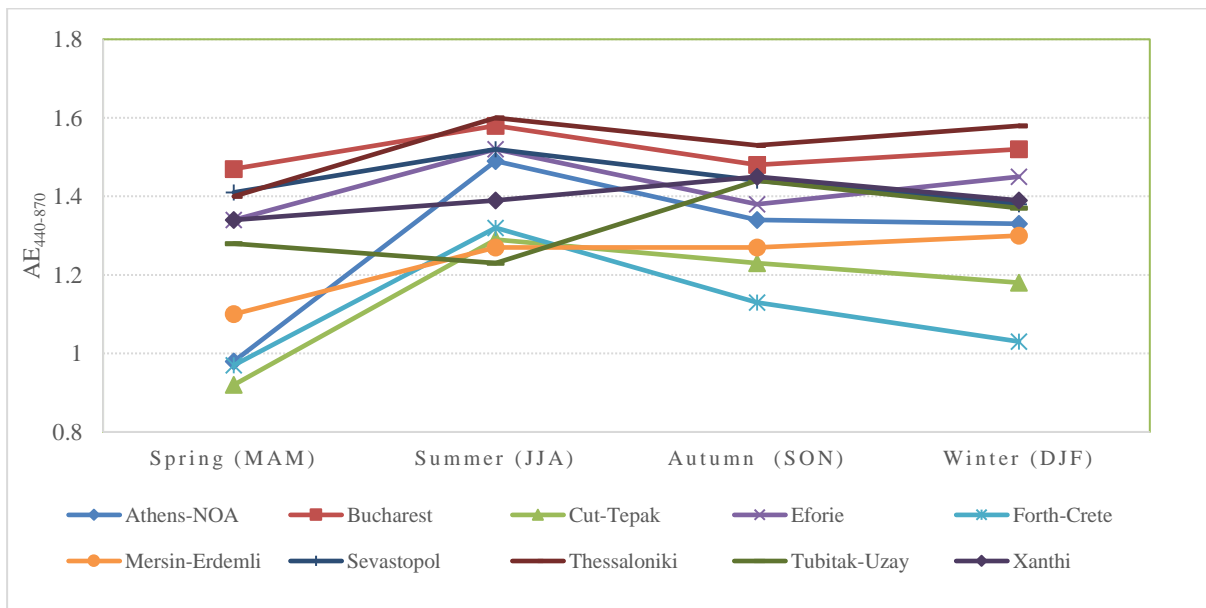


Figure 3. Seasonal variations of AE₄₄₀₋₈₇₀ at ten sites

3.2. Aerosol characterization

Aerosols were classified into four categories; i.e., maritime aerosol, biomass burning aerosol, desert dust aerosol and mixed-type aerosol. Mixed-type aerosol was found to be the most dominant aerosol type in the region. Apart from mixed-type aerosol, other aerosol types differed at each site due to local characteristics. Maritime aerosol was the highest contributing category at the sites of Forth-Crete (17%) and Cut-Tepak (13%), while the lowest contributing sites were Bucharest (1.1%) and Thessaloniki (1.4%). Maritime aerosols were higher at the coastal sites such as Forth-Crete and Cut-Tepak as expected. Biomass burning aerosols were highest at the sites of Thessaloniki (7.5%), Xanthi (7.4%) and Bucharest (6.4%), and lowest at Cut-Tepak (0.1%). Desert dust aerosol was found as the most contributing category at the sites of Cut-Tepak (6.2%), Forth-Crete (6.2%) and Mersin-Erdemli (5%) since these sites are close to the African region. Aerosol categories at all sites are shown in Figure 4.

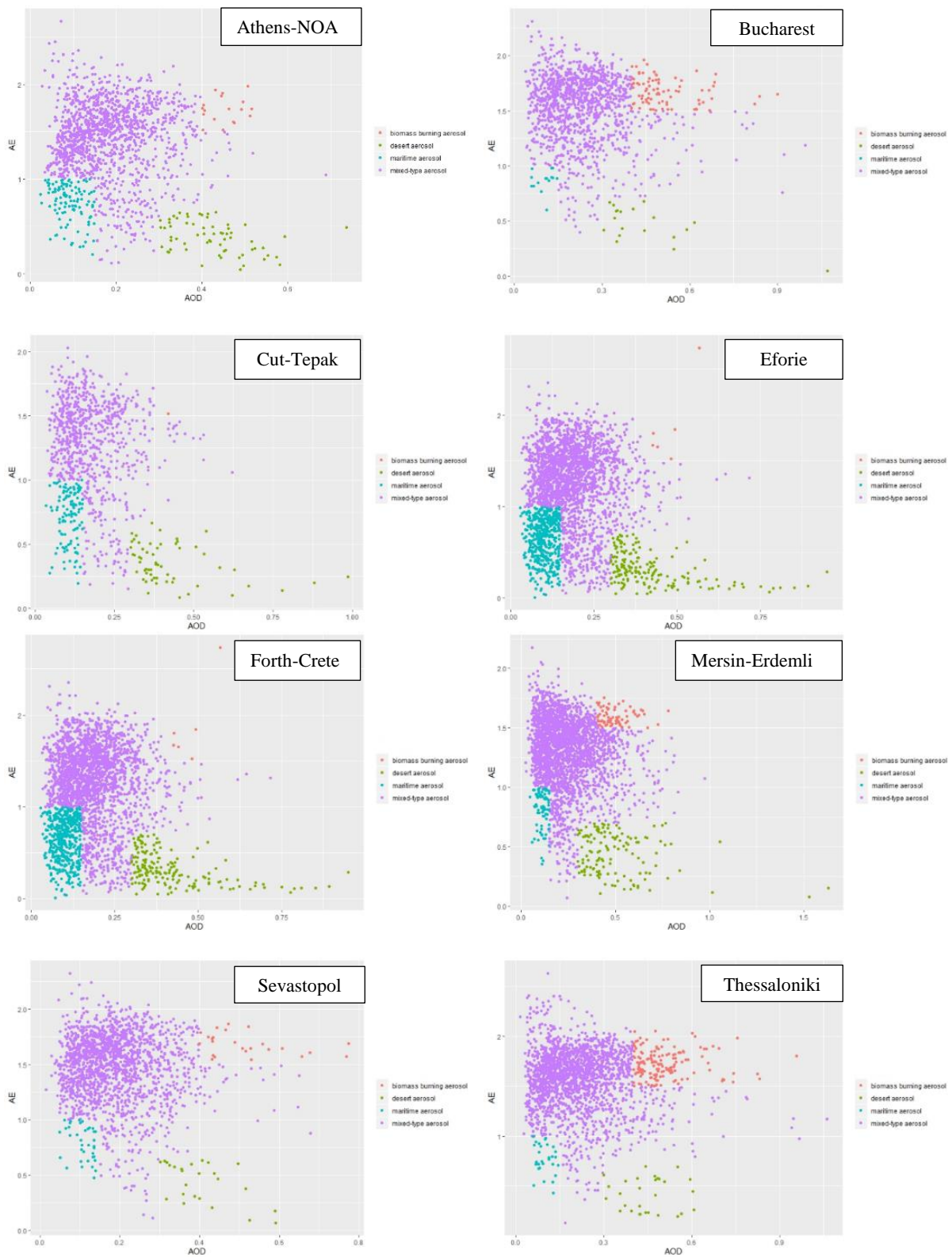


Figure 4. Scatter-plots of AOD at 500 nm vs. AE at 440-870 nm at ten sites

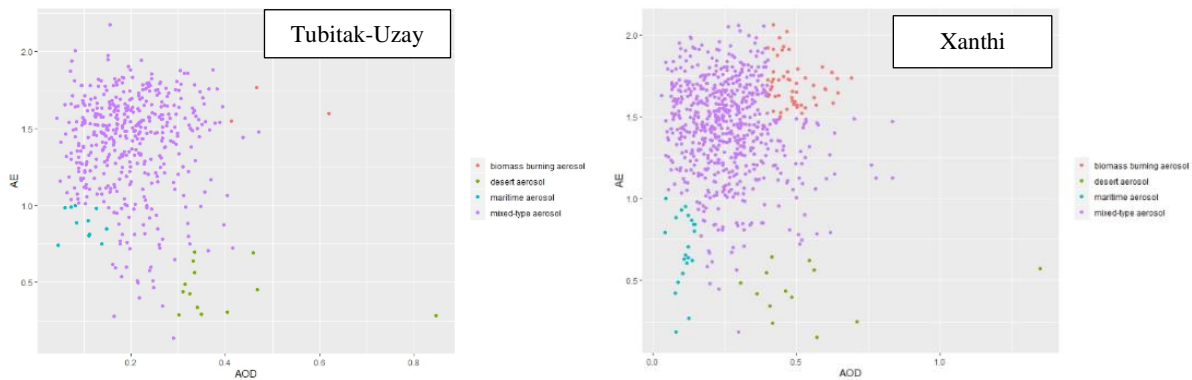


Figure 4. Scatter-plots of AOD at 500 nm vs. AE at 440-870 nm at ten sites (continue)

3.3. Influence of dust

In order to determine significant contribution of the dust particles to the total AOD, the dust particle was identified when the AOD is above 0.3 and AE is below 0.7. The results indicated that the number of dusty days varied significantly depending on the site. Number of dusty days and their mean AOD and AE values are given in Table 4.

Forth-Crete and Mersin-Erdemli sites had the highest number of dusty days. It represents 6% and 5% of the total number of observations in Forth-Crete and Mersin-Erdemli, respectively. These sites are effected by mineral dust from the Sahara and Middle East Deserts due to their locations that can explain higher dusty days than the other sites. On the other hand, Eforie, Tubitak-Uzay and Xanthi sites had the least dusty days because these sites are geographically far from desert dust transport. Dusty days occurred mainly in spring and summer due to meteorological conditions.

Table 4. Number of dusty days in sites

Aeronet Site	Dusty Days	Mean AOD	Mean AE
Athens-NOA	64	0.42	0.39
Bucharest	19	0.45	0.47
Cut-Tepak	58	0.43	0.35
Eforie	13	0.41	0.37
Forth-Crete	171	0.42	0.32
Mersin-Erdemli	129	0.5	0.44
Sevastopol	25	0.41	0.43
Thessaloniki	29	0.45	0.42
Tubitak-Uzay	13	0.4	0.45
Xanthi	13	0.54	0.44

Figure 6 shows corresponding average aerosol volume size concentration during dusty days for Forth-Crete and Mersin-Erdemli which were found most dusty stations over the region. Firstly dusty days and daily particle volume size distribution were paired. As a result of the pairing, particle size distribution was obtained for 77 and 60 days at Forth-Crete and Mersin-Erdemli stations, respectively.

The maximum of the volume size distribution was observed for a radius of 2.24 μm with a value of 0.14 $\mu\text{m}^3/\mu\text{m}^2$ for the Forth-Crete, for a radius of 1.7 μm with a value of 0.15 $\mu\text{m}^3/\mu\text{m}^2$ for the Mersin-Erdemli. In short, aerosol radius was between 1 and 10 μm . This represented coarse particles.

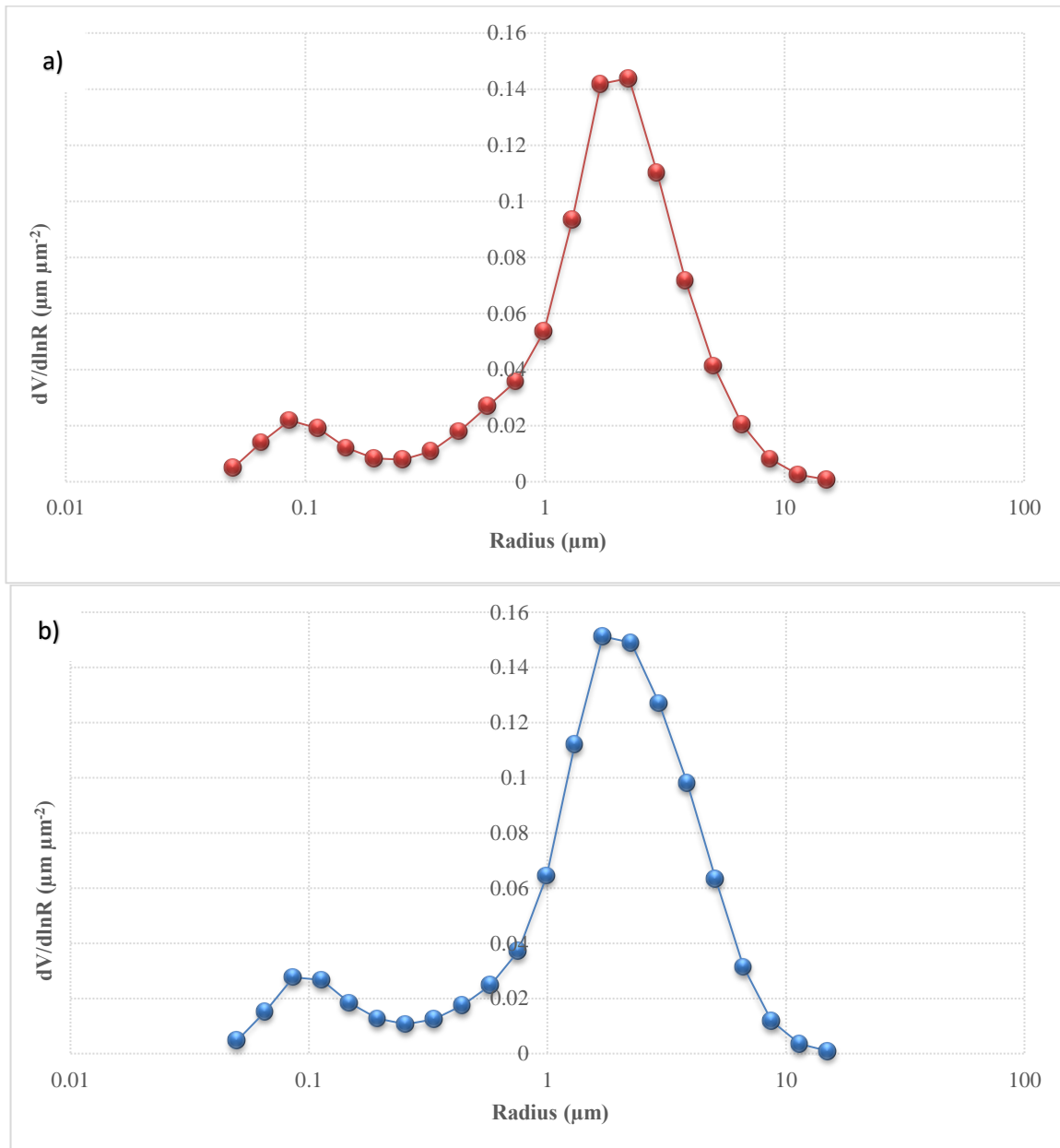


Figure 6. Average volume size distributions at a) Forth-Crete, b) Mersin-Erdemli for dusty days

4. Conclusions

A multi-year climatology of aerosol optical properties obtained from ten AERONET sites located in Turkey and its surrounding was presented in this study. In general, high AOD at 500 nm was principally characterized in summer due to high gas-to particle conversion, sluggish air masses and absence of rain. The lowest AOD values were mainly found in winter during rain or just the day after rain since wet deposition removes aerosol particles from atmosphere efficiently. The seasonality of the aerosol optical

and physical properties was remarkably modified by water vapour, temperature and rain events. The AE at the ten stations were higher in summer and lower in spring.

In general, it was found that main aerosol type is mixed with aerosols from long-range transport or aerosols from local sources over the study area. Apart from mixed-type aerosol, other aerosol types differed at the sites due to their different geographical characteristics. Forth-Crete and Mersin-Erdemli sites were mostly affected by desert dust. The desert-dust outbreaks reaching these stations, that are more frequent during the spring and summer months, have a clear influence on the seasonal pattern of the AOD and had an occurrence around 5% and 4% at Forth-Crete and Mersin-Erdemli sites, respectively. The volume size distributions for dusty days clearly demonstrate that variations in the size distributions over these two sites were mainly due to changes in the concentration of the coarse aerosol fraction. Aerosol radius was determined between 1 and 10 μm for both sites. This reveals the major influence of large dust particles.

The mean AOD and AE during dusty days were ranging 0.40 to 0.54 and 0.32 to 0.47, respectively. The mean AOD during dusty days was mainly ranging between 0.40 and 0.45, while it was found 0.50 and 0.54 at Mersin-Erdemli and Xanthi sites. The low Angstrom Exponent ($AE_{440-870}$) indicates an atmospheric situation corresponding to the dust controlled by a coarse particles.

5. References

- AERONET (Aerosol Robotic Network), 2019. AERONET web sites, <https://aeronet.gsfc.nasa.gov/>, access: August 2019.
- Banerjee, T., Kumar, M., Singh, N., 2018. Aerosol, Climate, and Sustainability. Reference Module in Earth Systems and Environmental Sciences. 2, 419-428.
- Bellouin, N., 2015. AEROSOLS | Role in Climate Change. Reference Module in Earth Systems and Environmental Sciences. 2015, 76-85.
- Dubovik, O., King, M.D., 2000. A flexible inversion algorithm for retrieval of aerosol optical properties from Sun and sky radiance measurements. *J. Geophys. Res.* 105, 20673–20696.
- Dubovik, O., Sinyuk, A., Lapyonok, T., Holben, B.N., Mishchenko, M., Yang, P., Eck, T.F., Volten, H., Muñoz, O., Veihelmann, B., van der Zande, W.J., Leon, J.F., Sorokin, M., Slutsker, I., 2006. Application of spheroid models to account for aerosol particle nonsphericity in remote sensing of desert dust. *J. Geophys. Res.* 111, D11208.
- Eck, T.F., Holben, B.N., Reid, J.S., Dubovik, O., Smirnov, A., O'Neill, N.T., Slutsker, I., Kinne, S., 1999. Wavelength dependence of the optical depth of biomass burning, urban and desert dust aerosols. *J. Geophys. Res.* 104, 31333–31350.
- Ghotbi, S., Sotoudeheian, S., Arhami, M., 2016. Estimating urban ground-level PM10 using MODIS 3km AOD product and meteorological parameters from WRF model. *Atmos. Environ.* 141, 333–346.
- Hansen, J., Sato, M., Ruedy, R., 1997. Radiative forcing and climate response. *Journal of Geophysical Research-Atmos.* 102, 6831–6864.
- Holben, B.N., Eck, T.F., Fraser, R.S., 1991. Temporal and spatial variability of aerosol optical depth in the Sahel region in relation to vegetation remote sensing. *Int. J. Remote Sens.* 12, 1147–1164.
- Holben, B.N., Tanre, D., Smirnov, A., Eck, T.F., Slutsker, I., Abuhassan, N., Newcomb, W.W., Schafer, J., Chatenet, B., Lavenue, F., Kaufman, Y., Vande Castle, J., Setzer, A., Markham, B., Clark, D., Frouin, R., Halthore, R., Karnieli, A., O'Neill, N.T., Pietras, C., Pinker, R.T., Voss, K., Zibordi, G., 2001. An emerging ground-based aerosol climatology: aerosol Optical Depth from AERONET. *J. Geophys. Res.* 106, 12 067–12 097.

- Horne, J.R., Dabdub, D., 2017. Impact of global climate change on ozone, particulate matter, and secondary organic aerosol concentrations in California: A model perturbation analysis. *Atmos. Environ.* 153, 1-17.
- Kaskaoutis, D.G., Kambezidis, H.D., 2008. The role of aerosol models of the SMARTS code in predicting the spectral direct-beam irradiance in an urban area. *Renewable Energy* 33, 1532–1543.
- Kaskaoutis, D. G. and Kambezidis, H. D., (2006). Investigation into the wavelength dependence of the aerosol optical depth in the Athens area, *Q. J. R. Meteorol. Soc.* 132, 2217–2234.
- Kaskaoutis, D.G., Kambezidis, H.D., Hatzianastassiou, N., Kosmopoulos, P.G., Badarinath, K.V.S., 2007. Aerosol climatology: On the Discrimination of aerosol types over four AERONET sites. *Atmospheric Chemistry and Physics Discussion.* 7, 6357–6411.
- Kaufman, Y., Gitelson, A., Karnieli, A., Ganor, E., Fraser, R., Nakajima, T., Mattoo, S., Holben, B.N., 1994. Size distribution and scattering phase function of aerosol particles retrieved from sky brightness measurements. *J. Geophys. Res.* 99 (D5), 10341–10356.
- Kloog, I., Sorek-Hamer, M., Lyapustin, A., Coull, B., Wang, Y., Just, A.C., Schwartz, J., Broday, D.M., 2015. Estimating daily PM_{2.5} and PM₁₀ across the complex geo-climate region of Israel using MAIAC satellite-based AOD data. *Atmos. Environ.* 122, 409–416.
- Mallet, M., Dubovik, O., Nabat, P., Dulac, F., Kahn, R., Sciare, J., Paronis, D., Leon, J., 2013. Absorption properties of Mediterranean aerosols obtained from multi-year ground-based remote sensing observations. *Atmos. Chem. Phys.* 13, 9195–9210.
- NASA (National Aeronautics and Space Administration), 2017. Atmospheric Aerosols: What Are They, and Why Are They So Important? <https://www.nasa.gov/centers/langley/news/factsheets/Aerosols.html>, access: August 2019.
- Rupakheti, D., Kang, S., Bilal, M., Gong, J., Xia, X., Cong, Z., 2019. Aerosol optical depth climatology over Central Asian countries based on Aqua-MODIS Collection 6.1 data: Aerosol variations and sources. *Atmos. Environ.* 207, 205-214.
- Russell, P.B., Bergstrom, R.W., Shinozuka, Y., Clarke, A.D., DeCarlo, P.F., Jimenez, J.L., Livingston, J.M., Redemann, J., Dubovik, O., Strawa, A., 2010. Absorption angstrom exponent in AERONET and related data as an indicator of aerosol composition. *Atmospheric Chemistry and Physics.* 10, 1155–1169.
- Smirnov, A., Holben, B.N., Dubovik, O., Frouin, R., Eck, T.F., Slutsker, I., 2003. Maritime component in aerosol optical models derived from Aerosol Robotic Network data. *Journal of Geophysical Research–Atmospheres.* 108, art. no. 4033.
- Smirnov, A., Holben, B.N., Kaufman, Y.J., Dubovik, O., Eck, T.F., Slutsker, I., Pietras, C., Halthore, R.N., 2002. Optical properties of atmospheric aerosol in maritime environments. *Journal of the Atmospheric Sciences.* 59, 501–523.
- Tan, F., Lim, H.S., Abdullah, K., Yoon, T.L., Holben, B., (2015). AERONET data-based determination of aerosol types. *Atmospheric Pollution Research.* 682-695.
- Toledano, C., Cachorro, V. E., Berjon, A., Frutos, A. M. De, Sorribas, M., Morenab, B. A. de la and Goloubc, P., (2007). Aerosol optical depth and Angstrom exponent climatology at El Arenosillo AERONET site (Huelva, Spain), 795-807.
- Tripathi, S.N., Dey, S., Chandel, A., Srivastava, S., Singh, R.P., Holben, B.N., 2005. Comparison of MODIS and AERONET derived aerosol optical depth over the Ganga Basin, India *Annales Geophysicae.* 23, 1093–1101.
- Tutsak, E., Kocak, M., 2019. Long-term measurements of aerosol optical and physical properties over the Eastern Mediterranean: Hygroscopic nature and source regions. *Atmos. Environ.* 207, 1-15.



18th World Clean Air Congress, 23-27 September 2019, Istanbul
organized by TUNCAP and IUAPPA

You, W., Zang, Z., Zhang, L., Zhang, M., Pan, X., Li, Y., 2016. A nonlinear model for estimating ground-level PM10 concentration in Xi'an using MODIS aerosol optical depth retrieval. *Atmos. Res.* 168, 169–179.

Zhang, T., H., Liao, H., 2016 Aerosol absorption optical depth of finemode mineral dust in eastern China. *Atmospheric and Oceanic Science Letters.* 9, 7-14.

Zhao, Hujia., Che, Huizheng., Zhang, Xiaoye., Ma, Yanjun, Wang Yangfeng, Wang Xuxin, Liu Chuang, Hou Bo, Che Haochi, 2013, Aerosol optical properties over urban and industrial region of Northeast China by using ground-based sun-photometer measurement , *Atmospheric Environment.* 270-278.

Acknowledgments

The authors gratefully acknowledge the AERONET and PHOTONS sun-photometer networks and their staff for their work to produce that dataset used in this study (<http://aeronet.gsfc.nasa.gov/>). In addition, this work was financially supported by the TUBITAK (1002) programme.

An overview of WRI experiences in impacts assessment on air quality and personal exposure to air pollutants of mobility interventions

Tugce Uzumoglu,¹ Cristina Albuquerque², Beatriz Cardenas³, Seth Contreras⁴, Luisa Oliveira², Jessica Seddon⁴ and Walter Simoni²

¹World Resources Institute Turkey, Muhurdar Cad. Uras Apt. 83/1, Moda, 34710 Kadıköy/Istanbul, Turkey

²World Resources Institute Brazil, Av. Independência, 1299 - Independência, Porto Alegre-RS, 90035-077, Brazil

³World Resources Institute Mexico, Belisario Dominguez No. 8 PA, Col. Alcaldía Coyoacán, 04000

⁴World Resources Institute, USA 10 G Street NE, Suite 800, Washington, DC 20002

beatriz.cardenas@wri.org

Abstract. Air pollution in cities is a major health threat considering the high density of people being exposed to air pollutants. Vehicular emissions are the major source of nitrogen oxides (NO₂), in most of the cities and in some cities major contributors of sulphur dioxides (SO₂), and particulate matter (PM). The objective of this paper is to present an overview of the work done by the World Resources Institute (WRI) in Brazil, Mexico and Turkey over the last years assessing the impacts on air quality and personal exposure of mobility interventions in Mexico city, Istanbul and Sao Paulo. Between 2004 and 2015, several studies showed that passengers personal exposure to air pollutants was reduced after bus rapid transport (BRT) lines were introduced in Mexico City. Commuter's personal exposure to carbon monoxide (CO), particulate matter 10 microns (PM₁₀), particulate matter 2.5 microns (PM_{2.5}) and benzene inside BRTs, showed PM_{2.5} and benzene were reduced up to 30% and 69% respectively, compared to buses and minibuses before BRT was implemented. In Istanbul, an assessment of the air quality impacts of pedestrianization on its historic peninsula was performed in 2014. Impacts on NO₂, SO₂, ozone (O₃) and PM_{2.5} ambient levels were assessed converting streets to public spaces in up to 300 streets. Air pollutants including criteria pollutants (NO₂, SO₂, O₃) and non-criteria pollutants, were measured using an array of monitoring equipment including passive samplers. As a result of the pedestrianization, ambient monitoring showed a reduction up to 42% and 80% of NO₂ and SO₂, respectively compared to a former air quality profile study of the Peninsula before pedestrianization in 2009-2010. Finally, preliminary results of a short study in 2018 to determine the impact of "care-free days" in Sao Paulo's central area in ambient air using low cost sensors for ambient air quality. Although no statistically significant reductions in local PM_{2.5} concentrations were observed, public perception of the citizens were very positive with respect of improvement of air quality. Lesson learned: assessing impacts on interventions, mainly to reduce emissions from vehicular emissions, personal exposure seem to be one of the best parameters to show benefits from emission reductions of interventions. Ambient measurements represent a real challenge considering the complexity of atmospheric pollutants. New devices and instruments represent great opportunities to expand pollutants, spatial and temporal coverage, however uncertainties associated to them may not allow to evaluate impacts of a specific intervention. WRI has learned a great deal from collaboration and synergies between the different stakeholders including scientific community, governments and non-governmental organizations in designing, performing and applying these studies into policies and programs both to improve air quality and.

Keywords: Air quality, Transport emissions, Interventions

1. Introduction

Air pollution in cities is a major health threat considering the high density of people being exposed to air pollutants. Vehicular emissions are the major source of nitrogen oxides (NO₂), in many cities and in some cities major contributors of sulphur dioxides (SO₂), and particulate matter (PM). Interventions to reduce vehicular emissions include a wide spectrum of actions including changes in fuels and or vehicular technology (renewal) or retrofit of existing fleet with or without a designated bus line or bus rapid transport (BRT), restrictions to circulation (“car free days”), closure of streets to vehicles (pedestrianization) among others. In all these cases, emissions reductions can be easily quantified by estimating emissions of a set of criteria pollutants and /or green house gases. Ideally, emissions reductions lead to a reduction of personal exposure to these pollutants, and eventually to an improvement of ambient air quality, assessing these reductions have been the objective of many studies over the last two decades (Shinohara et al., 2017).

In order to assess and to demonstrate there was impact of an intervention, measurements of any specific parameter (usually microenvironmental concentrations, personal exposure to pollutants and/or ambient concentrations) are measured (and compared) before and after the intervention is done. There is an extensive literature of studies reporting impacts of these interventions using a wide set of instruments both to sample and or to measure in real time, from the sophisticated reference ones, to the simple and low cost sensors now widely distributed.

Being emissions reductions from transportation one of the main strengths of the World Resources Institute, impact evaluation of intervention through a wide varied set of measurements arrays.

The objective of this paper is to present an overview of the work done by the World Resources Institute (WRI) in Brazil, Mexico and Turkey over the last years assessing the impacts on air quality and personal exposure of mobility interventions in Mexico city, Istanbul and Sao Paolo.

2. Methodology

The different types of studies here discussed are comprised a wide period since 2004. The intervention assessed varied in time and region as Table 1 shows. Methodology followed in each of these studies is described in Table 2.

Table 1. Studies assessing impact on air quality of specific interventions

Year	Location	Type of intervention	Impact assessment	References
2004-2014	Mexico City	Implementation of BRT lines.	Personal exposure to PM _{2.5} , CO and benzene	Worshimmel, 2010 INECC-CTS, 2008 INECC-CTS, 2010 INECC-CTS, 2014
2010-2014	Istanbul	Pedestrianization of 295 streets old town area	Ambient concentration at street level of NO ₂ , SO ₂	EMBARQ Turkey, 2015
2017-on going	Sao Paulo	Care-free days in selected downtown	Ambient concentration of PM _{2.5}	Albuquerque, 2019

2.1. Mexico City

Studies were done between 2004 and 2015, assessing impacts of implementing 4 lines of BRT during this period of time. Assessment of commuter's personal exposure included exposure to carbon monoxide (CO), particulate matter 10 microns (PM₁₀), particulate matter 2.5 microns (PM_{2.5}) and benzene inside buses and vehicles before and after BRT. Measurements were done in the same transect, time and season of the year in order to mimic the trip commuters do and to minimize other interferences such as meteorological conditions or congestion. Equipments used are described in Table 2.

Table 2. Methodology followed in the three cases studies

Intervention Assessed	Instrumentation	Measurements
BRT-Mexico City	PM ₁₀ and PM _{2.5} were collected with portable SKC sampling pumps with size selective impactors, using 37 mm Teflon filters. Mass in 1 and 5 were determined using a microscale. For benzene, samples were taken using SUMMA stainless steel canisters. Samples were analyzed under TO-14A (US-EPA, 1999) methods. CO measurements were done using Langan; Model T15 personal exposure monitors	4 to 6 weeks of daily measurements in morning schedules (6 to 9 h) in a specific transect before and after BRT lines were implemented. Base line measurements included diesel and gasoline buses and microbuses.
/Pedestrianization of historic peninsula Istanbul	Passive samplers	Measurements of NO ₂ , SO ₂ average concentration at street level in 23 points in 2014 compared to 50 points of measurements in 2010.
Car free days in São Paulo	21 AirBeam2 sensors used for the study 11 treated as FIXED sensors, located outside public buildings near and within the historic city center 2 "golden" sensors were placed near a ground reference monitor owned by CETESB (Public agency responsible for measuring air pollution) 5 sensors allocated for 5 different MOBILE routes 3 sensors kept as extras in case of possible theft or damage	Pre-collocation from 24 th to 25 th September/2018 Field deployment from 28 th Sep to 22 nd Nov/2018 Post-collocation from 23 rd to 26 th November/2018



2.2. Istanbul

In Istanbul, an assessment of the air quality impacts of pedestrianization on its historic peninsula was performed in 2014. Impacts on NO₂, SO₂, ozone (O₃) and PM_{2.5} ambient levels were assessed converting streets to public spaces in up to 300 streets. Air pollutants including criteria pollutants (NO₂, SO₂, O₃) and non-criteria pollutants were measured using an array of monitoring equipment including passive samplers.

2.3. Sao Paulo

The municipality of São Paulo has introduced Car-Free Fridays (CFF) as an access restriction measure to private vehicles, heavy-duty trucks and motorcycles on the last Friday of every month in selected areas of downtown. Particulate matter 2.5 microns (PM_{2.5}) was measured using Airbeam2 sensor, a low-cost sensor, and was followed by qualitative interviews in gathering user perception in the same area.

3. Results

In most of the cases the experimental design and measurements obtained generated data that show a reduction after the intervention was implemented. Differences were mainly due to the design of the experimental design as well as the type of equipment used.

Following a description of the main findings of each case study is described in Table 3.

3.1. Mexico City

Mexico City Commuter's personal exposure to carbon monoxide (CO), benzene and particulate matter 10 microns (PM₁₀), particulate matter 2.5 microns (PM_{2.5}) inside BRTs, showed reductions in CO, benzene and PM_{2.5}. Reductions determined were up to 45%, 69% and 30% respectively, compared to buses and minibuses before BRT was implemented. Although these studies did not measure other VOCs, similar reductions are expected to occurred as similar studies in Mexico City have demonstrated. Shinohara et al. 2011, showed reduction in commuter exposure to aldehydes and volatile organic compounds (VOCs) in 2011 compared to 2002 as a result of different measures implemented in transportation. Formaldehyde however, showed to have increased due to the increase of use of lpg vehicles.

3.2. Istanbul

As a result of the pedestrianization, ambient monitoring showed a reduction up to 42% and 80% of NO₂ and SO₂, respectively compared to a former air quality profile study of the Peninsula before pedestrianization in 2009-2010.

3.3. Sao Paulo

Preliminary results of a short study in 2018 to determine the impact of "car free days" in Sao Paulo central area in ambient air using low cost sensors for ambient air quality have shown that although no statistically significant reductions in local PM_{2.5} concentrations were observed, public perception of the citizens were very positive with respect of improvement of air quality. Currently analyses are being done and will be published in the near future.

Table 3. Key findings of impact of interventions

Location	Impact assessment/Other key findings	concentration reduction
BRT-Mexico City	Personal exposure reductions between 30% and 69%: varying in each of the assessed. High concentrations recorded after intervention up to 75 µg/m ³ of PM _{2.5} and 8 ppb of benzene in 60 to 90 min travel time.	High levels of olefins as indicator of lpg leaks in microbuses. Differences were observed in the different lines due to the congestion and to the technology and fuel of the vehicles. High reductions were observed by introducing Euro III, Euro IV and Euro V. Drastic emission reductions are expected in newer technologies would have been introduced originally.
Pedestrianization of historic peninsula Istanbul	Ambient concentration at street level of NO ₂ decreased by 32% and 87% of SO ₂ compared to 2014 measurements).	Still hot spots were found associated with congestion. (2010 Positive perception from residents and non residents, including air quality improvement. The residential area in the Northwest of the Historic Peninsula, which has not been pedestrianized, shows little or no reduction in traffic-related emissions. Only one sampling location is classified as safe in terms of air pollution profile according to EU Air Quality Standards.
Car free days in São Paulo	No statistically significant changes in air pollution levels detected by AirBeam2 sensors.	Qualitative interview showed positive changes in perception from local users regarding air quality.

4. Conclusions

In Mexico City, more than three quarter of the population use public transportation for commuting, reduction in personal exposure to air pollutants has a very important impact in reducing health risk. Although differences in concentrations and reductions were observed in all these studies due to the transect characteristics as well as the technology and fuel of the fleet, studies demonstrated that BRT implementation in Mexico City always resulted in reduction to personal exposure to CO, benzene and PM_{2.5}. Introduction of the cleanest technology available instead of the cleaner technology could have had better and faster impacts. Best technology should be introduced when replacing existing fleet and particularly when introducing BRT in order to maximize and expedite health impacts in commuters i.e. Euro VI/EPA 2010.



The three case studies here summarized show that interventions to reduce vehicular emissions could have an impact in personal exposure to commuters and pedestrians. The magnitude of reductions and type of pollutants may change considering the existing fleet technology, fuel and meteorological and geography of the city were the intervention is implemented. Experimental design impacts as well on the capacity of showing the reduction since time, spatial and pollutants coverage is a key issue in order to demonstrate impact in a very robust way.

Collaboration and synergies between the different stake holders including scientific community, governments and non governmental organizations in designing, performing and applying these studies into policies and programs both to improve air quality and mobility are part of the lessons learned.

Low cost sensors represent an important opportunity to expand and democratized these types of studies. They also represent challenges in terms of their accuracy and comparability with reference methods so technical and scientific experts should work closely to narrow these gaps. The result of qualitative interviews in São Paulo indicated an important component to be considered in future studies, which is the perception of those impacted by the interventions.

Results from these types of studies should be easily communicated in order to highlight the impact of these type of interventions both commuters, citizens and authorities, particularly those from transport sector. Transport experts should consider that health risks could be drastically reduced by introducing the cleanest technologies and should consider this criteria as a key one when designing interventions. As for citizens, requesting interventions that maximize the reductions of toxic pollutants in the shortest time should be one of the points in their agenda.

5. References

- Albuquerque, C, 2019. Preliminary results of car free days assessment on microenvironments. Personal communication.
- EMBARQ Turkiye, 2015. Assessment of the air quality effects of pedestrianization on Istanbul's historic peninsula. 2015. Issue Brief. 2015. EMBARQ Turkiye. www.embarqturkiye.org
- INECC-CTS Mexico, 2008. Evaluación de los beneficios en la exposición personal de usuarios de Eje Central por la instrumentación en cambios en el transporte. Primera Etapa. Reporte de Convenio de Concertación.
- INECC-CTS Mexico, 2010. Estudio de Impacto por exposición personal a contaminantes generados por fuentes móviles que circulan en el corredor eje 3 Oriente (Río de los Remedios – San Lázaro): Primera etapa. Reporte Instituto Nacional de Ecología Centro de Transporte Sustentable de México A.C. Informe de convenio de concertación.
- INECC_JICA, 2014. Exposición personal a carbonilos, CO, benceno y PM_{2.5} en microambientes de la ZMVM. Reporte Final. https://www.gob.mx/cms/uploads/attachment/file/370446/14._Informe_Exp_Per_ZMVM.pdf
- Shinohara N., Angeles, F., Basaldud, R., Cardenas, B., Wakamatsu., S., 2017. Reduction in commuter exposure to volatile organic compounds in Mexico City due to the environmental progress of Proaire 2002-2010. *Journal of Exposure and Environmental Epidemiology*. 339-345.
- Steinle, S., Reis, S, Sabel, C.E., Semple, S., Twigg, M.M., Braban, C.F., Leeson, S.R., Heal, M.R. , Harrison, D, Lin, C., Wu, H., 2015. Personal exposure monitoring of PM_{2.5} in indoor and outdoor microenvironments. *Science of the Total Environment*. 383-394.



18th World Clean Air Congress, 23-27 September 2019, Istanbul
organized by TUNCAP and IUAPPA

Wohrnschimmel, H., Zuk, M., Martinez Villa, G., Ceron, J.G., Cardenas, B., Rojas-Bracho, L., Fernandez, A., 2008. The impact Bus rapid transit system on commuter's exposure to benzene, CO, PM_{2.5} and PM₁₀ in Mexico City. *Atmospheric Environment*. 42, 8194-8203.

Acknowledgments

Authors would like to acknowledge the participants from the different institutions that have collaborated with WRI in these studies: As for the work done in Mexico City to evaluate BRT impacts was done as part of the collaboration between Centro de Transporte Sustentable –Embarq and the National Institute of Ecology and Climate Change with the support from the Hewlett Foundation.

Istanbul project was done in collaboration with Fatih University and Environmental Protection Department, Istanbul Metropolitan Municipality.

Dynamic spatio-temporal health impact assessments using geolocated population-based data: the PULSE project

Domenico Vito¹, Riccardo Bellazzi¹, Vittorio Casella², Cristiana Larizza¹,
Andrea Pogliaghi³ and Daniele Pala²

Università di Pavia LISRC Lab Pavia-Italy ¹, Università di Pavia Dipartimento di
Ingegneria Civile ed Architettura - Lab Geomatica Pavia-Italy ², Genegis Milan-Italy ³

dvito.pulse@gmail.com

Abstract. Despite the silent effects sometimes hidden to the major audience, air pollution is becoming one of the most impactful threat to global health.

Standing to the report of the European Environmental Agencies the number of deaths from cardiovascular disease that can be attributed only in Europe alone, is about 790.000 a year and each of these deaths affects an average reduction in life expectancy of more than two years: air pollution is addressed to be the cause of premature death in 41 European nations

This outcomes are enforced by the estimates of WHO, finding that air pollution is responsible for 120 extra deaths per year per 100,000 of the population.

Cities are the places where these deaths are concentrated most, as the consequences of bad air quality are more severe and localized. In order to correctly address intervention and prevention thus is essential to assess the risk and the impacts of air pollution spatially and temporally inside the urban spaces.

PULSE (Participatory Urban Living for Sustainable Environment) is a pioneer EU-financed project that aims to develop a set of models and technologies to predict and manage public health problems in cities and promote health. It aims to develop and test dynamic spatio-temporal health impact assessments using geolocated population-based data.

The project is currently active in eight pilot cities, Barcelona, Birmingham, New York, Paris, Singapore, Pavia, Keelung and Taiwan, following a participatory approach where citizen provide data through personal devices and the PulsAIR app, that are integrated with information from heterogeneous sources: open city data, health systems, urban sensors and satellites.

PULSE aims to design and build a large-scale data management system enabling real time analytics of flows of personal data

The objective is to reduce the environmental and behavioral risk of chronic disease incidence to allow timely and evidence-driven management of epidemiological episodes linked in particular to two pathologies; asthma and type 2 diabetes in adult populations. developing a policy-making across the domains of health, environment, transport, planning in the PULSE test bed cities.

The work will present the main frameworks of the project and the most relevant components of the decision support platform, such as satellite data processing, deployment of sensors, management of acquired spatial data, WebGIS and Dashboard tools to provide visualization of the correlations between epidemiologic and spatiotemporal data and models.act.

Keywords: Air Pollution, Health, Data, Participation.

1. Introduction

Despite progress in recent years, air pollution continues to be a serious environmental and health problem.



Air pollution consists of harmful or poisonous substances in outdoor or indoor air: this of course threatening for normal subject but also for people affected by respiratory and cardiovascular diseases like asthma and diabetes.

According to the WHO impacts deaths from air pollution reach 4.2 million annually due to air pollution (WHO, 2016), and one out of every nine deaths was the result of air pollution-related conditions.

The problem of air pollution currently affects all regions, settings, socioeconomics groups and of every age.

Standing to EEA, air pollution causes 790.000 new deaths per year and it reduces of 2 year the life expectancy and premature deaths in 41 EU countries.

The European Environmental Agency has estimated that 13 % of the EU-28 urban population was exposed to PM10 levels above the daily limit value and approximately 42 % was exposed to concentrations exceeding the stricter WHO AQG value for PM10 in 2016 (EEA, 2019).

Due to this urgency to intervene indeed air pollution has been identified as a global health priority in the sustainable development agenda.

Particularly air quality issues are addressed by Goal 3 related to health, Goal 7 related to energy and goal 11 “Sustainable cities and communities”.

On the purpose of address sustainability at a city level is inserted the european project PULSE.

PULSE (Participatory Urban Living for Sustainable Environment) is an EU-financed project that aims to develop a set of models and technologies to predict and manage public health problems in cities and promote health. It follows a participatory approach where citizen provide data through personal devices, that are integrated with information from heterogeneous sources: open city data, health systems, urban sensors and satellites. The project deals with various issues concerning air quality, lifestyle and personal behavior and it aims to investigate the correlations between the exposure to atmospheric pollutants, the citizen habits and the health of the citizen themselves, focusing on Asthma and T2 diabetes.

2. The PULSE project: system architecture

PULSE is a participative project focused on well-being in communities. The final goal is to build extensible models and technologies to predict, mitigate and manage public health problems, and promote population health, in cities.

The eight pilots of the project– Barcelona, Birmingham, New York, Paris, Singapore, Pavia, Keelung and Taiwan– can be defined as “Smart Cities”. “Smart Cities and Communities” embrace integrated IT infrastructure and solutions, and citizen services, across city sectors, including health.

To accomplish the transformation of public health systems, and stimulate the development of intersectorial policy in cities, PULSE leverages large amounts of data from city governments, health systems, and citizens.

Beyond the collection of existing data, PULSE undertakes the following:

- implement a novel environmental/health surveillance system on air quality within specific neighborhoods and model risk of exposure to polluted air for citizens, especially those with asthma;
- develop novel insights on the relationship between risk for the onset of T2D and environmental and behavioral factors;
- collect comprehensive data on individual and community well-being;
- model public health risk and resilience and develop tools and technologies to intervene and change behaviour, translating Big Data to Policy.

Currently the project pilots are running in 8 cities; the Consortium is implementing dashboards on support to Public Health Organization to visualize all the gathered data, the outputs of the health risk models and the simulation tools to assess neighbourhoods air quality conditions and the health status of the citizens.

The core of the PULSE project is the data management architecture: it is designed in order to collect and elaborate a multivariate set of data.

Figure 1 frames the basic concept and the main elements of PULSE architecture: it is made by several modules that are able to collect data from heterogeneous sources.

The different modules of the PULSE infrastructure enable the management of participative data from the PulsAIR App, geolocated Satellite (MODIS, Sentinel, Landstast) and also from static AIR sensors that can be from existing official AQ stations but also from from a dedicated dense networks of lowcost sensors, installed on test bed cities by the PULSE project.

The collected data are used to generate maps of environmental air quality, calculate personal exposure and to feed health risk models that assess the risk of asthma and diabetes T2 occurrence due both to air quality condition and subject health status. The PulsAIR app in facts is designed both to connect to a wearable connected to FitBit, Garmin Asus health tracker devices and to interact and to collect data from citizens by questionnaires and gamification techniques related to subjective health status, physiology and daily activity and current location.

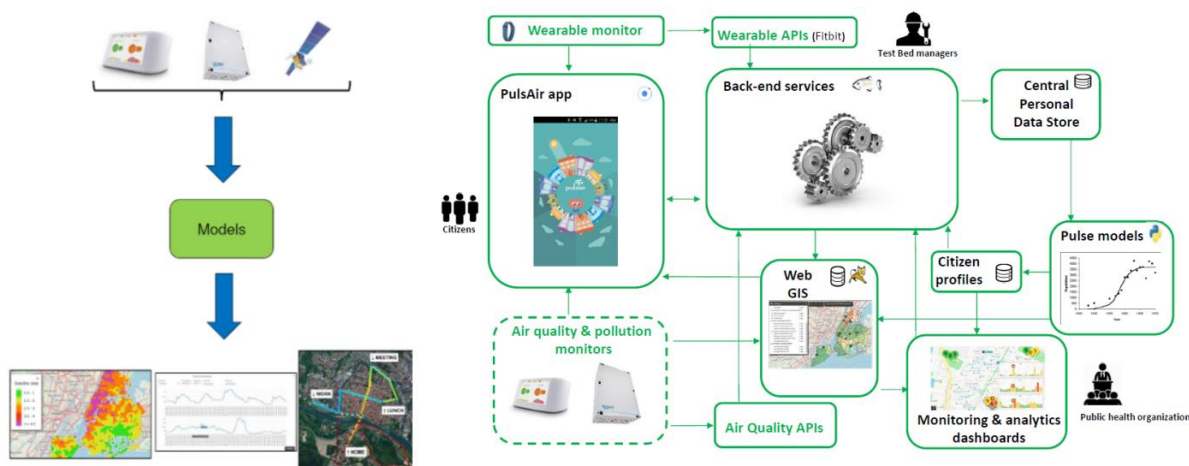


Figure 1. A. PULSE basic concept B. Pulse Architecture: Logic structure

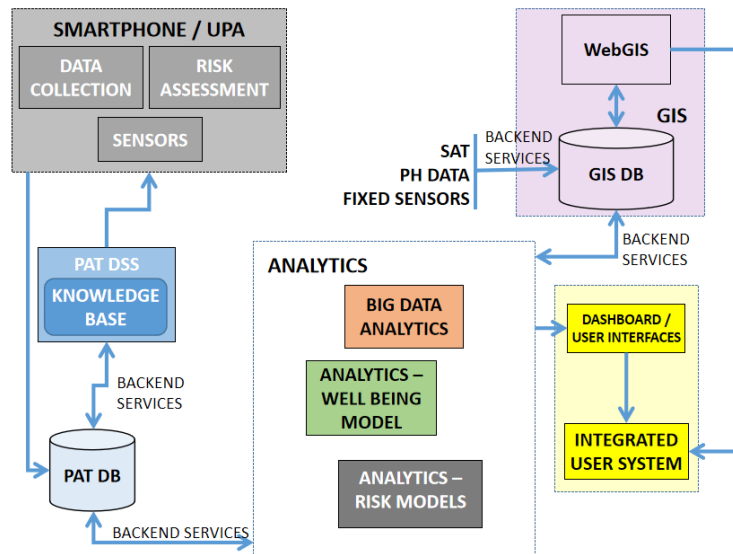
To manage the heterogeneous set of data the inner composition of the data architecture is structured in different modules and repositories.

Particularly the data related to health and behaviour coming directly from the users through PulsAIR are stored into a central personal data storage, and the outputs of the health model are backedup into a citizen profiles repository.

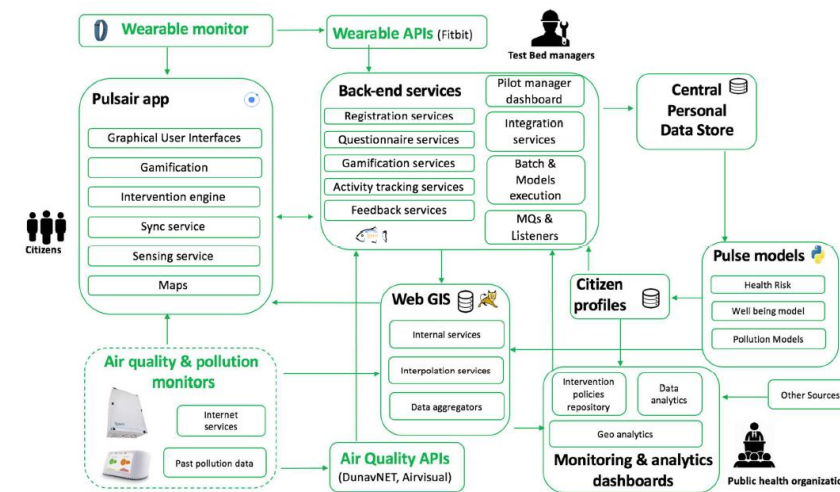
The environmental data, coming from the AQ stations and the diffuse network sensors, as well as the output environmental maps are stored into the WebGIS geodatabase (Figure 2.A).

The cross talking among the different repositories, the conversion between the different data within common measure units and timelapses is managed by a series of Backend Services hosted in a remote server.

The backend services also include all the necessary routines for user-data interactions provided by the PulsAIR app and the Fit-bit devices.



A. Database Structure



B. Full Overview of the interactions

Figure 2. PULSE architecture: service structure

2.1. PulsAIR App

PulsAIR is a novel participatory citizen science-based mobile application used to empower the citizens in their perceiving of urban environmental and health status.

The app has been developed to foster a healthy lifestyle and to make people more aware about the air pollution in the city.

PulsAIR is available both for iOS and Android and has been designed following a user-centred approach based on the goal-oriented design (GOD) methodology, in which end users and stakeholders guide the process, and ultimately validate the final product (Ottaviano et al 2019).

The main purpose of the app is of getting a positive behaviour change regarding healthy and green habits.

Figure 3 resumes the main interfaces of the PulsAIR app

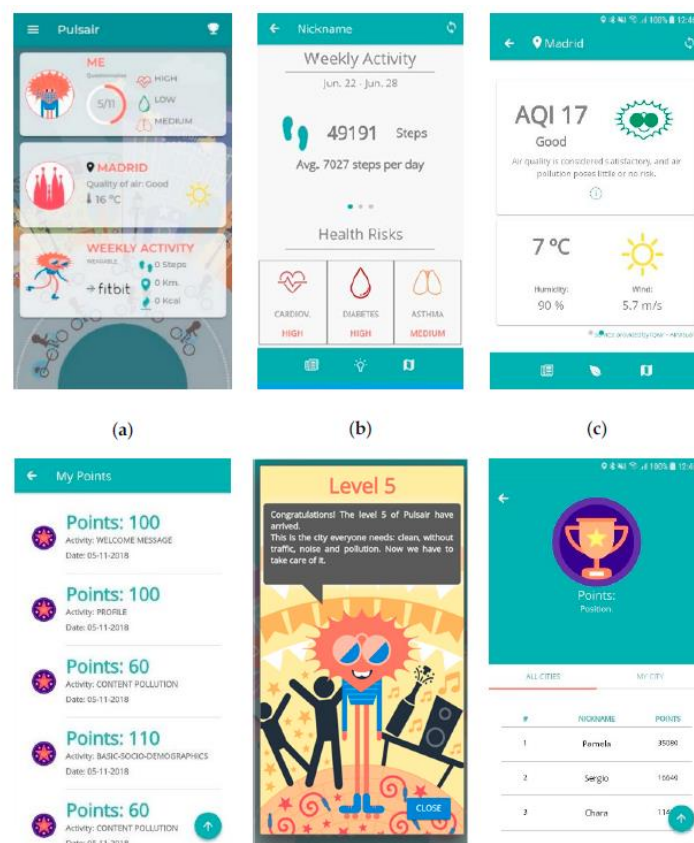


Figure 3. PulsAIR mobile application interface screenshots: (a) Home Menu; (b) “Me” module; (c) “My City” module; (d) “My Points” section; (e) Level up message; (f) Leaderboard

As schematized in Figure 4, PulsAIR can be connected to FitBit, Garmin and Asus health tracker devices: with this system the citizens can provide data on subjective health status through guided questionnaires and physiological and daily habits data for the wearable sensor.

The app can return back to the users health risks (of asthma and type 2 Diabetes) and it suggests specific behavioural changes for an improve on health that are delivered through a supportive feedback.

The app can also show user the exposure to the air pollutants by combining the information of the position (the GPS data) with the data coming from the environmental sensors that measure air pollutants (PM_{2.5} and CO etc..)



Figure 4. PulsAIR connection with FitBit Sensors and interaction with Air Quality Sensor Network

To foster the active engagement of the individuals in the air quality health policies, the PulsAIR has been developed integrating game-design elements, to allows an entertaining and informative engagement experience around several aspects such as encourage people to do things they consider otherwise boring, rise user engagement, enhance attention, and increase motivation.

Particularly it exploit a rewarding system on the performance of healthy habits and information on air quality as described in Figure 5.A and 5.B.

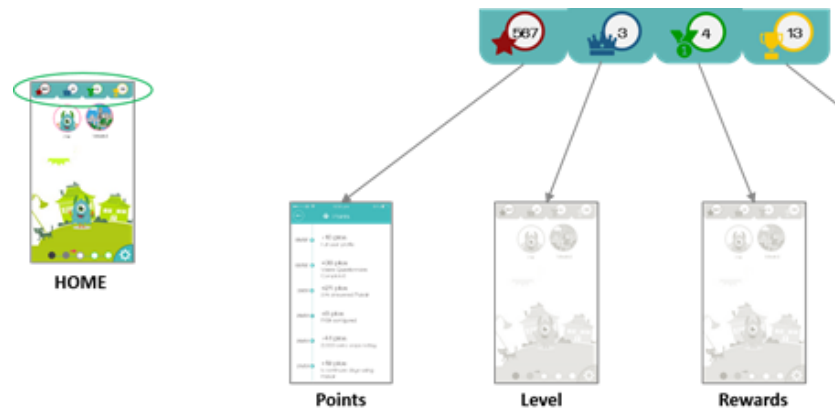


Figure 5.A PulsAIR App Game Views

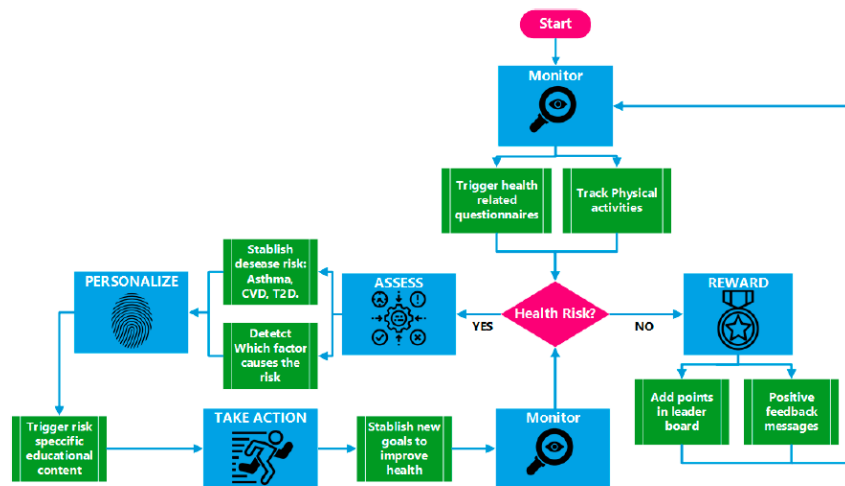


Figure 5.B PulsAIR workflow, CVD cardiovascular diseases (Ottaviano et al., 2019)

Inside the PULSE project, PulsAIR App is the first user interface for data collection from users to create a data back-end ecosystem.

The data back-end ecosystem has been implemented on support to the interoperability of the data flows. The ecosystem allows a continuous interaction with the mobile application, enabling a participative and real time data gathering and integration among different sources.

The data back-end ecosystem can be considered as framed on four overlapping data contextual layers that are mirrored into the back-end infrastructure for data processing and visualization and fed through the mobile application, enabling real-time information delivery (Figure 6)

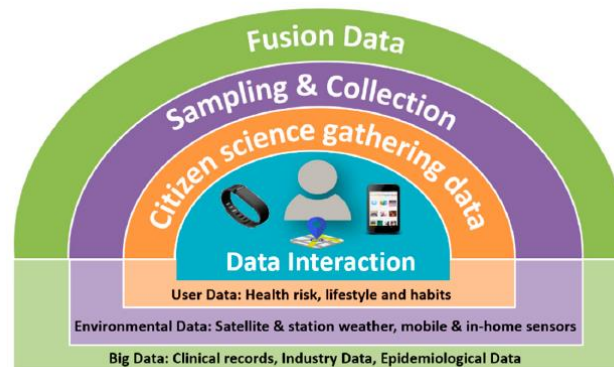


Figure 6. Data backend ecosystem framework (Ottaviano et al 2019)

Coupled with the data ecosystem on the backend it can be seen as a “toolkit” that collects and process information that is rarely integrated as health data from citizens and environmental data on pollution stored in the same repository.

This framework gives a citizen-centric set of applications and data services that can contribute to address in a remote manner, changing the way that environmental research, monitoring, and policy-making are carried out.

2.2. Dense network of air quality sensors

The PULSE air quality sensor’s system is composed of multiple type of sensors and sensor’s datasets, historic and real-time data, for all pollutants (PM_{2.5}, PM₁₀, NO₂, O₃, SO₂).

The network aims on monitor the variable trends in emission within urban areas with an high resolution, to appropriately address the temporal and spatial scales where usually pollutants are spread To have a capillary coverage of the sampling the project integrates mobile sensors and mobile network of sensors in order to establish a significantly enhanced monitoring system.

Two types of sensors are used across pilots that are the AQ10x of DunavNetn (20+, deployed in all pilots) and PurpleAir PA-II sensor (30+ in Pavia – started acquisition in 2018): they allowed to have an high frequency measurement providing a sample every minute.

Those two types of sensors are easily deployable in order to build both a mobile measurements station or a low-cost network of sensors, changing the paradigm to citizen participative urban network.

Before all the test bed acquisition the sensors has been tested and calibrated in the city of Barcelona for 2 weeks.

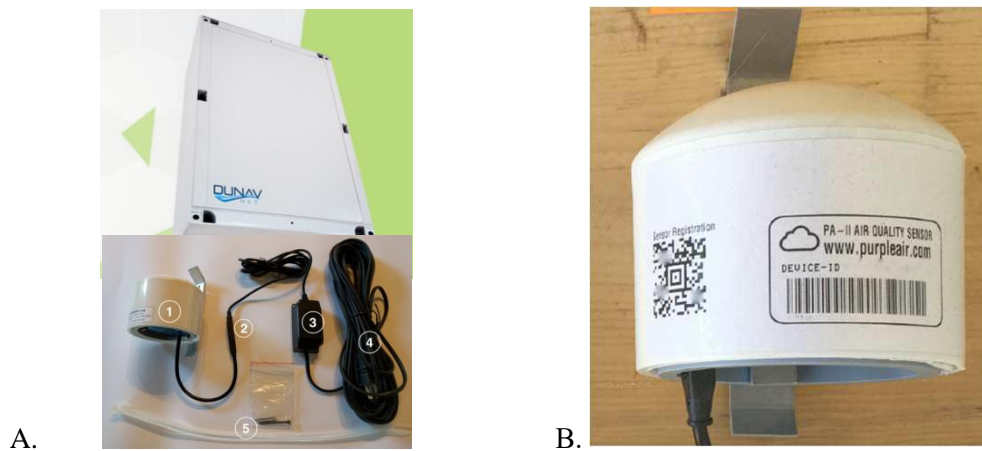


Figure 7. Network sensors: A. AQ10x of DunavNet sensor B. PurpleAir PA-II sensor

2.3. The WebGis Module

The pulse WebGIS module gathers and geo-refers the heterogeneous sets of data gathered in PULSE. The repositories of PULSE particularly collect socio-economic data (level of education, poverty rates, unemployment and violence rate), environmental data (concentration of fine dust $PM_{2.5}$ and PM_{10} , concentration of NO_x), demographic data (access to healthier food stores and dinners, ortotransport and mobility, use of public transport), health and subject behavioral data (hospitalizations for asthma and T2D, prevalence, mortality, alcohol, smoking, physical inactivity).

The WebGIS module allow to view the collected data using maps that help to graphically show relationships between data and models that would otherwise remain hidden without any geographical representation.

The module is basically composed by 8 WebGIS , one for each pilot site, working on 3 levels (Figure 8).The "Data Ingestion layer" level gathers the data from the different sources (sensors, apps, satellite) and allows also to integrate further data by uploading in .csv formats

The "Processing layer" processes and creates the geostatistics and the maps of interest and the "visualization layer" displays in maps that can be temporally and spatially explored for each pilot site.

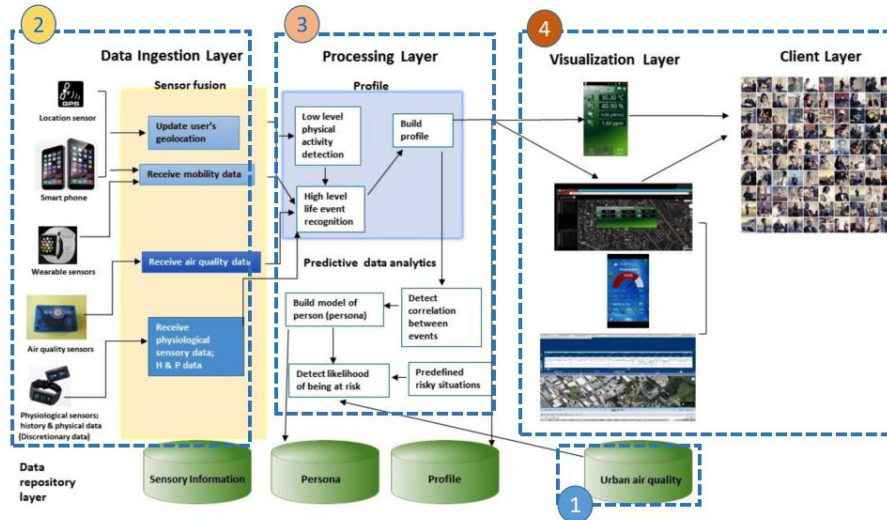


Figure 8. WebGIS module three layer structure

The WebGIS provides the geospatial services used by other Pulse components. It offers basic and advanced features by exploiting the data and maps (Figure 9).

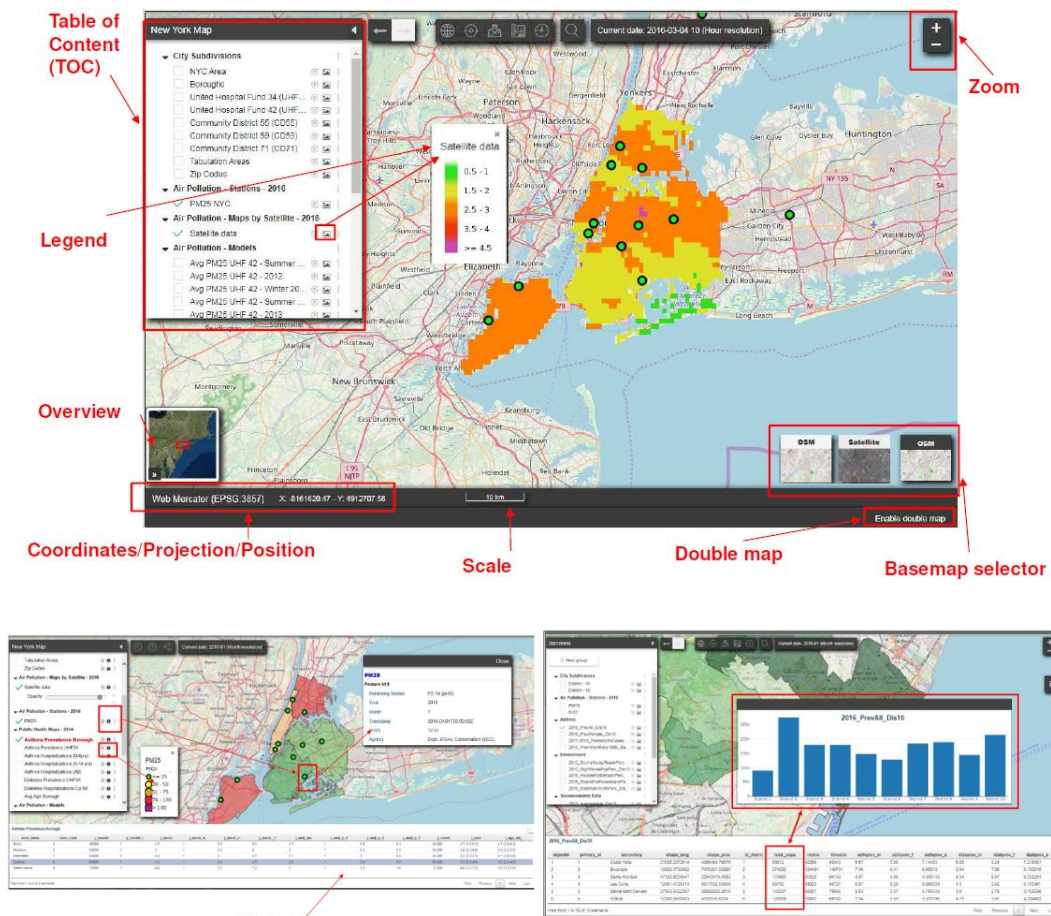


Figure 9. WebGIS module three layer structure

The standard functionality include zoom, pan extent, geocoding, current position, history navigation, the possibility to execute featured query and to show the table of attributes of the geodatabase, and finally to download of the data in .cvs format.

The WebGIS module is composed by two parts *the Viewer* and *the Configurator* (Figure 10)

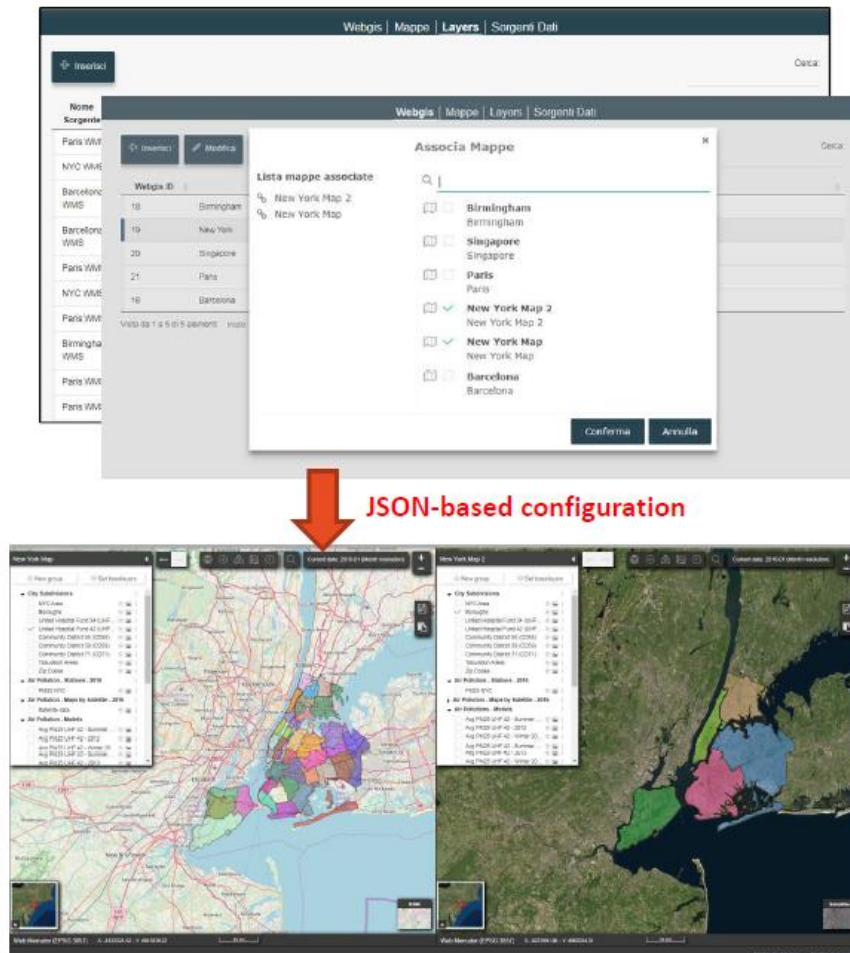


Figure 10. Architecture of the WebGIS module

The Viewer is the basic visualization interface of the module that shows the data as requested

The Configurator tool simplifies the creation of the WebGIS for the pilot cities, and the layer registry: it supports also the automatic data ingestion from external files, both combining with the existent layer from the WebGIS DB and GeoServer.

The Configurator is also a map composer, through the functionalities of layer choice and widgets to set the data and visualization permissions.

The Configurator is the underline element for the advanced functionalities of the WebGIS.

2.4. Advanced Application of WebGIS module

Beside the basic ones the WebGIS module has also some advanced functions for a deeper exploitation of the data.

First of all the WebGIS module allows to put two maps side-by-side (Figure 11) in order to visually make confrontations or visual interpretation of pattern and correlations and to compare data (e.g. asthma hospitalizations and air quality) or same data at different times (Figure 11). The side-by-side maps can support also geostatistical analysis to make more explicit the relationship between some parameters (for instance correlation between poverty and hospitalizations for asthma).

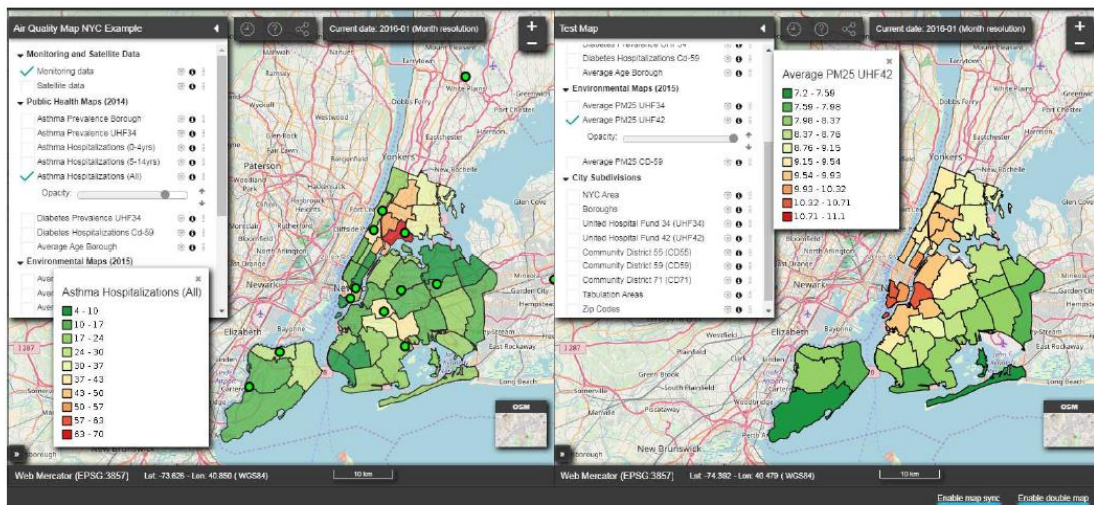


Figure 11. Two maps side-by-side feature

In addition to side-by-side maps, that can be useful to visually assess potential correlation, data can be analyzed also via geostatistical functions. These analysis allow to make more explicit the relationships between variables of different clusters. Figure 12 shows for instance the geostatistical correlation between poverty and hospitalizations for asthma.

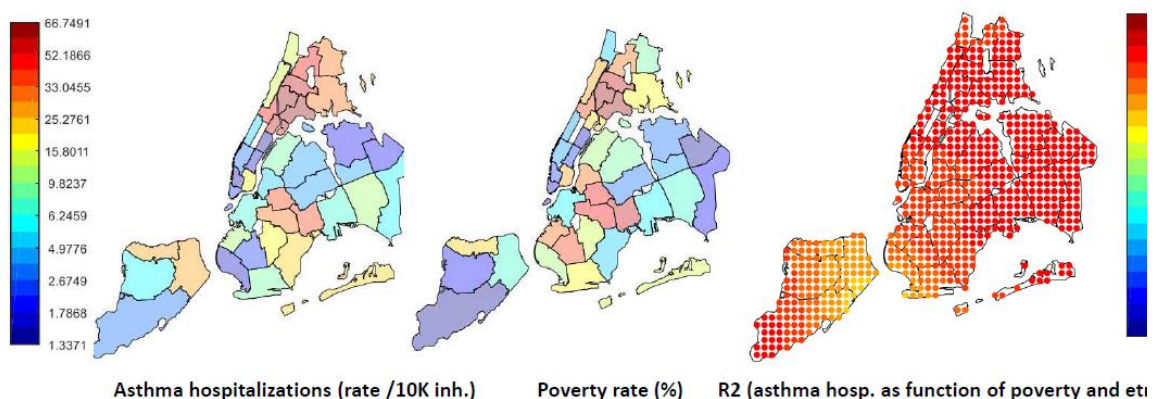


Figure 12. Geostatistical tool application between asthma hospitalization and poverty rate

Another advanced feature of the WebGIS is the *dynamic thematization* that is a data-driven on-the-fly definition and application of a style to a layer. It is possible to style an existing layer using external

parameters (via API or CSV): Figure 13 show an example of a district thematization applying different colors to the districts according to an external parameter A.

By the advanced features of WebGIS is possible to navigate data spatially but also temporally.

The *temporal navigator* manage to explore data series (e.g.: satellite data / air quality monitoring measurements) by time, allowing to analyze the evolution or variation of a phenomena in different in.

The navigator support different temporal resolutions: the native is hourly, but there are also aggregated as hourly, daily, monthly. It supports also different statistical operators as temporal and spatial average.

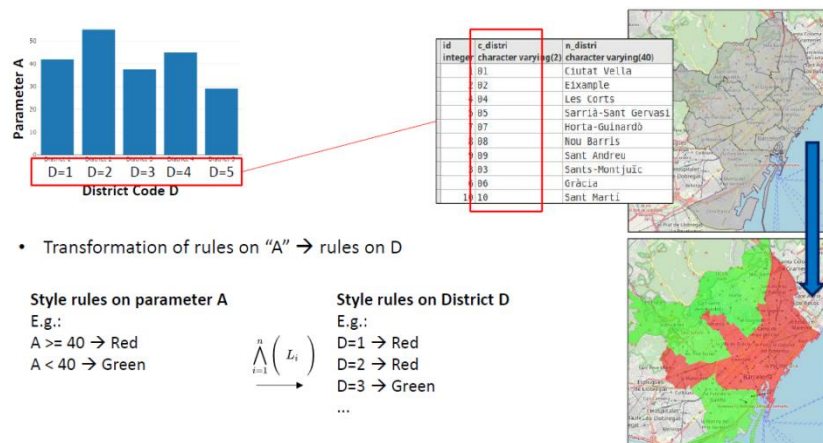
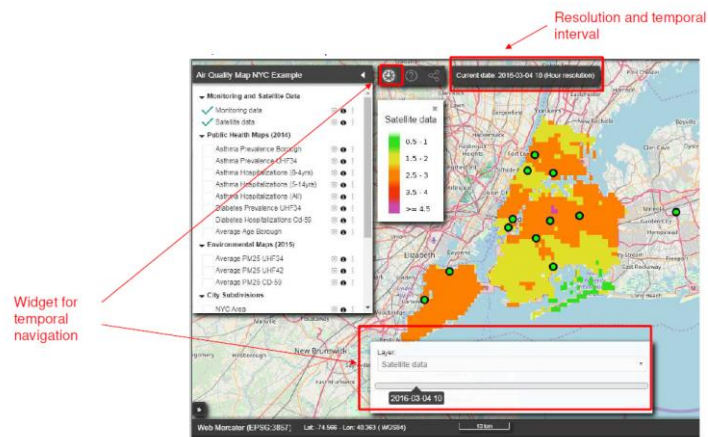


Figure 13. Example of a dynamic thematization of a "district style" based on an external parameter A



A.

Air quality satellite data (hour resolution)

Monitoring station data (NO_x, monthly/daily/hourly average values)

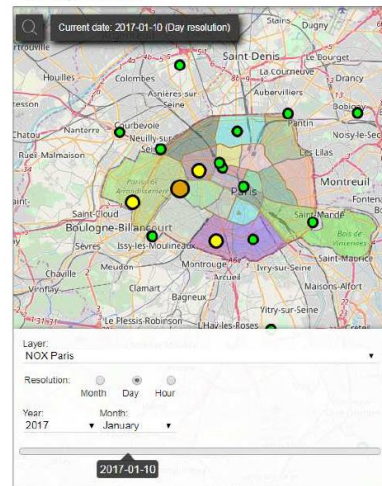
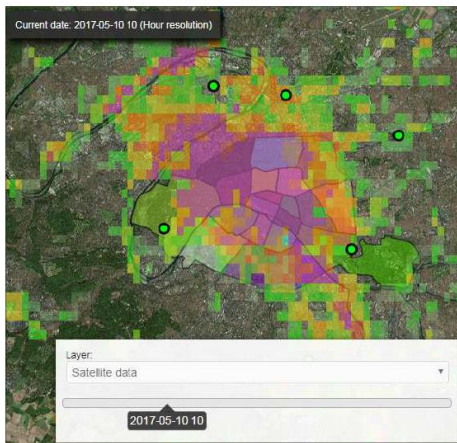


Figure 14. Screenshots of the WebGIS temporal navigator with A. basic interface and B. time lapse statistical data manipulation

2.5. The monitor & analytics dashboards

The PULSE project is provided by a dedicated for pilot management to follow-up the upper level and aggregated indicators . It is equipped by visual monitoring and analytics in order to assess the quality and statistic for the collected data.

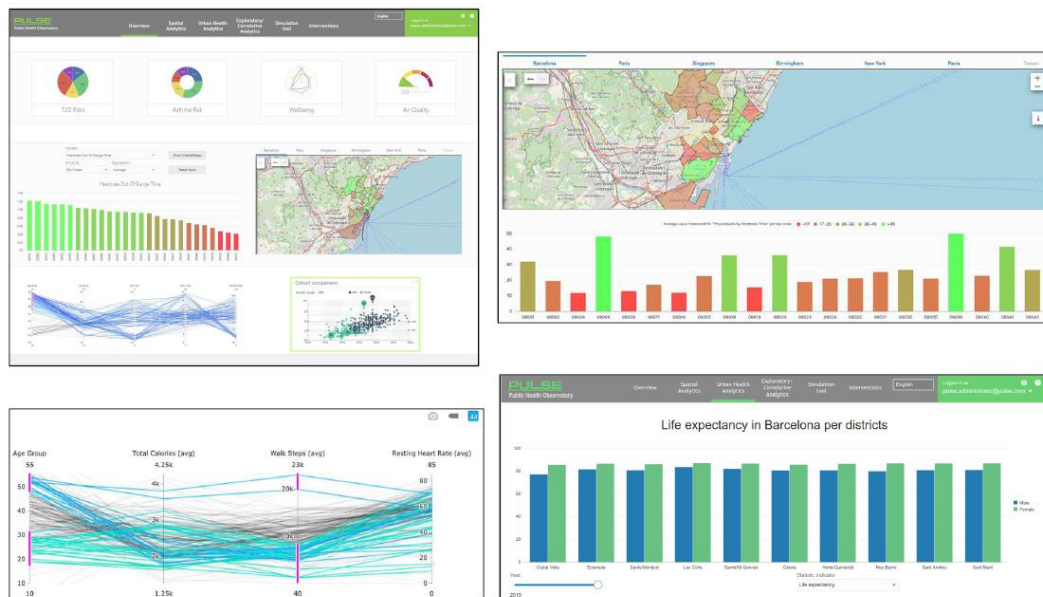


Figure 15. PULSE monitor and analytics dashboard

3. Example of spatio-temporal health impact assessments

On the following paragraph some examples of application of PULSE will be exposed showing how the combination of multivariate data can support the spatio-temporal assessment of the risk on health related to air quality.

Figure 16 reflect the schematic paradigm on how the PULSE platform works to reach this objective. Using existing open data and acquired data, and exploiting spatiotemporal models on health risks, asthma and diabetes T2D risk management data and environmental exposure can be assessed.

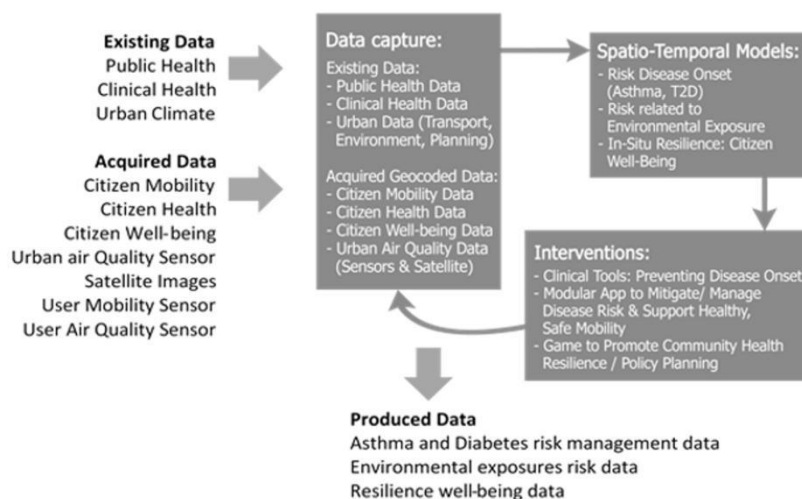


Figure 16. Spatio-temporal health impact assessments on PULSE; schematic paradigm

3.1. The MODIS satellite data for air quality

One of the source of external data integrated in PULSE has regarded the geographical distribution of air quality: particularly the data coming MODIS (Moderate Resolution Imaging Spectroradiometer) satellite sensor of NASA has been integrated to produce diffuse air quality maps.

The integration has required a suitable calibration and validation of parameters based on a relationship between the thermal band recorded by the space-borne sensor and the air pollutants. This technique permitted to reach a resolution of 500 meters, allowing the generation of one map per date at a fixed time corresponding to the transit time of the satellite.

In terms of numbers from the MODIS data, the test beds has been provided by more than 50 maps for NYC, more than 25 maps for Paris, and more than 20 for Barcelona.

3.2. Land surface maps to assess Urban Heat Island effect

Other types of satellite data used in PULSE have been the ones produced by Landsat-8 and Sentinel. These data have been exploited to assess the “Urban heat island” UHI effect (Manley, 1958).

The UHI phenomenon is generally considered as caused by a reduction in latent heat flux and an increase in sensible heat in urban areas as vegetated and evaporating soil surfaces are replaced by relatively impervious low albedo paving and building materials that have an higher heat capacity and conductivity compared to bare soil and vegetation such as concrete, asphalt, metal.

This creates a difference in temperature between urban and surrounding non-urban areas (Manley 1958). The UHI can be monitored through Land Surface Temperature maps obtained by the Landsat-8 and Sentinel satellite images (Imhoff et al. 2010). Land Surface Temperature (LST) is an important parameter to be assessed for air quality as an increase in LST determines an higher mobilization of air pollutants, greenhouse gasses and ground-level of ozone (smog) and particulate.

Figure 17 shows an example of LST map for the city of Pavia, with the LST calculation used in PULSE. The used calculation procedure is able to obtain maps for a spatial resolution of 30m and a temporal resolution of 2 week by the Landsat 8 images and maps of 10m of spatial resolution for a 5 days of temporal resolution.

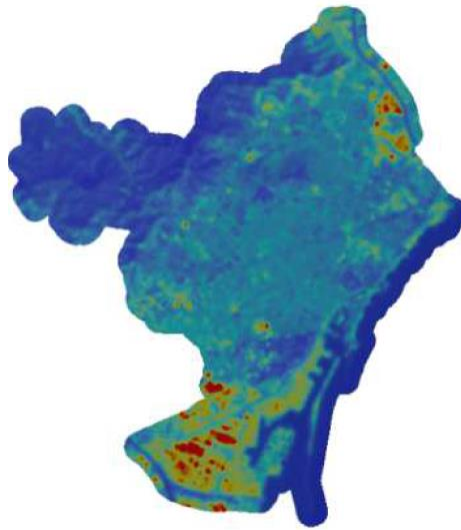


Figure 16. Example of Land Surface Temperature map for the city of Pavia

3.3. Personal Exposure evaluation

Personal exposure is a concept used by the epidemiologists to quantify the amount of pollution that each individual is exposed to, as a consequence of the living environment, habits etc.

Personal exposure has been evaluated in PULSE combining the information from the dense network of low-cost sensors and the data on habits coming from the PulsAIR app. Following the sampling rate of the sensors the data has been calculated.

Figure 17 shows a map for the personal exposure to PM₁₀ with an hourly frequency.

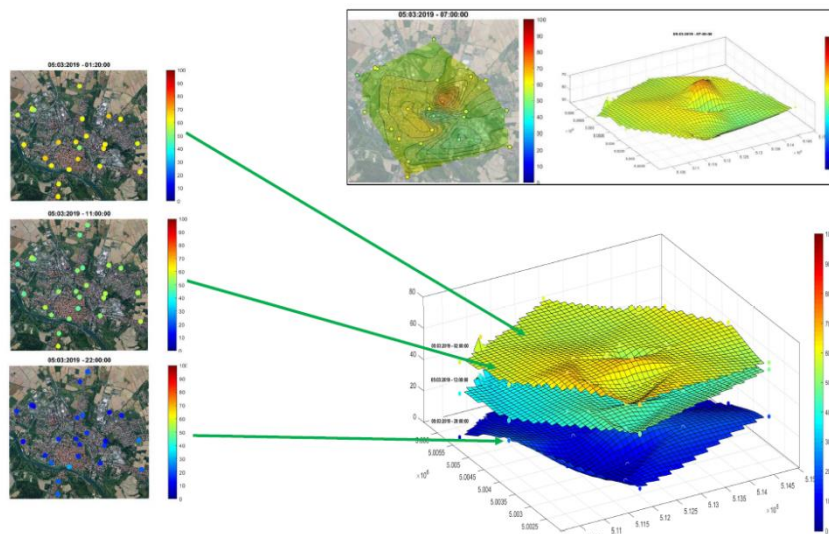


Figure 17. Personal Exposure Map to PM₁₀

Exploiting the data from the PulsAIR app, FitBit and the personal exposure, an estimate of inhaled pollutant has been calculated in association to three classes of movement by the speed of body translation; standing, walking and running, considering the breaths per minute and the air volume per breath (Table 1).

Table 1. Page setup and measurements

Speed [km/h]		#breaths per min	Air volume in litres per breath
>=0	<=2	15	0.6
>2	<=6	28	1.8
>6		40	2.5

Personal exposure result could be also traced into exposure paths as in Figure 18 each dot in the movement line correspond to a time-lapse of 1 minute.

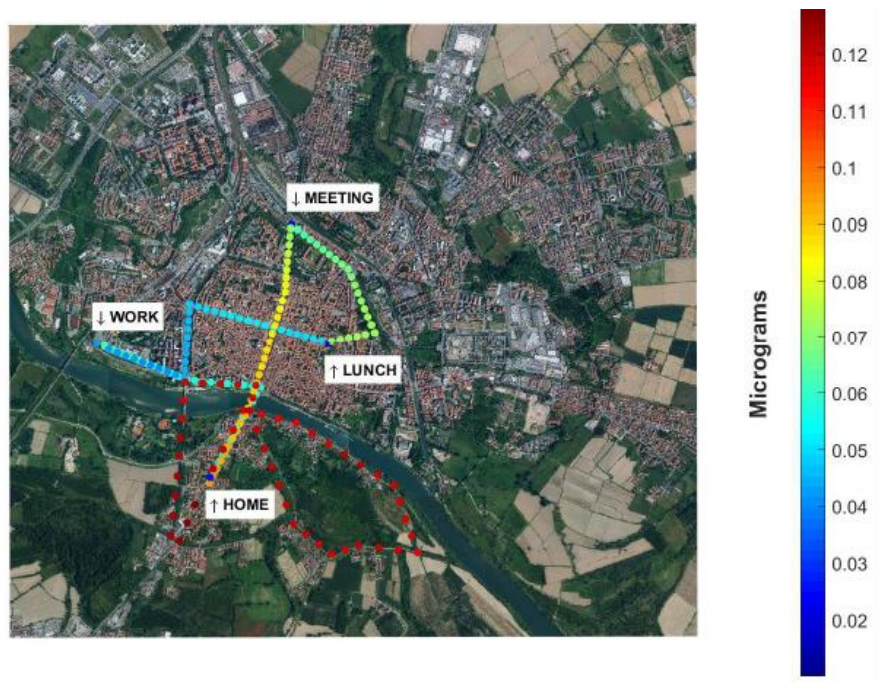


Figure 18. Personal Exposure Paths

4. The community of practices

The main aim of PULSE is to engage in a collaborative dialogue a range of stakeholders across the pilot studies to transform public health from a reactive to a predictive system focused on both risk and resilience.

On this aim PULSE works to raise awareness about those issues and empower stakeholders (Public Health Observatories, Community representatives, municipalities, health institutions, etc.) through innovative PULSE solutions.



Beside the development of the platform in each pilot site *communities of practices*, have been fostered in order to create the stakeholder ecosystems to transfer the collected data into knowledge and practices. The communities of practices are supported by PULSE through a dedicated blog that post articles related to air quality and health impact issues and by the organization of capacity building events for practitioners on PULSE innovative system.

5. Discussion

PULSE offers an example of data driven decision making support system to orient health policies in response to air quality.

It foster the paradigm of citizen science and “putting the human in the loop” (Fraternali, 2012), that mean engage the citizens in the feedback loops related to the sensing of the environment.

The extremely detailed organization of the internal architecture, helps to drive the exploitation of the collected data in very different manners.

PULSE represent an innovative support on the collection of air quality data and on the support to urban health policies.

The installation of the sensors and of all technologies requires low cost hardware and software and furthermore most of the software is open source (Ottaviano et al 2019). Beside the low cost hardware a great potential of the project is the direct involvement of the citizens.

The participatory approach indeed brings several advantage, both allowing a more capillar sensing of the environment and a direct feedback communication with the citizens. Currently PULSE has reached more than 1611 in all pilot cities and is open to engage more users in order to increase the statistical significance of the results. The objective will be to involve at least 300 participants in each pilot, for a total of 2400 users involved.

6. Conclusions

The PULSE project has been successfully deployed in 8 pilot cities and a data architecture to collect data from environmental sensors, from a participatory app and from external sources.

The data gathering process has been based on several methodologies following both qualitative (questionnaires/interviews) and quantitative (sensors, open public and private data) approaches.

The PULSE architecture furnishes the possibility to combine the collected data in several ways in order to have a dynamic spatio-temporal assessment effects of air quality on asthma risks and type 2 diabetes: the PULSE data in fact feed and validate dedicated predictive models on asthma risk and type 2 diabetes. Furthermore, the PULSE project offers the possibility to different stakeholders (PHOs, Community representatives, municipalities, health institutions, etc.) to join a common effort and collaborative work to raise awareness and address to a communitarian level the problem of urban air quality and its consequences on the health of the citizens.

7. References

EEA (European Environment Agency), 2017, European Union emission inventory report 1990-2015 under the UNECE Convention on Long-range Transboundary Air Pollution (LRTAP), Copenhagen, 149 pages



EEA (European Environment Agency), 2018. Air quality management. <https://www.eea.europa.eu/themes/air/explore-air-pollution-data#tab-air-quality-management> accessed in 2019.

Fraternali, P., Castelletti, A., Soncini-Sessa, R., Vaca Ruiz, C., Rizzoli, A.E., 2012. Putting humans in the loop: social computing for water resources management, *Environ Model Softw* 37, 68–77

Imhoff, M. L., Zhang, P., Wolfe, R. E., & Bounoua, L., 2010. Remote sensing of the urban heat island effect across biomes in the continental USA. *Remote sensing of environment*, 114(3), 504-513.

Manley, G. 1958. On the frequency of snowfall in metropolitan England. *Quarterly Journal of the Royal Meteorological Society*, 84, 70–72.

Ottaviano, M., Cabrera-Umpiérrez, M. F., & Waldmeyer, M. T. A., 2019. PULSE: Participatory Urban Living for Sustainable Environment. *Proceeding of IEEE 32nd International Symposium on Computer-Based Medical Systems (CBMS)*, Cordoba, Spain, pp. 62-63.

Ottaviano, M., Beltrán-Jaunsarás, M. E., Teriús-Padrón, J. G., García-Betances, R. I., González-Martínez, S., Cea, G., Arredondo Waldmeyer, M. T., 2019. Empowering Citizens through Perceptual Sensing of Urban Environmental and Health Data Following a Participative Citizen Science Approach. *Sensors*, 19(13), 2940.

Raaschou-Nielsen, O. 2012. 'Traffic air pollution and mortality from cardiovascular disease and all causes: a Danish cohort study', *Environmental Health* 11(60).

World Health Organization. (Ambient air pollution: a global assessment of exposure and burden of disease. World Health Organization), 2016. <https://apps.who.int/iris/handle/10665/250141>, burden of accessed in 2019

WHO (World Health Organization) Regional Office for Europe, 2012. *Environmental Health Inequalities in Europe*, 2012. http://www.euro.who.int/__data/assets/pdf_file/0010/157969/e96194.pdf accessed in 2019.

World Health Organization (World Health Organization) and UN Habitat, 2016. *Global report on urban health: equitable, healthier cities for urban development*. http://www.who.int/kobe_centre/publications/urban-global-report/en accessed on 2019.

World Health Organization (World Health Organization) and UN Habitat, 2016. *Global report on urban health: equitable, healthier cities for urban development*. http://www.who.int/kobe_centre/publications/urban-global-report/en accessed on 2019.

Acknowledgement

PULSE project has been founded by the European Union's Horizon 2020 research and innovation programme, and it is documented in the grant agreement No 727816. Specifically, PULSE has been founded under the call H2020-EU-3.1.5. in the topic SCI-PM-18-2016-Big Data supporting Public Health policies. More information on <http://www.project-pulse.eu>.

Temporal and spatial variability of atmospheric ammonia in the Lombardy region (Northern Italy)

Giovanni Lonati and Stefano Cernuschi

Civil and Environmental Engineering Department, Politecnico di Milano, Italy

giovanni.lonati@polimi.it

Abstract. This work investigates the spatial and temporal variability of atmospheric ammonia concentrations in the Lombardy region in Northern Italy, where its continuous measurement at hourly resolution began in 2007 at monitoring sites representative of three different land use areas (urban, rural, and mountain areas). Ammonia concentration data have been jointly elaborated with wind direction and speed to highlight the association between the origin of the air masses and the concentration levels observed at the monitoring sites far from the primary sources, essentially consisting of farming activities and cattle and pigs breeding activities located in the South-Eastern part of the region. The annual average concentrations of ammonia observed at urban (4-13 $\mu\text{g m}^{-3}$ range) and rural (17-35 $\mu\text{g m}^{-3}$ range) monitoring sites are in substantial agreement with literature data, which are however limited and strongly influenced by the measurement techniques used. The lowest concentration levels (0.4-5 $\mu\text{g m}^{-3}$ range) are observed at the monitoring sites in the mountain areas. Both the seasonal and daily time patterns of the concentrations appear strongly related to the features of the measurement sites, namely with regard to the monitoring sites most exposed to emissions of agricultural activities, whose seasonal practices determine emissions responsible for strong variations in the ammonia atmospheric presence. Conversely, in the mountain areas in the North of region, weather conditions of atmospheric circulation seem to play a more important role than local sources, with the highest concentrations occurring when the breezes transport ammonia-rich air masses from the Southern part of the region.

Keywords: Ammonia, Time pattern, Polar plots, Po valley

1. Introduction

The interest for atmospheric ammonia (NH_3) is linked to its fundamental role in the processes of ecosystems acidification and of water eutrophication originated by its deposition on sensitive environments (Zhang et al., 2012; Bobbink et al., 1998). Furthermore, NH_3 is the main basic compound capable of neutralizing atmospheric acid gases and thus is a precursor of secondary inorganic particulate material, whose effects are well known harmful to the environment and human health (Schlesinger and Cassee, 2003; Erisman and Schaap, 2004; Sutton et al., 2009). NH_3 can react with sulphur dioxide (SO_2) and nitrogen oxides (NO_x) to form ammonium sulphate ($(\text{NH}_4)_2\text{SO}_4$), ammonium bisulphate (NH_4HSO_4), and ammonium nitrate (NH_4NO_3), significantly contributing to fine particle mass ($\text{PM}_{2.5}$) with relevant implications for human health (Brunekreef and Holgate, 2002), for atmospheric visibility and for global radiation budgets (Clarisse et al., 2009; Horvath, 1992; Sutton et al., 1994). Modeling simulations (Heald et al., 2012; Schiferl et al., 2014) and air quality monitoring data (Gong et al., 2013) confirmed the specific role of NH_3 in the formation of secondary inorganic aerosol, with negative effects on both climate and air quality (Erisman et al., 2013; Paulot and Jacob, 2014). In spite of its environmental significance, atmospheric NH_3 still receives scarce attention and is not subject to air

quality standards. In the European Union atmospheric emission limits are fixed only for very few sources, such as waste incinerators where NH_3 is used in both catalytic and non-catalytic processes for NO_x emission control. However, national NH_3 emission reduction commitments for Member States are set by the National Emission Ceilings Directive for 2020 and 2030 (EU Directive 2016/2284/EU).

At the global scale NH_3 emissions have more than doubled since pre-industrial times because of both agricultural intensification and widespread use of fertilizer (Galloway et al., 2003). Actually, agricultural and livestock activities represent the largest and almost exclusive NH_3 source (Warner et al., 2016); people and traffic emissions may have an impact only in the non-agricultural regions, as suggested by the higher NH_3 ambient levels found in high densely populated areas (Suh et al., 1995). In the United States more than 82% of NH_3 emissions are attributable to the agricultural sector (US EPA National Emission Inventory, 2014) with a growing trend due to the combined effect of the increase of farming and animal husbandry and the use of nitrogen fertilizers. In the European Union, the agricultural sector is responsible for more than 94% of NH_3 emissions (EEA, 2017), but the limitations on the use of synthetic nitrogen fertilizers and the improvement of practices in the management of livestock waste have instead led to a slight emission reduction. However, increasing ambient concentration trends for NH_3 have been estimated in the orders of $2.6\% \text{ yr}^{-1}$ over the US, of $1.8\% \text{ yr}^{-1}$ over the European Union, and $2.3\% \text{ yr}^{-1}$ over China (Warner et al., 2017) also in consequence of the progressive decrease of acid gases in the atmosphere, in particular SO_2 , whose neutralization is an important pathway for the removal of ammonia.

Because of the combination of unfavourable morphology and climatology of the area and of the high density of emission sources, the river Po valley in Northern Italy is one of the European areas with critical issues for the values of the air quality indexes in general and also for the concentration levels of ammonia, making it one of the main NH_3 hot-spots worldwide (Figure 1, left panel). In particular, since also in the Lombardy region NH_3 emissions derive almost exclusively from agriculture, the major concern for atmospheric NH_3 is in the southernmost portion of the region, due to the high emission levels determined by the local agricultural and animal breeding activities (Figure 1, right panel).

Focusing on the Lombardy region, where for ten years the air quality monitoring network has been continuously collecting ambient NH_3 data, this work analyses the spatial variability and temporal evolution of its concentration levels, as well as the relationship between the observed concentrations and the features of the local anemological regime (wind speed and direction) in order to investigate the location of the sources that determine the most relevant impacts on air quality.

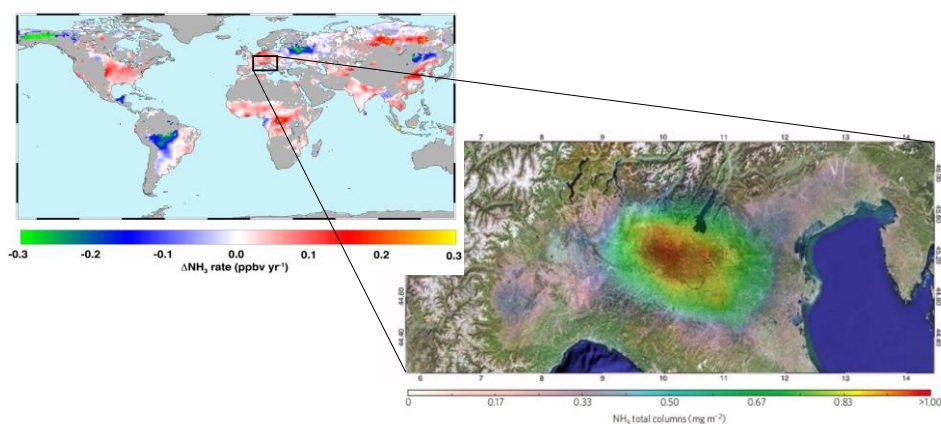


Figure 1. Left: annual change of NH_3 emission in 2002-2016 estimated from AIRS (Atmospheric Infrared Sounder, NASA) satellite measurements (Warner et al., 2017); right: average NH_3 concentration over Northern Italy in 2008 from IASI (Infrared Atmospheric Sounding Interferometer, MetOp satellite) satellite measurements (Clarisse et al., 2009)

2. Material and methods

2.1. NH_3 monitoring network in Lombardy

The air quality monitoring network operated by the Environmental Agency (ARPA) of the Lombardy region has begun to continuously collect data for atmospheric NH_3 at four sites in 2007. Progressively, the monitoring network has expanded and atmospheric NH_3 is currently measured at 11 stations, distributed almost all region at representative sites for air quality assessment, with generally very good annual data availability (more than 80% on annual basis, usually).

NH_3 concentrations are measured at hourly resolution with instruments based on the chemiluminescence technique that enables to determine NH_3 values indirectly. The measurement technique involves a sequential process with the catalytic transformation to NO of all the nitrogen compounds (NO , NO_2 , and NH_3) present in the air sample and the subsequent measurement of the total nitrogen N_t (expressed as NO). Thanks to the concurrent separate measurements of both NO and NO_2 (still expressed as NO), NH_3 concentration is obtained by difference, even taking into account the efficiency of the NH_3 catalytic conversion to NO. Such analytical determination is however complex and the final NH_3 ammonia may be inaccurate just because of the critical issues of the chemiluminescence technique (Villena et al., 2012; Dunlea et al., 2007) as related to the catalytic conversion efficiencies of the various compounds, in particular for NH_3 oxidation to NO (Capiaghi et al., 2014).

2.2. NH_3 datasets

In this work NH_3 data from 12 monitoring sites collected between 2007 and 2016 have been analyzed (Figure 2). Sites have been grouped together in three areas (urban, rural and mountain), according to the classification criteria adopted by ARPA for air quality monitoring sites. In particular, the urban group (sites S1-S5) includes the two sites in the city of Cremona (360000 inhab.), those in the metropolitan area of Milan (3200000 inhab.), and the site in the city of Pavia (70000 inhab.). In Cremona the monitoring sites are located North-Eastern of the city centre (S1-CR Fatebenefratelli), and on the outskirts of the city (S2-CR Gerre Borghi), close to the banks of the Po and potentially more exposed to the emissions generated in the surrounding countryside. In the metropolitan area of Milan sites are located in the heart of the city park of Monza (S3-Monza Parco), therefore not directly exposed to emission sources, and at an urban background site in the university area of Milan (S4-MI Pascal). In Pavia the monitoring site is located at the entrance of the city park North of the city centre (S5-Pavia-Folperti). The monitoring sites of the rural group (S6-S10) are all located in the Southern part of the region. In particular, S6-Corte de' Cortesi and S8-Bertonico site are placed in a territorial context which exposes them to the emissions of agricultural and livestock activities. Actually, S6 site is in a fairly isolated location, far from roads and industrial activities, but immediately near to a pig farm; S7 and S8 sites are in areas devoted to agricultural (cereals and fodder production) and livestock activities (beef and dairy cattle and pigs). The mountain group includes the sites of Colico (S11) and Moggio (S12). Actually, S11-Colico site is located in the last town on the Eastern shore of the Lake of Como, at about 250 m a.s.l.; thanks to its location the site is not exposed to ammonia sources but may be somewhat affected by transport phenomena of pollutants emitted in the plain area of the region because of the cyclic circulation of air masses that go up the Lake Como daily. Conversely, S12-Moggio site is really in a mountain area at about 1200 m a.s.l. in Valsassina valley, a pre-alpine area where there are no significant emission sources of ammonia. Nevertheless, as for S11 site, air masses coming from the plain, located to the South, can be channeled in the valley and reach the site affecting the local air quality. Wind speed and wind direction data used for bivariate analyses in order to investigate the relationship between the observed NH_3 concentrations of the characteristics of the local anemological regime, when not concurrently available at the air quality monitoring sites, have been taken from the nearest meteorological stations, as shown in Figure 2.

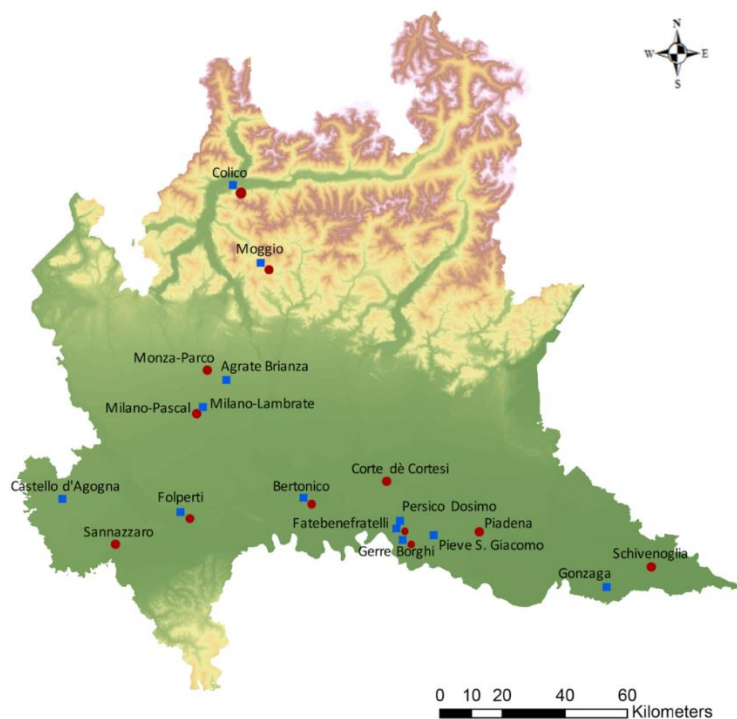


Figure 2. NH₃ monitoring sites (red circles) and meteorological stations for wind data (blue squares)

3. Results

3.1. NH₃ concentration levels

The range values for the annual average concentrations at the NH₃ monitoring sites of Lombardy are summarized in Table 1. At the sites of the urban group the minimum and maximum values are in the 4-8 $\mu\text{g m}^{-3}$ range and 10-13.5 $\mu\text{g m}^{-3}$ range, respectively. The urban sites, mostly located in urban background environments and not directly exposed to primary emissions, show significantly lower concentrations than those observed at the rural sites, and in particular of the sites (S6-Corte de' Cortesi, S7-Piadena, and S8-Bertonico) located in areas with a strong agricultural and animal husbandry vocation, where the annual average concentrations vary from a minimum of 21.9 $\mu\text{g m}^{-3}$ to a maximum of 81.7 $\mu\text{g m}^{-3}$. Interestingly, at the other two rural sites (S9 and S10) NH₃ levels are more similar to those of the urban sites, varying between a minimum of 4.8 $\mu\text{g m}^{-3}$ to a maximum of 15.5 $\mu\text{g m}^{-3}$.

The annual values observed at S6 site (41.5-81.7 $\mu\text{g m}^{-3}$), practically twice as high as those of sites S7 and S8 (17.7-35.8 $\mu\text{g m}^{-3}$), highlight the impact on air quality of the pig farm located at less than 100 m from the site itself: Thus, data from this site cannot be considered representative of an area with a generic rural vocation but of the local impact of NH₃ emissions from a very specific kind of human activity. On the other hand, the lower values observed at the S9 and S10 sites suggest that, despite their location in rural areas of the Lombardy plain, they are located in areas with a less intensive agricultural vocation and far from direct emission sources. The two sites of the mountain group display the lowest annual average concentrations, between 0.4 $\mu\text{g m}^{-3}$ and 5.8 $\mu\text{g m}^{-3}$, with maximum values substantially similar to the minimum values of urban sites. Thanks to their geographical position, especially for the S12-site, situated at relatively high altitude, in an area not densely populated and far from local emissive sources, the measured values can therefore be considered representative of the background level of ammonia in the atmosphere.

The time patterns of the annual average concentrations over the study period show irregular trends at the rural sites: from 2012 a strongly decreasing values are observed at S6 (from 70-80 $\mu\text{g m}^{-3}$ down to 40-45 $\mu\text{g m}^{-3}$), conversely a constant increase is observed at S8 (from 20 $\mu\text{g m}^{-3}$ up to 30 $\mu\text{g m}^{-3}$). At the urban sites and at the other rural sites the trends remain irregular and sometimes opposite, but with much smaller fluctuations; in general, the annual average concentrations at urban sites are around 10 $\mu\text{g m}^{-3}$ with a substantially stable temporal trend. A decreasing trend is observed instead for the mountain site S12-Moggio, with the annual average concentrations in the most recent past years getting down to a few $\mu\text{g m}^{-3}$.

Table 1. Range for NH_3 annual average concentration ($\mu\text{g m}^{-3}$, at 20 °C and 101.3 kPa) in Lombardy

Area	Monitoring site	Altitude (m a.s.l.)	Dataset	NH_3 annual average
Urban	S1-CR Fatebenefratelli	43	2011-2016	4.4 - 10.7
	S2-CR Gerre Borghi	36	2012-2016	8.2 - 13.2
	S3-Monza Parco	181	2013-2016	6 - 13.4
	S4-MI Pascal	122	2007-2016	5.8 - 12.6
	S5-PV Folperti	77	2013-2016	8.1 - 13.3
Rural	S6-Corte de' Cortesi	57	2007-2016	41.5 - 81.7
	S7-Piadena	30	2013-2014	17.7 - 23.5
	S8-Bertonico	65	2009-2016	21.9 - 35.8
	S9-Schivenoglia	12	2013-2016	11.3 - 15.5
Mountain	S10-Sannazzaro	87	2013-2016	4.8 - 7.6
	S11-Colico	229	2013-2016	0.4 - 5.8
	S12-Moggio	1194	2007-2016	0.4 - 4.1

The annual average levels measured at the sites are in substantial agreement with literature data, although the comparison is purely indicative as the methods of measurement, the temporal resolution and frequency of measurements may differ also noticeably. Nevertheless, especially for the urban sites of Lombardy, the NH_3 levels values are in line with those of similar sites, such as 5.4 $\mu\text{g m}^{-3}$ reported for Seoul in South Korea (Phan et al., 2013) and 15.9 $\mu\text{g m}^{-3}$ for Beijing in China (Meng et al., 2011). A substantial agreement is also observed for the rural sites, except for the S6-Corte de' Cortesi site, whose peculiarity has already been discussed. As for the sites in this study, both relatively low values, in the orders of 4-6 $\mu\text{g m}^{-3}$ (Wang et al., 2015; Zbieranowski and Aherne 2013; Meng et al., 2011) as at S10 site, and higher values, in the orders of 14-22 $\mu\text{g m}^{-3}$ (Erisman et al., 2001, Shen et al., 2011) as at sites S7, S8, and S9, are reported in the literature for rural sites worldwide.

3.2. Bivariate analyses

The association between the NH_3 concentration levels and the local features of the anemological regime has been investigated by means of graphic representations obtained by the joint analysis of the hourly NH_3 concentration and direction and wind speed data. In the resulting polar plot representations, the angle with respect to the y axis represents the direction of origin of the wind with respect to the North, the distance from the center, the speed of the wind, the color the average value of NH_3 concentration detected under such wind conditions (Carslaw and Ropkins, 2012). In practice, the color maps allow the concentration levels observed to be associated with certain wind conditions, thus providing indications on the location and distance of the emission sources that influence the quality of the air at the monitoring site. These representations can thus account for the presence of single sources (i.e.: large industrial complexes), highlighting the situations in which they are located upwind of the monitoring site, as well as for the presence of diffuse sources homogeneously distributed around the monitoring site (i.e.:

domestic heating in urban areas), for which, on the other hand, there is no clear association between high levels of concentration and wind direction.

This last case applies to the polar plots of this study that in general do not indicate a determining role of the wind but rather confirm the widespread nature of NH₃ emissions. However, the plots highlight some peculiarities of the different measurement sites. For the rural site S6, for example, in addition to a significant seasonal variability of NH₃ levels, the highest concentration associated to weak winds confirm the role of the nearby pig farm as a relevant local emission source. Furthermore, the substantial circular symmetry of the color plots reflects the location of the site at a point surrounded by agricultural land (Figure 3). Similar considerations apply to the S8 rural site, where however the effect of the local source responsible for the maximum values observed at site S6 is missing. The plots for the urban site in Milan also show a circular symmetry in correspondence of weak winds (Figure 4), but they show, regardless of the season, the lowest NH₃ concentration values for North-North Westerly strong winds (> 4 m s⁻¹). These conditions occur during foehn episodes, actually quite rare on an annual basis (7-10 events), which bring clean air masses from the Alps down to the plain of Lombardy, lowering the concentration levels of all the atmospheric pollutants (Mira-Salama et al., 2008).

Conversely, the association of high NH₃ concentration values with medium-intensity winds blowing from East to East South East in autumn suggests transport phenomena from the Southern part of the region, where concentration levels are particularly high, towards the foothills area of the Alps. The presence of these transport phenomena is also highlighted in the summer plot of the mountain site S12, where the highest concentrations are observed concurrently with winds blowing from South West (Figure 5). As already reported for other pollutants (Dosio et al., 2002), the masses of air moving towards the North are channeled along the Eastern branch of Lake Como, and from there to the Valsassina valley, bringing with it the ammonia emitted from agricultural activities in the plain area of Lombardy. In winter, this phenomenon is not evident and apparently we observe, instead, a separation between the air masses that insist on the plain and those of the mountain area, favored also by the frequent phenomena of thermal inversion typical of the Po valley during the cold seasons.

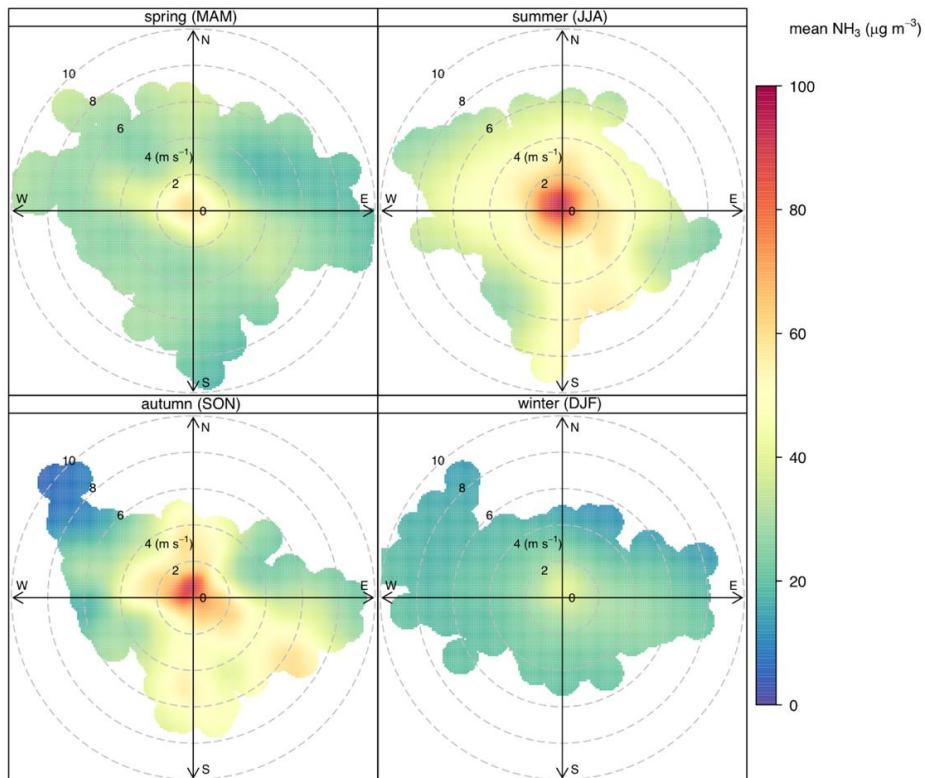


Figure 3. Seasonal polar plots for NH_3 hourly concentrations at rural site S6

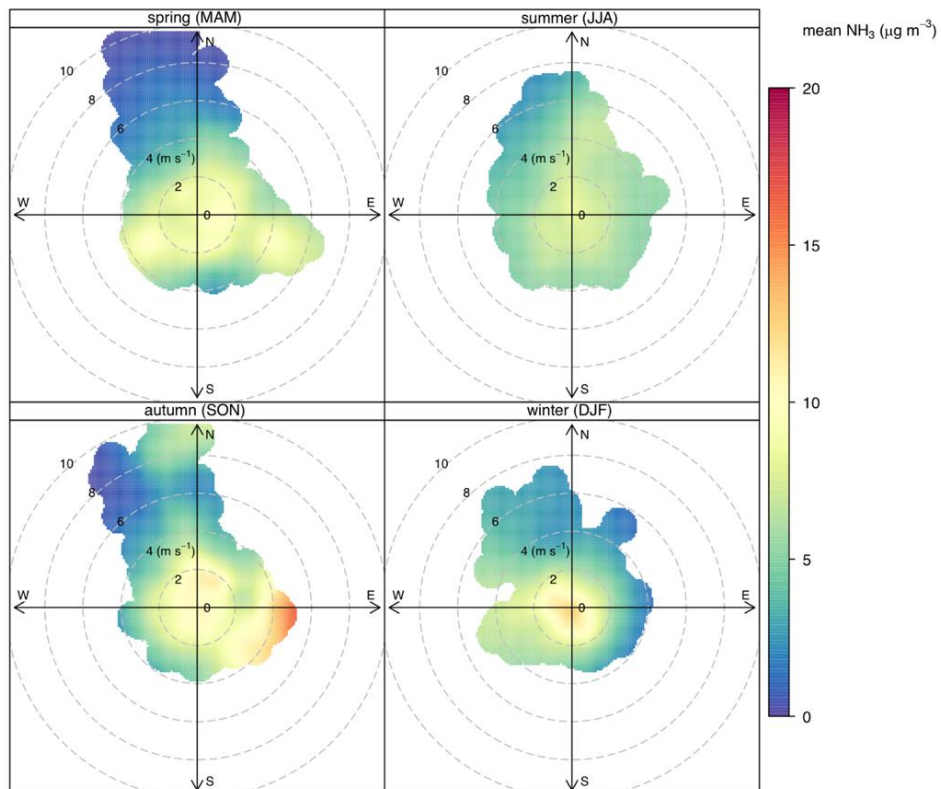


Figure 4. Seasonal polar plots for NH_3 hourly concentrations at urban site S4

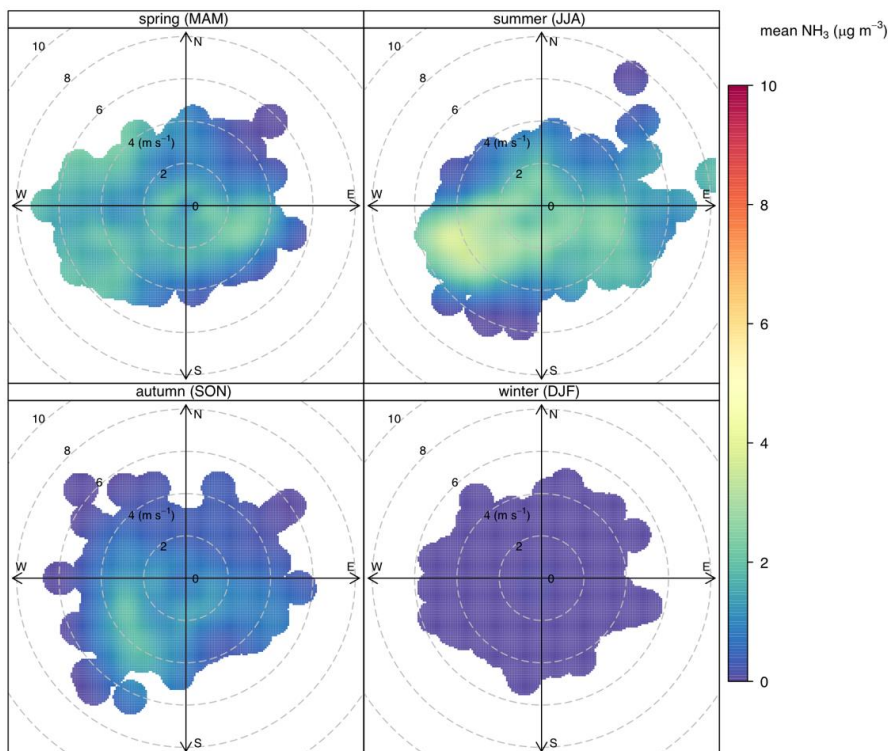


Figure 5. Seasonal polar plots for NH_3 hourly concentrations at mountain site S12

The association between high NH_3 concentrations and given wind conditions highlighted by the polar plots is further confirmed by the conditional wind roses for hourly concentration values higher than the 90th percentile of the entire NH_3 data series. This analysis confirms the presence of transport phenomena of NH_3 -rich air masses from the Southern part of the region to the northernmost areas. In particular, for the two sites in Milan metropolitan area the highest concentrations are observed more frequently in correspondence of South-easterly winds, while in the case of S12 mountain site of Moggio for winds blowing from West-South West.

4. Conclusions

In the Lombardy region atmospheric NH_3 levels show a marked spatial and temporal variability with the highest concentrations in rural areas (annual averages in the orders of 20-80 $\mu\text{g m}^{-3}$) and the lowest in at mountain sites (annual average less than 6 $\mu\text{g m}^{-3}$). At urban sites, the annual average concentrations are usually around 10 $\mu\text{g m}^{-3}$ with a substantially stable time trend from 2007. The NH_3 levels observed in Lombardy are substantially in agreement with literature data for similar sites, even though data are still limited and strongly influenced by the measurement techniques used.

The temporal pattern of concentrations is strongly dependent on the features of the measurement sites, namely for the rural sites more directly exposed to the emissions of agricultural activities. Seasonal practices of agricultural activities determine local emissions responsible for strong variations in atmospheric NH_3 concentration levels, especially in early spring and autumn. This variability, although attenuated, is also found at urban sites, confirming the absolutely dominant role of the emissions of the agricultural and zootechnical sector, already highlighted by the emission inventories. Furthermore, the joint analysis of the concentration data local wind conditions has highlighted the association between concentration levels and the origin of air masses, showing that the highest concentration values in urban

areas occur when the breezes carry NH₃-rich air masses from the areas at high emission intensity of the Po Valley.

5. References

- Bobbink, R., Hornung, M., Roelofs, J.G.M., 1998. The effects of air-borne nitrogen pollutants on species diversity in natural and semi-natural European vegetation. *Journal of Ecology*. 86, 717-738.
- Brunekreef, B., Holgate, S.T., 2002. Air pollution and health. *Lancet*. 360, 1233-1242.
- Capiaghi, V., Pirovano, G., Colombi, C., Lonati, G., Riva, G.M., Toppetti, A., Gianelle, V., Balzarini, A., 2014. Ricostruzione modellistica dell'ammoniaca atmosferica in Pianura Padana. Proceedings of PM2014 – Sesto convegno sul particolato atmosferico, May 20-23, 2014, Genova, Italy.
- Carslaw, D.C., Ropkins K., 2012, Openair - an R package for air quality data analysis. *Environmental Modelling & Software*. 27-28, 52-61.
- Clarisse, L., Clerbaux, C., Dentener, F., Hurtmans, D., Coheur, P.-F., 2009. Global ammonia distribution derived from infrared satellite observations. *Nature Geoscience*. 2, 479-483.
- Dosio, A., Galmarini, S., Graziani, G., 2002. Simulation of the circulation and related photochemical ozone dispersion in the Po plains (Northern Italy): Comparison with the observations of a measuring campaign. *Journal of Geophysical Research* 107, D18, 8189.
- Dunlea, E.J., et al. 2007. Evaluation of nitrogen dioxide chemiluminescence monitors in a polluted urban environment. *Atmospheric Chemistry and Physics*. 7, 2691-2704.
- Erismann, J.W., Otjes, R., Hensen, A., Jongejan, P., van den Bulk, P., Khlystov, A., Möls, H., Slanina, S., 2001. Instrument development and application in studies and monitoring of ambient ammonia. *Atmospheric Environment*. 35, 1913-1922.
- Erismann, J.W., Schaap, M., 2004. The need for ammonia abatement with respect to secondary PM reductions in Europe. *Environmental Pollution*. 129, 159-163.
- Erismann, J. W., Bleeker, A., Galloway, J., Sutton, M., 2007. Reduced nitrogen in ecology and the environment, *Environmental Pollution*. 150, 140-149.
- Erismann, J.W., Galloway, J.N., Seitzinger, S., Bleeker, A., Dise, N.B., Petrescu, R., Leach, A.M., de Vries, W., 2013. Consequences of human modification of the global nitrogen cycle, *Philosophical Transactions of The Royal Society*. 368, 20130116.
- European Environmental Agency 2017. European Union emission inventory report 1990–2015 under the UNECE Convention on Long-range Transboundary Air Pollution (LRTAP).
- European Union (EU), 2016. Directive 2016/2284 of the European Parliament and of the Council of 14 December 2016 on the reduction of national emissions of certain atmospheric pollutants, amending Directive 2003/35/EC and repealing Directive 2001/81/EC. OJ L 344, 17.12.2016, 1-31.
- Galloway, J.N., Aber, J.D., Erismann, J.W., Seitzinger, S.P., Howarth, R.W., Cowling, E.B., Cosby, B J., 2003. The nitrogen cascade. *BioScience*. 53, 341-353.
- Gong, L., Lewicki, R., Griffin, R.J., Tittel, F.K., Lonsdale, C.R., Stevens, R.G., Pierce, J.R., Malloy, Q.G.J., Travis, S.A., Bobmanuel, L.M., Lefer, B.L., Flynn, J.H., 2013. Role of atmospheric ammonia in particulate matter formation in Houston during summertime. *Atmospheric Environment*, 77, 893-900.
- Heald, C.L., Collett Jr., J.L., Lee, T., Benedict, K.B., Schwandner, F.M., Li, Y., Clarisse, L., Hurtmans, D.R., Van Damme, M., Clerbaux, C., Coheur, P.-F., Philip, S., Martin, R.V., Pye, H.O.T., 2012. Atmospheric ammonia and particulate inorganic nitrogen over the United States. *Atmospheric Chemistry and Physics*. 12, 10295-10312.



- Horvath, H., 1992. Effects on visibility, weather and climate, in: Atmospheric acidity: sources, consequences and abatement, edited by Radojevic, M. and Harrison, R. M., chapter 13, London: Elsevier Applied Science.
- Meng, Z.Y., Lin, W.L., Jiang, X.M., Yan, P., Wang, Y., Zhang, Y.M., Jia, X.F., Yu, X.L., 2011. Characteristics of atmospheric ammonia over Beijing, China. *Atmospheric Chemistry and Physics*. 11, 6139-6151.
- Mira-Salama, D., Van Dingenen, R., Gruening, C., Putaud, J.-P., Cavalli, F., Cavalli, P., Erdmann, N., Dell'Acqua, A., Dos Santos, S., Hjorth, J., Raes, F., Jensen, N.R., 2008. Using Föhn conditions to characterize urban and regional sources of particles. *Atmospheric Research*. 90, 159-169.
- Paulot, F., Jacob, D.J., 2014. Hidden cost of U.S. agricultural exports: Particulate matter from ammonia emissions. *Environmental Science and Technology*. 48, 903–908.
- Phan, N.-T., Kim, K.-H., Shon, Z.-H., Jeon, E.-C., Jung, K., Kim, N.-J., 2013. Analysis of ammonia variation in the urban atmosphere. *Atmospheric Environment*. 65, 177-185.
- Schiferl, L.D., Heald, C.L., Nowak, J.B., Holloway, J.S., Neuman, J.A., Bahreini, R., Pollack, I.B., Ryerson, T.B., Wiedinmyer, C., Murphy, J.G., 2014. An investigation of ammonia and inorganic particulate matter in California during the CalNex campaign. *Journal of Geophysical Research: Atmospheres*. 119, 1883–1902.
- Schlesinger, R.B., Cassee, F., 2003. Atmospheric secondary inorganic particulate matter: the toxicological perspective as a basis for health effects risk assessment. *Inhalation Toxicology*. 15, 197-235.
- Shen, J., Liu, X., Zhang, Y., Fangmeier, A., Goulding, K., Zhang, F., 2011. Atmospheric ammonia and particulate ammonium from agricultural sources in the North China Plain. *Atmospheric Environment* 45, 2011, 5033-5041.
- Suh, H.H., Allen, G.A., Koutrakis, P., Burton, R.M., 1995. Spatial variation in acidic sulphate and ammonia concentrations within metropolitan Philadelphia, *J. Air Waste Manage. Assoc.* 45, 442-452.
- Sutton, M.A., Asman, W.A.H., Schjørring, J.K., 1994. Dry deposition of reduced nitrogen. *Tellus*. 46B, 255-273.
- Sutton, M.A., Reis, S., Baker, S.M.H., 2009. *Atmospheric Ammonia. Detecting Emission Changes and Environmental Impacts*. Springer, pp. 464.
- Villena, I., Bejan, R., Kurtenbach, P., Wiesen, P., Kleffmann, J., 2012. Interferences of commercial NO₂ instruments in the urban atmosphere and in a smog chamber. *Atmospheric Measurement Techniques*. 5, 149-159.
- Warner, J.X., Wei, Z., Strow, L.L., Dickerson, R.R., Nowak, J.B., 2016. The global tropospheric ammonia distribution as seen in the 13-year AIRS measurement record. *Atmospheric Chemistry and Physics*, 16, 5467-5479.
- Warner, J.X., Dickerson, R.R., Wei, Z., Strow, L.L., Wang, Y., Liang, Q., 2017. Increased atmospheric ammonia over the world's major agricultural areas detected from space. *Geophysical research letters*. 44(6), 2875-2884.
- Zbieranowski, A.L., Aherne, J., 2013. Ambient concentrations of atmospheric ammonia, nitrogen dioxide and nitric acid in an intensive agricultural region., *Atmospheric Environment*. 70, 289-299.
- Zhang, L., Jacob, D.J., Knipping, E.M., Kumar, N., Munger, J.W., Carouge, C.C., van Donkelaar, A., Wang, Y.X., Chen, D., 2012. Nitrogen deposition to the United States: Distribution, sources, and processes. *Atmospheric Chemistry and Physics*. 12, 4539-4544.

Particle number concentrations in the Po valley (Northern Italy) in wintertime: comparison between urban and rural sites

Giovanni Lonati¹ and Arianna Trentini²

¹ Civil and Environmental Engineering Department, Politecnico di Milano, Italy

² ARPAE - Regional Agency for prevention, environment and energy of Emilia-Romagna, Bologna, Italy

giovanni.lonati@polimi.it

Abstract. The temporal and spatial variability of particle number concentration (PNC) levels and of the related particle number size distribution (PNSD) over the Po valley in Northern Italy is investigated based on data collected during an intensive multi-site monitoring campaign conducted in February 2014. Measurements were concurrently taken at three urban sites, in the cities of Milano, Bologna, and Padova, and at two rural sites, San Pietro Capofiume and Ispra, on the South-Eastern and North-Western side of the valley. PNC data have been collected by means of an Ultrafine Particle Monitor (UPM, TSI 3031), two Fast Mobility Particle Sizers (FMPS, TSI 3091), two Differential Mobility Particle Sizers (DMPS, TSI); investigated particle size ranges were 3-600 nm for both FMPS and DMPS and 20-1000 nm. Total PNC data and size-segregated PNC for 5 size bins (20-30 nm, 30-50 nm, 50-70 nm, 70-100 nm, and 100-200 nm), have been processed on hourly time resolution. Average hourly data for PNC were in the $5 \cdot 10^3$ - $1.1 \cdot 10^4$ cm⁻³ range, with the lowest values at the rural sites and the highest in the city of Milan. At the urban sites the PNC daily time pattern showed two main peaks on the morning and evening traffic rush hours; conversely, at the rural sites it was mainly driven by the boundary layer evolution and much less affected by source activity. Ultra fine particles (UFPs, 20-100 nm size range) accounted for about 75% of PNC at urban sites and for about 63% at the rural sites. On rush hours at the urban sites, PNC of the particles in the smallest size range (20-50 nm) greatly increased, thus confirming that motor vehicle emissions were the main source of UFPs, as also suggested by their correlation with NO_x and CO concentrations.

Keywords: Particle number, Size distribution, Po valley, Cluster analysis.

1. Introduction

The Po valley in Northern Italy is a well-known hot-spot for atmospheric pollution, especially for particulate matter (PM), whose air quality limits are frequently exceeded at monitoring sites. However, because the current air quality standards for PM are mass based, particle number concentration (PNC) and related size distribution (PNSD) are not routinely measured and their knowledge is still scarce for this area. Some literature studies focused on the nucleation and growth of new particles in Northern Italy (Hamed et al., 2007; Rodriguez et al., 2005); Rodriguez et al., 2007 compared number size distribution of urban fine aerosols in Milan, Barcelona and London; Lonati et al., 2011 investigated the multimodal structure of the PNSD at an urban background site in Milan while Bigi and Ghermandi, 2011 focused on the PNSD at an urban background site in the central part of the Po valley. Poluzzi et al., 2015 report seasonal data for particle number concentration in the Emilia-Romagna region and Wang et al., 2016 report size resolved PNC measured at different sites within a mid-sized city in the same region. A few studies investigated exposure concentration levels to ultrafine particles in urban microenvironments in Milan (Cattaneo et al., 2009; Ozgen et al., 2016) and in other cities in the Po valley (Lonati et al., 2017).

However, all these works usually rely on monitored data from just one single site and the comparison between concentration levels concurrently measured at different sites is not addressed, thus. This work brings a piece of knowledge of the latter issue as it discusses the temporal and spatial variability of PNC levels and PNSD over the Po valley with reference to five sites where concurrent measurements were taken during a dedicated monitoring campaign conducted in February 2014 in the framework of the POAIR (Po valley atmospheric Aerosol Intensive Research) project.

2. Material and methods

2.1. Monitoring period

The monitoring campaign was performed in 2014 from February 7th to February 27th, during an intensive multi-site field campaign intended to investigate the temporal and spatial variations of particle number concentration in the Po valley area. Compared with the typical winter weather conditions in this area, February 2014 was warmer, more unstable and rainy during the first and last decade and rather warm during the central decade because of an anticyclonic configuration extending its influence over the entire Po valley. Average values for the daily mean temperature, wind speed and relative humidity were respectively in the orders of 8.5 °C, 2 m s⁻¹, and 80%, with limited variations among monitoring sites. A few rain events occurred, with cumulative rainfall over the whole monitoring period ranging between 60 mm on the Eastern side and 95 mm on the Western side of the area.

2.2. Monitoring sites and instruments

Measurements were concurrently taken at five sites: three urban sites, in the cities of Bologna (BO - 400000 residents), Milano (MI - 1350000 res.), and Padova (PD - 200000 res.), and at two rural background sites, San Pietro Capofiume (SPC-R) and Ispra (ISP-R), on the South-Eastern and North-Western side of the valley (Figure 1). The urban sites in Bologna (BO-UB) and Milano (MI-UB) have the features of urban background sites, the former on the Northern outskirts of the city, nearby arterial roads and major highways, the latter in the University campus, not directly exposed to primary emission sources. The site in Padova (PD-MX) is actually in suburban area, located South-West of the city centre, with a mixture of urban, industrial and rural features. The SPC-R rural site is located in a flat area surrounded by cultivated fields; conversely, the site in Ispra shows an urban/rural mixed behaviour and recent studies identify this site as a rural background but still heavily influenced by human emissions (Henne et al., 2010; Sandrini et al., 2014).

Depending on the monitoring site PNC data have been collected by means of an Ultrafine Particle Monitor (UPM), a Fast Mobility Particle Sizer (FMPS), a Differential Mobility Particle Sizer (DMPS) and a Twin Differential Mobility Particle Sizer (T-DMPS). The instrument used at the monitoring sites, the corresponding investigated particle size range, time resolution, and number of size bins are summarized in Table 1. SMPS available at BO-UB site data were only used to correct FMPS data following Jeong and Evans, 2009. Raw PNC data have been processed in order to obtain total PNC data at actual ambient conditions on hourly time resolution and size-resolved PNC data for the same 6 size intervals (20-30 nm, 30-50 nm, 50-70 nm, 70-100 nm, 100-200 nm, and > 200 nm) at all the monitoring sites.

Table 1. Monitoring sites and instruments

Site	Size range	Time resolution	Size bins	Instrument
ISP-R	10-800 nm	10 min	45	TSI -DMPS
MI-UB	20-1000 nm	10 min	6	TSI UPM 3031
PD- MX	5.6-560 nm	1 min	32	TSI FMPS 3091
SPC-R	3-600 nm	10 min	119	TSI T-DMPS
BO-UB	5.6-560 nm	1 min	32	TSI FMPS 3091
	3-600 nm	5 min	148	TSI SMPS 3093

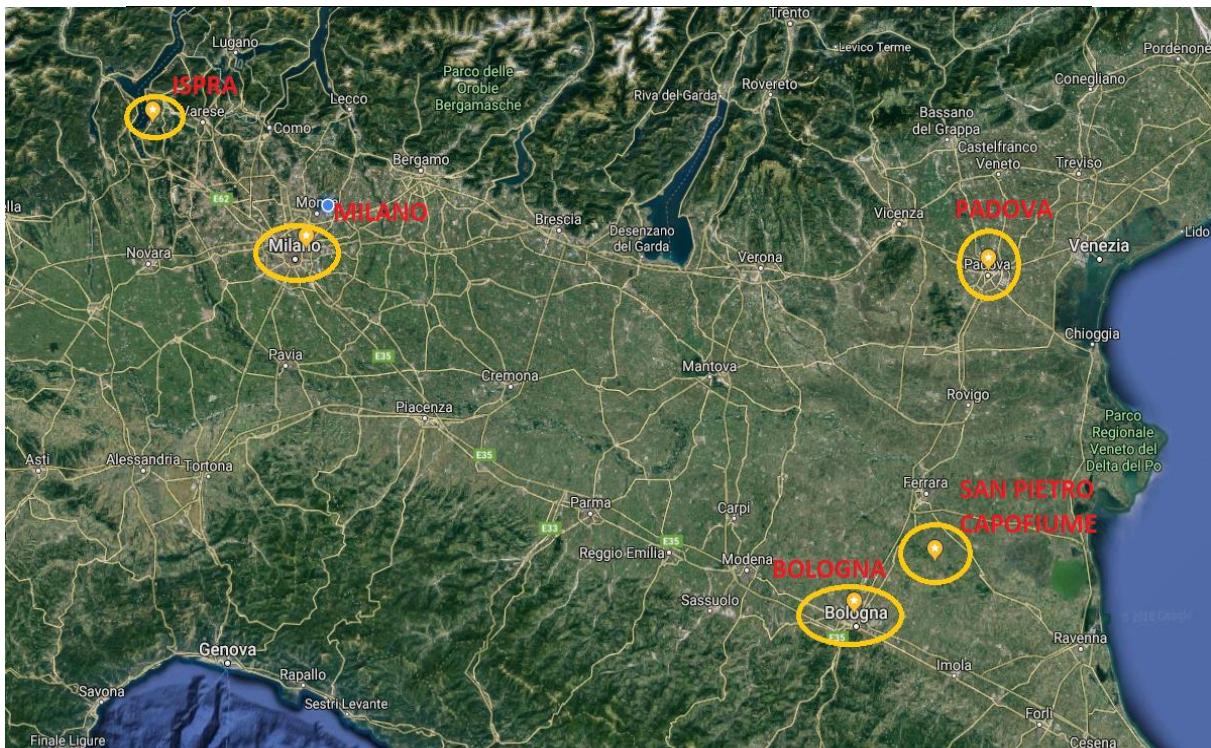


Figure 1. Location of the monitoring sites in the Po valley

3. Results

3.1. Particle number concentration

Box-plots for the hourly and daily average concentration for the total particle number are presented in Figure 2. For both the averaging times, the entire dataset from MI-UB site is shifted towards higher values than at the other sites. Hourly data for PNC are in the $3 \cdot 10^3$ - $3.8 \cdot 10^4$ cm^{-3} range, with a median of $1.0 \cdot 10^4$ cm^{-3} and a slightly higher mean of $1.1 \cdot 10^4$ cm^{-3} . Data distribution is right-skewed distribution, with a number of data in excess of $2.1 \cdot 10^4$ cm^{-3} and up to a maximum of $3.8 \cdot 10^4$ cm^{-3} . Because of the longer averaging time that smooths hourly peaks, the distribution of daily data is less scattered ($\text{CV} = 0.23$ vs. 0.45 for 1-h data) and skewed (Pearsons' skewness = 0.35 vs. 0.65 for 1-h data), with PNC values ranging between $8.1 \cdot 10^3$ - $1.7 \cdot 10^4$ cm^{-3} and almost coincident mean and median around $1.1 \cdot 10^4$ cm^{-3} . Among the other urban sites PD-MX is the most similar to MI-UB, though the median values of both distributions are well below 10^4 cm^{-3} ($7.5 \cdot 10^3$ and $8.5 \cdot 10^3$ cm^{-3} for 1-h and 24-h data, respectively); however, peak hourly data in excess of $2.0 \cdot 10^4$ cm^{-3} up to $3.4 \cdot 10^4$ cm^{-3} have been observed, even though less frequently than at MI-UB site. Conversely, BO-UB site is characterized by significantly lower concentration values ($8 \cdot 10^3$ - $1.8 \cdot 10^4$ cm^{-3} range, $4.5 \cdot 10^3$ cm^{-3} as median for 1-h data) not only with

respect for the urban sites but also for the SPC and ISP rural sites. In practice, PNC levels at BO-UB are similar to those of SPC-R, whereas ISP-R is actually characterized by intermediate PNC levels between the urban PD-MX site and the BO-UB and SPC-R sites. The peculiarity of PNC levels at BO-UB site compared with the other urban sites is likely due to the site location, not really in a densely built environment as on the city outskirts. Actually, the inspection of polar plots (Carslaw and Ropkins, 2012) for PNC levels in relation to wind speed and direction (Figure 3) points out that the whole urban agglomeration is the main source for airborne particles. Additionally, the similarity of BO-UB site with SPC-R site, which is only at about 30-km crow-fly distance, is also stated by the high correlation ($R = 0.86$) between PM_{2.5} daily concentrations measured during the monitoring campaign. Thus, BO-UB site has displayed rural and regional background features more than urban features, at least for the winter period of this campaign. On the other hand, PNC data collected at ISP-R site confirm its urban/rural mixed behaviour as suggested by both the concentration levels ($0.9 \cdot 10^3$ - $2.2 \cdot 10^4 \text{ cm}^{-3}$ range, $6.6 \cdot 10^3 \text{ cm}^{-3}$ as median for 1-h data) and the occurrence of relatively high concentration events, already observed at urban sites.

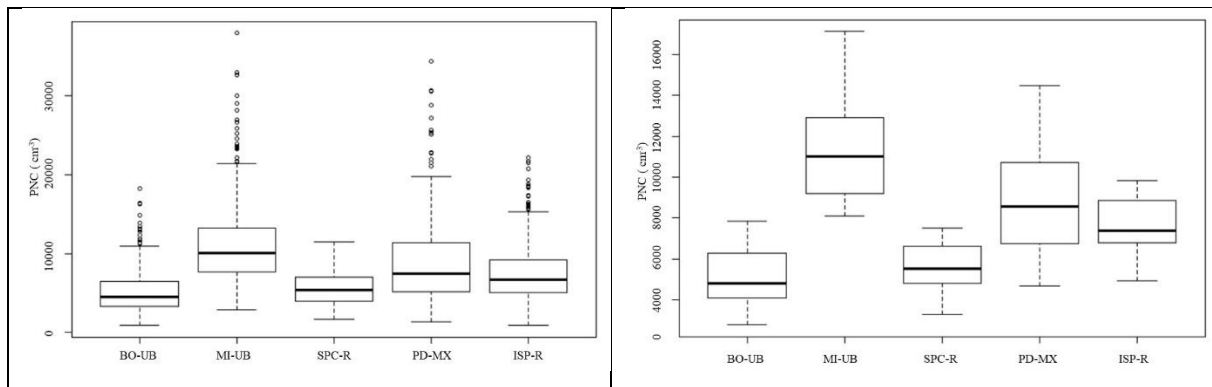


Figure 2. Hourly (left panel) and daily average total PNC (cm^{-3})

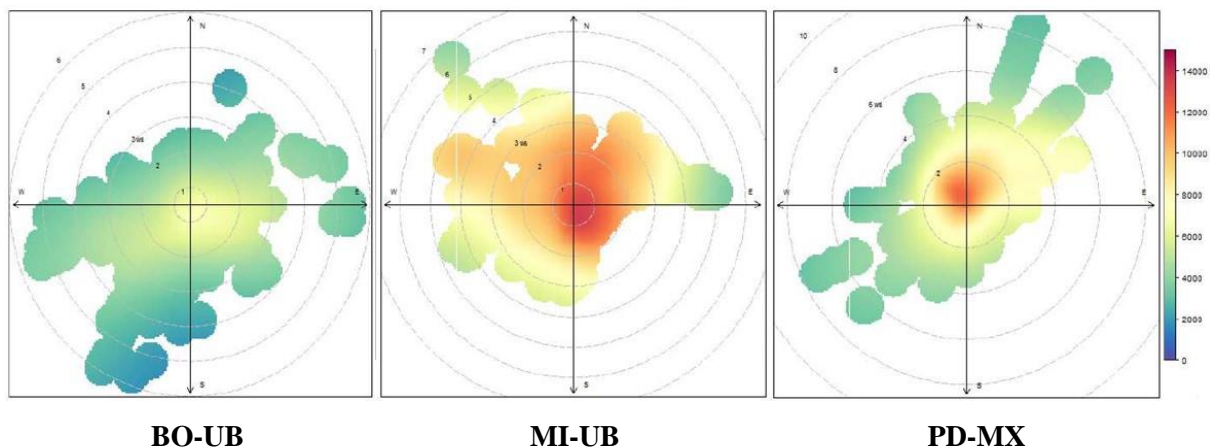


Figure 3. Polar plots for hourly total PNC (cm^{-3}) at urban sites

The measured PNC levels are in agreement with literature data for urban sites in Europe ($8 \cdot 10^3$ - $4 \cdot 10^4 \text{ cm}^{-3}$ range) and with previous results for the Po valley area: Poluzzi et al. 2015 report a wintertime mean concentration of $1.4 \cdot 10^4 \text{ cm}^{-3}$ ($6.8 \cdot 10^3$ - $2.2 \cdot 10^4 \text{ cm}^{-3}$ range); Lonati et al. 2013 report concentration levels in the $5 \cdot 10^3$ - $1.1 \cdot 10^4 \text{ cm}^{-3}$ range at an urban background site in a mid-sized city in the centre of the Po valley and in the $6 \cdot 10^3$ - $9 \cdot 10^3 \text{ cm}^{-3}$ range at a rural site. Based on data from the German Ultrafine Aerosol

Network for particles in the 20-800 nm size range, Sun et al., 2019 report multi-annual mean values for urban background and regional background sites of $4.9 \cdot 10^3 \text{ cm}^{-3}$, and $3.3 \cdot 10^3 \text{ cm}^{-3}$ respectively.

3.2. Particle size distribution and cluster analyses

Particle number size distribution (PNSD) analyses are performed for the same set of six size intervals (20-30 nm, 30-50 nm, 50-70 nm, 70-100 nm, 100-200 nm, and > 200 nm) common to all the monitoring sites. In general, all the PNSDs present an Aitken mode, located in the 60-100 nm range; however, the location and the magnitude of such mode are characterized by both spatial (i.e.: site-dependent) and temporal (i.e.: day, time of the day) variability. Because of the limited size range investigated, neither the presence of a nucleation mode nor that of a coarse mode can be observed. Nevertheless, especially at the urban sites, the structure of PNSDs suggests that a first mode below 20 nm, prevailing on the observed Aitken mode, is actually present, coherently with the multimodal structure of PNSDs reported in literature for urban sites (Lonati et al., 2011). The variability of daily averaged PNSDs was investigated through k-means cluster analysis, intended to group together days with a common pattern for the size distribution of airborne particles. Cluster analysis results are presented in Figure 4 for MI-UB site where four well-separated clusters were recognized; the four corresponding cluster-averaged PNSDs are shown in the right panel of Figure 4. Cluster #1 and cluster #4 group days with high ($1.5 \cdot 10^4 \text{ cm}^{-3}$ as cluster average) and low ($8 \cdot 10^3 \text{ cm}^{-3}$) PNC levels; Cluster #2 and cluster #3 group days with intermediate PNC levels (both around $1.1 \cdot 10^4 \text{ cm}^{-3}$ as cluster average) but with a different location of the Aitken mode, shifted towards a slightly larger diameter in Cluster #3. Similar 4-cluster results have been obtained for the other monitoring sites, though with site-related concentration levels and PNSDs. For each site the same k-means clustering approach was also performed based on daily averaged air pollution data (NO_x , PM_{10} , $\text{PM}_{2.5}$, SO_2 , CO) and meteorological parameters (temperature, wind speed, relative humidity, solar radiation, rainfall). The comparison with the clustering results for the PNSDs shows a stronger correspondence in the cluster composition with air quality levels than weather conditions. Actually, the high-PNC days of cluster#1 are concurrently characterized by high concentration levels for criteria pollutants (for cluster#1 at MI-UB site: $\text{PM}_{10} \mu\text{g m}^{-3}$ and $\text{PM}_{2.5}$ about $38 \mu\text{g m}^{-3}$).

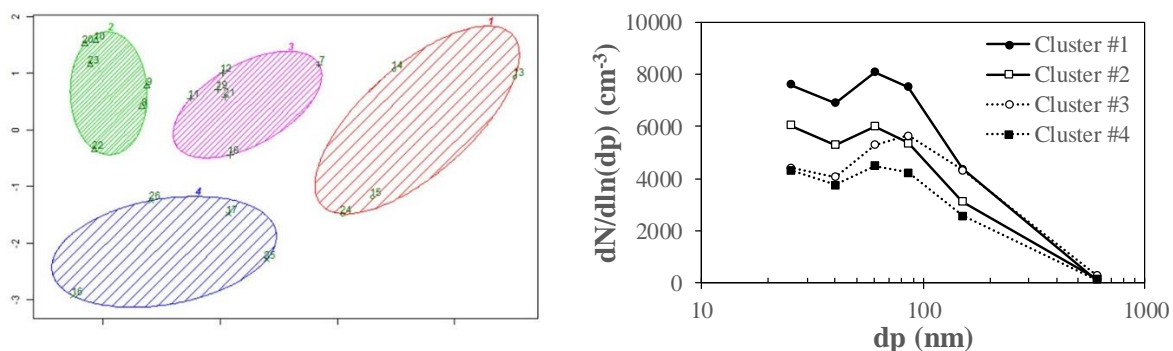


Figure 4. Principal components plot for daily averaged size distributions at MI-UB site (left); average PNC size distributions for the four identified clusters (right)

Intra-day variability of the PNSD was analysed through the investigation of the time pattern of size-resolved PNC. At the three urban sites and the ISP-R site the hourly pattern of the total PNC on weekdays displays two clear peaks on the morning and evening rush hour (Figure 5, top-left); conversely, at the SPC-R site the time pattern is quite flat, regardless for the day of the week, missing the two peaks generated by traffic emissions in the urban areas (Figure 5, top-right). The role of road traffic as a source of particles in urban areas is confirmed by the similar time patterns observed for NO_x and CO concentration as well as by the lack of the morning peak on Sundays. However, the influence of the diurnal evolution of the atmospheric conditions is also highlighted by the low PNC levels on the early afternoon due to the enhanced dispersion favoured by the vertical growth of the boundary layer.

The evolution of the boundary layer appears to be the main driver for the PNC time pattern at the SPC-R rural site, where PNC levels are much less affected by the activity of anthropogenic sources. Size-resolved analysis for urban sites shows that on both peak hours the PNSD is dominated by particles in the smallest size bins (20-30 nm and 30-50 nm), also suggesting the presence of a main mode below 20 nm (Figure 5, bottom-left). On the contrary on night time hours the PNSD is more uniform, likely without a sub-20 nm mode, and with a main Aitken mode around 100 nm also driven by phenomena of particulate formation and particle growth for condensation of semi-volatile precursors favoured by the low temperature.

3.3. Inter-site comparisons

As discussed in Section 3.1, PNC levels at the monitoring sites are quite different, essentially depending on the site location. Actually, the pairwise correlation analyses for the time series of the daily averaged PNC resulted in R values usually in the order of 0.5, with a highest R = 0.64 for PD-MX and ISP-R and a lowest R = 0.08 for SPC-R and ISP-R, confirming the already mentioned particular features of this latter site. Conversely, the hourly time patterns of both concentration levels and PNSD show stronger similarities, especially for the sites located in urban environments, with a behavior clearly different for the rural SPC-R site only. In order to gain a deeper insight of the temporal and spatial variability on both PNC levels and related size distributions, cluster analysis has been performed based on the entire dataset of the daily averaged size distributions. As shown in Figure 6, four clusters were identified have been rather different composition.

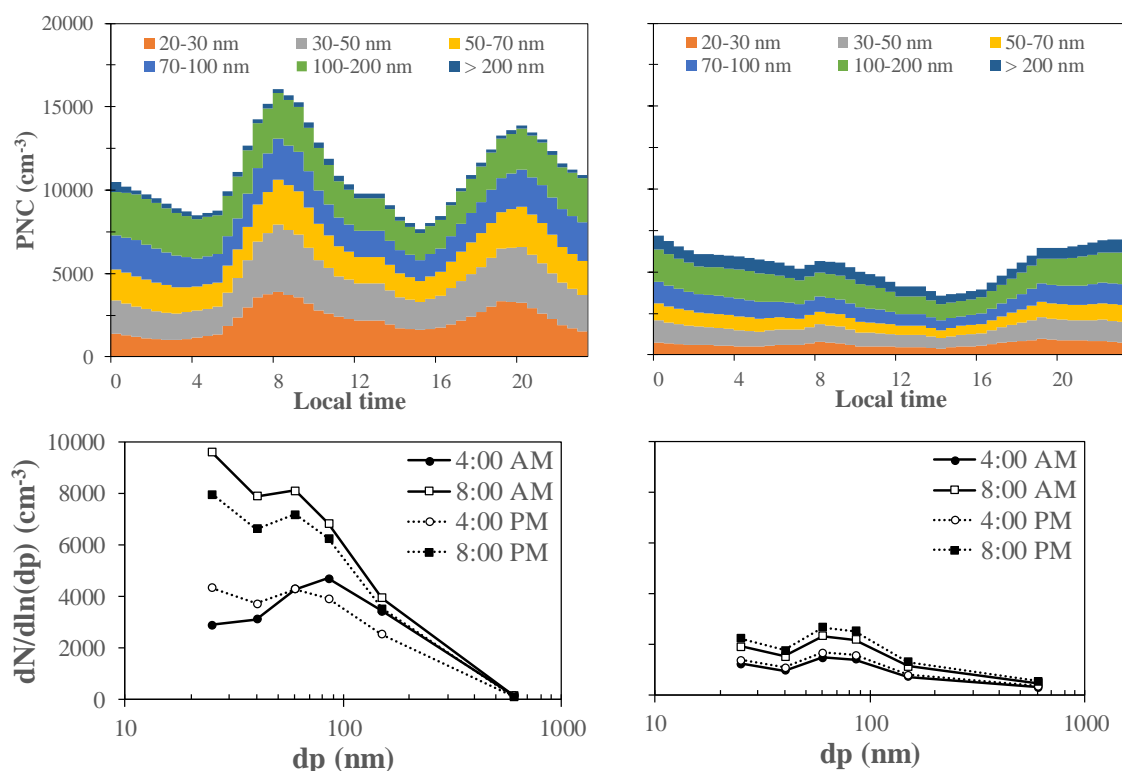


Figure 5. Hourly pattern of size-resolved PNC and related PNSDs at MI-UB site (left column) and at SPC-R site (right column)

Cluster #1 includes data only from MI-UB and PD-MX sites, corresponding to days with high PNC concentrations (cluster average: $1.2 \cdot 10^4 \text{ cm}^{-3}$), but mostly (68%) from the former site in Milan. Cluster #2 and Cluster #3 group together days with intermediate PNC levels ($7.3 \cdot 10^3 \text{ cm}^{-3}$ and $6.9 \cdot 10^3 \text{ cm}^{-3}$ as cluster average, respectively) but while the former mainly includes data from the urban sites (80%

overall) the latter conversely includes data from the two rural sites (84% overall), but mostly from the ISP-R site (50%). Finally, cluster #4 ($4.2 \cdot 10^3 \text{ cm}^{-3}$) is almost entirely formed by data from BO-UB and SPC-R, whose similarity in concentration levels has been already discussed in section 3.1. Figure 7 shows in details for each site the breakdown of the days of the monitoring period among the four clusters. Interestingly, we can observe that the daily data MI-UB and PD-MX sites not only fall in first two clusters mainly, but also that for 10 out of the 20 days considered in this analysis data from the two sites fall in the same cluster; the same consideration holds for the sites of BO-UB and SPC-R. Only in a few days the more than two sites fall in the same cluster (3 sites on Feb. 10th, 13th and 22nd; 4 sites on Feb. 9th) and only in one case (Sunday Feb. 16th) the PNC values and the shape of the PNSD have been such to have all the sites grouped in the same cluster. All these results indicate that the features of the site, namely its location within the urban context, have a significant influence on both the concentration levels and the particle size distribution.

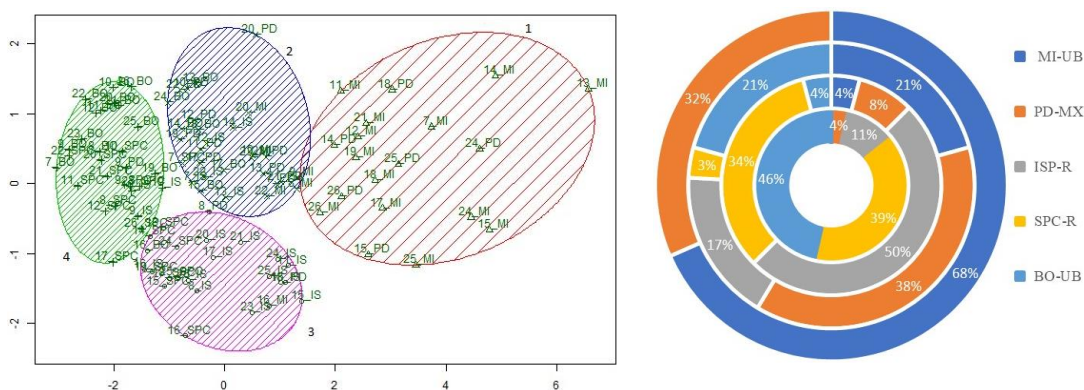


Figure 6. Principal components plot for the daily averaged size distributions (left); cluster compositions by site frequency (right: from cluster#1 on the outer to cluster#4 on the inner ring)

MI-UB	1	2	2	2	1	1	1	1	1	3	1	1	1	2	1	2	2	1	1	1
PD-MX	2	3	4	2	2	2	2	1	1	3	2	1	2	2	2	2	2	1	1	1
ISP-R	2	3	4	4	3	2	2	2	3	3	3	3	4	3	3	2	3	3	3	3
BO-UB	4	4	4	4	4	4	2	2	2	3	2	2	4	4	4	4	4	2	4	4
SPC-R	2	4	4	4	4	4	3	3	3	3	4	3	3	4	4	4	4	3	3	4
	7	8	9	10	11	12	13	14	15	16	17	18	19	20	21	22	23	24	25	26
	Calendar day																			

Figure 7. Breakdown by site of the days of the monitoring period among the four clusters

4. Conclusions

The results from a one-month winter campaign for particle number concentrations measurement at rural and urban sites in the Po valley show that concentration levels are in the same orders of those reported in literature for sites with similar features. At rural and urban sites average concentrations are about $5 \cdot 10^3 \text{ cm}^{-3}$ and $1.1 \cdot 10^4 \text{ cm}^{-3}$, respectively. In spite of the background position of the urban sites, however, concentrations up to $4 \cdot 10^4 \text{ cm}^{-3}$ occur on traffic rush hour. Actually, the monitoring sites location within the urban area strongly influences the concentration levels: the deeper the location into the urban conurbation the higher the generalized exposure of the site to the urban emission sources and, subsequently, the higher the particle concentration. At the urban sites located on the outskirts of the city or in suburban environments concentration similar to rural sites can be observed sometimes. As a consequence of the different features of the urban sites considered in this work, the correlation between the time series of the particle number concentration is rather weak, even though the sites share a common

time pattern hourly concentration, reflecting the diurnal pattern of the traffic flow in urban areas. Concentration values, size distribution and related time patterns markedly different from the urban sites are observed only at the rural site actually located in a regional background position, not directly affected by emission sources, where the levels of airborne particles are mainly driven by the daily evolution of the planetary boundary layer.

5. References

- Bigi, A., Ghermandi, G., 2011. Particle Number Size Distribution and Weight Concentration of Background Urban Aerosol in a Po Valley Site, *Water Air Soil Pollution* 220, 265-278
- Carslaw, D.C., Ropkins K., 2012, Openair - an R package for air quality data analysis. *Environmental Modelling & Software* 27-28, 52-61.
- Cattaneo, A., Garramone, G., Taronna, M., Peruzzo, C., Cavallo, D.M., 2009. Personal exposure to airborne ultrafine particles in the urban area of Milan. *Journal of Physics Conference Series* 151, 01203
- Hamed, A. et al., 2007. Nucleation and growth of new particles in Po Valley, Italy. *Atmospheric Chemistry and Physics* 7, 355-376
- Henne, S., Brunner, D., Folini, D., Solberg, S., Klausen, J., Buchmann, B., 2010. Assessment of parameters describing representativeness of air quality in-situ measurement sites. *Atmospheric Chemistry and Physics* 10, 3561-3581.
- Jeong, C.H., Evans, G.J., 2009. Inter-comparison of a Fast Mobility Particle Sizer and a Scanning Mobility Particle Sizer incorporating an Ultrafine Water-Based Condensation Particle Counter. *Aerosol Science and Technology* 43, 364-373.
- Lonati, G., Crippa, M. Gianelle, V., Van Dingenen, R., 2011. Daily patterns of the multi-modal structure of the particle number size distribution in Milan, Italy. *Atmospheric Environment* 45, 2434-2442.
- Lonati, G., Ozgen, S., Ripamonti, G. Signorini, S., 2017. Variability of Black Carbon and Ultrafine Particle Concentration on Urban Bike Routes in a Mid-Sized City in the Po Valley (Northern Italy). *Atmosphere* 8, 40.
- Ozgen, S., Ripamonti, G., Malandrini, A. Ragetti, M., Lonati, G., 2016. Particle number and mass exposure concentrations by commuter transport modes in Milan, Italy. *AIMS Environmental Science* 3, 168-184.
- Poluzzi V., et al., 2015. Preliminary result of the project “Supersito” concerning the atmospheric aerosol composition in Emilia-Romagna region, Italy: PM source apportionment and aerosol size distribution, in Brebbia C.A. (Ed.) Sustainable development. WIT Transaction on The Built Environment 168. WITpress, Southampton, pp. 689-698.
- Rodriguez, S. et al., 2007. A study on the relationship between mass concentrations, chemistry and number size distribution of urban fine aerosols in Milan, Barcelona and London. *Atmospheric Chemistry and Physics* 7, 2217-2232
- Rodriguez, S. et al. 2005. Nucleation and growth of new particles in the rural atmosphere of Northern Italy - relationship to air quality monitoring, *Atmospheric Environment* 39, 6734-6746
- Sandrini, S. et al., 2014. Spatial and seasonal variability of carbonaceous aerosol across Italy. *Atmospheric Environment* 99, 587-598.
- Sun, J. et al., 2019. Variability of black carbon mass concentrations, sub-micrometer particle number concentrations and size distributions: results of the German Ultrafine Aerosol Network ranging from city street to High Alpine locations. *Atmospheric Environment* 202, 256-268.



18th World Clean Air Congress, 23-27 September 2019, Istanbul
organized by TUNCAP and IUAPPA

Wang, F., Cernuschi, S., Ozgen, S., Ripamonti, G., Vecchi, R., Valli, G., Lonati, G., 2016. UFP and BC at a mid-sized city in Po valley, Italy: Size-resolved partitioning between primary and newly formed particles. *Atmospheric Environment* 142, 120-131.

Acknowledgments

The authors wish to acknowledge all the participants to the POAIR (PO valley atmospheric Aerosol Intensive Research) project.



Towards low carbon mobility in a developing country

Mohamed Rehan Muhammad Saifuddin^{1,2} and Mohamed Rehan Karim²

¹Department of Mechanical Engineering, International Islamic University Malaysia, 50728 Kuala Lumpur, Malaysia

²Transportation Science Society of Malaysia (TSSM), c/o Center for Transportation Research, University of Malaya, 50603 Kuala Lumpur, Malaysia

msaifuddin@iium.edu.my

Abstract. Malaysia as one of the participants of the United Nations Framework Convention on Climate Change (UNFCCC), ratified its commitment to the Kyoto Protocol in September 2002. Malaysia's Intended Nationally Determined Contribution (INDC) in reducing its GHG emissions intensity (per unit of GDP) by 45% by 2030 relative to the emissions intensity in 2005. Transport sector in Malaysia contributes 20% of the country's total GHG emissions, and the land transport sector makes up 90% of this transport sector emission contribution. This study focuses on potential approaches for land transport sector to enable the country to achieve low carbon mobility and fulfil its commitment to reduce its GHG emissions. A brief glance on road vehicle and public transport will be presented, including the vehicle numbers and volume share and the mode share of public transport. Baseline data will be presented and energy consumption and GHG emissions for land transport sector is then quantified. GHG emission comparisons have highlighted several possible measures that should be considered, including promoting vehicle with better fuel efficiency, promoting vehicle technology that improve energy consumption and GHG emission, promoting mode shift from private vehicle to public transport, and promoting the use of greener fuel. This paper will highlight the approach undertaken in developing the policies, strategies and action plans to reduce GHG emissions as compared with business-as-usual (BAU) scenario. The Avoid-Shift-Improve approach has been employed in the study, and a comprehensive set of strategies deemed necessary is highlighted.

Keywords: Transport, GHG emissions, Vehicle technology, Climate change, Energy.

1. Introduction

Malaysia's government has submitted its Intended National Determined Contribution (INDC) in January 2016 stating its target to reduce its greenhouse gas (GHG) emission intensity of GDP by 45 percent by 2030 relative to the emission intensity of GDP in 2005. The transport sector has consistently been the second largest GHG emitting sector in the country, with 20 percent of the country's total GHG emissions in 2014 (BUR, 2018). From the said 20 percent, 18 percent comes from road transportation. As such, land transport sector is one of the important sectors for GHG emission reduction, in order to help the country to meet its commitment.

Scenarios with multiple options across various subsectors have been analysed and it was confirmed that if substantial emission reductions are to be made, considerable action is needed on all fronts (McCollum and Yang, 2009).

2. A brief glance on road vehicles and public transport

Here a brief glance of an overview of some relevant information to the road vehicles and public transport scenario in Malaysia as a developing country.

2.1. Registered vehicles numbers and volume share

The number of vehicles in the country has been increasing throughout the years, from a total of 14.8 million in 2005 to 24.6 million in 2014. The vast majority of the registered vehicles are cars and motorcycle, where cars and motorcycle make up 45 percent and 47 percent, respectively, of the total vehicle numbers in 2014. With the increasing trend of vehicle number, mitigation measures may be required for the country to fulfil its commitment to reduce greenhouse gas (GHG) emissions.

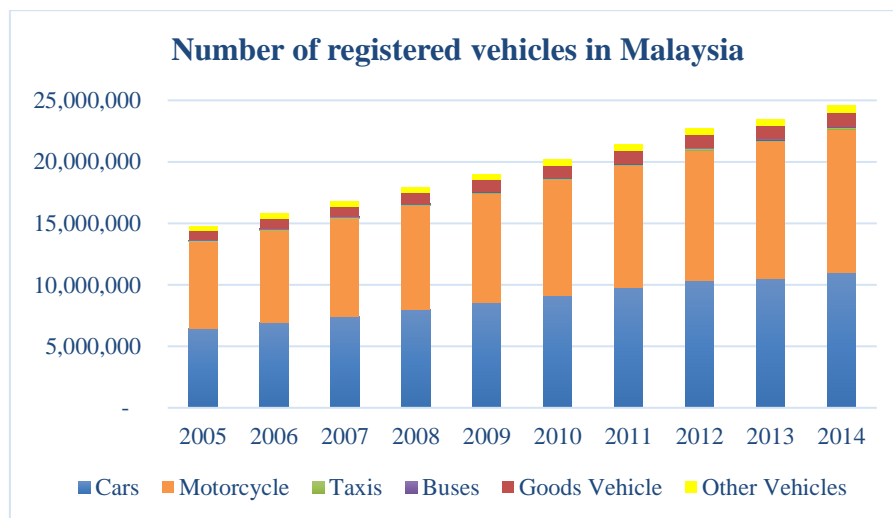


Figure 1. Total number of registered vehicles in Malaysia. Source data (EPU, 2017)

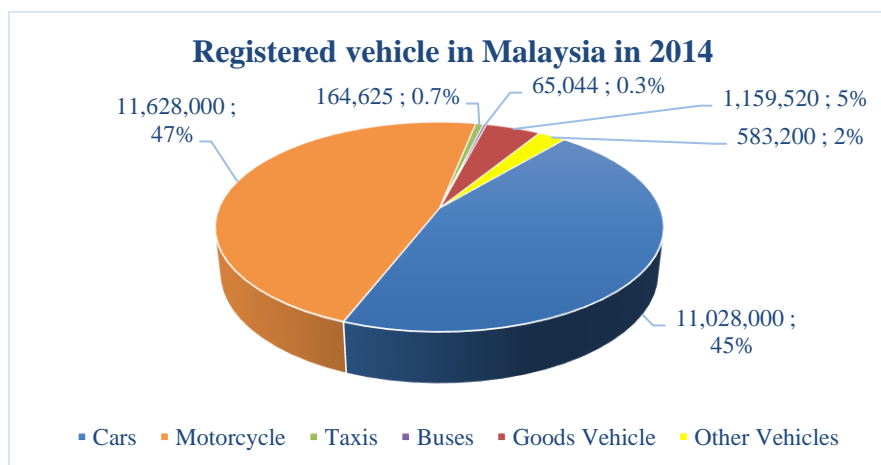


Figure 2. Number and percentage of registered vehicles in Malaysia. Source data (EPU, 2017)

2.2. Mode share of private and public transports

The country has seen a rapid growth of private vehicles as a transport mode of choice among the Malaysian public. Over a period of 20 years the registration of private cars and motorcycles has increased from 4.7 million in 1990 to 18.6 million in 2010 (SPAD, 2013). Within the same period the public transport modal share has been declining (Figure 3). Malaysia's land public transport vision is to have 40 percent of all commuters to use land public transport by 2030 (SPAD, 2017). Since 2010, the

government has invested heavily in improving public transport infrastructure under the Urban Public Transport (UPT) NKRA, and with concerted effort the modal share had grown to 20 percent in 2015. However, the modal share seems to hit a plateau, and some mitigation action may be required to meet the vision of 40 percent modal share.

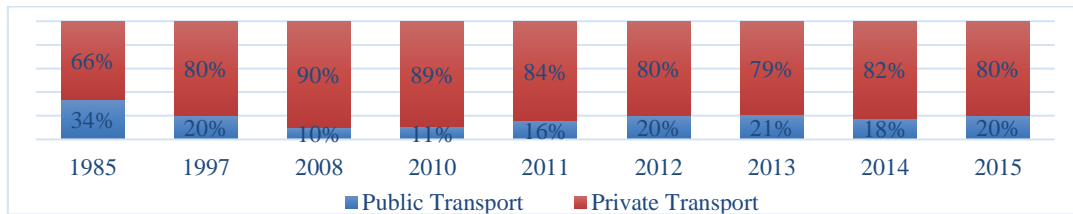


Figure 3. Percentage of mode share in Greater Kuala Lumpur/Klang Valley Area. (BUR 2018, SPAD 2017, SPAD 2013)

2.3. Registered vehicles by the type of fuels

Figure 4 presents the vehicle registration numbers by fuel type for the period of 2014-2018. For passenger vehicle, the vast majority is petrol vehicles, with diesel vehicle being a distance second. Other fuel type including EV has very small percentage, merely around 1.3 percent combined. For motorcycle, vast majority is petrol motorcycle, with electric motorcycle registration makes up less than 0.1 percent. For buses, the vast majority is diesel bus, with NGV and EV buses makes up only 4 percent combined. For goods vehicle the majority is diesel vehicles, with petrol vehicle a distance second.

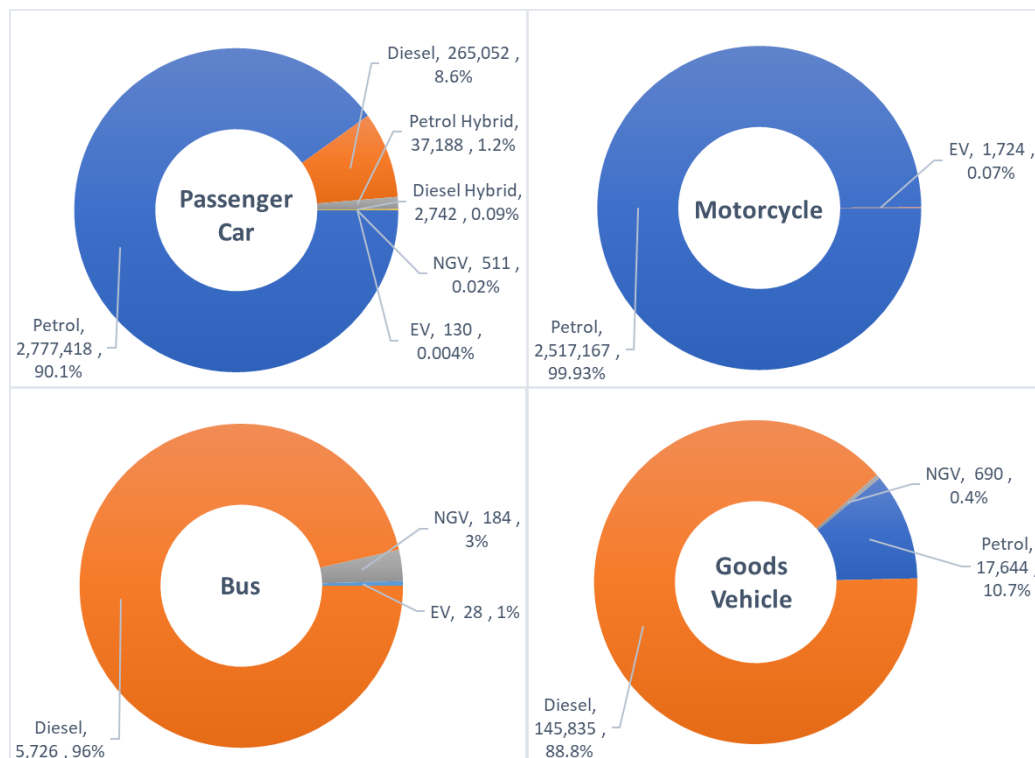


Figure 4. Number of vehicle registration by fuel type for the period of 2014-2018 (Jabatan Pengangkutan Jalan (JPJ) official portal)

One obvious observation is the vast majority of vehicle registered in the recent years run on fossil fuel, mainly petrol and diesel, with very insignificant number of vehicles run on greener fuel or renewable

energy sources. With the amount of vehicle registered, and the increasing number of vehicle trend, serious measures need to be looked into as mitigation efforts facing the increasing GHG emission from land transport sector.

3. GHG emission from land transport

This section will present the baseline data for the analysis, the estimation of vehicle kilometre travel, and the resulting energy consumption and GHG emission produced by each vehicle type.

3.1. Baseline data

GHG emission will be quantified using available data on land transport. Among the aspects that directly affect GHG emission are vehicle fuel efficiency, distance of travel, and type of fuel used. The vehicle fuel efficiency and kilometre travelled are listed in Table 1 and Table 2, and the emission factors for different fuel type are listed in Table 3.

Table 1. Fuel efficiency of land transport vehicles. Source data (EPU 2017, EPA website)

Vehicle Type	Fuel Type	Engine Size Range	Fuel Efficiency (km/L) *(km/kwh)	Fuel Efficiency (L/100km) *(kwh/100km)
Motorcycle	Petrol	All	46.53	2.15
Motorcycle	Electricity	-	26.00*	3.85*
Car	Petrol	All	12.24	8.17
Car	Diesel	2000 cc and above	8.74	11.44
Car	Electricity	-	5.36*	18.64*
Bus	Diesel	All	3.56	28.10
Taxi	Petrol	2500 cc and below	10.21	9.79
Taxi	NGV	2000 cc and above	11.90	8.40
Taxi	Diesel	2000 cc and below	8.76	11.42
Goods vehicle	Petrol	2000 cc and below	9.00	11.11
Goods vehicle	Diesel	All	4.63	21.59
Other vehicles	Petrol	4000 cc and below	7.52	13.30
Other vehicles	Diesel	All	5.51	18.14
Rail	Electricity	-	0.31*	322.58*

Table 2. Annual vehicle kilometre travelled for different vehicle types

Vehicle Type	Annual Vehicle Kilometer Travelled (km)	Data source
Motorcycle	21,500	(Shabadin, A., et al. 2017)
Car	28,000	(Shabadin, A., et al. 2017)
Taxi	86,000	(DSM 2017)
Bus	100,000	(DSM 2017)
Goods vehicles	70,000	(Briggs, A., et al. 2016)
Other Vehicles	10,000	(DSM 2017)

Table 3. Emission factor for different vehicle fuel

Vehicle Fuel	Emission Factor	Source
Petrol	72.309 t CO _{2eq} /TJ	(IPCC, 2006)
Diesel (B7)	70.085 t CO _{2eq} /TJ	(IPCC, 2006)
CNG	59.294 t CO _{2eq} /TJ	(IPCC, 2006)
Electricity	0.694 kg CO ₂ /kwh (192.7 t CO _{2eq} /TJ)	(MGTC, 2016)

3.2. Vehicle kilometer travel estimation

For the GHG emission calculation, the registered number of vehicles could not be directly used due to several reasons. First, the total registered number of vehicles of almost 25 million is much larger than the number of driving license issued of 14.3 million (JPJ, 2018). Hence it is not expected for all the registered vehicle to running on the road. Secondly, it would result in higher calculated values of energy consumption and GHG emission compared to what was reported in the National Energy Balance (NEB) report (Suruhanjaya Tenaga, 2015) and the Malaysia Third National Communication and Second Biennial Update to the UNFCCC (BUR) report (BUR, 2018), respectively. Hence the calculation uses an estimated vehicle kilometre travel (VKT) that is proportionately adjusted to satisfy these conditions: number of vehicles on the road cannot exceed the number of licenses, and energy consumption and GHG emission values matches the values reported in the NEB and BUR reports. The estimated VKT is presented in Figure 5.

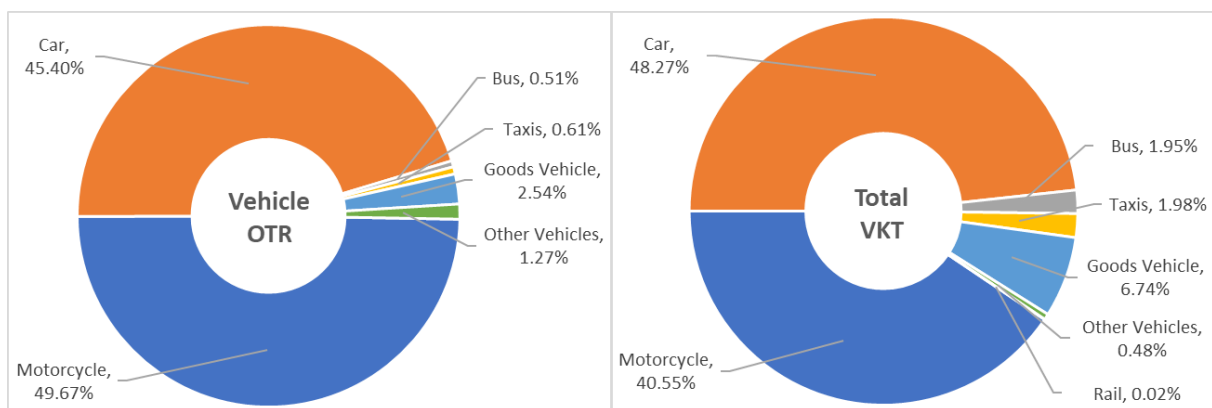


Figure 5. Number of vehicles on the road (OTR) and total vehicle kilometre travelled (VKT) by different vehicles in land transport for 2014

3.3. Resulting energy consumption and GHG emission for land transport

The resulting energy consumption and GHG emission from the various vehicle types in the land transport are illustrated in Figure 6.

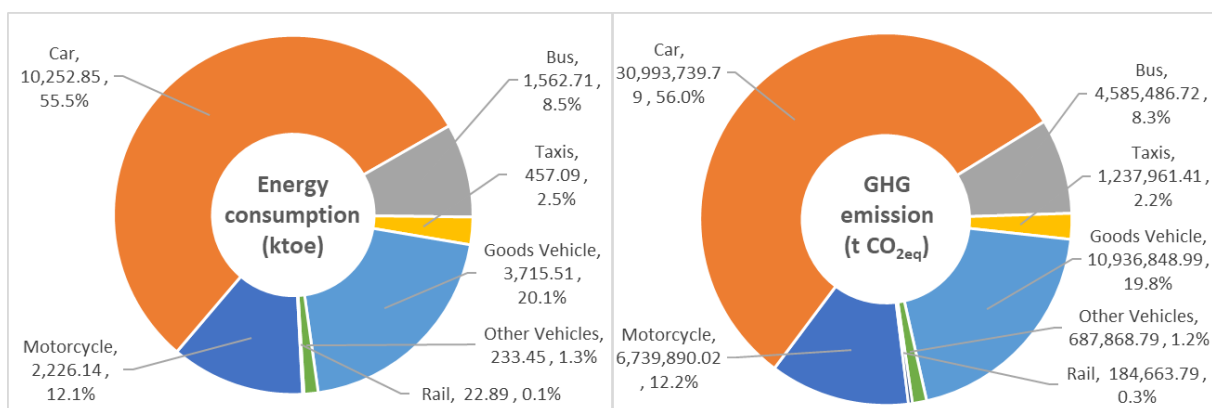


Figure 6. Calculated energy consumption and GHG emission by different vehicles in land transport for 2014

Passenger car is the biggest contributing vehicle type on energy consumption and GHG emission for land transport. This observation directly corresponds to the fact that passenger car having the biggest VKT compared to other vehicles (Figure 5). Motorcycle on the other hand, despite also having a major portion of the total VKT, have significantly lower energy consumption and GHG emission contributions.

This is due to the fact that motorcycle have relatively high fuel efficiency compared to passenger car and other vehicle types. Goods vehicles, despite having only less than 7 percent of the total VKT, contribute around 20 percent of the land transport energy consumption and GHG emission due to the significantly higher fuel consumption per unit vehicle. Buses also have big fuel consumption per unit vehicle, however the number of buses and hence VKT is very small compared to the total number of vehicles and the total VKT, resulting very small share of total energy consumption and GHG emission.

3.4. GHG emission comparison between different vehicle options

The GHG emission for each vehicle kilometre travel and also each passenger kilometre travel is presented in Table 4. There are a few important notes to be noted about the values presented in the table. Based on the registered vehicle data, certain fuel type is used for car or taxi only for certain engine size. For example, diesel cars and taxis are only available for cars with 2000 cc or higher. As a result, side by side comparison with cars or taxis running on petrol may not give an accurate deduction, as the weighted average fuel efficiency for the vehicles will not be able to compare. For instance, the majority of cars registered in the country are petrol cars below 2000 cc, hence the weighted average fuel consumption for petrol cars will be relatively low, compared to the weighted average fuel consumption for diesel cars will be relatively high. For bus comparison, the diesel bus category is divided into two subcategories, namely less than 5000 cc and 5000 cc and above, so that a valid comparison can be made with the electric bus data which is based on stage buses and express buses which correlates to diesel buses of 5000 cc and above.

Table 4. GHG emission comparison for various land transport vehicle in Malaysia. Source data for occupancy rate (Briggs et al., 2016)

Vehicle	Fuel	GHG emission per vehicle km (g CO _{2eq})	Occupancy Rate (passenger/vehicle)	GHG emission per passenger km (g CO _{2eq})
Motorcycle	Petrol	49.89	1.2	41.57
Motorcycle	Electricity	26.68	1.2	22.23
Car	Petrol	189.63	1.4	135.45
Car (>2000cc)	Diesel	287.12	1.4	205.08
Car	Electricity	129.43	1.4	92.45
Bus (<5000cc)	Diesel	560.68	18.4	30.47
Bus (>5000cc)	Diesel	836.35	18.4	45.45
Bus	Electricity	835.81	18.4	45.42
Taxi (<2500cc)	Petrol	227.34	1.55	146.67
Taxi (<2000cc)	CNG	159.94	1.55	103.19
Taxi (>2000cc)	Diesel	286.52	1.55	184.85
Rail	Electricity	2237.81	36.75	60.89

Several observations can be made from the GHG emission comparison. First, for any specific vehicle type the smaller vehicle tend to produce lower GHG emission than the bigger and heavier vehicle, due to the better fuel efficiency. One example is the comparison for buses between those with engine size less than 5000 cc and those with engine size more than 5000 cc. Figure 7 illustrates an example of GHG emission comparison from petrol and diesel vehicles within the same segment with varying vehicle weight, showing similar observation. This observation highlights the possible option of promoting vehicles with better fuel efficiency, which tend to be the smaller vehicles when the technology is the same or similar.

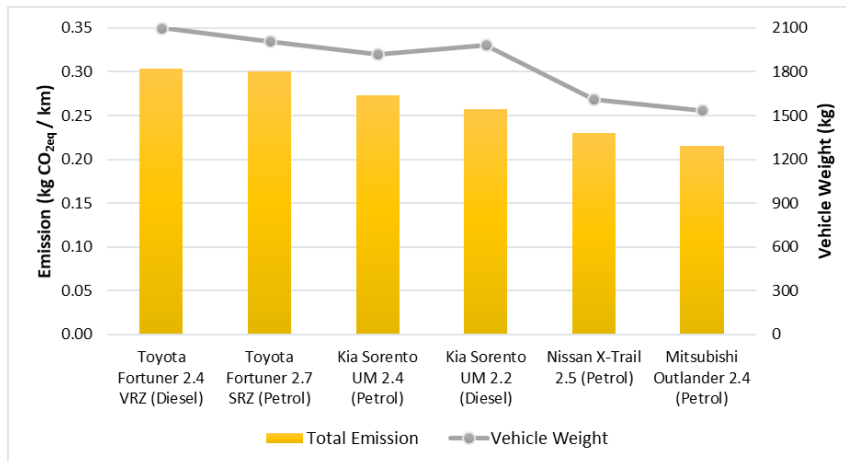


Figure 7. Total GHG emission from diesel and petrol vehicles within the same segment with varying vehicle weight

Second, different vehicle technology may also provide GHG emission reduction. Comparing petrol and electric motorcycle, electric motorcycle provides significant reduction in GHG emission. Similar observation can be made when comparing petrol and electric passenger car. This observation highlights the possible option of promoting electric vehicle that provide a relatively lower net GHG emission, for the type of vehicles where the option is available. It should be noted that the GHG emission level of electric vehicles is dependent on the electricity grid emission factor, for which the energy source for the electricity power generation is a significant contributing factor. Given the commitment of the government to significantly increase renewable energy portion in the energy mix, the corresponding electricity emission factor would be lower over time, and hence the calculated GHG emission would also be lower accordingly.

Third, from the perspective of the passenger travel, different choice of vehicle used can contribute to significant difference in GHG emission per passenger kilometre travelled. Between different choices of vehicle for travelling, it can be seen that the GHG emission footprint would be significantly lower if travel by bus or rail is chosen, compared to personal car or taxi. This highlight the importance of mode shift from private cars or even taxi towards public transport of buses and rails, if significant GHG emission reduction is to be achieved. In case where public transport is not an option and personal vehicle need to be used, motorcycle would be the best option among the private vehicle options.

Besides vehicle for people's mobility, the goods vehicle is also an important vehicle type in the perspective of GHG emission reduction. As established earlier goods vehicle have significant contribution towards the total GHG emission. Figure 8 illustrates GHG emission impact when higher blend of biodiesel is applied for diesel goods vehicle.

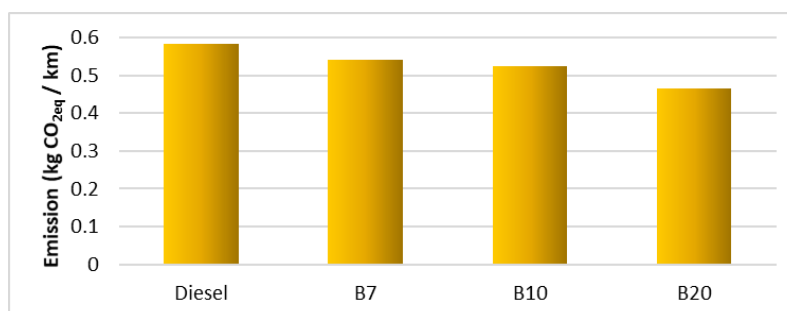


Figure 8. GHG emission comparison for diesel goods vehicle using biodiesel of different blend

5. Approach in addressing GHG emission

This section will present the possible approach for addressing the GHG emission. The general approach in addressing the GHG emissions from the land transport sector was formulated based on the basic understanding on the factors that influence the emissions of GHGs from the land transport sector itself. GHG emissions are from vehicles on the road that perform the function of moving people and goods from origin to destination for various trip purposes. As such, the trips made by various categories of vehicles on the road network for the specific purposes will determine the extent to which the GHG emissions are produced from the land transport sector.

Addressing the issue of GHG emissions from land transport may be considered as part of pursuing a more sustainable transport system, of which emissions from vehicular traffic affect the environment particularly the air quality within the vicinity. In this respect, the most appropriate approach to address the GHG emissions from land transport would be to utilize the Avoid-Shift-Improve (ASI) approach which is universally accepted as the approach to achieve a more sustainable transport system.

Adapting the ASI approach in this study was deemed most appropriate as can be understood from the following discussions. The Avoid strategy relates to the efficiency of the land use – transport system and means that the trip may not necessarily be made and can be avoided without jeopardizing the fulfilment of the purpose of the trip. It implies that a person can still perform a certain function without having to make the trip using a motorized vehicle. In this case, a motorized trip will be avoided, hence one less motorised vehicle on the road. As for the Shift strategy which relates to trip/travel efficiency implies that a person will choose a less carbon intensive mode of transport (such as public transit, cycling) instead of the regular private car. Finally, the Improve strategy refers to the improvements that can be made on the vehicle technology and fuel efficiency as well as improvement to the traffic control and management system for more optimal traffic flow.

It has been shown that shift from using private vehicle towards public transport can contribute towards significant GHG emission reduction. Measures that would encourage this mode shift may be in both 'carrot & stick' combination to make it more effective. Combination of improvement in the public transport system with traffic restraints measures that would discourage private car use in the city would be needed.

In term of vehicle and fuel consideration, comparison of GHG emission presented earlier has highlighted several measures that should be considered. Vehicle with better fuel efficiency should be promoted and encouraged, and usage of vehicle that have high level of fuel consumption should be discouraged. Vehicle technology that provides good alternative for GHG emission reduction, including electric vehicle, should be promoted. Among the aspects need to be addressed is the required infrastructure for the whole ecosystem to prosper. For goods vehicle alternative fuel including biodiesel should be considered.

One aspect specific to this country that makes it more challenging for any emerging green fuel or green vehicle technology to penetrate the market is the fact that the fuel price of petrol and diesel is relatively low. Figure 9 and Figure 10 show the comparison for the selling price of petrol and diesel fuel, respectively, with the break down of the ex-tax price and total tax price for which the data is available. It is clear that the selling price in Malaysia is comparatively very low, even when compared to the neighbouring developing countries. The reason may be the fact that Malaysia do not impose tax on the fuel, and may even to a certain extent subsidizing the fuel.

When the fuel price of petrol and diesel is very low, it will be very difficult for alternative fuel, for instance CNG or LNG, to enter the market at a competitive price, especially if considering that the vehicle for such fuel may come with a higher capital expenditure cost. The potential operating cost

saving from using for instance electrical vehicle would also be not big enough for the operators to justify the bigger upfront investment for the vehicle cost. To make room for the green alternatives to enter the market and be competitive, the policy of the country on the petrol and diesel fuel price may need to be looked into and revised.

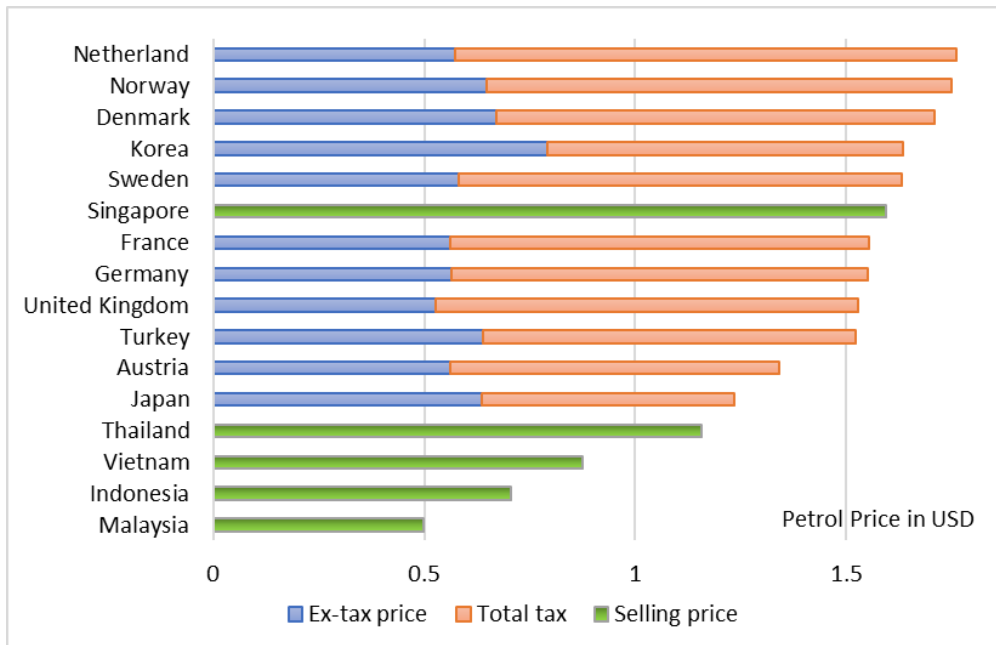


Figure 9. Petrol fuel price comparison between different countries. Ex-tax price and total tax is presented for which is available (OECD, 2018), and selling price is presented as of September 2019 (Global petrol prices website) for which the break down is not available

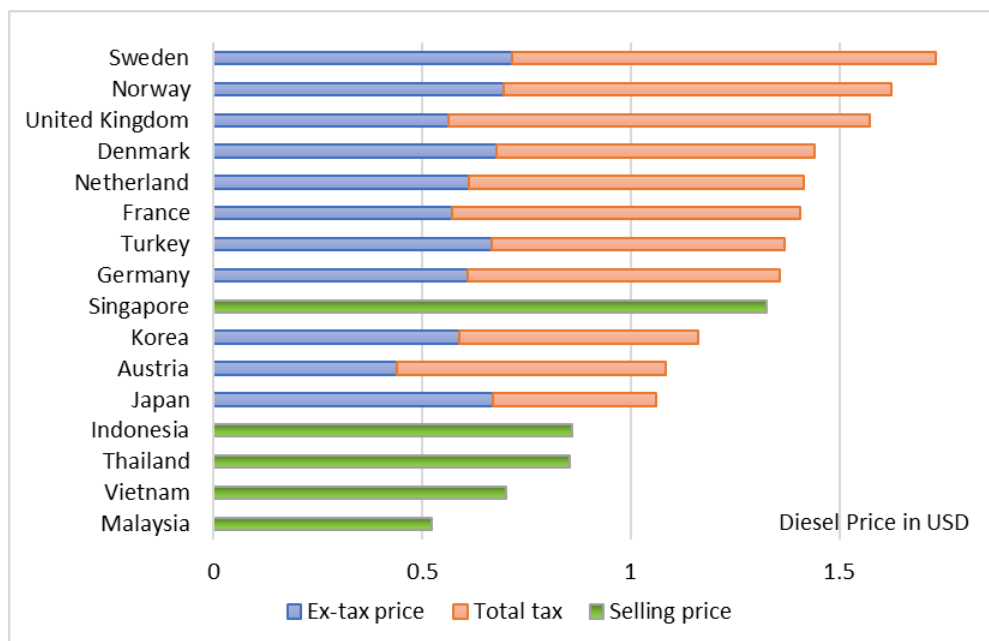


Figure 10. Diesel fuel price comparison between different countries. Ex-tax price and total tax is presented for which is available (OECD, 2018), and selling price is presented as of September 2019 (Global petrol prices website) for which the break down is not available



6. Conclusion

Transport sector is one of the most important sectors for the country to successfully reduce its total GHG emission. The continuously increasing number of vehicles indicate that mitigation measures are needed for the country to fulfil its commitment to reduce GHG emissions. To understand the current reality of land transport in Malaysia, this study has looked into the public transport mode share, the registered vehicle number by the type of fuels, and the baseline data directly related with GHG emission. GHG emission from various vehicle type in the land transport has been computed and analysed, and several observations were made. Possible measures include promoting vehicle with better fuel efficiency (which may be smaller vehicle), promoting vehicle technology that improve energy consumption and GHG emission (including electric vehicle), promoting mode shift from private vehicle to public transport, and promoting the use of greener fuel (including biofuels). The approach to promote all of the above may be in both 'carrot & stick' combination to make it more effective. One particular issue that may need to be looked into for revision is the petrol and diesel fuel price, as it may be a key enabler for alternative green fuel and vehicle technology to penetrate the market and be commercially attractive.

7. References

- Briggs, A., Leong Hau Kian, 2016. Malaysia stocktaking report on sustainable transport and climate change Nov 2016.
- BUR, 2018. Malaysia Third National Communication and Second Biennial Update to the UNFCCC, 2018.
- McCollum, D., Yang, C., 2009 Achieving deep reductions in US transport greenhouse gas emissions: Scenario analysis and policy implications *Energy Policy*. 37, 12, December 2009, 5580-5596.
- EPU, 2017. Final Report on Demand Side Management (DSM) Preliminary Study, July 2017.
- Global petrol prices website, <https://www.globalpetrolprices.com/>.
- IPCC, 2006. Guidelines for National Greenhouse Gas Inventories Volume 2 Energy: Chapter 3 Mobile Combustion (https://www.ipcc-nggip.iges.or.jp/public/2006gl/pdf/2_Volume2/V2_3_Ch3_Mobile_Combustion.pdf)
- JPJ, 2018. Jabatan Keselamatan Jalan Raya Malaysia, Buku Statistik Keselamatan Jalan Raya, April 2018.
- MGTC, 2016. Preliminary Findings: Mitigation Actions and Their Effects Chapter of Malaysia's Second Biennial Update Report (BUR), 2016 (http://oursphere.greentechmalaysia.my/wp-content/uploads/2016/10/Workshop-NRE_28Oct2016-after-workshop.pdf).
- OECD, 2018. Consumption Tax Trends 2018. VAT/GST and excise rates, trends and policy issues. https://read.oecd-ilibrary.org/taxation/consumption-tax-trends-2018_ctt-2018-en#page1
- SPAD, 2013. Land Public Transport Master Plan GKL/KV.
- SPAD, 2017. Land Public Transport Commission Annual Review 2017.
- Shabadin, A., Nusayba, M., Jamil, H. M, 2017. Car annual vehicle kilometer travelled estimated from car manufacturer data - An improved method, World Research & Innovation Convention on Engineering & Technology 2014, Putrajaya, Malaysia, 25-26 November 2014. 25, 171-180.
- Suruhanjaya Tenaga, National Energy Balance (NEB) 2015.
- US EPA website, comparison of EPA fuel economy of Nissan Leaf, (<https://www.fueleconomy.gov/feg/Find.do?action=sbs&id=37066&id=37067&id=34918&id=34699>)

Site-specific variation in ambient nanoparticles (PM_{0.1}) in North Sumatra Province-Indonesia

Rahmi Mulia Putri¹, Muhammad Amin¹, Tetra F. Suciari², Al Fattah Faisal M², Astri Novarina², Sri Rafiah Nam Bintang², Fumikazu Ikemori³, Masashi Wada⁴, Mitsuhiro Hata¹ and Masami Furuuchi^{1,5}

¹Graduate School of Natural Science and Technology, Kanazawa University, Kanazawa, Ishikawa, 920-1192, Japan

²Center for Environmental Health Engineering and Disease Control, Medan City - Medan-Indonesia

³Nagoya City Institute for Environmental Science, Nagoya, 460-8508, Japan

⁴Research Institute of Environment, Agriculture and Fisheries, Osaka Prefecture

⁵Faculty of Environmental Management, Prince of Songkla University, Hat Yai, Songkhla 90112, Thailand

mfuruch@staff.kanazawa-u.ac.jp

Abstract. In this study, to evaluate the present situation in Indonesia regarding air pollution by particulate matter, especially with respect to the status and characteristics of PM_{0.1} particles, air sampling using a cascade air sampler that can collect particles in different size ranges down to PM_{0.1} was conducted at several sites in North Sumatra Province. The sites were located in areas involving various aspects of land use and environmental categories, including roadside, a school adjacent to a road, an industrial area and an area near a volcano. Carbonaceous components as organic, elemental and total carbon (OC, EC, TC, respectively) in the PM_{0.1} range were analyzed using a thermal-optical carbon analyzer. The status of PM₁, PM_{2.5}, PM₁₀ and Total Suspended Particulate (TSP) as well as PM_{0.1} particles are discussed in relation to local emission sources, such as traffic, industries and open burning. Possible influences of long-range transportation are also discussed by taking into account the air mass trajectory and the distribution of hotspots or active fire distributions obtained from satellite images. The average PM₁₀ and PM_{2.5} values at urban sites were much larger than the WHO guidelines for 24 hours. However, the situation was rather moderate compared to other severe conditions, e.g., in Chiang Mai during the forest fire season. The first data on PM_{0.1} in Indonesia was reported and the level in urban sites was similar to those in large cities in the East Asia region. A small difference between diurnal and nocturnal PM concentration was observed at road side sites. A lower fraction of TC in PM_{0.1} at an industrial site may be attributed to particles from the secondary formation. The OC/EC ratio in PM_{0.1} was rather similar between the sites that were studied (4.26 ~ 6.49) and the char-EC/soot-EC ratio was always smaller than 1 (0.10 ~ 0.34), indicating that transportation or coal combustion as local emission sources appear to be the main air pollution sources in North Sumatra Province.

Keywords: PM_{0.1}; Mass concentration; Carbonaceous component; North Sumatra; Indonesia.

1. Introduction

North Sumatra is the largest province in Sumatera Island, Indonesia and is one of the most populous provinces in Indonesia with the Medan city as the capital city of this province, which is categorized as a metropolitan city (BPS North Sumatra Province, 2019). The total population of Medan city in 2018 was 2,247,425 with a growth rate since 2010 of around 5.39% (BPS Medan city, 2019). Growing

economics and populations have led to an increase in the number of vehicles as well as industrial activities and the associated energy consumption could lead to serious air quality problems. Although the emission of air pollutants must be managed carefully, as reported by Central Statistics Agency of Medan city (2015), more than a half of the vehicles that are comprised of 6,551,464 units of passenger cars, buses, trucks with 5,662,202 units of motorcycles in North Sumatera Province are not properly managed. Peatland land fires in the region is not as serious as local sources compared to other provinces, e.g., in Riau, Jambi and the South Sumatera region. However, Mt. Sinabung, one of the most active mountains in Indonesia is located in the province and this represents a huge source of temporary emissions, as it annually emits a huge amount of volcanic ash into the ambient air of North Sumatera (Hendrasto et al., 2012; Kriswati et al., 2018; Tampubolon et al., 2018).

Human health effects attributed to PMs depend on the level of concentration, size and chemical components of these particles (IPCC, 2001; Kaufman et al., 2002) so that a seriously contaminated situation in North Sumatera could lead to the development of diseases as neurology, respiratory, cardiovascular diseases (Akbarzadeh et al., 2018; Lee et al., 2018; Wu et al., 2018). Around 10% (221,635) of the total population in Medan city has registered as a respiratory disease patient with an acute respiratory infection (ARI) in 2014 and it is one of the top ten dominant diseases in Medan city (BPS Medan city, 2015). It is well known that particle size is a significant issue in the degree of health risk and this is particularly true for ultrafine particles most of which are emitted from anthropogenic sources such as traffic and open burning (Heinzerling et al., 2016; Manigrasso et al., 2017; Clifford et al., 2018).

Hence, the above situation in North Sumatera and Medan city may be closely related to the emission of fine and ultrafine particles. However, unfortunately, information on the status of ultrafine particles and the contribution of local emission sources is very limited not only in North Sumatera but also over the entire country of Indonesia as well as information on possible influences of transboundary air mass movement that plays an important role, e.g., during haze episodes in northern Thailand and peatland fire in Indonesia.

In this study, to evaluate the present situation in Indonesia on air pollution by particulate matter especially focusing on the status and characteristics of PM_{0.1}, air sampling using a cascade air sampler that can collect particles in different size ranges down to PM_{0.1} was conducted at several sites in North Sumatera Province that are located in areas with various land use and environmental categories, including roadsides, school adjacent to a road, an industrial area and an area near a volcano. Carbonaceous components in the form of organic, elemental and total carbon (OC, EC, TC, respectively) in the PM_{0.1} size range were analyzed using a thermal-optical carbon analyzer. The status of PM₁, PM_{2.5}, PM₁₀, and Total Suspended Particulate (TSP) as well as PM_{0.1} is discussed in relation to local emission sources including traffic, industrial output and open burning. Possible influences of long-range transportation are also discussed by taking into account the air mass trajectory and the distribution of hotspots or active fire distributions obtained from satellite images.

2. Methodology

2.1. Sampling sites

Four different sites located in the North Sumatera Province that have different characteristics were selected, or, 1) a roadside, 2) a school environment and 3) an industrial area in Medan City and 4) a near volcano area in the Karo Regency, were selected for the air sampling (See Figure 1).

The roadside site was located at Sisingamaraja St (N 3°33'37.4" E 98°41'38.0"), the main access of transportation from Amplas station to the center of Medan city and one of the busiest roads in this area with heavy traffic at almost all times. The selected school site was located at the 4th floor of Eria College School (N 3° 33' 38.0" E 98 ° 41' 38.4"), about 12 m away from the street. Eria College School is one of

private schools in Medan city consisting of four different grades (kindergarten, elementary school, Junior High School, and Senior High School) with a total student population of up to 600 students and it is open from 07:00 a.m. to 15:00 p.m. Monday to Saturday.

The industrial site was on the roof top of an office sector of PT. Gunung Gahapi Sakti in the 1st Medan Industrial Area (KIM 1)-Medan city (N 3° 40' 25.3" E 98° 39' 54.3") and is surrounded by various industries such as palm oil, rubber, chocolate, coffee, tea, seafood, canning fish, food and beverage, steel and agricultural industries.

The volcano area site was chosen at the roof top of Mt. Sinabung Observatory Agency (N 3° 08'28.3" E 98° 27'51.5") located in a local community around 8 km away from the top of Sinabung Mt., an active volcano since 2010 after had been dormant since the 16th century (around 400 years). This area contains a small community of local people. Land use in this area was predominantly for agricultural activities (e.g. rice field) with small scale open burning.

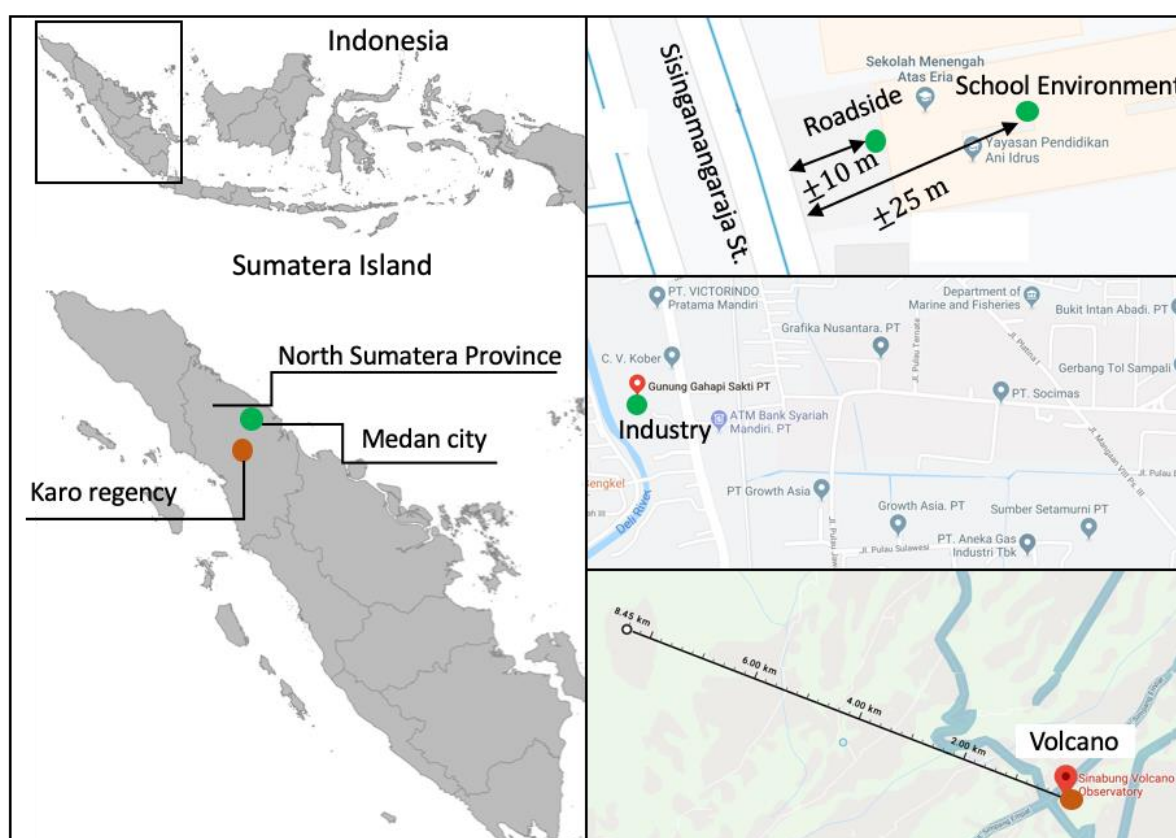


Figure 1. Locations of sampling sites in North Sumatera Province, Indonesia (roadside, school environment, industry, volcano)

2.2. Sampling methods and procedure

A cascade air sampler consisting of four impactor stages (10, 2.5, 1.0, 0.5 μm of cutoff sizes) and one inertial filter stage for the separation of particles less than 0.1 μm ($\text{PM}_{0.1}$) along with a backup filter for the collection of $\text{PM}_{0.1}$ (Furuuchi et al., 2010) was used at a flowrate of 40 l/min. Quartz fibrous filters (QFF) (Pallflex Tissuquartz 2500QAT-UP; Pall Corp., Japan) of $\text{Ø}55$ mm that had been pre-baked at 350°C in an oven for 1 hour then conditioned at $21.5 \pm 1.5^\circ\text{C}$, and $35 \pm 5\%$ RH in a $\text{PM}_{2.5}$ weighing chamber (PWS- $\text{PM}_{2.5}$; Tokyo Dylec Corp., Japan) for 48 hours before and after the sampling. Webbed stainless steel fibers (average fiber diameter of 9.8 μm , steel type SUS316; Nippon Seisen, Japan) were

located inside the nozzle of the inertial filter consisting of a duralumin cartridge with a 5.25 mm diameter nozzle that was 5.5 mm in length. To evaluate possible contaminants (e.g. gaseous carbon component adsorption), a travel blank filter was also prepared.

The air sampling was conducted for 7 days at each site. At the road side and school sites, day and night time samples were collected each for 12 hours so as to discuss the diurnal-nocturnal difference of PM level. The sampling duration was 24 hours for the other sites. The sampling information is summarized in Table 1.

Table 1. Information on sampling sites, sampling duration and period and meteorological conditions
(a)

Site	Method	Period	Start time	End time	Duration (hour)	Number of samples (n)
Roadside	day-time	Feb 19 th – 26 th	06:00	17:30	11.5	7
	night-time	Feb 19 th – 26 th	18:00	05.30 (same for following days)	11.5	7
School environment	day-time	Feb 19 th – 26 th	06:00	17:30	11.5	7
	night-time	Feb 19 th – 26 th	18:00	05.30 (same for following days)	11.5	7
Industry	day-night	Feb 26 th – March 5 th	09:00	08:30 (same for following days)	23.5	7
Volcano	day-night	March 5 th – March 12 th	16:00	15:30 (same for following days)	23.5	7

(b)							
Site	Method	Temp (°C)*	Wind Speed (km/h)*	Cloud (%)*	Humidity (%) *	Precipitation (mm)*	Sunlight (hour)**
Roadside	day-time	30.14	6.46	27.83	66.89	0.01	8.44
	night-time	26.74	5.37	25.46	83.40	0.11	0.00
School environment	day-time	30.14	6.46	27.83	66.89	0.01	8.44
	night-time	26.74	5.37	25.46	83.40	0.11	0.00
Industry	day-night	28.6	6.2	35.3	73.9	0.3	8.23
Volcano	Day-night	29.3	5.7	37.7	70.4	0.5	7.90

*www.worldweatheronline.com

**www.bmkg.go.id

2.3. Carbon analyses

Particle-bound carbonaceous components as organic carbon (OC) and elemental carbon (EC) were evaluated using a Sunset Laboratory Carbon Aerosol Analyzer with the IMPROVE_TOR protocol (Chow et al., 2004; Watson et al., 2005). An area of 1.5 cm² (1.5 cm x 1 cm) squarely punched from each filter sample was analyzed for four OC fractions (OC1, OC2, OC3, OC4 at 120°C, 250°C, 450°C, 550°C, respectively) in 100% Helium (He) while the EC fractions (EC1, EC2, and EC3 at 550 °C, 700 °C, 800 °C, respectively) were analyzed in a 2% O₂/98% He atmosphere. The total OC was defined as the sum of OC1-OC4 and a pyrolyzed carbon fraction (Py-OC) and the total EC was defined as EC1+EC2+EC3+(Py-OC). MDL (0.2) was confirmed to be small enough to a filter blank value.

2.4. Hotspot and Backward trajectory

Hotspots or active fire distributions were obtained from Web Fire Mapper produced by the US NASA (NASA, 2019) using the Moderate Resolution Imaging Spectroradiometer (MODIS) satellite. Air mass backward trajectories provided by Air Resources Laboratory with the Single-Particle Lagrangian Integrated Trajectory (HYSPPLIT) model (Draxler and Hess, 1998; Air Resource Laboratory (ALR), 2019) were used along with the hot spot distribution data. 24 hours backward trajectories were analyzed by a vertical motion calculation method of air masses that estimates the average ground level (AGL) of 500 meters above the monitoring site (Engling et al., 2014; Erel et al., 2007).

3. Results and Discussion

3.1. Mass concentration of particles

The average particle mass concentrations of different size categories, or, total suspended particulates (The average particle mass concentrations of different size categories, or, total suspended particulates (TSP), PM₁₀, PM_{2.5}, PM₁ and PM_{0.1} at four different sites are shown in Figure 2, in which PM₁ and PM_{0.1} respectively denote particles smaller than 1 and 0.1 μm. The mass concentration for each PM fraction and the ratios between fractions are also listed in Table 2 and compared with those from other locations in Table 3 (Kim et al., 2002; Hata et al., 2009; Thuy et al., 2018; Phairuang et al., 2019) Similar PM concentrations were observed at the road side (RS) and school sites (SE) both for a diurnal (D) and a nocturnal (N) sampling periods while definitely larger values for the industry site (IA) and smaller values for the volcano site (VA) were obtained. The average PM₁₀ and PM_{2.5} values were much larger than the WHO guidelines for 24 hours (50 and 25 μg/m³, respectively) except those at the volcano area. However, even at an industrial area site (IA), the PM concentration was rather moderate compared to corresponding values for the forest fire season in Indonesia (Kuwata et al., 2018). This may be related to a much less influence by air mass transportation through areas of a lower number of hot spots, as shown in Figure 3. The PM_{0.1} level in urban and industrial areas was similar to the annual average of Bangkok (14.80 ± 1.99) but lower than that in Chiang Mai (25.21±4.73 μg/m³), where the influence of forest fires is significant every February and March (Phairuang et al., 2019), and was larger than that in Hanoi, Vietnam (annual average 6.06 ± 2.71 μg/m³) (Thuy et al., 2018). PM_{0.1}/PM_{2.5} and PM_{2.5}/PM₁₀ ratios were 16.4 ~ 27.5% and 71.7 ~ 80.6%, respectively that were similar to other cities in East Asia region (Thuy et al., 2018); (Phairuang et al., 2019) (Kim et al., 2011a) (Kim et al., 2011b) (Liu et al., 2017).

Table 2. Mass concentration of each size fraction of particles and ratios between different fractions at studied sites

Mass concentration of PM fraction ($\mu\text{g}/\text{m}^3$)							
Size range (μm)	RSD	RSN	SED	SEN	IA	VA	
<0.1	15.56±6.05	10.70±2.01	17.23±3.15	15.39±2.84	16.78±4.02	7.09±2.47	
0.1-0.5	9.55±1.59	12.65±2.28	7.95±1.14	11.24±2.97	10.55±2.37	3.28±1.63	
0.5-1.0	18.96±7.30	20.58±6.59	18.00±3.68	25.61±4.40	31.29±5.90	9.73±3.54	
1.0-2.5	16.60±9.65	21.32±6.37	19.52±5.40	21.24±5.43	30.74±5.55	7.80±3.98	
2.5-10	21.22±7.39	17.85±6.22	21.96±7.09	19.74±5.49	35.29±7.03	6.70±3.45	
>10	13.33±6.69	6.58±3.17	11.59±3.68	10.25±5.45	23.96±6.54	3.77±3.89	
Ratio of mass fraction of particle (%)							
Size range (μm)	RSD	RSN	SED	SEN	IA	VA	
<0.1	16.38±4.08	12.27±3.18	17.89±2.02	14.83±2.27	11.26±1.59	18.77±2.52	
0.1-0.5	11.42±5.89	14.56±3.85	8.40±1.49	10.87±2.04	7.13±1.15	9.40±5.99	
0.5-1.0	20.77±6.81	22.56±5.51	18.64±2.05	24.97±2.59	21.11±2.00	26.43±7.97	
1.0-2.5	15.91±7.56	24.22±7.87	20.71±7.39	20.75±4.32	20.72±0.96	19.41±3.94	
2.5-10	22.55±3.91	19.37±4.30	22.47±5.72	19.04±3.08	23.78±1.98	17.36±4.61	
>10	12.96±5.36	7.03±2.75	11.88±2.40	9.54±4.29	16.00±2.60	8.64±7.82	
Ratio between different size fractions (-)							
PM _{0.1} /PM _{2.5}	25.66±6.50	16.40±3.40	27.47±4.39	20.95±3.19	18.78±2.77	25.40±6.04	
PM _{2.5} /PM ₁₀	74.08±4.26	78.52±5.03	74.07±6.57	78.82±3.22	71.69±1.80	80.64±6.27	

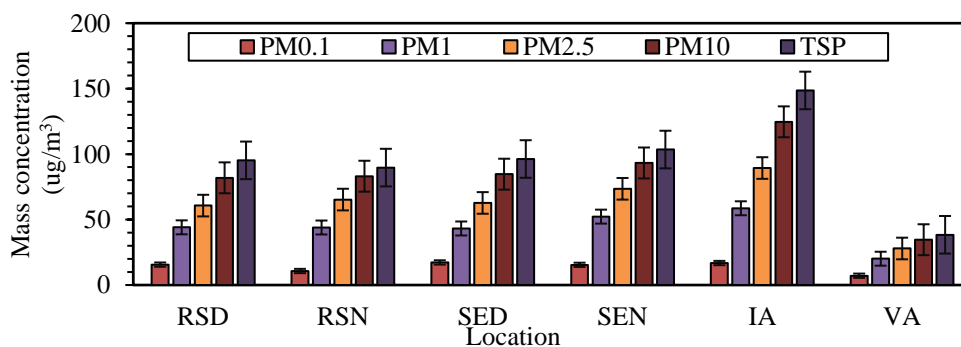


Figure 2. Mass concentration of each size category of particles (PM_{0.1}, PM₁, PM_{2.5}, PM₁₀, and TSP) at studied sites

Table 3. Mass concentration of PM_{0.1} in other countries compared with the present study

Location	Characteristic	Concentration (µg/m ³)	Reference
	Urban-traffic	13.13	This study
North Sumatera, Indonesia	Urban-traffic	16.31	This study
	Urban-industry	16.78	This study
	Rural-volcano	7.09	This study
Hanoi, Vietnam	Urban-Traffic	6.06 (annual ave.)	Thuy et al., 2018
	River side	1.34 (February-June 2001)	Kim et al., 2002
Los Angles, USA	Urban	4.11 (September 2000-January 2001)	Kim et al., 2002
	Mixed	4.7(May 2007)	Hata et al., 2009
Bangkok, Thailand	Urban	14.80 (annual ave.)	Phairuang et al., 2019
Chiang Mai, Thailand	Mixed	25.21 (annual ave.)	Phairuang et al., 2019

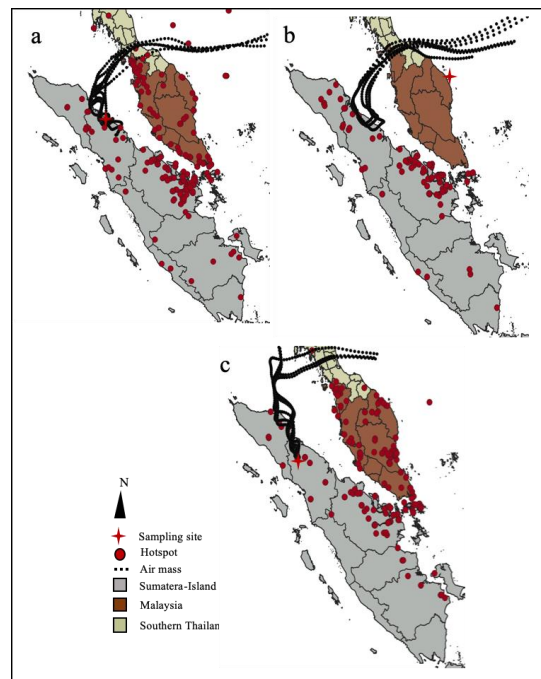
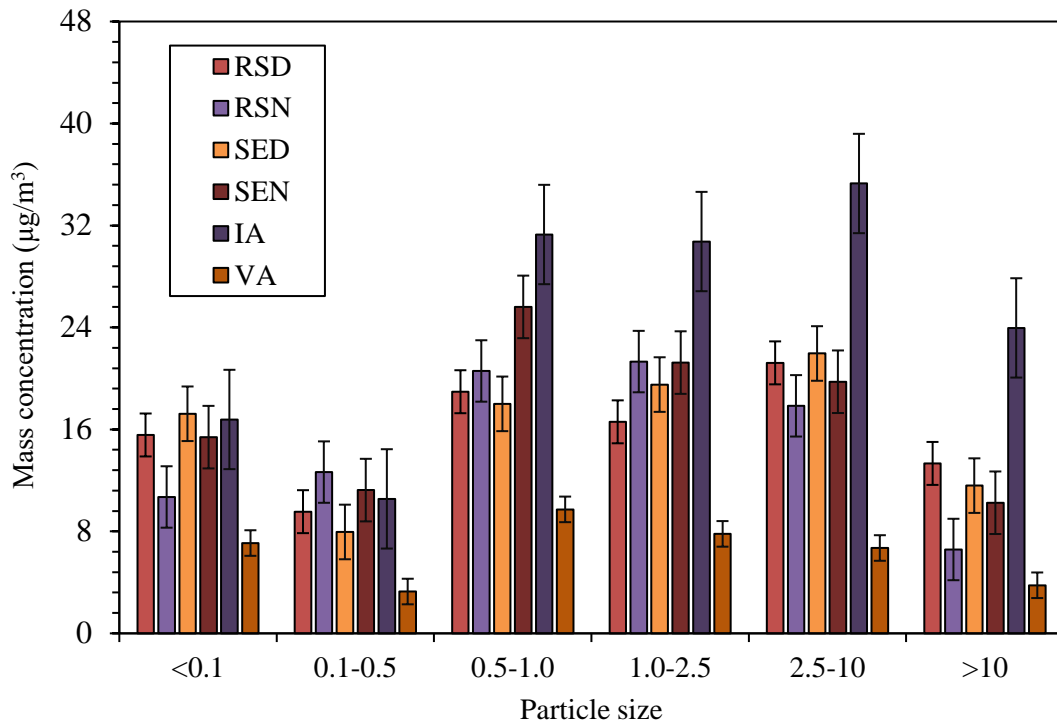
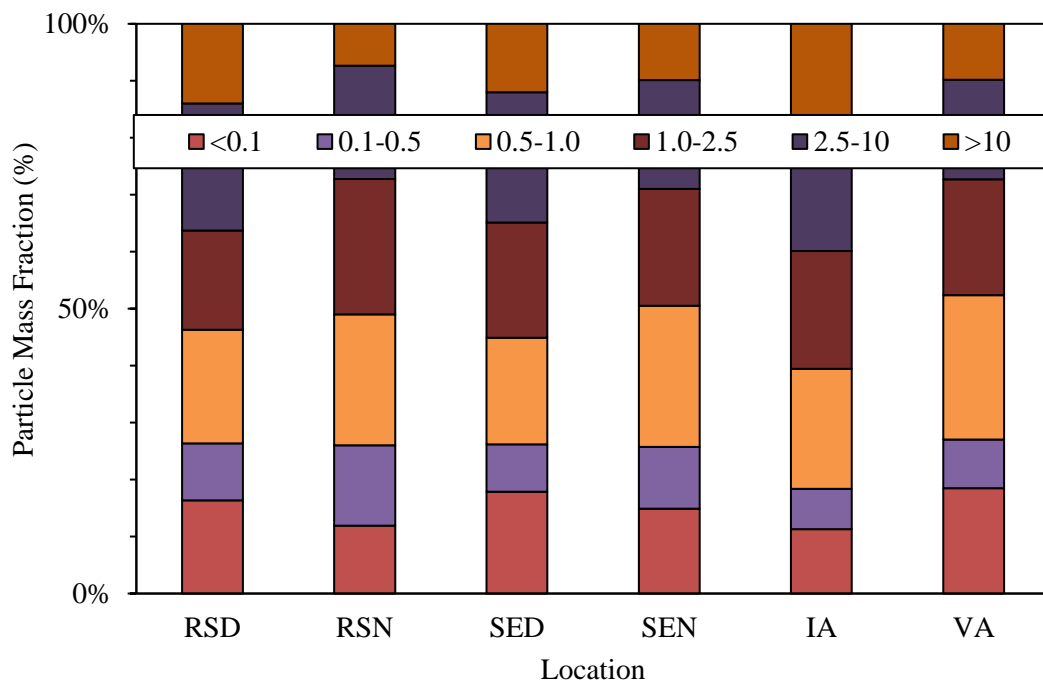


Figure 3. Distribution of hotspot and air mass trajectories corresponding to sites at (a) roadside and school environment, (b) industry and (c) volcano



(a)



(b)

Figure 4. Mass concentration (a) and fraction (b) of size fractionated particles evaluated at studied sites

In Figure 4, the particle mass concentration and the mass fraction of each category of particle sizes are summarized. Fractions of particles larger than 0.5 μm , particularly $> 1 \mu\text{m}$, at the IA site were clearly larger than at other locations while the particle concentration of particles $< 0.5 \mu\text{m}$ was similar to those at urban sites. This may suggest that a larger fraction ($>2.5\mu\text{m}$) of coarse particles may be caused by road dust produced by the transportation by heavy duty vehicles along with the diesel emissions (0.5-2.5 μm) while taking into account the rather short distance from Yos Sudarso Street nearby sampling site ($\sim 20 \text{ m}$).

Since the VA site was located in a rural area consisting of agricultural fields and vegetation including forest areas, emission sources in the area could be due to local household emissions, community traffic and the small-scale open burning of agricultural residues and wastes except when the volcano is actively erupting. Although this site may provide PM background data for North Sumatera, the $\text{PM}_{0.1}$ concentration was still larger than those in cleaner areas, e.g., 1.34 ~ 4.11 in Los Angeles, USA (Kim et al., 2002). 1~4 $\mu\text{g}/\text{m}^3$ in Japan (Hata et al., 2009) and the largest $\text{PM}_{0.1}$ fraction was observed at the VA site. These can be attributed to the influence of the above local sources.

The PM concentration and particle size distribution in the road side environments (RS, SE) were quite similar but this is reasonable given the fact that that the sites were at a similar distance from a main road (10~25 m). However, in spite of the fact that the traffic and children's activities as well as biomass fuel burning at a restaurant in the school should have some influence, only a slight difference was observed both in road side and school environments. Although this should be related to a decrease in the height of mixing layer, such a behavior suggests that the background environment in the corresponding area, e.g., as household, restaurants, traffic in a surrounding area, open burning of wastes etc. make constant contributions.

3.2. Carbonaceous components in $\text{PM}_{0.1}$

The average concentrations of OC and EC and their ratio for $\text{PM}_{0.1}$ are shown in Figure 5. The total carbon (TC) at the roadside and school sites was quite similar and clearly larger than the corresponding values at the other two sites (industry and volcano). A smaller TC fraction to PM mass at the industrial site (22.8%) than that at roadside, school and volcano sites (29.2~51.3%) can be attributed to chemicals from secondary particle formation, e.g., as sulfate corresponding to emission from industries that use coal as a main fuel. The OC/EC ratios at all sites were similar (4.26 ~ 6.49) and can be attributed to a large fraction of secondary organic carbon (SOC) that could be associated with a combination of vehicles, coal, and biomass combustion. It should also be noted that the char-EC/soot-EC ratio, an indicator of biomass burning to diesel emission (Chow et al., 2004; Cao et al., 2006; Zhu et al., 2010), was in the range of 0.10 ~ 0.34 that corresponds to a predominant influence of emission from vehicular traffic although there was a slight increase possibly caused by local open biomass burning in the vicinity of the volcano site and to cooking at a school restaurant during daytime (Phairuang, et al., 2019). The Py-OC/OC₄ ratio, an indicator of biomass burning (Fujii et al., 2016), was slightly larger at the industrial site than at the other sites, which is probably related to an emission from a biomass power plant located $\sim 130 \text{ m}$ away from the IA site.

4. Conclusion

The status and possible emission sources of ambient particles in North Sumatera Province, Indonesia were evaluated based on monitoring at four different sites that were located in different areas of land use during the rainy season (19, Feb.-12, Mar., 2019) using a cascade air sampler that can collect TSP and $\text{PM}_{10/2.5/1/0.5/0.1}$. The possible influence of transboundary air mass movement through areas of hot spots was also discussed. Carbonaceous components in ultrafine particles, or, $\text{PM}_{0.1}$ were analyzed in order to determine if these emission sources are a risk but unknown air pollutant to be managed. The average PM_{10} and $\text{PM}_{2.5}$ values at urban sites were much larger than the WHO guideline for 24 hours.

However, the situation was rather moderate compared to other severe conditions, e.g., in Chiang Mai in the forest fire season. This represents the first report of the collection of data for PM_{0.1} in Indonesia and

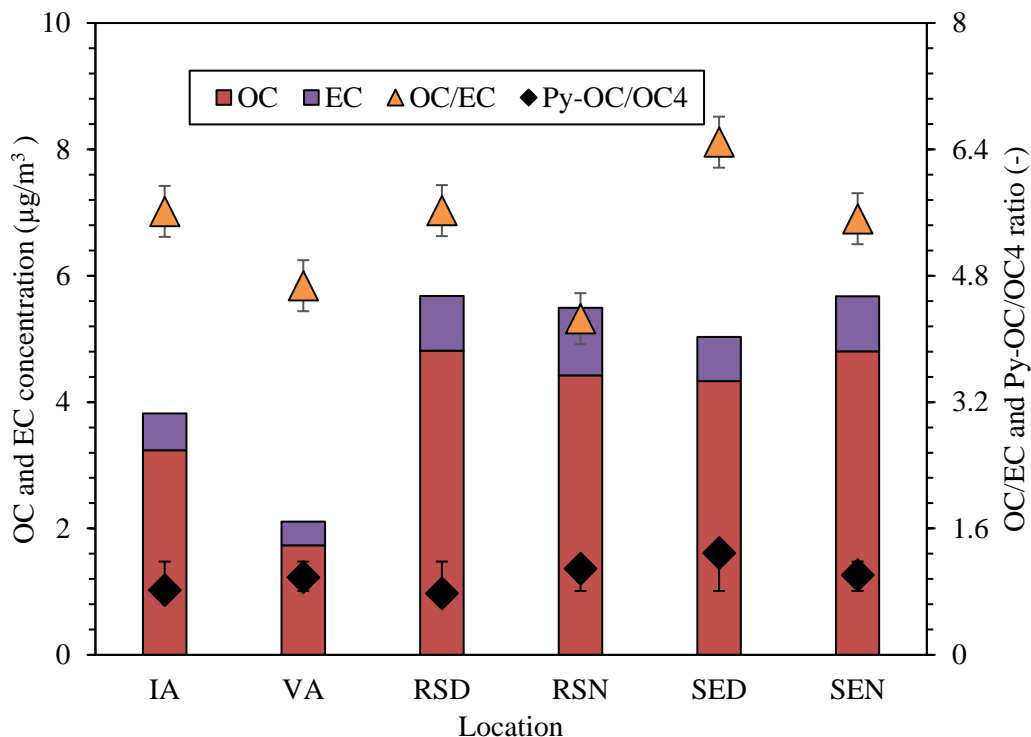


Figure 5. Carbonaceous components and indices in PM_{0.1}: OC, EC, OC/EC and Py-OC/OC4

its level in urban sites were similar to those in other large cities in East Asia region. A small difference between diurnal and nocturnal PM concentration was observed at road side sites. A smaller fraction of TC in the PM_{0.1} range at the industrial site can be attributed to particles from the secondary formation. The OC/EC ratio in PM_{0.1} was somewhat similar between the studied sites (4.26 ~ 6.49) and the char-EC/soot-EC ratio was consistently smaller than 1 (0.10 ~ 0.34), indicating that transportation or coal combustion as local emission sources appear to be the main sources of air pollution sources in North Sumatera Province. For a more detailed discussion, air quality during different seasons such as a peatland fire season in Indonesia should also be evaluated by using other chemicals in different size fractions.

5. References

Akbarzadeh, M.A., Khaheshi, I., Sharifi, A., Yousefi, N., Naderian, M., Namazi, M.H., Safi, M., Vakili, H., Saadat, H., Alipour Parsa, S., Nickdoost, N. 2018. The association between exposure to air pollutants including PM₁₀, PM_{2.5}, ozone, carbon monoxide, sulfur dioxide, and nitrogen dioxide concentration and the relative risk of developing STEMI: A case-crossover design. *Environ Res.*161, 299-303

Badan Pusat Statistik (BPS-Statistics of North Sumatera), 2019. North Sumatera in Figure. North Sumatera, Indonesia: BPS.

Badan Pusat Statistik (BPS-Statistics of Medan City), 2019. Medan City in Figure. Medan, Indonesia: BPS.

Badan Pusat Statistik (BPS-Statistics of Medan), 2015. Medan City in Figure. Medan, Indonesia: BPS



- Chow, J. C., Watson, J. G., Chen, L. W. A., Arnott, W. P., Moosmuller, H., 2004. Equivalence of elemental carbon by thermal/optical reflectance and transmittance with different temperature protocols. *Environmental Science & Technology*. 38, 4414–4422.
- Roland, D., Hess, G., 1998. An overview of the HYSPLIT_4 modeling system for trajectories, dispersion, and deposition. *Australian Meteorological Magazine*. 47, 295–308.
- Cao, J.J., Lee, S.C., Ho, K.F., Fung, K., Chow, J.C., Watson, J.G., 2006. Characterization of roadside fine particulate carbon and its eight fractions in Hong Kong. *Aerosol Air Qual. Res.* 6, 106–122.
- Chen Y.J., Zhi G.R., Feng Y.L., Fu J.M., Feng J.L., Sheng G.Y., Simoneit B.R.T., 2006. Measurements of emission factors for primary carbonaceous particles from residential raw-coal combustion in China. *Geophys. Res. Lett.* 33,382.
- Chow, J.C., Watson, J.W., Kuhns, H., Etyemezian, V., Lowenthal, D.H., Crow, D., Kohl, S.D., Engelbrecht, J.P., Green, M.C., 2004. Source profiles for industrial, mobile, and area sources in the Big Bend regional aerosol visibility and observational study. *Chemosphere*. 54, 185–208.
- Chow J.C., Watson J.G., Lu Z., Lowenthal D.H., Frazier C.A., Solomon P.A., Thuillier R.H., Magliano K., 1996. Descriptive analysis of PM_{2.5} and PM₁₀ at regionally representative locations during sjvaqs/auspex. *Atmos. Environ.* 30, 2079–2112.
- Clifford, S., Mazaheri, M., Salimi, F., Ezz, W.N., Yeganeh, B., Low-Choy, S., Walker, K., Mengersen, K., Marks, G.B., Morawska, L., 2018. Effects of exposure to ambient ultrafine particles on respiratory health and systemic inflammation in children. *Environment International*. 114, 167–180.
- Erel, Y., Kalderon-Asael, B., Dayan, U., Sandler, A., 2007. European atmospheric pollution imported by cooler air masses to the Eastern Mediterranean during the summer, *Environ. Sci. Technol.* 41, 5198–6003.
- Engling, G., He, J., Betha, R., Balasubramanian, R., 2014. Assessing the regional impact of Indonesian biomass burning emissions based on organic molecular tracers and chemical mass balance modeling. *Atmospheric Chemistry and Physics*. 14, 10.5194.
- Yusuke, F., Mastura, M., Masafumi, O., Susumu, T., Junko, M., Akira, M., 2016. A Key Indicator of Transboundary Particulate Matter Pollution Derived from Indonesian Peatland Fires in Malaysia. *Aerosol and Air Quality Research*. 16, 69–78.
- Furuuchi, M., Eryu, K., Nagura, M., Hata, M., Kato, T., Tajima, N., Sekiguchi, K., Ehara, K., Seto, T., Otani, Y., 2010. Development and performance evaluation of air sampler with inertial filter for nanoparticle sampling. *Aerosol and Air Quality Research*. 10, 185–192.
- Mitsuhiko, H., Bai, Y., Masami, F., Fukumoto, M. Yoshio, O., Kazuhiko, S., Tajima, N., 2009. Status and characteristics of ambient aerosol nano-particles in Kakuma, Kanazawa and comparison between sampling characteristics of air samplers for aerosol particle separation. *Japan See Reserch*. 40, 135–140.
- Heinzerling, A., Hsu, J., Yip, F., 2016. Respiratory Health Effects of Ultrafine Particles in Children: A Literature Review. *Water, Air, and Soil Pollution*, 227, 32.
- Hendrasto, M., Surono, Budianto, A., Kristianto, Triastuty, H., Haerani, N., Basuki, A., Suparman, Y., Primulyana, S., Prambada, O., Loeqman, A., Indrastuti, N., Andreas, A.S., Rosadi, U., Adi, S., Iguchi, M., Ohkura, T., Nakada, S., Yoshimoto, M., 2012. Evaluation of volcanic activity at sinabung volcano, after more than 400 years of quiet. *Journal of Disaster Research*. 7, 37–47.
- Intergovernmental Panel on Climate Change (IPCC), 2001. *Climate Change 2001: The Scientific Basis: Contribution of Working Group I to the Third Assessment Report of the Intergovernmental Panel on Climate Change*, edited by J. T. Houghton et al., pp. 881, Cambridge Univ. Press, New York.
- Lee, K.K., Miller, M.R., Shah, A.S.V., 2018. Air pollution and stroke. *J. Stroke*. 20, 2-11.

- Kaufman, Y., Tanré, J.D., Boucher, O., 2002. A satellite view of aerosols in the climate system, *Nature*. 419, 215–223.
- Kim, K.H., Sekiguchi, K., Furuuchi, M., Sakamoto, K., 2011a. Seasonal variation of carbonaceous and ionic components in ultrafine and fine particles in an urban area of Japan. *Atmospheric Environment*. 45, 1581–1590.
- Kim, K.H., Sekiguchi, K., Kudo, S., Sakamoto, K., 2011b. Characteristics of atmospheric elemental carbon (char and soot) in ultrafine and fine particles in a roadside environment, Japan. *Aerosol and Air Quality Research*. 11, 1–12.
- Kim, S., Shen, S., Sioutas, C., Zhu, Y., Hinds, W.C. 2002. Size distribution and diurnal and seasonal trends of ultrafine particles in source and receptor sites of the Los Angeles basin. *J. Air Waste Manage. Assoc.* 53, 297–307.
- Kriswati, E., Meilano, I., Iguchi, M., Abidin, H.Z., Surono., 2018. An evaluation of the possibility of tectonic triggering of the Sinabung eruption. *Journal of Volcanology and Geothermal Research*. 0–8.
- Kuwata, M., Neelam-Naganathan, G.G., Miyakawa, T., Khan, M.F., Kozan, O., Kawasaki, M., Sumin, S., Latif, M.T., 2018. Constraining the Emission of Particulate Matter From Indonesian Peatland Burning Using Continuous Observation Data. *Journal of Geophysical Research: Atmospheres*. 123, 9828–9842.
- Liu, L., Urch, B., Szyszkowicz, M., Speck, M., Leingartner, K., Shutt, R., Pelletier, G., Gold, D.R., Scott, J.A., Brook, J.R., Thorne, P.S., Silverman, F.S., 2017. Influence of exposure to coarse, fine and ultrafine urban particulate matter and their biological constituents on neural biomarkers in a randomized controlled crossover study. *Environment International*. 101, 89–95.
- Manigrasso, M., Natale, C., Vitali, M., Protano, C., Avino, P., 2017. Pedestrians in traffic environments: Ultrafine particle respiratory doses. *International Journal of Environmental Research and Public Health*. 14.
- NASA, 2019. <https://earthdata.nasa.gov/earth-observation-data/near-real-time/firms>.
- Phairuang, W., Suwattiga, P., Chetiyankornkul, T., Hongtieab, S., Limpaseni, W., Ikemori, F., Hata, M., Furuuchi, M., 2019. The influence of the open burning of agricultural biomass and forest fires in Thailand on the carbonaceous components in size-fractionated particles. *Environmental Pollution*. 247, 238–247.
- Tampubolon, J., Nainggolan, H.L., Ginting, A., Aritonang, J., 2018. Mount Sinabung Eruption: Impact on Local Economy and Smallholder Farming in Karo Regency, North Sumatra. *IOP Conference Series: Earth and Environmental Science*. 178.
- Thuy, N.T.T., Dung, N.T., Sekiguchi, K., Thuy, L.B., Hien, N.T.T., Yamaguchi, R., 2018. Mass Concentrations and Carbonaceous Compositions of PM_{0.1}, PM_{2.5}, and PM₁₀ at Urban Locations of Hanoi, Vietnam. *Aerosol and Air Quality Research*. 18, 1591–1605.
- Watson, J.G., Chow, J.C., Chen, L.-W.A., 2005. Summary of Organic and Elemental Carbon/Black Carbon Analysis Methods and Intercomparisons. *Aerosol and Air Quality Research*. 5, 65–102
- Wu, J.Z., Dan-Dan, G., Lin-fu, Z., Ling, Y., Ying, Z., Qi Yuan, L., 2018. Effects of particulate matter on allergic respiratory diseases. *Chronic Dis Transl Med*. 4, 95–102.
- Zhu, C.S., Chen, C.C., Cao, J.J., Tsai, C.J., Chou, C.C.K., Liu, S.C., Roam, G.D., 2010. Characterization of carbon fractions for atmospheric fine particles and nanoparticles in a highway tunnel. *Atmos. Environ*. 44, 2668–2673.

Acknowledgment

This studies was supported by an INPEX Foundation scholarship.

Commuter exposure to black carbon, fine particulate matter and particle number concentration in public marine transport in Istanbul

Burcu Onat, Ulku Alver Sahin, Burcu Uzun, Ozcan Akin, Fazilet Ozkaya and Coskun Ayvaz

Istanbul University-Cerrahpasa, Engineering Faculty, Environmental Engineering Department, Turkey

bonat@istanbul.edu.tr

Abstract. This paper presents a measurement and analysing of concentrations for black carbon (BC), particle number, and PM_{2.5} ($\leq 2.5 \mu\text{m}$) whilst commuting along by ferry in Istanbul. In this context, exposure to the mentioned pollutants was estimated for car ferry, fast ferry and at the pier, and for two travel routes, for a total of 89 trips. BC, particle number concentration (PNC) and PM_{2.5} measurements were simultaneously performed in a ferry and at the piers, and the correlation between pollutant concentrations, meteorological parameters, and environmental factors were analysed. The mean concentrations for all pollutants in car ferry were lower than the average concentrations in fast ferry. The ratio of fast ferry to car ferry for BC, PNC and PM_{2.5} was 6.4, 1.2 and 1.3, respectively. The high variability of the concentrations was observed at the piers and in ferry during berthing. The highest mean concentrations of BC ($14.3 \pm 10.1 \mu\text{g}/\text{m}^3$) and PNC ($42005 \pm 30899 \text{ \#/cm}^3$) were measured at Yalova pier. The highest total exposure to PNC and PM_{2.5} were in car ferry mode, the highest total exposure to BC was in fast ferry mode.

Keywords: Commuter exposure, Ferry, Pier, Black carbon, Particle number concentration, PM_{2.5}.

1. Introduction

Sea transport is an alternative public transport type in metropolitan cities. Passenger ferries in populous urban port cities are simply another commuting choice, alongside cars, trains, and buses. Passenger ferries provide a faster option to navigate metropolis cities. Travelling with fast ferry reduce the commute time and provide a comfortable trip (Corbett and Farrell, 2002). Passenger vessels maintain stability over time due to their regular services (Tichavska et al., 2015). Although passenger vessels not being as common as road vehicles and rail systems, the commuter exposure in marine transport is an important issue for passengers due to the high exhaust emission of vessels. The commuters are exposed to air pollutants sourced from passenger vessels during disembarking and boarding. Vessel traffic and passenger shipping are sources of air pollution in piers (Tichavska et al., 2015), shipping-related air pollutants are responsible for cardiopulmonary and lung cancer deaths, with most deaths occurring near coastlines (Corbett et al., 2007). There is no sufficient data nor detailed information available on commuter exposure in ferry and at the piers. Most of marine air quality studies are about the determination of emissions from ships. Only few studies were conducted in ferry. Lau and Chan (2003) investigated the VOC levels in ferry, road transport and railway, they revealed that the exposure levels in ferry were the lowest. Chan et al (2002) collected PM₁₀ samples in ferry in Hong Kong, they found PM₁₀ levels in ferries were higher than the air-conditioned roadway transport.

Particles with an aerodynamic diameter of less than 0.1 μm are defined as ultrafine particles (UFP) (Hinds, 1999). UFP contributes to 90% of particle number concentration (PNC) in urban areas and the major source of UFP is motor vehicle emissions (WHO, 2016; Morawska et al., 2008). Due to the small size of the UFP, it easily causes adverse effects on respiratory and cardiovascular systems (Valavanidis et al., 2008). Black carbon (BC), a component of fine particle ($\text{PM}_{2.5}$) (EPA, 2010), causes respiratory diseases and lung cancer (Fann et al., 2012), and is also considered as the second most major pollutant affecting climate change after CO_2 (Bond et al., 2013). Compared to $\text{PM}_{2.5}$ (aerodynamic diameter less than 2.5 μm), BC has more impact on cardiorespiratory morbidity and mortality (Janssen et al., 2011). The ship emissions at piers/harbours cause the most PM emissions emits during operating at low engine loads during stops (Cooper et al., 2001). The impact of in-port ships on PM_{10} concentration was estimated to be +28.9 and concerned mainly the PM_1 size fraction (40%) (Ledoux et al., 2018). Recently, there have been many studies on personal exposure to $\text{PM}_{2.5}$, UFP and BC (Li et al., 2015; Moreno et al., 2015; Rivas et al., 2017; Ham et al., 2017; Tan et al., 2017), however, most of these studies were performed for road transport (buses and personal cars), rail system and subway. The studies on the measurement of pollutant exposures in marine mass transport is very limited. This limited studies showed that passengers are exposed to air pollutants during the day when they are traveling in vessels and waiting at the piers (Chan et al., 2002; Knibbs et al., 2010; Velasco et al., 2013).

Istanbul city is located in the northwestern Turkey (latitude 41°00'N, longitude 28°97'E) with a population of 14.4 million (TUIK, 2018), and the Bosphorus that separates the Asian and European continents is located in the middle of the city. Approximately 70% of Istanbul city is surrounded by Marmara Sea, Black Sea and Istanbul strait. Small passenger vessels are widely used in Istanbul. The Istanbul strait (Bosphorus) separates the city into two parts, marine transport are mostly preferred between the two sides of the strait to avoid road traffic in rush-hours. The percentage of sea transportation in Istanbul is 3.2% among the urban public transport modes and the total number of people carried on a day is 341,854 (IATR, 2017). Different types of passenger vessels (slow ferry, fast ferry, car ferry and water taxi) are used for marine domestic commuting in Istanbul. Fast ferry and car ferry are preferred on the routes that require long travelling time, because they offer more comfort and shorter commute time in comparison to road transport. Studies were carried out to determine the concentration of PM_{10} , $\text{PM}_{2.5}$ and particle number in road transport vehicles (Onat et al., 2012; Onat et al., 2017) and in subway (Sahin et al., 2012; Onat et al., 2013) in Istanbul. This is the first comprehensive study conducted on personal exposure in marine transport taking into account the relationship between air pollutants and environmental factors. The aim of this study is to determine the in-vessel and outdoor concentrations of BC, PNC and $\text{PM}_{2.5}$ in fast ferry, car ferry and at the piers and to investigate the relationship between the pollutants and meteorological parameters.

2. Methodology

2.1. Features of ferry modes and piers

The measurement operation in this study was conducted in Bakirkoy-Bostanci fast ferry line and Yenikapi-Yalova car ferry line (Figure 1). Bakirkoy-Bostanci line is common for domestic trips with fast ferry, while Yenikapi-Yalova line provides transporting from Istanbul to the south of the Marmara sea with car ferry. Fast ferry has an enclosed space for passengers. Car ferry has two separate areas: enclosed space to carry passengers and partly enclosed vehicle park area. The number of trips and route characteristics were given in Table 1 and the ferry characteristics were given in Table 2. There is one stop – Kadikoy pier - on the fast ferry route. Kadikoy pier has very intense traffic of slow ferries which are preferred for short trips. Bakirkoy, Bostanci, Yenikapi and Yalova are terminal piers which are mostly used for departure of fast ferry and car ferry. The number of departures at the piers vary according to the season and route and the probable external emission sources at the piers are also different (Table 3).



Figure 1. Routes for fast ferry and car ferry

Table 1. The route characteristics

Transport mode	Route	Route Length (km)	Commute Time (min)	Number of trips	Travel route
Fast ferry	Bakirkoy - Bostanci	20	50	69	Along the coast of the city
Car ferry	Yenikapi - Yalova	50	75	20	Mostly through the Marmara sea, far from the city

Table 2. The ferry characteristics

Transport mode	Type	Width (m)	Length (m)	Speed (knot)	Passenger capacity	Car capacity
Fast ferry	Catamaran	10	35	32	400	-
Car ferry	Double ended	21	82.27	22	600	108

Table 3. Ferry activity and external emission sources at the piers

Piers	Departure/day (summer)	Departure/day (winter)	Local emission sources	External emission sources
Bakirkoy	6	6	Fast ferry	Poor road traffic, yacht marina activity near the pier
Kadikoy	149	147	Slow ferry (95%) Fast ferry (5%)	Very high road traffic, intense residential&commercial area,
Bostanci	76	53	Slow ferry (13%) Fast ferry (87%)	High road traffic, intense residential area, slow ferry activities near the pier.
Yenikapi	47	22	Fast ferry, car ferry	Very high road traffic High road traffic, shipping port activities (Yalova-Topcular port) about 5 km away from the pier.
Yalova	28	23	Car ferry	

2.2. Measurement and instrumentation

The mass concentration of BC, PM_{2.5}, and PNC within a range of 10-1000 nm were measured simultaneously, from June 2016 to September 2017 in two different ferry lines (Bakirkoy-Bostanci and Yenikapi-Yalova) and four piers (Bakirkoy, Bostanci, Yenikapi and Yalova piers). The measurement process was done in this way: first, the pollutants measurements were carried out for 15 minutes at the pier. Then, the in-ferry measurements were performed until the end of the ferry route. Lastly, measurements were taken for 15 minutes at the pier. Similarly, the measurements were performed on the return route. In the fast ferry and car ferry, the researchers always sat in the middle of the ferry. Fast ferry and car ferry were powered by diesel and were mechanically ventilated. We had no control over ventilation in ferries. It is not allowed to go out during travel for passengers security in fast ferry and the door just opens at the piers. In contrast, it is allowed to go to deck during travel in car ferry.

BC was monitored by using microAeth AE51, a portable aethalometer (AethLabs, USA). The microAeth was operated at a flow rate of 100 mL min⁻¹, the data was recorded every 10 seconds and was outfitted with a 2.5-µm inlet. MicroAeth, AE51 has noise (peak and negative values) because of instrument maintenance; measurement sensitivity, such as vibration; humidity; flow rate; and operating conditions. These deviations and negative values are needed for post-processing or smoothing. The Optimized Noise-reduction Averaging (ONA) algorithm (aethlabs.com), which was developed by Hagler et al. (2011), was first applied for smoothing the obtained BC data. After post processing, a correction was applied for filter loading (Kirchstetter and Novakov, 2007; Wang et al., 2011). Lastly, the data for all trips were checked and the measurements with error signals were excluded, hence 15% of all data were removed from analysis.

PNC was monitored with CPC Model 3007 portable condensation particle counter (TSI Inc., Shoreview, MN, USA). The measurement correction for preventing the underestimation of PNC was applied (Westerdahl et al., 2005). The pDR 1200 portable real-time aerosol monitor (Thermo-Fisher Scientific, USA) was used to measure PM_{2.5}. The measurement accuracy of pDR 1200 was tested through the reference method. The details of the data processing for BC, correction method for PNC, and the

accuracy measurement results for PM_{2.5} were given in the previous study conducted by Onat et al. (Onat et al., 2019). The calibration of CPC and microAeth was done by the manufacturers.

2.3. Exposure estimation

The personal exposure to pollutants in ferry and at the piers were estimated by the equation-1 (Ham et al., 2017). In this study, the ventilation rate for a ferry passenger were assumed as 12.7 L min⁻¹ given by Zuurbier et al. (Zuurbier et al., 2009) for bus passenger. The average waits at the pier was assumed to be 5 minutes.

$$\text{Commute Exposure } (\mu\text{g}) = \text{Concentration } (\mu\text{g}/\text{m}^3) \times \text{Time (min)} \times \text{Inhalation Rate (m}^3/\text{min)} \quad (1)$$

3. Results and discussion

The personal exposure to concentrations of BC, PM_{2.5} and PNC in ferry and at the piers were measured for 89 trips in two different commuting modes (fast ferry and car ferry) and two different routes, distributed between the winter (%) and summer (%). Knowing that 15% of BC measurements were ignored as they were considered ineligible (e.g. data with error signals or negative values). The overall trip mean concentration results of BC, PM_{2.5} and PNC in ferries and at the piers were given in Table 2. The results and discussion are presented in four parts; comparison of exposure concentrations and spatial variation in ferry and at the pier are discussed first. Next, the relation between pollutants and meteorological parameters were statistically analyzed. After that, the seasonal variation of exposure concentration was discussed. Lastly, commute exposure was estimated in ferry and at the pier.

3.1. Concentration in ferry

The overall mean concentration results showed that the pollutant concentrations in car ferry were lower than the concentrations in fast ferry (Table 4). Our PNC and PM_{2.5} mean concentration results were lower than the previous study conducted by Knibbs et al. (2010). They observed that PNC and PM_{2.5} mean concentrations in ferry were 55400 #/cm³ and 58.3 μg/m³, respectively. In Hong Kong, Chan et al. (2002) found that the mean concentration of PM₁₀ in ferry was 81 μg/m³ in winter, but they have not mentioned the rate of PM_{2.5} to PM₁₀. In another study conducted in Hong Kong, the mean PM_{2.5} concentration was found as 60 μg/m³ (three trips only), higher than in road transport (bus, car, minibus) modes (Yang et al., 2019). Our PM_{2.5} results were lower than bus, and higher than car (windows closed mode) in comparison to the previous study in Istanbul conducted by Onat et al (2019).

We observed that the mean concentrations of BC in fast ferry and car ferry were 7.7 and 1.2 μg/m³, respectively. To the best of our knowledge, the exposure concentration of BC in ferry was not investigated in the previous studies. We found only one study on BC exposure in canal boats in Bangkok conducted by Velasco et al. (2013). They found that the mean concentrations of BC ranged from 15 to 411 μg/m³ inside canal boats (the surroundings of boat was open).

We observed that the ratio of fast ferry to car ferry for PNC and PM_{2.5} were 1.2 and 1.3, respectively. The greatest difference was found for BC: the ratio of fast ferry to car ferry was 6.4. The in-ferry pollutant concentrations might be affected by the proximity to the city, the number of the stops along the route, and the pollutant concentration at pier.

The exposure concentration for all pollutants in car ferry was lower than the concentrations observed at the piers (Table 4). Fast ferry travels along the coast of the city while car ferry mostly travels through the Marmara sea, far from the city coast. The long travel time and operating of ventilation might cause the lower pollutant concentrations in car ferry. Particulate level is greatly affected by the ventilation system of the transport (Chan et al., 2002).

Table 4. Pollutants descriptive in ferry and at the pier

Comm ute Mode	PNC (pt/cm ³)		BC (µg/m ³)		PM _{2.5} (µg/m ³)	
	Mean (Std.dev)	Median	Mean (Std.Dev.)	Median	Mean (Std.Dev.)	Median
Fast ferry	25001 (13611)	15461	7.7 (5.2)	4.8	19.5 (9.5)	16.8
Bakirkoy pier	31620 (22883)	22488	6.0 (7.2)	2.7	24.7 (15.9)	22.4
Bostanci pier	20416 (15333)	13837	12.3 (13.0)	4.5	26.1 (11.5)	24.5
Car ferry	20399 (7222)	18711	1.2 (0.8)	0.9	14.4 (6.3)	14.4
Yenikapi pier	24386 (13474)	20623	5.4 (4.6)	2.5	25.8 (13.9)	20.2
Yalova pier	42005 (30899)	32249	14.3 (10.1)	8.5	23.4 (8.8)	20.1

3.2. Concentration at the pier

The mean concentration of the pollutants were variable at the piers (Figure 2). The daily mean concentrations of BC, PM_{2.5} and PNC at the piers ranged from 0.4 to 39.4 µg/m³, 4.1 – 88.6 µg/m³, and 5925 – 101886 #/cm³, respectively. Considering the mean of all measurements, PM_{2.5} concentrations at the piers were similar, ranged from 23.4 to 26.1 µg/m³, but higher than the PM_{2.5} concentrations in ferry. The highest mean concentrations of BC (14.3 ± 10.1 µg/m³) and PNC (42005 ± 30899 #/cm³) were measured at Yalova pier (Table 4).

The ferry activity at the piers is variable (Table 3). The second highest mean BC concentration (12.3 µg/m³) was measured at Bostanci pier. Fast ferry traffic is very intense throughout the day in Bostanci pier, since different modes of marine transport are available such as slow ferry and water taxi. Therefore, more than one pier is used in Bostanci. The intense vessel traffic might affect the pollutant concentrations at pier (Tichavska et al., 2015). If more than two boats approach to the pier at the same time, longer-term concentrations may occur during heavy passenger voyages (Velasco et al., 2013) and the time schedules of ferry vessels may increase the level of emission during acceleration-deceleration (Jalkanen et al., 2009). The marine transport contributes significantly to air pollution, particularly in coastal areas (Corbett et al., 2007).

3.2.1. Correlation between urban air and pier for PM_{2.5} concentration.

The urban air quality monitoring in Istanbul has been conducted by the Ministry of Environment and Urban Planning at 38 site air quality monitoring stations (AQMS) and, the conventional air pollutants (nitrogen dioxide (NO_x), sulfur dioxide (SO₂), carbon monoxide (CO), PM₁₀ and PM_{2.5}) were monitored continuously. For PM_{2.5}, we analysed the relation between the concentration at AQMS and the concentration at the pier. The nearest AQMS's to the pier were considered for the correlation analysis. The hourly PM_{2.5} data at AQMS were paired with PM_{2.5} concentrations at the pier by calculating the time-weighted average of the matching time period. The correlation results were given in Figure 2. We observed that there were significant correlation between AQMS and the pier concentrations. Figure 2 shows that the correlation for PM_{2.5} between Catladikapi AQMS and Bakirkoy pier was $r = 0.62$ ($p < 0.01$). The correlation between Bostanci pier and the AQMS in Umraniye1 and Umraniye 2 was found as $r = 0.569$ ($p < 0.01$) and 0.619 ($p < 0.01$), respectively.

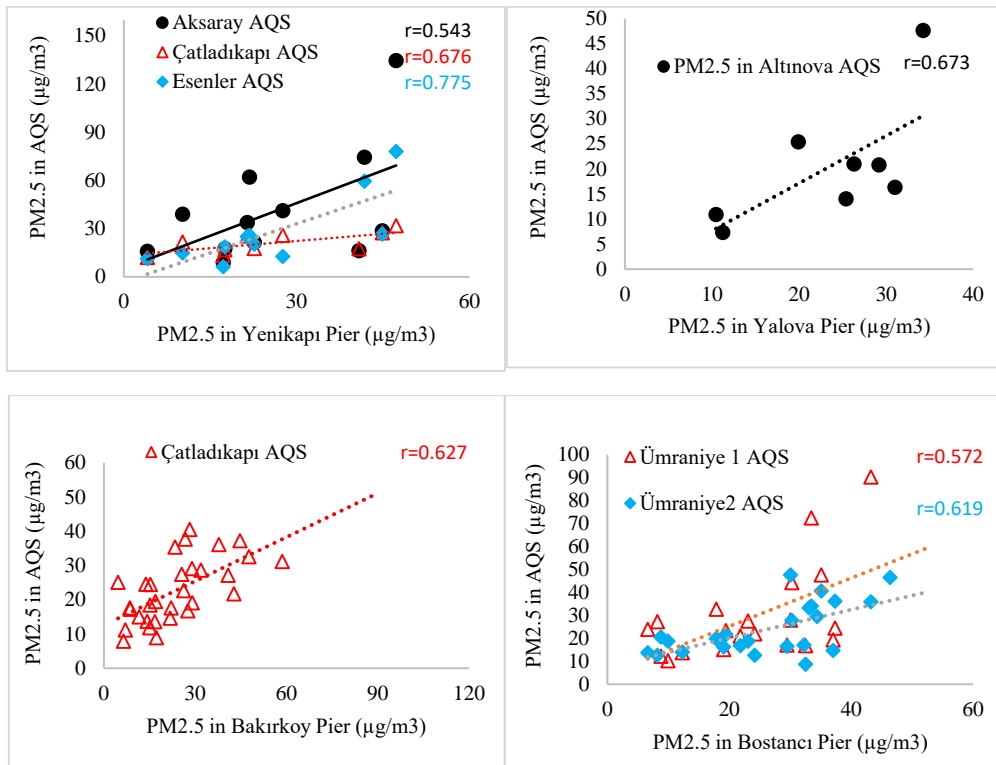


Figure 2. Scatterplots and Pearson correlation coefficient between the mean concentration of $PM_{2.5}$ in fixed Air Quality Station (AQS) and the mean concentration of $PM_{2.5}$ at the piers (Yenikapi, Yalova, Bakırköy and Bostancı)

For $PM_{2.5}$, we also observed significant correlations between AQMS and Yenikapi pier, and Yalova pier. The concentration of $PM_{2.5}$ at Yenikapi pier showed significant correlations with $PM_{2.5}$ concentration at Esenler AQMS ($r = 0.77$, $p < 0.01$), and Catladıkapi ($r = 0.67$, $p < 0.05$), and Aksaray AQMS ($r = 0.54$, $p < 0.06$). A correlation of ($r = 0.673$, $p < 0.06$) between Yalova pier and Altınova AQMS was found. These findings showed that the urban air quality could affect the concentration of $PM_{2.5}$ at the piers.

3.3. Estimation of commute exposure

The means and standard deviations of commuter exposures to PNC, BC and $PM_{2.5}$ per mile for in-ferry and at the piers were given in Table 5. The mean concentrations of pollutants provided in Table 2 were used for calculations. The highest average exposure per mile for BC was in fast ferry with $0.19 \mu\text{g mile}^{-1}$ ($0.08 \mu\text{g km}^{-1}$). The highest average exposures per mile for PNC and $PM_{2.5}$ were in car ferry with $10.7 \times 10^8 \text{ particles mile}^{-1}$ ($4.8 \times 10^8 \text{ particles km}^{-1}$) and $0.76 \mu\text{g mile}^{-1}$ ($0.34 \mu\text{g km}^{-1}$). When we took into account the total exposure during travel in ferry and waiting time at the pier, we explored that the highest total exposure to PNC and $PM_{2.5}$ were in car ferry mode, whereas the highest total exposure to BC was in fast ferry mode. In the previous study conducted by Onat et al (2019) in Istanbul, the commuter exposures to PNC, BC and $PM_{2.5}$ in road transport (bus, metrobus, car) were determined higher than the commuter exposure in car ferry and fast ferry, and we observed the commute exposure concentrations in car ferry and fast ferry were similar to the commute exposure to these pollutants in light rail mode.

Table 5. Exposure concentrations of PNC, BC and PM_{2.5} for ferry and pier

Commute mode	Exposure					
	PNC		BC		PM _{2.5}	
	particles	particles/mile	µg	µg/mile	µg	µg/mile
Fast ferry	158.8E ⁺⁸ ±86.4E ⁺⁸	6.0E ⁺⁸ ±3.3E ⁺⁸	4.9±3.3	0.19±0.13	12.4±6.0	0.47±0.23
Bakirkoy pier	20.1E ⁺⁸ ±14.5E ⁺⁸	-	0.4±0.5	-	1.6±1.0	-
Bostanci pier	13.0E ⁺⁸ ±9.7E ⁺⁸	-	0.8±0.8	-	1.7±0.7	-
Car ferry	194.3E ⁺⁸ ±68.8E ⁺⁸	10.7E ⁺⁸ ±3.8E ⁺⁸	1.1±0.8	0.06±0.04	13.7±6.0	0.76±0.33
Yenikapi pier	15.5E ⁺⁸ ±8.6E ⁺⁸	-	0.3±0.3	-	1.6±0.9	-
Yalova pier	26.7E ⁺⁸ ±19.6E ⁺⁸	-	0.9±0.6	-	1.5±0.6	-

4. Conclusion

The aim of the presented study was to investigate the exposure to pollutants for ferry passengers. PNC, BC and PM_{2.5} were measured in ferry and at the piers, using portable devices. To the best of our knowledge, this is the first comprehensive study on commute exposure in ferry travel mode. Mean commuter exposure to PNC, BC and PM_{2.5} varied with ferry route and the highest pollutant concentrations were observed during berthing. The location of the piers and the main external pollutant sources are important factors in determining commuter exposure at the piers. We also would like to note that there is an existing need for future studies to further investigate the influence of vessel ventilation parameters, ferry technical features, operational efficiency and fuel type on commuter exposure.

5. References

- Bond, T. C., Doherty, S. J., Fahey, D. W., Forster, P. M., Berntsen, T., DeAngelo, B. J., Kinne, S., et al. 2013. Bounding the role of black carbon in the climate system: A scientific assessment. *J. Geophys. Res. Atmos.* 118(11), 5380-5552.
- Chan, L.Y., Lau, W.L., Lee, S.C., Chan, C.Y., 2002. Commuter exposure to particulate matter in public transportation modes in Hong Kong. *Atmos. Environ.* 36, 3363-3373.
- Cooper, D.A., 2001. Exhaust emissions from high speed passenger ferries. *Atmos. Environ.* 35, 4189-4200.
- Corbett, J. J., Farrell, A., 2002. Mitigating air pollution impacts of passenger ferries. *Trans. Res. Part D: Trans. and Environ.* 7(3), 197-211.
- Corbett, J. J., Winebrake, J. J., Green, E. H., Kasibhatla, P., Eyring, V., Lauer, A., 2007. Mortality from ship emissions: a global assessment. *Environ. Sci. Technol.* 41(24), 8512-8518.
- EPA (Environmental Protection Agency), 2010. Report to Congress on Black Carbon. United States Environmental Protection Agency.
- Fann, N., Lamson, A. D., Anenberg, S. C., Wesson, K., Risley, D., Hubbell, B. J., 2012. Estimating the national public health burden associated with exposure to ambient PM_{2.5} and ozone. *Risk Anal.* An Int. Journ. 32(1), 81-95.
- Hagler, G. S., Yelverton, T. L., Vedantham, R., Hansen, A. D., Turner, J. R., 2011. Post-processing method to reduce noise while preserving high time resolution in aethalometer real-time black carbon data. *Aerosol Air Qual. Res.* 11(5), 539-546.
- Ham, W., Vijayan, A., Schulte, N., Herner, J. D., 2017. Commuter exposure to PM_{2.5}, BC, and UFP in six common transport microenvironments in Sacramento, California. *Atmos. Environ.* 167, 335-345.



- Hinds, W. C., 1999. *Aerosol technology: Properties, behavior, and measurement of airborne particles*. John Wiley & Sons. Inc. New York, 3-4.
- IATR (Istanbul Annual Transportation Report), 2017. Istanbul Metropolitan Municipality, 2017. <https://tuhim.ibb.gov.tr/İstatiksel-bilgiler/İbb-ulasim-raporu-2017/>, accessed on 14 June 2019.
- Jalkanen, J.P., Brink, A., Kalli, J., Pettersson, H., Kukkonen, J., Stipa, T., 2009. A modelling system for the exhaust emissions of marine traffic and its application in the Baltic Sea area. *Atmos. Chem. Phys.* 9, 9209-9223.
- Janssen, N. A., Hoek, G., Simic-Lawson, M., Fischer, P., Van Bree, L., Ten Brink, H., Cassee, F. R., et al. 2011. Black carbon as an additional indicator of the adverse health effects of airborne particles compared with PM10 and PM2.5. *Environ. Health Persp.* 119(12), 1691-1699.
- Kirchstetter, T. W., Novakov, T., 2007. Controlled generation of black carbon particles from a diffusion flame and applications in evaluating black carbon measurement methods. *Atmos. Environ.* 41(9), 1874-1888.
- Knibbs, L. D., de Dear, R. J., 2010. Exposure to ultrafine particles and PM2.5 in four Sydney transport modes. *Atmos. Environ.* 44 (26), 3224-3227.
- Lau, W.L., Chan, L.Y., 2003. Commuter exposure to aromatic VOCs in public transportation modes in Hong Kong. *Sci. Total Environ.* 308, 143-155.
- Ledoux, F., Roche, C., Cazier, F., Beaugard, C., Courcot, D., 2018. Influence of ship emissions on NOx, SO2, O3 and PM concentrations in a North-Sea harbor in France. *J. Environ. Sci.* 71, 56-66.
- Li, B., Lei, X. N., Xiu, G. L., Gao, C. Y., Gao, S., Qian, N. S., 2015. Personal exposure to black carbon during commuting in peak and off-peak hours in Shanghai. *Sci. Total Environ.* 524, 237-245.
- Morawska, L., Ristovski, Z., Jayaratne, E. R., Keogh, D. U., Ling, X., 2008. Ambient nano and ultrafine particles from motor vehicle emissions: Characteristics, ambient processing and implications on human exposure. *Atmos. Environ.* 42(35), 8113-8138.
- Moreno, T., Reche, C., Rivas, I., Minguillón, M. C., Martins, V., Vargas, C., Ealo, M. et al. 2015. Urban air quality comparison for bus, tram, subway and pedestrian commutes in Barcelona. *Environ. Res.* 142, 495-510.
- Onat, B., Alver Sahin, U., Sivri, N., 2017. The relationship between particle and culturable airborne bacteria concentrations in public transportation. *Indoor and Built Environ.* 26(10), 1420-1428.
- Onat, B., Sahin, U. A., Uzun, B., Akın, O., Ozkaya, F., Ayvaz, C., 2019. Determinants of exposure to ultrafine particulate matter, black carbon, and PM_{2.5} in common travel modes in Istanbul. *Atmos. Environ.* 206, 258-270.
- Onat, B., Stakeeva, B., 2012. Assessment of fine particulate matters in the subway system of Istanbul. *Indoor and Built Environ.* 1-10.
- Onat, B., Stakeeva, B., 2013. Personal exposure of commuters in public transport to PM_{2.5} and fine particle counts. *Atmos. Pol. Res.* 4 (3), 329-335.
- Rivas, I., Kumar, P., Hagen-Zanker, A., de Fatima Andrade, M., Slovic, A. D., Pritchard, J. P., Geurs, K. T., 2017. Determinants of black carbon, particle mass and number concentrations in London transport microenvironments. *Atmos. Environ.* 161, 247-262.
- Sahin, U. A., Onat, B., Stakeeva, B., Ceran, T., Karim, P., 2012. PM₁₀ concentrations and the size distribution of Cu and Fe-containing particles in Istanbul's subway system. *Trans. Res. Part D: Trans and Environ.* 17(1), 48-53.



- Tan, S. H., Roth, M., Velasco, E., 2017. Particle exposure and inhaled dose during commuting in Singapore. *Atmos. Environ.* 170, 245-258.
- Tichavska, M., Tovar, B., 2015. Port-city exhaust emission model: An application to cruise and ferry operations in Las Palmas Port. *Trans. Res. Part A*, 78, 347-360.
- TUIK (Turkish Statistical Institute), 2018. <http://tuik.gov.tr/Start.do>, accessed on 31 December 2018.
- Valavanidis, A., Fiotakis, K., Vlachogianni, T., 2008. Airborne particulate matter and human health: toxicological assessment and importance of size and composition of particles for oxidative damage and carcinogenic mechanisms, *J. Environ. Sci. Health, Part C*. 26, 339-362
- Velasco, E., Ho, K. J., Ziegler, A. D., 2013. Commuter exposure to black carbon, carbon monoxide, and noise in the mass transport khlong boats of Bangkok, Thailand. *Trans. Res. Part D: Trans. and Environ.* 21, 62-65.
- Wang, X., Westerdahl, D., Wu, Y., Pan, X., Zhang, K. M., 2011. On-road emission factor distributions of individual diesel vehicles in and around Beijing, China. *Atmos. Environ.* 45(2), 503-513.
- Westerdahl, D., Fruin, S.A., Sax, T., Fine, P.M., Sioutas, C., 2005. Mobile platform measurements of ultrafine particles and associated pollutant concentrations on freeways and residential streets in Los Angeles. *Atmos. Environ.* 39, 3597-3610.
- WHO (World Health Organization), 2016. *The world health report: working together for health*. Geneva: World Health Organization.
- Yang, F., Lau, C.F., Tong, V.W.T., Zhang, K.K., Westerdahl, D., Ng, S., Ning, Z., 2019. Assessment of personal integrated exposure to fine particulate matter of urban residents in Hong Kong. *J. Air Waste Manage. Assoc.* 69 (1), 47-57.
- Zuurbier, M., Hoek, G., Van den Hazel, P., Brunekreef, B., 2009. Minute ventilation of cyclists, car and bus passengers: an experimental study. *Environ. Health.* 8(1), 48.

Acknowledgments

We gratefully acknowledge the Scientific and Technical Research Council of Turkey (TUBITAK) for financially supporting this study with their project #115Y263. We also thank the Research Fund of the University of Istanbul for supporting this study with their project #25562.

Computational fluid dynamics modelling of air distributions and optimization of indoor air quality in classrooms

Norhayati Mahyuddin

Centre for Building, Construction & Tropical Architecture, Faculty of Built Environment, University of Malaya, Kuala Lumpur, Malaysia

hayati@um.edu.my

Abstract. Indoor air quality (IAQ) has been a global public concern for many years. Most people spend almost 90% of their time indoors, which further signifies the adverse effects of poor air quality. In most buildings, occupants are the main source of indoor Carbon Dioxide (CO₂) due to exhalation. Exhaled breath is a vehicle for the release of airborne infectious particles and thus contributes to the risk of airborne transmission of disease. Although CO₂ is not considered to pose serious health risks to occupants, elevated levels of CO₂ may serve as an indicator of insufficient ventilation. The limited air circulation in an enclosed space may lead to high concentrations of indoor air pollutants. Hence, this will negatively affect occupants who spend long hours indoor especially those in educational establishments. Most government school building design are mainly naturally ventilated due to energy saving and economical construction cost. Standard classrooms may have occupant levels anywhere from 1.8 m² per person to 2.4 m² square feet per person. Given so many individuals in a confined space, it is no wonder that schools IAQ are a major concern. Therefore, it is important for architects and engineers to accurately predict the performance of natural ventilation and the flow fields that would bring in the outdoor pollutants into the indoor classrooms, especially in the building design stage. This study investigated the airflow and contaminant (CO₂ spatial distribution) transport in enclosed spaces using Computational Fluid Dynamics (CFD) simulations. The conditions and the spatial distributions of CO₂ in the two classrooms were modelled using the ANSYS CFX to determine the most physically realistic combination of mass and energy transport models, fluid properties and boundary conditions. This would also enable the visualisation of sensitive aspects of the internal environment such as the prediction of airflow and accuracy of the results, which would otherwise not be possible experimentally. This paper considers the possibility of predicting both external and internal flow fields of wind profiles and the air distributions in a classroom. The overall findings would be of immense benefit to designers and building authority in enhancing classroom design guidelines for school buildings in the tropics.

Keywords: Airflow, Carbon dioxide, Computational fluid dynamics, Indoor air quality.

1. Introduction

Indoor air quality has been a global public concern for many years. As most people spend up to 90 % of their time indoors (Leech, Nelson et al. 2002, Hui, Wong L.T et al. 2006). the adverse effects of poor air quality have a far-reaching significance. In addition to residential and office buildings, educational buildings are predominantly occupied during the day and have associated health problems as reported by users (Kreiss 1989). Although the causes of occupants' complaints vary and are often elusive, air quality plays a major role because indoor pollutant levels are often higher than outdoor pollutant levels.

From a rational perspective, contaminant source control is the most effective general means for improving indoor air quality (IAQ) (Savenstrand Rado, Bakke et al. 2001). In many buildings the

occupants themselves are a major source of indoor air contamination, due to Carbon Dioxide (CO₂) exhalation. Although CO₂ (a gas produced through respiration) is not considered to pose serious health risks to occupants, some research has indicated that individuals in schools with high CO₂ concentrations tend to report drowsiness, lethargy, and a general perception that the air is stale. CO₂ is often used for evaluating the adequacy of classroom ventilation, particularly as it is believed to be related to the dilution of pollutants stemming from human metabolic activity (Daisey, Angell et al. 2003). Evidently, if the ventilation system is not controlling and maintaining CO₂ concentrations at acceptable levels, other indoor contaminants are probably accumulating proportionately. Proper monitoring of CO₂ levels will enable corrections to be made where necessary and consequently increase the IAQ of a space. The measurement strategy for determining CO₂ distribution is of the utmost importance not only for finding the sources of CO₂, but also for finding how it is distributed within the room and how its distribution is affected by occupant movement, heat sources, and room air distribution.

1.1. Carbon dioxide sampling points and the spatial variability of CO₂ concentration

The concentration of CO₂ within a building may vary from location to location due to gravitational settling and a non-uniform airflow field (Mahyuddin and Awbi 2010). Other factors that may affect the non-uniformity of spatial distribution are the location and strength of the source (mainly occupants), the types of ventilation systems present, and the internal air movements. They are all interrelated, therefore the sampling strategies needs to consider the spatial concentration gradient when choosing the representative locations, especially when evaluating the effectiveness of ventilation or any control system.

1.2. Ventilation in classrooms

Classrooms are complex indoor environments influenced by many factors such as number of students, seating arrangements and classroom activities. Hence, ventilation studies in classroom environments have increasingly become important. In a study of the relationship between classroom CO₂ concentrations and student attendance carried out in Washington and Idaho by Sundell et al.(2004), authors found that based on the CO₂ concentrations, the estimated ventilation rates in at least 50 % of the classrooms were < 7.5 l s⁻¹ per person, which is the minimum rate specified in most codes and standards.

The aim of this paper is to investigate the variation in CO₂ concentration within classrooms with different ventilation strategies. Factors that may affect the non-uniformity of CO₂ spatial distribution in the classroom will be studied using Computational Fluid Dynamics (CFD) model with ANSYS-CFX to establish the effects of spatial distribution of CO₂ concentration levels in these environments.

2. Research methodology

This paper is, however, limited to the parameters which influence the distribution of CO₂, air velocity and temperature to determine a relationship with the build-up of CO₂ in the classroom.

The simulations of the classrooms were carried out in two parts. These are listed below:

- i. The wind flow and velocity around the building where the classrooms are situated is determined. This simulation is carried out under steady state conditions.
- ii. The spatial distributions of CO₂ in the classroom subjected to the wind flow and impact on the outer wall are calculated (naturally ventilated and windcatcher system). For this situation, a transient calculation is carried out using the earlier steady-state results as the initial boundary conditions.

2.1. Modelling of the atmospheric boundary layer (ABL) in CFD

The modelling of the atmospheric boundary layer (ABL) in CFD is based on specifying appropriate inlet and wall boundary conditions. The 2 classrooms located in the Palmer Building were modelled and illustrated in Figure 1. In order to model the external and internal flow fields, it is necessary to model the structure of other buildings which are situated close to the selected classroom building in a simulated ABL. The construction of these domains was mapped using the layout of the whole campus.

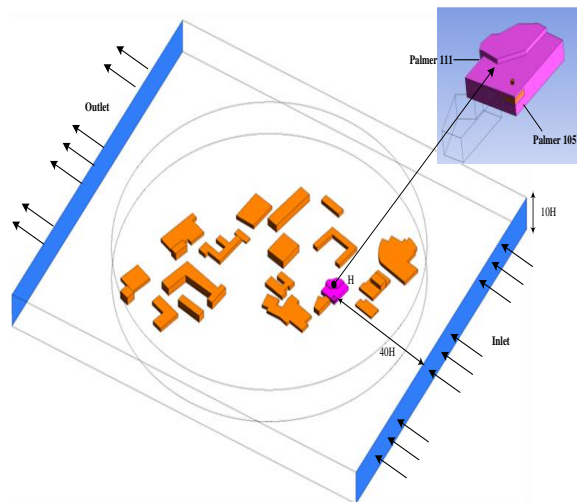


Figure 1. The computational domain of the building used in the CFD simulation

2.2. Transient simulation of the classrooms

In both CFD models, students occupying the classrooms were placed according to the sitting layout in respective classrooms. The numbers and locations of the students' sitting arrangement were 15 and 17 sedentary occupants in Palmer 105 and 111 respectively. These locations were modelled according to the field work measurements which is not highlighted in this paper. Figure 2 illustrates the layout of classrooms used in the field work. The design of individual classrooms is not the same, but they are similar in seating layout. All sampling devices (i.e. height of sensor in m) were placed at locations A, B, C, D and E.

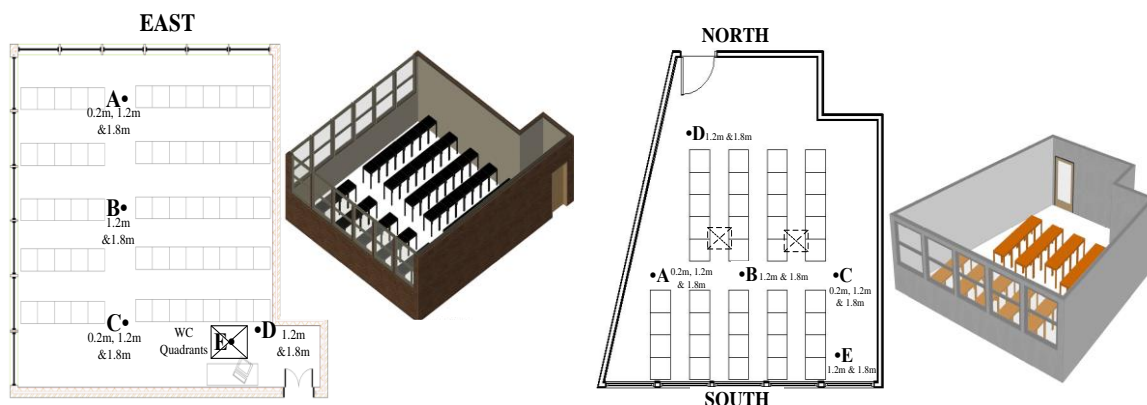


Figure 2. The floor plan and perspective layout of classroom Palmer 111 (left). The dotted squares are the extractor and supply fans on the ceiling. Palmer 105 (right) with dotted square where the location of the windcatcher on the ceiling

3. Results and discussion

3.1. Modelling of the atmospheric boundary layer (ABL) in CFD

Starting with the modelled profiles of the ABL, the predictions of external pressure and velocity profile around the test structure are discussed and compared for the 2 different wind directions. For classroom Palmer 105 (with windcatcher system), the wind direction implemented was from 0 °N while for classroom Palmer 111 (with extractor fan) the wind direction was from 216 °SW. In this study, the windcatcher on the roof of Palmer 105 was also modelled to visualise the flow fields of the external conditions into the classroom.

When the mean wind meets the windward face of the classroom structure, the velocity gradient leads to increased wind speeds at the top of the windward face as illustrated in Figure 3(a) due to the flow separation at the edge of the roof line. Above this line, higher velocity air flows upwards and over the roof of the classroom. A plane across of the windcatcher is also produced to show the flow into the classroom.

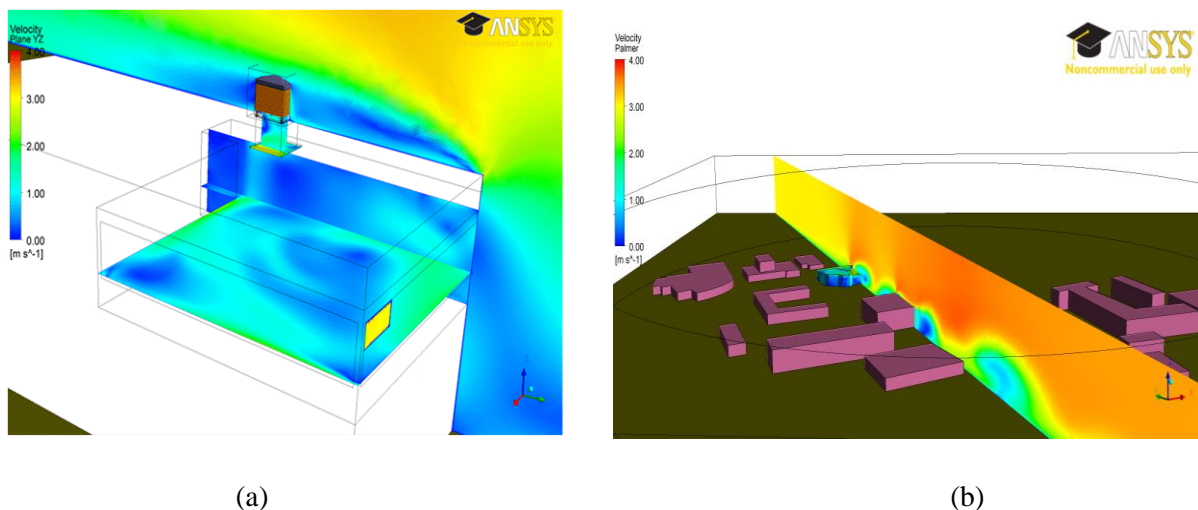


Figure 3. (a) The velocity contour plot in and around the test structure: classroom Palmer 105. (b) The external wind velocity distribution predictions across classroom 111 and adjacent buildings

The steady-state results for classroom Palmer 111 are different from classroom Palmer 105. Due to the wind direction and the location of the classroom in the domain, different velocity and pressure flow fields were observed. In this case, the wind direction was from the South West of the building domain, therefore greater obstacles (i.e. other buildings) were within the flow domain territory. Due to these obstacles, it is observed that the flow fields and the pressure distributions are significantly different. Figure 3(b) shows the velocity contour along a plane cutting through classroom Palmer 111. Higher air velocity from the wind side (3.24 ms⁻¹ from 216° SW) gradually decreases towards the opposite end and a much lower air velocity is also observed nearer to the buildings.

Transient simulation of the classroom Palmer 105. After simulating the airflow patterns for one-hour duration, plots are created to analyse the results obtained. Two vertical planes were created, one at the section corresponding to the windcatcher quadrant ($z = 1.2$ m) which is assumed as an opening and second, closer to the occupants ($z = 7.2$ m) as illustrated in Figure 4(a). The relative reference pressure (0.7 Pa) was taken from the external flow field in the ABL simulation results (see the insert in Figure 4). The velocity contours in these planes are observed to be higher towards the ceiling and the windcatcher. This was due to convection currents from heat sources rising from the occupant's plumes and the lamps. The plume flows is shown to spread laterally on reaching the ceiling. In addition, the inlet flow jet

through the back wall can be clearly observed causing a rise in velocity at the lower region. The downstream flow towards the floor is also due to the temperature difference from the outdoor (15.0 °C) and the classroom domain (average of 18.8 °C).

Based on Figure 4(b), it can be seen that the layers of high CO₂ concentration is driven by the buoyancy force produced by the manikins' thermal plumes. At this instance, natural convection around the human body is of particular interest since it interacts with respiration flows where, in a mixing ventilation condition, the exhaled air is entrained upwards by the warm plumes near the body. Hence, higher CO₂ concentrations are observed flowing towards the ceiling of the classroom. With regards to the number of sampling locations, it would be essential to locate sensors at varying locations as the variations in the mean CO₂ concentration with both height and location were significant.

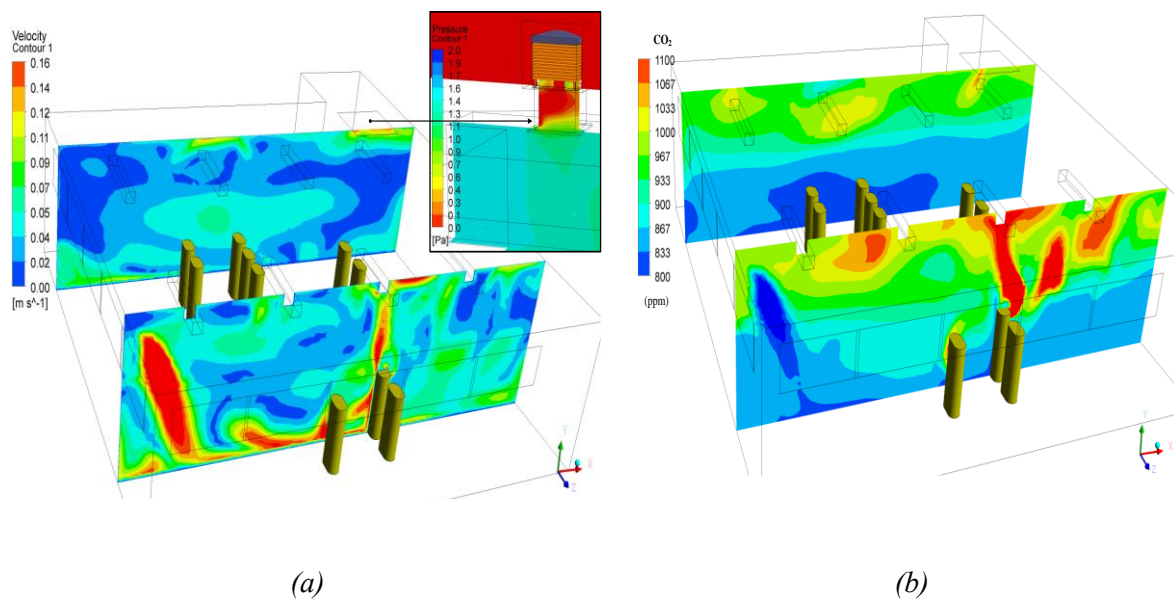


Figure 4. The airflow pattern (a) and the CO₂ concentration distribution pattern (b) in classroom 105 at vertical planes $z = 1.2$ m and 7.2 m

3.2. Transient simulation of the classroom Palmer 111.

In this simulation, it is demonstrated that the exhalation flow may indeed intensify because of density differences, and that high concentrations may occur locally. This is evident as the results of spatial distributions of CO₂ at the height of 1.2 m (Figure 5b) in the classroom show that high concentrations accumulate locally instead of rising due to positive buoyancy flow (see Figure 5c).

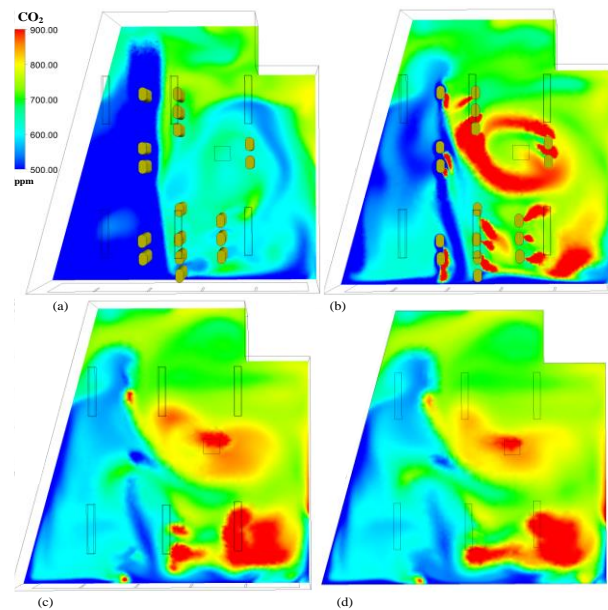


Figure 5. The airflow pattern in classroom 111 for horizontal planes of (a) $y = 0.2$ m, (b) $y = 1.2$ m, (c) $y = 1.8$ m and (d) $y = 3.0$ m (ceiling height)

However, another observation of the distributions of CO₂ concentration at this level (1.2 m) showing high values at the breathing zone, i.e. the concentration is seen to be transported behind the breathing manikins. This high concentration would probably penetrate into the breathing zone of the manikins seated at the back. This effect of airflow in a room should be avoided as the concentration of CO₂ could also be linked with contaminant source. Higher concentrations are also observed to be flowing towards the extract fan and into location E.

A clear difference in the spatial distributions of CO₂ can be observed. Although CO₂ concentrations in this case, are normally lower at lower regions (0.2 m), the CO₂ concentration at the back of the classroom is significantly lower compared to other locations at that level (see Figure 5a). This would have been due to the entrainment of warm air from the corridor via infiltration below the door forcing the accumulated CO₂ concentration from the corridor region to enter towards the side. This effect can be seen in Figure 5b where the high concentrations of exhaled CO₂ from the occupants in the back row tend to move towards this side.

4. Conclusion

In principle, in-situ measurement in an enclosed environment gives the most realistic information concerning airflow and air distribution. However, because measurements must be made at many locations, direct measurements of the air and contaminant distribution can be very expensive and time consuming. Generally, in most cases, spreading the sampling sensors across the horizontal locations in a classroom is more beneficial than vertically. This paper conclude that a sensor positioned at a height of 1.8 m is preferred as the highest CO₂ concentration levels are observed at this height. However, where vertical distributions are significant (i.e. in classrooms with natural ventilation), more sensors positioned at 1.2 m height and above are preferred. Overall, both findings indicate that when the extract fan is switched on, better vertical distribution was produced but significant variations occurred across the horizontal planes. These results suggest that if a limited number of sampling sensors is desired, the samplers can be distributed anywhere vertically (i.e. above 1.2 m height) but more samplers are needed in a few horizontal locations.



In light of these, the results obtained are of significance as it enables detailed analysis of spatial distribution of CO₂ amongst others to be predicted. These results are valuable and worth implementing for predictions and information for further studies. It is also important for architects and engineers to accurately predict the performance of natural ventilation and the flow fields that would bring in the outdoor pollutants into the indoor classrooms, especially in the building design stage.

5. References

- Daisey, J. M., W. J. Angell, Apte, M.G., 2003. Indoor air quality, ventilation and health symptoms in schools: an analysis of existing information. *Indoor Air*. 13(1), 53-64.
- Hui, P. S., Wong L.T., Mui K.W., 2006. Evaluation of professional choice of sampling locations for indoor air quality assessment. *Building and Environment*. article in press, 1-8.
- Kreiss, K., 1989. The epidemiology of building related complaints and illness. *Journal of Occupational and Environmental Medicine*. 4575-592.
- Leech, J., Nelson, W., Burnett, R., Aaron, S., Raizenne, M., 2002. It is about time: a comparison of Canadian and American time activity patterns. *Journal of Exposure Analysis and Environmental Epidemiology*. 12, 427-432.
- Mahyuddin, N., Awbi, H., 2010. The spatial distribution of carbon dioxide in an environmental test chamber. *Building and Environment*. 45(9), 1993-2001.
- Rado, S., Bakke, J.V., Ryden, E., 2001. Creation of healthy indoor environment in schools: IAQ Task Force on schools-A Nordic approach.
- Sundell, J., 2004. On the History of Indoor Air Quality and Health. *Indoor Air*. 14(7), 51-58.

Spatial variations of linear and cyclic volatile methyl siloxanes in a river basin and their air-water exchange patterns

Baris Yaman, Hakan Erkuzu, Fulya Okan and Mustafa Odabasi

Dokuz Eylul University, Tinaztepe Campus, Environmental Engineering Dept.,
35390, Buca, Izmir, Turkey

baris.yaman@deu.edu.tr

Abstract. Linear and cyclic volatile methylsiloxanes (VMS) are Si and O containing organic compounds that are increasingly subject to scientific studies in recent years. They are used as solvents and coating materials in personal care products, cleaning materials and industrial applications. In this study, it was aimed to investigate the spatial variations of VMS levels in river water and ambient air in Kucuk Menderes Basin and their air-water exchange patterns. Within the scope of the study, grab river water samples and passive ambient air samples collected from 10 sites throughout Kucuk Menderes Basin located in Izmir region in Turkey, and they were analyzed for VMSs. The concentrations of Σ VMS in river water and ambient air ranged from 48.4 to 148.0 ng/L and from 41.7 to 432.7 ng/m³, respectively. Among the VMS compounds, the predominant compounds were found to be D5 and D3 in ambient air and river water, respectively. In general, concentrations of all VMS congeners increased towards downstream of the river for both water and ambient air samples and there were substantial fluctuations between the sampling points. These fluctuations may be due to wastewater discharges at some sites (increase), followed by loss by volatilization along the river (decrease). The direction of the exchange between ambient air and river water was determined by fugacity fractions calculated using the air and water concentrations and Henry's Law constants of siloxanes. The calculated fugacity fractions for all compounds indicated net volatilization from river water to the atmosphere at all sampling sites.

Keywords: Volatile methyl siloxanes, River water, Air-water exchange, Fugacity fraction.

1. Introduction

Linear and cyclic volatile methylsiloxanes (VMS) are Si and O containing organic compounds that are increasingly subject to scientific studies in recent years. Since 1940's, these substances have been used as solvents and coating materials in personal care products, cleaning materials and industrial applications. Cyclic volatile methylsiloxanes (cVMS) are primarily used as carriers in personal care products such as deodorants, skin creams and lotions (Environment Canada, 2008c; 2008a; 2008b; 2008d; Brooke et al., 2009c, a, b). On a smaller scale cVMS are also used as solvents and building blocks in the production of silicon polymers (Environment Canada, 2008c; 2008a; 2008b; 2008d; Brooke et al., 2009c, a). The most commonly used cVMS are octamethylcyclotetrasiloxane (D4), decamethylcyclopentasiloxane (D5) and dodecamethylcyclohexasiloxane (D6) (Environment Canada, 2008c; 2008a; 2008b; 2008d; Brooke et al., 2009c, a). Linear volatile methylsiloxanes (lVMS) are mainly used as intermediates in the production of silicon polymers and on a smaller scale as carriers in personal care products (Brooke et al., 2009b). Usually the concentrations of cVMS in personal care products are higher than those of lVMS. Although they have large range of usage in most industries with number of commercial advantages and benefits on end products, VMSs currently have been identified as important pollutants in recent years. These compounds can accumulate in human bodies and other

organisms and even transport to the arctic regions. Recent studies focusing on health effects related to VMS exposure reported toxicity, endocrine disruptive effects and even carcinogenicity risks (Bondurant et al., 2000).

VMSs can easily reach to the environmental mediums like air, soil and water via the several transport mechanisms such as atmospheric dispersion, dry/wet deposition and partitioning between air-water, air-soil and air-biota (Kim et al., 2018). Since they are highly volatile, they can evaporate from industrial products, resulting high VMS concentrations in the atmosphere. VMSs' highly diffusive characteristics induced researchers to investigate these compounds in both quantitative and qualitative manner. Studies mostly focus on VMS levels in air (Genualdi et al., 2011; Buser et al., 2013; Kierkegaard and McLachlan, 2013; Yucuis et al., 2013; Gallego et al., 2017), soil (Xu, 1999; Wang et al., 2013), aquatic systems (Warner et al., 2010; Krogseth et al., 2013; Capela et al., 2017) and aquatic organisms (Kierkegaard et al., 2013; Warner et al., 2015). Krogseth et al. (2013) measured ambient air D3, D4, D5 and D6 levels in an Arctic region in Norway and they confirmed D5 and D6 have potential of long-range atmospheric transport. In another study, Sparham et al. (2011) investigated D5 levels in sediment samples collected from two rivers. In addition to monitoring studies, number of researchers surveyed occurrence, fate and behaviors of VMSs in environmental mediums by determining their physicochemical properties (Whelan, 2013; Gobas et al., 2015; Panagopoulos et al., 2015). For instance, Kozerski et al. (2014) determined soil-water sorption coefficients for D4, D5, L3 and L4 using gas chromatography-mass spectrometry (GC-MS) retention time method.

Although cyclic and linear VMSs have been addressed by number of researchers from all around the world in recent years, studies those focused on these compounds in Turkey are quite scarce. Within the scope of this study, it was aimed to investigate the spatial variations of VMS levels in river water and ambient air in Kucuk Menderes Basin and their air-water exchange patterns. Within the scope of the study, grab river water samples and passive ambient air samples collected from 10 sites throughout Kucuk Menderes River located in the South western part of Turkey, in Izmir City and analyzed for seven major VMS compounds (hexamethylcyclotrisiloxane, octamethylcyclotetrasiloxane, decamethylcyclopentasiloxane, dodecamethylcyclohexasiloxane, octamethyltrisiloxane, decamethyltetrasiloxane, dodecamethylpentasiloxane).

2. Materials and methods

2.1. Sampling site

Kucuk Menderes River located in the South western part of Turkey, in Izmir City was chosen as study area. The river has a tectonic subsidence basin with 140 km length and there are numerous of agricultural fields, several residential and industrial sites along it. Food and textile manufacturing plants are the most important industrial sectors followed by small, medium and large-sized machine, iron-steel, chemistry, construction materials, automotive, paper, forestry products and leather manufacturing plants within the four organized industrial zones located along the basin. Ten sampling points along the river basin were illustrated in Figure 1.

2.2. Collection and preparation of samples

Grab water samples and passive ambient air samples were collected from 10 sampling points designated between the spring and estuary of the river, as illustrated in Figure 1. Instant water samples were collected using pre-cleaned amber glass containers by avoiding headspace and they were immediately transferred to the laboratory and extracted. Extraction was carried out according to "Purge and Trap Method" that described by Horii et al. (2017). According to this method, each of 2-liter water samples were transferred to pre-cleaned gas washing bottles, then high purity nitrogen (N₂) gas with a constant flow rate was passed through the water for 2 hours. Gas phase VMS compounds desorbed from water were collected with a glass tubing filled with XAD-2 at the outlet of the gas washing bottle. The gas

washing bottle was held in an ultrasonic bath operated at 50°C during the purging period to provide proper desorption conditions. After 2 hours of purging, the gas washing bottle containing water sample was unmounted and N₂ gas flow continued to pass through the glass tubing for 30 minutes to remove humidity that might be accumulated in the tubing. XAD-2 was transferred from the glass tubing to a 40 ml amber vial and then 5 ml of hexane was also added to the vial as the extraction solvent. Extraction was conducted by sonicating the samples for 10 minutes after they were spiked with 50 µl internal standard (tetrakis (trimethylsilyloxy) silane, M4Q).

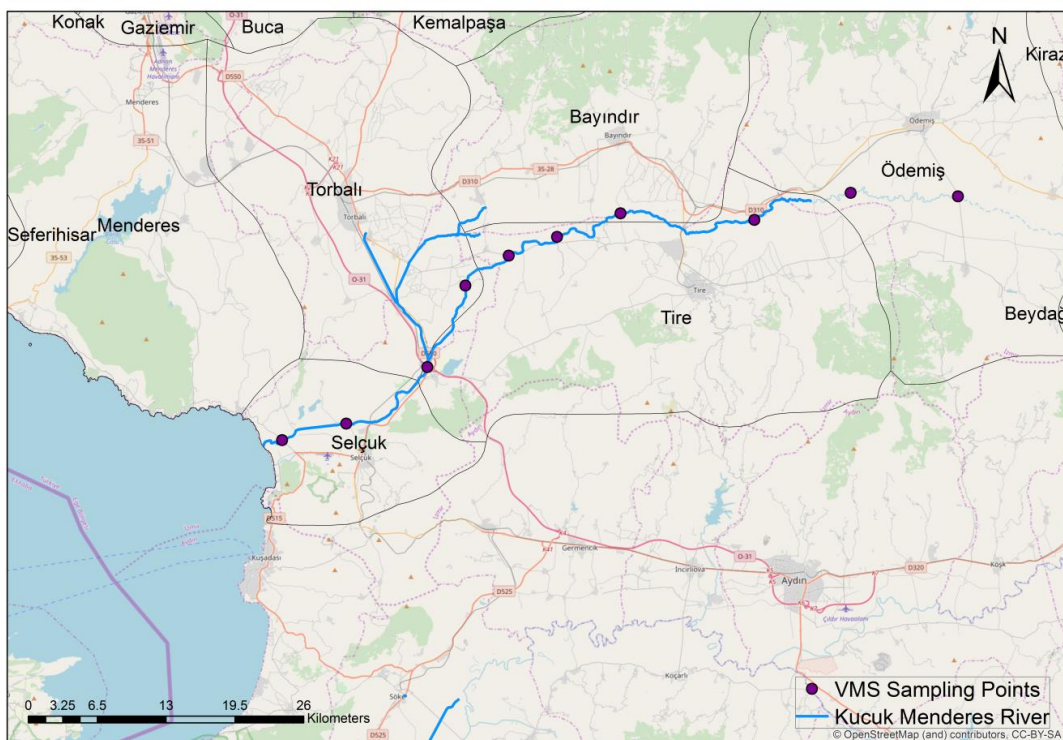


Figure 1. Sampling points

Ambient air samples were collected using stainless-steel meshed tubings containing XAD-2 resin by providing approximately 2 weeks of deployment. Before they were deployed in field, passive samplers were pre-cleaned by sonicating for 15 minutes in a solvent mixture (acetone:hexane 50:50) and the residual solvent was removed under high purity N₂ stream. After the sampling period, collected samplers were soaked into 2 ml of hexane, spiked with 20 µl internal standard and then extracted by sonicating for 10 minutes.

Ambient air VMS concentrations were determined using VMS amounts (ng) in samples and sampling volumes (m³). Sampling volumes (m³) were determined according to sampling times (day) and sampling rates (m³/day) those calculated using geometry of sampler and diffusion constants (cm²/sn). Determined sampling volumes were ranged between 0.63 (D6) and 0.92 (D3) m³.

2.3. Instrumental analysis

All samples were analyzed for 7 VMS compounds (D3, D4, D5, D6, L3, L4 and L5) using an Agilent 6890N GC-MS (Agilent 5973 inert MSD) at electron impact ionization and selected ion monitoring mode (SIM). An HP5-MS-UI capillary column (30 m, 0.25 mm, 0.25 µm) was utilized for the analysis and helium as the carrier gas. The initial oven temperature was held at 40 °C for 3 min and raised to

160 °C at 10 °C/min, 300 °C at 30 °C/min, and was held for 3 min. The injector, ion source, and quadrupole temperatures were 250, 230, and 150 °C, respectively while the injection volume was 1 µl.

2.4. Quality control and quality assurance

Accurate characterization of VMSs in environmental mediums is crucial to assess their effects on environment. Hence, the use of VMS containing materials (i.e. silicon containing septa) and personal care products during sampling, sample preparation, extraction and analysis were avoided. Samplers were stored in desiccator both before and after sampling until they were analysed. The contact time of sample with laboratory indoor air was minimized due to prevent possible contamination. Three blank samples for each air and water were prepared to detect any contamination from laboratory or field apparatus. The average analytical recoveries were calculated as 97.9±8.1% (avg. ± SD) and 87.0±3.7% (avg. ± SD) for water and air samples, respectively. Method detection limits were also ranged between 0.07 ng/L (L3) and 20.57 ng/L (D3) for water samples, 0.12 ng/m³ (L3) and 10.45 ng/m³ (D3) for ambient air samples.

3. Results and discussion

3.1. River water and ambient air VMS concentrations

The detection frequencies were 100% for all interested VMSs in both river water and ambient air samples. Σ VMS concentrations were ranged between 48.4 and 148.0 ng/L in water samples, and between 41.7 and 432.7 ng/m³ in ambient air samples. D3 and D5 were measured as the most predominant VMS species in water and air samples, respectively. In water samples D3 (36%) was measured as the most predominant VMS, followed by D5 (%31) and D4 (%17.8) while L3, L4 and L5 were the rarest compounds comprising 0.8%, 0.6% and 0.7% of Σ VMS, respectively. In ambient air samples D5 constituted more than 50% of Σ VMS, followed by D6 as illustrated in Table 1.

Table 1. River water and ambient air VMS concentrations

	Min.	Max.	Avg.	S.D.	%
River Water (ng/L)					
D3	22.79	55.24	35.7	10.0	36
L3	0.08	6.08	0.8	1.9	0.8
D4	5.96	33.38	17.7	8.8	17.8
L4	0.18	2.28	0.6	0.7	0.6
D5	8.86	51.48	30.7	14.1	31
L5	0.18	2.68	0.7	0.7	0.7
D6	5.08	34.45	12.8	10.2	12.9
Σ VMS	48.38	148.03	99.0	38.3	100
Ambient Air (ng/m³)					
D3	10.6	29.6	18.3	5.7	13.2
L3	0.2	0.4	0.3	0.1	0.2
D4	7.6	58.3	17.6	15.7	12.8
L4	0.3	1.0	0.6	0.3	0.4
D5	15.2	305.5	77.6	98.5	56.3
L5	0.3	1.5	0.8	0.4	0.6
D6	7.6	40.6	22.6	9.4	16.4
Σ VMS	41.7	432.7	137.8	123.8	100

Measured Σ VMS concentrations within the present study were mostly comparable those reported values in related studies. In a recent study carried out in Toronto, Canada ambient air Σ VMS concentrations were ranged from 91 to 414 and from 49 to 120 ng/m³ in an urban and a polar sites, respectively (Rauert et al., 2018). Σ cVMS concentrations one to five orders of magnitude higher than Σ IVMS as found out in the present study. However, there are few studies that reported VMS concentrations as lower as 8 ng/m³ in urban sites (Ratola et al., 2016). On the other hand, Horii et al. (2017) were investigated surface water VMS levels in river and sewage treatment plant effluent water samples. They measured Σ VMS concentrations with a wide range of <4.9 - 1700 ng/L, those comparable with the present study (48.4-148.0 ng/L).

3.2. Compound-specific compositions and spatial variations

In the basis of compound species, D3 and D5 were mostly dominated river water and ambient air samples, respectively. As it was strictly expected, cVMS concentrations were substantially higher than IVMSs in all samples. As an overall trend, all the VMS species showed increase in 10 sampling points from spring to estuary through the river, while there were significant fluctuations on consecutive samples. These fluctuations seem to be caused by the increase of VMS levels at particular sampling points nearby wastewater discharges and decrease due to evaporation of VMSs during the flow of the river. Concentrations of seven measured VMSs at particular sampling points were given in Table 2. As can be inferred from the table river water Σ VMS levels were significantly higher at sampling points 3, 5, 7 and 10, while ambient air concentrations were higher at 3 and 7. Sampling point based concentrations were also illustrated in Figure 2 for individual VMS species.

Table 2. River water and ambient air VMS concentrations for particular sampling points

River Water Cons. (ng/L)	N1	N2	N3	N4	N5	N6	N7	N8	N9	N10
D3	26.17	22.79	44.62	26.52	39.72	31.29	43.52	34.27	33.17	55.24
L3	0.08	0.13	0.15	0.13	0.28	0.18	6.08	0.18	0.20	0.58
D4	5.96	9.71	23.58	7.53	33.38	11.58	21.91	21.38	17.46	24.08
L4	0.20	0.18	0.30	0.18	0.45	0.33	2.28	0.40	0.48	1.15
D5	8.86	18.61	21.26	14.38	42.18	34.13	36.76	44.16	35.36	51.48
L5	0.18	0.25	0.28	0.28	0.68	0.63	0.73	0.73	1.00	2.68
D6	6.95	5.08	8.23	7.10	28.78	9.55	34.45	7.83	7.33	12.83
Σ VMSwater	48.4	56.7	98.4	56.1	145.5	87.7	145.7	108.9	95.0	148.0
Ambient Air Cons. (ng/m ³)	N1	N2	N3	N4	N5	N6	N7	N8	N9	N10
D3	18.05	10.56	25.78	14.31	16.72	13.22	18.62	17.07	29.57	19.12
L3	0.27	0.20	0.27	0.24	0.25	0.20	0.37	0.25	0.27	0.35
D4	13.20	7.58	58.30	10.39	12.29	7.58	30.12	12.34	14.29	10.00
L4	0.34	0.25	0.84	0.30	0.98	0.39	0.93	0.59	0.31	0.90
D5	24.02	15.17	305.53	19.60	53.86	26.62	208.32	27.44	29.19	65.86
L5	0.62	0.31	1.37	0.47	1.03	0.81	1.00	0.53	0.47	1.52
D6	25.68	7.59	40.61	16.63	26.64	24.69	24.88	17.40	12.61	29.55
Σ VMSair	82.2	41.7	432.7	61.9	111.8	73.5	284.2	75.6	86.7	127.3

As shown in Figure 3, the first 2 sampling points near to spring of the river had significantly lower VMS concentrations while there was a sharp increase in the 3rd sampling point which might be caused by

number of industrial facilities located in Odemis region. From the 3rd point to the estuary (10th point) concentrations followed an irregular trend. However river water VMS levels varied in a narrower range and the Σ VMS concentrations were slightly lower in the first four sampling points. The apparent water pollution in the river and publicly recognized odor problems may back up the outputs of the present study.

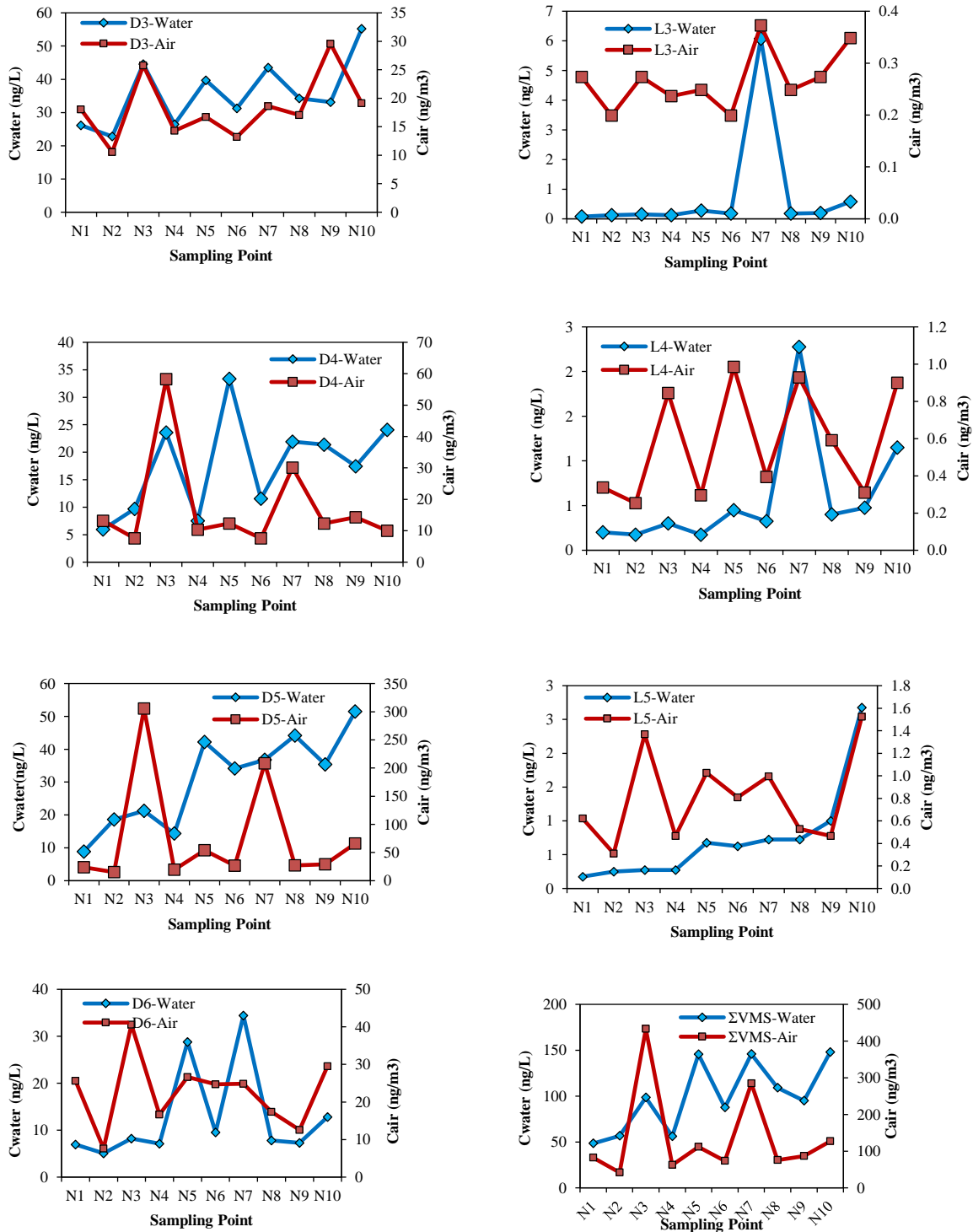


Figure 2. Sampling point based concentration variations for particular VMSs

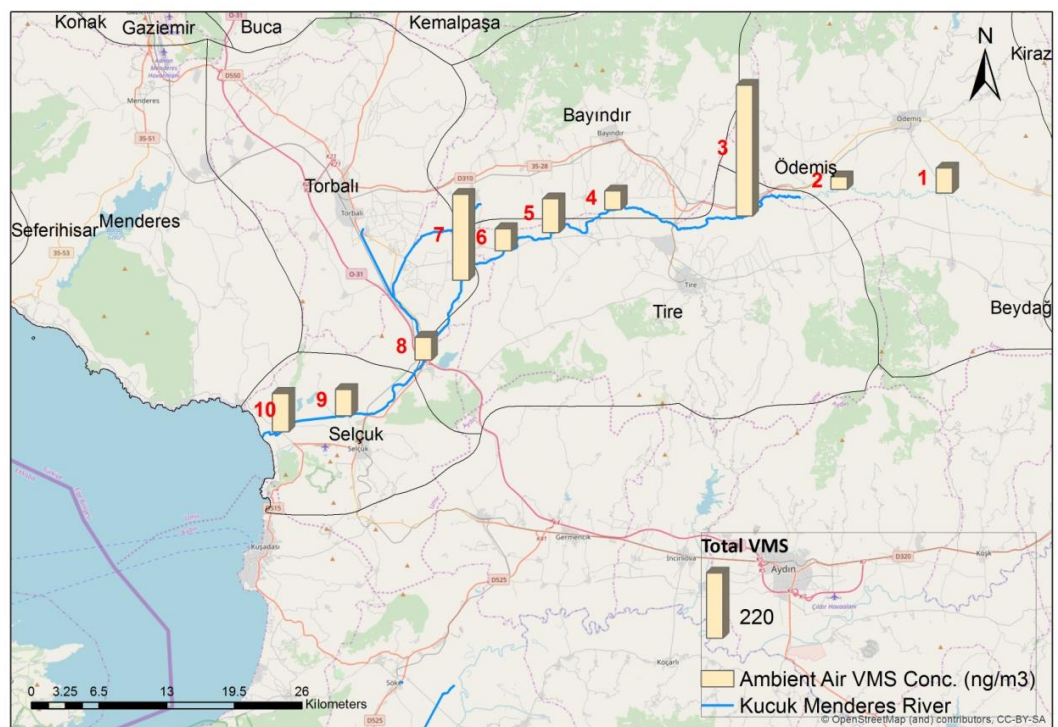
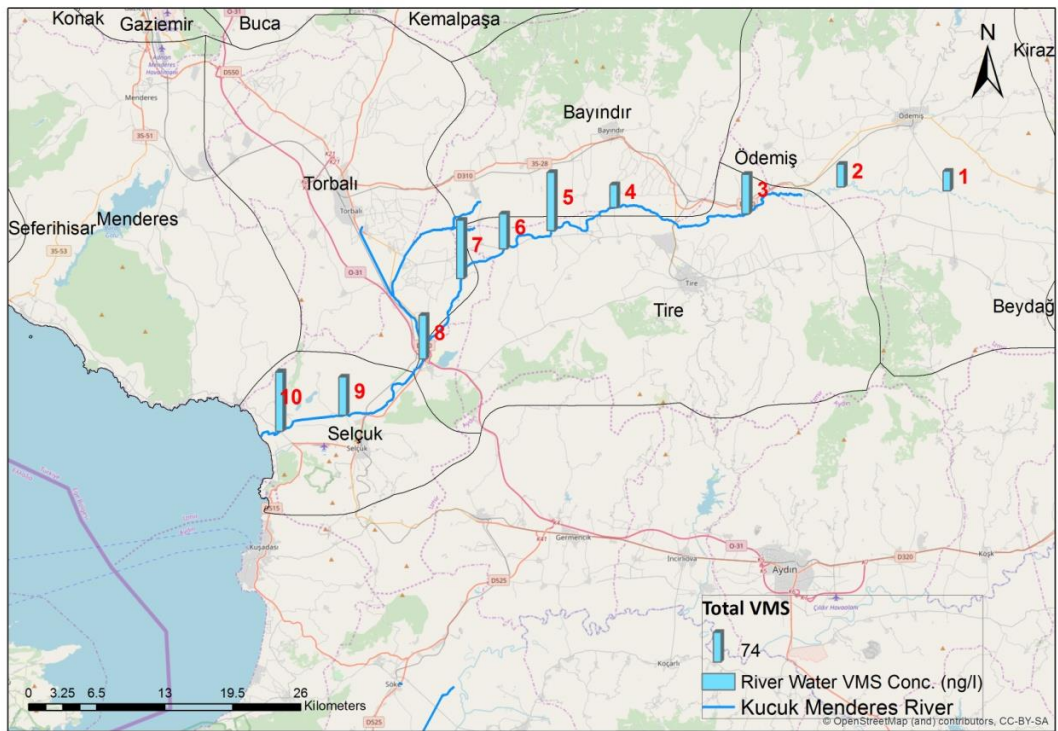


Figure 3. Spatial variations of VMSs

3.3. Ambient air – river water exchange patterns

As an important environmental transport mechanism, air-water exchange patterns of the studied VMSs were evaluated using fugacity fractions (*ff*). Fugacity is a quantity of chemical potential of a pollutant in a specific compartment that drives its transfer between media (Meijer et al., 2001). The direction of the transfer defined using *ff* value which calculated according to air (C_A) and water (C_W) concentrations of VMSs and dimensionless Henry's Law Constants (H'). *ff* value about 0.5 indicates the equilibrium state between air and water, while $ff > 0.5$ and $ff < 0.5$ implies net volatilization and gas phase deposition, respectively. The calculated *ff* values indicated net evaporation from river to atmosphere, for each VMS species in all samples (Table 3).

Table 3. Fugacity fractions

	Fugacity Fractions	
	$ff = f_w / (f_w + f_a) = H' * C_w / (H' * C_w + C_{air})$	
	Avg.	S.D.
D3	0.999998	0.000001
L3	0.999999	0.000001
D4	0.999996	0.000003
L4	0.999998	0.000001
D5	0.999983	0.000025
L5	0.999998	0.000002
D6	0.999976	0.000014

4. Conclusions

Cyclic and linear VMSs those commonly contained in personal care products and several industrial applications have been main subjects to number of studies in recent years due to their toxic and endocrine disruptive effects. However, studies those focus on these compounds in Turkey are quite scarce. Within the scope of this study ambient air and river water concentrations of VMSs were measured in a river basin, in Turkey. Additionally, spatial variations and air-water exchange patterns were also investigated. Σ VMS concentrations were ranged between 48.4 and 148.0 ng/L in water samples, and between 41.7 and 432.7 ng/m³ in ambient air samples. In the basis of compound species, D3 and D5 were mostly dominated river water and ambient air samples, respectively. As an overall trend, all the VMS species showed increase in 10 sampling points from spring to estuary through the river, while there were significant fluctuations on consecutive samples. VMS levels were dramatically increased in particular sampling points due to wastewater discharges into the river and then decreased due to evaporation of VMSs during the flow of the river.

Air-water exchange patterns of the studied VMSs were evaluated using fugacity fractions which calculated according to air and water concentrations of VMSs and dimensionless Henry's Law Constants. The calculated *ff* values indicated net evaporation from river to atmosphere, for each VMS species in all samples.

5. References

- Environment Canada, 2008a. Screening assessment for the challenge decamethylcyclopentasiloxane, in: Canada, E. (Ed.), Chemical abstracts service registry number 541-02-6.
- Environment Canada, 2008b. Screening assessment for the challenge dodecamethylcyclohexasiloxane, in: Canada, E. (Ed.), Chemical abstracts service registry number 540-97-6.

- Environment Canada, 2008c. Screening assessment for the challenge octamethylcyclotetrasiloxane, in: Canada, E. (Ed.), Chemical abstracts service registry number 556-67-2.
- Environment Canada, 2008d. Screening assessment for the challenge siloxanes and silicones, di-Me, hydrogen-terminated, in: Canada, E. (Ed.), Chemical abstracts service registry number 70900-21-9.
- Bondurant, S., Ernster, V., Herdman, R., 2000. Safety of Silicone Breast Implants. National Academies Press (US).
- Brooke, D.N., Crookes, M.J., Gray, D., Robertson, S., 2009a. Risk Assessment Report: Decamethylcyclopentasiloxane. Environment Agency of Great Britain.
- Brooke, D.N., Crookes, M.J., Gray, D., Robertson, S., 2009b. Risk Assessment Report: Dodecamethylcyclohexasiloxane. Environment Agency of Great Britain.
- Brooke, D.N., Crookes, M.J., Gray, D., Robertson, S., 2009c. Risk Assessment Report: Octamethylcyclotetrasiloxane. Environment Agency of Great Britain.
- Buser, A.M., Kierkegaard, A., Bogdal, C., MacLeod, M., Scheringer, M., Hungerbuhler, K., 2013. Concentrations in Ambient Air and Emissions of Cyclic Volatile Methylsiloxanes in Zurich, Switzerland. *Environ Sci. Technol.* 47, 7045-7051.
- Capela, D., Ratola, N., Alves, A., Homem, V., 2017. Volatile methylsiloxanes through wastewater treatment plants - A review of levels and implications. *Environ Int.* 102, 9-29.
- Gallego, E., Perales, J.F., Roca, F.J., Guardino, X., Gadea, E., 2017. Volatile methyl siloxanes (VMS) concentrations in outdoor air of several Catalan urban areas. *Atmos. Environ.* 155, 108-118.
- Genualdi, S., Harner, T., Cheng, Y., MacLeod, M., Hansen, K.M., van Egmond, R., Shoeib, M., Lee, S.C., 2011. Global Distribution of Linear and Cyclic Volatile Methyl Siloxanes in Air. *Environ Sci. Technol.* 45, 3349-3354.
- Gobas, F.A.P.C., Xu, S.H., Kozerski, G., Powell, D.E., Woodburn, K.B., Mackay, D., Fairbrother, A., 2015. Fugacity and activity analysis of the bioaccumulation and environmental risks of decamethylcyclopentasiloxane (D5). *Environ. Toxicol. Chem.* 34, 2723-2731.
- Horii, Y., Minomo, K., Ohtsuka, N., Motegi, M., Nojiri, K., Kannan, K., 2017. Distribution characteristics of volatile methylsiloxanes in Tokyo Bay watershed in Japan: Analysis of surface waters by purge and trap method. *Sci. Total Environ.* 586, 56-65.
- Kierkegaard, A., Bignert, A., McLachlan, M.S., 2013. Cyclic volatile methylsiloxanes in fish from the Baltic Sea. *Chemosphere.* 93, 774-778.
- Kierkegaard, A., McLachlan, M.S., 2013. Determination of linear and cyclic volatile methylsiloxanes in air at a regional background site in Sweden. *Atmos. Environ.* 80, 322-329.
- Kim, J., Mackay, D., Whelan, M.J., 2018. Predicted persistence and response times of linear and cyclic volatile methylsiloxanes in global and local environments. *Chemosphere.* 195, 325-335.
- Kozerski, G.E., Xu, S.H., Miller, J., Durham, J., 2014. Determination of Soil-Water Sorption Coefficients of Volatile Methylsiloxanes. *Environ Toxicol. Chem.* 33, 1937-1945.
- Krogseth, I.S., Kierkegaard, A., McLachlan, M.S., Breivik, K., Hansen, K.M., Schlabach, M., 2013. Occurrence and Seasonality of Cyclic Volatile Methyl Siloxanes in Arctic Air. *Environ Sci. Technol.* 47, 502-509.
- Meijer, S.N., Harner, T., Helm, P.A., Halsall, C.J., Johnston, A.E., Jones, K.C., 2001. Polychlorinated naphthalenes in UK soils: Time trends, markers of source, and equilibrium status. *Environ Sci. Technol.* 35, 4205-4213.



- Panagopoulos, D., Jahnke, A., Kierkegaard, A., MacLeod, M., 2015. Organic Carbon/Water and Dissolved Organic Carbon/Water Partitioning of Cyclic Volatile Methylsiloxanes: Measurements and Polyparameter Linear Free Energy Relationships. *Environ Sci. Technol.* 49, 12161-12168.
- Ratola, N., Ramos, S., Homem, V., Silva, J.A., Jimenez-Guerrero, P., Amigo, J.M., Santos, L., Alves, A., 2016. Using air, soil and vegetation to assess the environmental behaviour of siloxanes. *Environ Sci. Pollut. R* 23, 3273-3284.
- Rauert, C., Shoieb, M., Schuster, J.K., Eng, A., Harner, T., 2018. Atmospheric concentrations and trends of poly- and perfluoroalkyl substances (PFAS) and volatile methyl siloxanes (VMS) over 7 years of sampling in the Global Atmospheric Passive Sampling (GAPS) network. *Environ Pollut.* 238, 94-102.
- Sparham, C., van Egmond, R., Hastie, C., O'Connor, S., Gore, D., Chowdhury, N., 2011. Determination of decamethylcyclopentasiloxane in river and estuarine sediments in the UK. *J. Chromatogr. A.* 1218, 817-823.
- Wang, D.G., Alaei, M., Steer, H., Tait, T., Williams, Z., Brimble, S., Svoboda, L., Barresi, E., DeJong, M., Schachtschneider, J., Kaminski, E., Norwood, W., Sverko, E., 2013. Determination of cyclic volatile methylsiloxanes in water, sediment, soil, biota, and biosolid using large-volume injection-gas chromatography-mass spectrometry. *Chemosphere.* 93, 741-748.
- Warner, N.A., Evenset, A., Christensen, G., Gabrielsen, G.W., Borga, K., Leknes, H., 2010. Volatile Siloxanes in the European Arctic: Assessment of Sources and Spatial Distribution. *Environ Sci. Technol.* 44, 7705-7710.
- Warner, N.A., Krogseth, I.S., Whelan, M.J., 2015. Comment on "Unexpected Occurrence of Volatile Dimethylsiloxanes in Antarctic Soils, Vegetation, Phytoplankton, and Krill". *Environ Sci. Technol.* 49, 7504-7506.
- Whelan, M.J., 2013. Evaluating the fate and behaviour of cyclic volatile methyl siloxanes in two contrasting North American lakes using a multi-media model. *Chemosphere.* 91, 1566-1576.
- Xu, S.H., 1999. Fate of cyclic methylsiloxanes in soils. 1. The degradation pathway. *Environ Sci. Technol.* 33, 603-608.
- Yucuis, R.A., Stanier, C.O., Hornbuckle, K.C., 2013. Cyclic siloxanes in air, including identification of high levels in Chicago and distinct diurnal variation. *Chemosphere.* 92, 905-910.
- Horii, Y., Minomo, K., Ohtsuka, N., Motegi, M., Nojiri, K., Kannan, K., 2017. Distribution characteristics of volatile methylsiloxanes in Tokyo Bay watershed in Japan: Analysis of surface waters by purge and trap method. *Sci. Total Environ.* 586, 56-65.
- Meijer, S.N., Harner, T., Helm, P.A., Halsall, C.J., Johnston, A.E., Jones, K.C., 2001. Polychlorinated naphthalenes in UK soils: Time trends, markers of source, and equilibrium status. *Environ Sci. Technol.* 35, 4205-4213.
- Ratola, N., Ramos, S., Homem, V., Silva, J.A., Jimenez-Guerrero, P., Amigo, J.M., Santos, L., Alves, A., 2016. Using air, soil and vegetation to assess the environmental behaviour of siloxanes. *Environ. Sci. Pollut. R.* 23, 3273-3284.
- Rauert, C., Shoieb, M., Schuster, J.K., Eng, A., Harner, T., 2018. Atmospheric concentrations and trends of poly- and perfluoroalkyl substances (PFAS) and volatile methyl siloxanes (VMS) over 7 years of sampling in the Global Atmospheric Passive Sampling (GAPS) network. *Environ. Pollut.* 238, 94-102.

Monitoring and mapping of hydrogen sulphide emissions in a geothermal area in Turkey

Yetkin Dumanoglu

Dokuz Eylul University, Department of Environmental Engineering, Tinaztepe Campus, Buca, Izmir

yetkin.dumanoglu@deu.edu.tr

Abstract. Geothermal energy for electricity generation is likely to become increasingly important in Turkey in the future. There are several centres of thermal activity in Turkey, particularly in Aydin and Manisa. Hydrogen Sulphide (H₂S) from geothermal fluids need to be monitored with respect to their impacts on plants and animals. In this study, hydrogen sulfide concentrations in two different regions of Turkey were measured in air using passive/diffusive samplers (Radiello® traps). Ten suburban sites in Manisa and six suburban sites in Aydin characterized by intense degassing of H₂S-rich fluids were selected for measurements. Sampling time is 15 days. Two samples were taken between April and May 2019 in Manisa and one in July 2019 in Aydin. It was evaluated whether H₂S concentrations measured in the study areas were below 100 µg/m³ (1-14 days) as the limit value recommended by the World Health Organization. The results indicated that hydrogen sulphide levels varied between 12 and 70 µg/m³ around the geothermal power plants. Values below the limit value determined by the World Health Organization were determined. However, it is well above the hydrogen sulphide level detected at the remote point to geothermal sources. Since the unpleasant odor can be detected at concentrations as low as 7 µg/m³ (World Health Organization), it causes uncomfortable air quality for the people living in rural areas where the plants are located.

Keywords: Geothermal power plant, Hydrogen Sulphide, Turkey

1. Introduction

Technological developments, growth of industry, heating of houses and developments in transportation increase the need for energy resources in Turkey. The reserves of fossil fuel resources in the world are decreasing day by day and the energy demand is rapidly increasing. Turkey is dependent on foreign sources in terms of energy supply. It is becoming an important necessity to urgently bring new and renewable energy sources from our own domestic resources to the agenda in Turkey. Geothermal energy, which is one type of renewable energy has an important role in energy production to Turkey. US, Philippines, Indonesia, Turkey and New Zealand are the top five countries engaged in the production of electricity from geothermal energy (ETKB, 2018).

The largest share in the distribution of the primary energy source of power generation of the gas in Turkey. This is followed by hydraulics, coal (lignite+hard coal), imported coal, wind, liquid fuels, geothermal and other resources. In terms of energy resources, in 2017, 33.4% of total electricity production is from coal, 37.0% from natural gas, 20.0% from hydraulic resources, 6.1% from wind, 2.0 %, 0.7% from liquid fuels, 0.7% from biofuels and solar energy and 0.2% from waste heat. Turkey's geothermal potential, 78% in Western Anatolia, 9% in Central Anatolia, 7% in the Marmara Region, 5% is located in Eastern Anatolia and 1% is located in other regions.

Geothermal energy is a type of energy produced by the heat accumulated in the operable depths of the earth's crust. The water leaking into the ground is collected here in the reservoir rocks with porous and permeable properties. Geothermal energy is formed in the appropriate geological conditions with soundings overheated water, wet and dry steam is removed to the earth. This geothermal fluid is separated into water-vapour phases by decreasing pressure on it. The main process in generating electricity from geothermal energy is turbine cycle applications. The turbine needs an energy to rotate. This energy source is the steam obtained from geothermal reservoirs. The liquid taken from geothermal sources consists of 95-98% of steam and non-condensing gases. Non-condensable gases contain CO₂ (95%), CH₄ (2-3%) and H₂S (1-2%) (Bussotti et al., 2003; Thorsteinsson et al., 2013; Berstad and Nord, 2016).

H₂S is released from natural sources and human activities. H₂S is an odorous and highly toxic gas, produced by a number of industries and facilities, including sewage treatment plants, paper mills, oil and gas refineries, and concentrated animal feeding operations, as well as occurring naturally in geothermal and volcanic areas (Kourtidis et al., 2004, 2008; Colomer et al., 2012; Bates et al., 1992; WHO, 2003).

One of the most important environmental issues related to the use of geothermal fluids to generate electricity is the release of non-condensable gases into the atmosphere. Among these non-condensable gases, H₂S is important for human health due to its characteristic of being an odorous, irritating, suffocating, weakly acidic and toxic gas (Thorsteinsson et al., 2013; Cabassi et al., 2017). According to the World Health Organization report (WHO, 2003), the maximum permissible concentration of H₂S in outdoor air is 150 µg/m³ (average over 24 hours) and 100 µg/m³ (average over 1-14 days), but the value at which typical rotten egg odor occurs (0.7-42 µg/depending on individual sensitivity (Schiffman and Williams, 2005) should not exceed 7 µg/m³ (average over 30 minutes). H₂S is in gas phase and can be absorbed into the lungs by inhalation. There are respiratory, ocular, neurological, metabolic health effects and death effects at concentrations higher than 700 mg/m³ (Karapekmez and Dinçer, 2018).

Turkey is being used intensively in an area where electricity production from geothermal sources. It is thought that H₂S gas released during geothermal electricity production may harm human health and plants. However, there is no information about outdoor air concentrations in geothermal areas in Turkey. In this study, H₂S concentrations were measured in the region where geothermal power plants are located in Alasehir-Manisa and Germencik-Aydin. The levels of H₂S concentrations were determined in agricultural areas where geothermal power plants were installed.

2. Material and method

2.1. Sampling area

Two sampling regions were studied. This region is intense geothermal power plants are in the west of Turkey. First study area is located at the Alasehir, ~110 km east of the metropolitan city of Manisa, Turkey. The area contains eight geothermal power plant. The installed capacity of geothermal power plants operating in Alasehir varies between 10 and 45 mW. Secondary study area is located at the Germencik, ~25 km west of the metropolitan city of Aydin, Turkey. The area contains six geothermal power plant. The installed capacity of geothermal power plants operating in Germencik varies between 22.6 and 162.5 mW (Figure 1).

This sampler comprises a zinc acetate impregnated polyethylene adsorbing cartridge, surrounded by a cylindrical microporous diffusive body mounted on a supporting plate. When H₂S contacts the zinc acetate, it is converted to stable zinc sulphide, which is later extracted and assayed by sulphide ion (Radiello, 2001).

After sampling, cartridges were desorbed with 10 mL of ultrapure water followed by 0.5 mL of ferric chloride-amine solution. After stirring for 2 min, the samples were left to react at room temperature for 30 min. The leachate solutions of H₂S samples were analysed using a spectrophotometer (Hach Lange, DR6000) at a wavelength of 665 nm. A calibration curve was prepared with eight points in triplicate using standard methylene blue solution (Sigma-Aldrich, St. Louis, MO). The calibration curve had linear correlation coefficient $R^2 \approx 0.994$, indicating that 99.5% of the points can be described by the regression line. Procedural blanks were prepared as follows: unexposed cartridges from the same batch to those that were exposed were submitted to the same analysis protocol than the exposed cartridges.

Following the analysis, the H₂S concentrations in air (averaged over the exposure time interval) were calculated by a mass balance from the pollutant masses retained on the cartridge as in Equation (1):

$$C_{H_2S} = \frac{m_d - m_b}{Q_K \times t} \times 10^6 \quad (1)$$

where m_d is the adsorbed mass of compound (mg) sampled during time t (min) under the concentration in air C_{H_2S} (mg/m³), m_b the mass of compound (mg) on a non-exposed cartridge (blank) and Q_K is the sampling rate of the compounds (ml/min). Sampling rates vary with temperature as expressed by the following Equation (2):

$$Q_K = Q_{298} \times \left(\frac{T}{298}\right)^{1.5} \quad (2)$$

where Q_K is the sampling rate at the temperature Q_K (K) and Q_{298} is the reference value at 298 K. Q_K is invariant with humidity within the range of 10-90% and wind speed between 0.1 and 10 m/s. For the calculation of the H₂S concentrations during the sampling periods, sampling rates were adjusted using the corresponding average temperatures measured.

3. Results and discussion

H₂S concentrations were measured by passive sampling method at 10 different points in the region of geothermal power plants in Alaşehir. Figure 2 shows the spatial distribution of H₂S concentrations measured during the two sampling periods. Concentrations ranged from 11.18 µg/m³ to 57.94 µg/m³ in the first sampling period and from 12.15 µg/m³ to 79.89 µg/m³ in the second sampling period. In the two sampling periods, the lowest concentration was measured in the area where Power Plant-1, which is located at an altitude of 600 meters from the geothermal fields established in the Alaşehir plain. The highest concentrations were measured at the closest point to the 20 MW generation plant located in the north of the region during the first sampling period. The highest concentration measured in the second sampling period was measured at the sampling point in the settlement area located in the middle of Power Plant-2 and Power Plant-3.

H₂S concentrations were measured by passive sampling method at 6 different points in the region of geothermal power plants in Aydin. Figure 2 shows the spatial distribution of H₂S concentrations measured during the sampling period. Concentrations ranged from 28.76 µg/m³ to 66.69 µg/m³ in the sampling period. The highest concentration in Germencik was measured near the power plant with an installed capacity of 162.5 MW.

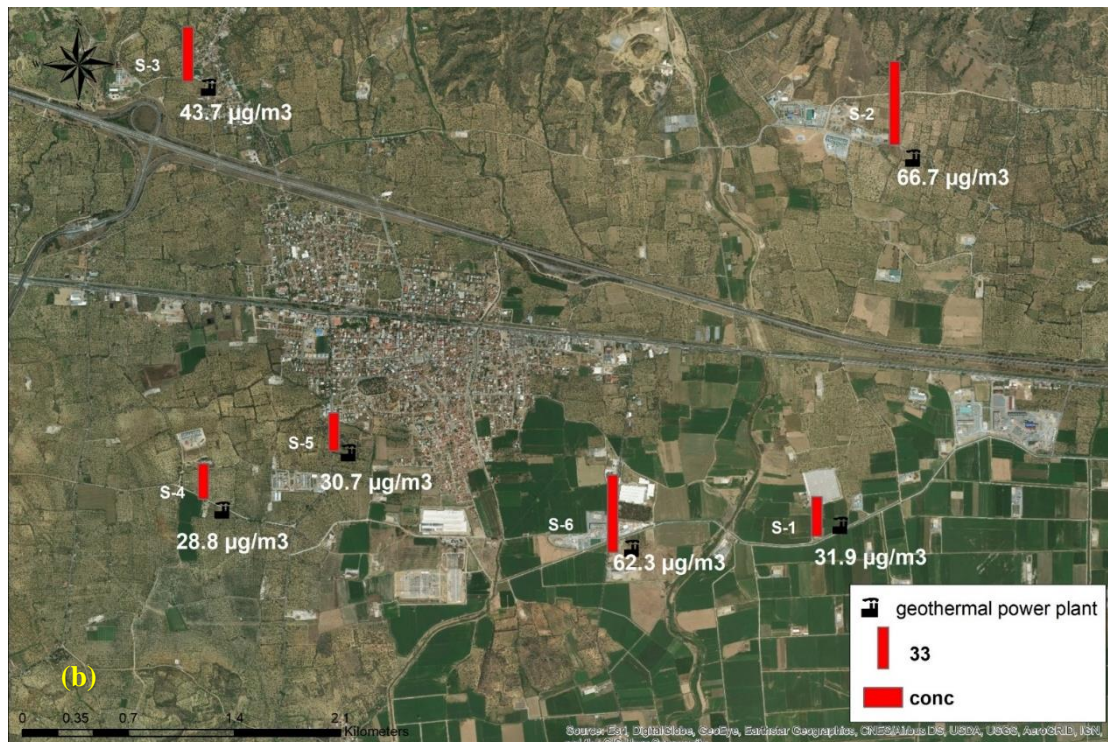
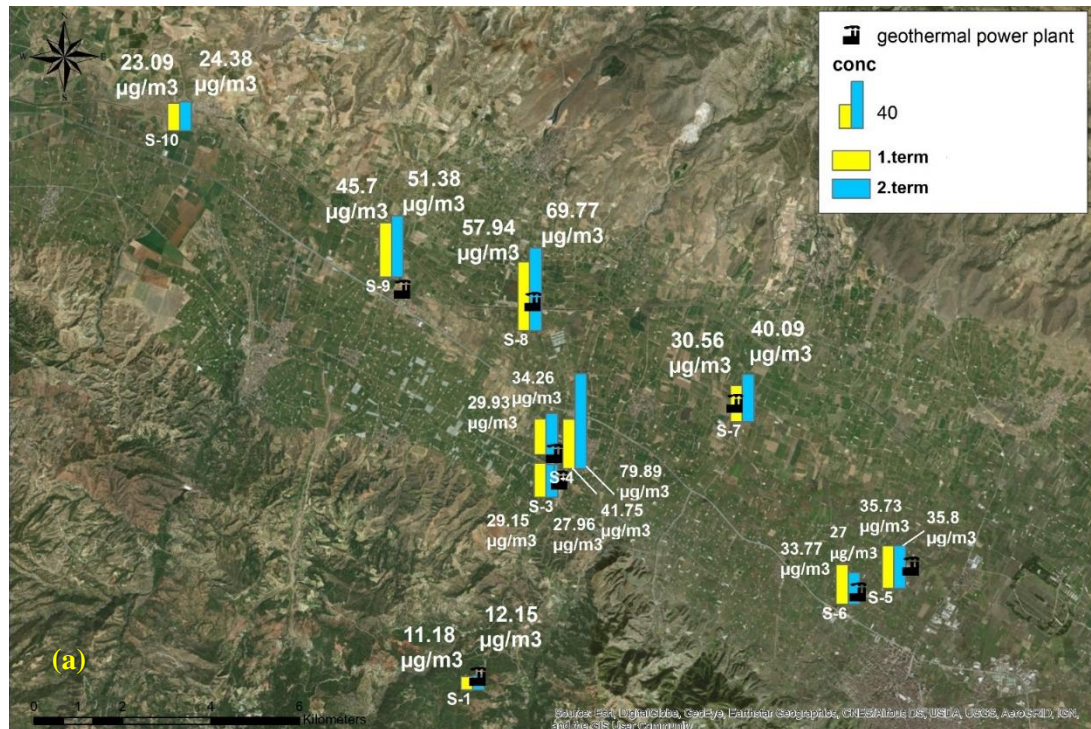


Figure 2. Spatial variation of H₂S concentrations (a) Alasehir-Manisa (b) Germencik-Aydin

It has also been observed how H₂S concentrations change at a point far from geothermal sources. For this purpose, measurements were made in the city of Izmir, which is 120 km away from both sampling regions. Two consecutive samples were sampled and concentrations were determined as 7.17 µg/m³ and 7.10 µg/m³ respectively.

According to the World Health Organization report (WHO, 2003), the maximum permissible concentration of H₂S in outdoor air is 150 µg/m³ (average over 24 hours) and 100 µg/m³ (average over 1-14 days), but the value at which typical rotten egg odor occurs (0.7-42 µg/depending on individual sensitivity (Schiffman and Williams, 2005) should not exceed 7 µg/m³ (average over 30 minutes). H₂S is in gas phase and can be absorbed into the lungs by inhalation. There are respiratory, ocular, neurological, metabolic health effects and death effects at concentrations higher than 700 mg/m³ (Karapekmez and Dincer, 2018). The 14-day average limit value was not exceeded at any of the sampling points. However, during field surveys, unpleasant odor of H₂S were exposed.

4. Conclusions

H₂S concentrations measured in the atmosphere, can be used to map of H₂S concentrations around geothermal power plants in the west side of Turkey. The results indicated that hydrogen sulphide levels varied between 12 and 70 µg/m³ around the geothermal power plants. The highest H₂S concentrations were measured at sites located near the geothermal power plant. Ambient air H₂S concentrations did not exceed the WHO limit value. While these H₂S concentrations are not toxic to humans or other living organisms, sensitive plant species may be affected by an exposure to 100 µg/m³ hydrogen sulphide, and although such a value is not toxic to humans it exceeds by more than one order of magnitude the nasal threshold, compromising air quality in a relatively large area (several square kilometres). H₂S is known to have toxic properties on living organisms. H₂S, which causes pollution in environmental environments and enters the ecosystem and causes permanent destruction, also threatens human health in various ways. Conducting studies like this in our country will help to determine human exposure to this compound.

5. References

- Bates, M.N., Garrett, N., Crane, J., Balmes, J.R., 2013. Associations of ambient hydrogen sulfide exposure with self-reported asthma and asthma symptoms. *Environmental Research*. 122, 81–87.
- Berstad, D., Nord, L.O., 2016. Acid gas removal in geothermal power plant in Iceland. *Energy Procedia*. 86, 32-40.
- Bussotti, F., Tognelli, R., Montagni, G., Borghini, F., Bruschi, P., Tani, C., 2002. Response of *Quercus pubescens* leaves exposed to geothermal pollutant input in southern Tuscany (Italy). *Environmental Pollution*. 121, 349-361.
- Cabassi, J., Tassi, F., Venturi, S., Calabrese, S., Capecchiacci, F., D'Alessandro, W., Vaselli, O., 2017. A new approach for the measurement of gaseous elemental mercury (GEM) and H₂S in air from anthropogenic and natural sources: Examples from Mt. Amiata (Siena, Central Italy) and Solfatara Crater (Campi Flegrei, Southern Italy). *Journal of Geochemical Exploration*. 175, 48–58.
- Colomer, F.L., Morato, H.E., Iglesias, E.M., 2012. Estimation of hydrogen sulfide emission rates at several wastewater treatment plants through experimental concentration measurements and dispersion modelling. *J. Air & Waste Manag. Assoc.* 62, 758-766. <http://dx.doi.org/10.1080/10962247.2012.674008>.
- ETKB (Enerji ve Tabii Kaynaklar Bakanlığı), 2018. <https://www.enerji.gov.tr/tr-TR/Sayfalar/Elektrik>, accessed in 30 Nisan 2019.
- Karapekmez, A., Dinçer, I., 2018. Modelling of hydrogen production from hydrogen sulfide in geothermal power plants. *International Journal of Hydrogen Energy*. 43, 10569-10579.



Kourtidis, K., Kelesis, A., Maggana, M., Petrakakis, M., 2004. Substantial traffic emissions contribution to the global H₂S budget. *Geophys. Res. Lett.* 31, L18107. <http://dx.doi.org/10.1029/2004GL020713>.

R&P-Co (Rupprecht and Patashnick Company), Radiello, 2001. *Passive Gas Sampling System for Industrial, Indoor/Outdoor and Personal Exposure Assessment*, 4 pp.

Schiffman, S.S., Williams, C.M., 2005. Science of odor as a potential health issue. *J. Environ. Qual.* 34, 129-138.

Thorsteinssona, T., Hackenbruchb, J., Sveinbjörnssonc, E., Jóhannsson, T., 2013. Statistical assessment and modeling of the effects of weather conditions on H₂S plume dispersal from Icelandic geothermal power plants. *Geothermics.* 45, 31– 40.

WHO, 2003. *Hydrogen Sulfide: Human Health Aspects. Concise International Chemical Assessment Document 53.* World Health Organization, Geneva, Switzerland.

Acknowledgments

I would like to thank very much to Abdurrahman Bayram, Hasan Altiok, Ersan Gunel and Gizem Tuna Tuygun (Dokuz Eylul University) for their very valuable support during the field studies.

Indoor air THM levels in an olympic and a semi-olympic swimming pool

Mesut Genisoglu¹, Yetkin Dumanoglu², Ersan Gunel², Ceren Nurlu², Begum Unsal¹, Merve Yolcular¹, Aysun Sofuoglu¹ and Sait C. Sofuoglu¹

^aIzmir Institute of Technology, Turkey

^bDokuz Eylul University, Turkey

yetkin.dumanoglu@deu.edu.tr

Abstract. Disinfection is essential for preventing growth of waterborne pathogens in swimming pools (SPs). Chlorination is the most commonly used disinfection method in SPs due to the superior properties e.g., effective pathogen inhibition, low operating cost, and ensured residual disinfectant. Increased temperature in SPs results in higher chlorine decay rates. Thus, higher doses are needed for compensation. Potential toxic disinfection by-products (DBPs) could be formed with the reaction between the disinfectant and precursors in SP source waters. Trihalomethanes are one of the most abundant DBP groups in SPs. CHCl_3 (chloroform), CHCl_2Br (bromodichloromethane, BDCM), CHClBr_2 (dibromochloromethane, DBCM), and CHBr_3 (bromoform) are regulated in drinking water. However, there are no regulations for swimming pools in Turkey. Increased water temperature increases the volatilization of THMs from the pool, which may result in higher indoor air levels. Inhalation exposure to THMs in indoor swimming pools may be of critical importance for swimmers and staff. Indoor air concentrations of two indoor swimming pools (an Olympic and a Semi-Olympic) in İzmir were investigated in this study. The average gas phase concentrations of chloroform, BDCM, DBCM, and bromoform were determined to be 3.99, 0.78, 0.37, and 0.24 $\mu\text{g}/\text{m}^3$ in the Semi-Olympic swimming pool while they were higher in the Olympic pool with average concentrations of 104, 7.86, 1.57, and 0.56 $\mu\text{g}/\text{m}^3$, respectively. Higher THM concentrations might be related to the differences in (1) source water characteristics, (2) the type and operation of HVAC system, and (3) higher swimmer counts. Measured concentrations in this study indicate magnitudes of inhalation exposure might vary and could be critical for health of swimmers and staff.

Keywords: Disinfection by-products, Indoor air, Swimming pools, Trihalomethanes.

1. Introduction

Public swimming pool waters are continuously disinfected for preventing growth of waterborne pathogens. Chlorine-based chemicals (chlorine gas, sodium hypochlorite, sodium and calcium hypochlorite) are the most common disinfectants due to the relatively low capital and operating costs, simplicity and providing residual disinfectant in water (Harman et al., 2017; Peng et al., 2016). Chlorine is a non-selective strong oxidizing agent that oxidize organic and inorganic compounds in water. Halogenated chlorination by-products are possibly formed due to the reaction of chlorine and organic/inorganic matters, named as disinfection by-products (DBPs). To date, more than 700 DBPs were determined in disinfected waters (Harman et al., 2017). Most of them are classified as carcinogenic, toxic, and possibly toxic. The presence of DBPs in swimming pools were reported for the first time in 1980 (Weil et al., 1980, Beech et al. 1980). The literature shows that the DBPs formation in swimming pools are higher than in drinking waters (Hang et al., 2016; Harman et al., 2017; Peng et al., 2016). Trihalomethanes (THMs) and haloacetic acids (HAA) are the most commonly determined DBPs in swimming pools. Haloacetic acids present in water, while THMs are partitioned between water and air due to their volatility. If ventilation rate is lower than the THM emission rate, THMs accumulate in gas

phase in indoor swimming pools. Emission rate is dependent on the concentration gradient between water and air phases. Thus, inhalation exposure to THMs in indoor swimming pools mainly depends on water concentration / emission rate and ventilation rate. If ventilation rate is kept at low levels due to energy consumption worries, accumulating THMs in indoor swimming pools may become an important concern.

Swimmers are exposed to THMs via ingestion, dermal adsorption, and inhalation routes in indoor swimming pools. The major exposure route of THMs in drinking water is ingestion. However, the main exposure routes are inhalation and dermal absorption in swimming pools (Hang et al., 2016). Also, swimming pool staff are exposed to THMs by inhalation route. Bladder cancer has been associated with swimming in chlorinated swimming pool water (Zwiener et al., 2007). Swimming pool water was determined to be more cytotoxic than drinking water (Plewa et al., 2011). Colon cancer frequency was determined to be increased with increasing THMs concentration and exposure duration (Jorgenson et al., 1985). Mutagenetic potential of swimming pool water and chlorinated drinking water were determined to be similar (Teo et al., 2015). Simultaneously determining the THMs concentrations of water and air in swimming pool is important for swimmer and occupational health mitigation efforts in swimming pools. This study measured both in two pools with different characteristics, which is the first study in Turkey that measured swimming-pool indoor air THM concentrations. Here we present the indoor air concentrations.

2. Materials and methods

Indoor air concentrations of two indoor swimming pools (an Olympic and a Semi-Olympic) in İzmir were investigated in this study. Sampling was performed between March-April 2019 for the Semi-Olympic swimming pool and April-May for the Olympic swimming pool. In addition to the swimming area, indoor air samples were taken from the dressing room and lobby in the Olympic and the Semi-Olympic swimming pools, and taken from management office and lifeguard resting room in the Semi-Olympic swimming pool. Swimming pool indoor air was sampled according to the ASTM D3686. Activated charcoal sorbent tubes (SKC, Anasorb) were used with the flow rate of 30 LPH for two hours. Calcium chloride was used as a dehumidifying agent. Activated charcoal in sampling tubes were ultrasonically extracted for 15 minutes with 1 mL carbon disulphide in 2-mL vials and centrifuged for 15 min for separation of the solvent and charcoal particles. The top clear solvent phase was then transferred to 2-mL chromatography vials. Field blank sorbent tubes were taken to the pool and returned to the laboratory without breaking before the extraction step. THMs were analysed in electron impact mode using gas chromatography – mass spectroscopy (Agilent 6890N GC – 5973 MSD) with HP5-MS (30 m, 0.25 mm, 0.25 µm). Split ratio and inlet temperature were set at 1.20 and 240 °C, respectively. Chloroform, BDCM, DCBM, and bromoform were the targeted analytes. Total organic carbon (TOC), temperature, UV₂₅₄, and pH were measured in pool water. Hach HQ11D portable pH meter was used to analyse pH and temperature. Shimadzu TOC-VCPH total organic carbon analyser was used to analyse TOC in water samples according to the Non-Purgeable Organic Carbon (NPOC) method. SUVA₂₅₄ was calculated using Equation 1.

$$SUVA_{254} = \frac{UV_{254}}{DOC} \times 100 \quad (1)$$

where; $SUVA_{254}$ is specific ultraviolet absorbance at 254 nm wavelength (L/mg C.m); UV_{254} is absorbance at 254 nm wavelength (cm⁻¹); DOC is dissolved organic carbon (TOC was assumed as DOC in this study, mg/L).

3. Results and discussion

Characteristics of sampling sites are different. The Semi-Olympic pool is in a university campus in İzmir and open for students and staff. The number of swimmers was much lower than the Olympic swimming pool. The Olympic swimming pool is for public use and training of athletic clubs in Izmir. So, the organic load from swimmers should be higher in the Olympic swimming pool. THM formation depends on disinfectant dose, precursors, temperature, and pH in water. The average TOC concentrations in the Semi-Olympic and the Olympic swimming pool waters were determined to be 4.66 ± 2.36 mg/L and 6.20 ± 2.42 mg/L, respectively. The average TOC concentrations in the source waters of the two pools were measured as 2.40 ± 1.65 mg/L and 2.43 ± 2.35 mg/L, respectively. $SUVA_{254}$ values of the Semi-Olympic and Olympic swimming pool waters were determined to be 0.72 ± 0.30 and 1.00 ± 0.28 L/mg C.m, respectively. The TOC concentrations being similar in the source waters but higher in the Olympic pool water point to higher organic load from swimmers in the Olympic pool. Generally, high $SUVA_{254}$ values, e.g., >4 L/mg C.m, indicate high contents of hydrophobic, aromatic and high molecular weight natural organic matter fractions, while $SUVA_{254}$ at $<2-3$ L/mg C.m indicates mostly hydrophilic, non-humic, and low molecular weight organic matter fractions (Edzwald and Tobiason, 1999). Low $SUVA_{254}$ value of the Semi-Olympic swimming pool water indicates that the lower THM formation potential compared to the Olympic pool. pH value of disinfected water directly effects the disinfection efficiency because due to pH dependent speciation of hypochlorous acid (HOCl) and hypochlorite ion (OCl⁻). HOCl is more effective than OCl⁻ in disinfection process. Increasing the pH value increases the disinfectant consumption and decreases the disinfection efficiency. pH values of the Semi-Olympic swimming pool and Olympic pool waters were determined to be 7.46 ± 0.30 and 7.40 ± 0.07 , respectively. At pH 7.40, both of the HOCl and OCl⁻ are presents in pool waters. Chlorine decay increases with increasing water temperature. So, disinfectant consumption increases with increasing temperature. Furthermore, concentration equilibrium is affected by the increase in the temperature, increasing THM volatilization from water. Because of relatively high pool water temperatures, higher indoor air THM levels can be expected (Harman et al., 2017). The average temperatures of the Semi-Olympic and Olympic pool waters were determined to be 25.8 ± 0.63 and 27.80 ± 0.68 °C, respectively.

Indoor and outdoor air concentrations of THMs were simultaneously measured (Table 1). The average concentrations of chloroform, BDCM, DBCM, and bromoform in the Semi-Olympic swimming pool were determined to be 3.98 ± 5.00 , 0.78 ± 0.71 , 0.37 ± 0.19 , and 0.23 ± 0.12 µg/m³, respectively. THM concentrations in the Olympic swimming pool were relatively higher than those measured in the Semi-Olympic swimming pool. The average concentrations of chloroform, BDCM, DBCM, and bromoform in the Olympic swimming pool were determined to be 104 ± 156 , 7.89 ± 15.2 , 1.57 ± 2.76 , and 0.33 ± 0.32 µg/m³, respectively. The average concentrations sum of four THM compounds (TTHM) in indoor air of Semi-Olympic and Olympic swimming pools were determined to be 4.79 ± 6.09 and 115 ± 179 µg/m³, respectively. Indoor air concentrations of THMs were much higher than those of outdoor air. THM concentrations in outdoor air of the Semi-Olympic swimming pool were determined to be lower than detection limits. However, THMs were detected in outdoor air of the Olympic swimming pool probably due to being located in a metropolitan city. TTHM concentration in outdoor air of the Olympic swimming pool was determined to be 1.43 ± 1.69 µg/m³.

Chloroform was determined to be the dominant THM compound in the samples. Speciation of the DBPs is dependent on the disinfection process and precursor characteristics. However, while the chlorine was used for disinfection, brominated DBPs were the dominant species found in seawater pools while chlorinated DBPs were the dominant species in the freshwater pool (Manasfi et al., 2016). Among the studied factors, there was a difference in TOC levels and the number of swimmers between the pools, while, the disinfectant doses, that may also have played an important role, were not measured. The average TTHM concentration in indoor air of Olympic swimming pool was 24-fold higher than in Semi-Olympic swimming pool. During the sampling, spectator stands of the Semi-Olympic swimming pool were under renovation, which may have had an effect on the number of swimmers.

Table 1. Indoor and outdoor air THM concentrations ($\mu\text{g}/\text{m}^3$).

	Semi-Olympic		Olympic	
	Indoor air	Outdoor air	Indoor air	Outdoor air
Chloroform	3.98±5.00	N.D.	104±156	0.90±1.47
BDCM	0.78±0.71	N.D.	7.89±15.2	0.14±0.11
DCBM	0.37±0.19	N.D.	1.57±2.76	0.06±0.02
Bromoform	0.23±0.12	N.D.	0.33±0.32	N.D.
TTHM	4.79±6.09	N.D.	115±179	1.43±1.69

N.D., not detected

Swimming pool staff and swimmers may be exposed to indoor air THMs in the other micro-environments of swimming pools, such as dressing rooms, lobby, lifeguard resting rooms, and management offices, which were sampled in the Semi-Olympic swimming pool. The average chloroform, BDCM, DBCM, bromoform, and TTHM concentrations in lifeguard resting room of the Semi-Olympic swimming pool were determined to be 1.01, 0.28, <BDL, <BDL, 1.14 $\mu\text{g}/\text{m}^3$, respectively. In the meantime, chloroform concentration was determined to be 0.38 and 0.43 $\mu\text{g}/\text{m}^3$ in lobby and management room of the Semi-Olympic swimming pool, respectively, while the remaining THMs concentrations were BDL. The average indoor air TTHM concentrations of dressing room and lobby in the Olympic swimming pool were determined to be 12.6 and 7.09 $\mu\text{g}/\text{m}^3$, respectively. The corresponding indoor to outdoor ratio values, 8.8 and 5.0, indicate the indoor levels measured in the dressing room and lobby were due to the pool.

The Semi-Olympic swimming pool is located on the shore outside the city, where groundwater is used as pool water. The groundwater is probably affected by sea water intrusion (Mansour, 2016). Formation potential of brominated DBPs could be increased due to the seawater intrusion. In the presence of bromine ions, chlorine oxidizes bromide and hypobromous acid and hypobromite ions are formed. Hypobromous acid and hypobromite ions react with organic matters and form brominated by-products (Manasfi et al., 2016). Concentration profile of THMs in indoor air of Semi-Olympic and Olympic swimming pools are shown in the Figure 1. Indoor air chloroform, BDCM, DBCM, and bromoform concentrations in the Semi-Olympic swimming pool represented 74.3%, 14.6%, 6.90%, and 4.29% of TTHM, respectively. The percentage of chloroform concentration is higher in the Olympic swimming pool, while the percentage of brominated by-products are lower (Figure 1a). Indoor air chloroform, BDCM, DBCM, and bromoform concentrations in the Olympic swimming pool represented 91.4%, 6.93%, 1.38%, and 0.29% of TTHM, respectively. Although the concentration of TTHM is higher in the Olympic swimming pool, the ratio of brominated DBPs concentration in the TTHM concentration is higher in the Semi-Olympic swimming pool probably due to the source water having higher bromine content.

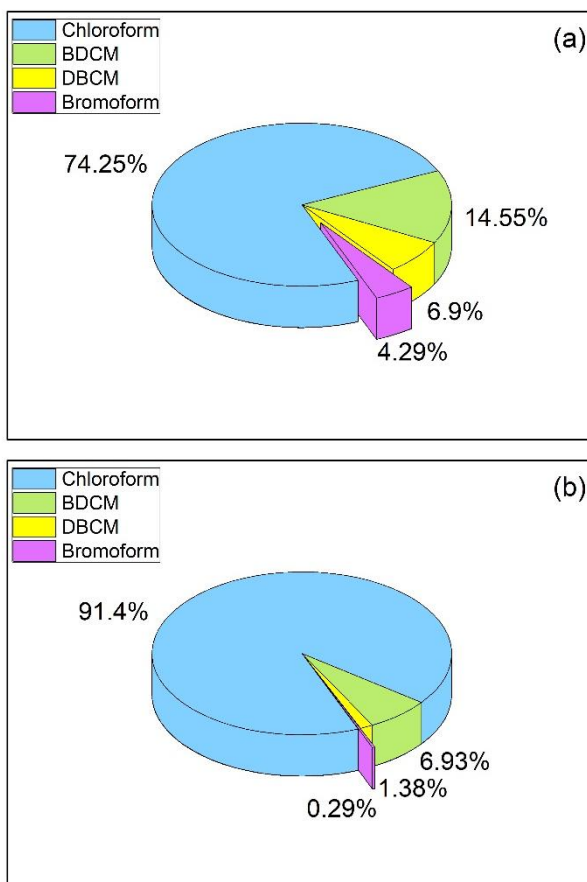


Figure 1. THM profile in indoor air of (a) the Semi-Olympic and (b) the Olympic swimming pools

In conclusion, indoor air THM concentrations of the studied swimming pools were significantly affected by the organic load from swimmers because indoor air concentrations of the heavily-used Olympic swimming pool was determined to be significantly higher than the Semi-Olympic swimming pool. Another reason for high indoor air THM concentrations may be poor ventilation due to the inefficient HVAC system. Source water characteristics affected the speciation of formed DBPs. Brominated-THM concentration in TTHM of possibly seawater-intrusion-affected groundwater filled Semi-Olympic swimming pool was determined to be higher than that of surface-water filled Olympic swimming pool. Low concentrations may also be of importance because the brominated by-products are known to be more toxic than the chlorinated ones. Long-term exposure to indoor air THMs may cause health effects for swimmers and pool staff. Higher THM concentrations compared to outdoors were also measured in other micro-environments of the Olympic pool. In this context, swimming pool workers are occupationally exposed even if they do not enter the pool space.

4. References

- Beech, J.A., Diaz, R., Ordaz, C., Palomeque, B., 1980. Nitrates, chlorates and trihalomethanes in swimming pool water, *Am. J. Public Health.* 70, 79-82.
- Edzwald, J., Tobiason, J., 1999. Enhanced coagulation: US requirements and a broader view. *J. Water Sci. and Technol.* 40, 63-70.
- Hang, C., Zhang, B., Gong, T., Xian, Q., 2016. Occurrence and health risk assessment of halogenated disinfection byproducts in indoor swimming pool water. *Sci. Total Environ.* 543, 425–431.



- Harman, B.I., Tanacan, E., Genisoglu, M., Kaplan, S.S., Al., E., 2017. Yuzme Havuzlarında Karbon Bazlı Dezenfeksiyon Yan Ürünlerinin Olusumu, DEU FMD. 63–78.
- Manasfi, T., De Méo, M., Coulomb, B., Di Giorgio, C., Boudenne, J.L., 2016. Identification of disinfection by-products in freshwater and seawater swimming pools and evaluation of genotoxicity. *Environ. Int.* 88, 94–102.
- Mansour, A.Y.S., 2016. The Investigation of Seawater Intrusion of Coastal Aquifer in Karareis (Karaburun Peninsula). MSc Thesis, Izmir Institute of Technology, İzmir, Turkey, 88 pages.
- Peng, D., Saravia, F., Abbt-Braun, G., Horn, H., 2016. Occurrence and simulation of trihalomethanes in swimming pool water: A simple prediction method based on DOC and mass balance. *Water Res.* 88, 634–642.
- Plewa, M.J., Wagner, E.D., Mitch, W.A., 2011. Comparative mammalian cell cytotoxicity of water concentrates from disinfected recreational pools, *Environ. Sci. Technol.*, 45, 4159–4165.
- Teo, L.L.T., Coleman, H.M., Khan, S.J., 2015. Chemical contaminants in swimming pools: Occurrence, implications and control, *Environ. Int.*, 76, 16-31.
- Weil, L., Jandik, J., Eichelsdorfer, D., 1980. Organic halogenated compounds in swimming pool water, I.Determination of volatile halogenated hydrocarbons, *Z.Wass. Abwass. Forsch.* 13, 165-169 (in German)
- Zwiener, C., Richardson, S.D., De Marini, D.M., Grummt, T., Glauner, T., Frimmel, F.H., 2007. Drowning in disinfection byproducts? Assessing swimming pool water. *Environ. Sci. Technol.* 41, 363–372.

Investigation of the effects of atmospheric particulate matter transported from deserts on photovoltaic module performance in Sanliurfa, Turkey

Tuba Rastgeldi Dogan¹, Nurettin Besli², Mehmet Azmi Aktacir³, Merne Nur Dinc¹, Mehmet Akif İlkhan³, Fatma Ozturk⁴ and Melek Yildiz¹

¹Harran Univ. Dept. of Environmental Engineering Sanliurfa-Turkey ,

²Harran Univ. Dept. of Electrical and Electronics Engineering Sanliurfa-Turkey,

³Harran Univ. Dept. of Mechanical Engineering Sanliurfa-Turkey ,

⁴Bolu Abant Izzet Baysal Univ. Dept. of Environmental Engineering Bolu-Turkey

tubarastgeldi@gmail.com

Abstract. In Turkey with its rich renewable energy resources the GAP (Southeastern Anatolia Project) region is the highest in terms of solar radiation level. However, the provinces in the GAP region are subject to Particulate Matter (PM) coming from atmospheric transport from the Sahara desert, the Syrian desert and even the Arabian desert. Sanliurfa often exceeds the daily limit of PM₁₀ and PM_{2.5} set by WHO for health. PM₁₀ and PM_{2.5} pollutants affect air quality and health as well as accumulate on the Photovoltaic (PV) panels and cause loss of PV panel performance. In this study, the effects of atmospheric dust accumulated on the panel surfaces for monocrystalline and polycrystalline PV technologies on panel performance was determined under Sanliurfa atmospheric conditions. In the experimental study, two panels with the same characteristics were used for each PV panel group from 2 different PV technologies. One of the panels in the PV panel group was cleaned by washing with distilled water while the other was not cleaned. Thus, the effect of the dust accumulation on the PV panel was determined by comparison to the cleaned PV panel. For this purpose, I-V values of all PV panels are measured with I-V meter. Panel surface temperature, solar radiation values and other meteorological values are measured simultaneously. In this study, the panels were washed every Monday. I-V measurements of PVs were taken every Monday, Wednesday and Friday at 12:00 am from May 1, 2019 to July 31, 2019. According to the measurements, it is observed that the dust accumulation on the PV surface reduces the energy obtained from the panel between 3-5% depending on the amount of radiation.

Keywords: Atmospheric particulate matter, Photovoltaic Module Performance, Desert, Transport, Sanliurfa

1. Introduction

Nowadays the use of renewable energy is encouraged and supported all over the world. Found abundant and fundamentally infinite in nature, sunlight is an energy resource disseminating unevenly on earth surface. Low latitude, dry and semi-dry territories, within 35N to 35S, get Direct Normal Irradiance (DNI) at the highest level. According to NASA Solar Insolation report (2008), while the Mojave Desert (latitude: 35 N) in southwestern United States annually receives 1920 kWh/m²-year sunlight, the Negev Desert (latitude: 30.5 N) in southern Israel receives 2007 kWh/m²-year. Some of the global energy needs can be satisfied by seven deserts situated between these two latitudes with the help of solar energy generation technologies, namely photovoltaic (PV), concentrated photovoltaic (CPV), and concentrated solar power (CSP) systems. Large-scale solar plants are commonly situated in semi-dry and desert lands

due to their abundant sunlight. The performance of these plants are mostly deteriorated by two environmental factors: high ambient temperature and high concentration of atmospheric dust. Soiling also decreases the energy yield of all solar panels. Dust and other particulate accumulation on solar panels result in transmittance losses in PV and CPV systems and reflection losses in CSP systems (Sayyah et al., 2014). With the development of PV related technologies, the cost of power plant components is decreasing and PV efficiency is increasing. This leads to further installation of PV power plants. Therefore, it gets even more important to examine the reasons for increasing and reducing efficiency of PV systems.

Turkey being located between latitudes 36N and 42N has rich solar energy potential. According to the Solar Energy Potential Atlas of Turkey, the total annual sunshine duration is estimated as 2.737 hours (average daily total is 7.5 hours) and the total annual incoming solar energy is 1.527 kWh/m² (daily total 4.2kWh/m²) (<http://www.enerji.gov.tr/tr-TR/Sayfalar/Gunes>). The Southeastern Anatolia Project (GAP) region is the highest in terms of solar radiation level. However, the provinces in GAP region are subject to Particulate Matter (PM) coming from atmospheric transport from the Sahara desert, the Syrian desert and even the Arabian desert, especially during the spring and autumn periods, which are the transitional seasons.

Many experimental studies have investigated the effect of dust accumulation on PV performance under outdoor conditions in various areas. The studies reported that weather conditions, panel slope angle and dust composition had a large effect on the accumulation of dust on the PV surface. Accumulation of dirt or dust on the surface of solar panels prevents or reduces the conversion of solar energy to electrical energy and is considered to be one of the main causes of energy loss of PV panels, especially in desert environments (Oh, 2019).

A thorough understanding of the effects of dust accumulation on solar panel performance is a complex process since it is a physical problem depending on various parameters. The size of the dust particles ranges from sub-micrometres to hundreds of micrometres, their shapes are irregular, and their compositions vary from region to region (Oh, 2019). Solar PV power plants have very long life-time, so the impact of dust accumulation on panel efficiency is important. Dust sources include small inorganic particles formed by the movement of sand, soil and wind, dust from industry, construction and transport, and organic particles that are dried particles of animals and plants (Chen et al., 2011; Wang et al., 2013; Chen et al., 2013).

The effects of dust pollution on PV panels have been investigated all over the world for many years. The dust can reduce the performance by covering the surface of the PV panel in a thin layer. The struggle to reduce power loss in PV systems (due to dust) is critically important in arid regions. These areas are exposed to high aerosol concentration levels and frequent sandstorms that cause a layer of dust on the surface (Parrott et al., 2018). Performance data from the installed power plants in desert areas in Rajasthan and Gujarat has reported that dust is a harmful factor (El-Shobokshy and Hussein 1993a, 1993b). Dust in a dry and less precipitation area has a greater effect on the efficiency of PV panels. In Bouzareah (Mediterranean coastal city in Algeria), performance data of seven PV systems have been collected for short periods (18 days) and a full year in different seasons (Koussa et al., 2011, 2012) and it has been found that the solar panel efficiency is reduced up to 50% at off-peak time due to the dust accumulation. The study (Parkin and Palgrave, 2005) found that glass permeability was reduced by 70% due to dust in the summer months in the United Arab Emirates.

In another study carried for about a year in Doha, the yields of PV panels were monitored. While the yield was expected to increase in the summer months, the yield was significantly reduced due to dust accumulation and high temperature. In the continuation of the study, the power efficiency of the solar panels was monitored before and after cleaning the dust on them. After cleaning the panels the power

went back to the former maximum levels; however, after a certain time the dust accumulated again and reduced the efficiency (Touati et al., 2017).

The effect of the dust on PV panels is quite different from one region to another due to the different environmental conditions of the regions. The performance of PV systems is also directly affected by actual weather conditions.

In this study, the effects of atmospheric dust accumulated on the panel surfaces for mono-crystalline and poly-crystalline PV technologies on panel performance was determined under Sanliurfa atmospheric conditions. In Section 2, the PV test setup used in this study and the Particulate matter measurement system will be described. In Section 3, case studies and numerical results will be given and discussed.

2. Material and methods

GAP Region has a semi-arid continental climate with very hot and dry summers and cold and often snowy winters. As for Sanliurfa, while the city center does not receive much snow, the provinces around Sanliurfa with higher altitude receive some snow in the winter. As mentioned earlier, GAP region is particularly exposed to dust from deserts.

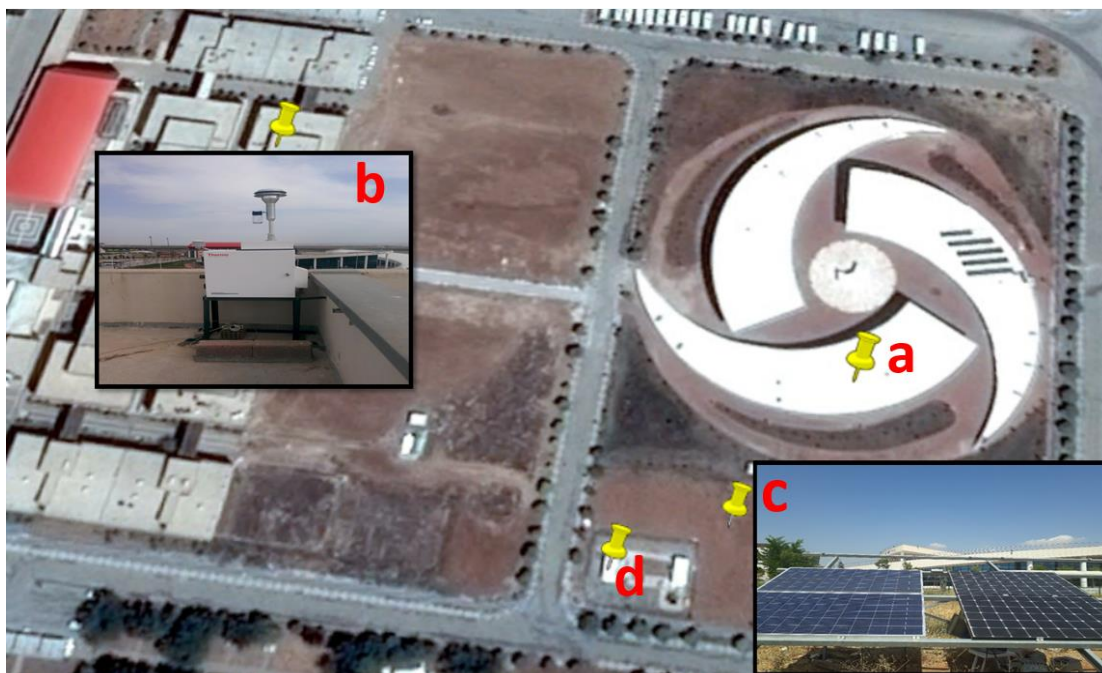


Figure 1. Work Area a) GAP YENEV Building, b) Partisol 2025ID Device from Environmental Engineering Dept., c) PV Panel Test Setup, d) Weather Station

As seen from Figure 1, the PV test setup is established in the expansion field of GAP YENEV center at the coordinates of (37° 10' 17" N, 39° 0' 15" E). In the PV test setup, two PV panels with the same characteristics formed a group. One group for monocrystalline PV panel technology and one group for polycrystalline PV panel technology are used. Their characteristics are given in Table 1. In each group, one of the panels was cleaned by washing with distilled water while the other was not cleaned except by rain. Thus, the effect of the dust accumulation on the PV panel was determined by comparison to the cleaned PV panel. For this purpose, I-V values of all PV panels are measured with I-V meter (MP-11 I-V checker). Panel surface temperature, solar radiation values and other meteorological values are also measured simultaneously.

Table 1. Characteristics of PV modules.

Values at STC(1000 W/m ² and 25 °C)	LG Electronics LG330N1C-A5 Monocrystalline	LEXRON LXR-330 M Polycrystalline
Maximum power (P _{max} -Wp)	330	330
MPP Voltage (V _{mpp} -V)	33.7	38.5
MPP Current (I _{mpp} -A)	9.8	8.57
Open Circuit Voltage (V _{oc} -V)	40.9	44.2
Short Circuit Current (I _{sc} -A)	10.45	8.93

In addition, PM₁₀ and PM_{2.5} particulates were daily collected with the Partisol 2025 ID device using filters PM₁₀ and PM_{2.5} and their concentrations were measured. Moreover, MODIS (Moderate Resolution Imaging Spectroradiometer) satellite image and HYSPLIT (Hybrid Single-Particle Lagrangian Integrated Trajectory) programs were used to determine the source where the dust has come from up to one year back. In literature on this topic for Turkey, there is not any detailed research and this study will be the first for the GAP region.

3. Results and Discussion

In this study, one of the panels in each group was washed with distilled water every Monday while the other was not cleaned except by rain. Thus, the effect of the dust accumulation on the PV panel was determined by comparison to the cleaned PV panel. I-V measurements of PVs were taken every Monday, Wednesday and Friday at 12:00 am from May 1, 2019 to July 31, 2019. During this term, it rained on June 9, 2019 and there were dusty days on May 13 and 24, on June 21 and 24, on July 8 to 10 and August 2, 6, 8, 19, 28 and 30, 2019.

Atmospheric dust transport is a natural phenomenon and can occur for long range distance with the effect of pressure differences and winds. Sanliurfa receives dust from the Sahara desert, the Syrian desert and even the Arabian desert. Despite the absence of advanced industrialization and the use of natural gas in residential heating, PM level in Sanliurfa often exceeds the healthy limit of 50 µg/m³ for PM₁₀ and 25 µg/m³ for PM_{2.5} which are determined by the World Health Organization (WHO). Measurements for PM₁₀ and PM_{2.5} were performed almost every day. The graph in Figure 2 shows the amount of PM₁₀ and PM_{2.5} particulates during the study period.

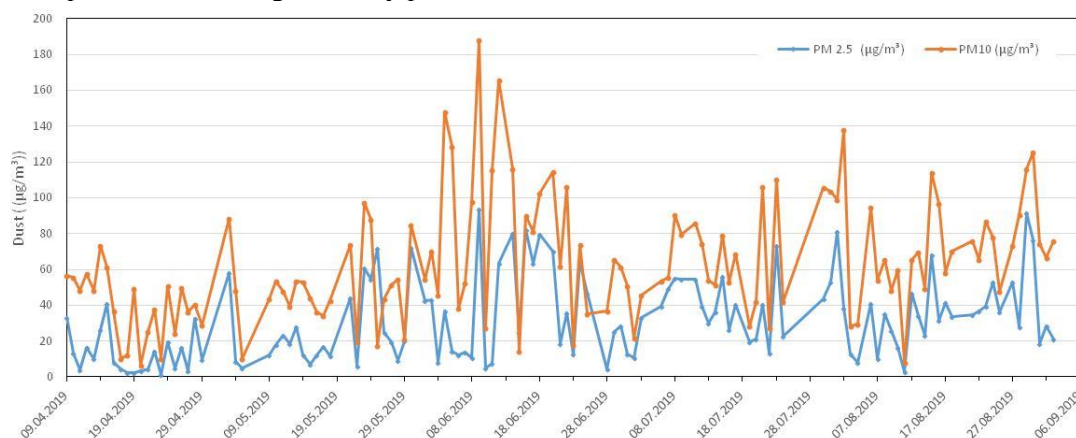


Figure 2. PM₁₀ and PM_{2.5} particulates collected during the study period

In order to follow the trails of dust deposited on the panels, MODIS satellite images and HYSPLIT images are used. While the MODIS image shows satellite picture, HYSPLIT image shows the movement of the dust originating from the Sahara desert, the Syrian desert and even the Arabian desert as seen in Figure 3.

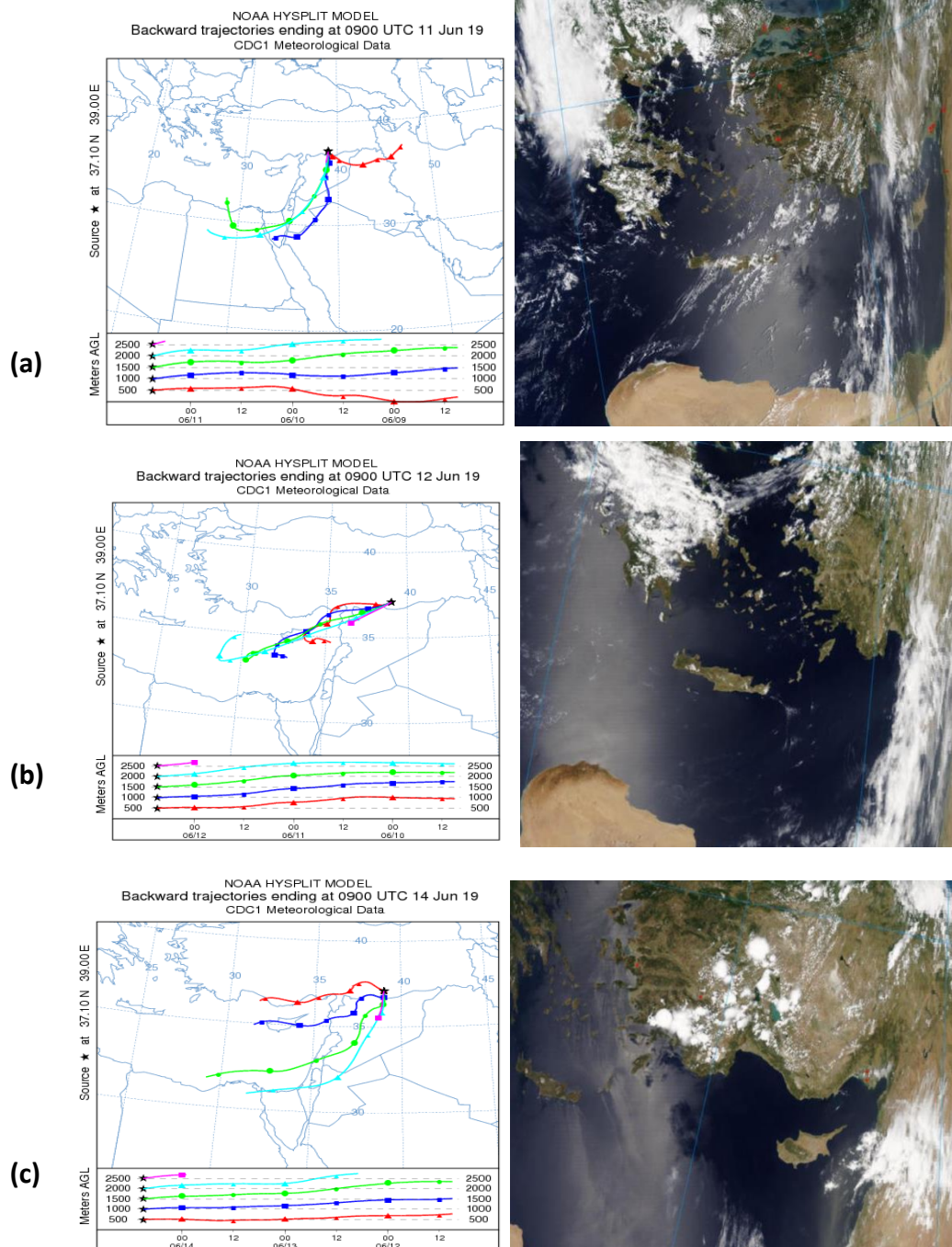


Figure 3. HYSPLIT and MODIS images on (a) June 11,2019, (b) June 12,2019, (c) June 14,2019

As mentioned earlier, one panel from each group is washed with distilled water every Monday. The pictures in Figure 4. show the differences between clean and uncleaned panels. Also it can be seen that rain can clean the panels. Therefore, it is very important to take the weather conditions and dust path into account before setting cleaning schedule.



Figure 4. Images of cleaned and uncleaned PV panel groups on different dates (Left: Polycrystalline and Right: Monocrystalline)

In order to evaluate the performance differences between clean and uncleaned panels, output power of all PV panels are measured with I-V meter. As seen in Figure 5.(a) and (b), the clean panels almost always produces higher output power for both PV technologies.

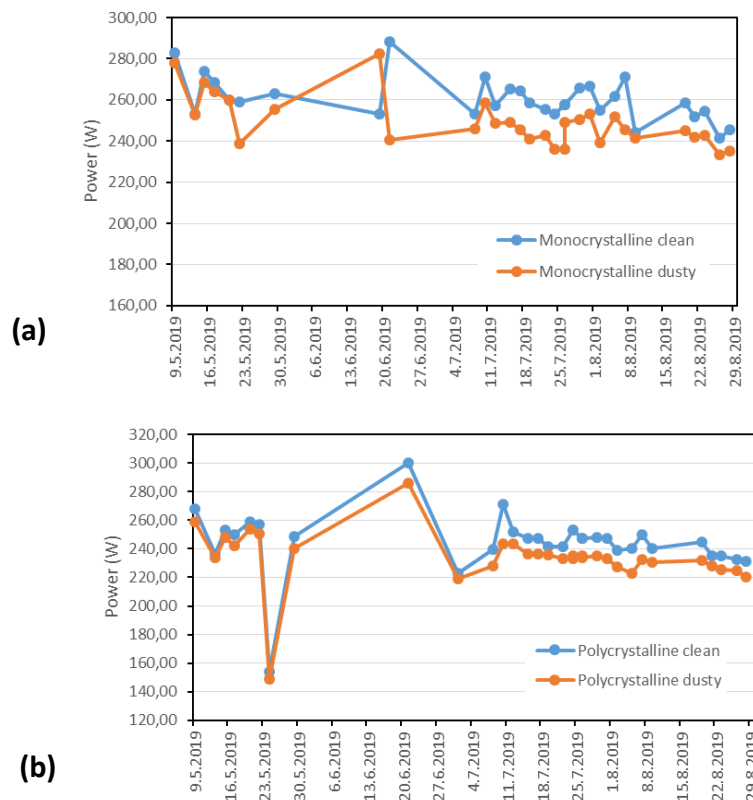


Figure 5. Power output of clean and uncleaned (a) Monocrystalline (b) Polycrystalline PV panels

After investigating power output of clean and uncleaned PV panels for both Monocrystalline and Polycrystalline technologies, the efficiency of clean Monocrystalline panel increases up to 6%, and 5% on the average. As for clean Polycrystalline panel, the efficiency increases up to 5% and 3% on the average. Therefore, cleaning panels in a PV power plants are very important.

Daily power loss of solar plants in different parts of the world were reviewed in the article by (Sayyah et al., 2014)(Figure 6). The cities are Dhaka, Bangladesh (latitude: 23.7N) (Rahman et al., 2012), Mountain View, CA (latitude: 37.4N) (Lam et al., 2009), Ogbomoso, Nigeria (latitude: 8.1N) (Sanusi, 2012), Kuwait, Kuwait (latitude: 29N) (AlBusairi and Möller, 2010), Limassol, Cyprus (latitude: 34.6N) (Kalogirou et al., 2013), Abu Dhabi, UAE (latitude: 24.5N) (Al Hanai et al., 2011), Riyadh, Saudi Arabia (latitude: 24.6N) (Salim et al., 1988), and Libya (latitude: 27N) (Mohamed and Hasan, 2012).

According to the Solar Energy Potential Atlas of Turkey, the total annual sunshine duration is estimated as 2.737 hours (average daily total is 7.5 hours) and the total annual incoming solar energy is 1.527 kWh/m² (average daily total is 4.2 kWh/m²). Average Daily Output Power Loss can be calculated as 0.8% for Polycrystalline panel. While the loss due to dust deposition on panels in Sanliurfa region (latitude: 37N) is as high as the one in neighbouring desert countries as seen in Figure 6, it is higher than the one in Mountain View, CA which has the similar latitude.

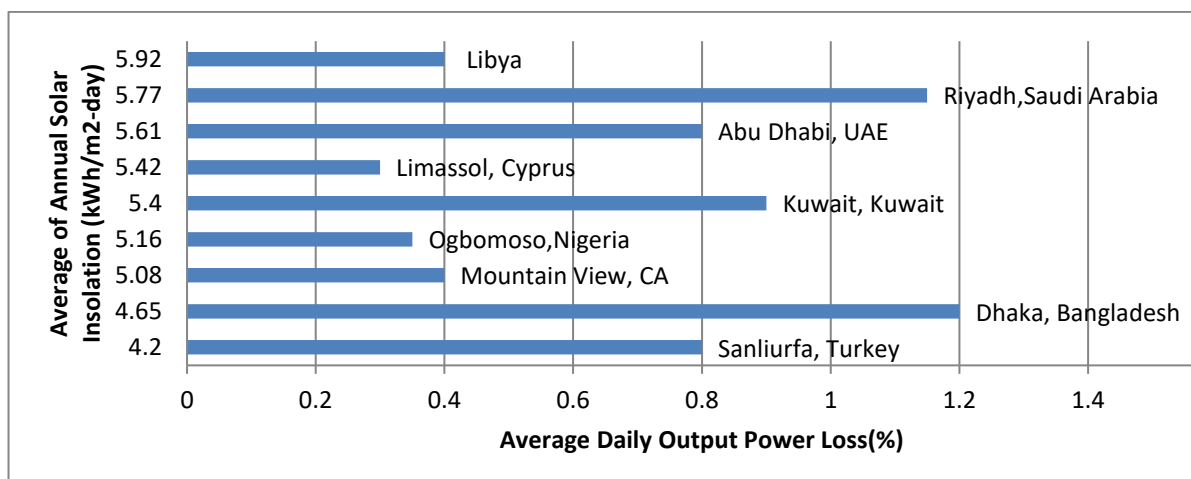


Figure 6. Daily power loss of solar plants in different parts of the world (Sayyah et al., 2014)

4. References

- AlBusairi, H. A., Möller, H. J., 2010. Performance evaluation of CdTe PV modules under natural outdoor conditions in Kuwait. In 25th European Solar Energy Conference and Exhibition/5th World Conference on Photovoltaic Energy Conversion, Valencia, Spain, September, pp. 6-10.
- Al Hanai, T., Hashim, R. B., El Chaar, L., Lamont, L. A., 2011. Environmental effects on a grid connected 900 W photovoltaic thin-film amorphous silicon system. *Renew Energ.* 36(10), 2615-2622.
- Chen, D.B., Li, D.S., Shi, J., 2011. The experiment and analysis of the dust and the poling shadow on the surface of solarpanel. *Sol Energy.* 9 (1), 39-41.
- Chen, X., Wu, C., Li, H., Feng, X., Li, Z. 2013. PV fouling detecting system based on neural network and fuzzy logic. *Intell Comput Smart Grid Electr Veh.* 463, 38-40.



- El-Shobokshy, M.S., Hussein, F.M., 1993. Effect of dust with different physical properties on the performance of photovoltaic cells. *Sol. Energy*. 51 (6), 505-511.
- El-Shobokshy, M.S., Hussein, F.M. 1993. Degradation of photovoltaic cell performance due to dust deposition on to its surface. *Renewable Energy*. 3 (6/7), 585-590.
- Kalogirou, S. A., Agathokleous, R., Panayiotou, G., 2013. On-site PV characterization and the effect of soiling on their performance. *Energy*, 51, 439-446.
- Koussa, M., Cheknane, A., Hadji, S., Haddadi, M., Noureddine, S. 2011. Measured and modelled improvement in solar energy yield from flat plate photovoltaic systems utilizing different tracking systems and under a range of environmental conditions. *Appl Energy*. 88 , 1756-1771.
- Koussa, M., Haddadi, M., Saheb, D., Malek, A., Hadji, S. 2012. Sun tracking mechanism effects on flat plate photovoltaic system performances for different step time and main parameters affecting the obtained gains: case of North Africa and Mediterranean site. *Energy Procedia*. 18 ,817-838.
- IEA, 2016. *World Energy Outlook 2016 (Executive Summary)*. World Energy Outlook 1–8. https://doi.org/http://www.iea.org/publications/freepublications/publication/WEB_WorldEnergyOutlo
- Lam, W., Nielsen, P., Ravitz, A., Cocosa, D. 2009. Getting the most energy out of Google's solar panels. Google Inc.: Mountain View.
- Mohamed, A. O., Hasan, A., 2012. Effect of dust accumulation on performance of photovoltaic solar modules in Sahara environment. *Journal of Basic and applied scientific Research*. 2(11), 11030-11036.
- NASA Solar Insolation, 2008. Solar Insolation in Different Parts of the World <http://eosweb.larc.nasa.gov/sse/global/text/global_radiation
- Oh, S., 2019. Analytic and Monte-Carlo studies of the effect of dust accumulation on photovoltaics. *Solar Energy*. 188, 1243-1247.
- Parkin, I. P., Palgrave, R.G. 2005. Self-cleaning coatings. *Mater Chem*. 15 (17), 1689-1695.
- Parrott, B., Zanini, P. C., Shehri, A., Kotsovos, K., & Gereige, I. 2018. Automated, robotic dry-cleaning of solar panels in Thuwal, Saudi Arabia using a silicone rubber brush. *Solar Energy*. 171, 526-533.
- Rahman, M. M., Islam, M. A., Karim, A. Z., Ronee, A. H., 2012. Effects of natural dust on the performance of PV panels in Bangladesh. *International Journal of Modern Education and Computer Science*. 4(10), 26.
- Salim, A.A., Huraib, F.S., Eugenio, N.N., 1988. PV power-study of system options and optimization. In: 8th International Photovoltaic Solar Energy Conference, 1988, Florence, Italy, pp. 688–692.
- Sanusi, Y., 2012. The performance of amorphous silicon PV system under Harmattan dust conditions in a tropical area. *Pacific Journal of Science and Technology*. 13(1), 168-175.
- Sayyah, A., Horenstein, M.N., Mazumder, M.K., 2014. Energy yield loss caused by dust deposition on photovoltaic panels. *Sol. Energy*. 107, 576-604.



18th World Clean Air Congress, 23-27 September 2019, Istanbul
organized by TUNCAP and IUAPPA

Touati, F., Chowdhury, N. A., Benhmed, K., Gonzales, A. J. S. P., Al-Hitmi, M. A., Benammar, M., Ben-Brahim, L. 2017. Long-term performance analysis and power prediction of PV technology in the State of Qatar. *Renewable Energy*. 113, 952-965.

Wang, F., Zhang, Y.Q., Cai, S. 2013. Research of the dust in Xi'an on distributed photovoltaic power station. *Sol. Energy*. 13, 38-40.

<http://www.enerji.gov.tr/tr-TR/Sayfalar/Gunes>).

Acknowledgments

This study was supported in part by the Scientific and Technological Research Council of Turkey (TUBITAK) (Project number: 118Y503).

Comparison of MODIS collection 6.1 and 6 aerosol optical depth based on finer resolution dark target dataset over Turkey

Gizem Tuna Tuygun, Esra Ozdemir and Tolga Elbir

gizem.tuna@deu.edu.tr

Dokuz Eylul University, Department of Environmental Engineering, 35390, Izmir, TURKEY

Abstract. This study aims to compare performance of the Moderate Resolution Imaging Spectroradiometer (MODIS) Collection 6.1 (C6.1) Dark Target 3-km aerosol optical depth (AOD) products with the Collection 6 (C6) products over Turkey between 2008 and 2016. The AOD retrievals were validated at two Turkish AERONET (V3) sites located in a coastal area (Erdemli) and an inner urban area (Tubitak). Since AERONET and MODIS measurements must be matched in space and time, matchups with the average of the AERONET AOD observations (at least two) at Terra and Aqua overpass time (10:30 and 13:30 local time, ± 30 min) and MODIS AOD pixels (at least five) within a radius of 25 km of the AERONET site were adopted in the study. The scientific data set (SDS) named “Optical_Depth_Land_And_Ocean” with quality assurance (QA) ≥ 1 over ocean and QA=3 over land was selected. For the statistical analysis, the correlation coefficient (R), root-mean-square error (RMSE), and the expected error (EE) were calculated. Since aerosol selection with the main focus on single scattering albedo (SSA) is important for data accuracy and seasonal variations affect the data quality, the seasonal differences of correlations and the effects of the accuracy of the SSA parameter on aerosol retrievals and the variability of the surface reflectance were also considered and discussed. Collection 6 DT algorithm Aqua-3km AOD products performed moderately with the correlation coefficients (R=0.51 for Tubitak site and R=0.54 for Erdemli site) over the region. Higher correlation coefficients for C6.1 DT Aqua-3km product were calculated as 0.65 and 0.85, respectively in the sites. The coastal site that has moderately vegetated surface indicated better statistical performance of DT C6 and C6.1 than the urban site. The reasonable performance of DT suggests that the surface reflectance scheme used in the inversion works well over. These products showed similar seasonal variation to the Aqua C6 and C6.1 products in Erdemli, with the values of R (>0.80) being the largest in spring; however, Aqua C6.1 products performs better in autumn in Tubitak. Performance of different MODIS collection data was also investigated under different SSA values in the coastal site. SSA values were mainly higher than 0.95. The results indicated that the Aqua C6.1 DT retrievals were significantly better than Aqua C6 DT retrievals especially when SSA was higher than 0.95 that indicates dominantly fine particles. The accuracy of C6.1 DT AOD retrievals was shown to be significantly improved (R=0.58 to 0.80) for SSA having the values higher than 0.95.

Keywords: MODIS, Aerosol Optical Depth, Collection 6.1, Dark Target Algorithm, Turkey

1. Introduction

Aerosol optical depth (AOD) is used for understanding the impact of aerosol on the Earth’s climate system, human health, atmospheric visibility, and air quality (Nichol and Bilal, 2016; Tian et al., 2018; Bilal et al., 2019). In order to perform continuous in-situ measurements of AOD, a large number of sun photometers have been deployed worldwide under the Aerosol Robotic Network (AERONET) (Holben et al., 1998) that provides AOD at relatively high spectral and temporal resolutions though at specific point-based locations. Therefore, to expand upon this framework, global AOD observations are required

for better understanding of aerosol distributions and their impacts on regional and larger scales. Various passive radiometric satellite sensors have been applied to retrieve AOD (Kahn et al., 2010), but the accuracy of AOD retrievals depends on instrument calibration, cloud screening fidelities, estimates of background surface reflectance, and available spectral aerosol models to support requisite radiance inversions (Li et al., 2009).

The Moderate Resolution Imaging Spectroradiometer (MODIS) can generate regular AOD products that are encouraging the understanding of the effects of aerosols at both local and global scales (Qin et al., 2018a, 2018b) with 36 spectral channels, a temporal resolution of 1–2 days, and moderate spatial resolutions of 250 m, 500 m, and 1000 m (King et al., 1992; Justice et al., 1998; Bisht et al., 2005). The accuracy of available land surface reflectance mostly limits the application of over-land AOD retrievals compared with over water (Levy et al., 2013; Gupta et al., 2016). Current satellite algorithms generally achieve a lower accuracy, especially in urban areas where the complexities in the physiochemical and optical properties of aerosol impose great challenges and introduce large uncertainty. Therefore, improvements to over-land retrieval algorithms as a whole are important to increase data availability globally.

MODIS aboard the NASA Terra and Aqua satellites features over-land AOD retrievals globally based on the Dark-Target (DT) (Levy et al., 2013) and the Deep-Blue (DB) algorithms (Hsu et al., 2013). For DT, pixels for dense vegetated surfaces are selected for a top-of-atmosphere (TOA) reflectance between 0.01 and 0.25 and corrected for gaseous absorption at 500 m spatial resolution. The selected pixels are arranged in a retrieval window of 20×20 pixels (400 pixels) and screened for clouds, snow/ice, and other bright surfaces. The remaining pixels are separated from land and water surfaces, and the 50% brightest pixels and the 20% darkest pixels are discarded to perform aerosol retrievals.

MODIS Collection 6.1 (C6.1) aerosol products have been recently released and replaced with the previous C6 products. In fact, the general principles behind the C6.1 products are similar to those of C6 as far as the DT algorithm is concerned. The new surface reflectance relationships between shortwave infrared and visible wavelength bands have been revised using a spectral surface reflectance product for urban areas. In addition, the MODIS sensor has now been in operation for around a decade longer than its design life. While it continues to function well, continual effort is required by the MODIS Adaptive Processing System (MODAPS) to improve the quality of MODIS' radiometric calibration. MODAPS produced a C6.1 Level-1B (L1B) product to replace the previous C6 L1B product. Improvements/changes for the DT C6.1 algorithm can be found at elsewhere (Bilal et al., 2018). However, the performance of the latest Collection 6.1 (C6.1) of MODIS APs is still unclear over different areas that feature complex surface characteristics and aerosol models. The most recent release of MODIS atmospheric product (Collection 6.1) has been used in the studies from different regions (Tian et al., 2018; Wei et al., 2018; Bilal et al., 2019). However, an assessment of the differences and similarities of the last updated and previous MODIS collections (6.1 and 6) for 3-km product is still missing in literature.

In this study, two different AERONET sites over Turkey were used for analysis. The coastal rural IMS-METU-Erdemli (here after Erdemli) atmospheric sampling site is located on the coastline of southern part of Turkey (36.57°N and 34.26°E, Figure 1). Depending on regional atmospheric dynamics, Erdemli aerosol population is mainly influenced by three aerosol sources namely; (i) anthropogenic particles from industrialized and semi-industrialized regions situated at North, (ii) mineral dust from the Sahara and Middle East Deserts located to the South and (iii) sea salt from the Mediterranean Sea (Kubilay et al., 2000; Koçak et al., 2007; Koçak et al., 2009). The inner urban TUBITAK-UZAY (hereafter Tubitak) site is temporarily instrumented. The site was located in inner part of Turkey and the instrument is mounted on the roof of TUBITAK UZAY's building (39.89°N and 32.78°E, Figure 1). The instrument is demounted for the field campaigns and moved to Tuz Golu salt lake. The site is in METU campus in Ankara city. It is exposed to any kind of aerosol sources in the city (AERONET, 2019).

This study mainly focused on comparison and analysis between MODIS C6 and C6.1 3 km-DT aerosol products over Turkey. For a better understanding of the spatiotemporal behavior and accuracy of MODIS aerosol products in urban and rural areas over Turkey, the MODIS Terra (MOD04) and Aqua (MYD04) aerosol products (collectively denoted as MxD04) at a 3 km resolution and AERONET ground observation sites were collected over the period of 2008–2016 and 2009–2012 for Erdemli and Tubitak, respectively. The performance of MODIS DT aerosol retrievals were compared and validated against AERONET AOD measurements. Meanwhile, the effects of the variability of the surface reflectance, and the accuracy of the SSA parameter on aerosol retrievals were also considered and discussed.

2. Material and Method

2.1. Datasets

AERONET provides measurements three-to-five times more accurate than satellite data in seven channels (0.340–1.020 μm) every 15 min with an uncertainty of ~ 0.01 – 0.02 in the absence of thin cirrus cloud contamination (Remer et al., 2009). AERONET data are available for January 2008 to December 2016 at Mersin-Erdemli site and for December 2009 to April 2012 at Tubitak-Uzay site. Since AERONET AOD data at 550 nm are not available, AOD is interpolated into 550 nm using Equation (1) based on the Angström exponent (440–675) (Tian et al., 2018):

$$AOD_{550nm} = AOD_{500nm} \times (550/500)^{-\alpha_{440-675nm}} \quad (1)$$

MODIS DT AOD product at 3 km is then developed from the spectral reflectance using a similar look-up-table (LUT) and inversion based on the ratio of visible and shortwave infrared, as the 10-km product (Gupta et al., 2016). The MYD04_3K is expected to resolve aerosol gradients and pollution sources such as smoke plumes that are missed at 10 km. However, since there are more pixels to select from in the deselection process at 10 km, dark or bright pixels discarded at 10 km might be retained at 3 km that makes the DT 3 km potentially noisier than the 10-km product. Accordingly, the expected error (EE) over land for the DT algorithm at 3 km is $\pm (0.05\% + 20\%)$, that is slightly less stringent than the $\pm (0.05\% + 15\%)$ for the 10-km product (Nichol and Bilal, 2016). In general, the quality of the MODIS aerosol retrievals depends on accuracy of the surface reflectance and of the aerosol model, and over- or underestimation during both clear and polluted conditions is normally caused by error in these two factors (Tian et al., 2018).

In this study, the performance of the Terra and Aqua MODIS DT C6 and C6.1 AOD retrievals at 3 km spatial resolution was evaluated on a local scale against two AERONET sites located at urban (Tubitak) and coastal rural (Erdemli) areas. Firstly, Terra and Aqua-MODIS DT, C6 and C6.1 aerosol products at 3-km spatial resolution for the two different AERONET sites located in Turkey were downloaded from “the Level-1 and Atmosphere Archive & Distribution System (LAADS) Distributed Active Archive Center (DAAC)”. The MODIS C6 level-three monthly NDVI product (MOD/MYD13A3) at 1-km resolution was used to define different land surface types. Collection 6 and 6.1 DT AOD retrievals were validated and compared by combining all available collocations for each AERONET site. The DT AOD retrievals were evaluated according to the seasons and seasonal NDVI values. NDVI values can be classified as non-vegetated surfaces ($\text{NDVI} < 0.2$), partially vegetated surfaces ($0.2 \leq \text{NDVI} \leq 0.3$), moderately vegetated surfaces ($0.3 < \text{NDVI} < 0.5$) and densely vegetated surfaces ($\text{NDVI} \geq 0.5$) (Tian et al., 2018) as defined by MOD13A3 NDVI static values (Figure 1). For the validation of the MOD/MYD04 AOD product, AERONET cloud-screened and quality-assured (Version 3, Level 2.0) data were downloaded from the AERONET website for two sites. The urban site is located over partially vegetated surface ($\text{NDVI} \sim 0.30$) while the rural site is located over moderately vegetated surface ($\text{NDVI} > 0.40$) (Figure 1). DT AOD retrievals were obtained from the scientific data set (SDS)

“Optical_Depth_Land_And_Ocean” containing the recommended high-quality flag (QF = 3) AOD retrievals over land.

2.2. Spatiotemporal matchup

As AERONET provides a point measurement that repeats frequently over time, the satellites provide a snapshot of a larger region at a single time. In order to take both the spatial and temporal variabilities of aerosol distribution into account, the AERONET measurements and the MODIS retrievals need to be co-located in time and space. In this study, it was considered that the differences in aerosol characteristics are small in the $15 \text{ km} \times 15 \text{ km}$ window. In addition, the 3-km AOD that averaged over $9 \text{ km} \times 9 \text{ km}$ is not suitable for reflecting the regional aerosol characteristics because the small statistical sample may reduce the correlation. Therefore, the daily MODIS 3-km product was averaged over the $15 \text{ km} \times 15 \text{ km}$ window size; this matched the AERONET measurements within 30 min of the MODIS overpass to calculate all of the validation spatial statistics. As AERONET does not make measurements at 550 nm, satellite retrieved AODs were interpolated to 550 nm using the standard Ångström exponent measured at 440–675 nm. Linear regression technique was used to estimate the slope and intercept of the datasets an accuracy of the collocated AOD retrievals were reported using the correlation coefficient (R), the root mean square error (RMSE), and the expected error (EE) ($0.05\% + 20\%$) of the DT algorithm over land.

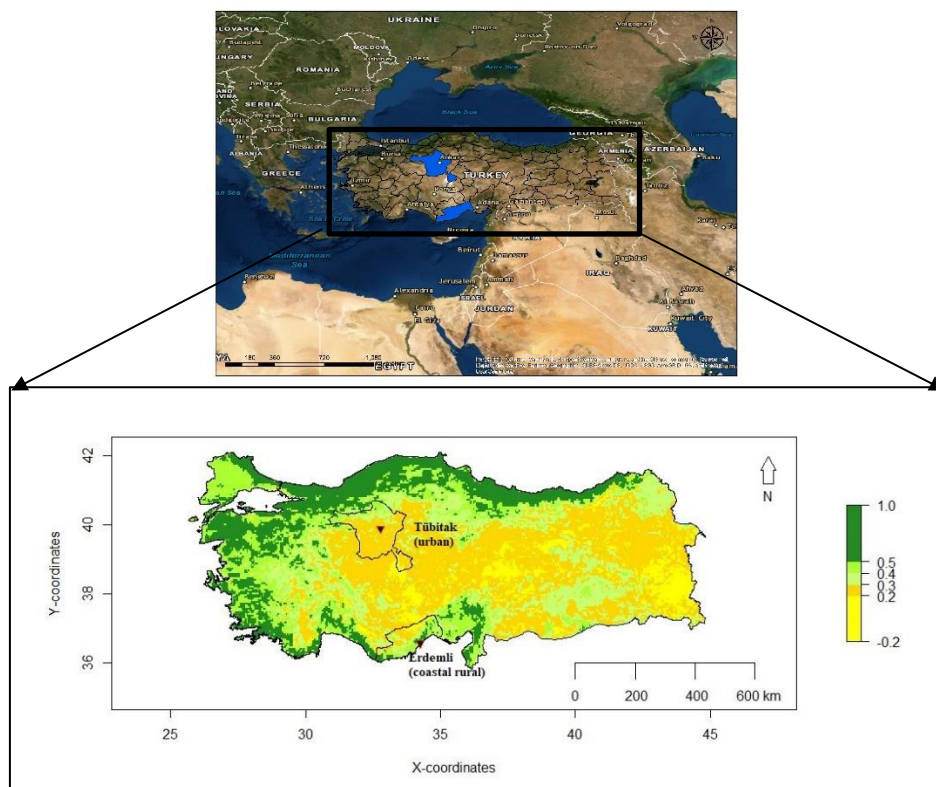


Figure 1. Locations of the stations and NDVI maps over Turkey

3. Results

3.1. Validation of the C6 and C6.1 Aerosol Products

Unlike the C6 DT algorithm, the C6.1 DT algorithm performed better over different regions, benefiting from the improved surface reflectance estimation model. The number of DT C6.1 collocations was relatively higher than DT C6. The C6.1 DT Aqua included more collocations than C6 DT Aqua mainly over the coastal rural site, because DT is designed to retrieve AOD over such regional surface. Based

on the statistical methods used in other studies, the root-mean-square error (RMSE), the correlation coefficient (R), and the percentage within expected error (PWE), defined as $\pm (0.05 + 0.20 \cdot \text{AOD AERONET})$ over land, were applied to evaluate the uncertainty in aerosol algorithms. It was found that modifications in DT C6.1 increased the percentage of retrievals EE and reduced the RMSE for both sites. Overall, similar to DT C6, DT C6.1 performed better over the rural site compared to the urban site. The percentage of DT-collocated AOD retrievals within EE was greater than 75% at the rural site, whereas less than 66% was observed at the urban site (Table 1). The reason is that the DT algorithm can accurately estimate the surface reflectance over vegetated ($\text{NDVI} > 0.30$) surfaces (Wei et al., 2018).

Validation showed that the DT C6 AOD retrievals (Figure 2 and Figure 3) were not correlated well with AOD measurements, as the range of R was between 0.54 and 0.51 for rural and urban sites, respectively. The C6 Aqua DT algorithm had not enough ability to represent the aerosol variation measured by AERONET for both sites. DT C6 Terra AOD retrievals performed better over rural and urban sites with R of 0.82 and 0.63, respectively. However, overall only 31.7% of retrievals fall within the EE at Tubitak site.

The accuracy of the C6 Terra DT product was consistent with the C6.1 Terra DT product mainly at the rural site. However, relatively significant improvement was found at the urban site. These relatively significant improvements may be due to the modified surface reflectance ratios for urban areas based on the MODIS operational surface reflectance (MOD09) (Bilal et al., 2019). Since the MxD04 C6 DT AODs were more overestimated at both sites due to underestimation of the surface reflectance and the use of inappropriate aerosol optical properties in the LUT, the PWE was only 58.6% and 42.1% for Aqua at rural and urban sites for C6 DT algorithm, respectively. With the new Collection the PWE increased by 76.1% and 83.3% and 48.5% and 60.0% for Terra and Aqua at rural and urban sites, respectively.

The moderately vegetated site (Erdemli) had better retrievals (76.1% for C6.1 Terra and 83.3% for C6.1 Aqua). However, overestimation at high AOD levels was observed mainly in summer over this region. The urban site (Tubitak) had poor quality of retrievals with only 48.5% for C6.1 Terra and 60% within EE for C6.1 Aqua. NDVI was relatively low at this site that is not ideal for the DT AOD algorithm. The relatively few collocations were also available in winter (only 5-6 over a 4-year period) due to cloud cover and short operating time. The urban site where AOD levels were ~ 2 times lower than the rural site showed the moderate correlation ($R = 0.69$ and 0.65 for C6.1 Terra and Aqua, respectively) as well as very low accuracy ($\text{PWE} < 66\%$), while the satellite retrievals and ground measurements exhibited good consistency, with $R = 0.82$ and 0.85 for C6.1 Terra and C6.1 Aqua at the rural site, respectively.

Figures 2 and 3 show scatter plots of the AODs derived from MxD04 C6 and C6.1 DT against the AODs obtained from ground-based sun photometer measurements at the rural and urban sites in spring, summer, autumn and winter. Large errors were observed at the urban site. It might be due to the errors in the estimated surface reflectance and aerosol scheme during low and high aerosol loadings. Similar results were reported by previous studies over the similar regions (Tian et al., 2018). DT C6 and C6.1 have similar collocation totals and R for Terra, but improvements and modifications in C6.1 significantly improved Aqua AOD quality. The percentage of retrievals increased from 58.6% to 83.3% and from 42.1% to 60% for Erdemli and Tübitak, respectively. RMSE decreased from 0.14 to 0.08 and 0.14 to 0.10 at Erdemli and Tubitak, respectively compared with C6. However, significant improvements and modifications are still required for DT to improve over the urban site. DT C6 and C6.1 collocated retrievals did not fulfil the requirements of EE for partially vegetated surface over Turkey, as the percentage of retrievals EE was less than 66%.

Table 1. Comparison of the retrieval accuracy between the MOD04/MYD04 C6 DT and C6.1 DT AOD products for two stations

Station	Sensor	N		R		RMSE		PWE (%)	
		C6	C6.1	C6	C6.1	C6	C6.1	C6	C6.1
Rural	Terra	1570	1575	0.82	0.82	0.09	0.09	75.2	76.1
	Aqua	1419	1625	0.54	0.85	0.14	0.08	58.6	83.3
Urban	Terra	202	203	0.63	0.69	0.17	0.12	31.7	48.5
	Aqua	140	149	0.51	0.65	0.14	0.10	42.1	60.0

N: number of matchups; PWE: percentage within the EE; R: correlation coefficient between the MODIS AOD product and the ground-observed data; RMSE: root-mean-square error.

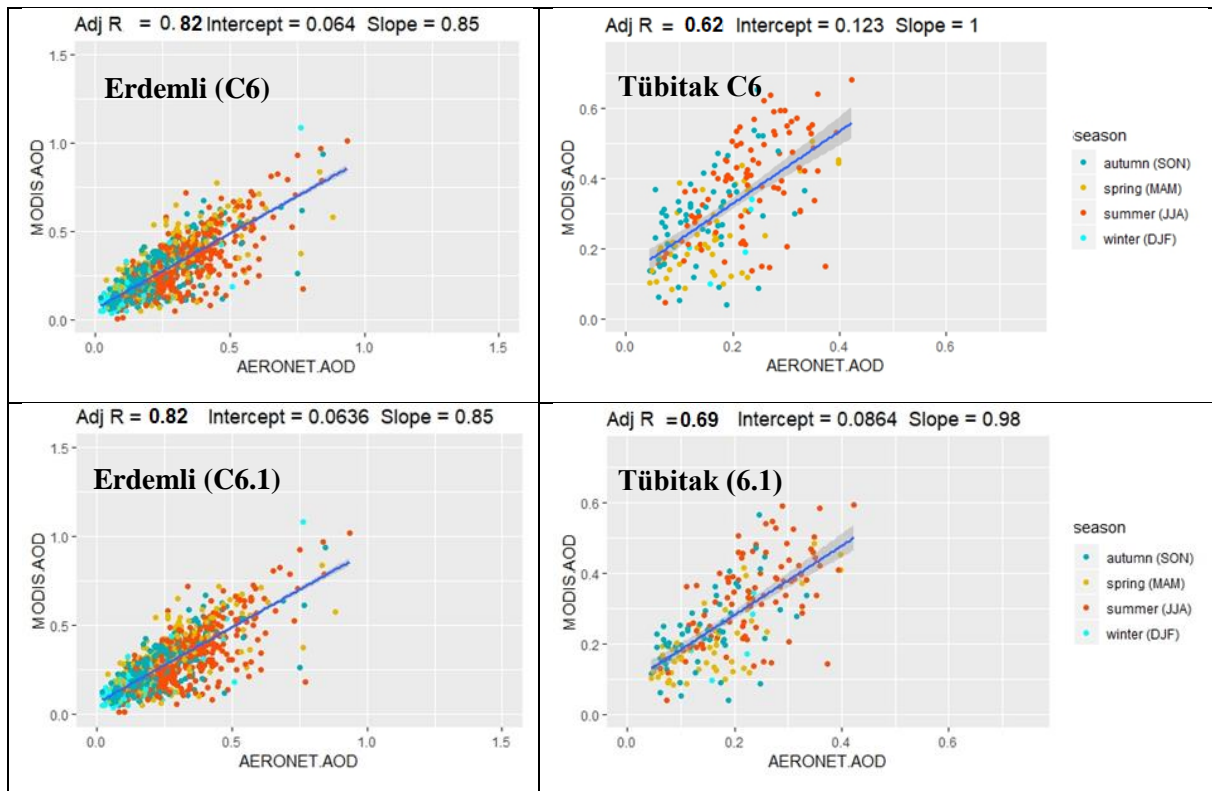


Figure 2. Validation of MODIS C6 and C6.1 DT AOD retrievals over urban and rural site for Terra. The blue line is the 1:1 line, and colors show seasons.

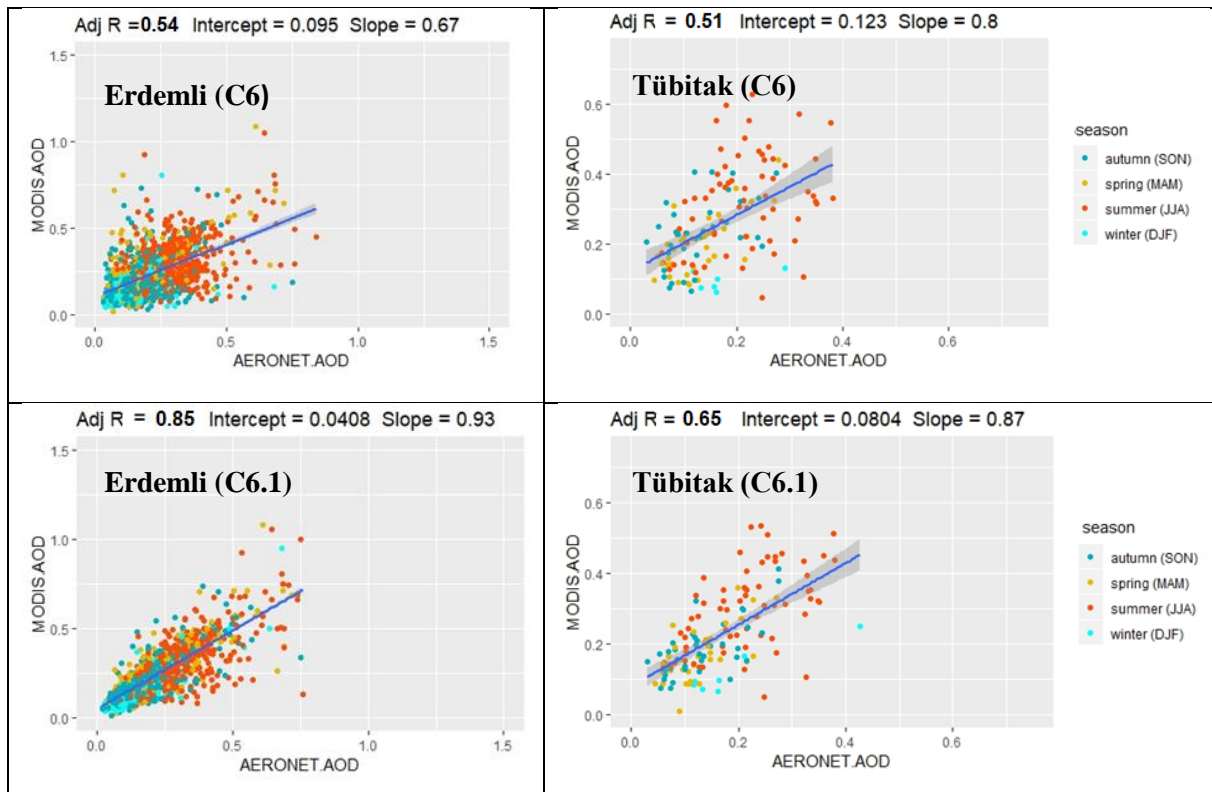


Figure 3. Validation of MODIS C6 and C6.1 DT AOD retrievals over rural and urban sites for Aqua, The blue line is the 1:1 line, and colors show seasons.

The numbers (N) of Aqua collocations were greater than numbers of Terra. The N for the DT was the largest during summer and autumn, while it was the smallest in winter. Tables 2 and 3 provide the statistics of MOD04/MYD04 C6 and C6.1 DT versus the AERONET AODs for the quarter seasons at rural and urban sites, respectively. The accuracy for both products showed obvious seasonal variation. Improvements were found significant for Aqua in all seasons mainly autumn at the rural site. Expected error increased from 65.3% to 86.5%. Improvements in summer and winter were found similar, while they were less significant in spring. Improvements were found significant for Aqua in all seasons mainly spring (~20%). Terra also showed significant improvements in spring at Tubitak. There were similar improvements were observed in summer and autumn. Both products (Terra and Aqua) showed similar seasonal variation to the MxD04 C6 and C6.1 products over two sites. However, the fraction of retrievals within EE from Aqua as 39.6% and 52.3% for C6 and C6.1, respectively was better than that of Terra as 37.9% and 45.8% for C6 and C6.1, respectively. In spring and summer, the PWE values of MOD04 and MYD04 were similar and smaller. These results indicated that the MxD04 C6.1 DT retrievals are significantly better than the MxD04 C6 DT retrievals over the both surfaces over Turkey. A similar seasonal variation was shown for the two products, with obvious seasonal and regional features.

Comparing the two products, the MYD04 showed more significant improvement than that of MOD04. However, the two products exhibited very lower accuracy over the urban site than that on the global scale (the PWE was approximately 67%) for the C6 and C6.1 DT algorithms except spring season. The C6.1 DT product had highest accuracy at the urban site with 65.5% and 74.7 PWE for Terra and Aqua, respectively. At the rural site, high accuracies were found for each season. PWE was ranging 65.5% to 89.5%. C6.1 Aqua product showed higher accuracy for each season mainly for winter.

Table 3. Comparison of the retrieval accuracy between the MOD04/MYD04 C6 DB and C6.1 DT AOD products in four seasons at the rural site

Season	Sensor	N	N	R	R	RMSE	RMSE	PWE(%)	PWE(%)
		C6	C6.1	C6	C6.1	C6	C6.1	C6	C6.1
spring	Terra	316	316	0.82	0.82	0.10	0.10	65.8	65.5
	Aqua	247	308	0.61	0.91	0.19	0.09	63.2	74.7
summer	Terra	563	563	0.78	0.78	0.09	0.09	80.3	80.8
	Aqua	583	599	0.50	0.76	0.13	0.09	67.4	82.5
autumn	Terra	425	429	0.82	0.82	0.08	0.08	74.1	75.3
	Aqua	372	423	0.38	0.82	0.12	0.07	65.3	86.5
winter	Terra	266	267	0.83	0.83	0.06	0.06	78.9	78.7
	Aqua	217	295	0.41	0.85	0.09	0.05	73.7	89.5

Table 4. Comparison of the retrieval accuracy between the MOD04/MYD04 C6 DB and C6.1 DT AOD products in the four seasons at the urban site

Season	Sensor	N	N	R	R	RMSE	RMSE	PWE(%)	PWE(%)
		C6	C6.1	C6	C6.1	C6	C6.1	C6	C6.1
spring	Terra	50	50	0.67	0.76	0.12	0.08	52.0	72.0
	Aqua	34	37	0.76	0.64	0.09	0.07	47.1	67.6
summer	Terra	89	90	0.56	0.59	0.19	0.14	27.0	43.3
	Aqua	66	67	0.59	0.52	0.17	0.13	39.4	47.8
autumn	Terra	58	58	0.49	0.55	0.18	0.12	20.7	32.8
	Aqua	34	38	0.55	0.69	0.13	0.08	38.2	57.9
winter	Terra	5	5	-	-	-	-	-	-
	Aqua	6	7	-	-	-	-	-	-

3.2. Comparison of C6 and C6.1 DT AOD

The monthly mean AODs for the C6 DT and C6.1 DT results at rural and urban sites are shown in Figures 4 and 5, respectively. A similar seasonal variation was shown for the two products, with obvious seasonal and regional features. Results indicate different temporal trends of C6 DT and C6.1 DT AODs over different regions. High DT AODs were observed in spring and summer months for both sites. In the case for DT, AOD was overestimated for C6 and C6.1 from March to May compared with AERONET at the rural site, while AOD was overestimated for C6 and C6.1 for all months compared with AERONET at the urban site.

No significant improvements in C6.1 DT Terra product were observed on a monthly basis compared with C6, as monthly averaged observations were the same for both datasets at the rural site. Some improvements were found in C6.1 DT Aqua product for spring and summer months (March to August). In general, the C6.1 data was lower than the C6 data for most seasons at both regions, but the difference was generally low at the rural site. However, the C6.1 data was much lower than the C6 data over mixed urban surface in all seasons. This means that C6 DT had a more serious underestimation of the surface reflectance than C6.1 over the region. The C6 and C6.1 DT algorithms also presented larger AOD loadings during spring and summer over the region. Overall, most C6.1 DT AODs were systematically lower than those obtained from C6 DT AODs over the urban site.

In terms of the comparison between C6.1 and C6, overestimation of DT in C6 was effectively mitigated in C6.1 just for Aqua at the rural site. Overestimation was found lowest in summer for both product,

while it was higher in spring. In terms of the comparison between C6.1 and C6, the overestimation of DT over urban areas (Tubitak site) in C6 is effectively mitigated in C6.1. The DT products could most accurately reflect the AOD over the region for both product. However, C6.1 overestimated AOD over the urban site mainly for summer months.

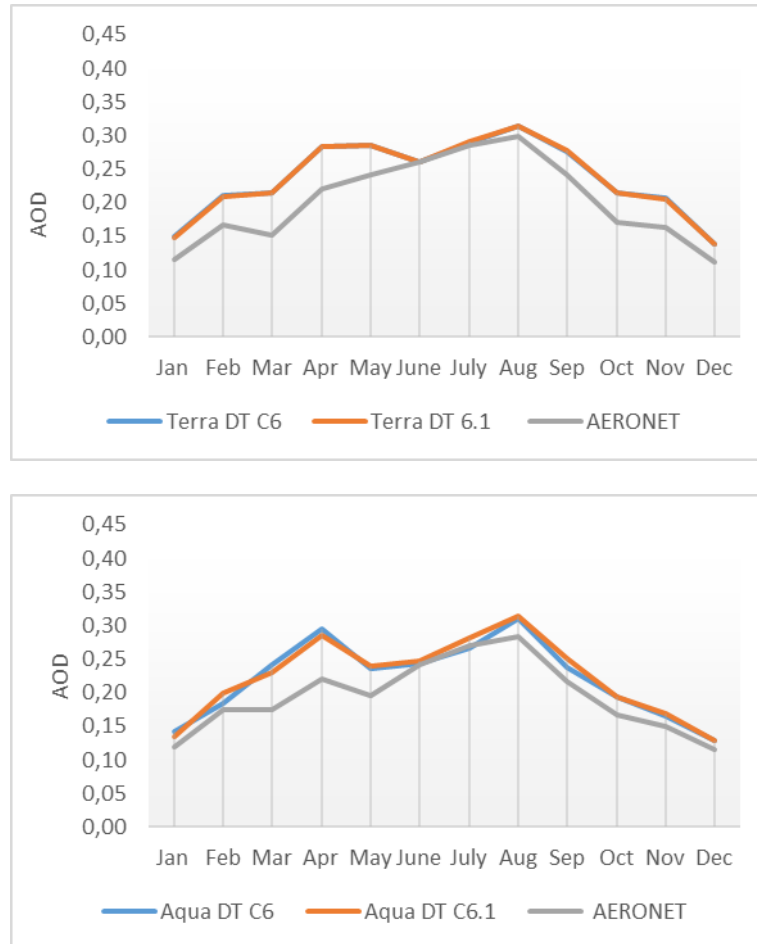


Figure 4. Monthly variation of C6 and C6.1 DT AOD at the rural site

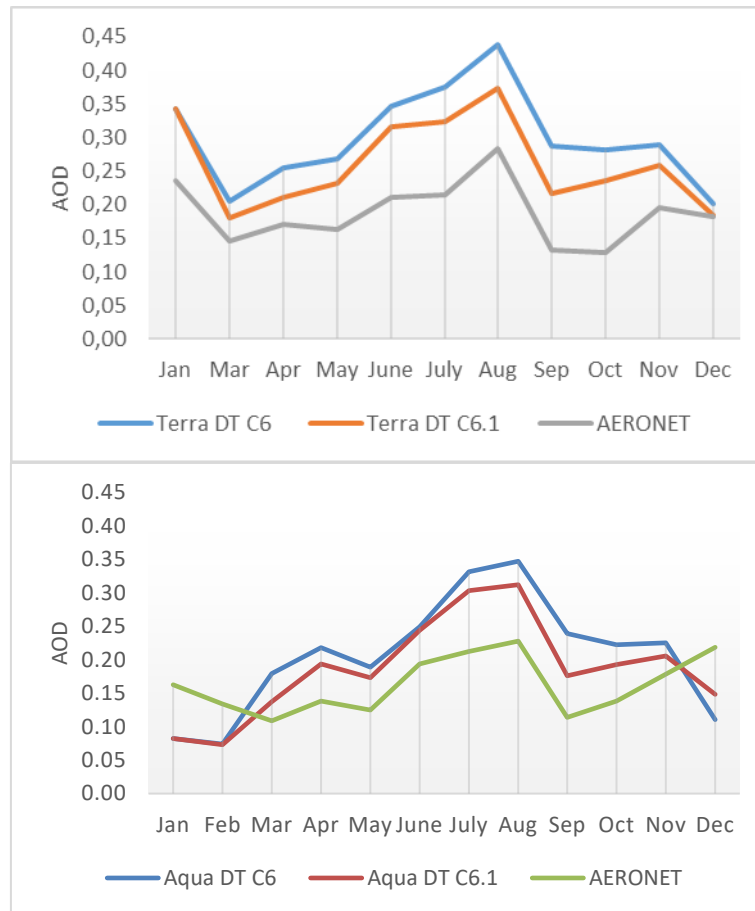


Figure 5. Monthly variation of C6 and C6.1 DT AOD at the urban site

3.3. Influence of surface estimation

In general, variance in the collocated AOD retrievals is mostly influenced by either the surface reflectance or the aerosol model used in the inversion process. Variance during high aerosol loading events is usually due to an error in the aerosol scheme. In contrast, variance in AOD retrievals during low aerosol loading events are usually due to the error in the estimated surface reflectance (Levy et al., 2013). High (low) agreement between satellite retrievals and AERONET AOD indicate that satellite retrievals follow (or do not follow) the aerosol variation as measured by the sun photometers. Improvements/changes in the DT C6.1 algorithm did not show significant improvements, as C6 and C6.1 collocated retrievals were comparable for all surfaces. Meanwhile, the regional discrepancies were also obvious, and there were much more significant regional differences over urban site than rural site. The overestimation of DT AOD retrievals over Tubitak was due to underestimation of the surface reflectance in the visible channels. Because, aerosol levels obtained from AERONET were generally low over the region and NDVI values were mainly low in winter and autumn (<0.30). Although the C6.1 DT algorithm improved serious overestimation issue over the urban site. In spring and summer, NDVI was relatively higher than other seasons, therefore overestimation was found higher in the urban site. The rural site had higher NDVI compared with the urban site. Therefore, DT algorithm performed better over the region for all seasons. The site has highest NDVI (0.46) in spring. More overestimated AODs observed at this site were the reason. Variation of seasonal NDVI values for both site was given in Figure 6.

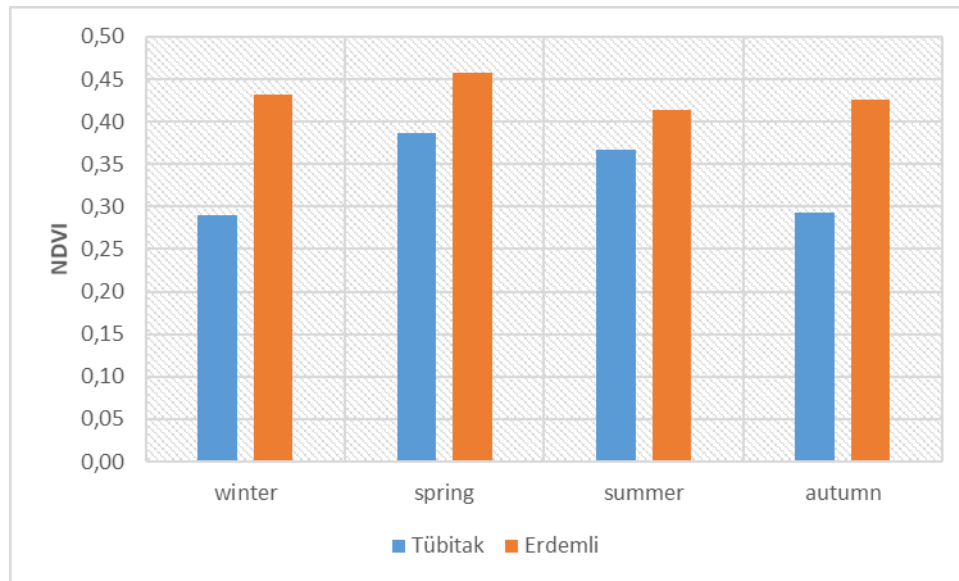


Figure 6. Seasonal variation of NDVI over the rural and urban sites

3.4. Influence of Aerosol Type Parameterization

The AOD dependence of uncertainty arises because in low-AOD conditions, the total uncertainty is dominated by surface reflectance assumptions, while as AOD increases, assumptions related to aerosol properties (most notably SSA) become increasingly dominant (Tian et al., 2018). The fine-dominated types were mainly separated through SSA, ranging from non-absorbing aerosol (SSA₄₇₀~0.95) in developed urban/industrial regions, to moderately absorbing aerosol (SSA₄₇₀~0.93) in forest fire burning and developing industrial regions, and absorbing aerosol (SSA₄₇₀~0.88) in regions of savanna/grassland burning (Tian et al., 2018). The selection of the fine-dominated aerosol model was based on the season and location. In addition, recent studies have shown that the aerosol particle shapes have significant impacts on fine-sized aerosol optical properties (He et al., 2015). Therefore, the particle shapes can also cause uncertainty in the MODIS aerosol products. Here, the aerosol type in the rural site through the AERONET was analyzed, and found that the aerosol type was non-absorbing in all seasons (SSA > 0.95) while moderately absorbing aerosol type was detected on June and November (~0.92). C6.1 and C6 DT AOD products were tested for Aqua under different SSA values (SSA = 0.90-0.95 and SSA > 0.95). It was found that improvements in both aerosol classes were consistent. Correlations increased from 0.58 to 0.80 for moderately absorbing aerosol and 0.62 to 0.80 for non-absorbing aerosols as seen in Figure 7.

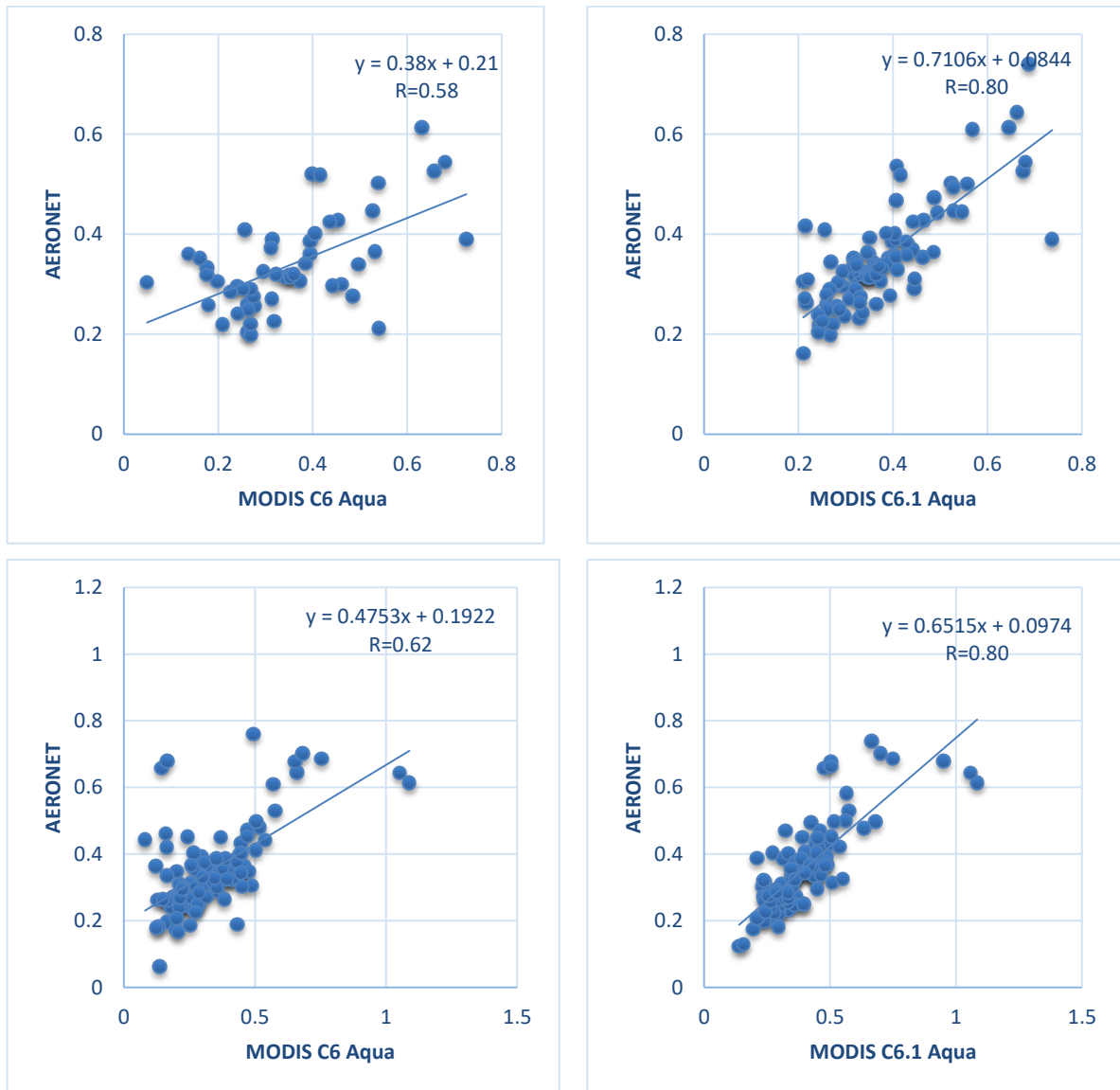


Figure 7. Validation of C6 and C6.1 Aqua DT product under different SSA values over rural site

4. Conclusions

This study comprehensively validated and analyzed the performance of the MODISAOD retrieval products (MOD04 and MYD04, separately) from C6/C6.1 DT algorithm using ground-based measurements from the AERONET dataset over the different surface types in Turkey. The results showed that the MxD04 C6/C6.1 DT algorithm greatly overestimated the AOD compared with AERONET measurements. However, the C6.1 DT was able to reduce the number of errors and retrieved AOD better than the C6 DT.

In addition, they have not only a large bias in the surface reflectance estimation in the urban site, but other factors (e.g., aerosol optical properties or cloud contamination) are also important error sources, and their effects on aerosol retrievals override the effects of non-ideality in aerosol model types. For more accurate DT AOD retrieval, improvements in the surface reflectance estimation as well as aerosol model schemes are required.

Compared with the MOD04/MYD04 C6 DT algorithm, the accuracy of MOD04/MYD04 C6.1 DT AOD retrievals was shown to be significantly improved. In addition, improvements in the MxD04 C6.1 DT algorithm for Terra were not evident, as the retrieval quality of the Terra C6.1 DT appeared similar to that of the C6 DT algorithm. Significant improvements were found for Aqua C6.1 DT product over Turkey. Overall, significant improvements and modifications are still required for DT to improve over the region that has lower NDVI.

5. References

- AERONET (Aerosol Robotic Network), 2019. Site information, https://aeronet.gsfc.nasa.gov/new_web/photo_db_v3/TUBITAK_UZAY_Ankara.html, Access: August 2019.
- Bilal, M., Nazeer, M., Nichol, J., Qiu, Z., Wang, L., Bleiweiss, M., Shen, X., Campbell, J.R, Lolli, S., 2019. Evaluation of Terra-MODIS C6 and C6.1 Aerosol Products against Beijing, Xiang He, and Xinglong AERONET Sites in China during 2004-2014. *Remote Sens.*, 11, 486.
- Bilal, M.; Nazeer, M.; Qiu, Z.; Ding, X.; Wei, J., 2018. Global Validation of MODIS C6 and C6.1 Merged Aerosol Products over Diverse Vegetated Surfaces. *Remote Sens.* 10, 475.
- Gupta, P.; Levy, R.C.; Mattoo, S.; Remer, L.A.; Munchak, L.A., 2016. A surface reflectance scheme for retrieving aerosol optical depth over urban surfaces in MODIS Dark Target retrieval algorithm. *Atmos. Meas. Tech* 9, 3293–3308.
- He, C.; Liou, K.N.; Takano, Y.; Zhang, R.; Zamora, M.L.; Yang, P.; Li, Q.; Leung, L.R., 2015. Variation of the radiative properties during black carbon aging: Theoretical and experimental intercomparison. *Atmos. Chem. Phys.* 15, 11967–11980.
- Holben, B.N.; Eck, T.F.; Slutsker, I.; Tanre, D.; Buis, J.P.; Setzer, A.; Vermote, E.; Reagan, J.A.; Kaufman, Y.J.; Nakajima, T., 1998. AERONET—A federated instrument network and data archive for aerosol characterization. *Remote Sens. Environ.* 66, 1–16.
- Hsu, N.C.; Jeong, M.-J.; Bettenhausen, C.; Sayer, A.M.; Hansell, R.; Seftor, C.S.; Huang, J.; Tsay, S.-C., 2013. Enhanced Deep Blue aerosol retrieval algorithm: The second generation. *J. Geophys. Res. Atmos.* 118, 9296–9315.
- Koçak, M., Mihalopoulos, N., Kubilay, N., 2007. Chemical composition of the fine and coarse fraction of aerosols in the Northeastern Mediterranean. *Atmos. Environ.* 41, 7351–7368.
- Koçak, M., Mihalopoulos, N., Kubilay, N., 2009. Origin and source regions of PM₁₀ in the eastern Mediterranean atmosphere. *Atmos. Res.* 92, 464–474.
- Kubilay, N., Nickovic, S., Moulin, C., Dulac, F., 2000. An illustration of the transport and deposition of mineral dust onto the eastern Mediterranean. *Atmos. Environ.* 34, 1293–1303.
- Levy, R.C.; Mattoo, S.; Munchak, L.A.; Remer, L.A.; Sayer, A.M.; Patadia, F.; Hsu, N.C. The Collection 6 MODIS aerosol products over land and ocean. *Atmos. Meas. Tech.* 2013, 6, 2989–3034.
- Li, Z.; Zhao, X.; Kahn, R.; Mishchenko, M.; Remer, L.; Lee, K.-H.; Wang, M.; Laszlo, I.; Nakajima, T.; Maring, H., 2009. Uncertainties in satellite remote sensing of aerosols and impact on monitoring its long-term trend: A review and perspective. *Ann. Geophys* 27, 2755–2770.



18th World Clean Air Congress, 23-27 September 2019, Istanbul
organized by TUNCAP and IUAPPA

Nichol J.E., Bilal, M., 2016. Validation of MODIS 3 km Resolution Aerosol Optical Depth Retrievals Over Asia. *Remote Sens.* 8, 328.

Remer, L.A.; Chin, M.; DeCola, P.; Feingold, G.; Halthore, R.; Kahn, R.A.; Quinn, P.K.; Rind, D.; Schwartz, S.E.; Streets, D., 2009. Executive Summary, in Atmospheric Aerosol Properties and Climate Impacts. In A Report by the U.S. Climate Change Science Program and the Subcommittee on Global Change Research; Chin, M., Kahn, R.A., Schwartz, S.E., Eds.; National Aeronautics and Space Administration: Washington, DC, USA.

Tian, X., Liu, Q., Li, X., Wei, J., 2018. Validation and Comparison of MODIS C6.1 and C6 Aerosol Products over Beijing, China. *Remote Sens.* 10, 2021.

Wei, J.; Sun, L.; Huang, B.; Bilal, M.; Zhang, Z.; Wang, L., 2018. Verification, improvement and application of aerosol optical depths in China Part 1: Inter-comparison of NPP-VIIRS and Aqua-MODIS. *Atmos. Environ.* 175, 221–233.

Acknowledgment

This study has been supported in part by the TUBITAK 2214/A Doctoral Research Scholarship Programme. We extend sincerest thanks to the AERONET and MODIS teams for their datasets.

An ecological assessment on the air pollution environment of Akhisar

M. Dogan Kantarci¹ and Arzu Yucel²

¹İst. Üni. Orman Fakültesi Toprak İlimi ve Ekoloji Abd. (EM) Bahçeköy-İstanbul

²Çevre Yüksek Müh. Ege Ormancılık Arşt. Enst. Md'üğü, Orman Ekolojisi ve Toprak Araştırmaları Başmühendisliği-İzmir-Türkiye

mdkant@istanbul.edu.tr

Abstract. The height of Akhisar level is 60-110 m. At the vest lies Yund-Berg and prevents the sea effect over Aegean Sea. The Massifs of Mount Görenez and Mount Katırcı in the east prevent the terrestrial climate effect in the east. The valleys, where the Akhisar Kırkağaç-Soma Road and the Akhisar-Sındırgı Road extend to the north, provide the north wind to reach the plain. The average annual temperatures in Akhisar between 1970-2017 show significant differences. It was 15.7 °C in the years 1970-1981, 15.8 °C in 1982-1993, 16.7 °C in 1994-2016 and 17.0 °C in 2007-2017. The average annual precipitation was calculated 616.3 mm in the period 1970-1981 and decreased to 483.2 mm from 1982-1993, to 586.1 mm from 1994-2006 and to 557.6 mm from 2007-2017. The rise in temperature and the fall in precipitation caused the humidity in the summer to drop between 20 and 30 % at 14 o'clock. The fact that the humidity in the summer at 7 o'clock in the morning between 50-65 %, indicates a serious lack of water. The winds number from the north is much higher in Akhisar than in the other directions. The average annual wind force is 28685, of which 66.8 % is from the north, 18.3 % from the south, 1 % from the west and 0.5 % from the west. The density of exhaust gases from Soma thermal power plants in and around Akhisar was calculated using a simple model as general values. According to a trapezoidal distribution area with a width of 10 km on Soma, 30 km on Akhisar and a distance of 40 km and a depth of 1 km. The total amount of coal incinerated in Soma A and B power plants in the period 1990-2008 is between 4.2 - 8.9 million tons/year and the amount of SO₂ released from the chimneys is 35806.27 to 86892.49 tons year. According to the model, the daily SO₂ concentration in Akhisar was calculated as 143.09-362.05 µg/m³/day. In dry and cold regions, the SO₂ limit is 30 µg/m³. The amount of NO_x released from the plants in the period 1990-2008 was 9432.06-22628.46 tons/year. Using the model, the daily NO_x concentration in Akhisar was calculated as 39.30-94.37 µg/m³/day. The limit value of the EU for NO_x is 30 µg / m³ and is exceeded during daytime rising air. In addition, ash and dust emissions from thermal power plants and dust from quarries and trucking on roads cause a remarkable air pollution.

Keywords: Akhisar, Sulfur dioxide, Nitrogen oxides, Thermal power plant, Olive trees.

1. Introduction

Akhisar is on the edge of a plain surrounded by mountainous terrain. The plain and the surrounding mountainous terrain form the transition between the western Aegean climate under the influence of the sea and the inner eastern area under the influence of the continental climate. The climate is "Western Aegean" in terms of temperature, and on the other hand as "continental climate" in terms of drought.

It is criticized that the exhaust gases of the Soma thermal power plants are transported to Akhisar and Manisa via the north winds and causes air pollution. In addition to news published in the local press in

Soma and Manisa, the problem of air pollution is being evaluated in "Air Pollution and Public Health" bulletins which are publishing annually.

2. Method

Firstly, ecological characteristics of Akhisar and its surrounding have been evaluated with its (1) land structure and (2) climate characteristics. The reason is that the flue gases of thermal power plants are more effective in arid or cold climate regions.

The density composed which is the exhaust gases of Soma thermal power plants, in and surround of Akhisar was calculated using a simple model as general values. The density of the exhaust gases is calculated according to a trapezoidal distribution area with a width of 10 km on Soma, 30 km on Akhisar and a distance of 40 km (bird flight distance) on Akhisar (Map 1).

It is assumed that the gases can rise during the day time to 1000 m with warm air current. This is a very rough estimate. The exhaust gases can reach at 1000 m altitude with warm air, but at night time the air will cool down and humid air will condense, so become heavier air masses sinks to the lowlands and valleys. The pollutants contained in the air masses precipitates on low terrain too. Thus the concentration of pollutant in the air increases.

In addition, the wind speeds, terrain structure, valleys and air currents along the valleys will affect the spread of polluted air. The transport distances of polluted air is a modeling study; in this study merely confine with general distribution calculation for give an idea.

3. Ecological characteristics of Akhisar and surroundings

3.1. Geomorphological structure of Akhisar and surroundings

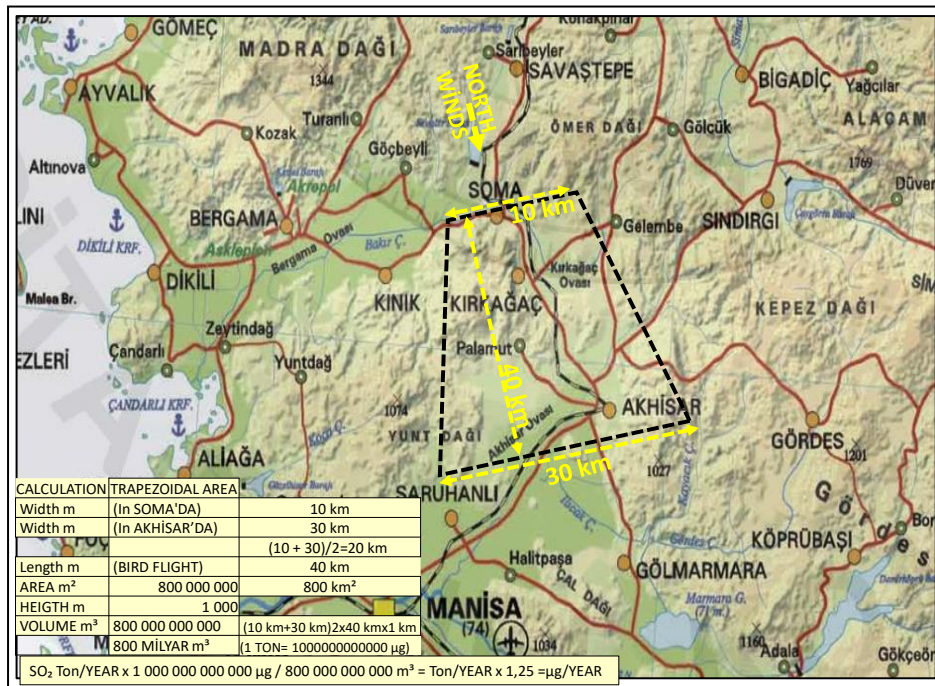
Akhisar and its surroundings can be described as a plain in the middle of horseshoe-like mountainous terrain. The Akhisar Plain extends south via the Saruhanlı, Manisa and Muradiye Plains to the Gediz Valley and via the Emiralem Strait into the Menemen Plain and the Aegean Sea (Map 1).

The Akhisar Plain has 60-110 m elevation, and the Yund Mountain (1014 m) Mass which is located of its west, block the sea effect from reaching the plain. If Görenez Mountain (1280 m) and Katırcı Mountain (1027 m) to the east, prevent the terrestrial climate effect of the east. The valleys where Akhisar-Kırkağaç-Soma road and Akhisar Sındırgı road pass in the north provide the northern winds to reach the plain. The effect of the Aegean Sea is insufficient and can reach the plain through Emiralem Pass (Map 1).

3.2. Climate characteristics of Akhisar and its surroundings

3.2.1. Average Temperature Values and Periodical Change in Akhisar

The average annual temperature values in Akhisar show significant differences between 1970 and 2017. The average annual temperatures was calculated as 15.7 ° C during 1970-1981, 15.8 ° C during 1982-1993, 16.7 ° C during 1994-2006, and 17.0 ° C during 2007-2017 (Figure 1). In 1982-1993 period, 5 volcano eruptions prevented the increase in temperature. Similar situations have been repeated in other eruptions and most notably in 2010-2011.



Map 1. Transport of the exhaust gases of the Soma power plants to Akhisar and surroundings

The reflection of the annual average temperature increase in the summer months is much more distinct. Monthly average temperature rises are; began 1.1 °C in IV month, and reach up to 2.9 °C in VIII. month, and its calculated to be 1.2 °C for in X. and XI. months (in the period 2007-2017 according to the period 1970-1981) (Figure 1).

3.2.2. Rainfall and periodical change in Akhisar

The average annual rainfall in Akhisar between 1970 and 2017 also shows remarkable differences. The average annual precipitation was calculated to be 616.3 mm in the period 1970-1981, decreased to 483.2 mm from 1982-1993, increased to 586.1 mm from 1994-2006 and to 557.6 mm from 2007-2017 (Figure 2). The relation were observed between 5 volcano eruptions and decrease in precipitation in 1982-1993 period.

3.2.3. Average evaporation amount in Akhisar

In the period 1970-2017, a total evaporation of 7 months (IV.-X. months) from the open water surface was measured in Akhisar between 1100 and 1700 mm/m² (Figure 3). The entire 7-month evaporation is very different over the years. Evaporation VI., VII. and VIII. higher in months.

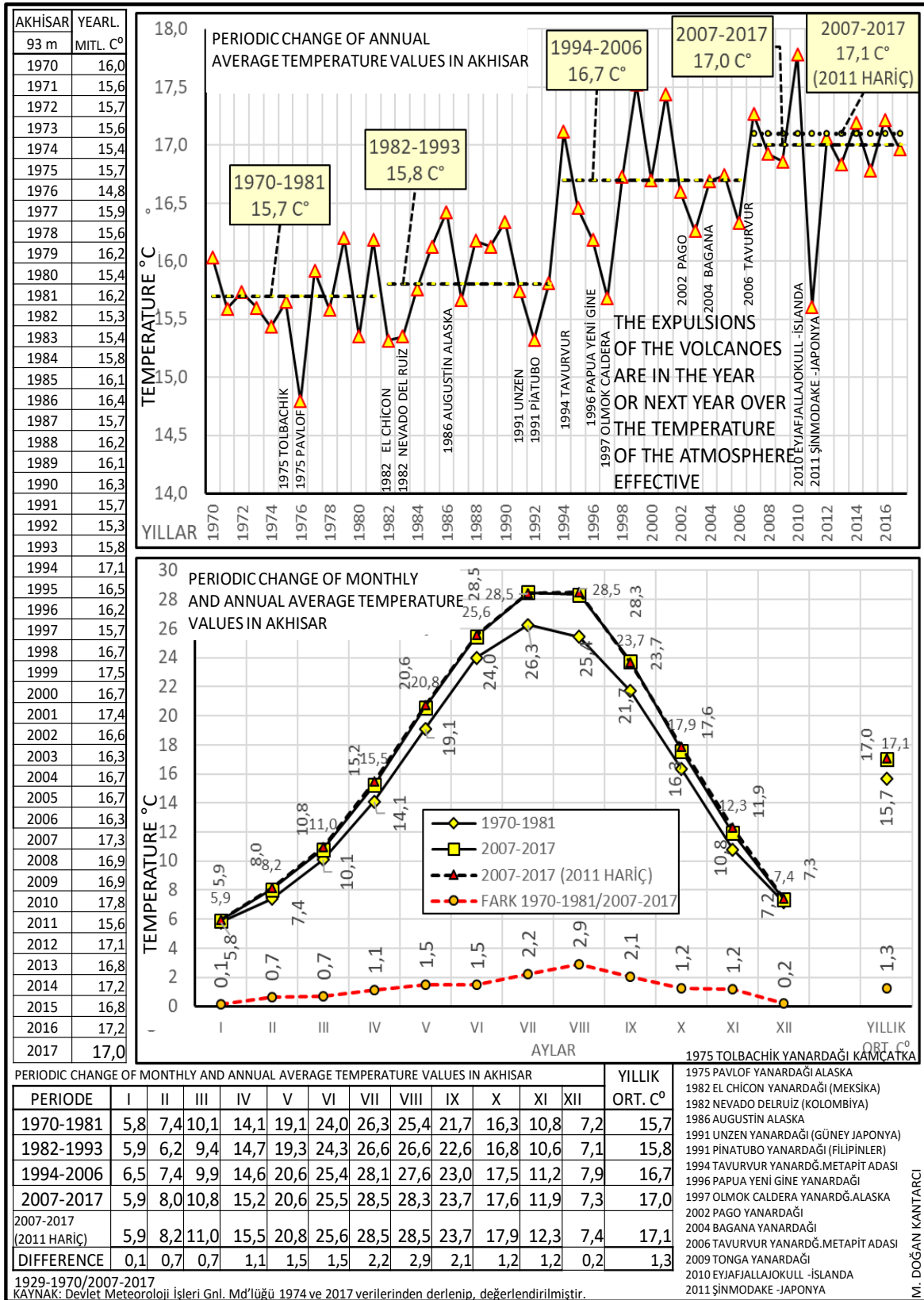


Figure 1. The periodic changes annual and monthly temperature values in Akhisar and the volcanoes effect

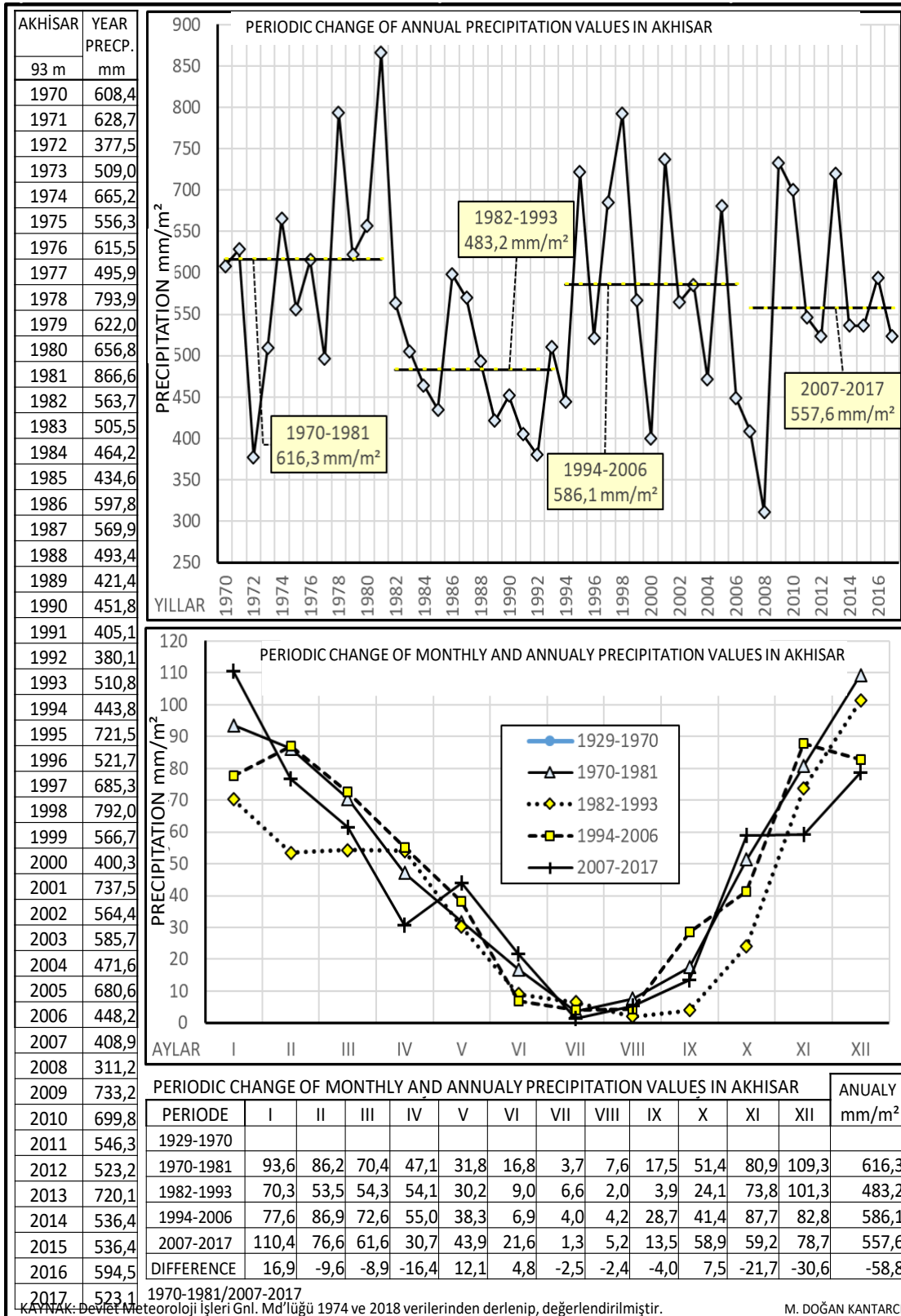


Figure 2. The periodic changes annual and monthly precipitation values in Akhisar

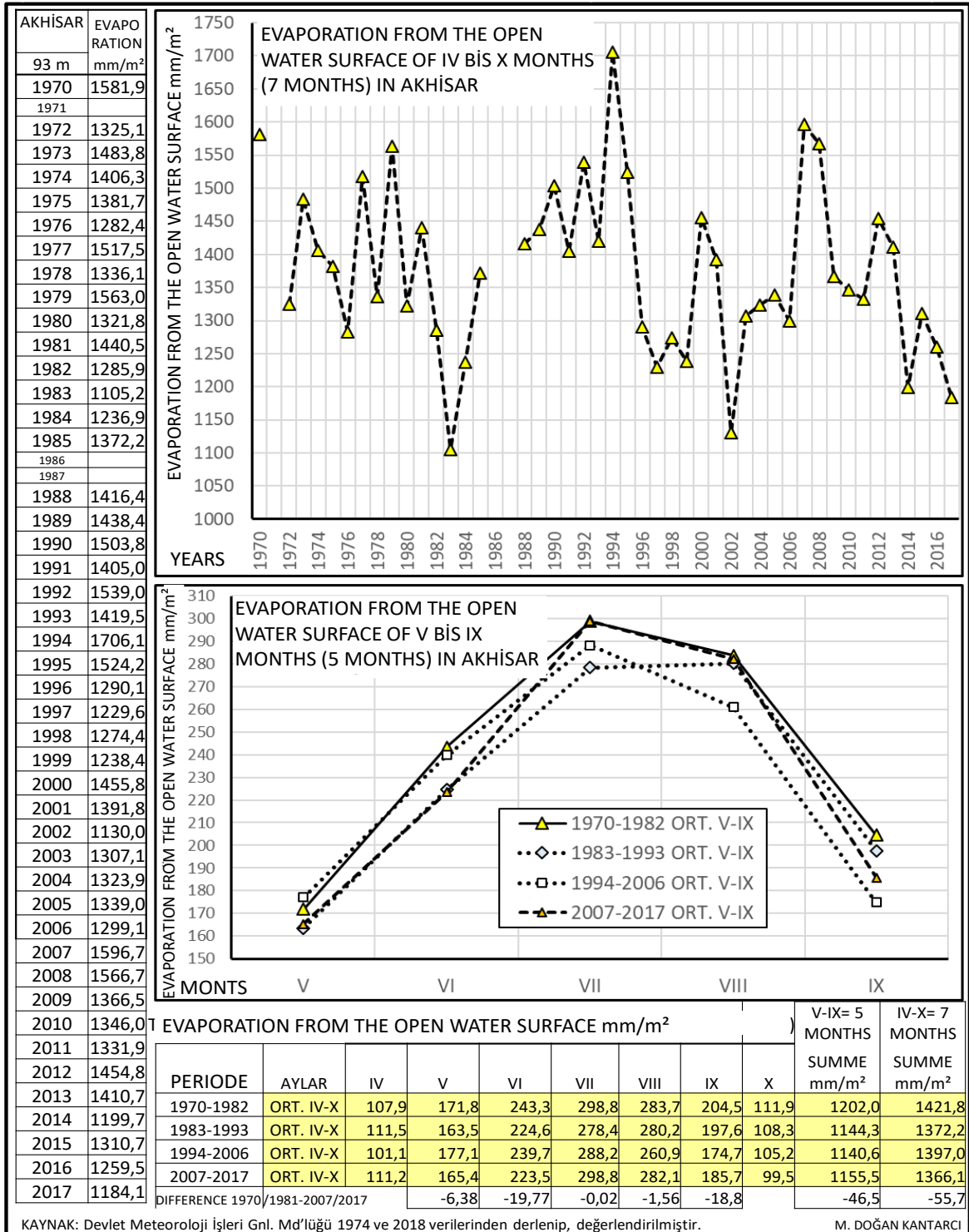


Figure 3. Periodic change of the total evaporation amount between V-X. months in Akhisar

3.2.4. Changing the humidity in Akhisar during the day in the morning (7:00 am), midday (2:00 pm), evening (9:00 pm)

Changes in air humidity values during the day and hours in Akhisar from 1970 to 2011 show very interesting results. The humidity in the summer months at 14 o'clock was between 35-40% in the period 1970-1981 and 1982-1993. But between 30-35% of the period 1994-2006 and between 25-35%. calculated in the period 2007-2011. The decrease in humidity compared to the periods depends on increasing temperature values in the summer up to 2 °C and the lack of water in the soil. Similar developments can be observed in the humidity at 7.00 and 21.00 (Table 1 and Figure 4).

The humidity measured at 7:00 am was lower in the period 2007-2011. This indicates that the moisture content of the air at night does not rise sufficiently and dew point can not occur. The lack of moisture during the night (and consequently the formation of dew) is very important for the water balance in the leaves. This phenomenon can be considered a typical drought effect.

Drought effect can be eliminated with irrigation. However, it is concluded that irrigation is insufficient to increase humidity during the night. Further irrigation is not possible or economical. Drip irrigation is used to prevent water loss.

Table 1. Variation of air humidity rates in Akhisar after morning, noon and evening times and periods

PERIODE	TIME 7.00												TIME 14.00												TIME 21.00											
	I	II	III	IV	V	VI	VII	VIII	IX	X	XI	XII	I	II	III	IV	V	VI	VII	VIII	IX	X	XI	XII	I	II	III	IV	V	VI	VII	VIII	IX	X	XI	XII
1970-1981	83	82	84	84	78	70	70	72	79	84	87	85	59	56	50	45	41	37	37	38	38	46	52	58	77	74	68	64	60	50	50	54	57	67	76	78
1982-1993	86	84	86	87	83	75	75	78	82	86	87	88	61	58	51	47	42	37	37	36	35	44	56	65	79	73	70	67	64	54	55	58	59	68	78	83
1994-2006	85	83	83	83	77	67	67	72	78	85	87	84	55	50	43	41	36	31	31	32	33	40	47	55	75	69	62	60	52	44	46	49	54	64	74	75
2007-2011	90	87	86	79	67	60	55	63	71	84	89	91	61	58	51	47	34	31	26	28	32	45	55	66	83	78	71	65	55	50	45	49	55	70	80	85

KAYNAK: Devlet Meteoroloji İşleri Genel Müdürlüğü 1974 ve 2017 verilerinden derlenip, değerlendirilmiştir.

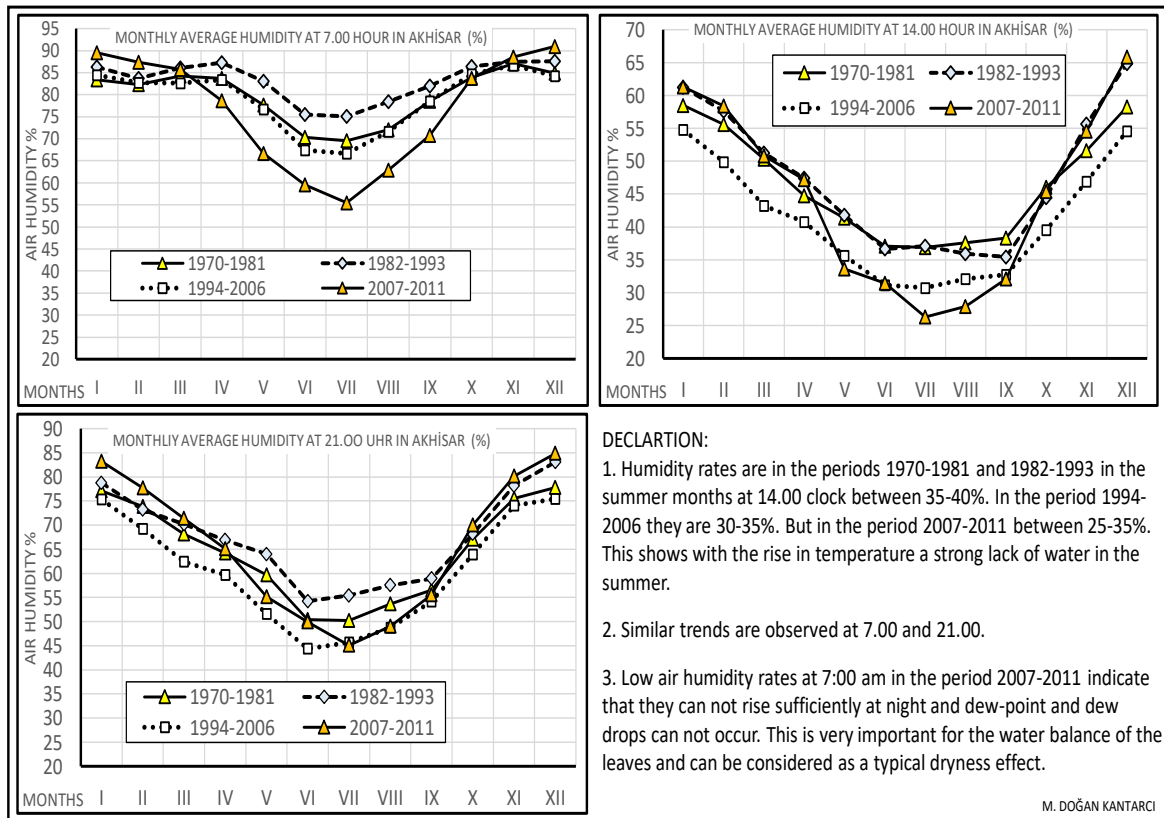


Figure 4. Periodical comparison of the Humidity rates in Akhisar by morning, midday and evening



3.2.5. Average wind blowing number according to winds directions in Akhisar

The number of winds from the north is much higher than in the other directions in Akhisar. The average annual wind force is 28685 winds, of which 66.8% (19176) is from the north, 18.3% from the south, 1% from the west and 0.5% from the west (Table 2, Figure 5). The Yund Mountain and the Turkmen mountain mass prevent the winds from coming from the west and obstructing the influence of the sea. North winds come through the valleys in the north.

The winds from the north direction have higher average speeds. Especially in the VIIth and VIIIth months, average north wind speeds are higher (Figure 5).

Table 2. Number of winds blowing directions in Akhisar (average from 1975 to 2006, 32 years)

DIRECTIONS GROUPS													ANNUALLY
DIRECTIONS	I	II	III	IV	V	VI	VII	VIII	IX	X	XI	XII	BLOW 28 685
NW	123	94	136	156	159	146	115	123	137	129	128	151	1597
NNW	431	423	409	366	507	531	663	750	616	471	348	433	5948
N	366	399	401	300	393	470	682	593	366	368	306	350	4994
NNE	355	336	427	266	374	494	643	618	444	427	320	274	4978
NE	140	133	145	127	127	95	177	139	147	173	134	122	1659
SUMME	1415	1385	1518	1215	1560	1736	2280	2223	1710	1568	1236	1330	19176 (% 67)
ENE	87	45	63	35	65	50	86	73	37	63	52	67	723
E	32	17	30	27	17	17	11	22	11	27	22	35	268
ESE	34	28	38	31	22	10	13	13	18	48	25	34	314
SUMME	153	90	131	93	104	77	110	108	66	138	99	136	1305 (%0,05)
SE	61	62	55	64	46	27	18	23	41	45	53	58	553
SSE	143	145	149	133	63	45	29	45	71	83	116	141	1163
S	124	140	152	134	76	68	31	40	63	80	116	146	1170
SSW	138	137	201	225	140	76	53	56	111	102	113	143	1495
SW	76	69	86	123	117	66	35	42	54	68	70	62	868
SUMME	542	553	643	679	442	282	166	206	340	378	468	550	5249 (% 18)
WSW	56	48	80	120	112	97	46	50	81	68	57	53	868
BW	48	51	69	96	116	99	51	35	80	60	64	52	821
WNW	101	80	86	133	121	181	88	84	115	108	90	79	1266
SUMME	205	179	235	349	349	377	185	169	276	236	211	184	2955 (%10)
GROUP OF WIND DIRECTIONS													ANNUALLY SUMME
ENE, E, ESE	153	90	131	93	104	77	110	108	66	138	99	136	1305
WSW, W, WNW	205	179	235	349	349	377	185	169	276	236	211	184	2955
SE, SSE, S, SSW, SW	542	553	643	679	442	282	166	206	340	378	468	550	5249
NW, NNW, N, NNE, NE	1415	1385	1518	1215	1560	1736	2280	2223	1710	1568	1236	1330	19176

KAYNAK: Devlet Meteoroloji İşleri Gn. Md'ü lüğü 1975-2006 verilerinden derlenip, değerlendirilmiştir.

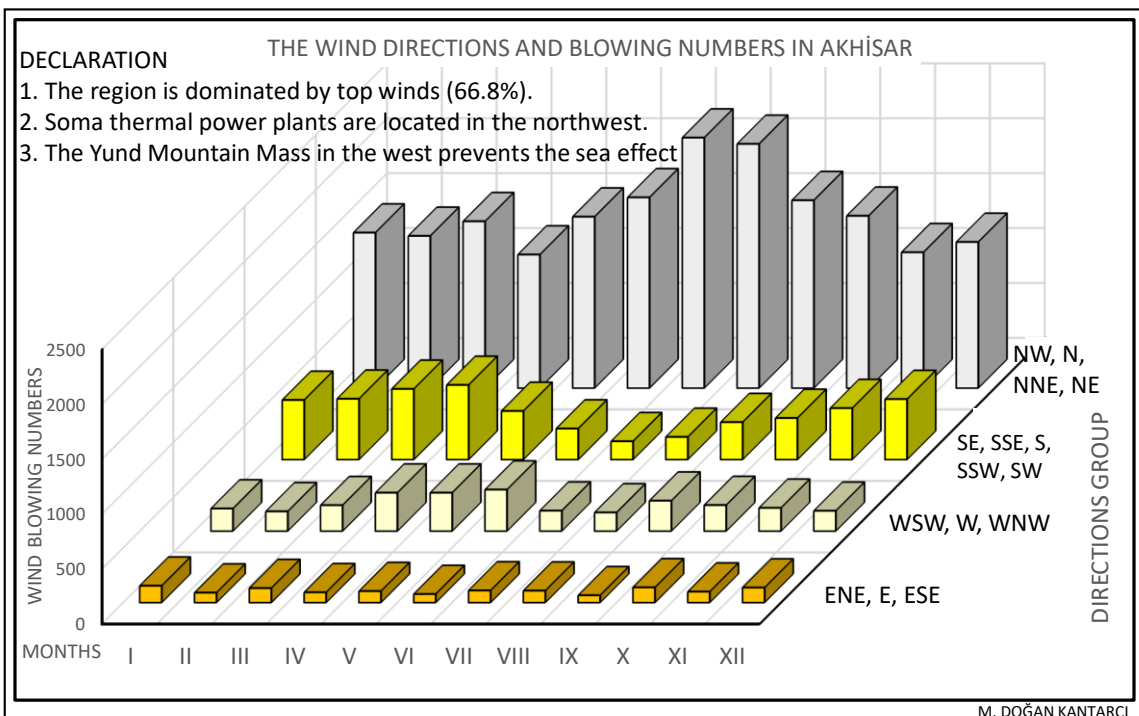


Figure 5. Comparison of Wind Blowing Numbers by Directions in Akhisar

4. The exhaust of thermal power plants in soma and the air pollution Akhisar environment

4.1. Sulfur dioxide (SO_2)

The combustible sulfur contained in the burned coal is discharged as exhaust gases in the form of sulfur dioxide (SO_2) into the air, and the non-combustible sulfur remains in the ash. In some thermal power plants exhaust gases are treated by fogging. In some thermal power plants, the resulting sulfur dioxide is retained by the addition of limestone powder to the coal by the fluidized bed process. Nevertheless, a significant amount of sulfur dioxide can be released from the chimney into the air. There are two forms of this exhaust.

First, the treatment plant of the thermal power plant is not enough. Or not enough works. Because the amount of electricity consumed by the treatment system is high.

The second; It comes from the mismanagement of thermal power plants. Coal power plants are kept hot at certain times of the day. However, they are activated during the hours in which the power consumption increases.

Because when commissioning the thermal power plant, a significant amount of ash and gas is discharged from the chimney. The electrostatic filters can only be operated when a certain (sufficient) current is generated. During the daytime, the natural gas power plant operates in Turkey. The coal power plants kept in hot (tow). In which hours the electricity demand rises during the day, the coal power plants are operated in normal function. The right management is to do the hydroelectric power plants in the hours of increased electricity demand or in the event of a thermal power plant failure.

The discharge of SO_2 from the 1 tonne of coal is shown in Table 3 and Figure 6 which was burned in Soma thermal power plants between 1990 and 2008. From the annual SO_2 release, average daily density (using the simple model described above) is calculated in Akhisar and surrounding area for 300 days (Table 3 and Figure 7). The destruction of SO_2 in chlorophyll cells in pine needles is shown in Figure 8.

4.2. Nitrogen oxides (NO_x and N_2O)

In coal-fired power plants, the combustion temperature is about 1000 °C. Nitrogen gas in the air from the temperature of 900 °C also begins to burn. Since the air contains 78% nitrogen and 21% oxygen, not all of the nitrogen can be oxidized as nitrogen dioxides. A part of the nitrogen gas is oxidized as dinitrogen monoxide (N_2O), a part as nitrogen monoxide (NO) and a part as nitrogen dioxide (NO_2). Dinitrogen monoxide takes up one atom of the oxygen molecule in the air and converts it into nitrogen monoxide, which takes up an atom of another oxygen molecule and converts it into nitrogen dioxide. In these reactions, the single remaining oxygen atom combines with an oxygen molecule to form ozone (O_3). Nitrogen dioxide is converted to nitrogen pentoxide by oxygen in ozone. Nitric oxide combines with moisture (H_2O) in the air to form nitric acid (HNO_3). Nitrogen pentoxide, like carbon dioxide (CO_2), is taken from plant leaves by the respiratory glands where it is converted into nitric acid and destroys chlorophyll. Humidity in the airways and lungs of humans and animals is converted to nitric acid and causes damage (Figure 8). The average concentration of nitrogen oxides for Akhisar and its environment is given in Table 4, 5 and Figure 9.

Table 3. The emitted Sulfur Dioxide (SO₂) from the burned Lignite In Soma (A) and (B) thermal Power Plants in the Period 1990-2008 and their Concentrations Around Akhisar

Table 3.1. Emission of Sulfur dioxide (SO ₂) into the atmosphere for a ton of lignite at Soma																			
FOR 1 TON COAL SO ₂	1990	1991	1992	1993	1994	1995	1996	1997	1998	1999	2000	2001	2002	2003	2004	2005	2006	2007	2008
SOMA(A) TPP SO ₂ kg/year	12611	12911	13664	13464	13792	13139	13847	13926	13015	13077	15103	14371	15764	12436	10997	19251	17294	11521	9223
SOMA(B) TPP SO ₂ kg/year	7756	7470	7532	7295	7248	7063	7023	7344	6763	6614	6979	9051	7437	10079	9799	6122	7843	12407	12692

Table 3.2. The amount of burned lignite in power plants Soma (A) and the emission of Sulfur dioxide (SO ₂)											
	1990	1991	1992	1993	1994	1995	1996	1997	1998	1999	
SOMA (A) TPP COAL (ton/year)	289223	304302	282063	267723	298446	300535	235346	306477	347661	314471	
SOMA (A) TPP SO ₂ (ton/year)	3647,45	3928,74	3853,97	3604,59	4116,30	3948,86	3258,73	4267,86	4524,69	4112,35	
	2000	2001	2002	2003	2004	2005	2006	2007	2008		
SOMA (A) TPP COAL (ton/year)	284726	274429	194372	144849	56292	61257	157051	244156	214839		
SOMA (A) TPP SO ₂ (ton/year)	4300,12	3943,72	3064,08	1801,39	619,05	1179,26	2715,96	2812,96	1981,41		

Table 3.3. The amount of burned lignite in power plants Soma (B) and the emission of Sulfur dioxide (SO ₂)											
	1990	1991	1992	1993	1994	1995	1996	1997	1998	1999	
SOMA (B) TPP COAL (ton/year)	3957604	4281854	6019591	6958061	7944968	6856834	7158269	8371305	8349451	9339762	
SOMA (B) TPP SO ₂ (ton/year)	30693,60	31986,64	45339,78	50760,96	57586,75	48432,43	50270,71	61482,74	56466,58	61776,07	
	2000	2001	2002	2003	2004	2005	2006	2007	2008		
SOMA (B) TPP COAL (ton/year)	8663775	7975692	7218844	4879890	4822340	5656580	4527445	5637674	6690066		
SOMA (B) TPP SO ₂ (ton/year)	60465,29	72188,44	53686,03	49186,79	47255,75	34627,01	35508,44	69947,84	84911,08		

Table 3.4. Total amount of burned lignite and emitting SO ₂ from the power plants Soma (A + B) and their density in the atmosphere around Akhisar environment. [Calculated as a flat rate for a trapezoidal area (10 + 30) / 2x40 km and an Air volume of 1 km depth.]											
SOMA (A+B) THERMAL POWER PLANT YEARS	1990	1991	1992	1993	1994	1995	1996	1997	1998	1999	
SOMA (A+B) TPP BURNED COAL (ton/year)	4246827	4586156	6301654	7225784	8243414	7157369	7393615	8677782	8697112	9654233	
SOMA (A+B) TPP TOTAL EMISSIONS SO ₂ (ton/year)	34341,05	35915,38	49193,75	54365,54	61703,05	52381,29	53529,44	65750,60	60991,27	65888,42	
SOMA (A+B) SO ₂ µg/m ³ /year	42926,31	44894,23	61492,19	67956,93	77128,82	65476,61	66911,79	82188,25	76239,09	82360,52	
SOMA (A+B) SO ₂ µg/m ³ /gün (for 300 days)	143,09	149,65	204,97	226,52	257,10	218,26	223,04	273,96	254,13	274,54	
SOMA (A+B) THERMAL POWER PLANT YEARS	2000	2001	2002	2003	2004	2005	2006	2007	2008		
SOMA (A+B) TPP BURNED COAL (ton/year)	8948501	8250121	7413216	5024739	4878632	5717837	4684496	5881830	6904905		
SOMA (A+B) TPP TOTAL EMISSIONS SO ₂ (ton/year)	64765,41	76132,16	56750,11	50988,17	47874,80	35806,27	38224,40	72760,80	86892,49		
SOMA (A+B) SO ₂ µg/m ³ /year	80956,76	95165,20	70937,63	63735,22	59843,50	44757,83	47780,50	90951,00	108615,62		
SOMA (A+B) SO ₂ µg/m ³ /gün (for 300 days)	269,86	317,22	236,46	212,45	199,48	149,19	159,27	303,17	362,05		

NOTICE: DRY REGIONS (such as Central Anatolia and Akhisar) AND COLD REGIONS (such as Sweden, Norway) LIMIT VALUE IS SO₂ 30 µg/m³/day
Literature: The values are compiled, calculated and arranged from TEAŞ exhaust measurements 1990-2008.

Declaration:
 Explanation: SO₂ dispersion volume in still air;
 Time of day (10 + 30) / 2 x 40 km = 800 km² and 1000 m depth (800 km³).
 The air is condensed the night after cooling and deposited in a thickness
 of about 100 m on the ground and the SO₂ density increases.

M. DOĞAN KANTARCI

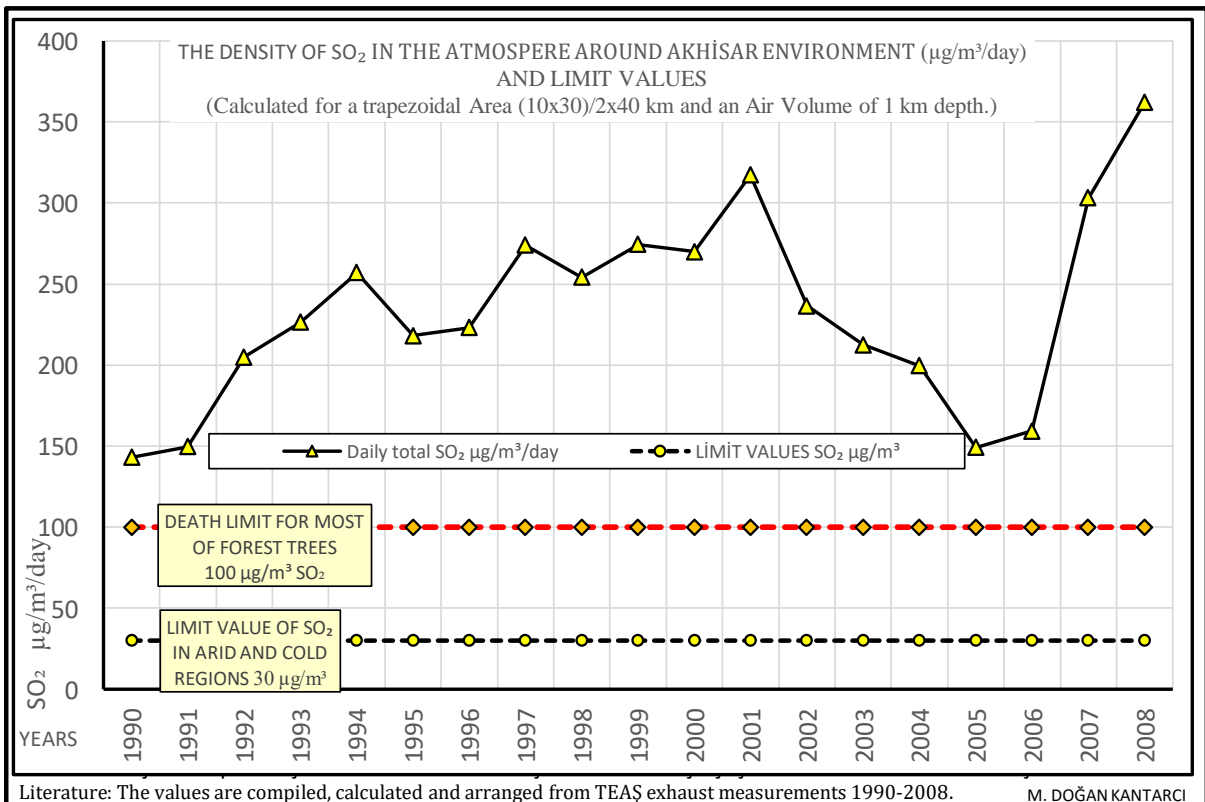
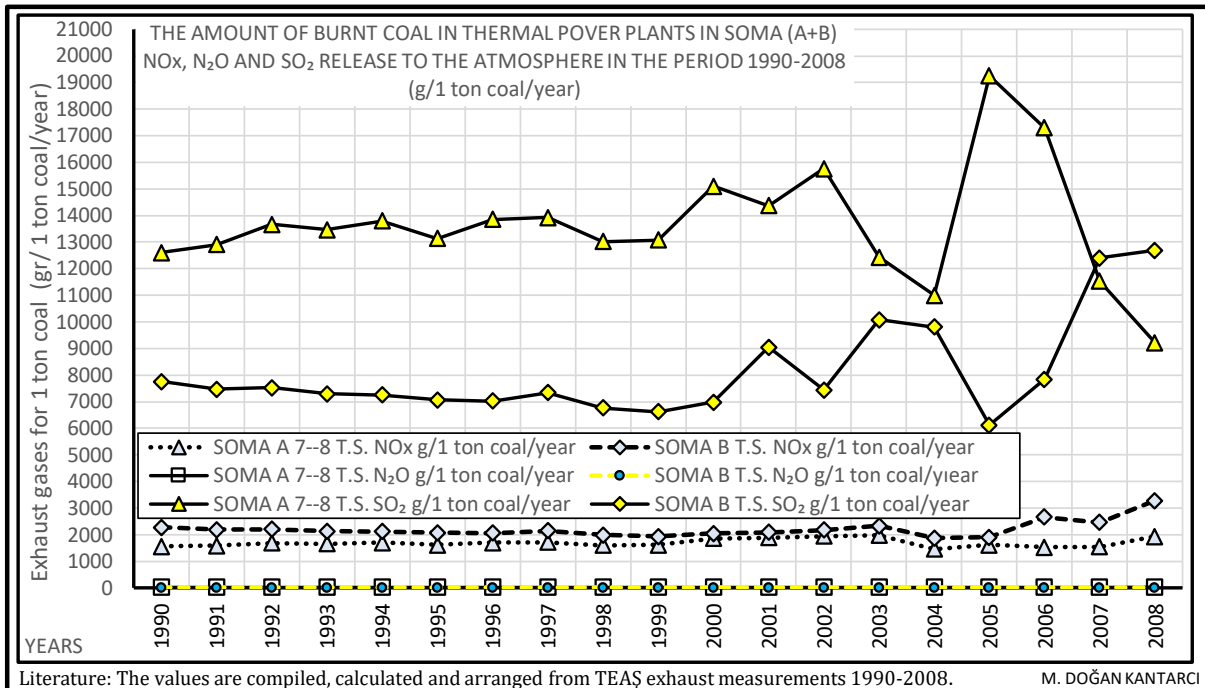


Figure 6. The waste gases from the chimney NO_x, N₂O and SO₂ from 1 ton lignite in Power Plants Soma A and B in the Period 1990 and 2008 (g/1 ton of coal/year)

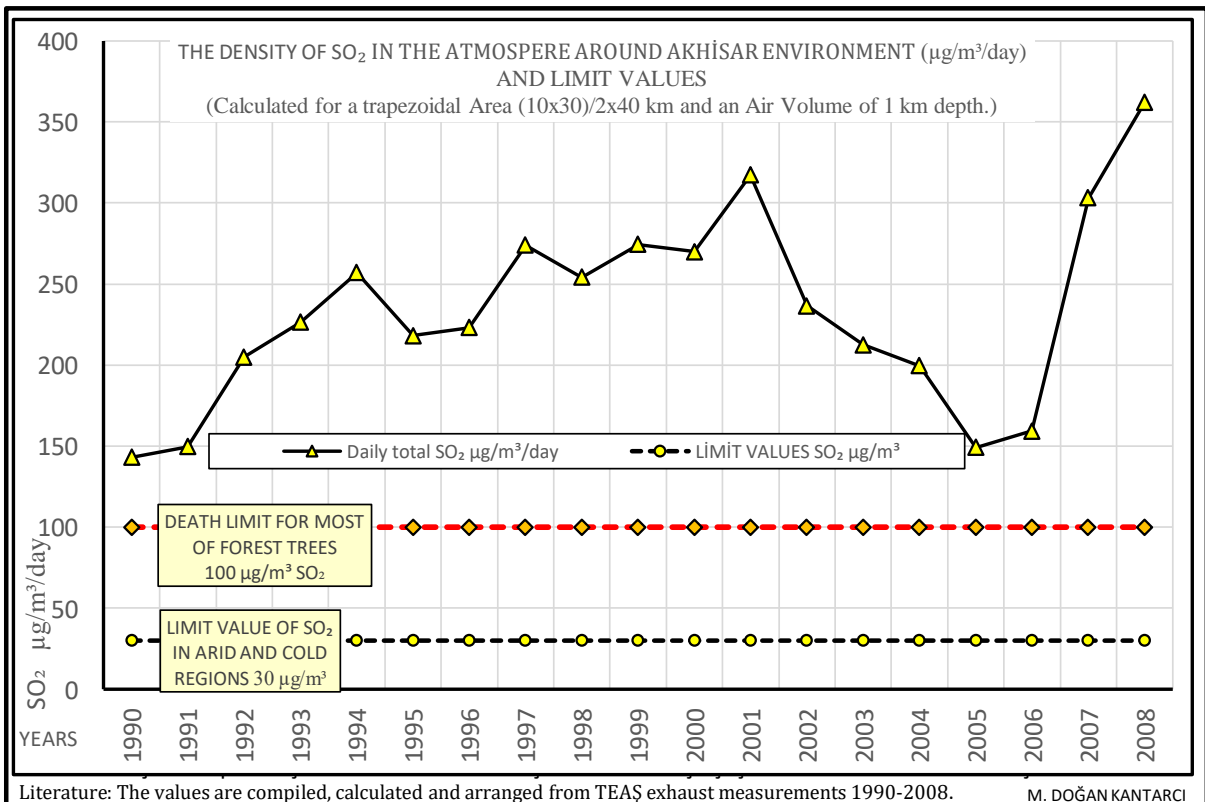
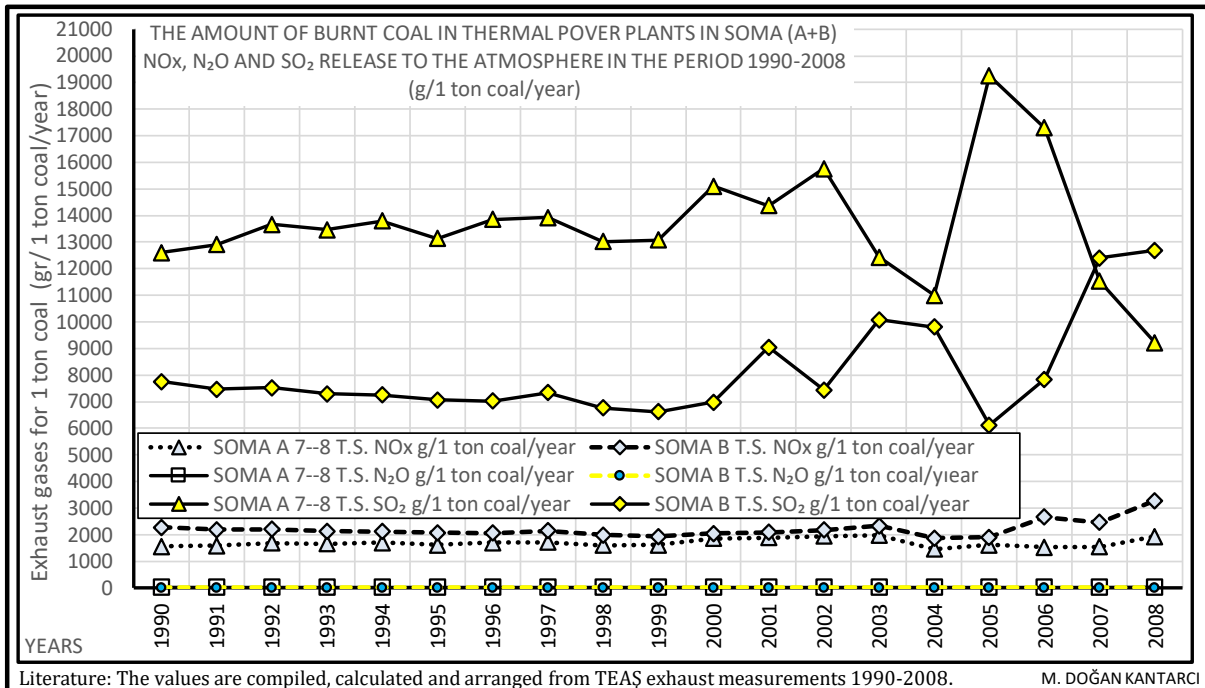
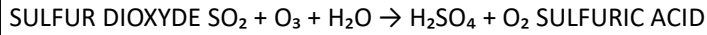


Figure 7. The emitted sulfur dioxide (SO₂) in Soma (A) and (B) thermal Power Plants in the Period 1990-2008 and their Concentrations around Akhisar.

TABLE 10.1. TRANSFORMATION OF SULFUR DIOXYDE TO SULFURIC ACID



NEEDLE AGE 1

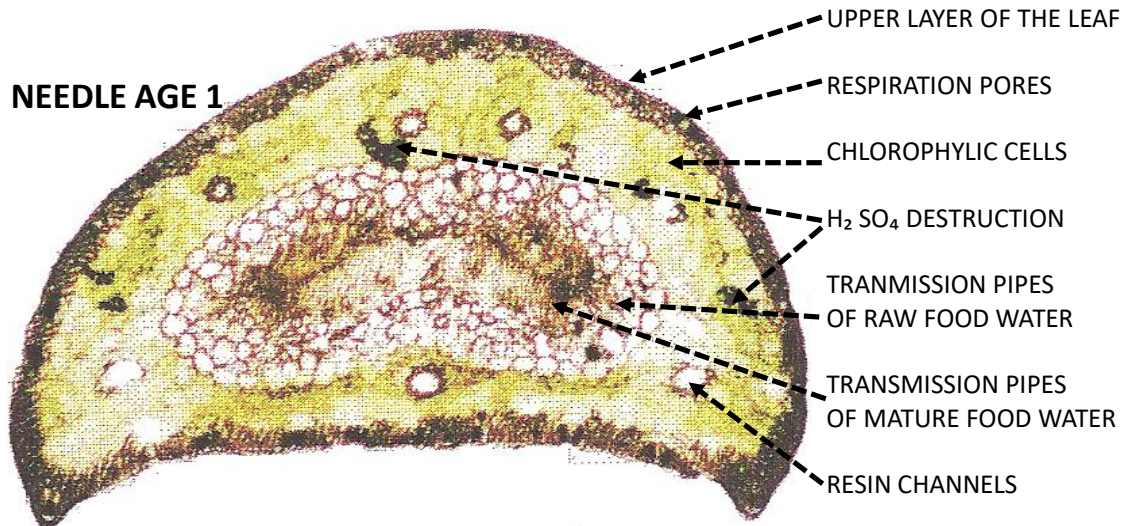


TABLE 10.2. TRANSFORMATION OF NITRIC OXIDES TO NITRIC ACID

DI NITROGEN MONOXIDE	$N_2O + O_2 \rightarrow 2NO + O$	NITROGEN MONOXIDE
NITROGEN MONOXIDE	$NO + O_2 \rightarrow NO_2 + O$	NITROGEN DIOXIDE
OXYGEN (atom)	$O + O_2 \rightarrow O_3$	OZON
NITROGEN DIOXIDE	$2NO_2 + O_3 \rightarrow N_2O_5$	NITROGEN PENTAOXIDE
NITROGEN PENTAOXIDE	$N_2O_5 + H_2O \rightarrow 2 HNO_3$	NITRIC ACID

NEEDLE AGE 3



SULFURIC ACID DESTROY THE CHLOROPHYLL CELL. THE CELL PHOTOSYNTHESIS IS NOT POSSIBLE, AND CARBOHYDRATE IS NOT PRODUCED. BECAUSE OF THE INSUFFICIENT NUTRIENT PRODUCTION, THE ANNUAL RING WIDTH OF THE TREE IS SMALL. LEAVES CAN NOT PRODUCE CARBOHYDRATES FOR RESPIRATION. LEAVES ARE DÏE.

Literature: Kantarci, M. D. 2011

M. DOĐAN KANTARCI

Figure 8. Impact of pine needles SO_2 and NO_x (at north northern slope of Kaz Mountains)

Table 4. The amount of burnt Coal in thermal Power Plants in Soma (A and B) and NO_x releas to the Atmosphere in the Period 1990-2008 and their Density in Akhisar Environment.

Table 4.1. Emission of nitrogen oxides (NO _x) into the atmosphere for a ton of lignite at Soma																			
FOR 1 TON COAL NO _x	1990	1991	1992	1993	1994	1995	1996	1997	1998	1999	2000	2001	2002	2003	2004	2005	2006	2007	2008
SOMA(A) TPP NO _x gr/year	1554	1591	1684	1659	1699	1619	1706	1716	1604	1611	1861	1880	1942	1978	1451	1619	1520	1535	1931
SOMA(B) TPP NO _x gr/year	2270	2186	2204	2135	2121	2067	2055	2149	1979	1936	2042	2087	2176	2326	1871	1905	2658	2455	3280

Table 4.2. The amount of burned lignite in power plants Soma (A) and the emission of nitrogen oxides (NO _x)											
	1990	1991	1992	1993	1994	1995	1996	1997	1998	1999	
SOMA (A) TPP COAL (ton/year)	289223	304302	282063	267723	298446	300535	235346	306477	347661	314471	
SOMA (A) TPP NO _x (ton/year)	449,41	484,07	474,86	444,13	507,18	486,55	401,52	525,86	557,50	506,70	
	2000	2001	2002	2003	2004	2005	2006	2007	2008		
SOMA (A) TPP COAL (ton/year)	284726	274429	194372	144849	56292	61257	157051	244156	214839		
SOMA (A) TPP NO _x (ton/year)	529,83	515,87	377,54	286,49	81,70	99,20	238,74	374,86	414,81		

Table 4.3. The amount of burned lignite in power plants Soma (B) and the emission of nitrogen oxides (NO _x)											
	1990	1991	1992	1993	1994	1995	1996	1997	1998	1999	
SOMA (B) TPP COAL (ton/year)	3957604	4281854	6019591	6958061	7944968	6856834	7158269	8371305	8349451	9339762	
SOMA (B) TPP NO _x (ton/year)	8982,65	9361,06	13268,93	14855,47	16853,07	14174,01	14711,99	17993,25	16525,25	18079,10	
	2000	2001	2002	2003	2004	2005	2006	2007	2008		
SOMA (B) TPP COAL (ton/year)	8663775	7975692	7218844	4879890	4822340	5656580	4527445	5637674	6690066		
SOMA (B) TPP NO _x (ton/year)	17695,49	16647,15	15711,50	11348,93	9023,94	10773,74	12033,24	13842,50	21943,54		

Table 4.4. Total amount of burned lignite and emitting NO_x from the power plants Soma (A + B) and their density in the atmosphere around Akhisar environment.
[Calculated as a flat rate for a trapezoidal area (10 + 30) / 2x40 km and an Air volume of 1 km depth.]

SOMA (A+B) THERMAL POWER PLANTS YEARS	1990	1991	1992	1993	1994	1995	1996	1997	1998	1999
SOMA (A+B) TPP Burned coal (ton/year)	4246827	4586156	6301654	7225784	8243414	7157369	7393615	8677782	8697112	9654233
SOMA (A+B) TPP Total emissions NO _x (ton/year)	9432,06	9845,13	13743,79	15299,60	17360,25	14660,56	15113,51	18519,11	17082,75	18585,79
SOMA (A+B) NO _x µg/m ³ /year	11790,07	12306,42	17179,74	19124,50	21700,32	18325,70	18891,89	23148,89	21353,44	23232,24
SOMA (A+B) NO _x µg/m ³ /day (for 300 day)	39,30	41,02	57,27	63,75	72,33	61,09	62,97	77,16	71,18	77,44
SOMA (A+B) TERMİK SANTRALI Years	2000	2001	2002	2003	2004	2005	2006	2007	2008	
SOMA (A+B) TPP Burned coal (ton/year)	8948501	8250121	7413216	5024739	4878632	5717837	4684496	5881830	6904905	
SOMA (A+B) TPP Total emissions NO _x (ton/yıl)	18225,32	17163,02	16089,04	11635,42	9105,64	10872,94	12271,99	14217,36	22648,46	
SOMA (A+B) NO _x µg/m ³ /year	22781,65	21453,77	20111,30	14544,27	11382,05	13591,18	15339,98	17771,70	28310,58	
SOMA (A+B) NO _x µg/m ³ /day (for 300 day)	75,94	71,51	67,04	48,48	37,94	45,30	51,13	59,24	94,37	

EUROPEAN UNION NO_x limit is 30 mg/m³/day

Literature: The values are compiled, calculated and arranged from TEAŞ exhaust measurements 1990-2008.

Declaration: NO_x and N₂O dispersion volume in still air;
 Explanation: NO_x and N₂O dispersion volume in still air;
 Time of day (10 + 30) / 2 x 40 km = 800 km² and 1000 m depth (800 km³).
 The air is condensed the night after cooling and deposited in a thickness
 of about 100 m on the ground and the NO_x density increases.

Table 5. The amount of burnt Coal in thermal Power Plants in Soma (A and B) and N₂O release to the Atmosphere in the Period 1990-2008 and their Density in Akhisar Environment.

Table 3.1. Emission of dinitrogen oxides (N ₂ O) into the atmosphere for a ton of lignite at Som																			
FOR 1 TON COAL N ₂ O	1990	1991	1992	1993	1994	1995	1996	1997	1998	1999	2000	2001	2002	2003	2004	2005	2006	2007	2008
SOMA (A) TPP N ₂ O kg/year	17,77	18,20	19,26	18,97	19,44	18,52	19,51	19,63	18,34	18,43	21,28	21,50	22,22	22,32	19,00	21,20	21,64	20,97	22,71
SOMA (B) TPP N ₂ O kg/year	12,27	11,82	11,92	11,54	11,47	11,17	11,11	11,62	10,70	10,46	11,04	11,28	11,76	12,42	11,74	11,24	11,07	12,12	12,70

Table 5.2. The amount of burned lignite in power plants Soma (A) and the emission of dinitrogen oxides (N ₂ O)											
	1990	1991	1992	1993	1994	1995	1996	1997	1998	1999	
SOMA (A) TPP COAL (ton/year)	289223	304302	282063	267723	298446	300535	235346	306477	347661	314471	
SOMA (A) TPP N ₂ O (ton/year)	5,140	5,537	5,431	5,080	5,801	5,565	4,593	6,015	6,377	5,796	
	2000	2001	2002	2003	2004	2005	2006	2007	2008		
SOMA (A) TPP (ton/year)	284726	274429	194372	144849	56292	61257	157051	244156	214839		
SOMA (A) TPP N ₂ O (ton/year)	6,060	5,901	4,318	3,232	1,069	1,299	3,399	5,119	4,878		

Table 5.3. The amount of burned lignite in power plants Soma (B) and the emission of dinitrogen oxides (N ₂ O)											
	1990	1991	1992	1993	1994	1995	1996	1997	1998	1999	
SOMA (B) TPP COAL (ton/year)	3957604	4281854	6019591	6958061	7944968	6856834	7158269	8371305	8349451	9339762	
SOMA (B) TPP N ₂ O (ton/year)	48,555	50,600	71,724	80,300	91,098	76,616	79,524	97,261	89,326	97,725	
	2000	2001	2002	2003	2004	2005	2006	2007	2008		
SOMA (B) TPP COAL (ton/year)	8663775	7975692	7218844	4879890	4822340	5656580	4527445	5637674	6690066		
SOMA (B) TPP N ₂ O (ton/year)	95,651	89,985	84,927	60,585	56,600	63,579	50,125	68,325	84,986		

Table 5.4. Total amount of burned lignite and emitting N ₂ O from the power plants Soma (A + B) and their density in the atmosphere around Akhisar environment. [Calculated as a flat rate for a trapezoidal area (10 + 30) / 2x40 km and an Air volume of 1 km depth.]											
SOMA (A+B) THERMAL POWER PLANT YEARS	1990	1991	1992	1993	1994	1995	1996	1997	1998	1999	
SOMA (A+B) TPP BURNET COAL (ton/year)	4246827	4586156	6301654	7225784	8243414	7157369	7393615	8677782	8697112	9654233	
SOMA (A+B) TPP Total emissions N ₂ O (ton/year)	53,70	56,14	77,16	85,38	96,90	82,18	84,12	103,28	95,70	103,52	
SOMA (A+B) N ₂ O µg/m ³ /year	67,12	70,17	96,44	106,72	121,12	102,73	105,15	129,09	119,63	129,40	
SOMA (A+B) N ₂ O µg/m ³ /day (for 300 days)	0,22	0,23	0,32	0,36	0,40	0,34	0,35	0,43	0,40	0,43	
SOMA (A+B) THERMAL POWER PLANT YEARS	2000	2001	2002	2003	2004	2005	2006	2007	2008		
SOMA (A+B) TPP BURNET COAL (ton/year)	8948501	8250121	7413216	5024739	4878632	5717837	4684496	5881830	6904905		
SOMA (A+B) TPP Total emissions N ₂ O (ton/year)	101,71	95,89	89,25	63,82	57,67	64,88	53,52	73,44	89,86		
SOMA (A+B) N ₂ O µg/m ³ /year	127,14	119,86	111,56	79,77	72,09	81,10	66,90	91,80	112,33		
SOMA (A+B) N ₂ O µg/m ³ /day (for 300 days)	0,42	0,40	0,37	0,27	0,24	0,27	0,22	0,31	0,37		

Literature: The values are compiled, calculated and arranged from TEAŞ exhaust measurements 1990-2008.

Declaration:
Explanation: NO_x and N₂O dispersion volume in still air;
Time of day (10 + 30) / 2 x 40 km = 800 km² and 1000 m depth (800 km³).
The air is condensed the night after cooling and deposited in a thickness of about 100 m on the ground and the NO_x density increases.

M. DOĞAN KANTARCI

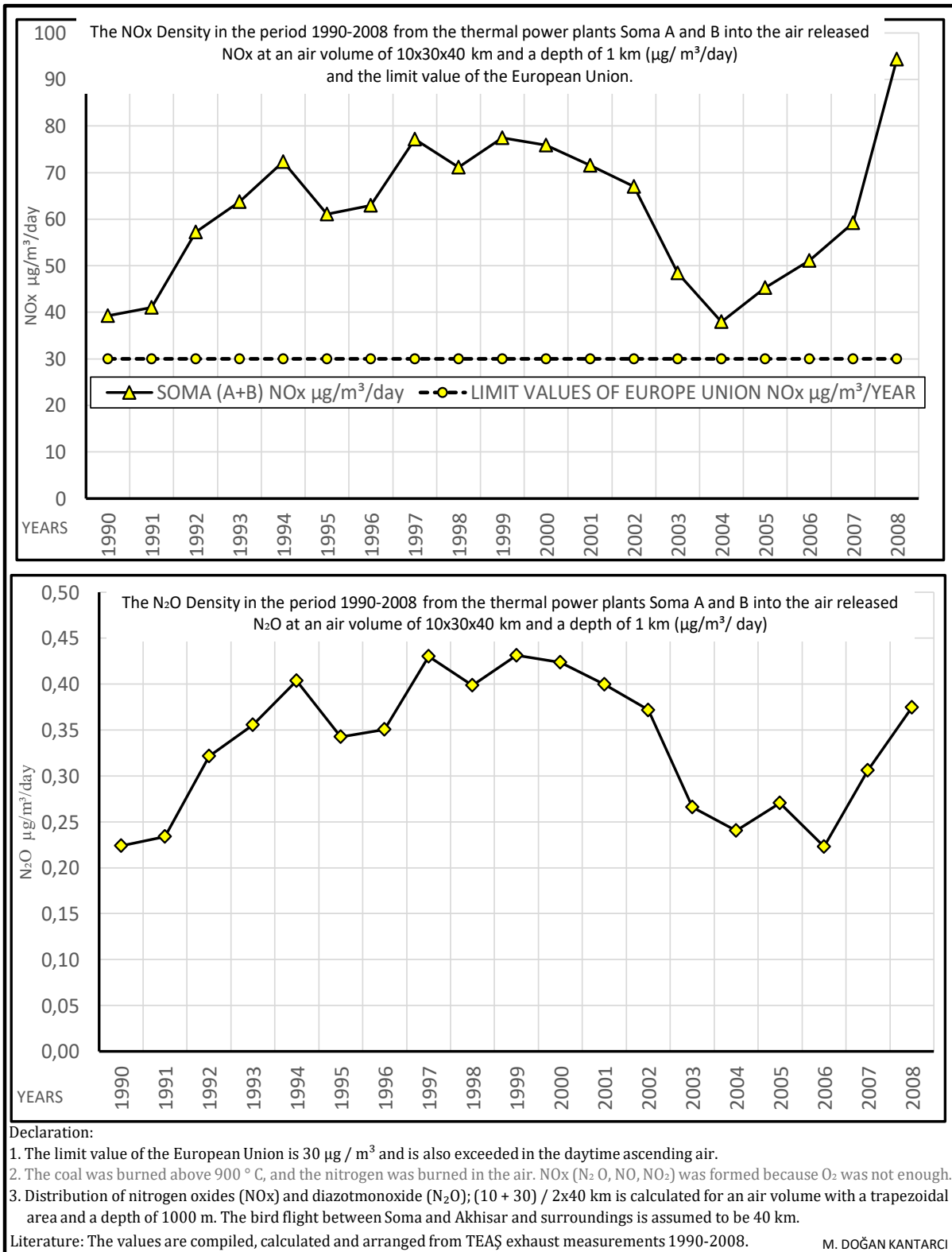


Figure 9. The amount of burnt Coal in thermal Power Plants in Soma (A and B) NO_x and N₂O release to the Atmosphere in the Period 1990-2008 and their density in Akhisar Environment

5. Ash and dust problem

Ash is discharged from the thermal power plant chimneys. During the operation of the power plants, very small diameters particulates ($<PM_{10}$ and $<PM_{2.5}$) escape through the electrostatic filters. These grains contain a significant amount of heavy metals. When the thermal power plants are put into operation, which are kept in stand-by (kept warm), a considerable amount of ash is thrown out of the chimney, since electrostatic filters can not be operated. In addition, significant amounts of dust from the coal, ash and limestone storage areas surrounding the thermal power plant, the operating areas of the open pit mines and the roads that connect those areas to the storage areas are removed and transported by wind. In addition to ash and dust carried by Soma thermal power plants in Akhisar and its surroundings, dust from the open quarry mining is also spreading.

As a very typical example; the dust that had accumulated in the leaves of the olive trees in Karacahisar and in the flue ash of the thermal power plant Yenikoy. It was placed in the water by shaking the leaves. The turbidity of the washed water suggests an accumulation of dust and ash on the leaves (Figure 10). Dust and sulfur dioxide (SO_2) have a dryer effects of the leaves and generative organs of plants.



Figure 10. Shaking water from olive leaves (From left to right the same olive leaves flushed by water 5 times.)

6. Conclusion

As a result;

- (1) Akhisar land is defined by a plain which is opens to the south, and surrounded by mountainous through western, northern and eastern directions (Map 1).
- (2) According to the measurements of the Akhisar Meteorological Station; the average annual temperatures were calculated as $15.7^{\circ}C$ between 1970 and 1981, increased to $17.1^{\circ}C$ over the period 2007-2017, and the reflection of this increase in summer months is between 1.5 and $2.9^{\circ}C$. On the other hand, the total annual precipitation amount was 616.3 mm between 1970 and 1982, while it was

557.6 mm between 2007 and 2017. The difference is -58.8 mm. High precipitation is generally determined to be 40-60 mm / day.

(3) The increase in temperature and the decrease in precipitation caused the humidity to fall between 20 and 30% at 14 o'clock in the summer months. The fact that the humidity in the summer at 7 o'clock in the morning between 50 and 65%, indicates a serious lack of water.

(4) The winds are much stronger from the north. The northern winds coming from the land are dry. Yund Mountain Mass to the west prevents the wet west winds from coming over the sea.

(5) Akhisar and its surroundings consume more groundwater due to these climatic characteristics and the effect of the heating / drought process. For this reason, in the land composed of limestones and marbles that leak rainwater and reach to groundwater; quarries mining, explosions, etc. operations are objectionable.

(6) The Soma thermal power plants, which are 40 km northwest of Akhisar and vicinity by airline, flue gases (SO₂, NO_x and N₂O) are transported by the northern winds and are considered to important air pollution in Akhisar. In addition, dust and ash emissions from thermal power plants, and withall dust from quarries, surface mining and truck transports on dirt roads cause a remarkable air pollution.

7. References

Avcı, M., Kantarcı, M.D., 2018. Güneybatı Anadolu'da (Muğla) açık kömür ocakları ve termik santrallardan atmosfere salınan tozların arıcılık ve zeytinciliğe etkileri üzerine ekolojik bir değerlendirme. 6. Uluslararası Muğla Arıcılık ve Çam Balı Kongresi (6th International Muğla Beekeeping and Honey Congress) 15-19.10.2018.

Devlet Meteoroloji İşleri Genel Müdürlüğü, Meteorolojik ölçmeler 1970-2017.

Güner, B., Boyraz, Z., Çitçi, M.D. 2010. Tütüncülükten zeytinciliğe geçiş. Karasaban 29.7.2019.

Hoşgören, Y. 1983; Akhisar Havzası-Jeomorfolojik ve Tatbiki Jeomorfolojik Etüt. İstanbul: İstanbul Üniv. Edebiyat Fak. Yayınları No: 3088.

Kantarcı, M.D., 2011. Vertical climate zones in Biga peninsula: The impact of climate change and air pollution on forests, *Procedia Social and Behavioral Sciences* 19 (2011) 797–810; Published by Elsevier Ltd. Selection and/or peer-review under responsibility of The 2nd International Geography Symposium-Mediterranean Environment doi:10.1016/j. sbspro. 2011.05.198.

Kantarcı, M. D., 2018. Güneybatı Anadolu'da üç termik santralin atmosfere saldığı kül+toz ile SO₂, NO_x gazları ve ekolojik etkileri üzerine bir değerlendirme. 6. Uluslararası Muğla Arıcılık ve Çam Balı Kongresi (6th International Muğla Beekeeping and Honey Congress) 15-19.10.2018.

Kayalı, A. C., Tokmakoğlu, U., Sesli, M., Kayalı, N.T., 2008. Development Potential of Olive Production Establishments in Akhisar-Manisa-Turkey. *Asian Journal of Scientific Research*, 1 (2), s. 103-112. <http://docsdrive.com/pdfs/ansinet/ajs/2008/103-112.pdf> (E.T: 01.02.2010).

MTA Gnl. Md'lüğü 1964; Türkiye Jeoloji Haritası (1/500 000) İzmir Paftası.

Source apportionment of fine particles simultaneously sampled at rural area versus urban area using receptor model application

Orhan Sevimoglu¹ and Wolfgang F. Rogge²

¹Gebze Technical University, Faculty of Engineering, Department of Environmental Engineering, Gebze, Kocaeli, Turkey.

²School of Engineering & Sierra Nevada Research Institute, University of California Merced (UCM), 5200 N. Lake Road, Merced, CA 95343, USA.

sevimoglu@gtu.edu.tr

Abstract. Inhalable fine particles cause health problems to population in urban area as well as in rural area that should be considered together to improve the air quality. The aim of this study is to use the data set of the trace organic concentrations for the collected ambient PM together with published fine particle source profiles in order to forecast the influences of major sources to the overall atmospheric fine particle in urban area (Delray Beach) and rural area (Belle Glade) in Palm Beach County, Florida, USA. The Chemical Mass Balance 8.2 (CMB8.2) software program was used to calculate the source apportionment from the particle emission sources by utilizing identified trace organic and metal compound concentrations. The sugarcane burning emissions were detected in both sampling sites in January. The urban site, neighboring the agricultural area, was affected during sugarcane foliage burning, due to the fact that the airborne particles were transported from rural site to the urban site. In May, there was only vegetative burning emission was detected in the agricultural area. The model results represented the fine particles sources as follows: road dust, sugarcane leaf burning, diesel and gasoline-powered vehicle exhaust, leaf surface abrasion particles, and a minor portion of meat cooking particles.

Keywords: Source apportionment, Trace organic compounds, Modelling, CMB8.2.

1. Introduction

Ambient aerosols cause many adverse negative environmental effects on human health (Dockery et al., 1993), climate change (Ramanathan and Feng, 2009), and reducing visibility (Eldering and Cass, 1996). Besides, ambient fine particles can be carried to remote distances. Therefore, the relative contributions from diverse natural and anthropogenic fine particle sources to ambient airborne particles on both the local and regional scales that should be extremely important to better understand the level of air quality (Motallebi et al., 2003). The conditions of meteorology can influence on contribution of the potential sources to the overall PM₁₀, causing the same location to experience different aerosol chemical compositions based upon the time of year. The relative contribution of different PM sources to ambient air should be considered by the policy makers in order to set applicable regulations that will allow these regions to achieve compliance. Therefore, elevated fine PM is considered an environmental concern in urban areas as well in rural areas (Sevimoglu and Rogge, 2016).

Respirable particulate matter is released from primary sources and as well formed from gaseous precursor via the mechanism of the volatile compounds to particle matter conversion in the atmosphere. Primary particulate matter is formed by contribution of both anthropogenic sources (fossil fuels burning,



waste and agricultural burning, vehicular emissions, wood burning for space heating, food cooking, and from numerous industrial activities) and natural sources (wind-blown dust, pollen, plant leaf surface abrasion and vegetation, wild fires) (Kalaitzoglou et al., 2004). So, the ambient particulate matter consists of hundreds to thousands of organic and inorganic compounds.

Nowadays, the available source apportionment (receptor) models are broadly used in the studies of air pollution. A calculation of receptor modeling pursues to find the best-fit linear combination of the chemical compositions of the discharges from particular emission sources that is needed to reconstruct the chemical composition of measured atmospheric concentrations of organic compounds and elements associated with airborne particulate matter at a site of interest (EPA, 2004; Schauer et al., 1996). Based on mass conservation law, the Chemical Mass Balance (CMB) receptor model was applied for organic trace compounds to Los Angeles area (Rogge et al., 1996), and subsequently to other areas, including San Joaquin Valley in California (Schauer and Cass, 2000) using source profiles generated by Rogge and colleagues (Rogge et al., 2007).

The Palm Beach County of Florida has the typical anthropogenic and biogenic emission sources, substantial seasonal agricultural burning activities (Gilbert et al., 2006). The pre-harvest foliage burning of sugarcane (*Saccharum officinarum*) is considered as a major PM source in the agricultural-rural area (Allen et al., 2004). Unfortunately, little information is known about the local rural (Belle Glade) and urban (Delray Beach) exposure levels to particulate matter released from pre-harvest sugarcane foliage burning. Therefore, the aim of this study is to determine the influence of major sources to the ambient particle burden at Belle Glade (near sugarcane field in the rural site) and Delray Beach (urban site) by using the CMB8.2 model.

2. Material and methods

2.1. Sampling area and sampling method

The sampling area and sampling method were explained in previous publication in detail (Sevimoglu and Rogge, 2016; Sevimoglu and Rogge, 2015). Palm Beach County is located along the southeast of Florida. The county area is 6181 km² and the population was about one million people in 2000s at the time of the project. The county has a large agricultural area with 10% the population and an urban area along the coastline in which about 90% of the population lives.

Figure 1 shows the sampling locations where are Belle Glade in rural site and Delray Beach in urban site in Palm Beach County. The city of Delray Beach is located in coastal urban area under the influence from both urban and industrial sources. The county includes the major industries that are electric power production, construction, aircraft testing, computer and electronics manufacturing, waste incineration, concrete and asphalt production. The size-segregated PM₁₀ samplers were located at the South County Government Center in Delray Beach, (latitude, 26.455174°; longitude, -80.092155°).

The rural area is located in the western part of Palm Beach County where an agricultural area is used based on the planting of sugarcane and winter vegetables. Sugarcane is the most important agricultural product in Florida. With more than 1800 km², the largest sugarcane producing industry in the United States is located within Palm Beach County and bordering counties. The sugarcane foliage is burned just before harvesting to reduce the quantity of sugarcane plant to be better controlled during the harvesting process (Sevimoglu and Rogge, 2015). The city of Belle Glade is located in a rural area in the middle of the Everglades Agricultural Area, where is periodically influenced by agricultural activities, especially pre-harvest sugarcane burning. Belle Glade is located near the southern shore of Lake Okeechobee which is the second largest fresh water lake in the United States. As a rule, the harvest season begins in the middle of October and is completed in the end of March, running nearly 150 days (Gilbert et al., 2006). The pre-harvest sugarcane burning season is considered for the months of

December, January, February, and March to evaluate harvesting season air quality in both sampling sites.

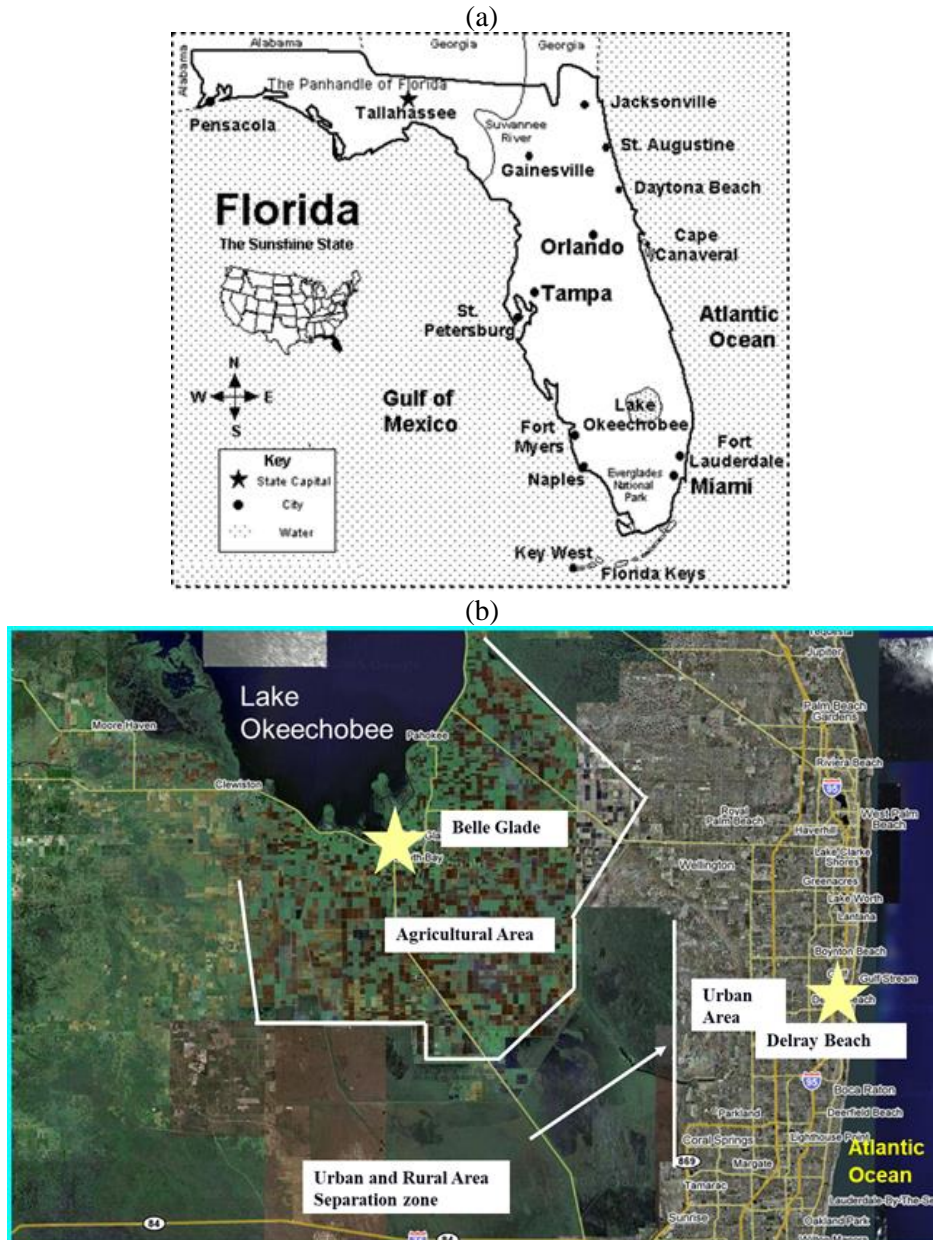


Figure 1. (a) The map of State of Florida (b) Ambient air sampling sites: Belle Glade represents rural area; Delray Beach represents urban area, in Palm Beach County

The rest of the months in a year are considered as sugarcane growing season. Pre-harvest sugarcane burning is directed by endorsement of the Florida Division of Forestry. Each selected field is independently permitted for burning on a daily basis between 9 a.m. and one hour before sunset. Permits are only issued when climatic conditions allow. Wind speed and wind direction are primary considerations for the transporting of fine particles. The growing agricultural area is separated into regions with tighter restrictions closer to the urban area to avoid ash deposition in the urban communities. Also, a wide-ranging air monitoring system operated by EPA and the Department of Environmental Protection (DEP), exists throughout the growing region to assure that all air quality

standards are met. The high volume PM₁₀ sampler of the rural area loaded with cascade impactor was placed at Belle Glade Civic Center (latitude, 26.692699°; longitude, -80.670927°).

The size segregated PM₁₀ sampling were conducted at both sampling sites simultaneously for 24-h and each sampling starting at midnight during January and May for organic compound analysis. The sampling procedure was explained in the previous publication in detail (Sornpoon et al., 2014).

2.2. Chemical mass balance model

The CMB8.2 air quality model is one of several receptor models that have been applied to air resources management. It is a 32-bit (Windows® 9x and higher) version software that substantially facilitates the estimation of source contributions to speciated PM₁₀, PM_{2.5} (EPA, 2004). In this study, the CMB8.2 model was used to determine source contribution to estimate PM₃ in Palm Beach County for the urban area and the rural area. The model helps to estimate the amount of each source that collectively elucidates the chemical composition of the ambient particle sample.

The CMB model uses the mass concentration of each chemical species in the ambient aerosol, which is assumed to be linear combination of the emissions of those species from individual sources. Therefore, source emission profiles are an essential part of these models. The basic equation used in these models is shown below:

$$c_{ik} = \sum_{j=1}^m a_{ij} f_{ijk} s_{jk}$$

Where c_{ik} is the mass fraction of chemical species i in ambient sample k , a_{ij} is the mass fraction of chemical species i in the emissions of sources j , f_{ijk} is the fractionation coefficient for species i as it travels from source j to ambient location k , s_{jk} is the mass fraction of ambient sample k that is due to all of the chemical species in emissions of source j , i.e., the fraction of the ambient sample mass that is contributed by sources j (Calhoun et al., 2003).

2.3. Data set

The CMB8.2 model was applied by using the atmospheric particulate data collected from Palm Beach County in 1997. The model helped estimate the amount of each source that collectively explains the chemical composition of the ambient sample. The compounds used in CMB8.2 were selected from the organic data set as shown in Table 1, which is the only data set for this region (Sevimoglu, 2007). The selected organic compounds and groups are representing the concentrations with standard deviations in PM₃ as following; n-Alkanes, Alkanoic Acids, Alkenoic Acids, Hopenes, PAHs, oxy-PAHs, Steroids (Cholesterol), sugar (Levogluconan).

The concentrations of Coronene, Cholesterol and Levogluconan were reported as below detection limit for the sampling sites and the sampling months in Table 1. Therefore, their concentrations were added to the calculation table as zero in order to run the program.

The CMB model used seven published different source profiles, which are accounted for major particulate matter sources in Palm Beach County as follow: gasoline-powered vehicle exhaust (Fraser et al., 1998), diesel-powered vehicle exhaust (Schauer et al., 1999), paved road dust (Rogge et al., 1993), meat charbroiling (Schauer et al., 1999), leaf surface abrasion (Rogge et al., 1993), tire dust (Rogge et al., 1993), sugarcane leaf burning (Oros et al., 2000). Each source profile used in the model contains different proportion of organic compounds as shown in Figure 2. The source profile is removed from the calculation if the compound concentration is not recorded in the ambient particle measurement. All mentioned particulate source profiles were used in CMB model application except the sugarcane source profile was not selected in calculation in May for Delray Beach because there was no Levogluconan measured.



3. Results and discussion

In the model application, selected 31 organic compounds including trace element, which is aluminum, were used representing the sources in the study area. The model produced modelled ambient concentrations for the selected compounds.

The modeled and measured ambient concentrations of each species were shown in Figure 3 and Figure 4 in January and May in Palm Beach County. Some compounds are very fit with measured and calculated values such as Aluminum, Hexadecanoic Acid.

The compounds 9, 10-Anthracenedione, Coronene, 7H-Benz[de]anthracen-7-one were measured in January in both sampling sites. However, the modeling did not give any result due to the proportion of selected source profile was very low for the model calculation.

Although Coronene was detected in the rural and urban sites in January, it was excluded in the model calculation in May. Cholesterol was only detected in the urban site Cholesterol not only derives from meat charbroiling but also meat fraying and zooplanktons on sea salt particles. The variation in between measured and calculated values is because of the only meat charbroiling source profiles used in the modeling. Levoglucosan represents biomass burning which is mainly from sugarcane leaf burning during the pre-harvest. There is no Levoglucosan measured in May in Delray Beach.

The calculation results are given in Table 2 with the standard error. The highest fine particle contribution was from road dust particles. Although sugarcane burning was also other important fine particle contributor during sugarcane burning period in the rural site in January, the model result shows that urban area biomass fine particle contribution was higher than rural site due to fine particles from sugarcane burning.

Table 1. Concentrations of organic compounds for use in receptor model

	Belle Glade January	Belle Glade May	Delray Beach January	Delray Beach May
<i>n-Alkanes</i>				
Tricosane	0,7989 ± 0,0253	0,6168 ± 0,0391	0,6390 ± 0,0202	0,8644 ± 0,0549
Tetracosane	0,8747 ± 0,0286	0,6584 ± 0,0298	0,5988 ± 0,0196	0,7597 ± 0,0343
Pentacosane	1,1456 ± 0,0483	1,1970 ± 0,0710	1,0052 ± 0,0424	1,0222 ± 0,0606
Hexacosane	0,9873 ± 0,0402	0,2890 ± 0,0195	0,8689 ± 0,0354	0,3055 ± 0,0206
Heptacosane	0,9743 ± 0,0585	0,4214 ± 0,0282	0,7343 ± 0,0441	0,3909 ± 0,0262
Octacosane	0,6787 ± 0,0299	0,2700 ± 0,0244	0,5479 ± 0,0241	0,2448 ± 0,0221
Nonacosane	1,2103 ± 0,0621	0,6146 ± 0,0371	0,8132 ± 0,0417	0,4557 ± 0,0275
Triacontane	0,4307 ± 0,0274	0,1620 ± 0,0134	0,3092 ± 0,0196	0,1006 ± 0,0083
Heneltriacontane	1,0310 ± 0,0575	0,4401 ± 0,0323	0,6086 ± 0,0340	0,3295 ± 0,0242
Dotriacontane	0,2442 ± 0,0182	0,1147 ± 0,0083	0,1576 ± 0,0118	0,0778 ± 0,0056
Tritriacontane	0,5602 ± 0,0323	0,1831 ± 0,0135	0,2869 ± 0,0165	0,1529 ± 0,0112
<i>n-Alkanoic Acids</i>				
Hexadecanoic Acid	8,6324 ± 0,1190	9,7586 ± 0,0740	11,0888 ± 0,1528	7,5701 ± 0,0574
Octadecanoic Acid	5,4761 ± 0,1395	4,0911 ± 0,0957	6,3715 ± 0,1623	3,3677 ± 0,0788
Hexacosanoic Acid	4,1144 ± 0,2396	3,5260 ± 0,1522	2,8751 ± 0,1674	2,0979 ± 0,0906
Octacosanoic Acid	5,4695 ± 0,3309	1,8455 ± 0,1180	2,4061 ± 0,1456	0,6976 ± 0,0446
Triacontanoic Acid	3,2993 ± 0,3766	1,8461 ± 0,1217	1,6246 ± 0,1855	0,7809 ± 0,0515
Dotriacontanoic Acid	1,5585 ± 0,1870	1,0445 ± 0,0989	1,0032 ± 0,1204	0,2990 ± 0,0283
<i>n-Alkenoic Acids</i>				
9-Octadecenoic Acid	0,2266 ± 0,0105	0,1493 ± 0,0115	0,4207 ± 0,0195	0,1094 ± 0,0084
<i>Hopanes</i>				
22,29,30-trisnonehopane	0,3803 ± 0,0245	0,1163 ± 0,0119	0,2505 ± 0,0161	0,2261 ± 0,0231
17a(H),21b(H)-hopane	1,5593 ± 0,0845	0,3330 ± 0,0158	0,8089 ± 0,0438	0,3841 ± 0,0182
22S-17a(H),21b(H)-30-homohopane	2,0100 ± 0,1329	0,3757 ± 0,0264	0,7017 ± 0,0464	0,7102 ± 0,0498
<i>PAH</i>				
Benzo[K] & [B]fluoranthene	0,8934 ± 0,0649	0,0647 ± 0,0049	0,3370 ± 0,0245	0,1886 ± 0,0142
Benzo[E]pyrene	0,7411 ± 0,0489	0,0317 ± 0,0016	0,1723 ± 0,0114	0,0471 ± 0,0024
Indeno[1,2,3-CD]pyrene	0,2770 ± 0,0188	0,0055 ± 0,0005	0,0362 ± 0,0025	0,0104 ± 0,0009
Benzo[ghi]perylene	1,4100 ± 0,0770	0,0333 ± 0,0031	0,3186 ± 0,0174	0,0450 ± 0,0041
Coronene	0,2396 ± 0,0133	0,0000 ± 0,0000	0,1205 ± 0,0067	0,0000 ± 0,0000
<i>Oxy-PAH</i>				
9,10-Anthracenedione	0,4267 ± 0,0224	0,0624 ± 0,0025	0,1629 ± 0,0086	2,1967 ± 0,0883
7H-Benz[de]anthracen-7-one	0,1752 ± 0,0090	0,0121 ± 0,0010	0,0434 ± 0,0022	0,0235 ± 0,0020
<i>Steroids</i>				
Cholesterol	0,0000 ± 0,0000	0,0000 ± 0,0000	0,4370 ± 0,0397	0,1027 ± 0,0083
<i>Sugar</i>				
Levoglocosan	6,9183 ± 0,3519	0,4929 ± 0,0235	5,0872 ± 0,2588	0,0000 ± 0,0000
<i>Ion</i>				
Aluminium	38,8800 ± 0,2400	67,7600 ± 0,3600	25,9600 ± 0,1600	45,1200 ± 0,2800

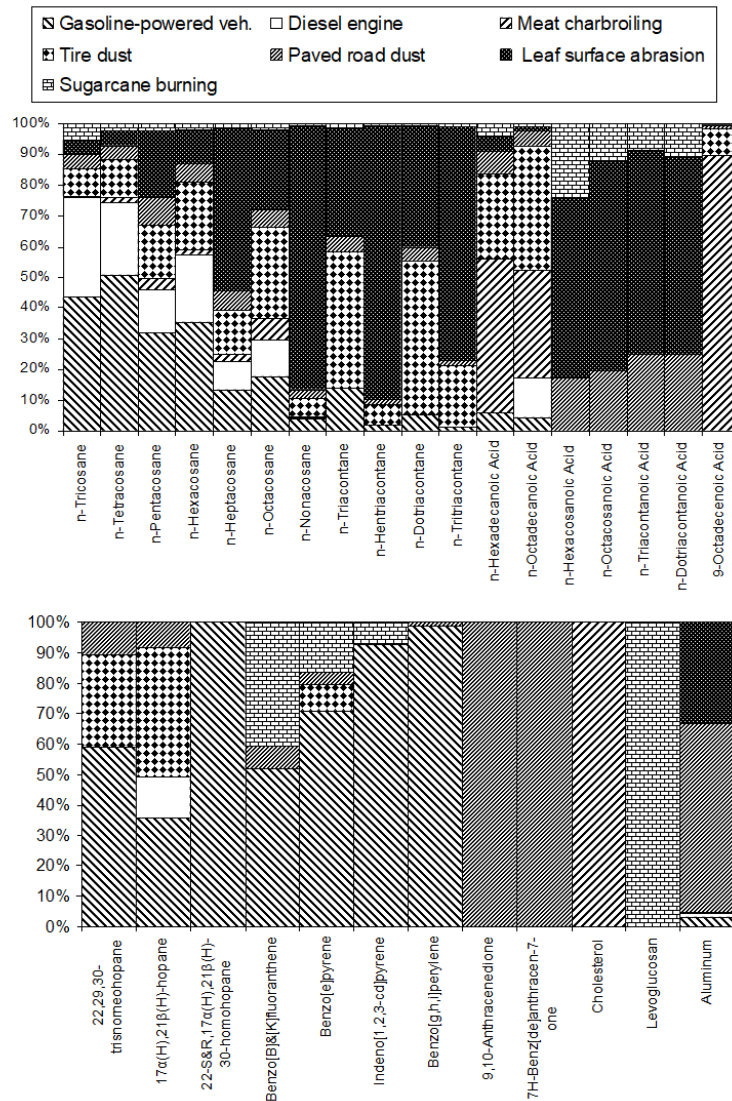


Figure 2. Ratios of particulate organic compound emissions by PM source type

There may be two reasons for this; one of the possibilities is that the fine particles could be carried out to the urban site or other possibility is that the biomass burning in urban site may elevate the concentration of Levoglucosan in significant level. The particle contribution from leaf surface was only seen in January in Belle Glade due to harvest activities that generates robbing monition on the leaf surface. The exhaust from vehicles on the field was also an important fine particle contributor in the rural site during the sugarcane harvest period. The biomass burning is mainly from sugarcane burning including small amount of wildfire and grass burning should be considered in South Florida. The source contribution in Belle Glade and Delray Beach during January and May is shown in Figure 5.

4. Conclusion

The modeling of CMB8.2 results show the contribution of fine particle matter from the sources in order from the highest ratio to lowest ratio, that are paved road dust, sugarcane foliage burning, gasoline-powered and diesel- powered vehicle exhaust, leaf surface abrasion particles, and a very minor fraction of meat cooking. The program did not did not produce only the concentration for tire dust.

The study area has a large agricultural area that includes a high-level fieldwork with diesel-equipped vehicle due to the sugarcane plantation. That also cause to emit the road dust from the farm area. In the urban site, the high traffic activity in the city was could be a considerable also another reason for the emission of paved road dust. The sugarcane burning emissions affected to the both sampling sites in January. The urban site, neighboring the agricultural area, was affected during sugarcane foliage burning, because the airborne particles were transported from Belle Glade to Delray Beach.

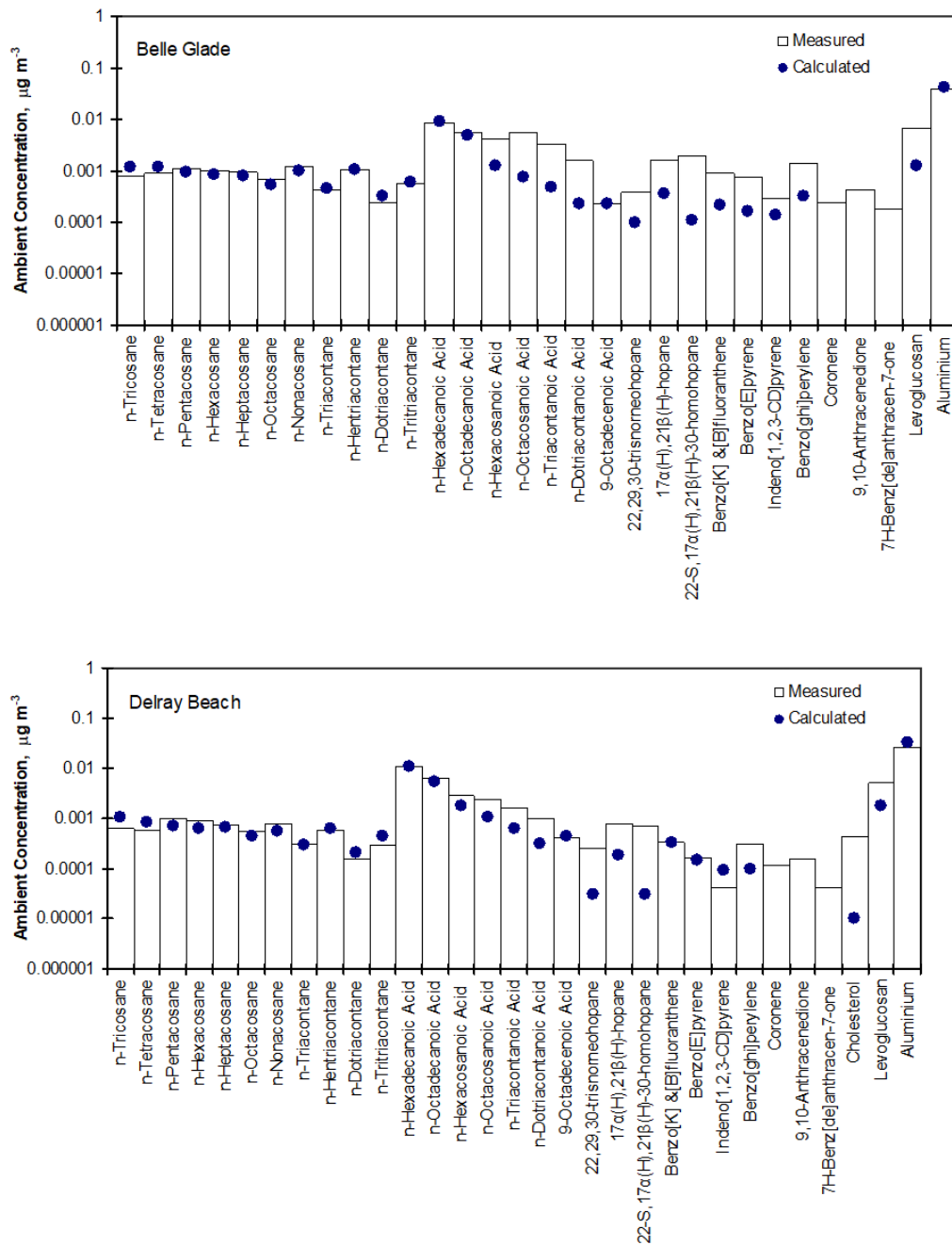


Figure 3. Comparison of model predictions to measured ambient concentrations for the selected compounds in January in Belle Glade and Delray Beach

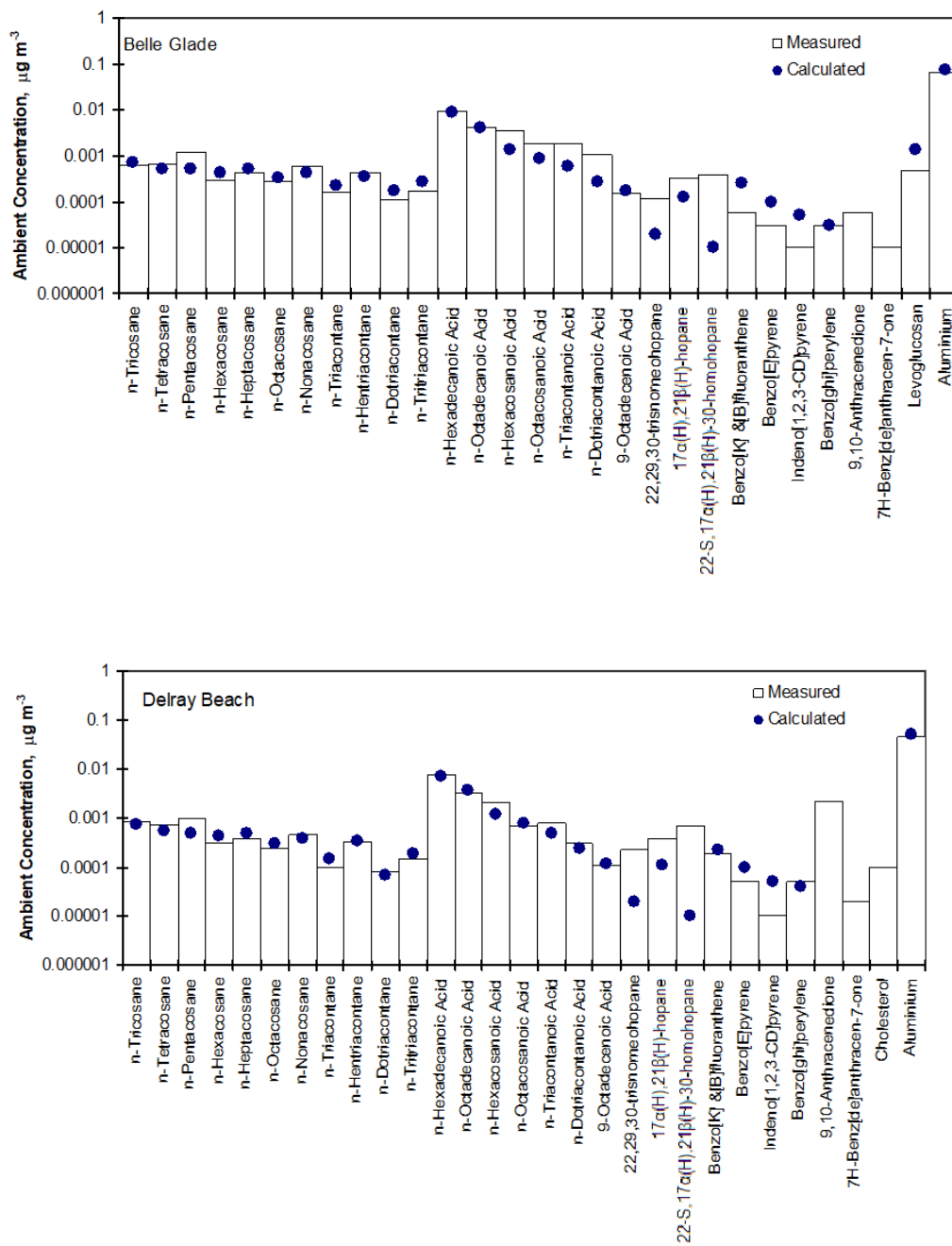


Figure 4. Comparison of model predictions to measured ambient concentrations for the selected compounds in May in Belle Glade and Delray Beach

Table 2. Source apportionment of primary sources of fine organic aerosol concentrations: Monthly average determined by chemical mass balance (avg. \pm std. in $\mu\text{g m}^{-3}$)

	Belle Glade January	Belle Glade May	Delray Beach January	Delray Beach May
Gasoline-powered vehicle	0,0119 \pm 0,0040	0,0008 \pm 0,0002	0,0035 \pm 0,0012	0,0012 \pm 0,0004
Diesel-powered engine	0,0041 \pm 0,0016	0,0039 \pm 0,0015	0,0054 \pm 0,0021	0,0046 \pm 0,0018
Meat charbroiling	0,0003 \pm 0,0000	0,0000 \pm 0,0000	0,0009 \pm 0,0000	0,0003 \pm 0,0000
Tire Dust	0,0000 \pm 0,0000	0,0000 \pm 0,0000	0,0000 \pm 0,0000	0,0000 \pm 0,0000
Paved road dust	0,0397 \pm 0,0005	0,0807 \pm 0,0010	0,0336 \pm 0,0004	0,0521 \pm 0,0007
Leaf surface abrasion	0,0010 \pm 0,0001	0,0000 \pm 0,0000	0,0000 \pm 0,0000	0,0000 \pm 0,0000
Sugarcane Burning	0,0143 \pm 0,0005	0,0156 \pm 0,0006	0,0211 \pm 0,0007	0,0000 \pm 0,0000

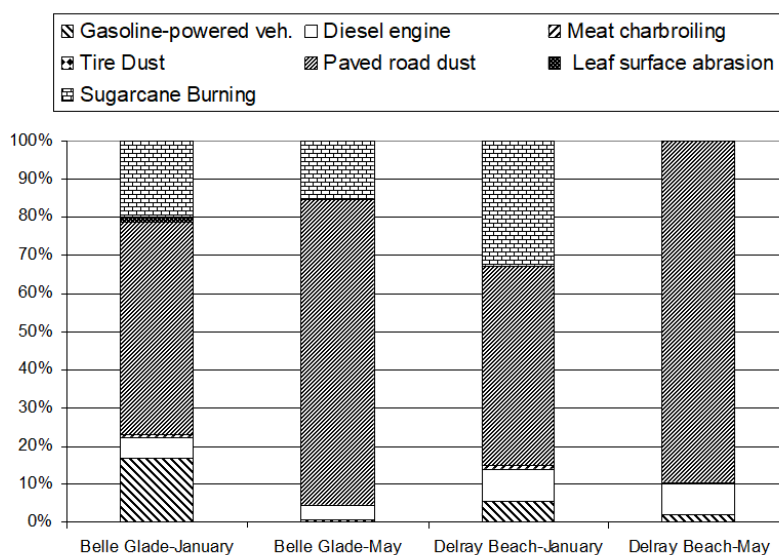


Figure 5. The proportion of sources selected in modeling in sugarcane burning and growing period

That elevates the fine PM concentrations due the wind from sugarcane agricultural area to urban area on January 7 and 20 of sampling year. However, Levoglucosan is not only derived from the sugarcane leaf burning, but also derived from other vegetative burning such as grass burning and biomass burning. In May, there was also biomass burning emission was detected in the rural area except the pre-harvest sugarcane burning period. There was possibility that the sugarcane foliage was also burned in the sugarcane mill facility to reduce the volume of waste foliage and to produce electricity.

Gasoline powered vehicles (catalytic and non-catalytic converter vehicles) were other source contributor in Belle Glade during the pre-harvest season though it has very low ratios in May. The ratios of diesel vehicle exhaust were very similar in January and May in Delray Beach. The result indicates that the number of diesel-powered vehicles in the road remained the same during these two sampling periods.

5. References

Dockery, D.W., Pope III, C.A., Xu, X., Spengler, J.D., Ware, J.H., Martha, E.F., Ferris, B.G., Speizer, F.E. 1993. An association between air pollution and mortality in six US cities. *New England Journal of Medicine*. 329(24), 1753-1759.



- Ramanathan, V., Feng Y. 2009. Air pollution, greenhouse gases and climate change: Global and regional perspectives. *Atmospheric Environment*. 43(1). 37-50.
- Eldering, A., Cass, G.R. 1996. Source-oriented model for air pollutant effects on visibility. *Journal of Geophysical Research*. 101, 19342-19369.
- Motallebi, N., Taylor, C.A., Turkiewicz, K., Croes B.E. 2003. Particulate matter in California: part 1- Intercomparison of several PM_{2.5}, PM_{10-2.5}, and PM₁₀ monitoring networks. *Journal of Air & Waste Management Association*. 53(12), 1509-1516.
- Sevimoglu, O., Rogge, W.F. 2016. Seasonal size-segregated PM₁₀ and PAH concentrations in a rural area of sugarcane agriculture versus a coastal urban area in Southeastern Florida, USA. *Particuology*. 28, 52-59.
- Kalaitzoglou, M., Terzi, E., Samara, C. 2004. Patterns and sources of particle-phase aliphatic and polycyclic aromatic hydrocarbons in urban and rural sites of western Greece. *Atmospheric Environment*. 38(16), 2545-2560.
- Environmental Protection Agency (EPA). 2004. EPA-CMB8.2 Users Manual. Report No. EPA-452/R-04-011. <https://www3.epa.gov/scram001/models/receptor/EPA-CMB82Manual.pdf>. U.S. Environmental Protection Agency, Research Triangle Park, NC. (accessed in 18.07.2019).
- Schauer, J.J., Rogge, W.F., Hildemann, L.M., Mazurek, M.A., Cass, G.R., Simoneit, B.R.T. 1996. Source apportionment of airborne particulate matter using organic compounds as tracers. *Atmospheric Environment*. 30 (22), 3837–3855.
- Rogge, W.F., Mazurek, M.A., Hildemann, L.M., Cass, G.R., Simoneit, B.R.T. 1996. Mathematical modeling of atmospheric fine particle-associated primary organic compound concentrations. *Journal of Geophysical Research-Atmosphere*. 101, 19379-19394.
- Schauer, J.J., Cass, G.R. 2000. Source apportionment of wintertime gas-phase and particle-phase air pollutants using organic compounds as tracers. *Environmental Science and Technology*. 34(9), 1821–1832.
- Rogge, W.F., Medeiros, P.M., Simoneit, B.R.T. 2007. Organic marker compounds in surface soils of crop fields from the San Joaquin Valley fugitive dust characterization study. *Atmospheric Environment*. 41(37), 8183-8204.
- Gilbert, R.A., Shine Jr., J.M., Miller, J.D., Rice, R.W., Rainbolt, C.R. 2006. The effect of genotype, environment and time of harvest on sugarcane yields in Florida, USA. *Field Crops Research*. 95, 156–170.
- Allen, A.G., Cardoso, A.A., Da Rocha, G.O. 2004. Influence of sugar cane burning on aerosol soluble ion composition in Southeastern Brazil. *Atmospheric Environment*. 38(30), 5025–5038.
- Sevimoglu, O., Rogge, W.F. 2015. Organic Compound Concentrations of Size-Segregated PM₁₀ in Sugarcane Burning and Growing Seasons at a Rural and an Urban Site in Florida, USA, *Aerosol and Air Quality Research*. 15(5), 1720–1736.
- Sornpoon, W., Bonnet, S., Poonpipope, K., Prasertsak, P., Garivait, S. 2014. Estimation of Emissions from Sugarcane Field Burning in Thailand Using Bottom-Up Country-Specific Activity Data. *Atmosphere*. 5(3), 669-685.
- Calhoun, D.D., Salmon, L.G., Schauer, J.J., Christoforou, C.S. 2003. PM_{2.5} characterization and source-receptor relations in South Carolina. *Journal of Environmental Engineering and Science*. 2(6), 441-451.
- Sevimoglu, O. 2007. Source/receptor reconciliation of ambient organic fine particulate matter in Palm Beach County. ProQuest ETD Collection for FIU. AAI3268663, pp.160.



Fraser, M.P., Cass, G.R., Simoneit, B.R.T. 1998. Gas-phase and particle-phase organic compounds emitted from motor vehicle traffic in a Los Angeles highway tunnel. *Environmental Science and Technology*. 32, 2051–2060.

Schauer, J.J., Kleeman, M.J., Cass, G.R., Simoneit, B.R.T. 1999. Measurement of emissions from air pollution sources.2: C–1 through C–30 organic compounds from medium duty diesel trucks. *Environmental Science and Technology*. 33(10), 1578–1587.

Rogge, W.F., Hildemann, L.M., Mazurek, M.A., Cass, G.R., Simoneit, B.R.T. 1993. Sources of fine organic aerosol. 3. Road dust, tire debris, and organometallic brake lining dust: roads as sources and sinks. *Environmental Science and Technology*. 27(9), 1892–1904.

Schauer, J.J., Kleeman, M.J., Cass, G.R., Simoneit, B.R.T. 1999. Measurement of emissions from air pollution sources. 1. C1 through C29 organic compounds from meat charbroiling. *Environmental Science and Technology*. 33(10), 1566–1577.

Rogge, W.F., Hildemann, L.M., Mazurek, M.A., Cass, G.R., Simoneit, B.R.T. 1993. Sources of fine organic aerosol. 4. Particulate abrasion products from leaf surfaces of urban plants. *Environmental Science and Technology*. 27(13), 2700–2711.

Oros, D.R., Abas, M.R., Omar, N.M.J., Rahman, N.A., Simoneit, B.R.T. 2006. Identification and emission factors of molecular tracers in organic aerosols from biomass burning Part 3. Grasses. *Applied Geochemistry*. 21(6), 919–940.

Acknowledgement

This air sampling study was supported by the Division of Air Pollution in Palm Beach County Health Department. The air sampling analysis was accomplished in the Air Pollution Laboratory at Florida International University in Miami, Florida, USA.

AUTHOR INDEX

A

Acikel, G.	627
Agouillal, F.	544
Akca, B.	591
Akin, Ö.	715
Akkoyunlu, B.	431, 447, 483
Aktacir, M.A.	755
Akyuz, E.	160, 184, 399, 483
Albuquerque, C.	647
Alp, K.	349
Amin, M.	244, 703
Anamarija, J.S.	38
Ante, C.	38
Arı, A.	554, 627
Arı, P.E.	554
Arslandaş, O.A.	265
Artun, G.	627
Atakul, H.	509
Atımtay, A.T.	389
Ayrı, I.	282, 476
Ayvaz, C.	715

B

Bakar, C.	576, 582
Bakar, S.A.	603
Balcı, E.	288
Barnes, J.	49
Baykara, M.	399
Beba, H.E.	265
Bellazzi, R.	654
Benadda, F.	544
Bešlić, H.I.	94
Bešlić, I.	112, 123
Bešli, N.	755
Bilgic, E.	146
Bingol, F.	597
Bintang, S.R.N.	703
Birgöl, A.	282
Boev, B.	492
Boev, I.	492
Burgaz, S.	554

C

Cačković, M.	123
Cakir, I.	27

Cakir, S.	1
Cakmak, E.G.	274
Cakmak, G.	554
Calısır, D.	627
Caliskan, B.	296
Callum, A.	49
Can, E.	627
Can-Guven, E.	518
Cardenas, B.	647
Casella, V.	654
Cernuschi, S.	674
Ceylan, O.	457, 467
Cherifi, N.	544
Chiarawatchai, N.	425
Cindoruk, S.S.	296
Cleo, K.	38
Contreras, S.	647
Ćosić, V.	57
Cotuker, O.	582
Csobod, E.	49
Cukurlu, H.	509
Cukurluoglu, S.	501
Cuzzolin, G.	567
Cvitković, A.	57

D

Dalvand, A.	525
Davila, S.	94, 112
De Vito, L.	49
Demir, G.	431
Demirhan, A.	27
Diafas, J.	49
Dinc, M.N.	755
Dincer, F.	457, 467
Dincer, F.K.	457, 467
Djadi, A.	544
Dogan Guzel, T.	349
Dogan, G.	597
Dogan, S.	597
Doğan, T.R.	755
Dortler, M.	63, 84
Dumanoglu, Y.	554, 742, 749
Dyson, L.L.	378
Džepina, K.	137

E

Eker Sanlı, G.	321
---------------------	-----

Elbir, T.	172, 533, 576, 582, 635, 764
Eraslan, F.N.....	560
Ercan, O.....	457, 467
Erdem, A.	597
Erguclu, M.E.	616
Erkuzu, H.	732

F

Faisal M.A.F.....	703
Fandi, N.F.M.	603
Ferrari, A.	567
Flores, R.M.....	431, 447
Fogg-Rogers, L.....	49
Furuuchi, M.	244, 703

G

Gaga, E.O.	554, 560, 627
Garland, R.M.....	378
Gaygisiz, H.	476
Gencil, C.D.	616
Genisoglu, M.	282, 288, 476, 749
Gertler, A.W.....	214
Ghasemi, R.	525
Giuponi, G.	567
Glušćić, V.....	123
Godec, R.	94, 105, 137
Gozdas, H.T.....	27
Gunduz, O.	146
Gunel, E.....	749

H

Han, J.W.....	13
Hassoli, N.....	13
Hata, M.....	244, 703
Hayes, E.	49
Himpe, W.	49
Hong, S.C.	73
Hrga, I.....	112
Hu, T.H.....	203
Huremović, J.	137
Husby, T.....	49
Hwang, J.S.....	203

I

Ikemori, F.....	244, 703
Ilhan, S.O.....	627
Ilkhan, M.A.	755
Incecik, S.....	412
Ivanova, O.	49

J

Jahangiri, A.....	525
Jakovljević, I.....	105, 137
Jalaludin, J.	603
Jang, E.S.	73
John, K.....	359

K

Kaced, A.	544
Kahya, C.	225
Kantarcı, M.D.	778
Karadeniz, H.....	93, 196
Karim, M.R.....	693
Kaynak, B.	160, 184, 399
Keivani, B.	389
Keskin, S.S.....	306
Kim, H.T.....	13
Kim, K.D.	13
Kim, K.S.	73
King, A.	49
Kuddusi, Y.....	509
Kurt-Karakus, P.B.	282
Kuzu, S.L.	483

L

Ladji, R.	544
Lakestani, S.....	27
Lange, A.D.....	378
Larizza, C.....	654
Latif, M.T.....	603
Lee, G.H.....	73
Lee, J.R.	13
Lee, K.S.	13
Lemou, A.	544
Liebenberg-Enslin, H.....	340
Lim, G.Q.	359
Lonati, G.....	674, 684
Longhurst, J.	49

M

Mahasurachaikul, E.	425
Mahyuddin, N.....	725
Marić, M.	112
Marijana, V.....	38
Mendaš, G.....	129
Mentese, S.....	576, 582, 591
Mertoglu, E.	447
Misirlioglu, C.....	597
Mihaljević, M.	94
Mirakovski, D.	492

Mirici, N.A.	576, 582
Moral, C.	597
Moshe, D.	214
Mumcuoglu, D.T.	582
Mwananawa, N.	340

N

Nikolova, M.H.	492
Novarina, A.	703
Nurlu, C.	749

O

Odabasi, M.	63, 84, 554, 627, 732
Oertzen, D.V.	340
Okan, F.	732
Oktay, B.	509
Okutan, H.	274, 509
Olgun, B.	597
Olgun, H.	389
Oliveira, L.	647
Onat, B.	715
Oruc, H.N.	431
Otkun, M.T.	576, 582
Ouakli, N.A.	544
Oymak, S.	576, 582
Ozdemir, B.	483
Ozdemir, E.	635, 764
Ozdemir, H.	431, 447
Ozengin, N.	296
Ozkaya, F.	715
Ozkurt, N.	306, 412
Ozturk, E.	370
Ozturk, F.	755
Ozturk, Z.	265

P

Pala, D.	654
Palaz, E.	533, 582
Panpanit, C.	425
Papics, P.	49
Park, Y.O.	13
Pecorari, E.	567
Pehnec, G.	76, 105, 123, 129, 137
Phairuang, W.	244
Pinprateep, W.	425
Piriyakarnsakul, S.	244
Pogliaghi, A.	654
Putri, R.M.	244, 703

R

Rampazzo, G.	567
Rinkovec, J.	76
Rizky, A.	244
Rogge, W.F.	797

S

Sahin, U.A.	715
Saifuddin, M.R.M.	693
Sakin, A.E.	330
Samavati, M.	160
Saral, A.	483
Sari, D.	306, 412, 457, 467
Saridikmen, B.	184
Schins, R.	554
Seddon, J.	647
Sevimoglu, O.	797
Sezen, I.	399, 431
Shijakova, T.	492
Silović, M.	94
Simić, I.	94, 129
Simoni, W.	647
Sita, M.	1
Sofuoglu, A.	282, 288, 476, 749
Sofuoglu, S.C.	282, 288, 476, 749
Song, S.N.	73
Strukil, Z.S.	105
Suciari, T.F.	703
Suer, S.N.	225

T

Tasdemir, Y.	321, 330
Tatjana, O.	38
Tayanc, M.	399, 431, 447
Tezel, M.N.	306
Tipsunave, V.	425
Toros, H.	265
Trentini, A.	684
Tuna Tuygun, G.	146, 172, 576, 635, 764
Turgut, E.T.	627

U

Ullah, A.	244
Unal, A.	399, 431, 447
Unsal, B.	749
Unsalan, F.	635
Uzmez, O.O.	560
Uzumoglu, T.	647
Uzun, B.	715



18th World Clean Air Congress, 23-27 September 2019, Istanbul
organized by TUNCAP and IUAPPA

V			
Valjetic, M.....	57	Yildiz, M.....	755
Vanherle, K.	49	Yilmaz, M.....	265
Vesna, C.....	38	Yigit, Y.	616
Vito, D.....	654	Yildiz, I.	27
		Yolcular, M.....	749
		Yu, S.Y.	73
		Yucel, A.....	778
W		Z	
Wada, M.....	703	Zendelska, A.	492
Y		Zero, S.....	137
Yaman, B.....	732	Zeydan, O.	370
Yavuz, E.....	483	Zužul, S.....	76
Yenisoy Karakas, S.	63, 84, 196		

KEYWORD INDEX

A		BTEX..... 591	
Active sampling.....	282, 330	Bulk..... 129	
AERONET	635	C	
Aerosol Optical Depth.....	635, 764	CAL3QHCR	370
Agriculture	73	Canakkale	576, 582
Air pollutants.....	1, 576, 591	Canakkale Harbor	591
Air pollution	49, 57, 225, 265, 597, 654	Carbon dioxide.....	725
Air pollution health effects.....	203	Carbon tetrachloride	476
Air pollution prevention	296	Carbonaceous Component	244, 703
Air quality	73, 457, 525, 647	Carbondioxide capture and storage.....	509
Air quality forecasting.....	533	Carcinogenic	105
Air Quality Management.....	340	Carcinogenic potency	137
Air quality modelling	370, 576	Cations	123
Air quality models	412	Cement.....	616
Airflow	725	Chloroform	476
Air-water exchange	330, 732	Chromosomal damage	603
Akhisar	778	Circulating fluidised bed combustion	389
Alternative fuels	616	Cities	49
Ambient monitoring	214	Citizen behaviour.....	49
Ammonia.....	73, 674	Climate change	274, 349, 693
Angstrom exponent	635	Cluster analysis.....	684
Anions	123	CMB8.2	797
Anthropogenic VOCs	63, 84	Coal-fired power plants	184
AOD	172	Collection 6.1.....	764
API	544	Commuter exposure.....	715
AQMeshPod.....	112	Computational fluid dynamics.....	725
Artificial Neural Network	1, 533	Concertation.....	492
Atmospheric dispersion model.....	146	Contribution.....	492
Atmospheric fallout.....	518	Conventional air pollutants.....	296, 483
Atmospheric particulate matter	755	Correlation	196, 483
AVGAS	627	Crop land	73
B		D	
Back trajectory	282	Dark Target Algorithm	764
Bacterial identification	544	Data.....	654
BaP	105	Day-night time periods	321
Barnett Shale	359	Deposited dust	467
Benzene	603	Deposition.....	330
Bibliometric analysis.....	597	Desert.....	755
Biga Peninsula.....	412	Diagnostic ratio.....	105, 137
Bioaerosols	544	Disinfection by-products.....	749
Biocoal	389	Dispersion modeling	457
Biogenic VOCs	63, 84	Dispersion of emissions	467
Biomass	389	Dry scrubbing	13
Biomonitor	525	Dust storms	146
Black carbon.....	483, 715		

E		Industrial emissions	296
Elemental carbon	94, 447	Inhalable particulate matter	340
Elemental composition	431	Inhalation	518
Emergency interventions	57	Integrated air quality assessment	399
Emission	274, 349, 476	Intelligent transportation systems	265
Emission Sources	244, 399	Interventions	647
Energy	693	Inventory	73
Energy efficiency	616	Ions	501
Entrained mixing reactor	13	Istanbul	447
Environmental impact of transportation	567	K	
Expected years of life lost	203	Kilitbahir Harbor	591
Exposure	306	Klang Valley	603
F		Konya	399
Factor analysis	501	L	
Ferry	715	Lead	525, 627
Fibers	518	Lichens	525
Fine particulate matter	203, 431	Linear Regression	1
Flame retardants	282	Livestock	73
Flue gas	509	Location optimization	184
Fugacity fraction	732	Long range atmospheric transport	282
G		Low-cost air sensors	112
Gas-particulate partitioning	288	M	
Genotoxicity	554	MALDI-TOF MS	544
Geothermal power plant	742	Management of transportation	567
Greenhouse gas	274, 349, 616, 693	Marmara Region	225
Grubb test	112	Mass concentration	703
<i>GSTT1</i> , <i>GSTM1</i> polymorphisms	603	Measuring site	123
H		MERRA	146
HCl removal	13	Metals	76
Health	654	Meteorological data	483
Health effects	425	Meteorological Parameters	1
Health impacts	340	Meteorology	399
Health risk	160	Microwave digestion	76
Heavy metals	431	Mobile sources	296
HPLC	105	Modelling	306, 797
Hydrate lime	13	MODIS	172, 764
Hydrogen Sulphide	57, 742	Moss	597
HYSPLIT	412	Motor vehicles	370
I		N	
ICP MS	76	Namibia	340
Indonesia	244, 703	Natural and man-made emissions	340
Indoor air	518, 749	Near-real time assessment	214
Indoor air quality	476, 582, 725	Nitrogen oxides	778
Indoor and outdoor air measurement	560	NO ₂	225
Indoor environment	288	North Sumatera	703
		NO _x pollution	306, 359

NQOI603

O

OC94
OC/EC ratio94
OCP321
Odor457
Oil and gas industry425
Olive trees778
Organic air pollutants591
Organic carbon447
Outdoor air518
Oxy-fuel combustion509
Oxygen enriched combustion389
Ozone359

P

PAHs 129, 554
Pamukkale501
Participation654
Particle fluorescence214
Particle number684
Particle number concentration715
Particle-gas phase321
Particulate matter57, 76, 146, 467, 533, 627
Particulates492
Passive air sampling544, 597
Patterns492
PBDEs282
PCA123
PCB129
Photovoltaic Module Performance755
Pier715
Piston engine aircraft627
Planetary Boundary Layer Height172
PM214
PM_{0.1}244, 703
PM₁₀137, 172, 184, 370, 597
PM_{2.5}160, 447, 560, 715
PMF492
Po valley674, 684
POC and SOC94
Polar plots674
Pollution525
Polycyclic Aromatic Hydrocarbons137
POPs330
Positive Matrix Factorization63, 84
Power generation274
Prediction533
Public engagement49
Pulmonary function576

R

Radiation exposure dose340
Rain196
Rainout-Washout Mechanism196
Remote sensing160
Respiratory function582
Respiratory health582
Respiratory symptoms576
River water732
Road traffic306

S

Sampling ratios330
Sanliurfa755
Seasonal variation84
Semi-rural area321
Shale gas359
Sick building syndrome582
Signal optimization370
Size distribution684
Size-segregated PM554
Slavonski Brod57
Small boats emissions567
Smoke-Haze244
SO₂184, 225
SO₂ removal13
Solid fuels274
Source apportionment49, 63, 214, 797
Source term146
Spatial distribution84
Sulfur dioxide778
Sumatera-Island244
Surface ozone412
Survival extrapolation203
Sustainable development616
Swimming pools749
Synthetic musk compounds288

T

Temporal variations63
Thailand425
Thermal power plant467, 778
Time pattern674
TIMES model349
TNMOC359
Toilet cleaning products476
Torrefaction389
Total deposited matter129
Trace elements501
Trace organic compounds797



Traffic.....	265
Transport	693, 755
Transport emissions.....	647
Transportation	265, 349
Trihalomethanes	749
Turkey	172, 635, 742, 764

U

Urban air quality.....	214
Urban traffic policemen.....	603

V

Vehicle technology.....	693
-------------------------	-----

Ventilation	476
VOCs Maximum.....	425
Volatile methyl siloxanes.....	732

W

Wastewater treatment plants.....	457
Water Soluble Inorganic Species.....	196
Waterborne transport	567
Wet deposition.....	501
Workplaces	560
WRF.....	412

SPONSORS



Istanbul Technical University



Dokuz Eylul University



Turkish Cooperation and
Coordination Agency



The World Bank



The Climate and Clean Air
Coalition



Enotek Ltd.



Kazan Soda Elektrik Uretim
Inc.



Pakmaya



The Foresters' Association of
Turkey



Turkish Cement
Manufacturers' Association



Teknozon Ozone Systems



TİTAS Inc.



GEBKIM Education
Foundation



Gebkim - Kocaeli Gebze V
(Chemistry) Specialized
Organized Industrial Zone



Ak-Tas Dis Ticaret Inc.



Izmir Demir Celik Sanayi Inc.